British Journal of Pharmacology

March 1994

Volume 111 Number 3 pages 649–968

Dr S J Coker
Department of Pharmacology
University of Liverpool
P.O. Box 147
LIVERPOOL L69 3BX

Br. J. Pharmacol. (1994), **111**, 649–651 © Macmillan Press Ltd, 1994

OBITUARY

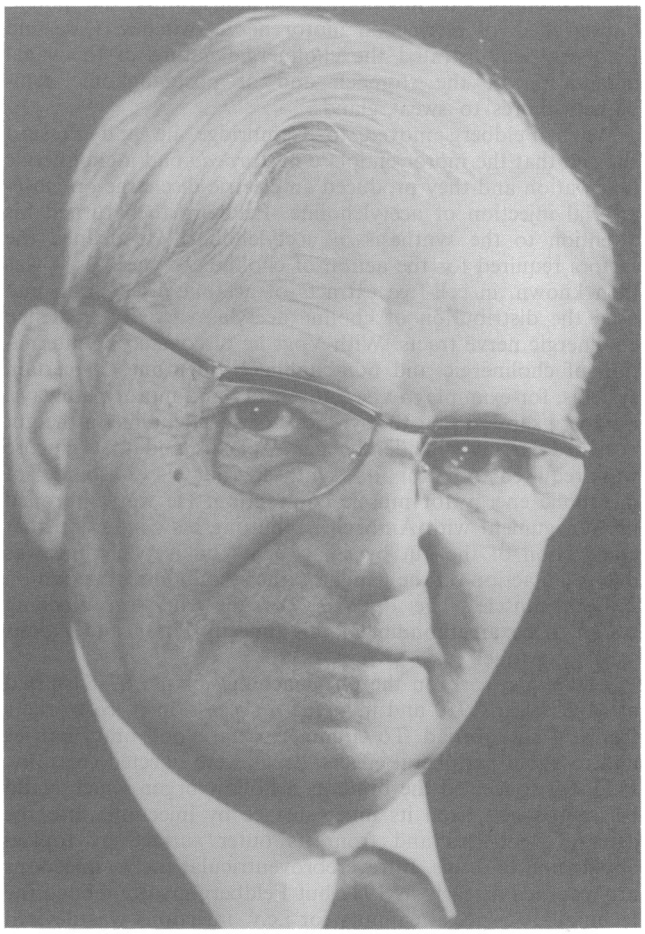
Wilhelm Feldberg, CBE, FRS (1900–1993)

We had looked forward to celebrating Wilhelm Feldberg's 93rd birthday on 19th November this year. He died on 23rd October, assured of a permanent place in the history of medical science by his outstanding work on neurochemical transmission and the actions of drugs on the central nervous system.

Feldberg was born in Hamburg. He studied medicine in Heidelberg and Munich. During his holidays he worked with E. Schilf at the Institute of Physiology in the University of Berlin and qualified M.D. Berlin in 1925. In the same year, he married Katherine, daughter of the art critic, Karl Scheffler and the next two years, which he fondly described as a prolonged honeymoon, were spent in England. He was inspired by Langley's book, *The Autonomic Nervous System*, which Schilf had translated into German and Schilf arranged for him to work with Langley in Cambridge. Langley died 6 months later and was succeeded by Joseph Barcroft. During the last 6 months of his stay in England, Feldberg worked with Dale in the National Institute for Medical Research which had been established in Hampstead. He acknowledged the formative influence of this early period on his approach to research and was particularly influenced by Dale who stressed the importance of first perfecting a method over months or years, if necessary, before carrying out the definitive experiment. 'Die methode ist alles' was in fact one of Feldberg's favourite aphorisms and underlies the whole of his work.

Feldberg returned to the Institute of Physiology in Berlin but in 1933, in a general purge of Jews in German universities, he was summarily dismissed. He had met Dale again at a meeting in Wiesbaden during the previous year and this prompted an invitation to work with him in his laboratory at Hampstead. There he met Gaddum, to be joined later by Marthe Vogt and G.L. Brown. He left Hampstead in 1936 to take up a 2 year scholarship with Kellaway in Australia and then returned to Cambridge where he was appointed Reader in Physiology. His distinguished career with the Medical Research Council began in 1949 with his appointment as Head of the Division of Physiology and Pharmacology in the National Institute for Medical Research. The Institute was then in the process of moving to its present site in Mill Hill but the Division was affectionately referred to as 'F4' in memory of the room which Dale had occupied in the old Institute at Hampstead. Feldberg retired as Head of Division in 1966 and a Laboratory of Neuropharmacology was set up for him. This was closed in 1974 but he continued to be supported by grants from the Council. Sadly in 1990, he encountered fierce opposition from Animal Rights activists and this led to unfavourable publicity and his finally retiring from the Institute. He had completed 65 years of continuous research with an output of 355 publications, revealing a capacity for work and self-discipline which few could hope to emulate.

It is instructive to trace the historical background to Feldberg's work on the identification of acetylcholine as a neurotransmitter. In 1904 Elliot, a student at Cambridge, was impressed by the similarity of responses to injections of adrenaline and stimulation of sympathetic nerves which he suggested might act by releasing an adrenaline-like substance. By similar reasoning, Dixon in 1907 proposed that parasympathetic nerves released a muscarine-like substance. In 1914 Dale published his classical paper on 'certain ethers and esters of choline', described acetylcholine as parasympathomimetic and predicted the existence of a choline esterase in blood. From 1921 to 26 Loewi carried out his famous experiments on the release of vagussstoff and acceleransstoff from the vagosympathetic nerve terminals in the perfused frog heart.



Professor Wilhelm Feldberg

In Berlin, Feldberg had decided to investigate the release of acetylcholine by nerve stimulation but the problem was to obtain a sufficiently sensitive method of bioassay. He adopted Fühner's preparation of the eserinized dorsal muscle of the Hungarian leech. The principle was to stimulate the nerve supply to an organ in the eserinized animal and to allow the venous outflow, after cooling, to pass over the leech muscle in an organ bath. Working with Krayer and Minz, Feldberg demonstrated release of acetylcholine from the tongue on stimulation of the chorda tympani in the lingual nerve, from the coronary sinus in the heart-lung preparation on stimulation of the vagus and from the adrenals after splanchnic stimulation. Feldberg introduced his leech muscle preparation to Dale's laboratory and in the following 3 years there followed a prodigious output of 24 papers or communications in the Journal of Physiology, in all of which he was a co-author, extending chemotransmission to the nicotinic action of acetylcholine at autonomic ganglia and the neuromuscular junction. Using the method devised by Kibjakow, Gaddum and Feldberg perfused the superior cervical ganglion and demonstrated the release, after stimulating the cervical sympathetic, of a substance which they identified as acetylcholine by the method of parallel

quantitative assay introduced by Gaddum and Chang. With Dale, the release of acetylcholine was demonstrated from skeletal muscle in a perfused leg preparation after stimulation of anterior spinal nerve roots. A crucial experiment was to produce contraction of skeletal muscle after close-arterial injection of acetylcholine. Brown introduced a new electrophysiological dimension into the work and added convincingly to the theory that acetylcholine was the transmitter at the neuromuscular junction by demonstrating the potentiating effect of eserine on motor nerve twitches. Dale and Feldberg demonstrated the cholinergic nature of the vagal innervation of the stomach and of postganglionic sympathetic fibres to sweat glands.

When Feldberg moved to Cambridge he and Fessard showed that the motor endplate in *Torpedo* had a cholinergic innervation and they produced an electric discharge on close-arterial injection of acetylcholine. Feldberg then turned his attention to the synthesis of acetylcholine. He defined the factors required for the action of choline acetylase, as it was then known, in cell-free extracts of acetone-dried brain and used the distribution of choline acetylase activity to define cholinergic nerve tracts. With Vogt he discovered an alternation of cholinergic and non-cholinergic neurones in certain systems, for example in afferent sensory and motor pathways. Feldberg showed that the synthesis of acetylcholine in the gut occurred largely outside the nerve plexus and that glucose was required not for its synthesis but as a source of metabolic energy for muscle contraction. He was embroiled in an argument with Ambache, rebutting his contention that contraction of the gut by small doses of acetylcholine was due to an action on the ganglia rather than a direct action on smooth muscle. The discovery of the ganglion blocking action of hexamethonium at this time by Paton and Zaimis was opportune.

Feldberg's work on the pharmacology of the CNS started at Mill Hill in 1950 and involved a succession of co-workers from F4 and abroad. To circumvent the blood brain barrier and to avoid peripheral effects, drugs were injected centrally. Feldberg conceived the brain as a hollow organ which could be approached from its inner surface by injections into the cerebral ventricles and from its outer surface by topical application of drugs. Intracerebroventricular (i.c.v.) injections are recorded as early as 1922 but Feldberg greatly refined the technique. A special cannula for i.c.v. injections was devised by Collison, his redoubtable Chief Technician whom he had inherited from Dale. The use of the Collison cannula was first described with Sherwood in 1953 and the characteristics of penetration and peripheral absorption of drugs injected i.c.v. were defined. A wide variety of effects was produced by drugs injected into a lateral ventricle. Among the most dramatic were sleep, anaesthesia, analgesia, loss of consciousness, convulsions, tremor, catatonia, scratching movements and fever. Experiments with dye distribution showed that a drug injected into a lateral ventricle passes into the third ventricle, through the cerebral aqueduct into the fourth ventricle and then through the lateral recesses of the fourth ventricle to reach the subarachnoid space surrounding the ventral and dorsal surfaces of the brain stem.

Feldberg devised techniques to localize the site of action of drugs and so discover the physiological function or pathological dysfunction of the underlying structures. Tubocurarine provides a good example. In contrast with its peripheral neuromuscular blocking action, tubocurarine injected into a lateral cerebral ventricle of the cat acted as a central stimulant, producing convulsions with an abnormal spike discharge in the electrocorticogram, accompanied by autonomic and motor effects. It was inactive when injected into the cisterna magna, from which access to the ventricles is excluded by the absence in the cat of the foramen of Magendie at the end of the IVth ventricle. It was still effective, however, when injected into a lateral ventricle after cannulation of the central aqueduct which prevents access to the IVth ventricle and subarachnoid space. By regional perfusion of the drug, the spike discharge was finally localized to the inferior horn of the lateral ventricle and the underlying hippocampus but the autonomic motor effects, which could be dissociated from this discharge, were shown to be elicited from structures in the IIIrd ventricle. This has an obvious bearing on the spread of an electrogenic focus in clinical epilepsy. Other central actions of tubocurarine were localized to different sites – scratching movements to the upper part of the dorsal cervical cord and release of vasopressin to the ventral surface of the brain stem.

Feldberg became interested in the mechanism of fever and this proved to be a contentious field. In the cat, on i.c.v. injection, 5-hydroxytryptamine (5-HT) caused a rise, and adrenaline a fall, of body temperature but species differences raised doubts about their significance in fever and the amines were supplanted in this role by prostaglandins. Prostaglandin E_2 (PGE_2) injected i.c.v. caused fever, it appeared in the CSF during fever induced by bacterial pyrogens and lipid A and disappeared when the fever was lowered by antipyretics which inhibit prostaglandin synthesis. A new area of study arose from an analysis of the hypotensive response to sodium pentobarbitone and glycine injected into a lateral ventricle. The site of action was traced to the ventral surface of the brain stem which Feldberg described as a 'scarcely explored area of pharmacological sensitivity'. The topical application of the drugs through perspex rings revealed a bilateral circumscribed zone from which the fall in blood pressure was elicited, revealing a possible physiological function of the underlying structures in the maintenance of normal blood pressure. A second area, the 'nicotine-sensitive zone' was discovered from which topical application of nicotine caused the release of vasopressin without oxytocin. This zone is now thought to be coincident with the A1 group of noradrenergic neurones on the ventral surface which selectively innervate vasopressin-secreting cells in the supraoptic and paraventricular nuclei. γ-Aminobutyric acid (GABA) applied to this zone blocked the physiological release of vasopressin in response to carotid occlusion and it was suggested that this zone acts as a relay station for afferent neural pathways to these nuclei which are relayed by the nucleus of the tractus solitarius from peripheral receptors in the cardiovascular system. Hypertonic saline injected i.c.v. in the cat also released vasopressin without oxytocin but the site of action was traced to the dorsal surface of the brain stem in the region of the obex, possibly revealing the presence of osmoreceptors in the area postrema. The obex and the NTS were found to be involved also in the action of morphine on the cardiovascular system. Topical application to the obex caused a fall in heart rate and blood pressure due to a selective inhibition of sympathetic tone to the heart and blood vessels, an action which could be important in the therapeutic use of morphine in left ventricular failure.

Feldberg's last experiments at Mill Hill were on hyperglycaemia. This had first been observed in response to morphine and adrenaline injected i.c.v. in the conscious animal. The effect of adrenaline was due to peripheral absorption from the fossa interpeduncularis. Morphine acted by central sympathetic stimulation of the adrenal medulla and the site of action was traced once again to the ventral surface of the brain stem in a region caudal to the trapezoid bodies. With a touch of serendipity, experiments with antagonists revealed an unexpected hyperglycaemic response to i.c.v. injection of naloxone, phentolamine and propranolol. The hyperglycaemic response to all these drugs was abolished by i.v. chloralose but, curiously, when injected i.c.v. in one hundredth of the i.v. dose, chloralose itself produced hyperglycaemia as well as anaesthesia. GABA i.c.v acted similarly. It was suggested that GABA and β-endorphin could act at synapses on the ventral surface in the central regulation of normal blood sugar levels and this has relevance to the aetiology of non-insulin dependent diabetes. One outcome of this work was the controversial suggestion that the chief physiological function of adrenaline in low concentrations is

to regulate the blood sugar level rather than the cardiovascular system.

An absorbing and continuing interest in histamine started from Feldberg's earliest days in Berlin with E. Schilf. With Kellaway, he worked on the release of histamine from the perfused lung by snake and bee venoms and bacterial toxins. It was shown that the perfusate contained not only histamine but another substance termed SRS or Slow Reacting Substance. This led subsequently to the discovery of SRS-A, the Slow Reacting Substance of Anaphylaxis and offered already at that time an explanation of the ineffectiveness of antihistamines for the treatment of bronchial asthma. The release of histamine by morphine, 5-HT, 48/80 and horse serum was investigated as well as its distribution within the skin and gut.

Feldberg was respected as much for his humanity as for his scientific achievement. He was a warm and generous man who worked tirelessly to promote both the personal and scientific interests of his staff in F4. He was a great wit and raconteur who collected a repertoire of inimitable jokes and stories for his after-dinner speeches. His good humour was unfailing to the end. His reputation attracted a large number of visiting workers from all parts of the world. Those who had worked with him were invited to contribute to a commemorative album presented to him on his 90th birthday. There were 71 contributors. He loved entertaining at 'Lavenham', his home in Mill Hill, educating his friends and colleagues in fine wines, surrounded by his collection of books, paintings and antiques. His particular joy was a complete set of Toulouse-Lautrec's 'Elles' series of lithographs which he had borrowed money to acquire as a young man.

Feldberg's reputation was international. He was awarded the CBE in 1963, elected FRS in 1947 and FRCP in 1948. He received honorary doctorates from many universities at home and abroad – MD from Freiburg, Berlin, Cologne, Liège, Würzburg and Heidelburg: DSc from Bradford and London and LLD from Glasgow and Aberdeen. He was awarded the Royal Medal of the Royal Society in 1983. His work was recognized in Germany by the award of the Grand Cross, Order of Merit of the German Federal Republic in 1961 and the Schmiedberg Plakette in 1969. With typical generosity, he used his restitution money and the pension he received as an Emeritus Professor in Germany to establish the Feldberg Foundation for exchange lectureships in medical research between England and Germany. It is most fitting that, 4 years before his death, the British Pharmacological Society paid our tribute to him by the award of the Wellcome Gold Medal.

Feldberg's first wife, Katherine, a literary scholar, translator and anthologist, died in 1976. In 1977 he married Kim O'Rourke, the secretary of the division who contributed so much to its efficiency and to the publication of his work. Tragically she died only 4 years later. Those who knew Feldberg were infected by his never failing excitement for his science; this shines out from the XVIth Sherrington Lecture in which he chronicled his extraordinary breadth of interests. He dedicated this lecture to Katherine and Kim. His son died in 1960. His daughter is a paediatric cardiologist in Seattle.

G.W. Bisset
National Institute for Medical Research, London

Br. J. Pharmacol. (1994), **111**, 652–654

SPECIAL REPORT

© Macmillan Press Ltd, 1994

Release of nitric oxide by angiotensin-(1-7) from porcine coronary endothelium: implications for a novel angiotensin receptor

[1]Ilkka Pörsti, Agnieszka T. Bara, Rudi Busse & [2]Markus Hecker

Centre of Physiology, Johann Wolfgang Goethe-University Clinic, Theodor-Stern-Kai 7, D-60590 Frankfurt/M., Germany

The angiotensin I (AI) metabolite, A(1-7), elicited a concentration-dependent dilator response ($ED_{50} \geqslant 2\ \mu M$) in porcine coronary artery rings which was markedly attenuated by the nitric oxide (NO) synthase inhibitor, N^G-nitro-L-arginine, and abolished after removal of the endothelium. This effect of the heptapeptide was not mimicked by AII, AIII or A(3-8) at comparable concentrations. The A(1-7)-induced relaxation was not affected by AT_1 or AT_2 receptor blockade or cyclo-oxygenase inhibition, but was attenuated by the B_2 receptor antagonist, Hoe 140, and augmented by the angiotensin-converting enzyme (ACE) inhibitor, quinaprilat. These findings suggest that the relaxation to A(1-7) was mediated by the release of NO from the coronary endothelium through activation of an, as yet unidentified, AT receptor, the occupation of which also seems to stimulate the release of vasoactive kinins. Since A(1-7) accumulates during ACE inhibition, this mechanism may contribute to the coronary dilator effect of ACE inhibitors *in vivo*.

Keywords: Angiotensin peptides; angiotensin-converting enzyme; angiotensin receptor antagonism; blood pressure; bradykinin; endothelium; nitric oxide; porcine coronary artery; relaxation

Introduction Angiotensin II (AII) is the most prominent member of the renin-angiotensin system due to its potent vasconstrictor activity which is mediated by stimulation of the AT_1 receptor on vascular smooth muscle (Timmermans *et al.*, 1993). However, recent findings suggest that AII may also be a vasodilator in certain vascular beds (Hasegawa *et al.*, 1993; Scheuer & Perrone, 1993), although it is not clear which AT receptor subtype is involved in this response. Moreover, other AI metabolites, such as AIII or A(1-7) are also biologically active (Ferrario *et al.*, 1991; Osei *et al.*, 1993). A(1-7), for example, is found in high concentrations in the central nervous system where it mimics some, but not all, of the biological actions of AII (Ferrario *et al.*, 1991). Although the plasma level of A(1-7) is much lower than that of AII, its concentration can be markedly increased by angiotensin-converting enzyme (ACE) inhibition (Ferrario *et al.*, 1991; Yamamoto *et al.*, 1992). Presumably neutral endopeptidase 24.11 (Yamamoto *et al.*, 1992) localized to the vascular endothelium (Santos *et al.*, 1992) converts AI into A(1-7). Interestingly A(1-7) seems to be a vasodilator rather than a vasoconstrictor in certain vascular beds (Benter *et al.*, 1992; Osei *et al.*, 1993). Here we have investigated the potential mechanisms by which A(1-7) exerts its dilator effect in the porcine coronary artery and the nature of the AT receptor involved.

Methods Freshly prepared porcine coronary arteries were cut into rings of 4 mm width, mounted between force transducers and a rigid support for measurement of isometric force, and superfused at 3.0 ml min^{-1} with warmed (37°C), oxygenated (95% O_2/5% CO_2) Krebs-Henseleit solution, pH 7.4 (composition in mM: Na^+ 144.0, K^+ 5.9, Cl^- 127.0, Ca^{2+} 1.6, Mg^{2+} 1.2, $H_2PO_4^-$ 1.2, SO_4^{2-} 1.2, HCO_3^- 25.0, D-glucose 11.1, diclofenac 0.003). Passive tension was adjusted over a 30 min equilibration period to 5 g; thereafter the segments were preconstricted to 10.7 ± 0.1 g of tension by infusing 9,11-dideoxy-11α,9α-epoxymethano-prostaglandin $F_{2\alpha}$ (U46619, 10–30 nM, $n = 62$) into the superfusate. In some experiments, the endothelium was removed mechanically, and its absence confirmed by the lack of a relaxant response to bradykinin injected as a bolus (10 pmol) into the superfusate. Data are expressed as mean ± s.e.mean of n experiments with ring segments from at least three different coronary artery preparations. Statistical evaluation was performed by one-way analysis of variance or Student's unpaired two-tailed t test, where appropriate, with a P value < 0.05 considered statistically significant.

Drugs used were 2-ethyl-4-[(2′-(1*H*-1,2,3,4-tetrazol-5-yl)biphenyl-4-yl)methoxy]quinoline (ICI-D8731; ICI Pharmaceuticals, Macclesfield, U.K.), losartan (MSD Sharp & Dohme, München, Germany), 1-(4-amino-3-methyl-phenyl)methyl-5-diphenyl-acetyl-4,5,6,7-tetrahydro-1H-imidazo[4,5-c]pyridine-6-carboxylic acid (PD123177), nicotinic acid-Tyr-N^{α}-benzyloxycarbonyl-Arg-Lys-His-Pro-Ile-OH (CGP42112A) and D-Arg[Hyp^3,Thi^5,D-Tic^7,Oic^8]-bradykinin (Hoe 140; Hoechst, Frankfurt/M., Germany), quinaprilat (Goedecke, Freiburg, Germany), and diclofenac (Voltaren; Ciba-Geigy, Wehr, Germany). The angiotensin peptides and bradykinin were obtained from Bachem (Heidelberg, Germany), and N^G-nitro-L-arginine from Serva (Heidelberg, Germany).

Results Bolus injections of A(1-7) into the superfusate elicited a dose-dependent relaxation of endothelium-intact, but not -denuded, coronary artery rings (Figure 1). High doses of AII also induced a weak relaxant response, whereas AIII and A(3-8) were inactive (Figure 1). In a separate series of experiments, the ED_{50}-value for A(1-7) was determined (with rings suspended in 5 ml organ chambers) to be $2.2 \pm 0.4\ \mu M$ ($n = 21$).

Pretreatment of the superfused rings with the nitric oxide (NO) synthase inhibitor, N^G-nitro-L-arginine, virtually abolished the relaxant response to the heptapeptide (Figure 2) which, on the other hand, was not affected by omission of the cyclo-oxygenase inhibitor, diclofenac, from the Krebs-Henseleit solution ($n = 6$). In contrast, superfusion with the AT_1 receptor antagonists, ICI-D8731 (Figure 2) or losartan (1 μM, $n = 3$), or the AT_2 receptor antagonists, PD123177 (Figure 2) or CGP42112A (1 μM, $n = 3$), had no effect on the A(1-7)-induced relaxation. ICI-D8731 and CGP42112A (1 μM) also failed to inhibit the dilator response to AII (10–30 nmol, $n = 3$).

[1] On leave from the Department of Biomedical Sciences, University of Tampere, P.O. Box 607, FIN-33101 Tampere, Finland.
[2] Author for correspondence.

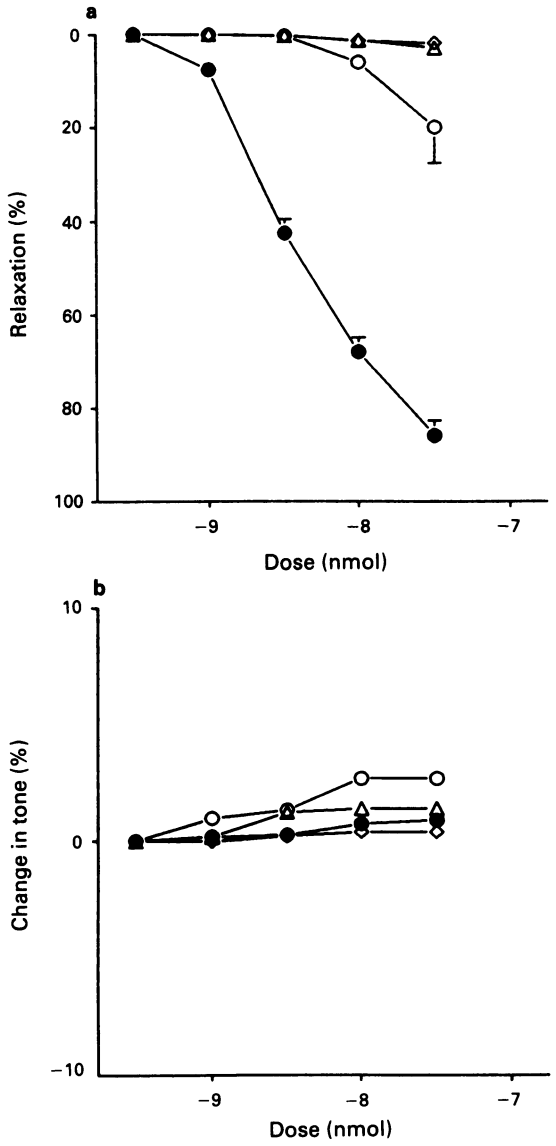


Figure 1 Relaxant effects (expressed as percentage of the U46619-induced tone) of angiotensin II (AII, ○, $n = 6-12$), AIII (△, $n = 6$), A(1-7) (●, $n = 9-26$) or A(3-8) in endothelium-intact (a) and -denuded (b) porcine coronary artery rings.

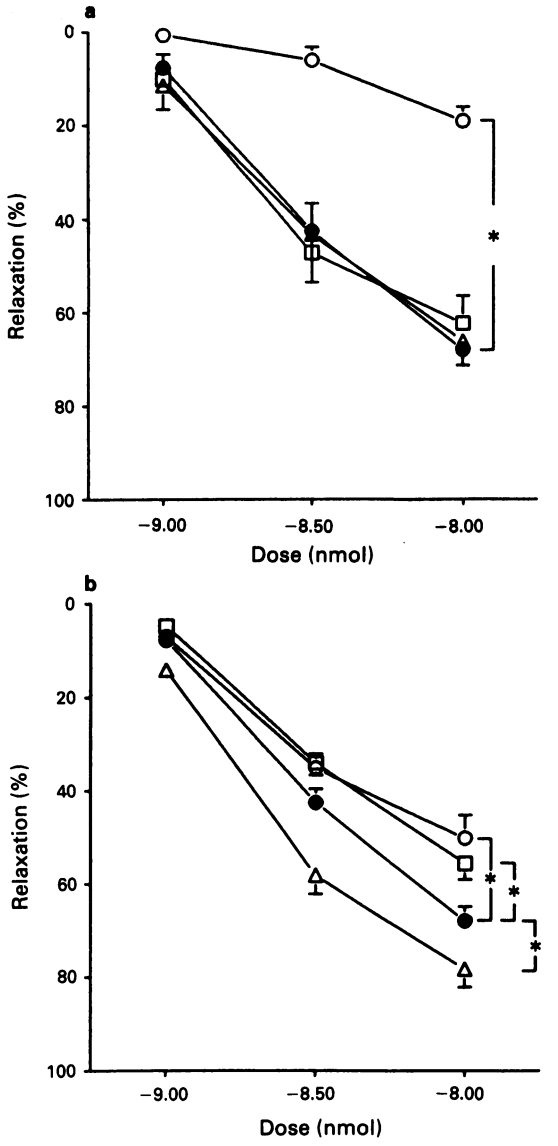


Figure 2 (a) Effects of N^G-nitro-L-arginine (○, superfusion at 100 μM, $n = 8$), ICI-D8731 (△, 0.3 μM, $n = 8$) or PD123177 (□, 1 μM, $n = 6$) on the endothelium-dependent dilator response to angiotensin-(1-7) (A(1-7), ●, $n = 26$; $^*P < 0.001$ as indicated). (b) Effects of Hoe 140 (○, superfusion at 1 μM, $n = 8$), quinaprilat (△, 0.3 μM, $n = 8$) or desensitization of the B_2 receptor (□, $n = 7$) on the endothelium-dependent dilator response to A(1-7) (●, $n = 26$; $^*P < 0.05$ as indicated).

Superfusion with the B_2 receptor antagonist, Hoe 140, attenuated the relaxation to A(1-7) which, on the other hand, was enhanced in the presence of the ACE inhibitor, quinaprilat (Figure 2). Hoe 140 (1 μM) abolished the dilator response to 10 pmol bradykinin (from 82 ± 6 to 0 ± 0% relaxation, $n = 8$, $P < 0.01$) while quinaprilat (0.3 μM) significantly enhanced the relaxation to 1 pmol bradykinin (from 17 ± 3 to 47 ± 6%, $n = 4$, $P < 0.01$). Desensitization of the B_2 receptor (1 ± 1 and 7 ± 4% relaxation in the presence of 1 and 10 pmol bradykinin respectively, $n = 5$, $P < 0.01$) by continuous superfusion of the rings with 10 nM bradykinin attenuated the relaxant response to A(1-7) to a similar extent to Hoe 140 (Figure 2).

Discussion This study demonstrates that A(1-7) is a potent vasodilator in the porcine coronary artery acting mainly through the release of NO from the vascular endothelium. Apart from a direct stimulation of NO formation via an endothelial AT receptor, A(1-7) also seems to elicit the release of vasoactive kinins from the coronary endothelium which can subsequently contribute to the relaxant response through activation of endothelial B_2 receptors (Schini *et al.*, 1990).

Neither AT_1 nor AT_2 receptor antagonists affected the dilator response to A(1-7) at concentrations which would abolish the biological activity of AII (Timmermans *et al.*, 1993), suggesting the involvement of a different receptor subtype. As AII was a relatively weak dilator and AIII and A(3-8) were virtually inactive, the amino-terminal aspartate residue rather than the phenylalanine residue at position 8 of the angiotensin peptide must be essential for its activation. A(1-7) produced very similar effects also in bovine coronary arteries (data not shown). Moreover, the heptapeptide has been reported to elicit endothelium-dependent dilatations in the mesenteric and hindquarters vascular beds of the cat (Osei *et al.*, 1993) and a decrease in mean arterial blood pressure in the pithed rat when injected intravenously (Benter

et al., 1992. Thus, besides its actions in the central nervous system (Ferrario *et al.*, 1991; Osei *et al.*, 1993), A(1-7) may also be an important component of the renin-angiotensin system in the circulation and help to balance the vasoconstrictor effects of AII.

Interestingly ACE inhibition has been shown to redirect the metabolism of AI towards an enhanced formation A(1-7) in a variety of species including man (Ferrario *et al.*, 1991; Yamamoto *et al.*, 1992). In view of its dilator activity, the accumulation of A(1-7) in or at the vascular wall in the presence of an ACE inhibitor may thus contribute to the blood pressure-lowering effect of this class of compounds *in vivo*.

This study was supported by the Alexander-von-Humboldt Stiftung (I.P.), the Boehringer Ingelheim Fonds (M.H.), the Deutsche Forschungsgemeinschaft (He 1587/3-1), the Paavo Nurmi Foundation (I.P.), Goedecke and Zeneca.

References

BENTER, I.F., KNOWLES, W.D. & FERRARIO, C.M. (1992). Angiotensin-(1-7) is vasoactive in the circulation of areflexic Sprague-Dawley rats. *FASEB J.*, **6**, A1735.

FERRARIO, C.M., BROSHINAN, K.B., DIZ, D.I., JAISWAL, N., KHOSLA, M.C., MILSTED, A. & TALLANT, E.A. (1991). Angiotensin-(1-7): a new hormone of the angiotensin system. *Hypertension*, **18** (Suppl. III), 126–133.

HASEGAWA, K., NISHIMURA, H. & KHOSLA, M. (1993). Angiotensin II-induced endothelium-dependent relaxation of fowl aorta. *Am. J. Physiol.*, **264**, R903–R911.

OSEI, S.Y., AHIMA, R.S., MINKES, R.K., WEAVER, J.P., KHOSLA, M.C. & KADOWITZ, P.J. (1993). Differential responses to angiotensin-(1-7) in the feline mesenteric and hindquarters vascular beds. *Eur. J. Pharmacol.*, **234**, 35–42.

SANTOS, R.A., BROSNIHAN, K.B., JACOBSEN, D.W., DICORLETO, P.E. & FERRARIO, C.M. (1992). Production of angiotensin-(1-7) by human vascular endothelium. *Hypertension*, **19** (Suppl. II), 56–61.

SCHEUER, D.H. & PERRONE, M.H. (1993). Angiotensin type 2 receptors mediate depressor phase of biphasic pressor response to angiotensin. *Am. J. Physiol.*, **264**, R917–R923.

SCHINI, V.B., BOULANGER, C., REGOLI, D. & VANHOUTTE, P.M. (1990). Bradykinin stimulates the production of cyclic GMP via activation of B_2-kinin receptors in cultured porcine aortic endothelial cells. *J. Pharmacol. Exp. Ther.*, **252**, 581–585.

TIMMERMANS, P.B.M.W.M., WONG, P.C., CHIU, A.T., HERBLIN, W.F., BENFIELD, P., CARINI, D.J., LEE, R.J., WEXLER, R.R., SAYE, J.M. & SMITH, R.D. (1993). Angiotensin II receptors and angiotensin II receptor antagonists. *Pharmacol. Rev.*, **45**, 205–251.

YAMAMOTO, K., CHAPPELL, M.C., BROSNIHAN, K.B. & FERRARIO, C.M. (1992). In vivo metabolism of angiotensin I by neutral endopeptidase (EC 3.4.24.11) in spontaneously hypertensive rats. *Hypertension*, **19**, 692–696.

(Received October 26, 1993
Accepted November 18, 1993)

Br. J. Pharmacol. (1994), **111**, 655–662 © Macmillan Press Ltd, 1994

Relaxation of rat thoracic aorta induced by the Ca^{2+}-ATPase inhibitor, cyclopiazonic acid, possibly through nitric oxide formation

[1]Hideki Moritoki, Tetsuhiro Hisayama, Shougo Takeuchi, Wataru Kondoh & Masayuki Imagawa

Department of Chemical Pharmacology, Faculty of Pharmaceutical Sciences, University of Tokushima, Shomachi, Tokushima 770, Japan

1 The effect of the Ca^{2+}-ATPase inhibitor, cyclopiazonic acid (CPA), was studied on rat thoracic aortic ring preparations.

2 At concentrations above 0.3 μM, CPA induced relaxation in the arteries precontracted with phenylephrine. Removal of the endothelium abolished CPA-induced relaxation.

3 The nitric oxide (NO) synthase inhibitor N^G-nitro L-arginine (3–300 μM), the free radical scavenger haemoglobin (0.1–3 μM), the soluble guanylate cyclase inhibitor, LY83583 (0.1–10 μM), each inhibited the endothelium-dependent relaxation to CPA. The potassium channel blocker, glibenclamide (10 μM) and cyclo-oxygenase inhibitor, indomethacin (100 μM for 60 min and then washed out) did not alter the action of CPA.

4 The calmodulin inhibitors calmidazolium (3–10 μM) and W-7 (100 μM) also abolished CPA-induced relaxation.

5 CPA (10 μM) increased guanosine 3':5'-cyclic monophosphate (cyclic GMP) levels in arteries with an intact endothelium, without affecting adenosine 3':5'-cyclic monophosphate (cyclic AMP) levels.

6 The inhibitors of NO synthesis and actions, the calmodulin inhibitor and removal of the endothelium abolished the CPA-stimulated increase in the levels of cyclic GMP.

7 In Ca^{2+}-free solution, CPA failed to induce relaxation or to stimulate cyclic GMP production. Relaxation to nitroprusside was not affected under these conditions.

8 These results suggest that CPA can stimulate NO synthesis, possibly by inhibiting a Ca^{2+}-ATPase, which replenishes Ca^{2+} in the intracellular storage sites in endothelial cells. Depletion of the Ca^{2+} store in the endothelium may then trigger influx of extracellular Ca^{2+}, contributing to an increase in free Ca^{2+} in the endothelial cells, which activates NO synthase and NO formation.

Keywords: Cyclopiazonic acid; rat aorta; relaxation; endothelium; nitric oxide; cyclic GMP; calcium; calmodulin; Ca^{2+}-ATPase inhibition

Introduction

Biosynthesis of nitric oxide (NO) is correlated to the free Ca^{2+} concentration in the cytoplasm of endothelial cells (Johns *et al.*, 1987; Mülsch *et al.*, 1989; Lückhoff *et al.*, 1988; Buchan & Martin, 1991). In the endothelial cells, an agonist-induced increase in Ca^{2+} concentration follows an influx of extracellular Ca^{2+} via Ca^{2+} channels and the release of intracellularly stored Ca^{2+} (Schilling *et al.*, 1988; 1989; 1992; Hallam *et al.*, 1989; Jacob, 1990; Dolor *et al.*, 1992).

Cyclopiazonic acid (CPA) is a specific inhibitor of Ca^{2+}-dependent ATPase in sarcoplasmic/endoplasmic reticulum vesicles (Goeger *et al.*, 1988), and inhibits Ca^{2+} uptake by the sarcoplasmic reticulum (Goeger *et al.*, 1988; Goeger & Riley, 1989; Seidler *et al.*, 1989). It has been documented that CPA can deplete inositol trisphosphate-sensitive Ca^{2+} stores, and subsequently activate Ca^{2+} influx in several cell types (Mason *et al.*, 1991; Foskett & Wong, 1992; Demaurex *et al.*, 1992). In vascular smooth muscle, CPA, besides raising resting tension (Shima & Blaustein, 1992) and inducing Ca^{2+}-dependent contraction (Deng & Kwan, 1991), has been shown to inhibit contractions induced by phenylephrine (Deng & Kwan, 1991) in Ca^{2+}-free solution, possibly by inhibiting ATP-dependent Ca^{2+} uptake into sarcoplasmic reticulum and subsequently depleting stored Ca^{2+}. However, an effect of CPA on the vascular endothelium has not been reported.

The present study was carried out to determine whether CPA could induce relaxation through the activation of NO synthase in the rat aorta, which may reflect an effect of Ca^{2+} entry.

A preliminary account of some of these data was presented at the 66th Annual Meeting of the Japanese Pharmacological Society, Yokohama, Japan, 1993 (Kondoh *et al.*, 1993).

Methods

Organ bath experiments

Male Wistar rats (9–11 weeks old) were killed by a blow to the head, cervical dislocation, and rapid exsanguination. The thoracic aortae were rapidly removed, freed of adjacent connective tissue under a dissecting microscope, and cut into ring segments of 3 mm length. The ring segments were placed in a 10 ml organ bath at 34°C containing oxygenated (95% O_2 and 5% CO_2) Krebs solution of the following composition (mM): NaCl 115.3, KCl 4.9, $CaCl_2$ 2.5, $MgSO_4$ 1.2, KH_2PO_4 1.2, $NaHCO_3$ 25.0 and glucose 11.1. Ca^{2+}-free solution was made by omitting $CaCl_2$ from the Krebs solution and adding 2 mM EGTA.

The ring preparations were maintained at 1.0 g resting tension, and equilibrated for 2 h before the start of an experiment. For the measurement of relaxation, the arteries were precontracted with phenylephrine (PHE) at a concentration corresponding to the EC_{80} (0.3 μM for the preparations with

[1] Author for correspondence.

endothelium and 0.1 μM for those without endothelium). In Ca^{2+}-free solution, the contraction induced by PHE was transient and greatly attenuated. However, under these conditions, as has been reported (Bradley & Morgan, 1987), prostaglandin $F_{2\alpha}$ ($PGF_{2\alpha}$) induced an attenuated, but sustained tonic contraction. In addition, a larger maximum contraction was produced by $PGF_{2\alpha}$ than by PHE. Therefore, in the experiments using Ca^{2+}-free conditions, an EC_{80} concentration of $PGF_{2\alpha}$ (around 10 μM) was used to produce tone.

Responses were recorded isometrically with a force displacement transducer (Nihon Kohden SB 1TH). Concentration-response curves were constructed by adding CPA cumulatively to the 10 ml organ bath in a volume of 10–20 μl, and relaxations were plotted as percentages of the contraction induced by the EC_{80} concentrations of PHE.

The endothelium was removed by rubbing the lumen of the artery with a cotton thread, and was assessed by a loss of relaxation to acetylcholine (ACh) at the start and end of each experiment.

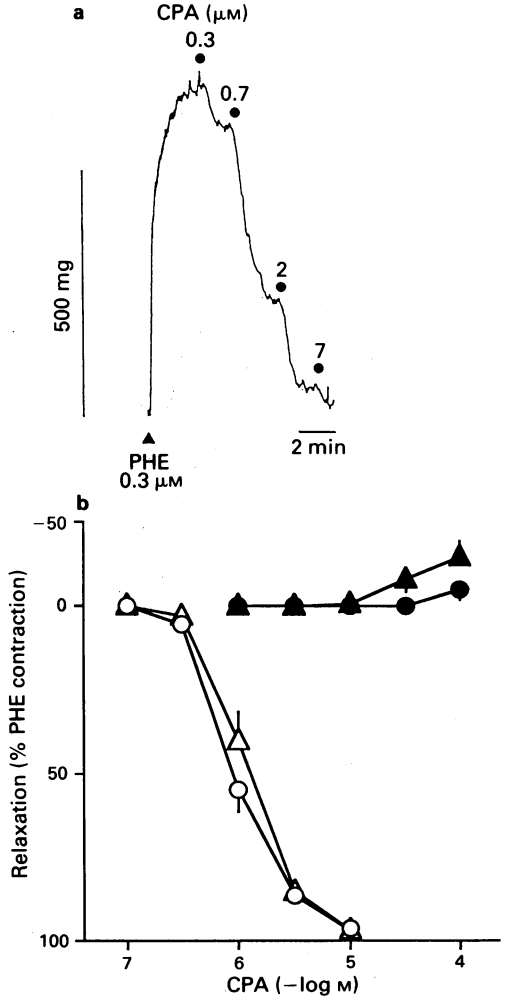


Figure 1 (a) Representative trace showing relaxation in the rat thoracic aorta induced by cyclopiazonic acid (CPA). The arteries were first contracted with an EC_{80} concentration of phenylephrine (PHE, 0.3 μM). (b) Effect of CPA on rat thoracic aorta with (○) and without endothelium (●). Initial tension, 576 ± 62 mg with endothelium and 994 ± 58 mg without endothelium. The ordinate scale shows the relaxation of the arteries expressed as a percentage of the contraction induced by 0.3 μM PHE. Preparations with matched levels of tension (386 ± 54 mg with (△) vs. 327 ± 47 mg without (▲) endothelium, $n = 6$) by lowering the concentration of PHE to 0.03–0.1 μM. Values are means with s.e.mean of preparations from 10 rats.

Assay of cyclic nucleotides

Segments of aorta were equilibrated in Krebs solution bubbled with O_2 containing 5% CO_2 for 2 h before the start of experiments. Arteries were first incubated with 0.3 μM PHE for 5 min, and then challenged with 3 or 10 μM CPA for 90 s. To study the effect of removal of Ca^{2+}, 2 min after replacing normal Krebs solution with Ca^{2+}-free EGTA-containing medium, the arteries were incubated with 10 μM $PGF_{2\alpha}$ for 5 min, and then challenged with 10 μM CPA. NO inhibitors, when used, were applied before and throughout the incubation with 10 μM CPA. After incubation with CPA for 90 s, the preparations were quickly frozen in liquid nitrogen and then homogenized in ice-cold 6% trichloroacetic acid in a Potter glass-glass homogenizer. The homogenates were centrifuged at 1700 *g* for 15 min at 4°C, and the supernatants were extracted with three volumes of water-saturated ether. Cyclic GMP and cyclic AMP were measured by radioimmunoassay. Briefly, the cyclic nucleotides in the supernatant were succinylated and incubated with [^{125}I]-succinyl cyclic GMP tyrosine methyl ester or [^{125}I]-succinyl cyclic AMP tyrosine methyl ester, and antisera for 18 h at 4°C. Then dextran-coated charcoal was added to the reaction medium to terminate the reaction. The radioactivity in the supernatant was counted in a gamma spectrophotometer. Amounts of cyclic nucleotides were expressed as pmol mg^{-1} protein.

Statistical analysis

Values are expressed as means ± s.e.mean. The statistical significance of differences was analyzed by Student's unpaired *t* test, and *P* values of less than 0.05 were considered as significant.

Materials

The drugs used were cyclopiazonic acid, acetylcholine chloride, sodium nitroprusside, methylene blue, haemoglobin, calmidazolium, W-7 (N-(6-aminohexyl)-5-chloro-1-naphthalene-sulphonamide), glibenclamide, indomethacin, phenylephrine hydrochloride (all from Sigma Chemical Co., St Louis, MO, U.S.A.), LY83583 (6-anilino-5,8-quinolinedione, Calbiochem, San Diego, CA, U.S.A.), N^G-nitro L-arginine and N^G-nitro D-arginine (Peptide Institute, Osaka, Japan) and prostaglandin $F_{2\alpha}$ (Ono Pharmaceutical Co. Ltd., Osaka, Japan). Kits for radioimmunoassay of cyclic GMP and cyclic AMP were obtained from Yamasa Shoyu Co. Ltd. (Choshi, Japan).

Results

Relaxation induced by cyclopiazonic acid

As shown in Figure 1a, the cumulative application of CPA at concentrations above 0.3 μM caused relaxation of the rat thoracic aorta with an EC_{50} value of 0.86 ± 0.16 μM ($n = 10$). The maximal relaxation caused by 10 μM CPA was sustained until CPA was washed out. CPA-induced relaxation was reproducible, but more than 60 min between exposures were necessary for a complete recovery of responses to either CPA or PHE.

In the arteries without endothelium, CPA did not induce relaxation, even at a concentration as high as 100 μM (Figure 1b). Although removal of the endothelium augmented the PHE-induced tone (576 ± 62 mg with and 994 ± 58 mg without endothelium, $n = 10$), nitroprusside-induced relaxation was not attenuated but slightly potentiated (EC_{50} values: 3.28 ± 0.49 nM with endothelium vs. 1.52 ± 0.25 nM without endothelium, $n = 6$, $P < 0.05$). Moreover, even when the initial tension was normalized by lowering the concentration of PHE, CPA did not induce relaxation.

Treatment with 100 μM indomethacin for 60 min (and then washed for 60 min) or 10 μM glibenclamide for 30 min did not affect the CPA-induced relaxation (data not shown).

In unstimulated, endothelium-denuded arteries, CPA at higher concentrations than those inducing relaxation (above 10 μM) evoked contraction. At a concentration of 100 μM, the contraction reached a plateau, and the maximal response was 11.0 ± 5.9% ($n = 4$) of that induced by 0.3 μM PHE. However, the contraction was not observed in endothelium-intact arteries

Effect of inhibitors of NO synthesis and action on CPA-induced relaxation

In arteries with a functional endothelium, N^G-nitro L-arginine (L-NOARG) inhibited CPA-induced relaxation (Figure 2). In the presence of 300 μM L-NOARG, CPA did not induce any relaxation. In contrast to L-NOARG, its enantiomer N^G-nitro D-arginine did not alter the CPA-induced relaxation. Haemoglobin (Hb, for 5 min) and LY83583 (for 20 min) had essentially similar inhibitory actions on the relaxation to CPA (Figure 2a).

Because inhibitors of the NO pathway augmented the initial tension caused by the EC_{80} concentration of PHE (Table 1), we examined whether the increased tone by the inhibitors of NO pathway attenuated the relaxant effect of CPA. However, even when the initial tensions were elevated by 100 μM L-NOARG, relaxations to nitroprusside and cromakalim were not weakened (the EC_{50} values of nitroprusside being 1.79 ± 0.30 nM in control and 2.01 ± 0.37 nM ($n = 5$) in treated rings, and those of cromakalim being 203.3 ± 40.1 nM in control and 236.4 ± 46.5 nM ($n = 5$) in treated rings).

Furthermore, even after the initial tension of the arteries treated with 100–300 μM L-NOARG, 1–3 μM LY83583 or

Table 1 Changes in the initial tensions in the presence of inhibitors of NO pathway

Inhibitor	μM	*Tension* (mg)
L-NOARG	0	608 ± 47
	10	1101 ± 136
	100	1070 ± 63
	300	1146 ± 92
LY 83583	0	707 ± 88
	0.3	1009 ± 114
	3	948 ± 83
Haemoglobin	0	582 ± 69
	0.3	698 ± 39
	3	803 ± 58
Calmidazolium	0	623 ± 97
	3	402 ± 69
	10	717 ± 61
W-7	0	675 ± 62
	10	238 ± 38

Tensions induced by 0.3 μM phenylephrine are expressed as mg. Values are mean ± s.e.mean ($n = 5$–8). L-NOARG: N^G-nitro-L-arginine.

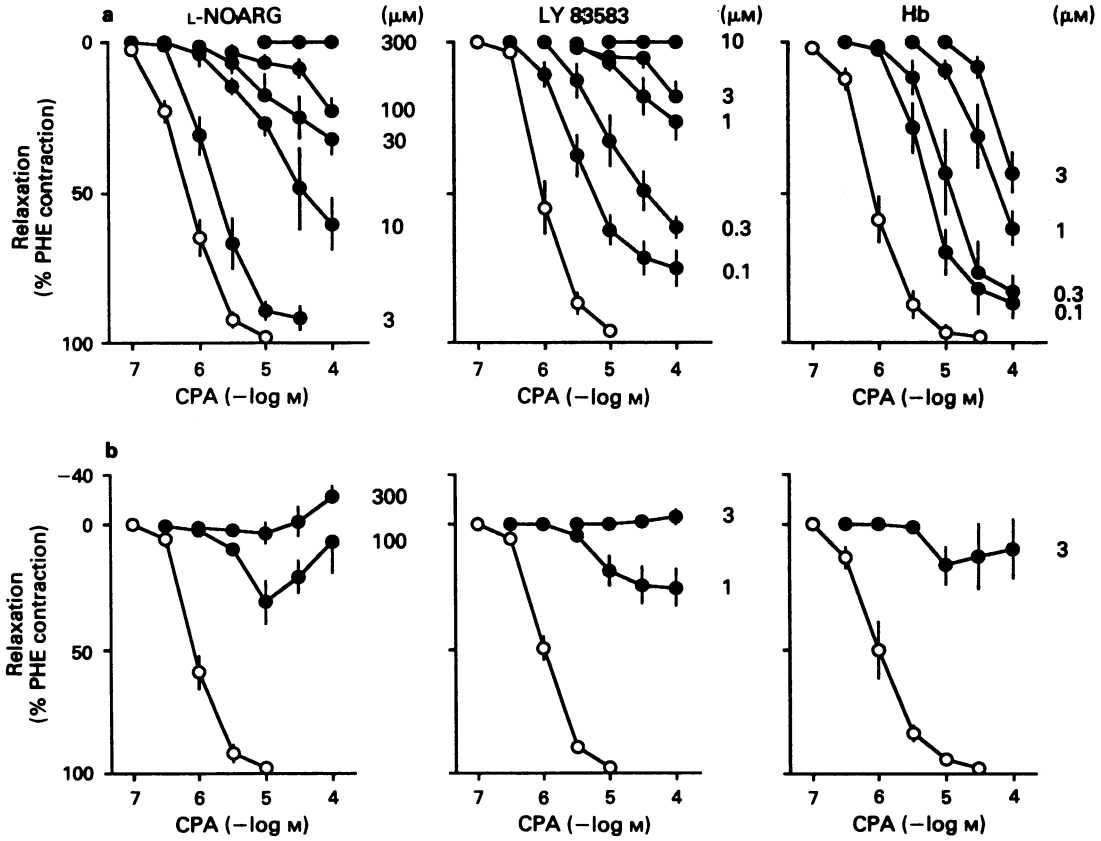


Figure 2 (a) Inhibitory effects of N^G-nitro L-arginine (L-NOARG), haemoglobin (Hb) and LY83583 on the cyclopiazonic acid (CPA)-induced relaxation in the rat thoracic aorta. Tissues were exposed to Hb for 5 min and to the other inhibitors for 20 min before the application of CPA. The ordinate scale shows the relaxation of the arteries expressed as a percentage of the contraction induced by 0.3 μM phenylephrine (PHE). (○), control; (●), in the presence of the inhibitors. (b) Effects of the inhibitors in preparations in which the initial tensions were matched by lowering the concentration of PHE to 0.03–0.1 μM. The ordinate scale shows the relaxation of the arteries expressed as a percentage of the respective initial tension. (○), control; (●), in the presence of the inhibitors. The initial tensions were as follows: L-NOARG (573 ± 48 mg in control vs. 546 ± 74 mg in treated rings), LY85383 (563 ± 52 mg in control vs. 642 ± 70 mg in treated rings), Hb (597 ± 43 mg in control vs. 620 ± 57 mg in treated rings). Experimental conditions were as for Figure 1. Values are means ± s.e.means of preparations from 6 rats.

3 μM Hb was adjusted to an equivalent level by lowering the concentration of PHE to 0.03 to 0.1 μM, the inhibitory effects of these inhibitors on the CPA-induced relaxation were not substantially different from those observed in un-normalized preparations (Figure 2b).

Effect of CPA on cyclic GMP formation

The time course of cyclic GMP formation in the rat aorta stimulated with 10 μM CPA is shown in Figure 3a. In preparations with a functional endothelium, CPA at a concentration of 10 μM increased the level of cyclic GMP from a basal level of 1.28 ± 0.32 pmol mg^{-1} protein, to 28.04 ± 2.40 pmol mg^{-1} protein within 90 s ($n = 5-6$). The level then decreased, but remained elevated (10.05 ± 1.70 pmol mg^{-1} protein) above basal, even after 20 min (Figure 3a). On the basis of the time course of cyclic GMP formation, amounts of the cyclic GMP were measured after incubation with CPA for 90 s. CPA-stimulated cyclic GMP formation was concentration-dependent (Figure 4).

In the endothelium-denuded preparations, 10 μM CPA did not increase the cyclic GMP level.

In contrast to the marked elevation of the cyclic GMP level, the cyclic AMP level was not significantly increased by 10 μM CPA (Figure 3b).

Effect of inhibitors of NO pathway on the CPA-stimulated cyclic GMP production

Treatment with 10 μM L-NOARG for 20 min, besides reducing the basal level of cyclic GMP to 0.12 ± 0.03 pmol mg^{-1} protein, suppressed the cyclic GMP production stimulated by 10 μM CPA from the control value of 28.04 ± 2.40 pmol mg^{-1} protein to 0.69 ± 0.07 pmol mg^{-1} protein, $n = 5-6$ (Figure 4).

Similarly, treatment with 3 μM Hb for 5 min or 1 μM LY83583 for 20 min suppressed the CPA-stimulated increase in cyclic GMP production. Removal of the endothelium also abolished any significant stimulation of cyclic GMP synthesis by CPA.

Effect of calmodulin inhibitors on CPA-induced relaxation and cyclic GMP formation

Pretreatment of artery segments with the calmodulin inhibitor, calmidazolium at a concentration of 3 μM for 20 min attenuated CPA-induced relaxation (Figure 5a). Increasing the concentration of calmidazolium to 10 μM completely suppressed CPA-induced relaxation and CPA-stimulated cyclic GMP production (Figure 5b). Under these conditions, ACh-induced relaxation and cyclic GMP production were similarly blocked by calmidazolium, whereas those induced by nitroprusside were not affected by the inhibitor (Figure 5).

W-7 at a concentration of 100 μM, which attenuated the contraction induced by the EC_{80} concentration of PHE (0.3 μM) to 38% (Table 1), completely suppressed CPA-induced relaxation (Figure 6) and CPA-stimulated cyclic GMP production (29 pmol mg^{-1} protein in control and 3.5 pmol mg^{-1} protein in treated preparation, $n = 5$). This concentration of W-7 nearly suppressed ACh-induced relaxation without affecting that induced by nitroprusside.

Effect of removal of Ca^{2+}

PHE-induced contraction was transient and greatly attenuated in the absence of Ca^{2+}; $PGF_{2\alpha}$ was therefore used to induce tone. Two minutes after replacing normal Krebs solution with Ca^{2+}-free EGTA-containing medium, the arteries were incubated with $PGF_{2\alpha}$ at a concentration corresponding to the EC_{80} (10 μM) to produce background tone. When the contraction induced by 10 μM $PGF_{2\alpha}$ reached a plateau, a single dose of CPA was applied. In Ca^{2+}-free conditions, although the $PGF_{2\alpha}$-induced contraction was reduced to 34% (528 ± 63 mg in control and 181 ± 21 in Ca^{2+}-free solution, $n = 6$), CPA at concentrations of up to 100 μM did not relax the arteries (Figure 7a). In addition, 10 μM CPA failed to stimulate cyclic GMP production (Figure 7b). Under these conditions, the relaxation and cyclic GMP production induced by 0.1 μM ACh were attenuated, whereas similar responses to 0.1 μM nitroprusside were not altered (Figure 7).

Discussion

CPA is a selective inhibitor of the Ca^{2+}-ATPase which mediates uptake of Ca^{2+} into endoplasmic/sarcoplasmic reticulum, and is known to deplete Ca^{2+} stores (Goeger & Riley, 1989; Seidler *et al.*, 1989).

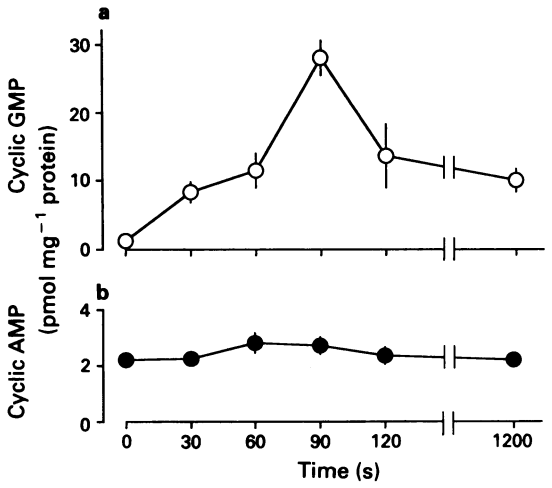


Figure 3 (a) Time course of cyclopiazonic acid (CPA)-stimulated formation of cyclic GMP in rat aortic preparations with a functional endothelium. The arteries were incubated with an EC_{80} concentration of phenylephrine for 5 min before exposure to 10 μM CPA. (b) Time course of cyclic AMP levels in the presence of 10 μM CPA. Each point represents mean ± s.e.mean of values ($n = 5-6$) in preparations from 8 to 12 rats.

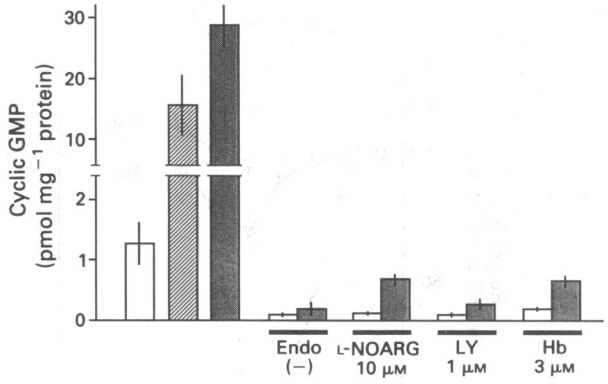


Figure 4 Effects of NO pathway inhibitors and removal of the endothelium on the cyclopiazonic acid (CPA)-induced formation of cyclic GMP in rat thoracic aorta. Amounts of cyclic GMP were measured after incubation with the EC_{80} concentration of phenylephrine (0.3 μM) for 5 min and then with CPA for 90 s. Open columns represent corresponding control values in the absence of CPA. Hatched and stippled columns show values in the presence of 3 μM and 10 μM CPA, respectively. N^G-nitro-L-arginine (L-NOARG) and LY 83583 (LY) were applied 20 min before and during incubation with CPA. Haemoglobin (Hb) was applied 5 min before and during application of CPA. Endo(−), removal of the endothelium. Each column represents the mean ± s.e.mean of values ($n = 5-6$) in preparations from 10 to 12 rats.

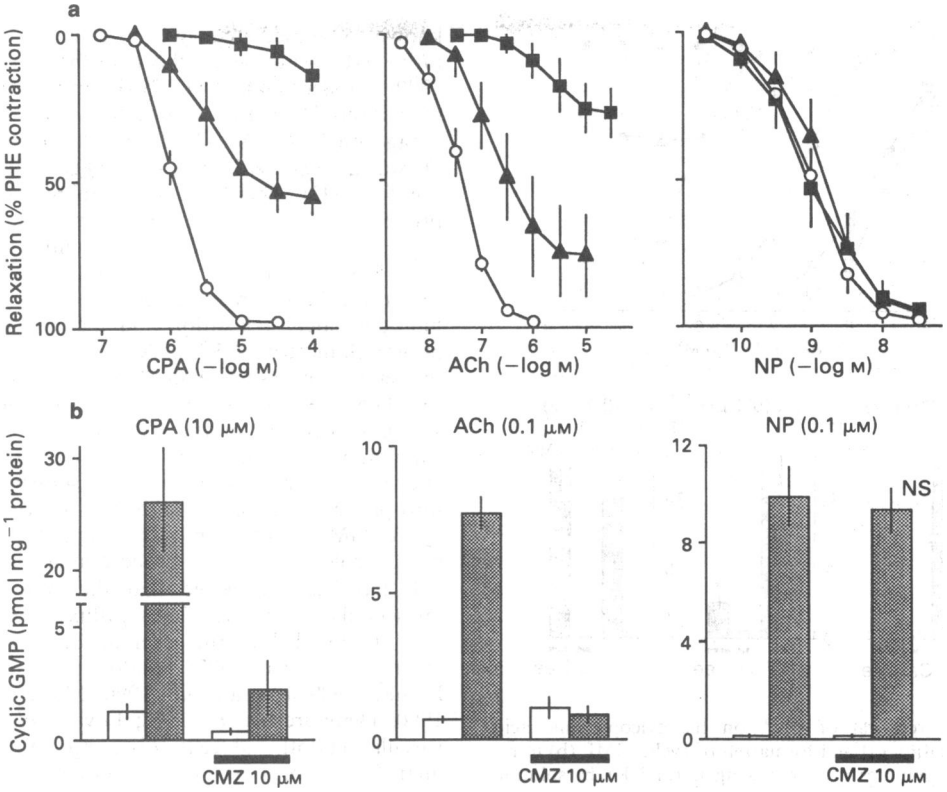


Figure 5 Effect of calmidazolium on cyclopiazonic acid (CPA)-induced relaxation (a) and cyclic GMP formation (b) in rat thoracic aorta with a functional endothelium. Calmidazolium, when used, was applied 20 min before and during incubation with CPA. Acetylcholine (ACh) and nitroprusside (NP) were used as reference relaxants. (○) Control; (▲) in the presence of 3 μM calmidazolium; (■) in the presence of 10 μM calmidazolium. Open columns, basal level of cyclic GMP; stippled columns, cyclic GMP level in the presence of 10 μM CPA, 0.1 μM ACh or 0.1 μM NP; underlined columns, cyclic GMP formation in the presence of 10 μM calmidazolium (CMZ). Other experimental conditions were as for Figures 1 and 4. Each point and column represent the mean ± s.e.mean of values ($n = 5$) in preparations from 6 to 8 rats. NS, not significantly different from the control preparations (unpaired t test).

It has been suggested that in aortic smooth muscle, CPA induced either contraction by increasing free Ca^{2+} as a result of inhibition of ATP-dependent Ca^{2+} uptake into storage sites (Deng & Kwan, 1991; Shima & Blaustein, 1992), or inhibition of PHE-induced contraction in Ca^{2+} free conditions (Deng & Kwan, 1991). However, the effect of CPA on the vascular endothelial cells has not been documented.

We demonstrated that in rat thoracic aorta, CPA induced relaxation, which was mediated by an endothelium-dependent mechanism. CPA-induced relaxation is not due to hyperpolarization via activation of glibenclamide-sensitive K^+-channels or production of prostanoids, because neither the K^+-channel blocker, glibenclamide nor the cyclo-oxygenase inhibitor, indomethacin affected the response.

The relaxant effect of CPA was found to be closely associated with an elevation of cyclic GMP level. It is known that cyclic GMP production is involved in endothelium-dependent vasorelaxation, and that NO stimulates cyclic GMP production by activating soluble guanylate cyclase. Therefore it is suggested that NO is involved in the CPA-induced relaxation of rat arteries. Further evidence supporting this idea is that the NO pathway inhibitors, such as the NO synthase inhibitor, L-NOARG (Moore *et al.*, 1990), the NO scavenger, haemoglobin (Gruetter *et al.*, 1981) and the soluble guanylate cyclase inhibitor with cyclic GMP-lowering activity, LY83583 (Malta *et al.*, 1988; Mülsch *et al.*, 1988) each suppressed both the CPA-induced relaxation and cyclic GMP formation.

It has been reported that the level of the initial tone is an important factor affecting relaxation (Furchgott, 1983; Dainty *et al.*, 1990). Indeed, blockers of the NO pathway and removal of the endothelium enhanced the PHE-induced tone of the aorta. Then the question arises of whether an increased initial tone due to blockade of the NO pathway or removal of the endothelium, in part contributes to abolition of CPA-induced relaxation. Therefore, the inhibitory effects of these blockers on the CPA-induced relaxation were examined at the equivalent level of the initial tension by lowering the concentration of PHE. However, the inhibitory effects of these blockers were not substantially altered, irrespective of whether the tone was normalized or not. In addition, the

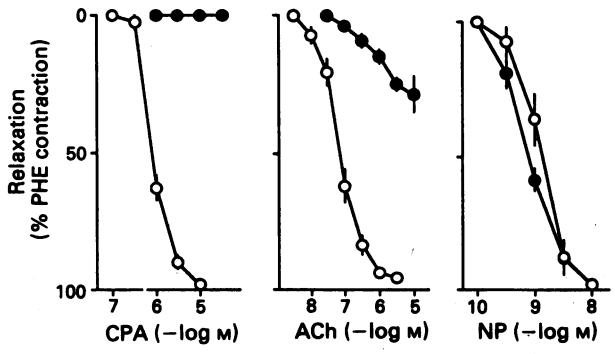


Figure 6 Effect of W-7 on cyclopiazonic acid (CPA)-induced relaxation in rat thoracic aorta with a functional endothelium. Arteries were stimulated with 10 μM prostaglandin $F_{2\alpha}$ for 5 min to produce tone. (○) Control; (●) in the presence of 100 μM W-7. W-7, when used, was applied 20 min before and during incubation with CPA. Other experimental conditions were as for Figures 1 and 4. Each point represents the mean ± s.e.mean of values ($n = 4$) in preparations from 4 rats.

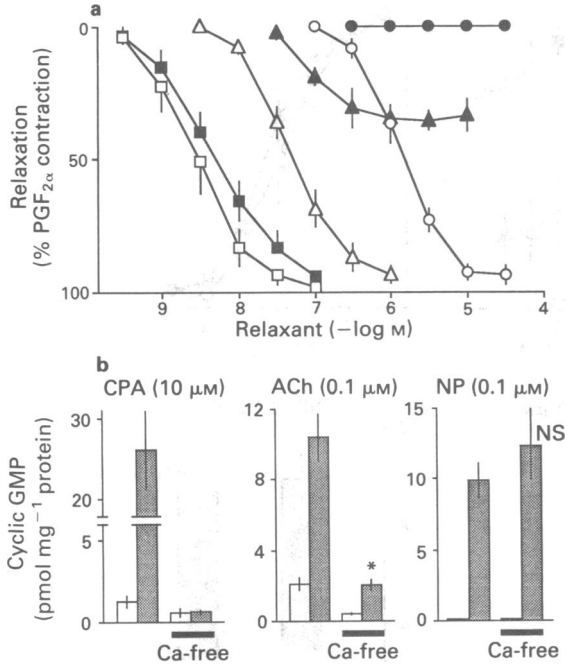


Figure 7 Effect of removal of Ca^{2+} on the cylcopiazonic acid (CPA)-induced relaxation (a) and formation of cyclic GMP (b) in rat thoracic aorta. Two minutes after replacing normal Krebs solution with Ca^{2+}-free Krebs solution, the arteries were incubated with 10 μM $PGF_{2\alpha}$ for 5 min to produce background tone, and then a single dose of CPA was applied. Acetylcholine (ACh) and nitroprusside (NP) were used as reference relaxants. (○ ●) CPA; (△ ▲) ACh; (□ ■) NP. Open symbols represent responses obtained in normal Krebs solution with 2.5 mM Ca^{2+} (initial tension, 528 ± 63 mg), and closed symbols represent those obtained in Ca^{2+}-free medium (initial tension, 181 ± 21 mg). Open columns, basal level of cyclic GMP; stippled columns, cyclic GMP level in the presence of 10 μM CPA, 0.1 μM ACh or 0.1 μM NP; underlined columns, cyclic GMP formation in Ca^{2+}-free medium. Other experimental conditions were as for Figures 1 and 4. Each point and column represent the means of values ($n = 5$) in preparations from 6 to 8 rats; vertical lines indicate s.e.mean. $^*P < 0.05$, compared with the value obtained in normal Krebs solution containing 2.5 mM Ca^{2+} (unpaired t test). NS, not significantly different from corresponding control value.

relaxant effects of cromakalim and nitroprusside were not substantially altered irrespective of the increased tone. Furthermore, L-NOARG, LY83583 and Hb also suppressed CPA-stimulated increases in the cyclic GMP level. Therefore, abolition of the CPA-induced relaxation does not seem to be secondary to this enhanced tone.

It is known that endothelium-derived hyperpolarizing factor (EDHF), distinct from NO, in part contributes to endothelium-dependent relaxation induced by A23187 or bradykinin (Nagao & Vanhoutte, 1991; 1992), and that the EDHF-mediated component of the relaxations is dependent on Ca^{2+}/calmodulin and resistant to L-NOARG (Illiano *et al.*, 1992). From these considerations, it is conceivable that CPA-induced relaxation is in part mediated by EDHF. However, we found that the relaxant effect of CPA was almost abolished by the inhibitors of the NO pathway, L-NOARG, Hb and LY83583. Therefore, it is suggested that the contribution of EDHF in CPA-induced relaxation is negligible, if any, and NO plays a major role in the CPA-induced relaxation.

Two types of NO synthase have been identified in the vasculatures; one is constitutive type present in the endothelial cells and Ca^{2+}.calmodulin-dependent (Busse & Mülsch, 1990), and the other is an inducible type found in macrophages and independent of Ca^{2+} and calmodulin (Hauschildt *et al.*, 1990). NO formation induced by ACh or bradykinin is known to be mediated by Ca^{2+}/calmodulin-dependent constitutive NO synthase in the endothelium (Busse & Mülsch, 1990; Förstermann *et al.*, 1991) and endothelium-dependent relaxations have been shown to be inhibited by calmodulin antagonists such as calmidazolium and W-7 (Weinheimer & Ossward, 1986; Adeagbo & Triggle, 1991; Schini & Vanhoutte, 1992). Therefore, calmodulin antagonists have been proposed as useful tools for identifying the type of NO synthase involved in relaxation (Schini & Vanhoutte, 1992).

In this respect, in the present experiments, it was found that the calmodulin inhibitors selectively abolished endothelium-dependent relaxation and increase in cyclic GMP formation induced by CPA as well as by ACh, without affecting the endothelium-independent nitroprusside-induced responses. These results provide evidence for the idea that the NO synthase involved in the CPA-induced relaxation is of the calmodulin-dependent constitutive type. In addition, the present results in the absence of Ca^{2+}, showing that CPA but not nitroprusside, failed to relax the arteries and to stimulate cyclic GMP formation, also suggests that Ca^{2+} plays a crucial role in the CPA-induced relaxation.

It has been suggested that the amount of Ca^{2+} in the intracellular stores regulates influx of Ca^{2+}; the influx of Ca^{2+} is coupled to the level of Ca^{2+} in the internal store (Merritt & Rink, 1987; Pandol *et al.*, 1987; Takemura & Putney, 1989; Kwan *et al.*, 1990; Mertz *et al.*, 1990; Putney, 1990; Demaurex *et al.*, 1992; Low *et al.*, 1992). In cultured vascular endothelial cells, discharge of Ca^{2+} from intracellular Ca^{2+} stores has been reported to trigger Ca^{2+} influx from the extracellular space via Ca^{2+} channels in the plasma membrane (Hallam *et al.*, 1989; Jacob, 1990; Dolor *et al.*, 1992; Schilling *et al.*, 1992). It has been shown that, in HL-60 cells, parotid acinar cells and thymic lymphocytes, CPA can induce a rapid release of Ca^{2+} from intracellular storage sites by inhibiting Ca^{2+}-ATPase and subsequently increasing the rate of influx of extracellular Ca^{2+} via the plasma membrane (Mason *et al.*, 1991; Demaurex *et al.*, 1992; Foskett & Wong, 1992), and that in vascular endothelial cells, Ca^{2+}-ATPase inhibitors increased the cytosolic Ca^{2+} (Dolor *et al.*, 1992; Schilling *et al.*, 1992). On the basis of these considerations, it is hypothesized that in rat thoracic aorta, the Ca^{2+}-ATPase inhibitor CPA prevents the Ca^{2+} uptake into intracellular stores in the endothelium and thereby depletes stored Ca^{2+}, which in turn triggers an influx of extracellular Ca^{2+} and stimulates NO synthase. Whether the Ca^{2+} influx pathway activated by CPA-induced depletion of the internal stores is the same as that activated by receptor agonists was not elucidated in the present study.

In endothelium-denuded arteries, in contrast to endothelium-intact preparations, high concentrations of CPA evoked contractions, suggesting that CPA elevates the cytosolic free Ca^{2+} level to trigger contraction. When the endothelium is present, the contractile effect is masked by a predominant endothelium-dependent relaxing effect.

Intracellular free Ca^{2+} is known to be sequestered into the sarcoplasmic reticulum via a Ca^{2+}-pump. In this respect, it is also possible that in the aortic endothelial cells, CPA prevents Ca^{2+} uptake into intracellular stores by inhibiting Ca^{2+}-ATPase (Ca^{2+} pump) and the Ca^{2+} thus accumulated stimulates constitutive NO synthase to trigger production of NO. If this were the case, CPA would induce relaxation and cyclic GMP production even in the absence of extracellular Ca^{2+}. However, this was not the case. In Ca^{2+}-free medium, CPA failed to induce relaxation of the arteries previously contracted with $PGF_{2\alpha}$, and did not stimulate cyclic GMP production. Under these conditions, ACh, although greatly attenuated, still induced relaxation and cyclic GMP production, which may be mediated in part by the Ca^{2+} released from the internal stores. From these results, it appears that the amount of intracellular free Ca^{2+} accumulated as a result of inhibition by CPA of Ca^{2+}-ATPase (Ca^{2+}-pump) is not sufficient for stimulation of the NO synthase. Therefore, the Ca^{2+}- that enters into the endothelial cells via plasma mem-

brane Ca^{2+}- channels subsequent to depletion by CPA of stored Ca^{2+} may activate NO synthase.

In summary, we have demonstrated that CPA induced relaxation of smooth muscle in the rat thoracic aorta by a mechanism involving NO synthesis. It seems likely that CPA blocks the Ca^{2+}-ATPase (Ca^{2+}-pump) in the endothelium. Depletion of the stored Ca^{2+} may then trigger an influx of extracellular Ca^{2+} by some as yet unknown mechanisms, which in turn activates Ca^{2+}/calmodulin-dependent constitutive NO synthase and produces NO.

This work was supported in part by a Grant-in-Aid for Scientific Research from the Ministry of Education, Science and Culture of Japan (03671054). We are grateful to the Fujisawa Foundation and The Suzuken Memorial Foundation for supplying grants.

References

ADEAGBO, A.S.O. & TRIGGLE, C.R. (1991). Effects of some inorganic divalent cations and protein kinase C inhibitors on endothelium-dependent relaxation in rat isolated aorta and mesenteric arteries. *J. Cardiovasc. Pharmacol.*, **18**, 511–521.

BRADLEY, A.B. & MORGAN, K.G. (1987). Alteration in cytoplasmic calcium sensitivity during porcine coronary artery contractions as detected by aequorin. *J. Physiol.*, **385**, 437–448.

BUCHAN, K.W. & MARTIN, W. (1991). Bradykinin induces elevations of cytosolic calcium through mobilization of intracellular and extracellular pools in bovine aortic endothelial cells. *Br. J. Pharmacol.*, **102**, 35–40.

BUSSE, R. & MÜLSCH, A. (1990). Calcium-dependent nitric oxide synthesis in endothelial cytosol is mediated by calmodulin. *FEBS Lett.*, **265**, 133–136.

DAINTY, I.A., MCGRATH, J.C., SPEDDING, M. & TEMPLETON, A.G. B. (1990). The influence of the initial stretch and the agonist-induced tone on the effect of basal and stimulated release of EDRF. *Br. J. Pharmacol.*, **100**, 767–773.

DEMAUREX, N., LEW, D.P. & KRAUSE, K.-H. (1992). Cyclopiazonic acid depletes intracellular Ca^{2+} stores and activates an influx pathway for divalent cations in HL-60 cells. *J. Biol. Chem.*, **267**, 2318–2324.

DENG, H.W. & KWAN, C.Y. (1991). Cyclopiazonic acid is a sarcoplasmic reticulum Ca^{2+}-pump inhibitor of rat aortic muscle. *Acta Pharmacol. Sinica*, **12**, 53–58.

DOLOR, R.J., HURWITZ, L.M., MIRZA, Z., STRAUSS, H.C. & WHORTON, A.R. (1992). Regulation of extracellular calcium entry in endothelial cells: role of intracellular calcium pool. *Am. J. Physiol.*, **262**, C171–181.

FÖRSTERMANN, U., POLLOCK, J.S., SCHMIDT, H.H.H.W., HELLER, M. & MURAD, F. (1991). Calmodulin-dependent endothelium-dependent relaxing factor/nitric oxide synthase activity is present in the particulate and cytosolic fractions of bovine aortic endothelial cells. *Proc. Natl. Acad. Sci. U.S.A.*, **88**, 1788–1792.

FOSKETT, J.K. & WONG, D. (1992). Calcium oscillations in parotid acinar cells induced by microsomal Ca^{2+}-ATPase inhibition. *Am. J. Physiol.*, **262**, C656–663.

FURCHGOTT, R.F. (1983). Role of endothelium in responses of vascular smooth muscle. *Circ. Res.*, **53**, 557–573.

GOEGER, D.E. & RILEY, R.T. (1989). Interaction of cyclopiazonic acid with rat skeletal muscle sarcoplasmic reticulum vesicles. Effect on Ca^{2+} binding and Ca^{2+} permeability. *Biochem. Pharmacol.*, **38**, 3995–4003.

GOEGER, D.E., RILEY, R.T., DORNER, J.W. & COLE, R.G. (1988). Cyclopiazonic acid inhibition of the Ca^{2+} transport ATPase in rat skeletal muscle sarcoplasmic reticulum vesicles. *Biochem. Pharmacol.*, **37**, 978–981.

GRUETTER, C.A., KADOWITZ, P.J. & IGNARRO, L.J. (1981). Methylene blue inhibits coronary arterial relaxation and guanylate cyclase activation by nitroglycerin, sodium nitrite, and amyl nitrite. *Can. J. Physiol.*, **59**, 150–156.

HALLAM, T.J., JACOB, R. & MERRITT, J.E. (1989). Influx of bivalent cations can be independent of receptor stimulation in human endothelial cells. *Biochem. J.*, **259**, 125–129.

HAUSCHILDT, S., LÜCKHOFF, A., MÜLSCH, A., KOHLER, J., BESSELE, W. & BUSSE, R. (1990). Induction and activity of NO synthase in bone-marrow-derived macrophages are independent of Ca^{2+}. *Biochem. J.*, **270**, 351–356.

ILLIANO, S., NAGAO, T. & VANHOUTTE, P.M. (1992). Calmidazolium, a calmodulin inhibitor, inhibits endothelium-dependent relaxations resistant to nitro-L-arginine in the canine coronary artery. *Br. J. Pharmacol.*, **107**, 387–392.

JACOB, R. (1990). Agonist-stimulated divalent cation entry into single cultured human umbilical vein endothelial cells. *J. Physiol.*, **421**, 55–77.

JOHNS, A., LATEGAN, T.W., LODGE, N.J., RYAN, U.S., VAN BREEMEN, C. & ADAMS, D.J. (1987). Calcium entry through receptor-operated channels in bovine pulmonary artery endothelial cell. *Tissue Cell*, **19**, 733–746.

KONDOH, W., KIDA, K., TAKEUCHI, S., HISAYAMA, T. & MORITOKI, H. (1993). Cyclopiazonic acid, a Ca^{2+}-ATPase inhibitor, stimulates NO formation in rat aortic endothelium. *Jpn. J. Pharmacol.*, **61**, 234p.

KWAN, C.Y., TAKEMURA, H., OBIE, J.F., THASTRUP, O. & PUTNEY, Jr. J.W. (1990). Effects of MeCh, thapsigargin, and La^{3+} on plasmalemmal and intracellular Ca^{2+} transport in lacrimal acinar cells. *Am. J. Physiol.*, **258**, C1006–C1015.

LOW, A.M., KWAN, C.Y. & DANIEL, E.E. (1992). Evidence for two types of internal Ca^{2+} stores in canine mesenteric artery with different refilling mechanisms. *Am. J. Physiol.*, **262**, H31–H37.

LÜCKHOFF, A., POHL, U., MÜLSCH, A. & BUSSE, R. (1988). Differential role of extra- and intracellular calcium in the release of EDRF and prostacyclin from cultured endothelial cells. *Br. J. Pharmacol.*, **95**, 189–196.

MALTA, E., MACDONALD, P.S. & DUSTING, G.J. (1988). Inhibition of vascular smooth muscle relaxation by LY83583. *Naunyn-Schmied. Arch. Pharmacol.*, **337**, 459–464.

MASON, M.J., GARCIA-RODRIGUEZ, C. & GRINSTEIN, S. (1991). Coupling between intracellular Ca^{2+} stores and the Ca^{2+} permeability of the plasma membrane. Comparison of the effects of thapsigargin, 2,5-di-(tert-butyl)-1,4-hydroquinone, and cyclopiazonic acid in rat thymic lymphocytes. *J. Biol. Chem.*, **266**, 20856–20862.

MERRITT, J.E. & RINK, T.J. (1987). Regulation of cytosolic free calcium in fura-2-loaded rat parotid acinar cells. *J. Biol. Chem.*, **262**, 17362–17369.

MERTZ, L.M., BAUM, B.J. & AMBUDKAR, I.S. (1990). Refill status of the agonist-sensitive Ca^{2+} pool regulates Mn^{2+} influx into parotid acini. *J. Biol. Chem.*, **265**, 15010–15014.

MOORE, P.K., AL-SWAYEN, O.A., CHONG, N.W.S., EVANS, R.A. & GIBSON, A. (1990). L-N^G-nitro arginine (L-NOARG), a novel L-arginine reversible inhibitor of endothelium-dependent vasodilatation *in vitro*. *Br. J. Pharmacol.*, **99**, 408–412.

MÜLSCH, A., BASSENGE, E. & BUSSE, R. (1989). Nitric oxide synthesis in endothelial cytosol: evidence for a calcium-dependent and a calcium-independent mechanism. *Naunyn-Schmied. Arch. Pharmacol.*, **340**, 767–770.

MÜLSCH, A., BUSSE, R. & FÖRSTERMANN, U. (1988). LY83583 interferes with the release of endothelium-derived relaxing factor and inhibits soluble guanylate cyclase. *J. Pharmacol. Exp. Ther.*, **247**, 283–288.

NAGAO, T. & VANHOUTTE, P.M. (1991). Hyperpolarization contributes to endothelium-dependent relaxation to acetylcholine in femoral veins of rats. *Am. J. Physiol.*, **261** (Heart Circ. Physiol. 30), H1034–1037.

NAGAO, T. & VANHOUTTE, P.M. (1992). Hyperpolarization as a mechanism for endothelium-dependent relaxations in the porcine coronary artery. *J. Physiol.*, **445**, 355–367.

PANDOL, S.J., SCHOEFFIELD, M.S., FIMMEL, C.J. & MUALLEM, S. (1987). The agonist-sensitive calcium pool in the pancreatic acinar cell: activation of plasma membrane Ca^{2+} influx mechanism. *J. Biol. Chem.*, **262**, 16963–16968.

PUTNEY, Jr, J.W. (1990). Capacitative calcium entry revisited. *Cell Calcium*, **11**, 611–624.

SCHILLING, W.P., CABELLO, O.A. & RAJAN, L. (1992). Depletion of the inositol 1,4,5,-trisphosphate-sensitive intracellular Ca^{2+} store in vascular endothelial cells activates the agonist-sensitive Ca^{2+}-influx pathway. *Biochem. J.*, **284**, 521–530.

SCHILLING, W.P., RAJAN, L. & STROBL-JAGER, E. (1989). Characterization of the bradykinin-stimulated influx pathway of cultured vascular endothelial cells. *J. Biol. Chem.*, **264**, 12838–12848.

SCHILLING, W.P., RITCHIE, A.K., NAVARRO, L.T. & ESKIN, S.C. (1988). Bradykinin-stimulated calcium influx in cultured bovine aortic endothelial cells. *Am. J. Physiol.*, **255**, (Heart Circ. Physiol. 24), H219–H227.

SCHINI, V. & VANHOUTTE, P.M. (1992). Inhibitors of calmodulin impair the constitutive but not the inducible nitric oxide synthase activity in the rat aorta. *J. Pharmacol. Exp. Ther.*, **261**, 553–559.

SEIDLER, N.W., JANA, I., VEGH, M. & MARTONOSI, A. (1989). Cyclopiazonic acid is a specific inhibitor of the Ca^{2+}-ATPase of salcoplasmic reticulum. *J. Biol. Chem.*, **264**, 17816–17823.

SHIMA, H. & BLAUSTEIN, M.P. (1992). Modulation of evoked contractions in rat arteries by ryanodine, thapsigargin, and cyclopiazonic acid. *Circ. Res.*, **70**, 968–977.

TAKEMURA, H. & PUTNEY, Jr. J.W. (1989). Capacitative calcium entry in parotid acinar cells. *Biochem. J.*, **258**, 409–412.

WEINHEIMER, G. & OSSWALD, H. (1986). Inhibition of endothelium-dependent smooth muscle relaxation by calmodulin antagonist. *Naunyn-Schmied. Arch. Pharmacol.*, **332**, 391–397.

(Received August 12, 1993
Revised October 26, 1993
Accepted October 29, 1993)

Br. J. Pharmacol. (1994), **111**, 663–672 © Macmillan Press Ltd, 1994

Local anaesthetic blockade of neuronal nicotinic ACh receptor-channels in rat parasympathetic ganglion cells

Javier Cuevas & [1]David J. Adams

Department of Molecular and Cellular Pharmacology, University of Miami School of Medicine, P.O. Box 016189 Miami, FL 33101, U.S.A.

1 The effects of the local anaesthetics QX-222 and procaine on nicotinic acetylcholine (ACh)-evoked currents in cultured parasympathetic cardiac neurones of the rat were investigated by use of the whole-cell, perforated-patch, and outside-out recording configurations of the patch clamp method.

2 QX-222 and procaine, applied to the extracellular surface, reversibly inhibited the peak amplitude of the whole-cell nicotinic ACh-evoked current in a concentration-dependent manner, with half-maximal inhibitory concentrations (IC_{50}) of 28 μM and 2.8 μM, respectively, at -80 mV. In these neurones, the sustained inward current mediated by M_1 muscarinic receptor activation was unaltered by QX-222, and neither local anaesthetic affected the adenosine 5'-triphosphate (ATP)-evoked current.

3 QX-222 and procaine block of nicotinic ACh-evoked inward current was voltage-dependent and enhanced by hyperpolarization. An e-fold change in their dissociation equilibrium constants (K_d) resulted from a 62 mV and a 122 mV change in membrane potential, respectively.

4 Both local anaesthetics produce a concentration-dependent increase in the half-time of decay of the nicotinic ACh-evoked inward current.

5 Measurements of unitary currents in outside-out patches showed that QX-222 reversibly increased the mean burst duration and closed time and reduced the mean channel open time and open-state probability of the nicotinic ACh receptor-channel (AChR) in a concentration-dependent manner.

6 The K_d and voltage sensitivity of local anaesthetic block of the nicotinic AChR in rat intracardiac neurones suggests that the pore-forming region of this channel differs from that of the AChR in frog and rat skeletal muscle and from the neuronal $\alpha_4\beta_2$ ACh receptor-channel.

Keywords: Cardiac ganglia; parasympathetic neurones; nicotinic receptor; muscarinic receptor; acetylcholine; adenosine 5'-triphosphate; local anaesthetic; single channel current; patch-clamp

Introduction

Neuronal nicotinic acetylcholine receptor (AChR) channels are distributed throughout the central and peripheral nervous systems, and are structurally and pharmacologically distinct from the AChR channels at the motor endplate. Whereas the muscle-type nicotinic AChR is a pentameric structure composed of two ACh-binding subunits (α_1) and three structural subunits (β_1, δ, and γ or ε), the neuronal nicotinic AChR appears to be comprised of only two subunit types, the ACh-binding, or α-subunit, and the β (or non-α) subunit. The stoichiometry for the neuronal AChR expressed in *Xenopus* oocytes has been defined as 2α, 3β (Anand *et al.*, 1991; Cooper *et al.*, 1991); however, it remains to be confirmed in neurones. At present, four α-subunits (α_2, α_3, α_4, α_7) and two β-subunits (β_2, β_4) have been demonstrated to be able to contribute to the formation of functional nicotinic AChRs (for review see Papke, 1993; Sargent, 1993). Muscle and neuronal AChRs exhibit differential sensitivity to receptor antagonists such as α-bungarotoxin and neuronal bungarotoxin (see Deneris *et al.*, 1991; Lukas & Bencherif, 1992). Among neuronal nicotinic AChRs composed of different subunit combinations, functional differences in agonist potency and block by neurotoxins have also been reported (Luetje *et al.*, 1990; Luetje & Patrick, 1991). The single channel properties of neuronal nicotinic AChRs are also dependent upon the subunit composition, the stage of development, and the host cell examined (for review see Deneris *et al.*, 1991; Papke, 1993). It would appear that AChRs are a heterogeneous family of neurotransmitter-activated channels with a diverse range of functional properties.

The membrane conductance change mediated by the activation of nicotinic AChRs can be modified by a variety of drugs which appear to act by blocking within the open channel. Single AChR channel currents show characteristic kinetic alterations in the presence of local anaesthetics, and the voltage-dependence of cationic drug binding indicates that the binding site is within the membrane electric field (see review Colquhoun, 1986). The binding site of the muscle AChR channel for the open-channel blocker QX-222, a quaternary ammonium derivative of lignocaine, was recently probed using site-directed mutagenesis. QX-222 interacts with adjacent turns of the M2 helix of the muscle AChR (Leonard *et al.*, 1988; Charnet *et al.*, 1990).

Anaesthetics have long been known to suppress the spike potential of neurones elicited by orthodromic stimulation, synaptic transmission, or exogenously applied acetylcholine in the central and peripheral nervous systems (Larrabee & Posternak, 1952; Galindo, 1969). Although local anaesthetics have been shown to depress synaptic transmission in rat sympathetic ganglia (Tabatabai & Booth, 1990), and to inhibit carbachol-evoked currents in bovine chromaffin cells (Charlesworth *et al.*, 1992), the precise mechanism of action of local anaesthetics on neuronal nicotinic AChRs remains unknown. Given that neuronal nicotinic AChRs are known to differ from muscle AChRs in their primary structure, ion permeation and pharmacological properties (Adams & Nutter, 1992; Sargent, 1993), investigation of the nature of the interaction of local anaesthetics with the neuronal nicotinic AChR may provide further insight into the functional properties of this ion channel.

In this study, we examine local anaesthetic block of ACh-evoked currents in cultured parasympathetic neurones from rat intracardiac ganglia. Mammalian intracardiac neurones possess both nicotinic and muscarinic ACh receptors (Hassall *et al.*, 1987; Seabrook *et al.*, 1990). In mammalian cultured cardiac neurones, ACh elicits a rapidly activating current

[1] Author for correspondence.

mediated by nicotinic ACh-receptors (Fieber & Adams, 1991a; Adams & Nutter, 1992; Selyanko & Skok, 1992) and a slowly activating current mediated by muscarinic ACh-receptors (Allen & Burnstock, 1990a; Selyanko & Skok, 1992). Our results show that the local anaesthetics, procaine and QX-222, selectively inhibit with high efficacy the nicotinic ACh-evoked current in parasympathetic neurones via a rapid transient block of the open channel. A preliminary report of some of these results has been published (Nutter *et al.*, 1991).

Methods

Preparation

The isolation and culture of parasympathetic neurones from rat intracardiac ganglia have been described previously (Fieber & Adams, 1991a). Briefly, neonatal rats, 3 to 5 days old, were killed by decapitation. The heart and lungs were excised as a single unit and placed in physiological saline solution (PSS) containing (mM): NaCl 140, KCl 3, $CaCl_2$ 2.5, $MgCl_2$ 1.2, glucose 7.7 and histidine 10 (pH to 7.2 with NaOH). Atria were removed and incubated in PSS solution containing collagenase (1 mg ml^{-1}, Worthington-Biomedical) at 37°C for 1 h. Individual ganglia were then dissected from the ganglion plexus, transferred to a sterile culture dish containing high glucose culture medium (Dulbecco's Modified Eagle Media, 10% (v/v) foetal calf serum, 100 u ml^{-1} penicillin and 0.1 mg ml^{-1} streptomycin), triturated with a fine-bore Pasteur pipette and plated onto 18 mm glass cover-slips coated with laminin. The dissociated cells were incubated at 37°C in a 95% air, 5% CO_2 atmosphere for 48–72 h. Following this incubation period, the glass cover-slips could be transferred to a 0.5 ml recording chamber mounted on an inverted, phase contrast microscope (Nikon Diaphot, 400 × magnification) and electrophysiological experiments conducted.

Electrical recordings and analysis

Acetylcholine-evoked currents in intracardiac neurones were studied under voltage clamp mode by standard whole-cell and outside-out recording configurations of the patch clamp technique (Hamill *et al.*, 1981). In some experiments electrical access to the cell was obtained by use of the perforated patch method (Horn & Marty, 1988), which prevents cell dialysis and the subsequent alterations in cell function due to loss of cytosolic components. Stock solutions of 25 mg ml^{-1} nystatin (Sigma) and 25 mg ml^{-1} pluronic (Molecular Probes), both in dimethylsulphoxide (DMSO), were prepared the day of the experiment and kept on ice, in the dark. Immediately prior to use, the pluronic and the nystatin stock solutions were diluted 500 fold in pipette solution and vortexed, yielding a final solution containing 50 μg ml^{-1} of both pluronic and nystatin in 0.4% DMSO. In order to prevent nystatin-induced disruption of gigaseal formation, the tips of the electrodes were first filled with nystatin-free pipette solution and then backfilled with the nystatin-containing solution.

Immediately following gigaseal formation, the neurones were held at − 70 mV and voltage pulses (20 ms) to − 80 mV were applied at 1 Hz. Nystatin incorporation into the membrane resulted in the appearance of a slow capacitive transient and a decrease in the series resistance (R_s). Experiments were continued only if R_s was less than 10 MΩ within 10 min of seal formation. Rupture of the membrane under the pipette tip was indicated by a rapid change in the holding current or a depolarization of the cell, at which time the experiment was stopped.

Electrodes were pulled from thick-walled borosilicate glass (GF 150F; Clark Electromedical Inst., UK) using a Sutter Instruments P-87 micropipette puller, and coated with Sylgard (Dow Corning Corp.) to within 100 μm of the tip. Final pipette resistance was 1–3 MΩ for normal and perforated patch whole-cell recordings and 4–6 MΩ for excised membrane patch recordings. Membrane currents evoked by agonist application were amplified and filtered (10 kHz) with a List patch clamp amplifier (L/M-EPC 7) and recorded on video tape using an analog to digital recorder adaptor (PCM 4, two channel mode; Medical Systems Corp., N.Y., U.S.A.). Membrane currents were continuously monitored on a digital oscilloscope (Nicolet 3091), and a chart recorder (Soltec 1242).

For analysis of ACh-evoked currents, data were played back from video-tape, filtered at 3 kHz (− 3 dB, 4 pole low-pass Bessel filter; Frequency Devices 902), and digitized at 20 kHz (Tecmar Labmaster TL1-125 DMA interface). Whole-cell currents were viewed and analyzed using the Axotape programme (Axon Instruments Inc., CA, U.S.A.). Unitary current records were transferred to a computer (Northgate PC 80386/33 MHz) using a threshold detection device (AI 2020A event detector; Axon Instruments Inc.), and analyzed using pClamp programmes (Axon Instruments Inc.). To minimize attenuation of unitary current amplitude, data used for determining mean unitary current amplitude were filtered at 5 kHz.

Amplitude distributions of single channel openings were obtained by measuring the difference between the amplitude of each event and the baseline current. Each individual opening contributed one point to the amplitude distribution of the whole record. An idealized reconstruction of open-closed transitions was created using a detection threshold for channel opening set at 50% of the amplitude of a single channel opening, and a minimum resolvable time of 150 μs for single channel events. Frequency distribution histograms were constructed for open and closed state durations, and fitted using the minimum X^2 method.

To analyze bursts of openings, the critical gap length below which a closure was classified as a gap within a burst was calculated for each experimental condition according to a method described previously (Colquhoun & Sigworth, 1983; Clapham & Neher, 1984). Under control conditions the critical gap length was found to be 1 ms, and increased to 1.1 ms and 1.4 ms in the presence of 30 μM and 100 μM QX-222, respectively. Total conduction time within a burst was determined using the equation (cf. Colquhoun & Sakmann, 1985):

$$T' = T_t/N_t \qquad (1)$$

where T' is the total conduction time within a burst, T_t is the total conduction time during time t, and N_t is the total number of bursts occurring during time t.

All numerical data are presented as mean ± standard error of the mean (s.e.mean).

Solutions

The control external solution for standard and peforated patch whole-cell recordings was normal PSS. The pipette solution for conventional whole-cell recordings consisted of (mM): $CsCl_4$ 140, MgATP 2, Cs_4BAPTA 2, HEPES 10 (pH to 7.2 with CsOH). The perforated patch pipette solution contained (mM): K_2SO_4 75, KCl 55, $MgSO_4$ 5, HEPES 10 (pH to 7.2 with *N*-methyl-(+)-glucamine). The recording chamber was continuously perfused (2 ml min^{-1}) with the indicated solutions at room temperature (22–23°C). Acetylcholine- and adenosine 5′-triphosphate-mediated responses were evoked during whole-cell recordings by focal application of 100 μM AChCl or 300 μM MgATP (Sigma Chemical Co., St. Louis, MO, U.S.A.) in PSS via pressure ejection (10 ms, 15 psi; Picospritzer II, General Valve Corp., N.Y., U.S.A.) from an extracellular pipette. The pressure ejection pipette was positioned ⩽ 50 μm from the neuronal soma to evoke maximal response to agonist under control conditions. The concentration of bath-applied drugs at the cell surface during pressure application of ACh or ATP was equal to or lower than that

of the bulk solution. Thus, the apparent dose-response curves for these drugs may be shifted towards higher antagonist concentrations. The external solution used for recording single channel currents contained (composition in mM): NaCl 136, $CaCl_2$ 2.5, $MgCl_2$ 1.2, glucose 7.7, histidine 5 (pH 7.2) and the intracellular pipette solution (mM): NaCl 130, Na_4 BAPTA 2, Na_2ATP 2, HEPES 10 (pH 7.2 with NaOH). The osmotic activity of the solutions was monitored with a vapor pressure osmometer (Wescor 5500). In outside-out patch experiments, 1 μM AChCl was bath-applied in the external solution, in the absence or presence of the local anaesthetic.

Procaine hydrochloride (Sigma Chemical Co.), the quaternary N-methyl lignocaine derivative QX-222 (Astra Pharmaceuticals; Westboro, MA, U.S.A.), and pirenzepine dihydrochloride (Research Biochemicals Inc., Natick; MA, U.S.A.) were bath applied at the indicated concentrations.

Results

Whole cell recordings of ACh-evoked currents

The effects of local anaesthetics on nicotinic and muscarinic ACh-currents were examined by the perforated-patch recording configuration to minimize the rundown of muscarinic ACh-induced current which occurs as a result of whole-cell dialysis. Figure 1 shows a typical series of inward currents elicited by pressure ejection of 100 μM ACh, obtained from a single cell. Application of ACh to the soma of cardiac neurones, voltage-clamped at 0 mV, evoked a slowly activating inward current (Figure 1a) previously undetected in whole-cell experiments (Fieber & Adams, 1991a). At negative potentials, ACh activated a transient inward current, followed by a steady-state inward current (Figure 1a). Bath application of QX-222 (100 μM) reversibly reduced the amplitudes of both the transient and sustained currents, but did not significantly depress the amplitude of the slow activating inward current (Figure 1b). The amplitude of the QX-222-insensitive, slow activating inward current was reduced by bath application of the muscarinic (M_1) receptor antagonist, pirenzepine (100 nM; Figure 1c).

Under standard, dialyzed whole-cell configuration, exogenous application of ACh elicited a transient current with a voltage-dependent amplitude, but the sustained inward current and the slowly inactivating inward current observed under perforated-patch recording conditions were absent. The ACh-evoked transient current was inward at negative potentials and reversed at approximately 0 mV (Figure 2a). The ACh-evoked current was outward at positive potentials, and the *I-V* relationship displayed strong inward rectification. Currents evoked by brief application (10 ms) of ACh decayed to baseline within 3 s, and the rate of current decay was independent of membrane potential over the range of − 100 to + 60 mV.

Effects of QX-222 on whole-cell currents

Figure 2b shows inward currents evoked by ACh in the presence of 10 μM QX-222. Externally applied QX-222 attenuated ACh-evoked current amplitude at negative membrane potentials, and produced a voltage-dependent decrease in the rate of current decay. The half-time of decay of the ACh-evoked current increased by ~7% in the presence of 10 μM QX-222 at − 40 mV and by ~33% at − 100 mV. The whole-cell *I-V* relationships obtained in the absence and presence of QX-222 reveals a concentration-dependent reduc-

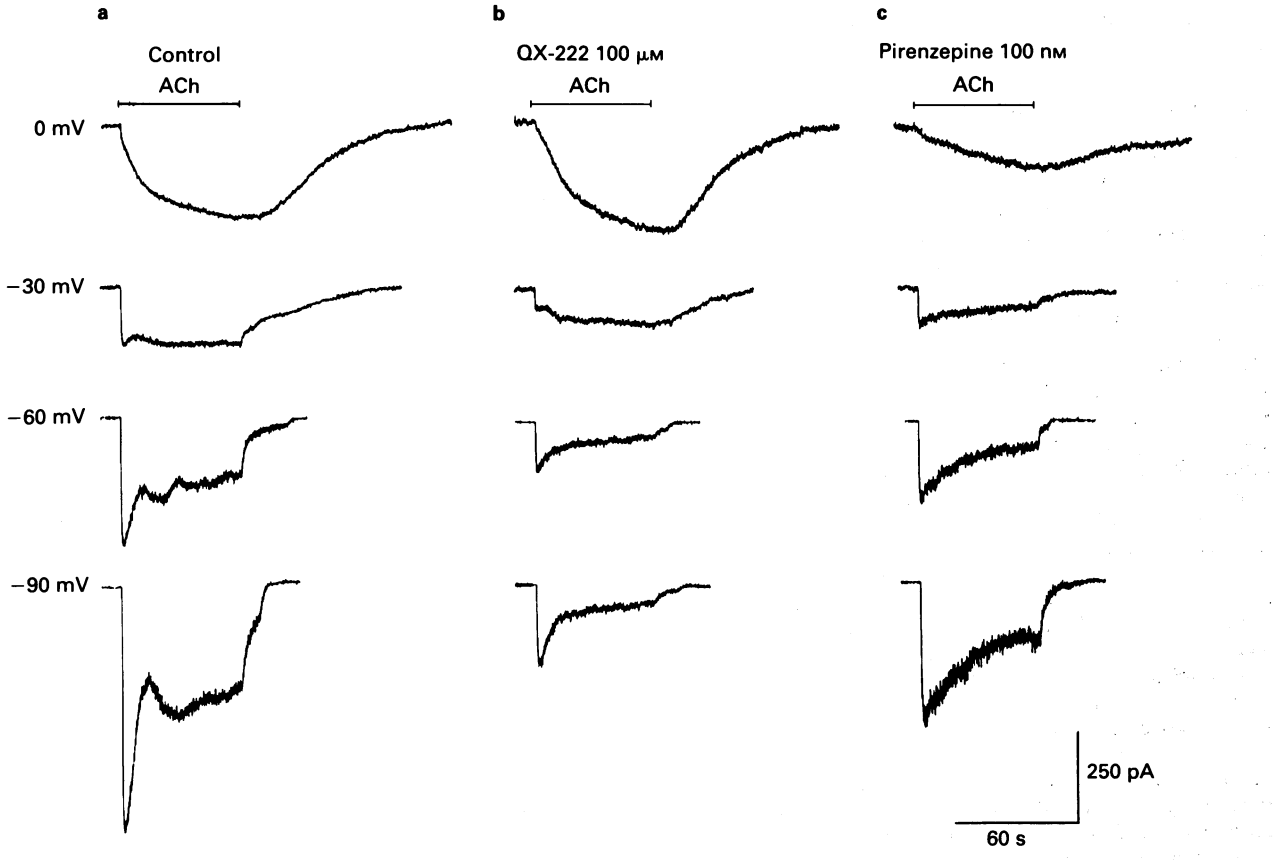


Figure 1 Whole-cell currents in rat parasympathetic neurones evoked by extracellular ACh (100 μM) by use of the perforated patch recording technique. (a) Whole-cell currents evoked by ACh at the membrane potentials indicated (− 90 to 0 mV). ACh-evoked currents obtained in the presence of bath applied 100 μM QX-222 (b) or 100 nM pirenzepine (c). ACh-evoked whole-cell currents shown in (a), (b) and (c) were recorded from the same neurone.

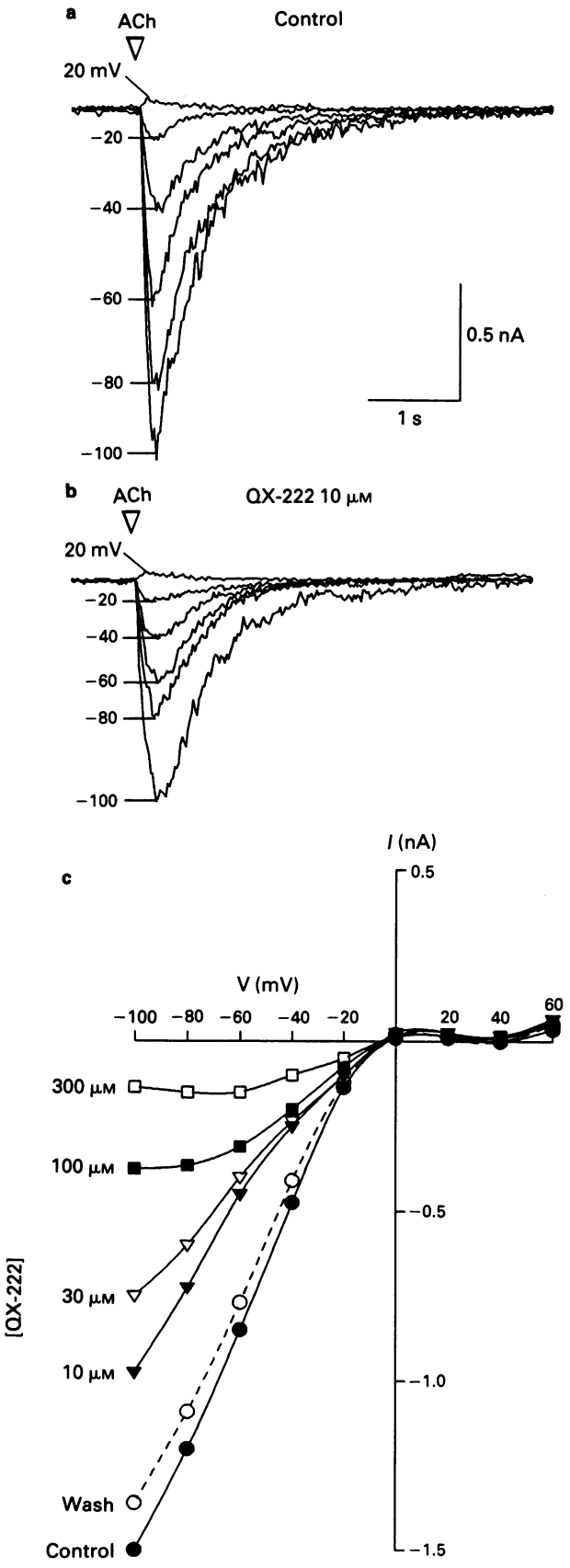


Figure 2 Inhibition of ACh-evoked currents by QX-222 in rat isolated parasympathetic neurones. (a) Family of currents evoked by brief pulses (10 ms) of ACh focally applied to an isolated neurone held at the indicated membrane potentials. (b) ACh-evoked currents obtained from the same neurone in the presence of bath applied 10 μM QX-222. (c) *I-V* relation of ACh-evoked currents obtained in the absence (control) and presence of QX-222 at the concentrations indicated.

tion of current amplitude at negative potentials (Figure 2c), but no alteration of the reversal potential, nor any significant reduction of current amplitude at positive potentials. The effects of QX-222 on the ACh-induced current amplitude and decay rate, were rapidly reversed upon washout.

Whole-cell recordings of representative ACh-evoked currents obtained at − 80 mV in the absence and presence of increasing concentrations of QX-222 are shown in Figure 3a. Raising the external QX-222 concentration reduced the ACh-evoked current amplitude, and increased the time course of decay in a concentration-dependent manner (Figure 3a). The half time of current decay increased from 0.40 ± 0.03 s (control) to 0.51 ± 0.05 s and 0.64 ± 0.05 s ($n = 5$ cells) in the presence of 30 μM and 100 μM QX-222, respectively. Figure 3b plots a normalized dose-response relationship obtained for the inhibition of ACh-evoked current by QX-222. The relationship was fit with a single-site adsorption isotherm with a half-maximal inhibition at 28 μM.

The influence of membrane potential on QX-222 inhibition of whole-cell ACh-evoked currents is shown in Figure 4. ACh-evoked current amplitude versus membrane potential, in the absence and presence of QX-222, is plotted in Figure 2c. Membrane hyperpolarization increased the inhibition of inward ACh-induced current amplitude: the change from − 20 mV to − 100 mV produced a 36% increase in inhibition of ACh-evoked current amplitude by 100 μM QX-222. The ratio (Λ) of the control ACh-evoked current amplitude to that obtained in the presence of 100 μM QX-222, was deter-

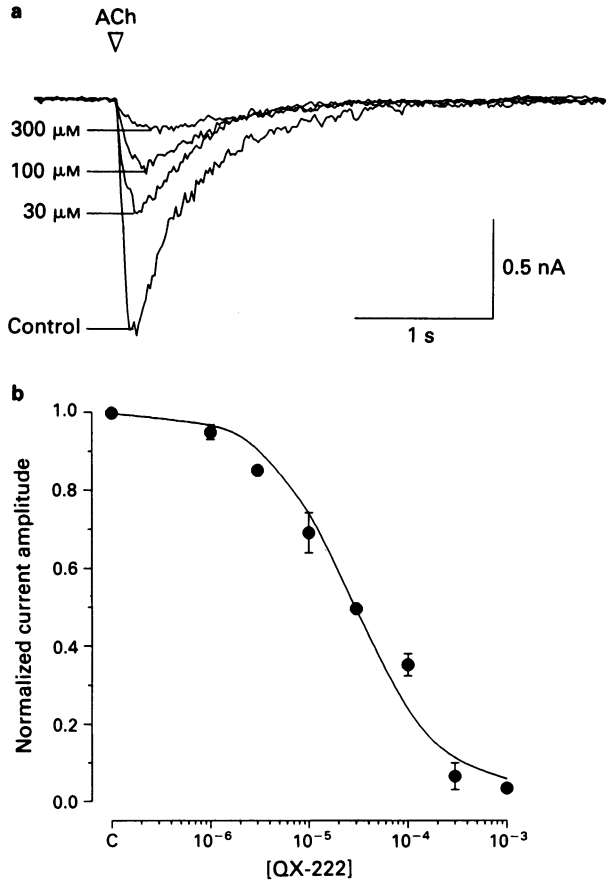


Figure 3 Concentration-dependence of QX-222 block of ACh-evoked currents. (a) ACh-evoked currents obtained in the absence (control) and presence of bath applied QX-222. Holding potential, − 80 mV. (b) Relative amplitude of ACh-evoked currents (at − 80 mV) normalized to control, as a function of QX-222 concentration. Data points represent the mean ± s.e.mean for five cells. The curve is a best fit of the data by a single-site adsorption isotherm with a half-maximal inhibition IC_{50} of 28 μM.

mined at different membrane potentials. A plot of Λ-1 as a function of membrane potential (Figure 4), revealed an e-fold change for a 62 mV change in membrane potential. The relationship between Λ-1 and the dissociation constant (K_d) for QX-222 binding to the ACh receptor-channel is approximated by the equation:

$$K_d \approx c_Q/\Lambda\text{-}1, \qquad (2)$$

where c_Q is the concentration of QX-222 (Ascher *et al.*, 1979). This implies that hyperpolarization by 62 mV reduces the apparent K_d e-fold.

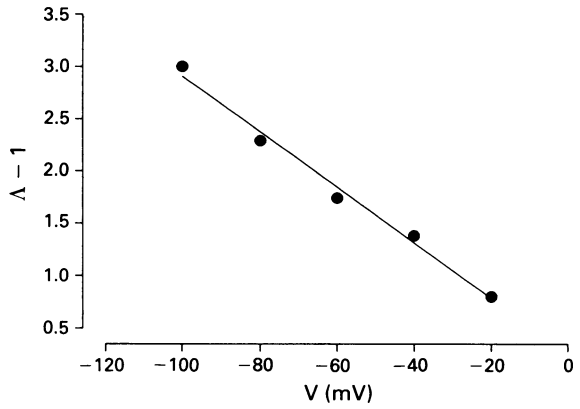


Figure 4 Voltage-dependence of QX-222 inhibition of ACh-activated currents in cardiac neurones. Λ-1 values calculated from the current amplitudes obtained in the absence and presence of 100 μM QX-222, plotted as a function of membrane potential. Data points were fitted by linear regression.

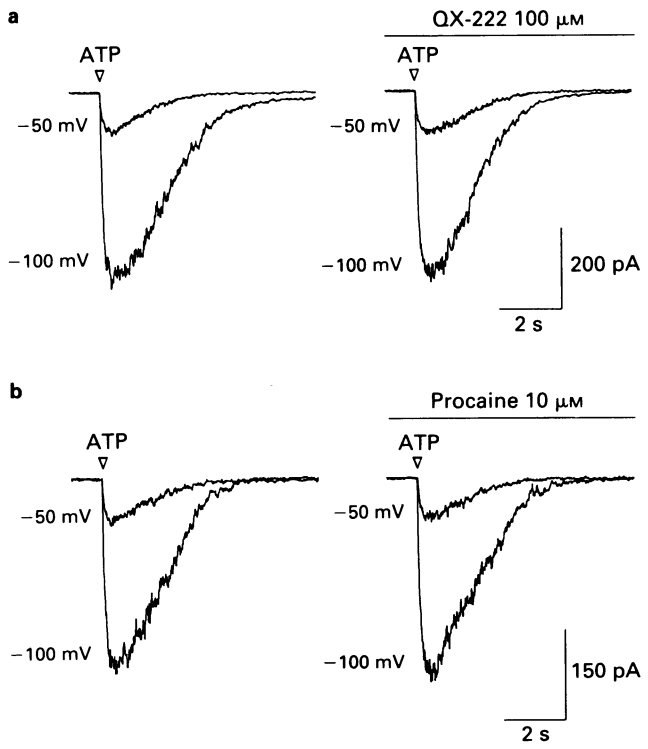


Figure 5 Lack of effect of local anaesthetics on adenosine 5'-triphosphate (ATP)-evoked currents in rat parasympathetic neurones. Currents evoked by brief (10 ms), focal application of ATP to the soma held at − 50 and − 100 mV. ATP-evoked currents obtained from the same cell in the absence and presence of PSS containing either 100 μM QX-222 (a) or 10 μM procaine (b).

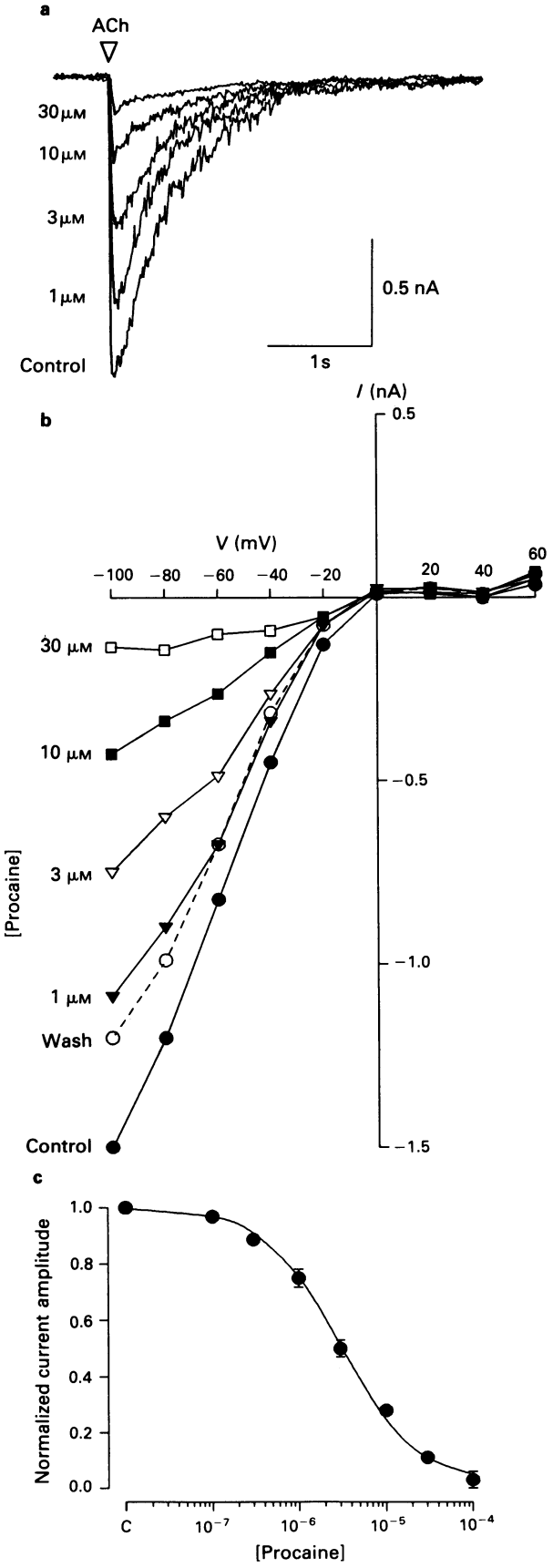


Figure 6 Inhibition of ACh-evoked currents by procaine in cultured parasympathetic neurones. (a) ACh-induced currents obtained in the absence (control) and presence of procaine. Holding potential, − 80 mV. (b) *I-V* relation of ACh-evoked currents obtained in the absence and presence of procaine. (c) Normalized current amplitude (at − 80 mV) plotted as a function of procaine concentration. Points represent mean ± s.e.mean for 3 cells. The curve was fitted according to a one-site adsorption isotherm with an IC_{50} of 2.8 μM.

ATP evoked a transient inward current in rat parasympathetic neurones with a time course and *I-V* relationship similar to that obtained with ACh (Fieber & Adams, 1991b). Bath application of either 100 μM QX-222 or 10 μM procaine failed to inhibit the ATP-induced current in these neurones (Figure 5).

Effects of procaine on whole cell currents

Procaine inhibited ACh-evoked currents in parasympathetic neurones similarly to QX-222. Bath application of procaine reduced the amplitude of the transient inward current evoked by focal application of ACh to the soma voltage-clamped at negative membrane potentials (Figure 6a). The inhibition of ACh-evoked current amplitude by procaine was concentration-dependent and reversible upon washout (Figure 6b). The dissociation equilibrium constant, calculated from equation 2, was 3 μM at − 80 mV. Procaine inhibition of ACh-current amplitude also was voltage-dependent, changing e-fold per 122 mV change in membrane potential. Procaine did not alter the reversal potential of the ACh-evoked current, nor affect the current amplitude at positive potentials. The half time of current decay at − 80 mV was increased from 0.41 ± 0.04 s (control) to 0.53 ± 0.05 s ($n = 3$ cells) in the presence of 30 μM procaine.

The dose-response relationship for the inhibition of ACh-evoked currents by procaine, normalized to the control condition, is shown in Figure 6c. Half-maximal inhibition was calculated to be 2.8 μM from the fit of a single-site adsorption isotherm to the data. Near complete block of the ACh-evoked current at − 80 mV was obtained with 100 μM procaine ($n = 3$).

Single-channel recordings

Single channel currents recorded from outside-out membrane patches in the absence and presence of QX-222, revealed complex gating kinetics. As described previously, unitary currents occurred in clusters separated by long shut periods (Mathie *et al.*, 1991). Within clusters, bursts of openings were separated by closures of intermediate length, whereas individual openings within a burst were separated by brief closings. Figure 7a shows unitary currents evoked by bath-application of 1 μM ACh recorded from an outside-out patch held at − 90 mV and − 120 mV in symmetrical 140 mM NaCl solutions. The traces were recorded within a cluster of channel

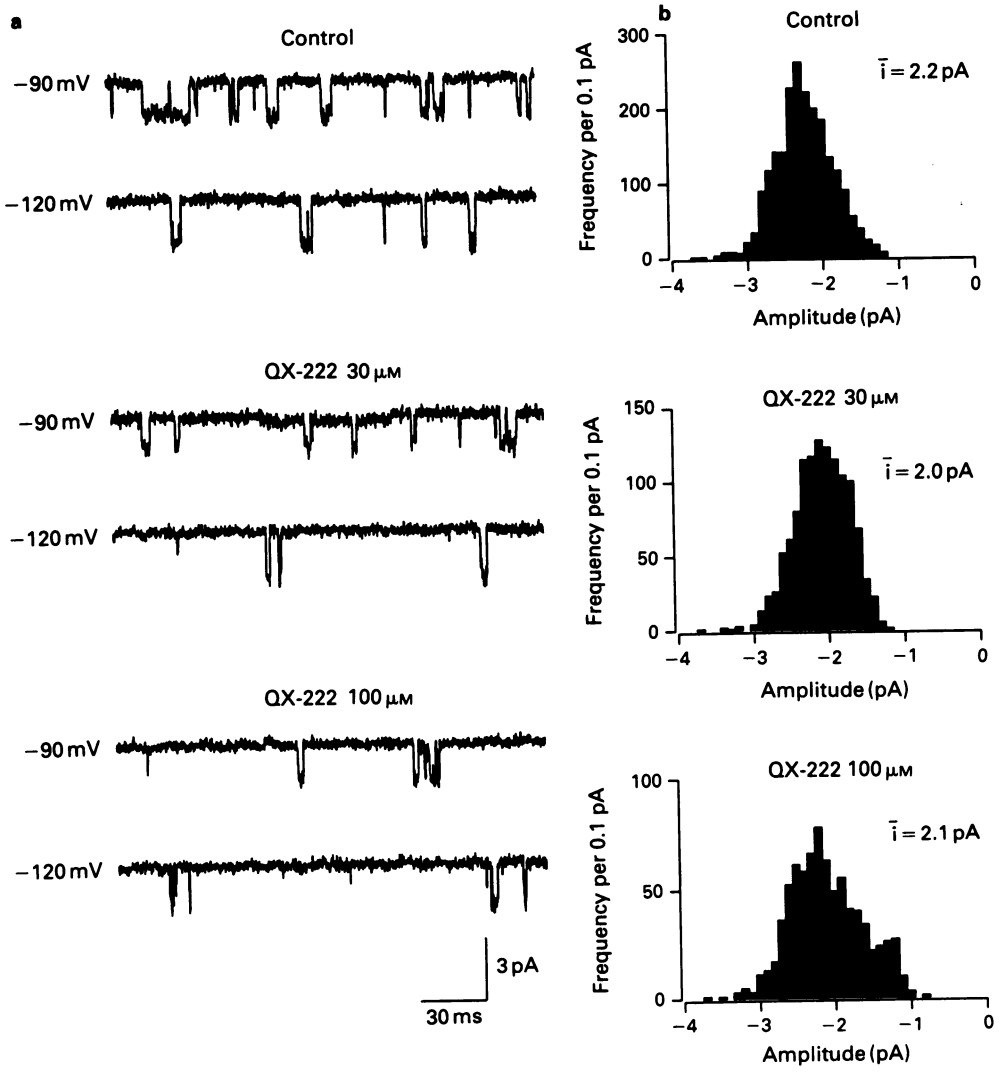


Figure 7 Neuronal ACh receptor single channel activity in the absence and presence of QX-222. (a) ACh-induced unitary currents recorded from an excised outside-out membrane patch held at − 90 mV and − 120 mV in the absence and presence of QX-222. (b) Current amplitude histograms (0.1 pA bin width) obtained for five outside-out membrane patches held at − 90 mV in 0, 30 and 100 μM QX-222. Single AChR-channels were activated by 1 μM ACh.

activity. The unitary *I-V* relationship was linear from − 120 to − 20 mV, and the mean single-channel slope conductance was 26 ± 3 pS ($n = 5$ cells).

The effects of QX-222 on the ACh-induced single channel currents were investigated in outside-out membrane patches exposed to bath applied QX-222 and 1 μM ACh. QX-222 reduced ACh-evoked single channel activity at negative potentials in a concentration-dependent manner, without a significant reduction of unitary current amplitude (Figure 7a). The unitary current amplitude at − 90 mV was 2.2 ± 0.4 pA for control, 2.0 ± 0.4 pA in 30 μM QX-222, and 2.1 ± 0.5 pA in 100 μM QX-222 ($n = 5$; Figure 7b).

QX-222 inhibition of ACh-evoked currents is reflected in the altered single channel kinetics. Figure 8a shows representative bursts of ACh-induced channel openings obtained at − 90 mV in the presence of 0, 30 and 100 μM QX-222. Open-time distributions for the combined data from five outside-out patches exposed to 1 μM ACh and the QX-222 concentrations indicated are shown in Figure 8b. The open-time distributions were best fit by the sum of two exponential functions. In the absence of QX-222, time constants of 0.30 ms and 1.28 ms were obtained whereas, in the presence of QX-222, a concentration-dependent shift of the distribution towards shorter open times was observed (Figure 8b; Table 1). Thus, bath application of QX-222 produced a significant decrease in the ACh receptor-channel apparent mean open time (t_o). At − 90 mV, t_o for the ACh-activated channel was 0.83 ± 0.01 ms (control), and decreased to 0.73 ± 0.01 ms and 0.55 ± 0.02 ms ($n = 5$) in the presence of 30 μM and 100 μM QX-222, respectively.

QX-222 also increased the time that the ACh receptor-channel remained in a non-conducting state in a concentration-dependent manner. The mean non-conducting interval within a burst (t_c) increased from 0.35 ± 0.01 ms (control) to 0.48 ± 0.01 and 0.55 ± 0.03 ms by 30 μM and 100 μM QX-222, respectively (− 90 mV, $n = 5$). This increased non-conducting time interval is also apparent from the closed time distributions obtained for these experiments, which were best fit with two exponentials. The time constant for the first exponential (τ_f), representing gaps within bursts, increased from 0.44 ms (control) to 0.60 ms and 0.80 ms in the presence of 30 μM and 100 μM QX-222, respectively. The time constant for the second exponential (τ_s), representing gaps between bursts, was also affected by QX-222, increasing from 10.64 ms (control) to 11.74 ms (30 μM QX-222) and 19.15 ms (100 μM QX-222). The open channel probability (P_o) at

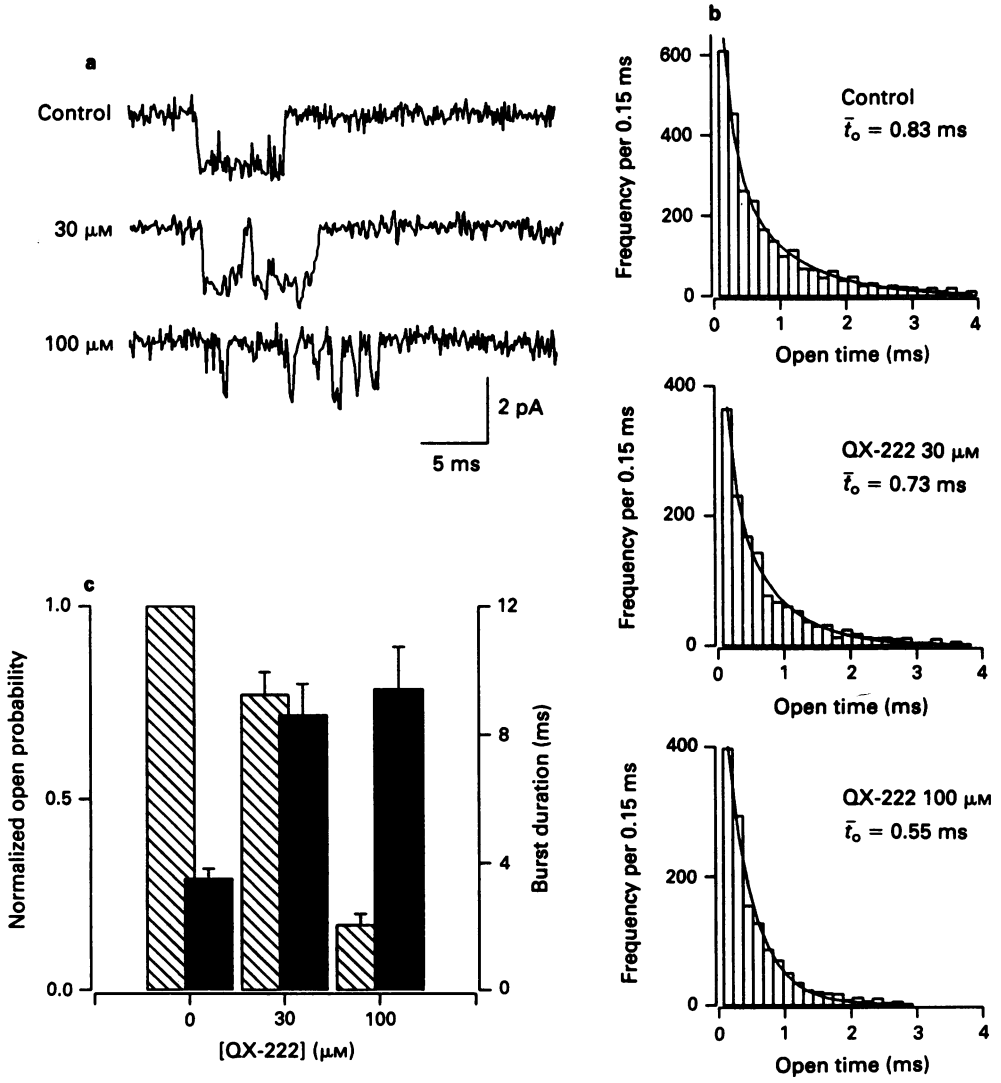


Figure 8 Effects of QX-222 on the kinetics of single neuronal ACh receptor channels. (a) Burst of activity recorded from single channel in the absence (control) and presence of 30 and 100 μM QX-222 at − 90 mV. (b) Distribution of open times (0.15 ms bin width) during a burst before and after addition of 30 and 100 μM QX-222 at − 90 mV for combined data from 5 patches. (c) Open probability (hatched columns) and mean burst duration (solid columns) obtained from five patches during a 5 min exposure to 0, 30 and 100 μM bath applied QX-222. Single AChR channels were activated by 1 μM ACh.

Table 1 Kinetics of neuronal nicotinic acetylcholine receptors (AChR) in the absence and presence of QX-222

	Control	*QX-222*	
		30 μM	100 μM
Open state			
τ_f (ms)	0.30 ± 0.04	0.25 ± 0.05	0.28 ± 0.12
τ_s (ms)	1.28 ± 0.29	0.92 ± 0.17	0.66 ± 0.37
A_f/A_s	1.05	0.84	1.13
Open time (ms)	0.83 ± 0.01	0.73 ± 0.01	0.55 ± 0.02
Closed state			
τ_f (ms)	0.44 ± 0.05	0.60 ± 0.10	0.80 ± 0.10
τ_s (ms)	10.64 ± 2.12	11.74 ± 1.50	19.15 ± 5.04
A_f/A_s	0.72	0.26	0.35
Closed time (ms)	0.35 ± 0.01	0.48 ± 0.01	0.55 ± 0.03
Burst			
Critical gap (ms)	1.0	1.1	1.4
Burst length (ms)	3.5 ± 0.3	8.6 ± 1.0	9.4 ± 1.3
Open probability (%)	3.0 ± 0.7	2.3 ± 0.2	0.5 ± 0.1

Mean ± s.e.mean values were calculated for five outside-out patches ($> 10^3$ events/patch). Each membrane potential was activated by bath application of 1 μM ACh in the absence and presence of 30 μM and 100 μM QX-222. Mean closed time represents the value obtained for gaps with duration greater than the minimum resolvable time and less than the critical gap time. A_f/A_s represents the ratio of the areas contributed by the components with the fast and slow time constants, respectively.

Table 2 Characteristics of local anaesthetic block of nicotinic acetylcholine receptor (AChR)-channel subtypes

	QX-222		*Procaine*		
Preparation	K_d (μM)	*Voltage sensitivity* (mV)	K_d (μM)	*Voltage sensitivity* (mV)	*References*
Rat neuronal	31	62	3	122	Present study
Rat $\alpha_4\beta_2$	> 2000	26			Charnet *et al.* (1992)
Rat muscle	20	64			Neher (1983)
Frog muscle (junctional)	9	50			Ruff (1982)
			20	50	Adams (1977)
			42	86	Gage *et al.*, (1983)
Frog muscle (extra-junctional)	80	32			Neher & Steinbach (1978)

– 90 mV decreased from 3.0 ± 0.7% (control) to 2.3 ± 0.2% and 0.5 ± 0.1% in membrane patches exposed to 30 μM and 100 μM QX-222, respectively ($n = 5$, Figure 8c). These changes in gating kinetics and P_o of the AChR channel produced by QX-222 were reversible upon washout.

QX-222 also produced a concentration-dependent increase in ACh receptor-channel burst duration. Burst duration increased from 3.5 ± 0.3 ms (control) to 8.6 ± 1.0 ms and 9.4 ± 1.3 ms in solutions containing 30 μM and 100 μM QX-222, respectively ($n = 5$, Figure 8c). While burst duration increased in the presence of QX-222, conduction time within a burst decreased from 2.3 ms (control) to 2.2 ms (100 μM QX-222) in the same patches. The equilibrium dissociation constant (K_d) may be estimated from the burst duration (T) and total conduction time (T') (Neher, 1983)

$$K_d = c_Q T'/(T - T') \qquad (3)$$

where c_Q is the concentration of QX-222 and (T-T') is the total blocked time. Here an apparent K_d of 31 μM was calculated for QX-222 at – 90 mV from the experimental values of 9.4 ms and 2.2 ms for T' and T', respectively.

Discussion

In rat intracardiac neurones, the local anaesthetics QX-222 and procaine inhibit nicotinic ACh-evoked current in a concentration- and voltage-dependent manner, without affecting muscarinic ACh-evoked currents. QX-222 inhibits the ACh-evoked current via a rapid transient block of the open channel, decreasing the ACh receptor-channel open probability. The sensitivity of the neuronal nicotinic ACh-evoked currents to local anaesthetics suggests a possible role for these channels in local anaesthetic inhibition of ganglionic transmission.

The pirenzepine-sensitive, slowly-activating ACh-evoked current observed using the perforated-patch recording configuration was unaffected by the quaternary amine QX-222. This current appears to be identical with the M_1-activated current described in cultured intracardiac neurones of the guinea-pig (Allen & Burnstock, 1990a). In contrast, QX-222 reversibly inhibited the ACh-evoked transient inward current and steady-state current. These currents were, however, insensitive to the muscarinic receptor antagonists, pirenzepine and atropine (data not shown) and thus constitute a nicotinic AChR-mediated current. An ATP-induced current has also been described in parasympathetic neurones of mammalian intracardiac ganglia (Allen & Burnstock, 1990b; Fieber & Adams, 1991b). However, ATP-evoked currents were unaffected by bath application of either 100 μM QX-222 or 10 μM procaine (Figure 5), concentrations 3 fold higher than that required to produce half-maximal inhibition of the nicotinic ACh-evoked currents.

QX-222 reversibly decreased the amplitude of the transient ACh-evoked current of rat parasympathetic neurones in a concentration-dependent manner similar to that described for the motor endplates of frog (Beam, 1976a,b; Neher & Steinbach, 1978; Ruff, 1982) and rat (Neher, 1983). A comparison of the K_d and voltage-dependence of QX-222 and procaine block of several nicotinic ACh receptor-channel subtypes is presented in Table 2. QX-222 inhibition of transient ACh-evoked currents was potentiated by membrane hyperpolarization. The K_d for QX-222 block of ACh-induced whole-cell current changed e-fold with a 62 mV change in membrane

potential. This voltage sensitivity suggests that QX-222 binds at a site within the electric field, presumably the pore-forming region, of the ACh receptor-channel in parasympathetic neurones. The magnitude of voltage sensitivity of the rat neuronal and muscle ACh receptor-channels to QX-222 inhibition correspond to a binding site approximately 40% into the membrane field of these channels (Woodhull, 1973) compared to 75% for frog muscle and 92% for rat $\alpha_4\beta_2$ neuronal receptors, respectively (Neher & Steinbach, 1978; Charnet *et al.*, 1992).

Procaine also produced a reversible, concentration-dependent block of the nicotinic ACh-evoked current in rat cardiac neurones. The K_d for procaine block occurred at a concentration of 3 μM (Table 2). Procaine block of the AChR channel was also voltage-dependent; however, this voltage-dependence was less than that observed for QX-222. An e-fold change in K_d was produced by a 122 mV change in membrane potential, indicating a binding site $\sim$20% into the membrane field. These values differ from those calculated for the ACh receptor-channel at the frog endplate (Gage *et al.*, 1983), where the voltage-dependance was 86 mV per e-fold change in K_d suggesting the binding site was $\sim$30% into the membrane field.

The effects of QX-222 on the kinetics of the ACh receptor-channels of rat intracardiac neurones are similar to those reported for muscle ACh receptor-channel in frog (Neher & Steinbach, 1978) and rat (Neher, 1983) (see Table 1). QX-222 binding to the ACh receptor-channel decreased t_o and total conduction time within a burst, and increased both t_c and mean burst duration. Furthermore, QX-222 increased the duration of gaps between bursts, and decreased the open channel probability.

Several models have been proposed to explain the kinetics of local anaesthetic block of nicotinic AChR channels. The sequential kinetic model of channel blockade (Adams, 1976; Ruff, 1977; Neher & Steinbach, 1978) accurately predicts the decrease in nicotinic AChR channel mean open time and increase in burst duration observed in the present study. However, this model fails to account for the concentration-dependent increase in the intra- and inter-burst gaps and the decrease in intra-burst conduction time and open probability observed in the presence of QX-222. Neher (1983) similarly found that AChR kinetic data obtained in the presence of high concentrations of QX-222 was inconsistent with predictions of the sequential block model and therefore proposed an alternative model in which a channel could enter multiple blocked states. If one of these blocked states were more long-lived than the closed state(s), then P_o would be expected to decrease, as found in the present study. The observed increase in inter-burst gaps may be due to the channel entering a long-lived blocked state, and not a closed state.

An apparent K_d of 31 μM was calculated for QX-222 at $-$90 mV from the changes in the ratio of total conduction time and total blocked time within a burst (see equation 3). The apparent K_d indicates that the affinity of QX-222 for the ACh receptor-channel in rat parasympathetic cardiac neurones is slightly less than that for the ACh receptor-channel in rat cultured muscle cells (Neher, 1983) and frog skeletal muscle (Ruff, 1982), but more than that observed for ACh receptor-channels of frog muscle extrajunctional membranes (Neher & Steinbach, 1978), and rat $\alpha_4\beta_2$ neuronal ACh receptor-channel expressed in *Xenopus* oocytes (Charnet *et al.*, 1992) at $-$90 mV.

The K_d of 3 μM for procaine block at $-$80 mV was significantly less than that determined for ACh receptor-channels at the frog endplate (Adams, 1977; Gage *et al.*, 1983). Thus, procaine, unlike QX-222, has a greater affinity for ACh receptor-channels in rat intracardiac neurones than in frog muscle. This difference is not surprising, given that procaine block of ACh receptor-channels has been shown to occur via a mechanism different from that of quaternary local anaesthetics (Gage *et al.*, 1983). Whereas quaternary local anaesthetics block the ACh-evoked current exclusively from the extracellular side of the membrane (Horn *et al.*, 1980), procaine is also able to act within the lipid environment.

The membrane spanning (M2) region of the ACh receptor-channel protein is proposed to line the ion channel pore (see Dani, 1989), and it has been suggested that the QX-222 binding site lies within the pore of the channel. This suggestion is substantiated by the finding that mutations of specific amino acids in this transmembrane region affect QX-222 binding to the receptor (Charnet *et al.*, 1990). Therefore, the difference between the affinity of QX-222 for rat neuronal and muscle junctional AChR channels may suggest a difference in the primary structure of these channels. Furthermore, the higher affinity of QX-222 for the ACh receptor-channel of rat intracardiac neurones compared to rat $\alpha_4\beta_2$ ACh receptor-channel, together with the difference in the estimated binding site of QX-222 within these channels, suggests a difference in their primary structure. These results also suggest that the ACh receptor-channel of rat parasympathetic neurones is not the $\alpha_4\beta_2$ receptor-channel studied by Charnet *et al.* (1992).

The effects of local anaesthetics on nerve conduction and synaptic transmission at the motor endplate are well documented, but, their action on ganglionic transmission is poorly understood. Tabatabi & Booth (1990) demonstrated that local anaesthetics can completely block synaptic transmission in sympathetic ganglia, acting at presynaptic and postsynaptic sites. One mechanism by which local anaesthetics inhibit synaptic transmission is via a decrease and eventual elimination of excitatory postsynaptic potentials (e.p.s.ps). The present study suggests that local anaesthetic block of ACh receptor-channels may be responsible for the attenuation of e.p.s.ps at cholinergic synapses.

In conclusion, the local anaesthetics, procaine and QX-222, have been shown to block selectively nicotinic ACh receptor-channels of rat parasympathetic cardiac neurones. The apparent K_ds and voltage-sensitivities calculated for QX-222 and procaine binding to these channels are significantly different from those obtained in other preparations, and suggest that their M2 region differs from that of frog and rat skeletal muscle and neuronal $\alpha_4\beta_2$ ACh receptor-channels. Local anaesthetics do not affect muscarinic or ATP-evoked currents in cardiac ganglia, indicating that the mechanism by which local anaesthetics affect ganglionic (vagal) transmission is via a block of nicotinic ACh receptor-channels.

This research was supported by National Institutes of Health grant RO1 HL 35422 to D.J.A. J.C. was supported by a NIH training grant HL 07188.

References

ADAMS, D.J. & NUTTER, T.J. (1992). Calcium permeability and modulation of nicotinic acetylcholine receptor-channel in rat parasympathetic neurons. *J. Physiol. (Paris)*, **86**, 67–76.

ADAMS, P.R. (1976). Drug blockade of open end-plate channels. *J. Physiol.*, **260**, 531–552.

ADAMS, P.R. (1977). Voltage jump analysis of procaine action at frog end-plate. *J. Physiol.*, **268**, 291–318.

ALLEN, T.G.J. & BURNSTOCK, G. (1990a). M_1 and M_2 muscarinic receptors mediate excitation and inhibition of guinea-pig intracardiac neurones in culture. *J. Physiol.*, **422**, 463–480.

ALLEN, T.G.J. & BURNSTOCK, G. (1990b). The actions of adenosine 5'-triphosphate on guinea-pig intracardiac neurones in culture. *Br. J. Pharmacol.*, **100**, 269–276.

ANAND, R., CONROY, W.G., SCHOEPFER, R., WHITING, P. & LINDSTROM, J. (1991). Neuronal nicotinic acetylcholine receptors expressed in *Xenopus* oocytes have a pentameric quaternary structure. *J. Biol. Chem.*, **266**, 11192–11198.

ASCHER, P., LARGE, W.A. & RANG, H.P. (1979). Studies on the mechanism of action of acetylcholine antagonists on rat parasympathetic ganglion cells. *J. Physiol.*, **295**, 139–170.

BEAM, K.G. (1976a). A voltage-clamp study of the effects of two lidocaine derivatives on the time course of end-plate currents. *J. Physiol.*, **258**, 279–300.

BEAM, K.G. (1979b). A quantitative description of end-plate currents in the presence of two lidocaine derivatives. *J. Physiol.*, **258**, 301–322.

CHARLESWORTH, P., JACOBSON, I., POCOCK, G. & RICHARDS, C.D. (1992). The mechanism by which procaine inhibits catecholamine secretion from bovine chromaffin cells. *Br. J. Pharmacol.*, **106**, 802–812.

CHARNET, P., LABARCA, C., LEONARD, R.J., VOGELAAR, N.J., CZYZYK, L., GOUIN, A., DAVIDSON, N. & LESTER, H. (1990). An open-channel blocker interacts with adjacent turns of α-helices in the nicotinic acetylcholine receptor. *Neuron*, **2**, 87–95.

CHARNET, P., LABARCA, C., COHEN, B.N., DAVIDSON, N., LESTER, H.A. & PILAR, G. (1992). Pharmacological and kinetic properties of α4β2 neuronal nicotinic acetylcholine receptors expressed in *Xenopus* oocytes. *J. Physiol.*, **450**, 375–394.

CLAPHAM, D.E. & NEHER, E. (1984). Substance P reduces acetylcholine-induced currents in isolated bovine chromaffin cells. *J. Physiol.*, **347**, 255–277.

COLQUHOUN, D. (1986). On the principles of postsynaptic action of neuromuscular blocking agents. In *New Neuromuscular Blocking Agents, Handbook of Experimental Pharmacology*, Vol. 79, ed. Kharkevich, D.A. pp. 59–113. Berline: Springer-Verlag.

COLQUHOUN, D. & SAKMANN, B. (1985). Fast events in single-channel currents activated by acetylcholine and its analogues at the frog muscle end-plate. *J. Physiol.*, **369**, 501–557.

COLQUHOUN, D. & SIGWORTH, F.J. (1983). Fitting and statistical analysis of single-channel records. In *Single Channel Recording*. ed. Sakmann, B. & Neher, E. Ch.11, pp. 191–263. New York: Plenum Press.

COOPER, E., COUTURIER, S. & BALLIVET, M. (1991). Pentameric structure and subunit stoichiometry of a neuronal nicotinic acetylcholine receptor. *Nature*, **350**, 235–238.

DANI, J.A. (1989). Site-directed mutagenesis and single channel currents define the ionic channel of the nicotinic acetylcholine-receptor. *Trends Neurosci.*, **12**, 125–128.

DENERIS, E.S., CONNOLLY, J., ROGERS, S.W. & DUVOISIN, R. (1991). Pharmacological and functional diversity of neuronal nicotinic acetylcholine receptors. *Trends Pharmacol. Sci.*, **12**, 34–40.

FIEBER, L.A. & ADAMS, D.J. (1991a). Acetylcholine-evoked currents in cultured neurones dissociated from rat parasympathetic cardiac ganglia. *J. Physiol.*, **434**, 215–237.

FIEBER, L.A. & ADAMS, D.J. (1991b). Adenosine triphosphate-evoked currents in cultured neurones dissociated from rat parasympathetic cardiac ganglia. *J. Physiol.*, **434**, 239–256.

GAGE, P.W., HAMILL, O.P. & WACHTEL, R.E. (1983). Sites of action of procaine at the motor end-plate. *J. Physiol.*, **335**, 123–137.

GALINDO, A. (1969). Effects procaine, pentobarbital and halothane on synaptic transmission in the central nervous system. *J. Pharmacol. Exp. Ther.*, **169**, 159–169.

HAMILL, O.P., MARTY, A., NEHER, E., SAKMANN, B. & SIGWORTH, F.J. (1981). Improved patch-clamp techniques for high-resolution current recording from cells and cell-free membrane patches. *Pflügers Archiv.*, **391**, 85–100.

HASSALL, C.J.S., BUCKLEY, N.J. & BURNSTOCK, G. (1987). Autoradiographic localization of muscarinic receptors on guinea pig intracardiac neurones and atrial myocytes in culture. *Neurosci. Lett.*, **74**, 145–150.

HORN, R., BRODWICK, M.S. & DICKEY, W.D. (1980). Asymmetry of the acetylcholine channel revealed by quaternery anesthetics. *Science*, **210**, 205–207.

HORN, R. & MARTY, A. (1988). Muscarinic activation of ionic currents measured by a new whole-cell recording method. *J. Gen. Physiol.*, **92**, 145–159.

LARRABEE, M.G. & POSTERNAK, J.M. (1952). Selective action of anesthetics on synapses and axons in mammalian sympathetic ganglia. *J. Neurophysiol.*, **15**, 91–114.

LEONARD, R.J., LABARCA, C., CHARNET, P., DAVIDSON, N. & LESTER, H. (1988). Evidence that the M2 membrane spanning region lines the ion channel pore of the nicotinic receptor. *Science*, **242**, 1578–1581.

LUETJE, C.W. & PATRICK, J. (1991). Both α- and β-subunits contribute to the agonist sensitivity of neuronal nicotinic acetylcholine receptors. *J. Neurosci.*, **11**, 837–845.

LUETJE, C.W., WADA, K., ROGERS, S., ABRAMSON, S.N., TSUJI, K., HEINEMANN, S. & PATRICK, J. (1990). Neurotoxins distinguish between different neuronal nicotinic acetylcholine receptor subunit combinations. *J. Neurochem.*, **55**, 632–640.

LUKAS, R.J. & BENCHERIF, M. (1992). Heterogeneity and regulation of nicotinic acetylcholine receptors. *Int. Rev. Neurobiol.*, **34**, 25–131.

MATHIE, A., CULL-CANDY, S.G. & COLQUHOUN, D. (1991). Conductance and kinetic properties of single nicotinic acetylcholine receptor channels in rat sympathetic neurones. *J. Physiol.*, **439**, 717–750.

NEHER, E. (1983). The charge carried by single-channel currents of rat cultured muscle cells in the presence of local anaesthetics. *J. Physiol.*, **339**, 663–678.

NEHER, E. & STEINBACH, J.H. (1978). Local anaesthetics transiently block currents through single acetylcholine receptor-channels. *J. Physiol.*, **277**, 153–176.

NUTTER, T.J., CUEVAS, J. & ADAMS, D.J. (1991). Local anesthetic and proton block of ACh-evoked currents in rat parasympathetic neurons. *Soc. Neurosci. Abst.*, **17**, 1332.

PAPKE, R.L. (1993). The kinetic properties of neuronal nicotinic receptors: Genetic basis of functional diversity. *Prog. Neurobiol.*, **41**, 509–531.

RUFF, R.L. (1977). A quantitative analysis of local anesthetic alteration of miniature end-plate currents and end-plate current fluctuations. *J. Physiol.*, **264**, 89–124.

RUFF, R.L. (1982). The kinetics of local anesthetic blockage of end-plate channels. *Biophys. J.*, **37**, 625–631.

SARGENT, P.B. (1993). The diversity of neuronal nicotinic acetylcholine receptors. *Annu. Rev. Neurosci.*, **16**, 403–443.

SEABROOK, G.R., FIEBER, L.A. & ADAMS, D.J. (1990). Neurotransmission in neonatal rat cardiac ganglion in situ. *Am. J. Physiol.*, **259**, H997–H1005.

SELYANKO, A.A. & SKOK, V.I. (1992). Acetylcholine receptors in rat cardiac neurones. *J. Autonom. Nerv. Sys.*, **40**, 33–48.

TABATABAI, M. & BOOTH, A.M. (1990). Mechanism of action of local anesthetics on synpatic transmission in the rat. *Anesth. Analg.*, **71**, 149–157.

WOODHULL, A.M. (1973). Ionic blockage of sodium channels in nerve. *J. Gen. Physiol.*, **61**, 687–708.

(Received June 8, 1993
Revised September 30, 1993
Accepted November 1, 1993)

Br. J. Pharmacol. (1994), **111**, 673–680 © Macmillan Press Ltd, 1994

Vasorelaxant effect of mexiletine in mesenteric resistance arteries of rats

[1]Yasuaki Dohi, Masayoshi Kojima & Koichi Sato

Division of Hypertension and Vascular Research, Second Department of Internal Medicine, Nagoya City University Hospital, Mizuho-ku, Nagoya 467, Japan

1 The vascular action of mexiletine, a class Ib antiarrhythmic agent, was investigated in the mesenteric resistance arteries of rats.

2 The second order branch of the mesenteric artery was cut into rings and changes in isometric tension were recorded.

3 Mexiletine (10^{-6}–10^{-3} M) evoked concentration-dependent, endothelium-independent relaxations in arteries contracted with noradrenaline.

4 Mexiletine (10^{-4} M) did not affect the contraction induced by noradrenaline in Ca^{2+}-free solution, while the compound inhibited the contraction induced by $CaCl_2$ in noradrenaline-activated arteries.

5 The relaxation induced by mexiletine was less pronounced in arteries contracted with high KCl than in those contracted with noradrenaline.

6 Mexiletine induced identical relaxations in arteries contracted with noradrenaline in high KCl solution containing verapamil and in Krebs solution.

7 Thus, mexiletine induces relaxations by inhibiting transmembrane Ca^{2+} movement, but not Ca^{2+} release from the intracellular store site in mesenteric resistance arteries of rats. It is speculated that mexiletine possesses greater inhibitory effects against noradrenaline-activated, verapamil-insensitive (receptor-operated) Ca^{2+} channels than against verapamil-sensitive (voltage-dependent) channels.

Keywords: 5-Hydroxytryptamine; rat mesenteric artery; mexiletine; noradrenaline; relaxation

Introduction

Mexiletine is widely used for the treatment of life-threatening ventricular arrhythmias (Monk & Brogden, 1990; Nagasako *et al.*, 1992). Intravenous mexiletine is one of the drugs of choice for emergency treatment of the arrhythmias. The antiarrhythmic drug is classified as a class Ib agent (Vaughan Williams, 1984). Like other drugs in class-I category, mexiletine blocks sodium current in cardiac muscle cells, leading to an inhibition of the depolarization of the cells (Singh & Vaughan Williams, 1972; Shirayama *et al.*, 1991). The action of the drug might also cause inhibition against contractions in vascular smooth muscle. Indeed, lignocaine which bears some resemblance to mexiletine, evokes relaxation in vascular smooth muscle (Altura & Altura, 1974; Wang & Jackson, 1988; Perlmutter *et al.*, 1990). Stabilizing effects on cell membrane and antagonistic effects on movement of calcium ions have been proposed for the mechanisms of the vasodilatation by lignocaine (Altura & Altura, 1974). However, effects of mexiletine on vascular smooth muscle have not been intensively studied. It is speculated that the inhibitory effects of mexiletine on vascular smooth muscle might be greater than those of lignocaine since mexiletine has a considerable blocking action on Ca^{2+} channels besides its well known action on the Na^+ channel in ventricular cells (Ono *et al.*, 1986). Modulation of vascular tone by mexiletine would be of clinical importance if it occurs in small resistance arteries where peripheral blood flow is regulated. Indeed, a fall in blood pressure or a decrease in peripheral resistance after intravenous administration of mexiletine has been reported in man (Fritz *et al.*, 1983; Greenspan *et al.*, 1984).

The present study was designed to investigate the vascular effect of mexiletine and the interaction of the antiarrhythmic drug with a neurotransmitter, noradrenaline, in mesenteric resistance arteries of rats.

[1] Author for correspondence.

Methods

Experimental animals and set-up

Male Wistar-Kyoto rats, 8–10 weeks of age, were obtained from Charles River Japan (Yokohama). The rat was stunned by a blow to the head and then exsanguinated. The entire mesenterium was removed and placed into cold modified Krebs-Ringer bicarbonate solution of the following composition (mM): NaCl 118.6, KCl 4.8, $CaCl_2$ 2.5, $MgSO_4$ 1.2, KH_2PO_4 1.2, $NaHCO_3$ 25.1, disodium calcium edetate (EDTA) 0.026, and glucose 10.1: pH 7.4 (Krebs solution). The second order branch of the mesenteric artery was carefully dissected and cleaned of adhering adipose tissue and cut into rings (intraluminal diameter: 200 μm, width: 1.5 mm) under a dissection microscope. In some preparations, the endothelium was removed by rubbing the intimal surface with a thin glass rod (diameter: 200 μm). The presence or absence of the endothelium was confirmed later by the presence or absence of a relaxation to acetylcholine (10^{-9}–10^{-6} M; Dohi *et al.*, 1990b). Unless otherwise stated in the text, the preparation used was without endothelium.

The ring preparation was suspended horizontally by means of two L-shaped stainless steel holders in the vessel lumen in a small chamber (5 ml) filled with Krebs solution (37°C) bubbled with a mixture of 95% O_2 and 5% CO_2. One of the holders was fixed and the other was connected to a force-displacement transducer (UM-203, Kishimoto, Kyoto) for the measurement of isometric tension development. The ring was equilibrated under a resting tension of 200 mg for 60 min. This tension was found to be optimal for contraction of the preparation as assessed by repeated exposure to 60 mM KCl under various resting tensions (50–500 mg). After the equilibration period, the rings were maximally contracted by

a 60 mM KCl solution two or three times at 45 min intervals until the responses were reproducible.

Protocol

Relaxation to mexiletine Concentration-response curves to mexiletine (10^{-6}–10^{-3} M) were obtained in arteries with or without endothelium which were precontracted half-maximally with noradrenaline (NA), 5-hydroxytryptamine (5-HT), KCl, or calcium ionophore A23187 (A23187). In some experiments, the response to mexiletine was obtained in the presence of meclofenamic acid (10^{-5} M) to block the vascular production of prostaglandins (Vane, 1971; Diedrich *et al.*, 1990), glibenclamide (10^{-5} M) or tetraethylammonium (TEA; 10^{-2} M) to inhibit ATP- or Ca^{2+}-sensitive K^+ channels, respectively (Sturgess *et al.*, 1985; Brayden & Nelson, 1992). The inhibitors were applied 30 min before the experiments began. In the experiments where effects of Na^+-free condition on the response to mexiletine were examined, the Krebs solution was replaced with a Na^+-free solution 20 min before the start of experiments.

Inhibitory effect of mexiletine against contractions Concentration-response curves to NA (3×10^{-8}–3×10^{-4} M) or 5-HT (3×10^{-8}–10^{-4} M) were constructed in arteries with or without endothelium. In arteries without endothelium, the first concentration-response curve was obtained in the absence of mexiletine, while the others were constructed in the presence of increasing concentrations of mexiletine (2.5×10^{-5}, 10^{-4}, 4×10^{-4} M). Arteries were exposed to mexiletine 20 min prior to the experiment. Results were plotted according to the method of Arunlakshana & Schild (1959) and the pA_2 value and slope of the regression for mexiletine versus NA or 5-HT were calculated. In time controls, the contraction induced by NA or 5-HT was reproducible throughout the experiment.

Caffeine-induced contractions were obtained by replacing the Krebs solution with a $CaCl_2$-free solution containing 10^{-2} M caffeine. NA-induced contractions in Ca^{2+}-free solution were obtained by adding 10^{-5} M NA, 2 min after the Krebs solution was replaced with a Ca^{2+}-free solution. The contractions induced by caffeine or NA were reproducible at 20 or 45 min intervals, respectively. In another series of experiments, Ca^{2+}-induced contractions in NA-activated arteries were investigated. Arteries were contracted with caffeine by replacing the Krebs solution with the Ca^{2+}-free solution containing 10^{-2} M caffeine and washed with the Ca^{2+}-free solution for 25 min. Then, 10^{-5} M NA was added to the solution for 20 min and the solution was replaced with the $CaCl_2$-free solution containing 10^{-5} M NA. After 2 min Ca^{2+}-induced contractions were obtained by addition of 2.5 mM $CaCl_2$ to the solution. These contractions were obtained in the presence or absence of 10^{-4} M mexiletine. Mexiletine was applied 20 min before contractions to caffeine or NA were obtained.

Drugs and solutions

The following drugs were used (unless otherwise stated from Sigma Chemical Co., St. Louis, Mo, U.S.A.): acetylcholine chloride, 4-bromo-calcium ionophore A23187 (A23187), caffeine, ethylene glycol-*bis* (β-aminoethyl ether) *N,N,N',N'*-tetra-acetic acid (EGTA), glibenclamide (Yamanouchi Medical Pharmacy Co. Ltd., Tokyo, Japan), 5-hydroxytryptamine creatinine sulphate complex (5-HT), meclofenamic acid, mexiletine hydrochloride (Nippon Boehringer Ingelheim Co. Ltd., Kawanishi, Japan), (−)-noradrenaline bitartrate (NA), N-methyl-D-glucamine (NMG), tetraethylammonium chloride (TEA), verapamil (Eisai Co., Tokyo). The stock solutions of A23187 and glibenclamide were prepared in ethanol and dimethylsulphoxide (DMSO), respectively, while all other compounds were dissolved in distilled water or the Krebs solution. Drugs were applied cumulatively and concentrations of drugs are expressed as final molar concentrations in the bath solution.

The $CaCl_2$-free solution was made by omitting $CaCl_2$ and EDTA from the Krebs solution and the Ca^{2+}-free solution was made by adding 2 mM EGTA to the $CaCl_2$-free solution. The high KCl solutions (40 and 60 mM KCl) were prepared by equimolar replacement of NaCl by KCl. A Na^+-free solution of the following composition (mM) was used: NMG 143.7, KCl 4.8, $CaCl_2$ 2.5, $MgSO_4$ 1.2, KH_2PO_4 1.2 and glucose 10.1 (osmotic pressure of the solution was not different from that of the Krebs solution, pH was adjusted to 7.4 with HCl).

Calculations and statistics

Contractions were expressed as a percentage of the contraction developed by 60 mM KCl and relaxations were expressed as percentage inhibition of preceding contractions. Data are given as mean ± s.e.mean. The concentration of an agonist causing half-maximal contraction (EC_{50} value) or half-maximal inhibition of a preceding contraction (IC_{50} value) was calculated for each experiment and expressed as negative log molar (pD_2 value). The shift of concentration-response curves was expressed as concentration shift at pD_2 values. In each set of experiments, *n* equals the number of animals studied. Statistical analysis was by Student's paired and unpaired *t* tests and by analysis of variance followed by Scheffe's *F* test (Scheffe, 1959). Means were considered to be significantly different when the *P* value was less than 0.05.

Results

In quiescent arteries mexiletine (10^{-6}–10^{-3} M) evoked no mechanical response ($n = 4$; data not shown).

Mexiletine (10^{-6}–10^{-3} M) evoked concentration-dependent relaxations in the resistance arteries with endothelium, precontracted with NA (pD_2 value: 4.69 ± 0.05, maximal response: 99.4 ± 0.6%; Figure 1). Removal of the endothelium did not alter the response to mexiletine (pD_2 value: 4.61 ±

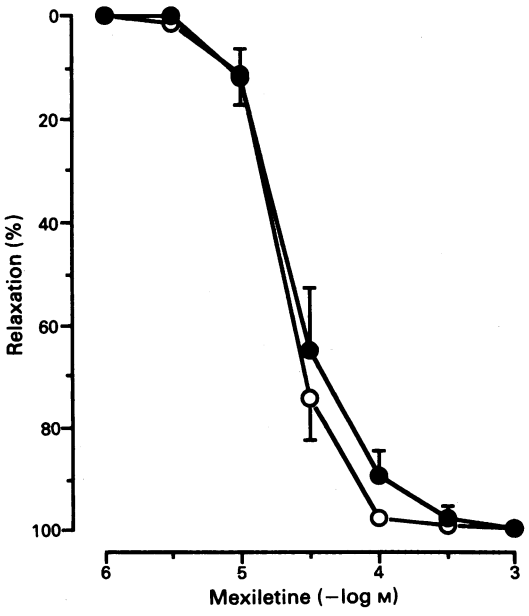


Figure 1 Concentration-response curves to mexiletine in mesenteric resistance arteries with (○) and without endothelium (●) contracted with noradrenaline obtained from 10–12 week old Wistar Kyoto rats. Note that the sensitivity and the maximal response to mexiletine are similar in arteries with and without endothelium. Each point represents mean ± s.e.mean from six experiments.

0.10, maximal response: 100 ± 0%; NS). The relaxation to mexiletine was not affected by meclofenamic acid (10^{-5} M) ($n = 5$, data not shown). Mexiletine also reversed contractions induced by 5-HT in arteries without endothelium. The pD_2 value and the maximal response in arteries precontracted with 5-HT (pD_2 value: 4.68 ± 0.04, maximal response: 99.3 ± 0.6%, $n = 6$; NS) were not different from those obtained in arteries precontracted with NA.

In arteries without endothelium, NA (3×10^{-8}–3×10^{-4} M) evoked concentration-dependent contractions (Figure 2a). Mexiletine (2.5×10^{-5}, 10^{-4}, 4×10^{-4} M) caused a significant shift to the right of the concentration-response curve to NA (Figure 2a, Table 1). Higher concentrations (10^{-4}, 4×10^{-4} M), but not a lower concentration of mexiletine (2.5×10^{-5} M) reduced the maximal response to NA (Table 1). In arteries with endothelium the contraction was also reduced by mexiletine (data not shown). The concentration shift by mexiletine (10^{-4} M) in arteries with and without endothelium was not different (5.0 ± 0.6-fold and 4.5 ± 0.6-fold, respectively; NS). Mexiletine also caused significant shifts of concentration-response curves to 5-HT (3×10^{-8}–10^{-4} M) to the right in arteries without endothelium (Figure 2b, Table 1). The maximal response to 5-HT was reduced by higher concentrations of mexiletine (10^{-4}, 4×10^{-4} M). The concentration shift by mexiletine was not different in arteries contracted with NA (2.5×10^{-5} M: 1.4 ± 0.1, 10^{-4} M: 4.5 ± 0.6, 4×10^{-4} M: 33 ± 3-fold) and 5-HT (2.5×10^{-5} M: 1.7 ± 0.2, 10^{-4} M: 3.6 ± 0.1, 4×10^{-4} M: 26 ± 2-fold; NS). Schild analysis of the inhibitory effect of the three concentrations of mexiletine against NA and 5-HT revealed a slope (1.9 ± 0.3, 1.4 ± 0.1, respectively) that differed from 1.0 ($P < 0.01$) and pA_2 values of 4.27 ± 0.08 and 4.42 ± 0.08, respectively. The pA_2 value and slope for mexiletine using NA as an agonist were not different from those obtained with 5-HT as an agonist.

Na^+-free solutions shifted concentration-response curves to mexiletine to the right (Figure 3). The pD_2 value for mexiletine was smaller in the Na^+-free solutions (4.31 ± 0.07) than in the Krebs solution (4.74 ± 0.05; $P < 0.001$), while the

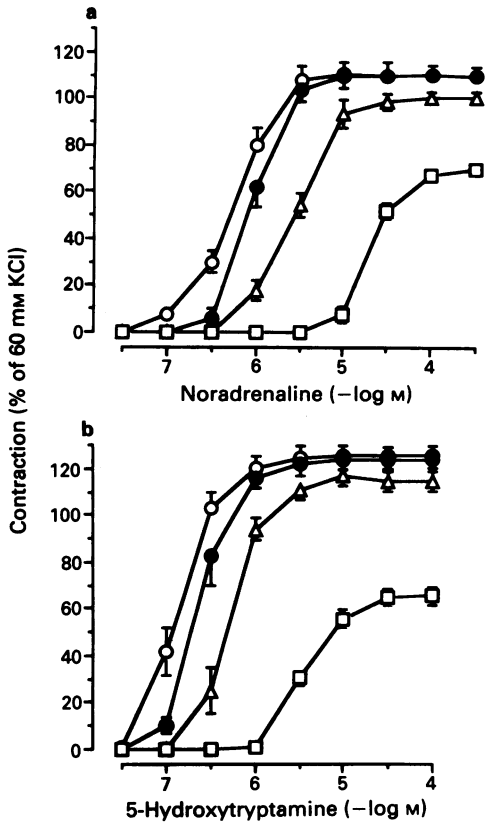


Figure 2 Concentration-response curves to noradrenaline (a) and 5-hydroxytryptamine (b) in the absence (○) and presence of increasing concentrations of mexiletine (2.5×10^{-5} M ●; 10^{-4} M △; 4×10^{-4} M □) in mesenteric resistance arteries without endothelium obtained from 10–12 week old Wistar Kyoto rats. Note that mexiletine causes a similar inhibition against the contraction induced by noradrenaline and 5-hydroxytryptamine. Each point represents mean from six experiments; s.e.mean shown by vertical bars.

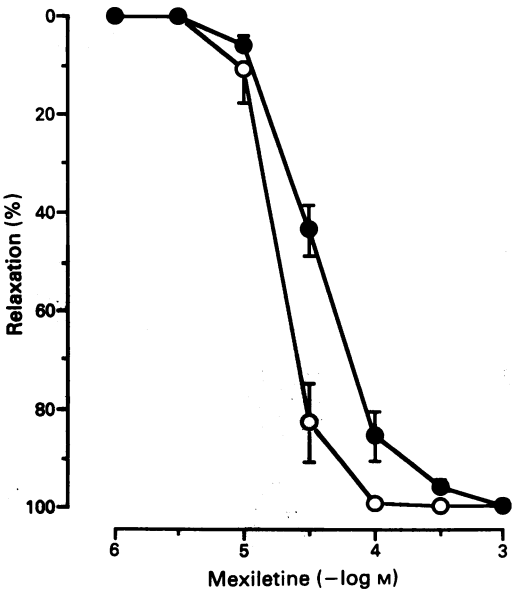


Figure 3 Effect of Na^+-free solution on concentration-response curves to mexiletine in mesenteric resistance arteries contracted with noradrenaline obtained from 10–12 week old Wistar Kyoto rats. The arteries were contracted half-maximally with noradrenaline in the Krebs solution (○) or the Na^+-free solution (●) and relaxations to mexiletine were obtained. Note the small inhibition of the relaxation to mexiletine by the Na^+-free solution. Each point represents mean ± s.e.mean from five experiments.

Table 1 Effect of mexiletine on pD_2 values and maximal responses for noradrenaline and 5-hydroxytryptamine

	Noradrenaline		*5-Hydroxytryptamine*	
	pD_2 value	*max*[a]	*pD_2 value*	*max*[a]
Control	6.21 ± 0.05	110 ± 5	6.85 ± 0.06	125 ± 5
With mexiletine:				
2.5×10^{-5} M	6.05 ± 0.06*	109 ± 5	6.62 ± 0.07*	124 ± 4
10^{-4} M	5.57 ± 0.05*	100 ± 3*	6.29 ± 0.05*	114 ± 4*
4×10^{-4} M	4.69 ± 0.03*	69 ± 2*	5.45 ± 0.03*	65 ± 4*

[a]Percentage of 60 mM KCl-induced contraction
*$P < 0.05$ vs control.

maximal response was not different (99.3 ± 0.7 and 99.6 ± 0.4%; NS).

Caffeine (10^{-2} M) induced transient contractions in the $CaCl_2$-free solution (Figure 4a). The amplitude of the contraction was 42.5 ± 6.3% of the 60 mM KCl-induced contraction. Mexiletine did not alter the contraction to caffeine (41.3 ± 5.6%; NS; Figure 4c). NA (10^{-5} M) also evoked transient contractions in the Ca^{2+}-free solution (58.4 ± 4.9%; Figure 4b). Mexiletine did not change the contraction (64.1 ± 6.2%; NS; Figure 4c). Replacement of the Ca^{2+}-free solution containing 10^{-5} M NA with Krebs solution evoked transient contractions, which were reduced by the pretreatment with mexiletine (Figure 4b).

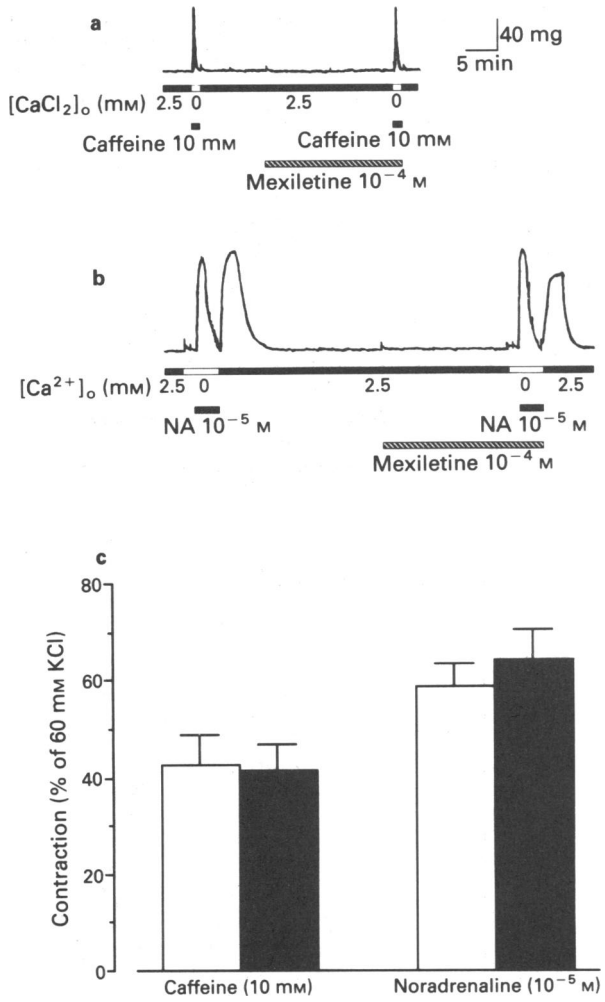


Figure 4 (a) Contractile responses to caffeine in mesenteric resistance arteries obtained from 10–12 week old Wistar Kyoto rats. The first response to 10 mM caffeine was assessed by replacing the Krebs solution with the $CaCl_2$-free solution containing 10^{-2} M caffeine. Then, the arteries were washed out with the Krebs solution for 10 min, followed by treatment of the arteries with 10^{-4} M mexiletine in the solution for 20 min. The second contraction to caffeine was obtained in the presence of mexiletine. $[CaCl_2]_o$ represents concentrations of $CaCl_2$ in the solutions. (b) Contractile responses to noradrenaline in mesenteric resistance arteries obtained from 10–12 week old Wistar Kyoto rats. The first response to 10^{-5} M noradrenaline (NA) was assessed in the Ca^{2+}-free solution after 2 min exposure of the arteries to the solution. After the contraction the arteries were washed out with the Krebs solution for 25 min and then treated with 10^{-4} M mexiletine in the solution for 20 min. The second contraction to noradrenaline was obtained in the Ca^{2+}-free solution in the presence of mexiletine after 2 min exposure to the solution. $[Ca^{2+}]_o$ represents concentrations of Ca^{2+} in the solutions. (c) Effect of mexiletine (open column: control, solid column: mexiletine 10^{-4} M) on the transient contraction induced by caffeine (10^{-2} M; in $CaCl_2$-free solution) and noradrenaline (10^{-5} M; in Ca^{2+}-free solution) in mesenteric resistance arteries obtained from 10–12 week old Wistar Kyoto rats. Note that mexiletine does not affect the contractions. Each column respresents mean from five experiments; s.e.mean shown by vertical bars.

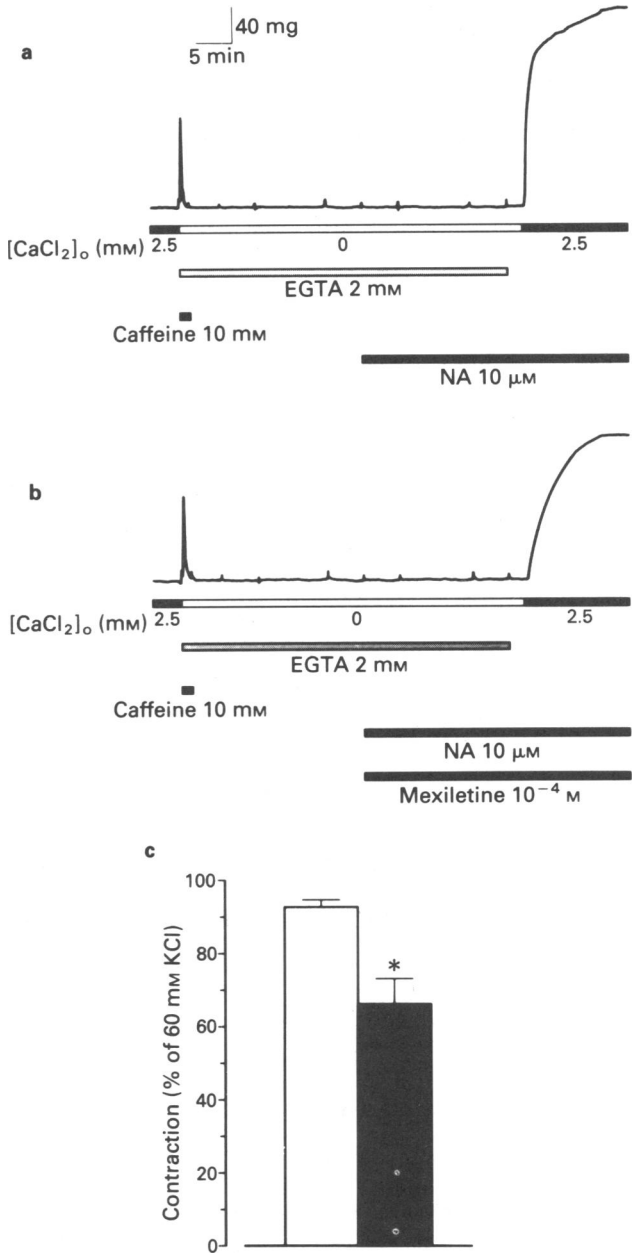


Figure 5 (a) Contractile response to 2.5 mM $CaCl_2$ in mesenteric resistance arteries obtained from 10–12 week old Wistar Kyoto rats. The arteries were contracted with caffeine by replacing the Krebs solution with the Ca^{2+}-free solution containing 10^{-2} M caffeine and washed out with the Ca^{2+}-free solution for 25 min. Then, 10^{-5} M noradrenaline (NA) was added to the solution for 20 min, and the solution was replaced with the $CaCl_2$-free solution containing 10^{-5} M noradrenaline. After 2 min, the contraction to $CaCl_2$ was obtained by an application of 2.5 mM $CaCl_2$. $[CaCl_2]_o$ represents concentrations of $CaCl_2$ in the solutions. (b) Effect of mexiletine on $CaCl_2$-induced contraction in 10^{-5} M noradrenaline-activated mesenteric resistance arteries obtained from 10–12 week old Wistar Kyoto rats. The same protocol as in (a) was carried out, but mexiletine was applied 20 min prior to the contraction to $CaCl_2$. (c) Effect of mexiletine (open column: control, solid column: mexiletine 10^{-4} M) on the amplitude of 2.5 mM $CaCl_2$-induced contraction in 10^{-5} M noradrenaline-activated mesenteric resistance arteries obtained from 10–12 week old Wistar Kyoto rats. $^*P < 0.01$. Each column represents mean with s.e.mean from five experiments.

After the application of caffeine, 10^{-5} M NA did not evoke contractions in the Ca^{2+}-free solution (Figure 5a) and the second application of caffeine at a 20 min interval was ineffective in the solution ($n = 5$, data not shown). Application of $CaCl_2$ (2.5 mM) to the $CaCl_2$-free solution containing 10^{-5} M NA induced tonic contractions (Figure 5a), while application of caffeine (10^{-2} M) to the solution did not evoke contractions in time matched controls (data not shown; $n = 5$). The amplitude of the tonic contraction (92.5 ± 2.2%) was reduced by 10^{-4} M mexiletine (66.1 ± 6.8%; $P < 0.01$; Figure 5b,c).

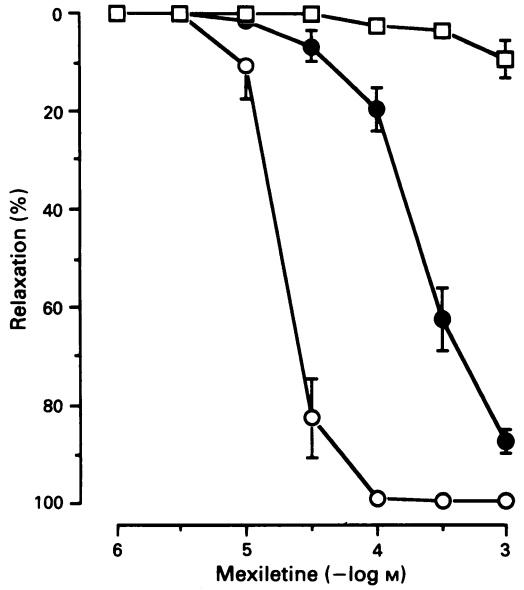


Figure 6 Effect of contractile agents on concentration-response curves to mexiletine in mesenteric resistance arteries obtained from 10–12 week old Wistar Kyoto rats. The arteries were contracted half-maximally with noradrenaline (○), KCl (●), or calcium ionophore A23187 (□) and relaxations to mexiletine were obtained. Note that mexiletine induces less potent relaxations in arteries contracted with KCl than in those contracted with noradrenaline. Mexiletine does not relax the arteries precontracted with A23187. Each point represents mean ± s.e.mean from six experiments.

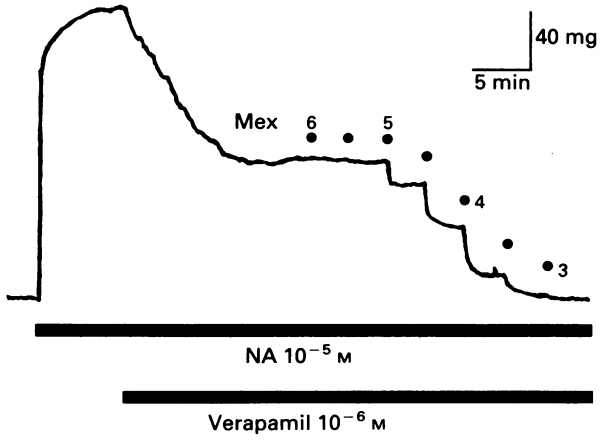


Figure 7 Relaxation to mexiletine in mesenteric resistance arteries precontracted with noradrenaline in the presence of verapamil obtained from 10–12 week old Wistar Kyoto rats. The arteries were contracted with 10^{-5} M noradrenaline (NA) and then 10^{-6} M verapamil was applied. After the relaxation to verapamil reached a steady state, mexiletine (Mex) was applied cumulatively. Numbers in the figure represent concentrations of mexiletine (− log M). Typical tracing is shown in the figure from similar experiments ($n = 4$).

In arteries precontracted with 40 mM KCl (which caused half-maximal contractions) mexiletine caused less pronounced relaxations (pD_2 value: 3.62 ± 0.07, maximal response: 88.2 ± 2.9%) than in those precontracted with NA (pD_2 value: 4.60 ± 0.08; $P < 0.0005$, maximal response: 100 ± 0%; $P < 0.05$; (Figure 6). Mexiletine did not induce relaxations in arteries precontracted with A23187 (Figure 6), while sodium nitroprusside (3×10^{-4} M) totally reversed the contraction ($n = 4$, data not shown). Verapamil (10^{-5} M) did not induce relaxations in arteries precontracted with A23187 ($n = 4$, data not shown).

In arteries precontracted with NA, mexiletine-induced relaxations (pD_2 value: 4.60 ± 0.08, maximal response: 100 ± 0%; $n = 5$) were not affected by 10^{-5} M glibenclamide (pD_2 value: 4.59 ± 0.07, maximal response: 97.6 ± 1.0%; $n = 5$;

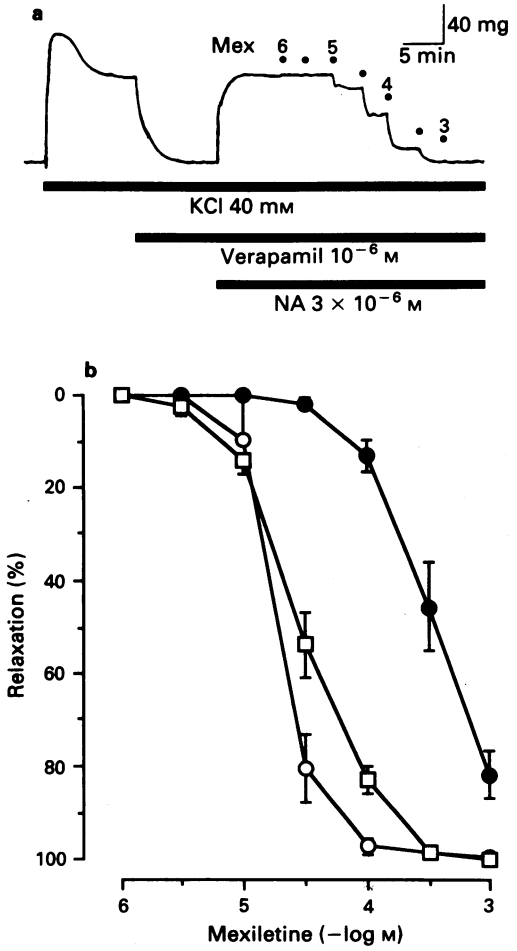


Figure 8 (a) Relaxation to mexiletine in mesenteric resistance arteries precontracted with noradrenaline in the 40 mM KCl solution containing 10^{-6} M verapamil obtained from 10–12 week old Wistar Kyoto rats. The arteries were contracted with the 40 mM KCl solution and then 10^{-6} M verapamil was applied. After the tension reached the basal level, the arteries were contracted again half-maximally with noradrenaline (NA) and then relaxations to mexiletine (Mex) were obtained. Numbers in the figure represent concentration of mexiletine (− log M). (b) Effect of KCl-induced depolarizations on mexiletine-induced relaxation in mesenteric resistance arteries contracted with noradrenaline obtained from 10–12 week old Wistar Kyoto rats. The arteries were contracted half-maximally with noradrenaline in the Krebs solution (○), with 40 mM KCl solution (●), or with noradrenaline in 40 mM KCl solution containing 10^{-6} M verapamil (□) and concentration-response curves to mexiletine were obtained. Note the similar relaxations to mexiletine in arteries contracted with noradrenaline in the Krebs solution and in the 40 mM KCl solution containing 10^{-6} M verapamil. Each point represents mean ± s.e.mean from six experiments.

NS) or 10^{-2} M TEA (pD_2 value: 4.58 ± 0.06, maximal response: 98.7 ± 0.9; $n = 5$; NS).

Contractions induced by 10^{-5} M NA were partially reversed by 10^{-6} M verapamil (Figure 7). The residual contraction after the application of the Ca^{2+} antagonist (verapamil-insensitive part; approximately a half of the maximal contraction to NA) was reversed by mexiletine (Figure 7). The pD_2 value and the maximal response to mexiletine in the condition were not different from those obtained in Figure 1 (data not shown).

Contractions induced by 40 mM KCl were totally reversed by 10^{-6} M verapamil (Figure 8a). After the tension reached the basal level by verapamil, the artery was again contracted half-maximally with NA and then the relaxation to mexiletine was investigated. In these conditions, mexiletine evoked relaxations with similar pD_2 value (4.56 ± 0.09) and maximal response (100 ± 0%) to those obtained in arteries contracted with NA in the Krebs solution (pD_2 value: 4.75 ± 0.04, maximal response: 99.6 ± 0.4%; NS), while the responses to 3×10^{-5} and 10^{-4} M mexiletine were different in the two groups (3×10^{-5} M: 53.9 ± 7.1 and 80.6 ± 7.3%; $P < 0.05$, 10^{-4} M: 82.9 ± 3.1 and 97.3 ± 1.9%; $P < 0.005$; Figure 8b). The relaxation was more pronounced in arteries precontracted with NA in the 40 mM KCl solution containing verapamil than in those precontracted with 40 mM KCl (pD_2 value: 3.47 ± 0.10; $P < 0.0005$, maximal response: 79.7 ± 5.5%; $P < 0.01$; Figure 8b).

Discussion

Mexiletine induced concentration-dependent relaxations in mesenteric resistance arteries precontracted with NA. Removal of the endothelium did not alter the relaxation, indicating that the relaxation is not endothelium-dependent. Mexiletine also shifted the concentration-response curves for NA and 5-HT to the right. Since the maximal responses to the agonists were reduced by higher concentrations of mexiletine and the slopes of the Schild plot were significantly different from 1.0, mexiletine does not act as a competitive α-adrenoceptor or 5-HT receptor antagonist. Furthermore, mexiletine shifted concentration-response curves to NA and 5-HT with identical pA_2 values and slopes. This suggests that NA and 5-HT activate a common pathway in pharmacomechanical (receptor-contraction) coupling and that mexiletine acts on the common pathway which is distal to the receptors. Indeed, mexiletine caused similar relaxations in arteries precontracted with NA and 5-HT. Involvement of prostaglandins in the relaxation to mexiletine can also be excluded since the cyclooxygenase inhibitor, meclofenamic acid, did not affect the relaxation.

There are only few reports investigating vascular effects of mexiletine: mexiletine induces small contractions in human saphenous vein, but not in arteries (Chiavarelli *et al.*, 1990), and does not affect NA-induced contraction in guinea-pig aorta (Kitagawa *et al.*, 1985). The discrepancy between the present observation and previous work in which large vessels were used can be explained, at least in part, by the difference in species or anatomical origin of the preparations. In contrast to mexiletine, there are many reports investigating vascular effects of lignocaine which possesses a chemical structure and pharmacological effects similar to those of mexiletine. The local anaesthetic causes relaxations (Altura & Altura, 1974; Wang & Jackson, 1988; Perlmutter, 1990) and, in some preparations, contractions (mainly in venous smooth muscles: Altura & Altura, 1974; Johns *et al.*, 1985; Monuszko *et al.*, 1989). Although inhibition of myosin light-chane kinase (Nosaka *et al.*, 1989) and phospholipase A_2 (Kunze *et al.*, 1976; Willman & Hendrickson, 1978), and antagonistic effects on movement of calcium ions (Josephson & Sperelakis, 1976) in smooth muscle by lignocaine have been reported, local anaesthetics are generally believed to induce nonspecific inhibition of vascular tone (Altura & Altura, 1974).

Caffeine induced transient contractions in $CaCl_2$-free solution, as in previous reports, by releasing Ca^{2+} from intracellular Ca^{2+} store site (sarcoplasmic reticulum; Endo, 1977; Dohi *et al.*, 1990a). Mexiletine did not change the contraction, indicating that mexiletine does not affect, at least at the concentration used, the release of Ca^{2+}. NA also evoked transient contractions in Ca^{2+}-free solution, confirming previous observations (Itoh *et al.*, 1983; Dohi *et al.*, 1990a) and suggesting that the contraction to NA in Ca^{2+}-free solution is independent of extracellular Ca^{2+}. The fact that mexiletine did not alter the contraction indicates that mexiletine does not inhibit the release of Ca^{2+} from the NA-sensitive Ca^{2+} store. In contrast, $CaCl_2$-induced contractions in NA-activated vessels were inhibited by mexiletine. The contraction was evoked by extracellular Ca^{2+} since the NA-sensitive intracellular Ca^{2+} store had been depleted (NA did not evoke contraction before the addition of $CaCl_2$ and application of caffeine instead of $CaCl_2$ did not evoke contraction). Thus, mexiletine inhibits NA-induced contraction by inhibiting the component of the contraction which depends on extracellular, but not intracellular Ca^{2+}.

A23187 produces a contraction which is dependent on the external Ca^{2+} in smooth muscles (Ishida & Shibata, 1980) by increasing the permeability of the membrane to Ca^{2+} (Swamy *et al.*, 1975). However, the contraction induced by A23187 was insensitive to verapamil and mexiletine did not induce relaxations in arteries contracted with A23187, indicating that mexiletine does not nonspecifically inhibit contractions which depend on extracellular Ca^{2+}. The compound might inhibit Ca^{2+} movement through Ca^{2+} channels. Indeed, in single ventricular cells of guinea-pig, mexiletine is effective in blocking Ca^{2+} channels (Ono *et al.*, 1986).

High K^+ depolarizes the membrane of vascular smooth muscle cells. In the present study, the contraction induced by 40 mM KCl was completely reversed by verapamil, indicating that the contraction depends on Ca^{2+} influx through verapamil-sensitive (voltage-dependent) Ca^{2+} channels. Mexiletine evoked less pronounced relaxations in arteries precontracted with KCl than in arteries precontracted with NA. This raises the following possibilities: (1) mexiletine causes the relaxation by hyperpolarizing the membrane (hyperpolarization might be prevented by KCl-induced depolarization), (2) mexiletine causes relaxations by opening K^+ channels (excess $[K^+]_o$ might prevent K^+ efflux through K^+ channels), and (3) inhibitory effects of mexiletine are more potent against NA- (or 5-HT-) sensitive Ca^{2+} channels than against verapamil-sensitive Ca^{2+} channels.

During the contraction to NA in arteries activated with high KCl in the presence of verapamil, the membrane potential of the mesenteric artery might be fixed by KCl-induced depolarization (Nagao & Vanhoutte, 1991). Even in this condition, mexiletine induced potent relaxations, indicating that KCl-induced depolarization itself has only minor effects on the relaxation to mexiletine. This suggests that a large part of the relaxation to mexiletine might not be due to hyperpolarization of the membrane caused by the drug. Although mexiletine inhibits depolarization of the membrane in cardiac muscle cells (Singh & Vaugham Williams, 1972; Shirayama *et al.*, 1991), the inhibitory effect against depolarization does not play a major role in the relaxation of the vascular smooth muscle. Mexiletine-induced relaxations in arteries contracted with NA in the high KCl solution containing verapamil were much more potent than in arteries contracted with high KCl. This finding further reinforces the concept that a large part of the inhibitory effect of mexiletine is not related to the hyperpolarizing effect of the drug. Mexiletine must have a greater inhibitory effect against NA- (or 5-HT-) activated, verapamil-insensitive Ca^{2+} channels than against verapamil-sensitive channels since the NA-induced contraction in the high KCl solution containing verapamil depends on Ca^{2+} influx through NA-activated, but not vera-

pamil-sensitive Ca^{2+} channels. Moreover, the fact that the pA_2 values (and slopes) for mexiletine using NA and 5-HT as agonists were identical suggests that 5-HT may act on NA-sensitive Ca^{2+} channels which might be the most important target of the antiarrhythmic drug in the vasorelaxant action. The failure of TEA and glibenclamide to inhibit the relaxation to mexiletine indicates that an activation of K^+ channels (at least those of TEA- and glibenclamide-sensitive) which may evoke relaxations by hyperpolarizing the membrane of the vascular smooth muscle is not involved in the relaxation.

In Na^+-free solution, where effects of Na^+-channel blockade may disappear, the relaxation to mexiletine was slightly inhibited. This suggests that mexiletine-induced relaxation might be related, at least in part, to Na^+ channel blockade which has hyperpolarizing effects on the membrane. Indeed, KCl-induced depolarization (in the presence of verapamil), which may reduce the hyperpolarizing effect of Na^+ channel blockade by fixing the membrane potential, slightly reduced the relaxation (see Figure 8). However, the Na^+ channel blockade contributes to only a small part of the relaxation induced by mexiletine.

Although mexiletine induces a fall in arterial pressure in dogs (Rossi *et al.*, 1984) and a decrease in total peripheral resistance and arterial pressure in rabbits (Beltrame *et al.*, 1984), it is not clear whether the vascular effect of mexiletine is clinically important especially since the effective concentration of mexiletine in the present study is slightly higher than the therapeutic concentration in man (2×10^{-6}–10^{-5} M; Vozeh *et al.*, 1982; Woosley *et al.*, 1984; Monk & Brogden, 1990). However, the possibility that the antiarrhythmic drug causes vasodilatation in man cannot be excluded. Indeed, reduction in blood pressure or total peripheral resistance has been reported in man (Fritz *et al.*, 1983; Greenspan *et al.*, 1984).

In conclusion, mexiletine induces potent relaxations in mesenteric resistance arteries contracted with NA. The mechanisms underlying the relaxation to mexiletine are related to the inhibitory effects of the drug against Ca^{2+} influx, but not release caused by NA. It is speculated that mexiletine possesses greater inhibitory effects against NA-activated, verapamil-insensitive (receptor-operated) Ca^{2+} channels than against verapamil-sensitive (voltage-dependent) Ca^{2+} channels.

References

ALTURA, B.M. & ALTURA, B.T. (1974). Effects of local anesthetics, antihistamines, and glucocorticoids on peripheral blood flow and vascular smooth muscle. *Anesthesiology*, **41**, 197–214.

ARUNLAKSHANA, O. & SCHILD, H.O. (1959). Some quantitative uses of drug antagonists. *Br. J. Pharmacol. Chemother.*, **14**, 48–59.

BELTRAME, J., AYLWARD, P.E., MCRITCHIE, R.J. & CHALMERS, J.P. (1984). Comparative haemodynamic effects of lidocaine, mexiletine, and disopyramide. *J. Cardiovasc. Pharmacol.*, **6**, 483–490.

BRAYDEN, J.E. & NELSON, M.T. (1992). Regulation of arterial tone by activation of calcium-dependent potassium channels. *Science*, **256**, 532–535.

CHIAVARELLI, M., CHIAVARELLI, R., FABI, F., STATI, T. & BASSO, P.D. (1990). Vascular effects of lignocaine after coronary artery surgery. *Lancet*, **335**, 1101–1102.

DIEDRICH, D., YANG, Z., BÜHLER, F.R. & LÜSCHER, T.F. (1990). Impaired endothelium-dependent relaxations in hypertensive resistance arteries involve the cyclooxygenase pathway. *Am. J. Physiol.*, **258**, H445–H451.

DOHI, Y., AOKI, K., FUJIMOTO, S., KOJIMA, M. & MATSUDA, T. (1990a). Alteration in sarcoplasmic reticulum-dependent contraction of tail arteries in responses to caffeine and noradrenaline in spontaneously hypertensive rats. *J. Hypertens*, **8**, 261–267.

DOHI, Y., THIEL, M.A., BÜHLER, F.R. & LÜSCHER, T.F. (1990b). Activation of endothelial L-arginine pathway in resistance arteries: effect of age and hypertension. *Hypertension*, **16**, 170–179.

ENDO, M. (1977). Calcium release from the sarcoplasmic reticulum. *Physiol. Rev.*, **57**, 71–108.

FRITZ, K.-W., LÜLLWITZ, E., SCHELD, H. & KIRCHNER, E. (1983). Haemodynamic effects of mexiletine and lidocaine in coronary surgery patients. *Anästh. Intensivther. Notfallmed.*, **18**, 125–128 (abstract in English).

GREENSPAN, A.M., WEBB, C.R., SPIELMAN, S.R. & HOROWITZ, L.N. (1984). Intravenous mexiletine therapy for ventricular tachyarrhythmias. *Clin. Res.*, **32**, 172A.

ISHIDA, Y. & SHIBATA, S. (1980). Characteristic contractile response to the calcium ionophore, A23187, in guinea-pig vas deferens. *Br. J. Pharmacol.*, **71**, 581–583.

ITOH, K., KURIYAMA, H. & SUZUKI, H. (1983). Differences and similarities in the noradrenaline- and caffeine-induced mechanical responses in the rabbit mesenteric artery. *J. Physiol.*, **337**, 609–629.

JOHNS, R.A., DIFAZIO, C.A. & LONGNECKER, D.E. (1985). Lidocaine constricts or dilates rat arterioles in a dose-dependent manner. *Anesthesiol.*, **62**, 141–144.

JOSEPHSON, I. & SPERELAKIS, N. (1976). Local anesthetic blockade of Ca^{2+}-mediated action potentials in cardiac muscle. *Eur. J. Pharmacol.*, **40**, 201–208.

KITAGAWA, H., TAKEDA, F. & KOHEI, H. (1985). Inhibition of sympathetic nervous system by mexiletine, an antiarrhythmic agent, and its antagonism against ouabain. *Drug Res.*, **35**, 356–359.

KUNZE, H., NAHAS, N., TRAYNOR, J.R. & WURL, M. (1976). Effects of local anaesthetics on phospholipases. *Biochim. Biophys. Acta*, **441**, 93–102.

MONK, J.P. & BROGDEN, R.N. (1990). Mexiletine: a review of its pharmacodynamic and pharmacokinetic properties, and therapeutic use in the treatment of arrhythmias. *Drugs*, **40**, 374–411.

MONUSZKO, E., HALEVY, S., FREESE, K. & LIU-BARNETT, M. (1989). Vasoactive actions of local anaesthetics on human isolated umbilical veins and arteries. *Br. J. Pharmacol.*, **97**, 319–328.

NAGAO, T. & VANHOUTTE, P.M. (1991). Hyperpolarization contributes to endothelium-dependent relaxations to acetylcholine in femoral veins of rats. *Am. J. Physiol.*, **261**, H1034–H1037.

NAGASAKO, S., HAYASHIBARA, M., KATAGIRI, Y. & IWAMOTO, K. (1992). Salivary excretion of mexiletine after bolus intravenous administration in rats. *J. Pharm. Pharmacol.*, **44**, 55–57.

NOSAKA, S., KAMAYA, H., UEDA, I. & WONG, K.C. (1989). Smooth muscle contraction and local anesthetics: calmodulin-dependent myosin light-chain kinase. *Anesth. Analg.*, **69**, 504–510.

ONO, K., KIYOSUE, T. & ARITA, M. (1986). Comparison of the inhibitory effects of mexiletine on the calcium current of single ventricular cells. *Life Sci.*, **39**, 1465–1470.

PERLMUTTER, N.S., WILSON, R.A., EDGAR, S.W., SANDERS, W., GREENBERG, B.H. & TANZ, R. (1990). Vasodilatory effects of lidocaine on epicardial porcine coronary arteries. *Pharmacol.*, **41**, 280–285.

ROSSI, F., RUGGIERO, E., SCAFURO, M.A., GIASI, M., MAZZEO, V., BILE, G., LAMPARELLI, E. & MARMO, E. (1984). Possible adverse effects on the cardiovascular system of an antiarrhythmic drug mexiletine. *Arch. Toxicol.*, Suppl. 7, 510–514.

SCHEFFE, H. (1959). *The Analysis of Variance*. New York: John Wiley & Sons.

SHIRAYAMA, T., INOUE, D., INOUE, M., TATSUMI, T., YAMAHARA, Y., ASAYAMA, J., KATSUME, H. & NAKAGAWA, M. (1991). Electrophysiological effects of sodium channel blockers on guinea pig left atrium. *J. Pharmacol. Exp. Ther.*, **259**, 884–893.

SINGH, B.N. & VAUGHAN WILLIAMS, E.M. (1972). Investigations of the mode of action of a new antidysrhythmic drug. Kö 1173. *Br. J. Pharmacol.*, **44**, 1–9.

STURGESS, N.C., ASHFORD, M.L.J., COOK, D.L. & HALES, C.N. (1985). The sulphonylurea receptor may be an ATP-sensitive potassium channel. *Lancet*, **ii**, 474–475.

SWAMY, V.C., TICKU, M., TRIGGLE, C.R. & TRIGGLE, D.J. (1975). The action of the ionophores, X-537A and A-23187, on smooth muscle. *Can. J. Physiol. Pharmacol.*, **53**, 1108–1114.

VANE, J.R. (1971). Inhibition of prostaglandin synthesis as a mechanism of action for aspirin-like drugs. *Nature*, **231**, 232–235.

VAUGHAN WILLIAMS, E.M. (1984). A classification of antiarrhythmic actions reassessed after a decade of new drugs. *J. Clin. Pharmacol.*, **24**, 129–147.

VOZEH, S., KATZ, G., STEINER, V. & FOLLATH, F. (1982). Population pharmacokinetic parameters in patients treated with oral mexiletine. *Eur. J. Clin. Pharmacol.*, **23**, 445–451.

WANG, H.-W. & JACKSON, R.T. (1988). Effects of lidocaine and procaine on canine nasal blood vessels. *Ann. Otol. Rhinol. Laryngol.*, **97**, 409–413.

WILLMAN, C. & HENDRICKSON, H.S. (1978). Positive surface charge inhibition of phospholipase A_2 in mixed monolayer systems. *Arch. Biochem. Biophys.*, **191**, 298–305.

WOOSLEY, R.L., WANG, T., STONE, W., SIDDOWAY, L., THOMPSON, K., DUFF, H.J., CERSKUS, I. & RODEN, D. (1984). Pharmacology, electrophysiology, and pharmacokinetics of mexiletine. *Am. Heart. J.*, **107**, 1058–1065.

(Received June 22, 1993
Revised October 23, 1993
Accepted November 4, 1993)

Br. J. Pharmacol. (1994), **111**, 681–686 © Macmillan Press Ltd, 1994

Interleukin-1β enhances capsaicin-induced neurogenic vasodilatation in the rat skin

[1]M.K. Herbert & *P. Holzer

[1]Department of Anaesthesiology, University of Würzburg, Germany, and *Department of Pharmacology, University of Graz, Austria

1 This study examined the effect of interleukin-1β (IL-1β) on the capsaicin-induced increase in cutaneous blood flow of anaesthetized rats as measured by laser Doppler flowmetry.

2 The substances were administered by intraplantar subcutaneous injection of 10 μl-volumes, saline being injected into one hindpaw and IL-1β into the other.

3 IL-1β (0.5–500 pg) was without effect on blood flow on its own but dose-dependently enhanced the hyperaemic response to intraplantar capsaicin (0.3 μg) up to 180% ($P<0.05$) of the response seen in saline-treated paws.

4 Il-1β-(163–171), a fragment devoid of proinflammatory activity, failed to enhance capsaicin-induced hyperaemia when given at a dose of 50 pg.

5 Indomethacin (10 mg kg^{-1}, i.p.) did not alter the capsaicin-induced vasodilatation but prevented IL-1β (50 pg) from augmenting the hyperaemic response to capsaicin.

6 The hyperaemia evoked by intraplantar calcitonin gene-related peptide (0.038–3.8 ng) was not altered by IL-1β (50 pg).

7 These data indicate that IL-1β enhances the cutaneous hyperaemic response to afferent nerve stimulation with capsaicin in a prostaglandin-dependent manner. This proinflammatory action of the cytokine appears to arise from sensitization of afferent nerve endings.

Keywords: Interleukin-1β; capsaicin; afferent nerve stimulation; cutaneous hyperaemia; neurogenic inflammation; sensitization of afferent nerve endings; proinflammatory action; prostaglandins; calcitonin gene-related peptide (CGRP)

Introduction

Intradermal injection of capsaicin leads to vasodilatation and increased vascular permeability (Hughes & Brain, 1991). These effects are elicited by activation of nociceptive afferent nerve fibres and release of vasoactive peptides from their peripheral endings. Among them, calcitonin gene-related peptide (CGRP) and substance P are the best studied candidate mediators (Holzer, 1992). The process of neurogenic inflammation is pathophysiologically relevant because it is potentially involved in a variety of diseases including inflammation of the skin, eye and respiratory tract, arthritis, migraine, and inflammatory bowel disease (Holzer, 1988; Maggi & Meli, 1988; Barnes, 1991; Basbaum & Levine, 1991; Moskowitz & Buzzi, 1991; Sharkey, 1992).

In addition to altering vascular functions, peptides released from afferent nerve endings can influence the activity of immunocompetent cells including mast cells, granulocytes, macrophages and lymphocytes (Donnerer *et al.*, 1990; McGillis *et al.*, 1990; Holzer, 1992). Mediators released from these cells, such as histamine and prostaglandins, can sensitize afferent nerve endings and in this way lead to hyperalgesia and prolong the inflammatory process (Handwerker, 1991). Sensitization is expected to facilitate the release of neuropeptides from afferent nerve endings and thus to reinforce the signs of neurogenic inflammation. Another putative link between the immune system and afferent nerve fibres is interleukin-1β (IL-1β). This cytokine is not only a major immune mediator but is also able to initiate inflammatory reactions or to exacerbate existing inflammation (Dinarello, 1992).

The present study was designed to examine the effect of IL-1β on neurogenic inflammation as measured by the cutaneous vasodilator response to the afferent nerve stimulant, capsaicin, in the rat hindpaw. As IL-1β was found to enhance the vasodilator action of capsaicin, further experiments were aimed at elucidating the mechanism of the sensitizing effect of this cytokine.

[1] Author for reprint requests: Department of Anaesthesiology, University of Würzburg, Josef-Schneider-Strasse 2, D-97080 Würzburg, Germany.

Methods

Animal preparation

The experiments of this study were approved by the Austrian Ministry of Science and Research. Female Sprague-Dawley rats (Versuchstierzuchtanstalt Himberg, Austria) weighing 180–245 g were anaesthetized with phenobarbitone, 250 mg kg^{-1} i.p. (Lippe & Holzer, 1992). Additional doses of phenobarbitone (25–50 mg kg^{-1}) were given as required to achieve a deep level of anaesthesia, which was checked by the absence of any reaction to pinching the forepaw in the interdigital web with a surgical clamp. In all animals the trachea was cannulated and blood pressure was monitored continuously via a catheter in the right carotid artery. Rectal temperature was monitored and maintained at a physiological level of 37.5 to 38°C with the aid of a heating pad.

A transparent probe holder for laser Doppler flowmetry (see below) was fixed rigidly with double-sided adhesive tape to the plantar skin of each paw. Then the probe holders were mounted to a frame keeping the paws in a vertical position. To ensure optimal paw perfusion, the rats were positioned supine and with their rostro-caudal axis inclined such that the level of the hindpaws was identical with that of the heart. The experimental procedure started after a 1 h resting period for stabilization of blood pressue, body temperature and plantar skin blood flow.

Measurement of cutaneous blood flow

Cutaneous blood flow was measured with a laser Doppler flowmeter (Periflux PF3, Perimed, Sweden) which operates on the principle that a virtually monochromatic laser beam (2 mW helium-neon laser) scattered by moving red blood cells undergoes a frequency shift according to the Doppler effect, while light scattered in static tissues remains unshifted in frequency. The laser light is guided to the skin surface by an optical fibre and permeates the skin up to a depth of 1 mm. Part of the reflected light is collected and transmitted by 2 optical fibres to 2 photodetectors. The output signal of the Periflux PF3 is expressed in dimensionless blood flow values (perfusion units, PU) and represents the red blood cell flow (determined by the number and velocity of these cells) in a semisphere with a radius of about 1 mm (Oberg *et al.*, 1984).

For the determination of the PU zero level, the laser probe was placed on a white static surface and the value of 250 PU was calibrated against the physical motility standard solution PF100 (Perimed) under the conditions recommended by Perimed. The band width of the instrument was set at 12 kHz and the time constant of the damping filter was set at 3 s in order to smooth out fluctuations due to the cardiac cycle.

For measurement of skin blood flow, the laser probe was inserted into the probe holder attached to the plantar skin and thus applied perpendicularly to the skin surface. After a 20–30 s period of stabilization, skin blood flow was determined as the average PU recorded during a period of 15–20 s.

Subcutaneous injection protocol

Intraplantar subcutaneous injections of 10 μl volumes were performed with a 50 μl Hamilton syringe and a 27 gauge needle (0.4 × 12 mm) which was inserted from the lateral aspect of the hindpaw. The tip of the needle was directed subcutaneously into the centre of the hole of the laser probe holder. With the tip of the needle in this position, the 10 μl volume was injected carefully under direct view. This small injection volume had the advantage of being readily absorbed by the tissue within a few minutes, as judged by the disappearance of the local blanching seen immediately after the injection.

The injection protocol was identical in all experiments inasmuch as the first injection was given into the right paw, while the second injection was given into the left paw after an interval of 45–60 s. This interval provided enough time to record the cutaneous blood flow in the right paw and then to place the laser probe on the left paw.

Experimental groups

All experimental groups consisted of 6 rats: treatment was as follows:

Groups 1–4 Doses of 0.5-500 pg IL-1β, dissolved in sterile saline, were injected into the left paw. The right paws served as controls and received an equal volume (10 μl) of saline. Forty min later 0.3 μg/10 μl capsaicin was injected into those areas of both paws which had been pretreated with IL-1β or saline (see Figure 1). The dose of 0.3 μg capsaicin was chosen after preliminary experiments had shown this dose to be suprathreshold in causing a reproducible increase in skin blood flow. Since desensitization to capsaicin is a characteristic consequence of topical application of the drug to the rat skin (Lynn *et al.*, 1992), capsaicin was administered only once to each paw.

Group 5 Rats were pretreated by injection of 50 pg IL-1β into both hindpaws. After 40 min 0.3 μg/10 μl capsaicin was injected into the left hindpaw while the right hindpaw received 10 μl saline.

Group 6 A dose of 50 pg of IL-1β-(163–171), a fragment of human IL-1β devoid of inflammatory activity (Antoni *et al.*, 1986), was injected into the left hindpaw, the contralateral paw receiving saline alone. Forty min later 0.3 μg/10 μl capsaicin was injected into both hindpaws (see Figure 2).

Groups 7–10 To examine the possible involvement of prostaglandins in the sensitizing effect of IL-1β, rats were pretreated with indomethacin (10 mg kg^{-1} body weight) or its vehicle (1 ml kg^{-1}), which were injected intraperitoneally 60 min prior to the subcutaneous injection of 50 pg IL-1β or saline. Forty min later 0.3 μg/10 μl capsaicin was injected into both paws (see Figure 3).

Groups 11–13 To study the effect of IL-1β on the cutaneous vasodilatation induced by calcitonin gene-related peptide (CGRP) this peptide (0.038, 0.38 and 3.8 ng in 10 μl saline) was injected into both hindpaws 40 min after IL-1β (50 pg) had been injected into the left paw and saline (10 μl) into the right paw (see Figure 4).

Group 14 In a separate experiment the change in the paw volume after intraplantar injection of saline (50 μl) into the right hindpaw and of capsaicin (1.5 μg in 50 μl saline) into the left hindpaw was examined with a plethysmometer (model 7150, Ugo Basile, Comerio-Varese, Italy). The paw volume was measured 5, 20 and 35 min post-injection.

Recording protocol

Cutaneous blood flow was measured three times at 15 min intervals before the first injection. In this way control recordings were made on each paw at − 35, − 20 and − 5 min. At time 0 the first injection (usually IL-1β or saline) was performed. A second series of recordings was made 5, 20 and 35 min after this injection. Forty min after the first injection, the second injection (usually capsaicin or CGRP) was carried out. The interval of 40 min was chosen because the effect of IL-1β in sensitizing nociceptors is fully developed within 1 h (Ferreira *et al.*, 1988) and because the time of the experiment was to be kept short as skin blood flow tended to fall slightly with time (Figure 1). The third series of recordings started 5 min after the second injection, i.e. 45 min after the first injection, and was continued at 60 and 75 min.

Statistics

The results are expressed as means ± s.e.mean. For statistical evaluation the PU values of the right and left paw, recorded 5 min after the capsaicin injection, were analysed with the Wilcoxon matched-pairs signed rank test (two-tailed). This test was also used to compare peak changes of blood flow induced by saline with those induced evoked by IL-1β or capsaicin. A value of $P<0.05$ was regarded as significant.

Substances

Human recombinant IL-1β and IL-1β-fragment-(163–171) were purchased from Sigma (Deisenhofen, Germany), calcitonin gene-related peptide (rat CGRP-α) from Bachem (Bubendorf, Switzerland), capsaicin from Fluka (Buchs, Switzerland), and indomethacin from Merck, Sharp and Dohme (Munich, Germany). All other chemicals were from commercial sources and were of analytical purity. Capsaicin was dissolved in absolute ethanol and dissolved with saline such that the ethanol concentration in the injection solution was 0.1% (weight/weight). Indomethacin was dissolved in 2% (wt/wt) Na_2CO_3 at a concentration of 30 mg ml^{-1} and further diluted with saline to a concentration of 10 mg ml^{-1}. CGRP was dissolved (100 μM) in, and diluted with, saline.

Results

General observations

Cutaneous blood flow during the control period (− 35, − 20, − 5 min) was similar in both paws of all groups and tended to fall slightly during the time of the experiment (Figure 1). The injection of 10 μl saline increased blood flow from 56.8 ± 6.5 to 79.5 ± 8.5 PU ($n = 6$) as measured 5 min post-injection while injection of 50 pg IL-1β enhanced skin blood flow from 59.3 ± 9.1 to 91.8 ± 12.2 PU ($n = 6$). The effect of IL-1β was not significantly different from that caused by saline and was not related to the dose of IL-1β injected (not shown). Twenty and 35 min post-injection skin blood flow had always returned to the level measured before the first injection.

Subcutaneous injection of 0.3 μg capsaicin into the saline-treated paw augmented plantar blood flow by 144.1 ± 61.0% ($n = 6$) (Figure 1), this increase being significantly ($P < 0.05$) higher than that caused by saline alone (26.7 ± 21.0%, $n = 6$). In the paw treated with 50 pg IL-1β, capsaicin enhanced blood flow by 223.0 ± 56.8% ($n = 6$). This hyperaemic reaction to capsaicin was significantly larger than that seen in the saline-treated paw (Figure 1). Blood flow returned to basal values within 20 min from the injection of capsaicin into the saline-treated paw, whereas blood flow in the paw treated with IL-1β took longer to return to the pre-capsaicin level (Figure 1).

In a control experiment both paws were pretreated with 50 pg IL-1β. Injection of 0.3 μg/10 μl capsaicin into the left paw increased cutaneous blood flow from 38.2 ± 7.8 PU to 106.8 ± 21.0 PU ($n = 6$). The effect of capsaicin was significantly ($P < 0.05$) higher than the minor effect of saline which after injection into the right paw increased blood flow from 36.8 ± 6.8 PU to 52.5 ± 10.2 PU ($n = 6$). This observation corroborates that the vasodilator reaction to capsaicin represents primarily a reaction to this algesic chemical and not a reaction to the needle insertion or injection of a 10 μl volume of fluid.

In another experiment it was observed that, at the doses used here, capsaicin failed to augment vascular permeability in the rat hindpaw as determined by plethysmometry. The maximal rise of the paw volume as seen 5 to 20 min after intraplantar injection of 1.5 μg capsaicin in 50 μl saline amounted to 14 ± 3% ($n = 6$), which did not differ from the rise evoked by 50 μl saline alone (13 ± 2%, $n = 6$).

Effect of IL-1β on capsaicin-induced hyperaemia

The effect of intraplantar IL-1β in enhancing the capsaicin-induced increase in cutaneous blood flow, for the sake of brevity referred to as 'sensitizing effect', depended on the dose of the cytokine (Figure 2). Doses as low as 0.5 pg IL-1β (Figure 2) tended to increase the capsaicin-evoked vasodilator effect but the response to this dose of the cytokine did not reach statistical significance. With 5 pg IL-1β, however, the capsaicin-induced cutaneous hyperaemia was significantly enhanced (Figure 2). A further increase in the dose of IL-1β to 50 pg did not further enhance the magnitude of the sensitizing effect (Figure 2) but caused a longer-lasting augmentation of the capsaicin-evoked hyperaemia than the dose of 5 pg IL-1β (not shown). Pretreatment of the hindpaw with 500 pg IL-1β also tended to enhance the hyperaemic response to capsaicin but the sensitizing effect of this cytokine dose did not reach statistical significance (Figure 2). It remains to be determined whether the failure of the highest dose of IL-1β was due to absorption of the cytokine into the circulation and augmentation of the capsaicin-induced hyperaemia in the contralateral paw. Mean arterial blood pressure was not affected by this dose of the cytokine ($n = 6$).

Effect of IL-1β-(163–171) on capsaicin-induced hyperaemia

The fragment IL-1β-(163–171) injected at a dose of 50 pg failed to exert any sensitizing effect on capsaicin-induced cutaneous vasodilatation. Five min post-injection the hyperaemic responses to capsaicin were identical in the IL-1β-(163–171)-treated and saline-treated paws (Figure 2), and this was also true for the recordings taken 60 and 75 min post-injection.

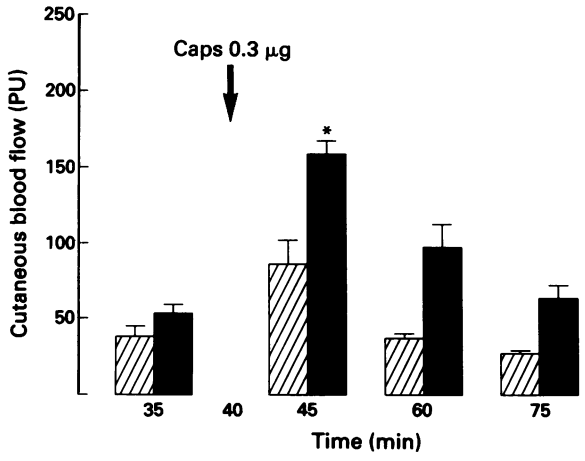


Figure 1 Time course of the effect of interleukin-1β in enhancing the cutaneous hyperaemia evoked by capsaicin (Caps). At time 0, saline (10 μl) was injected into the plantar side of the right paw whilst the left paw was treated with 50 pg interleukin-1β. Forty min later capsaicin (Caps, 0.3 μg) was injected into each paw. Cutaneous blood flow in the right saline-treated (hatched columns) and left IL-1β-treated (solid columns) hindpaw was recorded by laser Doppler flowmetry and expressed in perfusion units (PU). Results are mean with s.e.mean; $n = 6$. *$P < 0.05$ versus respective values measured in the saline-treated paw (two-tailed Wilcoxon matched-pairs signed rank test).

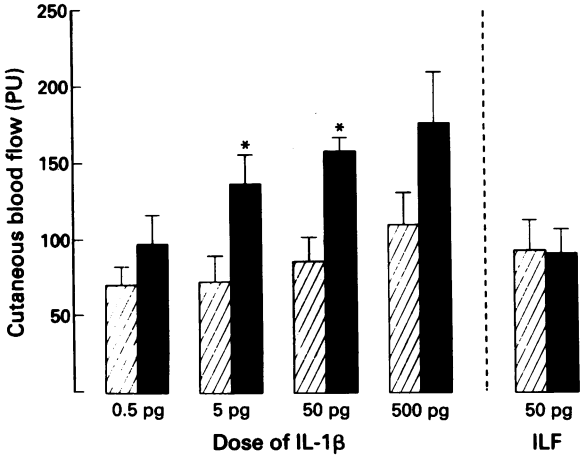


Figure 2 Dose-response relationship for the interleukin-1β (IL-1β)-induced enhancement of the cutaneous hyperaemia evoked by capsaicin and the lack of effect of the fragment IL-1β-(163–171) (ILF). Saline (10 μl) was injected into the plantar side of the right paw (hatched columns) whilst the left paw (solid columns) was treated with IL-1β or ILF. Forty min later capsaicin (0.3 μg) was injected into each paw. Cutaneous blood flow was recorded by laser Doppler flowmetry and expressed in perfusion units (PU). Results are mean with s.e.mean; $n = 6$. *$P < 0.05$ versus respective values measured in the saline-treated paw (two-tailed Wilcoxon matched-pairs signed rank test).

Effects of indomethacin

Neither basal blood flow in the hindpaw nor the vasodilator response to capsaicin was altered by intraperitoneal injection of indomethacin (10 mg kg^{-1}) when compared with the respective blood flow values measured after intraperitoneal injection of vehicle (Figure 3a). These experiments also showed that in both vehicle- and indomethacin-pretreated rats the hyperaemic reaction to intraplantar capsaicin in the left hindpaw was identical with that in the right paw when saline had been injected into either paw 40 min before capsaicin (Figure 3a). The injection of 50 pg/10 μl IL-1β to the left hindpaw of vehicle pretreated rats enhanced the vasodilator effect of capsaicin (Figure 3b) to an extent which was similar to that seen in untreated rats (Figures 1 and 2). This sensitizing effect of IL-1β was absent in rats treated with indomethacin (Figure 3b).

Effect of IL-1β on CGRP-induced hyperaemia

Intraplantar injection of CGRP (0.038–3.8 ng) caused a dose-dependent increase in cutaneous blood flow (Figure 4).

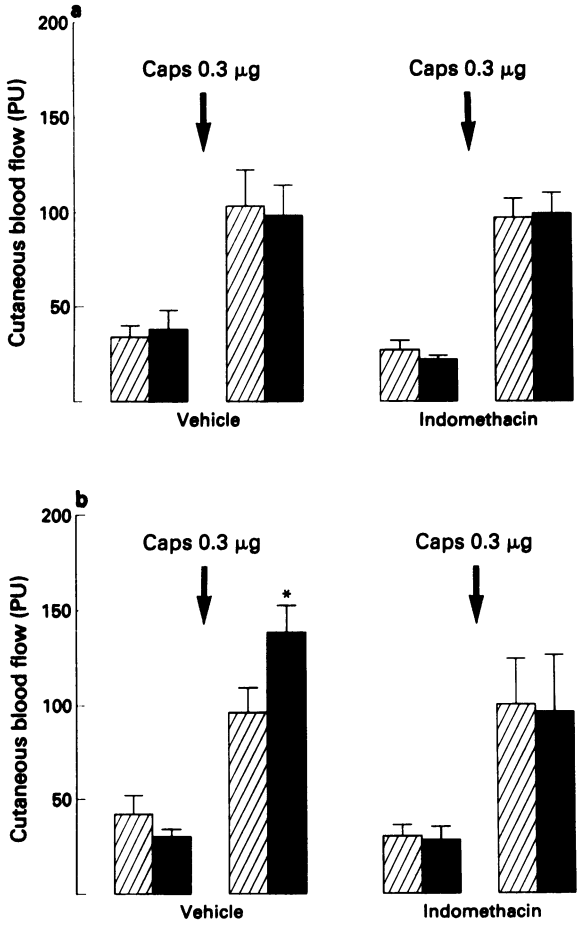


Figure 3 Effect of intraplantar capsaicin on cutaneous blood flow in rats pretreated with indomethacin or its vehicle. Indomethacin (10 mg kg^{-1}) or its vehicle was administered intraperitoneally 60 min before saline or interleukin-1β was injected into the plantar side of the hindpaw. In (a) saline (10 μl) was given to either paw whereas in (b) saline (10 μl) was injected into the right paw and interleukin-1β (50 pg) into the left paw. Forty min later capsaicin (Caps, 0.3 μg) was injected into each paw. Cutaneous blood flow in the right (hatched columns) and left (solid columns) hindpaw was recorded by laser Doppler flowmetry and expressed in perfusion units (PU). Results are mean with s.e.mean; $n = 6$. $^*P < 0.05$ versus respective values measured in the saline-treated paw (two-tailed Wilcoxon matched-pairs signed rank test).

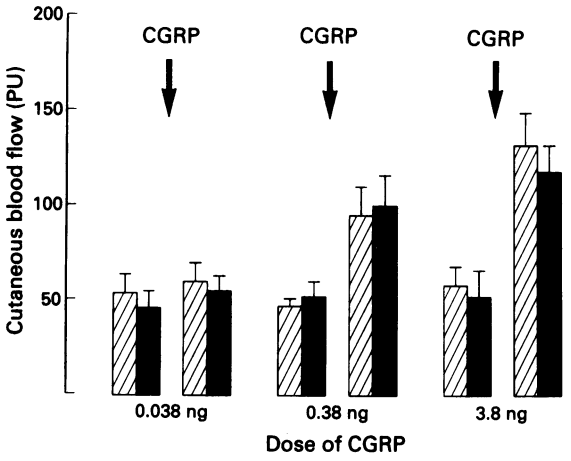


Figure 4 Effect of interleukin-1β on the cutaneous hyperaemia evoked by calcitonin gene-related peptide (CGRP). Saline (10 μl) was injected into the plantar side of the right hindpaw (hatched columns) whilst the left paw (solid columns) was treated with interleukin-1β (50 pg). Forty min later CGRP (doses as indicated) was injected into each paw. Cutaneous blood flow was recorded by laser Doppler flowmetry and expressed in perfusion units (PU). Results are mean with s.e.mean; $n = 6$.

The magnitude of the CGRP-evoked hyperaemia was the same when saline (10 μl) or IL-1β (50 pg) had been injected into the hindpaw 40 min before the administration of CGRP (Figure 4).

Effects on blood pressure

At the time of the first injection into the hindpaws mean arterial blood pressure was 104 ± 3 mmHg ($n = 78$). During the time of the experiment, blood pressure decreased on average by 10–20 mmHg. Rats were excluded from the study if blood pressure dropped below 80 mmHg during the experiment. In most of the rats, blood pressure rose transiently during/after insertion of the needle into the subcutaneous space of the hindpaw and the intraplantar injection of substances. Whilst pressor responses to intraplantar injection of saline or IL-1β did not differ from each other, the pressor responses to intraplantar capsaicin (0.3 μg/10 μl) were consistently higher than those to saline or IL-1β. The increase in blood pressure following capsaicin injection was about 20 mmHg and lasted usually less than 4 min.

Discussion

The major finding of the present study was the discovery that IL-1β enhanced the cutaneous vasodilator action of capsaicin. The sensitizing effect of IL-1β depended on the dose injected and was seen with picogram amounts of the cytokine. This high potency of IL-1β in augmenting capsaicin-evoked hyperaemia is comparable with the high activity of the cytokine in sensitizing the rat hindpaw to noxious pressure stimuli (Ferreira *et al.*, 1988; Follenfant *et al.*, 1989). The vasodilator action of capsaicin in the skin is due to stimulation of afferent nerve endings and subsequent release of vasodilator transmitters (Holzer, 1992), among which CGRP plays a major role, at least in the rabbit skin (Hughes & Brain, 1991). Since IL-1β failed to enhance the vasodilator response to CGRP it is inferred that this cytokine augmented the hyperaemic response to capsaicin by a sensitizing action on afferent nerve fibres but did not alter the sensitivity of blood vessels to the released vasodilator peptide. Together with the findings on nociception (Ferreira *et al.*, 1988; Follenfant *et al.*, 1989) the present data indicate

that IL-1β can sensitize afferent nerve fibres to both chemical and mechanical noxious stimuli, which results, on the one hand, in enhanced release of vasodilator transmitters from the peripheral nerve endings and, on the other hand, in hyperalgesia.

IL-1β is released from activated macrophages and a large variety of other cell types including B-lymphocytes and endothelial cells (Libby *et al.*, 1986; Howells *et al.*, 1988; Dinarello, 1991) and is considered to be a key mediator of the immune and inflammatory reactions to infectious and foreign agents (Dinarello, 1992). This cytokine is not only a proinflammatory substance (Stimpson *et al.*, 1988; Hom *et al.*, 1992; van de Loo *et al.*, 1992) but can *per se* induce inflammation and tissue destruction (Pettipher *et al.*, 1986; Chandrasekhar *et al.*, 1990). The finding that intra-articular injection of IL-1 induces release of substance P, presumably from afferent nerve fibres, into the synovial fluid (O'Byrne *et al.*, 1990a,b) suggests that cytokines themselves could evoke signs of neurogenic inflammation. The present study, though, failed to furnish conclusive evidence for IL-1β-induced inflammatory reactions in the rat hindpaw skin.

The ability of IL-1β to augment the neurogenic vasodilator response to capsaicin needs to be seen in context with its ability to influence the activity and function of various immune and connective tissue cells (O'Byrne *et al.*, 1991; Dinarello, 1992). Specifically, IL-1β stimulates lymphocytes to release other cytokines (Lowenthal *et al.*, 1986) and causes fibroblasts and synovial cells to produce prostaglandin E_2 (Antoni *et al.*, 1986; Mochan *et al.*, 1986; O'Byrne *et al.*, 1990b). In the present study twofold evidence was obtained that IL-1β enhanced capsaicin-induced hyperaemia in the rat hindpaw via secondary mediators released from immunocompetent or other cells.

A first hint of such a mechanism of action came from the use of IL-1β-(163–171), a fragment of human IL-1β that is devoid of inflammatory activity, such as the induction of prostaglandin formation, but which retains the immunological activity of the parent molecule in activating T-lymphocytes (Antoni *et al.*, 1986). The finding that IL-1β-(163–171) failed to enhance the capsaicin-evoked hyperaemia in the rat paw skin indicated, therefore, that immunological processes such as activation of, and cytokine release from, lymphocytes did not play a role in the sensitizing effect of IL-1β. The participation of inflammatory mediators such as prostaglandins was substantiated by the use of indomethacin. At a dose (10 mg kg^{-1}) that is known to block prostaglandin synthesis by more than 90% (Whittle & Vane, 1987), this drug prevented the IL-1β-induced augmentation of the vasodilator response to capsaicin whereas basal blood flow and the capsaicin-induced hyperaemia measured in the absence of IL-1β remained unchanged. It follows that cyclo-oxygenase products generated by IL-1β in the vicinity of afferent nerve endings are responsible for the enhancement of the hyperaemic response to capsaicin. This inference is in keeping with the reported involvement of prostaglandins in the IL-1β-induced hyperalgesia in the rat paw (Ferreira *et al.*, 1988) and rabbit ear (Schweizer *et al.*, 1988) but does not negate the possibility that other mediators could also participate (Follenfant *et al.*, 1989).

In conclusion, IL-1β has been shown to augment cutaneous hyperaemic responses to capsaicin by a sensitizing action on afferent nerve fibres, an action which involves prostaglandins as secondary mediators. The current findings suggest that cytokines released in the course of infection or inflammation amplify the ability of nociceptive afferent nerves to increase blood flow in the affected tissue and in this way contribute to the reinforcement of neurogenic inflammatory processes.

The authors wish to express their gratitude to Professor F. Lembeck for his advice during the course of this study and to Dr I. Haubitz, Rechenzentrum der Universität Würzburg, for her assistance in the statistical analysis of the data. Mrs I. Russa and Ms M. Jocič were of great help in providing secretarial and technical assistance, respectively. The study was supported by the Foundation for the Advancement of Research in Anaesthesia and Analgesia (e. V., Würzburg) and by the Austrian Science Foundation (grants P7845-MED and P9473-MED).

References

ANTONI, G., PRESENTINI, R., PERIN, F., TAGLIABUE, A., GHIARA, P., CENSINI, S., VOLPINI, G., VILLA, L. & BORASCHI, D. (1986). A short synthetic peptide fragment of human interleukin 1 with immunostimulatory but not inflammatory activity. *J. Immunol.*, **137**, 3201–3204.

BARNES, P.J. (1991). Neurogenic inflammation in airways. *Int. Arch. Allergy Appl. Immunol.*, **94**, 303–309.

BASBAUM, A.I. & LEVINE, J.D. (1991). The contribution of the nervous system to inflammation and inflammatory disease. *Can. J. Physiol. Pharmacol.*, **69**, 647–651.

CHANDRASEKHAR, S., HARVEY, A.K., HRUBEY, P.S. & BENDELE, A.M. (1990). Arthritis induced by interleukin-1 is dependent on the site and frequency of intraarticular injection. *Clin. Immunol. Immunopathol.*, **55**, 382–400.

DINARELLO, C.A. (1991). Interleukin-1 and interleukin-1 antagonism. *Blood*, **8**, 1627–1652.

DINARELLO, C.A. (1992). Role of interleukin-1 in infectious diseases. *Immunol. Rev.*, **127**, 119–146.

DONNERER, J., EGLEZOS, A. & HELME, R.D. (1990). Neuroendocrine and immune function in the capsaicin-treated rat: evidence for afferent neural modulation in vivo. In *The Neuroendocrine-Immune Network*, ed. Freier, S., pp. 69–83. Boca Raton: CRC Press.

FERREIRA, S.H., LORENZETTI, B.B., BRISTOW, A.F. & POOLE, S. (1988). Interleukin-1 beta as a potent hyperalgesic agent antagonized by a tripeptide analogue. *Nature*, **334**, 698–700.

FOLLENFANT, R.L., NAKAMURA-CRAIG, M., HENDERSON, B. & HIGGS, G.A. (1989). Inhibition by neuropeptides of interleukin-1β-induced, prostaglandin-independent hyperalgesia. *Br. J. Pharmacol.*, **98**, 41–43.

HANDWERKER, H.O. (1991). What peripheral mechanisms contribute to nociceptive transmission and hyperalgesia? In *Towards a New Pharmacotherapy of Pain*, ed. Basbaum, A.I. & Besson, J.-M. pp. 5–19. Chichester: Wiley.

HOLZER, P. (1988). Local effector functions of capsaicin-sensitive sensory nerve endings: involvement of tachykinins, calcitonin gene-related peptide and other neuropeptides. *Neuroscience*, **24**, 739–768.

HOLZER, P. (1992). Peptidergic sensory neurons in the control of vascular functions: mechanisms and significance in the cutaneous and splanchnic vascular beds. *Rev. Physiol. Biochem. Pharmacol.*, **121**, 49–146.

HOM, J.T., COLE, H., ESTRIDGE, T. & GLISZCZYNSKI, V.L. (1992). Interleukin-1 enhances the development of type II collagen-induced arthritis only in susceptible and not in resistant mice. *Clin. Immunol. Immunopathol.*, **62**, 56–65.

HOWELLS, G.L., CHANTRY, D. & FELDMANN, M. (1988). Interleukin 1 (IL-1) and tumour necrosis factor synergise in the induction of IL-1 synthesis by human vascular endothelial cells. *Immunol. Lett.*, **19**, 169–173.

HUGHES, S.R. & BRIAN, S.D. (1991). A calcitonin gene-related peptide (CGRP) antagonist ($CGRP_{8-37}$) inhibits microvascular responses induced by CGRP and capsaicin in skin. *Br. J. Pharmacol.*, **104**, 738–742.

LIBBY, P., ORDOVAS, J.M., AUGER, K.R., ROBBINS, A.H., BIRINYI, L.K. & DINARELLO, C.A. (1986). Endotoxin and tumor necrosis factor induce interleukin-1 gene expression in adult human vascular endothelial cells. *Am. J. Pathol.*, **124**, 179–185.

LIPPE, I.T. & HOLZER, P. (1992). Participation of endothelium-derived nitric oxide but not prostacyclin in the gastric mucosal hyperaemia due to acid back-diffusion. *Br. J. Pharmacol.*, **105**, 708–714.

LOWENTHAL, J.W., CEROTTINI, J.C. & MACDONALD, H.R. (1986). Interleukin 1-dependent induction of both interleukin 2 secretion and interleukin 2 receptor expression by thymoma cells. *J. Immunol.*, **137**, 1226–1231.

LYNN, B., YE, W. & COTSELL, B. (1992). The actions of capsaicin applied topically to the skin of the rat on C-fibre afferents, antidromic vasodilatation and substance P levels. *Br. J. Pharmacol.*, **107**, 400–406.

MAGGI, C.A. & MELI, A. (1988). The sensory-efferent function of capsaicin-sensitive sensory neurons. *Gen. Pharmacol.*, **19**, 1–43.

MCGILLIS, J.P., MITSUHASHI, M. & PAYAN, D.G. (1990). Immunomodulation by tachykinin neuropeptides. *Ann. New York Acad. Sci.*, **594**, 85–94.

MOCHAN, E., UHL, J. & NEWTON, R. (1986). Evidence that interleukin-1 induction of synovial cell plasminogen activator is mediated via prostaglandin E_2 and cAMP. *Arthritis Rheum.*, **29**, 1078–1084.

MOSKOWITZ, M.A. & BUZZI, M.G. (1991). Neuroeffector functions of sensory fibres: implications for headache mechanisms and drug actions. *J. Neurol.*, **238**, S18–S22.

OBERG, P.A., TENLAND, T. & NILSSON, G.E. (1984). Laser-Doppler flowmetry: a non-invasive and continuous method for blood flow evaluation in microvascular studies. *Acta Med. Scand.*, Suppl. **687**, 17–24.

O'BYRNE, E.M., BLANCUZZI, V., WILSON, D.E., WONG, M. & JENG, A.Y. (1990a). Elevated substance P and accelerated cartilage degradation in rabbit knees injected with interleukin-1 and tumor necrosis factor. *Arthritis Rheum.*, **33**, 1023–1028.

O'BRYNE, E.M., BLANCUZZI, V.J., WILSON, D.E., WONG, M., PEPPARD, J., SIMKE, J.P. & JENG, A.Y. (1990b). Increased intra-articular substance P and prostaglandin E_2 following injection of interleukin-1 in rabbits. *Int. J. Tissue React.*, **12**, 11–14.

O'BYRNE, E.M., BLANCUZZI, V., WILSON, D., WONG, M., PEPPARD, J., SIMKE, J.P. & JENG, A.Y. (1991). Effects of indomethacin, triamcinolone, and dexamethasone on recombinant human interleukin-1-induced substance P and prostaglandin E_2 levels in knee joints. *Agents Actions*, **34**, 46–48.

PETTIPHER, E.R., HIGGS, G.A. & HENDERSON, B. (1986). Interleukin 1 induces leukocyte infiltration and cartilage proteoglycan degradation in the synovial joint. *Proc. Natl. Acad. Sci. U.S.A.*, **83**, 8749–8753.

SCHWEIZER, A., FEIGE, U., FONTANA, A., MULLER, K. & DINARELLO, C.A. (1988). Interleukin-1 enhances pain reflexes. Mediation through increased prostaglandin E_2 levels. *Agents Actions*, **25**, 246–251.

SHARKEY, K.A. (1992). Substance P and calcitonin gene-related peptide (CGRP) in gastrointestinal inflammation. *Ann. New York Acad. Sci.*, **664**, 425–442.

STIMPSON, S.A., DALLDORF, F.G., OTTERNESS, I.G. & SCHWAB, J.H. (1988). Exacerbation of arthritis by IL-1 in rat joints previously injured by peptidoglycan-polysaccharide. *J. Immunol.*, **140**, 2964–2969.

VAN DE LOO, A.A., ARNTZ, O.J. & VAN DEN BERG, W.B. (1992). Flare-up of experimental arthritis in mice with murine recombinant IL-1. *Clin. Exp. Immunol.*, **87**, 196–202.

WHITTLE, B.J.R. & VANE, J.R. (1987). Prostanoids as regulators of gastrointestinal function. In *Physiology of the Gastrointestinal Tract*, ed. Johnson, L.R. Second Edition, Vol. 1, pp. 143–180. New York: Raven Press.

(Received June 28, 1993
Revised October 22, 1993
Accepted November 4, 1993)

Br. J. Pharmacol. (1994), **111**, 687–694 © Macmillan Press Ltd, 1994

Effect of cromakalim and glibenclamide on spontaneous and evoked motility of the guinea-pig isolated renal pelvis and ureter

[1]Carlo Alberto Maggi, Sandro Giuliani & Paolo Santicioli

Pharmacology Department, A. Menarini Pharmaceuticals, Via Sette Santi 2, 50131, Florence, Italy

1 We have investigated the effect of the potassium (K) channel opener, cromakalim, on the spontaneous myogenic activity of the guinea-pig isolated renal pelvis and on myogenic contractions evoked by direct electrical stimulation of the guinea-pig isolated ureter.

2 In the presence of Bay K 8644 (1 μM), electrical stimulation of the guinea-pig ureter (10 Hz for 1 s, pulse width 5 ms, 60 V) produced regular tetrodotoxin-(1 μM) resistant phasic contractions which were suppressed by 3 μM cromakalim. Glibenclamide (0.1–3 μM), 4-aminopyridine (4-AP, 0.1–2 mM) and tetraethylammonium (TEA, 1–10 mM) produced a concentration-dependent inhibition of the effect of cromakalim with the rank order of potency (EC_{50} in parentheses): glibenclamide (0.64 μM)>>4-AP (1.11 mM)>TEA (6.6 mM). Apamin (0.1–0.3 μM) was without effect.

3 Cromakalim (0.1–10 μM) produced concentration-dependent inhibition and suppression of spontaneous contractions of the guinea-pig isolated renal pelvis and of evoked contractions of the ureter with EC_{50} values of 0.71 and 0.47 μM, respectively.

4 Glibenclamide (1 μM) produced a rightward shift of the concentration-response curve to cromakalim in both the renal pelvis and ureter, without producing depression of the maximal inhibitory effect. Glibenclamide did not affect the spontaneous activity of the renal pelvis while it produced a slight enhancement (10–15% increase) of evoked contractions of the ureter. Glibenclamide did not affect the inhibitory action of the adenylate cyclase activator, forskolin, in the renal pelvis or ureter.

5 In electrophysiological experiments (sucrose gap), cromakalim (0.3 and 1 μM) produced hyperpolarization of ureter smooth muscle. Cromakalim also produced a transient suppression of action potentials and accompanying phasic contractions evoked by electrical stimulation. Before suppression of evoked contractions, a shortening of action potential duration was observed concomitant with the developing hyperpolarization produced by cromakalim. A lower concentration (0.1 μM) of cromakalim did not affect membrane potential but shortened action potential duration and reduced the evoked contraction.

6 Glibenclamide (1 μM) inhibited the hyperpolarizing action of cromakalim and prevented its inhibitory action on evoked action potentials and contractions of the ureter. Glibenclamide also produced a slight prolongation of action potential duration and increased the amplitude and duration of the accompanying mechanical response.

7 These findings demonstrate that activation of cromakalim- and glibenclamide-sensitive K channels produces a powerful mechanism for regulation of pyeloureteral motility and suppression of latent pacemakers of the ureter in guinea-pig. Glibenclamide-sensitive K channels take part in determining action potential shape and duration in the guinea-pig ureter.

Keywords: Potassium channels; guinea-pig ureter; electromechanical coupling; guinea-pig renal pelvis; cromakalim; glibenclamide; adenylate cyclase; forskolin

Introduction

Potassium (K) ions play an important role in determining the excitability of smooth muscle cells. Various types of outward K currents occur in smooth muscle, which influence the shape of the action potential, generation of spontaneous activity and the mechanical responses brought about by different stimuli. In the past few years, a number of pharmacological tools has been developed which affect in a selective manner only certain types of K channels (Cook & Quast, 1990). Among these, the development of the benzopyran derivative, BRL 34915, or cromakalim, which acts as a K channel opener, has represented one of the most interesting advances (Hamilton *et al.*, 1986; Weir & Weston, 1986; Quast, 1987). As expected from its agonist action on certain K channels, cromakalim produces smooth muscle hyperpolarization and reduces the probability of the opening of voltage-sensitive calcium channels (Cook & Quast, 1990, for review). These electrophysiological effects determine a remarkable relaxant action on smooth muscles, especially evident when cromakalim is challenged against stimuli which use voltage-dependent calcium channels to produce smooth muscle contraction.

The nature of K channels opened by cromakalim in smooth muscle has been a matter of debate (see Cook & Quast, 1990). In various preparations, the hyperpolarizing action of cromakalim and its smooth muscle relaxant activity are selectively blocked, in a competitive manner, by antidiabetic agents of the sulphonylurea group, such as glibenclamide (Quast & Cook, 1988; Wilson, 1989; Standen *et al.*, 1989). These findings support the idea that the K channel activated by cromakalim in smooth muscle could be an ATP-sensitive K channel, similar to that regulating insulin secretion, although the pharmacology of the ATP-sensitive K channels in smooth muscle and the peripheral nervous system may not be identical to that of the pancreatic and cardiac ATP-sensitive K channels (e.g. Zini *et al.*, 1991; Takano & Noma, 1993).

[1] Author for correspondence.

The smooth muscle relaxant activity of cromakalim has been documented in the urinary bladder from various species: at this level, cromakalim stimulates K efflux, produces hyperpolarization and reduces the spontaneous and stimulated activity of urinary bladder smooth muscle (Foster *et al.*, 1989; Fujii *et al.*, 1990; Grant & Zuzack, 1991). ATP-sensitive K channels activated by cromakalim and blocked by glibenclamide have recently been described in the guinea-pig urinary bladder (Bonev & Nelson, 1993). On the basis of these results, a possible therapeutic use of K channel openers in the treatment of motility disorders of the urinary tract has been suggested. However, the possible action of cromakalim on motility of the upper urinary tract has not been investigated. Since the activation of voltage-dependent calcium channels is very important for regulation of pyeloureteral motility (Weiss, 1992 for review), a powerful action of K channel openers at this level may be expected.

The aim of the present study was to evaluate the effect of cromakalim and glibenclamide, on the motility of the guinea-pig upper urinary tract. In a first series of experiments, we evaluated the effect of cromakalim on evoked contractions of the guinea-pig ureter and spontaneous contractions of the guinea-pig isolated renal pelvis. In a second series, the electrophysiological effect of cromakalim on membrane potential and evoked action potentials of the guinea-pig ureter were investigated by a sucrose gap technique.

Methods

Male albino guinea-pigs weighing 250–300 g were stunned and bled. The renal pelvis and ureter (from the inferior renal pole to its entry into the bladder) were excised, cleaned of adhering fat and connective tissue and placed in oxygenated and warmed (95% O_2 and 5% CO_2, pH 7.4 at 37°C) Krebs solution which was used in all experiments. Krebs solution had the following composition (mmol l^{-1}): NaCl 119, $NaHCO_3$ 25, KH_2PO_4 1.2, $MgSO_4$ 1.5, KCl 4.7, $CaCl_2$ 2.5 and glucose 11. Since experiments performed in the ureter required the application of pulses of electrical stimulation to evoke action potentials (see sucrose gap experiments) and contractions, and because of the existence of a capsaicin-sensitive inhibitory innervation of the guinea-pig ureter (Maggi & Giuliani, 1991), all experiments were performed in capsaicin-pretreated ureters to eliminate this neural inhibitory influence on ureteral excitability. With this aim, the ureters were incubated for 15 min in Krebs solution containing 10 μM capsaicin: this *in vitro* capsaicin desensitization technique has been shown to produce blockade of neuropeptide release from capsaicin-sensitive primary afferents in the guinea-pig ureter (Maggi & Giuliani, 1991).

Organ bath experiments

The renal pelvis, cleaned of adhering tissue, was opened, connected to silk threads and mounted in a 5 ml organ bath for isotonic recording (load 2 mN) of mechanical activity along its circular axis, as described previously (Maggi & Giuliani, 1992). The ureter was placed in a Petri dish, a segment about 2 cm long was excised from its middle portion and the specimen was mounted in a 5 ml organ bath for isotonic recording (load 3 mN) of mechanical activity along its longitudinal axis, as described previously (Maggi & Giuliani, 1991).

In the ureter, the effect of cromakalim on phasic contractions produced by electrical depolarization of smooth muscle was investigated: with this aim, trains of pulses (10 Hz for 1 s, 60 V) of long width (5 ms) were delivered automatically at 1 min intervals by means of platinum wire electrodes placed at the top and bottom of the organ bath (field stimulation) by means of a GRASS S88 stimulator. We found that the mechanical response produced by electrical field stimulation in these conditions undergoes a progressive fading and becomes irregular during prolonged periods of stimulation; addition of the calcium channel agonist, Bay K 8644 (1 μM) produced a prompt enhancement of the evoked response which then remains regular for several hours, enabling pharmacological analysis of drug action.

In a first series of experiments a concentration of cromakalim (3 μM) which invariably produces total suppression of evoked contractions of the ureter, was used to analyse the effect of potassium channel blockers on the response to cromakalim. The K channel blockers, glibenclamide, 4-aminopyridine (4-AP), tetraethylammonium (TEA) or apamin were added to the bath when the amplitude of the evoked contractions had reached a steady state and their effect was observed for 15 min or until a steady state had been reached. At this time, cromakalim (3 μM) was added to the bath.

In a second series of experiments a cumulative concentration-response curve to cromakalim was produced, the next concentration being added when the effect of the preceding one had reached a steady state. Cumulative response-curves to the adenylate cyclase activator, forskolin, were produced in the same manner. The effect of glibenclamide on the curve to cromakalim was determined after 15 min contact time.

In the spontaneously active renal pelvis preparation, cumulative concentration-response curves to cromakalim and forskolin were produced, in the absence or presence of glibenclamide, as described above for the ureter. In the renal pelvis, the effect of cromakalim was evident either as a progressive reduction in the amplitude of contractions with minor effect on frequency until suppression of contractility or as a mixed inhibitory effect on frequency and amplitude of contraction until suppression. In the latter case, the inhibitory effect of cromakalim on the amplitude of contraction was relatively minor (< 50% inhibition) until suppression of spontaneous contractions occurred. For this reason a motility index (arbitrary units) was calculated in each preparation by multiplying the frequency of spontaneous contractions (contraction min^{-1}) and their amplitude (in mm of chart); the inhibitory effect of cromakalim was calculated as % inhibition of the basal motility index.

Sucrose gap experiments

Male albino guinea-pigs (250–300 g) were stunned and bled. The ureters were excised and placed in oxygenated (95% O_2 and 5% CO_2) Krebs solution. A single sucrose-gap, modified as described in details by Artemenko *et al.* (1982) and Hoyle (1987) was used to investigate changes in membrane potential and mechanical activity in response to electrical stimulation. The ureters were superfused with oxygenated Krebs solution at a rate of 1 ml min^{-1}. The temperature of the solution was kept constant at 35 ± 0.5°C.

Electrical field stimulation with single pulses using parameters sufficient to produce direct excitation of smooth muscle (50–60 V, 2–5 ms pulse width) evoked an action potential and accompanying contraction of the guinea-pig ureter, as described in a number of previous studies. We found that electrical and mechanical responses evoked in this way need quite a long interstimulus interval to be consistently reproduced over the long periods of time required for a pharmacological analysis of drug action. This phenomenon has been referred to as the 'refractory period' of the ureter (e.g. Cuthbert, 1965). We found that *in vitro* capsaicin pretreatment (10 μM for 20 min) to eliminate the CGRP-mediated inhibitory innervation (cf. Maggi & Giuliani, 1991) and addition of the calcium channel agonist, Bay K 8644 (1 μM) both exert a favourable effect on the reproducibility of the electrical and mechanical responses of the guinea-pig ureter (Maggi, Giuliani & Santicioli, unpublished observations).

Cromakalim was applied in the superfusion fluid for 4 min. Glibenclamide was superfused for 15 min before application

of cromakalim, this contact time being sufficient to produce maximal effects on the action potential of the guinea-pig ureter. In some experiments, glibenclamide was applied to preparations which had not been exposed to cromakalim: in these experiments glibenclamide produced effects on the action potential of the guinea-pig ureter which were similar to those observed in the remainders and the pooled data of the experiments are presented in the Results section. In a few experiments, the effect of cromakalim and glibenclamide were assessed on preparations not subjected to electrical stimulation.

Statistical analysis

Each value is mean ± s.e. of the mean. Statistical analysis was performed by means of Student's t test or by means of analysis of variance, when appropriate. Linear regression was performed by the least squares method: EC_{50} and 95% confidence limits were calculated accordingly.

Drugs

Drugs used were: cromakalim (Beecham), nifedipine, glibenclamide, forskolin, capsaicin and 4-aminopyridine (Sigma), tetrodotoxin (Sankyo), tetraethylammonium (Serva), apamin (Peninsula), Bay K 8644 (methyl-1,4-dihydro-2,6-dimethyl-3-nitro-4-(2-trifluoromethylphenyl)-pyridine-5-carboxylate, Calbiochem).

Results

Guinea-pig ureter

The unstimulated guinea-pig isolated ureter is mechanically quiescent. Phasic contractions were produced by electrical field stimulation with train of pulses (10 Hz, 60 V, 5 ms pulse width for 1 s every 60 s, Figure 1). The phasic contractions evoked under these experimental conditions (capsaicin pretreatment, Bay K 8644 1 μM in the bath) are tetrodotoxin-(1 μM) resistant indicating that they depend upon direct activation of smooth muscle cells and are abolished by 10–30 μM nifedipine ($n = 4$) showing the involvement of voltage-dependent calcium channels.

Cromakalim (3 μM) produced a prompt suppression of evoked contractions of the guinea-pig ureter. This effect was concentration-dependently prevented (Figure 2) by glibenclamide (EC_{50} 0.64 μM, 95% c.l. 0.50–0.72 μM), 4-AP (EC_{50} 1.11 mM, 1.05–1.45 mM) and TEA (EC_{50} 6.6 mM, 3.5–36 mM). Glibenclamide, 4-AP and TEA also enhanced the amplitude of evoked ureteral contractions but the degree of enhancement was barely correlated with the extent of inhibition of the suppressive action of 3 μM cromakalim: the amplitude of evoked ureteral contractions was enhanced by 8 ± 2, 14 ± 3 and 14 ± 4% following 0.3, 1 and 3 μM glibenclamide, respectively ($n = 4–7$ for each concentration tested); by 5 ± 1, 10 ± 2, 14 ± 4 and 36 ± 5% following 0.1, 0.5, 1 and 2 mM 4-AP, respectively ($n = 4–6$); by 11 ± 2, 39 ± 6, 62 ± 13 and 82 ± 7% following 1, 2, 5 and 10 mM TEA, respectively ($n = 4–6$). Apamin (0.1–0.3 μM, $n = 4$) had no consistent effect on the amplitude of evoked contractions nor on the inhibitory action of 3 μM cromakalim.

Cromakalim (0.1–3 μM) produced a concentration-dependent inhibition and eventually suppressed the evoked contractions of the guinea-pig ureter (Figures 1 and 3). The EC_{50} was 0.47 μM (0.18–0.90 μM). The inhibitory effect of cromakalim was promptly reversed by washing or by addition of 1 μM glibenclamide (Figure 1). Glibenclamide (1 μM) produced a slight and steady enhancement of evoked contractions to 109 ± 2% of control value (Figure 1): although quantitatively small, this effect was consistently observed in all preparations tested ($n = 8$) and was statistically significant ($P < 0.05$). In the presence of glibenclamide, the concentration-dependent inhibitory effect of cromakalim was shifted rightward without depression of the maximal inhibitory effect attainable, i.e. a pattern consistent with competitive antagonism (Figure 3, Table 1).

Forskolin produced a concentration-dependent inhibition of evoked contractions of the guinea-pig ureter (Figure 3, Table 1): the maximal inhibitory effect averaged 57 ± 6%

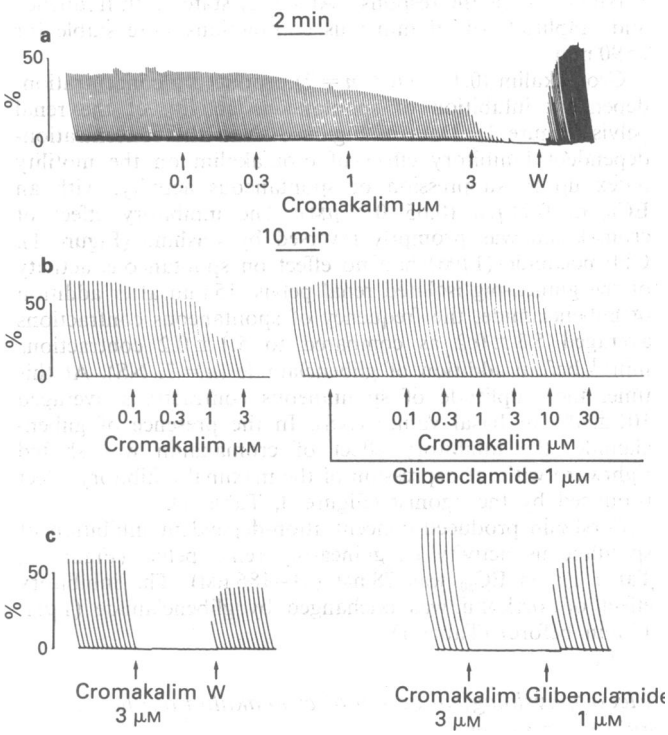


Figure 1 (a) Concentration-dependent inhibition by cromakalim of spontaneous activity of the guinea-pig isolated renal pelvis and reversal by washing (W). (b) Concentration-dependent inhibition by cromakalim of electrically-evoked contractions of the guinea-pig isolated ureter in the absence (left) and presence (right) of glibenclamide. Note that glibenclamide produced a small enhancement in amplitude of the evoked contractions. (c) Suppression by 3 μM cromakalim of electrically-evoked contractions of the guinea-pig isolated ureter and reversal of cromakalim inhibition by washing (W, left) and glibenclamide (right). In all panels, vertical bars indicate % of maximal contractile response to 80 mM KCl.

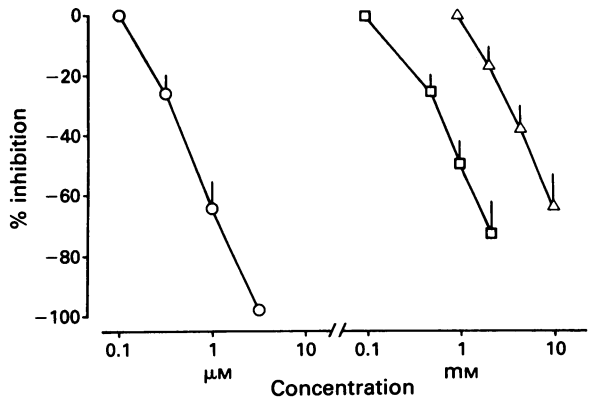


Figure 2 Concentration-dependent inhibition by glibenclamide (○), 4-aminopyridine (□) and tetraethylammonium (△) of the effect of cromakalim (3 μM) on electrically-evoked contractions of the guinea-pig isolated ureter. Each value is the mean ± s.e.mean of 4–7 experiments.

inhibition and its EC_{50} was 0.38 μM (0.11–3.2 μM). Glibenclamide (1 μM) did not significantly affect the inhibitory action of forskolin (Figure 3, Table 1).

Guinea-pig renal pelvis

The guinea-pig isolated renal pelvis showed spontaneous mechanical activity at a frequency of 4–7 contractions min^{-1} (Figure 1). At steady state (30–60 min from setup), the amplitude of spontaneous contractions averaged about 50% of maximal contractile response. At steady state, both frequency and amplitude of spontaneous contractions were stable for >90 min.

Cromakalim (0.1–10 μM, $n = 7$) produced a concentration-dependent inhibition of spontaneous activity of the renal pelvis (Figure 1). Data in Figure 3 show the concentration-dependent inhibitory effect of cromakalim on the motility index up to suppression of spontaneous activity, with an EC_{50} of 0.71 μM (0.65–0.75 μM). The inhibitory effect of cromakalim was promptly reversed by washing (Figure 1). Glibenclamide (1 μM) had no effect on spontaneous activity of the guinea-pig isolated renal pelvis: 15 min after addition of glibenclamide, the frequency of spontaneous contractions averaged 5.3 ± 0.2 as compared to 5.1 ± 0.2 contractions min^{-1} before addition of glibenclamide ($n = 7$, NS). At this time, the amplitude of spontaneous contractions averaged 101 ± 4% of basal values (NS). In the presence of glibenclamide, the inhibitory effect of cromakalim was shifted rightward without depression of the maximal inhibitory effect produced by the agonist (Figure 3, Table 1).

Forskolin produced concentration-dependent inhibition of spontaneous activity of guinea-pig renal pelvis (Figure 3, Table 1): its EC_{50} was 78 nM (41–186 nM). The inhibitory effect of forskolin was unchanged by glibenclamide (1 μM, 15 min before) (Table 1).

Electrophysiological action of cromakalim on the guinea-pig ureter

The effects of cromakalim and glibenclamide have been investigated in capsaicin-pretreated ureters and in the presence of 1 μM Bay K 8644: in these conditions, electrical stimulation with single shocks at 50–60 V and pulse width of 2–5 ms automatically delivered at 60 s intervals evoked reproducible electrical and mechanical responses (Figure 4a).

The action potential of the ureter elicited under these experimental conditions is characterized by a rapidly rising depolarization followed by a plateau with superimposed oscillations, repolarization and slight after-hyperpolarization (Figure 5). Quantitative data on action potential and accompanying contraction are given in Table 2.

Cromakalim (0.1 μM, applied by superfusion for 4 min, $n = 4$) did not affect membrane potential but produced a shortening (24% reduction) of action potential duration (from 1742 ± 220 to 1333 ± 210 ms, effect measured at 5 min from start of superfusion with cromakalim) without affecting the amplitude of the action potential (8.4 ± 1.3 and 8.8 ± 1.4 mV before and after cromakalim, respectively). The accompanying phasic contraction was slightly reduced (– 10%) in amplitude (from 3.9 ± 0.1 to 3.5 ± 0.09 mN) and shortened (– 22%) in duration (from 2071 ± 280 to 1612 ± 150 ms).

At higher concentrations (0.3–1 μM) cromakalim produced various effects (Figures 4, 5 and 6), summarized as follows: (a) hyperpolarization of the smooth muscle which averaged

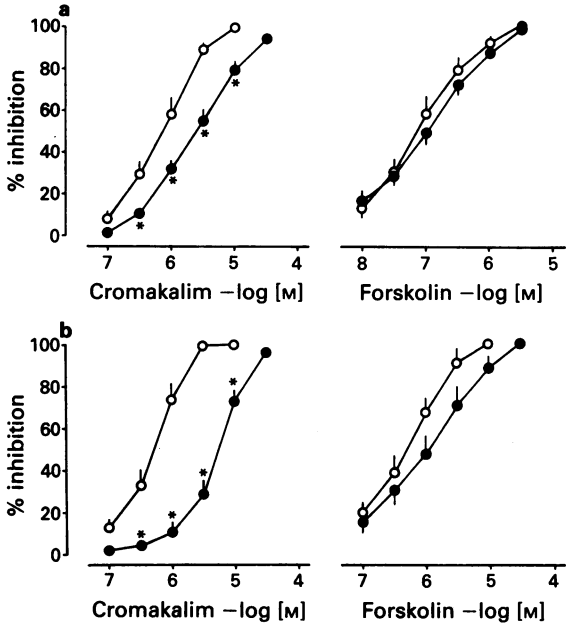


Figure 3 Concentration-dependent inhibition by cromakalim (left panels) and forskolin (right panels) of spontaneous activity of the guinea-pig isolated renal pelvis (a) and electrically-evoked contractions of the guinea-pig isolated ureter (b) in the absence (○) and presence (●) of glibenclamide. Each value is the mean ± s.e.mean of 6–8 experiments. *Significantly different from control, $P < 0.05$.

Table 1 EC_{50} (95% c.l. in brackets) of cromakalim and forskolin for inhibition of spontaneous (renal pelvis) and evoked (ureter) contractions of the guinea-pig pyeloureteral system in the absence and presence of glibenclamide (1 μM 15 min beforehand)

Guinea-pig renal pelvis	*Control*		*Glibenclamide* (1 μM)	
	EC_{50}	E_{max} (% inhibition)	EC_{50}	E_{max} (% inhibition)
Cromakalim	0.71 μM (0.65–0.75)	100	2.36 μM* (2.15–2.66)	100
Forskolin	78 nM (41–186)	100	93 nM (53–180)	100
Guinea-pig ureter	*Control*		*Glibenclamide* (1 μM)	
	EC_{50}	E_{max} (% inhibition)	EC_{50}	E_{max} (% inhibition)
Cromakalim	0.47 μM (0.18–0.90)	100	5.07 μM* (1.1–8.8)	100
Forskolin	0.38 μM (0.11–3.2)	57 ± 6	1.32 μM (1.2–1.4)	56 ± 6

*Significantly different from EC_{50} value recorded in the absence of glibenclamide. Each value is the mean of 6–8 experiments.

1.36 ± 0.16 and 1.85 ± 0.15 mV at 0.3 and 1 μM, respectively ($n = 8$); hyperpolarization produced by cromakalim developed fully in 4–6 min and recovered following washout; (b) the hyperpolarization was followed by progressive reduction in the duration of the action potential plateau and decrease in contraction amplitude (Figure 5); this inhibitory effect led to suppression of the action potential and accompanying contraction; both electrical and mechanical responses recovered following washout of cromakalim; after application of 0.3 and 1 μM cromakalim the evoked action potentials and contractions were suppressed for 2 ± 0.6 and 8 ± 2 min, respectively ($n = 8$).

Glibenclamide (1 μM, superfused for 15 min, $n = 10$) did not produce consistent changes of membrane potential: a slight depolarization was observed in 5 cases, a slight hyperpolarization in 2 cases and no change in 3 cases. Glibenclamide produced a slight but significant ($P < 0.05$) prolongation of action potential duration (20% increase), increased the number of spikes, amplitude (9% increase) and duration (15% increase) of accompanying contraction (Table 2, Figure 7). A shortening in the delay between stimulus application and onset of the action potential and an increased afterhyperpolarization were also observed in some preparations after glibenclamide (Figure 7), but these effects were not consistently observed in all preparations tested and did not reach statistical significance (Table 2).

In the presence of glibenclamide (1 μM, 15 min before), the hyperpolarizing action of cromakalim (0.3–1 μM) on membrane potential and the inhibitory effects on evoked action potential and contraction were significantly reduced; (Table 3, Figure 6). The inhibition by glibenclamide was overcome when a larger concentration of cromakalim (10 μM) was tested (Figure 6 and Table 3).

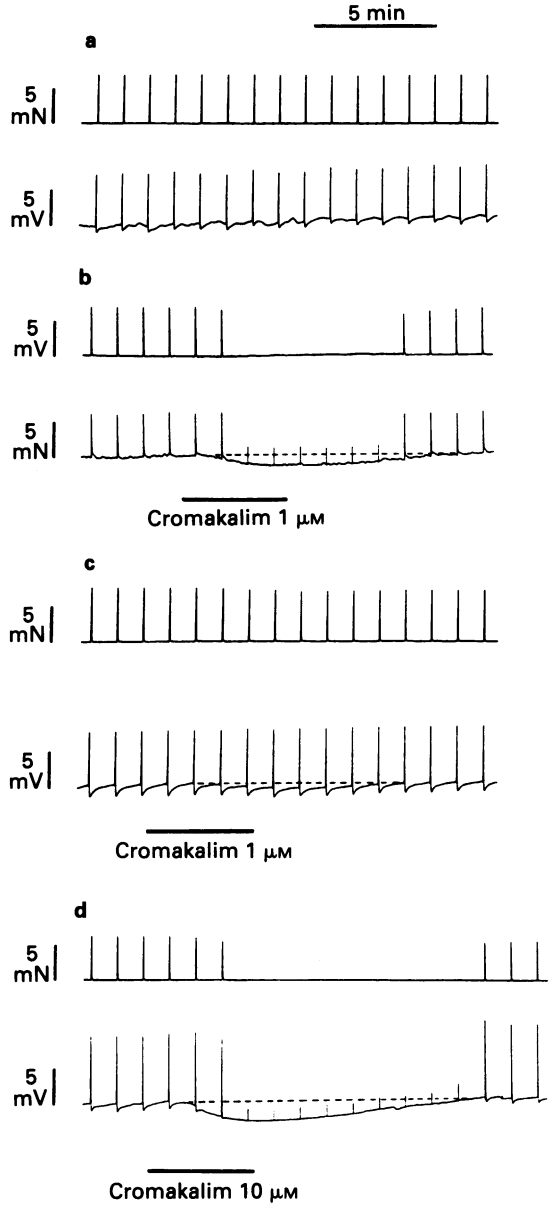


Figure 4 Electrical and mechanical activity of the guinea-pig isolated ureter evoked by electrical stimulation (sucrose gap recording). In capsaicin pretreated ureters and in the presence of Bay K 8644, electrical stimuli applied at intervals of 60 s produced regular action potentials (lower tracing in each panel) and accompanying phasic contractions of the ureter (upper tracing in each panel). (a) Shows reproducibility of the evoked responses. Cromakalim (b) produced hyperpolarization and suppression of evoked action potentials and contractions (the small upward deflections remaining during cromakalim action are artifacts of the stimulus). In the presence of glibenclamide (c and d) the hyperpolarization produced by 1 μM cromakalim and its inhibitory action on evoked action potentials and contractions were inhibited (c) but the inhibitory effect of glibenclamide was overcome by using a larger concentration of cromakalim (10 μM, d).

Discussion

The present findings demonstrate that the K channel opener, cromakalim, inhibits the contractile activity of the guinea-pig isolated renal pelvis and ureter at concentrations comparable to those found effective in other studies on vascular and nonvascular smooth muscles (e.g. Buckingham *et al.*, 1989;

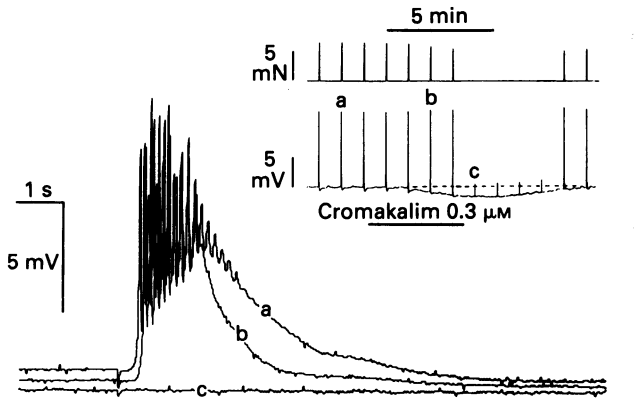


Figure 5 Superimposed tracings showing the reduction of action potential duration during the developing hyperpolarization produced by cromakalim in the guinea-pig ureter. Tracing (a) is control action potential; tracing (b) was obtained at 3 min after start of superfusion with 0.3 μM cromakalim; tracing (c) was obtained at 5 min from start of superfusion with cromakalim. The superimposed action potentials recorded in (a), (b) and (c) are shown in the inset at a low chart speed along with the accompanying mechanical response of the ureter.

Table 2 Membrane hyperpolarization produced by cromakalim in the guinea-pig ureter in the absence and presence of glibenclamide (1 μM, 15 min beforehand)

		Membrane hyperpolarization (mV)	
		Control	*After glibenclamide*
Cromakalim	0.3 μM	1.36 ± 0.16	0.40 ± 0.13*
	1.0 μM	1.85 ± 0.15	0.92 ± 0.13*
	10 μM	not tested	2.18 ± 0.34

Each value is mean ± s.e.mean of 4–8 experiments.
*Significantly different from control values, $P < 0.05$.

Foster et al., 1989; Fujii et al., 1990). Since the spontaneous activity of the renal pelvis and the electrically-evoked contractions of the ureter are highly if not exclusively dependent on activation of voltage-sensitive calcium channels (Shuba, 1977; Brading et al., 1983; Weiss, 1992 for review), we reasoned that cromakalim should exert a powerful suppressant activity on smooth muscle of the pyeloureteral complex. In both preparations, the contractile activity is abolished by nifedipine indicating the absolute requirement for activation of L-type voltage-sensitive calcium channels. In the ureter, relatively high (10–30 μM) concentrations of nifedipine were required to abolish contractility because of the presence of Bay K 8644 which was added to provide the regular and reproducible responses necessary for pharmacological analysis of the inhibitory action of cromakalim. Since cromakalim produces hyperpolarization of smooth muscles, including that of the urinary bladder (Foster et al., 1989; Fujii et al., 1990), its inhibitory activity in the pyeloureteral smooth muscle may be explained through a similar mechanism. This conclusion is supported by electrophysiological analysis of cromakalim action in the guinea-pig ureter, where developing hyperpolarization by cromakalim first produced a shortening of action potential duration and eventually suppressed the evoked electrical and mechanical activity. At 0.1 μM, cromakalim produced a small shortening of action potential duration and decreased the evoked contraction without producing overt changes of resting membrane potential. This effect is quite similar to that produced by nifedipine at low concentrations which do not abolish the action potential of the ureter (unpublished observations). Although cromakalim at high concentrations may possess calcium channel blocking properties (for e.g. 3–30 μM, Okabe et al., 1990), the present experiments have been performed in the presence of Bay K 8644 and it appears unlikely that direct blockade of calcium channels accounts for the reduced duration of action potential duration produced by 0.1 μM cromakalim. We speculate that the K channel agonist action of cromakalim may have been insufficient to produce membrane hyperpolarization at resting membrane potential but could have been efficient at the level of membrane potential attained during the plateau of the action potential.

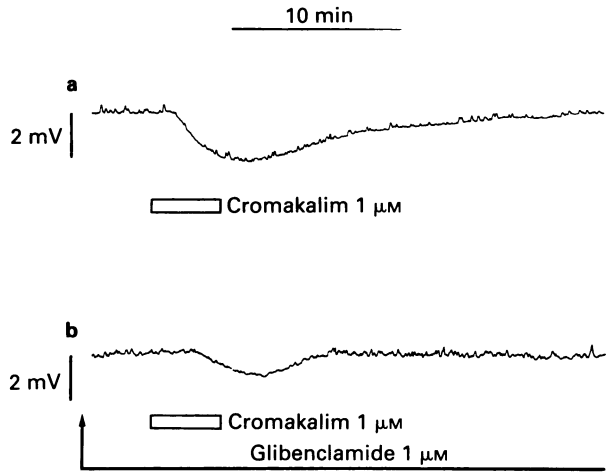


Figure 6 Membrane hyperpolarization produced by 1 μM cromakalim in the guinea-pig ureter (a) and its antagonism by 1 μM glibenclamide (b).

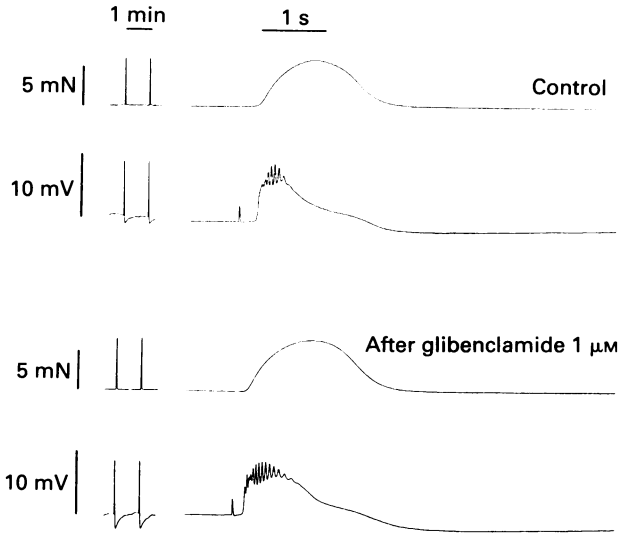


Figure 7 Effect of 1 μM glibenclamide on action potential and accompanying contraction produced by electrical stimulation of the guinea-pig ureter. The effect of glibenclamide is shown after 15 min superfusion with the drug. See text for details.

Although the nature of K channels activated by cromakalim in smooth muscle may not be identical to the ATP-dependent K channels regulating insulin secretion in the pancreas, the hyperpolarizing action and smooth muscle relaxant properties of cromakalim are sensitive to the inhibitory action of the sulphonylurea-type antidiabetics like glibenclamide (e.g. Buckingham et al., 1989; Cavero et al., 1989; Quast & Cook, 1989; Standen et al., 1989), including its actions on the guinea-pig urinary bladder smooth muscle (Fujii et al., 1990; Grant & Zuzack, 1991).

The present findings demonstrate that a similar mechanism occurs in the guinea-pig pyeloureteral system, based on the following results: (a) the inhibitory effect of cromakalim on motility of the renal pelvis and ureter was antagonized by glibenclamide in a manner consistent with competitive antagonism at a common target of action; (b) TEA and 4-AP were much weaker antagonists of the action of cromakalim as compared to glibenclamide (cf. Wilson et al., 1988; Winquist et al., 1989); (c) the antagonism by glibenclamide is selective because the depression of contractility produced by forskolin, a well known activator of adenylate cyclase

Table 3 Effect of glibenclamide (1 μM for 15 min) on action potential and contraction of the guinea-pig ureter

Action potential		*Control*	*After glibenclamide*
Delay	(ms)	172 ± 34	140 ± 30
Amplitude	(mV)	9.61 ± 0.7	9.05 ± 0.7
Duration	(90%, ms)	1431 ± 118	1821 ± 135 *
Afterhyperpolarization	(mV)	0.92 ± 0.14	1.19 ± 0.20
Contraction			
Amplitude	(mN)	4.52 ± 0.53	4.92 ± 0.61*
Duration	(90%, ms)	1953 ± 114	2240 ± 1.92*

Each value is mean ± s.e.mean of 8 determinations.
*Significantly different from control, $P<0.05$.

(Seamon *et al.*, 1981), was unaffected by glibenclamide; (d) the antagonism by glibenclamide of hyperpolarization of the ureter produced by cromakalim was overcome by increasing the concentration of cromakalim.

Interestingly, forskolin was unable to suppress totally the evoked contractions of the ureter, while it effectively abolished spontaneous mechanical activity of the renal pelvis. In contrast, cromakalim abolished spontaneous and evoked activity in the two preparations. Since forskolin reportedly blocks various types of K channels (Cook & Quast, 1990 for review), and K channel blockers (glibenclamide, TEA and 4-AP) enhance evoked ureteral contractions, it may be argued that the relaxant action of forskolin in the ureter could be counteracted by its K channel blocking activity, leading to an incomplete suppression of evoked motility. However, isoprenaline was similarly unable to totally suppress evoked contractions of the ureter under comparable experimental conditions (unpublished observations).

A somewhat unexpected finding of this study was the prolongation of action potential and enhancement of evoked contractility produced by glibenclamide in the guinea-pig ureter. Although quantitatively small, these effects were consistenly observed in all preparations tested. According to previous studies on mechanisms regulating the shape and duration of the action potential of the guinea-pig ureter (Shuba, 1977) the effect of glibenclamide would be consistent with a blockade of K channels. Although glibenclamide, even at high concentrations, does not affect electrical and mechanical activity of smooth muscles in general (e.g. Buckingham *et al.*, 1989, rat aorta and portal vein; Katayama *et al.*, 1993, guinea-pig stomach), previous studies have reported an increase in spontaneous mechanical activity (Fujii *et al.*, 1990) and membrane depolarization (Seki *et al.*, 1992) by 0.5–1 μM glibenclamide in the smooth muscle of the guinea-pig urinary bladder. These findings raise the possibility that glibenclamide-sensitive K channels play a role in determining action potential shape and duration in the guinea-pig ureter.

Blockade of calcium- and voltage-dependent K currents is likely to explain the enhancement of ureteral contractions produced by TEA and 4-AP, respectively. In fact, two major outward currents have been detected in ureter smooth muscle, a calcium-dependent K current which is blocked by TEA and a voltage-dependent A-current which is blocked by 4-AP (Imaizumi *et al.*, 1989; 1990; Lang, 1989). Although glibenclamide is remarkably selective in blocking the ATP-sensitive K channels (Cook & Quast, 1990), a few reports have described a blocking action on certain voltage-gated K currents in neuronal cells (Reeve *et al.*,1992; Crepel *et al.*, 1993) and this may explain the effect of glibenclamide on the action potential and contractility of the guinea-pig ureter.

In conclusion, the present findings demonstrate that cromakalim produces a powerful suppression of spontaneous and evoked contractility of the guinea-pig isolated renal pelvis and ureter, which is sensitive to blockade by glibenclamide. Since the motility of the pyeloureteral system is highly dependent upon activation of voltage-dependent calcium channels, the hyperpolarizing action produced by activation of cromakalim- and glibenclamide-sensitive K channels provides a powerful mechanism for regulating ureteral peristalsis. It is an important topic for future studies to assess whether mediators or transmitters present in the ureter may use this mechanism for producing inhibition of ureteral motility and suppression of latent pacemakers.

References

ARTEMENKO, D.P., BURY, V.A., VLADIMIROVA, I.A. & SHUBA, M.F. (1982). Modification of the single sucrose-gap method. *Physiol. Zhurn.*, **28,** 374–380.

BONEV, A.D. & NELSON, M.T. (1993). ATP-sensitive potassium channels in smooth muscle cells from guinea-pig urinary bladder. *Am. J. Physiol.*, **264,** C1190–C1200.

BRADING, A.F., BURDYGA, TH.V. & SCRIPNYUK, Z.D. (1983). The effects of papaverine on the electrical and mechanical activity of the guinea-pig ureter. *J. Physiol.*, **334,** 79–89.

BUCKINGHAM, R.E., HAMILTON, T.C., HOWLETT, D.R., MOOTOO, S. & WILSON, C. (1989). Inhibition by glibenclamide of the vasorelaxant action of cromakalim in the rat. *Br. J. Pharmacol.*, **97,** 57–64.

CAVERO, I., MONDOT, S. & MESTRE, M. (1989). Vasorelaxant effects of cromakalim in rats are mediated by glibenclamide-sensitive potassium channels. *J. Pharmacol. Exp. Ther.*, **248,** 1261–1268.

COOK, N.S. & QUAST, U. (1990). Potassium channel pharmacology. In *Potassium Channels.* ed. Cook, N.S. pp. 181–258. Chichester, England: Ellis Horwood Series in Pharmaceutical Technology.

CREPEL, V.,, KRNJEVIC, K. & BEN-ARI, Y. (1993). Sulphonylureas reduce the slowly inactivating D-type outward current in rat hippocampal neurons. *J Physiol.*, **466,** 39–54.

CUTHBERT, A.W. (1965). The relation between response and the interval between stimuli of the isolated guinea-pig ureter. *J. Physiol.*, **180,** 225–238.

FOSTER, C.D., FUJII, K., KINGDON, J. & BRADING, A.F. (1989). The effect of cromakalim on the smooth muscle of the guinea-pig urinary bladder. *Br. J. Pharmacol.*, **97,** 281–291.

FUJII, K., FOSTER, C.D., BRADING, A.F. & PAREKH, A.B. (1990). Potassium channel blockers and the effects of cromakalim on the smooth muscle of the guinea-pig bladder. *Br. J. Pharmacol.*, **99,** 779–785.

GRANT, T.L. & ZUZACK, J.S. (1991). Effects of K channel blockers and cromakalim (BRL 34915) on the mechanical activity of guinea-pig detrusor smooth muscle. *J. Pharmacol. Exp. Ther.*, **259,** 1158–1164.

HAMILTON, T.C., WEIR, S.W. & WESTON, A.H. (1986). Comparison of the effects of BRL 34915 and verapamil on electrical and mechanical activity in rat portal vein. *Br. J. Pharmacol.*, **88,** 103–111.

HOYLE, C.H.V. (1987). A modified single sucrose gap – junction potentials and electrotonic potentials in gastrointestinal smooth muscle. *J. Pharmacol. Methods*, **18,** 219–226.

IMAIZUMI, Y., MURAKI, K. & WATANABE, M. (1989). Ionic currents in single smooth muscle cells from the ureter of the guinea-pig. *J. Physiol.*, **411,** 131–159.

IMAIZUMI, Y., MURAKI, K. & WATANABE, M. (1990). Characteristics of transient outward currents in single smooth muscle cells from the ureter of the guinea-pig. *J. Physiol.*, **427,** 301–324.

KATAYAMA, N., HUANG, S.M., TOMITA, T. & BRADING, A.F. (1993). Effects of cromakalim on the electrical slow wave in the circular muscle of the guinea-pig gastric antrum. *Br. J. Pharmacol.*, **109,** 1097–1100.

LANG, R.J. (1989). Identification of the major membrane currents in freshly dispersed single smooth muscle cells of guinea-pig ureter. *J. Physiol.*, **412,** 375–395.

MAGGI, C.A. & GIULIANI, S. (1991). The neurotransmitter role of CGRP in the rat and guinea-pig ureter: effect of a CGRP antagonist and species-related differences in the action of omega conotoxin on CGRP release from primary afferents. *Neuroscience*, **43,** 261–271.

MAGGI, C.A. & GIULIANI, S. (1992). Nonadrenergic noncholinergic excitatory innervation of the guinea-pig isolated renal pelvis: involvement of capsaicin-sensitive primary afferent neurons. *J. Urol.*, **147,** 1394–1397.

OKABE, K., KAJIOKA, S., NAKAO, K., KITAMURA, K., KURIYAMA, H. & WESTON, A.H. (1990). Actions of cromakalim on ionic currents recorded from single smooth muscle cells of the rat portal vein. *J. Pharmacol. Exp. Ther.*, **252,** 832–839.

QUAST, U. (1987). Effect of the K efflux stimulating vasodilator BRL 34915 on ^{86}Rb efflux and spontaneous activity in guinea-pig portal vein. *Br. J. Pharmacol.*, **91,** 569–578.

QUAST, U. & COOK, N.S. (1988). Potent inhibitors of the effects of the K channel opener, BRL 34915 in vascular smooth muscle. *Br. J. Pharmacol.*, **93,** 204P.

QUAST, U. & COOK, N.S. (1989). In vitro and in vivo comparison of two K channel openers diazoxide and cromakalim and their inhibition by glibenclamide. *J. Pharmacol. Exp. Ther.*, **250,** 261–271.

REEVE, H.L., VAUGHAN, P.F.T. & PEERS, C. (1992). Glibenclamide inhibits a voltage-gated K current in the human neuroblastoma cell line SH-SY5Y. *Neurosci. Lett.*, **135**, 37–40.

SEAMON, K.B., PADGETT, W. & DALY, J.W. (1981). Forskolin: unique diterpene activator of adenylate cyclase in membranes and intact cells. *Proc. Natl. Acad. Sci. U.S.A.*, **78**, 3363–3367.

SEKI, N., KARIM, O.M.A. & MOSTWIN, J.L. (1992). Effect of pinacidil on the membrane electrical activity of guinea-pig detrusor muscle. *J. Pharmacol. Exp. Ther.*, **263**, 816–822.

SHUBA, M.F. (1977). The effect of sodium-free and potassium-free solutions ionic current inhibitors and ouabain on electrophysiological properties of smooth muscle of the guinea-pig ureter. *J. Physiol.*, **264**, 837–851.

STANDEN, N.B., QUAYLE, J.M., DAVIES, N.W, BRAYDEN, J.E., HUANG, Y. & NELSON, M.T. (1989). Hyperpolarizing vasodilators activate ATP-sensitive K channels in arterial smooth muscle. *Science*, **245**, 177–180.

TAKANO, M. & NOMA, A. (1993). The ATP-sensitive K channel. *Prog. Neurobiol.*, **41**, 21–30.

WEIR, S.W. & WESTON, A.H. (1986). The effects of BRL 34915 and nicorandil on electrical and mechanical activity and on 86Rb efflux in rat blood vessels. *Br. J. Pharmacol.*, **88**, 121–128.

WEISS, R.M. (1992). Physiology and pharmacology of renal pelvis and ureter. In *Campbell's Urology*, ed. Walsh, P.C., Retik, A.B., Stamey, T.A. & Vaughan, E.D. Volume I, pp. 113–144. Philadelphia PA: W.B. Saunders Co.

WILSON, C. (1989). Inhibition by sulphonylureas of vasorelaxation induced by K channels activators in vitro. *J. Autonom. Pharmacol.*, **9**, 71–78.

WILSON, C., COLDWELL, M.C., HOWLETT, D.R., COOPER, S.M. & HAMILTON, T.C. (1988). Comparative effects of K channel blockade on the vasorelaxant activity of cromakalim, pinacidil and nicorandil. *Eur. J. Pharmacol.*, **152**, 331–339.

WINQUIST, R.J., HEANEY, L.A., WALLACE, W.A., BASKIN, E.P., STEIN, R.B., GARCIA, M.L. & KACZOROWSKI, G.J. (1989) Glyburide blocks the relaxation response to BRL 34915 (cromakalim) minoxidil sulfate and diazoxide in vascular smooth muscle. *J. Pharmacol. Exp. Ther.*, **248**, 149–156.

ZINI, S., BEN-ARI, Y. & ASHFORD, M.L.J. (1991). Characterization of sulfonylurea receptors and the action of potassium channel openers on cholinergic neurotransmission in guinea-pig isolated small intestine. *J. Pharmacol. Exp. Ther.*, **259**, 566–573.

(Received October 13, 1993
Revised October 28, 1993
Accepted November 8, 1993)

Br. J. Pharmacol. (1994), **111**, 695–702 © Macmillan Press Ltd, 1994

Blockade of nicotinic responses by physostigmine, tacrine and other cholinesterase inhibitors in rat striatum

[1]P.B.S. Clarke, M. Reuben & H. El-Bizri

Department of Pharmacology and Therapeutics, McGill University, 3655 Drummond St, Montreal, Canada H3G 1Y6

1 The acetylcholinesterase inhibitors physostigmine, neostigmine, tetrahydroaminoacridine (tacrine; THA) and diisopropylfluorophosphate (DFP) were tested for possible direct nicotinic actions in rat striatal synaptosomes preloaded with [^{3}H]-dopamine. In this preparation, nicotinic cholinoceptor activation evoked [^{3}H]-dopamine release.

2 Antagonist activity was examined by giving a brief nicotine (1 μM) challenge after 30 min superfusion with an acetylcholinesterase (AChE) inhibitor (0.3–300 μM). Physostigmine, neostigmine and tacrine produced a concentration-dependent blockade. Physostigmine and tacrine were particularly potent (IC_{50}s approx. 10 μM and 1 μM, respectively). DFP reduced nicotinic responses only at the highest concentration tested (300 μM).

3 Nicotinic blockade produced by superfusion with physostigmine (30 μM) was insurmountable when tested against nicotine (0.1–100 μM).

4 Physostigmine (30 μM) also reduced responses to the nicotinic agonists 1,1-dimethyl-4-phenylpiperazinium iodide (DMPP) and cytisine, but did not alter responses to high K^+ or (+)-amphetamine. A higher concentration of physostigmine (300 μM) completely blocked responses to nicotine, somewhat reduced responses to amphetamine, and did not alter responses to high K^+. Tacrine (3 μM) reduced responses to nicotine and to high K^+ but did not affect responses to amphetamine.

5 Physostigmine (0.3–300 μM), given as a brief pulse, did not produce a nicotinic agonist-like effect.

6 Physostigmine, neostigmine, tacrine and DFP (all at 30 μM) each produced near-total (>96%) inhibition of AChE activity. However, DFP at a concentration (60 μM) that produced a degree of AChE inhibition equal to that of physostigmine 30 μM, did not significantly reduce nicotine-induced dopamine release.

7 It thus appears that physostigmine blocks CNS nicotinic receptors in an insurmountable and pharmacologically selective manner, independent of its ability to inhibit acetylcholinesterase. Tacrine reduced nicotinic responses, quite possibly by an indirect mechanism. The possibility of direct or indirect blockade of nicotinic receptor-mediated actions may complicate the interpretation of preclinical studies that have employed physostigmine and tacrine.

Keywords: Physostigmine; neostigmine; diisopropylfluorophosphate (DFP); tacrine; cholinesterase inhibitors; nicotine; nicotinic receptors; striatum; dopamine

Introduction

Acetylcholinesterase inhibitors (AChEIs) continue to be widely used in studies of cholinergic pharmacology and physiology. The peripheral actions of physostigmine, the prototypical AChEI, are almost entirely attributable to an inhibition of acetylcholinesterase, and classical experimental approaches have uncovered little evidence of direct postsynaptic actions (Taylor, 1990). However, single channel patch clamp recording techniques have revealed direct agonist and antagonist actions of physostigmine on nicotinic cholinoceptors (AChRs) of frog skeletal muscle (Shaw *et al.*, 1985) and of rat hippocampal neurones (Pereira *et al.*, 1993).

AChEIs form a chemically diverse group. The quaternary ammonium compound, neostigmine, exerts additional postsynaptic actions at autonomic ganglia (Haefely, 1980) and muscle endplate (Taylor, 1990); some of these actions appear mediated directly by nicotinic AChRs (Haefely, 1980; Fiekers, 1985). Tetrahydroaminoacridine (THA; tacrine) possesses a complex pharmacological profile, with AChE-independent actions reported on muscarinic receptors and on certain enzymes and voltage-gated ion channels (Freeman & Dawson, 1991). The organophosphorous compound, diisopropylfluorophosphate (DFP; dyflos), in contrast, appears quite selective for AChE over cholinoceptors (Taylor, 1990).

The purpose of the present study was to examine these commonly used AChEIs for possible direct nicotinic actions in the mammalian CNS. This issue has received little attention (Pereira *et al.*, 1993), and is important for at least two reasons. Firstly, in experimental studies, the use of AChEIs to define possible sites of nicotinic cholinergic transmission requires that these agents have negligible direct actions on receptors. Secondly, preliminary indications suggest that stimulation of CNS nicotinic receptors may be beneficial in Alzheimer's disease (Newhouse *et al.*, 1988; Jones *et al.*, 1992), whereas CNS nicotinic receptor blockade may impair cognition (Newhouse *et al.*, 1992). It thus becomes important to determine whether physostigmine and tacrine, two centrally-active AChEIs that have been administered to patients suffering from Alzheimer's dementia or other disorders (Davis *et al.*, 1983; Thal & Fuld, 1983; Summers *et al.*, 1986; Sahakian *et al.*, 1993), exert nicotinic actions.

Methods

Male Sprague-Dawley rats (Charles River, St. Constant, Quebec), weighing 200–250 g, were maintained on a 12 h/12 h light-dark cycle. Rats were housed four per cage, and food and water were available *ad libitum*. Subjects were allowed to accommodate to the housing conditions for 4 days after arrival, and were drug-naive prior to testing.

[1] Author for correspondence.

Dopamine release from superfused synaptosomes

Rats were decapitated, and both striata (combined wet weight 160–200 mg) were immediately dissected in ice-cold 0.32 M sucrose/5 mM HEPES at pH 7.5. Striata were homogenized in 20 vol of the sucrose/HEPES solution (12 up and down strokes, at 850 r.p.m., in a 0.25 mm clearance glass Teflon homogenizer). The homogenate was centrifuged at 1000 *g* for 10 min at 4°C. Supernatant was recentrifuged at 12000 *g* for 20 min at 4°C. The final pellet, consisting of the crude synaptosomal (P2) fraction, was resuspended in the superfusion buffer (5 ml g^{-1} of wet tissue weight). The superfusion buffer (SB) was composed of the following, in mM concentrations: NaCl 128, KCl 2.4, $CaCl_2$ 3.2, KH_2PO_4 1.2, $MgSO_4$ 1.2, HEPES 25, D-glucose 10, L-ascorbic acid 1 and pargyline 0.1 at pH 7.5. The synaptosomal preparation was incubated with [^{3}H]-dopamine (0.12 μM) for 5 min at 37°C. The synaptosomes were then centrifuged at 12000 *g* for 5 min at RT. The pellet was gently resuspended in an equal volume of SB.

Superfusion

The apparatus comprised 30 identical channels. Each channel consisted of a length of Tygon or silicone tubing (0.8 mm i.d.) leading to and from a retention chamber comprising a polypropylene filter unit (Millipore Corp., Bedford, MA, U.S.A.), fitted with a 13 mm diameter A/E glass fibre filter (1 μm pore size, Gelman Sciences Inc., Ann Arbor, MI, U.S.A.). The superfusate was continuously pumped downward through the chamber, at a rate of 0.4 ml min^{-1}, via a peristaltic pump (Masterflex, Cole-Parmer, Chicago, IL, U.S.A.) positioned downstream to the chamber. Drug (or SB for control channels) was introduced into the superfusate via a 1 ml syringe and 30 gauge needle (Becton Dickinson, NJ, U.S.A.) upstream to the chamber. In order to reduce the possibility of contaminants, all syringes used in these experiments were treated with bleach, followed by thorough washing with distilled water.

Each experiment comprised two or more assays. At the start of each assay, channels were thoroughly rinsed by superfusion with distilled water followed with SB. Next, 100 μl of the synaptosomal suspension was injected into the tubing immediately upstream to the superfusion chamber; synaptosomes were retained within the chamber on the filter. A superfusion period of 30 min followed, and AChE inhibitor was present in the buffer during this time, in the appropriate channels. Thirteen samples per channel were then collected in consecutive 1 min intervals into polypropylene minivials (Sarstedt, Montreal, Canada) containing 3 ml of scintillation fluid (BCS, Amersham, Montreal, Canada). After a 5 min baseline collection period, during which dopamine release showed little if any decline, a 1 min (0.4 ml) pulse of drug or SB (control channels) was injected. Finally, the filters holding the synaptosomes were removed in order to measure residual radioactivity. Samples were measured in a liquid scintillation counter (Wallac 1410, LKB, Sweden).

In each assay, data were collected simultaneously from all 30 channels. Four rats provided striatal tissue for each assay. Care was taken to include control (SB only) channels in all assays, and to counterbalance treatment conditions across channels and across invidual assays. Throughout the paper we shall refer to the tritium released as dopamine release, since it has been established that in similar synaptosomal preparations preloaded with [^{3}H]-dopamine, tritium released by nicotinic agonists or by depolarization largely corresponds to dopamine itself (Rapier *et al.*, 1988).

Acetylcholinesterase assay

AChE activity was measured in Experiment 5. This experiment comprised three parts, each part consisting of two or four assays. In each assay, striatal tissue from one rat was used, and quadruplicate determinations were made for each drug condition. Within each assay, AChE activity was expressed as a percentage of the mean of control samples, and the normalized data were then pooled across all assays for that part.

Synaptosomes were prepared, as for dopamine release experiments, and were resuspended in approx. 1 ml of super-

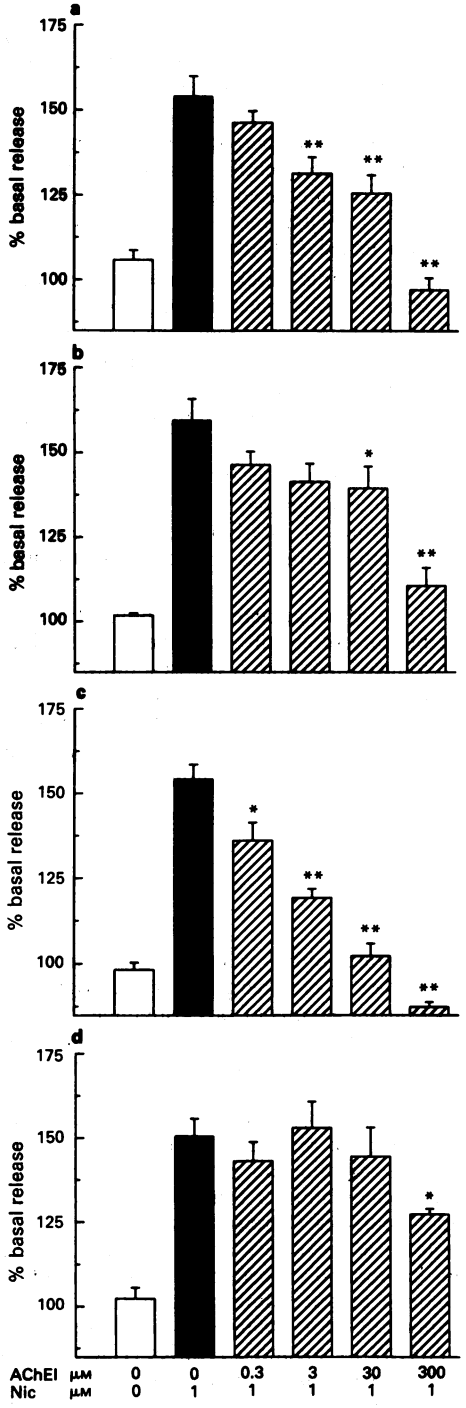


Figure 1 Effects of physostigmine (a), neostigmine (b), tacrine (c) and DFP (d) on [^{3}H]-dopamine release induced by nicotine from striatal synaptosomes (Experiment 1). Synaptosomes were superfused with buffer in the presence or absence of acetylcholinesterase inhibitor (AChEI) (0.3–300 μM) for 35 min prior to challenge with nicotine (Nic) 1 μM or buffer. The vertical axis shows mean ± s.e. mean peak release expressed as a percentage of basal release. Superfusion channels per condition: $n = 10$–20 (a), 8–11 (b), 7–10 (c), 7–14 (d). $^*P<0.05$; $^{**}P<0.01$ vs. nicotine alone (Dunnett's test).

fusion buffer (SB). Aliquots of 0.2 ml were incubated for 30 min at RT with or without addition of AChE inhibitor. AChE activity was determined colorimetrically by the method of Ellman *et al.* (1961). Briefly, 20 µl samples were added to 50 µl of 10 mM dithiobisnitrobenzoic acid and 1.395 ml of 0.1 M Na phosphate buffer, pH 8.0. Samples that had been incubated in the presence of AChEI were assayed in buffer containing the same concentration of the relevant AChEI. The reaction was started by the addition of 20 µl of 75 mM acetylthiocholine iodide (or Na phosphate buffer for the zeroing cuvette). The absorbance at 412 nm was measured with a spectrophotometer (Spectronic 2000, Bausch and Lomb, Rochester, NY, U.S.A.) and recorded every minute for 5 min. The rate of change of absorbance over time, determined by linear regression, was used to calculate the rate of reaction.

Data analysis

Basal release was defined as the mean radioactivity released (d.p.m. min^{-1}) over the five 1 min samples collected immediately prior to drug or SB administration. This basal [^{3}H]-dopamine release was approximately 2810 ± 210 d.p.m. min^{-1} (mean ± s.e.mean, $n = 9$ series of assays), which corresponds to approximately 3 fmol mg^{-1} of original wet tissue. Across experiments, basal release (min^{-1}) ranged from 0.7 to 2% of residual radioactivity collected on the tissue filters (304,000 ± 23,000 d.p.m. $filter^{-1}$). For each channel, the release occurring in each 1 min collection period was calculated as a percentage of basal release; evoked release was taken as the peak value that occurred in the first three periods after a drug challenge. This measure of drug effect was used since it is less likely to be affected by receptor desensitization than the time-averaged drug effect ('area under the curve'). Drug effects were examined by analysis of variance, using commercial software (Systat, Evanston, IL, U.S.A.). Multiple comparisons between all groups were made with Tukey's HSD test (Wilkinson, 1990); comparisons with a single control group were made with Dunnett's test (Dunnett, 1955); other multiple comparisons were made by Student's *t* test with Bonferroni's correction (Glantz, 1992). Probability values are 2-tailed.

Drugs

Chemicals and supplies were as follows: [^{3}H]-dopamine (dopamine, [8-^{3}H]-, specific activity 38.1 Ci $mmol^{-1}$; New England Nuclear, Boston, MA, U.S.A.), (−)-nicotine hydrogen tartrate, cytisine, 1,1-dimethyl-4-phenylpiperazinium iodide (DMPP), diisopropylfluorophosphate (DFP, dyflos) (Sigma Chemical Corp., St. Louis, MO, U.S.A.), physostigmine sulphate, neostigmine bromide, pargyline hydrochloride (Research Biochemicals Inc., Natick, MA, U.S.A.), 9-amino-1,2,3,4-tetrahydroacridine (tacrine, THA; gift of Pharmascience Inc., Montreal, Canada), (+)-amphetamine sulphate (gift of SmithKline Beecham Pharma, Oakville, Canada). Other chemicals and reagents were purchased from commercial sources. For *in vitro* administration, drugs were dissolved in superfusion buffer (SB).

Results

Experiment 1: Effects of physostigmine, neostigmine, tacrine and DFP on striatal [^{3}H]-dopamine release evoked by nicotine

The effects of each AChE inhibitor (0.3–300 µM) were examined in a different set of assays (Figure 1). In the absence of AChE inhibitor, nicotine increased dopamine release by 50–60% over baseline. Physostigmine (0.3–300 µM) reduced this effect in a concentration-dependent manner (main effect of concentration: $F = 19.17$, d.f. 4, 71, $P < 0.0001$). The IC_{50} of physostigmine fell between 3 and 30 µM, and complete blockade occurred at 300 µM (Figure 1a). Neostigmine (0.3–300 µM) reduced nicotinic responses in a concentration-related manner (main effect of concentration: $F = 10.36$, d.f. 4, 46, $P < 0.0001$), with an IC_{50} of approx. 100 µM (Figure 1b). Tacrine (0.3–300 µM) also produced a concentration-related inhibition of nicotine-induced dopamine release (main effect of concentration: $F = 31.68$, d.f. 4, 36, $P < 0.0001$), but appeared more potent than physostigmine or neostigmine (IC_{50} approx. 1 µM). Tacrine was effective even at 0.3 µM (Dunnett's test $P < 0.02$; Figure 1c). In the same concentration-range, DFP had no significant antagonist action as determined by ANOVA (main effect of concentration: $F = 2.33$, d.f. 4, 40, $P > 0.07$), and only at 300 µM was a significant reduction of nicotine-induced dopamine release detected (Dunnett's test: $P < 0.05$; Figure 1d).

Basal dopamine release was not significantly altered by superfusion with either physostigmine (main effect of concentration: $F = 1.92$, d.f. 4, 71, $P > 0.1$), neostigmine ($F = 0.13$, d.f. 4, 46, $P > 0.9$) or DFP ($F = 1.36$, d.f. 4, 40, $P > 0.2$). Tacrine did not significantly affect basal release at 0.3 or 3 µM (Dunnett's test, $P > 0.5$), but increased it markedly at 30 and 300 µM (Dunnett's test, $P < 0.0001$ for each). Mean (± s.e.mean) basal values of dopamine release for tacrine 0–300 µM were: 2419 ± 114, 2363 ± 134, 2759 ± 209, 5485 ± 330, and 6179 ± 326 DPM min^{-1}.

Experiment 2: Surmountable vs insurmountable blockade by physostigmine

The approximate IC_{50} of physostigmine (estimated from Experiment 1) was tested against graded concentrations of nicotine (Figure 2). The procedure was otherwise identical to that of Experimental 1. In the absence of physostigmine, nicotine increased dopamine release in a concentration-related manner. A maximal effect was attained at approximately 1 µM, and the EC_{50} was between 0.1 and 1 µM. Physostigmine significantly reduced the effect of nicotine at every concentration of the agonist ($P < 0.02$ to $P < 0.01$; Figure 2). Thus, blockade by physostigmine was not surmounted, even by high concentrations of nicotine. Perfusion with physostigmine did not significantly alter basal release ($F = 0.08$, d.f. 1.82, $P > 0.7$).

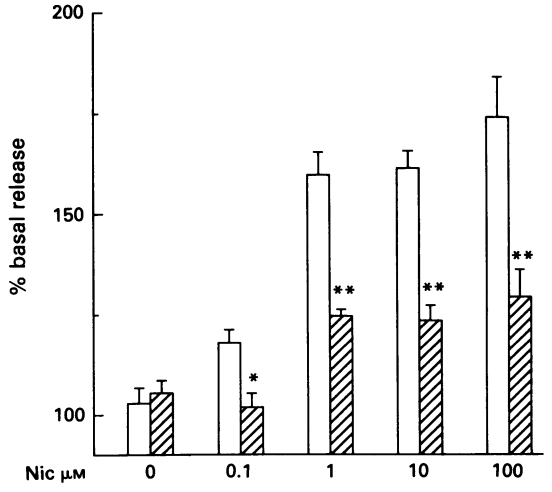
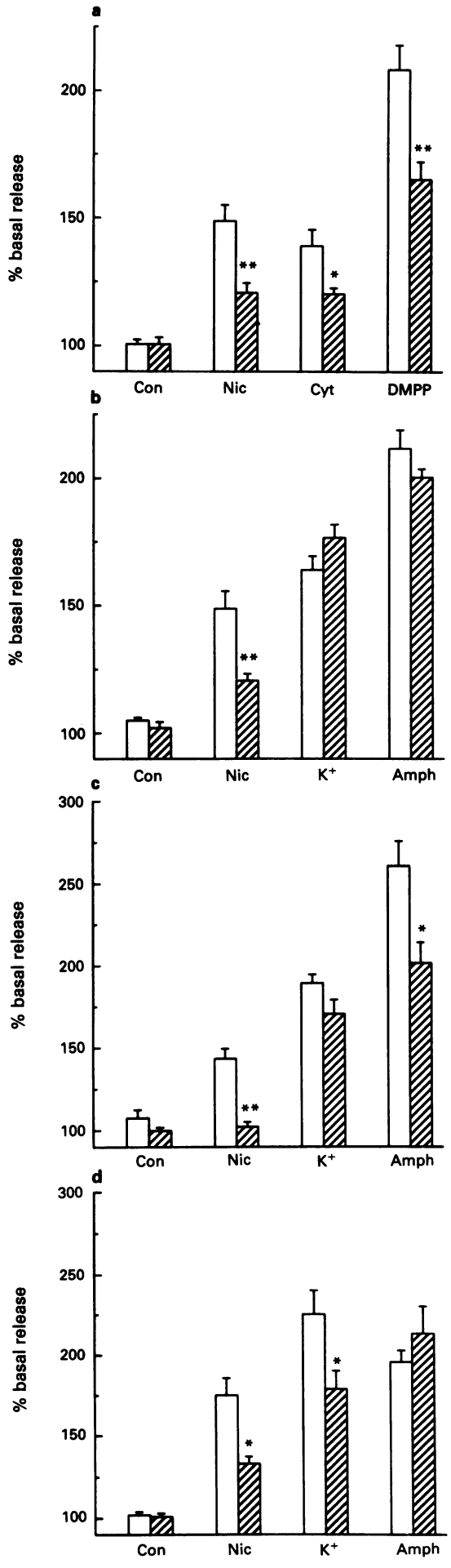


Figure 2 Insurmountable block by physostigmine (Experiment 2). Synaptosomes were challenged with nicotine (Nic, 0.1–100 µM) or with buffer alone, after a 35 min period of superfusion with (hatched columns) or without (open columns) physostigmine 30 µM. The vertical axis shows mean ± s.e.mean peak release expressed as a percentage of basal release ($n = 7$–11 superfusion channels). *$P < 0.02$, **$P < 0.01$ vs. physostigmine-free condition at same nicotine concentration (Student's *t* test with Bonferroni adjustment).



Experiment 3: Selectivity of blockade by physostigmine and tacrine

Four sets of assays were performed (Figure 3a–d). In the first set of assays (Figure 3a), physostigmine (30 μM) significantly reduced dopamine release evoked by nicotine (1 μM) ($t = 3.66$, d.f. 15, $P < 0.01$), cytisine (10 μM) ($t = 2.73$, d.f. 13.9, $P < 0.05$) and DMPP (10 μM) ($t = 3.69$, d.f. 15, $P < 0.01$). Basal release was not altered by physostigmine ($F = 0.01$, d.f. 1.76, $P > 0.8$).

In the second set of assays (Figure 3b), physostigmine (30 μM) reduced nicotine-induced dopamine release ($t = 3.79$, d.f. 16.9, $P < 0.005$), but did not significantly alter release induced by either 12 mM K^+ ($t = 1.69$, d.f. 30, $P > 0.1$) or 0.3 μM amphetamine ($t = 1.44$, d.f. 22.5, $P > 0.01$). Basal release was not affected by physostigmine ($F = 0.04$, d.f. 1, 112, $P > 0.8$).

A third set of assays was conducted in identical fashion, except that a higher concentration of physostigmine was used (300 μM). Here, physostigmine completely blocked nicotine-induced release, and somewhat reduced ampetamine-induced release ($t = 2.99$, d.f. 12, $P < 0.05$), but did not alter release induced by K^+ ($t = 1.91$, d.f. 13, $P > 0.2$) (Figure 3c). This high concentration of physostigmine also increased basal release ($F = 5.94$, d.f. 1, 47, $P < 0.02$), but the effect was small (13.4% increase).

A fourth set of assays was performed likewise, except that tacrine 3 μM was tested instead of physostigmine. Tacrine 3 μM (Figure 3d) attenuated dopamine release induced by nicotine ($t = 3.70$, d.f. 9.3, $P < 0.02$) and by high K^+ ($t = 2.79$, d.f. 23, $P < 0.05$), but not by amphetamine ($t = 1.67$, d.f. 13, $P > 0.1$). Tacrine also increased basal dopamine release ($t = 2.23$, d.f. 53, $P < 0.05$), but the effect was small (14.4% increase).

Experiment 4: Effects of a brief pulse of physostigmine on striatal [^{3}H]-dopamine release

In order to test for an agonist-like effect of physostigmine, synaptosomes were challenged with a 0.4 ml pulse containing nicotine 1 μM, physostigmine (0.3, 3, 30 or 300 μM), or SB alone. Physostigmine produced no clear effect. A significant main effect of drug ($F = 12.48$, d.f. 5, 54, $P < 0.0001$) was attributable to the effect of nicotine (Figure 4). Comparisons with the control condition (SB alone) revealed no significant effect of physostigmine, even at the highest concentration (Dunnett's test: $P > 0.8$).

Experiment 5: Acetylcholinesterase inhibition by physostigmine, neostigmine, tacrine and DFP

In the first set of assays, all three drugs tested (30 μM in each case) inhibited AChE activity almost completely (Table 1). ANOVA indicated that the degree of inhibition between the

Figure 3 Pharmacological selectivity of blockade by physostigmine or tacrine (Experiment 3). In all assays, synaptosomes were superfused for 35 min with or without acetylcholinesterase inhibitor (AChEI) (hatched and open column, respectively), prior to acute drug challenge. (a) Challenge with nicotine 1 μM (Nic), cytisine 10 μM (Cyt), DMPP 10 μM or buffer alone, with or without physostigmine (30 μM). (b) Challenge with nicotine 1 μM, K^+ 12 mM, (+)-amphetamine 0.3 μM (Amph) or buffer alone, with or without physostigmine 30 μM. (c) As for (b), except physostigmine 300 μM was used. (d) As for (b), except tacrine 3 μM was used. The vertical axis shows mean ± s.e.mean peak release expressed as a percentage of basal release. Superfusion channels per condition: $n = 8–12$ (a), 13–17 (b), 5–8 (c), 6–13 (d). $^*P < 0.05$; $^{**}P < 0.01$ vs. AChEI-free condition at same agonist concentration (Student's t test with Bonferroni's adjustment).

three drugs was not the same (drug main effect: $F = 3.70$, d.f. 2, 45, $P < 0.05$), but any differences were small and *a posteriori* tests did not reveal a significant difference between physostigmine and either neostigmine or DFP (respectively: $t = 2.26$, d.f. 21.2, $P > 0.06$, and $t = 1.38$, d.f. 18.9, $P > 0.3$). In control samples exposed only to SB, the mean ± s.e.mean AChE activity was 4.26 ± 0.52 nmol min^{-1} mg^{-1} original tissue ($n = 4$ assays).

A second set of two assays was performed in order to establish a concentration of tacrine that inhibited AChE activity as effectively as physostigmine 30 μM. Tacrine 0.3 μM and 3 μM produced significantly less AChE inhibition than physostigmine 30 μM (respectively: $t = 12.9$, d.f. 7.3, $P <$ 0.0001; $t = 5.32$, d.f. 13, $P < 0.001$), whereas tacrine 30 μM and physostigmine 30 μM produced comparable effects ($t = 0.68$, d.f. 9, $P > 0.5$; Table 1). In control samples exposed only to SB, the mean ± s.e.mean AChE activity was 4.59 ± 0.14 nmol min^{-1} mg^{-1} original tissue ($n = 2$ assays).

A third set of four assays was performed in order to establish a concentration of DFP that inhibited AChE activity as effectively as physostigmine 30 μM. Physostigmine and all three concentrations of DFP almost completely inhibited AChE activity (Table 1). The degree of inhibition differed to a small extent between drug conditions (drug main effect: $F = 14.98$, d.f. 3, 60, $P < 0.0001$); the lowest concentration of DFP (30 μM) gave significantly less inhibition than physostigmine 30 μM ($t = 7.66$, d.f. 25, $P < 0.0001$), whereas DFP 60 and 100 μM did not differ from physostigmine ($P > 0.6$ for each). In control samples exposed only to SB, the mean ± s.e.mean AChE activity was 5.49 ± 0.15 nmol min^{-1} mg^{-1} original tissue ($n = 4$ assays).

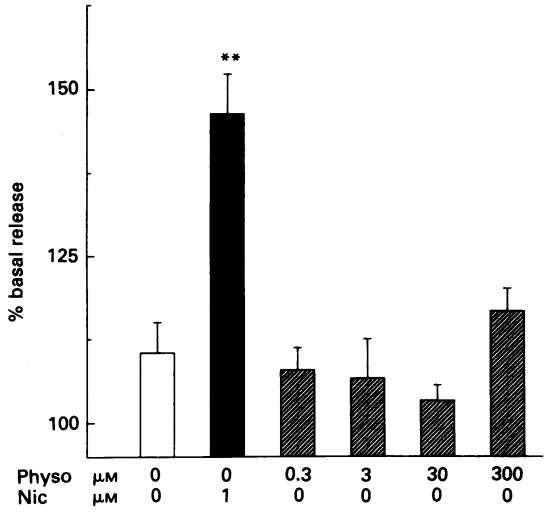


Figure 4 Test of physostigmine (Physo) as a nicotinic agonist (Experiment 4). Synaptosomes were challenged with brief (0.4 ml) pulses of nicotine 1 μM (Nic) (solid column), physostigmine 0.3–300 μM (hatched column), or buffer alone (open column). The vertical axis shows mean ± s.e.mean peak release expressed as a percentage of basal release ($n = 9$–13). **$P < 0.001$ vs. no drug control (Dunnett's test).

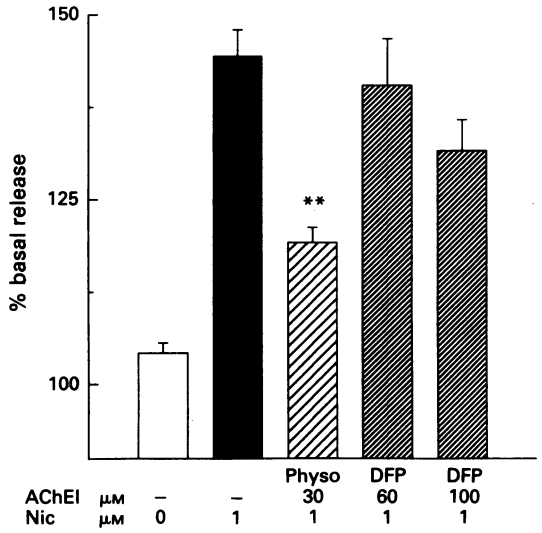


Figure 5 Comparison of physostigmine and DFP at concentrations giving equivalent degrees of acetylcholinesterase inhibition (AChEI) (Experiment 6). Synaptosomes were superfused with buffer in the presence or absence of physostigmine 30 μM or DFP 60 or 100 μM for 35 min, prior to challenge with nicotine 1 μM (Nic) or buffer. The vertical axis shows mean ± s.e.mean peak release expressed as a percentage of basal release ($n = 10$–22). **$P < 0.0005$ vs. nicotine alone and $P < 0.005$ vs. nicotine/DFP 60 μM (Tukey HSD test).

Table 1 Residual acetylcholinesterase (AChE) activity of synaptosomal preparations treated with AChE inhibitors (Experiment 5)

Drug	*Concentration* (μM)	*AChE activity**	n
Assay set No. 1			
Control		100.0 ± 3.0	16
Physostigmine	30	2.5 ± 0.4	16
Neostigmine	30	1.6 ± 0.2	16
DFP	30	3.9 ± 1.0	16
Assay set No. 2			
Control		100.0 ± 3.1	8
Physostigmine	30	2.2 ± 0.3	8
Tacrine	0.3	27.0 ± 1.9	8
Tacrine	3	4.6 ± 0.3	8
Tacrine	30	2.0 ± 0.2	4
Assay set No. 3			
Control		100.0 ± 2.0	16
Physostigmine	30	1.5 ± 0.1	16
DFP	30	2.6 ± 0.1	16
DFP	60	1.7 ± 0.2	16
DFP	100	1.6 ± 0.1	16

*Residual AChE activity (mean ± s.e.mean) expressed as a percentage of control samples not treated with AChE inhibitor.

Experiment 6: Effects of selected concentrations of physostigmine and DFP on striatal [^{3}H]-dopamine release evoked by nicotine

Nicotine-induced dopamine release was again studied, in order to test whether concentrations of physostigmine and DFP that had been found in Experiment 5 to give equivalent degrees of AChE inhibition would also produce equivalent degrees of nicotinic block (Figure 5). Dopamine release induced by nicotine challenge was significantly altered by treatment with AChE inhibitor (AChE inhibitor main effect: $F = 8.31$, d.f. 3, 62, $P < 0.001$). Multiple comparisons between nicotine-challenged drug conditions revealed no significant differences between control (SB alone), DFP 60 μM and DFP 100 μM conditions (Tukey's HSD test: $P > 0.1$ for each; Figure 5). In contrast, the nicotine response after treatment with physostigmine was significantly less than the nicotine response after perfusion with either SB alone ($P < 0.005$) or DFP 60 μM ($P < 0.005$). Basal release was not altered by treatment with AChE inhibitor ($F = 0.09$, d.f. 3, 72, $P < 0.9$).

Discussion

CNS nicotinic receptors are genetically diverse, but two main subfamilies can be distinguished, based on sensitivity to the antagonist α-bungarotoxin (Deneris *et al.*, 1991; Clarke, 1992). Evidence was recently provided for direct actions of physostigmine on CNS nicotinic receptors that are susceptible to blockade by α-bungarotoxin (Pereira *et al.*, 1993). Here, we describe effects of physostigmine and other AChEIs on nicotine-induced striatal dopamine release, a response mediated by nicotinic receptors that are not sensitive to α-bungarotoxin (Rapier *et al.*, 1990; Grady *et al.*, 1992).

In the present study, physostigmine antagonized nicotinic responses in a pharmacologically selective manner, insofar as dopamine release evoked by the nicotinic agonists DMPP and cytisine was reduced, whereas that evoked by high K^+ was not. Amphetamine-induced dopamine release was reduced, but only at a high concentration of physostigmine (300 μM). This suggests that physostigmine, at least at moderate concentrations, acts at nicotinic receptors and not on release mechanisms *per se*.

Physostigmine is reported to exert agonist actions when applied at submicromolar concentrations to frog skeletal muscle and to rat cultured hippocampal cells that express α-bungarotoxin-sensitive nicotinic receptors (Shaw *et al.*, 1985; Pereira *et al.*, 1993). These observations suggested that the nicotinic blockade seen following 30 min perfusion with physostigmine might reflect desensitization secondary to an initial receptor activation. However, when physostigmine was tested in a short pulse in the same manner as nicotine, no agonist activity was seen over a wide concentration range (Experiment 4). Consistent with its lack of agonist activity and with its insurmountable blocking action (observed in Experiment 2), physostigmine inhibits only weakly [^{3}H]-nicotine and [^{3}H]-ACh binding to brain tissue (Nilsson *et al.*, 1987; Perry *et al.*, 1988). Thus, it appears possible that physostigmine may act as an open channel blocker in the CNS, as proposed for nicotinic receptors in *Torpedo* electroplaque (Sherby *et al.*, 1985).

Physostigmine inhibited nicotinic responses at concentrations that inhibit AChE activity *in vitro*, and the three other AChEIs tested (neostigmine, tacrine, DFP) also inhibited nicotinic responses to some extent, as shown in Experiment 1. Conceivably, then, the nicotinic antagonist action of physostigmine could have been due to esterase inhibition, perhaps mediated via receptor desensitization resulting from increased concentrations of ACh in the superperfusate. This possibility appears unlikely in view of subsequent comparisons with DFP and tacrine. Thus, in Experiment 5, a concentration of DFP (60 μM) was determined that inhibited AChE to the same degree as physostigmine 30 μM; at these concentrations, physostigmine markedly inhibited nicotine-induced dopamine release, whereas DFP was inactive. Contrariwise, tacrine 3 μM was as effective as physostigmine 30 μM in inhibiting dopamine release (Experiment 1), but produced significantly less inhibition of AChE (Experiment 5).

The receptor subtype(s) mediating nicotine-induced dopamine release have not been classified with certainty. The association of [^{3}H]-nicotine binding sites with dopaminergic afferents (Clarke & Pert, 1985) suggests mediation by receptors containing alpha4 and beta2 subunits (Whiting *et al.*, 1991; Flores *et al.*, 1992), but other receptor subtypes are also expressed by dopaminergic neurones (Wada *et al.*, 1989) and may thus contribute. *In situ* hybridization experiments (Dineley-Miller & Patrick, 1992) indicate that receptors containing beta4 subunits, which appear to be prevalent at autonomic ganglia (Listerud *et al.*, 1991; Tarroni *et al.*, 1992), are probably not expressed by nigrostriatal dopaminergic neurones. Nevertheless, these are indications that physostigmine may exert an antagonist action in the periphery as well as in the CNS. Thus, in the myenteric plexus, physostigmine (10 μM) inhibited [^{3}H]-ACh release evoked by the direct nicotinic agonist DMPP (Briggs & Cooper, 1982), and physostigmine has also been shown to block carbachol-induced $^{86}Rb^+$ efflux from cultured cells derived from a peripheral neuroblastoma with an IC_{50} of 40 μM (Lukas *et al.*, 1993).

Physostigmine is commonly employed in concentrations of 10–50 μM in order to inhibit AChE *in vitro* (Murrin *et al.*, 1977; Lapchak & Collier, 1988; Suzuki *et al.*, 1993). Within this concentration-range, nicotinic actions were clearly inhibited in our assay. Moreover, the insurmountable nature of the block produced by physostigmine implies that this antagonist action would be apparent even at high agonist concentrations. The demonstration that moderate concentrations of physostigmine can block nicotinic response raises the possibility that the prevalence of nicotinic actions of ACh has been underestimated in the CNS: (1) The possibility of presynaptic nicotinic modulation of the ascending cholinergic innervation to cerebral cortex has been examined in synaptosomal preparations; in cerebral cortex, release of cortical ACh was enhanced by activation of nicotinic receptors in mouse (Rowell & Winkler, 1984) but not in rat (Meyer *et al.*, 1987). In the latter study, the use of physostigmine (50 μM) may have prevented a nicotinic action. (2) In another study, a lower concentration of physostigmine (10 μM) reduced nicotine-induced depolarization in rat cerebral cortical synaptosomes (Hillard & Pounds, 1991); the possibility of a direct blocking action on nicotinic receptors was not discussed. (3) In the substantia nigra pars compacta, a nicotinic cholinergic innervation has been described (Clarke *et al.*, 1987; Blaha & Winn, 1993). However, studies in which physostigmine has been applied directly to this area have emphasized a muscarinic component (Winn *et al.*, 1983; Smelik & Ernst, 1966). (4) Use of physostigmine perhaps also helps to account for the surprising absence of demonstrable nicotinic cholinergic transmission reported in the interpeduncular nucleus (Brown *et al.*, 1983).

A further issue relates to the interpretation of radioligand binding data obtained after chronic AChEI treatment. Brain nicotinic receptors can be identified by radioligand binding techniques, but the extent to which these receptors are cholinergically innervated remains uncertain. Initial reports of [^{3}H]-nicotine and [^{3}H]-ACh binding site downregulation following chronic AChEI treatment suggested that the nicotinic AChRs so identified are indeed targets for endogenous ACh in a number of brain regions (Schwartz & Kellar, 1983; 1985; Costa & Murphy, 1985). Subsequent reports indicate that AChEI-induced upregulation of nicotinic binding sites can also occur (De Sarno & Giacobini, 1989; Bhat *et al.*, 1990). The source of this variability has not been adequately explained. Hence, it may be significant that chronic treatment with physostigmine, which might be expected to exert an insurmountable nicotinic antagonism at the doses administered in these studies, upregulated nicotinic binding (De Sarno & Giacobini, 1989; Bhat *et al.*, 1990), whereas DFP, which appears to be at best a weak nicotinic antagonist, decreased binding (Schwartz & Kellar, 1983; 1985; Costa & Murphy, 1985; van de Kamp & Collins, 1992).

A nicotinic blocking effect of tacrine has not been identified previously (Experiment 1). The potency of this action is noteworthy; tacrine significantly reduced nicotinic responses even at the lowest concentration tested (0.3 μM), and the IC_{50} was around 1 μM. These values compare quite closely with IC_{50} values reported for AChE inhibition in brain (Freeman & Dawson, 1991), whereas the therapeutic dose-range of tacrine is associated with serum levels between 0.02 and 0.3 μM (Park *et al.*, 1986).

Tacrine also reduced dopamine release associated with the administration of buffer containing high K^+ (Experiment 3), and thus it is not clear whether this drug exerted a direct antagonist action at nicotinic receptors. Published attempts to demonstrate an interaction of tacrine with CNS nicotinic receptors have yielded mixed results. Tacrine has been reported to inhibit [^{3}H]-nicotine or [^{3}H]-ACh binding to rat or human brain tissue with IC_{50} or K_i values ranging from 1 μM

to 300 μM (Nilsson *et al.*, 1987; Perry *et al.*, 1988; Xiao *et al.*, 1993). However, in functional experiments designed to test nicotinic agonist activity, detectable activity was only reported at high micromolar concentrations (Nilsson *et al.*, 1987).

Certain reports have indicated that some of the cognitive impairments experienced in Alzheimer's disease may be alleviated by treatment with physostigmine (Thal & Fuld, 1983; Davis *et al.*, 1983) and tacrine (Summers *et al.*, 1986). However, other studies have shown little or no benefit with either drug (Ashford *et al.*, 1981; Caltagirone *et al.*, 1982; Sahakian *et al.*, 1983; Chatellier & Lacomblez, 1990; Gauthier *et al.*, 1990). In the light of recent evidence indicating that cognitive functioning can be enhanced by nicotinic receptor agonists and impaired by nicotinic blockers (Newhouse *et al.*, 1988; 1992; Jones *et al.*, 1992), it must be emphasized that the concentrations of physostigmine and tacrine shown to antagonize nicotinic responses in the present study, also inhibited AChE activity almost completely, and thus would not normally be achieved in the clinic.

We thank Ms Anna McNicoll for demonstrating the AChE assay, and Dr Brian Collier for advice and encouragement. We also thank Pharmascience and SmithKline Beecham for gifts of tacrine and (+)-amphetamine, respectively. This work was funded by the MRC of Canada (to P.B.S.C.). H.E.B. holds an MRC (Canada) Studentship. P.B.S.C. is a Chercheur Boursier Senior I of the FRSQ.

References

ASHFORD, J.W., SOLDINGER, S., SCHAEFFER, J., COCHRAN, L. & JARVIK, L.F. (1981). Physostigmine and its effect on six patients with dementia. *Am. J. Psychiatry*, **138**, 829–830.

BHAT, R.V., TURNER, S.L., MARKS, M.J. & COLLINS, A.C. (1990). Selective changes in sensitivity to cholinergic agonists and receptor changes elicited by continuous physostigmine infusion. *J. Pharmacol. Exp. Ther.*, **255**, 187–196.

BLAHA, C.D. & WINN, P. (1993). Modulation of dopamine efflux in the striatum following cholinergic stimulation of the substantia nigra in intact and pedunculopontine tegmental nucleus-lesioned rats. *J. Neurosci.*, **13**, 1035–1044.

BRIGGS, C.A. & COOPER, J.R. (1982). Cholinergic modulation of the release of [3H]acetylcholine from synaptosomes of the myenteric plexus. *J. Neurochem.*, **38**, 501–508.

BROWN, D.A., DOCHERTY, R.J. & HALLIWELL, J.V. (1983). Chemical transmission in the rat interpeduncular nucleus *in vitro*. *J. Physiol.*, **341**, 655–670.

CALTAGIRONE, C., GAINOTTI, G. & MASULLO, C. (1982). Oral administration of chronic physostigmine does not improve cognitive or mnesic performances in Alzheimer's presenile dementia. *Int. J. Neurosci.*, **16**, 247–249.

CHATELLIER, G. & LACOMBLEZ, L. (1990). Tacrine (tetrahydroaminoacridine; THA) and lecithin in senile dementia of the Alzheimer type: a multicentre trial. *Br. Med. J.*, **300**, 495–499.

CLARKE, P.B.S. (1992). The fall and rise of neuronal alpha-bungarotoxin binding proteins. *Trends Pharmacol. Sci.*, **11**, 407–413.

CLARKE, P.B.S., HOMMER, D.W., PERT, A. & SKIRBOLL, L.R. (1987). Innervation of substantia nigra neurons by cholinergic afferents from the pedunculopontine nucleus in rats: neuroanatomical and electrophysiological evidence. *Neuroscience*, **23**, 1011–1020.

CLARKE, P.B.S. & PERT, A. (1985). Autoradiographic evidence for nicotine receptors on nigrostriatal and mesolimbic dopaminergic neurons. *Brain Res.*, **348**, 355–358.

COSTA, L.G. & MURPHY, S.D. (1985). Antinociceptive effect of diisopropylphosphofluoridate: development of tolerance and lack of cross-tolerance to morphine. *Neurobehav. Toxicol. Teratol.*, **7**, 251–256.

DAVIS, K.L., MOHS, R.C., ROSEN, W.G., GREENWALD, B.S., LEVY, M.I. & HORVATH, T.B. (1983). Memory enhancement with oral physostigmine in Alzheimer's disease. *N. Engl. J. Med.*, **308**, 721.

DE SARNO, P. & GIACOBINI, E. (1989). Modulation of acetylcholine release by nicotinic receptors in the rat brain. *J. Neurosci. Res.*, **22**, 194–200.

DENERIS, E.S., CONNOLLY, J., ROGERS, S.W. & DUVOISIN, R. (1991). Pharmacological and functional diversity of neuronal nicotinic acetylcholine receptors. *Trends Pharmacol. Sci.*, **12**, 34–40.

DINELEY-MILLER, K. & PATRICK, J. (1992). Gene transcripts for the nicotinic acetylcholine receptor subunit, beta4, are distributed in multiple areas of the rat central nervous system. *Brain Res. Mol. Brain Res.*, **16**, 339–344.

DUNNETT, C.W. (1955). A multiple comparison procedure for comparing several treatments with a control. *J. Am. Statist. Assoc.*, **50**, 1096–1121.

ELLMAN, G.L., COURTNEY, K.D., ANDRES, V. & FEATHERSTONE, R.M. (1961). A new and rapid colorimetric determination of acetylcholinesterase activity. *Biochem. Pharmacol.*, **7**, 88–95.

FIEKERS, J.F. (1985). Concentration-dependent effects of neostigmine on the endplate acetylcholine receptor channel complex. *J. Neurosci.*, **5**, 502–514.

FLORES, C.M., ROGERS, S.W., PABREZA, L.A., WOLFE, B.B. & KELLAR, K.J. (1992). A subtype of nicotinic cholinergic receptor in rat brain is composed of 4 and β2 subunits and is up-regulated by chronic nicotine treatment. *Mol. Pharmacol.*, **41**, 31–37.

FREEMAN, S.E. & DAWSON, R.M. (1991). Tacrine: a pharmacological review. *Prog. Neurobiol.*, **36**, 257–277.

GAUTHIER, S., BOUCHARD, R., LAMONTAGNE, A., BAILEY, P. & et al. (1990). Tetrahydroaminoacridine-lecithin combination treatment in patients with intermediate-stage Alzheimer's disease. *N. Engl. J. Med.*, **322**, 1272–1276.

GLANTZ, S.A. (1992). *Primer of Biostatistics*. 3rd edn. New York: McGraw-Hill.

GRADY, S., MARKS, M.J., WONNACOTT, S. & COLLINS, A.C. (1992). Characterization of nicotinic receptor-mediated [^{3}H]dopamine release from synaptosomes prepared from mouse striatum. *J. Neurochem.*, **59**, 848–856.

HAEFELY, W.E. (1980). Non-nicotinic chemical stimulation of autonomic ganglia. *Handb. Exp. Pharmacol.*, **53**, 313–357.

HILLARD, C.J. & POUNDS, J.J. (1991). [^{3}H]Tetraphenylphosphonium accumulation in cerebral cortical synaptosomes as a measure of nicotine-induced changes in membrane potential. *J. Pharmacol. Exp. Ther.*, **259**, 1118–1123.

JONES, G.M.M., SAHAKIAN, B.J., LEVY, R., WARBURTON, D.M. & GRAY, J.A. (1992). Effects of acute subcutaneous nicotine on attention, information processing and short-term memory in Alzheimer's disease. *Psychopharmacology (Berlin)*, **108**, 485–494.

LAPCHAK, P.A. & COLLIER, B. (1988). Vasoactive intestinal peptide increases acetylcholine synthesis by rat hippocampal slices. *J. Neurochem.*, **50**, 58–64.

LISTERUD, M., BRUSSAARD, A.B., DEVAY, P., COLMAN, D.R. & ROLE, L.W. (1991). Functional contribution of neuronal AChR subunits revealed by antisense oligonucleotides. *Science*, **254**, 1518–1521.

LUKAS, R.J., NORMAN, S.A. & LUCERO, L. (1993). Characterization of nicotinic acetylcholine receptors expressed by cells of the SH-SY5Y human neuroblastoma clonal line. *Mol. Cell. Neurosci.*, **4**, 1–12.

MEYER, E.M., ARENDASH, G.W., JUDKINS, J.H., YING, L., WADE, C. & KEM, W.R. (1987). Effects of nucleus basalis lesions on the muscarinic and nicotinic modulation of [^{3}H]acetylcholine release in the rat cerebral cortex. *J. Neurochem.*, **49**, 1758–1762.

MURRIN, L.C., DEHAVEN, R.N. & KUHAR, M.J. (1977). On the relationship between [^{3}H]choline uptake activation and [^{3}H]acetylcholine release. *J. Neurochem.*, **29**, 681–687.

NEWHOUSE, P.A., POTTER, A., CORWIN, J. & LENOX, R. (1992). Acute nicotinic blockade produces cognitive impairment in normal humans. *Psychopharmacology (Berlin)*, **108**, 480–484.

NEWHOUSE, P.A., SUNDERLAND, T., TARIOT, P.N., BLUMHARDT, C.L., WEINGARTNER, H., MELLOW, A. & MURPHY, D.L. (1988). Intravenous nicotine in Alzheimer's disease: a pilot study. *Psychopharmacology (Berlin)*, **95**, 171–175.

NILSSON, L., ADEM, A., HARDY, J., WINBLAD, B. & NORDBERG, A. (1987). Do tetrahydroaminoacridine (THA) and physostigmine restore acetylcholine release in Alzheimer's brains via nicotinic receptors? *J. Neural Transm.*, **70**, 357–368.

PARK, T.H., TACHIKI, K.H., SUMMERS, W., KLING, D., FITTEN, J., PERRYMAN, P., SPIDELL, K. & KLING, A.S. (1986). Isolation and the fluorometric, high-performance liquid chromatographic determination of tacrine. *Anal. Biochem.*, **159**, 358–362.

PEREIRA, E.F.R., ALKONDON, M., TANO, T., CASTRO, N.G., FROES-FERRAO, M.M., ROZENTAL, R., ARONSTAM, R.S., SCHRATTENHOLZ, A., MAELICKE, A. & ALBUQUERQUE, E.X. (1993). A novel agonist binding site on nicotinic acetylcholine receptors. *J. Recept. Res.*, **13**, 413–436.

PERRY, E.K., SMITH, C.J., COURT, J.A., BONHAM, J.R., RODWAY, M. & ATACK, J.R. (1988). Interaction of 9-amino-1,2,3,4-tetrahydroamino-acridine (THA) with human cortical nicotinic and muscarinic receptor binding in vitro. *Neurosci. Lett.*, **91**, 211–216.

RAPIER, C., LUNT, G.G. & WONNACOTT, S. (1988). Stereoselective nicotine-induced release of dopamine from striatal synaptosomes: concentration dependence and repetitive stimulation. *J. Neurochem.*, **50**, 1123–1130.

RAPIER, C., LUNT, G.G. & WONNACOTT, S. (1990). Nicotinic modulation of ^{3}H-dopamine release from striatal synaptosomes: pharmacological characterisation. *J. Neurochem.*, **54**, 937–945.

ROWELL, P.P. & WINKLER, D.L. (1984). Nicotinic stimulation of [3H]acetylcholine release from mouse cerebral cortical synaptosomes. *J. Neurochem.*, **43**, 1593–1598.

SAHAKIAN, B.J., OWEN, A.M., MORANT, N.J., EAGGER, S.A., BODDINGTON, S., CRAYTON, L., CROCKFORD, H.A., CROOKS, M., HILL, K. & LEVY, R. (1993). Further analysis of the cognitive effects of tetrahydroaminoacridine (THA) in Alzheimer's disease: Assessment of attentional and mnemonic function using CANTAB. *Psychopharmacology (Berlin)*, **110**, 395–401.

SCHWARTZ, R.D. & KELLAR, K.J. (1983). Nicotinic cholinergic receptor binding sites in the brain: regulation in vivo. *Science*, **220**, 214–216.

SCHWARTZ, R.D. & KELLAR, K.J. (1985). In vivo regulation of ^{3}H-acetylcholine recognition sites in brain by nicotinic cholinergic drugs. *J. Neurochem.*, **45**, 427–433.

SHAW, K.-P., ARACAVA, Y., AWAIKE, A., DALY, J.W., RICKETT, D.L. & ALBUQUERQUE, E.X. (1985). The reversible cholinesterase inhibitor physostigmine has channel-blocking and agonist effects on the acetylcholine receptor-ion channel complex. *Mol. Pharmacol.*, **28**, 527–538.

SHERBY, S.M., ELDEFRAWI, A.T., ALBUQUERQUE, E.X. & ELDEFRAWI, M.E. (1985). Comparison of the actions of carbamate anticholinesterases on the nicotinic receptor. *Mol. Pharmacol.*, **27**, 343–348.

SMELIK, P.G. & ERNST, A.M. (1966). Role of nigro-striatal dopaminergic fibers in compulsive gnawing behavior in rats. *Life Sci.*, **5**, 1485–1488.

SUMMERS, W.K., MAJOVSKI, L.V., MARSH, G.M., TACHIKI, K. & KLING, A. (1986). Oral tetrahydryoaminoacridine in long-term treatment of senile dementia. *N. Engl. J. Med.*, **315**, 1241–1245.

SUZUKI, T., NONAKA, H., FUJIMOTO, K. & KAWASHIMA, K. (1993). Effects of physostigmine and some nitric oxide-cyclic GMP-related compounds on muscarinic receptor-mediated autoinhibition of hippocampal acetylcholine release. *J. Neurochem.*, **60**, 2285–2289.

TARRONI, P., RUBBOLI, F., CHINI, B., ZWART, R., OORTGIESEN, M., SHER, E. & CLEMENTI, F. (1992). Neuronal-type nicotinic receptors in human neuroblastoma and small-cell lung carcinoma cell lines. *FEBS Lett.*, **312**, 66–70.

TAYLOR, P. (1990). Anticholinesterase agents. In *The Pharmacological Basis of Therapeutics*, ed. Gilman, A.G., Rall, T.W., Nies, A.S. & Taylor, P. pp. 131–149. 8th ed. New York: Pergamon Press.

THAL, L.J. & FULD, P.A. (1983). Memory enhancement with oral physostigmine in Alzheimer's disease. *N. Engl. J. Med*,. **308**, 720.

VAN DE KAMP, J.L. & COLLINS, A.C. (1992). Species differences in diisopropylfluorophosphate-induced decreases in the number of brain nicotinic receptors. *Pharmacol. Biochem. Behav.*, **42**, 131–141.

WADA, E., WADA, K., BOULTER, J., DENERIS, E., HEINEMANN, S., PATRICK, J. & SWANSON, L.W. (1989). Distribution of alpha 2, alpha 3, alpha 4, and beta 2 neuronal nicotinic receptor subunit mRNAs in the central nervous system: a hybridization histochemical study in the rat. *J. Comp. Neurol.*, **284**, 314–335.

WHITING, P., SCHOEPFER, R., LINDSTROM, J. & PRIESTLEY, T. (1991). Structural and pharmacological characterization of the major brain nicotinic acetylcholine receptor subtype stably expressed in mouse fibroblasts. *Mol. Pharmacol.*, **40**, 463–472.

WILKINSON, L. (1990). *Systat: The System for Statistics*. Evanston, IL: Systat. Inc.

WINN, P., FARRELL, A., MACONICK, A. & ROBBINS, T.W. (1983). Behavioral and pharmacological specificity of the feeding elicited by cholinergic stimulation of the substantia nigra in the rat. *Behav. Neurosci.*, **97**, 794–809.

XIAO, W.-B., NORDBERG, A. & ZHANG, X. (1993). Effect of *in vivo* microdialysis of 1,2,3,4-tetrahydro-9-aminoacridine (THA) on the extracellular concentration of acetylcholine in the striatum of anesthetized rats. *J. Pharmacol. Exp. Ther.*, **265**, 759–764.

(Received July 6, 1993
Revised October 15, 1993
Accepted November 8, 1993)

Br. J. Pharmacol. (1994), **111**, 703–710 © Macmillan Press Ltd, 1994

Demonstration of the neurotransmitter role of calcitonin gene-related peptides (CGRP) by immunoblockade with anti-CGRP monoclonal antibodies

[1]K.K.C. Tan, M.J. Brown, *J. Longmore, C. Plumpton & *R.G. Hill

Clinical Pharmacology Unit, Addenbrooke's Hospital, Cambridge and *Merck Sharp and Dohme Research Laboratories, Neuroscience Research Centre, Terlings Park, Harlow

1 Monoclonal antibodies (MAbs) against rat α-calcitonin gene-related peptide (αCGRP) were produced. Those which bound CGRP in a radioimmunoassay and inhibited the binding of 2-[^{125}I]-iodohistidyl^{10}-CGRP in a receptor binding assay were selected for immunoblockade experiments.

2 The effect of MAbs on CGRP inhibition of electrically stimulated contractions of the rat isolated vas deferens was characterized. Four out of 11 MAbs tested shifted the concentration-response curve of CGRP to the right compared with vehicle or irrelevant MAb control. MAb C4.19 produced equipotent blockade of rat αCGRP and rat βCGRP and was chosen for further studies. MAb C4.19 had no pharmacologically significant effect on the concentration-response relationship of isoprenaline, rat β-endorphin or somatostatin.

3 We demonstrated that the pharmacological response to CGRP in the presence of MAb C4.19 could be predicted when the dissociation constant and concentration of binding sites of the antibody were known. Comparison of experimental and computer simulated data showed good agreement for EC_{50} and maximum effect of CGRP in the presence of MAb C4.19.

4 Capsaicin at 1 μM inhibited the electrically stimulated contractions by 60.8% (95% confidence interval 51.8% to 69.9%). This effect was significantly attenuated by MAb C4.19 to 26.0% (95% confidence interval 15.2% to 36.8%; $P<0.0003$).

5 The immunoblockade of exogenous and endogenous CGRP described here, together with complementary evidence from other studies, strongly suggest that CGRP has a major neurotransmitter role at the neuroeffector junction of the rat vas deferens.

Keywords: Calcitonin gene-related peptide; monoclonal antibodies, rat isolated vas deferens; immunoblockade; neurotransmission; capsaicin

Introduction

Calcitonin gene-related peptide (CGRP) is produced by alternative processing of the primary mRNA transcripts of the calcitonin gene (Rosenfeld *et al.*, 1983). A second CGRP gene encoding another 37-amino acid peptide was subsequently identified (Amara *et al.*, 1985; Steenbergh *et al.*, 1985). This peptide (βCGRP) differs from the originally discovered CGRP (αCGRP) by only one amino acid at position 35 in the rat. Unlike calcitonin, CGRP is primarily localized in the brain and peripheral nervous tissue. Diverse biological effects have been attributed to CGRP but its physiological importance remains to be established in many organ systems. The localization of CGRP-like immunoreactivity in primary afferent neurones innervating many different tissues and the wide distribution of CGRP binding sites suggest that CGRP may be a physiologically important neurotransmitter.

One important criterion that must be fulfilled for any neurotransmitter is that modulation of the effects of the exogenous putative neurotransmitter by drugs should have corresponding effects on responses to nerve stimulation. Pharmacological blockade is normally achieved through the use of specific receptor antagonists. A number of C-terminal fragments of CGRP have been demonstrated to behave as receptor antagonists (Mimeault *et al.*, 1991). The C-terminal (8–37) fragment of human αCGRP has been well characterized and is commercially available. However, CGRP (8–37) demonstrates variable antagonistic potency in different tissues and is a relatively poor antagonist in the rat isolated vas deferens preparation (Dennis *et al.*, 1990). This has led to the postulation that multiple receptor subtypes exist for CGRP. An alternative approach to pharmacological blockade is the use of antibodies which bind to and inhibit the biological activities of putative neurotransmitter peptides. Immunoblockade may be a more general approach to the elucidation of the physiological roles of neuropeptides since no assumptions have to be made concerning receptor multiplicity and the relative selectivity of receptor antagonists.

The major objective of the present study was to investigate the role of CGRP as a principal neurotransmitter, using the neuroeffector junction of the rat isolated vas deferens as a model for neurotransmission. The release of endogenous CGRP from nerves was achieved through the use of capsaicin. Capsaicin is the pungent ingredient of hot peppers of the genus *Capsicum* which selectively stimulates a sub-population of primary afferent neurones (reviewed by Holzer, 1991). It has been widely used as a pharmacological tool to investigate the 'efferent' function of primary afferent neurones (reviewed by Maggi & Meli, 1988). Stimulation of capsaicin-sensitive sensory neurones leads to release of neuropeptides stored in nerve terminals which may, in turn, mediate various efferent functions. Both capsaicin and CGRP inhibit the nerve-mediated contractions of the isolated vas deferens. It is therefore reasonable to hypothesize that CGRP may be involved in neurotransmission at the neuroeffector junction of the rat vas deferens.

Analysis of the effects of individual endogenous neuropeptides is often difficult because of the co-release of several neuropeptides by capsaicin in many tissues. In particular, tachykinins co-released with CGRP often produce a similar biological response (e.g. dilatation of arteries). In the electrically stimulated isolated vas deferens, neurokinin A and susbtance P enhance contractions (Moritoki *et al.*, 1987) in

[1] Author for correspondence.

contrast to the inhibitory effect of CGRP (Goto et al., 1987). Tissue concentrations of tachykinins are low in the rat vas deferens and substance P-like and neurokinin-like immunoreactivity were undetectable by immunocytochemistry in this tissue (Saito et al., 1987). In this respect, the rat vas deferens is a particularly useful model for the investigation of CGRP as a major neurotransmitter.

Immunoblockade of biologically-active peptides is a relative new pharmacological tool which has not been subject to rigorous scientific evaluation. Therefore a further objective of the present investigations was to validate the use of immunoblockade as an experimental tool for probing the physiological role of CGRP. We have done this by the use of monoclonal antibodies (MAbs) and appropriate experimental designs to confirm the specificity of blockade. In addition, we have fitted appropriate models to the observed data and performed limited simulations in order to compare observations with theoretical predictions.

Methods

Production of monoclonal antibodies

Rat αCGRP was conjugated to bovine serum albumin using 1-ethyl-3(3-dimethylaminopropyl)-carbodiimide hydrochloride (O'Shaughnessy, 1982). The conjugate was mixed with Freund's adjuvant to produce a water-in-oil emulsion. Two hundred μl of the mixture, containing 35 μg of the immunogen, was injected into each mouse by the intraperitoneal route. Ten female Balb/C mice were immunized. Freund's complete adjuvant was used for the priming dose and Freund's incomplete adjuvant used for the first and second booster injections. The first and second booster injections were given at 4 weekly intervals. A final aqueous injection was given 3 days prior to fusion.

Sera collected 8 days following the second booster injection were screened by indirect enzyme-linked immunoadsorbent assay (ELISA; described below) and were found to be positive for antibodies against CGRP. Fusion between Sp2 myeloma cells and spleen cells from mice was performed by a modification of the method described by Galfre & Milstein (1981). Hybridoma cells were co-cultured with feeder layer cells (irradiated MRC-5 human lung diploid fibroblasts; Long et al., 1986). Supernatants from the fusion were screened by indirect ELISA. Prior to cloning, 100 positive hybridomas detected by the primary ELISA screen were subjected to secondary screening assays which included further ELISAs, radioimmunoassay (RIA) and receptor binding assay using a rat liver membrane preparation (Nakamuta et al., 1986). These assays are described fully below. Four hybridomas (coded C4.19, C4.6, R1.50, R2.73) were strongly positive in the RIA and the receptor binding assay. The hybridoma lines were cloned twice by limiting dilution (Goding, 1986).

MAbs were produced in bulk by growing hybridoma cells as ascitic tumours (Galfre & Milstein, 1981) in Balb/C mice which had been previously primed with a 100 μl intraperitoneal injection of pristance (2,6,10,14-tetramethyl-pentadecane). MAbs were purified by ammonium sulphate precipitation (Goding, 1986) followed by re-suspension in phosphate-buffered saline (PBS). Protein concentrations were estimated using a Coomassie brilliant blue dye binding assay (Bio-Rad) with bovine γ-globulin as standard.

Indirect enzyme-linked immunoadsorbent assay (ELISA)

Ninety-six well microtitre plates (Linbro EIA plus titration plates; Flow) were coated with 50 μl of 400 nM CGRP solution or PBS vehicle per well, sealed with film, and left overnight at 4°C. Further steps were performed at room temperature. Plates were washed three times with 300 μl PBS/Tween 20 0.05% between each step of the ELISA. Wells were incubated with 100 μl porcine gelatin 0.25% in PBS pH 7.4 (blocking step) for 2 h. Fifty μl serum or hybridoma culture supernatant, diluted as appropriate, was added to each well and incubated for 2 h. Serial dilutions were made in PBS/Tween 20 0.05%/gelatin 0.25%. Controls used were normal mouse immunoglobulin (10 μg ml^{-1}), culture medium and Sp2 myeloma cell culture supernatant. Wells were incubated with 50 μl horseradish peroxidase-conjugated rabbit anti-mouse antibody (1 in 1000 in PBS/Tween 20 0.05%/gelatin 0.25%) for 1 h. One hundred μl substrate reagent (0.006% hydrogen peroxide, 0.1 M acetate-citrate buffer pH 6) containing tetramethylbenzidine (100 μg ml^{-1}) as chromogen (Bos et al., 1981) was added to each well. Positive wells developed a blue colour when 25 μl of 2 M sulphuric acid was added to give a yellow colour with greater intensity. Absorbance was measured at 450 nm using an ELISA plate reader (Titertek Multiskan Plus Mk II, Flow Laboratories).

Selectivity of antibodies for different CGRPs was assessed by coating plates with the α and β forms of rat and human CGRP. Relative affinity of antibodies for CGRP was assessed by serial dilution of hybridoma supernatants. The validity of this simple method of determining relative affinity (van Heyningen et al., 1983) depends on prior knowledge that the variation of immunoglobulin concentration in supernatants from confluent hybridomas is generally less than ten fold.

Receptor binding assay

Livers dissected from Wistar rats were homogenized in 50 mM Tris HCl pH 7.4 containing 0.1 mM phenyl-methyl-sulphonyl-fluoride (PMSF). The homogenate was centrifuged at 15000 *g* for 20 min at 4°C. Supernatant was decanted and centrifuged at 48000 *g* for 60 min at 4°C. The pellet was resuspended in buffer and centrifuged at 48000 *g* for 60 min at 4°C. The supernatant was discarded and pellet resuspended in binding assay buffer containing aprotinin (20 u ml^{-1}), bacitracin (0.1%), PMSF (0.1 mM), $MgCl_2$ (5 mM), bovine serum albumin (0.5%) in 50 mM Tris HCl pH 7.4 (at 4°C).

The binding assay incubation mixture consisted of 50 μl hybridoma supernatant (diluted as appropriate), 50 μl binding buffer, 50 μl (2-[^{125}I]-iodohistidyl^{10}-human αCGRP (40,000 c.p.m.) and 100 μl liver membrane suspension (3 mg ml^{-1}). Non-specific binding was assessed using excess rat αCGRP (10^{-6} M). Cell culture medium, Sp2 myeloma supernatant and normal mouse immunoglobulin (10 μg ml^{-1}) were used as controls. The mixture was incubated at 4°C for 2 h, vacuum filtered through Whatman GF/C filter paper presoaked in polyethyleneimine (250 μl in 200 ml 50 mM Tris HCl pH 7.4), and washed thrice with 3 ml ice-cold buffer (50 mM Tris HCl pH 7.4 containing bovine serum albumin 0.5%). Radioactivity on the filter paper was counted in a Beckman Gamma 5500 counter.

Radioimmunoassay (RIA)

For screening procedures, the RIA incubation mixture consisted of 50 μl hybridoma supernatant, 50 μl 2-[^{125}I]-iodohistidyl^{10}-human αCGRP (40,000 c.p.m.) and 400 μl of assay buffer (50 mM sodium phosphate buffer pH 7.4 containing 10 mM EDTA and 0.3% bovine serum albumin). Tissue culture medium, myeloma (Sp2) culture supernatant, normal mouse immunoglobulin (10 μg ml^{-1}) and a blank without supernatant were used as controls. The assay was performed at 4°C with a 4 day incubation period. Bound and free CGRP was separated by charcoal precipitation. One dextran-coated charcoal tablet (Steranti Separex; Steranti Research) was stirred in 15 ml separation buffer (assay buffer containing 0.25% gelatin) for 30 min at 4°C. Two hundred and fifty μl of the dextran/charcoal suspension was added to each assay tube followed by centrifugation at 2000 *g* for 20 min.

Supernatant and charcoal were separated and the pellet counted in a Beckman Gamma 5500 counter.

RIA was also performed to estimate the dissociation constants (K_d) of MAbs and the maximum binding capacity (B_{max}) of purified ascites. The displacement of 2-[^{125}I]-iodohistidyl^{10}-human αCGRP binding to MAb C4.19 by rat α and β CGRP was investigated. No difference in binding was found whether assay buffer or Krebs buffer was used in the RIA. MAb C4.19 did not cross-react with substance P at 1 μM.

Tissue bath experiments

Approximately 1.5 cm sections of the prostatic portion of the vas deferens were obtained from male Sprague-Dawley rats (220–300 g). Left and right vas deferens from the same animal were used as test and control tissues. The tissues were mounted for isometric tension recordings in 3 ml siliconized (Sigmacote, Sigma) tissue baths containing Krebs physiological salt solution (PSS) maintained at 37°C, pH 7.4, oxygenated with 95% O_2 and 5% CO_2. The Krebs PSS had the following composition (mM): NaCl 118, KCl 4.8, $CaCl_2$ 2.5, KH_2PO_4 1.2, $MgSO_4$ 1.2, $NaHCO_3$ 25, and glucose 11.1. A resting load of 0.5 g tension was applied. Isometric tension changes along the longitudinal axis were recorded with a force transducer connected to a Grass Model 7D Polygraph recorder. Platinum wire electrodes were placed at the top and bottom of the organ bath for electrical field stimuation. The tissues were electrically stimulated using a Multistim System-D330 (Digitimer Limited) stimulator. The following stimulation parameters were used: frequency 0.2 Hz; pulse width 0.5 ms; voltage 60–80 V.

Following a 90 min equilibration period, over which the tissues were electrically stimulated, anti-CGRP MAbs or controls (see below) were added to the tissue baths. Experiments were performed to determine whether pre-incubation with MAb for different periods affected the response to 10 nM rat αCGRP (Table 1). In all other experiments, tissues were pre-incubated with MAb or control for 10 min prior to the determination of cumulative concentration-response relationships to the appropriate agonists (either CGRP, isoprenaline, rat β-endorphin, or somatostatin). Preliminary experiments with CGRP showed that a second concentration-response determination produced a lower maximal effect. Therefore, only one cumulative concentration-response relationship was obtained for CGRP in each tissue. Since tachyphylaxis develops rapidly to somatostatin (Vizi *et al.*, 1984), the response to a single concentration of somatostatin was tested only once in each tissue. Responses to isoprenaline and rat β-endorphin did not desensitize. Cross-over experiments were therefore performed in which the same tissue was pre-incubated for 10 min with anti-CGRP MAb or control.

Time course experiments were performed to investigate the influence of MAb incubation time on the response to capsaicin (Table 1). The effect of MAb C4.19 on the response to capsaicin was compared with controls following a 45 min incubation. A concentration of capsaicin producing maximal response (1 μM) was used (Maggi *et al.*, 1993). Individual tissues were exposed to a single concentration of capsaicin.

MAbs were added in the form of crude ascites or MAbs purified as described above. Seven MAbs against human CGRP C- and N-terminal fragments (from C. Plumpton) were tested along with the four MAbs obtained from immunization of mice with rat αCGRP described above. The MAb vehicle (PBS) was used as a control. A mouse anti-rat MAb MAR 18.5 or a mouse anti-thyroid-stimulating hormone (TSH) MAb was also used as irrelevant antibody controls at the same protein concentration as anti-CGRP MAbs.

Data analysis

The K_d and B_{max} of the MAb C4.19 for rat αCGRP and rat βCGRP were estimated by fitting the following model to binding data from RIA displacement experiments:

$$B(C) = \frac{B_{max} \times C}{K_d \times (1 + D/K_{dD}) + C} + NS \times C$$

where B(C) is the binding B of ligand (2-[^{125}I]-iodohistidyl^{10}-human αCGRP) concentration C in the presence of displacer (rat αCGRP or βCGRP) concentration D. K_d and K_{dD} are the dissociation constants of ligand and displacer respectively. B_{max} is the concentration of binding sites and NS is the non-specific binding parameter.

For a given total concentration of ligand, the concentration of ligand bound was predicted from the following binding model for simulation purposes:

$$B(C) = \frac{B_{max} \times C}{K_d + C}$$

The concentration of unbound CGRP was simulated for the range of concentrations used in organ bath experiments. The pharmacological response in the presence of MAb could then be simulated with the pharmacodynamic model described below.

The inhibitory effect of CGRP in organ bath experiments was expressed as % inhibition relative to stable pre-dosing contractions. The following sigmoidal E_{max} (logistic) model was fitted to concentration-response data obtained from individual tissues:

$$E = E_0 + \frac{E_{max} \times C^N}{EC_{50}{}^N + C^N}$$

Where E_0 is the baseline effect, E_{max}, the maximum effect, EC_{50} the concentration which produces half-maximal effect and N the steepness factor (Hill coefficient).

Parameter estimation and simulation were performed by use of the non-linear extended least-squares regression package MKMODEL version 4.72 (Biosoft, Cambridge). EC_{50} was assumed to be log-normally distributed (Carpenter, 1986). The paired *t* test was performed for comparison of test and control data from paired tissues. One-way analysis of variance followed by Tukey's test for multiple comparisons were performed to assess the influence of incubation time on immunoblockade of CGRP and capsaicin responses in unpaired tissues. Ninety-five percent confidence intervals were used to indicate the precision of estimates (Gardner & Altman, 1989). Differences discernible at the 0.05 level were

Table 1 Effect of incubation time of MAb C4.19 on the mean responses (95% confidence interval) to rat αCGRP and capsaicin (% inhibition: tissues from 6 animals at each time point)

Incubation time (min)	*Response to rat αCGRP* (10 nM)	*Response to capsaicin* (1 μM)
10	14.3 (7.6 to 21.0)	55.0 (46.9 to 63.2)*
45	17.8 (9.4 to 26.2)	26.0 (19.0 to 33.1)
90	20.2 (11.8 to 28.6)	29.4 (21.2 to 37.5)

*$P < 0.05$ compared with responses at 45 or 90 min.
Inhibition of electrically stimulated contractions of the rat isolated vas deferens is expressed as % inhibition relative to stable contractions recorded immediately before addition of rat αCGRP or capsaicin.

considered statistically significant. Statistical analysis was performed by use of the Statgraphics-Plus package (STSC, Inc., Rockville, U.S.A.).

Materials

Rat αCGRP, rat βCGRP, human αCGRP, human βCGRP and rat β-endorphin were obtained from Peninsula. Bacitracin, polyethleneimine, PMSF, 1-ethyl-3(3-dimethylaminopropyl)-carbodiimide hydrochloride, pristane, capsaicin, (−)-isoprenaline hydrochloride and somatostatin were purchased from Sigma. 2-[^{125}I]-iodohistidyl^{10}-human αCGRP was supplied by Amersham. Aprotinin was obtained from Bayer. Tetramethylbenzidine and horseradish peroxidase-conjugated rabbit anti-mouse antibody were from ICN Flow. Anti-thyroid stimulating hormone MAb (Code MA/732.162) and mouse anti-rat MAb 18.5 (ATCC No. TIB 216) were from Serono and the European Collection of Animal Cell Cultures, Porton Down, respectively. A 10 mg ml^{-1} stock solution of capsaicin was prepared in 70% ethanol and further diluted with Krebs solution for addition to organ baths. All other drugs were diluted in Krebs solution.

Results

The four MAbs C4.19, C4.6, R1.50, R2.73 bound CGRP by ELISA and RIA. All four MAbs cross-reacted with the α and β forms of rat and human CGRP by ELISA. CGRP binding was inhibited by these antibodies in the receptor binding assay which served as the screening system for blocking MAbs.

Rat αCGRP and rat βCGRP produced concentration-dependent inhibition of electrically stimulated contractions of

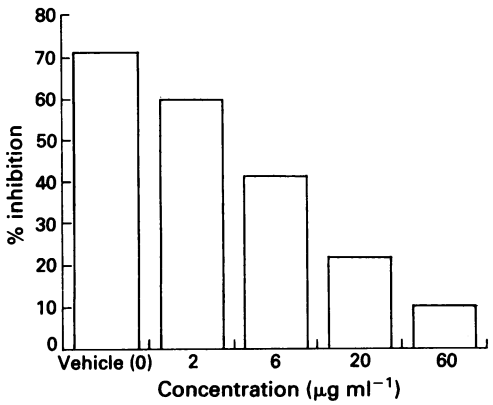


Figure 1 Effect of MAb C4.19 at various protein concentrations on the inhibitory effect of 10 nM rat αCGRP. The effect of CGRP was expressed as % inhibition relative to stable pre-dosing contractions. Mean responses from 2 experiments are shown.

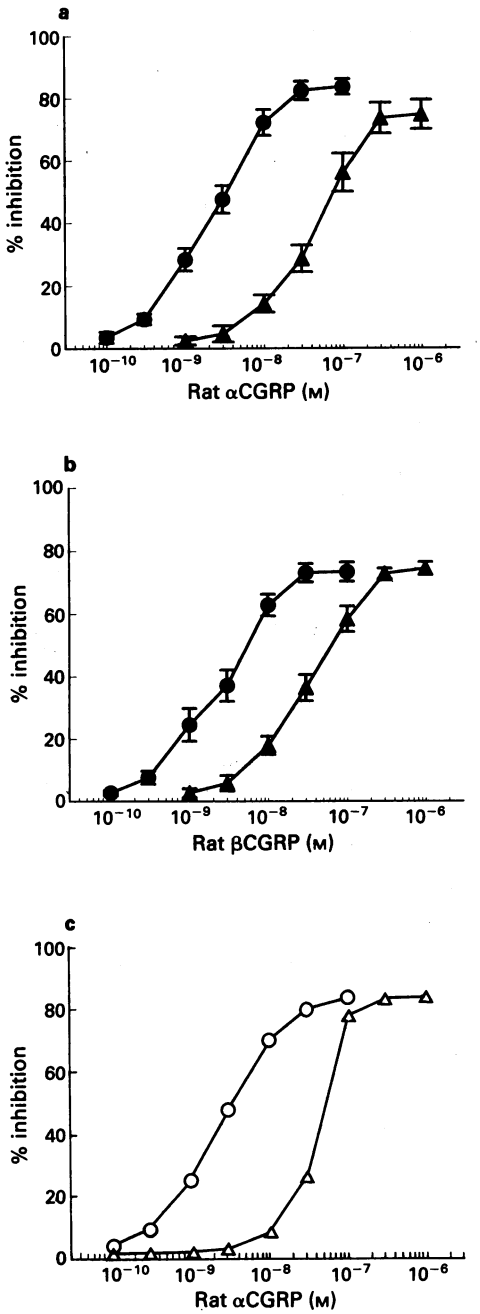


Figure 2 Concentration-response curves observed for rat αCGRP (a) or βCGRP (b) in the presence of PBS vehicle (●) or purified MAb C4.19 ascites at 60 μg ml^{-1} protein (▲). The effect of CGRP is expressed as % inhibition relative to stable pre-dosing contractions. Mean responses (n = 6 to 8) are plotted with standard error bars. (c) Shows simulated concentration-response curves to rat αCGRP in the presence of PBS vehicle control (○) or MAb C4.19 (△) at 60 μg ml^{-1} protein using estimated K_d of 1.9 nM and B_{max} of 79 nM.

Table 2 Estimated geometric mean EC_{50} (95% confidence interval) of drugs following pre-incubation of the electrically stimulated rat isolated vas deferens with MAb C4.19 or control (nM: n = 6 to 8)

Drug	*EC_{50} in presence of MAb C4.19 at 60 μg ml^{-1}*	*Control EC_{50} (PBS vehicle[a] or irrelevant MAb MAR 18.5 at 60 μg ml^{-1}[b])*	*Ratio of MAb: Control EC_{50} (95% confidence interval)*
Rat αCGRP	52 (27 to 98)	2.3 (1.5 to 3.6)[a]	21.9 (13.3 to 36.2)
Rat αCGRP	38 (26 to 54)	4.4 (2.8 to 7.1)[b]	8.5 (7.5 to 9.6)
Rat βCGRP	32 (21 to 49)	2.4 (1.3 to 4.4)[a]	13.3 (6.2 to 28.4)
Isoprenaline	25 (7.9 to 77)	19 (6.4 to 58)[a]	1.3 (0.3 to 4.8)
Rat β-endorphin	56 (32 to 98)	44 (25 to 76)[a]	1.3 (1.0 to 1.6)

the rat isolated vas deferens. The two forms of CGRP were equipotent (Table 2). Effective blocking concentrations of MAbs were found by assessing the effect of various concentrations of MAbs on the response to 10 nM rat αCGRP. For example, it was found that 60 μg ml^{-1} of purified MAb C4.19 ascites was required to block most of the response to 10 nM rat αCGRP (Figure 1). The effect of a single concentration of MAb on the concentration-response relationship of CGRP was then examined to assess whether an approximate ten fold $\log_{10}$ shift to the right could be obtained. None of the MAbs tested had any effect on baseline contractions. Four out of 11 MAbs tested, including MAb C4.19, C4.6 and R2.73 described above, shifted the concentration-response curve of CGRP to the right compared with vehicle or irrelevant MAb control. The use of RIA and a receptor binding assay as biochemical screens was generally successful in predicting blocking MAbs. An interesting exception was MAb R1.50 which clearly showed the greatest activity in these assays and in the ELISA. Although raised in mice immunized with rat αCGRP, it was highly potent at blocking human αCGRP but blocked rat αCGRP poorly. The unexpected selective blocking activity of MAb R1.50 highlighted the need to perform positive control experiments with exogenous peptide of the form known to be present in the tissue. MAb R2.73 was effective at blocking rat αCGRP but not βCGRP despite cross-reaction with both forms of CGRP in the ELISA.

MAb C4.19 was found to block rat αCGRP (Figure 2a) and rat βCGRP (Figure 2b) effectively and was chosen for detailed studies at a protein concentration of 60 μg ml^{-1} (8.5 μl of a stock solution of 21.1 mg ml^{-1} added to tissue bath). Time-course experiments showed that a 10 min incubation period with MAb C4.19 was sufficient for optimal immunoblockade (Table 1). The onset of effect of CGRP was more gradual in tissues incubated with MAb C4.19 than in tissues incubated with PBS vehicle or irrelevant MAb MAR 18.5 (Figure 3). The magnitude of the rightward shift (ratio of MAb: control EC_{50}; Table 2) of the concentration-response curves for rat αCGRP and βCGRP due to MAb C4.19 were not significantly different. The dissociation constants (K_d) of MAb C4.19 for rat αCGRP and βCGRP were very similar (1.9 and 2.5 nM respectively). Irrelevant mouse MAb MAR 18.5 did not significantly affect the concentration-response relationship of αCGRP compared with PBS vehicle (Table 2). The MAb was purified from ascites fluid by ammonium sulphate precipitation in the same manner as anti-CGRP MAbs. MAb C4.19 had no pharmacologically significant effect on the concentration-response relationship of isoprenaline, rat β-endorphin or somatostatin (Table 2, Figure 4).

The pharmacological response to CGRP in the presence of MAb C4.19 could be predicted when the dissociation constant and concentration of binding sites of the antibody were known. Comparison of experimental and computer simulated data showed good agreement for EC_{50} and E_{max} of CGRP in the presence of MAb C4.19 (Figure 2c). The EC_{50} derived from simulated data was 44 nM. This result was close to the mean EC_{50} of 52 nM (95% confidence interval 27 to 98 nM) estimated from data observed in the presence of MAb C4.19. However, the steepness factor (N) of the theoretical concentration-response curve in the presence of C4.19, 1.81, was

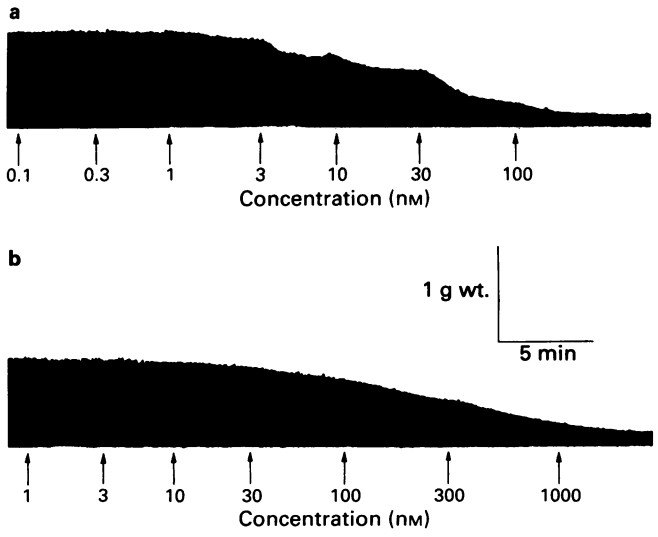


Figure 3 Original traces showing the inhibitory effect of rat αCGRP on electrically stimulated contractions of the rat isolated vas deferens in the presence of irrelevant control MAb MAR 18.5 (a) or MAb C4.19 at 60 μg ml^{-1} protein (b). The examples are from an experiment using paired tissues from a single animal.

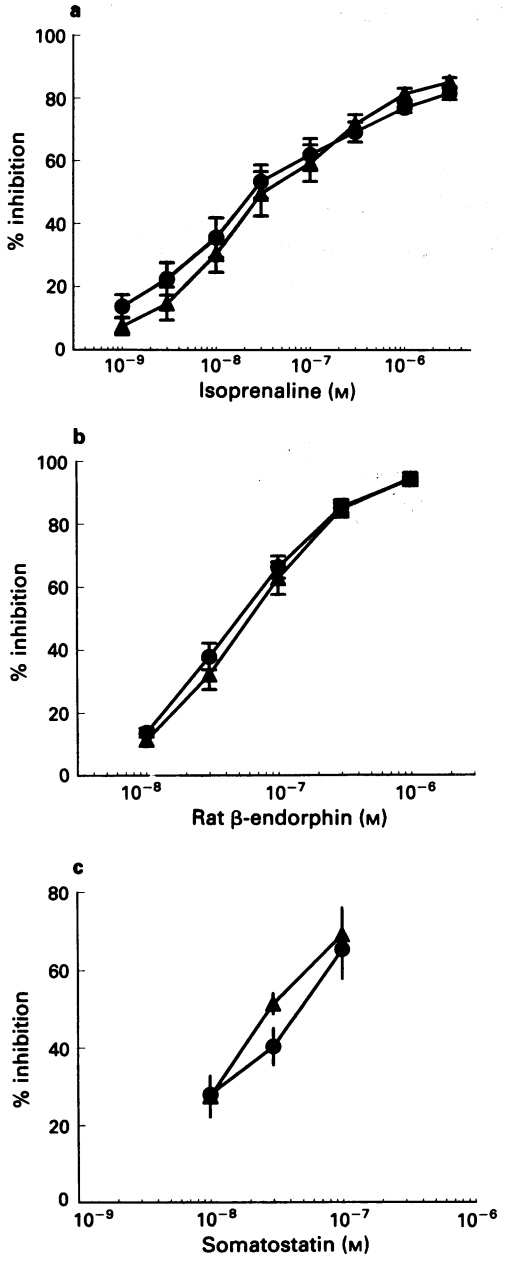


Figure 4 Concentration-response curves observed for isoprenaline (a), rat β-endorphin (b) and somatostatin (c) in the presence of PBS vehicle (●) or MAb C4.19 at 60 μg ml^{-1} protein (▲). Mean responses ($n = 6$) are plotted ± s.e.mean.

Table 3 Mean inhibitory effect of 1 μM capsaicin (95% confidence interval) in the presence of MAb C4.19 or control ($n = 6$ to 8)

% inhibition in presence of MAb C4.19 at 60 μg ml^{-1}	*Control % inhibition (PBS vehicle[a] or irrelevant anti-TSH MAb at 60 μg ml^{-1}[b])*	*Mean MAb-Control difference (95% confidence interval)*
26.0 (15.2 to 36.8)	60.8 (51.8 to 69.9)[a]	− 34.8 (− 22.6 to − 47.0)*
36.1 (16.6 to 55.5)	67.0 (50.0 to 83.9)[b]	− 30.9 (− 14.3 to − 47.5)**

*$P = 0.0003$; **$P = 0.005$

Inhibition of electrically stimulated contractions of the rat isolated vas deferens was expressed as % inhibition relative to stable contractions recorded immediately before addition of capsaicin.

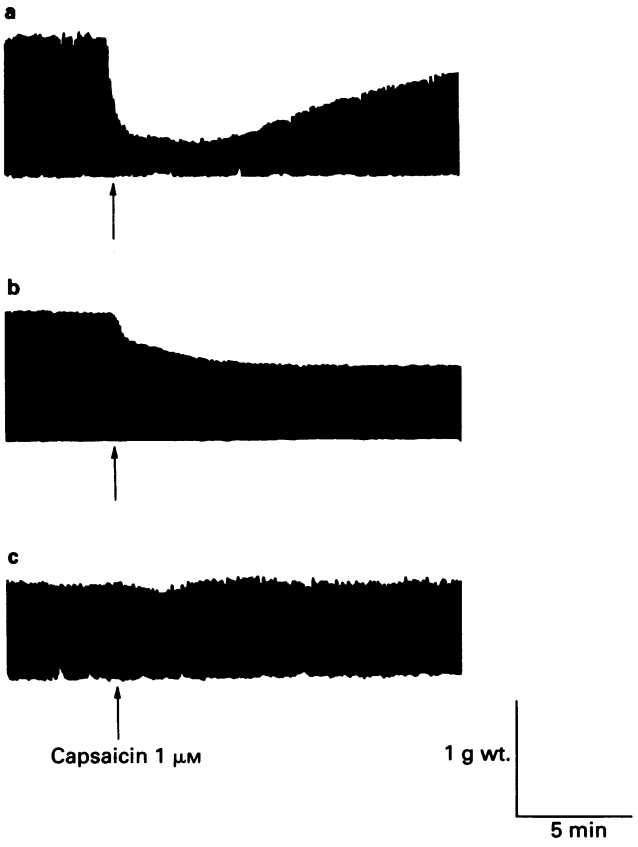


Figure 5 Original traces showing the inhibitory effect of 1 μM capsaicin on the electrically stimulated contractions of the rat isolated vas deferens in the presence of irrelevant control MAb directed against thyroid-stimulating hormone (a) or MAb C4.19 at 60 μg ml^{-1} protein (b and c). The degree of immunoblockade was variable, with partial (b) or almost complete (c) blockade of the capsaicin effect observed in different tissues compared with control.

significantly higher than the steepness factor of 1.12 (95% confidence interval 0.75 to 1.51) estimated from experimental data.

Capsaicin inhibited the electrically stimulated contractions of the isolated vas deferens (Figure 5, Table 3). The response to 1 μM capsaicin was completely desensitized on second administration to tissues. This suggested that the response to capsaicin was due to a specific action on sensory nerves (Maggi *et al.*, 1987; Maggi & Meli, 1988). The effect of capsaicin was significantly attenuated by a 45 min pre-incubation with MAb C4.19. Time-course experiments showed that an antibody incubation period of 45 min produced optimal immunoblockade (Table 1). The peak effect of capsaicin was observed rapidly in the presence of vehicle, followed by a gradual recovery. The time to peak effect was slower and recovery more gradual in the presence of MAb C4.19. Blockade was evident when the response in every pair of tissue obtained from the same animal was compared. The blockade of the effect of capsaicin by MAb C4.19 was also significant compared with an irrelevant mouse anti-TSH MAb (Table 3). The mean responses to capsaicin in the presence of MAb C4.19 or control were in reasonable agreement with the magnitude of immunoblockade of exogenous CGRP responses.

Discussion

We have identified several MAbs which block a biological effect of CGRP. The effects of MAb C4.19 have been characterized in detail, with particular reference to specificity of immunoblockade. Good agreement of observed and predicted immunoblockade of exogenous CGRP with MAb C4.19 provided the basis for attempts to block endogenous CGRP released by capsaicin. Our findings suggest that endogenous CGRP released from primary afferent neurones is partly responsible for inhibition of nerve-mediated contractions of the rat vas deferens.

Immunoblockade has been used to investigate the role of endogenous CGRP in mediating the effect of capsaicin in the rat vas deferens (Maggi *et al.*, 1987). However, a rabbit antiserum was used, the blockade of exogenous rat βCGRP was not characterized, and no attempt was made to model the dynamics of immunoblockade. The low dilution of antiserum (1 in 25) required for immunoblockade in this study raised issues of specificity. The authors proposed immunoblockade as a pharmacological tool to study the possible physiological roles of CGRP as a neurotransmitter. We have performed a further evaluation of immunoblockade as an experimental tool.

The binding of an antibody to a peptide does not always result in blockade of biological activity. Indeed, some workers have reported potentiation of the biological effects of peptides by anti-peptide antibodies (Tilders *et al.*, 1990; Shaw *et al.*, 1992). This was not observed in the present investigation. Our pharmacological screening studies with a panel of anti-CGRP MAbs allowed selection of those that blocked both species of rat CGRP effectively. A MAb such as C4.19 which equipotently blocks the biological activity for both forms is likely to be more generally useful than MAbs which are selective for either form (e.g. MAb R2.73). It is unclear at present whether αCGRP or βCGRP is the major form found in the vas deferens. αCGRP appears to be the major form found in peripheral sensory nerves whereas βCGRP appears to predominate in enteric nerves (Mulderry *et al.*, 1988; Sternini & Anderson, 1992). However, both forms of CGRP are expressed in peripheral sensory nerves innervating many tissues (Noguchi *et al.*, 1990; Sternini & Anderson, 1992).

The time-course experiments showed that due consideration must be paid to antibody incubation periods. However, a distinction should be drawn between requirements for the blockade of exogenous CGRP added to the tissue bath and endogenous CGRP released into the synaptic cleft compart-

ment. Antibodies which are effective in immunoblockade should achieve maximum binding of antigen within a time frame of seconds (van Oers & Tilders, 1991). Therefore it was not suprising that incubation of MAb C4.19 for longer than 10 min produced no enhancement of blockade of exogenous CGRP. No difference is expected because 10 min should be sufficient for the antibody to distribute homogeneously within the tissue bath and antibody concentration did not change with time. In contrast, an incubation time of 10 min was clearly inadequate to achieve blockade of the capsaicin response, indicating that more time must be allowed for the MAb C4.19 to diffuse into the synaptic cleft. The results of the time-course experiment suggested that the concentration of the antibody had reached equilibrium in the synaptic cleft after 45 min since incubation with MAb C4.19 for 90 min did not enhance blockade of the capsaicin response.

The use of MAbs does not obviate the need to demonstrate specificity. The very specificity of an MAb could result in cross-reaction with other peptides or proteins bearing the same epitope. The potential non-specific binding of the MAb C4.19 to CGRP was characterized by controlled experiments with a MAb directed against an irrelevant epitope (MAb MAR 18.5). The potential of the anti-CGRP MAb C4.19 to cross-react with other drugs and peptides producing similar pharmacological responses was assessed by experiments with isoprenaline, rat β-endorphin and somatostatin. Similarly, a non-specific blockade of endogenous CGRP released by capsaicin was excluded by an experiment using an irrelevant anti-peptide (TSH) MAb as a control. We were also able to confirm the specificity of MAb C4.19 in immunocytochemistry experiments. Pre-incubation of the MAb C4.19 with 1 μM rat αCGRP for 90 min at room temperature completely abolished immunostaining in rat spinal cord sections (K. Tan, unpublished observations).

Apparent parallel rightward shifts in the CGRP concentration-response curves were observed in the presence of MAb C4.19. The magnitude of the rightward shift was predicted well by the binding and pharmacodynamic models. However, the theoretical curve was steeper because of the non-linear relationship between total and bound concentration of CGRP predicted by the antibody binding model. One reason for the discrepancy between observed data and theoretical prediction might be experimental error. Another explanation is the assumption of equilibrium conditions for antibody binding prior to consideration of receptor binding. However, the antibody has to compete with receptor for binding, initially under non-equilibrium conditions, when CGRP is added to the tissue bath. A steady-state, corresponding to stable pharmacodynamic response observed, is eventually achieved. Under non-saturating conditions, the proportion of CGRP bound to antibody or receptor is likely to depend on the relative on- and off-rates of antibody and receptor binding and the relative concentrations of antibody and receptor. Modelling of the competitive binding of CGRP to antibody or receptor clearly requires more complex mathematical treatment. However, the present analysis has shown that the assumption of an equilibrium antibody binding model is sufficient to explain the magnitude of the rightward shift in the CGRP concentration-response relationship in the presence of MAb C4.19. It is interesting to note that a steeper non-parallel rightward shift of the CGRP concentration-response relationship, similar to the one simulated here, has been observed in the presence of an anti-CGRP antiserum in the guinea-pig isolated bladder base (Maggi *et al.*, 1988). However, a near-parallel shift of the CGRP concentration-response relationship was observed with the antiserum in the rat isolated vas deferens preparation (Maggi *et al.*, 1987).

Inmunoblockade should be considered as a complementary tool to immunocytochemical, electrophysiological and pharmacological studies using receptor antagonists. CGRP-like immunoreactive outflow from the rat vas deferens is increased 4.5 fold by 10 μM capsaicin (Santicioli *et al.*, 1988). This effect was desensitized on second application of capsaicin. Desensitization is a feature of the specific action of capsaicin on sensory nerves (Maggi & Meli, 1988). CGRP immunoreactive nerves are found around the deferential artery, in the smooth muscle layer and in the lamina propria (Goto *et al.*, 1978). Pre-incubation with capsaicin *in vitro* causes disappearance of CGRP-like immunostaining in the rat vas deferens (Saito *et al.*, 1987). The capsaicin antagonist, capsazepine, blocks the effect of capsaicin on the electrically-evoked contractions of rat isolated vas deferens but not the inhibitory effect of CGRP (Maggi *et al.*, 1993).

Several lines of evidence point to a direct effect of CGRP on smooth muscle rather than a prejunctional effect on sympthetic nerves. Rat αCGRP does not alter the uptake or release of tritiated noradrenaline in mouse vas deferens (Al-Kazwini *et al.*, 1987). In electrophysiological studies of transmural nerve stimulation in the rat isolated vas deferens, CGRP did not affect the amplitude of excitatory junction potentials which are associated with nerve excitation or transmitter release. In contrast, CGRP inhibited the contraction of rat vas deferens induced by direct stimulation of smooth muscles (Goto *et al.*, 1987). The C-terminal fragment human αCGRP (8–37) blocked the effect produced by a low concentration of capsaicin (30 nM) in the rat isolated vas deferens (Maggi *et al.*, 1991). The results of our immunoblockade experiments, together with the complementary evidence reviewed, provide strong evidence that CGRP partly mediates the efferent function of capsaicin-sensitive primary afferent neurons in the rat vas deferens.

This work was supported in part by the British Heart Foundation and the East Anglian Regional Health Authority (Locally Organized Research Scheme).

References

AL-KAZWINI, S.J., CRAIG, R.K. & MARSHALL, I. (1986). Postjunctional inhibition of contractor responses in the mouse vas deferens by rat and human calcitonin gene-related peptides (CGRP). *Br. J. Pharmacol.*, **88**, 173–180.

AMARA, S.G., ARRIZA, J.L., LEFF, W.E., SWANSON, L.W., EVANS, R.M. & ROSENFELD, M.G. (1985). Expression in brain of a messenger RNA encoding a novel neuropeptide homologous to calcitonin gene-related peptide. *Science*, **229**, 1094–1097.

BOS, E.S., VAN DER DOELEN, A.A., VAN ROOY, N. & SCHUURS, A.H.W.M. (1981). 3,3',5,5'-tetramethylbenzidine as an Ames test negative chromogen for horse-radish peroxidase in enzyme immunoassay. *J. Immunoassay*, **2**, 187–204.

CARPENTER, J.R. (1986). A method for presenting and comparing dose-response curves. *J. Pharmacol. Methods*, **15**, 283–303.

DENNIS, T., FOURNIER, A., CADIEUX, A., POMERLEAU, F., JOLICOEUR, F.B., ST. PIERRE, S. & QUIRION, R. (1990). $hCGRP_{8-37}$, a calcitonin gene-related peptide antagonist revealing calcitonin gene-related peptide receptor heterogeneity in brain and periphery. *J. Pharmacol. Exp. Ther.*, **254**, 123–128.

GALFRE, G. & MILSTEIN, C. (1981). Preparation of monoclonal antibodies: strategies and procedures. *Methods Enzymol.*, **73**, 3–46.

GARDNER, M.J. & ALTMAN, D.G. (1989). *Statistics with Confidence*. London: British Medical Journal.

GODING, J.W. (1986). *Monoclonal Antibodies: Principles and Practice*. 2nd ed., London: Academic Press.

GOTO, K., KIMURA, S. & SAITO, A. (1987). Inhibitory effect of calcitonin gene-related peptide on excitation and contraction of smooth muscles of the rat vas deferens. *J. Pharmacol. Exp. Ther.*, **241,** 635–641.

HOLZER, P. (1991). Capsaicin: cellular targets, mechanisms of action, and selectivity for thin sensory neurons. *Pharmacol. Rev.*, **43,** 143–201.

LONG, W.J., McGUIRE, W., PALOMBO, A. & EMINI, E.A. (1986). Enhancing the establishment efficiency of hybridoma cells; use of irradiated human diploid fibroblast feeder layers. *J. Immunol. Methods*, **86,** 89–93.

MAGGI, C.A., BEVAN, S., WALPOLE, C.S.J., RANG, H.P. & GIULIANI, S. (1993). Comparison of capsazepine and ruthenium red as capsaicin antagonists in the rat isolated bladder and vas deferens. *Br. J. Pharmacol.*, **108,** 801–805.

MAGGI, C.A., CHIBA, T. & GIULIANI, S. (1991). Human α-calcitonin gene-related peptide-(8–37) as an antagonist of exogenous and endogenous calcitonin gene-related peptide. *Eur. J. Pharmacol.*, **192,** 85–88.

MAGGI, C.A. & MELI, A. (1988). The sensory-efferent function of capsaicin-sensitive sensory neurones. *Gen. Pharmacol.*, **19,** 1–43.

MAGGI, C.A., SANTICIOLI, P., PATACCHINI, R., GEPPETTI, P., GIULIANI, M., ASTOLFI, M., BALDI, E., PARLANI, M., THEODORSSON, E., FUSCO, B. & MELI, A. (1988). Regional differences in the motor response to capsaicin in the guinea-pig urinary bladder: relative role of the pre- and postjunctional factors related to neuropeptide-containing sensory nerves. *Neuroscience*, **27,** 675–688.

MAGGI, C.A., SANTICIOLI, P., THEODORSSON-NORHEIM, E. & MELI, A. (1987). Immunoblockade of response to capsaicin in the rat vas deferens: evidence for the involvement of endogenous calcitonin gene-related peptide. *Neurosci. Lett.*, **78,** 63–68.

MIMEAULT, M., FOURNIER, A., DUMONT, Y., ST-PIERRE, S. & QUIRON, R. (1991). Comparative affinities and antagonistic potencies of various human calcitonin gene-related peptide fragments on calcitonin gene-related peptide receptors in brain and periphery. *J. Pharmacol. Exp. Ther.*, **258,** 1084–1090.

MORITOKI, H., IWAMOTO, T., KANAYA, J., ISHIDA, Y., ANDO, K. & KITAGAWA, K. (1987). Capsaicin enhances the non-adrenergic twitch response of rat vas deferens. *Br. J. Pharmacol.*, **92,** 469–475.

MULDERRY, P.K., GHATEI, M.A., SPOKES, R.A., JONES, P.M., PIERSON, A.M., HAMID, Q.A., KANSE, S., AMARA, S.G., BURRIN, J.M., LEGON, S. & POLAK, J.M. (1988). Differential expression of α-CGRP and β-CGRP by primary sensory neurons and enteric autonomic neurons of the rat. *Neuroscience*, **25,** 195–205.

NAKAMUTA, H., FUKUDA, Y. & KOIDA, M. *et al.* (1986). Binding sites of calcitonin gene-related peptide (CGRP); abundant occurrence in visceral organs. *Jpn. J. Pharmacol.*, **42,** 175–180.

NOGUCHI, K., SENBA, E., MORIT, Y., SATO, M. & TOHYAMA, M. (1990). Co-expression of α-CGRP and β-CGRP mRNAs in the rat dorsal root ganglion cells. *Neurosci. Lett.*, **108,** 1–5.

O'SHAUGHNESSY, D.J. (1982). Antibodies. In *Radioimmunoassay of Gut Regulatory Peptides*. ed. Bloom, S.R. & Long, R.G. London: W.B. Saunders.

ROSENFELD, M.G., MERMOD, J., AMARA, S.G., SWANSON, L.W., SAWCHENKO, P.E., RIVIER, J., VALE, W.W. & EVANS, R.M. (1983). Production of a novel neuropeptide encoded by the calcitonin gene via tissue-specific RNA processing. *Nature*, **304,** 129–135.

SAITO, A., TOMOBE, Y. & GOTO, K. (1987). Effect of capsaicin on smooth muscles of rat vas deferens: involvement of calcitonin gene-related peptide? *J. Pharmacol. Exp. Ther.*, **242,** 666–672.

SANTICIOLI, P., MAGGI, C.A., GEPPETTI, P., DEL BIANCO, E., THEODORSSON, E. & MELI, A. (1988). Release of calcitonin gene-related peptide-like immunoreactivity (CGRP-LI) from organs of the genitourinary tract in rats. *Neurosci. Lett.*, **92,** 197–201.

SHAW, N.E., FOULKES, R., ANDREW, D.P., BROWN, D.T. & HUGHES, B. (1992). The effect of monoclonal antibodies to calcitonin gene-related peptide (CGRP) on CGRP-induced vasodilatation in pig coronary artery rings. *Br. J. Pharmacol.*, **106,** 196–198.

STEENBERGH, P.H., HOPPENER, J.W.M., ZANDBERG, J., LIPS, C.J.M. & JANSZ, H.S. (1985). A second human calcitonin/CGRP gene. *FEBS Lett.*, **183,** 403–407.

STERNINI, C. & ANDERSON, K. (1992). Calcitonin gene-related peptide containing neurons supplying the rat digestive system: differential distribution and expression pattern. *Somatosens. Mot. Res.*, **9,** 45–59.

TILDERS, F.J.H., VAN OERS, J.W.A.M., WHITE, A., MENZAGHI, F. & BURLET, A. (1990). Antibodies to neuropeptides: biological effects and mechanisms of action. In *Circulatory Regulatory Factors and Neuroendocrine Function*. eds. Porter, J.C. & Jezova, D. pp. 135–145. New York: Plenum Press.

VAN HEYNINGEN, V., BROCK, D.J.H. & VAN HEYNINGEN, S. (1983). A simple method for ranking the affinities of monoclonal antibodies. *J. Immunol. Methods*, **62,** 147–153.

VAN OERS, J.W.A.M. & TILDERS, F.J.H. (1991). Affinities in passive immunization studies: characteristics and consequences. *Endocrincology*, **128,** 496–503.

VIZI, E.S., HORVATH, T. & SOMOGYI, G.T. (1984). Evidence that somatostatin releases endogenous substances responsible for its presynaptic inhibitory effect on rat vas deferens and guinea pig ileum. *Neuroendocrinology*, **39,** 142–148.

(Received September 24, 1993
Revised November 3, 1993
Accepted November 8, 1993)

Br. J. Pharmacol. (1994), **111**, 711–716 © Macmillan Press Ltd, 1994

Inhibition of hypoxia-induced relaxation of rabbit isolated coronary arteries by N^G-monomethyl-L-arginine but not glibenclamide

Canwen Jiang & [1]Peter Collins

Department of Cardiac Medicine, National Heart & Lung Institute, University of London, Dovehouse Street, London SW3 6LY

1 The effects of N^G-monomethyl-L-arginine, tetrodotoxin and glibenclamide on hypoxia-induced coronary artery relaxation, induced by bubbling Krebs solution with 95% N_2 and 5% CO_2 instead of 95% O_2 and 5% CO_2, were assessed by measuring the changes in isometric tension in isolated epicardial coronary artery rings of the rabbit. In addition, the effects of glibenclamide on the relaxation induced by adenosine were investigated.

2 Hypoxia caused a transient relaxation of 38 ± 3% ($P<0.01$) and 17 ± 2% ($P<0.01$) in endothelium-intact or -denuded arteries respectively. N^G-monomethyl-L-arginine (30 and 100 μM) inhibited the relaxation in endothelium-intact rings to 31 ± 2% ($P<0.05$) and 16 ± 2% ($P<0.01$) respectively and slightly but significantly attenuated the relaxation in endothelium-denuded rings to 15 ± 1% and 13 ± 1% ($P<0.05$) respectively.

3 Glibenclamide, a potassium channel inhibitor, did not significantly affect the hypoxia-induced relaxation.

4 Incubation with tetrodotoxin (3 and 10 μM) for 30 min reduced the relaxation to 31 ± 3% ($P<0.05$) and 14 ± 2% ($P<0.01$), and 14 ± 2% ($P<0.05$) and 11 ± 1% ($P<0.05$) in endothelium-intact and -denuded rings respectively. However, indomethacin (10 μM), atropine (1 μM), propranolol (10 μM) and phentolamine (10 μM) did not significantly affect the relaxation.

5 Adenosine (1, 10 and 100 μM) caused relaxation of 6 ± 1%, 52 ± 3% and 97 ± 2% respectively in endothelium-denuded rings precontracted with prostaglandin $F_{2\alpha}$ ($PGF_{2\alpha}$, 3 μM) and the relaxation was markedly inhibited by 8-phenyltheophylline. Furthermore, glibenclamide (1 and 10 μM) reduced the relaxation induced by adenosine (1, 10 and 100 μM) to 2 ± 1% ($P<0.05$), 38 ± 3% ($P<0.05$) and 85 ± 2% ($P<0.05$), and 0.6 ± 0.4% ($P<0.05$), 27 ± 4% ($P<0.05$) and 72 ± 4% ($P<0.01$) respectively, in these endothelium-denuded preparations.

6 These data suggest that hypoxia-induced relaxation is mediated by the release of nitric oxide rather than by the activation of glibenclamide-sensitive potassium channels in rabbit isolated coronary arteries. A neurogenic mechanism partially modulates the relaxation, possibly by activating non-adrenergic and non-cholinergic nerve endings. The inhibition by glibenclamide on adenosine-induced relaxation in isolated coronary arteries may help to explain the fact that glibenclamide inhibits hypoxic coronary relaxation in perfused hearts but not in isolated coronary preparations.

Keywords: Adenosine; hypoxia; relaxation; nitric oxide; neurogenic; ATP-sensitive potassium channels; coronary artery

Introduction

Hypoxia can cause either relaxation or contraction of vascular tissue depending on vessel and species and the degree of hypoxia (Rubanyi & Vanhoutte, 1985a; Wadsworth *et al.*, 1990; Vanhoutte & Lüscher, 1990). Various mechanisms underlying coronary artery relaxation induced by hypoxia have been proposed. The release of endothelium-derived relaxing factor (EDRF), recognised as nitric oxide or a closely related moiety (Palmer *et al.*, 1987; Ignarro *et al.*, 1987), and prostaglandin I_2, may be involved in the hypoxia-induced coronary artery relaxation (Busse *et al.*, 1984; Pohl & Busse, 1989). It is now known that an endothelium-derived hyperpolarization factor (EDHF), identified in certain vascular beds, may contribute to endothelium-dependent relaxation (Chen *et al.*, 1988; Edwards & Weston, 1990; Jiang *et al.*, 1991). Whether EDHF is involved in the mechanism of hypoxia-induced, endothelium-dependent relaxation is not known.

Recent experiments suggest that activation of glibenclamide-sensitive potassium channels may mediate hypoxia-induced relaxation of coronary arteries in perfused heart preparations (Daut *et al.*, 1990; von Beckerath *et al.*, 1991). These authors have proposed that activation of the channel mediates the hypoxia-induced relaxation. However, it is well known that adenosine and other metabolites can be released from the hypoxic myocardium (Newby *et al.*, 1985; Deussen *et al.*, 1986). These vasoactive substances may affect coronary artery tone (Wei *et al.*, 1989). Indeed, adenosine has been found to activate directly glibenclamide-sensitive potassium channels in cardiac myocytes (Kirsch *et al.*, 1990) and dog coronary artery *in vivo* (Belloni & Hintze, 1991). Conversely, endothelium-dependent relaxation induced by acetylcholine has been shown to be mediated partially by the activation of glibenclamide-sensitive potassium channels in some vessels, including rabbit coronary arteries (Jiang *et al.*, 1991).

In order to assess the possible interaction of the endothelium-dependent and adenosine triphosphate-sensitive potassium (K_{ATP}) channel mechanisms, we investigated the effects of N^G-monomethyl-L-arginine (L-NMMA), an inhibitor of nitric oxide synthase, and glibenclamide, which is an inhibitor of the K_{ATP} channels, on hypoxia-induced relaxation in isolated epicardial coronary artery preparations of the rabbit. The possible involvement of non-adrenergic, non-cholinergic and capsaicin nerve endings was assessed by use of tetrodotoxin and capsaicin. Furthermore, the effects of glibenclamide on adenosine-induced relaxation in similar preparations were investigated.

Methods

Animals and tissues

Adult male New Zealand white rabbits (2.5–3 kg) were anaesthetized by an injection of pentobarbitone (60 mg kg^{-1}) into the

[1] Author for correspondence.

ear artery after an injection of heparin (150 units kg^{-1}). The hearts were removed and immediately immersed in ice-cold modified Krebs solution. The epicardial coronary artery was dissected free of connective tissue. Rings (2–3 mm length) were prepared and, in alternate rings, endothelium was removed by gently rubbing the intimal surface with a wooden probe. The presence or absence of endothelium was verified by the relaxation in response to substance P (0.3, 1, 3 and 10 nM).

Coronary artery rings with, or without, endothelium were suspended horizontally between two stainless steel hooks for measurement of isometric tension in individual organ baths containing 7 ml modified Krebs solution at 37°C, bubbled with 95% O_2 and 5% CO_2. The millimolar composition of modified Krebs solution was as follows: NaCl 118.3, KCl 4.7, $CaCl_2$ 2.5, $MgSO_4$ 1.2, K_2PO_4 1.2 and glucose 11.1. Rings were equilibrated for 90 min under a resting tension of 1 g before drugs were added. All experiments were performed in rings with, or without, endothelium in the presence of indomethacin (10 μM).

Coronary artery relaxation induced by hypoxia

Concentration-dependent constrictor response curves to prostaglandin $F_{2\alpha}$ ($PGF_{2\alpha}$) were performed in endothelium-intact and -denuded coronary arteries. The EC_{70} concentration of $PGF_{2\alpha}$ was used to pre-contract individual rings. Hypoxia was induced by bubbling modified Krebs solution with 95% N_2 and 5% CO_2 instead of 95% O_2 and 5% CO_2 after which a stable plateau of contraction was achieved. Po_2 was measured by rapid anaerobic collection of the Krebs solution from the organ bath and its immediate analysis with a Corning 178 pH/blood gas analyser (Corning, Essex), at the time of maximal transient relaxation.

Effects of L-NMMA or glibenclamide on hypoxia-induced relaxation

In groups of endothelium-intact or -denuded rings, L-NMMA (30 and 100 μM), L-NMMA (30 and 100 μM) plus L-arginine (1 mM) or D-arginine (1 mM) or glibenclamide (1 and 3 μM, dissolved in ethanol) were added to coronary arteries precontracted with $PGF_{2\alpha}$. Hypoxia was induced 5 min after the addition of the agent. Because of possible impairment of nitric oxide-dependent relaxation by hypoxia and reoxygenation, these experiments were performed in different tissues. Time-matched controls were performed in the presence of the solvent, ethanol (1/2000, v/v).

Effects of tetrodotoxin (TTX) or capsaicin pretreatment on hypoxia-induced relaxation

A group of endothelium-intact or -denuded arteries was incubated with atropine (10 μM) plus propranolol (10 μM) and phentolamine (10 μM). In the presence of these three agents, another group of endothelium-intact or -denuded arteries was incubated with TTX (3 μM) or capsaicin (1 μM) for 20 min. Rings were then precontracted with $PGF_{2\alpha}$ 10 min after washout of TTX or capsaicin. Hypoxia was subsequently induced.

Effects of 8-phenyltheophylline or glibenclamide on adenosine-induced relaxation

In endothelium-denuded rings the dose-dependent relaxing responses to adenosine (1, 10 and 100 μM) were performed after the rings had been preconstricted with $PGF_{2\alpha}$ (3 μM). In different rings preconstricted with $PGF_{2\alpha}$ (3 μM), glibenclamide (1 and 10 μM), 8-phenyltheophylline (10 μM) or the solvent ethanol (1/2000, v/v) were added. Adenosine dose-dependent relaxant responses were then obtained 5 min later. In two endothelium-denuded rings, precontracted by $PGF_{2\alpha}$ (3 μM), hypoxia was induced 5 min after the addition of 8-phenyltheophylline (10 μM).

Drugs

The following drugs were used: adenosine, N^G monomethyl-L-arginine, tetrodotoxin, indomethacin, atropine sulphate, propranolol hydrochloride, phentolamine hydrochloride, (all supplied by Sigma chemical company and of analytical grade); glibenclamide (gift from Hoechst, UK.).

Statistics

Coronary artery relaxation was expressed as a percentage of the contraction induced by $PGF_{2\alpha}$. Data are shown as mean ± s.e.mean. Student's unpaired t tests were used to analyse the data. In some experiments, the values between groups were compared by one-way analysis of variance, differences between groups being confirmed by the use of an unpaired t test with Bonferronis' modification. A probability of less than 0.05 ($P<0.05$) was considered significantly different.

Results

Coronary artery relaxation induced by hypoxia

The EC_{70} concentration of $PGF_{2\alpha}$ induced comparable contractions of 0.9 ± 0.1 and 0.9 ± 0.2 g respectively ($n = 8$) in endothelium-intact or -denuded rings ($P>0.05$). Hypoxia (Po_2 20–30 torr) caused a transient relaxation in endothelium-intact and -denuded coronary arteries pre-contracted by $PGF_{2\alpha}$ followed by contraction. The relaxation occurred 2–7 min after hypoxia was induced. However, the relaxation was greater in endothelium-intact than -denuded rings ($P<0.05$, Figure 1). In time-matched controls, the contraction induced by $PGF_{2\alpha}$ was no different.

Effects of L-NMMA, L-NMMA plus L-arginine, or L-NMMA plus D-arginine, on hypoxia-induced relaxation

L-NMMA (100 μM) caused a small further contraction (0.06 ± 0.04 g) in endothelium-intact rings precontracted by $PGF_{2\alpha}$, but none in endothelium-denuded arteries. L-NMMA (30 and 100 μM) significantly reduced hypoxia-induced relaxation in endothelium-intact and -denuded arteries in the presence of

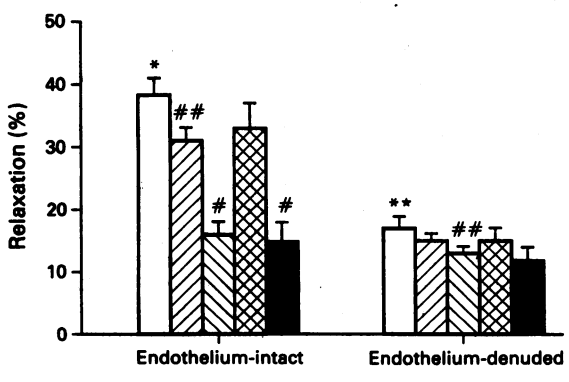


Figure 1 The effects of N^G-monomethyl-L-arginine (L-NMMA, 30 and 100 μM, left slide- and right slide-hatched columns respectively), L-NMMA (100 μM) plus L-arginine (1 mM, cross-hatched columns) or L-NMMA (100 μM) plus D-arginine (1 mM, solid columns) on the relaxation induced by hypoxia (open columns) in rabbit coronary arteries with, or without endothelium. Data (mean ± s.e.mean, $n \geq 6$) are expressed as percentage relaxation of contraction induced by prostaglandin $F_{2\alpha}$ (EC_{70} concentration). *$P<0.01$ compared to time-matched non-hypoxic controls; **$P<0.01$ between endothelium-intact and -denuded arteries; #$P<0.05$ and ##$P<0.01$ compared with corresponding hypoxia alone groups.

Table 1 The effects of glibenclamide (1 and 3 μM), atropine plus propranolol plus phentolamine (10 μM, Atr + Prop + Phent) or capsaicin (1 μM) on hypoxia-induced relaxation in endothelium-intact or -denuded rabbit coronary arteries, precontracted by an EC_{70} dose of prostaglandin $F_{2\alpha}$

	Endothelium-intact	*Endothelium-denuded*
Hypoxia control	38 ± 3%	17 ± 2%
Glibenclamide (1 μM)	38 ± 4%	15 ± 2%
Glibenclamide (3 μM)	36 ± 2%	15 ± 3%
Capsaicin	34 ± 2%	14 ± 3%
Atr + Prop + Phent	39 ± 4%	19 ± 2%

Data are expressed as percentage relaxation of contraction to prostaglandin $F_{2\alpha}$ (mean ± s.e.mean, $n \geq 6$).

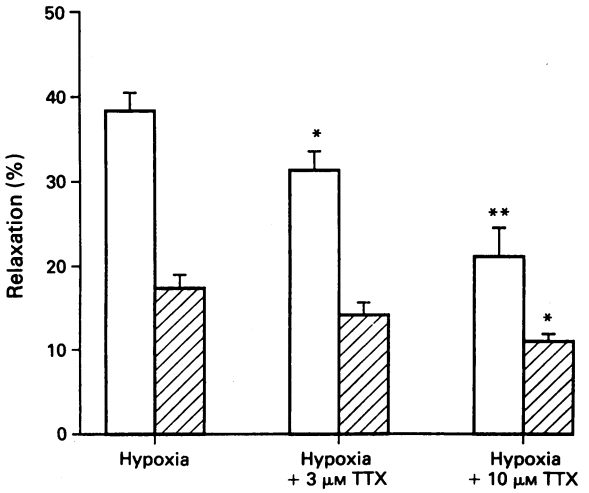


Figure 2 The effects of tetrodotoxin (TTX, 3 and 10 μM) on hypoxia-induced relaxation of rabbit coronary arteries with, or without endothelium (open and cross-hatched columns respectively). Data (mean ± s.e.mean, $n \geq 6$) are expressed as percentage relaxation of contraction induced by prostaglandin $F_{2\alpha}$ (EC_{70} concentration). $^*P<0.05$ and $^{**}P<0.01$ compared with corresponding hypoxia alone groups.

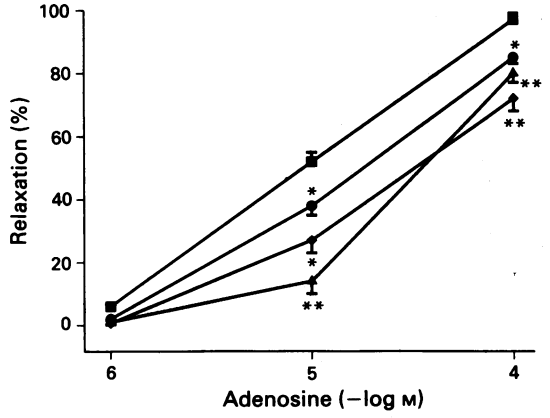


Figure 3 The effects of glibenclamide (1 (●) and 10 μM (▲)) or 8-phenyltheophylline (10 μM, ◆) on adenosine-induced relaxation (controls, ■) in endothelium-denuded rabbit coronary arteries, precontracted with prostaglandin $F_{2\alpha}$ (3 μM). Data (mean ± s.e.mean, $n \geq 8$) are expressed as percentage relaxation of contraction. $^*P<0.05$ and $^{**}P<0.01$ compared to controls.

atropine (10 μM), propranolol (10 μM) and phentolamine (10 μM). Neither L-arginine nor D-arginine had an effect on contraction induced by $PGF_{2\alpha}$. L-Arginine (1 mM) partially reversed this reduction in relaxation, whilst D-arginine (1 mM) had no effect (Figure 1).

Effects of glibenclamide on hypoxia-induced relaxation

Glibenclamide (1 and 3 μM) did not cause significant constrictor responses in endothelium-intact or -denuded arteries precontracted with $PGF_{2\alpha}$. Hypoxia-induced relaxation was slightly but not significantly decreased in the presence of glibenclamide ($n = 7$, $P \geq 0.05$, Table 1). The solvent ethanol (1/2000, v/v) did not affect hypoxia-induced relaxation in time-matched controls (data not shown).

Effects of TTX or capsaicin pretreatment on hypoxia-induced relaxation

Incubation with capsaicin for 30 min slightly, but non-significantly, reduced hypoxia-induced relaxation in endothelium-intact and -denuded coronary arteries (Table 1). However, pretreatment with TTX significantly reduced hypoxia-induced relaxation ($P<0.05$) though the relaxation was not completely abolished. The reduction was greater in endothelium-intact than -denuded arteries (Figure 2). In a group of endothelium-intact or -denuded arteries, atropine, propranolol and phentoalmine (10 μM) did not affect hypoxia-induced relaxation ($n = 6$, $P<0.05$, Table 1).

Effects of glibenclamide and 8-phenyltheophylline on adenosine-induced relaxation

Adenosine caused relaxation of endothelium-denuded rabbit coronary artery rings precontracted with $PGF_{2\alpha}$. 8-Phenyltheophylline (10 μM) had no effect on $PGF_{2\alpha}$-induced contraction. The relaxation was reduced by the adenosine-receptor antagonist, 8-phenyltheophylline (10 μM). Glibenclamide (1 and 3 μM) inhibited the adenosine-induced relaxation (Figure 3), whilst the solvent ethanol (1/2000, v/v) had no effect. In two endothelium-denuded rings, 8-phenyltheophylline (10 μM) did not alter the relaxation induced by hypoxia.

Discussion

We have demonstrated that hypoxia causes a transient relaxation in isolated epicardial coronary arteries of the rabbit. This hypoxia-induced relaxation was reduced significantly by L-NMMA whilst glibenclamide and atropine plus propranolol plus phentolamine did not significantly affect the relaxation. The relaxation was also significantly reduced by pretreatment with TTX but not capsaicin.

It has been suggested that anoxia inhibits the release of nitric oxide from the endothelium (De Mey & Vanhoutte, 1983), and endothelium-dependent contraction is induced by the release of endothelium-dependent constricting factor(s) (Rubanyi & Paul, 1984; Rubanyi & Vanhoutte, 1985a). It has also been proposed that hypoxia may promote a more rapid inactivation of the released nitric oxide, possibly due to the enhanced production of superoxide anions (Gryglewski *et al.*, 1986; Rubanyi & Vanhoutte, 1986). However, it has been

demonstrated that hypoxia (P_{O_2} <300 mmHg) stimulates release of EDRF in rabbit aorta or femoral arteries (Bassenge & Busse, 1988; Pohl & Busse, 1989). In the present study, we observed that transient hypoxia-induced relaxation occurred within 2–3 min in both endothelium-intact and -denuded arteries. The relaxation was greater in endothelium-intact than -denuded rings ($P<0.05$). L-NMMA, a specific inhibitor of nitric oxide biosynthesis, significantly attenuated hypoxia-induced relaxation in endothelium-intact coronary arterial rings. L-Arginine, but not D-arginine, partially reversed this effect. This may be evidence that nitric oxide partially mediates hypoxia-induced relaxation in rabbit coronary arteries. The mechanism by which hypoxia stimulates the release of nitric oxide is unknown. However, endothelial cells may release substance P and other metabolites such as ATP and ADP under hypoxic conditions (Burnstock *et al.*, 1988; Milner *et al.*, 1989; Burnstock, 1989). The release of nitric oxide may therefore be secondary to the release of receptor- or non-receptor-mediated stimuli from endothelial cells in endothelium-intact tissues. Prostaglandin I_2 has been implicated in the mechanism of hypoxia-induced coronary relaxation (Busse *et al.*, 1984; Pohl & Busse, 1989). In the present study, experiments were performed in the presence of indomethacin, therefore precluding the effects of these vasodilator prostanoids.

We found that hypoxia induced a small but significant transient relaxation in endothelium-denuded rings. We tested the hypothesis that activation of glibenclamide-sensitive potassium channels may mediate the hypoxia-induced relaxation, since hypoxia-induced coronary relaxation in perfused guinea-pig hearts is inhibited by glibenclamide and mimicked by the potassium channel opener, cromakalim (Daut *et al.*, 1990; von Beckerath *et al.*, 1991). Glibenclamide significantly inhibits endothelium-independent relaxation induced by lemakalim, a potassium channel opener, in similar preparations of the rabbit epicardial coronary artery (Jiang *et al.*, 1991). However, the same concentration of glibenclamide did not significantly affect hypoxia-induced relaxation in our experiments. These results are consistent with the findings that inhibition of the glibenclamide-sensitive potassium channel does not affect hypoxia-induced relaxation in rat isolated aortic preparations (Rodman *et al.*, 1990). This would argue against the activation of glibenclamide-sensitive potassium channels being responsible for the relaxation demonstrated in these experiments. Furthermore, hypoxia may stimulate the release of endothelium-independent vasoactive substances. It is also possible that hypoxia directly affects intracellular pathways which modulate smooth muscle relaxation.

Adenosine may be the substance that is involved in this relaxation. It is a potent coronary arterial relaxing agent (Kusachi *et al.*, 1984) and an important cardiac metabolite in the regulation of coronary arterial tone (Olsson & Bünger, 1987). EDRF mediates adenosine-induced relaxation in certain arteries, including canine coronary arteries (Rubanyi & Vanhoutte, 1985b). However, in other arteries, including rabbit coronary arteries (De Mey & Vanhoutte, 1981; Furchgott, 1983; Corr, 1992), adenosine causes endothelium-independent relaxation. It has been shown that the relaxation induced by adenosine is mediated by a stimulation of the A_2 receptor (Mustafa, 1980; Cushing *et al.*, 1991; Mathie *et al.*, 1991) and a receptor-linked activation of adenylate cyclase (Kukovetz *et al.*, 1981; Cassis *et al.*, 1987). The release of adenosine may be responsible for the observed coronary arterial relaxation, since adenosine has been shown to be released from hypoxic myocardium (Newby *et al.*, 1985; Deussen *et al.*, 1986; Headrick & Willis, 1988). Adenosine has been shown directly to activate K_{ATP} channels in cardiac myocytes (Kirsch *et al.*, 1990) and the coronary artery *in vivo* (Belloni & Hintze, 1991). It can mediate hypoxic coronary dilatation (Merrill *et al.*, 1986; 1988: Wei *et al.*, 1988; 1989) and has also been shown to hyperpolarize coronary arterial smooth muscle (Sabouni *et al.*, 1989). In the present study, we have demonstrated that adenosine induces relaxation which is inhibited by the adenosine-receptor antagonist, 8-phenyltheophylline. Glibenclamide significantly reduced this relaxation. Thus, adenosine may be responsible for the glibenclamide-sensitive hypoxia-induced relaxation in guinea-pig coronary arteries in perfused hearts. It is possible that mechanisms may vary between different preparations with differing degrees of hypoxia. It should also be noted that there may be differences between the epicardial coronary arteries used in our experiments and the resistance vessels in perfused hearts, and that the hypoxia-induced relaxation may vary from one species to the other. K_{ATP} channel activity has been demonstrated in vascular smooth muscle (Standen *et al.*, 1989; Nelson *et al.*, 1990). This is inhibited by glibenclamide and opened by potassium-channel openers such as cromakalim (Standen *et al.*, 1989). Some authors propose that glibenclamide-antagonized relaxation may be due to the activation of K_{ATP} channels (Nelson *et al.*, 1990; Kirsch *et al.*, 1990; Belloni & Hintze, 1991). Thus, it is a possibility that adenosine may act on K_{ATP} channels. However, further investigation is required to clarify the precise mechanisms of smooth muscle relaxation by adenosine.

Glibenclamide did not significantly inhibit the hypoxia-induced relaxation in endothelium-intact arteries. However, the same concentration of glibenclamide has been shown to inhibit significantly the endothelium-dependent relaxation induced by acetylcholine in similar preparations (Edwards & Weston, 1990; Jiang *et al.*, 1991). It is well established that nitric oxide induces relaxation by increasing the levels of cyclic GMP in smooth muscle, while EDHF has been proposed to activate K_{ATP} channels (Chen *et al.*, 1989). EDHF can be released by acetylcholine and contributes to a small part of the endothelium-dependent relaxation in certain vascular beds (Edwards & Weston, 1990; Jiang *et al.*, 1991). Either EDHF is not released during hypoxia, or, if it is, not in sufficient amounts to make a significant contribution to relaxation.

The modulation by autonomic nerves of coronary vasomotor tone is becoming increasingly recognised. Autonomic nerve endings, which contain neuropeptides, have been demonstrated by functional and immunocytochemical studies in coronary artery tissue (Maggi & Meli, 1988; Gaw *et al.*, 1991). The activation of these nerve endings in response to chemical or electrical stimulation induces endothelial-dependent or -independent relaxation in the presence of adrenergic and cholinergic antagonists (Hynes *et al.*, 1986; Kawasaki *et al.*, 1988; Han *et al.*, 1990). Non-adrenergic and non-cholinergic (NANC) nerves may release endothelium-dependent or -independent vasodilators such as substance P (Hökfelt *et al.*, 1980; Ellis & Burnstock, 1989) and ATP (MacKenzie *et al.*, 1988). It has been proposed that NO itself may be a neurotransmitter in non-adrenergic and non-cholinergic nerves in certain vascular beds (for review see Moncada *et al.*, 1991). It is not known whether a neurogenic mechanism is involved in hypoxia-induced relaxation. However, the neuropeptides, ATP and ADP, may be released from NANC nerve endings by electrical and chemical stimulation as well as hypoxia in some tissues (Hökfelt *et al.*, 1980). In the present study, we have observed that pretreatment with TTX significantly reduced the hypoxia-induced relaxation. Atropine and propranolol did not affect the relaxation. These results suggest that the hypoxia-induced relaxation is partially mediated via a neurogenic mechanism, possibly by stimulating NANC nerve endings. This possible mechanism might explain why L-NMMA attenuates hypoxia-induced relaxation in endothelium-denuded tissues by inhibiting the release of NO from NANC in response to hypoxia. Recent reports suggest that L-NMMA partially inhibits endothelium-independent relaxation induced by vasoactive intestinal polypeptide (VIP) (Gaw *et al.*, 1991). Therefore, we cannot exclude the possibility that L-NMMA may directly inhibit the action of VIP, possibly released from NANC nerve endings. In some tissues, capsaicin-sensitive sensory nerves are responsible for the autonomic nerve-mediated actions (Fujimori *et*

al., 1990). In this study, capsaicin incubation *in vitro* did not significantly affect the hypoxia-induced relaxation. We suggest that capsaicin-sensitive fibres are not involved in the mechanism underlying hypoxia-induced relaxation in rabbit epicardial coronary artery preparations.

In summary, these results suggest that hypoxia-induced relaxation is mediated by the release of endothelium-derived relaxing factor rather than by the activation of K_{ATP} in rabbit isolated coronary arteries. A neurogenic mechanism partially modulates the relaxation, possibly by activating non-adrenergic and non-cholinergic nerve endings. Adenosine-induced relaxation may explain the different effects of glibenclamide on hypoxic coronary artery relaxation in perfused hearts and isolated coronary arterial preparations.

References

BASSENGE, E. & BUSSE, R. (1988). Endothelial modulation of coronary tone. *Prog. Cardiovasc. Dis.*, **30**, 349–380.

BELLONI, F.L. & HINTZE, T.H. (1991). Glibenclamide attenuates adenosine-induced bradycardia and coronary vasodilatation. *Am. J. Physiol.*, **261**, H720–H727.

BURNSTOCK, G. (1989). Vascular control by purines with emphasis on the coronary system. *Eur. Heart J.*, **10**, Suppl F, 15–21.

BURNSTOCK, G., LINCOLN, J., FEHÉR, E., HOPWOOD, A.M., KIRKPATRICK, K., MILNER, P. & RALEVIC, V. (1988). Serotonin is localized in endothelial cells of coronary arteries and released during hypoxia: a possible new mechanism for hypoxia-induced vasodilatation of the rat heart. *Experientia*, **44**, 705–707.

BUSSE, R., FÖRSTERMANN, U., MATSUDA, H. & POHL, U. (1984). The role of prostaglandins in the endothelium-mediated vasodilatory response to hypoxia. *Pflügers Arch.*, **401**, 77–83.

CASSIS, L.A., LOEB, A.L. & PEACH, M.J. (1987). Mechanisms of adenosine- and ATP-induced relaxation in rabbit femoral artery: role of the endothelium and cyclic necleotides. In *Topics and Perspectives in Adenosine Research*. ed. Gerlach, E. & Becker, B.F. pp. 486–496. Berlin: Springer-Verlag.

CHEN, G., HASHITANI, H. & SUZUKI, H. (1989). Endothelium-dependent relaxation and hyperpolarization of canine coronary artery smooth muscles in relation to the electrogenic Na-K pump. *Br. J. Pharmacol.*, **98**, 950–956.

CHEN, G., SUZUKI, H. & WESTON, A.H. (1988). Acetylcholine releases endothelium-derived hyperpolarizing factor and EDRF from rat blood vessels. *Br. J. Pharmacol.*, **95**, 1165–1174.

CORR, L.A. (1992). Peptidergic, purinergic and adrenergic neurotransmitters in the control of the coronary artery. *PhD Thesis, University of London.*

CUSHING, D.J., BROWN, G.L., SABOUNI, M.H. & MUSTAFA, S.J. (1991). Adenosine receptor-mediated coronary artery relaxation and cyclic nucleotide production. *Am. J. Physiol.*, **261**, H343–H348.

DAUT, J., MAIER-RUDOLPH, W., BECKERATH, N,. MEHRKE, G., GÜNTHER, K. & GOEDEL-MEINEN, L. (1990). Hypoxic dilation of coronary arteries is mediated by ATP-sensitive potassium channels. *Science*, **247**, 1341–1344.

DE MEY, J.G. & VANHOUTTE, P.M. (1981). Role of the intima in cholinergic and purinergic relaxation of isolated canine femoral arteries. *J. Physiol.*, **316**, 347–355.

DE MEY, J.G. & VANHOUTTE, P.M. (1983). Anoxia and endothelium-dependent reactivity of the canine femoral artery. *J. Physiol.*, **335**, 65–74.

DEUSSEN, A., MÖSER, G. & SCHRADER, J. (1986). Contribution of coronary endothelial cells to cardiac adenosine production. *Pflügers Arch.*, **406**, 608–614.

EDWARDS, G. & WESTON, A.H. (1990). Potassium channel openers and vascular smooth muscle relaxation. *Pharmacol. Ther.*, **48**, 237–258.

ELLIS, J.L. & BURNSTOCK, G. (1989). Modulation of neurotransmission in the guinea-pig vas deferens by capsaicin: involvement of calcitonin gene-related peptide and substance P. *Br. J. Pharmacol.*, **98**, 707–713.

FUJIMORI, A., SAITO, A., KIMURA, S. & GOTO, K. (1990). Release of calcitonin gene-related peptide (CGRP) from capsaicin-sensitive vasodilator nerves in the rat mesenteric artery. *Neurosci. Lett.*, **112**, 173–178.

FURCHGOTT, R.F. (1983). Role of endothelium in responses of vascular smooth muscle. *Circ. Res.*, **53**, 557–573.

GAW, A.J., ABERDEEN, J., HUMPHREY, P.P.A., WADSWORTH, R.M. & BURNSTOCK, G. (1991). Relaxation of sheep cerebral arteries by vasoactive intestinal polypeptide and neurogenic stimulation: inhibition by L-N^G-monomethyl arginine in endothelium-denuded vessels. *Br. J. Pharmacol.*, **102**, 567–572.

GRYGLEWSKI, R.J., MONCADA, S. & PALMER, R.M. (1986). Bioassay of prostacyclin and endothelium-derived relaxing factor (EDRF) from porcine aortic endothelial cells. *Br. J. Pharmacol.*, **87**, 685–694.

HAN, S.P., NAES, L. & WESTFALL, T.C. (1990). Calcitonin gene-related peptide is the endogenous mediator of nonadrenergic-noncholinergic vasodilation in rat mesentry. *J. Pharmacol. Exp. Ther.*, **255**, 423–428.

HEADRICK, J. & WILLIS, R.J. (1988). Mediation by adenosine and bradycardia in rat heart during graded global ischaemia. *Pflügers Arch.*, **412**, 618–623.

HÖKFELT, T., JOHANSSON, O., LJUNGDAHL, A., LUNDBERG, J.M. & SCHULTZBERG, M. (1980). Peptidergic neurones. *Nature*, **284**, 515–521.

HYNES, M.R., BANNER, W.Jr., YAMAMURA, H.I. & DUCKLES, S.P. (1986). Characterization of muscarinic receptors of the rabbit ear artery smooth muscle and endothelium. *J. Pharmacol. Exp. Ther.*, **238**, 100–105.

IGNARRO, L.J, BYRNS, R.E., BUGA, G.M. & WOOD, K.S. (1987). Endothelium-derived relaxing factor from pulmonary artery and vein possesses pharmacologic and chemical properties identical to those of nitric oxide radical. *Circ. Res.*, **61**, 866–879.

JIANG, C., POOLE-WILSON, P.A. & COLLINS, P. (1991). Comparison of rabbit coronary artery relaxation induced by acetylcholine and lemakalim: activation of ATP sensitive potassium channels. *Cardiovasc. Res.*, **25**, 930–935.

KAWASAKI, H., TAKASAKI, K., SAITO, A. & GOTO, K. (1988). Calcitonin gene-related peptide acts as a novel vasodilator neurotransmitter in mesenteric resistance vessels of the rat. *Nature*, **335**, 164–167.

KIRSCH, G.E., CODINA, J., BIRNBAUMER, L. & BROWN, A.M. (1990). Coupling of ATP-sensitive K^+ channels to A_1 receptors by G proteins in rat ventricular myocytes. *Am. J. Physiol.*, **259**, H820–H826.

KUKOVETZ, W.R., POCH, G. & HOLZMANN, S. (1981). Cyclic nucleotides and relaxation of vascular smooth muscle. In *Vasodilatation*. ed. Vanhoutte, P.M. & Leusen, I. pp. 339–353. New York: Raven Press.

KUSACHI, S., BUGNI, W.J. & OLSSON, R.A. (1984). Forskolin potentiates the coronary vasoactivity of adenosine in the open-chest dog. *Circ. Res.*, **55**, 116–119.

MACKENZIE, I., KIRKPATRICK, K.A. & BURNSTOCK, G. (1988). Comparative study of the actions of AP5A and α, β-methylene ATP on nonadrenergic, noncholinergic neurogenic excitation in the guinea-pig vas deferens. *Br. J. Pharmacol.*, **94**, 699–706.

MAGGI, C.A. & MELI, A. (1988). The sensory-efferent function of capsaicin-sensitive sensory neurons. *Gen. Pharmacol.*, **19**, 1–43.

MATHIE, R.T., ALEXANDER, B., RALEVIC, V. & BURNSTOCK, G. (1991). Adenosine-induced dilatation of the rabbit hepatic arterial bed is mediated by A_2-purinoceptors. *Br. J. Pharmacol.*, **103**, 1103–1107.

MERRILL, G.F., DOWNEY, H.F. & JONES, C.E. (1986). Adenosine deaminase attenuates canine coronary vasodilation during systemic hypoxia. *Am. J. Physiol.*, **250**, H579–H583.

MERRILL, G.F., DOWNEY, H.F., YONEKURA, S., WATANABE, N. & JONES, C.E. (1988). Adenosine deaminase attenuates canine coronary vasodilatation during regional non-ischaemic myocardial hypoxia. *Cardiovasc. Res.*, **22**, 345–350.

MILNER, P., RALEVIC, V., HOPWOOD, A.M., FEHÉR, E., LINCOLN, J., KIRKPATRICK, K.A. & BURNSTOCK, G. (1989). Ultrastructural localisation of substance P and choline acetyltransferase in endothelial cells of rat coronary artery and release of substance P and acetylcholine during hypoxia. *Experientia*, **45**, 121–125.

MONCADA, S., PALMER, R.M.J. & HIGGS, E.A. (1991). Nitric oxide: physiology, pathophysiology, and pharmacology. *Pharmacol. Rev.*, **43**, 109–142.

MUSTAFA, S.J. (1980). Cellular and molecular mechanism(s) of coronary flow regulation be adenosine. *Mol. Cell. Biochem.*, **31**, 67–87.

NELSON, M.T., HUANG, Y., BRAYDEN, J.E., HESCHELER, J. & STANDEN, N.B. (1990). Arterial dilations in response to calcitonin gene-related peptide involve activation of K^+ channels. *Nature*, **344**, 770–773.

NEWBY, A.C., WORKU, Y. & HOLMQUIST, C.A. (1985). Adenosine formation. Evidence for a direct biochemical link with energy metabolism. *Adv. Myocardiol.*, **6**, 273–284.

OLSSON, R.A. & BÜNGER, R. (1987). Metabolic control of coronary blood flow. *Prog. Cardiovasc. Dis.*, **29**, 369–387.

PALMER, R.M., FERRIGE, A.G. & MONCADA, S. (1987). Nitric oxide release accounts for the biological activity of endothelium-derived relaxing factor. *Nature*, **327**, 524–526.

POHL, U. & BUSSE, R. (1989). Hypoxia stimulates release of endothelium-derived relaxant factor. *Am. J. Physiol.*, **256**, H1595–H1600.

RODMAN, D.M., HASUNUMA, K., PEACH, J.L. & MCMURTRY, I.F. (1990). Inhibitor of ATP-sensitive K^+ channel alters neither hypoxic contraction nor relaxation of rat aorta. *Blood vessels*, **27**, 365–368.

RUBANYI, G. & PAUL, R.J. (1984). O_2-sensitivity of beta adrenergic responsiveness in isolated bovine and porcine coronary arteries. *J. Pharmacol. Exp. Ther.*, **230**, 692–698.

RUBANYI, G. & VANHOUTTE, P.M. (1985a). Endothelium-removal decreases relaxations of canine coronary arteries caused by beta-adrenergic agonists and adenosine. *J. Cardiovasc. Pharmacol.*, **7**, 139–144.

RUBANYI, G.M. & VANHOUTTE, P.M. (1985b). Hypoxia releases a vasoconstrictor substance from the canine vascular endothelium. *J. Physiol.*, **364**, 45–56.

RUBANYI, G.M. & VANHOUTTE, P.M. (1986). Superoxide anions and hyperoxia inactivate endothelium-derived relaxing factor. *Am. J. Physiol.*, **250**, H822–H827.

SABOUNI, M.H., HARGITTAI, P.T., LIEBERMAN, E.M. & MUSTAFA, S.J. (1989). Evidence for adenosine receptor-mediated hyperpolarization in coronary smooth muscle. *Am. J. Physiol.*, **257**, H1750–H1752.

STANDEN, N.B., QUAYLE, J.M., DAVIES, N.W., BRAYDEN, J.E., HUANG, Y. & NELSON, M.T. (1989). Hyperpolarizing vasodilators activate ATP-sensitive K^+ channels in arterial smooth muscle. *Science*, **245**, 177–180.

VANHOUTTE, P.M. & LÜSCHER, T.F. (1990). Endothelium-dependent vasoconstriction. In *Endothelium-Derived Contracting Factors*. ed. Rubanyi, G.M. & Vanhoutte, P.M. pp. 1–7. Basel: Karger.

VON BECKERATH, N., CYRYS, S., DISCHNER, A. & DAUT, J. (1991). Hypoxic vasodilatation in isolated, perfused guinea-pig heart: an analysis of the underlying mechanisms. *J. Physiol.*, **442**, 297–319.

WADSWORTH, R.M., AMATYA, M.P., KWAN, Y.W., KANE, K.A. & ZEITLIN, I.J. (1990). Modulation by hypoxia of the release of endothelium-derived mediators from sheep coronary artery rings. In *Endothelium-derived Contracting Factors*. ed. Rubanyi, G.M. & Vanhoutte, P.M. pp. 32–38. Basel: Karger.

WEI, H.M., KANG, Y.H. & MERRILL, G.F. (1988). Coronary vasodilatation during global myocardial hypoxia: effects of adenosine deaminase. *Am. J. Physiol.*, **254**, H1004–H1009.

WEI, H.M., KANG, Y.H. & MERRILL, G.F. (1989). Canine coronary vasodepressor responses to hypoxia are abolished by 8-phenyltheophylline. *Am. J. Physiol.*, **257**, H1043–H1048.

(Received April 15, 1993
Revised September 16, 1993
Accepted November 9, 1993)

Br. J. Pharmacol. (1994), **111**, 717–722 © Macmillan Press Ltd, 1994

Class I and III antiarrhythmic actions of prazosin in guinea-pig papillary muscles

[1]Onésima Pérez, Carmen Valenzuela, Eva Delpón & Juan Tamargo

Department of Pharmacology, School of Medicine, Universidad Complutense, 28040 Madrid, Spain

1 The electrophysiological effects of prazosin, a highly specific α_1-adrenoceptor antagonist, on transmembrane action potential characteristics were studied in guinea-pig papillary muscles.

2 At concentrations between 10^{-6} M and 10^{-5} M, prazosin produced a concentration-dependent decrease in the maximum upstroke velocity ($\dot{V}_{max}$) and a progressive lengthening of the action potential duration at 50% (APD_{50}) and 90% (APD_{90}) of repolarization. The prolongation of the APD_{50} and APD_{90} values was independent of the frequency of stimulation. The prolongation of the APD_{90} was accompanied by a parallel lengthening of the effective refractory period (ERP) and thus, the ERP/APD_{90} ratio remained unaltered at all drug concentrations tested.

3 In the presence of prazosin, 5×10^{-6} M, the percentage of $\dot{V}_{max}$ block increased with the frequency of stimulation, the inhibitory effect being more marked at fast driving rates (frequency-dependent $\dot{V}_{max}$ block). At 3 Hz, the onset kinetics of the frequency-dependent $\dot{V}_{max}$ block was better fitted by a biexponential function, the K values of the fast (K_1) and slow components (K_2) being 0.254 ± 0.037 AP^{-1} and 0.045 ± 0.010 AP^{-1}, respectively. However, prazosin did not produce tonic $\dot{V}_{max}$ block.

4 The recovery time constant (τ_{re}) from the frequency-dependent $\dot{V}_{max}$ block was prolonged from 19.6 ± 2.5 ms to 24.4 ± 5.5 s. This result indicated that prazosin can be considered as a slow kinetics Na channel blocker.

5 Prazosin, 5×10^{-6} M, shifted the membrane responsiveness curve in a hyperpolarizing direction, which indicated that the blockade of sodium channels increased at less negative potentials (voltage-dependent $\dot{V}_{max}$ block).

6 It is concluded that in guinea-pig papillary muscles, prazosin inhibited the $\dot{V}_{max}$ and lengthened the duration of the action potentials, thus exhibiting both class I and class III antiarrhythmic actions, respectively, that were possibly unrelated to blockade of myocardial α_1-adrenoceptors.

Keywords: Prazosin; ventricular muscles; action potentials; action potential duration; frequency-dependent $\dot{V}_{max}$ block

Introduction

The effectiveness of α_1-adrenoceptor antagonists on catecholamine-induced cardiac arrhythmias in animals has been known for more than 40 years (for review, see Benfey 1980; 1982). Phentolamine and prazosin inhibited the ventricular arrhythmias occurring after coronary oclussion and during reperfusion (Sheridan *et al.*, 1980; Stewart *et al.*, 1980) as well as those induced by ouabain (Ettinger *et al.*, 1969) and chloroform (Vargaftig & Coignet, 1969). In addition, α_1-adrenoceptor antagonists suppressed ventricular tachyarrhythmias in patients with myocardial infarction (Gould *et al.*, 1975) and in circumstances where β-adrenoceptor antagonists were inactive (Sheridan *et al.*, 1980; Benfey, 1982). Even although it may be expected that at high concentrations α_1-adrenoceptor antagonists might antagonize arrhythmias in conditions not involving α_1-adrenoceptor stimulation, the mechanisms responsible for the antiarrhythmic effects are still unknown (Benfey, 1982; Ferrier & Carmeliet, 1990).

Previous electrophysiological studies in different animal species have demonstrated that α_1-adrenoceptor antagonists inhibited the maximum upstroke velocity ($\dot{V}_{max}$) and lengthened the action potential duration (Quadbeck & Reiter, 1975; Sada, 1978; Northover, 1983; Dukes & Vaughan Willians, 1984; Rosen *et al.*, 1984; Tohse *et al.*, 1986; Himmel *et al.*, 1991). These results suggested that α_1-adrenoceptor antagonists may exhibit class I (Na channel blocking properties) and class III antiarrhythmic properties, respectively, according to the classification of Vaughan Williams (1984). Most sodium (Na) channel blocking drugs have been shown to have important frequency (use)-dependent effects on the $\dot{V}_{max}$ of the cardiac action potential (Hondeghem & Katzung, 1977; Tamargo *et al.*, 1992) and the analysis of the onset and offset kinetics of the frequency-dependent $\dot{V}_{max}$ block has been used for the subclassification of cardiac Na channel blockers into three subgroups, i.e., fast, intermediate, and slow kinetics drugs (Campbell, 1983; Vaughan Williams, 1984). In contrast, the prolongation of the action potential duration produced by most class III antiarrhythmic drugs decreased at fast rates, i.e., they exhibited a 'reversed use-dependence' (Hondeghem & Snyders, 1990). Even when in some studies the inhibitory effects of phentolamine and prazosin on $\dot{V}_{max}$ increased with the frequency of stimulation (Sada, 1978; Northover, 1983; Tohse *et al.*, 1986) the frequency-dependent effects of α_1-adrenoceptor antagonists on $\dot{V}_{max}$ and APD have not been thoroughly studied.

Therefore, the present study was undertaken to: (1) investigate the frequency-dependent effects of prazosin, a highly specific α_1-adrenoceptor antagonist (Williams *et al.*, 1981), on $\dot{V}_{max}$ and APD in guinea-pig papillary muscles, and (2) compare its effects with those previously described in this cardiac tissue with other antiarrhythmic drugs.

Methods

Experimental procedure

Guinea-pigs of either sex, weighing 250–350 g, were killed by a blow on the neck. The hearts were rapidly excised, and papillary muscles (< 1 mm in diameter) were dissected from the right ventricle and superfused continuously at a constant rate of 7 ml min^{-1} with Tyrode solution of the following composition (mM): NaCl 125, KCl 5.4, $CaCl_2$ 1.8, $MgCl_2$ 1.05, $NaHCO_3$ 24, NaH_2PO_4 0.42 and glucose 11. The solu-

[1] Author for correspondence.

tions were bubbled with 95% O_2:5% CO_2 (pH = 7.4) and the temperature was kept constant at 34 ± 0.5°C. The preparations were initially driven at 1 Hz and a period of at least 1 h was allowed for equilibration during which a stable impalement was obtained. Driving stimuli were rectangular pulses (2 ms duration, twice threshold strength) delivered to the preparation from a multipurpose programmable stimulator (Cibertec CS-220).

Transmembrane action potentials were conventionally recorded through glass microelectrodes filled with 3 M KCl (tip resistance of 8–15 MΩ). The microelectrode was connected via Ag-AgCl wire to a high-input impedance, capacity neutralizing amplifiers (WPI model 701). The $\dot{V}_{max}$ of the action potential was obtained by electronic differentiation (Delpón *et al.*, 1992). Stimulus intensity and duration were adjusted throughout each experiment to maintain a constant latency (1–2 ms) between stimulus and upstroke of action potential. Both action potential and $\dot{V}_{max}$ were displayed on a storage oscilloscope (Tektronix 5104N) and photographed with a kymographic Grass camera (Model C-4). Film analysis was used to measure resting membrane potential (RMP), action potential amplitude (APA), $\dot{V}_{max}$, action potential duration at 50% (APD_{50}) and 90% of repolarization (APD_{90}) and effective refractory period (ERP). The ERP was determined by introducing premature test-stimuli of twice threshold strength at progressively earlier diastolic intervals applied every 8th basic beat (Delpón *et al.*, 1992). All experimental results were obtained from a single continuous impalement through the whole experiment. In some experiments following the equilibration period, the effects of prazosin on APD_{50} and APD_{90} values at steady state were studied in muscles stimulated at different driving rates (0.1–3 Hz).

To study the frequency-dependent effects of prazosin on $\dot{V}_{max}$, preparations were driven at a basal rate of 0.02 Hz. Following the equilibration period, the preparations were driven by trains of stimuli at various rates ranging from 0.5 to 3 Hz for 40 s (0.5, 1 and 2 Hz) and 16 s (3 Hz). Resting periods of 5 min, which were sufficient to ensure full recovery from the frequency-dependent decrease in $\dot{V}_{max}$, were interposed between the trains of stimuli (Delpón *et al.*, 1992). The rate of onset of $\dot{V}_{max}$ block in the presence of prazosin was quantified by determining the rate constant of this process, described as the reciprocal of the action potential number (AP^{-1}). Recovery of $\dot{V}_{max}$ from the frequency-dependent block was studied by applying a single test stimulus at various coupling intervals after a stimulation train for 20 s at 3 Hz (Delpón *et al.*, 1992).

The effect of prazosin on the relationship between $\dot{V}_{max}$ and the resting membrane potential, i.e., membrane responsiveness, was studied in papillary muscles driven at 0.01 Hz and the resting potential was depolarized in a stepwise manner by increasing the $[K]_o$ from 2 to 15 mM (Delpón *et al.*, 1992). The $\dot{V}_{max}$ was measured each time after an equilibration period of 8 min. After obtaining control data, $[K]_o$ was returned to 2 mM and the procedure repeated 30 min after exposure to prazosin, 5×10^{-6} M.

Drugs

Prazosin hydrochloride (Sigma Chemical Ltd., London) as a powder was initially dissolved in distilled deionized water and further dilutions were carried out in Tyrode solution to obtain the desired final concentrations.

Throughout the paper, data are expressed as the mean ± s.e.mean and Student's *t* test for paired observations was used to estimate the significance of differences from control values. For statistical comparison of more than two groups, a one-way analysis of variance was performed (Wallenstein *et al.*, 1980). A *P* value of less than 0.05 was considered as significant. A nonlinear least squares fitting routine was used to determine the rate constant for the onset block of $\dot{V}_{max}$ and the time constant of recovery from block $\dot{V}_{max}$.

Results

Effects on action potential characteristics

The effects of prazosin in a range of concentrations between 10^{-7} M and 10^{-5} M on the electrophysiological characteristics of the ventricular action potentials were studied in nine guinea-pig papillary muscles constantly driven at 1 Hz. The results obtained under control conditions and 30 min after each increment in drug concentration are summarized in Table 1. At 10^{-7} M, prazosin had no significant effects on the characteristics of the action potential. At higher concentrations it produced a progressive decrease ($P<0.05$) in $\dot{V}_{max}$, which reached significant values at 5×10^{-6} M and 10^{-5} M. This effect was not accompanied by significant changes in action potential amplitude or in the resting membrane potential. However, the most representative effect of prazosin was a progressive slowing in the rate of repolarization during phases 2 and 3 of the ventricular action potential, leading to a concentration-dependent lengthening of the APD_{50} and APD_{90} values. This prolongation reached significant values at concentrations $\geq$ than 10^{-6} M ($P<0.05$). The prolongation of the APD_{90} was accompanied by a parallel lengthening of the ERP and hence, the ERP/APD_{90} ratio remained unaltered at all drug concentrations tested. Thus, in seven papillary muscles driven at 1 Hz the values for the ERP and ERP/APD_{90} ratio averaged 194.8 ± 18.4 ms and 1.03 ± 0.07 in the absence and 225.7 ± 30.3 ms and 1.04 ± 0.04 in the presence of 10^{-5} M prazosin, respectively.

Frequency-dependent $\dot{V}_{max}$ block

The effectiveness of Na channel blockers in inhibiting the fast inward Na current (I_{Na}) is strongly dependent on the frequency of stimulation (Hondeghem & Katzung, 1977; Campbell, 1983; Tamargo *et al.*, 1992). In order to study the effect of the stimulation frequency on the $\dot{V}_{max}$ block induced by prazosin, preparations were driven at a basal rate of 0.02 Hz and trains of pulses at different rates (0.5–3 Hz) separated

Table 1 Electrophysiological effects of prazosin on action potentials in guinea-pig ventricular papillary muscles driven at 1 Hz

Drug concentration (M)	*RMP* (mV)	*APA* (mV)	$\dot{V}_{max}$ ($V\ s^{-1}$)	*APD_{50}* (ms)	*APD_{90}* (ms)
0	86 ± 1	120 ± 1	179 ± 18	154 ± 11	186 ± 9
10^{-7}	86 ± 1	120 ± 1	179 ± 19	157 ± 10	190 ± 9
10^{-6}	86 ± 1	119 ± 1	178 ± 17	168 ± 10	202 ± 8*
5×10^{-6}	85 ± 1	118 ± 2	161 ± 15*	171 ± 12*	208 ± 12*
10^{-5}	85 ± 1	118 ± 1	145 ± 14*	182 ± 11**	223 ± 13**

x ± s.e.mean, $n = 9$
*$P<0.05$; **$P<0.001$.

from one another by a rest period of 5 min were applied. In the presence of prazosin, 5×10^{-6} M, the inhibition of the $\dot{V}_{max}$ of the first action potential of each train, i.e. tonic $\dot{V}_{max}$ block, averaged $0.6 \pm 0.3\%$ ($n = 8$), this effect being independent of the frequency of stimulation tested. In fact, as previously reported by Tohse *et al.* (1986), sometimes prazosin slightly increased, instead of decreasing, the $\dot{V}_{max}$ of the first action potential. These results suggested that at this concentration, prazosin had no affinity for the rested state of the Na channel.

In the absence of prazosin the repetitive stimulation of the papillary muscles produced a gradual decrease of $\dot{V}_{max}$ from the value of the first action potential to a new steady-state and this decrease increased with the frequency of stimulation (frequency-dependent $\dot{V}_{max}$ block). Table 2 shows that when the stimulation rate increased from 0.5 to 3 Hz the $\dot{V}_{max}$ block progressively augmented from $0.7 \pm 0.3\%$ to $16.1 \pm 1.5\%$. Figure 1 shows the percentage decrease in $\dot{V}_{max}$ from the first action potential of the train to the new steady-state level obtained in a typical experiment in the presence of prazosin, 5×10^{-6} M. It can be observed that the percentage of $\dot{V}_{max}$ block increased with the frequency of stimulation. As summarized in Table 2, prazosin induced a significant frequency-dependent $\dot{V}_{max}$ block at all the rates of stimulation tested but the inhibitory effect was more marked at fast (1–3 Hz, $P < 0.001$) than at slow driving rates (0.5 Hz, $P < 0.05$).

The onset kinetics of frequency-dependent $\dot{V}_{max}$ block can be defined as an event-dependent process, that can be fitted by a single or biexponential function (Courtney, 1987; Delpón *et al.*, 1992). The onset rate constant per action potential [K/AP] at which $\dot{V}_{max}$ decreased to a new steady-state level in the presence of 5×10^{-6} M prazosin was calculated from the exponential fit of the $\dot{V}_{max}$ values obtained during the train of action potentials. As is shown in Table 3, the onset rate constant of $\dot{V}_{max}$ block was dependent on the stimulation frequency, being always higher at lower stimulation frequencies. In muscles driven at 0.5 and 1 Hz, the onset kinetics were fitted by a single exponential curve, the K values being 0.177 ± 0.039/AP and 0.064 ± 0.004/AP, respectively. However, at 2 Hz and 3 Hz, the onset kinetics of the frequency-dependent $\dot{V}_{max}$ block was better fitted by a biexponential function, the K values of the fast (K_1) and slow components (K_2) being 0.301 ± 0.036/AP and 0.040 ± 0.006/AP at 2 Hz and 0.254 ± 0.037/AP and 0.045 ± 0.010/AP at 3 Hz, respectively.

Table 2 Effects of prazosin (5×10^{-6} M) on the frequency-dependent $\dot{V}_{max}$ block in guinea pig papillary muscles

Frequency of stimulation (Hz)	*Frequency-dependent $\dot{V}_{max}$ block (%)* *Control* (%)	*Prazosin* (%)
0.5	0.7 ± 0.3	2.4 ± 0.5*
1	3.4 ± 0.8	9.9 ± 1.3**
2	10.7 ± 1.1	21.9 ± 1.6**
3	16.1 ± 1.5	28.6 ± 2.4**

x ± s.e.mean, $n = 8$
*$P < 0.05$; **$P < 0.001$.

Table 3 Rate constants of development of frequency-dependent $\dot{V}_{max}$ block (K) in the presence of prazosin (5×10^{-6} M)

Frequency of stimulation (Hz)	*Onset rate per AP* K_1/AP	K_2/AP
0.5	–	0.177 ± 0.039
1.0	–	0.064 ± 0.004
2.0	0.301 ± 0.036	0.040 ± 0.006
3.0	0.254 ± 0.037	0.045 ± 0.010

x ± s.e.mean, $n = 7$

Effects of prazosin on the recovery process of $\dot{V}_{max}$

The effects of prazosin on the recovery kinetics of frequency-dependent $\dot{V}_{max}$ block were also studied in papillary muscles driven every 5 min by a train of stimuli at a frequency of 3 Hz for 20 s and a test-stimulus was applied at variable coupling intervals from 500 ms to 10 s. Recovery from fre-

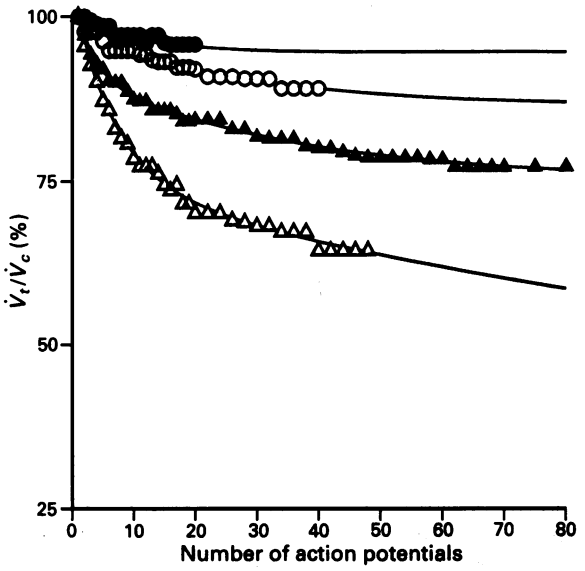


Figure 1 Frequency-dependent $\dot{V}_{max}$ block obtained in the presence of prazosin (5×10^{-6} M) in guinea-pig papillary muscles driven by trains of stimuli at various rates of stimulation (0.5, 1, 2 and 3 Hz). The percentage of $\dot{V}_{max}$ normalized by the value of the first action potential of the train [$\dot{V}_t/\dot{V}_c$ (%), $\dot{V}_t = \dot{V}_{max}$ of the action potentials of the train, $\dot{V}_c = \dot{V}_{max}$ of the first action potential of the train] was plotted against the number of consecutive beats of the train: (●) 0.5 Hz; (○) 1 Hz; (▲) 2 Hz; (△) 3 Hz.

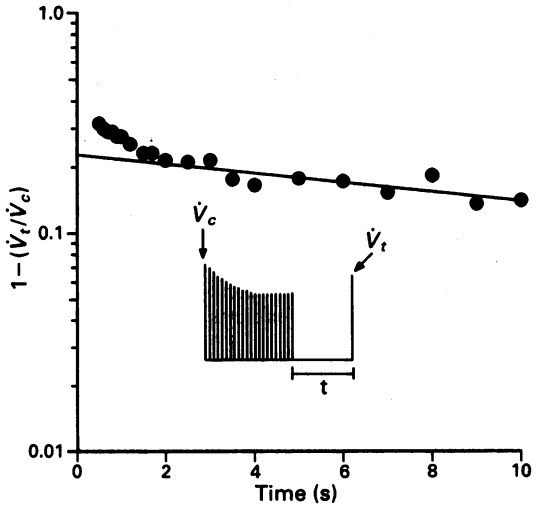


Figure 2 Effects of prazosin (10^{-5} M) on the recovery process of $\dot{V}_{max}$ block after trains of action potentials at 3 Hz for 20 s. $\dot{V}_c$: $\dot{V}_{max}$ of the first action potential of the train; $\dot{V}_t$: $\dot{V}_{max}$ of the test response. Time:interval (s) between the last action potential of the train and the test response. First-order regressions of the slow component were fitted by the method of least squares.

Table 4 Duration of action potential at 50% (APD_{50}) and 90% (APD_{90}) of repolarization in absence and presence of prazosin 5×10^{-6} M at different frequencies of stimulation

Frequency of stimulation (Hz)	*Control*		*Prazosin*	
	APD_{50}	APD_{90}	APD_{50}	APD_{90}
0.1	170 ± 10	199 ± 10	195 ± 12*	233 ± 14*
0.5	172 ± 9	202 ± 10	197 ± 9*	239 ± 11*
1	163 ± 9	195 ± 9	191 ± 13*	235 ± 13*
2	134 ± 5	166 ± 6	162 ± 10*	203 ± 11*
3	112 ± 3	145 ± 4	133 ± 6*	175 ± 7*

x ± s.e.mean, $n = 6$
*$P < 0.01$.

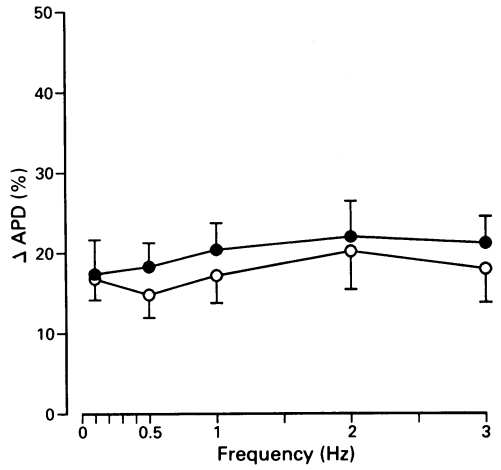


Figure 3 Relationship between the increment of the action potential duration values measured at 50% (APD_{50}, ○) and 90% (APD_{90}, ●) repolarization induced by prazosin (5×10^{-6} M) and the frequency of stimulation. The increment of action potential duration values was obtained from paired experiments. Each point represents the mean ± s.e.mean of six experiments.

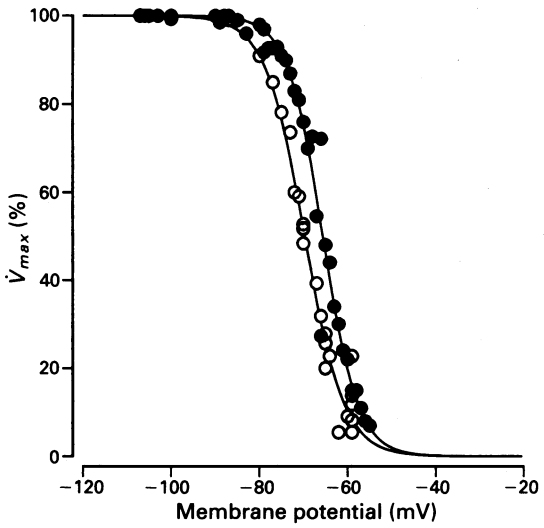


Figure 4 Effect of prazosin 5×10^{-6} M on the relationship between $\dot{V}_{max}$ and the resting membrane potential at which the action potential is generated (i.e., membrane responsiveness). Ordinate scale: normalized $\dot{V}_{max}$ values ($V\,s^{-1}$). Absicissa scale: membrane potential (mV). Controls (●), prazosin (○).

quency-dependent $\dot{V}_{max}$ block occurred as a biexponential process for which the time constant of the slow component can be taken as the recovery time constant (τ_{re}). Figure 2 shows the recovery process of $\dot{V}_{max}$. In order to ensure a high degree of $\dot{V}_{max}$ block, these experiments were performed in the presence of a high concentration of prazosin (10^{-5} M) and the duration of the conditioning train was increased to 20 s. Under control conditions, the τ_{re} was 19.6 ± 2.5 ms, whereas in the presence of prazosin the τ_{re} was prolonged to 24.4 ± 5.5 s ($P < 0.001$). The y-intercept of the recovery of $\dot{V}_{max}$, which can be taken as the fraction of Na channels blocked (Valenzuela *et al.*, 1989), rose to a value of 26.1 ± 4.1%. In another three muscles prazosin, 5×10^{-6} M, prolonged the τ_{re} to a similar extent (24.4 ± 5.3 s, $P > 0.05$). These results indicated that prazosin can be considered as a slow kinetics Na channel blocker, i.e. it exhibits class Ic antiarrhythmic actions.

Effects of prazosin on APD at different frequencies

The lengthening of the ventricular action potential produced by 5×10^{-6} M prazosin was studied in six papillary muscles driven at various frequencies of stimulation. The basic driving rate was changed at 5 min intervals from 0.1 to 3 Hz. In the absence of prazosin an increase in the frequency of stimulation progressively shortened both the APD_{50} and APD_{90} values. Prazosin significantly prolonged the APD_{50} and APD_{90} values ($P < 0.01$) at all driving rates over control values (Table 4). However, as is shown in Figure 3, when the results were expressed as a percentage change, the prolongation of the APD values was similar at all driving rates tested ($P > 0.05$). These results indicated that the effects of prazosin on APD_{50} and APD_{90} values were independent of the frequency of stimulation.

Effect on membrane responsiveness

The relationship between $\dot{V}_{max}$ and the membrane resting potential from which the action potential arises, i.e. membrane responsiveness, was studied in four papillary muscles driven at a basal rate of 0.01 Hz, so that the diastolic interval was much longer than the τ_{re}. The resting membrane potential was depolarized stepwise to approximately − 60 mV by increasing the $[K]_o$ from 2 to 15 mM and the $\dot{V}_{max}$ value was measured when the resting membrane potential reached steady-state values at each $[K]_o$. Results of a typical experiment are shown in Figure 4. It can be observed that 5×10^{-6} M prazosin shifted the membrane responsiveness curve along the voltage axis in a hyperpolarizing direction by 4.1 ± 0.5 mV. These results indicated that the blockade of Na channels produced by prazosin increased at less negative potentials (voltage-dependent block).

Discussion

The results of the present study demonstrated that prazosin, a highly selective α_1-adrenoceptor blocking drug, inhibited

$\dot{V}_{max}$, an indirect index of the I_{Na}, and prolonged the APD of the guinea-pig ventricular muscle fibres in a concentration-dependent manner. The inhibition of $\dot{V}_{max}$ appeared at concentrations at which prazosin had no effect on the resting membrane potential which suggested that the drug exhibits Na channel blocking properties, e.g., class I antiarrhythmic actions. These results confirmed and extended previous evidence that prazosin inhibited the $\dot{V}_{max}$ in rat (Northover, 1983), guinea-pig (Himmel *et al.*, 1991) and rabbit ventricular muscles (Dukes & Vaughan Williams, 1984; Tohse *et al.*, 1986) and dog Purkinje fibres (Rosen *et al.*, 1984).

The voltage- and frequency-dependent blockade of $\dot{V}_{max}$ produced by prazosin can be interpreted within the framework of the 'modulated receptor hypothesis' proposed to explain the interactions between local anaesthetic and antiarrhythmic drugs with Na channels (Hondeghem & Katzung, 1977; Tamargo *et al.*, 1992). According to this hypothesis, the affinity of the drug receptor differs in the three different receptor conformations (rested, activated and inactivated). In our experiments prazosin decreased only slightly, and sometimes increased, the $\dot{V}_{max}$ of the first beat of the train. These results indicated that prazosin has no affinity for rested channels at concentrations at which the drug produced frequency-dependent $\dot{V}_{max}$ block.

During repetitive stimulation, Na channels spend proportionately more time in the activated and/or inactivated state and the time for recovery during the diastole is shortened. Thus, if prazosin exhibited a higher affinity for the activated or inactivated state than for the resting state of the channel and prolonged the τ_{re}, an accumulation of blocked channels would be expected at increasing driving rates (i.e., frequency-dependent $\dot{V}_{max}$ block). At 3 Hz the onset rate value of the frequency-dependent $\dot{V}_{max}$ block produced by 5×10^{-6} M prazosin was 0.045 ± 0.010/AP, a value between that described for procainamide, an intermediate kinetics Na channel blocker, and flecainide, a slow kinetics blocker (Hondeghem & Katzung, 1977; Campbell, 1983; Tamargo *et al.*, 1992). In rabbit papillary muscles treated with 10 μM prazosin and driven at 1 Hz, Tohse *et al.* (1986) obtained a K value of 0.042 ± 0.006/AP, which is slower than that obtained in the present experiments at the same driving rate (0.064 ± 0.004/AP). The discrepancy between these values can be attributed not only to the fact that the experiments were performed in different animal species but also at different drug concentrations, since the value of K increased with drug concentration (Courtney, 1987). As previously described for phentolamine (Northover, 1983), prazosin-induced $\dot{V}_{max}$ block increased when the extracellular K concentration was raised. Since the inactivated state of the Na channel predominates at depolarized membrane potentials, this result suggests that the drug exhibits a high affinity for the inactivated state of the Na channel.

The recovery kinetics of $\dot{V}_{max}$ from the frequency-dependent block is one of the most reliable parameters to subdivide Na channel blockers (Hondeghem & Katzung, 1977; Campbell, 1983; Tamargo *et al.*, 1992). In the present experiments prazosin prolonged the τ_{re} value to 24 s, suggesting that it binds with a slow dissociation constant to the inactivated Na channels. The τ_{re} value is similar to that described for encainide (20.3 s; Campbell, 1983) and thus, it may be considered as a member of the Na channel blockers with slow kinetics, i.e., class Ic antiarrhythmic drugs. This value, however, is significantly shorter than that described in rabbit papillary muscles (39.97 ± 1.2 s; Tohse *et al.*, 1986). Since the τ_{re} is independent of drug concentration and in both experimental designs its value was determined after applying a train of pulses until a steady-state $\dot{V}_{max}$ block was achieved, the discrepancy may result from the different species used (rabbit vs guinea-pig). The main repolarizing current in rabbit ventricular muscle fibres is the transient outward current, I_{to} (Giles & Imaizumi, 1988), which is not present in guinea-pig ventricular cells, where the delayed rectifier K current (I_K) is the main determinant for repolarization (Matsuura *et al.*, 1987). Because the I_{to} is rapidly activated (Giles & Imaizumi, 1988), the $\dot{V}_{max}$ observed in rabbit papillary muscles may reflect not only changes of the I_{Na}, but also of the I_{to}. In contrast, since I_K activates only after several hundred milliseconds (Matsuura *et al.*, 1987), this current would possibly not interfere with the determination of the $\dot{V}_{max}$ values.

The most characteristic effect of prazosin was a decrease in the slopes of phases 2 and 3 of repolarization that prolonged the APD_{50} and APD_{90} values. This effect was accompanied by a parallel prolongation of the ERP, and thus, the ERP/APD_{90} ratio remained unchanged. These results are consistent with those previously described with prazosin in rat (Northover, 1983), guinea-pig ventricular muscle (Himmel *et al.*, 1991), rabbit (Dukes & Vaughan Williams, 1984; Tohse *et al.*, 1986) and dog Purkinje fibres (Rosen *et al.*, 1984), and suggest that prazosin may also exhibit class III antiarrhythmic actions according to Vaughan Williams' classification (1984). Although this paper is not concerned with the ionic mechanisms that determine the prazosin effect on repolarization, the prolongation of the APD can be related to an increase in the slowly inactivating Na and the inward L-type Ca currents (I_{Ca}) and/or to a decrease in outward K currents. The former possibility can be excluded since inhibition of inward Na currents would shorten, but not lengthen, the APD. Moreover, at concentrations at which prazosin lengthened the APD it had no effect on the slowly inactivating Na channels (Ferrier & Carmeliet, 1990). Thus, the most likely explanation for the prolongation of the APD would be an inhibition of the I_K (Ferrier & Carmeliet, 1990). Since stimulation of α_1-adrenoceptor agonists also prolonged the APD in papillary muscles, it seems unlikely that the prolongation of the APD induced by prazosin could be related to the blockade of α_1-adrenoceptors (Dukes & Vaughan Williams, 1984).

It has been shown that the ability of most class III antiarrhythmic drugs to prolong the APD is diminished at fast heart rates and augmented by bradycardia, i.e. they exhibited reverse frequency-dependence (Hondeghem & Snyders, 1990). In the present experiments, prazosin prolonged the APD to a similar extent at all stimulations tested. Thus, prazosin as previously described with amiodarone (Hondeghem & Snyders, 1990; Nattel, 1991) can be considered as a class III drug without reverse frequency-dependence. A homogeneous prolongation of the APD reducing the dispersion of ventricular refractoriness can explain the effectiveness of prazosin against ischaemia- and reperfusion-induced ventricular arrhythmias (Sheridan *et al.*, 1980; Davey, 1980).

Prazosin plasma levels present a marked intersubject-variability, but in patients with chronic heart failure, peak plasma concentrations after 1 and 4 mg of prazosin averaged 23 ± 10.5 and 254 ± 48 ng ml^{-1} (Wood *et al.*, 1976; Silke *et al.*, 1981). These levels are higher than those used in the present experiments and suggests that possibly its antiarrhythmic properties may be unrelated to its specific α_1-adrenoceptor blocking properties. In fact, it has been proposed that prazosin might have antiarrhythmic efficacy in the settings in which sympathetic activity is not a prominent factor in the induction of the arrhythmia (Dukes & Vaughan Williams, 1984; Ferrier & Carmeliet, 1990).

In conclusion, in guinea-pig papillary muscles prazosin inhibited the $\dot{V}_{max}$ and lengthened the duration of the action potentials, thus exhibiting both class I and class III antiarrhythmic actions, respectively, which were possibly unrelated to blockade of myocardial α-adrenoceptors.

This work was supported by CICYT (SAF92-0157) and FIS (91/0648) Grants.

References

BENFEY, B.G. (1980). Cardiac α-adrenoceptors. *Can. J. Physiol Pharmacol.*, **58**, 1145–1157.

BENFEY, B.G. (1982). Function of myocardial α-adrenoceptors. *Life Sci.*, **31**, 101–112.

CAMPBELL, T.J. (1983). Importance of physicochemical properties in determining the kinetics of the effects of class I antiarrhythmic drugs on maximum rate of depolarization in guinea-pig ventricle. *Br. J. Pharmacol.*, **80**, 33–40.

COURTNEY, K. (1987). Review: quantitative structure/activity relations based on use-dependent block and repriming kinetics in myocardium. *J. Mol. Cell. Cardiol.*, **19**, 319–330.

DAVEY, M.J. (1980). Relevant features of the pharmacology of prazosin. *J. Cardiovasc. Pharmacol.*, **2** (Suppl. 3), S287–S301.

DELPON, E., VALENZUELA, C., PEREZ, O. & TAMARGO, J. (1992). Electrophysiological effects of CRE-1087 in guinea-pig ventricular muscles. *Br. J. Pharmacol.*, **107**, 515–520.

DUKES, I. & VAUGHAN WILLIAMS, E. (1984). Electrophysiological effects of α-adrenoceptor antagonists in rabbit sino-atrial node, cardiac Purkinje cells and papillary muscles. *Br. J. Pharmacol.*, **83**, 419–426.

ETTINGER, S., GOULD, L., CARMICHAEL, J.A. & TASHJIAN, R.J. (1969). Phentolamine: Use in digitalis induced arrhythmias. *Am. Heart J.*, **77**, 636–640.

FERRIER, G.R. & CARMELIET, E. (1990). Effects of α-adrenergic agents on transient inward current in rabbit Purkinje fibers. *J. Mol. Cell. Cardiol.*, **22**, 191–200.

GILES, W.R. & IMAIZUMI, Y. (1988). Comparison of potassium currents in rabbit atrial and ventricular cells. *J. Physiol.*, **405**, 123–145.

GOULD, L., REDDY, C.V.R., WEINSTEIN, T. & GOMPRECHT, R.F. (1975). Antiarrhythmic prophylaxis with phentolamine in acute myocardial infarction. *J. Clin. Pharmacol.*, **15**, 191–197.

HIMMEL, H., GLOSSMANN, H. & RAVENS, U. (1991). Naftopidil, a new α-adrenoceptor blocking agent with calcium antagonistic properties: characterization of Ca^{2+} antagonistic effects. *J. Cardiovasc. Pharmacol.*, **17**, 213–221.

HONDEGHEM, L.M. & KATZUNG, B. (1977). Time- and voltage-dependent interactions of antiarrhythmic drugs with cardiac sodium channels. *Biochim. Biophys. Acta*, **472**, 377–398.

HONDEGHEM, L.M. & SNYDERS, D.J. (1990). Class III antiarrhythmic agents have a lot of potential, but a long way to go. Reduced effectiveness and dangers of reverse use-dependence. *Circulation*, **81**, 686–690.

MATSUURA, H., EHARA, T. & IMOTO, Y. (1987). An analysis of the delayed outward current in single ventricular cells of the guinea-pig. *Pflügers Arch.*, **410**, 596–603.

NATTEL, S. (1991). Antiarrhythmic drug classifications. A critical appraisal of their history, present status, and clinical relevance. *Drugs*, **41**, 672–701.

NORTHOVER, B. (1983). A comparison of the electrophysiological actions of phentolamine with those of some other antiarrhythmic drugs on tissues isolated from the rat heart. *Br. J. Pharmacol.*, **80**, 85–93.

QUADBECK, J. & REITER, M. (1975). Adrenoceptors in cardiac ventricular muscle and changes in duration of action potential caused by noradrenaline and isoprenaline. *Naunyn-Schmied. Arch. Pharmacol.*, **288**, 403–414.

ROSEN, M.R., WEISS, R.M. & DANILO, P. Jr. (1984). Effect of alpha adrenergic agonist and blockers on Purkinje fiber transmembrane potentials and automaticity in the dog. *J. Pharmacol. Exp. Ther.*, **231**, 566–571.

SADA, H. (1978). Effect of phentolamine, alprenolol and prenylamine on maximum rate of rise of action potential in guinea-pig papillary muscles. *Naunyn-Schmied. Arch. Pharmacol.*, **304**, 191–201.

SHERIDAN, D.J., PENKOSKE, P.A., SOBEL, B.E. & CORR, P.B. (1980). Alpha adrenergic contributions to dysrhythmia during myocardial ischemia and reperfusion in cats. *J. Clin. Invest.*, **65**, 161–171.

SILKE, B., LAKHANI, Z.M. & TAYLOR, S.H. (1981). Pharmacokinetic and pharmacodynamic studies with prazosin in chronic heart failure. *J. Cardiovasc. Pharmacol.*, **3**, 329–355.

STEWART, J.R., BURMEISTER, W.E., BURMEISTER, J. & LUCCHESI, B.F. (1980). Electrophysiologic and antiarrhythmic effects of phentolamine in experimental coronary artery occlusion and reperfusion in the dog. *J. Cardiovasc. Pharmacol.*, **2**, 77–91.

TAMARGO, J., VALENZUELA, C. & DELPON, E. (1992). New insights into the pharmacology of sodium channel blockers. *Eur. Heart J.*, **13** (Suppl F), 2–13.

TOHSE, N., NAKAYA, H. & KANNO, M. (1986). Electrophysiological effects of amosulalol, a new α- and β-adrenoceptor blocker, in isolated rabbit papillary muscles. *Eur. J. Pharmacol.*, **125**, 411–419.

VALENZUELA, C. & SANCHEZ CHAPULA, J. (1989). Electrophysiologic interactions between mexiletine-quinidine and mexiletine-ropitoin in guinea pig papillary muscles. *J. Cardiovasc. Pharmacol.*, **14**, 783–789.

VARGAFTIG, B. & COIGNET, J.L. (1969). A critical evaluation of three methods for the study of adrenergic beta-blocking and antiarrhythmic effects. *Eur. J. Pharmacol.*, **6**, 49–55.

VAUGHAN WILLIAMS, E. (1984). A classification of antiarrhythmic actions reassessed after a decade of new drugs. *J. Clin. Pharmacol.*, **24**, 129–147.

WALLENSTEIN, S., ZUCKER, S. & FLEISS, J. (1980). Some statistical methods useful in circulation research. *Circ. Res.*, **47**, 1–9.

WILLIAMS, R.S., DUKES, D.F. & LEFKOVITZ, R.J. (1981). Subtype specificity of α-adrenergic receptors in rat heart. *J. Cardiovasc. Pharmacol.*, **3**, 522–531.

WOOD, A.J., BOLLI, P. & SIMPSON, F.O. (1976). Prazosin in normal subjects: plasma levels, blood pressure and heart rate. *Br. J. Clin. Pharmacol.*, **3**, 199–201.

(Received May 7, 1993
Revised November 3, 1993
Accepted November 10, 1993)

Br. J. Pharmacol. (1994), **111**, 723–728 © Macmillan Press Ltd, 1994

Differential regulation of inositol 1,4,5-trisphosphate by co-existing P_{2Y}-purinoceptors and nucleotide receptors on bovine aortic endothelial cells

John R. Purkiss, Graeme F. Wilkinson & [1]Michael R. Boarder

Department of Pharmacology & Therapeutics, University of Leicester, Medical Sciences Building, University Road, Leicester LE1 9HN

1 We have examined the inositol 1,4,5-trisphosphate ($Ins(1,4,5)P_3$) responses in bovine aortic endothelial (BAE) cells to purines (ATP, ADP and analogues) and the pyrimidine, uridine triphosphate (UTP).

2 Exchange of medium on BAE cells in the absence of agonist was found to be a stimulus for $Ins(1,4,5)P_3$ generation. BAE cells stimulated with 100 μM ATP, 30 μM 2MeSATP (an agonist at P_{2Y}-purinoceptors but not nucleotide receptors) or 100 μM UTP (an agonist at nucleotide receptors but not P_{2Y}-purinoceptors) gave $Ins(1,4,5)P_3$ responses above that caused by exchange of medium. The time course was rapid, with peak response within the first 5 s and levels returning close to basal after 30 s of stimulation.

3 Significant differences in $Ins(1,4,5)P_3$ responses to 100 μM UTP and 30 μM 2MeSATP stimulation were observed. The response to UTP was reproducibly more sustained than that to 2MeSATP.

4 Stimulation of BAE cells with 100 μM UTP plus 30 μM 2MeSATP produced a response statistically indistinguishable from that predicted by addition of the responses to the two agonists in isolation.

5 The $Ins(1,4,5)P_3$ response to UTP was attenuated to 25% of control by pretreatment of BAE cells with pertussis toxin. Responses to 2MeSATP and ADP were essentially unaffected. ATP stimulation was reduced to 65% of control.

6 Activation of protein kinase C with tetradecanoyl phorbol acetate (TPA) profoundly inhibited $Ins(1,4,5)P_3$ responses to 2MeSATP and ADP but had no effect on UTP stimulation. The protein kinase C inhibitor, Ro 31-8220, enhanced responses to 2MeSATP, ADP and ATP but no effect was observed on UTP stimulation.

7 These observations show that nucleotide and P_{2Y}-receptors mobilise the second messenger $Ins(1,4,5)P_3$ by separate routes resulting in different patterns of generation and suggest that while ATP activates both receptors, ADP principally influences these cells by interacting with the P_{2Y}-purinoceptors.

Keywords: Purinoceptors; endothelial cells; nucleotide receptors; phospholipase C; inositol phosphates; UTP receptors

Introduction

Regulation of free intracellular Ca^{2+} in vascular endothelial cells contributes to the control of several aspects of local vascular function, such as vascular permeability, smooth muscle contraction and platelet aggregation. One of the mechanisms controlling Ca^{2+} is the generation of inositol 1,4,5-trisphosphate ($Ins(1,4,5)P_3$) by receptors which are linked to hydrolysis of phosphatidylinositol 4,5-bisphosphate by phospholipase C (PLC). $Ins(1,4,5)P_3$, the primary hydrophilic product of this activity, mobilizes intracellular Ca^{2+} stores (see Berridge, 1993, for review); in addition it is the precursor to $Ins(1,3,4,5)P_4$, which in endothelial cells is reported to play a role in entry of extracellular Ca^{2+} (Luckhoff & Clapham, 1992). It is well established that ATP and ADP act on cell surface receptors to regulate vascular endothelial cells by this PLC-linked mechanism (Boynaems & Pearson, 1990). Following the proposals of Burnstock & Kennedy (1985) it is also widely accepted that this is by action at P_{2Y}-purinoceptors. The principal evidence for this is the potency of the P_{2Y}-selective agonist 2 methylthioadenosine 5′-trisphosphate (2MeSATP) and the lack of effect of β,γ-methylene ATP (a P_{2X}-purinoceptor agonist) on aortic endothelial cells (Martin *et al.*, 1985; Houston *et al.*, 1987; Pirotton *et al.*, 1987; Allsup & Boarder, 1990).

Recently it has become apparent that the situation is more complex, with the recognition that the pyrimidine nucleotide, UTP can also elicit a PLC response from these endothelial cells. Work of ours and others has established that there are two populations of co-existing receptors for ATP on these cells, the P_{2Y}-purinoceptors and nucleotide receptors. The P_{2Y}-purinoceptors respond to ATP and 2MeSATP but not to UTP, while the nucleotide receptors respond to both ATP and UTP but not to 2MeSATP (Wilkinson & Boarder, 1992; Wilkinson *et al.*, 1993; Motte *et al.*, 1993). ADPβS has been shown to be an agonist at P_{2Y}-purinoceptors but not nucleotide receptors and β,γ-methylene ATP acts at neither (Wilkinson *et al.*, 1993).

To pursue the significance of regulation of responses to ATP and ADP by two receptor populations, we have investigated the accumulation of $Ins(1,4,5)P_3$. Here we describe for the first time the mass measurement of $Ins(1,4,5)P_3$ in endothelial cells in response to purinoceptor activation and provide evidence that this primary second messenger is differentially regulated by P_{2Y}-purinoceptors and nucleotide receptors co-existing on bovine cultured aortic endothelial cells.

Methods

Cell culture

BAE cells were prepared from fresh aortae by digestion with 2 to 5 mg ml^{-1} collagenase (Booyse *et al.*, 1975) and cultured in Minimum Essential Medium D-valine with 10% foetal calf serum, 10% new-born calf serum, 25 iu ml^{-1} penicillin, 25 μg ml^{-1} streptomycin, 10 mg ml^{-1} gentamycin, 250 μg ml^{-1} fungizone and 27 mg ml^{-1} glutamine in 95:5% air:CO_2 at 37°C. Cells formed a confluent monolayer of homogeneous cells

[1] Author for correspondence.

positive for Von Willebrand factor immunofluorescence and were used up to passage nine in 24 well plates.

Measurement of Ins(1,4,5)P_3

Cells cultured in 24 well multiwells were gently washed twice with balanced salt solution (BSS) with the following composition (mM): NaCl 125, KCl 5.4, $NaHCO_3$ 16.2, N-2-hydroxyethylpiperazine-N-2-ethanesulphonic acid 15, NaH_2PO_4 1, $MgSO_4$ 0.8, $CaCl_2$ 1.8, glucose 5.5 and gassed with 95% O_2, 5% CO_2. Agonists and drugs were all made up in this solution. Preincubations when included were for 5 min (at 37°C) with tetradecanoyl phorbol acetate (TPA), Ro 31 8220 or control balanced salt solution. The preincubation was in place of the second wash. When present during the preincubation, TPA and Ro 31 8220 were included in the 0.2 ml incubation, which was for 5 s (except where indicated) in the presence of the appropriate purine or pyrimidine. Where there was no preincubation the final wash was left for 5 min before removal and addition of incubate. The incubation was stopped by addition of 0.1 ml of cold (4°C) trichloroacetic acid (1.5 M). The acid extract was washed with 3 × 2 ml of H_2O saturated diethyl ether, buffered to pH 7 with $NaHCO_3$ and assayed for mass of Ins(1,4,5)P_3 by the procedure of Challiss *et al.* (1991). Results are given as mean ± s.e.mean.

Materials

[^{3}H]-Ins(1,4,5)P_3 for the mass assay was purchased from NEN Du Pont (UK) Ltd., Stevenage, Herts. 2MeSATP was from Research Biochemicals, Semat, St. Albans, Herts. Other chemicals were from Sigma, Poole, Dorset or Fisons, Loughborough, Leics. Ro 31 8220 (a *bis*-indolymaleimide derivative, compound 3 in Davis *et al.*, 1989) was a kind gift from Dr G. Lawton, Roche Products Ltd., Welwyn Garden City, Herts.

Results

Figure 1 shows results of experiments in which the concentration-effect relationship for various nucleotides were determined, stimulating for 5 s and measuring accumulation of Ins(1,4,5)P_3. Data were pooled from three separate experiments, resulting in computer generated (Graph-Pad) EC_{50} values (in μM) as follows, in order of decreasing potency: (2MeSATP (1.11 ± 0.54); ADPβS (2.07 ± 0.56); ADP (3.17 ± 0.88); ATPγS (31.0 ± 12.3); ATP(36.3 ± 12.9); UTP(64.2 ± 6.84).

Experiments were set up to examine the time course of the Ins(1,4,5)P_3 response to some of these nucleotide agonists. Preliminary experiments indicated that there was a rapid fluctuation in levels in control wells to which no agonist was added (Figure 2). In these experiments the culture medium was removed and the cells gently washed twice. After 5 min the final wash was removed and BSS with no agonist added for the times shown, followed by addition of TCA. The zero time point was determined by removal of wash and direct addition of 0.3 ml of 0.5 M TCA. Without drugs there was a rapid increase in Ins(1,4,5)P_3 levels at 5 and 10 s, followed by a gradual decline. This pattern was followed when 100 μM ATP was present but was enhanced approximately 2 fold (Figure 2a). In all the data reported in this paper a control (no agonist added) value was established in each experiment for each condition of stimulation and has been deducted from the level obtained on stimulation with agonist. Subtraction of the basal from the ATP stimulation illustrated in Figure 2a is shown in Figure 2b.

The time course of response to 30 μM 2MeSATP and 100 μM UTP is shown in Figure 3. We characteristically obtained a fast response to 2MeSATP, peaking within 5 s followed by a rapid decline to control levels by 20–30 s. Stimulation with UTP gave a reproducibly more sustained response. In some experiments this was a slower response (maximal at 15 s), in others (Figure 3) it was rapid (maximal at 5 s) and in all cases sustained compared with the response to 2MeSATP. The statistically significant differences were not due to differential breakdown: both these agonists were susceptible to ectonucleotidase attack, but this was not significant within the time course of these experiments (determined by high performance liquid chromatography – data not shown).

Figure 4 shows that the response to a mixture of 2MeSATP (30 μM) and UTP (100 μM) was rapid and followed by a decline. This response to a maximally effective concentra-

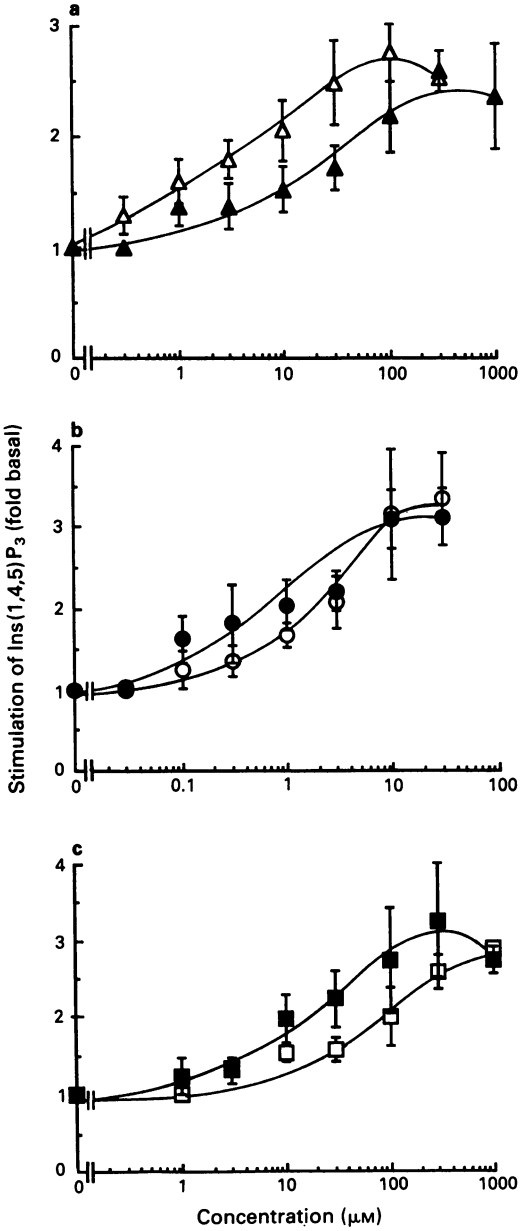


Figure 1 Concentration-effect curves for inositol 1,4,5-trisphosphate (Ins(1,4,5)P_3) responses in bovine aortic endothelial (BAE) cells stimulated for 5 s with increasing concentrations of: (a) ATP (▲) and ADP (△), (b) 2MeSATP (●) and ADPβS (○) and (c) ATPγS (■) and UTP (□). Stimulations of Ins(1,4,5)P_3 are expressed as fold increases over basal ± s.e.mean. Data are pooled from 3 separate experiments, each carried out in triplicate. Typical values were basal, 11.06 ± 0.49; 300 μM ATP, 32.13 ± 0.30; 100 μM ADP, 29.11 ± 0.81; 30 μM 2MeSATP, 30.74 ± 1.00; 30 μM ADPβS, 29.28; 300 μM ATPγS, 40.84 ± 1.85 and 1 mM UTP, 38.41 ± 0.84 pmol Ins(1,4,5)P_3 per well.

tion of 2MeSATP and submaximal UTP was additive and was statistically indistinguishable from that predicted by addition of the two individual responses (Figure 3).

Experiments were undertaken to determine whether the responses to the agonists differed in the involvement of a pertussis toxin sensitive G-protein. The data in Table 1 show that the responses to 2MeSATP were unaffected by pertussis toxin at 5, 15 and 30 s of stimulation. The response to UTP was significantly reduced by toxin pretreatment at each of three times. The inhibition of the ATP response by pertussis toxin varied somewhat between experiments, but assumed in general, an intermediate position between UTP and 2MeSATP (e.g. Table 1). Over three separate experiments (each in triplicate) the responses to 5 s stimulation after pertussis toxin treatment as a percentage of control stimulations were: ATP (64.5 ± 5.0%); 2MeSATP (90.2 ± 9.4%); UTP (19.5 ± 2.1%). Further experiments with ADP at 5 s stimulation showed no effect of pertussis toxin (102 ± 18.7%) ($n = 4$). After pertussis toxin the basal (no agonist) response fell to 48.6 ± 9.7%.

It is a common observation that activation of protein kinase C with TPA can attenuate agonist-stimulated PLC responses. In some cases this has been related to a short feedback loop: agonist stimulation of PLC leads to protein kinase C activation which attenuates the PLC response. In this case downregulation or inhibition of protein kinase C augments the response to the agonist. The extent to which this occurs is very variable (see for example Helper *et al.*, 1988; Pfeilschifter *et al.*, 1989; Boarder & Challiss, 1992; Challiss *et al.*, 1993). Here we looked at the effect of protein

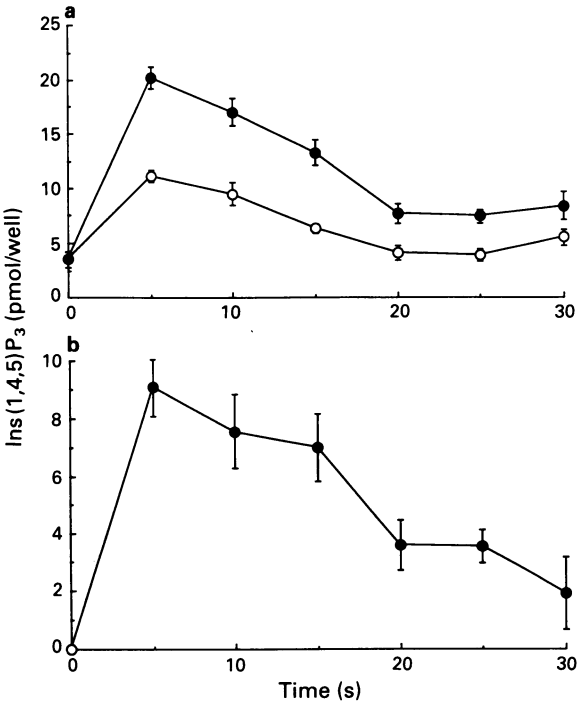


Figure 2 Time courses of inositol 1,4,5-trisphosphate ($Ins(1,4,5)P_3$) generation in bovine aortic endothelial (BAE) cells. (a) Responses to BSS alone (○) and 100 μM ATP (●). (b) Response to 100 μM ATP with BSS response (basal) subtracted. Data expressed as pmol $Ins(1,4,5)P_3$ per well ± s.e.mean, $n = 6$ pooled from two separate experiments.

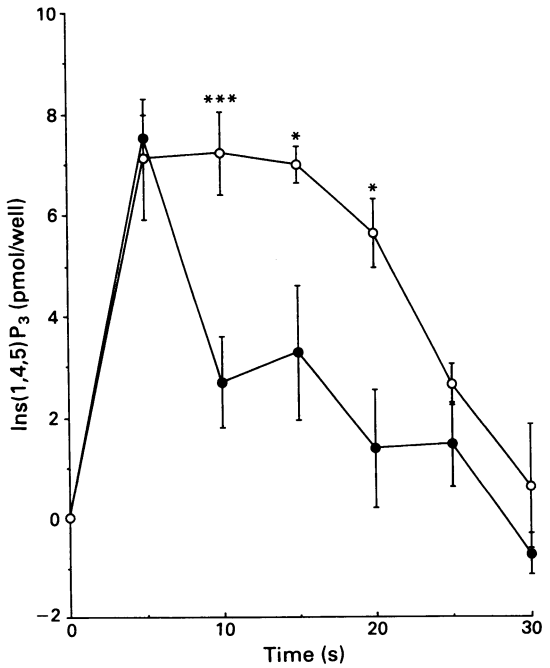


Figure 3 Time courses of inositol 1,4,5-trisphosphate ($Ins(1,4,5)P_3$) generation in bovine aortic endothelial (BAE) cells in response to 100 μM UTP (○) and 30 μM 2MeSATP (●) with basal response subtracted. Data expressed as pmol $Ins(1,4,5)P_3$ per well ± s.e.mean, $n = 6$ pooled from two separate experiments. Significant differences in the response to the two agonists indicated by $***P < 0.001$ or $*P < 0.01$.

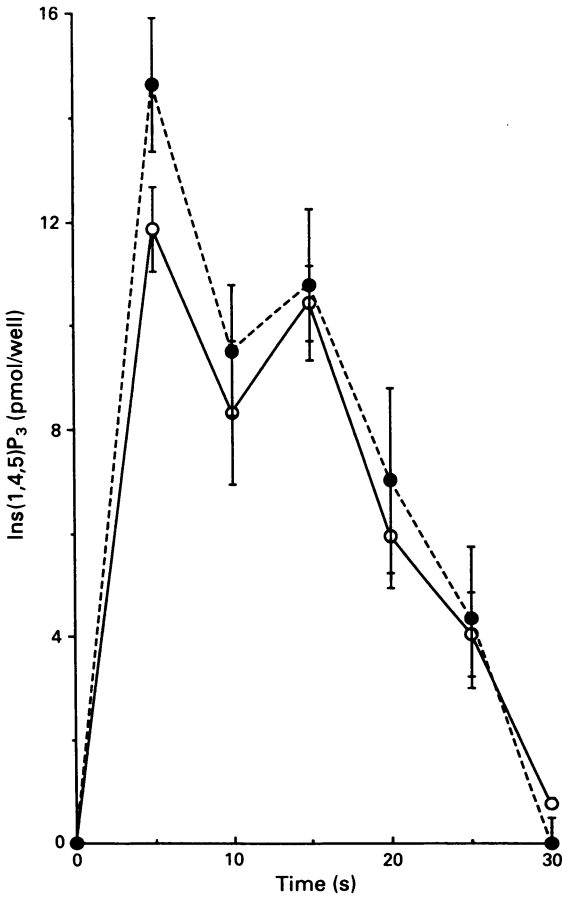


Figure 4 Time course of inositol 1,4,5-trisphosphate ($Ins(1,4,5)P_3$) generation in bovine aortic endothelial (BAE) cells in responses to 100 μM UTP plus 30 μM 2MeSATP (○, solid line) and the response predicted for the two agonists acting additively (●, dotted line). The predicted response is the addition of response from paired wells into which *either* 30 μM 2MeSATP or 100 μM UTP were added. Basal response (no agonist) was subtracted in each case. No significant difference was seen between observed and predicted values. Data expressed as pmol $Ins(1,4,5)P_3$ per well ± s.e.mean, $n = 6$ pooled from two separate experiments.

Table 1 The effect of pertussis toxin treatment on the inositol 1,4,5-trisphosphate ($Ins(1,4,5)P_3$) responses

Time	*Treatment*	*ATP*	*2MeSATP*	*UTP*
5 s	Control	15.36 ± 4.26	10.18 ± 0.70	9.73 ± 0.10
	PTX	8.37 ± 1.50*	9.34 ± 0.84	2.28 ± 1.34*
15 s	Control	6.84 ± 3.07	4.99 ± 1.55	8.7 ± 1.10
	PTX	3.56 ± 1.89	5.87 ± 1.01	4.15 ± 1.35*
30 s	Control	3.97 ± 1.72	4.74 ± 1.88	6.03 ± 2.26
	PTX	1.35 ± 0.09*	5.16 ± 0.78	0.08 ± 0.07*

Stimulation with ATP (300 μM), 2MeSATP (30 μM) and UTP (300 μM) were for the times indicated. Basal values were determined for each condition and have been deducted. Data are pmol per well of $Ins(1,4,5)P_3$, mean ± s.e.mean, $n = 3$, from a single experiment in each case (see text for data pooled across experiments). PTX = pertussis toxin treated (100 ng ml^{-1} for 16 h). The asterisks denote difference from control (no PTX) values was significant at the $P < 0.05$ level or greater (Student's t test).

Table 2 The effect of tetradecanoyl phorbol acetate (TPA) on the inositol 1,4,5-trisphosphate ($Ins(1,4,5)P_3$) responses

Agonist	*Control stimulation* (pmol/well)	*Stimulation + TPA* (pmol/well)	P *value*
ATP (300 μM)	20.20 ± 1.62	12.47 ± 1.8	<0.05
UTP (300 μM)	9.69 ± 2.37	14.87 ± 1.46	NS
2MeSATP (30 μM)	13.79 ± 1.68	4.86 ± 0.55	<0.01
ADP (100 μM)	9.09 ± 0.34	− 0.66 ± 1.01	0.001

Stimulation was for 5 s. Unstimulated values (control = 6.29 ± 1.61, TPA = 3.36 ± 1.39) have been deducted. TPA was at 100 nM. Data (pmol per well of Ins(1,4,5)P) are mean ± s.e.mean ($n = 3$) from a single representative experiment (see text for data pooled across experiments). The P values are by Student's t test, NS = non significant.

kinase C stimulation with TPA, and inhibition with Ro 31 8220 on the stimulation of $Ins(1,4,5)P_3$ levels by purinoceptor agonists and UTP. There was a significant attenuation of response to the purinoceptor agonists by TPA: the response to ADP and to 2MeSATP was substantially attenuated while the response to ATP was down to 61% of control stimulation (Table 2). By contrast the UTP response was not inhibited by TPA. Over three such experiments (each in triplicate) the percentage of original response left by TPA was: ADP (12 ± 4.1%); 2MeSATP (41 ± 15%); ATP (68 ± 4%); UTP (123 ± 27%) ($n = 3$). TPA treatment reduced the control (no agonist) response to 51.4 ± 10.4% ($n = 4$).

The effect of the protein kinase C inhibitor Ro 31 8220 on $Ins(1,4,5)P_3$ responses was largely the inverse of the TPA effect: responses to 2MeSATP, ADP and ATP were increased by the protein kinase C inhibitor. For example, the response to ATP was increased by 10 μM Ro 31 8220 from 24.1 ± 4.4 to 48.6 ± 4.0; to 2MeSATP from 21.9 ± 3.8 to 46.7 ± 6.3 and to ADP from 22.4 ± 3.0 to 35.9 ± 2.7 (data are pmol/well, $n = 3$). However, there was no effect on the UTP response (112 ± 15% of response with no Ro 31 8220, $n = 5$ separate experiments). Ro 31 8220 raised the control (no agonist) response to 132 ± 12% ($n = 6$ separate experiments).

Discussion

In the absence of selective antagonists or cloning studies, the P_2-purinoceptors are classified on the basis of rank order of agonist potency. While this can yield only working hypotheses for classification, the significance of this approach can be seen in the value which has been attached to the subdivision into P_{2X} and P_{2Y} subtypes, based principally on the relative potencies of 2MeSATP and β,γ-methylene ATP (Burnstock & Kennedy, 1985). A number of receptors responding to ATP and ADP have been described which do not fall into this classification: recently interest has focussed on nucleotide receptors, which respond to both the purine ATP (or its stable analogue ATPγS) and the pyrimidine UTP, but do not respond to either 2MeSATP or β,γ-methylene ATP.

This pattern has been described in a variety of cell types (e.g. Demolle *et al.*, 1988; Fine *et al.*, 1989; Pfeilschifter, 1990; Davidson *et al.*, 1990; Brown *et al.*, 1991; Murrin & Boarder, 1992). In vascular endothelial cells, nucleotide receptors are known to be present on endothelial cells from aorta (Wilkinson & Boarder, 1992; Wilkinson *et al.*, 1993; Motte *et al.*, 1993) and from microvasculature of the adrenal medulla (Purkiss *et al.*, 1993). While in adrenal medulla cells nucleotide receptors are the sole PLC linked receptors for ATP (Allsup & Boarder, 1990; Purkiss *et al.*, 1993), in BAE cells we have shown that ATP regulates vascular function by interacting with two co-existing receptor populations, P_{2Y}-purinoceptors and nucleotide receptors, linked to both PLC (Wilkinson *et al.*, 1993) and phospholipase D (Purkiss & Boarder, 1992). Using precontracted rings of bovine aortic collateral artery (vessels supplying the intercostal muscles), we have shown that both receptors mediate relaxant responses to ATP, but with differential sensitivity to indomethacin: the response to P_{2Y} stimulation (2MeSATP) was indomethacin-sensitive while the response to nucleotide stimulation (UTP) was not (Wilkinson *et al.*, 1994). This shows that the two receptors generate differential release of relaxant factors. Since they co-exist on the same cells and both are PLC-linked, this suggests that the pattern of second messenger generation must differ according to which receptor population is activated. Here we have initiated the study of this difference by investigating the generation of $Ins(1,4,5)P_3$, the primary product of phosphoinositide(4,5)bisphosphate hydrolysis by PLC.

The principal observations to emerge from this study are: (i) there was differential sensitivity to pertussis toxin depending on whether P_{2Y} or nucleotide receptors were stimulated; (ii) the pattern of $Ins(1,4,5)P_3$ accumulation was dependent on the type of receptor stimulated; (iii) there was differential regulation of this stimulation by protein kinase C.

The observations on pertussis toxin sensitivity unequivocally show that the P_{2Y} response is not mediated by pertussis toxin-sensitive G-proteins. We can therefore exclude a role for the G_i family of G-proteins, which includes G_o. It seems likely that a member of the G_q family is involved: $G_{q/11}$ has been shown to stimulate phosphoinositide directed PLC activity (Smrcka *et al.*, 1991). The observations for stimulation of nucleotide receptors by UTP shows pertussis toxin-sensitivity, from which we can conclude that a member of the

G_i family is involved in linking the receptor to PLC. The two receptor populations acting on the same cell therefore differ in the G-proteins used to elicit the PLC response. With respect to the two principal endogenous agonists of these receptors (ATP and ADP), the data show an intermediate sensitivity of the ATP response to pertussis toxin, consistent with this being a natural agonist for both receptors. However, ADP was unaffected by pertussis toxin, suggesting that the influence of ADP was principally via the P_{2Y}-purinoceptors.

With respect to the different time course of Ins(1,4,5)P_3 accumulation, it is of importance to consider how this comes about if we are to understand how activation of the two PLC linked receptor populations can effect different physiological responses. Three possibilities will be introduced: (1) Activation of P_{2Y}-purinoceptors may result in more rapid desensitization than activation of nucleotide receptors. Rapid desensitization (i.e. within a few seconds) has been described for PLC linked receptors (Tobin *et al.*, 1993) and so may be involved.

(2) The rate at which the G-protein activation of PLC is terminated by GTPase activity may vary. When an effector such as PLC is activated by a G-protein linked receptor, the activation is terminated by the intrinsic GTPase activity of the α-subunit converting PLC*-α_{GTP} to PLC and α_{GDP}, where PLC* is active and PLC is inactive. The hydrolysis rate for GTP bound to purified α-subunits is slow, e.g. 50 s for $G_{q/11}$ (Berstein *et al.*, 1992a) and may therefore play a role in the events shown in Figure 3. This rate varies according to the specific G-proteins involved, but it is also regulated by the GTPase activating characteristics of PLC (Berstein *et al.*, 1992b). The involvement of G-proteins with different intrinsic GTPase activity, or of PLC species with differing GTPase activating characteristics, could therefore generate within the same cells the differential kinetics seen in Figure 3.

(3) Activation of P_{2Y}-purinoceptors may generate conditions in which breakdown of Ins(1,4,5)P_3 is faster than that which occurs following nucleotide receptor activation. For example it has been shown that elevation of Ca^{2+} may cause enhanced 3-kinase activity, leading to increased metabolism of Ins(1,4,5)P_3 to Ins(1,3,4,5)P_4 (Shears, 1991). Both the 3-kinase and 5-phosphatase pathways for Ins(1,4,5)P_3 metabolism are subject to regulation by protein kinase C (King & Rittenhouse, 1989; Sim *et al.*, 1990). Therefore if there is differential control of Ca^{2+} or protein kinase C by P_{2Y}-purinoceptors or nucleotide receptors it may result in differential rates of Ins(1,4,5)P_3 metabolism.

The final observations from this paper which require discussion are those involving protein kinase C. It is apparent that the nucleotide response is unusual amongst receptor stimulation of G-protein-regulated PLC in that TPA does not attenuate the agonist-stimulated PLC activity. The P_{2Y}-purinoceptor stimulation is much more typical in that activation of protein kinase C by TPA severely attenuated the response. The consequences of protein kinase C inhibition on agonist-stimulated PLC described in the literature show considerable variation, with instances of major enhancement (e.g. Challiss *et al.*, 1993) indicating an active short inhibitory feedback loop, alongside reports in which only a small effect is seen (e.g. Boarder & Challiss, 1992). The outcome of the present paper is that the P_{2Y}-purinoceptor agonists activate this short protein kinase C feedback loop while the nucleotide agonist, UTP, does not. The observation that TPA does not attenuate the UTP response suggests that this is not because UTP fails to activate protein kinase C. Possibly the reason for the differential sensitivity to protein kinase C activation lies in the involvement of different G-proteins.

Of the principal endogenous agonists, the responses to ATP and ADP were both decreased by TPA and enhanced by Ro 31 8220. The effect of TPA on ADP was more profound than the effect on ATP. These results are consistent with ATP acting at both receptors (as suggested by our earlier work), but also with ADP acting principally at the P_{2Y}-purinoceptor and not at the nucleotide receptor. The notion that ADP, unlike ATP, is not an effective agonist at nucleotide receptors is supported by other evidence, including the pertussis toxin data discussed above, our work on relaxant responses of aortic collateral artery rings (Wilkinson *et al.*, 1994) and a recent publication describing a cloned receptor with the characterization of a nucleotide receptor (Lustig *et al.*, 1993).

In conclusion, the data presented here show that there are two separate routes for activation of PLC by co-existing nucleotide receptors and P_{2Y}-purinoceptors on BAE cells, leading to a different pattern of second messenger generation. This may involve modulation of separate populations or subtypes of PLC, but the interpretation discussed here suggests that the differential responses could arise from different receptors acting through different G-proteins on a common pool of PLC activity. The different pattern of second messenger generation which we have described here may provide an explanation for the differential physiological responses elicited by two receptors for ATP co-existing on the same cells. They may also contribute to understanding how ATP and ADP may differentially regulate vascular endothelial cells.

This work was supported by a grant from The Wellcome Trust and an MRC/Fisons plc studentship to G.F.W. We thank Lyn McCarthy for preparing the manuscript and Dr G. Lawton, Roche Products Ltd., for supplying Ro 31 8220.

References

ALLSUP, D.J. & BOARDER, M.R. (1990). Comparison of P_2 purinergic receptors of aortic endothelial cells with those of adrenal medulla. Evidence for heterogeneity of receptor subtype and of inositol phosphate response. *Mol. Pharmacol.*, **38**, 84–91.

BERRIDGE, M.J. (1993). Inositol trisphosphate and calcium signalling. *Nature*, **361**, 315–325.

BERSTEIN, G., BLANK, J.L., SMRCKA, A.V., HIGASHIJIMA, T., STERNWEISS, P.C., EXTON, J.H. & ROSS, E.M. (1992a). Reconstitution of agonist stimulated phosphoinositide (4,5) bisphosphate hydrolysis using purified ml muscarinic receptor, G_q/11 and phospholipase C-β1. *J. Biol. Chem.*, **267**, 8081–8088.

BERSTEIN, G., BLANK, J.L., JHON, D.-Y., EXTON, J.H., RHEE, S.G. & ROSS, E.M. (1992b). Phospholipase C-β1 is a GTPase-activating protein for G_q/11, its physiological regulator. *Cell*, **70**, 411–418.

BOARDER, M.R. & CHALLISS, R.A.J. (1992). Role of protein kinase C in the regulation of histamine and bradykinin stimulated inositol polyphosphate turnover in adrenal chromaffin cells. *Br. J. Pharmacol.*, **107**, 1140–1145.

BOEYNAMES, J.-M. & PEARSON, J.D. (1990). P_{2Y}-purinoceptors as vascular endothelial cells: physiological significance and transduction mechanisms. *Trends Pharmacol. Sci.*, **11**, 34–37.

BOOYSE, F.M., SEDLACK, B.J. & RAFELSON, M.E. (1975). Culture of arterial endothelial cells: characterisation and growth of bovine adrenal cells. *Thrombos. Diath. Haemorrh.*, **34**, 825– 839.

BROWN, H.A., LAZAROWSKI, E.R., BOUCHER, R.C. & HARDEN, T.K. (1991). Evidence that UTP and ATP regulate phospholipase C through a common extracellular 5'-nucleotide receptor in human airway epithelial cells. *Mol. Pharmacol.*, **40**, 648–655.

BURNSTOCK, G. & KENNEDY, C. (1985). Is there a basis for distinguishing two types of P_2-purinoceptor. *Gen. Pharmacol.*, **16**, 433–440.

CHALLISS, R.A.J., BATTY, I.H. & NAHORSKI, S.R. (1988). Mass measurements of inositol 1,4,5-trisphosphate in rat cerebral cortical slices using a radioceptor assay: effects of neurotransmitters and depolarisation. *Biochem. Biophys. Res. Commun.*, **157**, 684–691.

CHALLISS, R.A.J., WILKES, L., PATEL, V., PURKISS, J.R. & BOARDER, M.R. (1993). Evidence that phospholipase D can regulate endothelin stimulated phospholipase C activity in SK-N-MC cells. *Br. J. Pharmacol.*, **108**, 111P.

DAVIDSON, J.S., WAKEFIELD, I.K., SOHNIUS, U., VAN DER MERWE, R.A. & MILLAR, R.P. (1990). A novel extracellular nucleotide receptor coupled to phosphoinositidase C in pituitary cells. *Endocrinology*, **126**, 80–87.

DAVIS, P.D., HILL, C.H., KEECH, E., LAWTON, G., NIXON, J.S., SEDGWICK, A.D., WADSWORTH, J., WESTMACOTT, D. & WILKINSON, S.E. (1989). Potent selective inhibitors of protein kinase C. *FEBS Lett.*, **259**, 61–63.

DEMOLLE, D., LAGNEAU, C. & BOEYNAEMS, J.M. (1988). Stimulation of prostacyclin release from aortic smooth muscle cells by purine and pyrimidine nucleotides. *Eur. J. Pharmacol.*, **155**, 339–343.

FINE, J., COLE, P. & DAVIDSON, J.S. (1989). Extracellular nucleotides stimulate receptor mediated calcium mobilisation and inositol phosphate production in human fibroblasts. *Biochem. J.*, **263**, 371–376.

HELPER, J.R., BARP, H.S. & HARDEN, T.K. (1988). Longterm phorbol ester treatment down-regulates protein kinase C and sensitises the phosphoinositide signalling pathway to hormone growth factor stimulation. *J. Biol. Chem.*, **263**, 7610–7619.

HOUSTON, D.A., BURNSTOCK, G. & VANHOUTTE, P.M. (1987). Different P_2-purinergic subtypes of endothelium and smooth muscle in canine blood vessels. *J. Pharmacol. Exp. Ther.*, **241**, 501–509.

KING, W.G. & RITTENHOUSE, S.E. (1989). Inhibition of protein kinase C by staurosporine promotes elevated accumulations of inositol trisphosphates and tetrakisphosphate in human platelets exposed to thrombin. *J. Biol. Chem.*, **264**, 6070–6074.

LUCKHOFF, A. & CLAPHAM, D.E. (1992). Inositol 1,3,4,5-tetrakisphosphate activates an endothelial Ca^{2+} permeable channel. *Nature*, **355**, 356–358.

LUSTIG, K.D,. SHIAU, A.K., BRAKE, A.J. & JULIUS, D. (1993). Expression cloning of an ATP receptor from mouse neuroblastoma cells. *Proc. Natl. Acad. Sci. U.S.A.*, **90**, 5113–5117.

MARTIN, W., CUSACK, N.J., CARLETON, J.S. & GORDON, J.L. (1985). Specificity of P_2-purinoceptor that mediates endothelium dependent relaxation of the pig aorta. *Eur. J. Pharmacol.*, **108**, 295–299.

MOTTE, S., PIROTTON, S. & BOEYNAEMS, J.M. (1993). Heterogeneity of ATP receptors in aortic endothelial cells. *Circ. Res.*, **72**, 504–510.

MURRIN, R.J.A. & BOARDER, M.R. (1992). A neuronal 'nucleotide' receptor linked to phospholipase C and phospholipase D? Stimulation of PC12 cells by ATP analogues and UTP. *Mol. Pharmacol.*, **41**, 561–568.

PFEILSCHIFTER, J. (1990). Comparison of extracellular ATP and UTP signalling in rat renal mesangial cells. No indications for the involvement of separate purino- and pyrimidino-ceptors. *Biochem. J.*, **272**, 469–472.

PFEILSCHIFTER, J., OCHSNER, M., WHITEBREAD, S. & DEGASPARO, M. (1989). Down-regulation of protein kinase C potentiates angiotensin II-stimulated phosphoinositide hydrolysis in vascular smooth muscle cells. *Biochem. J.*, **262**, 285–291.

PIROTTON, S., RASPE, E., DEMOLLE, D., ERNEAUX, C. & BOEYNAEMS, J.-M. (1987). Involvement of inositol 1,4,5-trisphosphate and calcium in the action of adenine nucleotides on aortic endothelial cells. *J. Biol. Chem.*, **262**, 17461–17466.

PURKISS, J.R. & BOARDER, M.R. (1992). Stimulation of phosphatidate synthesis in endothelial cells in response to P_2-receptor activation: Evidence for phospholipase C and phospholipase D involvement, phosphatide and diacyglycerol interconversion and the role of protein kinase C. *Biochem. J.*, **287**, 31–36.

PURKISS, J.R., WILKINSON, G.F. & BOARDER, M.R. (1993). Evidence for a nucleotide receptor on adrenal medullary endothelial cells linked to phospholipase C and phospholipase D. *Br. J. Pharmacol.*, **108**, 1031–1037.

SHEARS, S.D. (1991). Regulation of the metabolism of 1,2-diacylglycerols and inositol phosphates that respond to receptor activation. *Pharmacol. Ther.*, **49**, 79–104.

SIM, S.S., KIM, J.W. & RHEE, S.G. (1990). Regulation of D-myo-inositol 1,4,5-trisphosphate 3-kinase by cAMP-dependent protein kinase and protein kinase C. *J. Biol. Chem.*, **265**, 10367–10372.

SMRCKA, A.V., HELPER, J.R., BROWN, K.O. & STERNWEIS, P.C. (1991). Regulation of phosphoinositide-specific phospholipase C activity by purified G_q. *Science*, **251**, 804–807.

TOBIN, A.B., LAMBERT, D.G. & NAHORSKI, S.R. (1993). Rapid desensitisation of muscarinic m3 receptor-stimulated polyphosphoinositide responses. *Mol. Pharmacol.*, **42**, 1042–1048.

WILKINSON, G.F. & BOARDER, M.R. (1992). Evidence for two distinct receptors for ATP on bovine aortic endothelial cells, both linked to phospholipase C activation. *Br. J. Pharmacol.*, **107**, 107P.

WILKINSON, G.F., PURKISS, J.R. & BOARDER, M.R. (1993). The regulation of aortic endothelial cells by purines and pyrimidines involves co-existing P_{2Y}-purinoceptors and nucleotide receptors linked to phospholipase C. *Br. J. Pharmacol.*, **108**, 689–693.

WILKINSON, G.F., MCKECHNIE, K., DAINTY, I.A. & BOARDER, M.R. (1994). P_{2Y} purinoceptor and nucleotide receptor induced relaxation of precontracted bovine aortic collateral artery rings: differential sensitivity to suramin and indomethacin. *J. Pharmacol. Exp. Ther.* (in press).

(Received October 13, 1993
Accepted November 11, 1993)

Br. J. Pharmacol. (1994), **111**, 729–732 © Macmillan Press Ltd, 1994

ET_A receptor-mediated responses to endothelin-1 and big endothelin-1 in the rat kidney

[1]David M. Pollock & Terry J. Opgenorth

Pharmaceutical Discovery, Abbott Laboratories, D-47V AP9, Abbott Park, IL 60064, U.S.A.

1 Renal clearance experiments were conducted in anaesthetized Sprague-Dawley rats to determine the effect of the ET_A receptor antagonist, BQ-123, on the renal haemodynamic response to endothelin-1 (ET-1) and its precursor, big endothelin-1 (big ET-1) at doses that produce an equivalent degree of renal vasoconstriction.

2 Infusion of either big ET-1 at 100 pmol kg^{-1} min^{-1} or ET-1 at 12 pmol kg^{-1} min^{-1} for 60 min produced almost identical decreases in renal blood flow (RBF) and glomerular filtration rate (GFR). Big ET-1 produced an increase in mean arterial pressure (MAP) that was significantly larger than the increase produced by ET-1.

3 Co-infusion with BQ-123 (0.1 mg kg^{-1} min^{-1}) prevented the rise in MAP produced by big ET-1 and completely blocked the renal response. Similarly, BQ-123 inhibited both the increase in MAP and the decrease in RPF and GFR produced by ET-1.

4 Big ET-1 but not ET-1, produced a significant increase in water and sodium excretion. BQ-123 had no effect on the diuretic and natriuretic response to big ET-1 consistent with possible ET_B-mediated inhibition of tubular reabsorption.

5 We have previously shown that at higher doses of ET-1, BQ-123 was unable to inhibit the renal vasoconstrictor response despite blockade of the pressor response. Taken together, these results indicate that ET-1 activates primarily ET_A receptors at moderately low doses to produce renal vasoconstriction while higher doses also involve non-ET_A receptors.

6 Since ET-1 has a similar binding affinity for both ET_A and ET_B receptors, we suggest that there may be a third type of ET-1 receptor in the rat kidney with lower affinity for ET-1 that is coupled to a vasoconstrictor mechanism.

Keywords: Endothelin-1 (ET-1); big endothelin-1 (big ET-1); endothelin receptors; endothelium; renal haemodynamics

Introduction

Endothelin-1 (ET-1) produces contraction of vascular smooth muscle by activation of ET_A receptors and, in some tissues, via ET_B receptors (Clozel *et al.*, 1992; Cristol *et al.*, 1992; Pollock & Opgenorth, 1993). The rat kidney contains a predominance of ET_B receptors (Nambi *et al.*, 1992; Terada *et al.*, 1992; Karet *et al.*, 1993) and several lines of evidence have suggested that ET-1 activates primarily ET_B receptors to produce decreases in renal blood flow (RBF) and glomerular filtration rate (GFR). First, the receptor-selective ET_B, agonist, sarafotoxin 6c, has been reported to produce renal vasoconstriction in this species (Clozel *et al.*, 1992; Cristol *et al.*, 1992). We and others have also reported that the ET_A receptor antagonist, BQ-123, effectively blocks the systemic pressor response to a high dose of exogenously administered ET-1 but has no effect on decreases in RBF or GFR (Cristol *et al.*, 1992; Pollock & Opgenorth, 1993). Furthermore, a non-selective receptor antagonist, PD145065, can block the effects of ET-1 in the kidney (Wellings *et al.*, 1993). These findings bring into question the physiological role of ET_A receptors in the rat kidney. In addition to haemodynamic effects, ET_B receptors may also play a role in fluid-electrolyte balance. Evidence suggests that ET-1 inhibits the actions of vasopressin in the kidney through ET_B receptor activation (Ohta *et al.*, 1990; Terada *et al.*, 1992; Migas *et al.*, 1993).

The ET-1 precursor, referred to as big ET-1, is thought to produce effects similar to ET-1 as a result of proteolytic cleavage by an endothelin converting enzyme (Opgenorth *et al.*, 1992). Big ET-1 is a less potent renal vasoconstrictor than ET-1 despite being capable of producing much larger increases in systemic arterial pressure (Hoffman *et al.*, 1990; Pollock & Opgenorth, 1991). Due to the apparent autocrine and/or paracrine nature of endothelin, a common hypothesis is that the site of conversion of big ET-1 to ET-1 represents a location where the endothelin system plays a physiological and pathophysiological role. Thus, infusion of big ET-1 may provide insight into the relevant actions of ET-1.

The purpose of the current study was first to compare the haemodynamic and renal excretory effects of i.v. administered ET-1 and big ET-1 at doses that produce similar degrees of renal vasoconstriction in the anaesthetized rat, and secondly, to elucidate the role of ET_A receptors in these responses by determining the effect of the ET_A receptor antagonist, BQ-123, on the response to ET-1 and big ET-1.

Methods

Experiments were conducted on male Sprague-Dawley rats (200–300 g; Charles River, Cambridge, MA, U.S.A.) anaesthetized with Inactin (100 mg kg^{-1}, i.p.; 5-*sec*-butyl-5-ethyl-2-thiobarbituric acid; synthesized in-house) and placed on a servo-controlled heating table to maintain rectal temperature at 37°C. A tracheostomy was performed to allow for unobstructed breathing. Two catheters (PE-50) were placed in the jugular vein for infusion of endothelin peptides (0.9% NaCl vehicle was infused during the control periods at 10 µl min^{-1}) and BQ-123 (0.25 M $NaHCO_3$ vehicle was infused during the control periods and in the control groups at 10 µl min^{-1}). A catheter was placed in the femoral artery (PE-50) for measurement of mean arterial pressure (MAP; Modular Instruments Inc., Southeastern, PA, U.S.A.) and blood sampling. [^{3}H]-inulin (0.75 µCi kg^{-1} min^{-1}; Amersham, Arlington Heights, IL) and [^{14}C]-*p*-aminohuppurate (PAH: 2 µCi kg^{-1} min^{-1}; New England Nuclear, Boston, MA,

[1] Author for correspondence.

U.S.A.) were infused via a catheter (PE-50) placed in the femoral vein (10 $\mu l\ min^{-1}$ in 0.9% NaCl). Urine was collected via a bladder catheter (PE-90).

After surgery, a 90 min equilibration period was allowed before starting a 30 min control clearance period. Animals then received one of four infusions regimens: ET-1 alone (12 $pmol\ kg^{-1}\ min^{-1}$), ET-1 in combination with BQ-123 (0.1 $mg\ kg^{-1}\ min^{-1}$), big ET-1 alone (100 $pmol\ kg^{-1}\ min^{-1}$), and big ET-1 in combination with BQ-123 ($n = 6$ in each group). BQ-123 infusion was initiated 2–5 min prior to ET-1 or big ET-1. Thirty min after starting the infusions, a 30 min experimental clearance period was obtained. An arterial blood sample (40–50 μl) was collected into a heparinized capillary tube at the midpoint of each clearance period for determination of haematocrit and plasma radioactivity. At the end of the clearance protocol, a terminal blood sample (1.5 ml) was collected into a heparinized centrifuge tube for determination of plasma electrolyte concentrations. Kidneys were then removed, decapsulated and weighed.

Urine and plasma sodium and potassium concentrations were measured with ion-selective electrodes (EL-*ISE*, Beckman, Instruments, Brea, CA, U.S.A.). Activity of [^{3}H]-inulin and [^{14}C]-PAH in urine and plasma was determined by liquid scintillation counting (Beckman Instruments, Fullerton, CA, U.S.A.).

Human endothelin-1-(1-21) and human big endothelin-1-(1-38) were purchased from American Peptide, Santa Clara, CA, U.S.A.). BQ-123 (cyclo(-D-Trp-D-Asp-Pro-D-Val-Leu)) was synthesized in-house.

Renal blood flow (RBF) was calculated as the clearance of [^{14}C]-PAH/(1-haematocrit). Using 5 mmHg as an estimate of renal venous pressure, renal vascular resistance was calculated as (MAP-5)/RBF. Glomerular filtration rate (GFR) was determined from the clearance of inulin. Fractional excretion rates were calculated as the absolute excretion rate as a percentage of the filtered load.

Student's t test for paired data was used to determine significant differences between control vs. experimental periods and for unpaired data to determine the effect of BQ-123 (Statview II, Abacus Concepts, Berkeley, CA, U.S.A.). $P < 0.05$ was considered significant. All values are reported as mean ± s.e.mean.

Results

By design, i.v. infusion of ET-1 or big ET-1 at 12 and 100 $pmol\ kg^{-1}\ min^{-1}$ produced nearly identical decreases in RBF and GFR, approximately 60% and 50%, respectively, in both groups (Figure 1). Renal vascular resistance values were increased to a similar level at these doses. MAP and haematocrit were also significantly increased although the changes produced by big ET-1 were more than 2 fold larger. MAP was increased by 22 ± 3% and 49 ± 7% by ET-1 and big ET-1, respectively ($P < 0.05$), while haematocrit was increased by 11 ± 2% and 28 ± 1% by ET-1 and big ET-1, respectively ($P < 0.05$).

Simultaneous infusion of BQ-123 in rats receiving either ET-1 or big ET-1 significantly inhibited the systemic and renal haemodynamic responses (Figure 1). Infusion of BQ-123 and ET-1 resulted in no significant change in MAP, HCT, renal vascular resistance, or RBF. However, a small (16 ± 5%), but significant decrease in GFR was observed. BQ-123 completely prevented all of the responses to big ET-1.

The effect of ET-1 and big ET-1 with or without co-infusion of BQ-123 on water and sodium excretion is depicted in Figure 2. Big ET-1, but not ET-1, produced a significant increase in both urine flow rate and sodium excretion as well as fractional excretion of water and sodium. Water and sodium excretion rates were also unchanged during co-administration of BQ-123 and ET-1. During infusion of both big ET-1 and BQ-123, a significant diuresis and natriuresis was still observed despite blocking the increase in MAP and the decreases in RBF and GFR. The increases in urine flow rate and sodium excretion were actually larger when big ET-1 was infused along with BQ-123 than with big ET-1 alone although the difference in sodium excretion did not achieve statistical significance ($0.1 < P < 0.05$).

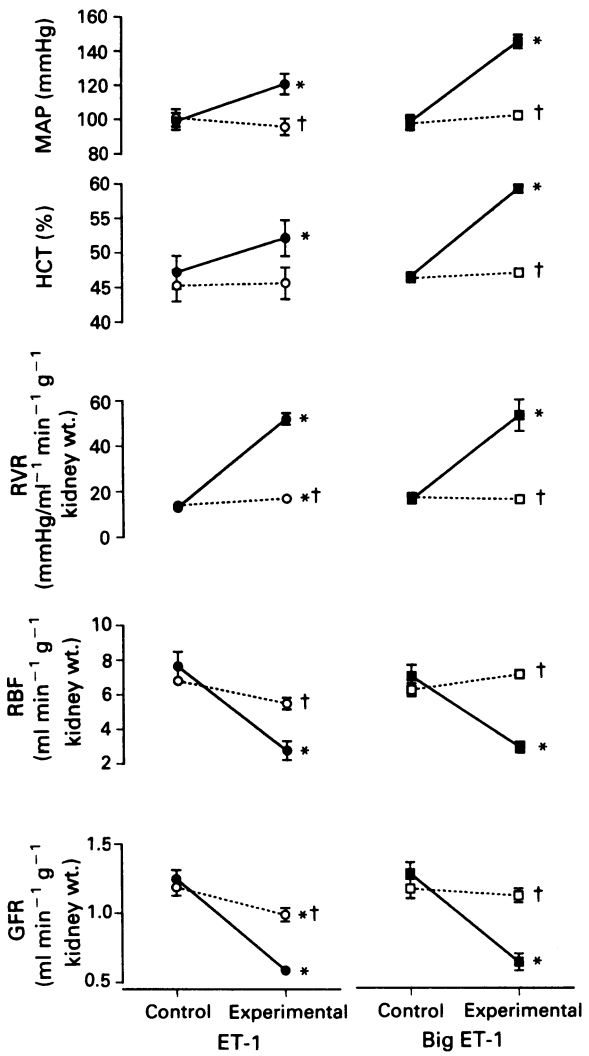


Figure 1 Haemodynamic responses to endothelin-1 (ET-1) and big ET-1 in anaesthetized rats during infusion of BQ-123 or vehicle (0.25 N $NaHCO_3$). ET-1 was infused at 12 $pmol\ kg^{-1}\ min^{-1}$ with (○) or without (●) simultaneous infusion of BQ-123 at 0.1 $mg\ kg^{-1}\ min^{-1}$. Big ET-1 was infused at 100 $pmol\ kg^{-1}\ min^{-1}$ with (□) or without (■) simultaneous infusion of BQ-123. Values are mean ± s.e.mean. $n = 6$ in all four groups of rats. *$P < 0.05$ vs. control; †$P < 0.05$ vs. ET-1 or big ET-1 alone. MAP, mean arterial pressure; HCT, haematocrit; RVR, renal vascular resistance; RBF, renal blood flow; GFR, glomerular filtration rate.

Discussion

Our study provides new information regarding the role of ET_A receptors in the rat kidney. Since the ET_A-selective antagonist, BQ-123, was capable of blocking the haemodynamic responses to ET-1 and big ET-1, we have provided evidence that ET_A receptor activation is capable of producing a significant degree of renal vasoconstriction in the rat. Furthermore, we provide evidence to suggest that big ET-1 infusion activates non-ET_A receptors, presumably ET_B, to inhibit tubular sodium and water reabsorption.

We have previously reported that the renal haemodynamic effects of a relatively high dose of ET-1, 25 $pmol\ kg^{-1}\ min^{-1}$,

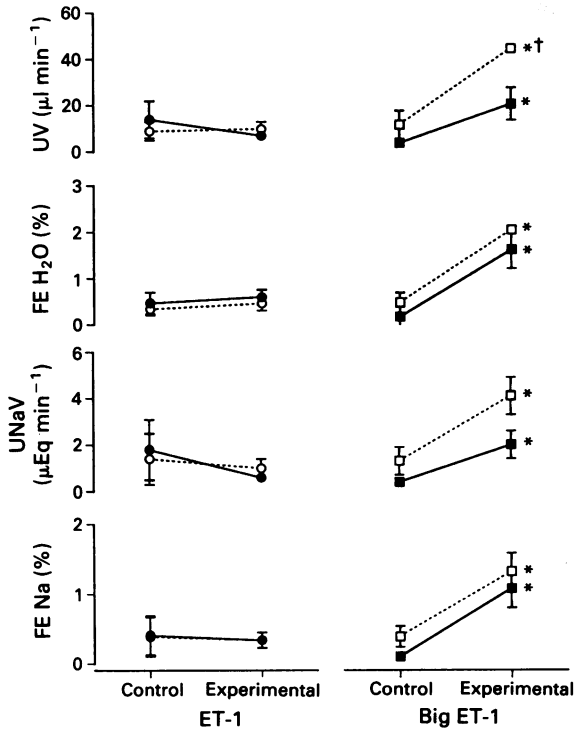


Figure 2 Renal excretory responses to endothelin-1 (ET-1) and big ET-1 in anaesthetized rats during infusion of BQ-123 or vehicle (0.25 N $NaHCO_3$). ET-1 was infused at 12 pmol kg^{-1} min^{-1} with (○) or without (●) simultaneous infusion of BQ-123 at 0.1 mg kg^{-1} min^{-1}. Big ET-1 was infused at 100 pmol kg^{-1} min^{-1} with (□) or without (■) simultaneous infusion of BQ-123. Values are mean ± s.e.mean. $n = 6$ in all four groups of rats. $^*P < 0.05$ vs. control; $^\dagger P < 0.05$ vs. ET-1 or big ET-1 alone. UV, urine flow rate; FE H_2O, fractional excretion of water; UNaV, sodium excretion; FE Na, fractional excretion of sodium.

cannot be inhibited by BQ-123. Since the renal haemodynamic effects of a lower (yet probably still pharmacological) dose of ET-1 can be inhibited by ET_A receptor antagonism, it is possible that a non-ET_A receptor with a lower affinity for ET-1 may exist in the kidney that is insensitive to BQ-123. Furthermore, Cirino *et al.* (1992) reported that ET_A receptor blockade could not completely prevent the vasoconstrictor actions of ET-1 in the pig kidney. ET_A receptor blockade has been shown to inhibit completely the renal vasoconstrictor response to ET-1 in the dog and rabbit (Brooks *et al.*, 1994; Télémaque *et al.*, 1993).

One of the goals of the current study was to determine the role of ET_A receptors in the renal response to big ET-1. Our finding that big ET-1-induced renal vasoconstriction is mediated by ET_A receptors agrees with a preliminary report of Slee *et al.* (1993) who observed that BQ-123 inhibits the increase in renal vascular conductance produced by big ET-1 in anaesthetized rats. Big ET-1 is a less potent renal vasoconstrictor than ET-1 despite being capable of producing a higher degree of systemic hypertension (Pollock & Opgenorth, 1991). In order to make the comparison between big ET-1 and ET-1 more meaningful for the study of renal haemodynamics and excretion, we utilized a lower dose of ET-1 that produced a similar degree of renal vasoconstriction to a high dose of big ET-1. Under these conditions, we observed that the renal vasoconstriction produced by both peptides is mediated by ET_A receptors. The difference in potency between big ET-1 and ET-1 to produce haemodynamic changes in the kidney as compared to other vascular beds has been previously reported (Hoffman *et al.*, 1990; Pollock & Opgenorth, 1991). Although the reason for this observation has not been elucidated, it can be postulated that conversion of big ET-1 by the endothelin converting enzyme may occur at a lower rate in the kidney.

Our results confirm the findings of Hoffman and colleagues (1990) that big ET-1, but not ET-1, is a diuretic agent. However, their results were somewhat complicated by the use of doses of ET-1 that produced a much larger decrease in GFR compared to big ET-1. In our experiments, the divergent effects of big ET-1 and ET-1 on sodium and water excretion were somewhat unexpected given our experimental design that the doses be chosen based on equivalent degrees of renal vasoconstriction. We observed that ET-1 had no natriuretic activity at the dose used and that ET_A receptor antagonism prevented the haemodynamic but not the renal excretory response to big ET-1. Several possible mechanisms could explain these findings. First, since it is known that ET-1 can be metabolized by brush-border endopeptidases (Abassi *et al.*, 1992; Asaad *et al.*, 1993), it is possible that the additional 11 amino acids on big ET-1 could protect it from proteolytic degradation thus facilitating access of mature ET-1 to tubular endothelin receptors. Also, there are a few studies that suggest a direct effect of big ET-1, producing certain haemodynamic effects independent of conversion to ET-1 (Auguet *et al.*, 1992; Salvati *et al.*, 1992). Since the ET_B receptor has been linked to endothelium-dependent vasodilatation (Warner *et al.*, 1989), we can hypothesize that big ET-1 may produce ET_B receptor mediated increases in medullary blood flow as a mechanism for producing diuresis and natriuresis. However, there is no direct evidence to support this idea at present. Other possibilities are that big ET-1 may directly activate a non-ET_A receptor or that big ET-1 is converted by an endothelin converting enzyme that allows it to gain access to a site not accessible to exogenous ET-1.

Our results are consistent with the idea that the diuretic and natriuretic effects of big ET-1 are mediated by non-ET_A receptors since BQ-123 did not prevent these effects. In fact, the potentiation of the diuretic and natriuretic responses by BQ-123 suggest that the intense renal vasoconstriction decreases the filtered load thus attenuating the increases in water and sodium excretion. Although the mechanism of inhibiting reabsorption is not clear, it does not appear to be a pressure-dependent phenomenon since BQ-123 blocked the pressor response to big ET-1 yet the changes in urine flow rate and sodium excretion remained intact. Zeidel *et al.* (1989) have reported that ET-1 can inhibit tubular Na^+-K^+-ATPase activity as a means of inhibiting tubular sodium reabsorption. There is also increasing evidence that ET_B receptors located on inner medullary collecting duct cells may be responsible for inhibiting vasopressin-stimulated increases in water reabsorption (Terada *et al.*, 1992; Migas *et al.*, 1993).

While ET-1 was roughly 10 fold more potent than big ET-1 in terms of renal vasoconstriction, this difference was not evident with respect to changes in mean arterial pressure and haematocrit. We have now observed that ET-1 can activate multiple receptor subtypes in the kidney, yet increases in mean arterial pressure and haematocrit appear to be mediated exclusively by ET_A receptors. Big ET-1 also increases these variables via ET_A receptor activation.

In conclusion, we have provided evidence that ET-1 can activate ET_A receptors to produce vasoconstriction in the rat kidney. Since ET-1 has been proposed as a mediator of detrimental haemodynamic effects in various forms of renal failure, ET_A receptor antagonists may provide useful pharmacological tools for elucidating the physiological and pathophysiological role of ET-1 in the kidney (Benigni *et al.*, 1993; Mino *et al.*, 1993). This does not preclude an important role for non-ET_A receptors in the renal vasculature. Our study also demonstrated that big ET-1 inhibits tubular reabsorption of sodium and water by a non-ET_A receptor and non-pressure-dependent mechanism. Therefore, the role of ET_B receptors in the control of sodium and water excretion warrants further investigation.

The authors wish to thank Barbara J. Divish for her outstanding assistance in conducting these studies. We also thank Gerard Sullivan for his efforts in the synthesis of BQ-123.

References

ABASSI, Z.A., TATE, J.E., GOLOMB, E. & KEISER, H.R. (1992). Role of neutral endopeptidase in the metabolism of endothelin. *Hypertension*, **20**, 89–95.

ASAAD, M.M., DORSO, C.R. & MORELAND, S.M. (1993). Effects of neutral endopeptidase inhibition on the clearance of exogenously administered endothelin in Sprague-Dawley rats. *J. Cardiovasc. Pharmacol.*, **21**, 633–636.

AUGUET, M., DELAFLOTTE, S., CHABRIER, P.-E. & BRAQUET, P. (1992). The vasoconstrictor action of big endothelin-1 is phosphoramidon-sensitive in rabbit saphenous artery but not in saphenous vein. *Eur. J. Pharmacol.*, **224**, 101–102.

BENIGNI, A., ZOJA, C., CORNA, D., ORISIO, S., LONGARETTI, L., BERTANI, T. & REMUZZI, G. (1993). A specific endothelin subtype A receptor antagonist protects against injury in renal disease progression. *Kidney Int.*, **44**, 440–444.

BROOKS, D.P., DEPALMA, P.D., PULLEN, M. & NAMBI, P. (1994). Characterization of canine renal endothelin receptor subtypes and their function. *J. Pharmacol. Exp. Ther.* (in press).

CIRINO, M., MOTZ, C., MAW, J., FORD-HUTCHINSON, A.W. & YANO, M. (1992). BQ-153, a novel endothelin $(ET)_A$ antagonist, attenuates the renal vascular effects of endothelin-1. *J. Pharm. Pharmacol.*, **44**, 782–785.

CLOZEL, M., GRAY, G.A., BREU, V., LÖFFLER, B.-M. & OSTERWALDER, R. (1992). The endothelin ETB receptor mediates both vasodilatation and vasoconstriction *in vivo*. *Biochem. Biophys. Res. Commun.*, **186**, 867–873.

CRISTOL, J.-P., WARNER, T.D., THIEMERMANN, C. & VANE, J.R. (1993). Mediation via different receptors of the vasoconstrictor effects of endothelins and sarafotoxins in the systemic circulation and renal vasculature of the anaesthetized rat. *Br. J. Pharmacol.*, **108**, 776–779.

HOFFMAN, A., GROSSMAN, E. & KEISER, H.R. (1990). Opposite effects of endothelin-1 and Big endothelin-1(1-39) on renal function in rats. *Eur. J. Pharmacol.*, **182**, 603–606.

KARET, F.E., KUC, R.E. & DAVENPORT, A.P. (1993). Novel ligands BQ123 and BQ3020 characterize endothelin receptor subtypes ETA and ETB in human kidney. *Kidney Int.*, **44**, 36–42.

MIGAS, I., BÄCKER, A., MEYER-LEHNERT, J., MICHEL, H., WULFHEKEL, U. & KRAMER, H.J. (1993). Characteristics of endothelin receptors and intracellular signaling in porcine inner medullary collecting duct cells. *Am. J. Hypertens.*, **6**, 611–618.

MINO, N., KOBAYASHI, M., NAKAJIMA, A., AMANO, H., SHIMAMOTO, K., ISHIKAWA, K., WATANABE, K., NISHIKIBE, M., YANO, M. & IKEMOTO, F. (1993). Protective effect of a selective endothelin receptor antagonist, BQ-123, in ischemic acute renal failure in rats. *Eur. J. Pharmacol.*, **221**, 77–83.

NAMBI, P., WU, H.L., PULLEN, M., AIYAR, N., BRYAN, H. & ELLIOTT, J. (1992). Identification of endothelin receptor subtypes in rat kidney cortex using subtype-selective ligands. *Mol. Pharmacol.*, **42**, 336–339.

OHTA, K., NONOGUCHI, H., TOMITA, K. & MARUMO, F. (1991). Endothelin-1 inhibits AVP-stimulated osmotic water permeability in rat inner medullary collecting duct. *Am. J. Physiol.*, **261**, F951–F956.

OPGENORTH, T.J., WU-WONG, J.R. & SHIOSAKI, K. (1992). Endothelin converting enzyme. *FASEB J.*, **6**, 2653–2659.

POLLOCK, D.M. & OPGENORTH, T.J. (1991). Evidence for metalloprotease involvement in the in vivo effects of big endothelin 1. *Am. J. Physiol.*, **261**, R257–R263.

POLLOCK, D.M. & OPGENORTH, T.J. (1993). Evidence for endothelin-induced renal vasoconstriction independent of ET_A receptor activation. *Am. J. Physiol.*, **264**, R222–R226.

SALVATI, P., DHO, L., CALABRESI, M., ROSA, B. & PATRONO, C. (1992). Evidence for a direct vasoconstrictor effect of big endothelin-1 in the rat kidney. *Eur. J. Pharmacol.*, **221**, 267–273.

SLEE, S.-J., HEYS, C. & WILSON, C. (1993). Effect of BQ123 on regional hemodynamic responses to big endothelin-1 in anaesthetized rats. *Br. J. Pharmacol.*, **108**, 195P.

TÉLÉMAQUE, S., GRATTON, J.-P., CLAING, A. & D'ORLÉANS-JUSTE, P. (1993). Endothelin-1 induces vasoconstriction and prostacyclin release via the activation of endothelin ET_A receptors in the perfused rabbit kidney. *Eur. J. Pharmacol.*, **237**, 275–281.

TERADA, Y., TOMITA, K., NONOGUCHI, H. & MARUMO, F. (1992). Different localizations of two types of endothelin receptor mRNA in microdissected rat nephron segments using reverse transcription and polymerase chain reaction assay. *J. Clin. Invest.*, **90**, 107–112.

WARNER, T.D., MITCHELL, J.A., DE NUCCI, G. & VANE, J.R. (1989). Endothelin-1 and endothelin-3 release EDRF from isolated perfused arterial vessels of the rat and the rabbit. *J. Cardiovasc. Pharmacol.*, **13** (Suppl. 5), S85–S88.

WELLINGS, R.P., WARNER, T.D., CORDER, R., THIEMERMANN, C. & VANE, J.R. (1993). A new non-selective endothelin antagonist blocks the vasoconstriction induced by endothelin in the rat. *Br. J. Pharmacol.*, **108**, 110P.

ZEIDEL, M.L., BRADY, H.R., KONE, B.C., GULLANS, S.R. & BRENNER, B.M. (1989). Endothelin, a peptide inhibitor of Na^+-K^+-ATPase in intact renal tubular epithelial cells. *Am. J. Physiol.*, **257**, C1101–C1107.

(Received September 21, 1993
Revised November 8, 1993
Accepted November 11, 1993)

Br. J. Pharmacol. (1994), **111**, 733–738 © Macmillan Press Ltd, 1994

Modulation of noradrenaline release from the sympathetic nerves of the human saphenous vein and pulmonary artery by presynaptic EP_3- and DP-receptors

[1]Gerhard J. Molderings, Emile Colling, *James Likungu, †Jens Jakschik & Manfred Göthert

Institut für Pharmakologie und Toxikologie, *Klinik für Herz-und Gefäßchirurgie and †Chirurgische Klinik und Poliklinik, Rheinische Friedrich-Wilhelms-Universität Bonn, Reuterstr. 2 b, D-5300 Bonn 1, Germany

1 Spirally cut strips of the human saphenous vein and pulmonary artery were used to determine the pharmacological properties of the presynaptic prostanoid receptors involved in the modulation of sympathetic [^{3}H]-noradrenaline release. Strips preincubated with [^{3}H]-noradenaline were superfused with physiological salt solution containing inhibitors of uptake$_1$ and uptake$_2$ and rauwolscine to eliminate involvement of presynaptic α_2-adrenoceptors. Tritium overflow was evoked by transmural electrical stimulation (standard frequency: 2 Hz).

2 In the saphenous vein, prostaglandin E_2 (PGE_2) inhibited the electrically-evoked tritium overflow; at the highest concentration investigated, tritium overflow was inhibited by more than 75% and the pEC_{50} value was 7.00. These effects were mimicked by prostaglandin E_1, the EP_1/EP_3 receptor agonist, sulprostone and the EP_2/EP_3 receptor agonist, misoprostol with the rank order (pEC_{50}): sulprostone (8.60) > PGE_1 (7.25) > misoprostol (6.96). This rank order of potency suggests that the inhibitory effect of the drugs is mediated by presynaptic EP_3-receptors. In contrast, $PGF_{2\alpha}$ did not inhibit evoked tritium overflow; the IP/EP_1 receptor agonist iloprost and the stable thromboxane A_2 analogue U 46619 (9, 11-dideoxy-11α,9α-epoxy-methanoprostaglandin $F_{2\alpha}$) produced inhibition only at concentrations above 1 μM.

3 The EP_1-receptor antagonist, AH 6809 (6-isopropoxy-9-oxoxanthene-2-carboxylic acid) had no effect on the evoked tritium overflow nor did it modify the inhibitory effect of PGE_2, further excluding involvement of inhibitory presynaptic EP_1-receptors.

4 PGD_2 caused a facilitation of evoked tritium overflow in the saphenous vein; this facilitation is probably mediated by presynaptic DP-receptors, since it was abolished by the selective DP-receptor antagonist, BW A868C (3-benzyl-5-(6-carboxyhexyl)-1-(2-cyclohexyl-2-hydroxyethylamino)hydantoin).

5 In the pulmonary artery, sulprostone (pEC_{50} value 8.35), misoprostol (7.70) and PGE_2 (6.80) inhibited electrically-evoked tritium overflow. This rank order of potency is consistent with the involvement of inhibitory presynaptic EP_3-receptors.

6 These results suggest that the sympathetic nerve fibres of both human saphenous vein and pulmonary artery are endowed with presynaptic inhibitory EP_3 receptors. The EP_3-receptors do not interact with the α_2-autoreceptors. In addition, the human saphenous vein seems to be endowed with presynaptic facilitatory DP-receptors.

Keywords: Human saphenous vein; human pulmonary artery; EP_3-receptors; DP-receptors; presynaptic receptors; noradrenaline release

Introduction

Presynaptic prostanoid EP-receptors mediate inhibition of noradrenaline release from sympathetic nerve fibres in a variety of tissues from different species (for reviews, see Güllner, 1983; Malik & Sehic, 1990). These presynaptic inhibitory EP-receptors belong to the EP_3-subtype in guinea-pig atria and vas deferens (Coleman *et al.*, 1987; Mantelli *et al.*, 1991), rat trachea, stomach and vena cava (Racké *et al.*, 1991; Möhlig *et al.*, 1992; Molderings *et al.*, 1992a) as well as in human iris-ciliary body (Ohia & Jumblatt, 1991). Other studies suggest that presynaptic facilitatory DP-receptors may also exist, for example, on the sympathetic nerves in human corpus cavernosum (Molderings *et al.*, 1992b) and canine mesenteric artery (Nakajima & Toda, 1984).

Few reports have so far described the modulation of noradrenaline release via EP-receptors in human blood vessels and none has characterized precisely the EP-receptor subtype involved. Therefore, the aims of the present study were (1) to investigate whether modulatory presynaptic EP- and DP-receptors are present on the sympathetic nerves of the human saphenous vein and pulmonary artery, and (2) if present, to determine the subtype (EP_1, EP_2, EP_3) to which the EP-receptors belong. A preliminary account of this study has been given at the 34th Spring Meeting of the Deutsche Gesellschaft für Pharmakologie und Toxikologie (Molderings *et al.*, 1993).

Methods

Segments of macroscopically intact human saphenous veins and pulmonary arteries were obtained from normotensive 35 to 70 year-old male or female patients undergoing surgery for aorta-coronary bypass grafting or lung surgery, respectively. The patients were not treated with adrenoceptor agonists or antagonists or with drugs influencing the storage or release of noradrenaline. Meperidine and promethazine were used for premedication. Patients were anaesthetized (both induction and maintenance) with flunitrazepam and fentanyl. During maintenance of anaesthesia, they were ventilated with mixtures of oxygen and air. Pancuronium was administered for neuromuscular blockade.

Vascular segments were cut into spiral strips (3 × 20 mm) and incubated for 60 min in 1.5 ml physiological salt solution

[1] Author for correspondence.

(37°C; composition see below) containing (−)-[ring-2,5,6-^{3}H]noradrenaline 0.2 μM (specific activity 52.3 Ci mmol^{-1}). Subsequently, the strips were mounted vertically in an organ bath (tension adjusted to 2.0 g) between two parallel platinum electrodes and superfused with physiological salt solution of 37°C at a rate of 2 ml min^{-1}. The composition of the solution was (mM): NaCl 118, NaH_2PO_4 1.2, $NaHCO_3$ 25, KCl 4.7, $CaCl_2$ 1.6, $MgSO_4$ 1.2, glucose 11.0, ascorbic acid 0.3, Na_2 EDTA 0.03 (aerated with 95% O_2 and 5% CO_2). Throughout superfusion this solution contained desipramine 0.6 μM and corticosterone 40 μM to block neuronal and extraneuronal uptake of noradrenaline, respectively.

The superfusate was collected in 4-min fractions. Five (in some experiments three or four) 3 min periods of transmural electrical stimulation (2 Hz, rectangular pulses of 150 mA and 0.3 ms) were applied to each vascular strip after 94 (S_1), 126 (S_2), 158 (S_3), 190 (S_4) and 222 (S_5) min of superfusion. In a few experiments, the vascular strips were stimulated at 0.66 Hz for 9 min (otherwise identical time schedule). Antagonist drugs were introduced into the superfusion fluid from 4 min before S_1 until the end of the experiment, naproxen from 18 min before S_1 until the end of the experiment and agonist drugs at concentrations increasing by a factor of 10 from 12 min before S_3, S_4 and S_5 until 20 min after the onset of the respective stimulation period. Separate time-matched control experiments (if relevant, in the presence of the respective antagonist) were carried out for each series of experiments. At the end of superfusion the strips were solubilized with Soluene, and the radioactivity in the superfusate samples and blood vessels was determined by liquid scintillation counting.

Tritium efflux was calculated as the fraction of tritium present in the strip at the start of the respective collection period. Tritium content in the strips at the start of each period of superfusate sampling was calculated by adding the radioactivity in the respective and subsequent superfusate samples to that in the solubilized blood vessel. Basal tritium efflux was expressed as the ratio of tritium efflux per min during the collection period immediately before S_3, S_4 or S_5 (t_3, t_4, t_5) over that immediately before S_2 (t_2). Stimulation-evoked tritium overflow was calculated by subtraction of the basal efflux from the total efflux during stimulation and in the subsequent 13 min (basal efflux decreased linearly from the collection period before to that 16–20 min after the start of stimulation; not shown). The tritium overflow evoked by the five stimulation periods is given as a percentage of tissue tritium at the start of stimulation and is denoted as S_1, S_2, S_3, S_4 and S_5 after the respective stimulation period (as generally accepted for studies of presynaptic receptors; see e.g. papers quoted in Westfall, 1977; Langer, 1981; Starke et al., 1989). The ratios of the overflow evoked by S_3, S_4 or S_5 over that evoked by S_2 were determined. The ^{3}H overflow ratios (S_3/S_2. S_4/S_2 and S_5/S_2) obtained in the experiments with the prostanoid under study, were expressed as percentage of the overflow ratios in the respective control experiments (performed in the absence of the prostanoid).

The negative logarithm of the agonist concentration at which the evoked tritium overflow was inhibited by 50% (pEC_{50}) was determined as an estimate of the potency of the compound from the concentration-response curves shown in the figures. Results are given as the mean ± s.e.mean. Student's t test was used for comparison of the mean values.

Drugs used

(−)-[ring-2,5,6-^{3}H]-noradrenaline (New England Nuclear, Dreieich, Germany); desipramine hydrochloride (Ciba-Geigy, Wehr, Germany); corticosterone, prostaglandins D_2, E_1, E_2, $F_{2\alpha}$ (Sigma, München, Germany); AH 6809 (6-isopropoxy-p-oxoxanthene-2-carboxylic acid; Glaxo, Ware, England); iloprost, sulprostone (Schering, Berlin, Germany); misoprostol (Searle, Skokie, IL, U.S.A.), rauwolscine hydrochloride (Roth, Karlsruhe, Germany); U46619 (9, 11-dideoxy-11α,9α-epoxy-methano-prostaglandin $F_{2\alpha}$; Biosigma, Munich, Germany); BW A868C (3-benzyl-5-(6-carboxyhexyl)-1-(2-cyclohexyl-2-hydroxyethylamino)hydantoin; Wellcome Research Laboratories, Kent, England). Stock solutions were prepared with water (AH 6809, desipramine, rauwolscine), saline (iloprost), 1,2-propandiol (corticosterone), ethanol (misoprostol, sulprostone, PGE_1, PGE_2, PGD_2, $PGF_{2\alpha}$, BW A868C) or dimethylsulphoxide (U46619) and diluted with physiological salt solution to the concentration required. The solvents did not affect basal or evoked tritium overflow.

Results

Common features of basal and stimulation-evoked tritium-overflow in saphenous veins and pulmonary arteries

In strips of human saphenous vein and pulmonary artery preincubated with [^{3}H]-noradrenaline, basal tritium efflux under control conditions decreased with time, as reflected by

Table 1 Effect of rauwolscine, AH 6809, naproxen and BW A868C on the electrically-evoked tritium overflow from strips of human saphenous vein (**A**) and pulmonary artery (**B**)

Drugs (μM)	*Frequency of stimulation* (Hz)	S_2[a]	S_3/S_2[b]	S_4/S_2[b]	S_5/S_2[b]
A None	2	0.30 ± 0.04[c]	1.02 ± 0.12	0.97 ± 0.10	0.91 ± 0.07
Rauwolscine 1	2	0.98 ± 0.20[d]	1.03 ± 0.06	0.97 ± 0.05	0.95 ± 0.03
Rauwolscine 1	0.66	0.34 ± 0.12	1.00 ± 0.09	1.02 ± 0.17	0.93 ± 0.11
Rauwolscine 1 + AH 6809 10	2	0.65 ± 0.11	0.94 ± 0.04	0.89 ± 0.05	0.82 ± 0.04
Rauwolscine 1 + naproxen 10	2	0.60 ± 0.08	1.04 ± 0.13	1.03 ± 0.17	1.01 ± 0.15
Rauwolscine 1 + BW A868C 0.1	2	1.05 ± 0.28	0.89 ± 0.04	0.83 ± 0.05	0.90 ± 0.11
B Rauwolscine 1	2	0.43 ± 0.07[e]	1.02 ± 0.10	0.93 ± 0.08	1.00 ± 0.08

The values were obtained in a representative series of control experiments. Five 3- or 9-min periods (2 and 0.66 Hz, respectively) of transmural electrical stimulation (S_1, S_2, S_3, S_4 and S_5) were applied in each preparation. Data are means ± s.e.means of 5–9 experiments. Representative absolute values for basal efflux and tritium overflow evoked by S_2 (in nCi) are given below.
[a]Evoked tritium overflow by S_2 above basal efflux, expressed as percentage of tissue tritium. [b]Tritium overflow evoked by S_3, S_4 and S_5 is given as ratio over the respective tritium overflow evoked by S_2. [c]Corresponding to 3.4 ± 0.8 nCi (basal efflux amounted to 1.3 ± 0.2 nCi min^{-1}). [d]Corresponding to 7.8 ± 2.4 nCi (basal efflux amounted to 1.1 ± 0.2 nCi min^{-1}). [e]Corresponding to 2.3 ± 0.4 nCi (basal efflux amounted to 1.1 ± 0.2 nCi min^{-1}).

a decrease of the ratios t_3/t_2 to t_5/t_2 (all ratios <1.0; not shown). Basal tritium efflux was not significantly altered by rauwolscine (1 μM; see e.g. Table 1, footnotes c and d) or by the other drugs applied at the concentrations investigated (results not shown).

Transmural electrical stimulation of strips of human saphenous vein and pulmonary artery elicited an overflow of tritium above basal efflux. In the presence of rauwolscine 1 μM from 4 min before S_1 until the end of the experiments, the tritium overflow evoked by S_2 at 2 Hz (360 impulses) was increased about 3 fold compared to the experiments without rauwolscine (Table 1) whereas overflow evoked by S_2 at 0.66 Hz (360 impulses as well) was in a similar range as in the experiments without previous α-adrenoceptor blockade at 2 Hz (Table 1). At both frequencies of stimulation and under all experimental conditions studied, the evoked overflow either slightly decreased from S_2 to S_5 or remained approximately constant, as reflected by S_n/S_2 ratios close to unity (Table 1).

Saphenous veins

PGE_2 produced a concentration-dependent inhibition of electrically-evoked tritium overflow that was unaffected by rauwolscine (1 μM; Figure 1). The pEC_{50} of PGE_2 was 6.80 in the presence of rauwolscine (Table 2) and 7.00 in its absence. All further experiments were performed in the presence of rauwolscine 1 μM, to eliminate any possible drug interactions with α_2-autoreceptors. This manipulation enhanced evoked tritium overflow by about 3 fold (Table 1), facilitating quantitation of inhibitory drug effects.

Since modulation of [^{3}H]-noradrenaline release by presynaptic receptors has been shown to increase with decreasing frequency of stimulation (see Starke *et al.*, 1989), it was of interest to examine whether such an effect also occurred with PGE_2. When the frequency of stimulation was decreased from 2 Hz to 0.66 Hz, PGE_2 was more potent as reflected by leftward shift of the concentration-response curve (pEC_{50} of PGE_2 at 0.66 Hz, 7.85; Figure 2).

Naproxen 10 μM did not significantly modify the tritium overflow evoked by electrical impulses at the standard frequency of 2 Hz (compare relevant S_2 values in Table 1). In the presence of this drug, PGE_2 was clearly more potent (about 7 fold) in inhibiting the evoked tritium overflow than in the absence of the cyclo-oxygenase inhibitor (Figure 3a; pEC_{50} value 7.62). On the other hand, the inhibitory effect of PGE_2 on tritium overflow was not affected by a high concentration (10 μM) of the selective EP_1-receptor antagonist, AH 6809 (Figure 3b; pEC_{50} value 6.85), which given alone did also not significantly modify the evoked tritium overflow (compare relevant S_2 values in Table 1).

Further experiments were carried out to determine the EP-receptor subtype which mediates the inhibitory effect of PGE_2. The EP_1/EP_3-receptor agonist sulprostone was about 63 fold and PGE_1 3 fold more potent than PGE_2; the EP_2/EP_3-receptor agonist, misoprostol, exhibited about the same potency as PGE_2 (Figure 4a, for pEC_{50} values determined from these concentration-response curves, see Table 2). The thromboxane analogue, U46619 and the IP/EP_1 receptor agonist, iloprost, inhibited the electrically-evoked tritium overflow only at concentrations of 1 and 10 μM, respectively (by less than 40%), and $PGF_{2\alpha}$ at concentrations of up to 1 μM failed to affect the evoked overflow (Figure 4b). Taken together, the following rank order of potency of the inhibitory drugs was obtained: sulprostone $>>$ PGE_1 $>$ misoprostol = PGE_2 $>>$ U46619 and iloprost (see also Table 2).

In contrast, PGD_2 enhanced the evoked tritium overflow (Figure 5). The facilitatory effect of PGD_2 on evoked

Table 2 Potencies of prostanoids (given as their pEC_{50} values) for their inhibitory effect on the electrically evoked tritium overflow from superfused strips of human saphenous vein and pulmonary artery preincubated with [^{3}H]-noradrenaline and superfused in the presence of rauwolscine 1 μM

Prostanoid	pEC_{50}[a] *Saphenous vein*	*Pulmonary artery*
Sulprostone	8.60 (10)	8.35 (3)
Prostaglandin E_1	7.25 (6)	
Misoprostol	6.96 (8)	7.70 (3)
Prostaglandin E_2	6.80 (8)	6.80 (6)
U46619	<6.00 (5)	
Iloprost	<5.20 (7)	

Number of experiments in parentheses. [a]pEC_{50} values were determined from the concentration-response curves shown in Figures 1, 4 and 6.

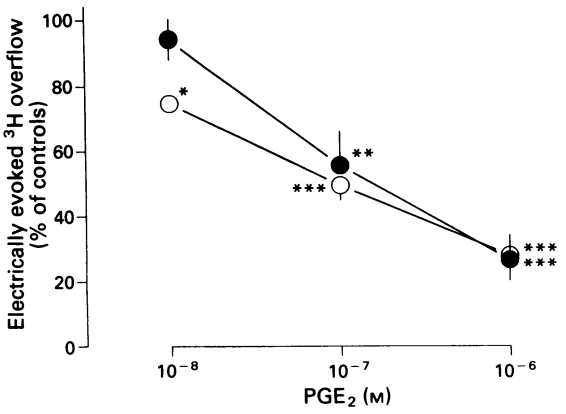


Figure 1 Inhibitory effect of prostaglandin E_2 (PGE_2) in the absence (●) or presence (○) of rauwolscine 1 μM on the electrically (2 Hz)-evoked tritium overflow from strips of the human saphenous vein preincubated with [^{3}H]-noradrenaline. Ordinate scale: ^{3}H overflow ratios, expressed as percentage of ratios in prostaglandin E_2-free control experiments. Means ± s.e.means of 8 experiments each. $*P<0.05$; $**P<0.025$; $***P<0.001$ (compared with the corresponding controls).

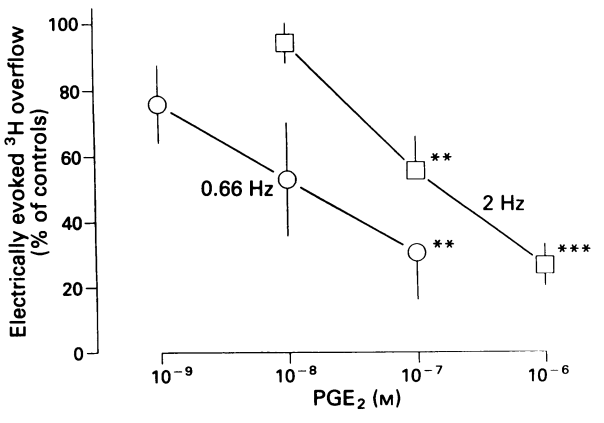


Figure 2 Frequency-dependence of prostaglandin E_2 (PGE_2) induced inhibition of electrically-evoked tritium overflow in strips of human saphenous vein. α_2-Autoreceptors were blocked with rauwolscine 1 μM. Ordinate scale: ^{3}H overflow ratios, expressed as percentage of ratios in prostaglandin E_2-free control experiments at 0.66 Hz (○) and 2 Hz (□). Means ± s.e.means of 6 to 8 experiments. $**P<0.025$; $***P<0.001$ (compared with the corresponding controls).

overflow was abolished in the presence of the selective DP-receptor antagonist, BW A868C (0.1 μM; Figure 5). The antagonist itself did not affect evoked tritium overflow (compare relevant S_2 values in Table 1).

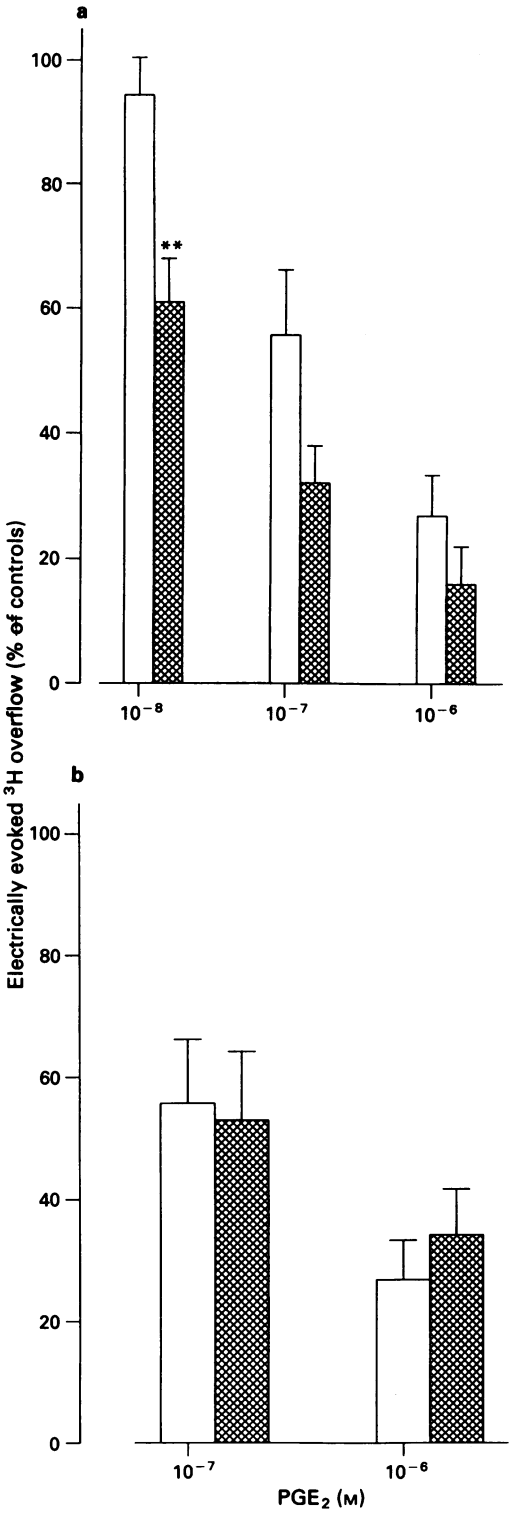


Figure 3 Influence of naproxen (1 μM, a) and AH 609 (10 μM, b) on the inhibitory effect of postaglandin E_2 (PGE_2) (in the presence of rauwolscine 1 μM) on electrically (2 Hz)-evoked tritium overflow from strips of the human saphenous vein. Experiments without naproxen and AH 6809 (open columns); experiments with naproxen 1 μM or AH 6809 10 μM (cross-hatched columns). Ordinate scale: ^{3}H overflow ratios, expressed as percentage of ratios in PGE_2-free control experiments. Means ± s.e.means of 6 to 7 experiments. $^{**}P<0.025$ (compared with the response to PGE_2 in the experiments without naproxen).

Pulmonary arteries

All experiments using pulmonary artery strips were performed in the presence of rauwolscine (1 μM). Electrically-evoked tritium overflow was concentration-dependently inhibited by PGE_2, misoprostol and sulprostone (Figure 6). As in the saphenous vein, sulprostone was considerably more potent in inhibiting tritium overflow than PGE_2. Misoprostol exhibited a lower potency than sulprostone but a higher one than PGE_2 (Figure 6). The pEC_{50} values of sulprostone and PGE_2 were in a similar range to those in the saphenous vein and that of misoprostol was moderately higher than in the latter blood vessel (Table 2).

Discussion

The aim of the present study was to identify and characterize presynaptic prostanoid receptors on sympathetic neurones in the human saphenous vein and pulmonary artery. Under the conditions applied here (blockade of neuronal and extraneuronal uptake), electrically evoked tritium overflow from these blood vessels has been shown to be tetrodotoxin-sensitive and Ca^{2+}-dependent (Göthert *et al.*, 1984; Göthert & Hentrich, 1985). The electrically-evoked tritium overflow consists mainly of [^{3}H]-noradrenaline and reflects action potential-induced release of unlabelled noradrenaline from

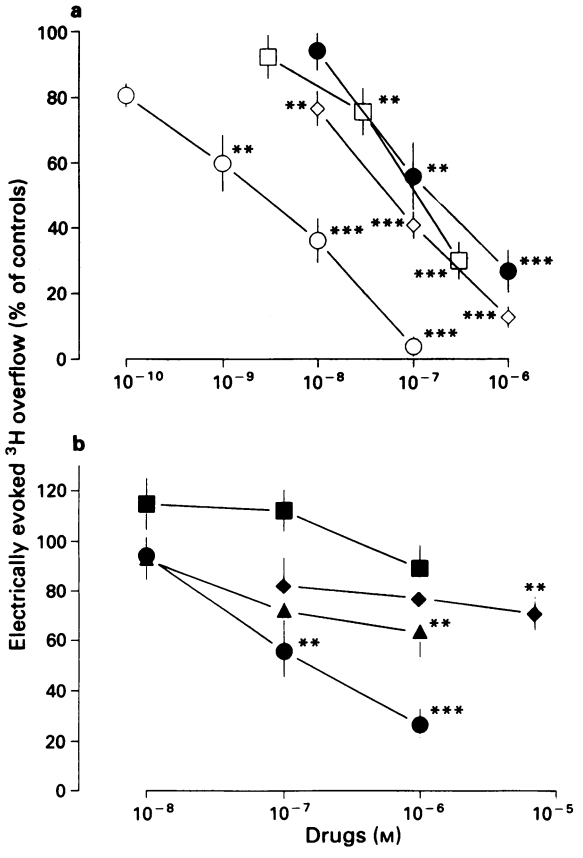


Figure 4 Effects of prostanoids in the presence of rauwolscine 1 μM on the electrically (2 Hz)-evoked tritium overflow from strips of human saphenous vein preincubated with [^{3}H]-noradrenaline. (a) Prostaglandin E_2 (●); prostaglandin E_1 (◇); sulprostone (○); misoprostol (□); (b) prostaglandin E_2 (●); iloprost (◆); prostaglandin $F_{2\alpha}$ (■); U 46619 (▲). Ordinate scale: ^{3}H overflow ratios, expressed as percentage of ratios in prostanoid-free control experiments. Means ± s.e.means from 5 to 10 experiments. $^{**}P<0.025$; $^{***}P<0.001$ (compared with the corresponding controls).

the sympathetic neurones contained in the blood vessels (for discussion of this point, see Göthert *et al.*, 1984; Göthert & Hentrich 1985).

Both in the saphenous vein and in the pulmonary artery, PGE_2 inhibited the electrically-evoked noradrenaline release from the sympathetic neurones. It has been suggested that this inhibitory effect of PGE_2 (which is in agreement with previous findings obtained in a variety of other sympathetically innervated tissues from various species) may be mediated by presynaptic EP-receptors (for references, see introduction). The substantial increase of the potency of PGE_2 in the human saphenous vein when the frequency of stimulation was decreased from 2 Hz to 0.66 Hz is a typical feature of responses mediated by presynaptic receptors (Starke *et al.*, 1989) and, therefore, is compatible with the involvement of presynaptic EP receptors in the PGE_2-induced inhibition.

In view of the possibility that presynaptic EP receptors might interact with the presynaptic α_2-autoreceptors, our experiments on both blood vessels were, as a rule, carried out in the presence of rauwolscine in the superfusion fluid. Such an interaction occurs in peripheral (Ohia & Jumblatt, 1990) and central noradrenergic neurones (Allgaier *et al.*, 1989). When in those studies, the autoreceptors which are tonically activated by endogenous noradrenaline were blocked by an α_2-adrenoceptor antagonist, the inhibitory effect of PGE_2 was increased. However, in the present experiments on human saphenous veins, blockade of the α_2-adrenoceptor by rauwolscine did not enhance the inhibitory effect of PGE_2. Thus, the possibility was ruled out that activation of α_2-autoreceptors attenuates the inhibitory effect mediated by the presynaptic EP-receptors. This finding in the human saphenous vein resembles that previously obtained in the rat vena cava (Molderings *et al.*, 1992a). Two further advantages can be derived from the routine presence of rauwolscine in the superfusion fluid: firstly, in view of the increased noradrenaline release in its presence, a more exact quantitative evaluation of the inhibitory effect of drugs was possible, and secondly, the theoretical possibility of an action of any of these drugs on α_2-adrenoceptors was excluded.

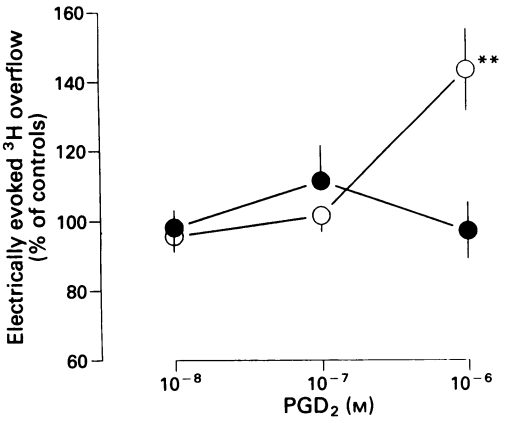


Figure 5 Effect of prostaglandin D_2 (PGD_2) and the DP-receptor antagonist, BW A868C, on electrically (2 Hz)-evoked tritium overflow from strips of the human saphenous vein (in the presence of rauwolscine 1 μM). Experiments without BW A868C, (○); experiments with BW A868C 0.1 μM, (●). Ordinate scale: ^{3}H overflow ratios, expressed as percentage of ratios in PGD_2-free control experiments. Means ± s.e.means of 8 to 9 experiments. $^{**}P<0.025$ (compared with the corresponding controls).

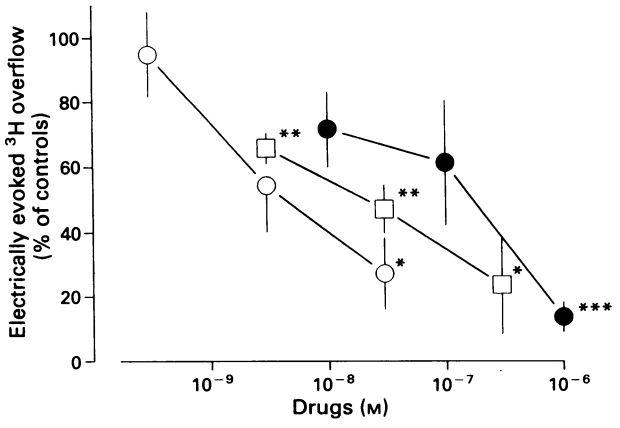


Figure 6 Inhibitory effects of prostanoids on electrically (2 Hz)-evoked tritium overflow from strips of the human pulmonary artery (in the presence of rauwolscine 1 μM). Prostaglandin E_2 (●); sulprostone (○); misoprostol (□). Ordinate scale: ^{3}H overflow ratios, expressed as percentage of ratios in prostanoid-free control experiments. Means ± s.e.means of 3 to 6 experiments. $^{*}P<0.05$; $^{**}P<0.025$; $^{***}P<0.001$ (compared with the corresponding controls).

The pharmacological characteristics of the EP receptor mediating inhibition of noradrenaline release in both human blood vessels clearly conform to an EP_3-receptor according to the classification criteria of Coleman and coworkers (1990). Thus, the effect of PGE_2 was mimicked with greater potency by the non-selective agonist PGE_1 in the saphenous vein, and, in both blood vessels, by the EP_2/EP_3 receptor agonist, misoprostol and the EP_1/EP_3-receptor agonist, sulprostone. In the pulmonary artery, misoprostol was considerably more potent than in the saphenous vein. This difference cannot be explained satisfactorily on the basis of our data. The potency of the drugs in inhibiting noradrenaline release in the human saphenous vein is in good agreement with their potency in inhibiting neurotransmitter release from guinea-pig vas deferens, a preparation recognised to possess EP_3-receptors (Coleman *et al.*, 1987; 1990). In the latter preparation, potency ratios of PGE_1 and sulprostone relative to PGE_2 (= 1) were 0.8 and 0.02, respectively. In the human saphenous vein they were 0.35 and 0.02, respectively, and in the human pulmonary artery, the potency ratio of sulprostone related to PGE_2 was 0.03. Iloprost, a stable analogue of prostacyclin (the main product of arachidonic acid released in response to sympathetic nerve stimulation in blood vessels; see Malik & Sehic, 1990), was only a weak agonist at the presynaptic EP-receptor in human saphenous vein. This drug has been shown to be equipotent with PGE_2 at EP_1-receptors and markedly less potent than PGE_2 at EP_2- and EP_3-receptors (Sheldrick *et al.*, 1988). Moreover, the EP_1-receptor antagonist, AH 6809, at a concentration which is at least 30 fold higher than its pA_2 value at EP_1-receptors (Coleman *et al.*, 1985), failed to affect that PGE_2-induced inhibition. Taken together, it may be concluded that the effect of PGE_1 and PGE_2 in both human blood vessels is mediated via EP_3-receptors. This is in agreement with findings for the presynaptic EP-receptors on postganglionic sympathetic nerves innervating other vascular and non-vascular tissues, namely the rat vena cava (Molderings *et al.*, 1992a), the rat trachea (Racké *et al.*, 1991), the guinea-pig vas deferens (Coleman *et al.*, 1987; 1990) and atrium (Beckman & Knirk, 1991; Mantelli *et al.*, 1991), and the human iris-ciliary body (Ohia & Jumblatt, 1991).

Experiments with the cyclo-oxygenase inhibitor, naproxen, were performed to determine whether or not, under the present experimental conditions, [^{3}H]-noradrenaline release is also inhibited by endogenously formed prostanoids. Gryglewski (1979) has shown that naproxen (1 μM) effectively inhibits cyclo-oxygenase. If the EP receptors were tonically activated by endogenous arachidonic acid metabolites, the exogenous prostaglandin would compete with the endogenously formed prostanoids resulting in an apparently lower potency of the exogenous agonist. In such circumstances, inhibition of the formation of these endogenous prostanoids with naproxen would be expected to enhance the inhibitory effect of

exogenous PGE_2 on [^{3}H]-noradrenaline release. Indeed, such an enhancement was found in the present study. This finding is in agreement with results reported for several other vascular preparations (for review, see e.g. Malik & Sehic, 1990). Interestingly, naproxen might be expected to facilitate noradrenaline release by itself, by abolishing the inhibitory effect produced by endogenous prostanoids. However, such an enhancement of evoked noradrenaline release was not observed in our experiments, a discrepancy which may be related to the simultaneous inhibition of the synthesis of prostanoids with facilitatory action on noradrenaline release.

In the human saphenous vein, PGD_2 increased the evoked noradrenaline release. An enhancement of noradrenaline release has also been found in human corpus cavernosum (Molderings *et al.*, 1992b) and canine mesenteric artery (Nakajima & Toda, 1984), but not e.g. in rat vena cava (Molderings *et al.*, 1992a). The facilitatory effect of PGD_2 on noradrenaline release was abolished by a low concentration of the highly selective DP-receptor antagonist, BW A868C (Giles *et al.*, 1989; Trist *et al.*, 1989). Therefore, the data suggest that presynaptic DP-receptors are involved in PGD_2-induced facilitation of electrically-evoked noradrenaline release.

The lack of an effect of the FP receptor agonist, $PGF_{2\alpha}$ (at concentrations up to 1 μM) on noradrenaline release and the low potency and efficacy of the stable thromboxane analogue, U46619, in inhibiting noradrenaline release suggest that the sympathetic nerve endings in the human saphenous vein are devoid of FP- and thromboxane receptors.

In conclusion, the present data indicate that the sympathetic nerves of the human saphenous vein and pulmonary artery are endowed with presynaptic inhibitory EP_3-receptors and presynaptic facilitatory DP receptors, respectively. The EP_3-receptors may be tonically activated by endogenous PGE_2 and do not interact with the presynaptic α_2-autoreceptors.

The technical assistance of Mrs K. Thur and Mrs D. Funccius is gratefully acknowledged. We wish to thank the pharmaceutical companies for generous gifts of drugs.

References

ALLGAIER, C., JÄGER, T. & HERTTING, G. (1989). Endogenous noradrenaline impairs the prostaglandin-induced inhibition of noradrenaline release. *Naunyn-Schmied. Arch. Pharmacol.*, **340**, 472–474.

BECKMAN, R. & KNIRK, U. (1991). Presynaptic effects of prostaglandins on adrenergic neurotransmission in guinea pig atria in vitro. *Naunyn-Schmied. Arch. Pharmacol.*, **344**, (Suppl), R83.

COLEMAN, R.A., HUMPHREY, P.P.A. & KENNEDY, I. (1985). Prostanoid receptors in smooth muscle: further evidence for a proposed classification. In *Trends in Autonomic Pharmacology*, Vol. 3, ed. Kalsner, S. pp. 35–49. London: Taylor and Francis.

COLEMAN, R.A., KENNEDY, I., HIMPHREY, P.P.A., BUNCE, K. & LUMLEY, P. (1990). Prostanoids and their receptors. In *Comprehensive Medicinal Chemistry. The Rational Design, Mechanistic Study and Therapeutic Application of Chemical Compounds*, Vol. 3, ed. Emmet, J.C. pp. 643–714. Oxford: Pergamon.

COLEMAN, R.A., KENNEDY, I., SHELDRICK, R.L.G. & TOLOWINSKA, I.Y. (1987). Further evidence for the existence of three subtypes of PGE_2-sensitive (EP)-receptors. *Br. J. Pharmacol.*, **91**, 407P.

GILES, H., LEFF, P., BOLOFO, M.L., KELLY, M.G. & ROBERTSON, A.D. (1989). The classification of prostaglandin DP-receptors in platelets and vasculature using BW A868C, a novel, selective and potent competitive antagonist. *Br. J. Pharmacol.*, **96**, 291–300.

GÖTHERT, M. & HENTRICH, F. (1985). Identification of presynaptic β_2-adrenoceptors on the sympathetic nerve fibres of the human pulmonary artery. *Br. J. Pharmacol.*, **85**, 933–941.

GÖTHERT, M., SCHLICKER, E., HENTRICH, F., ROHM, N. & ZERKOWSKI, H.R. (1984). Modulation of noradrenaline release in human saphenous vein via presynaptic α_2-adrenoceptors. *Eur. J. Pharmacol.*, **102**, 261–267.

GRYGLEWSKI, R.J. (1979). Screening and assessment of the potency of antiinflammatory drugs in vitro. In *Antiinflammatory Drugs. Handb. Exp. Pharmacol.*, Vol. 50, ed. Vane, J.R. & Ferreira, S.H. pp. 3–43. Berlin: Springer Verlag.

GÜLLNER, H.G. (1983). The interactions of prostaglandins with the sympathetic nerve system – a review. *J. Autonom. Ner. Syst.*, **8**, 1–12.

LANGER, S.Z. (1981). Presynaptic regulation of the release of catecholamines. *Pharmacol. Rev.*, **32**, 337–362.

MALIK, K.U. & SEHIC, E. (1990). Prostaglandins and the release of the adrenergic transmitter. *Ann. N.Y. Acad. Sci.*, **604**, 222–236.

MANTELLI, L., AMERINI, S., RUBINO, A. & LEDDA, F. (1991). Prejunctional prostanoid receptors on cardiac adrenergic terminals belong to the EP_3 subtype. *Br. J. Pharmacol.*, **102**, 573–576.

MÖHLIG, A., REIMANN, A., BRÄUTIGAM, M. & RACKÉ, K. (1992). Release of endogenous noradrenaline from the rat stomach is inhibited via prostanoid receptors. *Naunyn-Schmied. Arch. Pharmacol.*, **345** (Suppl. 2), R63.

MOLDERINGS, G.J., COLLING, E. & GÖTHERT, M. (1993). EP_3 receptor-mediated inhibition of noradrenaline release from the postganglionic sympathetic nerve fibres of the human saphenous vein. *Naunyn-Schmid. Arch. Pharmacol.*, **347** (Suppl.), R122.

MOLDERINGS, G.J., MALINOWSKA, B. & SCHLICKER, E. (1992a). Inhibition of noradrenaline release in the rat vena cava via prostanoid receptors of the EP_3-subtype. *Br. J. Pharmacol.*, **107**, 352–355.

MOLDERINGS, G.J., VAN AHLEN, H. & GÖTHERT, M. (1992b). Modulation of noradrenaline release in human corpus cavernosum by presynaptic prostaglandin receptors. *Int. J. Impotence Res.*, **4**, 19–25.

NAKAJIMA, M. & TODA, N. (1984). Neuroeffector actions of prostaglandin D_2 on isolated dog mesenteric arteries. *Prostaglandins*, **27**, 407–419.

OHIA, S.E. & JUMBLATT, J.E. (1990). Prejunctional inhibitory effects of prostanoids on sympathetic neurotransmission in the rabbit iris-ciliary body. *J. Pharmacol. Exp. Ther.*, **255**, 11–16.

OHIA, S.E. & JUMBLATT, J.E. (1991). Prejunctional prostaglandin receptors in the human iris-ciliary body. *Current Eye Res.*, **10**, 967–975.

RACKÉ, K., BÄHRING, J. & WESSLER, I. (1991). Release of endogenous noradrenaline from rat isolated trachea is inhibited via prostaglandin receptors of the EP_3-subtype. *Naunyn-Schmied. Arch. Pharmacol.*, **344** (Suppl. 2), R128.

SHELDRICK, R.L.G., COLEMAN, R.A. & LUMLEY, P. (1988). Iloprost – a potent EP_1 – and IP-receptor agonist. *Br. J. Pharmacol.*, **94**, 334P.

STARKE, K., GÖTHERT, M. & KILBINGER, H. (1989). Modulation of neurotransmitter release by presynaptic autoreceptors. *Physiol. Rev.*, **69**, 864–989.

TRIST, D.G., COLLINS, B.A., WOOD, J., KELLY, M.G. & ROBERTSON, A.D. (1989). The antagonism by BW A868C of PGD_2 and BW245C activation of human platelet adenylate cyclase. *Br. J. Pharmacol.*, **96**, 301–306.

WESTFALL, T.C. (1977). Local regulation of adrenergic neurotransmission. *Physiol. Rev.*, **57**, 659–728.

(Received June 8, 1993
Revised November 8, 1993
Accepted November 11, 1993)

Br. J. Pharmacol. (1994), **111**, 739–746 © Macmillan Press Ltd, 1994

Tachykinin NK_1 receptor subtypes in the rat urinary bladder

Stefania Meini, Riccardo Patacchini & Carlo Alberto Maggi

Pharmacology Department, A. Menarini Pharmaceuticals, Via Sette Santi 3, 50131, Florence, Italy

1 Following the recent proposal that the selective agonist septide, ([*p*Glu^6,Pro^9]SP(6-11)), acts on a novel tachykinin receptor distinct from the 'classical' NK_1 receptor, the aim of the study was to investigate the possible heterogeneity of tachykinin NK_1 receptors in the rat urinary bladder.

2 The synthetic tachykinin receptor agonists, septide (pD_2 7.87) and [Sar^9]substance P (SP) sulphone (pD_2 7.64) produced concentration-dependent contractions of the rat isolated urinary bladder.

3 The NK_1 receptor antagonists GR82,334, (±)-CP96,345, and RP67,580 competitively antagonized (slopes of Schild plot not significantly different from unity) the response to septide with the rank order of potency (pK_B values in parentheses): RP 67,580 (7.57) > GR 82,334 (7.01) > (±)-CP 96,345 (6.80). The same antagonists were significantly less potent when tested against [Sar^9]SP sulphone, while maintaining the same rank order of potency: RP 67,580 (7.00) > GR 82,334 (5.93) > (±)-CP 96,345 (< 6). The antagonists did not affect the concentration-response curve to bombesin.

4 To exclude the involvement of the NK_2 receptor, a second series of experiments was performed in the presence of the potent nonpeptide NK_2 receptor antagonist, SR 48,968. SR 48,968 (1 μM) produced a rightward shift of the concentration-response curve to the NK_2 receptor selective agonist, [βAla^8]neurokinin A (NKA) (4-10). SR 48,968 did not significantly modify the response to SP, NKA, neurokinin B (NKB), neuropeptide K (NPK), neuropeptide γ (NPγ), SP(4-11), SP(6-11), septide or [Sar^9]SP sulphone.

5 In the absence or presence of SR 48,968, RP 67,580 antagonized in a competitive manner the response to septide, [Sar^9]SP sulphone, SP(4-11) and SP(6-11): pK_B values obtained in the absence and presence of SR 48,968 were not significantly different for any of these four agonists.

6 RP 67,580 antagonized the response to SP and NKA both in the absence and presence of SR 48,968. In both cases, the slopes of the Schild plots were significantly different from unity. Mean dose-ratios produced by RP 67,580 in the presence of SR 48,968 were larger than those measured without NK_2 receptor blockade for both SP and NKA.

7 RP 67,580 (3 μM) did not antagonize the response to NKB in the absence of SR 48,968. In the presence of SR 48,968, RP 67,580 acted as a competitive antagonist of NKB-induced contractions with a pK_B value (7.63) not significantly different from that measured towards septide. In the present of SR 48,968, RP 67,580, GR 82,334 and (±)-CP 96,345 antagonized the response to NKB with a rank order of potency identical to that measured towards septide or [Sar^9]SP sulphone.

8 In the absence of SR 48,968, RP 67,580 (3 μM) produced a small shift of the concentration-response curve to neuropeptide K and was ineffective toward neuropeptide γ. In the presence of SR 48,968 a clear shift of the curve to both agonists was observed.

9 These findings are compatible with the idea that a septide-sensitive tachykinin receptor may exist in the rat urinary bladder. The septide-sensitive receptor is recognized by NK_1 receptor antagonists with higher affinity than the 'classical' NK_1 receptor recognized by [Sar^9]SP sulphone. Our data suggest that NKB, after NK_2 receptor blockade, is a more suitable ligand than SP for activation of the 'septide-sensitive' receptor. While the final proof for the existence of possible NK_1 receptor subtypes must await confirmation at the molecular level, the present findings provide strong pharmacological evidence that either NK_1 receptor subtypes or a novel type of tachykinin receptor exist in the rat urinary bladder.

Keywords: Neurokinin B; NK_1 receptor; rat urinary bladder; receptor subtypes; substance P; tachykinins

Introduction

The tachykinin NK_1 receptors are defined by the rank order of potency of natural tachykinins, substance P (SP) > neurokinin A (NKA) > neurokinin B (NKB). A number of agonists and antagonists have been developed which selectively interact with NK_1 receptors. Selective NK_1 receptor agonists are [Sar^9]SP sulphone and septide ([pGlu^6,Pro^9]SP(6-11)) (Wormser *et al.*, 1986; Dion *et al.*, 1987; Laufer *et al.*, 1988). Amongst the antagonists, the undecapeptide GR 82,334 (Hagan *et al.*, 1991), and the non-peptide ligands CP 96,345 (Snider *et al.*, 1991) and RP 67,580 (Garret *et al.*, 1991) block NK_1 receptor-mediated responses with high affinity, with little activity at NK_2 or NK_3 sites. The development of selective antagonists for the NK_1 receptor has revealed a species-related heterogeneity: thus, CP 96,345 is more potent that RP 67,580 in blocking NK_1 receptor-mediated responses in human, guinea-pig or rabbit than in rat preparations, while RP 67,580 is more potent than CP 96,345 at the rat compared to human or guinea-pig NK_1 receptors (Snider *et al.*, 1991; Gitter *et al.*, 1991; Garret *et al.*, 1991; Patacchini *et al.*, 1992; Barr & Watson, 1993). This species-related difference in antagonist potencies is linked to species-related variations at discrete sites in the amino acid sequence of the NK_1 receptor (Fong *et al.*, 1992c). Although a short form of the human NK_1 receptor protein has been isolated (Fong *et al.*, 1992d), it is unclear whether it represents a functional receptor site. A recent report (Kage *et al.*, 1993) provided evidence suggesting that two forms of the NK_1 receptor, differing in their amino acid composition, may be present in rat salivary glands. At the present time, however, no conclusive evidence has been obtained from molecular biology to support the idea of the

[1] Author for correspondence.

existence of NK_1 receptor subtypes (intraspecies heterogeneity) (Gerard et al., 1993 for recent review).

Petitet et al. (1992) presented evidence indicating that septide does not interact with classical NK_1 receptors in the guinea-pig ileum which are labelled with high affinity by, for example, [Pro^9]SP or [Sar^9]SP sulphone. Petitet et al. (1992) found that septide potently contracts the guinea-pig isolated ileum (cf. Laufer et al., 1988), its effect being blocked by GR 71,251 (Ward et al., 1990), a NK_1 receptor antagonist. In sharp contrast, septide is only a weak displacer of SP binding in this preparation: following this discrepancy, the hypothesis has been proposed that septide is acting at a 'novel' type of tachykinin receptor (Petitet et al., 1992).

In the first part of this study we have compared the ability of three NK_1 receptor selective antagonists, CP 96,345, RP 67,580 and GR 82,334 to antagonize the contractile response to the rat isolated urinary bladder produced by septide or the selective NK_1 receptor agonist, [Sar^9]SP sulphone. The latter agonist is known to interact with high affinity with 'classical' NK_1 receptors recognized by SP in binding assays (Dion et al., 1987; Tousignant et al., 1991). From this first set of experiments (Meini et al., 1993), the three antagonists were significantly more potent in antagonizing the response to septide than that to [Sar^9]SP sulphone. On this basis, a second series of experiments was planned in which the action of RP 67,580 was investigated against a panel of tachykinin receptor agonists, both natural and synthetic. Since both NK_1 and NK_2 receptors are known to mediate smooth muscle contraction in the rat isolated urinary bladder (Maggi et al., 1988) and some of the test ligands also act as NK_2 receptor agonists, experiments were performed in the presence and absence of SR 48,968, a potent non peptide NK_2 receptor antagonist (Emonds-Alt et al., 1992).

Methods

Experimental protocol

Male albino rats of Wistar strain weighing 320–350 g were stunned and bled. The urinary bladder was removed, placed in oxygenated and gassed Krebs solution containing indomethacin (10 μM), bestatin, captopril and thiorphan (1 μM each) and strips of detrusor muscle were prepared for isotonic tension recording as described in Patacchini et al. (1992). The composition of Krebs solution was as follows (mM): NaCl 118, KCl 4.7, $CaCl_2 2H_2O$ 2.5, $MgCl_2 6H_2O$ 0.5, $NaH_2PO_4 H_2O$ 1.0, $NaHCO_3$ 25 and glucose 10. After an equilibration period of 45 min, the preparations were exposed to KCl (80 mM), which was used as an internal standard. Thereafter the strips were repeatedly exposed to a maximally effective concentration of the chosen tachykinin receptor agonist at 20–30 min intervals until two reproducible responses were obtained. At this time, a cumulative concentration-response curve to the agonist was constructed, the next concentration being added when the effect of the preceding one had reached a steady state. After the first curve, there was a washout period (45 min) until basal resting conditions had been re-established. Then, the chosen concentration of the antagonist was added, and a new curve to the agonist obtained. Preliminary experiments had shown that the concentration-response curve to the agonists was fully reproducible using this protocol. Contact time for the antagonists was 15 min.

For experiments involving the effect of antagonists towards bombesin, a different experimental protocol was used, since reproducible curves to this peptide cannot be obtained in the rat urinary bladder, owing to the difficulty of washing out the bombesin effect (Maggi et al., 1992). Concentration-response curves to bombesin were carried out in parallel strips from the same animal in the absence or presence of the antagonist.

For experiments involving the NK_2 receptor antagonist, SR 48,968, it was present at a concentration of 1 μM in the Krebs solution throughout the experiment. This concentration of SR 48,968 was selected from preliminary experiments (Figure 3) indicating that it produces a rightward shift of the concentration-response curve to the selective NK_2 receptor agonist [βAla^8]NKA(4-10).

Data analysis

Regression analysis was made by the least squares method, EC_{50} values and 95% confidence limits (c.l.) were calculated accordingly.

The competitive nature of the interaction of each antagonist with tachykinin NK_1 receptors was checked by the 'Schild Regression' method as follows: antagonist-induced parallel shifts of concentration-response curves to the agonist were calculated graphically at the level of the half-maximal response as the ratio (dose-ratio) of equieffective concentrations of agonist. Estimates of log [dose ratio − 1] were plotted against log [antagonist concentration], (Arunlakshana & Schild, 1959). Antagonists providing plots with linear regression lines and slopes not significantly different from unity were considered competitive. The affinity of competitive antagonists was expressed in terms of pK_B from the equation: pK_B = log [dose ratio − 1] − log [antagonist concentration] (Kenakin, 1984; Jenkinson, 1991).

For each antagonist, at least three different concentrations were investigated. When a Schild plot slope so determined was significantly different from unity, only the dose-ratio was calculated.

All values in text, Figures and Tables are mean ± s.e. of the mean, or mean (95% c.l. in brackets).

Drugs

Drugs used were: bestatin, substance P, [Sar^9]SP sulphone, neurokinin B, substance P (4-11), substance P (6-11) neuropeptide K, neuropeptide γ and septide ([*p*Glu^6,Pro^9]SP(6-11)) (Peninsula), GR 82,334 ([D-Pro^9,(spiro-γ-lactam)Leu^{10}, Trp^{11}] physalaemin(1-11)) (Neosystem), indomethacin and captopril (Sigma), thiorphan (Bachem). RP 67,580 ([3α**R**,7α**R**]-7,7-diphenyl-2-[1-imino-2-(2-methoxyphenyl)ethyl]perhydroisoindol-4-one) was a kind gift of Dr C. Garret, Rhone Poulenc, Vitry, France, whilst SR 48,968 ((**S**)-N-methyl-*N*[4-(4-acetylamino-4-phenylpiperidino)-2-(3,4- dichlorophenyl)butyl] benzamide) was kindly supplied by Dr X. Emonds-Alt, Sanofi Recherche, Montpellier Cedex, France. (±)-CP 96,345 ([*cis*-2-(diphenylmethyl)-*N*-[(2-methoxyphenyl)-methyl]-1-azabicyclo[2.2.2]octan-3-amine]) NKA and [βAla^8]NKA(4-10) were synthesized in the Chemistry Department of Menarini Pharmaceuticals.

Results

Effect of (±)-CP 96,345, GR 82,334 and RP 67,580 on the contractile responses to septide and [Sar^9]SP sulphone

Septide (1–300 nM) and [Sar^9]SP sulphone (1 nM–1 μM) produced concentration-dependent contractions of the rat isolated urinary bladder approaching 75–85% of the maximal response to KCl (80 mM). EC_{50} values were 19.9 (18.8–21.2) nM and 12.5 (10.4–16.6) nM for [Sar^9]SP sulphone and septide, respectively.

(±)-CP 96,345 (1–5 μM), RP 67,580 (0.3–3 μM) and GR 82,334 (1–10 μM) produced concentration-dependent rightward shifts of the concentration-response curve to septide; slopes of Schild plots (Figure 1, Table 1) were not significantly different from unity, indicating a competitive antagonism. The rank order of potency was RP 67,580 > GR 82,334 > (±)-CP 96,345 (Table 1).

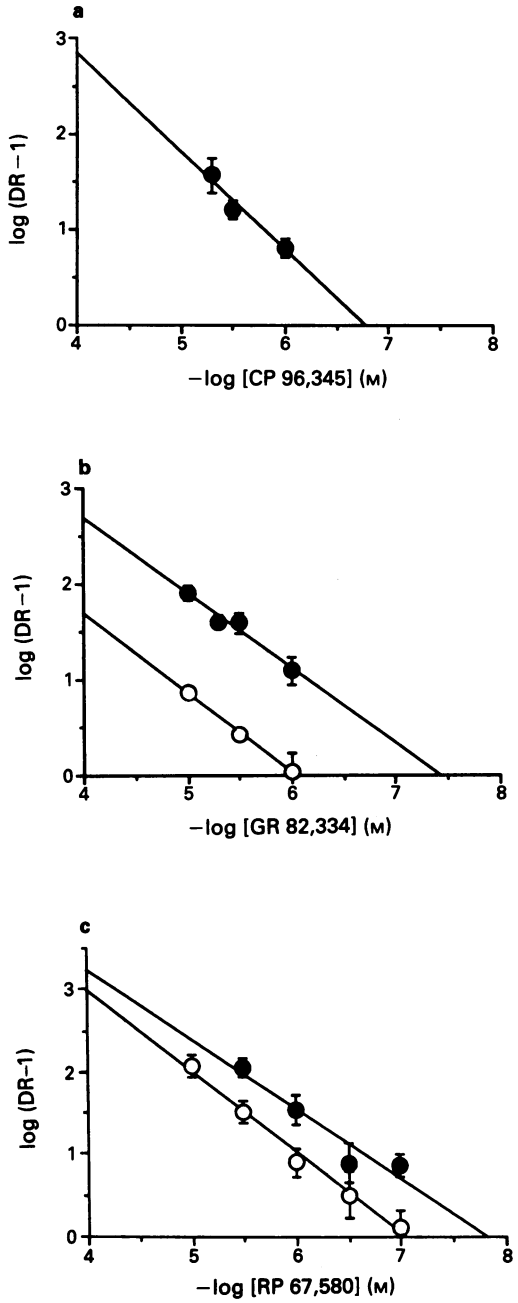


Figure 1 Schild plots for antagonism of contraction produced by septide (●) or [Sar^9]SP sulphone (○) by the NK$_1$ receptor antagonists (±)-CP 96,345 (a), GR 82,334 (b) and RP 67,580 (c). Each value is the mean ± s.e.mean of at least four determinations at the stated concentration of the antagonist. Slopes of regression lines are shown in Table 1.

RP 67,580 (1–10 μM) and GR 82,334 (1–10 μM) also produced concentration-dependent rightward shifts of the response to [Sar^9]SP sulphone with slopes of Schild plots indicative of competitive antagonism (Table 1, Figure 1). (±)-CP 96,345 was ineffective against [Sar^9]SP sulphone up to 1 μM. At 3 μM, (±)-CP 96,345 produced a rightward shift of the curve to the agonist without depression of the maximal response (mean dose-ratio 6.01 ± 2.03, $n = 5$). At 5 μM, the shift of the curve to the agonist produced by (±)-CP 96, 345 (dose-ratio 4.01 ± 0.77, $n = 5$) was not larger than that observed at 3 μM and a reduction (20–30%) of the maximal response to the agonist was observed in some experiments (data not shown).

Data shown in Table 1 indicate that the affinity of various antagonists against septide is significantly higher than that measured against [Sar^9]SP sulphone, because of the non-overlapping of 95% c.l. of pK_B values (Table 1). In particular, GR 82,334 was about 10 times more potent against septide than against [Sar^9]SP sulphone (1.08 log unit difference in pK_B values). The ability of RP 67,580 to discriminate between the two agonists was less than that of GR 82,334 (0.58 log unit difference) but was still statistically significant (Table 1).

The selectivity of action of the NK$_1$ receptor antagonists was tested against bombesin (1 nM–1 μM) (Figure 2). Bombesin produced concentration-dependent contractions of the rat isolated urinary bladder, with an EC_{50} value of 17.1 nM (8.4–69.2 nM) (Figure 2). The response to bombesin was unaffected by RP 67,580, GR 82,334 or (±)-CP 96,345 (Figure 2) at a concentration (3 μM), which effectively antagonized responses to septide.

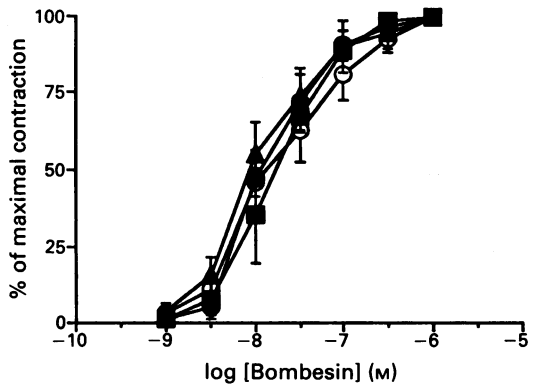


Figure 2 Concentration-response curves to bombesin in control rat urinary bladder strips (○) or in strips previously incubated with the NK$_1$ receptor antagonists RP 67,580 (●), GR 82,334 (■) or (±)-CP 96,345 (▲), 3 μM each. All data are expressed as mean ± s.e.mean of four experiments. Control and antagonist-treated strip preparations were obtained from the same animal.

Table 1 Antagonism by (±)-CP 96,345, GR 82,334 and RP 67,580 of the contractile responses produced by septide or [Sar^9]SP sulphone in the rat urinary bladder

Antagonist		*Agonist* [Sar^9]SP sulphone	*Septide*
(±)-CP 96,345	pK_B	<6	6.80 (6.63–6.97)
	slope	–	−1.05 (0.48–1.62)
GR 82,334	pK_B	5.93 (5.82–6.04)	7.01 (6.89–7.13)
	slope	−0.83 (0.52–1.14)	−0.79 (0.47–1.12)
RP 67,580	pK_B	7.00 (6.86–7.28)	7.57 (7.38–7.76)
	slope	−0.98 (0.76–1.20)	−0.86 (0.51–1.22)

95% confidence limits of pK_B values and slopes of Schild regression are shown in parentheses. Data were calculated from at least 12 experiments.

Effect of the NK_2 receptor antagonist SR 48,968 on the activity of synthetic tachykinin receptor agonists and natural tachykinins

Since the rat urinary bladder contains both NK_1 and NK_2 receptors (Maggi *et al.*, 1988; Hall *et al.*, 1992), it was important to exclude the possibility that septide and [Sar^9]SP sulphone interact with NK_2 receptors. The selective NK_2 receptor agonist, [βAla^8]NKA(4-10) produced concentration-dependent contractions of the rat isolated bladder with an EC_{50} value of 46.2 nM (33.7–67.1, $n = 12$, Table 2). The response to [βAla^8]NKA(4-10) was antagonized by the non peptide NK_2 receptor antagonist, SR 48,968 (Figure 3). At 1 μM, SR 48,968 produced a rightward shift of the concentration-response curve to the NK_2 agonist without depression of the maximal response. The dose-ratio, calculated from the EC_{50} values obtained in the presence and absence of the antagonist was 70.4, which, assuming competitive antagonism, corresponds to an apparent pK_B value of 8.59.

In subsequent experiments, the effect of 1 μM SR 48,968 on the response to natural tachykinins, C-terminal fragments of substance P and synthetic neurokinin receptor agonists was determined (Table 2). As shown by the data in Table 2, responses to septide, [Sar^9]SP sulphone, SP, SP(4-11), SP(6-11), NKA, NKB, NPK or NPγ were unaffected by SR 48,968 (Table 2).

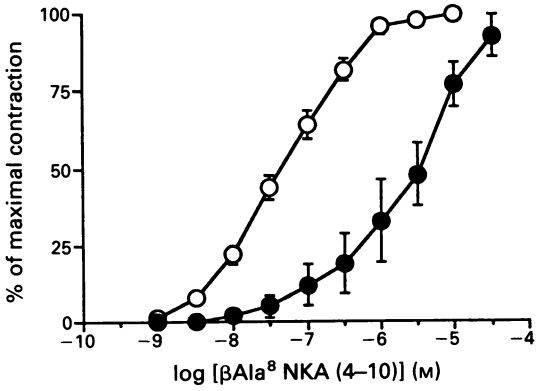


Figure 3 Concentration-response curves to [βAla^8]NKA(4-10) in rat urinary bladder strips in the absence (○) or in the presence of the NK_2 receptor antagonist SR 48,968 (1 μM) (●). Data are expressed as mean ± s.e.mean of four experiments.

Table 2 EC_{50} values of natural or synthetic tachykinin agonists in the rat isolated urinary bladder in the absence or presence of the NK_2 receptor antagonist, SR 48,968 (1 μM)

	EC_{50} values (95% c.l.) [nM]	
Tachykinin agonist	*No drug*	*In the presence of SR 48,968* [1 μM]
Substance P	37.3 (18.2–123.2)	29 (19.9–47.1)
[Sar^9]SP sulphone	19.9 (18.8–21.2)	17.5 (14–22.8)
Septide	12.5 (10.4–16.6)	17.3 (14.8–19.1)
SP(4-11)	14.8 (11.3–20.7)	16.7 (10.3–35.3)
SP(6-11)	16.9 (13–23.3)	16.1 (13.3–20.1)
Neurokinin A	29.4 (18.5–55.3)	96.9 (45.7–297.0)
Neurokinin B	89.6 (60.3–144.9)	61.0 (38.6–109.9)
Neuropeptide K	10.8 (6.5–25.9)	17.5 (16.6–18.6)
Neuropeptide γ	6.8 (4.8–11.6)	13.5 (9.0–24.5)
[βAla^8]NKA(4-10)	46.2 (33.7–67.1)	3251 (1507–8404)*

Data are expressed as mean EC_{50} values from at least five preparations each obtained from a different animal. 95% confidence limits (95% c.l.) are shown in parentheses (*$P < 0.05$, significantly different from EC_{50} value obtained in absence of SR48,968).

Effect of RP 67,580 on the contractile response to natural and synthetic tachykinin receptor agonists in the absence and presence of SR 48,968

Data in Table 3 and Figure 4 indicate that RP 67,580 antagonized in a competitive manner (slope of Schild plot not significantly different from unity) responses to septide, [Sar^9]SP sulphone, SP(4-11) and SP(6-11) both in the absence and presence of 1 μM SR 48,968. The affinity of RP 67,580 for these four agonists was not significantly affected by blockade of NK_2 receptors.

Also, in the presence of 1 μM SR 48,968, the pK_B value of RP 67,580 towards septide (pK_B 7.72) was significantly higher than that measured towards [Sar^9]SP sulphone (pK_B 7.08). pK_B values measured for SP(4-11) and SP (6-11) were somewhat intermediate between those measured against septide and [Sar^9]SP sulphone (Table 3).

Displacement of the concentration-response curve to SP by RP 67,580 was not compatible with competitive antagonism both in the absence and presence of SR 48,968 so that a pK_B value could not be determined (Tables 3 and 4). Nevertheless, the mean dose-ratio at the SP EC_{50} level obtained with 3 μM RP 67,580 was significantly larger in the presence than in the absence of SR 48,968 (26.8 ± 5.2 vs. 9.5 ± 2.5, $n = 4$ and 3, respectively, $P < 0.05$).

In the absence of SR 48,968, RP 67,580 (3 μM) had no effect against the concentration-response curve to NKA. In

Table 3 Effect of incubation with the NK_2 receptor antagonist SR 48,968 on the affinity of RP 67,580 at NK_1 receptors against several tachykinin agonists

	RP 67,580 affinity mean pK_B (95% c.l.)	
Tachykinin agonist	*No drug*	*In the presence of SR 48,968* [1 μM]
Substance P	Slope < 1	Slope < 1
[Sar^9]SP sulphone	7.00 (6.86–7.28)	7.08 (6.87–7.28)
Septide	7.57 (7.38–7.76)	7.72 (7.41–8.03)
SP(4-11)	7.32 (7.09–7.56)	7.45 (7.32–7.57)
SP(6-11)	7.17 (6.89–7.47)	7.45 (7.24–7.66)
Neurokinin A	Inactive up to 3 μM	Slope < 1
Neurokinin B	ND	7.63 (7.41–7.85)

pK_B values are expressed as the mean of single determinations in at least 12 separate preparations. Slopes of Schild plots were not significantly different from unity. Slope < 1: slope of Schild plot less than unity, $P < 0.05$, and pK_B could not be calculated. ND: pK_B could not be determined (antagonist concentration-range not sufficient to analyse according to Schild calculations).

Table 4 Effect of RP 67,580 (3 μM) on tachykinin-induced contractions of the rat isolated urinary bladder

	RP 67,580 (3 μM) *mean dose-ratio* (DR)	
Tachykinin agonist	*Without SR 48,968*	*In the presence of SR 48,968* [1 μM]
Substance P	9.5 ± 2.5 (3)	26.8 ± 5.2 (4)
Neurokinin A	*DR* < 2 (3)	62.1 ± 23.0 (7)
Neurokinin B	*DR* < 2 (4)	87.0 ± 39.0 (6)
Neuropeptide K	9.8 ± 3.2 (4)	51.5 ± 14.2 (3)
Neuropeptide γ	*DR* < 2 (3)	49.3 ± 27.0 (4)

Each value is the mean ± s.e.mean of n determinations (number shown in parentheses) obtained from different animals.

the presence of SR 48,968, RP 67,580 (3 μM) antagonized the concentration-response curve to NKA with a mean dose-ratio of 62.1 ± 23 ($n = 3$) (Tables 3 and 4).

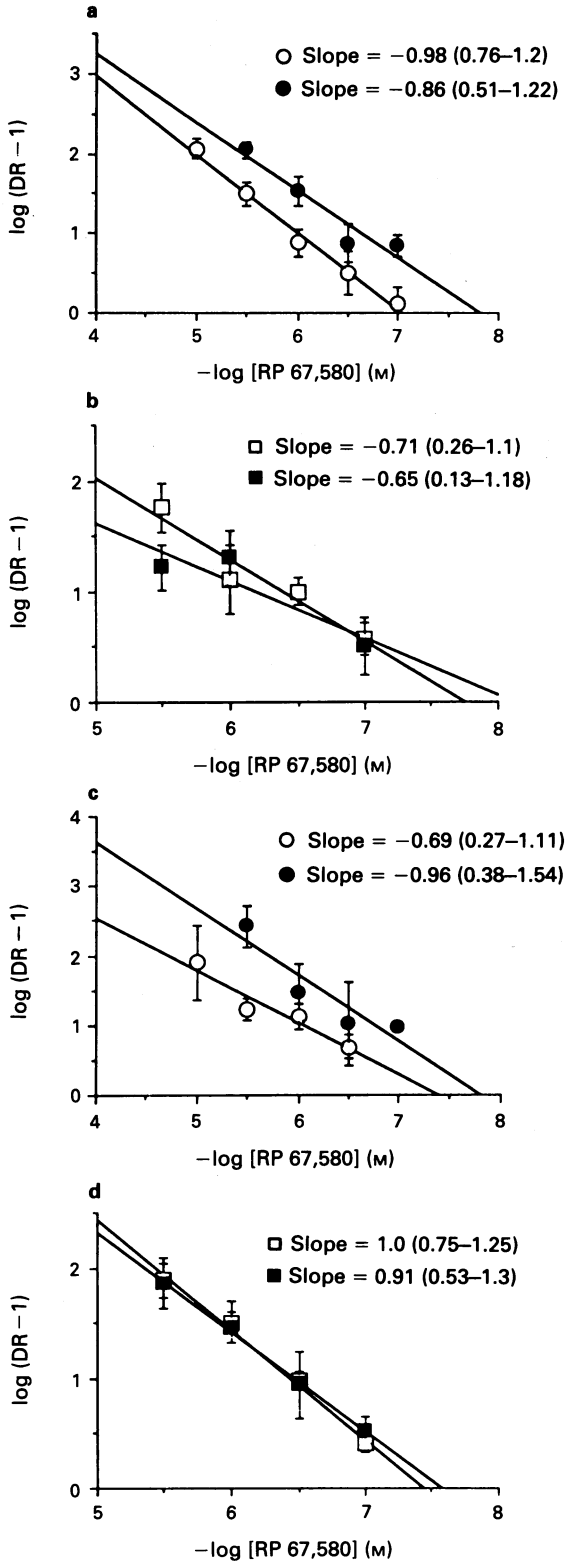


Figure 4 Schild plots for antagonism elicited by the NK_1 receptor competitive antagonist RP 67,580 on concentration-response curves to [Sar^9]SP sulphone (O), septide (●), SP(4-11) (□) or SP(6-11) (■). Experiments were performed in control conditions (a and b) or in preparations incubated throughout the experiment with the NK_2 receptor antagonist, SR 48,968 (1 μM) (c and d). Each value is the mean ± s.e.mean of at least four determinations at the stated concentration of the antagonist. Slopes of Schild plots (95% confidence limits in brackets) are shown in the figure.

In the absence of SR 48,968, RP 67,580 (1–10 μM) depressed the contractile response induced by the lower concentrations of NKB (Tables 3 and 4, Figure 5a). This inhibitory effect was not concentration-dependent. In the presence of SR 48,968, RP 67,580 (0.1–3 μM) produced a concentration-dependent, competitive antagonism of NKB-induced contractions (Figure 5b). The Schild plot approximated to a straight line with a slope of 1.0 (0.47–1.53 c.l.) (Figure 5c). The pK_B for RP 67,580 [7.63 (7.41–7.85 c.l.)] (Tables 3 and 4), was not significantly different from that measured against septide, but was significantly greater than that measured against [Sar^9]SP sulphone (Table 3).

RP 67,580 (3 μM) produced a rightward displacement of the concentration-response curve to NPK in the absence of

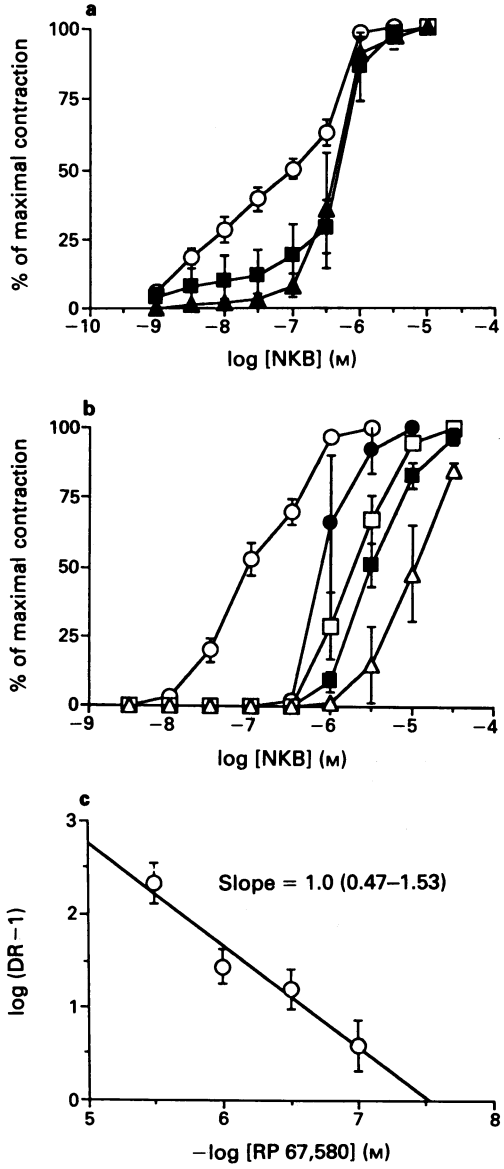


Figure 5 Antagonism by the NK_1 tachykinin antagonist, RP 67,580 of NKB-induced contractions of the rat urinary bladder. (a) Reponse to NKB in the absence (O) and in the presence of 1 μM (■) or 10 μM (▲) RP 67,580. (b) Concentration-dependent antagonism elicited by RP 67,580 (0.1–3 μM) towards NKB in preparations incubated throughout the experiment with the NK_2 tachykinin antagonist, SR 48,968 (1 μM). (c) Schild plot of the antagonism produced by RP 67,580 against NKB contractile responses, in the presence of SR 48,968 (1 μM). Data were calculated from results shown in (b). Slope of Schild plot (95% confidence limits in parentheses) is shown. Each value is mean ± s.e.mean of four determinations.

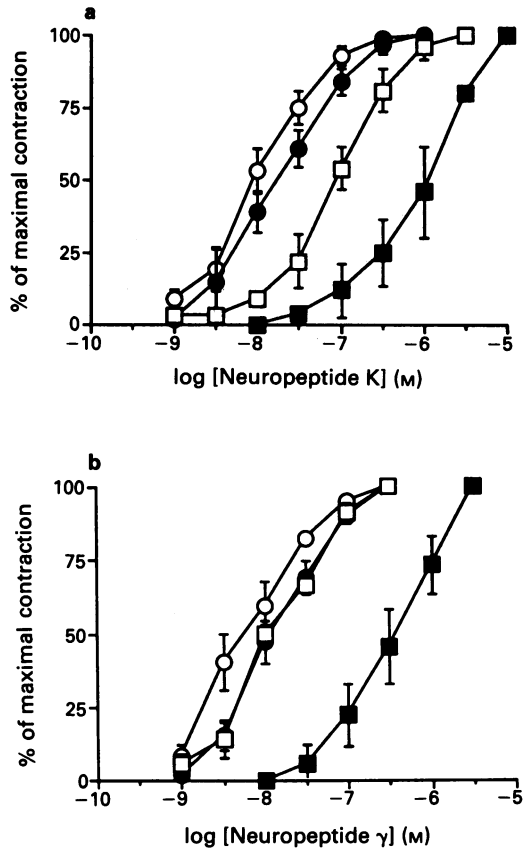


Figure 6 Concentration-response curves produced by neuropeptide K (a) or neuropeptide γ (b) (○) in the rat isolated urinary bladder; effect of incubation with the NK_2 tachykinin antagonist SR 48,968 (1 μM) (●), and the NK_1 tachykinin antagonist RP 67,580 (3 μM) in the presence (■) and absence (□) of SR 48,968 (1 μM). Data are expressed as mean ± s.e.mean of four experiments.

SR 48,968 (mean dose-ratio 9.8 ± 3.2, $n = 4$) (Table 4, Figure 6a) and a much larger shift in the presence of the NK_2 receptor antagonist (51.5 ± 14, $n = 3$, $P < 0.05$, Figure 6a, and Table 4).

RP 67,580 (3 μM) had no effect on the concentration-response curve to NPγ in the absence of SR 48,968 (Table 4, Figure 6b). In the presence of the NK_2 receptor antagonist, RP 67,580 (3 μM) produced a rightward shift of the curve to NPγ (mean dose-ratio 49.3 ± 27, $n = 4$, Table 4; Figure 6b).

From the above experiments it appears that, in the presence of SR 48,968, NKB is antagonized in a competitive manner by RP 67,580 with a pK_B value comparable to that measured against septide. For this reason, further experiments were performed with the other NK_1 receptor antagonists, (±)-CP 96,345 and GR 82,334, towards NKB in the presence of SR 48,968. The rank order of antagonist potencies in these conditions was the same as that observed against septide: RP 67,580 > GR 82,334 > (±)-CP 96,345. Mean dose-ratios produced by the three antagonists at a concentration of 3 μM were 87 ± 39 ($n = 6$), 56.6 ± 28.4 ($n = 7$), and 30.5 ± 9 ($n = 6$), for RP 67,580, GR 82,334 and (±)-CP 96,345, respectively.

Discussion

Septide ([pGlu^6,Pro^9]SP(6-11) was developed as a highly selective NK_1 receptor agonist (Wormser *et al.*, 1986; Laufer *et al.*, 1988). This hexapeptide derivative of the SP C-terminal sequence is very effective in various bioassays for NK_1 receptor activity (Laufer *et al.*, 1988; Hall & Morton, 1991) while having negligible affinity for NK_2 or NK_3 receptors (Wormser *et al.*, 1986; Lee *et al.*, 1986; Dion *et al.*, 1987; Laufer *et al.*, 1988; Maggi *et al.*, 1991).

Petitet *et al.* (1992) presented evidence that septide interacts with a class of tachykinin receptors which are pharmacologically distinguishable from 'classical' NK_1 receptors in the guinea-pig ileum. They showed that septide is as potent as SP in producing contractions of the guinea-pig ileum in the presence of atropine, but at least two orders of magnitude less potent than SP in displacing [^{3}H]-[Pro^9]SP binding to NK_1 receptors in the ileum (Petitet *et al.*, 1992). Such a discrepancy between the agonist potency of septide and its binding affinity for NK_1 receptors had been previously observed. For example, Lee *et al.* (1986) reported that septide was 293 and 87 times less potent than SP in displacing binding of radiolabelled SP from NK_1 receptors in rat salivary glands and guinea-pig urinary bladder membranes, respectively.

Our present findings show that (±)-CP 96,345, GR 82,334 and RP 67,580, which are highly selective and competitive NK_1 receptor antagonists, preferentially interact with septide- rather than with [Sar^9]SP sulphone-stimulated receptors in the rat urinary bladder. Against both agonists, RP 67,580 was more potent than (±)-CP 96,345, in agreement with previously reported data in the rat (Gitter *et al.*, 1991; Garret *et al.*, 1991; Patacchini *et al.*, 1992; Barr & Watson, 1993).

The NK_1 receptor was originally defined by the rank order of potency of natural tachykinins, SP > NKA > NKB, SP being its preferred natural ligand. If NK_1 receptor subtypes exist, it appears logical to ask what is the relative affinity of SP and other natural tachykinins for these sites. With this in mind, we assessed the ability of RP 67,580 to antagonize the responses to SP, NKA, NKB and the two N-terminally extended forms of NKA, neuropeptide K and neuropeptide γ. Since septide is a substituted derivative of the C-terminal sequence of SP, we also investigated the effect of RP 67,580 towards the C-terminal SP fragments, SP(4-11) and SP(6-11).

The rat urinary bladder contains NK_1 and NK_2 receptors which mediate contractile responses, but not NK_3 receptors (Maggi *et al.*, 1988; Burcher & Buck, 1986; Hall *et al.*, 1992). For this reason, we used the non peptide NK_2 receptor antagonist, SR 48,968 (Emonds-Alt *et al.*, 1992; Advenier *et al.*, 1992; Maggi *et al.*, 1993) to exclude the interaction of agonists with NK_2 receptors. Interestingly, SR 48,968 did not produce a significant displacement of any of the various tachykinin receptor agonists tested, with the exception of the NK_2 selective agonist [βAla^8]NKA(4-10). This is not surprising in the case of [Sar^9]SP sulphone and septide which are known to be ineffective at NK_2 receptors (Wormser *et al.*, 1986; Dion *et al.*, 1987; Laufer *et al.*, 1988). For the other ligands tested, we interpret the ineffectiveness of SR 48,968 as an indication that natural tachykinins and C-terminal SP fragments are capable of producing full contractile responses by interacting with receptor(s) that are SR 48,968-insensitive.

The most interesting findings were obtained when comparing the action of RP 67,580 towards natural tachykinins and SP fragments in the absence and presence of SR 48,968. We may expect that, if a natural tachykinin had preferential activity at the septide-sensitive receptor, then RP 67,580 should act as a competitive antagonist with a pK_B value similar or identical to that measured against septide itself. Of the various peptides for which Schild analysis was performed, this condition was observed only for NKB, in the presence of SR 48,968. In the presence of SR 48,968, not only RP 67,580 but also GR 82,334 and (±)-CP 96,345 antagonized the response to NKB with a rank order of potency (RP 67,580 > GR 82,334 > (±)-CP 96,345) identical to that found towards septide or [Sar^9]SP sulphone.

The antagonist activity of RP 67,580 against SP and NKA was clearly increased after blockade of NK_2 receptors by SR 48,968 but, for both peptides, slopes of the Schild plots were not compatible with competitive antagonism. These findings may indicate the presence of a mixed receptor population, i.e.

the 'classical' NK_1 receptor and the septide-sensitive receptor, SP and NKA having little ability to discriminate between them. Unlike SP, the C-terminal fragments SP(4-11) and SP(6-11) were competitively antagonized by RP 67,580 both in the presence and absence of SR 48,968. This may suggest a lower affinity of C-terminal SP fragments for NK_2 receptor in the rat urinary bladder as compared to SP. Since septide itself is a derivative of the C-terminal sequence of SP, this may suggest a preferential interaction of SP C-terminal residues with the septide-sensitive receptor. However, the affinity of RP 67,580 towards SP(4-11) and SP(6-11) is somewhat intermediate between that found against septide and [Sar^9]SP sulphone, which could suggest an additional effect of the Pro/Gly substitution in position 9 to increase affinity for the septide-sensitive receptor. The limited amounts of NPK and NPγ available to us prevented us from performing a complete analysis of responses to these agonists using various concentrations of RP 67,580. It is interesting to note, however, that the antagonist activity of RP 67,580 against these two elongated forms of NKA was increased after occlusion of NK_2 receptors by SR 48,968. A high affinity interaction of the N-terminally extended forms of NKA with both NK_1 and NK_2 receptors has been reported previously (Takeda & Krause, 1989a,b; van Giersbergen *et al.*, 1992).

Summarizing, it is evident from our analysis that if a septide-sensitive receptor does indeed exist in the rat urinary bladder smooth muscle, distinct from classical NK_1 receptor sites, NKB may be a natural tachykinin endowed with preferential activity at this receptor site. The real question opened by the present findings is whether the pharmacological differences described in this study reflect the existence of a distinct receptor which is preferentially stimulated by septide and NKB and blocked by various NK_1 receptor antagonists, RP 67,580, GR 82,334 and (±)-CP 96,345. At present, no indication for intraspecies heterogeneity of the NK_1 receptor has been documented with the molecular biology approach and, until now, only three tachykinin receptors, corresponding to the classical NK_1, NK_2 and NK_3 classes have been isolated from the mammalian genome (Gerard *et al.*, 1993 for review). While these 'negative' findings do not preclude *a priori* the existence of receptor subtypes or of a fourth type of tachykinin receptor, the lack of evidence from the molecular biology approach calls for a word of caution on this matter.

In particular, recent evidence has shown (Fong *et al.*, 1992b) that the interaction of (±)-CP 96,345 with the NK_1 receptor occurs at recognition sites (epitopes) that are at least partially distinct from those recognizing SP and other agonists. Evidence is also available to indicate that the interaction of NKB with NK_1 receptors could involve a site(s) partially distinct from that of SP (Fong *et al.*, 1992a). These observations raise the possibility that NK_1 receptor antagonists, by acting at sites distinct from those which recognize the agonist(s), prevent the binding of the agonists without physically competing for the same epitopes of the NK_1 receptor protein. If epitopes recognizing septide and NKB compared to [Sar^9]SP sulphone were at least partially distinct, then the NK_1 receptor antagonists might preferentially prevent or disturb the binding of one agonist compared to the other. In this case pharmacological differences could arise from different binding domains of NK_1 receptor agonists and antagonists on a single NK_1 receptor type.

On the other hand, septide is distinctly less potent (about one order of magnitude) than SP in producing an electrophysiological response in *Xenopus* oocytes transfected with the rat NK_1 receptor (Fong *et al.*, 1992b). Moreover, mutation experiments indicate that aminoacids 21–29 in the N-terminal sequence of the rat NK_1 receptor are extremely important for binding of both septide and SP (Fong *et al.*, 1992a). The latter findings suggest that septide and SP may have common recognition sites on the rat NK_1 receptor protein and, consequently, make it more difficult to account for the present results if only one NK_1 receptor exists in the rat bladder.

In conclusion, our findings support the idea, raised by Petitet *et al.* (1992), that the hexapeptide SP analogue septide (Wormser *et al.*, 1986; Laufer *et al.*, 1987) may be an agonist at a class of tachykinin receptors that is distinct from that stimulated by other NK_1 receptor agonists, such as [Sar^9]SP sulphone and that NKB could be a better ligand than SP at this septide-sensitive receptor. However, the possibility that septide and other agonists bind to different epitopes of the NK_1 receptor cannot be excluded on the basis of present findings. The high affinity of both peptide and non peptide NK_1 receptor antagonists for the septide-sensitive receptor in the rat bladder suggests that it may be an NK_1 receptor subtype. Thus both species-related and intraspecies (subtypes) differences should be considered in the pharmacology of the tachykinin NK_1 receptor.

We wish to thank Dr C. Garret, Rhone Poulenc, Vitry, France for the kind gift of RP 67,580 and Dr X. Emonds-Alt, Sanofi Recherche, Montpellier Cedex, France for the kind gift of SR 48,968.

References

ADVENIER, C., ROUISSI, N., NGUYEN, Q.T., EMONDS-ALT, X., BRELIERE, J.-C., NELIAT, G., NALINE, E. & REGOLI, D. (1992). Neurokinin A (NK_2) receptor revisited with SR 48968, a potent non-peptide antagonist. *Biochem. Biophys, Res. Commun.*, **184**, 1418–1424.

ARUNLAKSHANA, O. & SCHILD, H.O. (1959). Some quantitative uses of drug antagonists. *Br. J. Pharmacol. Chemother.*, **14**, 48–58.

BARR, A.J. & WATSON, S.P. (1993). Non-peptide antagonists, CP 96,345 and RP 67,580, distinguish species variants in tachykinin NK_1 receptors. *Br. J. Pharmacol.*, **108**, 223–227.

BURCHER, E. & BUCK, S.H. (1986). Multiple tachykinin binding sites in hamster, rat and guinea-pig urinary bladder. *Eur. J. Pharmacol.*, **128**, 165–177.

DION, S., D'ORLEANS-JUSTE, P., DRAPEAU, G., RHALEB, N.E., ROUISSI, N., TOUSIGNANT, C. & REGOLI, D. (1987). Characterization of neurokinin receptors in various isolated organs by the use of selective agonists. *Life Sci.*, **41**, 2269–2278.

EMONDS-ALT, X., VILAIN, P., PROIETTO, V., VAN BROECK, D., ADVENIER, C., NALINE, E., NELIAT, G., LE FUR, G. & BRELIERE, J.C. (1992). A potent and selective non-peptide antagonist of the neurokinin A (NK_2) receptor. *Life Sci.*, **50**, 101–106.

FONG, T.M., HUANG, R.-R.C. & STRADER, C.D. (1992a). Localization of agonist and antagonist binding domains of the human neurokinin-1 receptor. *J. Biol. Chem.*, **267**, 25664–25667.

FONG, T.M., YU, H., HUANG, R.-R.C. & STRADER, C.D. (1992b). The extracellular domain of the neurokinin-1 receptor is required for high-affinity binding of peptides. *Biochemistry*, **31**, 11806–11811.

FONG, T.M., YU, H. & STRADER, C.D. (1992c). Molecular basis for the species selectivity of the neurokinin-1 receptor antagonist CP 96,345 and antagonist RP 67,580. *J. Biol. Chem.*, **267**, 25668–25671.

FONG, T.M., YU, H. & STRADER, C.D. (1992d). Differential activation of intracellular effector by two isoforms of human neurokinin-1 receptor. *Mol. Pharmacol.*, **41**, 24–30.

GARRET, C., CARRUETTE, A., FARDIN, V., MOUSSAOUI, S., PEYRONEL, J.F., BLANCHARD, J.C. & LADURON, P.M. (1991). Pharmacological properties of a potent and selective nonpeptide substance P antagonist. *Proc. Natl. Acad. Sci. U.S.A.*, **88**, 10208–10211.

GERARD, N.P., BAO, L., XIAO-PING, H. & GERARD, C. (1993). Molecular aspects of the tachykinin receptors. *Regul. Pept.*, **43**, 21–35.

GITTER, B.D., WATERS, D.C., BRUNS, R.F., MASON, N.R., NIXON, J.A. & HOWBERT, J.J. (1991). Species differences in affinities of nonpeptide antagonists for substance P receptors. *Eur. J. Pharmacol.*, **197**, 237–238.

HAGAN, R.M., IRELAND, S.J., BAILEY, F., MCBRIDE, C., JORDAN, C.A. & WARD, P. (1991). A spirolactam conformationally-constrained analogue of physalaemin which is a peptidase resistant, selective NK-1 receptor agonist. *Br. J. Pharmacol.*, **102**, 168P.

HALL, J.M., FLOWERS, J.M. & MORTON, I.K.M. (1992). A pharmacological study of NK_1 and NK_2 tachykinin receptor characteristics in the rat isolated urinary bladder. *Br. J. Pharmacol.*, **107**, 777–784.

HALL, J.M. & MORTON, I.K.M. (1991). Novel selective agonists and antagonists confirm neurokinin NK_1 receptors in guinea-pig vas deferens. *Br. J. Pharmacol.*, **102**, 511–517.

JENKINSON, D.H. (1991). How we describe competitive antagonists: three questions of usage. *Trends Pharmacol. Sci.*, **12**, 53–54.

KAGE, R., LEEMAN, S.E. & BOYD, N.D. (1993). Biochemical characterization of two different forms of the substance P receptor in rat submaxillary gland. *J. Neurochem.*, **60**, 347–351.

KENAKIN, T.P. (1984). The classification of drugs and drug receptors in isolated tissues. *Pharmacol. Rev.*, **36**, 165–222.

LAUFER, R., GILON, C., CHOREV, M. & SELINGER, Z. (1988). Desensitization with a selective agonist discriminates between multiple tachykinin receptors. *J. Pharmacol. Exp. Ther.*, **245**, 639–643.

LEE, C.-M., CAMPBELL, N.J., WILLIAMS, B.J. & IVERSEN, L.L. (1986). Multiple tachykinin binding sites in peripheral tissues and in brain. *Eur. J. Pharmacol.*, **130**, 209–217.

MAGGI, C.A., COY, D.H. & GIULIANI, S. (1992). Effect of [D-Phe^6]bombesin(6-13) methylester, a bombesin receptor antagonist, towards bombesin-induced contractions in the guinea-pig and rat isolated urinary bladder. *J. Auton. Pharmacol.*, **12**, 215–222.

MAGGI, C.A., PARLANI, M., ASTOLFI, M., SANTICIOLI, P., ROVERO, P., ABELLI, V., SOMMA, V., GIULIANI, S., REGOLI, D., PATACCHINI, R. & MELI, A. (1988). Neurokinin receptors in the rat lower urinary tract. *J. Pharmacol. Exp. Ther.*, **246**, 308–315.

MAGGI, C.A., PATACCHINI, R., GIULIANI, S. & GIACHETTI, A. (1993). In vivo and in vitro pharmacology of SR48,968, a non-peptide tachykinin NK_2 receptor antagonist. *Eur. J. Pharmacol.*, **234**, 83–90.

MAGGI, C.A., PATACCHINI, R., QUARTARA, L., ROVERO, P. & SANTICIOLI, P. (1991). Tachykinin receptors in the guinea-pig isolated bronchi. *Eur. J. Pharmacol.*, **197**, 167–174.

MEINI, S., PATACCHINI, R. & MAGGI, C.A. (1993). Tachykinin NK_1 receptor subtypes in the rat urinary bladder. *Br. J. Pharmacol.*, **108**, 177P.

PATACCHINI, R., SANTICIOLI, P., ASTOLFI, M., ROVERO, P., VITI, G. & MAGGI, C.A. (1992). Activity of peptide and non-peptide antagonists at peripheral NK-1 tachykinin receptors. *Eur. J. Pharmacol.*, **215**, 93–98.

PETITET, F., SAFFROY, M., TORRENS, Y., LAVIELLE, S., CHASSAING, G., LOEUILLET, D., GLOWINSKI, J. & BEAUJOUAN, J.C. (1992). Possible existence of a new tachykinin receptor subtype in the guinea-pig ileum. *Peptides*, **13**, 383–388.

SNIDER, R.M., CONSTANTINE, J.W., LOWE III, J.A., LONGO, K.P., LEBEL, W.S., WOODY, H.A., DROZDA, S.E., DESAI, M.C., VINICK, F.J., SPENCER, R.W. & HESS, H.J. (1991). A potent nonpeptide antagonist of the substance P (NK-1) receptor. *Science*, **251**, 435–437.

TAKEDA, Y. & KRAUSE, J.E. (1989a). γ-Preprotachykinin-(72-92)-peptide amide potentiates substance P-induced salivation. *Eur. J. Pharmacol.*, **161**, 267–271.

TAKEDA, Y. & KRAUSE, J.E. (1989b). Neuropeptide K potently stimulates salivary gland secretion and potentiates substance P-induced salivation. *Proc. Natl. Acad. Sci. U.S.A.*, **86**, 392–396.

TOUSIGNANT, C., GUILLEMETTE, G. & REGOLI, D. (1991). Binding sites for [^{3}H][Sar^9,Met(O$_2$)^{11}]substance P in rat brain and guinea pig ileum. *Brain Res.*, **560**, 1–11.

VAN GIERSBERGEN, P.L., SHATZER, S.A., BURCHER, E. & BUCK, S.H. (1992). Comparison of the effects of neuropeptide K and neuropeptide y with neurokinin A at NK_2 receptors in the hamster urinary bladder. *Naunyn-Schmied. Arch. Pharmacol.*, **345**, 51–56.

WARD, P., EWAN, G.B., JORDAN, C.C., IRELAND, S.J., HAGAN, R.M. & BROWN, J.R. (1990). Potent and highly selective neurokinin antagonists. *J. Med. Chem.*, **33**, 1848–1851.

WORMSER, U., LAUFER, R., HART, Y., CHOREV, M., GILON, C. & SELINGER, Z. (1986). Highly selective agonists for substance P receptor subtypes. *EMBO J.*, **5**, 2805–2808.

(Received February 26, 1993
Revised November 8, 1993
Accepted November 12, 1993)

Br. J. Pharmacol. (1994), **111**, 747–752 © Macmillan Press Ltd, 1994

The origin of the effects of an anticholinesterase on the latencies of action potentials in mouse skeletal muscles

[1]S.S. Kelly & C.B. Ferry

Pharmacological Laboratories, Pharmaceutical Sciences Institute, Aston University, Birmingham B4 7ET

1 Subcutaneous injection in mice of a single dose of an organophosphorous anticholinesterase, ecothiopate (0.5 μmol kg^{-1}), produced increased variability in the latency (jitter) of indirectly-elicited action potentials in diaphragm muscles 5 days after treatment, but there was no effect on the variability of latencies of endplate potentials. This study was designed to elucidate the mechanism(s) of the increase in action potential jitter.

2 Action potentials evoked directly by electrical stimulation at one end of muscle fibres and recording near the other end had less jitter than indirectly-evoked action potentials and ecothiopate had no effect on directly-evoked action potentials.

3 In preparations with uncut fibres, pretreatment with ecothiopate reduced by about 20% both muscle fibre input resistance and the amplitude of spontaneous miniature endplate potentials. Ecothiopate had no effect on muscle fibre resting membrane potential or on the threshold potential for excitation.

4 In untreated preparations, indirectly-evoked action potentials recorded at the endplate had similar jitter to action potentials recorded at the tendon when latencies were measured at 10% of peak amplitude. However, when latencies were measured at peak, there was greater jitter of action potentials at the endplate. Ecothiopate increased jitter of action potentials recorded at the endplate at 10% of peak but did not significantly increase jitter of action potentials recorded at the endplate when measured at the peak.

5 In cut-fibre preparations, the first endplate potential of trains was significantly increased after ecothiopate but there was no effect of ecothiopate on the amplitude of plateau endplate potentials later in the train. Analysis of plateau endplate potentials showed that 5 days after administration, ecothiopate produced an increase in the variance of endplate potential amplitudes and changes in the binomial parameters n and p.

6 It was concluded that the increased jitter produced by ecothiopate is not a generalized effect on the plasma membrane and that none of the above observations could explain the increased jitter. The possibility is discussed that increased jitter is produced by variability in times to threshold of endplate potentials and/or by variability in the locus of generation of the action potential in the perijunctional area.

Keywords: Organophosphorous anticholinesterases; action potentials; quantum content; mouse skeletal muscle

Introduction

Experiments reported by Kelly *et al.* (1990) showed that the 'jitter' i.e. the variability of latencies of indirectly-elicited diaphragm muscle action potentials was increased 5 days after administration of a single dose (0.5 μmol kg^{-1}) of ecothiopate, a quaternary organophosphate. Two other anticholinesterase organophosphates also increased jitter, and this effect appeared to be related to the degree and duration of the initial inhibition of acetylcholinesterase, although the increased jitter lasted for several days after acetylcholinesterase activity had returned to control values. Furthermore, later studies (Kelly *et al.*, 1992) also showed that the increased jitter could be reduced or prevented by protection or early reactivation of acetylcholinesterase. This indicates that prolonged inhibition of acetylcholinesterase is at least the initiator of the increased jitter.

In untreated preparations, jitter of endplate potentials and action potential jitter were not different from each other. After ecothiopate, the increased jitter of the action potentials recorded at the tendon end of the muscle fibres was not accompanied by a change in endplate potential jitter. It was concluded that normal jitter in untreated mice was possibly presynaptic in origin, or at least influenced by the endplate potential jitter. However, the increased jitter after ecothiopate was not caused by altered timing of transmitter release but may have originated after the production of the endplate potential and before the arrival of the action potential at the tendon end of the fibre. Increased jitter of muscle action potentials may be produced during generation of the action potentials and/or during their conduction along the muscle fibre. The purpose of this study was to elucidate the origin of the increased jitter produced by ecothiopate.

In order to determine if altered conduction of the action potential along the muscle fibre might contribute to the increased jitter after ecothiopate, action potentials were produced by direct electrical stimulation of the muscle fibre, thus bypassing the process of neuromuscular transmission. In other experiments, indirectly-evoked action potentials were recorded at the endplate region of muscle fibres to determine whether the jitter of these action potentials after ecothiopate was increased similarly to jitter of action potentials near the tendon or was unchanged as with endplate potentials. Evoked endplate potentials were studied in cut-fibre preparations so that any prejunctional changes produced by ecothiopate might be identified. A further investigation was made of the effect of ecothiopate on the safety factor of neuromuscular transmission which might produce an increased jitter by affecting the generation of the action potential in the endplate region.

[1] Author for correspondence at present address: Department of Environmental and Occupational Medicine, The Medical School, University of Newcastle upon Tyne, NE2 4HH.

Methods

The anticholinesterase used was ecothiopate (S-(2-trimethylammoniumethyl)phosphorothioate iodide). Ecothiopate was made up from Phospholine Eyedrops powder (Ayerst). This powder consisted of 12.5 mg ecothiopate and 40 mg potassium acetate, but when dissolved and diluted the amount of potassium injected was negligible (approximately 6.0 μmol kg^{-1}).

Male albino mice aged 6–7 months were used in all experiments. At various times after subcutaneous injection of ecothiopate iodide (0.5 μmol kg^{-1}) with atropine (0.7 μmol kg^{-1}), animals were killed by decapitation. The inclusion of atropine in the injection prevents muscarinic effects caused by inhibition of acetylcholinesterase. The acute toxic effect of a subcutaneous injection of a mixture of atropine sulphate and ecothiopate was fasciculation, which usually began about 20 min after the injection and lasted up to 2 h. During this period animals were able to move around, but usually remained quiet with reduced exploratory behaviour. Dosing was in the morning so that the reduced mobility did not coincide with the normal feeding/activity pattern. None of the many human studies refer to any association of pain with fasciculation after organophosphate poisoning (Heath & Vale, 1992; Johnson & Vale, 1992).

The left hemidiaphragm, together with its phrenic nerve, was rapidly removed from each animal and pinned to Sylgard 184 (Dow Corning) in a Perspex bath through which flowed physiological saline of the following composition (mM): NaCl 137, $NaHCO_3$ 12, NaH_2PO_4 1, KCl 5, $CaCl_2$ 2, $MgCl_2$ 1 and glucose 25. The saline was gassed with a mixture of 95% O_2 and 5% CO_2 and the temperature was maintained at 37.0 ± 0.5°C. The phrenic nerve was stimulated via a suction electrode with supramaximal pulses of 0.05 ms duration. For direct stimulation of the muscle, two silver wires about 0.5 mm apart and embedded in Araldite with only the tips exposed, were used to deliver pulses of duration of 0.2 ms and amplitude twice threshold. For both direct and indirect stimulation the stimulus frequency was 30 Hz.

Glass capillary microelectrodes filled with 3 M KCl were used to record intracellularly resting membrane potentials, action potentials, endplate potentials and spontaneous miniature endplate potentials. When recording action potentials, many pins were used to fix the muscle to the Sylgard and, if necessary, some muscle fibres were cut to minimize muscle movement in response to nerve stimulation. In order to record endplate potentials and to prevent the muscle twitching in response to nerve stimulation, the muscle fibres were cut (Barstad, 1962; Hubbard & Wilson, 1973).

Recording of action potentials

When elicited by nerve stimulation, action potentials were recorded either focally at the endplate or at the end of uncut muscle fibres near the tendon. However, when action potentials were elicited by direct stimulation close to the central tendon of the muscle, recordings were made either close to the costal tendon or close to the endplate region but on the rib side of the endplate. Recordings were made from these two sites in order to detect any incremental changes which might take place during conduction, although at both sites the action potential was conducted through the endplate region. Action potentials were displayed on an oscilloscope and recorded on an FM tape recorder (Racal Store 4) with a tape speed of 30 inches per second (i.p.s.). These recordings were then replayed at 15/16 i.p.s. and were analysed with an analogue-to-digital (AD) converter and a PDP 11/03 minicomputer. With an AD sampling rate of 20 kHz and a record/replay ratio of 32, the effective sampling rate of the recordings was 640 kHz. Trains of 30 action potentials were recorded from each muscle fibre and approximately 10 fibres were sampled from each muscle. Data from a fibre were rejected if, during the train, the resting membrane potential fell by more than 5 mV or the action potential amplitude fell by more than 10%.

Recording of miniature endplate potentials and endplate potentials

Miniature endplate potentials and endplate potentials were recorded on an FM tape recorder and on replay were displayed on an oscilloscope and were analysed on-line using an analogue-to-digital converter and a PDP 11/03 minicomputer. The recording of miniature endplate potentials with a rise-time to amplitude ratio of less than 1.1 ms/mV was the criterion for the focal location of the microelectrode at the endplate. Between 50 and 200 miniature endplate potentials were recorded from each muscle fibre and approximately 10 fibres were sampled from each muscle. The amplitude of spontaneous and evoked endplate potentials was corrected for non-linear summation and to a standard resting membrane potential. In intact fibres the standard resting membrane potential for correction was − 70 mV assuming the reversal potential to be − 15 mV, and in cut fibres the standard resting membrane potential was − 50 mV. The mean amplitude and frequency of miniature endplate potentials were calculated at each end-plate. Martin's correction for non-linear summation (Martin, 1955) was empirically trimmed by a factor of 0.7 in cut fibres so that corrected endplate potential amplitudes would not exceed the reversal potential of − 5 mV in these preparations (McLachlan & Martin, 1981).

Analysis of evoked potentials

Computer programmes were devised which measured the amplitude, time course, and latency of each evoked potential, the latency being the interval between the stimulus and a point on the rising phase at 10% of peak amplitude. Those data were used to calculate (i) the mean consecutive difference of latencies of action potentials 11–30 (plateau) and (ii) individual latencies of the first 16 action potentials with respect to the first action potential of the train. The formula used to calculated the mean consecutive difference was:

$$\text{mean consecutive difference} = [(L_{11}-L_{12}) + (L_{12}-L_{13}) + \ldots(L_{29}-L_{30})]/19$$

Where L_n is the latency of evoked potential number n.

Using the mean consecutive difference as a measure of variability is thought to reduce the effects of any long-term drifts in latency, but might hide any initial changes at the beginning of trains of action potentials (Ekstedt *et al.*, 1974). In our experiments, the initial change is measured as the 'delay' of the sixteenth action potential relative to the first action potential (i.e. latency of sixteenth action potential minus latency of first action potential). Using a pulse generator accurate to 1 in 10^6 (Digitimer) to simulate action potentials at 10 Hz, the value obtained for mean consecutive difference was 2.4 μs, which represents the intrinsic error of the process of record/replay/analysis.

Analysis of miniature endplate potentials and endplate potentials

A train of 50 endplate potentials was recorded from each muscle fibre and the mean amplitude of the last 40 (plateau) endplate potentials was calculated. The mean quantum content of the endplate potentials in each muscle fibre was determined directly by dividing the mean corrected endplate potential amplitude by the mean corrected miniature endplate potential amplitude. The binomial parameters n and p were calculated from amplitudes of miniature endplate potentials and endplate potentials at the plateau (Miyamoto, 1975; McLachlan, 1978). Values were accepted only from data which conformed to binomial statistics. For this reason, the observed and calculated distributions of endplate potential

amplitudes were compared by the Chi-squared test. The equations used to calculate the endplate potential amplitudes expected if the distribution were binomial (Miyamoto, 1975) were incorporated into a computer programme, the validation of which has been described elsewhere (Kelly & Robbins, 1987).

Measurement of input resistance and threshold

Two electrodes were put into the same fibre within 50 μm of each other at the endplate region, detected by the presence of focal miniature endplate potentials, and a hyperpolarizing current of 10^{-8} A was injected through one electrode. The voltage change was recorded through the other electrode, enabling the input resistance to be calculated. To determine the threshold for excitation, a depolarizing current of 5 ms duration was passed and the resting potential and response to depolarization were recorded on a digital storage oscilloscope. The voltage at which the action potential was initiated was taken as the threshold of that fibre.

Statistical analysis

Unless otherwise stated, all results are expressed as mean ± 1 s.d. of values from two to five animals, with the number of muscle fibres in parentheses. To test for significance of differences between groups of data, non-parametric tests were used and differences were taken to be significant if $P<0.05$ (2-tail). For data on jitter, i.e. delay and mean consecutive difference, usually the Kolmogorov-Smirnov test was used as this is more sensitive to changes in the skewness of the distributions under test. Because reciprocal transformation of mean consecutive difference values normalizes its distribution (Baker *et al.*, 1987), the Mann-Whitney test was also applied to groups of mean consecutive difference data thus transformed. Groups of other data were compared by the Mann-Whitney test.

Results

Characteristics of action potentials produced by direct stimulation

The characteristics of directly-evoked action potentials, recorded either close to the costal tendon or more centrally, i.e. closer to the endplate, are shown in Table 1. Treatment with ecothiopate had no effect on the mean consecutive difference or on the delay. The latency of action potentials elicited by direct stimulation usually decreased throughout the early part of the train. This decreased latency may be artefactual, perhaps due to movement of muscle relative to the stimulating electrodes during the contraction, or it may be due to some use-dependent biological phenomenon. With direct stimulation the action potentials recorded near the tendon had a mean consecutive difference significantly less than that recorded after nerve stimulation, irrespective of whether or not the mice had been treated with ecothiopate (see also Table 3 and data of Kelly *et al.*, 1990, their Table 2).

Effect of ecothiopate at the endplate of intact fibres

Five days after treatment with ecothiopate there was a decrease in the amplitude and frequency of miniature endplate potentials and also a decrease in the input resistance of the muscle fibres (Table 2). At this time there was no effect of ecothiopate on the half-decay time of miniature endplate potentials, on resting membrane potential or on the threshold depolarization required to initiate a muscle action potential. The mean amplitude of miniature endplate potentials in ecothiopate-treated fibres was 83% of the value in untreated fibres, and the input resistance at the endplate was similarly decreased to 80% of that of untreated diaphragms. As the resting membrane potential was unaltered and if it were assumed that the reversal potential of the miniature endplate potentials was also unchanged, these results suggest that the reduction in miniature endplate potential amplitude after ecothiopate was due to the smaller input resistance.

Indirectly-evoked action potentials at the endplate

Measuring latencies at 10% of peak amplitude, jitter of endplate potentials and of action potentials recorded at the endplate both measure the variability of latencies of the endplate potential but at different levels. Jitter of action potentials recorded at the endplate at a trigger of 10% would still represent the jitter of the endplate potential, but at a more depolarized trigger level than the usual endplate potential measurements. To measure the jitter of the action potentials at the endplate, the trigger level must be higher than 10%. Records of action potentials at the endplate were analysed twice at two different trigger levels. One was the usual 10% of peak amplitude, the other trigger level was the peak itself; the results are shown in Table 3. In untreated

Table 1 Characteristics of action potentials produced by direct stimulation of the muscle close to the central tendon

	Untreated	*Ecothiopate*
A *Tendon*		
Resting membrane potential (mV)	− 72 ± 6 (27)	− 73 ± 5 (28)
Amplitude (mv)	81 ± 9 (27)	81 ± 7 (28)
Time to peak (μs)	219 ± 32 (27)	213 ± 32 (28)
Mean consecutive difference (μs)	5.6 ± 3.8 (27)*	4.2 ± 1.3 (28)*
Delay (μ)	− 57 ± 50 (27)*	− 70 ± 51 (28)*
B *Central*		
Resting membrane potential (mV)	− 73 ± 5 (18)	− 71 ± 4 (27)
Amplitude (mV)	79 ± 6 (18)	79 ± 8 (27)
Time to peak (μs)	226 ± 12 (18)	231 ± 36 (27)
Mean consecutive difference (μs)	3.8 ± 1.9 (18)	4.5 ± 2.0 (27)
Delay (μs)	− 40 ± 42 (18)	− 24 ± 71 (27)

Stimuli of 0.2 ms duration were twice threshold amplitude; action potentials were recorded either close to the ribs (tendon) or close to the endplate between the endplate and the ribs (central). Values are mean ± 1 s.d., with the number of muscle fibres in parentheses. Ecothiopate (0.5 μmol kg^{-1}) given 5 days before recording had no effect. There was no difference between values in untreated animals and values after ecothiopate. Asterisk indicates value is significantly different from that found with indirect stimulation (see Table 3 and Kelly *et al.*, 1990).

Table 2 Electrophysiological parameters at the endplate in intact muscle fibres 5 days after treatment with ecothiopate (0.5 μmol kg^{-1})

Parameter	*Untreated*	*Ecothiopate*
Resting membrane potential (mV)	− 71 ± 3 (48)	− 71 ± 3 (30)
Miniature endplate potential amplitude (mV)	0.93 ± 0.23 (48)	0.77 ± 0.18 (30)*
Miniature endplate potential half-decay (ms)	1.5 ± 0.3 (48)	1.8 ± 0.5 (30)
Miniature endplate potential frequency (Hz)	4.9 ± 2.4 (48)	2.6 ± 1.3 (30)*
Input resistance (kohm)	627 ± 151 (31)	502 ± 145 (26)*
Threshold (mV)	14.8 ± 2.5 (15)	14.0 ± 1.9 (14)

Values are mean ± 1 s.d., with the number of muscle fibres sampled in parentheses. Asterisk indicates significant difference between value after ecothiopate and value in untreated animals.

Table 3 (**A**) The delay of action potential 16 with respect to the first action potential and (**B**) mean consecutive difference of endplate potentials or action potentials recorded at the endplate or at the tendon with measurement point for analysis of latencies set at 10% of action potential or at its peak

A *Delay* (μs)

		Tendon action potential	*Endplate action potential*	*Endplate potential*
Untreated	10%	32 ± 22 (42)	44 ± 11 (14)	38 ± 16 (17)
	Peak		42 ± 15 (14)	
Ecothiopate	10%	88 ± 74 (24)*	70 ± 25 (28)*	42 ± 15 (24)
	Peak	94 ± 78 (24)	83 ± 36 (28)*	

B *Mean consecutive difference* (μs)

		Tendon action potential	*Endplate action potential*	*Endplate potential*
Untreated	10%	9.9 ± 3.6 (42)	8.1 ± 1.7 (14) †	9.2 ± 3.2 (17)
	Peak		11.6 ± 3.1 (14)	
Ecothiopate	10%	24.7 ± 31.0 (24)*	14.6 ± 7.4 (28)*	8.9 ± 3.2 (24)
	Peak	21.3 ± 16.0 (24)	13.8 ± 4.7 (28)*	

Values are mean ± 1 s.d. with the number of muscle fibres in parentheses. Asterisk indicates significant difference between values in untreated animals and after ecothiopate (0.5 μmol kg^{-1}). †Value at peak different from the value at 10% trigger level.

Table 4 Neuromuscular transmission in cut fibres 5 days after treatment with ecothiopate (0.5 μmol kg^{-1})

Parameter	*Untreated*	*Ecothiopate*
Resting membrane potential (mV)	− 51 ± 3 (32)	− 50 ± 3 (26)
Miniature endplate potential amplitude (mV)	0.53 ± 0.16 (32)	0.49 ± 0.16 (26)
Miniature endplate potential half-decay time (ms)	0.78 ± 0.19 (32)	0.94 ± 0.38 (26)
First endplate potential amplitude (mV)	25.6 ± 10.1 (32)	35.9 ± 10.8 (26)*
Plateau endplate potential amplitude (mV)	17.5 ± 6.1 (32)	20.1 ± 6.2 (26)
Plateau endplate potential variance	1.6 ± 1.3 (32)	4.6 ± 5.4 (26)*
Ratio $\frac{\text{Plateau endplate potential}}{\text{First endplate potential}}$	0.70 ± 0.08 (32)	0.56 ± 0.07 (26)*
Plateau direct m	35 ± 12 (32)	43 ± 15 (26)
Plateau binomial m	35 ± 12 (27)	44 ± 15 (24)
Plateau binomial n	41 ± 15 (27)	63 ± 20 (24)*
Plateau binomial p	0.86 ± 0.08 (27)	0.71 ± 0.15 (24)*

Endplate potentials were elicited at 30 Hz. Values are mean ± 1 s.d., with the number of muscle fibres sampled in parentheses. Asterisk indicates significant difference between value after ecothiopate and in untreated animals.

preparations the mean consecutive difference, (but not delay) was greater at the peak than at 10% of peak. At both trigger levels after ecothiopate the delay was greater than in controls, and there was no difference between values at the two trigger levels. Ecothiopate produced an increase in mean consecutive differences measured at 10% of peak but no significant increase when measured at the peak and after ecothiopate there was no longer a difference between mean consecutive differences at the two trigger levels.

Statistics of transmitter release

Cutting the muscle fibres to prevent the generation of action potentials also halved the half-decay time of miniature end-

plate potentials compared with uncut fibres in both untreated and ecothiopate-treated preparations. Five days after treatment with ecothiopate there was no significant change in the half-decay time of miniature endplate potentials in cut fibres. After recording a sample of miniature endplate potentials, the nerve was stimulated at 30 Hz and the resulting train of endplate potentials was recorded. The amplitude of these endplate potentials ran down to a plateau of 0.5–0.7 of the first endplate potential. The mean amplitude of plateau endplate potentials after ecothiopate was not different from that in untreated preparations, but the variance of the plateau endplate potentials was significantly greater after ecothiopate treatment. The results of these experiments are summarised in Table 4. After ecothiopate there was an increase in the amplitude of the first endplate potential of trains and of the tetanic run-down i.e. the ratio of plateau endplate potential to first endplate potential. The distribution of the amplitudes of the plateau endplate potentials was binomial in the majority of the fibres from which records were made in untreated mice and after ecothiopate. After ecothiopate, the binomial parameters n and m were increased and the value of p was reduced.

Discussion

Five days after ecothiopate there was a large increase in jitter of indirectly-evoked action potentials 11 to 30 recorded near the tendon and in the delay of action potential number 16 relative to the first action potential of trains. Ecothiopate had no effect on the jitter or delay of endplate potentials, so altered latency of transmitter release is ruled out as a source of the increased jitter. Other possible causes of increased jitter might be altered conduction along the muscle fibre, altered muscle membrane characteristics or a decreased safety factor of neuromuscular transmission. The observation that in untreated preparations the mean consecutive difference of directly-evoked action potentials was less than that of indirectly-evoked action potentials indicates that much of the jitter can be attributed to the process of neuromuscular transmission.

There was no effect of ecothiopate on the conduction of directly-elicited action potentials along the muscle fibre, even though the action potential had to pass through the endplate region before reaching the recording electrode. Therefore, the increased jitter produced by ecothiopate is not caused by a general effect on the plasma membrane of the muscle fibre and it is concluded that the increased jitter did not originate from some persistent defect in action potential conduction.

Although ecothiopate has no effect on the delay of endplate potentials, it may be that the increased rundown of the endplate potential amplitude at the beginning of trains contributes to the increased delay of action potentials after ecothiopate. This is because smaller endplate potentials would excite nearer their peak than would larger endplate potentials. Furthermore, ecothiopate does have some prejunctional effects which might influence the jitter of indirectly-evoked muscle action potentials. For example, the quantum content of plateau endplate potentials and their calculated binomial parameters were altered by ecothiopate. This effect of ecothiopate on binomial characteristics could not have been due to an acute anticholinesterase effect because adding ecothiopate to cut fibre preparations *in vitro* had no effect on binomial parameters (Ferry & Kelly, 1988).

The effectiveness of endplate potentials in exciting action potentials can be assessed by the safety factor for transmission. The safety factor can be expressed as the amplitude of endplate potential divided by the threshold depolarization, both corrected for non-linear summation. In these experiments, the resting membrane potentials, the threshold and the mean amplitude of plateau endplate potentials were not different after ecothiopate. This indicates no change in the mean safety factor. However, in the context of the timing of excitation, it may be the variation in safety factor for individual endplate potentials that is important.

Although the overall mean amplitude of plateau endplate potentials recorded in fibres from animals treated with ecothiopate was not different from that in untreated animals (Table 4), the variance of endplate potential amplitude at the plateau in individual fibres was significantly increased after ecothiopate. Thus after ecothiopate the amplitude of successive plateau endplate potentials in a train had a greater variability, which might contribute to an increased jitter, especially if the bottom end of the range of endplate potential amplitudes were extended. However, close inspection and analysis of the data did not show any increase in the proportion of lower-amplitude endplate potentials after ecothiopate.

In whole (i.e. uncut) muscle fibres, the initial (subthreshold) portion of a potential recorded at the endplate will be the rising phase of the endplate potential which will then give rise to an action potential. Calculating jitter of action potentials at the endplate at 10% of peak might, therefore, be expected to give similar results to measuring endplate potential jitter, and in control preparations this was found to be true (Table 3). However, the jitter at the peak of the action potential at the endplate is greater than the jitter at 10% of peak. This indicates that much of the jitter at the peak of action potentials at the endplate in untreated fibres must originate in their excitation. Furthermore, latencies were measured at 10% of the peak amplitude of the endplate potential, i.e. about 2 mV and near the resting membrane potential. For an action potential at the endplate, the measurement point (10% of peak) is about 8–10 mV, i.e. on the rising phase of the endplate potential about half way between the resting membrane potential and the threshold depolarization. If the rise-time of the response varied, then the value of the latency would depend upon the point on the response at which the latency is measured. This may be the reason why after ecothiopate, the jitter of action potentials recorded at the endplate is greater than the jitter of endplate potentials.

Jitter measured at the peak of the action potentials recorded at the endplate was not further increased after ecothiopate, despite an increase in mean consecutive difference at 10% trigger level by some 6 μs, which suggests that ecothiopate had no effect. However, the rise time of untreated action potentials measured from trigger at 10% peak to the peak was 234 ± 37 μs (20) and although this was not different from after ecothiopate, 244 ± 35 μs (29), these values are such that the moderate increase of latency represented by a mean consecutive difference increased by 6 μs is likely to be contained in the variance of the rise time after ecothiopate.

The concept of a varying safety factor for transmission, which relates amplitude of endplate potentials and threshold has so far been discussed in terms of varying endplate potentials and constant threshold. However, variation in the threshold for action potential generation would also be expected to result in jitter, as suggested by Stalberg & Trontelj (1979). Thus the timing of excitation of action potentials would depend on interaction of endplate potentials of variable amplitude with a possibly variable threshold. We have not attempted to measure variations in threshold which might occur over time periods as short as a few milliseconds.

Another possible explanation of the increased jitter of action potentials after ecothiopate is that, due to acetylcholine (ACh) action, there may be variation in the velocity of conduction of action potentials in the locus of excitation. Furthermore, the locus of generation of the action potential may vary between stimuli. The repetitive muscle action potentials after acute intoxication with ecothiopate are generated ectopically from the prolonged endplate potential and after a single stimulus the excitability of the postjunctional membrane is reduced for several tens of milliseconds (Ferry, 1988). To what extent this applies 5 days after ecothiopate and with trains at 30 Hz is unknown, but repetitive firing was recorded in about 20% of fibres (Kelly *et al.*, 1990), so this is admissible for consideration. Although the reduction of input

resistance at the endplate indicates a change there in the length constant of the membrane, this did not affect conduction along the fibre after direct stimulation.

In conclusion increased jitter of indirectly-evoked action potentials after ecothiopate is not caused by either changes in latency or transmitter release or by changes in the conduction of action potentials along the muscle fibre. The increased mean consecutive difference is probably caused by alterations in the process of generation of the action potential at the endplate. This increased variability of excitation at the endplate may be due to an increased variability of time to threshold after ecothiopate and/or it may involve changes in the locus of generation of the action potential. There may also be a postsynaptic component such as variation of threshold for excitation, which may itself depend upon ACh action. If the threshold were influenced by the immediate history of transmitter action, it may be that with stimulation at 30 Hz, a slight degree of inhibition of functional acetylcholinesterase may become important. Experiments to investigate the possibility that the locus of excitation or the velocity of propagation away from the perijunctional region may change throughout the train may further elucidate the mechanism(s) by which ecothiopate produces increased jitter of indirectly-elicited action potentials.

References

BAKER, D.J., CROSS, N.L. & SEDGWICK, E.M. (1987). Normality of single fibre electromyographic jitter: a new approach. *J. Neurol. Neurosurg. Psychiatry*, **50**, 471–475.

BARSTAD, J.A.B. (1962). Presynaptic effect of neuromuscular transmitter. *Experientia*, **18**, 579–581.

EKSTEDT, J., NILSSON, G. & STALBERG, G. (1974). Calculation of the electromyographic jitter. *J. Neurol. Neurosurg. Psychiatry*, **37**, 526–539.

FERRY, C.B. (1988). The origin of the anticholinesterase-induced repetitive activity of the phrenic nerve-diaphragm preparation of the rat *in vitro*. *Br. J. Pharmacol.*, **94**, 169–179.

FERRY, C.B. & KELLY, S.S. (1988). The nature of the presynaptic effects of (+)-tubocurarine at the mouse neuromuscular junction. *J. Physiol.*, **403**, 425–437.

HEATH, A.J.W. & VALE, J.A. (1992). Clinical presentation and diagnosis of acute organophosphate insecticide and carbamate poisoning. In *Clinical and Experimental Toxicology of Organophosphates and Carbamates*. ed. Ballantyne, B. & Marrs, T.C. pp. 513–519. Oxford: Butterworth-Heinemann.

HUBBARD, J.I. & WILSON, D.F. (1973). Neuromuscular transmission in a mammalian preparation in the absence of blocking drugs and the effect of d-tubocurarine. *J. Physiol.*, **228**, 307–325.

JOHNSON, M.K. & VALE, J.A. (1992). Clinical management of acute diagnosis of acute organophosphate poisoning: an overview. In *Clinical and Experimental Toxicology of Organophosphates and Carbamates*. ed. Ballantyne, B. & Marrs, T.C. pp. 528–535. Oxford: Butterworth-Heinemann.

KELLY, S.S., FERRY, C.B. & BAMFORTH, J.P. (1990). The effects of anticholinesterases on the latencies of action potentials in mouse skeletal muscles. *Br. J. Pharmacol.*, **99**, 721–726.

KELLY, S.S., FERRY, C.B., BAMFORTH, J.P. & DAS, S.K. (1992). Protection against the effects of anticholinesterases on the latencies of action potentials in mouse skeletal muscles. *Br. J. Pharmacol.*, **107**, 867–872.

KELLY, S.S. & ROBBINS, N. (1987). Statistics in neuromuscular transmitter release in young and old mouse muscle. *J. Physiol.*, **385**, 507–516.

MCLACHLAN, E. (1978). The statistics of transmitter release at chemical synapses. *Int. Rev. Physiol.*, **17**, 49–117.

MCLACHLAN, E.M. & MARTIN, A.R. (1981). Non-linear summation of end-plate potentials in the frog and mouse. *J. Physiol.*, **311**, 307–324.

MARTIN, A.R. (1955). A further study of the statistical composition of the endplate potential. *J. Physiol.*, **130**, 114–122.

MIYAMOTO, M.D. (1975). Binomial analysis of quantal transmitter release at glycerol treated frog neuromuscular junctions. *J. Physiol.*, **250**, 121–142.

STALBERG, E. & TRONTELJ, J.V. (1979). *Single Fibre Electromyography*. Old Woking, Surrey: The Miravelle Press.

(Received July 20, 1993
Revised November 1, 1993
Accepted November 12, 1993)

Br. J. Pharmacol. (1994), **111**, 753–758 © Macmillan Press Ltd, 1994

Reduction by intracellular calcium chelation of acetylcholine secretion without occluding the effects of adenosine at frog motor nerve endings

[1]J.M. Hunt, R.S. Redman & [2]E.M. Silinsky

Department of Pharmacology, Northwestern University Medical School, 303 E. Chicago Avenue, Chicago, Illinois 60611, U.S.A.

1 The calcium chelators *bis*-(aminophenoxy)ethane-tetraacetic acid (BAPTA) or dimethyl-BAPTA (DMBAPTA) were introduced into the cytoplasm of frog motor nerve endings by use of the AM loading technique. The effects of intracellular Ca^{2+} chelation were studied on quantal acetylcholine (ACh) release and on the action of adenosine.

2 Intracellular BAPTA or DMBAPTA prevented the increases in quantal ACh secretion normally evoked by caffeine.

3 Intracellular DMBAPTA decreased the number of ACh quanta released by individual nerve impulses and virtually eliminated the fast phase of facilitation in response to paired nerve impulses.

4 Adenosine reduced both spontaneous and evoked secretion of ACh quanta with its usual potency and efficacy in the presence of intracellular DMBAPTA. Adenosine had no significant effect on facilitation.

5 The results, which suggest that adenosine and intracellular DMBAPTA reduce ACh secretion by different mechanisms, are consistent with the hypothesis that adenosine inhibits ACh release by reducing the ability of Ca^{2+} to promote ACh secretion from frog motor nerve endings.

Keywords: Neurotransmitter release; frog neuromuscular junction; adenosine; BAPTA; DMBAPTA; calcium

Introduction

The neuromodulator, adenosine, has been shown to inhibit neurotransmitter release in both the central and peripheral nervous systems (for reviews see Phillis, 1985; Ribeiro & Sebastiao, 1986; Fredholm & Dunwiddie, 1988; Silinsky, 1989). Exogenous adenosine reduces both the rate of spontaneous secretion of single acetylcholine (ACh) quanta, and the number of ACh quanta synchronously released by an action potential to approximately 50% of the control value at the neuromuscular junctions of the rat (Ginsborg & Hirst, 1972), and frog (Silinsky, 1980; 1984). To produce this decrease in ACh secretion, adenosine must be either reducing the amount of secretion triggered by a given amount of Ca^{2+} or reducing the amount of Ca^{2+} available to trigger secretion. Previous results suggest that adenosine inhibits ACh secretion in frog without reducing Ca^{2+} influx through voltage-dependent Ca^{2+} channels (Silinsky, 1981, 1984; Silinsky & Solsona, 1992; Hunt & Silinsky, 1993). We have now investigated the possibility that adenosine reduces the amount of cytoplasmic Ca^{2+} available to trigger secretion by increasing the rate at which Ca^{2+} is removed from the cytoplasm adjacent to the active zone.

If adenosine inhibits evoked ACh release by increasing Ca^{2+} clearance, it would be expected to diminish both the peak and duration of the local Ca^{2+} concentration change at the secretory apparatus. This would lead to a decrease in the number of ACh quanta released by a nerve impulse and a reduction in the fast phase of facilitation, which is thought to depend on residual Ca^{2+} (Katz & Miledi, 1968; Silinsky, 1985; Kijima & Tanabe, 1988; Bain & Quastel, 1992).

The Ca^{2+} chelator *bis*-(aminophenoxy)ethane-tetraacetic acid (BAPTA) (Tsien, 1980), or its dimethyl derivative (DMBAPTA) when introduced into nerve terminal cytoplasm, has been shown to reduce the fast phase of facilitation (Kijima & Tanabe, 1988; Tanabe & Kijima, 1988; Robitaille & Charlton, 1990; 1992), the number of ACh quanta released synchronously (Robitaille & Charlton, 1992), and the frequency of occurrence of spontaneous quantal events (Kijima & Tanabe, 1988). These effects are identical to what would be expected for an increase in the rate of Ca^{2+} clearance, and suggest that intracellular BAPTA derivatives are able to compete successfully with cytosolic Ca^{2+} binding proteins (see Blaustein, 1988) and decrease cytoplasmic free Ca^{2+} more rapidly than the endogenous mechanisms (Robitaille & Charlton, 1992). Thus, if adenosine is increasing the rate at which Ca^{2+} is removed from the cytoplasm adjacent to the active zone, its effects should be occluded by intracellular BAPTA derivatives.

In this paper, we describe the effects of introducing BAPTA derivatives into the cytoplasm of frog nerve terminals and the interaction of DMBAPTA with adenosine. Some of these results have been presented previously as an abstract (Hunt & Silinsky, 1989).

Methods

General

Cutaneous pectoris nerve-muscle preparations of the frog *Rana pipiens* were dissected and superfused with flowing Ringer solution. Supramaximal stimulation pulses were delivered to the nerve supply through a suction electrode. Intracellular recordings were made at endplate regions by use of glass microelectrodes filled with 3 M KCl and with resistances of 8–25 Mohms. Signals from the microelectrode were fed into a conventional high input impedance preamplifier, the output of which was delivered to an oscilloscope, a microcomputer for on-line data collection (coupled through a TL-1 DMA interface, Axon Instruments Inc.) and an Indec IR-2 Instrumentation Recorder for further analysis if needed.

Evoked ACh release in response to individual nerve impulses (endplate potentials, e.p.ps), were recorded on line and later analyzed with the pCLAMP software package (Axon

[1] Present address: Department of Neurobiology, Duke University Medical Center, Durham, NC 27706.
[2] Author for correspondence.

Instruments, Inc). Spontaneous quantal events (miniature endplate pontentials, m.e.p.ps) were recorded on line and later analyzed with the Axotape software package (Axon Instruments, Inc.).

Measurement of quantal ACh release and facilitation

The mean number of ACh quanta released synchronously by a nerve impulse, i.e. mean quantal content (m), was calculated by one of the following two methods: (1) the direct method, namely, the ratio of the mean computer averaged e.p.p. amplitude to the mean m.e.p.p. amplitude (Del Castillo & Katz, 1954), or (2) the method of failures, when levels of release are low enough for Poisson statistics to apply (Del Castillo & Katz, 1954). In some experiments both methods were used and gave comparable results (see e.g. Figure 3). The experimental protocol for most experiments was to deliver a pair of stimuli (interstimulus interval 20 ms) to the nerve at the rate of one pair per second. This protocol allowed both quantal content (m in response to the first stimuli) and the fast phase of facilitation (m in response to the second stimulus/m in response to the first stimuli) to be measured simultaneously. M.e.p.p. frequency was determined by continuously monitoring membrane potential and counting the number of m.e.p.ps per second. As neither DMBAPTA nor adenosine changed m.e.p.p. amplitudes (Silinsky, 1984 and Results), inhibitory effects of these agents on e.p.p. amplitudes reflect the presynaptic inhibitory action of these agents on ACh release.

The statistical procedures are identical to those described previously (see Silinsky, 1984). In most instances, appropriate averaging techniques were used to make statistically significant differences at $P<<0.01$ (see Silinsky 1984). In instances where significance was at the $P<0.05$ level, this is stated within the text. Mean values presented in the text are ± 1 standard error of the mean.

Loading of BAPTA derivatives

The active Ca^{2+} chelating forms of BAPTA derivatives are not membrane permeable and frog motor nerve terminals are too small to microinject these Ca^{2+} chelators. Therefore, we used the AM loading procedure to introduce BAPTA and DMBAPTA into the nerve terminal cytoplasm (Tsien, 1981). In this procedure the nerve terminal was exposed to a solution containing the acetoxymethyl ester of BAPTA (BAPTA-AM) or DMBAPTA (DMBAPTA-AM) which is able to cross the plasma membrane. These AM compounds diffuse into the cell, but upon entering the cytoplasm the acetoxymethyl esters are removed by non-specific esterases, trapping the Ca^{2+} chelating form of the BAPTA derivative within the cytoplasm.

We experimented with two protocols for loading BAPTA derivatives into the nerve terminal cytoplasm. The first protocol was a modification of the procedure of Tanabe & Kijima (1988). Immediately following dissection, we placed the preparation in a beaker containing 25 ml of normal Ringer solution. A mixture of BAPTA-AM and dimethylsulphoxide (DMSO) was then added, to produce final concentrations of 100 μM BAPTA-AM and 0.2% v/v DMSO. The preparation was maintained in this solution for 1 h in darkness before beginning any electrophysiological procedures. This protocol, while apparently effective in loading BAPTA into the nerve terminal (see Figure 1), generally resulted in a preparation which could not generate action potentials in response to nerve stimulation (J.M.H., unpublished). Upon addition of BAPTA-AM, a white precipitate formed which apparently damaged the preparation. Increasing the concentration of DMSO to 1% v/v, and sonication of the BAPTA-AM solution was not sufficient to solubilize the BAPTA-AM completely.

As it was our purpose to examine the effect of Ca^{2+}-chelation by BAPTA derivatives whilst maintaining microelectrode impalements, we abandoned this protocol in most experiments in favour of the protocol of Robataille & Charlton (1992), in which DMBAPTA-AM was used to chelate cytoplasmic calcium. DMBAPTA has a slightly greater affinity for Ca^{2+} than BAPTA (Robataille & Charlton, 1992). In this protocol, the preparation was superfused with 25 μM DMBAPTA-AM. After 20–30 min of continuous superfusion with 25 μM DMBAPTA-AM, the decreases in e.p.p. amplitude and facilitation reach a plateau (Robataille & Charlton, 1992) indicating that further increases in the concentration of DMBAPTA within the nerve terminal have little effect on the localized, transient Ca^{2+} influx which triggers ACh secretion. Whilst most of the experiments focussed on the effects of DMBAPTA, both BAPTA and DMBAPTA protocols were employed to study the effects of adenosine after Ca^{2+} chelation (see Results). An equal concentration of DMSO was routinely included in all solutions to avoid any solvent effects.

To assess effective Ca^{2+} buffering by BAPTA derivatives, we used one or both of the following electrophysiological indices: (see Results): (1) the occlusion of the effects of caffeine on m.e.p.p. frequency by BAPTA derivatives (Figure 1) and/or (2) the virtual elimination of facilitation after exposure to DMBAPTA (Figure 2).

Solutions

Normal frog Ringer contained (mM): NaCl 115, KCl 2, $CaCl_2$ 1.8, $NaHCO_3$ 1.8, and HEPES buffer 2 (pH 7.2–7.4) and was used in the majority of experiments. In most experiments reduced Ca^{2+} Ringer was used to control the level of ACh release. Reduced Ca^{2+} Ringer contained 0.9 mM $CaCl_2$ and 9 mM $MgCl_2$, and 1 mg l^{-1} neostigmine methylsulphate. Chemicals were purchased from Sigma Chemicals (St. Louis MO, U.S.A.) with the exception of BAPTA-AM and DMBAPTA-AM which were purchased from Molecular Probes (Eugene OR, U.S.A.). Stock solutions of BAPTA-AM and DMBAPTA-AM were prepared in DMSO, divided into aliquots, and frozen until their use.

Results

BAPTA-derivatives buffer caffeine-induced Ca^{2+} release

Intracellular BAPTA derivatives have been shown to block processess stimulated by the release of Ca^{2+} from intracel-

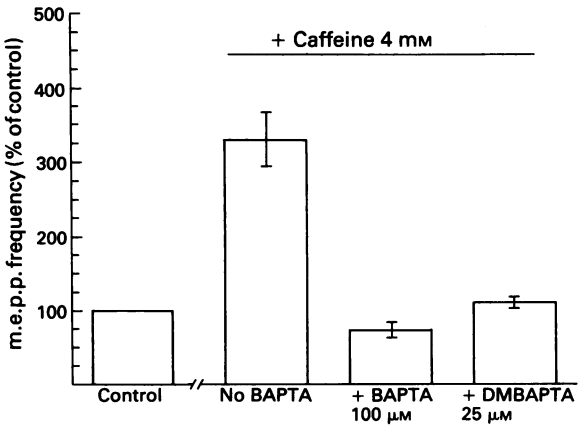


Figure 1 Intracellular BAPTA derivatives buffer the Ca^{2+} released from intracellular stores by 4 mM caffeine. Preparations were pretreated with no BAPTA-AM ($n=9$), 100 μM BAPTA-AM for 60 min ($n=4$ – for protocol see methods), or superfused with 25 μM DMBAPTA-AM for approximately 30 min ($n=5$) prior to exposure to caffeine.

lular storage sites (see e.g., Silver, 1989). We thus reasoned that intracellular BAPTA should be able to block the increase in m.e.p.p. frequency due to a caffeine-stimulated release of Ca^{2+} from intracellular storage sites (Onodera, 1973; Neering & McBurney, 1984; Silinsky, 1984). Figure 1 demonstrates that intracellular BAPTA or DMBAPTA is indeed able to buffer the Ca^{2+} released by 4 mM caffeine. Similarly, ACh secretion evoked by 4 mM caffeine has been shown to be reduced in the presence of TMB-8 (Hunt *et al.*, 1990), which is thought to block the uptake and release of Ca^{2+} from intracellular stores. Based on these results we established one criterion for effective loading of the calcium chelator; if, at the end of an experiment, the m.e.p.p. frequency did not increase by more than 50% when the preparation was exposed to 4 mM caffeine, then the motor nerve ending Ca^{2+} concentration was considered to be suitably buffered by BAPTA or DMBAPTA. (The other criterion was the complete elimination of facilitation by DMBAPTA-see below and methods). Figure 1 also supports previous results (Robataille & Charlton, 1992), suggesting that the degree of intracellular Ca^{2+} chelation using the DMBAPTA superfusion method compares favourably with the BAPTA-AM loading protocol, which does not allow for continuous monitoring of the electrophysiological correlates of ACh release during the experiment (see methods). Consequently, the remaining experiments were all carried out using continuous superfusion with DMBAPTA whilst maintaining the microelectrode impalement throughout the course of the experiment.

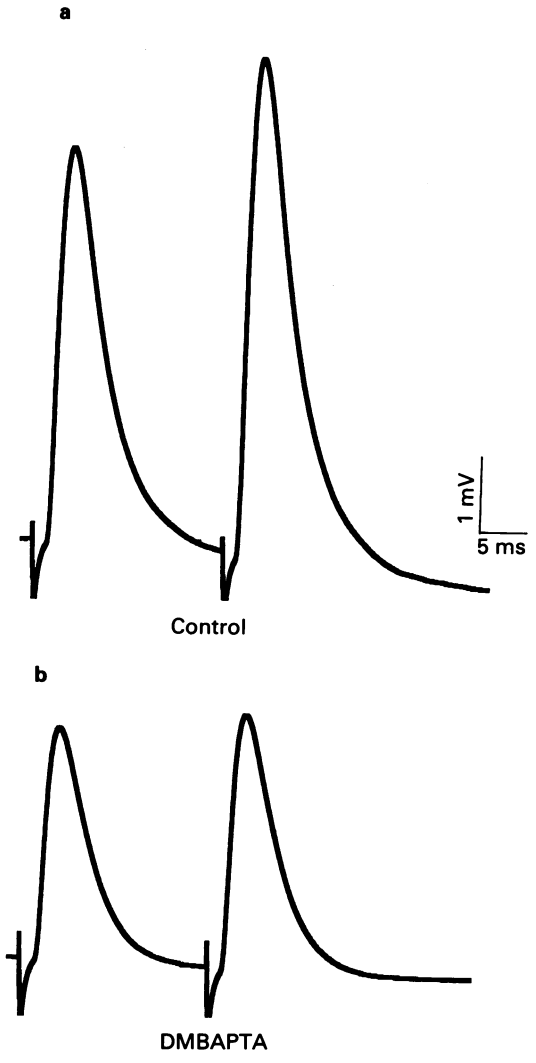


Figure 2 Typical effect of DMBAPTA (25 μM) on evoked ACh release (e.p.ps) and facilitation. The motor nerve was stimulated with a rapid pair of stimuli (interstimulus interval 20 ms) repeated at a frequency of 1 Hz. E.p.ps in this and in the remaining figures represent the average of 64 stimuli. As m.e.p.p. amplitudes were unchanged by DMBAPTA, changes in e.p.p. amplitudes accurately reflect the effect of this Ca^{2+} chelator on evoked ACh release. Note the reduction evoked ACh release (first e.p.p. in a and b) to 58% of the control (a) after DMBAPTA (b). Facilitation of the e.p.p. was reduced from 1.23 (a) to 1.06 (b) by DMBAPTA, a virtual elimination of the facilitatory process. Calibration bars apply to all four records. For further details see text.

Intracellular DMBAPTA reduces neurally-evoked ACh secretion and effectively eliminates facilitation

Figure 2a illustrates the typical control response to two closely-spaced stimuli (50 Hz) in low Ca^{2+}, high Mg^{2+} Ringer prior to the addition of DMBAPTA-AM (average response to 64 stimuli). Note the facilitation of the second e.p.p. in the control condition. Twenty minutes after superfusion with 25 μM DMBAPTA-AM, the amplitude of the first e.p.p. (and e.p.p. quantal content) decreased to 58% of the control level and facilitation was virtually eliminated (Figure 2b). This result was typical of seven experiments using the paired-pulse protocol for facilitation shown in Figure 2 (see also Figure 4). The mean percentage decrease in e.p.p. produced by DMBAPTA treatment was 63% ± 2.8% of the control value (the range was from 52% to 73% of control). Control facilitation, quantified as the ratio of amplitudes of the facilitated to the control e.p.p. (1.34 ± 0.02, $n = 10$) was reduced to 1.02 ± 0.01 (where 1 = no facilitation).

An experiment in which facilitation was especially dramatic (greater than 10 fold, Figure 3) further demonstrated the high buffering capacity of DMBAPTA. In addition, this experiment revealed a decrease in m.e.p.p. frequency concomitant with the presynaptic inhibitory effects of BAPTA on evoked ACh release (much as is seen with adenosine). As the mean amplitude of the m.e.p.p. remained at approximately 1 mV for the duration of this experiment (see legend to Figure 3), the average e.p.p. amplitude in Figure 3 is approximately equal to the average number of quanta of ACh released. In the experiment of Figure 3, we studied the facilitatory response to three consecutive stimuli (50 Hz, one series of three stimuli delivered each second). As shown in Figure 3a, the first control e.p.p. was of very low quantal content ($m \approx 0.04$). The second response was an order of magnitude larger ($m = 0.55$), representing a 12.4 fold facilitation of evoked ACh release in this experiment. Within 10 min after the beginning of superfusion with DMBAPTA (Figure 2b), m of the first e.p.p. was diminished and all detectable facilitation of the second e.p.p. was eliminated ($m \approx 0.02$ for both e.p.ps). The amplitude of the third e.p.p. was reduced to 55% of the control level by DMBAPTA (see figure legend for further details). The m.e.p.p. frequency in this cell was inhibited to 56% of the control value by DMBAPTA. These effects of DMBAPTA in inhibiting evoked and spontaneous ACh release are similar to the effects of near maximal concentrations of adenosine, showing that DMBAPTA is capable of mimicking the effects of exogenous adenosine (see Introduction and Silinsky, 1984).

Interactions of DMBAPTA and adenosine

The results thus far suggest that DMBAPTA can compete with the normal intracellular Ca^{2+} buffering mechanisms and decrease local subplasmalemmal Ca^{2+} concentrations more rapidly than endogenous buffering systems. If adenosine and BAPTA derivatives are sharing a common mode of action, then inhibition of ACh release by DMBAPTA derivatives should at least partially occlude the effects of adenosine. Furthermore, if adenosine is capable of rapidly removing Ca^{2+} that has entered in response to a previous nerve impulse, then this purine might be expected to reduce facilita-

tion of ACh release. Figures 4 and 5 show that none of these predictions was borne out.

Figure 4 illustrates the effects of 20 μM adenosine prior to and during treatment with DMBAPTA. Note that in the absence of DMBAPTA, 20 μM adenosine (Figure 4b) reduces ACh to 63% of the control level (Figure 4a) without affecting facilitation of ACh release (control facilitation, 1.38; facilitation in adenosine, 1.41). In contrast, in the same cell, DMBAPTA treatment reduced the amplitude of the first e.p.p. to a similar value to that produced by adenosine in the absence of DMBAPTA, yet completely eliminated facilitation (Figure 4c). Finally, 20 μM adenosine produced a similar percentage inhibition of ACh release in the presence of DMBAPTA (60%, Figure 4d) as was observed before treatment with this calcium chelator.

Figure 5 illustrates dose-response curves for adenosine made prior to (a) and after treatment with DMBAPTA (b). Note that in Figure 5c, the first e.p.ps of the pairs recorded after DMBAPTA treatment are scaled upwards to the control level for comparison of the potency and efficacy of adenosine in the two conditions. In this and in five other experiments, DMBAPTA inhibited ACh release without

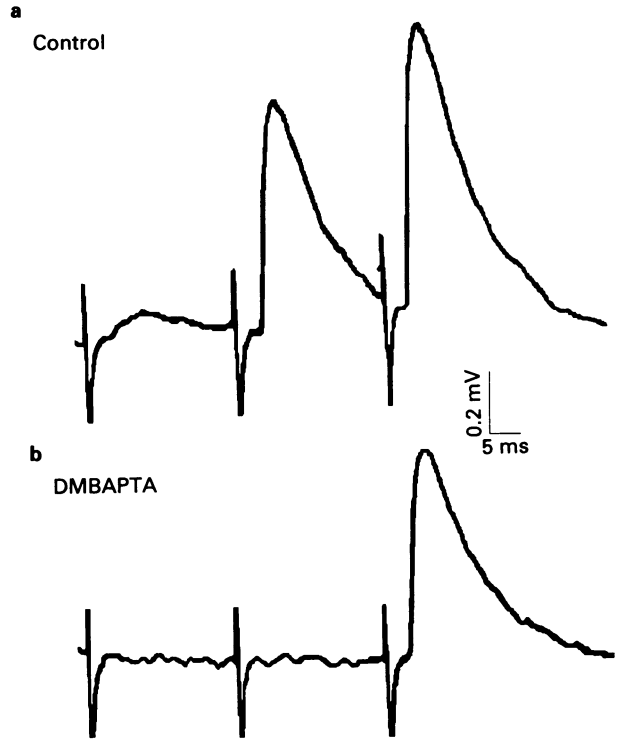


Figure 3 Effect of DMBAPTA (25 μM) on evoked ACh release (e.p.ps) and facilitation in a cell particularly sensitive to the buffering action of DMBAPTA. The mean amplitude of the m.e.p.p. in the control condition was 1.01 ± .05 mV ($n = 54$) and 30 min after DMBAPTA 1.01 ± 0.04 ($n = 32$). In this experiment, the facilitatory response to three consecutive stimuli (50 Hz, one series of three stimuli derived each second) was examined. In (a), the first e.p.p. was of very low quantal content (m≈0.046 by the method of failures; m∼0.043 by the direct method, $n = 192$ stimuli). The facilitation of the second response (m = 0.55, direct method, $n = 192$ stimuli) was 12.4. The facilitation between the second and third response in this cell was 1.8. As (b) shows, within 10 min after the beginning of superfusion with DMBAPTA, all detectable facilitation of the second e.p.p. was eliminated, (m∼0.02 for both e.p.ps). The amplitude of the third e.p.p. was reduced to 55% of the control level by DMBAPTA. M.e.p.p. frequency in this cell was reduced from 2.3 ± 0.25 s^{-1} ($n = 23$ s) to 1.28 ± 0.20 s^{-1}, ($n = 32$ s), a 56% inhibition of spontaneous quantal ACh release. After DMBAPTA treatment in this cell, 10 μM adenosine inhibited e.p.ps to 80% of control and 20 μM adenosine inhibited e.p.ps to 40% of control. These effects of adenosine were reversible (data not shown).

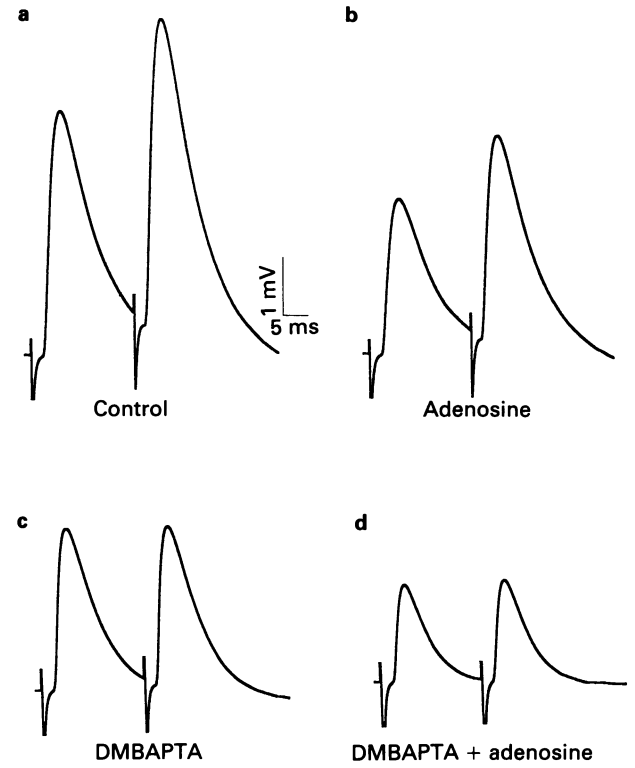


Figure 4 The effects of adenosine (20 μM) before (b) and after treatment with DMBAPTA (d). (a) Shows the control condition in which facilitation of the second response was 1.38; (b) shows that after treatment with 20 μM adenosine, ACh release (i.e. the first e.p.p.) was reduced to 63% of control whilst facilitation was unchanged (facilitation = 1.41); (c) shows that DMBAPTA reduced evoked ACh release to 66% of control and eliminated facilitation (facilitation = 0.99). (d) Shows that after DMBAPTA treatment, 20 μM adenosine inhibited e.p.ps to 60% of control (facilitation = 1.01).

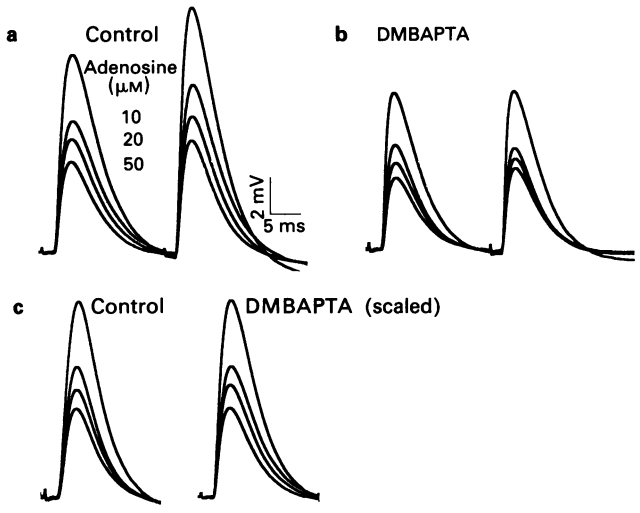


Figure 5 Dose-response relationship for adenosine before (a) and after superfusion with DMBAPTA (b). In (c) the adenosine dose-response relationship for the e.p.ps produced by the first of the two stimuli in the presence of DMBAPTA (b) was scaled upwards and juxtaposed with the control dose-response relationship of the first e.p.ps from (a) for comparison. In the absence of DMBAPTA (a), 10, 20 and 50 μM adenosine inhibited ACh release respectively to 68%, 59% and 46% of the control level. After treatment with DMBAPTA, these concentrations of adenosine respectively inhibited release to 68%, 57% and 47% of the control value. Calibrations refer to (a) and (b) and the control data in (c). In five other experiments, DMBAPTA failed to produce any significant alteration of the concentration-effect relationship for adenosine.

affecting the concentration-dependence of the action of adenosine or the maximal inhibitory effect of adenosine (see legend to Figure 5). Even in the experiment of Figure 3, in which DMBAPTA exhibited extremely efficacious buffering ability, adenosine had its conventional inhibitory effect on ACh release (see legend to Figure 3). In a series of experiments using the BAPTA-AM loading protocol (see methods), the effects of maximal concentrations of adenosine (50 μM adenosine) were examined. The results were indistinguishable from those reported previously from this laboratory in the absence of BAPTA (approximately 50% inhibition of evoked and spontaneous ACh release – see Silinsky, 1980; 1984). Specifically, in seven experiments, adenosine (50 μM) decreased evoked ACh release to 47% ± 3% of control and m.e.p.p. frequency to 49% ± 5% of control after DMBAPTA treatment.

With respect to adenosine and facilitation, in contrast to the elimination of facilitation by DMBAPTA, adenosine (10–50 μM) inhibited ACh release without affecting facilitation (control facilitation 1.34 ± 0.02, $n = 10$; facilitation in adenosine 1.32 ± 0.02, $n = 6$, see also Figure 4).

Discussion

These results suggest that BAPTA derivatives are able to bind and buffer the Ca^{2+} transients stimulated either by caffeine or by a nerve impulse, the latter as shown by the virtual elimination of the fast phase facilitation (which is generally attributed to the presence of residual Ca^{2+} – see Katz & Miledi, 1968). As a result of such cytoplasmic Ca^{2+} chelation, the number of ACh quanta released by a temporally-isolated nerve stimulus (m) is reduced. BAPTA derivatives thus appear to mimic the behaviour of the normal rapid mechanism by which Ca^{2+} is removed from active sites of secretion after a prejunctional nerve impulse (i.e. cytoplasmic Ca^{2+} binding proteins, see Blaustein, 1988).

DMBAPTA can be far more efficacious than any hypothetical rapid buffering system linked to adenosine receptor activation (see e.g. Figure 3 and results). Intracellular BAPTA or DMBAPTA should thus occlude any rapid Ca^{2+} buffering effects of adenosine. This is indeed not the case as the ability of adenosine to reduce ACh secretion was unimpaired by BAPTA derivatives. Furthermore whilst DMBAPTA virtually eliminated paired pulse facilitation of evoked ACh release, adenosine had no effect on this facilitatory process. These results suggest that adenosine is not increasing the rate or the amount of cytoplasmic buffering as such changes in Ca^{2+} levels would be expected to decrease facilitation. In further support of this view, when TMB-8 is used to prevent the uptake and release of intracellular Ca^{2+} from storage sites in the nerve terminal, the ability of adenosine to inhibit ACh secretion is also unaffected (Hunt *et al.*, 1990).

The previous literature on BAPTA and frog motor nerve endings is not without controversy, even in the same laboratory. For example, Kijima & Tanabe (1988) originally reported intracellular BAPTA to reduce facilitation and m.e.p.p. frequency. In more recent experiments, Tanabe & Kijima (1992) have shown only a decrease in the fast phase of facilitation, with m.e.p.p. frequency and quantal content being relatively unaffected by intracellular BAPTA. However, in the experiments in their more recent paper, the data of Kijima & Tanabe (1992) show that quantal content is decreased in the presence of 100 μM BAPTA-AM (see e.g. Figure 6b and c in their paper). In contrast, Charlton and colleagues have reported intracellular DMBAPTA to reduce quantal content and facilitation (Robitaille & Charlton, 1990; 1992). All of these data, when taken together, suggest that intracellular BAPTA derivatives are able to reduce ACh release evoked by electrical stimulation of the motor nerve or by displacement from storage sites (e.g. caffeine, Figure 1) as a consequence of reducing the amount of Ca^{2+} available to trigger release.

One apparently anomalous result was an increase m.e.p.p. frequency after treatment with DMBAPTA (M. Charlton, personal communication). In some experiments we too saw increases in m.e.p.p. frequencies. Other experiments revealed decreases in m.e.p.p. frequency (see e.g. Figure 3) or no effect of DMBAPTA on spontaneous ACh release. The reason for these discrepant results is unknown. Because of the variable effects of BAPTA derivatives on m.e.p.p. frequency, with different results reported by different investigators, we chose to focus our studies on the sources of apparent agreement between laboratories, namely the reduction in evoked ACh release and the occlusion of facilitation by intracellular DMBAPTA.

Adenosine, in order to reduce ACh secretion, must either reduce the amount of free Ca^{2+} available to trigger secretion, or impair the ability of Ca^{2+} to promote secretion (Silinsky, 1984). Previous reports from this laboratory have shown that adenosine does not reduce the Ca^{2+} influx via voltage-dependent Ca^{2+} channels in the frog (Silinsky & Solsona, 1992). In addition, adenosine inhibits ACh secretion triggered by methods which bypass active Ca^{2+} channels, i.e., Ca^{2+}-filled liposomes (Silinsky, 1984) or Ca^{2+} ionophores (Hunt & Silinsky, 1993). The evidence presented in this paper, when combined with previous work, strongly suggests that adenosine inhibits ACh secretion by modulating the ability of cytoplasmic Ca^{2+} to trigger secretion.

A recent study of the effects of BAPTA on the electrically-evoked release of tritiated noradrenaline (NA) in rat hippocampal slices (Fredholm & Hu, 1992) revealed similar results to those presented here. Briefly, these authors found that intracellular Ca^{2+} chelation by BAPTA reduced evoked NA release but not as effectively as reductions in extracellular Ca^{2+} concentrations. Furthermore, the inhibitory effect of the adenosine receptor agonist N^6-cyclohexyl adenosine was unchanged in the presence of BAPTA. Fredholm & Hu (1992) thus suggested that adenosine derivatives regulate NA release either by limiting Ca^{2+} entry or by acting at a step beyond Ca^{2+} entry. It thus appears that the suggestion that adenosine affects a Ca^{2+} binding site associated with evoked ACh release (Silinsky, 1981; 1984; see also Fredholm & Hu, 1992) and thus impairs the ability of Ca^{2+} to promote ACh release provides the most parsimonious interpretation of the results at frog neuromuscular junctions and at catecholaminergic terminals in rat hippocampus (see also Scholz & Miller, 1992).

This work was supported by a research grant (NS 12782) and a training grant (NS 07140) from the National Institutes of Health. We thank Dr Milt Charlton for personal communication of unpublished data.

References

BAIN, I.A. & QUASTEL, D.M.J. (1992). Multiplicative and additive Ca^{2+}-dependent components of facilitation at mouse endplates. *J. Physiol.*, **455**, 383–405.

BLAUSTEIN, M.P. (1988). Calcium transport and buffering in neurones. *Trends Neurosci.*, **11**, 438–443.

DEL CASTILLO, J. & KATZ, B. (1954). Quantal components of the end-plate potential. *J. Physiol.*, **124**, 560–573.

FREDHOLM, B.B. & DUNWIDDIE, T.V. (1988). How does adenosine inhibit transmitter release? *Trends Pharmacol. Sci.*, **9**, 130–134.

FREDHOLM, B.B. & HU, P.-S. (1992). Effect of an intracellular calcium chelator on the regulation of electrically-evoked [3H]-noradrenaline release from rat hippocampal slices. *Br. J. Pharmacol.*, **108**, 126–131.

GINSBORG, B.L. & HIRST, G.D.S. (1972). The effect of adenosine on the release of the transmitter from the phrenic nerve of the rat. *J. Physiol.*, **224**, 629–645.

HUNT, J.M. & SILINSKY, E.M. (1989). BAPTism of frog motor nerve terminals does not impair the inhibitory actions of adenosine on acetylcholine release. *Soc. Neurosci. Abs.*, **15**, 484.

HUNT, J.M. & SILINSKY, E.M. (1993). Ionomycin-induced acetylcholine release and its inhibition by adenosine at frog motor nerve endings. *Br. J. Pharmacol.*, **110**, 828–832.

HUNT, J.M., SILINSKY, E.M., HIRSH, J.K., AHN, D. & SOLSONA, C. (1990). The effects of TMB-8 on acetylcholine release from frog motor nerve; interactions with adenosine. *Eur. J. Pharmacol.*, **178**, 259–266.

KATZ, B. & MILEDI, R. (1968). The role of calcium in neuromuscular facilitation. *J. Physiol.*, **195**, 481–492.

KIJIMA, H. & TANABE, N. (1988). Calcium-independent increase of transmitter release at frog end-plate by trinitrobenzene sulphonic acid. *J. Physiol.*, **403**, 135–149.

NEERING, I.R. & MCBURNEY, R.N. (1984). Role for microsomal Ca storage in mammalian neurones? *Nature*, **309**, 158–160.

ONODERA, K. (1973). Effect of caffeine on the neuromuscular junction of the frog, and its relation to external calcium concentration. *Jpn. J. Physiol.*, **23**, 587–597.

PHILLIS, J.W. (1985). The pharmacology of purines in the CNS: Interactions with psychoactive agents. In *Purines: Pharmacology and Physiological Roles*. ed. Stone, T.W. pp. 45–56. London: The MacMillan Press, Ltd.

RIBEIRO, J.A. & SEBASTIAO, A.M. (1986). Adenosine receptors and calcium; basis for proposing a third (A3) type of adenosine receptor. *Prog. Neurobiol.*, **26**, 179–209.

ROBITAILLE, R. & CHARLTON, M.P. (1990). Frequency facilitation is not caused by residual ionized calcium at the frog neuromuscular junction. *Soc. Neurosci. Abs.*, **16**, 503.

ROBITAILLE, R. & CHARLTON, M.P. (1992). Presynaptic calcium signals and transmitter release are modulated by calcium-activated potassium channels. *J. Neurosci.*, **12**, 297–305.

SCHOLZ, K.P. & MILLER, R.J. (1992). Inhibition of quantal transmitter release in the absence of calcium influx by a G protein-linked adenosine receptor at hippocampal synapses. *Neuron*, **8**, 1139–1150.

SILINSKY, E.M. (1980). Evidence for specifical adenosine receptors at cholinergic nerve endings. *Br. J. Pharmacol.*, **71**, 191–194.

SILINSKY, E.M. (1981). On the calcium receptor that mediates depolarization-secretion coupling at cholinergic motor nerve terminals. *Br. J. Pharmacol.*, **73**, 413–429.

SILINSKY, E.M. (1984). On the mechanism by which adenosine receptor activation inhibits the release of acetylcholine from frog motor nerve endings. *J. Physiol.*, **346**, 243–256.

SILINSKY, E.M. (1985). The biophysical pharmacology of calcium-dependent acetylcholine secretion. *Pharmacol. Rev.*, **37**, 81–132.

SILINSKY, E.M. (1989). Adenosine derivatives and neuronal function. *Sem. Neurosci.*, **1**, 155–165.

SILINSKY, E.M. & SOLSONA, C.S. (1992). Calcium currents at motor nerve endings: absence of effects of adenosine receptor agonists in the frog. *J. Physiol.*, **457**, 315–328.

SILVER, R.B. (1989). Nuclear envelope breakdown and mitosis in sand dollar embryos is inhibited by microinjection of calcium buffers in a calcium-reversible fashion, and by antagonists of intracellular Ca^{2+} channels. *Devel. Biol.*, **131**, 11–26.

TANABE, N. & KIJIMA, H. (1988). Transmitter release at frog end-plate loaded with a Ca^{2+}-chelator, BAPTA: Hypertonicity and erythrosin B augment the release independently of internal Ca^{2+}. *Neurosci. Lett.*, **92**, 52–57.

TANABE, N. & KIJIMA, H. (1992). Ca^{2+}-dependent and -independent components of transmitter release at the frog neuromuscular junction. *J. Physiol.*, **455**, 271–289.

TSIEN, R.Y. (1980). New calcium indicators and buffers with high selectivity against magnesium and protons: Design, synthesis and properties of prototype structures. *Biochem.*, **19**, 2396–2404.

TSIEN, R.Y. (1981). A non-disruptive technique for loading calcium buffers and indicators into cells. *Nature*, **290**, 527–528.

(Received September 1, 1993
Revised November 11, 1993
Accepted November 17, 1993)

Br. J. Pharmacol. (1994), **111**, 759–768 © Macmillan Press Ltd, 1994

Characterization of NK_1 and NK_2 tachykinin receptors in guinea-pig and rat bronchopulmonary and vascular systems

[1]Anne Floch, Véronique Fardin & Icilio Cavero

Rhone-Poulenc Rorer S.A., Centre de Recherche de Vitry-Alfortville, 13, quai Jules Guesde, BP 14, 94403 Vitry sur Seine Cedex, France

1 NK_1 and NK_2 tachykinin receptors were characterized in guinea-pig and rat bronchopulmonary systems and in the vasculature of the rat by use of radioligand binding and/or functional studies.

2 The radioligands for NK_1 and NK_2 receptors ([^{3}H]-SP and [^{3}H]-pNKA, respectively) did not label tachykinin receptors in homogenates of rat lungs or bronchi. In contrast, in the guinea-pig, [^{3}H]-SP bound with high affinity to these tissues ($K_D = 0.23 \pm 0.08$ nM and 0.34 ± 0.05 nM, for lungs and bronchi, respectively). The total number of binding sites was 4.6 fold greater in bronchus ($B_{max} = 135 \pm 27$ fmol mg^{-1} protein) than in lung homogenates ($B_{max} = 29.3 \pm 0.1$ fmol mg^{-1} protein). Furthermore, this binding was markedly displaced by CP-96,345 ($pK_i = 9.5 \pm 0.1$) and RP 67580 ($pK_i = 7.6 \pm 0.1$), antagonists of NK_1 receptors, slightly displaced by SR 48968 ($pK_i = 6.6 \pm 0.1$), but not affected by actinomycin D or L-659,877, antagonists of NK_2 receptors. Specific binding of [^{3}H]-pNKA, detected in guinea-pig bronchi ($K_D = 5.2 \pm 0.1$ nM, and $B_{max} = 203 \pm 19$ fmol mg^{-1} protein) but not in lungs, was similarly (40 to 53%) displaced by RP 67580 (1 μM), CP-96,345 (10 and 100 nM) or SR 48968 (10 and 100 nM). The displacement approximately doubled (87 to 91%) when SR 48968 (10 nM) was combined with either RP 67580 (1 μM) or CP-96,345 (10 nM), but not when RP 67580 was combined with CP-96,345.

3 In urethane-anaesthetized guinea-pigs, i.v. injections of the NK_1 receptor agonists SP, [Pro^9]-SP, [Sar^9,Met(O$_2$)^{11}]-SP and septide, as well as the NK_2 receptor agonists NKA and [Lys^5,MeLeu^9,NLeu^{10}]-$NKA_{(4-10)}$ (0.1–10 μg kg^{-1}, i.v.), dose-dependently increased lung inflation pressure. The most potent of these peptides were septide and [Lys^5, MeLeu^9,NLeu^{10}]-$NKA_{(4-10)}$ ($EC_{50} = 0.38 \pm 0.07$ and 0.07 ± 0.02 μg kg^{-1}, respectively). Interestingly, septide was 130 fold less potent than SP in displacing [^{3}H]-SP from its binding sites in the guinea-pig lung, whereas it was 14 fold more potent than SP as a bronchoconstrictor. RP 67580 (0.3–5 mg kg^{-1}, i.v.) and CP-96,345 (0.01–3 mg kg^{-1}, i.v.) dose-dependently reduced the bronchoconstriction produced by the NK_1 receptor agonists. Conversely, the NK_2 receptor antagonists actinomycin D (1–10 mg kg^{-1}, i.v.) and SR 48968 (0.03–0.3 mg kg^{-1}, i.v.) inhibited specifically the responses induced by NK_2 receptor agonists.

4 In pentobarbitone-anaesthetized rats, the NK_1 and NK_2 receptor agonists (0.01–4 μg kg^{-1}, i.v.) produced dose-dependent hypotensive responses. The order of potency was SP = [Sar^9, Met(O$_2$)^{11}]-SP = [Pro^9]-SP > septide = NKA > [Lys^5, MeLeu^9, NLeu^{10}]-$NKA_{(4-10)}$. RP 67580 (0.13–0.5 mg kg^{-1}, i.v.) and CP-96,345 (0.5–2 mg kg^{-1}, i.v.) antagonized in a dose-related manner (20 to 64%) the vascular effects of both NK_1 and NK_2 receptor agonists, whereas actinomycin D (3 mg kg^{-1}, i.v.) and SR 48968 (2 mg kg^{-1}, i.v.) did not. RP 67580 was approximately 4 times more potent than CP-96,345.

5 These studies indicate that NK_1 and NK_2 receptors are both present in the guinea-pig bronchopulmonary system whereas only NK_1 receptors are detectable in the rat vasculature under our experimental conditions. Furthermore, NK_1 receptors in the guinea-pig bronchopulmonary system are pharmacologically distinct from those present in the rat vascular system, since both agonist potencies and antagonist affinities differ between the two species.

Keywords: Vascular system of rat; bronchopulmonary systems of rat, guinea-pig; bronchoconstriction; hypotension; tachykinin receptor; RP 67580; CP-96,345; SR 48968; actinomycin D

Introduction

Substance P (SP), neurokinin A (NKA) and neurokinin B (NKB) are members of a family of structurally related peptides, called tachykinins, that are involved in the regulation of various biological processes, particularly the modulation of bronchial smooth muscle contraction. These endogenous susbtances interact with three distinct types of tachykinin receptor, named NK_1, NK_2 and NK_3, as suggested by pharmacological and radioligand binding experiments, for which SP, NKA and NKB are the preferred endogenous agonists, respectively (Guard & Watson, 1991; Maggi *et al.*, 1993, for review). Recently, several novel, highly selective agonists of these receptors have been identified: [Pro^9]-SP (Lavielle *et al.*, 1986), [Sar^9, Met(O$_2$)^{11}]-SP (Regoli *et al.*, 1988) and septide (Wormser *et al.*, 1986) for the NK_1 receptor, [Lys^5, MeLeu^9, NLeu^{10}]-$NKA_{(4-10)}$ (Chassaing *et al.*, 1991) for the NK_2 receptor and senktide (Laufer *et al.*, 1986) for the NK_3 receptor. The availability of selective antagonists of these receptors, such as RP 67580 (Garret *et al.*, 1991) and CP-96,345 (Snider *et al.*, 1991) for NK_1, as well as SR 48968 (Advenier *et al.*, 1992; Emonds-Alt *et al.*, 1992) and L-659,877 (Williams *et al.*, 1988; McKnight *et al.*, 1991) for NK_2 receptors, provides an additional opportunity to characterize further the pharmacology and tissue location of these receptor sites (Watling, 1992). NK_2 receptor-mediated responses are also blocked by high doses of the antibiotic, actinomycin D (Lundberg & Lou, 1991; Delay-Goyet & Lundberg, 1991).

Tachykinins are known to contract bronchial smooth muscle (Karlsson & Persson, 1989; Frossard & Advenier, 1991, for review) and to cause hypotension (Couture *et al.*, 1989). However, the distribution of the different tachykinin receptors along the bronchopulmonary tree, as well as the partic-

[1] Author for correspondence.

ular receptor type involved in these responses, is not well understood. Therefore, the aim of the present investigation was to determine the distribution and function of the different tachykinin receptors at the bronchopulmonary level. To this end, binding experiments on homogenates prepared from rat and guinea-pig bronchi and lungs were performed and tachykinin receptor-mediated bronchopulmonary and vascular responses were measured in guinea-pigs and rats, respectively. For these studies, we used various selective agonists and antagonists of NK_1 and NK_2 receptors.

Methods

Radioligand binding assays

Binding to NK_1 and NK_2 tachykinin receptor sites was performed using [^{3}H]-SP and [^{3}H]-propionyl-NKA ([^{3}H]-pNKA), respectively, according to published procedures (Lee *et al.*, 1983; Bergström *et al.*, 1987) with slight modifications in order to increase levels of specific binding (Fardin & Garret, 1991; Garret *et al.*, 1991).

Preparation of homogenates of guinea-pig and rat bronchopulmonary tissues Male Sprague-Dawley rats (250–300 g, Iffa Credo, France) and male Dunkin-Hartley guinea-pigs (250–350 g, Charles River, France) were decapitated and their lungs and bronchi removed rapidly. The tissues were washed several times in ice-cold binding buffer which contained Tricine buffer (50 mM, pH 7.4 at 20°C), glucose (5.6 mM) and $MgCl_2$ (10 mM) for NK_1 or Tris buffer (50 mM, pH 7.4 at 20°C) for NK_2 receptor assays. The lungs were then freed from all non-lung tissue and weighed. Large and small bronchi were prepared by scraping off the parenchymal tissue of the lungs. Then, these tissues were cut into thin pieces and homogenized with a polytron sonicator in 15 vol (w/v) of appropriate binding buffer. Peptidase inhibitors (bacitracin 40 mg l^{-1}, leupeptin 4 mg l^{-1} and bestatin 5 mg l^{-1}) were added to the buffer used for the homogenization and all washing steps. The homogenates were centrifuged (50,000 *g* for 10 min at 4°C) twice and the final pellets suspended in 5 vol (w/v) of buffer. This suspension was divided into aliquots and frozen at − 80°C until use (generally 1 to 8 weeks after preparation). Protein content, measured according to the method of Smith *et al.* (1985) using bovine serum albumin (BSA) as the standard, yielded approximately 9 and 5 mg ml^{-1} for lung and bronchus homogenates, respectively.

Binding assays On the day of experiment, the homogenate preparations were adjusted to a protein concentration of 0.3 mg ml^{-1} by dilution with the appropriate binding buffer, containing BSA (0.02%), $MnCl_2$ (3 mM for NK_2 assays) and protease inhibitors [bacitracin (40 mg l^{-1}), chymostatin (4 mg l^{-1}, except for ^{3}[H]-SP assays for which bestatin 5 mg l^{-1} was used), leupeptin (4 mg l^{-1}) and kelatorphan (1 μM) or phosphoramidon (10 μM)]. The binding interaction was initiated by the addition of 1 ml of the homogenate suspension to 0.1 ml of the solution containing the ligand and 0.1 ml of binding buffer either alone (determination of total binding) or containing the competing drugs (final volume 1.2 ml). Incubations were performed at 25°C for 20 min ([^{3}H]-SP) or 90 min ([^{3}H]-pNKA). Non-specific binding was measured in the presence of non-radioactive SP (1 μM) and NKA (10 μM) for NK_1 and NK_2 assays, respectively.

For distribution studies, three different concentrations of [^{3}H]-SP (0.3, 2 and 5 nM) and [^{3}H]-pNKA (1, 3 and 6 nM) were used, whereas saturation binding assays were conducted over a ligand concentration range of 0.1–5 nM for [^{3}H]-SP and 0.2–15 nM for [^{3}H]-pNKA. In these studies, total and non-specific binding were measured in triplicate. Tachykinin binding was characterized by drug competition experiments. Guinea-pig lung homogenates were incubated with a single concentration of [^{3}H]-SP (0.3 nM) and 6 to 8 concentrations of tachykinin agonists SP, NKA, [Pro^9]-SP, [Sar^9, Met(O$_2$)^{11}]-SP, septide, [Lys^5, MeLeu^9,NLeu^{10}]-$NKA_{(4-10)}$ or senktide) or antagonists (CP-96,345, RP 67580, RP 68651, SR 48968, L-659,877 or actinomycin D). These experiments allowed the determination of the IC_{50} values (concentration inducing 50% inhibition of specific binding) for each competing agent. Guinea-pig bronchi homogenates were incubated with [^{3}H]-pNKA (1, 3 and 6 nM) in the presence of SR 48968 (100 nM) or RP 67580 (1 μM). Additional experiments were performed with [^{3}H]-pNKA (3 nM) in the presence of SR 48968 (10 or 100 nM), RP 67580 (100 nM or 1 μM) or CP-96,345 (10 or 100 nM) or the combinations SR 48968 (10 nM) plus RP 67580 (1 μM). SR 48968 (10 nM) plus CP-96,345 (10 nM) or CP-96,345 (10 nM) plus RP 67580 (1 μM).

In all assays, incubations were terminated by rapid filtration (Skatron cell harvester), through Whatman GF/B glass fibre filters presoaked with 0.3% polyethylenimine. Filters were immediately rinsed with ice-cold buffer, and the radioactivity trapped on the filters measured by liquid scintillation counting.

Analysis of data Binding data were analysed by the curve fitting programmes LIGAND (Munson & Rodbard, 1980) and EBDA (McPherson, 1985), which allowed equilibrium dissociation constants (K_D) and total number of binding sites (B_{max}) to be determined from saturation studies, and IC_{50} values to be determined from drug competition experiments. IC_{50} values were then transformed into inhibition constants (K_i) according to the equation of Cheng & Prusoff (1973). These affinity values were expressed as mean pK_i values ± s.e. mean, which are the negative logarithms of the K_i values and which are reported in the result section.

Tachykinin-induced bronchoconstriction in guinea-pigs

Animals and treatments Male Dunkin-Hartley guinea-pigs (Charles River, St Aubin Lès Elbeuf, France) weighing 400–500 g were anaesthetized with an intraperitoneal injection of urethane (1.25 g kg^{-1}) and prepared according to the method of Konzett & Rössler (1940). The animals were ventilated with a respiratory pump (60 cycles min^{-1}, 10 ml air kg^{-1}). The right jugular vein was catheterized for drug injections and spontaneous breathing was suppressed by the administration of gallamine triethiodide (6 mg kg^{-1}, i.v.). The bronchial resistance to inflation was measured with a bronchospasm transducer (Ugo Basile 7020) connected to a recorder (Graphtec, Mark VII). The right carotid artery was cannulated with a catheter connected to a blood pressure transducer (Gould P23XL) and the mean carotid blood pressure was recorded on the polygraph. The intratracheal cannula was clipped for 3 s before the experiment to calibrate the bronchospasm transducer. After a 15 min equilibration period, bronchial reactivity was tested with an intravenous bolus injection of acetylcholine (30 μg kg^{-1}). Only animals responding with an increase of more than 8 cmH_2O in lung inflation pressure were retained for the full experimental procedure.

In studies with agonists, animals received 10 min later three or four consecutive i.v. bolus injections of increasing doses of SP, [Pro^9]-SP, [Sar^9, Met(O$_2$)^{11}]-SP, septide, NKA or [Lys^5, MeLeu^9,NLeu^{10}]-$NKA_{(4-10)}$. A 10 min interval was allowed to elapse between successive doses, so that lung inflation pressure could return to pre-injection values.

In studies with antagonists, guinea-pigs received an intravenous injection of a submaximal dose of tachykinins twice. The bronchoconstrictor response to the second dose was taken as a control value. Then, animals received RP 67580, RP 68651, CP-96,345, actinomycin D, SR 48968 or their solvent, given over 1 min as 1 ml kg^{-1}, i.v. A third dose of tachykinin (the same as the previous two) was injected 5 min after treatment.

Analysis of data Experimental data are presented as means ± s.e.mean, whereas ED_{50} and ID_{50} values are reported with their s.d. Bronchoconstrictor responses are reported as the absolute increase (cmH_2O) in lung inflation pressure from baseline values. The potency of the agonists was evaluated by determining the ED_{50}, which is the dose producing 50% of the maximal response obtained with the highest dose of agonist studied ($E_{max} = 100\%$), by analysing the dose-response curve with the sigmoidal function $y = E_{max} + [(E_{min} - E_{max})/(1 + x/ED_{50})n]$ where y = measured bronchoconstrictor response, E_{min} = minimal effect, x = dose of agonist and n = slope coefficient (Gomeni & Gomeni, 1980). This programme allowed more than one dose-response curve to be drawn simultaneously and the ED_{50} ± s.d. to be calculated. For the antagonists, the dose inhibiting by 50% the response to a submaximal dose of agonist (ID_{50} ± s.d.) was determined by fitting simultaneously all the experimental results with the same sigmoidal function as above, where y = inhibition (%) of the bronchoconstrictor response. Statistical significance was evaluated with Student's unpaired or paired *t* test and the effect was assumed to be significant when $P \leqslant 0.05$.

Tachykinin-induced hypotension in rats

Animals and treatments Male Sprague-Dawley rats (Charles River, France) weighing 250 to 270 g were anaesthetized with sodium pentobarbitone (60 mg kg^{-1}, intraperitoneally) and artifically ventilated with room air (60 strokes min^{-1}, 10 ml kg^{-1}). The left carotid artery and the right femoral vein were cannulated for blood pressure measurement and drug administration, respectively. After a 15 min equilibration period, RP 67580, RP 68651, CP-96,345, actinomycin D, SR 48968 or vehicles were given as 10 min intravenous infusions. Ten minutes later, dose-response curves to i.v. bolus injections of SP, [Pro^9]-SP, [Sar^9, $Met(O_2)^{11}$]-SP, septide, NKA or [Lys^5, $MeLeu^9$,$NLeu^{10}$]-$NKA_{(4-10)}$ were determined. Blood pressure was recorded on a polygraph (Graphtec, Mark VII) via a pressure transducer (Gould P23XL).

Analysis of data Results are reported as means ± s.e.mean of at least five rats/group. Hypotensive responses are given as maximal changes in blood pressure from baseline values. The potency of agonists was determined by calculating the dose that reduced blood pressure by 30 mmHg. This was done by computer-assisted curve fitting with the Sigma-plot programme (Jandel). The areas under the $dose_{(a\rightarrow b)}$-hypotensive curves ($AUC_{(a\rightarrow b)}$), as illustrated in Figure 7, were calculated. These parameters were used to evaluate the inhibitory effects of the antagonist over the full dose-response curve (Cavero *et al.*, 1980). This inhibition was calculated as the percentage of reduction of the $AUC_{(a\rightarrow b)}$ obtained after the administration of the antagonist, taking the $AUC_{(a\rightarrow b)}$ obtained after vehicle pretreatment as 100%. The significance ($P \leqslant 0.05$) of the difference between responses to vehicle and to treatment was assessed by means of a Student's *t* test for unpaired data.

Materials

([^{3}H]-prolyl^{2,4}-3,4)-SP (specific activity 48.5–60 Ci $mmol^{-1}$; 1 Ci = 37 GBq) and ([^{3}H]-propionyl-lysyl-3)-NKA (specific activity 93.8–106 Ci $mmol^{-1}$, synthesis on request) were obtained from Amersham (Les Ulis, France). [L-Pro^9]-SP and [Lys^5, $MeLeu^9$, $NLeu^{10}$]-$NKA_{(4-10)}$ were synthesized by Drs S. Lavielle and G. Chassaing (University Paris VI, Paris, France). RP 67580 ((3a**R**,7a**R**)-7,7-diphenyl-2-[imino-2-(2-methoxyphenyl)-ethyl]perhydroisoindol-4-one), its inactive enantiomer RP 68651, and the active enantiomers (CP-96,345 ((2S,3S)-cis-2-(diphenylmethyl)-N-[(2-methoxyphenyl)-methyl]-1-azabicyclo[2.2.2]octan-3-amine) and SR 48968 ((**S**)-N-methyl-N-[4-(4-acetylamino-4-phenyl piperidino)-2-(3,4-dichlorophenyl)butyl]benzamide) were synthesized by Dr J.F. Peyronel and collaborators (Chemistry Department, Rhône-Poulenc Rorer, Centre de Recherche de Vitry-Alfortville, France). SP, [Sar^9,$Met(O_2)^{11}$]-SP and septide were obtained from Bachem (Bachem A.G., Bubendorf, Switzerland). NKA and L-659,877 were purchased from Novabiochem (Meudon, France) and CRB (Cambridge Research Biochemicals, Cheshire, UK), respectively. Other chemicals and reagents were obtained from Sigma (Sigma Chemical, St Louis, MO, U.S.A.) or Prolabo (Paris, France), except polyethylenimine which was obtained from Janssen Chemica (Noisy Le Grand, France). Kelatorphan was a generous gift from Prof. B. Roques (University Paris V, Paris, France).

Results

Binding studies

Effects of the metalloprotease inhibitors, phosphoramidon and kelatorphan In initial experiments, we studied the effects of either phosphoramidon (10 μM) or kelatorphan (1 μM) on the specific binding of [^{3}H]-SP and [^{3}H]-pNKA in guinea-pig tissues since it has been reported recently that phosphoramidon increases tachykinin binding in the lung (Aharony *et al.*, 1991; Geraghty *et al.*, 1991). In these assays, the peptidase inhibitors leupeptin, bacitracin, and either bestatin or chymostatin were present as described in the Methods section. In guinea-pig bronchi, kelatorphan increased the bind-

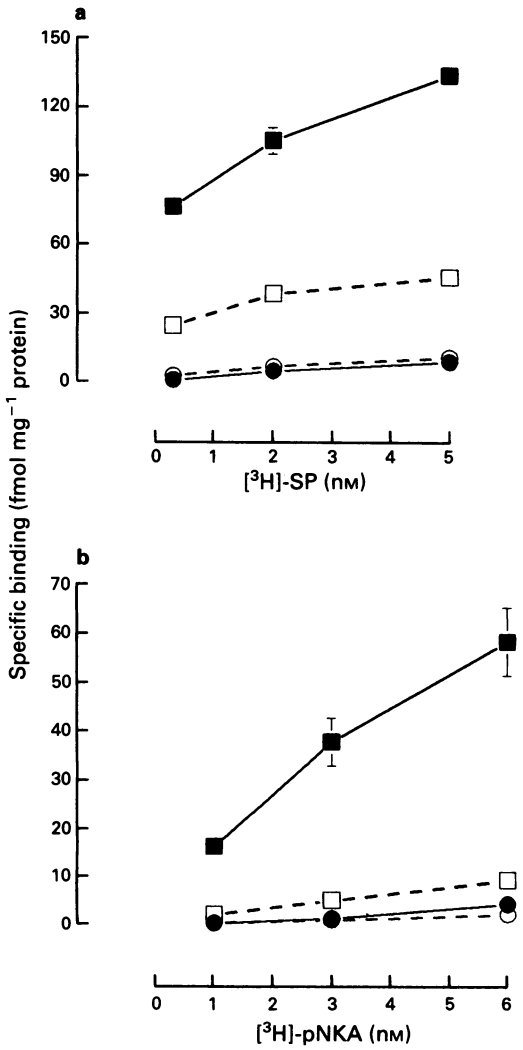


Figure 1 Distribution of tachykinin receptors labelled by [^{3}H]-substance P ([^{3}H]-SP) (a) and [^{3}H]-propionyl-neurokinin A ([^{3}H]-pNKA) (b) in homogenates of rat lung (○) and bronchus (●), and guinea-pig lung (□) and bronchus (■). The results are given as means ± s.e.mean of 3–4 independent experiments run in triplicate.

ing of [^{3}H]-pNKA, at concentrations of 1, 3 and 6 nM, by 270 ± 23, 230 ± 20 and 190 ± 10% (n = 3), respectively. Similar increases were found with phosphoramidon. In contrast, these metalloprotease inhibitors did not significantly ($\leq$ 22% of control values) modify [^{3}H]-SP (0.3, 2 and 5 nM) binding. On the basis of these results, kelatorphan (1 μM) was routinely used for all the studies described below.

Distribution of tachykinin receptors in the bronchopulmonary system In the rat, no significant specific binding of [^{3}H]-SP or [^{3}H]-pNKA to lung or bronchial tissue was detected, except when these ligands were used at high concentrations (5 or 6 nM, respectively), in which case the specific binding was slight (about 400 d.p.m. for [^{3}H]-SP and about 250 d.p.m. for [^{3}H]-pNKA).

In contrast, in the guinea-pig, [^{3}H]-SP displayed specific, concentration-dependent binding in both tissues. In the lungs, the specific binding of 0.3 nM [^{3}H]-SP was 85% of total binding, resulting in 24.4 ± 2.4 fmol mg^{-1} protein (n = 3, about 1000 d.p.m.); in bronchus homogenates, it resulted in 76 ± 4 fmol mg^{-1} protein (n = 3). Thus, the binding of [^{3}H]-SP was greater in the bronchi than in the lungs (Figure 1). Concentration-dependent specific binding, again predominant in the bronchi, was also obtained with [^{3}H]-pNKA. Only high concentrations (6 nM) of this ligand labelled lung homogenates and this occurred with some interassay variability (9.4 ± 2.3 fmol, about 700 d.p.m., n = 3). Moreover, within the range of concentrations used, the [^{3}H]-pNKA binding appeared lower (i.e. 58.5 ± 7.0 fmol mg^{-1} protein at 6 nM, n = 4) than that observed with [^{3}H]-SP in guinea-pig bronchi (134 ± 5 fmol mg^{-1} protein at 5 nM, n = 3).

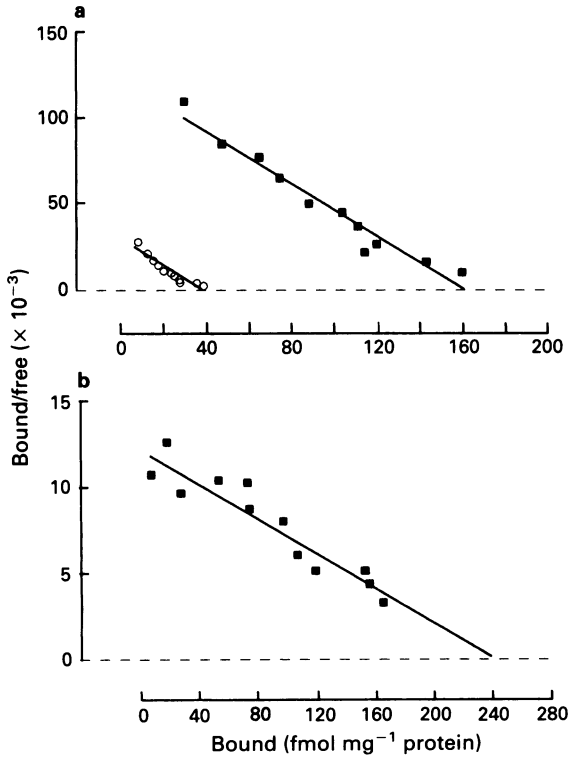


Figure 2 Scatchard analysis of [^{3}H]-substance P ([^{3}H]-SP) (a) and [^{3}H]-propionyl-neurokinin A ([^{3}H]-pNKA) (b) binding in guinea-pig lung (○) and bronchus (■) homogenates. Saturation studies were conducted over a concentration range of 0.1 to 5 nM for [^{3}H]-SP and 0.2 to 15 nM for [^{3}H]-pNKA. Data are taken from single representative experiments carried out in triplicate. The K_D and B_{max} values from this single experiment determined with [^{3}H]-SP were 0.374 nM and 38.1 fmol mg^{-1} protein, respectively, for lung homogenates. The corresponding values for bronchi were 0.390 nM and 162 fmol mg^{-1} protein. For [^{3}H]-pNKA, the K_D and B_{max} values for bronchi were 5.8 nM and 240 fmol mg^{-1} protein, respectively.

To examine further the binding in guinea-pig tissues, saturation experiments were conducted with [^{3}H]-SP (0.1–5 nM) and [^{3}H]-pNKA (0.2–15 nM). Specific binding exhibited saturability for the two ligands and Scatchard plots obtained from typical experiments are shown in Figure 2. Assays performed with lung and bronchus homogenates showed that [^{3}H]-SP labelled an apparently homogeneous population of sites with high affinity. The equilibrium dissociation constants were in the same range for both tissues: K_D = 0.23 ± 0.08 nM (n = 3) for lungs and K_D = 0.34 ± 0.05 nM, (n = 2) for bronchi. The total number of binding sites was 4.6 fold greater in bronchi (B_{max} = 135 ± 27 fmol mg^{-1} protein) than in lung homogenates (B_{max} = 29.3 ± 0.1 fmol mg^{-1} protein).

The transformation of the raw data obtained from experiments on [^{3}H]-pNKA binding to guinea-pig bronchi gave rise to linear Scatchard plots with the following equilibrium constants: K_D = 5.2 ± 0.1 nM and B_{max} = 203 ± 19 fmol mg^{-1} protein (n = 3). Thus, in guinea-pig bronchi, the total number of sites labelled by [^{3}H]-pNKA was 1.5 fold greater than that labelled by [^{3}H]-SP.

Pharmacological profile of tachykinin binding in guinea-pig lungs and bronchi The pharmacological profile of the specific binding of [^{3}H]-SP at a low concentration (0.31 ± 0.01 nM, n = 8) in guinea-pig lung homogenates was in agreement with that expected for NK_1 binding sites. SP and the two selective NK_1 receptor agonists, [Pro^9]-SP and [Sar^9, Met $(O_2)^{11}$]-SP, potently displaced specific [^{3}H]-SP binding, with IC_{50} values lower than 1 nM (pK_i values between 9.48 and 9.72, Table 1). Septide, another selective NK_1 receptor agonist, was found to be 130 fold less potent than SP (pK_i = 7.60). The selective NK_2 ([Lys^5, MeLeu^9,NLeu^{10}]-$NKA_{(4-10)}$) and NK_3 (senktide) receptor agonists exhibited very low affinities (at least 7000 fold lower than that of SP). However, NKA, the preferred endogenous ligand for NK_2 receptors, displaced the specific binding of [^{3}H]-SP with a pK_i value of 7.0; thus, it was about 500 fold less potent than SP itself.

We further characterize [^{3}H]-SP specific binding in the lungs by determining the affinities of several NK_1 and NK_2

Table 1 Affinities of several tachykinins and related compounds for [^{3}H]-substance P ([^{3}H]-SP, 0.3 nM) binding sites in guinea-pig lung

Competitor	pK_i
Agonists	
SP	9.72 ± 0.06
NKA	7.03 ± 0.15
[Pro^9]-SP	9.48 ± 0.09
[Sar^9, Met$(O_2)^{11}$]-SP	9.62 ± 0.07
Septide	7.60 ± 0.02
[Lys^5,MeLeu^9,NLeu^{10}]-$NKA_{(4-10)}$	5.86 ± 0.10
Senktide	inactive
Antagonists	
CP-96,345	9.47 ± 0.10
RP 67580	7.63 ± 0.06
RP 68651	inactive
SR 48968	6.59 ± 0.07
L-659,877	inactive
Actinomycin D	inactive

Data are expressed as pK_i values (the negative logarithm of the K_i). Results are the means ± s.e.mean of at least 3 independent determinations, each one performed in duplicate. Hill coefficients were close to 0.9 for CP-96,345 and RP 67580 and were 0.68 ± 0.04 and 0.58 ± 0.01 for septide and [Lys^5, MeLeu^9,NLeu^{10}]-$NKA_{(4-10)}$, respectively. Inactive indicates either no inhibition, or less than 50% inhibition, with a 10 μM concentration of the competitor (pK_i < 5.4).

receptor antagonists. The NK_1 antagonists used, CP-96,345 (0.01–100 nM) and RP 67580 (1 nM–3 μM), dose-dependently inhibited this binding (Figure 3). A clear enantioselectivity existed for this binding since RP 68561, the inactive enantiomer of RP 67580, exhibited no affinity for the sites labelled by [^{3}H]-SP in the lungs. The NK_2 receptor antagonists, L-659,877 and actinomycin D, even at high concentrations (10 μM) did not displace [^{3}H]-SP binding, whereas SR 48968, a selective NK_2 receptor antagonist, exhibited a slight affinity for lung NK_1 receptors, but this was over 1000 fold lower than that of SP (Table 1).

The small amount of tissue obtained from guinea-pig bronchi limited our pharmacological characterization of the bronchial [^{3}H]-pNKA binding site. The specific binding of

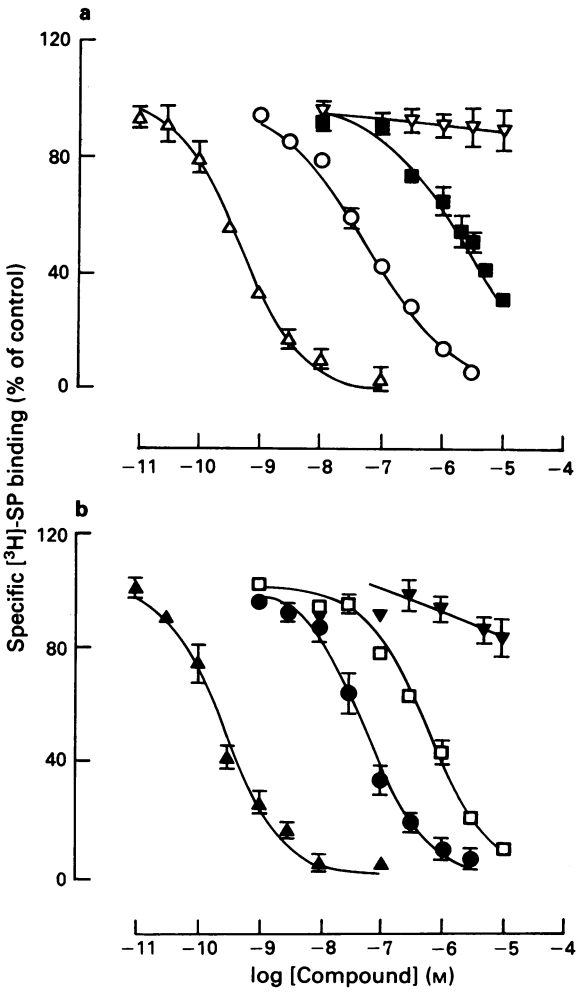


Figure 3 Displacement of [^{3}H]-substance P ([^{3}H]-SP) binding to guinea-pig lung homogenates by various tachykinin agonists: SP (△), septide (○), [Lys^5, MeLeu^9,NLeu^{10}]-$NKA_{(4-10)}$ (■) and senktide (▽) (a) and antagonists: CP-96,345 (▲), RP 67580 (●), SR 48968 (□) and L-659,877 (▼) (b). Values are given as percentages of control [^{3}H]-SP specific binding and are the means ± s.e.mean of three to four experiments performed in duplicate. Non-specific binding corresponded to 5–15% of total binding.

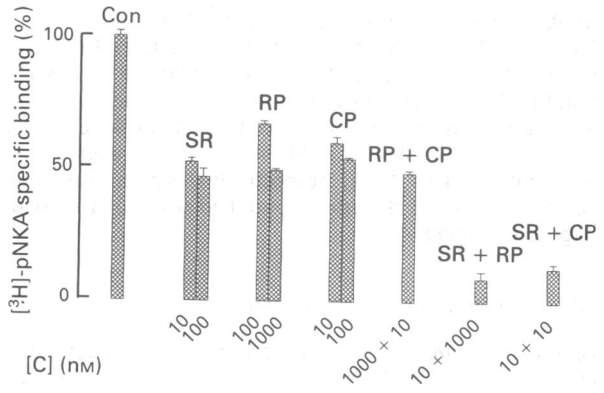


Figure 4 Specific binding of [^{3}H]-propionyl-neurokinin A ([^{3}H]-pNKA, 3 nM) to guinea-pig bronchi in the absence (controls: Con) or presence of RP 67580 (RP), CP-96,345 (CP), SR 48968 (SR) or their combination. Results are given as percentages of control [^{3}H]-pNKA specific binding and are the means ± s.e.mean of 3 independent experiments run in duplicate. Non-specific binding corresponded to 10–20% of total binding. Statistical significance was evaluated by ANOVA followed by a Wilcoxon's test. Inhibition of binding in comparison to controls was significant ($P<0.01$) for all groups. Significantly ($P<0.01$) greater displacements were obtained when SR 48968 was combined with either CP-96,345 or RP 67580, than when only one antagonist was used.

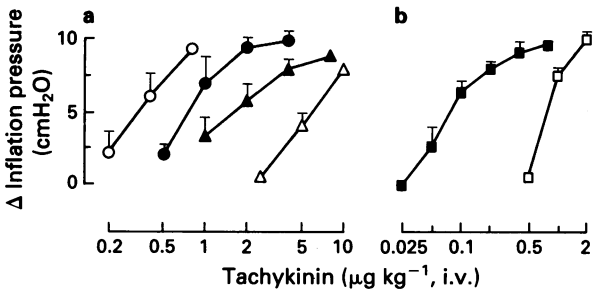


Figure 5 Bronchoconstrictor effects (Δ in intratracheal pressure from baseline) produced in anaesthetized guinea-pigs by i.v. bolus injections of several NK_1 agonists: substance P (SP) (△), [Pro^9]-SP (▲), [Sar^9, Met$(O_2)^{11}$]-SP (●) and septide (○) (a) and NK_2 agonists: neurokinin A (NKA) (□) and [Lys^5, MeLeu^9,NLeu^{10}]-$NKA_{(4-10)}$ (■) (b). Results are expressed as means ± s.e.mean of 4 to 6 guinea-pigs per group.

Table 2 Bronchopulmonary response to various tachykinin receptor agonists in the guinea-pig expressed as means ± s.e.mean of E_{max} (maximal increase in intratracheal pressure from baseline obtained with the highest dose of agonist studied) and means ± s.d. of ED_{50} (dose producing 50% of the E_{max}) values

Agonist	E_{max} (cmH_2O)	ED_{50} (μg kg^{-1}, i.v.)
SP	9.0 ± 0.3	5.17 ± 0.66
[Pro^9]-SP	9.0 ± 0.2	1.19 ± 0.26*
[Sar^9, Met$(O_2)^{11}$]-SP	9.6 ± 0.2	0.72 ± 0.17*
Septide	9.4 ± 0.3	0.38 ± 0.07*
NKA	9.6 ± 0.2	0.82 ± 0.05*
[Lys^5, MeLeu^9,NLeu^{10}]-$NKA_{(4-10)}$	9.5 ± 0.5	0.07 ± 0.02*

$n = 4–6$ guinea-pigs per group. *Value significantly ($P<0.05$, Student's t test) different from that obtained in the SP group.

[^{3}H]-pNKA was determined in the presence of 1 μM RP 67580, a concentration that totally (over 90%) inhibited the binding of [^{3}H]-SP to the NK_1 receptor in guinea-pig lungs. Under these conditions, the binding of [^{3}H]-pNKA (6 nM) was decreased significantly by 43%. The presence of NK_2 binding sites was indicated by the displacement of about 50% of [^{3}H]-pNKA binding by a relatively low concentration (100 nM) of SR 48968, which did not significantly inhibit the binding of [^{3}H]-SP in guinea-pig lungs. Furthermore, [^{3}H]-pNKA (3 nM) binding was similarly displaced (40 to 53%) by SR 48968 (10 and 100 nM), RP 67580 (1 μM) and CP-96,345 (10 and 100 nM) (Figure 4). When CP-96,345 (10 nM) and RP 67580 (1 μM) were combined, the displacement (49%) did not change. However, the combination of SR 48968 (10 nM) with either RP 67580 or CP-96,345 produced a greater displacement (91 and 87%, respectively), which was almost equal to the sum of the effects obtained with each individual antagonist (Figure 4).

Guinea-pig bronchopulmonary studies

Responses to agonists In guinea-pigs, the intravenous administration of the NK_1 receptor agonists SP, [Pro^9]-SP, [Sar^9, Met(O$_2$)^{11}]-SP and septide, and the NK_2 receptor agonists NKA and [Lys^5, MeLeu^9,NLeu^{10}]-$NKA_{(4-10)}$ (0.1–10 μg kg^{-1}, i.v.), dose-dependently increased lung inflation pressure (Figure 5). In this respect, [Lys^5, MeLeu^9,NLeu^{10}]-$NKA_{(4-10)}$ and septide were the most potent compounds, being 74 and 14 fold more potent, respectively, than SP (ED_{50} = 0.07, 0.38 and 5.17 μg kg^{-1}, respectively). Their maximal effects did not differ significantly (Table 2). For studies with antagonists, equiactive doses of SP (5 μg kg^{-1}, i.v.), [Pro^9]-SP (3 μg kg^{-1}, i.v.), [Sar^9, Met(O$_2$)^{11}]-SP (2 μg kg^{-1}, i.v.), septide (0.5 μg kg^{-1}, i.v.), NKA (1 μg kg^{-1}, i.v.) and [Lys^5,MeLeu^9,NLeu^{10}]-$NKA_{(4-10)}$ (0.15 μg kg^{-1}, i.v.) were chosen (Δ inflation pressure = 7.5 ± 0.3, 8.6 ± 0.3, 8.6 ± 0.9, 8.6 ± 0.3, 7.2 ± 0.4 and 8.5 ± 0.4 cmH_2O, respectively, n = 8–11 guinea-pigs/group).

Effects of antagonists None of the antagonists studied modified the baseline bronchomotor tone. CP-96,345 (0.01–3 mg kg^{-1}, i.v.) dose-dependently reduced the bronchoconstriction produced by SP, [Pro^9]-SP, [Sar^9, Met(O$_2$)^{11}]-SP and septide (ID_{50} = 0.86 ± 0.25, 0.11 ± 0.02, 0.07 ± 0.02 and 0.024 ± 0.004 mg kg^{-1}, i.v., respectively, n = 4 to 5 guinea-pigs per dose). In contrast, RP 67580 (0.3–5 mg kg^{-1}, i.v.) did not affect SP-evoked bronchoconstriction but inhibited the pulmonary responses to [Pro^9]-SP, [Sar^9, Met(O$_2$)^{11}]-SP and septide (ID_{50} = 3.30 ± 0.69, 3.52 ± 0.36 and 0.75 ± 0.11 mg kg^{-1}, i.v., respectively), whereas RP 68651 (5 mg kg^{-1}, i.v.), the inactive enantiomer of RP 67580, failed to antagonize septide-induced bronchoconstriction. Neither actinomycin D (10 mg kg^{-1}, i.v.) nor SR 48968 (1 mg kg^{-1}, i.v.) modified the response induced by SP or septide (n = 4 to 6/group).

Responses to NKA and to [Lys^5, MeLeu^9,NLeu^{10}]-$NKA_{(4-10)}$ were not affected by either RP 67580 (5 mg kg^{-1}, i.v.) or CP-96,345 (3 mg kg^{-1}, i.v.). Conversely, actinomycin D (1–10 mg kg^{-1}) and SR 48968 (0.03–0.3 mg kg^{-1}) dose-dependently inhibited the effects induced by NKA (ID_{50} = 1.94 ± 0.46 and 0.07 ± 0.01 mg kg^{-1}, i.v., respectively) and by [Lys^5, MeLeu^9,NLeu^{10}]-$NKA_{(4-10)}$ (ID_{50} = 5.5 ± 1.1 and 0.08 ± 0.02 mg kg^{-1}, i.v., respectively, n = 4 to 6/group).

Rat vascular studies

Responses to agonists In rats, the NK_1 (SP, [Pro^9]-SP, [Sar^9, Met(O$_2$)^{11}]-SP and septide) and NK_2 (NKA and [Lys^5, MeLeu^9,NLeu^{10}]-$NKA_{(4-10)}$) receptor agonists induced dose-dependent hypotension (Figure 6). The rank order of potency, established for doses decreasing blood pressure by 30 mmHg (Table 3), was SP = [Sar^9, Met(O$_2$)^{11}]-SP = [Pro^9]-SP > septide = NKA > [Lys^5, MeLeu^9,NLeu^{10}]-$NKA_{(4-10)}$. SP was 2.7, 7.3 and 70 fold more potent than septide, NKA and [Lys^5, MeLeu^9,NLeu^{10}]-$NKA_{(4-10)}$, respectively.

Effects of antagonists The intravenous infusion of RP 67580 (2 mg kg^{-1}), RP 68651 (10 mg kg^{-1}), actinomycin D (3 mg kg^{-1}) or SR 48968 (2 mg kg^{-1}) did not modify blood pres-

Table 3 Vascular response to various tachykinin receptor agonists in rats

Agonist	$ED_{-30\,mmHg}$ (μg kg^{-1}, i.v.)
SP	0.189 ± 0.054
[Pro^9]-SP	0.148 ± 0.029
[Sar^9, Met(O$_2$)^{11}]-SP	0.165 ± 0.025
Septide	0.628 ± 0.164*
NKA	1.054 ± 0.379*
[Lys^5, MeLeu^9,NLeu^{10}]-$NKA_{(4-10)}$	20.67 ± 3.88*

Results are expressed in terms of $ED_{-30\,mmHg}$ ± s.e.mean, which is the dose producing a blood pressure decrease of 30 mmHg. Initial MAP values were not significantly different from one group to another (from 124 ± 3 to 131 ± 2 mmHg, n = 5–6 rats per group).
*Value significantly (P<0.05, Student's t test) different from that obtained in the SP group.

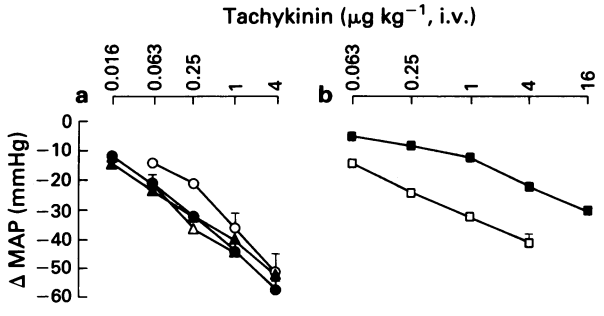


Figure 6 Hypotensive effects (Δ MAP) produced in anaesthetized rats by i.v. bolus injections of several NK_1 agonists: substance P (SP) (△), [Pro^9]-SP (▲), [Sar^9, Met(O$_2$)^{11}]-SP (●) and septide (○) (a) and NK_2 agonists: neurokinin A (NKA) (□) and [Lys^5, MeLeu^9,NLeu^{10}]-$NKA_{(4-10)}$ (■) (b). Results are expressed as means ± s.e.mean of 4 to 6 rats per group.

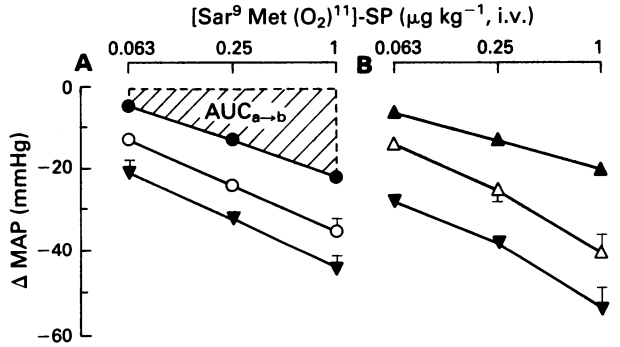


Figure 7 Effects of RP 67580 (A) and CP-96,345 (B) on [Sar^9, Met(O$_2$)^{11}]-substance P-induced hypotension in anaesthetized rats (n = 4–6 rats/group). The different treatments [(RP 67580, 0.13 (○) or 0.5 (●) mg kg^{-1}, CP 96,345, 0.5 (△) or 2 (▲) mg kg^{-1} and vehicle (▼)] were infused over a 10 min period, 10 min before the agonist. Similar displacements of the dose-response curves to substance P (SP), [Pro^9]-SP and septide were obtained with RP 67580 (0.13–0.5 mg kg^{-1}) and CP-96,345 (0.5–2 mg kg^{-1}, i.v.). $AUC_{a\to b}$ represents the area under the dose-response curve for doses ranging from the lowest (a) to the highest (b) dose studied.

Table 4 Hypotensive responses of several agonists expressed as the area under the dose-response curve ($AUC_{a\to b}$ ± s.e.mean) in rats pretreated with antagonsts (AUC ant) or their vehicle (AUC veh), as graphically represented in Figure 7 ($n = 5-6$ rats/group)

			$AUC_{a\to b}$ (% of inhibition)					
	Dose a→b	*Vehicle* –	*RP 67580* (mg kg^{-1})		*CP-96,345* (mg kg^{-1})		*Actinomycin D* (mg kg^{-1})	*SR 48968* (mg kg^{-1})
Agonist	(μg kg^{-1}, i.v.)	–	0.13	0.5	0.5	2	3	2
SP	0.016→1	35 ± 1	28 ± 2* (20)	16 ± 2* (54)	25 ± 1* (29)	19 ± 1* (46)	36 ± 2 (0)	35 ± 2 (0)
[Pro^9]-SP	0.016→1	34 ± 2	26 ± 2* (24)	22 ± 2* (35)	26 ± 2* (24)	19 ± 1* (44)	ND	ND
[Sar^9, Met(O$_2$)^{11}]-SP	0.063→1	34 ± 2	25 ± 1* (26)	15 ± 1* (56)	28 ± 3 (18)	14 ± 1* (59)	ND	ND
Septide	0.063→4	151 ± 10	115 ± 11* (24)	64 ± 8* (58)	104 ± 7* (31)	60 ± 5* (60)	ND	ND
NKA	0.016→1	25 ± 1	16 ± 2* (36)	12 ± 1* (52)	17 ± 1* (32)	9 ± 1* (64)	24 ± 2 (4)	24 ± 2 (4)
[Lys^5, MeLeu^9, NLeu^{10}]-NKA$_{(4-10)}$	0.25→16	334 ± 23	ND	191 ± 19* (43)	ND	203 ± 26* (39)	ND	371 ± 34 (0)

Antagonist effects are given, in parentheses, according to $\frac{\text{AUC veh} - \text{AUC ant}}{\text{AUC veh}} \times 100$. The $AUC_{a\to b}$ are reported in arbitrary units.

*Value significantly ($P < 0.05$, Student's t test) different from that obtained in the vehicle-treated group.
ND = not determined.

sure, whereas CP-96,345 (2 mg kg^{-1}) caused significant hypotension (from 126 ± 2 to 85 ± 3 mmHg at the end of the 10 min infusion), which faded 10 min after ending the administration. This transitory effect may be attributed to the ability of CP-96,345 to interact with Ca^{2+} channels (Schmidt *et al.*, 1992). RP 67580 (0.13–0.5 mg kg^{-1}) and CP-96,345 (0.5–2 mg kg^{-1}) each antagonized to a similar degree the hypotensive effects of SP, [Pro^9]-SP, [Sar^9, Met(O$_2$)^{11}]-SP or septide (Table 4, Figure 7). In this respect, RP 67580 was approximately four times more potent than CP-96,345. However, SP-induced hypotension was not modified by RP 68651, the inactive enantiomer of RP 67580, at doses up to 10 mg kg^{-1}, i.v., by actinomycin D (3 mg kg^{-1}, i.v.) or by SR 48968 (2 mg kg^{-1}, i.v.). Finally, RP 67580 (0.5 mg kg^{-1}) and CP-96,345 (2 mg kg^{-1}) inhibited the vascular effects of NKA and [Lys^5, MeLeu^9,NLeu^{10}]-NKA$_{(4-10)}$, whereas actinomycin D (3 mg kg^{-1}, i.v.) and SR 48968 (2 mg kg^{-1}, i.v.) did not (Table 4).

Discussion

The existence of NK_1 receptors in the guinea-pig lung is strongly supported by the results of previous (Castairs & Barnes, 1986; Aharony *et al.*, 1991; Geraghty *et al.*, 1991; Morimoto *et al.*, 1992) and present radioligand binding studies with [^{3}H]-SP. Since most of the available data on tachykinin receptors in the bronchopulmonary system were obtained by studying the entire lung, one goal of the present work was to assess whether tachykinin binding sites are present in the bronchi. A higher density of NK_1 binding sites (4.6 fold) was found in the guinea-pig bronchus, as compared with the entire lung. The apparent affinity of [^{3}H]-SP for guinea-pig lungs ($K_D = 0.23$ nM) is close to that found for bronchi ($K_D = 0.34$ nM) and is virtually the same as that reported by Morimoto *et al.* (1992) for the lung ($K_D = 0.27$ nM).

Furthermore, we were able to obtain evidence for the first time, to our knowledge, that NK_2 binding sites exist in the bronchi. These results are in agreement with available functional studies showing that both NK_1 and NK_2 receptors mediate bronchoconstriction in the guinea-pig (Maggi *et al.*, 1991; see also Maggi *et al.*, 1993). A major problem for identifying NK_2 sites is the lack of sufficiently selective ligands for this receptor. This problem was brought to light by Geraghty *et al.* (1991), who reported that a low concentration (50 pM) of the NK_2 ligand, [^{125}I]-iodohystidyl-NKA, labelled an NK_1-type receptor in guinea-pig lungs. However, the binding of [^{3}H]-pNKA that we observed in guinea-pig bronchi was compatible with a simultaneous labelling of NK_1 and NK_2 sites since it was displaced to a similar degree (approximately 50%) by low concentrations of the selective antagonists of both NK_1 receptors (RP 67580 and CP-96,345) and NK_2 receptors (SR 48968). Although we have no direct evidence that would exclude the possibility that the inhibition of [^{3}H]-pNKA binding by the NK_1 antagonists is due to their affinity for NK_2 receptors in the tissues studied, we consider this very unlikely because RP 67580, at a concentration of 10 μM, does not modify the binding of [^{3}H]-pNKA to the rat duodenum (Garret *et al.*, 1991), nor does CP-96,345 display significant affinity for NK_2 binding sites (Snider *et al.*, 1991). Furthermore, the combination of SR 48968 with either CP-96,345 or RP 67580 resulted in a greater inhibition of this binding, which was almost equal to the sum of the inhibitory effects produced by each individual compound. That [^{3}H]-pNKA labelled both NK_1 and NK_2 receptors is further supported by the absence of additional effects when RP 67580 and CP-96,345, each at a concentration inhibiting significantly [^{3}H]-pNKA binding, were combined.

The present results, which extend those of Hua *et al.* (1984), also clearly indicate that stimulation of NK_1 or NK_2 receptors with appropriate agonists produces bronchoconstriction in guinea-pigs. We found that the NK_1 receptor agonists, SP, [Pro^9]-SP, and [Sar^9, Met(O$_2$)^{11}]-SP all displaced [^{3}H]-SP from its binding sites in guinea-pig lungs with a similar degree of potency, and all produced bronchoconstriction. Furthermore, we antagonized the effects of these agonists with novel, selective antagonists of these receptors. RP 67580, which exhibited a 50 fold lower affinity for [^{3}H]-SP binding sites than CP-96,345, was also approximately 30 times less potent than CP-96,345 in inhibiting NK_1 receptor agonist-induced bronchoconstriction in guinea-pigs.

Interestingly, septide, another selective NK_1 receptor agonist, was 130 fold less potent than SP in displacing [^{3}H]-SP from its binding sites in the guinea-pig lung, whereas it was 14 fold more potent than SP as a bronchoconstrictor. We have already observed that septide was 350 to 7000 fold less potent than SP in inhibiting binding to NK_1 sites in various animal species and tissues (Fardin *et al.*, 1993). The poor correlation between affinity and functional activity has already been reported for the guinea-pig ileum, where septide is as potent as SP in producing contraction, whereas its affinity

for NK_1 receptors (labelled by either [^{3}H]-SP or [^{3}H]-Pro^9-SP) is at least 200 fold lower than that of SP (Wormser *et al.*, 1986; Fardin & Garret, 1991; Petitet *et al.*, 1992). A possible explanation for these findings is that septide may stimulate a subtype of the NK_1 receptor for which [^{3}H]-SP is not the best ligand (Fardin & Garret, 1991; Petitet *et al.*, 1992). This suggestion is supported by the finding of Petitet *et al.* (1992) showing that GR 71251, a selective NK_1 peptide antagonist (Ward *et al.*, 1990), is 25 fold more potent in antagonizing the contractile effects of septide ($pK_B = 7.9$) than those of Pro^9-SP ($pK_B = 6.5$) in the guinea-pig ileum. However, if a specific 'septide receptor site' exists, the present as well as previous results (Garret *et al.*, 1991; Carruette *et al.*, 1992) indicate that RP 67580 and CP-96,345 can block the activation of both the classical NK_1 and also the putative septide receptor sites. Moreover, recent studies involving the use of a recombinant rat NK_1 receptor, have yielded evidence that septide interacts with the NK_1 receptor at a site distinct from that of SP (Pradier *et al.*, 1993).

In the rat, SP and NKA, even at very high i.v. doses, produced only weak and not easily reproducible bronchoconstrictor responses (Joos *et al.*, 1988). These results suggest that NK_1 and NK_2 receptors are either absent or functionally silent (e.g. absence of coupling) in this species. We favour the former suggestion since, in contrast to what was observed with guinea-pigs, [^{3}H]-SP and [^{3}H]-pNKA specific binding was not detectable in either rat lungs or bronchi under experimental conditions identical to those used for guinea-pigs. However, it has been reported that some NK_1 agonists increase plasma protein extravasation in the rat airways (Saria *et al.*, 1983; Abelli *et al.*, 1991). Therefore, we cannot exclude the possibility that tachykinin receptors are present in the bronchopulmonary region of this species, but only in some discrete areas, particularly at the vascular level. Such species variations have also been found by experiments on isolated tracheal preparations, which failed to demonstrate tachykinin receptor-mediated contractile responses in the rat but did reveal them in the guinea-pig, rabbit and pig (Sheldrick *et al.*, 1990). However, this conclusion is perhaps not entirely valid for the cardiovascular system, since both the rat and guinea-pig respond to NK_1 receptor stimulation with a decrease in blood pressure (Goel & Biggs, 1987). That SP, [Pro^9]-SP, [Sar^9, Met$(O_2)^{11}$]-SP and septide interact with the NK_1 receptor is supported by the ability of RP 67580 and CP-96,345 to antagonize the hypotensive effects of these peptides.

Even though it is known that endopeptidases are present in the lung, the potency of SP as a bronchoconstrictor was only slightly (2.2 fold) enhanced in animals pretreated with phosphoramidon, an inhibitor of the enzyme that inactivates SP (data not shown). Thus, that septide was more potent than SP cannot be totally accounted for by the endogenous degradation of SP. Furthermore, although septide was significantly less potent than SP as a hypotensive agent, similar doses of NK_1 receptor antagonists (RP 67580 or CP-96,345) were needed to antagonize the effect of an equiactive dose of SP or septide. In contrast, septide was not only more potent than SP in inducing bronchospasm in guinea-pigs, but the dose of CP-96,345 inhibiting its effects was 30 fold smaller than that inhibiting the effects of an equiactive dose of SP.

Furthermore, in the rat cardiovascular system, CP-96,345 was found to be less potent than RP 67580 as an antagonist of NK_1 agonist-induced responses. Thus, RP 67580 appears to block NK_1 receptors better in the rat vasculature than in the guinea-pig bronchopulmonary system. The reverse holds true for CP-96,345. Therefore, although NK_1 receptors are present in the rat vascular system, they are not the identical counterpart of those in guinea-pig bronchi. Our *in vivo* results are in agreement with *in vitro* functional and binding studies which have demonstrated that CP-96,345 is a weaker NK_1 antagonist in the rat and mouse than in guinea-pig and human preparations and that the reverse holds true for RP 67580 (Beresford *et al.*, 1991; Fardin *et al.*, 1992).

These findings could be explained by the subtle difference in the amino-acid sequence of the rat and guinea-pig NK_1 receptors, which nevertheless have a high degree of homology (94.6%) (Gorbulev *et al.*, 1992). Indeed, for human and rat NK_1 receptors, the differences in affinities between RP 67580 and CP-96,345 are due to amino-acid differences at position 116 and 290 of the NK_1 receptor (Fong *et al.*, 1992; Pradier *et al.*, 1992). Interestingly, at those two positions, the amino-acids in the human and guinea-pig receptors are identical. An analogous case is the recent demonstration that the human 5-HT_{1B} receptor can be transformed into the rodent 5-HT_{1B} receptor by replacing threonine with asparagine at residue 355 (Oksenberg *et al.*, 1992). This single change renders the pharmacology of those two receptors essentially identical.

As already mentioned, we have also demonstrated the specific binding of [^{3}H]-pNKA to NK_2 receptor sites in guinea-pig bronchi. This biochemical observation is confirmed by functional studies which demonstrate that NKA and [Lys^5, MeLeu^9,NLeu^{10}]-$NKA_{(4-10)}$ produce bronchoconstriction in the guinea-pig, which is blocked specifically by the NK_2 receptor antagonists, actinomycin D and SR 48968. In the rat, the NK_2 receptor agonists, NKA and [Lys^5, MeLeu^9,NLeu^{10}]-$NKA_{(4-10)}$ decreased blood pressure. This observation may indicate the presence of NK_2 receptors in the vascular system of the rat; moreover, NKA and a more selective NK_2 receptor agonist, $NKA_{(4-10)}$, have been reported to be poorly hypotensive peptides (Couture *et al.*, 1989). However, in the present study, the hypotensive effects evoked by NKA and [Lys^5, MeLeu^9,NLeu^{10}]-$NKA_{(4-10)}$ were not modified by the selective NK_2 receptor antagonists, actinomycin D and SR 48968, but were antagonized by the NK_1 receptor antagonists, RP 67580 and CP-96,345. Thus, the rat NK_1 vascular receptor can also be stimulated by NK_2 receptor agonists, suggesting that the active site (or sites) of the NK_1 receptor on the rat vascular system discriminates poorly NK_1 from NK_2 agonists.

In conclusion, radioligand binding and functional studies indicate that NK_1 and NK_2 receptors are present in the bronchopulmonary system of the guinea-pig. A functional NK_1 receptor is present in the rat vasculature, but it differs from that of the guinea-pig bronchopulmonary system, since NK_1 receptor agonists exhibit differential potencies in inducing bronchoconstriction in guinea-pigs and hypotension in rats. The possible activation of NK_2 receptors in guinea-pigs does not appear to explain the differences in potency, since NK_2 antagonists did not modify the responses to NK_1 agonists at the bronchopulmonary level under our experimental conditions. Furthermore, RP 67580 is a more potent antagonist of the rat than of the guinea-pig NK_1 receptor, whereas the reverse relationship exists for CP-96,345, another non-peptide antagonist of NK_1 receptors. Finally, the NK_1 vascular receptor in the rat does not discriminate between NK_1 and NK_2 receptor agonists, since the effects of these substances can be inhibited by NK_1 antagonists but not by NK_2 antagonists. However, this is not the case for the bronchoconstrictor responses to NK_1 and NK_2 receptor agonists which are discriminated only by their respective antagonists. Biochemical (Beresford *et al.*, 1991; Fardin *et al.*, 1992; 1993) and molecular (Gobulev *et al.*, 1992) studies have indicated that the human and guinea-pig NK_1 receptors resemble each other. Therefore, the optimization of chemical series of NK_1 receptor antagonists for human application should employ experimental animal preparations, such as the bronchopulmonary system of the guinea-pig, in which the NK_1 receptors have the same pharmacological characteristics as the human NK_1 receptor.

The authors wish to thank warmly Ms O. Flamand, A. Jolly, N. Massa and C. Thiry for their excellent and patient excution of all experimental procedures described herein. Our warm thanks are extended to Dr S. Lavielle, G. Chassaing and Professor B. Roques for providing [Pro^9]-SP, [Lys^5, MeLeu^9,NLeu^{10}]-$NKA_{(4-10)}$ and kelatorphan, respectively and to Dr K. Pepper for restyling our English.

References

ABELLI, L., MAGGI, C.A., ROVERO, P., DEL BIANCO, E., REGOLI, D., DRAPEAU, G. & GIACHETTI, A. (1991). Effect of synthetic tachykinin analogues on airway microvascular leakage in rats and guinea-pigs: evidence for the involvement of NK-1 receptors. *J. Auton. Pharmacol.*, **11**, 267–275.

ADVENIER, C., EMONDS-ALT, X., VILAIN, P., GOULAOUIC, P., PROIETTO, V., VAN BROECK, D., NALINE, E., NELIAT, G. & LE FUR, G. (1992). SR 48968, a potent and selective non-peptide antagonist of the neurokinin A (NK_2) receptor. *Br. J. Pharmacol.*, **105**, 77P.

AHARONY, D., CATANESE, C.A. & WOODHOUSE, D.P. (1991). Binding of the novel ligand [4,5-^{3}H-Leu^{10}] Substance P to high-affinity NK_1 receptors on guinea-pig lung membranes: Modulation by GTP analogue and sulfhydryl modifying agents. *J. Pharmacol. Exp. Ther.*, **259**, 146–155.

BERESFORD, I.J.M., BIRCH, P.J., HAGAN, R.M. & IRELAND, S.J. (1991). Investigation into species variants in tachykinin NK_1 receptors by use of the non-peptide antagonist, CP-96,345. *Br. J. Pharmacol.*, **104**, 292–293.

BERGSTRÖM, L., BEAUJOUAN, J.C., TORRENS, Y., SAFFROY, M., GLOWINSKI, J., LAVIELLE, S., CHASSAING, G., MARQUET, A., D'ORLEANS-JUSTE, P., DION, S. & REGOLI, D. (1987). [^{3}H]-neurokinin A labels a specific tachykinin-binding site in the rat duodenal smooth muscle. *Mol. Pharmacol.*, **32**, 764–771.

CARRUETTE, A., MOUSSAOUI, S.M., CHAMPION, A., COTTEZ, D., GONIOT, P. & GARRET, C. (1992). Comparison in different tissue preparations of the in vitro pharmacological profile of RP 67580, a new non-peptide substance P antagonist. *Neuropeptides*, **23**, 245–250.

CASTAIRS, J.R. & BARNES, P.J. (1986). Autoradiographic mapping of substance P-receptors in lung. *Eur. J. Pharmacol.*, **127**, 295–296.

CAVERO, I., GOMENI, R., LEFEVRE-BORG, F. & ROACH, A.G. (1980). Comparison of mianserin with desipramine, maprotiline and phentolamine on cardiac presynaptic and vascular postsynaptic α-adrenoceptors and noradrenaline reuptake in pithed normotensive rats. *Br. J. Pharmacol.*, **68**, 321–332.

CHASSAING, G., LAVIELLE, S., LOEUILLET, D., ROBILLIARD, P., CARRUETTE, A., GARRET, C., BEAUJOUAN, J.C., SAFFROY, M., PETITET, F., TORRENS, Y. & GLOWINSKI, J. (1991). Selective agonists of NK_2 binding sites, highly active on rat portal vein (NK_3 bioassay). *Neuropeptides*, **1**, 91–95.

CHENG, Y.C. & PRUSOFF, W.H. (1973). Relationship between the inhibition constant (K_i) and the concentration of inhibitor which causes 50% inhibition (I_{50}) of an enzymatic reaction. *Biochem. Pharmacol.*, **22**, 3099–3108.

COUTURE, R., LANEUVILLE, O. GUIMOND, C., DRAPEAU, G. & REGOLI, D. (1989). Characterization of the peripheral action of neurokinins and neurokinin receptor selective agonists on the rat cardiovascular system. *Naunyn Schmied. Arch. Pharmacol.*, **340**, 547–557.

DELAY-GOYET, P. & LUNDBERG, J.M. (1991). Dactinomycin is a competitive neurokinin-2 receptor antagonist. *Biochem. Biophys. Res. Commun.*, **180**, 1342–1349.

EMONDS-ALT, X., VILAIN, P., GOULAOUIC, P., PROIETTO, V., VAN-BROECK, D., ADVENIER, C., NALINE, E., NELIAT, G., LE FUR, G. & BRELIERE, J.C. (1992). A potent and selective non-peptide antagonist of the neurokinin A (NK_2) receptor. *Life Sci.*, **50**, 101–106.

FARDIN, V., FOUCAULT, F., BOCK, M.D., FLAMAND, O., JOLLY, A., CLERC, F. & GARRET, C. (1993). Variations in affinities for the NK1 receptor: differences between the non-peptide substance P antagonists RP 67580 and CP-96,345 and the agonist septide. *Regul. Pept.*, **46**, 300–303.

FARDIN, V., FOUCAULT, F., BOCK, M.D. & GARRET, C. (1992). Binding profile of RP 67580, a new non-peptide substance P antagonist: Comparison with CP-96,345. *Br. J. Pharmacol.*, **105**, 80P.

FARDIN, V. & GARRET, C. (1991). Species differences between (^{3}H)-Substance P binding in rat and guinea-pig shown by the use of peptide agonists and antagonists. *Eur. J. Pharmacol.*, **201**, 231–234.

FONG, T.M., YU, H. & STRADER, C.D. (1992). Molecular basis for the species selectivity of the neurokinin-1 receptor antagonists CP-96,345 and RP 67580. *J. Biol. Chem.*, **267**, 25668–25671.

FROSSARD, N. & ADVENIER, C. (1991). Tachykinin receptors and the airways. *Life Sci.*, **49**, 1941–1953.

GARRET, C., CARRUETTE, A., FARDIN, V., MOUSSAOUI, S., PEYRONEL, J.F., BLANCHARD, J.C. & LADURON, P.M. (1991). Pharmacological properties of a potent and selective non-peptide substance P antagonist. *Proc. Natl. Acad. Sci. U.S.A.*, **88**, 10208–10212.

GERAGHTY, D.P., MUSSAP, C.J. & BURCHER, E. (1991). Radioiodinated substance P, neurokinin A and eledoïsin bind predominantly to NK_1 receptors in guinea pig lung. *Mol. Pharmacol.*, **41**, 147–153.

GOEL, V. & BIGGS, D.F. (1987). Comparison of the bronchoconstrictor and cardiovascular effects of some tachykinins in guinea-pigs. *Life Sci.*, **40**, 1007–1015.

GOMENI, R. & GOMENI, C. (1980). A conversational graphic program for the analysis of the sigmoid curve. *Comput. Biomed. Res.*, **13**, 489–499.

GORBULEV, V., AKHUNDOVA, A., LUZIUS, H. & FAHRENHOLZ, F. (1992). Molecular cloning of substance P receptor cDNA from guinea-pig uterus. *Biochim. Biophys. Acta*, **1131**, 99–102.

GUARD, S. & WATSON, S.P. (1991). Tachykinin receptor types: classification and membrane signaling mechanisms. *Neurochem. Int.*, **18**, 149–165.

HUA, X., LUNDBERG, J.M., THEODORSSON-NORHEIM, E. & BRODING, E. (1984). Comparison of cardiovascular and bronchoconstrictor effects of substance P, substance K and other tachykinins. *Naunyn Schmied. Arch. Pharmacol.*, **328**, 196–201 and 361 (erratum).

JOOS, G.F., PAUWELS, R.A. & VAN DER STRAETEN, M.E. (1988). The mechanism of tachykinin-induced bronchonconstriction in the rat. *Am. Rev. Respir. Dis.*, **137**, 1038–1044.

KARLSSON, J.A. & PERSSON, C.G.A. (1989). Novel peripheral neurotransmitters and control of the airways. *Pharmacol. Ther.*, **43**, 397–423.

KONZETT, H. & RÖSSLER, R. (1940). Versuchsanordnung zu Untersuchungen an der Bronchialmusculatur. *Arch. Exp. Path. Pharmakol.*, **195**, 71–74.

LAUFER, R., GILON, C., CHOREV, M. & SELINGER, Z. (1986). Characterization of a neurokinin B receptor site in rat brain using a highly selective radioligand. *J. Biol. Chem.*, **261**, 10257–10263.

LAVIELLE, S., CHASSAING, G., JULIEN, S., MARQUET, A., BERGSTROM, L., BEAUJOUAN, J.C., TORRENS, Y. & GLOWINSKI, J. (1986). Specific recognition of SP and NKB receptors by analogues of SP substituted at positions 8 and 9. *Eur. J. Pharmacol.*, **125**, 461–462.

LEE, C.M., JAVITCH, J.A. & SNYDER, S.H. (1983). [^{3}H]-Substance P binding to salivary gland membranes: regulation by guanyl nucleotides and divalent cations. *Mol. Pharmacol.*, **23**, 563–569.

LUNDBERG, J.M. & LOU, Y.P. (1991). Dactinomycin inhibits noncholinergic bronchoconstriction by capsaicin-sensitive sensory nerves in the guinea-pig by antagonizing neurokinin 2 receptor activation. *Acta Physiol. Scand.*, **141**, 141–142.

MAGGI, C.A., PATACCHINI, R., ROVERO, P. & GIACHETTI, A. (1993). Tachykinin receptors and tachykinin receptor antagonists. *J. Auton. Pharmacol.*, **13**, 23–93.

MAGGI, C.A., PATACCHINI, R., ROVERO, P. & SANTICIOLI, P. (1991). Tachykinin receptors and non cholinergic bronchoconstriction in the guinea-pig isolated bronchi. *Am. Rev. Resp. Dis.*, **144**, 363–367.

MCKNIGHT, A.T., MAGUIRE, J.J., ELLIOTT, N.J., FLETCHER, A.C., FOSTER, A.C., TRIDGETT, R., WILLIAMS, B.J., LONGMORE, J. & IVERSEN, L.L. (1991). Pharmacological specificity of novel, synthetic, cyclic peptides as antagonists at tachykinin receptors. *Br. J. Pharmacol.*, **104**, 355–360.

MCPHERSON, G.A. (1985). Analysis of radioligand binding experiments. A collection of computer programs for the IBM PC. *J. Pharmacol. Methods*, **14**, 213–228.

MORIMOTO, H., MURAI, M., MAEDA, Y., HAGIWARA, D., MIYAKE, H., MATSUO, M. & FUJII, T. (1992). FR 113680: a novel tripeptide substance P antagonist with NK_1 receptor selectivity. *Br. J. Pharmacol.*, **106**, 123–126.

MUNSON, P.J. & RODBARD, D. (1980). A versatile computerized approach for characterization of ligand-binding systems. *Anal. Biochem.*, **107**, 220–239.

OKSENBERG, D., MARSTERS, S.A., O'DOWD, B.F., JIN, S., PEROUTKA, S.J. & ASHKENAZI, A. (1992). A single amino-acid difference confers major pharmacological variation between human rodent 5-HT_{1B} receptors. *Nature*, **360**, 161–163.

PETITET, F., SAFFROY, M., TORRENS, Y., LAVIELLE, S., CHASSAING, G., LOEUILLET, D., GLOWINSKI, J. & BEAUJOUAN, J.C. (1992). Possible existence of a new tachykinin receptor subtype in the guinea-pig ileum. *Peptides*, **13**, 383–388.

PRADIER, L., EMILE, L., HABERT, E., MERCKEN, L., LE GUERN, S., MORAS, V., LOQUET, I., CLOT, J., FARDIN, V., DOBLE, A. & MAYAUX, J.F. (1992). Molecular characterization of the NK_1 antagonist species selectivity on rat and human recombinant receptors. *Soc. Neurosci. Abst.*, **18**, 400.

PRADIER, L., MENAGER, J., LE GUERN, J., BOCK, M.D., HEUILLET, E., FARDIN, V., DOBLE, A. & MAYAUX, J.F. (1993). Septide: an agonist of the NK_1 receptor acting at a site distinct from substance P. *Br. J. Pharmacol.*, **110**, 57P.

REGOLI, D., DRAPEAU, G., DION, S. & COUTURE, R. (1988). New selective agonists for neurokinin receptors: pharmacological tools for receptor characterization. *Trends Pharmacol. Sci.*, **9**, 290–295.

SARIA, A., LUNDBERG, J.M., SKOFITSCH, G. & LEMBECK, F. (1983). Vascular protein leakage in various tissues induced by substance P, capsaicin, bradykinin, serotonin, histamine and by antigen challenge. *Naunyn Schmied. Arch. Pharmacol.*, **324**, 212–218.

SHELDRICK, R.L.G., BALL, D.I. & COLEMAN, R.A. (1990). Characterization of the neurokinin receptors mediating contraction of isolated tracheal preparations from a variety of species. *Agents Actions* (Suppl), **31**, 205–209.

SCHMIDT, A.W., MCLEAN, S. & HEYM, J. (1992). The substance P receptor antagonist CP-96,345 interacts with Ca^{2+} channels. *Eur. J. Pharmacol.*, **219**, 491–492.

SMITH, P.K., KROHN, R.I., HERMANSON, G.T., MALLIA, A.K., GARTNER, F.H., PROVENZANO, M.D., FUJIMOTO, E.K., GOEKE, N.M., OLSON, B.J. & KLENK, D.C. (1985). Measurement of protein with bicinchoninic acid. *Anal. Biochem.*, **150**, 76–85.

SNIDER, R.M., CONSTANTINE, J.W., LOWE III, J.A., LONGO, K.P., LEBEL, W.S., WOODY, H.A., DROZDA, S.E., DESAI, M.C., VINICK, F.J., SPENCER, R.W. & HESS, H.J. (1991). A potent nonpeptide antagonist of the substance P (NK1) receptor. *Science*, **251**, 435–437.

WARD, P., EWAN, G.B., JORDAN, C.C., IRELAND, S.J., HAGAN, R.M. & BROWN, J.R. (1990). Potent and highly selective neurokinin antagonists. *J. Med. Chem.*, **33**, 1848–1851.

WATLING, K.J. (1992). Nonpeptide antagonists herald new era in tachykinin research. *Trends Pharmacol. Sci.*, **131**, 266–269.

WILLIAMS, B.J., CURTIS, N.R., MCKNIGHT, A.T., MAGUIRE, J., FOSTER, A. & TRIDGETT, R. (1988). Development of NK-2 selective antagonists. *Regul. Pept.*, **22**, 189–194.

WORMSER, U., LAUFER, R., HART, Y., CHOREV, M., GILON, C. & SELINGER, Z. (1986). Highly selective agonists for substance P receptor subtypes. *EMBO J.*, **5**, 2805–2808.

(Received September 13, 1993
Revised November 11, 1993
Accepted November 17, 1993)

Br. J. Pharmacol. (1994), **111**, 769–776 © Macmillan Press Ltd, 1994

The effects of phorbol 12,13-diacetate on responses of guinea-pig isolated trachea to methylxanthines, isoprenaline and ryanodine

[1]J. Cortijo, [2]C.M. Sanz, V. Villagrasa, E.J. Morcillo, & †R.C. Small

Department of Pharmacology, Faculty of Medicine, University of Valencia, Valencia, Spain and †Smooth Muscle Research Group, School of Biological Sciences, University of Manchester, Oxford Road, Manchester, M13 9PT

1 Using guinea-pig isolated trachea, we have studied how phorbol 12,13-diacetate (PDA) modulates mechanical responses of the tissue to methylxanthines, isoprenaline and ryanodine.

2 Caffeine (10 μM–5 mM), theophylline (10 μM–5 mM) and isoprenaline (1 nM –1 μM), each inhibited the spontaneous tone of the trachea. Pretreatment with PDA (0.1–10 μM) converted relaxant responses to high concentrations of the methylxanthines into contractions. PDA produced no equivalent effect against isoprenaline. Pretreatment with verapamil (1 or 10 μM), nifedipine (0.1 μM) or incubation with Ca^{2+}-free, EGTA (0.1 mM)-containing physiological salt solution (PSS) suppressed the contraction produced by caffeine or theophylline in PDA (5 μM)-treated tissues.

3 The ability of PDA (5 μM) to convert caffeine-induced relaxation into caffeine-induced contraction was retained in tissues pretreated with a combination of atropine (1 μM) and mepyramine (1 μM) and in tissues denuded of the airway epithelium.

4 Caffeine (10 μM–5 mM), theophylline (10 μM–5 mM) and isoprenaline (1 nM–1 μM), each relaxed trachea contracted with histamine (0.1 mM). The relaxation induced by caffeine, theophylline and isoprenaline was markedly reduced in the presence of PDA (5 μM) and the responses to high concentrations of caffeine and theophylline, but not those to isoprenaline, were reversed to contractions. Verapamil (10 μM) prevented the effects of PDA against caffeine- or theophylline-induced relaxation.

5 PDA (1 μM) enhanced the tracheal spasm produced by caffeine (10 mM) and theophylline (10 mM) in indomethacin (2.8 μM)-treated trachea maintained at 20°C. This enhancement was reduced in the presence of verapamil (10 μM).

6 Tested in trachea bathed by K^+-rich (40 mM), Ca^{2+}-free PSS, $CaCl_2$ (0.1–20 mM) caused concentration-dependent spasm. PDA (1–5 μM) did not significantly modify the shape or position of the log concentration-effect curve for $CaCl_2$. In contrast, verapamil (1 and 10 μM) antagonized $CaCl_2$.

7 Tested in trachea bathed by indomethacin (2.8 μM)-containing PSS, ryanodine (1–100 μM) caused concentration-dependent spasm. PDA (5 μM) potentiated ryanodine. Verapamil (10 μM) inhibited ryanodine in inducing spasm and suppressed the ability of PDA to potentiate ryanodine.

8 It is concluded that, in guinea-pig isolated trachea, PDA augments the spasmogenic activity of the methylxanthines and ryanodine. This effect of PDA does not result from PDA-induced suppression of spontaneous tone, from increased cellular entry of Ca^{2+} through L-type channels or from sensitization of the intracellular contractile machinery to activator Ca^{2+}. The evidence suggests, instead, that PDA facilitates methylxanthine- or ryanodine-induced release of Ca^{2+} from the intracellular store.

Keywords: Trachealis muscle; Ca^{2+}-free media; caffeine; isoprenaline; nifedipine; papaverine; phorbol 12,13-diacetate; ryanodine; theophylline; verapamil

Introduction

The proposal that protein kinase C (PKC) can mediate mechanical responses to agonist-induced activation of Ca^{2+}-mobilizing receptors has received considerable experimental support (Nishizuka, 1986). Furthermore, the finding that phorbol esters directly bind to, and activate, PKC (Castagna *et al.*, 1982) has led to the use of such esters as tools for investigating the role of PKC in intact tissues. The effects of phorbol esters on the spontaneous tone of airways smooth muscle *in vitro* seem complex. For example, Schramm & Grunstein (1989) reported that, in rabbit trachealis, low (⩽ 1 μM) concentrations of 12-deoxy-phorbol 13-isobutyrate (DPB) were spasmogenic while high (> 1 μM) concentrations evoked relaxation. In guinea-pig trachealis, phorbol 12-myristate 13-acetate (PMA), phorbol 12,13-diacetate (PDA) and DPB (each 10 μM) produced biphasic responses comprising an initial spasmogenic response, a secondary relaxation and a final, more sustained spasmogenic response (Souhrada & Souhrada, 1989). In the same tissue, phorbol esters have been reported to suppress spontaneous tone at 37°C (Menkes *et al.*, 1986; Huang *et al.*, 1987) but to increase tone at 22°C (Huang *et al.*, 1987).

Several authors have investigated the interaction between phorbol esters and spasmogenic agents acting on airways smooth muscle. In low concentrations (⩽ 1 μM) the phorbol esters have been reported to augment contraction induced by structurally-specific spasmogens (Schramm & Grunstein, 1989) or by KCl (Huang *et al.*, 1987). However, higher concentrations (⩾ 1 μM) of phorbol esters inhibited spasm evoked by carbachol, 5-hydroxytryptamine or prostaglandin $F_{2\alpha}$ (Menkes *et al.*, 1986).

Little study has so far been made of the effects of phorbol esters in modulating the actions of relaxant drugs in airways smooth muscle. The object of the present experiments was therefore to determine, in guinea-pig isolated trachealis, the influence of PDA on the relaxant actions of caffeine, theophylline and isoprenaline.

[1] Author for correspondence.
[2] Present address: Department of Clinical Biopathology, University Hospital 'La Fe', Valencia, Spain.

Methods

Preparation of tissues

Tricoloured guinea-pigs (350–500 g) of either sex were killed by stunning and bleeding. Tracheae were excised, cleaned of extraneous tissues, opened by cutting longitudinally through the cartilage rings diametrically opposite the trachealis, and divided into strips of about 3 mm width. Tracheal strips were suspended in jacketted 10 ml tissue chambers containing physiological salt solution (PSS). Tension changes were recorded with isometric transducers (Grass FT03C) coupled to a multi-channel polygraph. The tracheal strips were subjected to an initial, imposed tension of 2.5 g. Changes of the PSS were made at 15 min intervals for a period of 1 h before any pharmacological intervention occurred.

Effects of PDA on spontaneous tracheal tone

Following 60 min tissue equilibration with PSS, PDA (0.1, 1, 5 or 10 μM) or its vehicle was added to the tissue bath and changes in tissue tone were monitored for up to 80 min.

Effects of PDA on the actions of caffeine, theophylline and isoprenaline in suppressing the spontaneous tone of the trachea

A cumulative log concentration-relaxation curve for caffeine (10 μM–5 mM), theophylline (10 μM–5 mM) or isoprenaline (1 nM–1 μM) was constructed in each tissue. Following washout of the relaxant drug, the tissues were allocated randomly in equal numbers to test and control groups. All tissues were then incubated with PSS for 40 min before the addition of PDA (0.1, 1, 5 or 10 μM; test tissues) or vehicle (time-matched control tissues) to the bath fluid; 20 min later a second cumulative log concentration-effect curve for the relaxant drug was constructed in the presence of PDA (test tissues) or vehicle (control tissues). Similar experiments were performed in which papaverine (0.1, 1 or 10 μM) was substituted for PDA.

In order to analyse the mechanisms underlying spasm evoked by alkylxanthines in PDA-treated tissues, several further types of experiment were performed. The interaction between PDA (5 μM) and caffeine was, for example, studied by the protocol outlined above in tissues where the epithelium had been removed by rubbing with a cotton-wool tipped swab. In such experiments the efficacy of epithelial removal was assessed by low power light microscopy, essentially as described by Small et al. (1990). Further study of the interaction between PDA (5 μM) and caffeine was performed in tissues treated with a combination of atropine (1 μM) and mepyramine (1 μM), these substances being added to the bathing medium 20 min before the addition of PDA or its vehicle.

In a further series of experiments an initial log concentration-effect curve for caffeine or theophylline was constructed against spontaneous tracheal tone. Following alkylxanthine washout, all tissues were incubated in PSS for 40 min. Test tissues were then treated according to one of two protocols. In the first of these protocols, PDA (5 μM) and either verapamil (1 or 10 μM) or nifedipine (0.1 μM) were added to the bath fluid 20 min before reconstructing the log concentration-effect curve to the alkylxanthine. In the second protocol the bath fluid was exchanged for Ca^{2+}-free PSS containing PDA (5 μM) and EGTA (0.1 mM) 20 min before constructing the second alkylxanthine log concentration-effect curve. In each case time-matched control tissues were treated identically to test tissues but were not exposed to the modifying agents (PDA and verapamil; PDA and nifedipine; PDA and Ca^{2+}-free, EGTA-containing PSS).

Effects of PDA on the actions of caffeine, theophylline and isoprenaline in suppressing tracheal tone induced by histamine

Following an initial period of tissue equilibration with PSS (see above), test tissues were treated with caffeine (5 mM) in order to determine the recorder pen position at zero tone. The caffeine was subsequently washed from the tissues and, when spontaneous tone was fully regained, indomethacin (2.8 μM) was added to the bath fluid. Following tone suppression by indomethacin (40 min), histamine (0.1 mM) was added to the bath fluid. Once the spasm evoked by histamine had reached a plateau, PDA (5 μM) was added to the bath fluid; 20 min later a cumulative concentration-response curve for caffeine (10 μM–5 mM), theophylline (10 μM–5 mM) or isoprenaline (1 nM–1 μM) was constructed. In a subset of test tissues, verapamil (10 μM) was added to the indomethacin-containing bath fluid 20 min before the histamine challenge. Time-matched control tissues were treated identically to test tissues but were treated with vehicle instead of PDA.

Effect of PDA on the spasmogenic effects of caffeine and theophylline in trachea maintained at low temperature

Segments of trachea were prepared for observation of the spasmogenic effects of alkylxanthines essentially as described by Small et al. (1988). In brief, the spontaneous tone of the tissues was dissipated by incubating (40 min) the tracheal segments with PSS containing indomethacin (2.8 μM). The bath temperature was then lowered to 20°C. All tissues were next challenged with caffeine (10 mM). Once the caffeine-induced spasm had equilibrated, the bath fluid was changed several times to dissipate the effects of the caffeine. The caffeine challenge was repeated 60 min after the first challenge.

Two groups of test tissues were used. For the first of these tissue groups, PDA (0.01, 0.1 or 1 μM) was added to the bath fluid 40 min before the second caffeine challenge. For the second group of test tissues, PDA (1 μM) was added 40 min before, and verapamil (10 μM) added 20 min before the second caffeine challenge. In each case time-matched control tissues were treated identically to test tissues but were not exposed to PDA. Similar experiments were performed in which caffeine (10 mM) was substituted by theophylline (10 mM).

Effects of PDA and verapamil on log concentration-response curves to $CaCl_2$ in K^+-depolarized trachea

Cumulative log concentration-effect curves to $CaCl_2$ (0.1–20 mM) were constructed in trachea equilibrated with K^+-rich (40 mM), Ca^{2+}-free PSS essentially as described by Foster et al. (1984). Following construction of the initial log concentration-effect curve for $CaCl_2$, test tissues were incubated (20 min) either with PDA (1 or 5 μM) or with verapamil (10 μM) before reconstructing the $CaCl_2$ log concentration-effect curve in the presence of the modifying agent. Time-matched control tissues were treated similarly but were not exposed to PDA or verapamil.

Effects of PDA and verapamil on spasm evoked by ryanodine

Tracheal segments were equilibrated (1 h) in Krebs solution containing indomethacin (2.8 μM). Tissues were then challenged with a single concentration (1, 10 or 100 μM) of ryanodine. Once ryanodine-induced spasm had reached its peak (20–30 min), acetylcholine (10 mM) was added to the bath fluid to identify the maximum contractile response of the tissue. In test tissues the ryanodine challenge was performed in the presence (20 min pre-incubation) of PDA (5 μM), or verapamil (10 μM) or a combination of these

agents. Time-matched control tissues were treated similarly but were not exposed to PDA or verapamil.

Drugs and solutions; statistical analysis of results

The PSS used in the majority of experiments had the following composition (mM): NaCl 118.4, KCl 4.7, $CaCl_2$ 2.5, $MgSO_4$ 0.6, KH_2PO_4 1.2, $NaHCO_3$ 25.0 and dextrose 11.1 The PSS (pH 7.4) was gassed with 5% CO_2 in O_2 and maintained at 37°C. Ca^{2+}-free PSS was prepared by substituting ethyleneglycol-*bis* (β-amino-ethylether)-*N,N'*-tetraacetic acid (EGTA; 0.1 mM) for $CaCl_2$. The K^+-rich (40 mM), Ca^{2+}-free PSS (Foster *et al.*, 1984) was prepared by omitting $CaCl_2$ from the formulation and raising the KCl concentration to 38.8 mM. The concentration of NaCl was reduced to preserve isosmolality.

The following drugs were used: atropine sulphate, caffeine, EGTA, histamine hydrochloride, indomethacin, (−)-isoprenaline hydrochloride, mepyramine maleate, papaverine, phorbol 12,13-diacetate (PDA), theophylline (each from Sigma), nifedipine (Bayer), ryanodine (Calbiochem) and verapamil hydrochloride (Biosedra-Knoll). A stock solution of PDA was prepared in dimethyl sulphoxide and stored at −20°C until the day of use. A stock solution of isoprenaline was prepared in 0.1 M HCl and dilutions made into PSS containing ascorbic acid (0.57 mM). A stock solution of nifedipine was prepared in absolute ethanol and was protected from light. Other substances were dissolved in PSS immediately before use. Drug concentrations are throughout expressed as the bath concentrations of the active species.

Data are presented as means ± s.e.mean. The significance of differences between means was assessed by the application of parameteric (analysis of variance followed by Duncan's test) or non-parametric (Wilcoxon matched pairs, signed rank tests) statistical tests as appropriate. Differences were considered significant when $P<0.05$.

Results

Effects of PDA on spontaneous tracheal tone and on the relaxant actions of caffeine, theophylline and isoprenaline

At 37°C, PDA produced a small and transient contraction followed by a sustained reduction in the spontaneous tone of the trachea. These effects were concentration-dependent (Figures 1 and 2). In the absence of PDA, caffeine (10 μM–5 mM), theophylline (10 μM–5 mM) and isoprenaline (1 nM–1 μM), each produced concentration-dependent inhibition of spontaneous tracheal tone. In the presence of PDA, concentration-response curves for caffeine, theophylline and isoprenaline started from a lower level of tone than those constructed in the absence of PDA (Figures 2 and 3). In the presence of PDA (1, 5 and 10 μM), the responses to high (>100 μM) concentrations of caffeine and theophylline were reversed to contraction. In contrast, PDA produced no equivalent effect against responses to high concentrations of isoprenaline. In the presence of PDA (5 or 10 μM), spasm induced by caffeine or theophylline (each 5 mM) raised tissue tone to a level above that existing at the beginning of the experiment (Figures 2b,3a and 3b). Papaverine (0.1, 1 or 10 μM) reduced spontaneous tracheal tone but, when concentration-effect curves for caffeine and theophylline were constructed in the presence of papaverine, the alkylxanthines failed to exhibit spasmogenic activity (data not shown). The spasmogenic effects of caffeine and theophylline observed in the presence of PDA (5 μM) were markedly inhibited by pretreatment of the tissue with verapamil (1 or 10 μM), nifedipine (0.1 μM) or tissue incubation with Ca^{2+}-free, EGTA (0.1 mM)-containing PSS (Figure 4).

Pre-incubation of tracheal segments with a combination of atropine (1 μM) and mepyramine (1 μM) did not alter either the effects of PDA (5 μM) itself on tracheal tone or the ability of PDA to convert relaxant responses induced by high (>100 μM) concentrations of caffeine into spasmogenic responses. For example, in tissues treated with PDA, the spasmogenic responses to caffeine (5 mM) observed in the absence and presence of the atropine/mepyramine combination were of amplitude 1695 ± 248 mg and 1745 ± 298 mg respectively (mean ± s.e.mean; $n=5$; $P>0.05$).

Low power light microscopy of transverse sections of

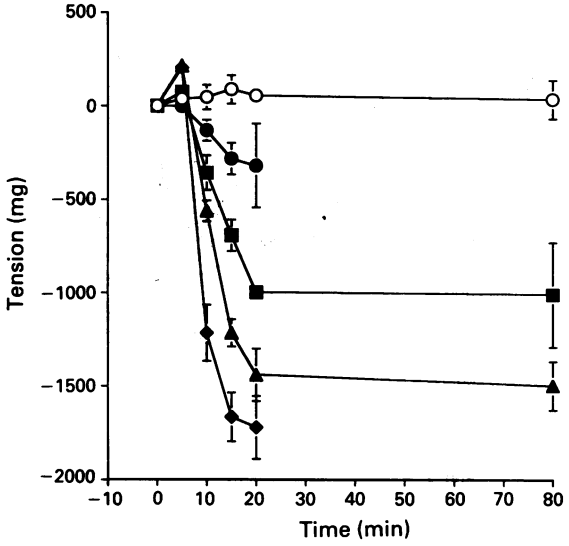


Figure 1 Time course of the effects of phorbol 12,13-diacetate (PDA) (0.1 μM, ●; 1 μM, ■; 5 μM, ▲; 10 μM, ◆) or vehicle (○) on the spontaneous tone of guinea-pig isolated trachea. Abscissa scale: time after administration of PDA or vehicle. Ordinate scale: tension change measured from initial level (0) of spontaneous tone. Data represent means ± s.e.mean of values from 6 tissues.

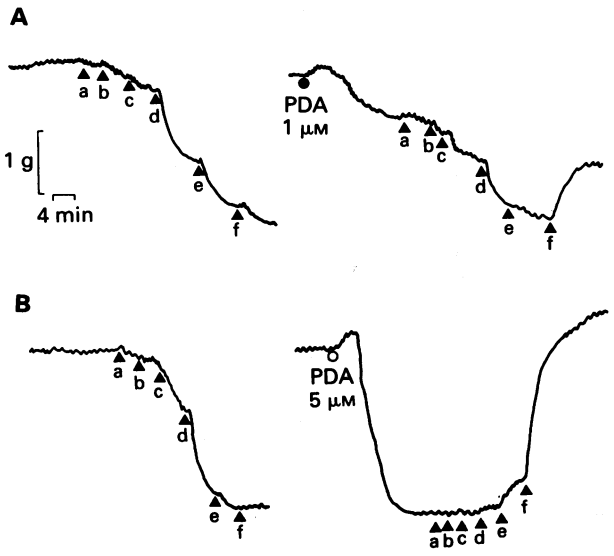


Figure 2 The effect of phorbol 12,13-diacetate (PDA) on the action of caffeine in reducing the spontaneous tone of guinea-pig isolated trachea. In (A) and (B) the left hand trace indicates the initial log concentration-effect curve for caffeine and the right hand panel indicates the log concentration-effect curve for caffeine obtained after incubating (20 min) the tissue with PDA (1 and 5 μM respectively). The arrows (▲) indicate the bath concentration (a,b,c,d,e,f = 10 μM, 50 μM, 100 μM, 500 μM, 1 mM, 5 mM, respectively) of caffeine.

trachea revealed that rubbing the luminal surface of opened tracheal segments with a cotton wool-tipped swab effectively removed the epithelium without damaging the underlying trachealis muscle. Removal of the epithelium in this way did not alter the effects of PDA (5 μM) itself on tracheal tone, nor did it alter the ability of PDA to convert relaxant responses induced by high (>100 μM) concentrations of caffeine into spasmogenic responses. In tissues treated with PDA, the spasmogenic responses to caffeine (5 mM) observed in epithelium-intact and epithelium-denuded tissues were of amplitude 1695 ± 248 mg and 1274 ± 273 mg respectively (mean ± s.e.mean; $n = 5$; $P > 0.05$).

Effects of PDA on the actions of caffeine, theophylline and isoprenaline in suppressing tracheal tone induced by histamine

Tested in the absence of PDA, caffeine (10 μM–5 mM), theophylline (10 μM–5 mM), and isoprenaline (1 nM–1 μM) each produced concentration-dependent inhibition of histamine (0.1 mM)-induced spasm in trachealis treated with

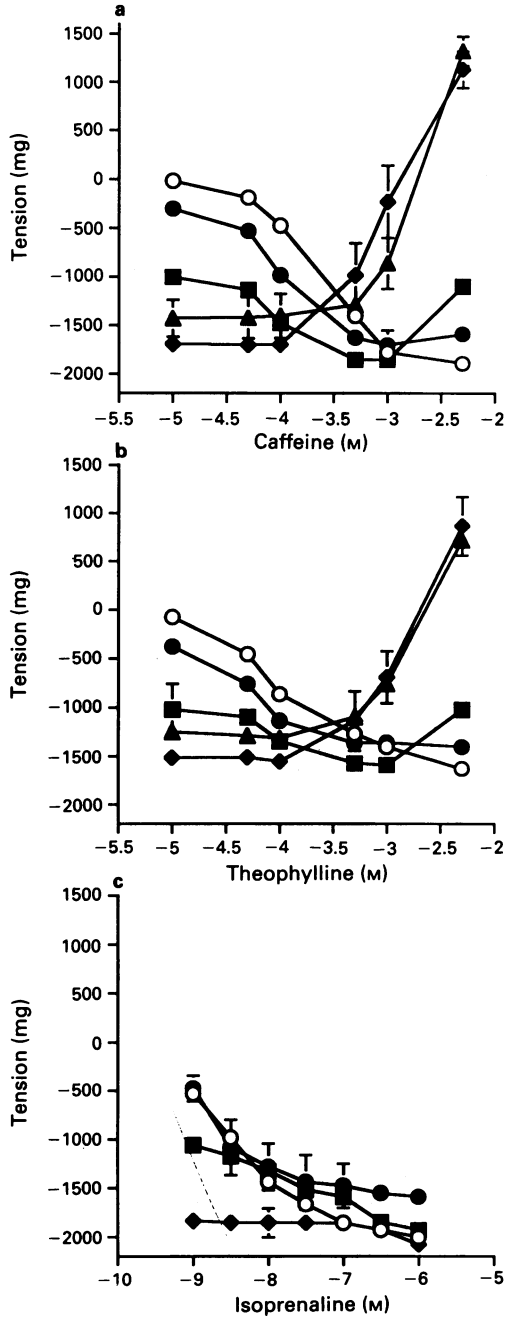


Figure 3 The effect of phorbol 12,13-diacetate (PDA) on the log concentration-response curves of caffeine (a), theophylline (b) and isoprenaline (c) against the spontaneous tone of the guinea-pig isolated trachea: (○) indicates time-matched control log concentration-response curves for the relaxant agents; (●), (■), (▲) and (◆) represent curves obtained in the presence of PDA 0.1, 1, 5 and 10 μM respectively. The abscissae indicate the molar concentration of the relaxant drugs on a log scale. The ordinate scale indicates responses expressed as mg of tension above (+) or below (−) the level of spontaneous tone observed immediately before the administration of PDA (test tissues) or its vehicle (time-matched control tissues). Data are means ± s.e.mean of values from 6 tissues.

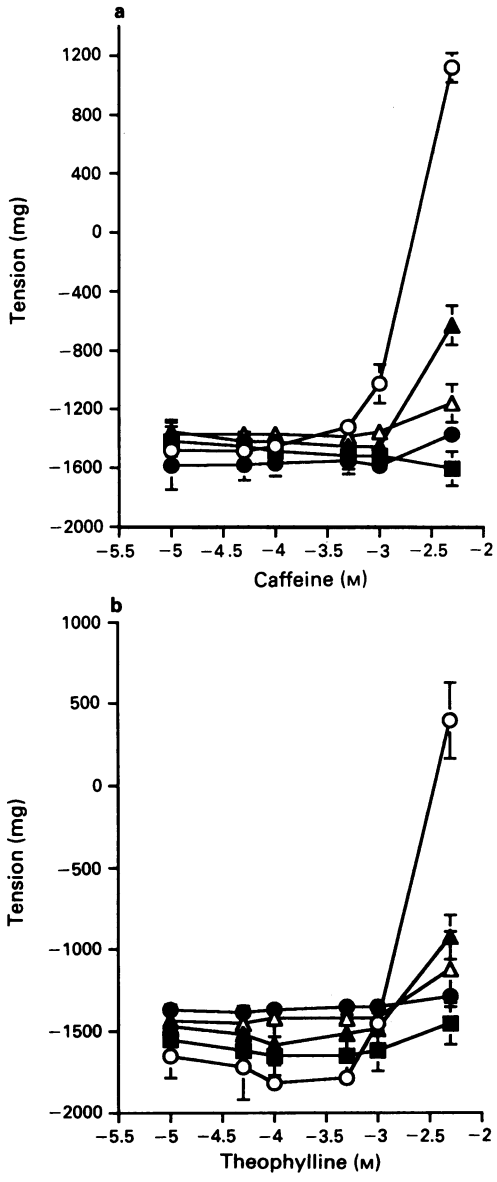


Figure 4 The influence of verapamil, nifedipine and Ca^{2+}-free, EGTA-containing PSS on the effects of phorbol 12,13-diacetate (PDA) on the log concentration-response curves of caffeine (a) and theophylline (b) against the spontaneous tone of guinea-pig isolated trachea. The log concentration-response curves for caffeine were obtained in PDA (5 μM)-treated tissues in the absence (○) or presence of 1 μM (▲) or 10 μM (△) verapamil, 0.1 μM (■) nifedipine, or (●) Ca^{2+}-free EGTA (0.1 mM) solution. The abscissae indicate the molar concentration of caffeine (a) or theophylline (b) on a log scale. The ordinate scale indicates responses as mg of tension above (+) or below (−) the spontaneous tone of the preparation observed immediately before the administration of PDA. Data are means ± s.e.mean of values from 6 tissues.

indomethacin (2.8 μM). PDA (5 μM) evoked little or no change in histamine-induced tone. The relaxant effects of caffeine, theophylline and isoprenaline were reduced in the presence of PDA (5 μM). When caffeine (5 mM) or theophylline (5 mM) were tested in the presence of PDA, both alkylxanthines evoked tracheal spasm. No equivalent spasmogenic activity was observed for isoprenaline (Figure 5).

The administration of verapamil (10 μM) did not reduce histamine (0.1 mM)-induced spasm in trachealis muscle treated with indomethacin (2.8 μM). Tested in the presence of both PDA (5 μM) and verapamil (10 μM), caffeine, theophylline and isoprenaline each produced concentration-dependent relaxation equivalent to that observed in the absence of PDA (Figure 5). The effect of PDA on responses to the three tracheal relaxant agents was therefore ablated by verapamil.

Effects of PDA on the spasmogenic effects of caffeine and theophylline in trachea maintained at low temperature

When caffeine (10 mM) or theophylline (10 mM) were applied to trachea pretreated with indomethacin (2.8 μM) and maintained at 20°C, the two alkylxanthines each evoked spasm, confirming the earlier observations of Small *et al.* (1988). When a second challenge with caffeine or theophylline was performed 60 min after the first challenge, the spasm evoked was not significantly different from that evoked by the first challenge with the alkylxanthine (Table 1). Tested in trachea pretreated with indomethacin (2.8 μM) and maintained at 20°C, PDA (0.01, 0.1 and 1.0 μM) caused concentration-dependent tension development. The spasm evoked by PDA (0.18 ± 0.03 g at 0.01 μM; 0.22 ± 0.06 g at 0.1 μM; 0.43 ± 0.08 g at 1 μM) was slow to develop but was well-sustained. When tissues treated with PDA (1 μM) were subjected to the second challenge with caffeine (10 mM) or theophylline (10 mM), the spasmogenic response to these alkylxanthines was significantly increased compared with the equivalent response observed in control tissues (Table 1).

Verapamil (10 μM) did not itself modify the spasmogenic responses of cooled, indomethacin-treated trachea to either caffeine or theophylline. However, verapamil (10 μM) reduced the spasmogenic effects of PDA (1 μM) and reduced the ability of PDA (1 μM) to enhance the spasm evoked by caffeine and theophylline (Table 1).

Effects of PDA and verapamil on log concentration-response curves to $CaCl_2$ in K^+-depolarized trachea

The addition of $CaCl_2$ (0.1–40 mM) to the K^+-rich (40 mM), Ca^{2+}-free PSS bathing strips of trachea, caused concentration-dependent spasm, confirming the observations of Foster *et al.* (1984). The mean (± s.e.mean) − log EC_{50} values for $CaCl_2$ in the absence and presence of PDA 1 and 5 μM (2.88 ± 0.09, 2.80 ± 0.16 and 2.85 ± 0.12 respectively) did not significantly differ ($P > 0.05$). Furthermore, the shape of the log concentration-effect curve for $CaCl_2$ was unaltered by the presence of PDA 1 or 5 μM (Figure 6). In contrast, verapamil (1–10 μM) shifted the log concentration-effect curve for $CaCl_2$ to the right in a concentration-dependent manner and caused some reduction in the maximal response to $CaCl_2$ (Figure 6).

Effects of PDA and verapamil on spasm evoked by ryanodine

Tested in trachea bathed by indomethacin (2.8 μM)-containing PSS, ryanodine (1–100 μM) caused concentration-dependent spasm which required 20–30 min to reach peak amplitude. PDA (5 μM) markedly augmented the spasm evoked by all tested concentrations of ryanodine. Verapamil (10 μM) suppressed the spasm induced by ryanodine and inhibited the ability of PDA to augment the effects of ryanodine (Figure 7).

Discussion

PDA-induced suppression of the spontaneous tone of the trachealis muscle

The present observation (Figures 1 and 2) that PDA (0.1–10 μM) transiently promotes but then more markedly inhibits

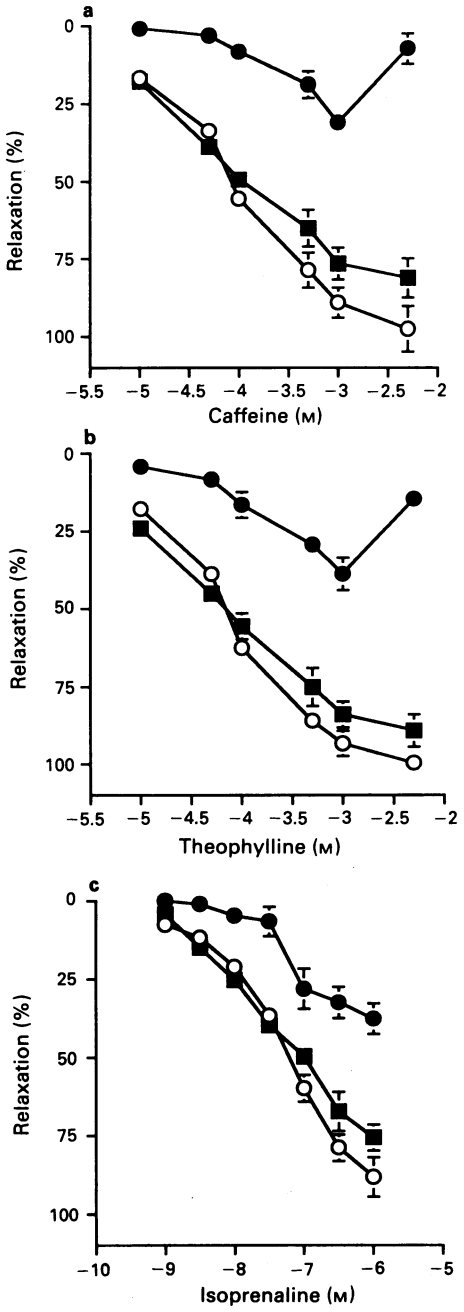


Figure 5 The effects of phorbol 12,13-diacetate (PDA) on the log concentration-response curve of caffeine, theophylline and isoprenaline in suppressing histamine (0.1 mM)-induced tone of guinea-pig isolated trachealis. Abscissae: concentration of caffeine (a), theophylline (b) or isoprenaline (c) on a log scale. Ordinates: relaxation expressed as a percentage of the maximal relaxation induced by caffeine. Indomethacin (2.8 μM) was present throughout the experiments. (○) indicates the log concentration-effect curve for the relaxant drug obtained in the absence of PDA or verapamil; (●) indicates the log concentration-effect curve for the relaxant drug in the presence of PDA (5 μM); (■) indicates the log concentration-effect curve for the relaxant drug in the presence of PDA (5 μM) and verapamil (10 μM). Data points indicate the means ± s.e.mean of values from 6 tissues.

Table 1 Effect of phorbol 12,13-diacetate (PDA) and/or verapamil on caffeine (10 mM)- or theophylline (10 mM)-induced spasm of guinea-pig isolated trachea treated with indomethacin (2.8 μM) and cooled to 20°C

	n	*Caffeine*	*Theophylline*
Control	16	99.7 ± 7.3	96.2 ± 5.3
PDA (0.01 μM)	8	93.7 ± 5.1	99.1 ± 12.1
PDA (0.1 μM)	8	131.1 ± 10.3	121.6 ± 12.3
PDA (1 μM)	8	205.1 ± 8.6*	193.1 ± 7.9*
Verapamil (10 μM)	6	109.1 ± 10.3	102.7 ± 9.8
PDA (1 μM) + verapamil (10 μM)	6	153.2 ± 12.1*†	147.2 ± 7.9*†

Two consecutive challenges with the alkylxanthines were performed. In test tissues, the second challenge was performed in the presence of PDA or verapamil alone, or in combination, as indicated. Data are means ± s.e.mean of n experiments and are expressed as percentages of responses obtained to the initial challenge with the methylxanthine. *$P<0.05$ compared to control; †$P<0.05$ compared to PDA (1 μM).

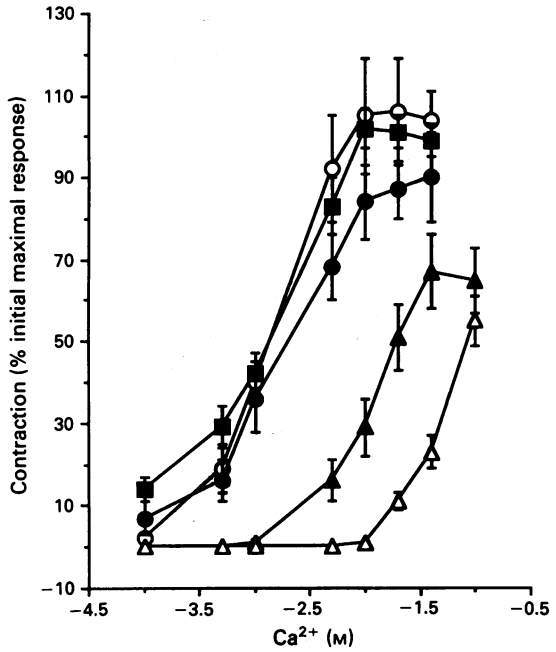


Figure 6 Guinea-pig trachealis bathed by K^+-rich (40 mM), Ca^{2+}-free PSS: the effects of phorbol 12,13-diacetate (PDA) and verapamil on log concentration-effect curves for $CaCl_2$. Abscissa scale: molar concentration of $CaCl_2$ on a log scale. Ordinate scale: spasm as a percentage of the initial maximal response to $CaCl_2$. Log concentration-effect curves for $CaCl_2$ were obtained in the absence of modifying agents (○) (time-matched control tissues) and in the presence of PDA (1 μM ● or 5 μM ■) or verapamil (1 μM ▲ or 10 μM △). Data points indicate the means ± s.e.mean of values from 6 tissues.

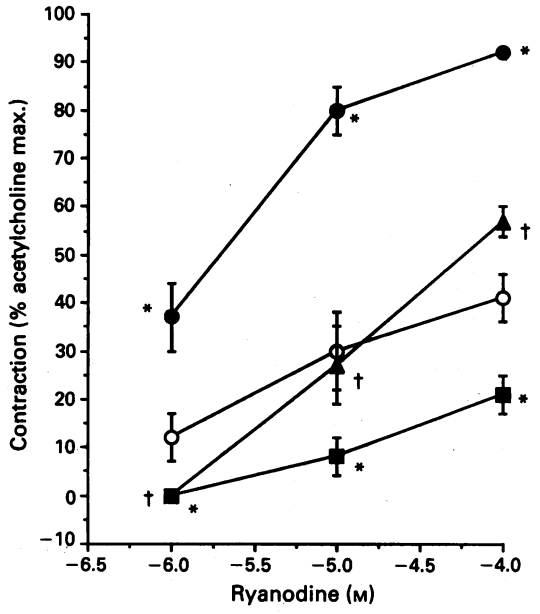


Figure 7 Guinea-pig trachea bathed by indomethacin (2.8 μM)-containing PSS: the effects of phorbol 12,13-diacetate (PDA) and verapamil on spasmogenic responses to ryanodine. Abscissa scale: molar concentration of ryanodine on a log scale. Ordinate scale: spasm expressed as a percentage of that induced by acetylcholine (10 mM). Log concentration-effect curves for ryanodine were obtained in the absence (○, time-matched control tissues) of modifying agents and in the presence of 5 μM PDA (●), 10 μM verapamil (■) or a combination of 5 μM PDA and 10 μM verapamil (▲). Data points indicate means ± s.e.mean of values from 6 tissues. *Indicates a significant ($P<0.05$) difference from the corresponding data point in the ryanodine alone curve; †indicates a significant ($P<0.05$) difference from the corresponding data point in the ryanodine + PDA curve.

the spontaneous tone of guinea-pig isolated trachea confirms the findings of earlier workers (Huang *et al.*, 1987; Souhrada & Souhrada, 1989). The ability of PDA transiently to increase the spontaneous tone of the tissue may reflect the ability of the phorbol ester to facilitate the release of Ca^{2+} from the intracellular store or, in some way, to augment the contractile activity of Ca^{2+} released from the store (see below). It is more difficult to explain why PDA subsequently suppresses the spontaneous tone of the trachea.

An inhibitory effect of this kind could reflect an ability of the phorbol ester to interfere with the intracellular disposition or action of Ca^{2+}. Na^+/K^+-ATPase is a substrate for PKC (Nishizuka, 1986) and it may be that, by activating PKC, PDA can stimulate the activity of Na^+/K^+-ATPase. In trachealis muscle, enhanced activity of Na^+/K^+-ATPase results in cellular hyperpolarization (Souhrada & Souhrada, 1989). This change in membrane potential would reduce the opening of L-type, voltage-dependent Ca^{2+}-channels in the plasmalemma. Hence, PDA could be envisaged as inhibiting the cellular influx of Ca^{2+} by this indirect mechanism. However, in contrast to PDA, organic inhibitors of Ca^{2+} influx through L-type channels (e.g. nifedipine and verapamil) have relatively little effect against the spontaneous tone of guinea-pig trachea (Foster *et al.*, 1984; Ahmed *et al.*, 1985). Furthermore, we have now observed (Figure 6) that PDA (1–5 μM) fails to mimic verapamil (1–10 μM) in inhibiting the spasm evoked by $CaCl_2$ in K^+-depolarized trachealis muscle. These findings suggest that the ability of PDA to suppress the spontaneous tone of the trachea cannot be explained by the phorbol ester acting either directly or indirectly to inhibit the cellular influx of Ca^{2+} through L-type channels.

The present findings that PDA (5 μM) did not suppress

histamine-induced contraction of the trachea and augmented contractile responses to alkylxanthines and ryanodine (Figures 2, 3 and 7) suggests that PDA does not directly reduce the Ca^{2+} sensitivity of the intracellular contractile machinery. This notion receives strong support from the observation (Cortijo *et al.*, 1992) that PDA (0.1–1 μM) does not antagonize Ca^{2+} acting on Triton X-100 skinned trachealis muscle.

The ability of PDA to suppress the spontaneous tone of guinea-pig trachea at concentrations that (a) do not reduce histamine-induced spasm and that (b) augment the spasm induced by alkylxanthines or ryanodine indicates that PDA exerts a selective inhibitory effect against the mechanisms that underlie the generation of the spontaneous tone. There is convincing evidence (Farmer *et al.*, 1974; Gryglewski *et al.*, 1976) to suggest that the spontaneous tone of guinea-pig trachea results from prostaglandin production. Furthermore, in human amnion cells, phorbol esters have been shown to inhibit the biosynthesis of prostaglandins (Mitchell *et al.*, 1991). If PDA produces a similar inhibition of prostaglandin synthesis in guinea-pig trachea, this could well explain the ability of PDA to suppress the spontaneous tone of the trachea without concomitantly reducing the spasm evoked by histamine, alkylxanthines and ryanodine.

Influence of verapamil and PDA on the spasmogenic activity of ryanodine

The present observations that ryanodine (1–100 μM) evokes spasm of guinea-pig trachealis and that such spasm may be inhibited by verapamil (Figure 7) are consistent with an earlier report (Bourreau *et al.*, 1991) that contraction of canine trachealis induced by ryanodine (30 μM) can be suppressed by nifedipine. However, the sensitivity of ryanodine-induced spasm to inhibitors of L-type, voltage-dependent Ca^{2+}-channels does not necessarily imply that ryanodine-induced tension development results from the entry of extracellular activator Ca^{2+} via L-type channels directly into the cytosol. Bourreau *et al.* (1991) have suggested that, in airways smooth muscle, ryanodine acts to promote the release of Ca^{2+} from intracellular stores. These workers also envisaged that, during store refilling, extracellular Ca^{2+} gains access to the store directly (i.e. does not involve prior Ca^{2+} entry into the cytosol) via L-type Ca^{2+}-channels. Hence the suppression of ryanodine-induced spasm of trachealis muscle produced by inhibitors of L-type Ca^{2+}-channels (Bourreau *et al.*, 1991; present study) may reflect interference, by these inhibitors, with the mechanism by which the Ca^{2+} store is refilled from the extracellular milieu.

That ryanodine acts to cause the release of Ca^{2+} from intracellular stores is suggested by the observation that pretreatment of airways smooth muscle with ryanodine (10 μM) inhibits the action of acetylcholine (a spasmogen the actions of which are believed to depend upon an intracellular source of activator Ca^{2+}) in causing tension development either when the tissue is bathed by Ca^{2+}-containing PSS (Al-Hassani *et al.*, 1993) or when the tissue is bathed by a Ca^{2+}-free medium (Chideckel & Anireddy, 1991). Furthermore, by using permeabilized cells cultured from rabbit trachealis muscle, Chopra *et al.* (1991) have directly demonstrated the ability of ryanodine to promote Ca^{2+} release from an intracellular pool. That this pool might overlap that releasable by methylxanthines (see below) is suggested by the observation (Chopra *et al.*, 1991) that pretreatment of the permeabilized cells with ryanodine prevented the Ca^{2+} release induced by caffeine (50 mM).

In the present study PDA very clearly augmented the spasmogenic effects of ryanodine (Figure 7). Since PDA does not appear to promote the influx of Ca^{2+} through L-type channels or to increase the Ca^{2+} sensitivity of the intracellular contractile machinery (Figure 6; Cortijo *et al.*, 1992), the ability of PDA to augment ryanodine-induced spasm indicates that PDA facilitates ryanodine-induced Ca^{2+} release from the intracellular store.

Interactions between PDA and bronchodilator substances acting on trachealis muscle

Treatment of guinea-pig trachea with PDA (0.5–5 μM) suppressed the spontaneous tone of the tissue (Figures 1 and 2) and when high concentrations (500 μM–5 mM) of caffeine and theophylline were administered in the presence of PDA, the two alkylxanthines induced spasm rather than relaxation (Figures 2 and 3). A combination of atropine (1 μM) and mepyramine (1 μM) modified neither the effects of PDA itself on tracheal tone nor the ability of PDA to convert the relaxation induced by high (>100 μM) concentrations of caffeine into spasms. Furthermore, removal of the epithelium failed to modify the action of PDA or its interaction with caffeine. Collectively these findings suggest that neither the action of PDA on the spontaneous tone of the trachea, nor its interaction with caffeine involve the release of acetylcholine from nerve terminals, the release of histamine from intramural sites of sequestration or the release of mediator substances from the airways epithelium.

Several observations suggest that PDA-induced conversion of the relaxant effects of high concentrations of alkylxanthines into spasmogenic effects was not a simple consequence of PDA having lowered the tissue tone. Small *et al.* (1988) showed that, for guinea-pig trachea maintained at 37.5°C, suppression of spontaneous tone using indomethacin (2.8 μM) did not convert caffeine (10 mM)-induced relaxation into a spasmogenic response. In the present study papaverine (0.1–10 μM) was used to reduce the spontaneous tone of the trachea yet, unlike PDA, papaverine did not convert the relaxation induced by caffeine or theophylline into a spasmogenic response. Furthermore, when PDA was applied to trachea treated with indomethacin and histamine (100 μM), it had negligible effect against histamine-induced tone yet converted the relaxation induced by high concentrations of alkylxanthines into spasmogenic responses (Figure 5). We therefore propose that PDA converts the tracheal relaxation induced by high concentrations of alkylxanthines into tracheal spasm by mechanisms other than the simple reduction of tissue tone.

Small *et al.* (1988) and Ortiz *et al.* (1991) have shown that alkylxanthines can evoke spasm of guinea-pig trachea treated with indomethacin (2.8 μM) and maintained at 20°C. That such spasmogenic effects result from alkylxanthine-induced release of Ca^{2+} from intracellular sites of sequestration is suggested by the relative resistance of caffeine-induced spasm to Ca^{2+}-free PSS (Small *et al.*, 1988; Chideckel & Anireddy, 1991). The direct demonstration (Chopra *et al.*, 1991) that caffeine (50 mM) liberates Ca^{2+} from permeabilized cells cultured from rabbit trachealis muscle lends support to this idea.

We considered the possibility that the ability of PDA to augment the spasmogenic activity of alkylxanthines (Figures 2 and 5) represents a PDA-induced increase in the Ca^{2+} sensitivity of the intracellular contractile machinery, perhaps via stimulation of protein kinase C (Rodger & Small, 1991). However, in view of the failure of PDA to potentiate Ca^{2+} acting on K^+ depolarized trachea (Figure 6) or to sensitize skinned trachealis muscle fibres to Ca^{2+} (Cortijo *et al.*, 1992), a more likely explanation for the ability of PDA to augment the spasmogenic activity of the alkylxanthines is that PDA facilitates alkylxanthine-induced release of Ca^{2+} from the intracellular store. As discussed above in the context of ryanodine, the susceptibility of the interaction between PDA and the alkylxanthines to inhibition by a Ca^{2+}-free medium, by nifedipine or by verapamil (Figures 4 and 5) is a reflection of the fact that refilling of the intracellular Ca^{2+} store may require the entry of extracellular Ca^{2+} directly into the store via L-type Ca^{2+}-channels (Bourreau *et al.*, 1991).

As far as we are aware, there have been no reports that isoprenaline can promote the release of Ca^{2+} from the intracellular stores of airways smooth muscle. This may explain why PDA was able to reveal/augment the spasmogenic act-

ivity of alkylxanthines and ryanodine but failed to endow isoprenaline with equivalent activity (Figures 2 and 5).

The authors wish to thank Mr Pedro Santamaría for technical assistance and Mrs Dora Martí for graphical work. This study was supported in part by grants FAR90-680 and FAR91-875 from CICYT (Ministerio de Industria y Energía; Spain).

References

AHMED, F., FOSTER, R.W. & SMALL, R.C. (1985). Some effects of nifedipine in guinea-pig isolated trachealis. *Br. J. Pharmacol.*, **84**, 861–869.

AL-HASSANI, M.H., GARCIA, J.G.N. & GUNST, S. (1993). Differences in Ca^{2+} mobilization by muscarinic agonists in tracheal smooth muscle. *Am. J. Physiol.*, **264**, L53–L59.

BOURREAU, J.P., ABELA, A.P., KWAN, C.Y. & DANIEL, E.E. (1991). Acetylcholine Ca^{2+} stores refilling involves a dihydropyridine-sensitive channel in dog trachea. *Am. J. Physiol.*, **261**, C497–C505.

CASTAGNA, M., TAKAI, Y., KAIBUCHI, K., SANO, K., KIKKAWA, U. & NISHIZUKA, Y. (1982). Direct activation of calcium-activated, phospholipid-dependent protein kinase by tumor-promoting phorbol esters. *J. Biol. Chem.*, **257**, 7847–7851.

CHIDECKEL, E.W. & ANIREDDY, D.R. (1991). Effect of caffeine on tone and intracellular Ca^{2+} release in guinea-pig and human trachealis. *Arch. Int. Pharmacodyn.*, **311**, 166–176.

CHOPRA, L.C., TWORT, C.H., CAMERON, I.R. & WARD, J.P. (1991). Inositol 1,4,5,trisphosphate- and guanosine 5'-O-(3-thiotriphosphate)-induced Ca^{2+} release in cultured airway smooth muscle. *Br. J. Pharmacol.*, **104**, 901–906.

CORTIJO, J., GONZALEZ, M., ORTIZ, J.L. & MORCILLO, E. (1992). Effects of low temperature and pharmacological interventions on the responses of the guinea-pig isolated trachea. *Naunyn-Schmied. Arch. Pharmacol.*, **346**, 573–580.

FARMER, J.B., FARRAR, D.G. & WILSON, J. (1974). Antagonism of tone and prostaglandin-mediated responses in a tracheal preparation by indomethacin and SC-19220. *Br. J. Pharmacol.*, **52**, 559–565.

FOSTER, R.W., OKPALUGO, B.I. & SMALL, R.C. (1984). Antagonism of Ca^{2+} and other actions of verapamil in guinea-pig isolated trachealis. *Br. J. Pharmacol.*, **81**, 499–507.

GRYGLEWSKI, R.J., DEMBINSKA-KIEC, A., GRODZINSKA, L. & PANCZENKO, B. (1976). Differential generation of substances with prostaglandin-like and thromboxane-like activities by guinea-pig trachea and lung strips. In *Lung Cells in Disease*, pp. 289–307. Amsterdam: Elsevier, North Holland Biomedical Press.

HUANG, C.K., MUNAKATA, M., BARABAN, J.M. & MENKES, H. (1987). Protein kinase C and tracheal contraction at low temperature. *J. Pharmacol. Exp. Ther.*, **243**, 270–280.

MENKES, H., BARABAN, J.M. & SNYDER, S.H. (1986). Protein kinase C regulates smooth muscle tension in guinea-pig trachea and ileum. *Eur. J. Pharmacol.*, **122**, 19–27.

MITCHELL, M.D., EDWIN, S.S., LEPERA, R. & LUNDIN-SCHILLER, S. (1991). Epidermal growth factor and the regulation of amnion prostaglandin synthesis. *Prostaglandins, Leukotr. Essent: Fatty Acids*, **44**, 57–59.

NISHIZUKA, Y. (1986). Studies and perspectives of protein kinase C. *Science*, **233**, 305–312.

ORTIZ, J.L., CORTIJO, J., MORCILLO, E.J., SANZ, C., PERPIÑÁ, M. & ESPLUGUES, J. (1988). The spasmogenic effect of caffeine in trachealis isolated from control and actively sensitized guinea-pigs. *Eur. J. Pharmacol.*, **158**, 243–249.

RODGER, I.W. & SMALL, R.C. (1991). Pharmacology of airway smooth muscle. In *Handbook of Experimental Pharmacology*, Vol. 98. ed. Page, C.P. & Barnes, P.J. pp. 107–141. Berlin: Springer-Verlag.

SCHRAMM, C.M. & GRUNSTEIN, M.M. (1989). Mechanisms of protein kinase C regulation of airway contractility. *J. Appl. Physiol.*, **66**, 1935–1941.

SMALL, R.C., BOYLE, J.P., CORTIJO, J., CURTIS-PRIOR, P.B., DAVIES, J.M., FOSTER, R.W. & HOFER, P. (1988). The relaxant and spasmogenic effects of some xanthine derivatives acting on guinea-pig isolated trachealis muscle. *Br. J. Pharmacol.*, **94**, 1091–1100.

SMALL, R.C., GOOD, D.M., DIXON, J.S. & KENNEDY, I. (1990). The effects of epithelium removal on the actions of cholinomimetic drugs in opened segments and perfused tubular preparations of guinea-pig trachea. *Br. J. Pharmacol.*, **100**, 516–522.

SOUHRADA, M. & SOUHRADA, J.F. (1989). Sodium and calcium influx induced by phorbol esters in airway smooth muscle cells. *Am. Rev. Respir. Dis.*, **139**, 927–932.

(Received September 16, 1993
Revised November 17, 1993
Accepted November 18, 1993)

Br. J. Pharmacol. (1994), **111**, 777–786 © Macmillan Press Ltd, 1994

5-Hydroxytryptamine receptor-mediated phosphoinositide hydrolysis in canine cultured tracheal smooth muscle cells

[1]Chuen Mao Yang, Ying-Ling Yo, Jen-Tsung Hsieh & Richard Ong

Cellular and Molecular Pharmacology Laboratory, Department of Pharmacology, Chang Gung Medical College, Kwei-San, Tao-Yuan, Taiwan

1 5-Hydroxytryptamine (5-HT) has been shown to induce contraction of tracheal smooth muscle. However, the mechanisms of action of 5-HT are not known. We therefore investigated the effects of 5-HT on phospholipase C (PLC)-mediated phosphoinositide (PI) hydrolysis and its regulation in canine cultured tracheal smooth muscle cells (TSMCs) labelled with [^{3}H]-inositol. 5-HT-induced inositol phosphates (IPs) accumulation was time- and dose-dependent with a half-maximal response (EC_{50}) and a maximal response at 0.38 ± 0.05 and 10 μM, respectively.

2 Ketanserin and mianserin (10 and 100 nM), 5-HT_2 receptor antagonists, were equipotent in blocking the 5-HT-induced IPs accumulation with pK_B values of 8.46 and 8.21, respectively. In contrast, the dose-response curves of 5-HT-induced IPs accumulation were not shifted until the concentrations of NAN-190 and metoclopramide (5-HT_{1A} and 5-HT_3 receptor antagonists, respectively) were increased up to 10 μM.

3 Pretreatment of TSMCs with pertussis toxin or cholera toxin did not inhibit the 5-HT-induced IPs accumulation, but partially inhibited the AlF_4^--induced IPs response.

4 Stimulation of IPs accumulation by 5-HT required the presence of external Ca^{2+} and was blocked by EGTA. The addition of Ca^{2+} (3–620 nM) to digitonin-permeabilized TSMCs directly stimulated IPs accumulation. A further Ca^{2+}-dependent increase in IPs accumulation was obtained by inclusion of either guanosine 5'-O-(3-thiotriphoshate) (GTPγS) or 5-HT. The combination of GTPγS and 5-HT elicited an additive effect on IPs accumulation.

5 Treatment with phorbol 12-myristate 13-acetate (PMA, 1 μM, 30 min) abolished the 5-HT-induced IPs accumulation. The concentrations of PMA that gave a half-maximal and maximal inhibition of 5-HT-induced IPs accumulation were 2.2 ± 0.4 nM and 1 μM, $n = 3$, respectively. The protein kinase C (PKC) activator, 4α-phorbol 12,13-didecanoate, at 1 μM, did not influence this response. The inhibitory effect of PMA was reversed by staurosporine, a PKC inhibitor, suggesting that the inhibitory effect of PMA is mediated through the activation of PKC.

6 The site of this inhibition was further investigated by examining the effect of PMA on AlF_4^--induced IPs accumulation in canine TSMCs. AlF_4^--stimulated IPs accumulation was inhibited by PMA treatment, suggesting that the effect of PMA is distal to the 5-HT receptor.

7 Acetylcholine-induced IPs accumulation was completely inhibited by atropine, but not affected by ketanserin or mianserin, suggesting that 5-HT-induced IPs accumulation is not due to release of acetylcholine.

8 These results demonstrate that 5-HT directly stimulates PLC-mediated PI hydrolysis via a pertussis toxin- and cholera toxin-insensitive GTP binding protein in canine TSMCs and that this coupling process is negatively regulated by PKC. 5-HT_2 receptors may be predominantly mediating IPs accumulation and presumably IP-induced Ca^{2+} release may function as the transducing mechanism for 5-HT-stimulated contraction of tracheal smooth muscle.

Keywords: 5-Hydroxytryptamine; protein kinase C; inositol phosphates; phorbol ester; G protein

Introduction

5-Hydroxytryptamine (5-HT) has been shown to increase phosphoinositide (PI) hydrolysis in a variety of tissues, including rat cerebral cortex (Kendall & Nahorski, 1985), vascular smooth muscle (Roth *et al.*, 1986), cardiomyocytes (Hamamori *et al.*, 1990), and tracheal smooth muscle (Cohen & Wittenauer, 1987). Phospholipase C (PLC)-mediated PI hydrolysis produced diacylglycerol (DAG) and inositol phosphates (IPs), inositol 1-monophosphate, inositol 1,4-bisphosphate, and inositol 1,4,5-trisphosphate (IP_3), in response to various agonists (Berridge & Irvine, 1989). These two intracellular messenger systems are involved in the regulation of a variety of cellular functions includng exocytosis, gene expression, Na^+-H^+ exchange, and Ca^{2+} influx in different cell types (Berridge & Irvine, 1989). In tracheal smooth muscle, several agonists, such as muscarinic agonists (Grandordy *et al.*, 1986; Meurs *et al.*, 1988; van Amsterdam *et al.*, 1989; Yang *et al.*, 1991; Rosenberg *et al.*, 1991), histamine (Kotlikoff *et al.*, 1987), and bradykinin (Marsh & Hill, 1992) have been shown to stimulate PLC reactions. These agents are believed to mediate smooth muscle contraction via activation of PLC.

5-HT receptors have been classified on the basis of radioligand binding studies, signal transduction mechanisms and molecular cloning techniques, into at least seven subtypes (Frazer *et al.*, 1990). 5-HT_{1A}, 5-HT_{1B} and 5-HT_{1D} are negatively coupled to adenylate cyclase (Schoeffter & Hoyer, 1989), whereas 5-HT_4 receptors are positively coupled to adenylate cyclase (Bockaert *et al.*, 1990). 5-HT_{1C} and 5-HT_2 receptors stimulate PI hydrolysis and result in the generation of DAG and IP_3 which serve as second messengers (Coughlin *et al.*, 1984; Roth *et al.*, 1986; Roth & Chuang, 1987). In

[1] Author for correspondence.

contrast, the 5-HT_3 receptor is a ligand-gated ion channel, which causes a fast depolarization response when activated (Maricq *et al.*, 1991).

5-HT is a potent bronchoconstrictor which has been widely studied in rat and guinea-pig (Baumgartner *et al.*, 1990; Watts & Cohen, 1992). The contractile response of 5-HT is attributed to the direct action of 5-HT on tracheal smooth muscle (Baumgartner *et al.*, 1990; Watts & Cohen, 1992) and to indirect actions mediated by the release of acetylcholine (ACh) from parasympathetic nerve terminals (Macquin-Mavier *et al.*, 1991; Rizzo *et al.*, 1993). 5-HT-induced contraction was also inhibited by the 5-HT_2 receptor antagonists, ketanserin and LY53857 (Cohen *et al.*, 1985; Lemoine & Kaumann, 1986; Baumgartner *et al.*, 1990; Buckner *et al.*, 1991). Moreover, 5-HT did not markedly increase PI turnover in guinea-pig trachea (Cohen & Wittenauer, 1987; Baumgartner *et al.*, 1990), a finding which suggests that the contractile response of 5-HT in trachea may be different from other 5-HT_2 receptors. The mechanisms for actions of 5-HT in canine TSMCs are poorly understood because of the lack of knowledge of relevant molecular mechanisms involved in their receptor activation. Non smooth muscle cells (Breeze & Wheeldon, 1977), which occupy a large part of the whole trachea and tracheal tissue preparation, create a major obstacle in the study of 5-HT receptors and their actions in the trachea. Therefore, it is necessary to use a highly enriched TSMC preparation to delineate molecular mechanisms of 5-HT actions in the trachea.

There is evidence that PLC is coupled to a variety of cell surface receptors via a guanine nucleotide binding protein (Gq) (Sternweis & Smrcka, 1992). A stable analogue of GTP, guanosine 5-*O*-(3-thiotriphosphate) (GTPγS), has been shown to increase IPs accumulation in permeabilized tracheal smooth muscle of rabbits (Rosenberg *et al.*, 1991) and cows (van Amsterdam *et al.*, 1989). Furthermore, a G protein α subunit purified from bovine brain has been shown to selectively stimulate PI hydrolysis by a partially purified PLC (Smrcka *et al.*, 1991). The requirement of calcium for agonist-stimulated PI hydrolysis remains controversial. In some studies, PI hydrolysis has been shown to be dependent on calcium, presumably due to the requirement of this ion for PLC activity (Fisher *et al.*, 1989; Eberhard & Holz, 1991). In another report, no dependence on calcium was observed (Berridge & Irvine, 1989). However, potentiation by GTPγS of 5-HT-induced IPs accumulation under various free Ca^{2+} concentrations has not been investigated in canine TSMCs. Gq proteins have been classified into two distinct groups based on their sensitivity to pertussis toxin (PTX). PTX has been shown to modify various G proteins by ADP-ribosylation (Ui, 1984). Both PTX-sensitive and insensitve G proteins have been reported in several types of cells (Ui, 1984). Therefore, the involvement of G protein(s) in the 5-HT signal transduction requires investigation in TSMCs.

Agonist-activation of PI hydrolysis also leads to the formation of DAG. The ability of phorbol esters, such as phorbol 12-myristate 13-acetate (PMA) which mimics the effect of DAG, to activate PKC (Castagna *et al.*, 1982), has provided a useful tool for examination of the role of the DAG-PKC pathway in cellular functions. In rat aorta, phorbol ester has been found to inhibit 5-HT-induced IPs accumulation and contraction (Roth *et al.*, 1986). Since DAG is one of the products of PI hydrolysis, it is believed that activation of PKC by DAG may serve as a feedback inhibitor in this signal transduction (Watson & Lapetina, 1985).

To define the mechanisms of action of 5-HT in tracheal smooth muscle, the present study was undertaken to determine the effects of 5-HT on PLC-mediated PI hydrolysis and its regulation in canine cultured TSMCs, using 5-HT receptor antagonists, PTX, cholera toxin (CTX), PKC activator, and AlF_4^-, an activator of the regulatory proteins. These results demonstrate that 5-HT induces PLC-mediated PI hydrolysis through the activation of 5-HT_2 receptors in canine TSMCs and that this reaction is negatively regulated by PKC activation. 5-HT_2 receptors may be coupled to PLC via a PTX- and CTX-insensitive Gq protein.

Methods

Animals

Mongrel dogs, 10–20 kg, of either sex were purchased from a local supplier and used throughout this study. Dogs were housed in our animal facilities under automatically controlled temperature and light cycle and fed standard laboratory chow and tap water *ad libitum*. Dogs were anaesthetized with pentobarbitone (30 mg kg^{-1}, intravenously) and the lungs were ventilated mechanically via an orotracheal tube. The tracheae were surgically removed.

Isolation of tracheal smooth muscle cells

The TSMCs were isolated according to the methods described previously (Yang *et al.*, 1991). The trachea was cut longitudinally through the cartilage rings and the smooth muscle was dissected. The muscle was minced and transferred to the dissociation medium containing 0.1% collagenase IV, 0.025% DNase I, 0.025% elastase IV, and antibiotics in physiological solution. The physiological solution contained (mM): NaCl 137, KCl 5, $CaCl_2$ 1.1, $NaHCO_3$ 20, NaH_2PO_4 1, glucose 11 and HEPES 25 (pH 7.4). The tissue pieces were gently agitated at 37°C in a rotary shaker for 1 h. The released cells were collected and the residual was again digested with fresh enzyme solution for an additional 1 h at 37°C. The released cells were washed twice with DMEM/F-12 medium. The cells, suspended in Dulbecco's Modified Eagle's Medium (DMEM)/F-12 containing 10% foetal bovine serum (FBS), were plated onto a 60 mm culture dish and incubated at 37°C for 1 h to remove fibroblasts. The cell number was counted and the suspension diluted with DMEM/F-12 to 2×10^5 cells ml^{-1}. The cell suspension (1 ml/well) was plated onto 12-well culture plates. The medium was changed after 24 h and then every 3 days. After a 5-day culture, cells were moved to DMEM/F-12 containing 1% FBS for 24 h at 37°C. Then, the cells were cultured in DMEM/F-12 containing 1% FBS supplemented with IGF-I (10 ng ml^{-1}) and insulin (1 μg ml^{-1}) for 12–14 days.

In order to characterize the isolated and cultured TSMCs and to exclude contamination by epithelial cells and fibroblasts, the cells were identified by indirect immunofluorescence using a monoclonal antibody of light chain myosin (Gown *et al.*, 1985). Over 95% of the cell preparation was composed of smooth muscle cells.

Accumulation of inositol phosphates

The effect of 5-HT on the hydrolysis of PI was assayed by monitoring the accumulation of ^3H-labelled IPs as described by Berridge *et al.* (1983). Cultured TSMCs were incubated with 5 μCi ml^{-1} of *myo*-[2-^3H]-inositol at 37°C for 2 days. TSMCs were washed two times with PBS and incubated in Krebs-Henseleit buffer (KHS, pH 7.4) containing (in mM) NaCl 117, KCl 4.7, $MgSO_4$ 1.1, KH_2PO_4 1.2, $NaHCO_3$ 20, $CaCl_2$ 2.4, glucose 1, HEPES 20 and LiCl 10, at 37°C for 30 min. After 5-HT had been added at the concentration indicated, incubation was continued for another 60 min. Reactions were terminated by addition of 5% perchloric acid followed by sonication and centrifugation at 3000 *g* for 15 min.

The perchloric acid soluble supernatants were extracted four times with ether, neutralized with potassium hydroxide, and applied to a column of AG1-X8, formate form, 100–200 mesh (Bio-Rad). The resin was washed successively with 5 ml of water and 5 ml of 60 mM ammonium formate-5 mM sodium tetraborate to eliminate free *myo*-[^3H]-inositol and glycerophosphoinositol, respectively. Total IPs was eluted with

5 ml of 1 M ammonium formate-0.1 M formic acid. The amount of [^{3}H]-IPs was determined in a radiospectrometer (Beckman LS5000TA, Fullerton, CA, U.S.A.).

Permeabilized cells

After the prelabelling period, TSMCs were washed two times with PBS and then permeabilized in potassium glutamate-EGTA-HEPES buffer (KGEH) containing (mM): K^+ glutamate 139, ATP 2, $MgCl_2$ 4, LiCl 10, EGTA 2, HEPES 20 (pH 7.4), and digitonin 10 μM, as described by Eberhard & Holz (1987). Cells were allowed to permeabilize for 5 min at 37°C. The permeabilizing buffer was discarded and cells were washed twice with KGEH buffer without digitonin. Incubations were continued for 15 min at 37°C. The required free Ca^{2+} concentrations ($[Ca^{2+}]_f$) were achieved by the addition of various amounts of $CaCl_2$ to the KGEH buffer containing 2 mM EGTA. The $[Ca^{2+}]_f$ was determined by the addition of 10 μM fura-2 (K^+-salt) with an SLM spectrofluorometer (Aminco SLM, Urban, IL, U.S.A.). 5-HT at the indicated concentration was added and incubation continued for 60 min. Reactions were terminated by the addition of 5% perchloric acid. The procedures for extraction, separation, and quantification of IPs were the same as those used for intact cells.

Analysis of data

The EC_{50} of 5-HT for stimulating IPs accumulation was estimated by Graph Pad Programme (Graph Pad, San Diego, CA, U.S.A.). The dissociation constants (K_B) of 5-HT antagonists were estimated by the method of Furchgott (1972), from their ability to antagonize 5-HT-mediated IPs accumulation.

The data were expressed as the mean ± s.e.mean of at least four experiments with statistical comparisons based on a two-tailed Student's t test at a $P<0.01$ level of significance.

Chemicals

Dulbecco's modified Eagle's Medium (DMEM)/F-12 and foetal bovine serum (FBS) were purchased from J.R. Scientific (Woodland, CA, U.S.A.). Insulin and insulin-like growth factor I (IGF-I) were from Boehringer Mannheim (GmbH, Germany). Fura-2 was from Molecular Probes Inc (Eugene, OR, U.S.A.). *Myo*-[^{3}H]-inositol (18 Ci mmol^{-1}) was from Amersham (Buckinghamshire, England). Enzymes and other chemicals were from Sigma Co (St. Louis, MO, U.S.A.).

Results

5-HT-induced IPs accumulation

To study 5-HT-stimulated IPs accumulation, canine cultured TSMCs were labelled for 48 h with [^{3}H]-inositol, treated with 5-HT and extracted. The aqueous phase of cell extracts was used to determine the amount of [^{3}H]-IPs. As shown in Figure 1, 5-HT-induced IPs accumulation increased rapidly up to 10 min of incubation and reached a maximal value at 60 min in the presence of 10 mM LiCl. LiCl alone caused no significant accumulation of IPs within 60 min (data not shown).

Effects of 5-HT receptor antagonists on 5-HT-induced IPs accumulation

As shown in Figure 2, the effect of 5-HT on IPs accumulation was dose-dependent over the range of 1 nM to 100 μM with an EC_{50} of 0.38 ± 0.05 μM and maximal effect at 10 μM, $n = 3$, respectively. Preincubation of TSMCs with 5-HT receptor antagonists inhibited the 5-HT-induced IPs accumulation. The concentration-effect relationship of 5-HT was shifted to the right in a nearly parallel fashion upon addition of ketanserin (10 and 100 nM), mianserin (10 and 100 nM), 1-(2-methoxyphenyl)-4-[4-(2-phthlimido)butyl]piperazine hydrobromide (NAN-190; 10 μM), and metoclopramide (10 μM). The dissociation constants (K_B) were calculated from the dose-ratios by the method developed by Furchgott (1972). There was no significant difference between these two pK_B values for ketanserin and mianserin in antagonizing the 5-HT-induced IPs accumulation (Table 1). Whereas the dose-response curves of 5-HT-induced IPs accumulation were not shifted until the concentrations of the 5-HT_{1A} and 5-HT_3 receptor antagonists, NAN-190 and metoclopramide, increased up to 10 μM. Based on the pK_B values of 8.46, 8.21, 6.34 and 5.80 for ketanserin, mianserin, NAN-190, and metoclopramide, respectively, the 5-HT receptors mediated IPs accumulation were in good agreement with the pharmacological properties of 5-HT_2 receptors in this response (Leysen *et al.*, 1981; Roth *et al.*, 1986; Zifa & Fillion, 1992).

Effect of PTX and CTX on 5-HT-induced IPs accumulation

To gain insight into the identity of the coupling G protein in the 5-HT signal transduction mechanism, cultured TSMCs were preincubated with either CTX or PTX, and IPs accumulation in response to 5-HT was examined. As shown in Figure 3, pretreatment of TSMCs with either PTX (100 ng ml^{-1}, 4 h) or CTX (10 μg ml^{-1}, 4 h) produced no inhibition of the basal or 5-HT-stimulated IPs accumulation. However, both PTX and CTX caused about 40% inhibition of AlF_4^--induced IPs accumulation ($P<0.01$, $n = 5$).

Effect of phorbol esters on 5-HT-induced IPs accumulation

In order to determine whether PKC activation by phorbol esters caused an inhibition of 5-HT-induced IPs accumula-

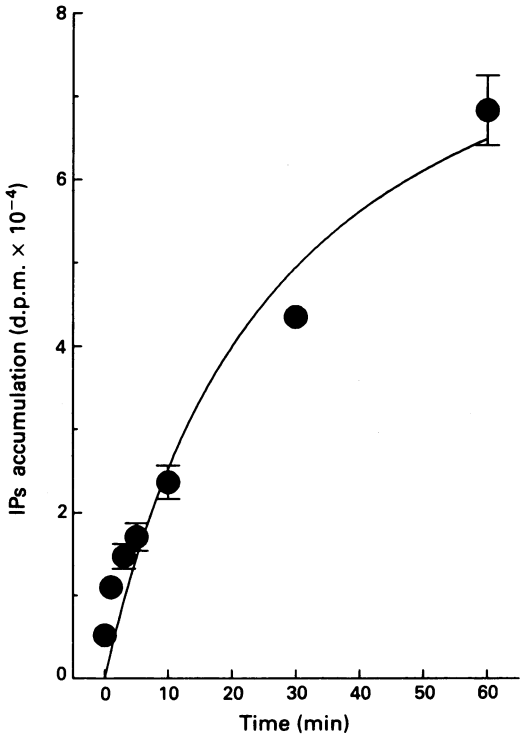


Figure 1 Time response for 5-HT-stimulated [^{3}H]-inositol phosphates ([^{3}H]-IPs) accumulation in cultured TMSCs. 5-HT (100 μM) was added and the reaction was stopped at the time indicated. [^{3}H]-IPs was determined as described under Methods. Results presented are the mean ± s.e.mean of three separate experiments determined in triplicate.

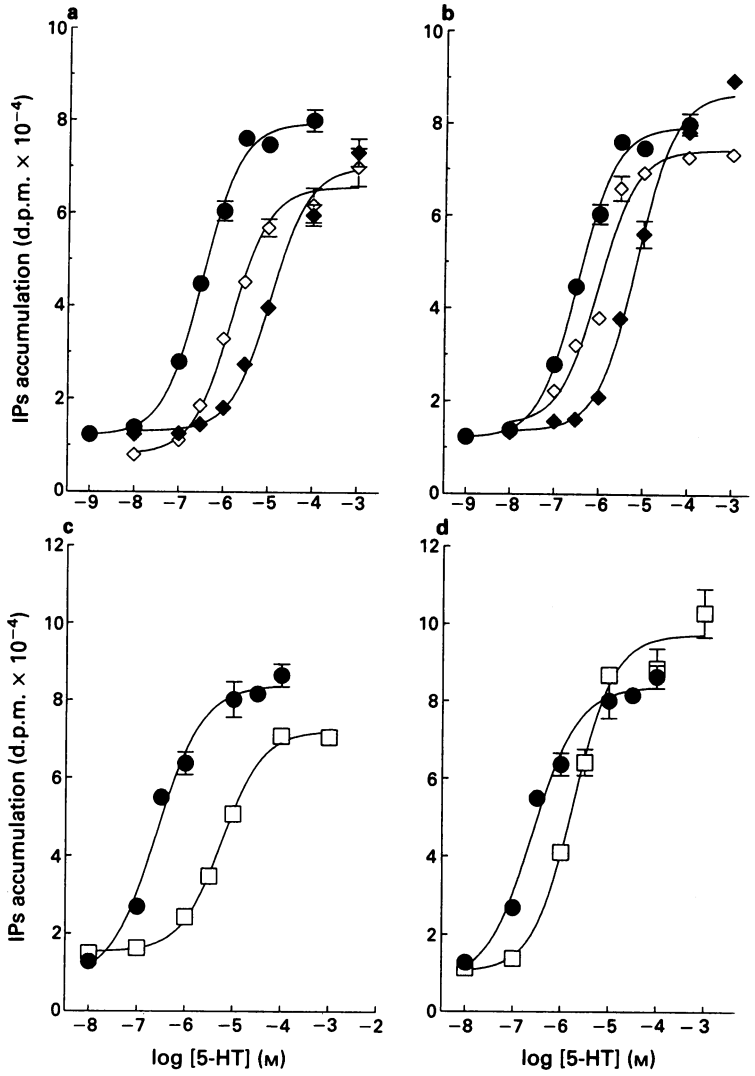


Figure 2 Competitive antagonism of 5-HT-mediated stimulation of inositol phosphates (IPs) accumulation in TSMCs by (a) ketanserin, (b) mianserin, (c) NAN-190, and (d) metoclopramide. 5-HT-stimulated IPs accumulation was measured in the absence (●) and presence of ketanserin (◇, 10 nM; ◆, 100 nM), mianserin (◇, 10 nM; ◆, 100 nM), NAN-190 (□, 10 μM) or metoclopramide (□, 10 μM). 5-HT (1 nM–1 mM) was added and the reaction was stopped after 60 min incubation. [^{3}H]-IPs were determined as described under Methods. Each value represents the mean ± s.e.mean of three experiments determined in triplicate.

tion, the concentration-response relationship for PMA inhibition of 5-HT-stimulated IPs accumulation was examined in cultured TSMCs. As shown in Figure 4, PMA induced half-maximal and maximal inhibition of 5-HT-stimulated IPs accumulation at 2.2 ± 0.4 nM and 1 μM, ($n = 3$) respectively. PMA had no effect on the basal levels of IPs accumulation at any of the concentrations tested. The inhibitory action of PMA appeared to result from a decrease in the maximal response, rather than a shift to the right in the concentration curve for 5-HT-induced IPs accumulation (Figure 5). Furthermore, [^{3}H]-inositol-labelled TSMCs were treated with phorbol esters (1 μM) and then stimulated with 100 μM 5-HT in the continuous presence of phorbol esters (Figure 6). Treatment of TSMCs with 1 μM PMA for 30 min led to an inhibition of 5-HT-stimulated IPs accumulation by 60% ($P < 0.001$, $n = 4$, as compared with the control). The inactive phorbol ester, 4α-phorbol 12,13-didecanoate (4α-PDD, 1 μM), did not block 5-HT-induced IPs accumulation (Figure 6). When TSMCs were pretreated with staurosporine (1 μM), a potent PKC inhibitor, the inhibitory effect of PMA on 5-HT-stimulated IPs accumulation was reversed and the 5-HT-mediated response was significantly enhanced ($P < 0.001$, $n = 4$; Figure 6).

Effect of PMA on direct stimulation of G proteins

To determine whether PMA treatment uncoupled G proteins from PLC, AlF_4^- was used to stimulate G proteins directly and IPs accumulation was measured in TSMCs. Data in Figure 7 reveal that 100 μM 5-HT or 10 μM AlF_4^- elicited essentially identical IPs accumulation in intact TSMCs. Pretreatment of TSMCs with 1 μM PMA for 30 min, inhibited the IPs accumulation induced by 5-HT or AlF_4^- ($P < 0.001$, $n = 3$, as compared with non-treated cells). Parallel experiments were performed on digitonin-permeabilized TSMCs and GTPγS to activate G proteins directly. IPs accumulation induced by GTPγS was also inhibited by PMA treatment (data not shown). These results suggest that the inhibitory effect of PMA on IPs accumulation can be due to activation of PKC and subsequent uncoupling of G proteins from PLC.

Dependence of 5-HT-stimulated IPs accumulation on extracellular Ca^{2+}

To determine whether Ca^{2+} influx is required for the activation of PLC, 5-HT-induced IPs accumulation was performed in Ca^{2+}-free KHS buffer. Results in Figure 8 illustrate the

Table 1 The dissociation constants (K_B) for 5-HT receptor antagonists antagonizing the 5-HT-mediated inositol phosphates (IPs) accumulation

Antagonist	*EC_{50} (μM)*	*Dose-ratio*	*pK_B*
Ketanserin			
(10 nM)	1.5 ± 0.3	3.95 ± 0.23	8.47 ± 0.11
(100 nM)	11 ± 2	28.95 ± 3.16	8.45 ± 0.14
Mianserin			
(10 nM)	0.96 ± 0.13	2.52 ± 0.08	8.18 ± 0.09
(100 nM)	7.1 ± 1.7	18.68 ± 0.19	8.25 ± 0.14
NAN-190			
(10 μM)	5.9 ± 1.4	15.42 ± 1.67	6.16 ± 0.12
Metoclopramide			
(10 μM)	1.9 ± 0.4	4.87 ± 0.75	5.59 ± 0.45

Values (mean ± s.e. for three experiments) were calculated from the dose-response curves for 5-HT as shown in Figure 3. EC_{50} for 5-HT-stimulated IPs accumulation was 0.38 ± 0.05 μM.

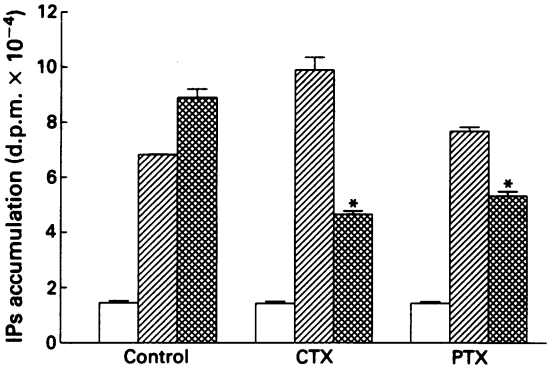


Figure 3 Effects of cholera toxin and pertussis toxin on 5-HT-stimulated [^{3}H]-inositol phosphates ([^{3}H]-IPs) accumulation in cultured TMSCs. Cells were treated with either cholera toxin (CTX, 10 μg ml^{-1}) or pertussis toxin (PTX, 100 ng ml^{-1}) for 4 h and then exposed to 5-HT (100 μM) or AlF_4^- (10 μM $AlCl_3$ and 10 mM NaF) for 60 min. [^{3}H]-IPs were determined as described under Methods. Results presented are the mean ± s.e.mean of five separate experiments determined in triplicate. *$P < 0.001$, as compared with control cells. Open columns, basal; hatched columns, exposed to 5-HT; cross-hatched columns, exposed to AlF_4^-.

dependence of 5-HT-induced IPs accumulation on extracellular Ca^{2+}. TSMCs preincubated in Ca^{2+}-free KHS or in Ca^{2+}-free KHS plus 0.5 mM EGTA for 5 min, led to a significant attenuation of the 5-HT-induced response ($P <$ 0.001, $n = 3$, as compared with Ca^{2+}-containing KHS). Furthermore, 5-HT-induced IPs accumulation was only slightly affected by pretreatment with the Ca^{2+}-channel blockers, diltiazem and verapamil at a concentration of 10 μM (Figure 9). However, Ni^{2+} (5 mM) significantly inhibited 5-HT-induced IPs accumulation (Figure 9; $P < 0.001$, $n = 3$, as compared with control). Moreover, ω-conotoxin and dimethadione had no effect on 5-HT-induced IPs accumulation.

To assess more directly the role played by physiologically relevant Ca^{2+} concentrations in the regulation of the activity of PLC, [^{3}H]-inositol-labelled TSMCs were first permeabilized in digitonin-containing KGEH buffer and then exposed to Ca^{2+}-EGTA buffer. IPs accumulation was measured after 60 min incubation. Elevation of $[Ca^{2+}]_f$ from 3 to 620 nM resulted in a 35% increase in IPs accumulation, with an EC_{50} of 120 ± 29 nM, $n = 3$ (Figure 10). The addition of 50 μM GTPγS further potentiated this Ca^{2+}-dependent IPs accumulation with an EC_{50} for Ca^{2+} of 25 ± 5 nM, $n = 3$. The effect of 5-HT was potentiated by the inclusion of 50 μM GTPγS,

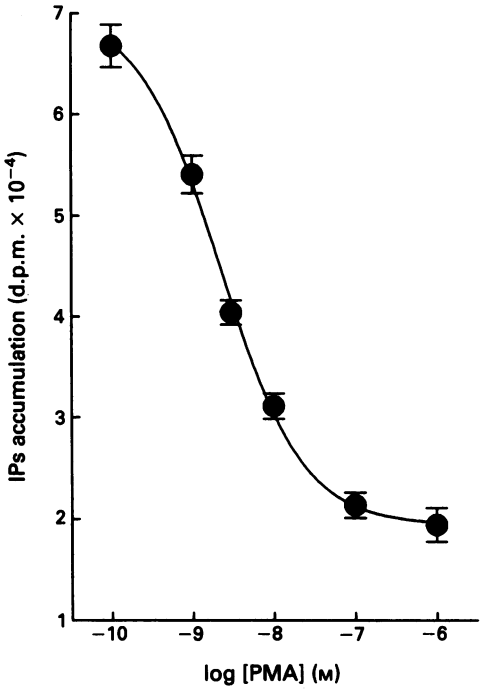


Figure 4 Concentration-dependence of phorbol 12-myristate 13-acetate (PMA) inhibition of 5-HT-stimulated [^{3}H]-inositol phosphates ([^{3}H]-IPs) accumulation in cultured TSMCs. Cells prelabelled with [^{3}H]-inositol were washed with KHS, treated with various concentrations of PMA for 30 min and then exposed to 5-HT (100 μM) for 60 min. [^{3}H]-IPs were determined as described under Methods. Results presented are the mean ± s.e.mean of three separate experiments determined in triplicate. The basal level and 5-HT-induced IPs accumulation were 13430 ± 3500 and 78600 ± 3200 d.p.m./well, respectively.

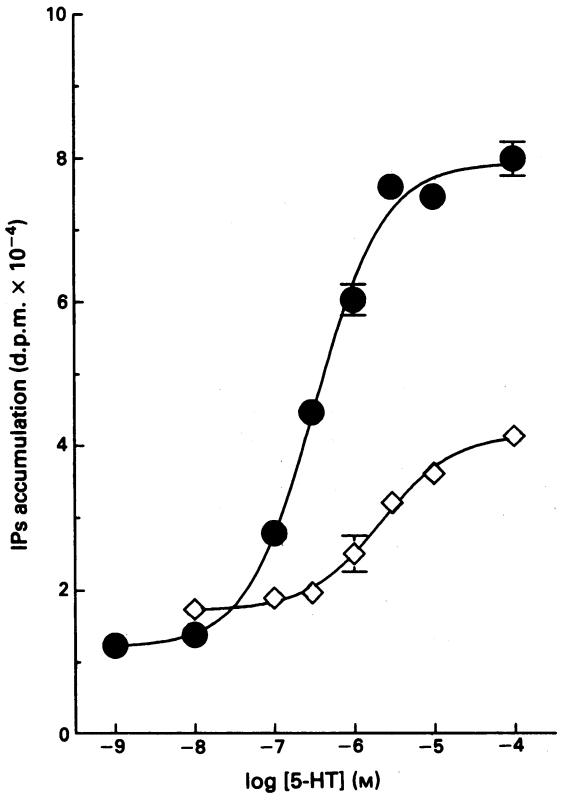


Figure 5 Effect of phorbol 12-myristate 13-acetate (PMA) on concentration curve for 5-HT-induced inositol phosphates (IPs) accumulation. TSMCs were incubated with 10 nM PMA for 30 min and then exposed to various concentrations of 5-HT (10 nM–100 μM) for 60 min. [^{3}H]-IPs were determined as described under Methods. Results presented are the mean ± s.e.mean of three separate experiments determined in triplicate.

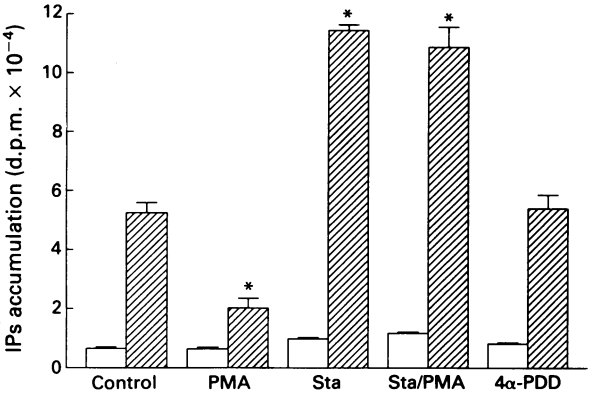


Figure 6 Effects of phorbol ester and staurosporine treatment on 5-HT-stimulated [^{3}H]-inositol phosphates ([^{3}H]-IPs) accumulation in cultured TSMCs. [^{3}H]-inositol-labelled TSMCs were pretreated with phorbol 12-myristate 13-acetate (PMA, 1 μM), staurosporine (Sta, 1 μM), Sta plus PMA, or 4α-phorbol 12,13-didecanoate (4α-PDD, 1 μM) for the indicated time and then exposed to 5-HT (100 μM) for 60 min. [^{3}H]-IPs were determined as described under Methods. Results presented are the mean ± s.e.mean of four separate experiments determined in triplicate. *$P < 0.001$, as compared with non-treated cells stimulated by 5-HT. Open columns, basal level; hatched columns, stimulated by 5-HT.

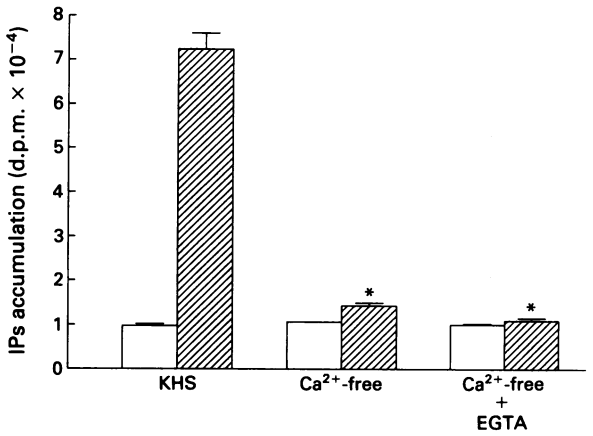


Figure 8 Calcium-dependence of 5-HT-stimulated [^{3}H]-inositol phosphates ([^{3}H]-IPs) accumulation in cultured TSMCs. Cells were prelabelled with [^{3}H]-inositol for 2 days. Labelled cells were incubated in either KHS, Ca^{2+}-free KHS or Ca^{2+}-free KHS plus 0.5 mM EGTA. Then 5-HT (100 μM) was added and continuously incubated for 60 min. [^{3}H]-IPs were determined as described under Methods. Results are the mean ± s.e.mean of three separate experiments determined in triplicate. *$P < 0.001$, as compared with that of cells treated with 5-HT alone in KHS buffer. Open columns, basal level; hatched columns, stimulated by 5-HT.

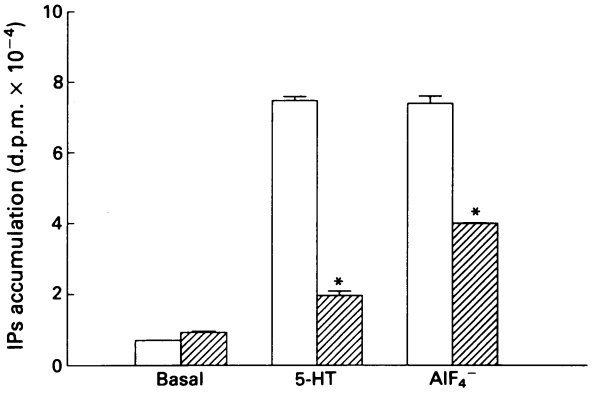


Figure 7 Effect of phorbol 12-myristate 13-acetate (PMA) on direct stimulation of G proteins coupling to phosphoinositide (PI) hydrolysis in intact TSMCs. Cells prelabelled with [^{3}H]-inositol were washed with KHS and incubated in the presence or absence of 1 μM PMA for 30 min. The cells were then exposed to 100 μM 5-HT or 10 μM AlF_4^- (10 μM $AlCl_3$ and 10 mM NaF) for 60 min. The accumulation of inositol phosphates (IPs) was determined as described under Methods. Values are expressed as the mean ± s.e.mean from three separate experiments determined in triplicate. *$P < 0.001$, as compared with untreated cells stimulated with 5-HT. Open columns, control; hatched columns, treated with PMA.

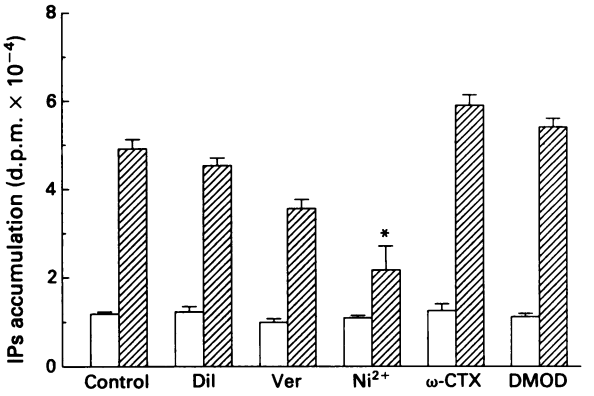


Figure 9 Effects of Ca^{2+}-channel blockers on 5-HT-stimulated [^{3}H]-inositol phosphates ([^{3}H]-IPs) accumulation in cultured TSMCs. [^{3}H]-inositol-labelled cells were preincubated with diltiazem (Dil, 10 μM), verapamil (Ver, 10 μM), Ni^{2+} (5 mM), ω-conotoxin (ω-CTX, 0.1 μM), or dimethadione (DMOD, 0.5 mM) for 30 min and then exposed to 5-HT (100 μM) for 60 min. [^{3}H]-IPs were determined as described under Methods. Results are the mean ± s.e.mean of three separate experiments determined in triplicate. *$P < 0.001$, as compared with control. Open columns, basal level; hatched columns, stimulated by 5-HT.

such that, under these conditions, the $[Ca^{2+}]_f$ required to elicit a half-maximal increase in IPs accumulation was reduced from 65 ± 22 nM to 5.0 ± 0.5 nM, $n = 3$. When 5-HT and GTPγS were added simultaneously, the stimulated accumulation of IPs was 223 ± 36% of control ($n = 3$), a value that compares favourably with the degree of stimulation obtained in intact cells. Therefore, GTPγS and 5-HT together elicit an additive increase in IPs accumulation.

Inability of atropine to inhibit 5-HT-induced IPs accumulation

The contractile response to 5-HT has been shown to be indirectly mediated by release of ACh from parasympathetic nerve terminals (Macquin-Mavier *et al.*, 1991; Rizzo *et al.*, 1993). In addition, muscarinic agonists have been known to induce PI hydrolysis in tracheal smooth muscle (Grandordy *et al.*, 1986; Meurs *et al.*, 1988; van Amsterdam *et al.*, 1989; Rosenberg *et al.*, 1991; Yang *et al.*, 1991). Therefore, it may be argued that in the present study, 5-HT responses can be due to ACh release from nerve cells contaminating the culture. To exclude this possibility, we examined the effect of atropine, a muscarinic antagonist, on 5-HT-induced IPs accumulation (Figure 11). Indeed, ACh (100 μM) induced IPs accumulation in TSMCs. Pretreatment with 10 μM atropine for 30 min completely inhibited the effect of ACh ($P < 0.001$, $n = 3$), but not the effect of 5-HT. These findings indicate that the 5-HT-induced IPs accumulation is not mediated by

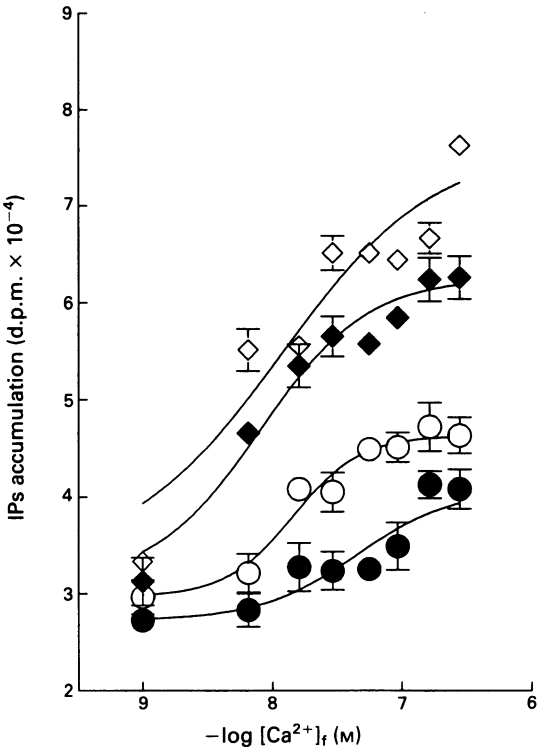


Figure 10 Increase in $[Ca^{2+}]_f$ causes the release of inositol phosphates (IPs) from digitonin-permeabilized TSMCs. [^{3}H]-inositol-prelabelled cells were permeabilized and incubated in KGEH buffer with added Ca^{2+} to achieve the required $[Ca^{2+}]_f$ (as measured by the addition of fura-2). Cells were incubated for 60 min in the absence (●) or presence of either 5-HT (○, 100 μM), GTPγS (◆, 50 μM), or 5-HT plus GTPγS (◇). The EC_{50} values for basal, 5-HT, GTPγS, and 5-HT plus GTPγS were 120, 65, 25 and 5 nM, respectively. Results are expressed as means ± s.e.mean from three separate experiments determined in triplicates. $[Ca^{2+}]_f$ values of 3.03, 16.61, 39.89, 56.35, 100.4, 207.3 and 616.8 nM were obtained at Ca^{2+}/EGTA molar ratios of 0.25, 0.38, 0.50, 0.63, 0.75, 0.88 and 1, respectively, with EGTA maintained at a concentration of 2 mM.

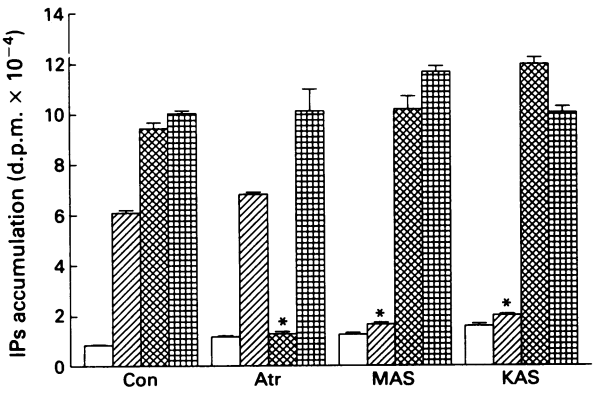


Figure 11 Effects of atropine, mianserin, and ketanserin on agonist-induced [^{3}H]-inositol phosphates ([^{3}H]-IPs) accumulation in canine TSMCs. [^{3}H]-inositol labelled cells were washed with KHS and incubated in the presence of vehicle (control), atropine (Atr, 10 μM), mianserin (MAS, 10 μM), or ketanserin (KAS, 10 μM) for 30 min and then exposed to vehicle (open columns), 5-HT (100 μM, hatched column), ACh (100 μM, cross-hatched column), or AlF_4^- (10 μM $AlCl_3$ and 10 mM NaF, squared column) for 60 min. [^{3}H]-IPs were determined as described under Methods. Each column represents the mean with s.e.mean of three separate experiments determined in triplicate. *$P < 0.001$ as compared with the untreated cells stimulated with respective agonist.

the release of ACh. In contrast, ketanserin and mianserin at concentrations of 10 μM completely inhibited the 5-HT-induced IPs accumulation ($P < 0.001$, $n = 3$), but not the effect induced by ACh (Figure 11). Moreover, both muscarinic and 5-HT receptor antagonists did not affect the AlF_4^--induced IPs accumulation (Figure 11). These results suggest that different agonists induce IPs accumulation which is mediated through specific agonist receptors in canine TSMCs.

Discussion

It has been demonstrated that activation of receptors by neurotransmitters, growth factors, hormones and light causes rapid PI hydrolysis (Rana & Hokin, 1990). The present study demonstrates the 5-HT activation of PLC-mediated hydrolysis of PI through 5-HT_2 receptors and its regulation in canine cultured TSMCs. 5-HT has been shown to produce contractile activity in the trachea and vascular smooth muscle via 5-HT_2 receptors (Roth *et al.*, 1986; Lemoine & Kaumann, 1988; Baumgartner *et al.*, 1990; Buckner *et al.*, 1991; Watts & Cohen, 1992). These observations are consistent with those of several contractile agents including muscarinic agonists, bradykinin and histamine that stimulate tracheal smooth muscle contraction through the same mechanism (Grandordy *et al.*, 1986; Kotlikoff *et al.*, 1987; Meurs *et al.*, 1988; van Amsterdam *et al.*, 1989; Rosenberg *et al.*, 1991; Yang *et al.*, 1991; Marsh & Hill, 1992). 5-HT-stimulated IPs accumulation is time- and dose-dependent and regulated by $[Ca^{2+}]_f$ and GTPγS, a nonhydrolyzable analogue of GTP. 5-HT-stimulated inositol phospholipid-specific PLC may be regulated by PKC stimulation via the formation of DAG. Treatment of TSMCs with PMA dramatically inhibits 5-HT-stimulated IPs accumulation. One possible consequence for the activation of this arm of the second messenger pathway is the presence of a short inhibitory feedback loop in which DAG formation and PKC activation cause an attenuation of agonist-stimulated PLC activity. This mechanism has been proposed for this regulation of agonist-stimulated PLC in a number of cell types (Castagna *et al.*, 1982; Leeb-Lundberg *et al.*, 1985; Orellana *et al.*, 1985). Therefore, studies on the regulatory mechanisms of the PLC activation by 5-HT may lead to a better understanding of functional role of 5-HT in the trachea.

Seven subtypes of 5-HT receptors have been characterized by pharmacological studies, signal transduction mechanisms and molecular cloning techniques (Frazer *et al.*, 1990). Two of these receptors, 5-HT_{1C} and 5-HT_2, are coupled to G proteins which activate PLC (Frazer *et al.*, 1990; Zifa & Fillion, 1992). For example, PI hydrolysis appears to be linked to 5-HT_2 receptors in the brain (Conn *et al.*, 1986), smooth muscle preparations (Coughlin *et al.*, 1984), rat aorta (Roth *et al.*, 1986), and rat cerebral cortex (Roth & Chuang, 1987). However, in the rat choroid plexus it is linked to 5-HT_{1C} receptors (Roth & Chuang, 1987). In the present study, we investigated the effects of ketanserin and mianserin (5-HT_2 receptor antagonists), NAN-190 (5-HT_{1A} antagonist), and metoclopramide (5-HT_3 antagonist) (Leysen *et al.*, 1981; Roth *et al.*, 1986; Frazer *et al.*, 1990; Zifa & Fillion, 1992), on the 5-HT-stimulated IPs accumulation to determine which type of 5-HT receptor is coupled to PLC in canine TSMCs. The dissociation constants, $pK_B = 8.46$ and 8.21, of ketanserin and mianserin (Table 1), respectively, for antagonizing the 5-HT-mediated IPs accumulation, are consistent with that of 5-HT_2 receptors (Leysen *et al.*, 1981; Roth *et al.*, 1986; Frazer *et al.*, 1990; Zifa & Fillion, 1992), since ketanserin possesses a low affinity for antagonizing the 5-HT_{1C}-mediated PLC activation (Conn *et al.*, 1986). Moreover, the 5-HT_{1A} and 5-HT_3 receptor antagonists, NAN-190 and metoclopramide antagonized the 5-HT-induced IPs accumulation with low affinity. These results demonstrate that it is predominantly the 5-HT_2 receptors that mediate IPs accumulation. Presumably IP-induced Ca^{2+} release functions as the trans-

ducing mechanism for 5-HT-stimulated contraction of tracheal smooth muscle.

The involvement of G proteins in receptor coupling to PLC activity has been established for several agonists (Sternweis & Smrcka, 1992). Our results demonstrate that 5-HT stimulation of PLC activity is not inhibited by PTX and CTX (Figure 3), although the latter caused a little increase in the 5-HT-induced IPs accumulation. These results suggest that a coupling process occurs in these cells through a mechanism which is not inhibited by PTX or CTX treatment. To confirm that there is a GTP binding protein coupled to PLC (Sternweis & Smrcka, 1992) in canine TSMCs, we investigated the effect of AlF_4^- on IPs accumulation. It has been proposed that AlF_4^- binds to the nucleotide-binding subunit of transducin when GDP is present in the site (Bigay *et al.*, 1985). This complex would thus mimic the γ-phosphate of GTP and confer on the α-subunit its activated conformation. A similar model can account for AlF_4^- activation of Gq proteins. In fact, we found that AlF_4^- (10 μM) induced an identical magnitude of IPs accumulation to 5-HT. This stimulatory effect of AlF_4^- on IPs accumulation was partially inhibited by CTX or PTX treatment (Figure 3). These results indicate that there are at least two types of Gq proteins, toxin-sensitive and insensitive, in canine TSMCs. 5-HT_2 receptors are coupled to a toxin-insensitive Gq protein. Similar results have been reported for several cell types by others (Garlon *et al.*, 1990; Gutowski *et al.*, 1991). Signal transduction processes have been reported that required GTP but are not affected by these toxins (Martin *et al.*, 1985; Aub *et al.*, 1986).

Agonist-activation of PI hydrolysis also leads to the formation of DAG which is generally accepted to be the physiological activator of the Ca^{2+} and phospholipid-dependent PKC, an enzyme involved in the regulation of a variety of cellular functions (Nishizuka, 1988). There are several lines of evidence that PKC provides a negative feedback regulation over various steps of the cell-signalling processes. First, phosphorylation of a cell surface receptor by PKC may lead to their sequestration (Leeb-Lundberg *et al.*, 1985). Second, PKC-catalyzed phosphorylation of the G protein coupling to PLC results in the attenuation of IPs accumulation (Scherer & Nathanson, 1990). Third, PKC can phosphorylate the PLC enzyme itself (Ryu *et al.*, 1990), and fourth, PKC phosphorylates inositol 5'-phosphomonoesterase and increases phosphatase activity (Connolly *et al.*, 1986). Therefore, phorbol esters are thought to inhibit PLC reactions through activation of PKC. In the present study, the 5-HT-induced PLC activation was inhibited by PMA (Figure 4 and 5), a PKC activator, but not by 4α-PDD which does not affect PKC. Furthermore, staurosporine, a PKC inhibitor, can reverse the inhibitory effect of PMA on the 5-HT-induced IPs accumulation. Taken together, PKC may serve as a feedback inhibitor and attenuate the 5-HT-induced IPs accumulation in canine TSMCs.

The other possibility, that the 5-HT responses observed can be mediated by the ACh release from the contaminating nerve cells (Macquin-Mavier *et al.*, 1991; Rizzo *et al.*, 1993) was excluded, since the muscarinic antagonist, atropine, cannot inhibit the 5-HT-induced IPs accumulation (Figure 11), whereas ACh-induced IPs accumulation was almost completely blocked by atropine (Figure 11). These results suggest that 5-HT activates PLC reactions by directly binding to 5-HT_2 receptors in canine TSMCs. This is consistent with previous findings, which showed that (1) PLC reactions may be the main signal transduction pathway for the tracheal smooth muscle contraction stimulated by several agonists (Grandordy *et al.*, 1986; Kotlikoff *et al.*, 1987; van Amsterdam *et al.*, 1989; Rosenberg *et al.*, 1991; Yang *et al.*, 1991; Marsh & Hill, 1992), and (2) IP_3 has been shown to raise cytosolic Ca^{2+} concentration thereby leading to smooth muscle contraction (Hashimoto *et al.*, 1985).

5-HT-stimulated IPs accumulation is almost completely dependent on the presence of extracellular Ca^{2+} (Figure 8). This calcium dependence is similar to the PI response to agonists in several types of cells (Eberhard & Holz, 1991; Fisher *et al.*, 1989; Yang & Chou, 1992). In the present study, TSMCs exposed to 5-HT, caused a rapid release of IPs in the presence of external Ca^{2+}. However, Ca^{2+}-free buffer or inclusion of 0.5 mM EGTA almost completely abolished the 5-HT-induced increase in IPs accumulation. Furthermore, the 5-HT-induced effect was slightly affected by the presence of the Ca^{2+}-channel blockers diltiazem and verapamil (Figure 9), suggesting that the dihydropyridine-sensitive L type Ca^{2+}-channel may not be involved in the Ca^{2+} influx. However, the non-selective Ca^{2+}-channel blocker Ni^{2+} (Tsien, 1983) did inhibit the 5-HT-stimulated response (Figure 9), indicating that Ca^{2+} influx may be required for the activation of PLC.

Further indications for the requirement of Ca^{2+} for PI hydrolysis have been obtained from experiments with digitonin-permeabilized TSMCs (Figure 10). In the presence of 5-HT and GTPγS, the extent of PI breakdown in permeabilized TSMCs appears to be the same as that obtained in intact cells stimulated by 5-HT alone. Since GTPγS alone could also stimulate IPs accumulation in permeabilized cells, a guanine nucleotide binding protein might be involved in the transduction process (Merritt *et al.*, 1986; Jones *et al.*, 1988). Although 5-HT does enhance IPs accumulation without the addition of GTPγS, this ability presumably reflects the presence of residual endogenous guanine nucleotides within the permeabilized cells. However, the combination of 5-HT and GTPγS have an additive effect on IPs accumulation. GTPγS may play a role in the breakdown of PI that reduces the requirement of $[Ca^{2+}]_f$ for PLC activity (Bradford & Rubin, 1986; Smith *et al.*, 1986). The availability of $[Ca^{2+}]_f$ is required for stimulation of PI hydrolysis. A half-maximal (EC_{50}) increase of IPs accumulation induced by 5-HT alone occurs at a $[Ca^{2+}]_f$ greater than 65 nM, while in the presence of GTPγS, only 5 nM $[Ca^{2+}]_f$ is required for 5-HT to induce a half-maximal increase in IPs accumulation. Therefore, guanine nucleotides appear to sensitize the transduction process such that 5-HT effectively initiates PI hydrolysis at a $[Ca^{2+}]_f$ that is encountered in quiescent cells.

In conclusion, our results demonstrate that 5-HT directly stimulates PLC-mediated PI hydrolysis via 5-HT_2 receptors and that this coupling process is not inhibited by CTX and PTX treatment. The activation of PLC is dependent on the external Ca^{2+}. PMA treatment results in a negative feedback regulation on agonist-induced IPs accumulation. These results suggest that physiological activation of PKC might serve as a modulator of cellular responses induced by IP_3.

This work was supported by grants CMRP-340 and 273 from Chang Gung Medical Research Foundation and NSC83-0412-B182-026 from National Science Council, Taiwan. The authors are greatly indebted to Dr Anthony Herp at Chang Gung Medical College for his critical reading of the manuscript and suggestions. Appreciation is also expressed to Dr Delon Wu for his encouragement.

References

AUB, D.L., FREY, E.A., SEKURA, R.D. & COTE, T.E. (1986). Coupling of the thyrotropin-phospholipase C by GTP-binding protein distinct from the inhibitory or stimulatory GTP-binding protein. *J. Biol. Chem.*, **261**, 9333–9340.

BAUMGARTNER, R.A., WILLS-KARP, M., KAUFMAN, M.J., MUNAKATA, M. & HIRSHMAN, C. (1990). Serotonin induces constriction and relaxation of the guinea pig airway. *J. Pharmacol. Exp. Ther.*, **255**, 165–173.

BERRIDGE, M.J., DAWSON, R.M.C., DOWNES, C.P., HESLOP, J.P. & IRVINE, R.F. (1983). Changes in the levels of inositol phosphates after agonist-dependent hydrolysis of membrane phosphoinositides. *Biochem. J.*, **212**, 473–482.

BERRIDGE, M.J. & IRVINE, R.F. (1989). Inositol phosphates and cell signalling. *Nature*, **341**, 198–205.

BIGAY, J., DETERRE, P., PFISTER, C. & CHABRE, M. (1985). Fluoroaluminates activate transducin-GDP by mimicking the γ-phosphate of GTP in its binding sites. *FEBS Lett.*, **191**, 181–185.

BOCKAERT, J., SEBBEN, M. & DUMUIS, A. (1990). Pharmacological characterization of 5-hydroxytryptamine 4 (5-HT_4) receptors positively coupled to adenylate cyclase in adult guinea-pig hippocampal membranes: effect of substituted benzamide derivatives. *Mol. Pharmacol.*, **37**, 408–411.

BRADFORD, P.G. & RUBIN, R.P. (1986). Guanine nucleotide regulation of phospholipase C activity in permeabilized rabbit neutrophils. *Biochem. J.*, **239**, 97–102.

BREEZ, R.G. & WHEELDON, E.B. (1977). The cells of the pulmonary airways. *Am. Rev. Respir. Dis.*, **116**, 705–777.

BUCKNER, C.K., DEA, D., LIBERATI, N. & KRELL, R.D. (1991). A pharmacological examination of receptors mediating serotonin-induced bronchoconstriction in the anesthetized guinea pig. *J. Pharmacol. Exp. Ther.*, **257**, 26–34.

CASTAGNA, M., TAKAI, Y., KAIBUCHI, K., SANO, K., KIKKAWA, U. & NISHIZUKA, Y. (1982). Direct activation of calcium-activated phospholipid-dependent protein kinase by tumor-promoting phorbol esters. *J. Biol. Chem.*, **257**, 7847–7851.

COHEN, M.L., SCHENCK, K.W., COLBERT, W. & WITTENAUER, L.A. (1985). Role of 5-HT_2 receptors in serotonin-induced contractions of non vascular smooth muscle. *J. Pharmacol. Exp. Ther.*, **232**, 770–774.

COHEN, M.L. & WITTENAUER, L.A. (1987). Serotonin receptor activation of phosphoinositide turnover in uterine, fundal, vascular and tracheal smooth muscle. *J. Cardiovasc. Pharmacol.*, **10**, 176–181.

CONN, P.U., SANDERS-BUSH, E., HOFFMAN, B.J. & HARTIG, P.R. (1986). A unique serotonin receptor in choroid plexus is linked to phosphatidylinositol turnover. *Proc. Natl. Acad. Sci. U.S.A.*, **83**, 4086–4088.

CONNOLLY, T.M., LAWING, W.J. Jr. & MAJERUS, P.W. (1986). Protein kinase C phosphorylates human platelet inositol trisphosphate 5'-phosphomonoesterase, increasing the phosphates activity. *Cell*, **46**, 951–958.

COUGHLIN, S.R., MOSKOWITZ, M. & LEVINE, L. (1984). Identification of a serotonin type-2 receptor linked to prostacyclin synthesis in vascular smooth muscle cells. *Biochem. Pharmacol.*, **33**, 692–695.

EBERHARD, D.A. & HOLZ, R.W. (1987). Cholinergic stimulation of inositol phosphate formation in bovine adrenal chromaffin cells: distinct nicotinic and muscarinic mechanisms. *J. Neurochem.*, **49**, 1634–1643.

EBERHARD, D.A. & HOLZ, R.W. (1991). Regulation of the formation of inositol phosphates by calcium, guanine nucleotides and ATP in digitonin-permeabilized bovine adrenal chromaffin cells. *Biochem. J.*, **279**, 447–453.

FISHER, S.K., DOMASK, L.M. & ROLAND, R.M. (1989). Muscarinic receptor regulation of cytoplasmic Ca^{2+} concentrations in human SK-N-SH neuroblastoma cells: Ca^{2+} requirements for phospholipase C activation. *Mol. Pharmacol.*, **35**, 195–204.

FRAZER, A., MAAYANI, S. & WOLFE, B.B. (1990). Subtypes of receptors for serotonin. *Annu. Rev. Pharmacol. Toxicol.*, **30**, 307–348.

FURCHGOTT, R.F. (1972). The classification of adrenoceptors (adrenergic receptors). An evaluation from the standpoint of receptor theory. In *Catecholamines, Handbook of Experimental Pharmacology*, Vol. 33, ed. Blaschko, H. & Muscholl, E. pp. 283–335. Berlin, Heidelberg, New York: Springer.

GARLON, R., BDOLAH, A., KLOOG, Y. & SOKOLOVSKY, M. (1990). Endothelin/sarafotoxin receptor induced phosphoinositide turnover: effects of pertussis and cholera toxins and of phorbol ester. *Biochem. Biophys. Res. Commun.*, **171**, 949–954.

GOWN, A.M., VOGEL, A.N., GORDON, D. & LU, P.L. (1985). A smooth muscle-specific monoclonal antibody recognizes smooth muscle actin isozymes. *J. Cell. Biol.*, **100**, 807–813.

GRANDORDY, B.M., CUSS, F.M., SAMPSON, A.S., PALMER, J.B. & BARNES, P.J. (1986). Phosphatidylinositol response to cholinergic agonists in airway smooth muscle: relationship to contraction and muscarinic receptor occupancy. *J. Pharmacol. Exp. Ther.*, **238**, 273–279.

GUTOWSKI, S., SMRCKA, A., LOWAK, L., WU, D., SIMON, M. & STERNWEIS, P.C. (1991). Antibodies to the α_q subfamily of guanine nucleotide-binding regulatory protein α subunits attenuate activation of phosphatidylinositol 4,5-bisphosphate hydrolysis by hormones. *J. Biol. Chem.*, **266**, 20519–20524.

HAMAMORI, Y., YOKOYAMA, M., YAMADA, M., AKITA, H., GOSHIMA, K. & FUKUZUKI, H. (1990). 5-Hydroxytryptamine induces phospholipase C-mediated hydrolysis of phosphoinositides through 5-hydroxytyrptamine-2 receptors in cultured fetal mouse ventricular myocytes. *Circ. Res.*, **66**, 1474–1483.

HASHIMOTO, T., MIRATA, M. & ITO, Y. (1985). A role for inositol 1,4,5-trisphosphate in the initiation of agonist-induced contractions of dog tracheal smooth muscle. *Br. J. Pharmacol.*, **86**, 191–199.

JONES, L.G., GOLDSTEIN, D. & BROWN, J.H. (1988). Guanine nucleotide-dependent inositol trisphosphate formation in chick heart cells. *Circ. Res.*, **62**, 299–305.

KENDALL, D.A. & NAHORSKI, S.R. (1985). 5-Hydroxytryptamine-stimlated inositol phospholipid hydrolysis in rat cerebral cortex slices: pharmacological characterization and effects of antidepressants. *J. Pharmacol. Exp. Ther.*, **233**, 473–479.

KOTLIKOFF, M.I., MURRAY, R.K. & REYNOLDS, E.E. (1987). Histamine-induced calcium release and phorbol antagonism in cultured airway smooth muscle cells. *Am. J. Physiol.*, **253**, C561–C566.

LEEB-LUNDBERG, L.M.F., COTECCHIA, S., LOMASNEY, J.W., DEBERNARDIS, J.F., LEFKOWITZ, R.J. & CARON, M.G. (1985). Phorbol esters promote alpha$_1$-adrenergic receptor phosphorylation and receptor uncoupling from inositol phospholipid metabolism. *Proc. Natl. Acad. Sci. U.S.A.*, **82**, 5651–5655.

LEMOINE, H. & KAUMANN, A.J. (1986). Allosteric properties of 5-HT_2 receptors in tracheal smooth muscle. *Naunyn-Schmied. Arch. Pharmacol.*, **333**, 91–97.

LEYSEN, J.E., NIEMEBEERS, J.E., VAN NUETEN, J.M. & LADURON, P.M. (1981). [^{3}H]Ketanserin (R41 468), a selective ^{3}H-ligand for serotonin$_2$ receptor binding sites. *Mol. Pharmacol.*, **21**, 301–314.

MACQUIN-MAVIER, I., PIERRE-HENRI, J., ISTIN, N. & HARF, A. (1991). 5-Hydroxytryptamine-induced bronchoconstriction in the guinea-pig: effect of 5-HT_2 receptor activation on acetylcholine release. *Br. J. Pharmacol.*, **102**, 1003–1007.

MARICQ, A.V., PETERSON, A.S., BRAKE, A.J., MYERS, R.M. & JULIUS, D. (1991). Primary structure and functional expression of the 5-HT_3 receptor, a serotonin-gated ion channel. *Science*, **254**, 432–437.

MARSH, K.A. & HILL, S.H. (1992). Bradykinin B_2 receptor-mediated phosphoinositide hydrolysis in bovine cultured tracheal smooth muscle cells. *Br. J. Pharmacol.*, **107**, 443–447.

MARTIN, U.W., EVANS, T. & HARDEN, T.K. (1985). Further evidence that muscarinic cholinergic receptors of 1321N1 astrocytoma cells, couple to a guanine nucleotide regulatory protein that is not Ni. *Biochem. J.*, **229**, 539–544.

MERRITT, J.E., TAYLOR, C.W., RUBIN, R.P. & PUTNEY, J.W. Jr. (1986). Evidence suggesting that a novel guanine nucleotide regulatory protein couples receptors to phospholipase C in exocrine pancreas. *Biochem. J.*, **236**, 337–343.

MEURS, H., ROFFEL. A.F., POSTEMA, J.B., TIMMERMANS, A., ELZINGA, C.R.S., KAUFFMAN, H.F. & ZAAGSMA, J. (1988). Evidence for a direct relationship between phosphoinositide metabolism and airway smooth muscle contraction induced by muscarinic agonists. *Eur. J. Pharmacol.*, **156**, 271–274.

NISHIZUKA, Y. (1988). The molecular heterogeneity of protein kinase C and implications for cellular regulation. *Nature*, **334**, 661–665.

ORELLANA, S.A., SOLSKI, P.A. & BROWN, J.H. (1985). Phorbol ester inhibits phosphoinositide hydrolysis and calcium mobilization in cultured astrocytoma cells. *J. Biol. Chem.*, **260**, 5236–5239.

RANA, R.S. & HOKIN, L.E. (1990). Role of phosphoinositides in transmembrane signaling. *Physiol. Rev.*, **70**, 115–164.

RIZZO, C.A., KREUTNER, W. & CHAPMAN, R.W. (1993). 5-HT_3 receptors augment neuronal, cholinergic contractions in guinea pig trachea. *Eur. J. Pharmacol.*, **234**, 109–112.

ROSENBERG, S.M., BERRY, G.T., YANDRASITZ, J.R. & GRUNSTEIN, M.M. (1991). Maturational regulation of inositol 1,4,5-trisphosphate metabolism in rabbit airway smooth muscle. *J. Clin. Invest.*, **88**, 2032–2038.

ROTH, B.L. & CHUANG, D.-M. (1987). Multiple mechanisms of serotoninergic signal transduction. *Life Sci.*, **41**, 1051–1064.

ROTH, B.L., NAKAKI, T., CHUANG, D.-M. & COSTA, E. (1986). 5-Hydroxytryptamine$_2$ receptors coupled to phospholipase C in rat aorta: modulation of phosphoinositide turnover by phorbol ester. *J. Pharmacol. Exp. Ther.*, **238**, 480–485.

RYU, S.H., KIM, U.-H., WAHL, M.I., BROWN, A.B., CARPENTER, G., HUANG, K.-P. & RHEE, S.G. (1990). Feedback regulation of phospholipase C-β- by protein kinase C. *J. Biol. Chem.*, **265**, 17941–17945.

SCHERER, N.M. & NATHANSON, N.M. (1990). Differential regulation by agonist and phorbol ester of cloned m1 and m2 muscarinic acetylcholine receptors in mouse Y1 adrenal cells and in Y1 cells deficient in cAMP-dependent protein kinase. *Biochemistry*, **29**, 8475–8483.

SCHOEFFTER, P. & HOYER, D. (1989). 5-Hydroxytryptamine 5-HT$_{1B}$ and 5-HT$_{1D}$ receptors mediating inhibition of adenylate cyclase activity: pharmacological comparison with special reference to the effects of yohimbine, rauwolscine and some B-adrenergic antagonists. *Naunyn-Schmied. Arch. Pharmacol.*, **340**, 285–292.

SMITH, C.D., COX, C.C. & SNYDERMAN, R. (1986). Receptor-coupled activation of phosphoinositide-specific phospholipase C by an N protein. *Science*, **232**, 97–100.

SMRCKA, A.V., HELPER, J.R., BROWN, K.O. & STERNWEIS, P.C. (1991). Regulation of phosphoinositide-specific phospholipase C activity by purified Gq. *Science*, **251**, 804–807.

STERNWEIS, P.C. & SMRCKA, A.V. (1992). Regulation of phospholipase C by G proteins. *Trends Biochem. Sci.*, **17**, 502–506.

TSIEN, R.W. (1983). Calcium channels in excitable cell membranes. *Annu. Rev. Physiol,*. **45**, 341–356.

UI, M. (1984). Islet-activating protein, pertussis toxin: A probe for functions of the inhibitory guanine nucleotide regulatory component of adenylate cyclase. *Trends Pharmacol. Sci.*, **5**, 277–279.

VAN AMSTERDAM, R.G.M., MEURS, H., BROUWER, F., POSTEMA, J.B., TIMMERMANS, A. & ZAAGSMA, J. (1989). Role of phosphoinositide metabolism in functional antagonism by airway smooth muscle contraction by β-adrenoceptor agonists. *Eur. J. Pharmacol.*, **172**, 175–183.

WATSON, S.P. & LAPETINA, E.G. (1985). 1,2-Diacylglycerol and phorbol ester inhibit agonist-induced formation of inositol phosphates in human platelets: possible implications for negative feedback regulation of inositol phospholipid hydrolysis. *Proc. Natl. Acad. Sci. U.S.A.*, **82**, 2623–2626.

WATTS, S.W. & COHEN, N.L. (1992). Characterization of the contractile serotonergic receptor in guinea pig trachea with agonists and antagonists. *J. Pharmacol. Exp. Ther.*, **260**, 1101–1106.

YANG, C.M. & CHOU, S.-P. (1992). Muscarinic regulation of cytoplasmic Ca^{2+} concentrations in dog tracheal smooth muscle cells: Ca^{2+} requirements for phospholipase C activation. *Mol. Biol. Cell*, **3**, 249a.

YANG, C.M., CHOU, S.-P., & SUNG, T.-C. (1991). Muscarinic receptor subtypes coupled to generation of different second messengers in isolated tracheal smooth muscle cells. *Br. J. Pharmacol.*, **104**, 613–618.

ZIFA, E. & FILLION, G. (1992). 5-Hydroxytryptamine receptors. *Pharmacol. Rev.*, **44**, 401–458.

(Received September 16, 1993
Accepted November 18, 1993)

Br. J. Pharmacol. (1994), **111**, 787–792 © Macmillan Press Ltd, 1994

Studies on the mechanism of [^{3}H]-noradrenaline release from SH-SY5Y cells: the role of Ca^{2+} and cyclic AMP

R. Atcheson, [1]D.G. Lambert, R.A. Hirst & D.J. Rowbotham

University Department of Anaesthesia, Leicester Royal Infirmary, Leicester LE1 5WW

1 The roles of both Ca^{2+} and adenosine 3':5'-cyclic monophosphate (cyclic AMP) in carbachol and K^+-stimulated [^{3}H]-noradrenaline release from SH-SY5Y human neuroblastoma cells were examined.

2 Both carbachol and K^+ caused a time- and dose-related stimulation of [^{3}H]-noradrenaline release. The release event in perfused cells was monophasic. Half-maximum stimulation measured in statically incubated (3 min) cells was 38 ± 4 μM and 63 ± 4 mM respectively. K^+ (100 mM, added)-evoked release was greater than that produced by carbachol (1 mM).

3 Both carbachol and K^+ caused a time- and dose (measured at 3 min)-related stimulation of cyclic AMP formation with half-maximum stimulation occurring at 5 ± 1 μM and 49 ± 2 mM respectively. In contrast to its effects on release, carbachol produced a greater stimulation of cyclic AMP formation than K^+.

4 K^+-stimulated [^{3}H]-noradrenaline release was entirely dependent on Ca^{2+} entry as 2.5 mM Ni^{2+} abolished release. However, carbachol-evoked (1 mM) release appeared to be unaffected by Ni^{2+} pretreatment.

5 These data suggest that in SH-SY5Y cells, elevated cyclic AMP levels are not directly involved in [^{3}H]-noradrenaline release. In addition, carbachol-stimulated release is largely independent of extracellular Ca^{2+} possibly implying a role for intracellular stored Ca^{2+} in the release process.

Keywords: SH-SY5Y neuroblastoma cells; [^{3}H]-noradrenaline release; adenosine 3':5'-cyclic monophosphate; calcium

Introduction

Neurotransmitter release at both central and peripheral synapses is Ca^{2+}-dependent. Indeed, the release of many neurotransmitters can be blocked by inhibition of voltage-sensitive Ca^{2+} channels (VSCC), where action potential-mediated presynaptic depolarization is the stimulus for their opening (Miller, 1990). However, there is a good deal of evidence to support the existence of Ca^{2+}-independent neurotransmitter release (Burgoyne, 1984; Illes, 1986; Knight *et al.*, 1989; Neher, 1993; Zucker, 1993). In contrast, the direct involvement of adenosine 3':5'-cyclic monophosphate (cyclic AMP) in transmitter release is speculative, with either stimulatory or no effects observed (Wemer *et al.*, 1982; Mulder *et al.*, 1991; Heijna *et al.*, 1992). In rat pineal gland addition of dibutryl cyclic AMP enhanced K^+-stimulated [^{3}H]-noradrenaline release (Pelayo *et al.*, 1978). This enhancement was also demonstrated by Shuntoh *et al.* (1988) in guinea-pig brain cortical slices. In addition, forskolin enhanced K^+-stimulated [^{3}H]-noradrenaline release which was blocked by cyclic AMP-dependent protein kinase inhibition with KT5720. Furthermore, K^+-stimulated [^{3}H]-noradrenaline release from rat brain slices was inhibited by omission of extracellular Ca^{2+} or addition of Cd^{2+} to the incubation buffer (Schoffelmeer & Mulder, 1983) confirming a role for Ca^{2+} in evoked [^{3}H]-noradrenaline release.

SH-SY5Y human neuroblastoma cells represent a useful model of noradrenergic neurones capable of both the uptake and release of [^{3}H]-noradrenaline, with release being evoked by both muscarinic receptor occupancy and K^+ depolarization (Scott *et al.*, 1986; Murphy *et al.*, 1991; 1992; Atcheson *et al.*, 1993a,b). Interestingly, muscarinic receptor occupation in these cells increases cyclic AMP levels, that is secondary to a substantial rise in intracellular Ca^{2+} (Nakagawa-Yagi *et al.*, 1991; Hirst & Lambert, 1993). Furthermore, we have observed that the opiates morphine and fentanyl, caused a dose-dependent and naloxone-reversible, inhibition of forskolin-stimulated cyclic AMP formation, but failed to inhibit carbachol (and K^+) evoked [^{3}H]-noradrenaline release in a naloxone reversible manner (Lambert & Hirst, 1993; Lambert *et al.*, 1993; Atcheson *et al.*, 1993a; and unpublished). In addition, Seward *et al.* (1991) demonstrated that opiate receptor occupancy in these cells closed VSCC. To address these discrepancies we have examined the roles played by intracellular Ca^{2+} and cyclic AMP in the control of [^{3}H]-noradrenaline release in response to both carbachol and K^+ stimulation.

[1] Author for correspondence.

Methods

Cell culture and miscellaneous methods

SH-SY5Y human neuroblastoma cells, passages 69–90 (a gift from Dr J. Beidler, Sloan-Kettering Institute for Cancer Research, Rye, NY, U.S.A.) were maintained in minimum essential medium supplemented with 2 mM glutamine, 100 iu ml^{-1} penicillin, 100 μg ml^{-1} streptomycin, 2.5 μg ml^{-1} fungizone and 10% foetal calf serum in 5% CO_2/humidified air at 37°C. Stock cultures were fed twice weekly and passaged weekly by use of trypsin/EDTA. For some [^{3}H]-noradrenaline release studies, cells (1.25×10^5) were seeded into 12 well multitrays and cultured to confluence (6–7 days) prior to use (see below). All experiments were performed with undifferentiated cells. In an earlier series of studies examining the effects of opioids on [^{3}H]-noradrenaline release, we compared the release profiles of undifferentiated cells with that of retinoic acid (10 μM) differentiated cells. Differentiation decreased the absolute release of [^{3}H]-noradrenaline. Furthermore, the reported lack of opioid receptor-mediated inhibition of release was seen both in undifferentiated and differentiated cells (Atcheson *et al.*, 1993a and unpublished data). Except for [^{3}H]-noradrenaline release from multiwell cultured cells, all other experiments were performed with suspensions (harvested by brief exposure to EDTA 0.02%) of cells in Krebs/HEPES buffer pH 7.4, the composition of which has been described by Atcheson *et al.* (1993b). Gross morphological examination showed no evidence of differentiation as a result of the experimental manipulations reported here.

[^{3}H]-noradrenaline release

Loading of [^{3}H]-noradrenaline and subsequent release from multiwell cultured cells was performed in Krebs/HEPES buffer supplemented with pargyline (0.2 mM) and ascorbic acid (0.2 mM) at 37°C as described previously (Murphy et al., 1991; 1992; Atcheson et al., 1993b). Monolayers of SH-SY5Y cells were first rinsed with two 2 ml aliquots of Krebs/HEPES buffer then loaded with 0.5 ml of [^{3}H]-noradrenaline (48 nM in Krebs/HEPES buffer) for 1 h. [^{3}H]-noradrenaline-loaded cells were then incubated with 1 ml of fresh buffer for 15 min. This 15 min incubation was repeated twice more in order to remove any [^{3}H]-noradrenaline not taken up. Cells loaded and rinsed were then challenged with carbachol (0.1–1000 μM), K^+ (0–100 mM added, with Na^+ adjusted), forskolin (10 μM) or 3-isobutyl-1-methylxanthine (IBMX, 1 mM), for 3 min. In some experiments atropine (1 μM) and Ni^{2+} (2.5 mM) were included. Unreleased [^{3}H]-noradrenaline was extracted for 30 min with perchloric acid (0.4 M) and release expressed as a % of total content. In order to confirm the identity of the released tritium, PCA (0.4 M) acidified supernatants from K^+-stimulated (100 mM added with Na^+ adjustment) samples were separated by h.p.l.c. (Partisil reverse-phase, C18, 5 μM column) according to Herdon et al. (1985). Profiles were compared with PCA (0.4 M) – acidified authentic [^{3}H]-noradrenaline. For perfusion experiments SH-SY5Y cells were harvested and loaded with [^{3}H]-noradrenaline (48 nM) in 3 ml of Krebs/HEPES buffer for 1 h at 37°C. The loaded cells were centrifuged (1500 r.p.m./5 min MSE Chilspin 2), resuspended in 1 ml of fresh buffer and incubated for 15 min at 37°C. This 15 min incubation was repeated twice in order to remove [^{3}H]-noradrenaline not taken up. [^{3}H]-noradrenaline-loaded cells were then pumped into the perfusion chamber (see below). The chamber was made from a 2 ml syringe barrel with the plunger replaced by a perspex flow spreader. The chamber was packed at the needle end with fine nylon mesh then glass wool and the flow spreader inserted. [^{3}H]-noradrenaline-loaded cells were then sucked (0.5 ml min^{-1}, Gilson Minipuls) into the chamber which was then reversed to enable the cells to be perfused. Cells were perfused at 0.5 ml min^{-1} for 10 min and then 0.5 min fractions were collected (over 12–15 min). The system had a dead volume of 0.85 ml, which at a flow rate of 0.5 ml min^{-1} gave a response time of 1.7 min. Cells were perfused with Ca^{2+} containing or Ca^{2+}-free buffer supplemented with carbachol (1 mM), K^+ (100 mM added, with Na^+ adjustment) or Ni^{2+} (2.5 mM) in various combinations. To control for differences in cell densities, and hence [^{3}H]-noradrenaline loading in perfusion experiments, all data are presented relative to the first fraction collected.

Cyclic AMP determinations

Whole cell suspensions (300 μl) were incubated in Krebs/HEPES buffer containing IBMX (1 mM), forskolin (10 μM), carbachol (0.1–1000 μM), atropine (1 μM) and K^+ (0–100 mM added with Na^+ adjustment) in various combinations for 3 min at 37°C. Reactions were terminated with HCl (10 M) and neutralized with NaOH (10 M) followed by Tris (1 M) pH 7.4. The incubation tubes were then centrifuged at 12,000 r.p.m. for 5 min (Sarstedt, Desaspeed MH-2) and aliquots of the supernatant were frozen for the subsequent estimation of cyclic AMP by a radioreceptor assay (Brown et al., 1971; Lambert & Nahorski, 1990a). The radioreceptor assay was based on the competition between [^{3}H]-cyclic AMP and unlabelled cyclic AMP (from samples or authentic standards) for binding to a protein prepared from bovine adrenal glands. There was no significant release of cyclic AMP from SH-SY5Y cells into the incubation buffer. In 27 determinations, 11 were below the detection limits of the assay. Furthermore, the level of cyclic AMP in the buffer was not increased by addition of carbachol (1 mM) or K^+ (100 mM added, with Na^+ adjustment) over 3 or 15 min of incubation. The mean cyclic AMP in the buffer was 1.5 ± 0.3 pmol mg^{-1} protein ($n = 16$) and probably represents limited cell lysis during pipetting.

Drugs and reagents

Tissue culture media, foetal calf serum, penicillin, streptomycin, fungizone, glutamine, trypsin/EDTA and plasticware (NUNC) were from Life Technologies (UK). (−)-[7,8-^{3}H]-noradrenaline (41 Ci mmol^{-1}) was from Amersham (UK). [2,8-^{3}H]-cyclic AMP (28 Ci mmol^{-1}) was from NEN DuPont (Boston, MA, U.S.A.). Carbachol, atropine, forskolin and 3-isobutyl-1-methylxanthine (IBMX) were from Sigma (UK). All other reagents were of the highest purity available.

Statistical analysis

All data are presented as mean ± s.e.mean of at least three independent experiments. Dose-response curves were analysed statistically by ANOVA, and EC_{50} (concentration producing half maximum response) values obtained by computer assisted curve fitting (non linear regression model) using GraphPAD (V2.0). In dose-response analyses a maximum effect was assumed to have been achieved when there was no statistical difference with the next lowest concentration used, i.e., 10^{-3} and 10^{-4} M for carbachol and 100 and 80 mM added K^+. Where appropriate, statistical comparisons were made by Student's paired or unpaired t test and considered significant when $P < 0.05$.

Results

Both carbachol and K^+ stimulated a monophasic (Figure 1a) and dose-dependent (Figure 1b,c) increase in [^{3}H]-noradrenaline release from SH-SY5Y cells with K^+ (100 mM added with Na^+ adjustment) producing a 2.1 fold greater release than carbachol (1 mM). Significant release above basal occurred from 0.1 μM and 20 mM (added, with Na^+ adjustment) for carbachol and K^+ respectively. The EC_{50} values for carbachol and K^+-evoked release were 38 ± 4 μM and 63 ± 4 mM ($n = 5$) with the response to 1 mM carbachol being inhibited 91 ± 4% ($n = 3$) by 1 μM atropine. High performance liquid chromatography (h.p.l.c.) analysis of the released tritium from K^+-stimulated (100 mM added) monolayers showed that over 90% was [^{3}H]-noradrenaline (data not shown).

In addition to the dose- and time-related stimulation of [^{3}H]-noradrenaline release, both carbachol and K^+ caused a time (Figure 2a) and dose-related increase in cyclic AMP formation, that, in the case of carbachol, was atropine-sensitive (Figure 2b,c). The short (3 min) time course for cyclic AMP formation is included for comparison with noradrenaline release and is in agreement with our previously published data for carbachol (Hirst & Lambert, 1993) where a maximum effect was not observed until 5–10 min of incubation. In contrast to the release data, carbachol (1 mM)-stimulated cyclic AMP formation was 2.4 fold greater than that caused by K^+ (100 mM, added with Na^+ adjustment). Significant stimulation above basal occurred from 1 μM and 25 mM (added) for carbachol and K^+ respectively. The EC_{50} values for carbachol- and K^+-stimulated cyclic AMP formation were 5 ± 1 μM and 49 ± 2 mM ($n = 4$) respectively. The EC_{50} values for cyclic AMP formation by both carbachol and K^+ were significantly ($P < 0.05$) more potent than for [^{3}H]-noradrenaline release. Forskolin 10 μM, whilst increasing basal cyclic AMP formation 9 fold, failed to evoke [^{3}H]-noradrenaline release (Table 1). In order to allow comparison of release and cyclic AMP experiments the effects of IBMX on basal, carbachol- and K^+-stimulated release were examined. Basal and carbachol-stimulated (1 mM) release were unaffected by inclusion of IBMX (1 mM) in the release

(3 min) buffer. The response to 100 mM added K^+ was significantly reduced (16%, $P<0.05$) compared with control (Table 2). The reason for this inhibition is unclear but may be as a result of inhibition of voltage-sensitive Ca^{2+} channels. However, if an elevation in cyclic AMP were responsible for neurotransmitter release then IBMX would be expected to enhance, not inhibit release. A small inhibitory effect of IBMX on [^{3}H]-noradrenaline release has also been reported by Wemer *et al.* (1982).

Ca^{2+} channel blockade with 2.5 mM Ni^{2+} abolished K^+-evoked (100 mM added) release without significantly affecting either basal or carbachol-stimulated (1 mM) release when measured in multitray cultured cells (Table 2). These data were confirmed in perfused cells with K^+-evoked (100 mM added) release again being abolished and carbachol-evoked (1 mM) release remaining largely unaffected (Figure 3). It is worthy of note that the first time point after carbachol stimulation plus Ni^{2+} is reduced ($P<0.05$) compared with the carbachol control. We further analysed the carbachol-evoked release in the absence and presence of Ni^{2+} by comparing the areas under the normalized curves (AUC). Whilst

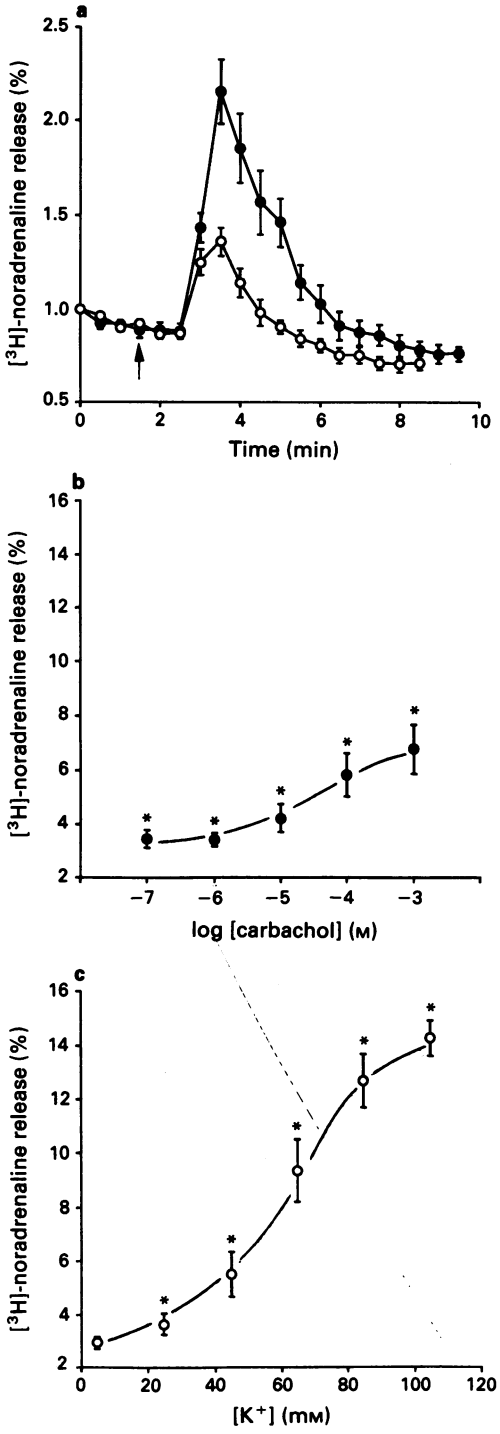


Figure 1 Carbachol and K^+ caused a time- (a) and dose-related (b,c) increase in [^{3}H]-noradrenaline release from SH-SY5Y cells. Data are mean ± s.e.mean (a, $n=6$; b,c, $n=5$). *$P<0.05$ increased compared with basal. In (a) [^{3}H]-noradrenaline release data in response to K^+, 100 mM (●) and carbachol, 1 mM (○) stimulation are expressed relative to the first fraction collected. Stimulus addition is noted by the arrow.

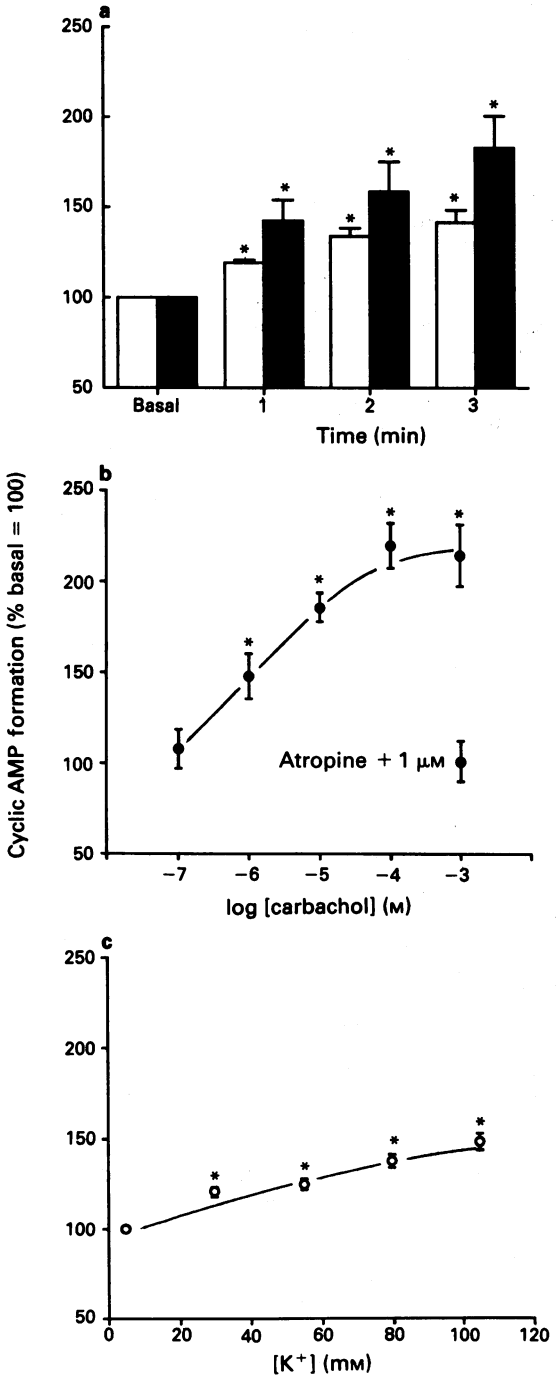


Figure 2 Carbachol and K^+ caused a time- (a) and dose-related (b,c) increase in cyclic AMP formation in SH-SY5Y cells. Data are mean ± s.e.mean (a, open columns, K^+ 100 mM, $n=5$; solid columns, carbachol 1 mM, $n=7$; b,c, $n=4$). *$P<0.05$ increased compared with basal.

Table 1 Effects of increased cyclic AMP on [^{3}H]-noradrenaline ([^{3}H]-NA) release from SH-SY5Y cells

	Cyclic AMP (pmol mg^{-1} protein)	*[^{3}H]-NA release* (%)
Basal	24 ± 6	4.3 ± 0.2
Forskolin 10 μM	220 ± 23*	4.7 ± 0.1

All data are mean ± s.e.mean $n = 4$. *$P < 0.05$ increased compared with basal. Basal samples contained 0.1% dimethylsulphoxide the vehicle for forskolin.

Table 2 The effects of 3-isobutyl-1-methylxanthine (IBMX, 1 mM) and Ni^{2+} (2.5 mM) on [^{3}H]-noradrenaline release from statically incubated SH-SY5Y human neuroblastoma cells

	[^{3}H]-noradrenaline release (%)		
	Control	*+ IBMX*	n
Basal	2.8 ± 0.2	2.8 ± 0.3	7
Carbachol (1 mM)	4.8 ± 0.4*	4.9 ± 0.7*	7
K^+ (100 mM)	8.1 ± 0.7*	6.8 ± 0.8*‡	7
	Control	*+ Ni^{2+}*	–
Basal	2.9 ± 0.3	3.4 ± 0.4	12
Carbachol (1 mM)	5.7 ± 0.6*	5.1 ± 0.7*	12
K^+ (100 mM)	8.9 ± 1.6*	4.1 ± 0.5‡	12

All data are mean ± s.e.mean and represent paired samples (i.e. both IBMX and Ni^{2+} have their own control) measured in duplicate. Ni^{2+} was added 5 min prior to stimulation. *$P < 0.05$ significantly increased compared with basal. ‡$P < 0.05$ significantly reduced compared with paired control. *n*, represents the number of independent experiments performed.

a small reduction was observed this did not reach statistical significance ($AUC_{control}$:1.94 ± 0.25 ($n = 6$), $AUC_{+Ni^{2+}}$:1.35 ± 0.41 ($n = 4$), $P > 0.05$).

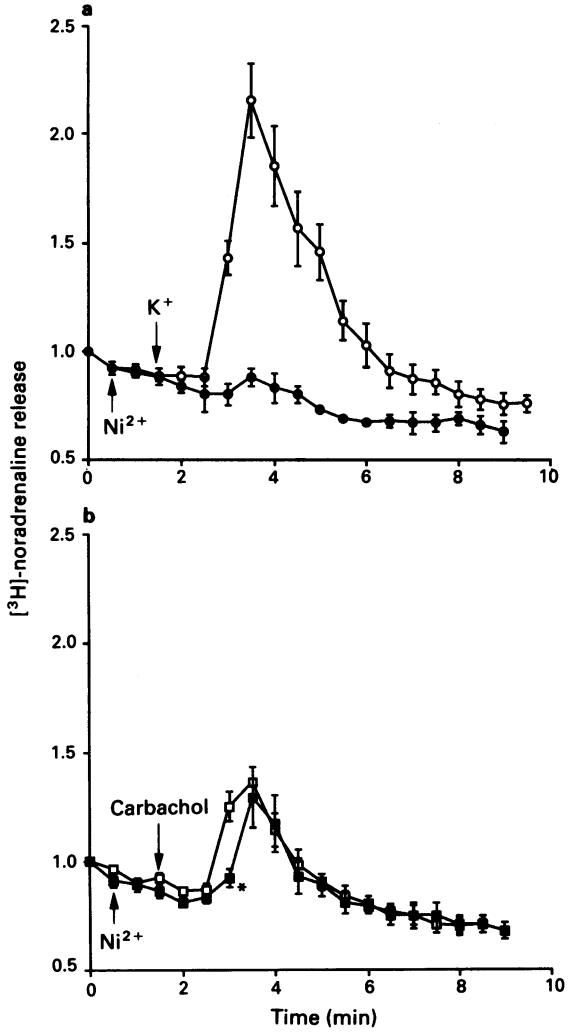


Figure 3 Effect of Ni^{2+} (2.5 mM in nominally Ca^{2+}-free buffer, added at the first arrow) on K^+- (100 mM, —○—; + Ni^{2+}, ●) (a) and carbachol- (1 mM □; + Ni^{2+}, ■ added at the second arrow) (b) evoked [^{3}H]-noradrenaline release from perfused SH-SY5Y cells. Data are mean ± s.e.mean. *$P < 0.05$ reduced compared with carbachol control.

Discussion

The SH-SY5Y human neuroblastoma cell line has been described as a useful model of sympathetic ganglia with which to study noradrenergic neurotransmission (Ross *et al.*, 1983; Ross & Biedler, 1985; Scott *et al.*, 1986; Murphy *et al.*, 1991). Both tyrosine hydroxylase and dopamine-β-hydroxylase activities have been reported (Ross *et al.*, 1983; Ross & Biedler, 1985) and these cells express muscarinic M_3 receptors (Lambert *et al.*, 1989), α_2-adrenoceptors (Kazmi & Mishra, 1989) and μ and δ opioid receptors (Kasmi & Mishra, 1987). In a previous study we have shown that SH-SY5Y cells take up substantial amounts of [^{3}H]-noradrenaline with a $t_{\frac{1}{2}}$ of 5.7 min (Atcheson *et al.*, 1993b).

Scott and colleagues (1986) demonstrated (in differentiated cells) that both K^+ (50 mM) depolarization and acetylcholine (100 μM) evoked a modest monophasic increase in the release of [^{3}H]-noradrenaline; these data are confirmed and extended in this manuscript. Furthermore, in two papers Murphy *et al.* (1991, 1992) reported a dose-dependent increase in [^{3}H]-noradrenaline release in response to both K^+ and carbachol with EC_{50} values for K^+ similar to that reported here but with an EC_{50} for carbachol around 3 fold more potent. The identity of the muscarinic receptor subtype mediating noradrenaline release from SH-SY5Y cells was described by Murphy *et al.* (1991) as M_3 based on the affinities of the M_1 selective antagonist pirenzepine (K_i 1.2 μM) and the M_3-selective antagonist, hexahydrosiladiphenidol (K_i 18 nM). This is in agreement with the expression (in our hands) of an homogeneous M_3 muscarinic receptor complement on these cells (Lambert *et al.*, 1989). In addition, both carbachol and K^+ evoked release were enhanced by protein kinase C activation and reduced by protein kinase C inhibitors but only the K^+ response was extracellular Ca^{2+}-dependent, although EGTA treatment did reduce carbachol stimulated release (Murphy *et al.*, 1991; 1992). In these latter studies, 1 min preincubation with EGTA reduced carbachol (1 mM)-stimulated release 19% and K^+ (100 mM) by 79%. A longer (3 min) preincubation reduced carbachol and K^+ stimulated release by 56 and 86% respectively. However EGTA pretreatment may have partially emptied (consistent with the inhibition being time-dependent) the intracellular stores of Ca^{2+}. In this study we adopted a more gentle approach to investigate the roles of extracellular and intracellular Ca^{2+}, using a combination of nominally Ca^{2+}-free buffer (no added Ca^{2+}) and Ni^{2+} (2.5 mM) preincubation (Lambert *et al.*, 1990). Using these approaches in both static and dynamic release studies we clearly showed that K^+-evoked release is extracellular Ca^{2+}-dependent and carbachol-stimulated release is largely extracellular Ca^{2+}-independent. Certainly, muscarinic M_3 receptor activation in SH-SY5Y cells produce a marked and biphasic increase in $Ins(1,4,5)P_3$ mediating a

substantial rise in intracellular Ca^{2+} (Lambert & Nahorski, 1990b; Lambert *et al.*, 1991). It is also worthy of note here that whilst K^+ (100 mM added) produced a greater release of [^{3}H]-noradrenaline than carbachol (1 mM) challenge, K^+ produces a smaller rise in intracellular Ca^{2+} than carbachol (Lambert *et al.*, 1990). Moreover bradykinin stimulated [^{3}H]-dopamine release from PC12 cells was only inhibited 60% by removal of extracellular Ca^{2+} with 40% of the response being extracellular Ca^{2+}-independent. In the same experiment 50 mM K^+-evoked release was abolished (Appell & Barefoot, 1989).

Muscarinic receptor occupation in SH-SY5Y cells also leads to elevated cyclic AMP concentrations that are both Ca^{2+}- and calmodulin-dependent (Nakagawa-Yagi *et al.*, 1991; Hirst & Lambert, 1993) and there is evidence that raised intracellular concentrations of this second messenger may be involved in neurotransmitter release (Mulder *et al.*, 1991). For example, in rat cerebral cortex slices, K^+-stimulated [^{3}H]-noradrenaline release was enhanced by dibutyryl-cyclic AMP (dbcyclic AMP) and 8-bromo-cyclic AMP (8-Brcyclic AMP) (around 160%) but surprisingly, and in agreement with this study, phosphodiesterase inhibition with IBMX reduced release (Wemer *et al.*, 1982). Also, in electrically stimulated rat cortical slices, forskolin, 8-Br-cyclic AMP, dbcyclic AMP, (not 8-bromo-cyclic GMP) and IBMX all caused a modest dose-dependent enhancement of [^{3}H]-noradrenaline release (Schoffelmeer *et al.*, 1985). However, in slices of rat nucleus accumbens, 8-Br-cyclic AMP did not affect either [^{14}C]-acetylcholine or [^{3}H]-dopamine release. It could be argued that [^{3}H]-noradrenaline release is more susceptible to cyclic AMP regulation than either [^{14}C]-acetylcholine or [^{3}H]-dopamine but Ca^{2+} stimulated [^{3}H]-dopamine release from rat synaptosomes was enhanced by forskolin and IBMX (Bowyer & Weiner, 1989). We show that a carbachol and K^+ challenge over 3 min caused a dose-related increase in cyclic AMP formation with the EC_{50} for carbachol being 7.6 fold more potent than for release. The dose-related rise in cyclic AMP mirrors the previously reported rise in intracellular Ca^{2+} (carbachol spike $EC_{50} = 8\ \mu M$, Lambert & Nahorski 1990b) rather than release suggesting that the rise in intracellular Ca^{2+} is tightly coupled to cyclic AMP formation and the activation of a Ca^{2+} calmodulin-sensitive isoform of adenylate cyclase. The discrepancy between the EC_{50} for carbachol-mediated cyclic AMP formation and release suggests that the two events are not linked. These data, coupled with the ineffectiveness of adenylate cyclase activation with forskolin, indicate that cyclic AMP is not directly involved in the release process. Whether cyclic AMP-dependent protein kinase A-mediated phosphorylation events (Nestler & Greengard, 1983; Mulder *et al.*, 1991) play a role in the longer term control of neurotransmission in these cells will require further study.

R.A. is a British Journal of Anaesthesia research fellow. The authors would like to thank Jonathon Willets for performing some of the h.p.l.c. analyses of released catecholamines.

References

APPELL, K.C. & BAREFOOT, D.S. (1989). Neurotransmitter release from bradykinin-stimulated PC12 cells. Stimulation of cytosolic calcium and neurotransmitter release. *Biochem. J.*, **263**, 11–18.

ATCHESON, R, ROWBOTHAM, D.J. & LAMBERT, D.G. (1993a). Carbachol and potassium evoked release of [^{3}H]-noradrenaline are inhibited dose-dependently by fentanyl in SH-SY5Y cells. *Br. J. Pharmacol.*, **108**, 283P.

ATCHESON, R., ROWBOTHAM, D.J. & LAMBERT D.G. (1993b). Fentanyl inhibits the uptake of [^{3}H]-noradrenaline in cultured neuronal cells. *Br. J. Anaesthesia*, **71**, 540–543.

BOWYER, J.F. & WEINER, N. (1989). K^+ channel and adenylate cyclase involvement in regulation of Ca^{2+}-evoked release of [^{3}H]-dopamine from synaptosomes. *J. Pharmacol. Exp. Ther.*, **248**, 514–520.

BROWN, B.L., ALBANO, J.D.M., EKINS, R.P. & SGHERZI, A.M. (1971). A simple and sensitive saturation assay method for the measurement of adenosine 3':5'-cyclic monophosphate. *Biochem. J.*, **121**, 561–562.

BURGOYNE, R.D. (1984). Mechanisms of secretion from adrenal chromaffin cells. *Biochim. Biophys. Acta*, **779**, 201–216.

HEIJNA, M.H., HOGENBOOM, F., MULDER, A.H. & SCHOFFELMEER, A.N.M. (1992). Opioid receptor-mediated inhibition of ^{3}H-dopamine and ^{14}C-acetylcholine release from rat nucleus accumbens slices. *Naunyn-Schmied. Arch. Pharmacol.*, **345**, 627–632.

HERDON, H., STRUPISH, J. & NAHORSKI, S.R. (1985). Differences between the release of radiolabelled and endogenous dopamine from superfused rat brain slices: effects of depolarizing stimuli, amphetamine and synthesis inhibition. *Brain. Res.*, **348**, 309–320.

HIRST, R.A. & LAMBERT, D.G. (1993). Carbachol stimulated cAMP formation in SH-SY5Y cells is dependent on both extracellular and intracellular calcium. *Biochim. Soc. Trans.* (in press. Sheffield 647th meeting).

ILLES, P. (1986). Mechanisms of receptor-mediated modulation of transmitter release in noradrenergic, cholinergic and sensory neurons. *Neuroscience*, **17**, 909–928.

KAZMI, S.M.I. & MISHRA, R.K. (1987). Competitive pharmacological properties and functional coupling of μ and δ opioid receptor sites in human neuroblastoma SH-SY5Y cells. *Mol. Pharmacol.*, **32**, 109–118.

KAZMI, S.M.I. & MISHRA, R.K. (1989). Identification of alpha2-adrenergic receptor sites in human retinoblastoma (Y79) and neuroblastoma (SH-SY5Y) cells. *Biochem. Biophys. Res. Commun.*, **158**, 921–928.

KNIGHT, D.E., VONGRAFENSTEIN, H. & ATHAYDE, C.M. (1989). Calcium-dependent and calcium-independent exocytosis. *Trends Neurol. Sci.*, **12**, 451–458.

LAMBERT, D.G., ATCHESON, R., HIRST, R.A. & ROWBOTHAM, D.J. (1993). Effects of morphine and its metabolites on opiate receptor binding, cAMP formation and [^{3}H]-noradrenaline release from SH-SY5Y cells. *Biochem. Pharmacol.*, **45**, 1145–1150.

LAMBERT, D.G., GHATAORRE, A.S. & NAHORSKI, S.R. (1989). Muscarinic receptor binding characteristics of a human neuroblastoma SK-N-SH and its clones SH-SY5Y and SH-EP1. *Eur. J. Pharmacol.*, **165**, 71–77.

LAMBERT, D.G. & HIRST, R.A. (1993). Effects of morphine and its metabolites on opiate receptor binding and cyclic adenosine-3',5'-monophosphate (cAMP) formation in human neuroblastoma cells. *Br. J. Pharmacol.*, **70**, 475P–476P.

LAMBERT, D.G. & NAHORSKI, S.R. (1990a). Pertussis toxin inhibits alpha2-adrenoceptor mediated inhibition of adenylate cyclase without affecting muscarinic regulation of $[Ca^{2+}]_i$ or inositol phosphate generation in SH-SY5Y human neuroblastoma cells. *Biochem. Pharmacol.*, **40**, 2291–2295.

LAMBERT, D.G. & NAHORSKI, S.R. (1990b). Muscarinic-receptor mediated changes in intracellular Ca^{2+} and inositol 1,4,5-trisphosphate mass in a human neuroblastoma cell line, SH-SY5Y. *Biochem. J.*, **265**, 555–562.

LAMBERT, D.G., CHALLISS, R.A.J. & NAHORSKI, S.R. (1991). Accumulation and metabolism of Ins(1,4,5)P_3 and Ins(1,3,4,5)P_4 in muscarinic receptor stimulated SH-SY5Y neuroblastoma cells. *Biochem. J.*, **273**, 791–794.

LAMBERT, D.G., WHITHAM, E.M., BAIRD, J.G. & NAHORSKI, S.R. (1990). Different mechanisms of Ca^{2+} entry induced by depolarization and muscarinic receptor stimulation in SH-SY5Y human neuroblastoma cells. *Mol. Brain. Res.*, **8**, 263–266.

MILLER, R.J. (1990). Receptor-mediated regulation of calcium channels and neurotransmitter release. *FASEB J.*, **4**, 3291–3299.

MULDER, A.H., SCHOFFELMEER, A.N.M. & STOOF, J.C. (1991). On the role of adenylate cyclase in presynaptic modulation of neurotransmitter release mediated by monoamine and opioid receptors in the brain. *Ann. N.Y. Acad. Sci.*, **604**, 237–249.

MURPHY, N.P., BALL. S.G. & VAUGHAN, P.F.T. (1991). Potassium- and carbachol-evoked release of [^{3}H]-noradrenaline from human neuroblastoma cells, SH-SY5Y. *J. Neurochem.*, **56**, 1810–1815.

MURPHY, N.P., MCCORMACK, J.G., BALL, S.G. & VAUGHAN, P.F.T. (1992). The effect of protein kinase C activation on muscarinic-M_3 and K^+-evoked release of [^{3}H]-noradrenaline and increases in intracellular Ca^{2+} in human neuroblastoma SH-SY5Y cells. *Biochem. J.*, **282,** 645–650.

NAKAGAWA-YAGI, Y., SAITO, Y., TAKADA, Y. & TAKAMA, M. (1991). Carbachol-enhances forskolin-stimulated cyclic AMP accumulation via activation of calmodulin system in human neuroblastoma SH-SY5Y cells. *Biochem. Biophys. Res. Commun.*, **178,** 116–123.

NEHER, E. (1993). Spatial and temporal aspects of Ca changes in secretion control. *Biochem. Soc. Trans.*, **21,** 420–423.

NESTLER, E.J. & GREENGARD, P. (1983). Protein phosphorylation in the brain. *Nature*, **305,** 583–588.

PELAYO, F., DUBOCOVICH, M.L. & LANGER, S.Z. (1978). Possible role of cyclic nucleotides in regulation of noradrenaline release from rat pineal through presynaptic adrenoceptors. *Nature*, **274,** 76–78.

ROSS, R.A. & BIEDLER, J.L. (1985). Presence and regulation of tyrosinase activity in human neuroblastoma cell varients in vitro. *Cancer Res.*, **45,** 1628–1632.

ROSS, R.A., SPENGLER, B.A. & BIEDLER, J.L. (1983). Coordinate morphological and biochemical interconversion of human neuroblastoma cells. *J. Natl. Cancer. Inst.*, **71,** 741–749.

SCHOFFELMEER, A.N.M., HOGENBOOM, F. & MULDER, A.H. (1985). Evidence for a presynaptic adenylate cyclase system facilitating [^{3}H]-norepinephrine release from rat brain neocortex and synaptosomes. *J. Neurosci.*, **5,** 2685–2689.

SCHOFFELMEER, A.N.M. & MULDER, A.H. (1983). [^{3}H]-noradrenaline release from brain slices induced by an increase in intracellular sodium concentration: Role of intracellular calcium stores. *J. Neurochem.*, **40,** 615–621.

SCOTT, I.G., AKERMAN, K.E.O., HEIKKILA, J.E., KAILA, K. & ANDERSSON, L.C. (1986). Development of a neural phenotype in differentiating ganglion cell-derived human neuroblastoma cells. *J. Cell. Physiol.*, **128,** 285–292.

SEWARD, E., HAMMOND, C. & HENDERSON, G. (1991). μ-opioid receptor mediated inhibition of N-type calcium-channel current. *Proc. R. Soc. B.*, **244,** 129–135.

SHUNTOH, H., TANIYAMA, K., FUKUZAKI, H. & TANAKA, C. (1988). Inhibition by cyclic AMP of phorbol ester-potentiated norepinephrine release from guinea pig brain cortical synaptosomes. *J. Neurochem.*, **51,** 1565–1572.

WEMER, J., SCHOFFELMEER, A.N.M. & MULDER, A.H. (1982). Effects of cyclic AMP analogues and phospodiesterase inhibitors on K^+-induced [^{3}H]-noradrenaline release from rat brain slices and on its presynaptic alpha-adrenergic modulation. *J. Neurochem.*, **39,** 349–356.

ZUCKER, R.S. (1993). Calcium and transmitter release at nerve terminals. *Biochem. Soc. Trans.*, **21,** 395–401.

(Received November 8, 1993
Accepted November 19, 1993)

Br. J. Pharmacol. (1994), **111**, 793–796 © Macmillan Press Ltd, 1994

Insulin requirement for the antihyperglycaemic effect of metformin

[1]C.J. Bailey & K.J. Mynett

Department of Pharmaceutical and Biological Sciences, Aston University, Birmingham B4 7ET

1 Insulin-dependent diabetic BB/S rats with little or no endogenous insulin were used to determine whether insulin is required for the acute antihyperglycaemic effect of metformin (dimethylbiguanide).

2 Metformin (250 mg kg^{-1}, intrajejunally) did not lower the hyperglycaemia in BB/S rats in the absence of exogenous insulin, but metformin increased by 69% ($P<0.05$) the blood glucose-lowering effect of exogenous insulin.

3 Metformin (250 mg kg^{-1}, intrajejunally) improved glucose disposal in rats with a normal insulin response to an intravenous glucose challenge. Plasma glucose disappearance was increased from 0.7 ± 0.1 to $2.5 \pm 0.1\%$ min^{-1} ($P<0.05$).

3 When the insulin response to glucose was suppressed with somatostatin and diazoxide, metformin improved glucose disposal to a similar extent to that in rats with a normal insulin response. Plasma glucose disappearance was increased from 0.24 ± 0.02 to $1.0 \pm 0.1\%$ min^{-1} ($P<0.01$).

5 The results indicate that insulin is required for the acute antihyperglycaemic effect of metformin, but the extent of this effect is not proportional to the prevailing insulin concentration.

Keywords: Metformin; insulin requirement; glucose metabolism

Introduction

The antihyperglycaemic drug metformin (dimethylbiguanide) is an established treatment for non-insulin dependent diabetes mellitus (NIDDM) (Bailey & Nattrass, 1988; Bailey, 1992). It acts mainly by increasing glucose utilization and decreasing hepatic glucose production, but the cellular mechanisms responsible for these effects have not been resolved (Bailey, 1993). In particular, controversy exists concerning a possible association between the mode of action of metformin and that of insulin. Metformin cannot sustain life in totally pancreatectomized animals (Sterne, 1969), but it increases the blood glucose-lowering efficacy of insulin in hyperglycaemic and insulin resistant states (Pagano *et al.*, 1983; Gin *et al.*, 1985; Prager *et al.*, 1986; Leblanc *et al.*, 1987; Nosadini *et al.*, 1987; Hother-Nielsen *et al.*, 1989; Reaven *et al.*, 1992). Thus it has been assumed, but not actually demonstrated, that the blood glucose-lowering effect of metformin requires the presence of insulin. Studies in NIDDM patients have failed to show an association between the prevailing insulin concentration and the extent to which metformin lowers blood glucose (Hermann, 1979; Bailey, 1992), but a possible association could be disguised by the variable extent of insulin resistance in these patients.

The present study investigates the requirement for insulin of metformin by determining the blood glucose-lowering efficacy of metformin in normal rats with normal and reduced insulin concentrations, and in diabetic BB/S rats with no measurable insulin.

Methods

Animals

Adult male Wistar rats weighing approximately 150 g and diabetic BB/S rats weighing about 300 g were maintained as described previously (Bailey *et al.*, 1992). BB/S rats were obtained courtesy of Professor A.J. Bone from the colony at Southampton University, which originated from the colony at Mollegaard Breeding Centre, Ejby, Denmark. Each BB/S rat had overt insulin-dependent diabetes mellitus (IDDM) for >1 month, and was maintained on a single daily s.c. injection of human insulin (Ultratard, 4-9 iu per rat). The dosage was adjusted to eliminate glucosuria and ketonuria, and maintain body weight without incurring hypoglycaemia (venous plasma glucose <2 mmol l^{-1}).

Intravenous glucose tolerance test (IVGTT)

Rats were 24 h-fasted, anaesthetized with sodium pentobarbitone (60 mg kg^{-1}, i.p.) and maintained under anaesthesia with further doses of 15 mg kg^{-1} h^{-1}. Rectal temperature was maintained at 35–37°C. The right internal jugular vein was cannulated. Metformin hydrochloride (250 mg kg^{-1}) or vehicle only (PBS 10 ml kg^{-1}) was administered into the proximal jejunum (time -60 min), and glucose (0.5 g kg^{-1} in a 20% w/v solution) was delivered as an i.v. bolus via the jugular cannula at 0 min.

For experiments in which the plasma insulin response to glucose was reduced, somatostatin (0.5 μg kg^{-1} min^{-1}) was infused i.v. from time -60 min throughout the study, and diazoxide (30 mg kg^{-1}) was administered i.p. at times -60 and 0 min.

In the BB/S diabetic rats, a smaller i.v. glucose challenge at 0.25 g kg^{-1} was given at 0 min because these rats were already severely hyperglycaemic (plasma glucose >20 mmol l^{-1}). At 90 min an i.v. bolus of human actrapid insulin (0.5 iu kg^{-1}) was administered, and the subsequent fall in plasma glucose was used to assess insulin sensitivity.

Blood samples were taken from the tail at intervals (shown in the figures) for plasma glucose and insulin assay. The rate of plasma glucose disappearance (% min^{-1}) after an i.v. glucose challenge was determined ($69.3/t_{\frac{1}{2}}$) between 5 and 30 min.

Glucose and insulin assays

Plasma glucose was determined by an automated glucose oxidase procedure (Stevens, 1971) and plasma insulin was measured by radioimmunoassay using a polyethylene glycol

[1] Author for correspondence.

separation method (Desbuquois & Aurbach, 1971). The assay sensitivity was 0.1 ng ml^{-1}.

Chemicals

All chemicals were obtained from Sigma Chemical Company, Poole or BDH, Poole, except PBS tablets from Unipath, Basingstoke, metformin hydrochloride from Lipha Pharmaceuticals, West Drayton, sodium pentobarbitone (Sagatal) from RMB Animal Health Ltd, Dagenham, human insulin for injection from Novo Nordisk, Crawley, and diazoxide (Eudemine) from Evans Medical, Horsham.

Statistical analysis

Data are presented as mean ± s.e.mean. Data were evaluated for the effect of metformin by one-way analysis of variance and differences between individual groups were compared by Student's t test. Differences were considered to be significant if $P<0.05$.

Results

IVGTT with normal insulin response

Intrajejunal administration of metformin (250 mg kg^{-1}) did not alter basal glucose and insulin concentrations (− 60 to 0 min) in normal fasted rats (Figure 1). An i.v. glucose challenge at 0 min resulted in a faster rate of plasma glucose disappearance in the group treated with metformin (2.5 ± 0.1% min^{-1}) than controls (1.7 ± 0.1% min^{-1}). The plasma insulin response to glucose was not affected by metformin.

IVGTT with reduced insulin response

The i.v. infusion of somatostatin (0.5 μg kg^{-1} min^{-1}) throughout the experiment, and i.p. administration of diazoxide (30 mg kg^{-1}) at − 60 and 0 min suppressed basal and glucose-stimulated insulin release (Figure 2), compared with normal insulin concentrations (Figure 1). Metformin did not affect these insulin concentrations.

Basal glucose concentrations were not significantly affected by somatostatin and diazoxide, but the rate of plasma glucose disappearance was slower with the somatostatin-diazoxide regimen (0.24 ± 0.02% min^{-1}, $P<0.05$) than normal controls (1.7 ± 0.1% min^{-1}). With metformin treatment glucose disappearance was increased (1.00 ± 0.15% min^{-1}, $P<0.01$) in the somatostatin-diazoxide-treated rats.

IVGTT in diabetic BB/S rats

The insulin-dependent diabetic BB/S rats had been receiving daily insulin injections (4–9 iu per rat) to sustain life, and the last injection was given 50 h before experimentation. At 20 h before experimentation the plasma insulin concentration was <0.3 ng ml^{-1}. During experimentation (up to 90 min) plasma insulin was not detected (<0.1 ng ml^{-1}). The severe hyperglycaemia in these rats was unaffected by metformin either before or after the i.v. glucose challenge (Figure 3).

At 90 min an i.v. bolus of insulin (0.5 iu kg^{-1}) was administered. Plasma glucose disappearance (90–150 min) was 0.71 ± 0.09 and 1.20 ± 0.15% min^{-1} ($P<0.05$) in the control and metformin-treated groups respectively, indicating a greater plasma glucose-lowering effect in those treated with metformin.

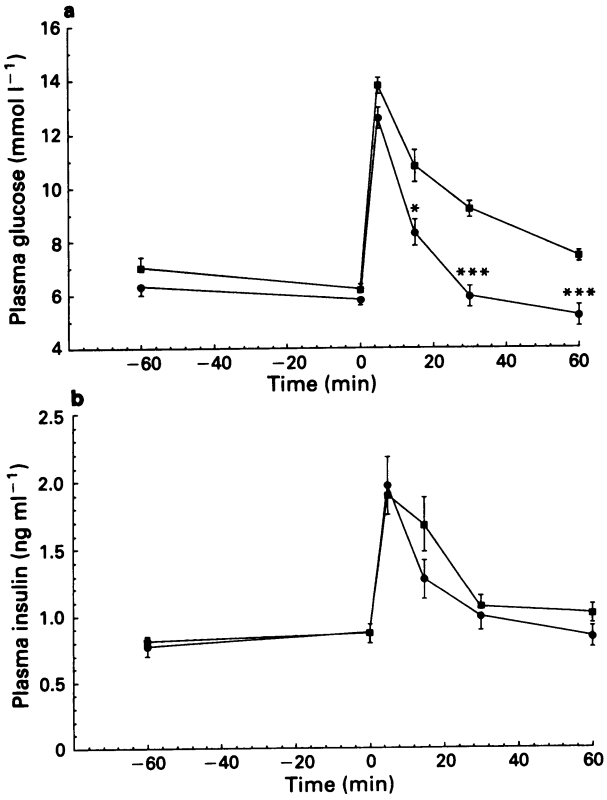


Figure 1 Plasma glucose (a) and insulin (b) concentrations of 24 h fasted normal rats receiving an i.v. glucose challenge at 0 min. At time − 60 min, 250 mg kg^{-1} metformin (●) or saline as control (■) was given intrajejunally. Values are mean with s.e.mean, $n=7$. *$P<0.05$; ***$P<0.001$ versus control, Student's unpaired t test.

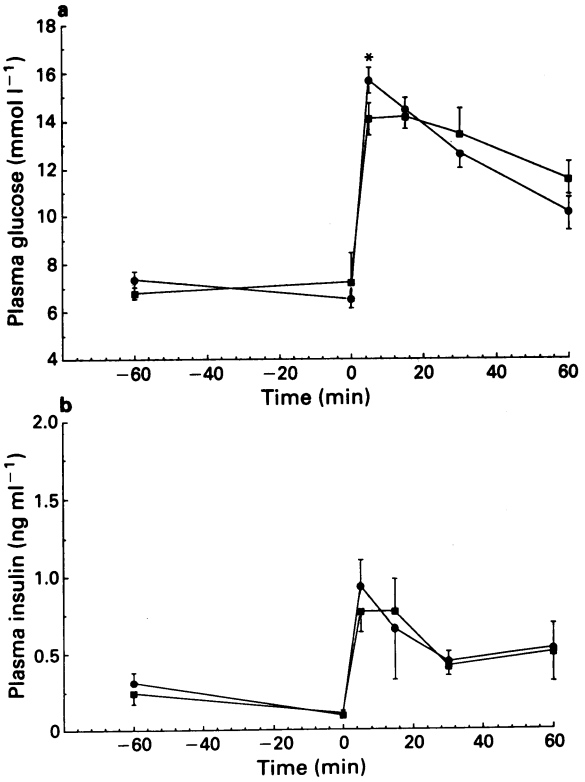


Figure 2 Plasma glucose (a) and insulin (b) concentrations of 24 h fasted normal rats receiving an infusion of somatostatin (0.5 μg kg^{-1} min^{-1}, i.v., starting at − 60 min) and injections of diazoxide (30 mg kg^{-1}, i.p. at − 60 and 0 min) and an i.v. glucose challenge at 0 min. At time − 60 min, 250 mg kg^{-1} metformin (●) or saline as control (■) was given intrajejunally. Values are mean with s.e.mean, $n=6$. *$P<0.05$ versus control, Student's unpaired t test.

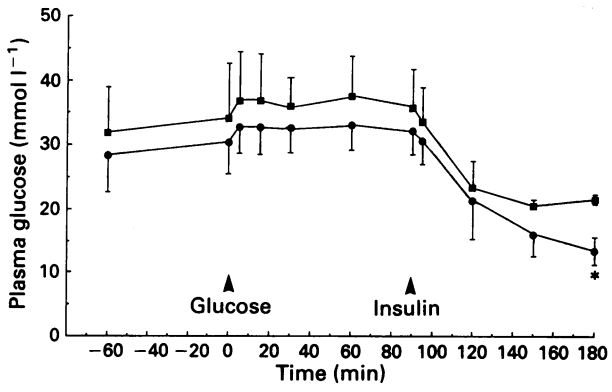


Figure 3 Plasma glucose concentrations of 24 h fasted BB/S rats receiving an i.v. glucose challenge at 0 min and an i.v. bolus of insulin at 90 min. At time − 60 min, 250 mg kg^{-1} metformin (●) or saline as control (■) was given intrajejunally. Values are mean with s.e.mean, $n = 6$ for metformin-treated and $n = 4$ for control. *$P < 0.05$ versus control, Student's unpaired t test.

Discussion

This study provides evidence that insulin is required for the acute antihyperglycaemic effect of metformin but the extent of this effect is not a function of the absolute level of insulinaemia. The study has demonstrated an antihyperglycaemic effect of metformin in rats with normal and reduced insulin concentrations. The effect was lost in diabetic BB/S rats in which insulin concentrations were negligible or absent, and re-established when insulin was introduced.

BB rats offer a model of insulin-dependent diabetes resulting from autoimmune destruction of the insulin-secreting pancreatic β-cells (Nakhooda *et al.*, 1976; Bone, 1991). These animals require the administration of insulin to sustain life. Thus the failure of metformin to reduce the hyperglycaemia in BB/S rats substantiates the view that a therapeutic concentration of metformin does not mimic the actions of insulin in conditions of severe insulinopenia (Sterne, 1969; Bailey, 1992). However, the hypoglycaemic effect of exogenous insulin was augmented by metformin, as noted in other diabetic states (Lord *et al.*, 1983; Pagano *et al.*, 1983; Gin *et al.*, 1985; Leblanc *et al.*, 1987).

The ability of somatostatin (Cherrington *et al.*, 1978) and diazoxide (Henquin *et al.*, 1992) to suppress basal and glucose-stimulated insulin concentrations was exploited in the present study to induce a state of low insulin. Predictably, this was associated with impaired glucose disposal during an IVGTT. However, the extent to which metformin improved glucose disappearance with low insulin (from 0.24 to 1.00% min^{-1}) was similar to the improvement in normal rats (from 1.7 to 2.5% min^{-1}), i.e. improvements of 0.76 and 0.80% min^{-1} respectively. Since this observation was made in non-diabetic rats, it excludes the variable impingement of insulin resistance which complicates the interpretation of studies in diabetic individuals (Hermann, 1979; Bailey, 1992). Thus it appears that the efficacy of metformin is *not* directly related to the prevailing insulin concentration, provided that at least some insulin is present.

Since metformin typically exerts little effect on basal glycaemia in the euglycaemic state, but does improve glucose disposal during glucose tolerance tests and hyperglycaemic clamp procedures, it has been mooted that metformin might enhance the mass action effect of glucose to increase glucose utilization (Hother-Nielsen *et al.*, 1989; DeFronzo *et al.*, 1991). The present observations in BB/S rats indicate that if this occurs it is not quantitatively sufficient to alter the level of hyperglycaemia in an insulinopenic situation.

The IVGTT procedures are primarily a measure of insulin-stimulated glucose disposal (Bergmann *et al.*, 1985). Thus the present observations are consistent with *in vitro* evidence that metformin increases insulin-stimulated glucose uptake into skeletal muscle and fat (Frayn & Adnitt, 1972; Bailey & Puah, 1986; Galuska *et al.*, 1991; Matthaei *et al.*, 1991). It has also been reported that metformin increases glucose uptake by cultured L6 muscle cells of the rat in the presence of insulin and in the period immediately after insulin has been removed from the medium (Hundal *et al.*, 1992). The metformin-induced increase in glucose uptake appears to involve increased translocation of glucose transporters from the microsomal fraction into the plasma membrane, without changing the total cellular pool of transporters (Matthaei *et al.*, 1991; Hundal *et al.*, 1992). In normal fat cells there was increased translocation of both GLUT-4, the main insulin-responsive transporter, and GLUT-1, which is only slightly responsive to insulin (Matthaei *et al.*, 1991). In rat cultured L6 muscle cells, metformin increased translocation of GLUT-1 (but not GLUT-4) into the plasma membrane (Hundal *et al.*, 1992). While it is premature to extrapolate from these *in vitro* models to the *in vivo* situation, the possibility exists that metformin could exert different effects on glucose transporters in different tissues. Tissue-specific differences in transporter regulation are known to occur in various physiological and pathological states (Pessin & Bell, 1992). Indeed the intestine, which has a very different glucose transporter complement from muscle and fat, shows increased glucose utilization in response to metformin in both the basal and post-prandial states (Bailey *et al.*, 1992). Increased glucose recycling, for example via lactate, could then contribute to the maintenance of blood glucose concentrations in the basal state (Penicaud *et al.*, 1989).

Consistent with the reported effects of metformin on the translocation of glucose transporters, the present study suggests that the presence, or recent presence of insulin is required for metformin to augment glucose utilization. Thus it is possible that insulin is necessary to activate the cellular processes upon which metformin operates. However, metformin does not potentiate insulin action in a manner proportional to the prevailing insulin concentration.

The authors gratefully acknowledge the expert help of Susan Turner, Tracey Buck and Karen Taylor and thank Lipha Pharmaceuticals for support and constructive discussion.

References

BAILEY, C.J. (1992). Biguanides in NIDDM. *Diabetes Care*, **15**, 755–772.

BAILEY, C.J. (1993). Metformin – an update. *Gen Pharmacol.*, **24**, 1299–1309.

BAILEY, C.J. & NATTRASS, M. (1988). Treatment-metformin. *Clin. Endocrinol. Metab.*, **2**, 455–476.

BAILEY, C.J. & PUAH, J.A. (1986). Effect of metformin on glucose metabolism in mouse solens muscle. *Diabete Metab.*, **12**, 212–218.

BAILEY, C.J., WILCOCK, C. & DAY, C. (1992). Effect of metformin on glucose metabolism in the splanchnic bed. *Br. J. Pharmacol.*, **105**, 1009–1013.

BERGMANN, R.N., FINEGOOD, D.T. & ADER, M. (1985). Assessment of insulin sensitivity in vivo. *Endocrine Revs.*, **6**, 45–86.

BONE, A.J. (1991). Animal models of insulin-dependent diabetes mellitus. In *Textbook of Diabetes*. ed. Pickup, J.C. & Williams, G. pp. 151–163. Oxford: Blackwell Scientific.

CHERRINGTON, A.D., LACY, W.W. & CHAISSON, J.-L. (1978). Effect of glucagon on glucose production during insulin deficiency in the dog. *J. Clin. Invest.*, **62**, 664–677.

DEFRONZO, R.A., BARZILAI, N. & SIMONSON, D.C. (1991). Mechanism of metformin action in obese and lean noninsulin-dependent diabetic subjects. *J. Clin. Endocrinol. Metab.*, **73**, 1294–1301.

DESBUQUOIS, B. & AURBACH, G.D. (1971). Use of polyethylene glycol to separate free and antibody-bound peptide hormones in radioimmunoassays. *J. Clin. Endocrinol. Metab.*, **33**, 732–738.

FRAYN, K.N. & ADNITT, P.I. (1972). Effect of metformin on glucose uptake by isolated diaphragm from normal and diabetic rats. *Biochem. Pharmacol.*, **21**, 3153–3162.

GALUSKA, D., ZIERATH, J., THORNE, A., SONNENFELD, T. & WALLBERG-HENRIKSSON, H. (1991). Metformin increases insulin-stimulated glucose transport in insulin-resistant human skeletal muscle. *Diabete Metab.*, **17**, 159–163.

GIN, H., MESSERSCHMITT, C., BROTTIER, E. & AUBERTIN, J. (1985). Metformin improved insulin resistance in type 1, insulin-dependent, diabetic patients. *Metabolism*, **34**, 923–925.

HENQUIN, J.C., DEBUYSER, A., DREWS, G. & PLANT, T.D. (1992). Regulation of K^+ permeability and membrane potential in insulin-secreting cells. In *Nutrient Regulation of Insulin Secretion* ed. Flatt, P.R. pp. 173–191. London: Portland Press.

HERMANN, L.S. (1979). Metformin: a review of its pharmacological properties and therapeutic use. *Diabete Metab.*, **5**, 233–245.

HOTHER-NIELSEN, O., SEHMITZ, O., ANDERSEN, P.H., BECK-NIELSEN, H. & PEDERSEN, O. (1989). Metformin improves peripheral but not hepatic insulin action in obese patients with type II diabetes. *Acta Endocrinol.*, **120**, 257–265.

HUNDAL, H.S., RAMLAL, T., REYES, R., LEITER, L.A. & KLIP, A. (1992). Cellular mechanism of metformin action involves glucose transporter translocation from an intracellular pool to the plasma membrane in L6 muscle cells. *Endocrinol.*, **131**, 1165–1173.

LEBLANC, H., MARRE, M., BILLAULT, B. & PASSA, Ph. (1987). Combined continuous subcutaneous insulin infusion in 10 overweight insulin requiring diabetic patients. *Diabete Metab.*, **13**, 613–617.

LORD, J.M., ATKINS, T.W. & BAILEY, C.J. (1983). Effect of metformin on hepatocyte insulin receptor binding in normal, streptozotocin diabetic and genetically obese diabetic (ob/ob) mice. *Diabetologia*, **25**, 108–113.

MATTHAEI, S., HAMANN, A., KLEIN, H.H., BENECKE, H., KREYMANN, G., FLIER, J.S. & GRETEN, H. (1991). Association of metformin's effect to increase insulin-stimulated glucose transport with potentiation of insulin-induced translocation of glucose transporters from intracellular pool to plasma membrane in rat adipocytes. *Diabetes*, **40**, 850–857.

NAKHOODA, A.F., LIKE, A.A., CHAPPEL, C.I., MURRAY, F.T. & MARLISS, E.B. (1976). The spontaneously diabetic Wister rat. Metabolic and morphologic studies. *Diabetes*, **26**, 100–112.

NOSADINI, R., AVOGARO, A., TREVISAN, R., VALERIO, A., TESSARI, P., DUNER, E., TIENGO, A., VELUSSI, M., DEL PRATO, S., DE KREUTZENBERG, S., MUGGEO, M. & CREPALDI, G. (1987). Effect of metformin on insulin binding to receptors in type II diabetes. *Diabetes Care*, **10**, 62–67.

PAGANO, G., TAGLIAGERRO, V., CARIA, Q., CASELLE, MLT., BOZZO, C., VITELLI, F., TROVATI, M. & COCUZZA, E. (1983). Metformin reduces insulin requirement in type 1 (insulin-dependent) diabetes. *Diabetologia*, **24**, 351–354.

PENICAUD, L., HITIER, Y., FERRE, P. & GIRARD, J. (1989). Hypoglycaemic effect of metformin in genetically obese (fa/fa) rats results from an increased utilization of blood glucose by intestine. *Biochem. J.*, **262**, 881–885.

PESSIN, J.E. & BELL, G.I. (1992). Mammalian facilitative glucose transporter family: structure and molecular regulation. *Annu. Rev. Physiol.*, **544**, 911–930.

PRAGER, R., SCHERNTHANER, G. & GRAF, H. (1986). Effect of metformin on peripheral insulin sensitivity in non insulin dependent diabetes mellitus. *Diabete Metab.*, **12**, 346–350.

REAVEN, G.M., JOHNSTON, P., HOLLENBECK, C.B., SKOWRONSKI, R., ZHANG, J.C., GOLDFINE, I.D. & CHEN, Y.D.I. (1992). Combined metformin-sulfonylurea treatment of patients with noninsulin-dependent diabetes in fair to poor glycaemic control. *J. Clin. Endocrinol. Metab.*, **74**, 1020–1026.

STERNE, J. (1969). Pharmacology and mode of action of hypoglycaemic guanidine derivatives. In *Oral Hypoglycaemic Agents* ed. Campbell, G.D. pp. 193–245. London: Academic Press.

STEVENS, J.F. (1971). Determination of glucose by an automatic analyser. *Clin. Chim. Acta*, **32**, 199–201.

(Received October 4, 1993
Accepted November 22, 1993)

Br. J. Pharmacol. (1994), **111**, 797–802 © Macmillan Press Ltd, 1994

In vivo properties of SB 200646A, a 5-$HT_{2C/2B}$ receptor antagonist

[1]G.A. Kennett, M.D. Wood, A. Glen, S. Grewal, *I. Forbes, *A. Gadre & T.P. Blackburn

Department of Psychiatry and *Department of Medicinal Chemistry, SmithKline Beecham, Coldharbour Road, The Pinnacles, Harlow, Essex CM19 5AD

1 SB 200646A, N-(1-methyl-5-indolyl)-*N'*-(3-pyridyl) urea hydrochloride, the first reported selective 5-$HT_{2C/2B}$ over 5-HT_{2A} receptor antagonist, (pK_i rat 5-HT_{2C} receptor 6.9, pA_2 rat 5-HT_{2B} receptor 7.5, pK_i rat 5-HT_{2A} receptor 5.2) dose-dependently blocked a putative rat model of 5-HT_{2C} receptor activation; 1-(3-chlorophenyl)piperazine (mCPP, 5 mg kg^{-1}, i.p. 20 min pretest)-induced hypolocomotion (estimated ID_{50} 19.2 mg kg^{-1}, p.o.).

2 SB 200646A also blocked another putative *in vivo* model of 5-HT_{2C} receptor function; mCPP (5 mg kg^{-1}, i.p. 20 min pretest)-induced hypophagia in 23 h food-deprived rats (estimated ID_{50} 18.3 mg kg^{-1}, p.o.).

3 SB 200646A did not antagonize 1-(2,5-dimethoxy-4-iodophenyl)-2-aminopropane (DOI)-induced head shakes in rats at doses up to 200 mg kg^{-1}, p.o., an effect thought to be mediated by 5-HT_{2A} receptors for which SB 200646A has its next highest affinity (50 fold less) after the 5-HT_{2C} and 5-HT_{2B} sites.

4 SB 200646A (20, 40 mg kg^{-1}, p.o., 1 h pretest) also reversed mCPP (0.5 mg kg^{-1}, i.p., 30 min pretest)-induced anxiety in the social interaction test, under low light familiar conditions.

5 When given alone, under high light unfamiliar conditions, SB 200646A (2–40 mg kg^{-1}, p.o.) increased active social interaction without affecting locomotor activity in the rat social interaction test. This is consistent with an anxiolytic action of SB 200646A.

6 These results indicate that SB 200646A has *in vivo* efficacy and that 5-HT_{2C} or 5-HT_{2B} receptors are indeed likely to mediate mCPP-induced hypolocomotion, hypophagia and anxiogenesis. They also suggest that 5-$HT_{2C/2B}$ receptor blockade induces anxiolysis.

Keywords: 5-HT_{2C} receptors; 5-HT_{2A} receptors; 5-HT_{2B} receptors; 5-HT; anxiety; SB 200646A

Introduction

The 5-HT_{1C} receptor was first characterized by Pazos *et al.* (1984). However, it is now recognised as belonging to the 5-HT_2 receptor family on the basis of marked amino acid sequence homology (Pritchett *et al.*, 1988; Saltzman *et al.*, 1991), and has therefore been renamed as the 5-HT_{2C} receptor site (Humphrey *et al.*, 1993). The receptor is reported to act through the phosphoinositide hydrolysis secondary messenger system (Conn *et al.*, 1986) and is widely distributed in both rat (Pazos & Palacios, 1985) and human (Pazos *et al.*, 1987) brain, with particularly high density in the choroid plexus (Pazos & Palacios 1985; Pazos *et al.*, 1987). In rats, several *in vivo* responses to the putative 5-HT_{2C} receptor agonist, 1-(3-chlorophenyl) piperazine (mCPP) have been suggested to be mediated by 5-HT_{2C} receptor activation. These include mCPP-induced hypolocomotion (Kennett & Curzon, 1988a), hypophagia (Kennett & Curzon, 1988b) and anxiety (Kennett *et al.*, 1989). mCPP-induced anxiety is of particular interest as it has been widely reported in healthy volunteers and to a greater extent in patients with either panic disorders or obsessive compulsive disorder (OCD) (see Kennett, 1993). Unfortunately mCPP is not a selective 5-HT_{2C} receptor agonist and the pharmacological characterization of its effects *in vivo* result from the use of non-selective 5-HT_{2C} receptor antagonists. In the present study we have investigated the effects of the *in vivo* administration of SB 200646A (N-(1-methyl-5-indolyl)-*N'*-(3-pyridyl) urea hydrochloride), the first reported antagonist with selectivity for the 5-HT_{2C} over the 5-HT_{2A} receptor (Forbes *et al.*, 1993; Wood *et al.*, 1993). This compound had 50 fold selectivity for the rat 5-HT_{2C} over the 5-HT_{2A} receptor, and 80 fold or greater selectivity over other neurotransmitter receptors tested (Table 1, Forbes *et al.*, 1993). However, SB 200646A is also equipotent at the 5-HT_{2B} (rat stomach fundus) receptor with which the 5-HT_{2C} receptor shares a high degree of sequence homology (Foquet *et al.*, 1992; Kursar *et al.*, 1992) and at which mCPP has agonist properties (Clineschmidt *et al.*, 1985).

[1] Author for correspondence.

Methods

Animals

Male Sprague-Dawley (CD) rats 220–250 g were housed in groups of six under a 12 h light/dark cycle (lights on 07 h 00 min) with free access to food (CRMX, Special Diet Services) and water.

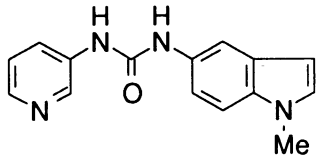
mCPP-induced hypolocomotion

Rats were placed in a room adjacent to the experimental room on the day of the procedure. They were dosed orally 1 h pretest with SB 200646A or vehicle, and injected i.p. 20 min pretest with mCPP or saline, in groups of four. Rats were returned to their home cages after dosing. At 0 h they were each placed in automated locomotor activity cages (57 × 16.6 × 25.3 cm) made of black perspex with a clear perspex lid and sawdust-covered floor, under red light for 10 min. During this time locomotion was recorded by means of alternately breaking two photocell beams traversing opposite ends of the box 3.9 cm above floor level.

mCPP-induced hypophagia

Rats were individually housed on day 1 and deprived of food. Twenty three hours later they were dosed orally with

Table 1 Receptor binding profile of SB 200646A



Receptor	*Affinity* (pK_I)	*Receptor*	*Affinity* (pK_I)
5-HT_{2C}	6.9	Adrenoceptorα_1	<5.0
5-HT_{2B}	7.5*	Adrenoceptorα_{2A}	<5.0
5-HT_{2A}	5.2	Adrenoceptorα_{2B}	<5.0
5-HT_{1A}	<5.0	Adrenoceptorβ_1	<4.0
5-HT_{1D}	<5.0	Adrenoceptorβ_2	<4.0
5-HT_3	<5.0	Dopamine D_1	<5.0
BDZ	<5.0	Dopamine D_2	<4.5
$GABA_A$	<5.0	Histamine H_1	<5.0
GABA/Cl^- channel (TBPS)	<5.0		

*pA_2 value in the rat stomach fundus preparation. For experimental details see Forbes *et al.* (1993) except affinities for benzodiazepine (BDZ) receptors ([^{3}H]-flunitrazepam in rat cortex), histamine H_1 ([^{3}H]-mepyramine in rat cortex) and ter-butylbicyclophosphorothionate (TBPS) ([^{3}H]-TBPS) which were carried out as in Sanger & Nelson (1989) and those for $GABA_A$ ([^{3}H]-muscimol in rat cortex as described by Peters *et al.* (1988)).

antagonist or vehicle and returned to their home cages. Forty minutes later they were given mCPP or saline i.p. and again returned to their home cages. After a further 20 min, weighed aliquots of their normal food pellets were placed in their food hoppers and the amount remaining after 2 h was measured.

Social interaction

Rats were housed singly in a room adjacent to the testing room on day 1. On day 5 they were dosed orally with SB 200646A or vehicle in treatment- and weight-matched (± 5 g) pairs, which had not previously been housed together, and returned to their home cage. Rats were then placed in a white perspex test box (54 × 37 × 26 cm) for 15 min under bright white light (150 lux) in an adjacent darkened room containing a fan to generate white noise. Active social interaction (sniffing, following, grooming, biting, boxing and crawling over or under) was scored by a 'blind' observer by remote video monitoring and a computerised score pad. At the end of each test the box was thoroughly wiped with moistened tissue paper. Alternatively rats were individually pre-exposed to test boxes of black perspex under red light for 10 min on days 3 and 4 and tested under the same conditions on day 5.

DOI-induced head shakes

Rats were dosed orally with SB 200646A 30 min before being placed in individual clear perspex observation cages (25.4 × 25.4 × 22.2 (height) cm). Thirty minutes later 1-(2,5-dimethoxy-4-iodophenyl)-2-aminopropane (DOI) was given i.p. and the number of head shakes produced over the next 30 min were counted using a computerised score pad.

Drugs

SB 200646A (SB) and mianserin (Organon, Newhouse, Scotland) were ground into 1% methyl cellulose in 0.9% NaCl with a drop of BRIJ 35 (Sigma Chemical Co., Poole, Dorset) dispersant using a mortar and pestle and given orally as a suspension in a 2 ml kg^{-1} injection volume 1 h pretest. SB 200646A was neutralised to pH 4.5. SB 200646A controls were given 1% methyl cellulose in 0.9% NaCl and a drop of BRIJ 35 acidified to pH 4.5 with HCl. DOI (Research Biochemcials Inc, Natick, Massachusetts, U.S.A.) and mCPP (Sigma Chemical Co., Poole, Dorset) were dissolved in saline and given i.p. in 1 ml kg^{-1} injection volume 1 and 20 min pretest respectively.

Statistics

The effect of SB 200646A on mCPP-induced hypolocomotion was determined by one-way ANOVA and Newman-Keuls test, and on hypophagia and anxiogenesis by two-way ANOVA and Newman-Keuls test. All other data were subjected to one-way ANOVA and Dunnett's test. Estimates of the dose producing 50% inhibition (ID_{50}) of mCPP-induced hypolocomotion or hypophagia were made using the iterative curve-fitting programme 'Allfit' (DeLean *et al.*, 1978). All data are cited as means ± s.e.mean.

Results

Effect of SB 200646A on mCPP-induced hypolocomotion

SB 200646A alone at 40 mg kg^{-1}, p.o., had no effect on locomotor activity, neither did lower doses in previous experiments (data not shown) or mianserin at 4 mg kg^{-1}, p.o. (Table 2). mCPP (5 mg kg^{-1}, i.p.) markedly reduced the number of transits over 10 min and this effect was significantly reversed by SB 200646A (20 and 40 mg kg^{-1}, p.o.) and mianserin, used here as a positive control. The iterative curve-fitting programme 'Allfit', estimated the ID_{50} value of SB 200646A against mCPP-induced hypolocomotion as 19.2 ± 0.2 mg kg^{-1}, p.o. The ANOVA test result for this study was $F(8,178) = 25.0$, $P<0.01$).

Effect of SB 200646A on mCPP-induced hypophagia

SB 200646A had no significant effect on the food intake of 23 h food-deprived rats over 2 h ($F(4,81) = 1.63$, NS), although food intake was somewhat reduced after 40 and 60 mg kg^{-1}, p.o. (Table 3). mCPP (5 mg kg^{-1}, i.p.) significantly reduced food intake ($F(1,81) = 22.3$, $P<0.01$) and this effect was significantly, and dose-dependently, reversed by SB 200646A (10–60 mg kg^{-1}, p.o.) ($F(4,81) = 100.7$, $P<0.01$) (Table 3). The estimated ID_{50} for this action was 18.3 ± 10.3 mg kg^{-1}, p.o.

Effect of SB 200646A on DOI-induced head shakes

DOI (3 mg kg^{-1}, i.p.) induced 27.9 ± 3.0 head shakes over 30 min. SB 20064A, at doses up to 200 mg kg^{-1}, p.o. 1 h pretest, did not alter this response ($F(4,58) = 0.9$, NS) (Figure 1) and did not cause head shake behaviour when given alone at 100 or 200 mg kg^{-1}, p.o. (vehicle-treated 2.3 ± 1.2, SB 200646A 100 mg kg^{-1}, p.o. 2.8 ± 0.8; 200 mg kg^{-1}, p.o., 1.7 ± 2.0 $n = 4$ per group).

Effect of SB 200646A on 'anxiogenic-like' responses to mCPP

mCPP (0.5 mg kg^{-1}, i.p.) significantly reduced total interaction scores ($F(1,49) = 11.5$, $P < 0.01$), but had no effect on locomotor activity ($F(1,49) = 0.86$, NS). SB 200646A had no effect on total interaction scores when given alone, but significantly reversed the effect of mCPP ($F(2,49) = 3.36$, $P < 0.05$). SB 2006464A also caused a significant effect on locomotion ($F(2,49) = 6.07$, $P < 0.01$), but this did not result in a significant effect between vehicle- and SB 200646A-treated groups, whether given mCPP or not, when analysed by the Newman-Keuls test (Figure 2).

Effect of SB 200646A on rat social interaction

SB 200646A dose-dependently increased time spent in active social interaction over 15 min ($F(6,67) = 28.2$, $P < 0.01$) (Fig-

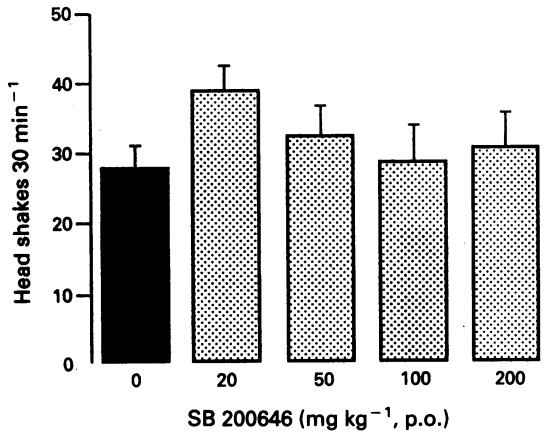


Figure 1 Effect of SB 200646A, given p.o. 1 h pretest, on 1-(2,5-dimethoxy-4-iodophenyl)-2-aminopropane (DOI, 3 mg kg^{-1}, i.p. 1 min pretest)-induced head shakes over 30 min. All columns means ± s.e.mean. $n = 12-14$ per group. No significant differences.

Table 2 Effect of SB 200646A on 1-(3-chlorophenyl) piperazine (mCPP)-induced hypolocomotion

Pretreatment	*Treatment*	*Transits/10 min*
Vehicle	Saline	16.6 ± 0.7
SB 200646A 40 mg kg^{-1}	Saline	16.8 ± 0.9
Mianserin 4 mg kg^{-1}	Saline	15.7 ± 1.3
Vehicle	mCPP	2.1 ± 0.7**
SB 200646A 10 mg kg^{-1}	mCPP	2.5 ± 0.6
SB 200646A 20 mg kg^{-1}	mCPP	7.7 ± 1.5†
SB 200646A 40 mg kg^{-1}	mCPP	11.4 ± 2.3††
Mianserin 4 mg kg^{-1}	mCPP	13.3 ± 2.5††

ID_{50} = 19.2 ± 0.2 mg kg^{-1}, p.o. by 'Allfit'
mCPP (5 mg kg^{-1}, i.p.) given 20 min pretest, SB 200646A and mianserin given p.o. 1 h pretest. All points means ± s.e.mean, $n = 15-20$. Significantly different from vehicle + saline-treated group: $^{**}P < 0.01$; from vehicle + mCPP-treated group. $^{\dagger}P < 0.05$; $^{\dagger\dagger}P < 0.01$ by Newman-Keuls test following 1-way ANOVA.

Table 3 Effect of SB 200646A on 1-(3-chlorophenyl) piperazine (mCPP)-induced hypophagia

Pretreatment	*Treatment*	*2 h Food intake* (g)
Vehicle	Saline	4.3 ± 0.4
SB 200646A 10 mg kg^{-1}	Saline	3.7 ± 0.4
SB 200646A 20 mg kg^{-1}	Saline	4.6 ± 0.3
SB 200646A 40 mg kg^{-1}	Saline	3.6 ± 1.4
SB 200646A 60 mg kg^{-1}	Saline	3.2 ± 0.3
Vehicle	mCPP	1.0 ± 0.7**
SB 200646A 10 mg kg^{-1}	mCPP	2.5 ± 0.3†
SB 200646A 20 mg kg^{-1}	mCPP	2.4 ± 0.5†
SB 200646A 40 mg kg^{-1}	mCPP	3.6 ± 0.6††
SB 200646A 60 mg kg^{-1}	mCPP	3.5 ± 0.5††

ID_{50} = 18.3 ± 10.3 mg kg^{-1}, p.o. by 'Allfit'
mCPP (5 mg kg^{-1}, i.p.) given 30 min pretest, SB 200646A given p.o. 1 h pretest. All points means ± s.e.mean, $n = 9$. Significantly different from vehicle + saline-treated group: $^{**}P < 0.01$; from vehicle + mCPP-treated group: $^{\dagger}P < 0.05$; $^{\dagger\dagger}P < 0.01$ by Newman-Keuls test following significant 2-way ANOVA.

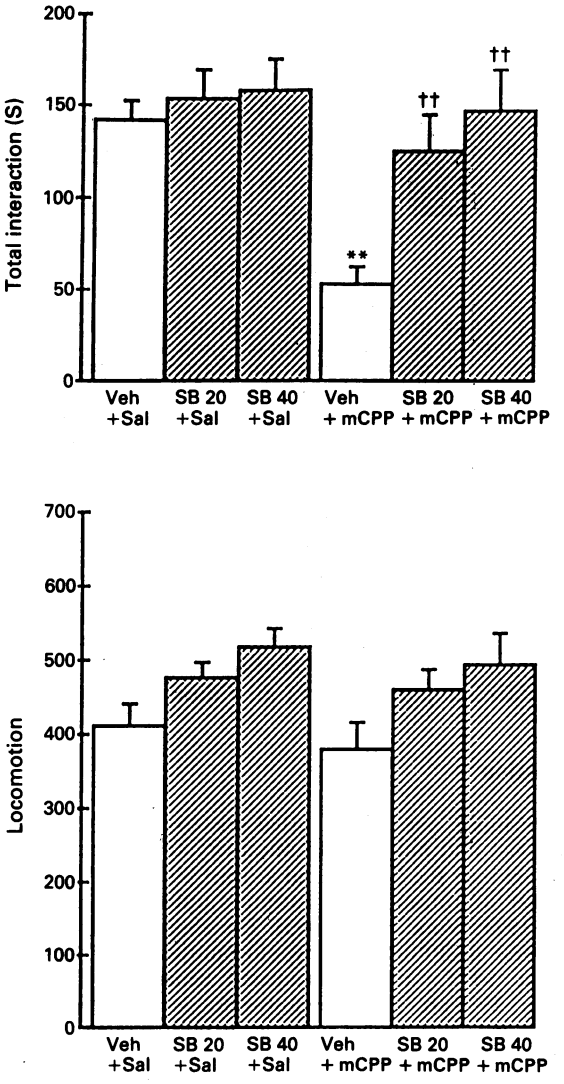


Figure 2 Effect of SB 200646A (20–40 mg kg^{-1}, p.o. 1 h pretest) on 1-(3-chlorophenyl)piperazine (mCPP, 0.5 mg kg^{-1}, i.p., 30 min pretest)-induced anxiety in the rat social interaction test. Veh = vehicle, SB = SB 200646A. All columns means ± s.e.mean, $n = 8-12$ per group. Significantly different from vehicle + saline (Sal)-treated group: $^{**}P < 0.01$; from vehicle + mCPP-treated group: $^{\dagger\dagger}P < 0.01$ by Newman-Keuls test following significant 2-way ANOVA.

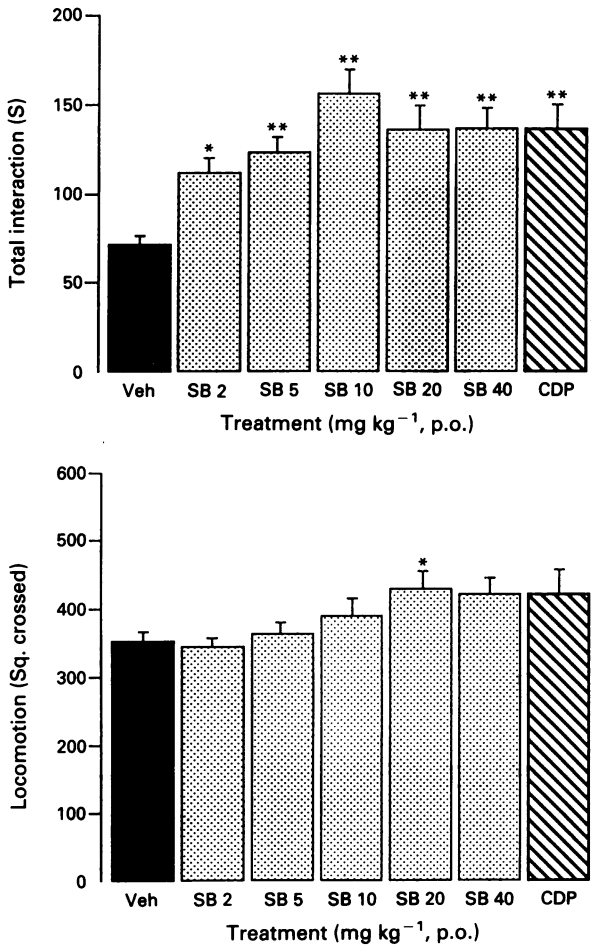


Figure 3 Effect of SB 200646A (2–40 mg kg^{-1}), chlordiazepoxide 5 mg kg^{-1} (CDP) and vehicle (Veh) (all given p.o., 1 h pretest) in the rat 15 min social interaction test under high light unfamiliar conditions. All columns means ± s.e.mean. $n = 8-12$ per group. Significantly different from vehicle-treated group: $*P<0.05$; $**P<0.01$ by Dunnett's test following significant 1-way ANOVA.

ure 3). The drug also caused a small increase in locomotion at 20 mg kg^{-1}, p.o. but at no other dose ($F(6,67) = 2.4$, $P<0.05$) (Figure 3). The magnitude of the increase in total interaction induced by SB 200464A was equal to that seen after chlordiazepoxide (CDP) at a dose of 5 mg kg^{-1}, p.o.

Discussion

SB 200646A is the first reported selective 5-HT$_{2C/2B}$ receptor antagonist and has 50 fold selectivity for the rat 5-HT$_{2C/2B}$ receptors over the 5-HT$_{2A}$ and at least 80 fold selectivity over all other neurotransmitter receptors tested (Table 1, Forbes *et al.*, 1993; Wood *et al.*, 1993). The ability of the compound to reverse mCPP-induced hypolocomotion and hypophagia, putative 5-HT$_{2C}$ receptor-mediated behaviours (Kennett & Curzon, 1988a,b; 1991) demonstrates *in vivo* efficacy. Since SB 200646A has similar potency in both models it is likely that a similar mechanism of action is indeed involved and this is likely to be via blockade of the 5-HT$_{2C}$ site, as previously proposed, or of the recently characterized 5-HT$_{2B}$ site. However, given the relatively low potency of the compound in these tests it might be suggested that SB 200646A is blocking some other site, despite its 50 fold selectivity for 5-HT$_{2C/2B}$ receptors. The inability of SB 200646A, at much higher doses (200 mg kg^{-1}, p.o.), to antagonize 5-HT$_{2A}$-mediated DOI-induced head shakes (Pranzatelli, 1990; Kennett & Curzon, 1991) argues against this, as after the 5-HT$_{2C/2B}$ site, its next highest affinity is for the 5-HT$_{2A}$ receptor (Table 1).

Although both mCPP-induced hypophagia and hypolocomotion appear to be mediated by the same receptor they are independent behaviours. Thus, hypophagia caused by mCPP is blocked by cyanopindolol and (−)-propranolol (Kennett & Curzon, 1988b) unlike the hypolocomotor response (Kennett & Curzon, 1988a) while intrahypothalamic trifluoromethyl phenylpiperazine (TFMPP), a closely related 5-HT$_{2C}$ agonist, causes only hypophagia (Hutson *et al.*, 1988). That SB 200646A fully reversed the hypophagic effect of mCPP but only partially reversed hypolocomotion (Tables 2 and 3) is, however, probably due to not having administered high enough doses, although it may conceivably indicate the presence of an additional mechanism.

SB 200646A also antagonized the anxiogenic-like effect of mCPP in the rat social interaction model at similar doses to those which were effective against mCPP-induced hypolocomotion and hypophagia. Thus, the anxiogenic response is also likely to be mediated by 5-HT$_{2C/2B}$ receptors. This is consistent with previous evidence that non-selective 5-HT$_{2C/2B}$, but not selective 5-HT$_{2A}$ or 5-HT$_{1A}$ and 5-HT$_{1B}$ receptor antagonists blocked the effect of mCPP in this paradigm (Kennett *et al.*, 1989). It is also consistent with antagonism of mCPP-induced anxiety in man by both the non-selective 5-HT$_1$ and 5-HT$_2$ receptor blockers metergoline (Kalus *et al.*, 1990; Pigott *et al.*, 1991) and methysergide (Kalus *et al.*, 1990) and, in particular, by the relatively selective (see Kennett, 1993) 5-HT$_{2C/2B/2A}$ receptor antagonist, ritanserin (Seibyl *et al.*, 1991).

Since activation of 5-HT$_{2C}$ (or 5-HT$_{2B}$) receptors seems to cause anxiety, their blockade might be anxiolytic if the system is activated during stress. Indeed, immobilisation stress (Shimzu *et al.*, 1992), tail pinch and handling (Kalen *et al.*, 1989) and placement on the open arms of the elevated X-maze (Wright *et al.*, 1992) have all been shown to enhance extraneuronal 5-HT in either the hypothalamus or the hippocampus. mCPP infusion into this latter region in the rat, which contains high levels of 5-HT$_{2C}$ receptor mRNA (Hoffman & Mezey, 1989; Molineaux *et al.*, 1989) and receptors (Mengod *et al.*, 1990), has been reported to induce anxiogenic-like responses (Whitton & Curzon, 1990). mCPP has also been reported to potentiate periaqueductal grey-induced anxiety (Beckett *et al.*, 1992). The anxiolytic-like response to SB 200646A in the social interaction test may therefore be caused by antagonism of these responses and is in agreement with previous findings of the anxiolytic effects of non-selective 5-HT$_{2C/2B}$, but not of 5-HT$_{2A}$ or other receptor antagonists, in both the rat social interaction and Geller-Seifter models of anxiety (Kennett, 1992; Kennett *et al.*, 1993). The lack of an anxiolytic-like response in the social interaction test when SB 200646A was given alone under low light unfamiliar conditions (Figure 2) is probably due to low intrinsic levels of anxiety under these conditions (File, 1985). As SB 200646A has low affinity for the benzodiazepine, GABA$_A$ and TBPS binding sites (Table 1) the GABA/Cl$^-$ complex is unlikely to be the primary site of its anxiolytic action while the presence of 5-HT$_{2B}$ receptors in rat brain, let alone the hippocampus is as yet unknown.

In conclusion, experiments with SB 200646A, the first selective 5-HT$_{2C/2B}$ receptor antagonist, indicate that the compound has *in vivo* activity and that 5-HT$_{2C/2B}$ receptors are likely to mediate the hypolocomotion, hypophagia and anxiety induced by mCPP. Furthermore, the results suggest that selective antagonists of 5-HT$_{2C/2B}$ receptors possess anxiolytic-like properties. These may be of clinical relevance given reports of the clinical anxiolytic efficacy of the non-selective 5-HT$_{2C/2B}$ receptor antagonists, mianserin (Murphy, 1978; Russell *et al.*, 1978; Conti & Pinder, 1979; Khan *et al.*, 1983) and ritanserin (Ceulemans *et al.*, 1985; Bressa *et al.*, 1987; Pangalila-Ratu *et al.*, 1988). However, although there is as yet no pharmacological evidence to differentiate between

5-HT$_{2C}$ or 5-HT$_{2B}$ receptor mediation of the above effect, the 5-HT$_{2B}$ receptor has, to date, been identified only in mouse brain at extremely low density (Loric *et al.*, 1992). Furthermore while mCPP is an almost full agonist on the 5-HT$_{2C}$ receptor functions so far examined (see Kennett, 1993) it is only a weak partial agonist on the rat stomach fundus (Clineschmidt *et al.*, 1985). This suggests that the 5-HT$_{2C}$ receptor is the more likely mediator of the hypolocomotion, hypophagia and anxiety responses to mCPP. Identification of the exact functions of the 5-HT$_{2C}$, 5-HT$_{2B}$ and indeed of the pharmacologically similar rat and porcine endothelial receptors (Glusa & Richter, 1993; Bodelson *et al.*, 1993), awaits the development of selective ligands.

References

BECKETT, S.R.G., MARSHALL, P.W. & MARSDEN, C.A. (1992). Intraperiaqueductal grey administration of mCPP potentiates a chemically-induced defence response. *Br. J. Pharmacol.*, **107**, 8P.

BODELSON, M., TORNEBRANDT, K. & ARNEKLO-NOBIN, B. (1993). Endothelial relaxing 5-hydroxytryptamine receptors in the rat jugular vein: similarity with the 5-hydroxytryptamine $_{1C}$ receptor. *J. Pharmacol. Exp. Ther.*, **264**, 709–716.

BRESSA, G.M., MARINI, S. & GREGORI, S. (1987). Serotonin S2 receptor blockade and generalised anxiety disorder. A double-blind study on ritanserin and lorazepam. *Int. J. Clin. Pharmacol. Res.*, **VII**, 111–119.

CEULEMANS, D.L.S., HOPPENBROUWERS, M.L.J.A., GELDERS, Y.G. & REYNTJENS, A.J.M. (1985). The influence of ritanserin, a serotonin antagonist, in anxiety disorders: A double-blind placebo controlled study versus lorazepam. *Pharmacopyschiatry*, **18**, 303–305.

CLINESCHMIDT, B.V., REISS, D.R., PETTIBONE, D.J. & ROBINSON, J.L. (1985). Characterization of 5-hydroxytryptamine receptors in rat stomach fundus. *J. Pharmacol. Exp. Ther.*, **235**, 696–708.

CONN, C.J., SANDERS-BUSH, E., HOFFMAN, B.J. & HARTIG, P.R. (1986). A unique serotonin receptor in choroid plexus is linked to phosphatidylinositol turnover. *Proc. Natl. Acad. Sci. U.S.A.*, **83**, 4086–4088.

CONTI, L. & PINDER, R.M. (1979). A controlled comparative trial of mianserin and diazepam in the treatment of anxiety states in psychiatric outpatients. *J. Int. Med. Res.*, **7**, 285–289.

DELEAN, A., MUNSON, P.J. & ROBARD, D. (1978). Simultaneous analysis of families of sigmoidal curves: application to bioassay, radioligand assay and physiological dose-response curve. *Am. J. Physiol.*, **235**, E97–E102.

FILE, S.E. (1985). Animal models for predicting clinical efficacy of anxiolytic drugs: social behaviour. *Neuropsychobiology*, **13**, 55–62.

FOQUET, M., NGUYEN, H., LE, H. & LUBBERT, H. (1992). Structure of the mouse 5-HT$_{1C}$, 5-HT$_2$ and stomach fundus serotonin receptor genes. *Neuroreport*, **3**, 345–348.

FORBES, I.T., KENNETT, G.A., GADRE, A., HAM, P., HAYWARD, C.J., MARTIN, R.T., THOMPSON, M., WOOD, M.D., BAXTER, G.S., GLEN, A., MURPHY, O.E., STEWART, B. & BLACKBURN, T.P. (1993). N-(1-methyl-5-indolyl)-N'-(3-pyridyl)urea hydrochloride: The first selective 5-HT$_{1C}$ receptor antagonist. *J. Med. Chem.*, **36**, 1104–1107.

GLUSA, E. & RICHTER, M. (1993). Endothelium-dependent relaxation of porcine pulmonary arteries via 5-HT$_{1C}$-like receptors. *Naunyn Schmied. Arch. Pharmacol.*, **347**, 471–477.

HOFFMAN, B.J. & MEZEY, E. (1989). Distribution of serotonin 5-HT$_{1C}$ receptor mRNA in adult rat brain. *FEBS Lett.*, **247**, 453–462.

HUMPHREY, P.P.A., HARTIG, P. & HOYER, D. (1993). A proposed new nomenclature for 5-HT receptors. *Trends Pharmacol. Sci.*, **14**, 233–236.

HUTSON, P.H., DONOHOE, T.P. & CURZON, G. (1988). Infusion of the 5-hydroxytryptamine agonists RU 24969 and TFMPP into the paraventricular nucleus of the hypothalamus causes hypophagia. *Psychopharmacology*, **95**, 550–552.

KALUS, O., KAHN, R.S., WETZLER, S., ASNIS, G.M. & VAN PRAAG, H.M. (1990). Hypersensitivity to m-chlorophenyl piperazine in a subject with subclinical panic attacks. *Biol. Psychiat.*, **28**, 1053–1057.

KALEN, P., ROSENGREN, E., LINDVALL, O. & BJORKLUND, A. (1989). Hippocampal noradrenaline and serotonin release over 24 hours as measured by the dialysis technique in freely moving rats: correlation to behavioural activity state, effect of handling and tail pinch. *Eur. J. Neurosci.*, **1**, 181–186.

KENNETT, G.A. (1992). 5-HT$_{1C}$ receptor antagonists have anxiolytic-like actions in the rat social interaction test. *Psychopharmacology*, **107**, 397–402.

KENNETT, G.A. (1993). 5-HT$_{1C}$ receptors and their therapeutic relevance. *Curr. Opin. Invest. Drugs*, **2**, 317–362.

KENNETT, G.A. & CURZON, G. (1988a). Evidence that mCPP may have behavioural effects mediated by 5-HT$_{1C}$ receptors. *Br. J. Pharmacol.*, **94**, 137–147.

KENNETT, G.A. & CURZON, G. (1988b). Evidence that hypophagia induced by mCPP and TFMPP requires 5-HT$_{1C}$ and 5-HT$_{1B}$ receptors; hypophagia induced by RU 24969 only requires 5-HT$_{1B}$ receptors. *Psychopharmacology*, **96**, 93–100.

KENNETT, G.A. & CURZON, G. (1991). Potencies of antagonists indicate that 5-HT$_{1C}$ receptors mediate 1-3(chlorophenyl) piperazine-induced hypophagia. *Br. J. Pharmacol.*, **103**, 2016–2020.

KENNETT, G.A., PITTAWAY, K. & BLACKBURN, T.P. (1993). Evidence that 5-HT$_{1C}$ receptor antagonists are anxiolytic in the Geller-Seifter model of anxiety. *Psychopharmacology* (in press).

KENNETT, G.A., WHITTON, P., SHAH, K. & CURZON, G. (1989). Anxiogenic-like effects of mCPP and TFMPP in animal models are opposed by 5-HT$_{1C}$ receptor antagonists. *Eur. J. Pharmacol.*, **164**, 445–454.

KHAN, M.C., BENNIE, E.H., STULEMEIJER, S.M. & RAVENS, M.A. (1983). Mianserin and doxepin in the treatment of outpatient depression with anxiety. *Br. J. Clin. Pharmacol.*, **15**, 213S–218S.

KURSAR, J.D., NELSON, D.L., WAINSCOTT, D.B., COHEN, M.L. & BAEZ, M. (1992). Molecular cloning, functional expression, and characterization of a novel serotonin receptor (5-hydroxytryptamine$_{2F}$) from rat stomach fundus. *Mol. Pharmacol.*, **42**, 547–557.

LORIC, S., LAUNAY, J.-M., COLAS, J.-F. & MAROTEAUX, L. (1992). New mouse 5-HT$_2$-like receptor: Expression in brain, heart and intestine. *F.E.B.S.*, **312**, 203–207.

MENGOD, G., NGUYEN, H., LE, H., WAEBER, C., LUBBERT, H. & PALACIOS, J.M. (1990). The distribution and cellular localization of the serotonin 1C receptor mRNA in the rodent brain examined by in situ hybridization histochemistry. Comparison with receptor binding distribution. *Neuroscience*, **35**, 577–591.

MOLINEAUX, S.M., JESSELL, T.M., AXEL, R. & JULIUS, D. (1989). 5-HT$_{1C}$ receptor is a prominent serotonin receptor subtype in the central nervous system. *Proc. Natl. Acad. Sci. U.S.A.*, **86**, 6793–6797.

MURPHY, J.E. (1978). Mianserin in the treatment of depressive illness and anxiety states in general practice. *Br. J. Clin. Pharmacol.*, **5**, 81S–85S.

PANGALILA-RATU LANGI, E.A. & JANSSEN, P.A.J. (1988). Ritanserin in the treatment of generalised anxiety disorders: a placebo-controlled trial. *Human Psychopharmacology*, **3**, 207–212.

PAZOS, A., HOYER, D. & PALACIOS, J.M. (1984). The binding of serotonergic ligands to the porcine choroid plexus: Characterization of a new type of serotonin recognition site. *Eur. J. Pharmacol.*, **106**, 539–546.

PAZOS, A. & PALACIOS, J.M. (1985). Quantitative autoradiographic mapping of serotonin receptors in the rat brain. I. Serotonin-1 receptors. *Brain Res.*, **346**, 205–230.

PAZOS, A., PROBST, A. & PALACIOS, J.M. (1987). Serotonin receptors in the human brain-III. Autoradiographic mapping of serotonin-1 receptors. *Neuroscience*, **21**, 97–122.

PETERS, J.A., KIRKNESS, E.F., CALLACHAN, H., LAMBERT, J.J. & TURNER, A.J. (1988). Modulation of the GABA$_A$ receptor by depressant barbiturates and pregnone steroids. *Br. J. Pharmacol.*, **94**, 1257–1269.

PIGOTT, T.A., ZOHAR, J., HILL, J.L., BERNSTEIN, S.E., GROVER, G.N., ZOHAR-KADOUCH, R.C. & MURPHY, D.L. (1991). Metergoline blocks the behavioural and neuroendocrine effects of oral mCPP in obsessive-compulsive disorder. *Biol. Psychiatry*, **29**, 418–426.

PRANZATELLI, M.R. (1990). Evidence for involvement of 5-HT_2 and 5-HT_{1C} receptors in the behavioural effects of the 5-HT agonist 1-(2,5-dimethoxy-4-iodophenyl aminopropane)-2 (DOI). *Neurosci. Letts*, **115**, 74–80.

PRITCHETT, D.B., BACH, A.W.J., WOZNY, M., TALEB, O., DAL TOSO, R., SHIH, J.C. & SEEBURG, P.H. (1988). Structure and functional expression of cloned rat serotonin 5-HT_2 receptor. *EMBO J.*, **7**, 4135–4140.

RUSSELL, G.F.M., NIAZ, U., WAKELING, A. & SLADE, P.D. (1978). Comparative double-blind trial of mianserin hydrochloride (Organon GB94) and diazepam in patients with depressive illness. *Br. J. Pharmacol.*, **5**, 57S–65S.

SANGER, G.J. & NELSON, D.R. (1989). Selective and functional 5-hydroxytryptamine$_3$ receptor antagonism by BRL 43694 (granistron). *Eur. J. Pharmacol.*, **159**, 113–124.

SALTZMAN, A.G., MORSE, B., WHITMAN, M.M., IVANSCHENKO, Y., JAYE, M. & FELDER, S. (1991). Cloning of the human serotonin 5-HT_2 and 5-HT_{1C} receptor subtypes. *Biochem. Biophys. Res. Commun.*, **181**, 1469–1478.

SEIBYL, J.P., KRYSTAL, J.H., PRICE, L.H., WOODS, S.W., HENNINGER, G.R. & CHARNEY, D.S. (1989). 5-HT function in the biochemical and behavioural responses to mCPP in healthy subjects and schizophrenics. *Am. Soc. Neurosci.*, 1236.

SHIMZU, N., TAKE, S., HORI, T. & OOMURA, Y. (1992). In vivo measurement of hypothalamic serotonin release by intracerebral microdialysis: Significant enhancement by immobilization stress in rats. *Brain Res. Bull.*, **28**, 727–734.

WHITTON, P. & CURZON, G. (1990). Anxiogenic-like effect of infusing 1-(3-chlorophenyl) piperazine (mCPP) into the hippocampus. *Psychopharmacology*, **100**, 138–140.

WOOD, M.D., GLEN, A., MURPHY, O., STEWART, B.R. & BLACKBURN, T.P. (1993). SB 200646A: a selective 5-HT_{2C} receptor antagonist. *Br. J. Pharmacol.* (in press).

WRIGHT, I.K., UPTON, N. & MARSDEN, C.A. (1992). Effect of established and putative anxiolytics on extracellular 5-HT and 5-HIAA in the ventral hippocampus of rats during behaviour on the elevated X-maze. *Psychopharmacology*, **109**, 338–346.

(Received October 4, 1993
Revised November 18, 1993
Accepted November 22, 1993)

Br. J. Pharmacol. (1994), **111**, 803–810

© Macmillan Press Ltd, 1994

Species-dependent functional properties of non-NMDA receptors expressed in *Xenopus laevis* oocytes injected with mammalian and avian brain mRNA

[1]Derek Bowie & Trevor G. Smart

Department of Pharmacology, The School of Pharmacy, University of London, 29–39 Brunswick Square, London WC1N 1AX

1 Species-dependent variation in the functional properties of non-NMDA receptors was investigated by intracellular recording in *Xenopus laevis* oocytes injected with rat, chick and calf brain mRNA.

2 In all mRNA-injected oocytes, kainic acid (KA), domoic acid (Dom) and 5-bromowillardiine (BrW) evoked large, maintained membrane currents, in contrast to the smaller, desensitizing responses elicited by α-amino-3-hydroxy-5-methyl-4-isoxazolepropionic acid (AMPA), quisqualic acid (QA) and L-glutamic acid (L-Glu). Dose-response curves for KA in oocytes injected with calf ($EC_{50} = 96.4 \pm 12.3$ μM; mean ± s.e.mean), chick (87.0 ± 8.9 μM) or rat (88.7 ± 4.3 μM) brain mRNA were similar.

3 Current-voltage ($I-V$) relationships determined with KA inwardly rectified in oocytes injected with calf or chick mRNA; whereas, outward rectification was observed in oocytes injected with rat brain mRNA.

4 In oocytes injected with rat brain mRNA, AMPA antagonized responses evoked by KA in a competitive manner. The absolute amplitudes of KA and AMPA responses in the same oocytes were significantly correlated, which is consistent with both agonists acting on the same receptor-ionophore complex.

5 In contrast, in oocytes injected with calf or chick brain mRNA, AMPA (QA and L-Glu) antagonized the response evoked by KA in a non-competitive manner. The response amplitudes of KA compared to AMPA, QA or L-Glu in the same oocytes were not correlated suggesting discrete receptor-ionophores.

6 This study favours the existence of distinct non-NMDA receptor subtypes that are equi-sensitive to KA. The expressed receptors from different species of mRNA may be distinguished by their voltage-sensitivities and the type of antagonism exerted by AMPA on KA-activated responses. Our observations may reflect further heterogeneity of non-NMDA receptors in the central nervous system of different vertebrate species.

Keywords: Kainate; intracellular recording; glutamate receptor heterogeneity; mRNA translation; *Xenopus laevis* oocyte

Introduction

In the central nervous system (CNS), heterogeneity amongst neurotransmitter receptor subtypes has been established as a general phenomenon from radioligand binding, electrophysiological and molecular cloning studies. For non-N-methyl-*D*-aspartate (non-NMDA) receptors, multiple cDNAs coding for distinct receptor subunits in the rat exist which display diverse functional properties (Gasic & Hollmann, 1992; Sommer & Seeburg, 1992; Barnes & Henley, 1992). In some cases, correlations between the functional properties of recombinant and native neuronal non-NMDA receptors are evident. For example, high (Robinson & Deadwyler, 1981; Ben-Ari & Gho, 1988) and low (Perouansky & Grantyn, 1989; Patneau & Mayer, 1990) binding affinities at neuronal non-NMDA receptors by kainate (KA) have also been noted on recombinant receptors (Wisden & Seeburg, 1993). In addition, KA-induced membrane currents in neurones can exhibit inward (Iino *et al.*, 1990; Gilbertson *et al.*, 1991) or outward (Mayer & Westbrook, 1984) rectification. Similar rectifying behaviour has been observed with recombinant non-NMDA receptors (Boulter *et al.*, 1990; Verdoorn *et al.*, 1991). In these studies, membrane currents induced on receptors comprising either GluR1 and/or GluR3 subunits, possessed inwardly rectifying properties. Co-expression of GluR1 or GluR3 with GluR2 formed heteromeric ion channels devoid of inward rectification.

Although most neuronal or cloning studies have been performed in the rat, it is assumed, by analogy, that a similar functional heterogeneity exists for non-NMDA receptors in other vertebrate species. In view of this, the present investigation was initiated to determine whether non-NMDA receptors from different vertebrate species possess similar functional properties to native receptors in the rat. For this, the *Xenopus laevis* oocyte was used to compare the functional properties of non-NMDA receptors expressed from calf and chick brain mRNA with those expressed from rat brain mRNA. Our results suggest that receptor heterogeneity can occur between different vertebrate species. Preliminary accounts of this work have been published previously in abstract form (Bowie & Smart, 1989; 1990; 1991b).

Methods

Extraction of messenger RNA

Messenger ribonucleic acid (mRNA) was extracted from 3-month old calf brain cortices, 1 day old chick whole brains and 3–6 week old rat whole brains (all devoid of the cerebellum) using a guanidinium thiocyanate/caesium chloride method (Chirgwin *et al.*, 1979). The poly (A)-mRNA was isolated by oligo-(dT)-cellulose chromatography, then resuspended in water at 1 mg ml^{-1} and stored at − 70°C.

Preparation of oocytes and microinjection with mRNA

Mature female *Xenopus laevis* toads were anaesthetized by immersion in a cold solution of 0.2% w/v ethyl-*m*-amino-

[1] Author for correspondence at present address: Laboratory of Cellular and Molecular Neurophysiology, N.I.C.H.D., Building 49, National Institutes of Health, Bethesda, Maryland 20892, U.S.A.

benzoate (tricaine) for 15–30 min. Part of an ovary containing up to 100–200 oocytes was excised and transferred directly into a modified Barth's solution (MBS) containing (mM): NaCl 110, KCl 1, $NaHCO_3$ 2.4, Tris/HCl 7.5, $Ca(NO_3)_2$ 0.33, $CaCl_2$ 0.41, $MgSO_4$ 0.82 streptomycin 10 mg ml^{-1}, pH 7.6. Healthy oocytes at stages V and VI were preferentially selected for injection. Each oocyte, with an intact follicular layer, was injected with approximately 50 nl of mRNA solution (1 mg ml^{-1}) into the equatorial region. Injected oocytes were transferred into fresh MBS and incubated at 17–18°C for 2–3 days to permit the translation of mRNA. The MBS was replaced on alternate days. Once the oocytes became responsive to the test agonists they were then stored at 10°C which prolonged their survival for up to 4–5 weeks. Under these conditions, the survival of injected and uninjected oocytes were almost the same. In the first 5 days *in vitro*, 83.1 ± 2.5% (1496 oocytes, 18 batches, 4 donors) of follicular oocytes survived after being injected with calf brain mRNA. In comparison, 80 ± 11% (640 oocytes, 8 batches, 3 donors) of uninjected oocytes survived over the same period. The survival of injected oocytes did not apparently vary throughout the year which was monitored consecutively over a 3 year period.

Electrophysiology

Electrophysiological recordings were performed in a Perspex recording chamber (adjustable volume: 0.15–1 ml) lined with Sylgard and superfused at 8–10 ml min^{-1} with an amphibian Ringer containing (mM): NaCl 110, KCl 2, HEPES 5, $CaCl_2$ 1.8, pH 7.4. Oocytes were impaled with two microelectrodes manufactured from thin-walled borosilicate glass and filled with 3 M KCl, providing resistances of 5–10 MΩ for the voltage-recording and 1–2 MΩ for the current-injecting microelectrodes. All electrophysiological experiments were performed using an Axoclamp 2A in two electrode voltage clamp recording mode. Only oocytes with a membrane input resistance (R_{IN}) and membrane potential (E_m) of 1–5 MΩ and −40 to −60 mV respectively were accepted for experimentation. Experiments were performed at room temperature and drugs were dissolved in Ringer and bath-applied.

Calculation of membrane conductance

The membrane potential was voltage-clamped at a holding potential (V_H) of −50 mV to −60 mV. The membrane conductance evoked by the agonist was determined by subtraction after applying voltage command steps in the presence and absence of the agonist. Membrane conductance data were used to construct dose-response curves which were fitted using a logistic equation (see Figure 1 legend) employing a Marquadt non-linear least squares routine.

Determination of agonist current-voltage relationships

Current-voltage ($I-V$) relationships were studied in voltage clamped oocytes by stepping the holding potential (V_H = −40 mV to −60 mV) with voltage command steps (20 mV increments, 1.5 s duration, applied every 20 s) in the presence and absence of agonist. Instantaneous currents were measured after the command step achieved a steady state (usually within 10 ms). The $I-Vs$ were only determined in the presence of agonist after the agonist-evoked membrane current attained a steady-state. The agonist $I-V$ was determined by subtracting the control $I-V$ from the $I-V$ determined in the presence of the agonist. To determine the voltage sensitivity of the agonist-induced conductances, the membrane chord conductances evoked by agonists at different membrane potentials were calculated using the equation,

$$\text{Chord } G = I/(E_m - V_{rev})$$

where chord G and I are the chord conductance and membrane current evoked by the agonist, E_m represents the membrane potential and V_{rev} the agonist reversal potential. The $I-V$ relationship evoked by KA in *Xenopus laevis* oocytes can be contaminated by a chloride conductance ($I_{Cl(Ca^{2+})}$) which is activated by calcium entering the cell through non-NMDA ion channels. We have previously shown in oocytes injected with calf and chick brain mRNA that activation of $I_{Cl(Ca^{2+})}$ influences the $I-V$ relationship to KA producing outward rectification at positive membrane potentials (Bowie & Smart, 1993a). Therefore, to ensure the agonist $I-Vs$ were not contaminated by $I_{Cl(Ca^{2+})}$, $I-Vs$ were also constructed in the presence of the chloride channel blocker, anthracene-9-carboxylic acid (1 mM A9C). In the present study, all the $I-Vs$ were unaffected by the inclusion of A9C suggesting that $I_{Cl(Ca^{2+})}$ did not contaminate $I-V$ plots determined for non-NMDA receptor agonists.

Drugs

(RS)-α-amino-3-hydroxy-5-methyl-4-isoxazolepropionic acid (AMPA), quisqualic acid (QA), (±)-willardiine and 5-bromowillardiine (BrW) were obtained from Tocris Neuramin. Kainic acid (KA) and L-glutamic acid (L-Glu) were obtained from Sigma and Professor E.A. Barnard kindly supplied domoic acid.

Results

Two types of response for non-NMDA receptor agonists

In oocytes injected with any of the different mRNA species, KA (80 μM; $n = 182$) produced a large, apparently non-desensitizing response which was associated with an increase in membrane conductance. In contrast, the responses evoked by AMPA (100 μM; $n = 40$) were much smaller and showed signs of desensitization (Figure 1a). To highlight these differences, the peak response of a variety of non-NMDA receptor agonists were compared in 50 oocytes injected with calf brain mRNA. Similar to 80 μM KA (51 ± 5 nA, $n = 27$), the responses evoked by 20 μM Dom (59 ± 7 nA, $n = 6$) and 20 μM BrW (56 ± 10 nA, $n = 7$) were large and non-desensitizing. However, membrane currents evoked by 6 μM QA (4 ± 0.7 nA, $n = 13$), 50 μM L-Glu (5.7 ± 0.9 nA, $n = 11$) and 100 μM AMPA (3.2 ± 0.6 nA, $n = 11$) were smaller and desensitizing. Similar observations were also made on oocytes injected with chick and rat brain mRNA.

Equilibrium dose-response curves to kainate

Equilibrium dose-response curves were constructed to KA to make a direct quantitative comparison between non-NMDA receptors expressed from different vertebrate species. The expressed non-NMDA receptors showed a similar degree of sensitivity to KA in oocytes injected with calf, chick or rat brain mRNA where the estimated EC_{50} values were 96.4 ± 12.3 μM ($n = 20$), 87.0 ± 8.9 μM ($n = 6$) and 88.7 ± 4.3 μM ($n = 5$) respectively (Figure 1b).

Current-voltage relationships to kainate

Two distinct types of current-voltage ($I-V$) relationship for KA were revealed in oocytes injected with different mRNA species. With calf or chick brain mRNA, the membrane current evoked by 80 μM KA exhibited pronounced inward rectification at positive membrane potentials. In contrast, the membrane current evoked by 80 μM KA in oocytes injected with rat brain mRNA showed only slight outward rectification (Figure 2a). The voltage sensitivity of the two types of KA response was further demonstrated by determining the chord conductance-voltage (G–V) relationships (Figure 2b). In oocytes injected with calf ($n = 4$) or chick ($n = 3$) brain mRNA, KA (80 μM) produced a bell-shaped chord $G-V$ plot which described a region of maximum membrane conduc-

tance between − 60 to − 100 mV membrane potential (Figure 2b). The minimum membrane conductance was approached at positive membrane potentials (i.e. > + 10 mV). In comparison, the membrane conductance produced by 80 μM KA ($n = 6$) in oocytes injected with rat brain mRNA increased at depolarised potentials greater than + 20 mV, but was relatively voltage-insensitive at membrane potentials more negative than − 20 mV (Figure 2b).

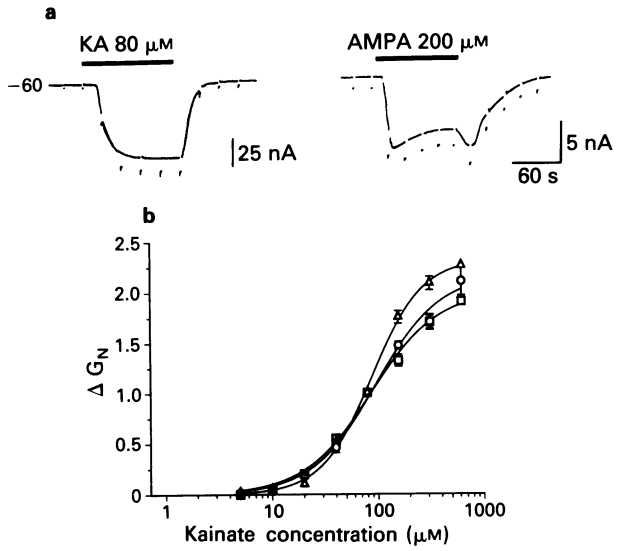


Figure 1 Membrane current profiles and concentration-response relationships for non-NMDA receptor agonists in mRNA-injected oocytes. (a) Typical membrane currents (holding potential, V_H − 60 mV) evoked by 80 μM kainic acid (KA) and 200 μM α-amino-3-hydroxy-5-methyl-4-isoxazole propionic acid (AMPA) in an oocyte injected with calf brain mRNA. Negative voltage command steps (− 5 to − 10 mV, 1.5 s duration, 0.05 Hz) were used to monitor the membrane conductance. Agonists were applied for the duration indicated by the solid line. (b) Equilibrium dose-response curves constructed for KA applied to oocytes injected with calf (○, $n = 20$), rat (△, $n = 5$) or chick (□, $n = 6$) brain mRNA. The membrane conductances induced by KA were normalized in each dose-response curve to the response evoked by 80 μM KA and expressed as the mean ± s.e.mean (ΔG_N). The curves were fitted by a logistic function of the form, $I/I_{max} = 1/\{1 + (EC_{50}/[A]^n)\}$, where I and I_{max} represent the agonist-induced current at a given concentration and the maximum current induced by a saturating concentration of agonist. EC_{50} defines the concentration of agonist ([A]) which induces 50% of the maximum response and n, is the Hill coefficient. The following estimates of EC_{50} s and n were obtained for KA; calf brain mRNA, $EC_{50} = 96.4 \pm 12.3$ μM, $n = 1.42 \pm 0.2$; chick brain mRNA, $EC_{50} = 87.0 \pm 8.9$ μM, $n = 1.36 \pm 0.1$; rat brain mRNA, $EC_{50} = 88.7 \pm 4.3$ μM, $n = 1.78 \pm 0.1$. To avoid receptor desensitization, dose-response curves were constructed by applying high and low agonist concentrations alternately and supramaximal concentrations of KA (> 640 μM) were avoided.

The voltage-dependency of the response evoked by a variety of non-NMDA receptor agonists and at different agonist concentrations were compared using a chord conductance ratio (G_R) (Table 1; cf. Bowie & Smart, 1991a). The non-NMDA receptor agonists, BrW and Dom, evoked responses which exhibited the same type of voltage-dependency to that observed with KA. For example, the G_R value for 80 μM KA ($G_R = 0.45 \pm 0.06$, $n = 7$) in oocytes injected with chick brain mRNA was similar to that determined for equi-effective concentrations of Dom (20 μM; 0.51 ± 0.05, $n = 4$) and BrW (20 μM; 0.47 ± 0.06, $n = 5$) (Table 1). Similar observations were made in oocytes injected with calf brain mRNA (Table 1). In addition, the degree of rectification observed in oocytes injected with calf or chick brain mRNA was dependent on the agonist concentration (Table 1). A comparison of the G_R values calculated for KA (20–160 μM) revealed that the ability of the KA-activated channel to pass outward current was further compromised at increasing agonist concentrations (Figure 2c; see also Table 1). An example of a series of $I-V$ plots in the same oocyte determined with different concentrations of KA is shown in Figure 2c. The rectification was not dependent on the absolute amplitude of the membrane current evoked by the agonists in each oocyte, since similar G_R values were observed at a given agonist concentration in oocytes exhibiting markedly different levels of receptor expression. In contrast to oocytes injected with calf or chick brain mRNA, the voltage-sensitivity of the response evoked by KA in oocytes injected with rat brain mRNA was apparently independent of agonist concentration (Table 1).

Interactions between kainate and other non-NMDA receptor agonists

The different $I-V$ relationships observed to KA may be a consequence of several distinct receptor-channel complexes activated only by KA. This possibility was examined by studying the interaction of KA with AMPA, QA and L-Glu on non-NMDA receptors expressed from the different species of mRNA. In all mRNA-injected oocytes ($n = 52$), near saturating concentrations of QA (6 μM), AMPA (100 μM) and L-Glu (50 μM) reduced the membrane current evoked by 80 μM KA. For example, AMPA (100 μM) reduced the response to 80 μM KA by 55 ± 5% ($n = 5$), 47 ± 4% ($n = 4$) and 54 ± 2% ($n = 10$) in oocytes injected with calf, chick and rat brain mRNA respectively. The antagonism of the KA-induced response by preincubation or co-application of QA, AMPA or L-Glu had a rapid onset and recovery. Furthermore, the antagonism did not show any use-dependency and was fully reversible. Responses to other agonists, such as BrW and Dom were similarly antagonized by QA. In oocytes injected with calf brain mRNA, the order of potency for inhibition of the KA-activated response, assessed from the IC_{50}s, was: QA ($IC_{50} = 5$ μM) >> L-Glu (30 μM) > AMPA (50 μM) ($n = 4$).

Table 1 Mean chord conductance rectification ratios (G_R) for non-NMDA receptor agonists calculated from individual $I-V$ relationships determined in calf, chick and rat brain mRNA-injected oocytes

Agonist	*Calf*	*Chick*	*Rat*
KA 20 μM	0.81 ± 0.16 (4)	0.78 ± 0.14 (3)	1.42 ± 0.19 (3)
KA 80 μM	0.44 ± 0.06 (9)	0.45 ± 0.06 (7)	1.49 ± 0.15 (6)
Dom 20 μM	0.55 ± 0.04 (5)	0.51 ± 0.05 (4)	ND
BrW 20 μM	0.52 ± 0.08 (3)	0.47 ± 0.06 (5)	ND

G_R was determined by calculating the chord conductances at + 30 mV and − 50 mV and using these values to define the ratio ($G_R = G(+30)/G(-50)$). All agonists tested had similar reversal potentials ($V_{rev} = -6 \pm 2$ mV, $n = 72$). G_R values less than one were associated with an $I-V$ relationship which displayed inward rectification, whereas values greater than one predicted outward rectification. The values in parentheses indicate the number of oocytes examined. All values are mean ± s.e.mean; ND: not determined. KA: kainic acid; Dom: domoic acid; BrW: 5-bromowillardiine.

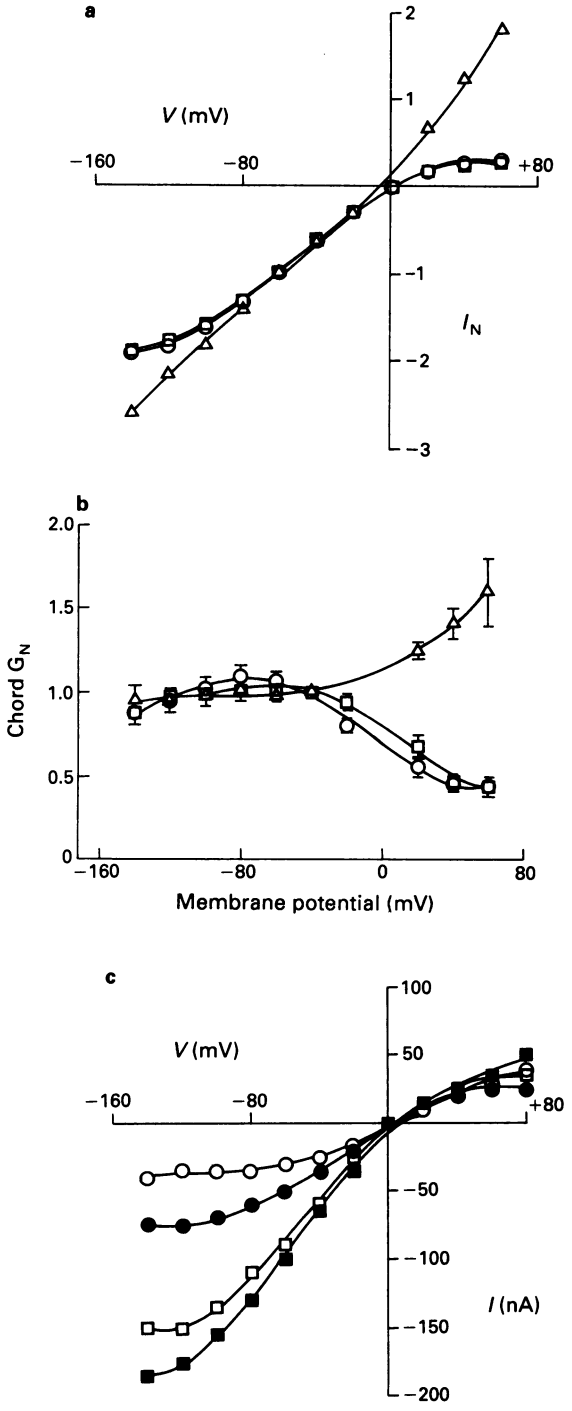


Figure 2 Current voltage ($I-V$) relationships for kainic acid (KA)-activated responses. (a) $I-V$s were determined in oocytes injected with either calf (○), chick (□) or rat brain (△) mRNA (V_H − 60 mV). For comparison, the agonist-evoked currents at different membrane potentials were normalized to the current induced by 80 μM KA in each oocyte at − 60 mV. KA characteristically produced inward rectification at membrane potentials near to 0 mV in oocytes injected with calf or chick brain mRNA. The membrane current evoked by KA in the oocyte injected with rat brain mRNA exhibited outward rectification. The curves fitted to data points in the $I-V$s were generated from third order polynomials. These equations were used to calculate the reversal potentials and chord conductances. (b) Chord conductance-membrane potential ($G-V$) relationships for kainate. $I-V$ relationships to 80 μM KA were used to generate the $G-V$ plots (see Methods). For comparison, the agonist-evoked chord conductances were normalized to the chord conductance obtained at − 40 mV membrane potential (G_N). Normalised $G-V$ relationships were obtained for KA using oocytes injected with rat (△, $n = 6$), calf (○, $n = 4$) or chick (□, $n = 3$) brain mRNA. (c) $I-V$ relationships at different concentrations of KA (20 μM − 160 μM) were determined in the same oocyte injected with calf brain mRNA (V_H − 50 mV). Increasing KA concentration apparently increased the rectification for 20 μM (○), 40 μM (●), 80 μM (□) and 160 μM (■) KA where the G_R values are 0.81 ± 0.10, 0.70 ± 0.08, 0.43 ± 0.11 and 0.35 ± 0.02 respectively ($n = 4$). Curve fits were generated from fourth order polynomials.

Competitive and non-competitive antagonism of kainate responses

In oocytes injected with rat brain mRNA, AMPA 100 μM produced an apparent parallel shift of the KA dose-response curve without any modification to the maximum KA-induced response (Figure 3a). The estimated EC_{50} values for KA in the absence and presence of AMPA were 97 μM and 327 μM respectively. These observations are consistent with competitive antagonism and indicated that both agonists are probably binding to the same receptor-ionophore complex.

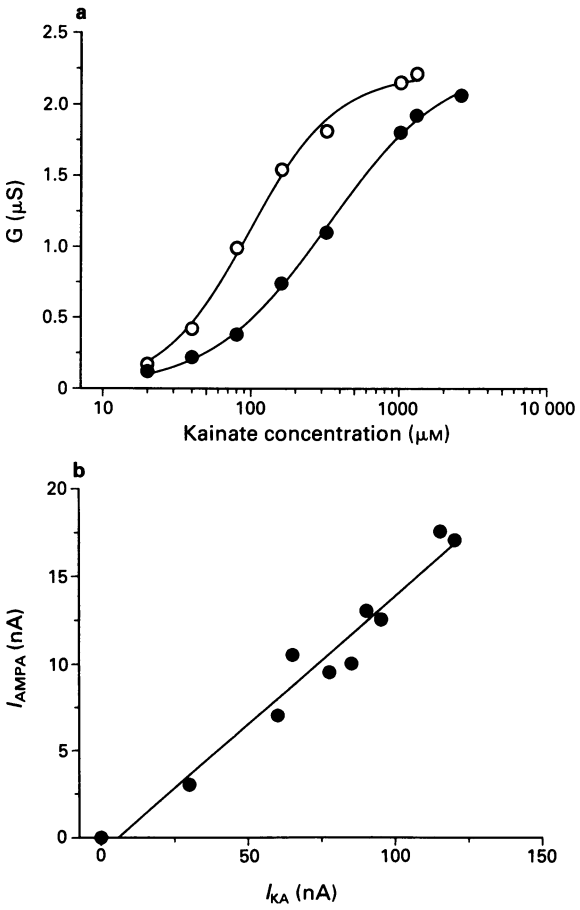


Figure 3 Competitive interaction of kainic acid (KA) and α-amino-3-hydroxy-5-methyl-4-isoxazole propionic acid (AMPA) on expressed non-NMDA receptors. (a) Equilibrium dose-response curves for KA-induced membrane conductance (G) in the absence (○) and presence (●) of 100 μM AMPA determined in an oocyte injected with rat brain mRNA at V_H − 60 mV. The curves were fitted to the data points using a logistic function providing the following estimates of the EC_{50} and n for the control curve, 97 ± 6 μM and 1.5 ± 0.1; and in the presence of AMPA, 327 ± 26 μM and 1.2 ± 0.1 respectively. (b) The amplitude of membrane currents (V_H − 60 mV) evoked by 80 μM KA (I_{KA}) were compared with currents induced by 100 μM AMPA (I_{AMPA}) in the same rat brain mRNA-injected oocytes. The correlation was assessed using unweighted linear regression with $r = 0.9785$, $t = 13.4$ and $P = 9.16E\text{-}7$.

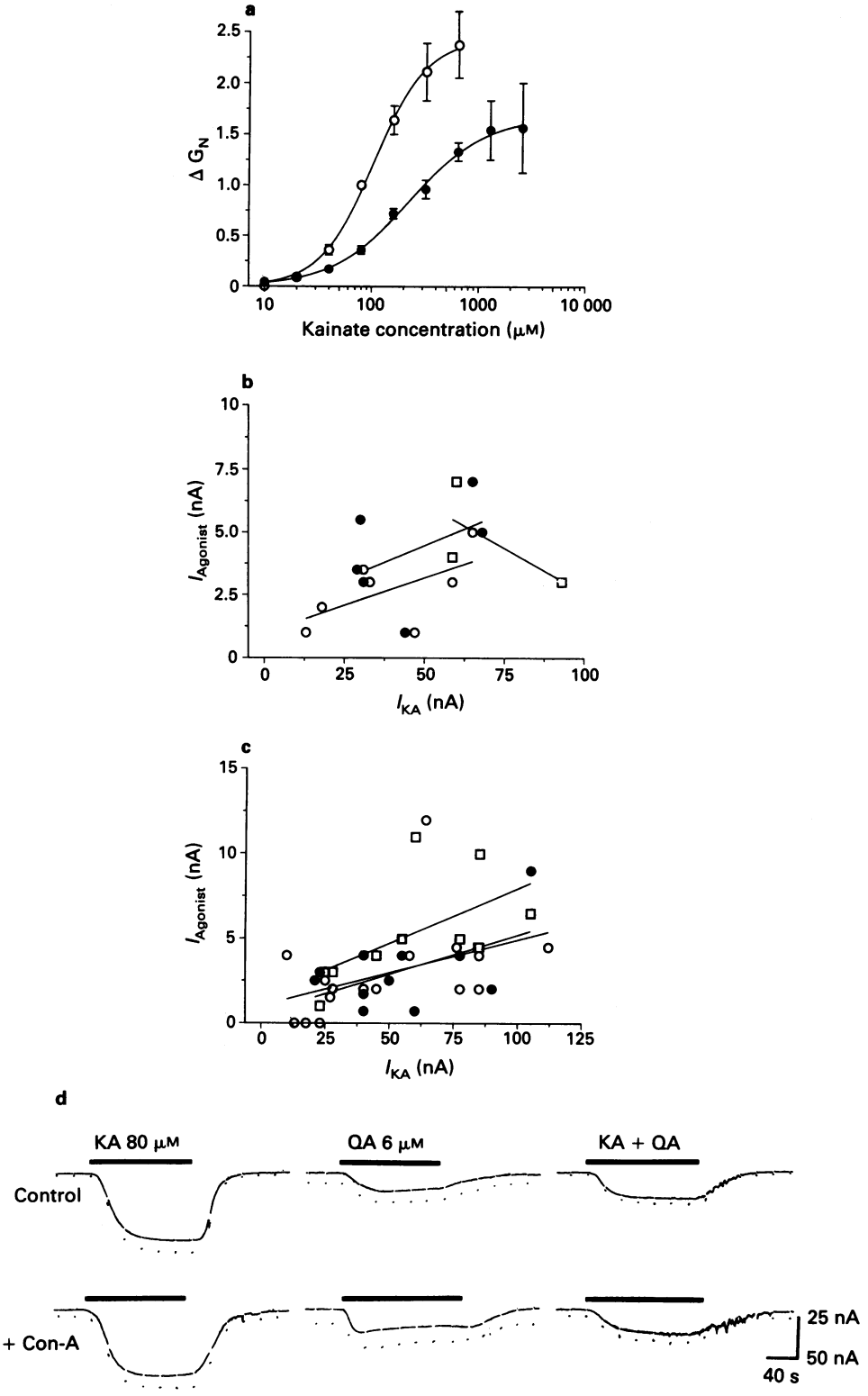


Figure 4 Apparent non-competitive interaction of kainic acid (KA) and quisqualic acid (QA) on expressed non-NMDA receptors. (a) Equilibrium dose-response curves for normalised conductances (ΔG_N) induced by KA in the absence (○) and presence (●) of 6 μM QA determined in oocytes injected with calf brain mRNA ($n = 6$; V_H − 60 mV). KA-activated responses were normalized to the control 80 μM KA response and expressed as the mean ± s.e.mean. The logistic function was used to fit curves to the data points providing the following estimates of EC_{50} and n; control, 103 ± 5 μM and 1.7 ± 0.1; and in the presence of QA 222 ± 19 μM, 1.2 ± 0.1. (b and c) The amplitudes of membrane currents evoked by 80 μM KA were compared at − 60 mV with those induced ($I_{Agonist}$) by 6 μM QA (○), 100 μM AMPA (●) and 50 μM L-glutamic acid (L-Glu, □) in the same oocytes injected with either chick (b; $n = 16$) or calf (c; $n = 36$) brain mRNA. Correlations were assessed between I_{KA} and $I_{Agonist}$ using unweighted linear least squares analyses providing the following values for chick brain mRNA: I_{QA}, $r = 0.6023$, $t = 1.6872$; I_{AMPA}, $r = 0.4541$, $t = 1.0196$; and I_{Glu}, $r = -0.6698$, $t = -0.9021$. For calf brain mRNA: I_{QA}, $r = 0.4280$, $t = 1.7719$; I_{AMPA}, $r = 0.5463$, $t = 1.9565$; and I_{Glu}, $r = 0.5953$, $t = 2.0955$. All correlations were insignificant at the 5% level. (d) In an oocyte injected with calf brain mRNA, responses were evoked to 80 μM KA, 6 μM QA and 80 μM KA + 6 μM QA in control Ringer and after incubation with 10 μM concanavalin A (Con-A) for 30 min. Con-A enhanced the response evoked by QA; however, the antagonism of the KA response by QA was unaffected (54% in control Ringer, 56% with Con-A). The 25 nA calibration applies to the traces for 6 μM QA.

This notion was supported by the significant correlation ($P<0.001$) between the membrane current amplitudes evoked by KA (80 μM) and AMPA (100 μM) in the same oocytes, reflecting the relative level of receptor expression (Figure 3b). All the oocytes injected with rat brain mRNA ($n=9$) consistently exhibited a sensitivity to both KA and AMPA.

In contrast, in oocytes injected with either calf or chick brain mRNA, QA or AMPA antagonized the KA dose-response curve in an apparently non-competitive manner. The equilibrium dose-response curve constructed for KA ($n=6$, calf mRNA) in the presence of QA (6 μM) was shifted slightly to the right with a clear reduction in the maximum response to KA (Figure 4a). The estimated EC_{50} values for KA in the absence and presence of QA were 103 μM and 222 μM respectively. At low concentrations of KA (<20 μM), the membrane current evoked by combinations of KA and QA was larger than that recorded to KA alone. In this case, the net response observed during co-application of these agonists was the summation of their individual responses.

Interestingly, unlike rat brain mRNA-injected oocytes, a comparison of the membrane current amplitudes evoked by 80 μM KA with currents evoked by QA (6 μM, $n=22$), AMPA (100 μM, $n=17$) or L-Glu (50 μM, $n=13$) in the same oocytes injected with chick ($n=16$; Figure 4b) or calf ($n=36$; Figure 4c) brain mRNA were not significantly correlated ($P>0.05$). This result is apparently inconsistent with the agonists sharing the same receptor but could be accounted for by assuming discrete receptor-ionophore complexes. Moreover, in some oocytes, a response to KA could be observed in the absence of any measurable QA response; even at concentrations of QA which would be regarded as saturating. In these QA-insensitive oocytes ($n=3$), the response to KA was still antagonized by QA.

To test the possibility that the absence of measurable QA-responses was due to a rapid and full receptor desensitization induced by QA, the plant lectin, concanavalin-A (Con-A), was used to reduce receptor desensitization (Mayer & Vyklicky, 1989). Figure 4d shows a typical example of the effect of Con-A (10 μM) on the antagonism of KA (80 μM) responses by 6 μM QA. In oocytes injected with calf ($n=4$) or chick ($n=3$) brain mRNA, Con-A increased the response to QA; however, the reduction of the KA-response by QA following Con-A treatment was similar to the inhibition in control Ringer. This suggested that the level of Con-A-sensitive receptor desensitization does not affect the degree of antagonism.

Discussion

Our primary objective in this study was to examine the possibility of species-dependent variation in the functional properties of non-NMDA receptors expressed from three vertebrate species. The *Xenopus laevis* oocyte was used since it was possible to study each expressed non-NMDA receptor in the same membrane environment. In this study, non-NMDA receptors expressed from rat brain mRNA were apparently activated by both KA and AMPA and possessed similar properties to previously described native neuronal and expressed recombinant glutamate receptors derived from the rat. In oocytes injected with calf and chick brain mRNA, our data were compatible with the existence of distinct non-NMDA receptors activated by KA and AMPA. As yet, non-NMDA receptors from calf and chick have not been cloned nor has there been any extensive electrophysiological studies of neurones derived from these species. Non-NMDA receptors expressed from calf and chick brain mRNA are typified by a novel non-competitive antagonism of KA responses by AMPA, QA or L-Glu. We propose that these observations may reflect further heterogeneity of non-NMDA receptor subtypes present in the CNS of a variety of vertebrates.

Expression of non-NMDA receptors equi-sensitive to kainate

The mRNAs in this study have been extracted from brain tissue which includes a variety of cell types of neuronal, glial, ependymal and vascular origin. Neurones are a favourable candidate for the source of mRNA since, in addition to their large number in the CNS, the receptors expressed in this study displayed similar properties to their neuronal counterparts. For example, expressed receptors from different species were equi-sensitive to KA with a similar potency to that determined in mammalian (Perouansky & Grantyn, 1989; Patneau & Mayer, 1990), avian (O'Brien & Fischbach, 1986; Zorumski & Yang, 1988) and fish (Ishida & Neyton, 1985) neurones. In addition, the different $I-V$ relationships determined for KA in this study have also been observed in neuronal studies (Ozawa *et al.*, 1991). However, non-NMDA receptors are not solely confined to neurones since glial cells, which may outnumber neurones by 10:1 (Kuffler *et al.*, 1984), also respond to excitatory amino acid receptor agonists (Usowicz *et al.*, 1989; Wyllie *et al.*, 1991; Muller *et al.*, 1992; Burnashev *et al.*, 1992). Although non-NMDA receptors expressed by glial cells have not yet been characterized as thoroughly as their neuronal counterparts, electrophysiological studies have revealed similar pharmacological and biophysical properties (Usowicz *et al.*, 1989; Wyllie *et al.*, 1991; Muller *et al.*, 1992; Burnashev *et al.*, 1992). In addition, it was also difficult to compare the receptor properties between species at the same developmental stage and thus eliminate the possibilty that our data may be explained by a differential age-dependent expression of glutamate receptor subunits.

Interaction of KA and AMPA with non-NMDA receptors

In neurones or mRNA-injected oocytes, the responses to KA can be antagonized by other non-NMDA agonists in either a competitive or non-competitive manner. Usually, the antagonism was competitive and could be relieved by increasing the concentration of KA (O'Brien & Fischbach, 1986; Perouansky & Grantyn, 1989; Patneau & Mayer, 1991; Thio *et al.*, 1991; Bowie & Smart, 1993b), as also observed for the AMPA inhibition of KA-induced responses in oocytes injected with rat brain mRNA. This is consistent with a common receptor-ionophore for KA and AMPA, supported by the correlation between the amplitudes of KA and AMPA-induced responses measured in the same oocytes. It is not known whether KA and AMPA bind to the same agonist recognition site on the receptor-ionophore complex or if discrete binding sites exist (cf. Patneau & Mayer, 1991). However, thiocyanate ions can pharmacologically distinguish between KA- and AMPA-evoked responses on the same receptor ionophore complex which would favour discrete agonist binding sites (Bowie & Smart, 1993b).

Rarely, the antagonism of KA responses by QA (AMPA or L-Glu) was non-competitive (Ishida & Neyton, 1985; Aizenman *et al.*, 1988; Bowie & Smart, 1990; 1991b). This antagonism could also occur in the absence of any response to QA, favouring distinct receptor-channel complexes for KA and QA (or AMPA) (Ishida & Neyton, 1985; Aizenman *et al.*, 1988; Bowie & Smart, 1990; 1991b). However, Thio *et al.* (1991) observed non-competitive antagonism of KA-induced responses by QA on rat hippocampal neurones and concluded that both non-NMDA receptor agonists activated a single receptor-channel complex. Non-competitive antagonism was only observed when QA was applied before KA. QA was assumed to desensitize some of the non-NMDA receptors, since wheat germ agglutinin abolished the antagonism. Although in our study, non-compeitive antagonism of KA responses was observed when QA was pre- or co-applied with KA, we cannot discount the possibility that in some oocytes, QA may induce a rapid and full desensitization of

non-NMDA receptors. This could have three consequences, firstly, QA-activated responses may no longer be resolved; secondly, QA could still compete for a common binding site with KA thereby acting as an antagonist; and thirdly, the desensitization may cause a reduction in the maximum response evoked by KA. Cross desensitization between QA or L-Glu and KA-activated responses has been proposed to account for agonist interactions on the same receptor-ionophore in hippocampal pyramidal neurones (Kiskin *et al.*, 1986; 1990; Thio *et al.*, 1991). However, in the present study, a reduction in the level of QA-induced desensitization by Con-A did not affect the antagonism of KA-induced responses (Figure 4d; cf. Mayer & Vyklicky, 1989). An alternative explanation is that QA desensitizes the receptor by additional Con-A insensitive mechanisms.

The failure to correlate KA- and QA- (AMPA or L-Glu) induced response amplitudes in the same oocytes injected with calf or chick brain mRNA is consistent with the activation of discrete receptor ionophores. However, if the degree of desensitization induced by QA varies between oocytes, this would account for the lack of any correlation in response amplitudes. A less likely hypothesis to explain our data would involve a direct occlusion of KA-activated ion channels by QA, AMPA or L-Glu. This has been discounted since the voltage-dependency expected for this type of antagonism was not observed (Bowie, 1991).

A more complex model compatible with our results, involves the allosteric modulation by QA (AMPA or L-Glu) of a receptor sensitive to KA, causing a conformational change in the receptor channel complex to a non-conducting state. In this model, QA binds to two sites; a receptor specific for this agonist and an allosteric site where QA acts only as an antagonist. The ability of QA to antagonize responses to KA in the absence of any measurable agonist response to QA and the lack of any correlation between the amplitudes of QA and KA responses are both consistent with QA acting at an allosteric site on a KA receptor. It is an interesting correlation that non-competitive antagonism was only observed on non-NMDA receptors which mediate voltage-sensitive KA-activated responses.

Heterogeneity amongst non-NMDA receptors activated by kainate

The functionally diverse properties of expressed non-NMDA receptors from different species, may be accounted for by assuming the existence of a number of distinct non-NMDA receptors, with equal sensitivity to KA. In the CNS of a variety of species, heterogeneous populations of non-NMDA receptors may exist which are selective for QA and AMPA (Aizenman *et al.*, 1989; Henley & Barnard, 1989b; Yoneda & Ogita, 1989), KA and AMPA (Honore & Drejer, 1988; Henley & Barnard, 1989a; Henley *et al.*, 1989) or KA alone (Agrawal & Evans, 1986). The physiological significance of non-NMDA receptor heterogeneity has not been fully resolved. Ozawa *et al.* (1991) have suggested that different types of KA-receptor may be associated with particular neurones since inward rectification was observed in smaller hippocampal neurones whereas outward rectification was found in larger cells that were probably young pyramidal neurones; although, inward rectifying excitatory synaptic currents in hippocampal interneurones are not associated with any particular cellular morphology (McBain & Dingledine, 1993). More recent studies have suggested a further complexity since more than one type of non-NMDA receptor may be expressed by a single neurone (Wyllie *et al.*, 1993) and that each receptor may have selective subcellular localization (Craig *et al.*, 1993). In view of this, one possible role for receptor heterogeneity (e.g. at central synapses) may be to provide a subtle modification of the neurotransmitter response through the expression of a mosaic of several non-NMDA receptor subtypes.

This work was supported by the SERC, MRC and Wellcome Trust. We wish to thank Professor Eric A. Barnard and Drs Mark Darlison, Margaret Sutherland and Mike Webb for the provision of mRNA. We are grateful to Fernanda Alves for secretarial assistance.

References

AGRAWAL, S.G. & EVANS, R.H. (1986). The primary afferent depolarising action of kainate in the rat. *Br. J. Pharmacol,*. **87,** 345–355.

AIZENMAN, E., FROSCH, M.P. & LIPTON, S.A. (1988). Responses mediated by excitatory amino acid receptors in retinal ganglion cells from the rat. *J. Physiol.*, **396,** 75–91.

AIZENMAN, E., KARSCHIN, A. & LIPTON, S.A. (1989). Two pharmacological classes of quisqualate-induced electrical responses in rat retinal ganglion cells in vitro. *Eur. J. Pharmacol.*, **174,** 9–22.

BARNES, J.M. & HENLEY, J.M. (1992). Molecular characteristics of excitatory amino acid receptors. *Prog. Neurobiol.*, **39,** 113–133.

BEN-ARI, Y. & GHO, M. (1988). Long-lasting modification of the synaptic properties of rat CA3 hippocampal neurones induced by kainic acid. *J. Physiol.*, **404,** 365–384.

BOULTER, J., HOLLMANN, M., O'SHEA-GREENFIELD, A., HARTLEY, M., DENERIS, E., MARON, C. & HEINEMANN, S. (1990). Molecular cloning and functional expression of glutamate receptor subunit genes. *Science*, **249,** 1033–1037.

BOWIE, D. (1991). Functional properties of vertebrate non-NMDA excitatory amino acid receptors expressed in *Xenopus laevis* oocytes. *University of London, PhD thesis.*

BOWIE, D. & SMART, T.G. (1989). Properties of a kainate receptor expressed in *Xenopus laevis* oocytes after injection with bovine brain mRNA. *J. Physiol.*, **418,** 196P.

BOWIE, D. & SMART, T.G. (1990). Antagonism of kainate responses by excitatory amino acid antagonists and agonists in *Xenopus* oocytes injected with bovine brain mRNA. *Neurochem. Int.*, **16** suppl. 1.

BOWIE, D. & SMART, T.G. (1991a). Interaction of 5-bromowillardiine with non-NMDA receptors expressed in *Xenopus laevis* oocytes injected with chick brain mRNA. *Neurosci. Lett.*, **121,** 68–72.

BOWIE, D. & SMART, T.G. (1991b). Functional diversity of non-NMDA receptors expressed from avian and mammalian brain mRNA-injected *Xenopus laevis* oocytes. *Br. J. Pharmacol.*, **104,** 340P.

BOWIE, D. & SMART, T.G. (1993a). Interplay between expressed non-NMDA receptors and endogenous calcium-activated chloride currents in *Xenopus laevis* oocytes. *Neurosci. Lett.*, **151,** 4–8.

BOWIE, D. & SMART, T.G. (1993b). Thiocyanate ions selectively antagonize AMPA-evoked responses in *Xenopus laevis* oocytes microinjected with rat brain mRNA. *Br. J. Pharmacol.*, **109,** 779–787.

BURNASHEV, N., KHODOROVA, A., JONAS, P., HELM, P.J., WISDEN, W., MONYER, H., SEEBURG, P.H. & SAKMANN, B. (1992). Calcium-permeable AMPA-kainate receptors in fusiform cerebellar glial cells. *Science*, **256,** 1566–1570.

CHIRGWIN, J.M., PRZYBYLA, A.E., MCDONALD, R.J. & RUTTER, W.J. (1979). Isolation of biologically active ribonucleic acid from sources enriched in ribonuclease. *Biochemistry*, **18,** 5294–5299.

CRAIG, A.M., BLACKSTONE, C.D., HUGANIR, R.L. & BANKER, G. (1993). The distribution of glutamate receptors in cultured rat hippocampal neurons: Postsynaptic clustering of AMPA-selective subunits. *Neuron*, **10,** 1055–1068.

GASIC, G.P. & HOLLMANN, M. (1992). Molecular neurobiology of glutamate receptors. *Annu. Rev. Physiol.*, **54,** 507–536.

GILBERTSON, T.A., SCOBEY, R. & WILSON, M. (1991). Permeation of calcium ions through non-NMDA glutamate channels in retinal bipolar cells. *Science*, **251,** 1613–1615.

HENLEY, J.M. & BARNARD, E.A. (1989a). Kainate receptors in Xenopus central nervous system: solubilisation with n-octyl-β-D-glucopyranoside. *J. Neurochem.*, **52,** 31–37.

HENLEY, J.M. & BARNARD, E.A. (1989b). Solubilisation and characterisation of a putatuve quisqualate-type glutamate receptor from chick brain. *J. Neurochem.*, **53**, 140–148.

HENLEY, J.M., AMBROSINI, A., KROGSGAARD-LARSEN, P. & BARNARD, E.A. (1989). Evidence for a single glutamate receptor of the ionotropic kainate/quisqualate type. *The New Biologist*, **1**, 153–158.

HONORE, T. & DREJER, J. (1988). Chaotropic ions affect the conformation of quisqualate receptors in rat cortical membranes. *J. Neurochem.*, **51**, 457–461.

IINO, M., OZAWA, S. & TSUZUKI, K. (1990). Permeation of calcium through excitatory amino acid receptor channels in cultured rat hippocampal neurones. *J. Physiol.*, **424**, 151–165.

ISHIDA, A.T. & NEYTON, J. (1985). Quisqualate and L-glutamate inhibit retinal horizontal cell responses to kainate. *Proc. Natl. Acad. Sci. U.S.A.*, **82**, 1837–1841.

KISKIN, N.I., KRISHTAL, O.A. & TSYNDRENKO, A.YA. (1986). Excitatory amino acid receptors in hippocampal neurons: kainate fails to desensitize them. *Neurosci. Lett.*, **63**, 225–230.

KISKIN, N.I., KRISHTAL, O.A. & TSYNDRENKO, A.Y. (1990). Cross-desensitization reveals pharmacological specificity of excitatory amino acid receptors in isolated hippocampal neurons. *Eur. J. Neurosci.*, **2**, 461–470.

KUFFLER, S.W., NICHOLLS, J.G. & MARTIN, A.R. (1984). Physiology of neuroglial cells: In *From Neuron to Brain*, pp. 323–360. Sutherland, M.A.: Sinauer.

MCBAIN, C.J. & DINGLEDINE, R. (1993). Heterogeneity of synaptic glutamate receptors on CA3 stratum radiatum interneurones of rat hippocampus. *J. Physiol.*, **462**, 373–392.

MAYER, M.L. & WESTBROOK, G.L. (1984). Mixed-agonist action of excitatory amino acids on mouse spinal cord neurons under voltage clamp. *J. Physiol.*, **354**, 29–53.

MAYER, M.L. & VYKLICKY, L. (1989). Concanavalin-A selectively reduces desensitization of mammalian neuronal quisqualate receptors. *Proc. Natl. Acad. Sci.*, **86**, 1411–1415.

MULLER, T., MOLLER, T., BERGER, T,. SCHNITZER, J. & KETTENMANN, H. (1992). Calcium entry through kainate receptors and resulting potassium-channel blockade in Bergmann glial cells. *Science*, **256**, 1563–1566.

O'BRIEN, R.J. & FISCHBACH, G.D. (1986). Characterization of excitatory amino acid receptors expressed by embryonic chick motoneurons in vitro. *J. Neurosci.*, **6**, 3275–3283.

OZAWA, S., IINO, M. & TSUZUKI, K. (1991). Two types of kainate response in cultured rat hippocampal neurones. *J. Neurophysiol.*, **66**, 2–11.

PATNEAU, D.K. & MAYER, M.L. (1990). Structure-activity relationships for amino acid transmitter candidates acting at N-methyl-D-aspartate and quisqualate receptors. *J. Neurosci.*, **10**, 2385–2399.

PATNEAU, D.K. & MAYER, M.L. (1991). Kinetic analysis of interactions between kainate and AMPA. Evidence for activation of a single receptor in mouse hippocampal neurons. *Neuron*, **6**, 785–798.

PEROUANSKY, M. & GRANTYN, R. (1989). Separation of quisqualate- and kainate-selective glutamate receptors in cultured neurons from the rat superior colliculus. *J. Neurosci.*, **9**, 70–80.

ROBINSON, J.H. & DEADWYLER, S.A. (1981). Kainic acid produces depolarization of CA3 pyramidal cells in the *in vitro* hippocampal slice. *Brain Res.*, **221**, 117–127.

SOMMER, B. & SEEBURG, P.H. (1992). Glutamate receptor channels: novel properties and new clones. *Trends Pharmacol. Sci.*, **13**, 291–296.

THIO, L.L., CLIFFORD, D.B. & ZORUMSKI, C.F. (1991). Characterization of quisqualate receptor desensitization in cultured postnatal rat hippocampal neurons. *J. Neurosci.*, **11**, 3430–3441.

VERDOORN, T.A., BURNASHEV, N., MONYER, H., SEEBURG, P.H. & SAKMANN, B. (1991). Structural determinants of ion-flow through recombinant glutamate receptor channels. *Science*, **252**, 1715–1718.

USOWICZ, M., GALLO, V. & CULL-CANDY, S.G. (1989). Multiple conductance channels in type-2 cerebellar astrocytes activated by excitatory amino acids. *Nature*, **339**, 380–383.

WISDEN, W. & SEEBURG, P.H. (1993). Mammalian inotropic glutamate receptors. *Curr. Opin. Neurobiol.*, **3**, 291–298.

WYLLIE, D.J.A., MATHIE, A., SYMONDS, C.J. & CULL-CANDY, S.G. (1991). Activation of glutamate receptors and glutamate uptake in identified macroglial cells in rat cerebellar cultures. *J. Physiol.*, **432**, 235–258.

WYLLIE, D.J.A, TRAYNELIS, S.F. & CULL-CANDY, S.G. (1993). Evidence for more than one type of non-NMDA receptor in outside-out patches from cerebellar granule cells of the rat. *J. Physiol.*, **463**, 193–226.

YONEDA, Y. & OGITA, K. (1989). Solubilization of quisqualate-sensitive [3H] glutamate binding activity from rat retina. *J. Neurochem.*, **52**, 1501–1507.

ZORUMSKI, C.F. & YANG, J. (1988). AMPA, kainate and quisqualate activate a common receptor-channel complex on embryonic chick motoneurons. *J. Neurosci.*, **8**, 4277–4286.

(Received July 14, 1993
Revised November 8, 1993
Accepted November 22, 1993)

Br. J. Pharmacol. (1994), **111**, 811–818 © Macmillan Press Ltd, 1994

Role of CD18 in the accumulation of eosinophils and neutrophils and local oedema formation in inflammatory reactions in guinea-pig skin

M.M. Teixeira, S. Reynia, *M. Robinson, *A. Shock, T.J. Williams, F.M. Williams, A.G. Rossi & [1]P.G. Hellewell

Department of Applied Pharmacology, National Heart and Lung Institute, Dovehouse Street, London SW3 6LY and *Celltech Limited, 216 Bath Road, Slough SL1 4EN

1 Intradermal injection of the complement fragment C5a des Arg induces local oedema formation that, in rabbits and man, is dependent on circulating neutrophils. Monoclonal antibodies to the leukocyte adhesion molecule CD11/CD18 block neutrophil accumulation and prevent neutrophil-dependent oedema formation. The role of CD11/CD18 in mediating eosinophil accumulation *in vivo* is less established. In this study we have used an anti-human CD18 monoclonal antibody, 6.5E, to investigate the neutrophil-dependency of oedema formation induced by C5a des Arg in guinea-pig skin. We also studied the role of CD18 in mediating eosinophil accumulation in the same model.

2 Stimulated adhesion of ^{111}In-labelled guinea-pig neutrophils and eosinophils to serum-coated plastic was inhibited in a dose-dependent manner by 6.5E suggesting that the monoclonal antibody recognizes and blocks the guinea-pig CD18 adhesion molecule.

3 The accumulation of ^{111}In-labelled neutrophils induced by zymosan-activated plasma (ZAP, as a source of C5a des Arg) in skin sites was reduced by up to 89% in animals treated intravenously with F(ab')$_2$ fragments of 6.5E. ZAP-induced accumulation of ^{111}In-labelled eosinophils was also greatly reduced (by up to 78%) by treatment with 6.5E.

4 Despite the inhibition of ZAP-induced neutrophil accumulation by 6.5E, local oedema formation in the same skin sites was unaffected, except at the top dose of ZAP, by treatment with the anti-CD18 monoclonal antibody, suggesting that the oedema response was largely neutrophil-independent. Indeed, ZAP-induced oedema formation was reduced by up to 81% by the H_1 receptor antagonist, mepyramine.

5 Accumulation of ^{111}In-labelled eosinophils in a passive cutaneous anaphylactic (PCA) reaction was also blocked by treatment with 6.5E, while oedema formation in the same skin sites was unaffected. Intradermal injection of cationic protein-containing extracts of *Schistosoma mansoni* larvae also induced the accumulation of ^{111}In-labelled neutrophils and eosinophils which was abrogated by intravenous 6.5E. In contrast, extract-induced local oedema formation was similar in control and 6.5E-treated guinea-pigs.

6 In summary, the local accumulation of radiolabelled neutrophils at sites of inflammation in guinea-pig skin was dependent on the adhesion molecule CD18 while, in contrast, there was no evidence for neutrophil-dependent oedema formation in this species. Accumulation of radiolabelled eosinophils was also dependent on CD18.

Keywords: Eosinophils; neutrophils; inflammation; oedema; CD18; adhesion molecules; guinea-pig skin

Introduction

Intradermal injection of the complement fragment, C5a and its metabolite, C5a des Arg, induces an increase in microvascular permeability leading to local oedema formation. In rabbit skin, C5a-induced oedema formation is delayed compared with 'direct-acting' mediators such as histamine and bradykinin and is dependent on circulating neutrophils (Issekutz, 1981; Jose *et al.*, 1981; Wedmore & Williams, 1981; Williams & Jose, 1981). Moreover, there is little evidence in the rabbit for the involvement of mast cell products such as histamine (Jose *et al.*, 1981; Williams & Jose, 1981). Studies in man have shown that the wheal response to i.d. injection of zymosan-activated autologous serum (ZAS), as a source of C5a des Arg, was attenuated in neutropaenic subjects but only marginally reduced by an anti-histamine (Williamson *et al.*, 1986). In contrast, i.d. injection of C5a or C5a des Arg from a number of species into guinea-pig skin induces an immediate increase in vascular permeability that is reduced by anti-histamines (Davies & Lowe, 1960; 1962; Dias da Silva & Lepow, 1967; Cochrane & Muller-Eberhard, 1968). The exception is human C5a des Arg which has little permeability-increasing activity in guinea-pig skin although intact C5a is very potent (Fernandez *et al.*, 1978; Webster *et al.*, 1980). However, the neutrophil-dependency of the permeability response in guinea-pig skin remains to be established.

Neutrophil accumulation at sites of cutaneous inflammation is dependent on several adhesion pathways including the leukocyte β_2 integrin CD11/CD18. For example, monoclonal antibodies (mAbs) directed against CD18 are very effective inhibitors of neutrophil accumulation in the skin of rats and rabbits (Arfors *et al.*, 1987; Nourshargh *et al.*, 1989; Doerschuk *et al.*, 1990; Mulligan *et al.*, 1992). These observations are consistent with the inability of neutrophils to migrate to sites of local cutaneous inflammation in patients suffering from leukocyte adhesion deficiency (LAD), whose neutrophils lack the CD18 molecule (Bowen *et al.*, 1982; Hawkins *et al.*, 1992). In contrast to the well-established role of CD18 in mediating neutrophil accumulation *in vivo*, the involvement of this molecule in eosinophil accumulation *in vivo* has been less studied. Indeed, evidence suggests that the β_1 integrin VLA-4, present on eosinophils but not neutrophils, plays an important role in eosinophil accumulation (Weg *et al.*, 1993).

[1] Author for correspondence.

In the present study, we used an anti-human CD18 mAb 6.5E, that recognizes the guinea-pig homologue, to determine the role of neutrophils in mediating local oedema formation in guinea-pig skin. We also examined the effect of the mAb on the accumulation of radiolabelled neutrophils and eosinophils in response to a number of inflammatory mediators, in a passive cutaneous anaphylactic (PCA) reaction and in response to cationic protein-containing extracts of *Schistosoma mansoni* larvae.

Methods

Preparation of zymosan-activated plasma

Zymosan-activated plasma (ZAP) was used as a source of guinea-pig C5a des Arg. Guinea-pig heparinized (10 iu ml^{-1}) plasma was incubated with zymosan (5 mg ml^{-1}) at 37°C. After 30 min, zymosan was removed by centrifugation (2 × 10 min at 3,000 *g*). The ZAP was then desalted on a PD-10 Sephadex G-25M column (Pharmacia) and stored in aliquots at − 20°C.

Anti-CD18 monoclonal antibody

The anti-CD18 mAb 6.5E was generated from a mouse immunized with the human B lymphoblastoid cell line JY. 6.5E is a murine IgG_1 monoclonal antibody and blocks CD18 function on both human (Andrew *et al.*, 1993) and rabbit cells (Galea-Lauri *et al.*, 1993). The antibody was purified from hybridoma supernatant by Protein-A affinity chromatography and $F(ab')_2$ fragments generated as described in Hudson & Hay (1989). Endotoxin was assayed by the Coatest LAL assay (Kabi Pharmacia Diagnostics, Milton Keynes); the stock $F(ab')_2$ preparation (4.8 mg ml^{-1}) used in these experiments contained less than 1 Eu mg^{-1}. In some experiments the mouse myeloma protein MOPC21 (IgG_1, Celltech) was used as a control antibody.

Preparation of passive cutaneous anaphylaxis sera and reactions

Details of the preparation of sera and doses of antigen are described elsewhere (Weg *et al.*, 1991). Briefly, male guinea-pigs (Harlan Porcellus, Oxon; 350–400 g) were immunized with BGG in Freund's complete adjuvant followed by a boost on day 21 and serum collected on day 30. Recipient animals received an i.d. injection of 50 µl of a 1/50 dilution of the anti-serum followed, 16–20 h later, by the injection of antigen (BGG, 0.01–1 µg per site). Most of the tissue-fixing antibody was of the IgG_1 isotype (Weg *et al.*,1991).

Induction, purification and radiolabelling of guinea-pig eosinophils

The method is described in detail elsewhere (Faccioli *et al.*, 1991; Teixeira *et al.*, 1993b). Briefly, ex-breeder female guinea-pigs (Harlan Porcellus; 700–800 g) were treated with neat horse serum (1 ml i.p.) every other day for 2 weeks and the cells collected by peritoneal lavage with heparinized saline (10 iu ml^{-1}) 2 days after the last injection. The cells obtained were layered onto a discontinuous Percoll-HBSS (calcium and magnesium-free) gradient followed by centrifugation (1,500 *g*, 25 min at 20°C). Eosinophils (>95% pure, >98% viable) were collected from the 1.085/1.090 and 1.090/1.095 g ml^{-1} density interfaces. The purified eosinophils were radiolabelled by incubation with $^{111}InCl_3$ (100 µCi in 10 µl) chelated to 2-mercaptopyridine-*N*-oxide (merc; 40 µg in 0.1 ml of 50 mM PBS, pH 7.4) for 15 min at 20°C. The cells were then washed twice in HBSS (calcium- and magnesium-free) containing 10% guinea-pig platelet-poor plasma and resuspended at a final concentration of 10^7 cells ml^{-1} prior to injection. The labelling efficiency for eosinophils was 78–90%.

Induction, purification and radiolabelling of guinea-pig neutrophils

Neutrophils were elicited in the peritoneal cavity of naive ex-breeder guinea-pigs by the i.p. injection of 15 ml of a 5% (w/v) solution of casein as previously described (Teixeira *et al.*, 1993b). After 8–12 h, the animals were killed and the peritoneal cavity washed with heparinized saline (10 iu ml^{-1}). The rest of the procedure was followed as described for the eosinophils. The cells were also collected from the 1.085/1.090 and 1.090/1.095 g ml^{-1} interfaces. The purity of the preparation was always greater than 99% and the rare contaminants were eosinophils and occasional mononuclear cells. Viability, tested by trypan blue exclusion, was greater than 98%. Neutrophils were also radiolabelled with ^{111}In-merc and resuspended at a concentration of 10^7 cells ml^{-1}. The labelling efficiency for neutrophils was 80–83%.

Measurement of local oedema formation and leukocyte accumulation in guinea-pig skin

Radiolabelled leukocyte infiltration and oedema formation were measured simultaneously in the skin. ^{125}I-human serum albumin (5 µCi) was added to the ^{111}In-labelled eosinophils or neutrophils prior to i.v. injection (2.5 × 10^6 cells per animal) into recipient guinea-pigs (Harlan Porcellus; 350–400 g) anesthetized with Hypnorm (0.2 ml i.m.). Experiments were conducted in pairs, one guinea-pig receiving the vehicle (pyrogen-free saline, 1 ml kg^{-1}) and the other receiving 6.5E (0.24–2.4 mg kg^{-1}). The antibody or saline were injected i.v. 5 min before infusion of radiolabelled leukocytes. Preliminary studies established that ZAP-induced inflammatory responses were no different in animals that received saline or a control antibody (MOPC21, 2.4 mg kg^{-1}, i.v.); thus, saline was considered to be a suitable control. Five min after injection of cells, inflammatory mediators, schistosomal extracts (CH or cCTF) or antigen were injected i.d. in 0.1 ml volumes into the dorsal skin of the shaved animals. Each animal received a duplicate of each treatment following a randomized injection plan and the inflammatory response (^{111}In-labelled cell accumulation and oedema formation) was assessed after 2 h. Experiments were carried out over 2 h since previous time course studies indicated that the majority of plasma leakage or leukocyte accumulation was complete at this time (Faccioli *et al.*, 1991; Weg *et al.*, 1992; Collins *et al.*, 1993). At this time, blood was obtained by cardiac puncture and the animals were sacrificed by an overdose of sodium pentobarbitone. The dorsal skin was removed, cleaned free of excess of blood and the skin sites punched out with a 17 mm punch. The samples were counted in an automatic 5-head gamma-counter (Canberra Packard Ltd, Pangbourne, Berks) and the counts were cross-channel corrected for the two isotopes, Two h after infusion of ^{111}In-labelled eosinophils or neutrophils, greater than 95% of total plasma ^{111}In remained associated with either cell type.

The number of leukocytes accumulating in each site is expressed as ^{111}In-labelled cells per skin site and oedema formation as the ratio of ^{125}I counts of the skin sample divided by the ^{125}I counts in 1 µl of plasma.

Adhesion of leukocytes to serum-coated plastic

The wells of microtitre tissue culture plates (Nunc, Life Technologies Ltd.) were coated with serum by incubation for at least 2 h at 37°C with RPMI containing 10% FCS. Plates were washed twice before the addition of 100 µl of ^{111}In-labelled guinea-pig eosinophils or neutrophils (2 × 10^6 ml^{-1}) in HBSS containing 0.25% BSA (w/v). This was followed by whole 6.5E (final concentration 0.1–30 µg ml^{-1}) or MOPC21 (30 µg ml^{-1}) and 15 min later the cells were stimulated with

PMA since this is known to be a potent and effective activator of leukocyte β_2 integrins (Figdor & Kooyk, 1992). Based on dose-response studies, PMA was used at a final concentration of 10^{-8} M. After incubation for 30 min at 37°C, the medium was removed and the plate washed three times with PBS containing 2.5% heat-inactivated newborn calf serum. Adherent leukocytes were solubilized with neat formic acid and an aliquot counted for radioactivity. Results are expressed as number of adherent eosinophils or neutrophils per mm^2. Experiments were carried out with six replicates on cells from each animal.

Reagents

The following compounds were purchased from Sigma Chemical Company (Poole, Dorset): bradykinin, histamine, substance P, mepyramine maleate, casein, phorbol myristate acetate (PMA), bovine gamma globulin (BGG) and zymosan. Hanks solutions, HEPES, foetal calf serum (FCS), newborn calf serum, RPMI 1640 medium and horse serum were purchased from Life Technologies Limited (Paisley, Scotland). Percoll was from Pharmacia (Milton Keynes) and C16 PAF from Bachem (Saffron Walden, Essex). ^{125}I-labelled human serum albumin (^{125}I-HSA) and $^{111}InCl_3$ were purchased from Amersham International plc (Amersham).

Cercarial homogenates and cercarial transformation fluid supernatants were prepared as previously described (Teixeira *et al.*, 1993a). Briefly, snails with patent *Schistosoma mansoni* infections were induced to shed cercariae, excess water was removed by filtration and the residual larvae sedimented. Cercarial homogenate (CH) was prepared by homogenizing approximately 3×10^6 cercariae in 2 ml isotonic saline followed by centrifugation. CH was adjusted to 150 μg protein ml^{-1} and stored at −20°C until use. For preparation of cercarial transformation fluid (CTF), sedimented live cercariae were resuspended in culture medium (1.5×10^6 larvae in 10 ml Medium 199) and aspirated by syringe 12 to 14 times through a 0.8 × 40 mm needle. CTF in the supernatant was concentrated (using an Amicon YM2 filter) to produce cCTF which was adjusted to approximately 50 μg protein ml^{-1} and stored at −20°C.

Statistics

Data were analysed by two-way analysis of variance on normally distributed data. P values were assigned by the Neuman-Keuls procedure and considered significant if $P<0.05$.

Results

Effect of the anti-CD18 mAb on leukocyte adhesion to protein-coated plastic

The effect of 6.5E on the adhesion of guinea-pig neutrophils and eosinophils to serum-coated plastic is shown in Figure 1. Basal adhesion of neutrophils and eosinophils ranged from 295–1202 (three experiments) and 160–2490 (four experiments) cells per mm^2, respectively. PMA (10^{-8} M)-stimulated adhesion of both types of leukocyte was inhibited in a dose-dependent manner by 6.5E with IC_{50} values for neutrophil and eosinophil adhesion in these particular experiments of 1 and 0.6 μg ml^{-1}, respectively. Mean IC_{50} values for neutrophil and eosinophil adhesion in pooled experiments were 1.8 ± 0.6 and 0.9 ± 0.1 μg ml^{-1}, respectively (means ± s.e.mean of three neutrophil and four eosinophil assays). The control antibody MOPC21 (30 μg ml^{-1}) had no effect on adhesion of either leukocyte type. For example, in one experiment basal adherence of neutrophils (384 ± 57 cells per mm^2; mean ± s.d. of six replicates) was increased to 5245 ± 129 in the presence of 10^{-8} M PMA which was unaffected by the presence of MOPC21 (5197 ± 354). In the same experiments, PMA-stimulated adhesion of eosinophils was reduced to 34 ± 10 cells per mm^2 in the presence of 6.5E (30 μg ml^{-1}). In all experiments, 6.5E inhibited the basal adhesion of neutrophils (95.3 ± 2.1% inhibition, $n = 3$) but not eosinophils (2.4 ± 1.6% inhibition, $n = 4$).

Effect of 6.5E on the distribution of radiolabelled leukocytes in vivo

In our inital *in vivo* studies, we used 6.5E as a whole antibody administered i.v. at a dose of 0.24 mg kg^{-1} based on studies in the rabbit (Rutter *et al.*, 1992). While this dose of 6.5E had no significant effect on the number of circulating unlabelled leukocytes (data not shown), it resulted in enhanced clearance of ^{111}In-eosinophils from the circulation such that after 2 h, only 0.5 ± 0.1% of ^{111}In-eosinophils were circulating compared with 9.3 ± 2.9% in the controls (means ± s.e.mean, $n = 5$). The majority of radiolabelled cells were found in the liver (data not shown). Experiments were then carried out using F(ab')$_2$ fragments of 6.5E. Maximum inhibition of radiolabelled leukocyte accumulation in skin was achieved with a dose of 2.4 mg kg^{-1} (see below), however, this did not result in a significant alteration in the blood and tissue distribution of either ^{111}In-eosinophils or ^{111}In-

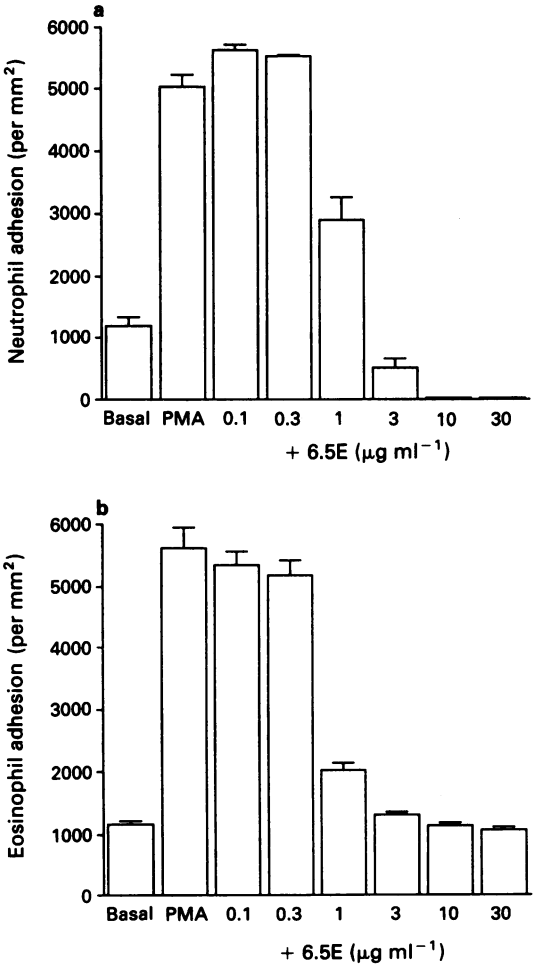


Figure 1 Effect of 6.5E (whole antibody) on adhesion of (a) ^{111}In-labelled guinea-pig neutrophils and (b) ^{111}In-labelled guinea-pig eosinophils to serum-coated plastic. Adhesion was stimulated by phorbol myristate acetate (PMA, 10^{-8} M) and quantified after 30 min at 37°C. Values are means ± s.e.mean of six replicates. In three neutrophil studies, 6.5E reduced PMA-stimulated adhesion in each experiment by >100% (i.e. to below basal adherence) while in four eosinophil studies 6.5E blocked PMA-stimulated adhesion by 99.8 ± 1.5%.

neutrophils (Table 1). This dose of 6.5E F(ab')$_2$ was used in all further experiments.

Effect of 6.5E on ZAP-induced inflammation in skin

Intradermal injection of ZAP induced a dose-dependent increase in the local accumulation of ^{111}In-labelled neutrophils (Figure 2a) or ^{111}In-labelled eosinophils (Figure 2b) in control animals (saline-treated). In animals treated with 6.5E F(ab')$_2$ (2.4 mg kg^{-1}), ^{111}In-neutrophil accumulation was inhibited by 80–89% (Figure 2a). The inhibitory effect of 6.5E F(ab')$_2$ was dose-dependent. Thus, ZAP (10–90%)-induced accumulation of ^{111}In-neutrophils was inhibited by 34–46% and 70–83% by 0.48 mg kg^{-1} and 0.96 mg kg^{-1} 6.5E F(ab')$_2$, respectively. The small number of ^{111}In-neutrophils accumulating after injection of saline was also inhibited ($P<0.05$). Interestingly, in another group of 6.5E F(ab')$_2$-treated guinea-pigs, ZAP-induced ^{111}In-eosinophil accumulation was also suppressed by 70–78% (Figure 2b).

The effect of 6.5E F(ab')$_2$ on ZAP-induced oedema formation in guinea-pig skin is shown in Figure 3 (oedema formation was measured in the same skin sites in which ^{111}In-neutrophil accumulation was assessed; neutrophil data are shown in Figure 2a). ZAP-induced oedema formation was slightly reduced in 6.5E F(ab')$_2$-treated animals compared with saline controls, with the response to 90% ZAP showing the largest dependency on CD18. However, local administration of the H_1 receptor antagonist, mepyramine, at a dose (2.5×10^{-8} mol per site) which effectively reduced (by 84%) oedema formation induced by exogenous histamine (2.5×10^{-8} mol per site; Figure 3), revealed that oedema formation induced by the lower doses of ZAP was almost all due to endogenous histamine. Oedema formation induced by 90% ZAP was inhibited by 45% ($P<0.05$) in the presence of mepyramine, but was not further reduced in animals treated with 6.5E F(ab')$_2$ (Figure 3). Histamine-induced oedema formation was not significantly affected by 6.5E F(ab')$_2$ (Figure 3).

Effect of 6.5E F(ab')$_2$ on oedema formation and eosinophil accumulation in a PCA reaction

Intradermal injection of antigen (BGG) into sensitized skin sites induced a dose-dependent increase in the local accumulation of ^{111}In-eosinophils and local oedema formation (Figure 4). In animals treated with 6.5E F(ab')$_2$, accumulation of ^{111}In-eosinophils in response to 0.01, 0.1 and 1 μg of BGG was inhibited by 84%, 89% and 92%, respectively (Figure 4a). Local oedema formation in the same sites was not significantly affected by 6.5E F(ab')$_2$ treatment (Figure 4b).

Table 1 Effect of 6.5E F(ab')$_2$ on the blood and tissue distribution of ^{111}In-neutrophils and ^{111}In-eosinophils in guinea-pigs

		% of ^{111}In-labelled leukocytes infused	
		Saline	*6.5E F(ab')$_2$*
^{111}In-eosinophils	Blood	7.4 ± 1.8	5.5 ± 1.6
	Lung	9.2 ± 0.8	10.3 ± 2.0
	Spleen	12.6 ± 2.6	11.9 ± 3.4
	Liver	56.6 ± 9.0	55.0 ± 8.2
^{111}In-neutrophils	Blood	2.0 ± 0.5	2.1 ± 0.5
	Lung	12.0 ± 2.6	14.1 ± 2.8
	Spleen	5.7 ± 1.0	8.2 ± 1.0
	Liver	70.3 ± 9.3	63.2 ± 3.1

The effect of i.v. treatment with 6.5E F(ab')$_2$ (2.4 mg kg^{-1}) on the distribution of ^{111}In-labelled leukocytes was assessed after 2 h. Results are expressed as mean ± s.e.mean for 4–5 guinea-pigs.

Effect of 6.5E F(ab')$_2$ on inflammation in skin induced by extracts of Schistosoma mansoni *larvae*

We have previously shown that i.d. injection of cercarial homogenate (CH) or concentrated cercarial transformation fluid (cCTF) induce the local accumulation of neutrophils and eosinophils and local oedema formation in guinea-pig skin (Teixeira *et al.*, 1993a). The ability of these extracts to induce inflammation correlates with their proteolytic activity. Figure 5 shows that 6.5E F(ab')$_2$ effectively inhibited both cCTF- and CH-induced accumulation of ^{111}In-neutrophils (Figure 5a) and ^{111}In-eosinophils (Figure 5b) while there was no detectable change in oedema formation at the same sites (Figure 5c).

Discussion

It is well established that C5a and C5a des Arg increase vascular permeability leading to oedema formation in several species. In the rabbit, i.d. injection of rabbit C5a des Arg, human C5a and C5a des Arg or pig C5a des Arg leads to oedema formation (Jose *et al.*, 1981; Williams & Jose, 1981) that is histamine-independent but requires circulating neutrophils (Wedmore & Williams, 1981). The nature of the neutrophil requirement remains undefined but is thought to involve

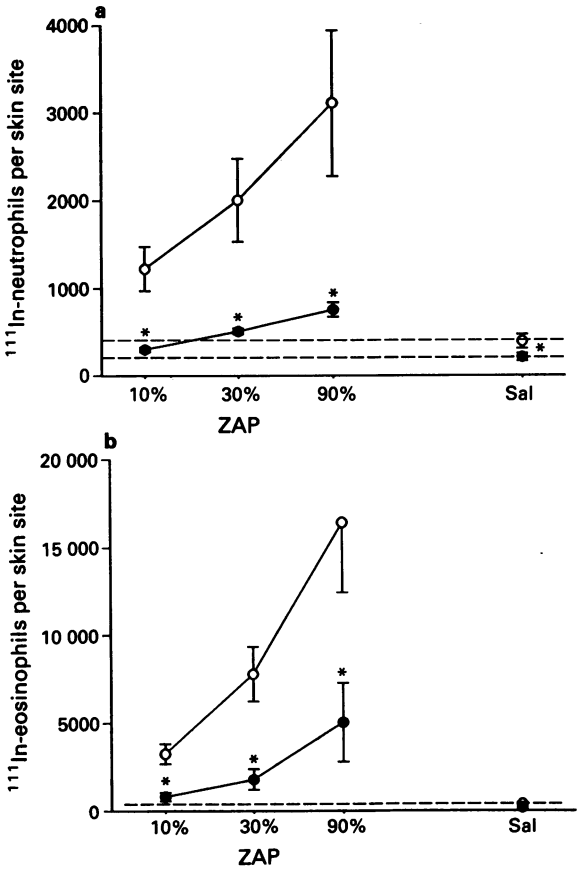


Figure 2 Effect of 6.5E F(ab')$_2$ on the local accumulation of (a) ^{111}In-labelled neutrophils and (b) ^{111}In-labelled eosinophils induced by i.d. injection of ZAP in guinea-pig skin. Animals were treated with saline (1 ml kg^{-1}, i.v.; ○) or 6.5E F(ab')$_2$ (2.4 mg kg^{-1}, i.v.; ●). Zymosan activated plasma (ZAP) (10–90% in saline) and saline were injected i.d. and radiolabelled leukocyte accumulation was assessed over a 2 h period. Results are expressed as the mean ± s.e.mean of six animals. The dashed lines represent the background values in sites injected with saline (Sal) alone. *$P<0.01$ when responses in control and 6.5E F(ab')$_2$-treated guinea-pigs are compared.

a rapid interaction (occurring within min) of the circulating neutrophils with the venular endothelium leading to oedema formation (Wedmore & Williams, 1981). Topical application of human C5a to the superfused hamster cheek pouch also leads to an increase in vascular permeability in the venules that shows some neutrophil-dependency and is largely histamine-independent (Bjork *et al.*, 1983). In the guinea-pig, i.d. injection of human C5a, but not C5a des Arg, leads to local oedema formation; a response abrogated by H_1 anti-histamine drugs (Fernandez *et al.*, 1978; Webster *et al.*, 1980). This activity correlates with the spasmogenic activity of human C5a on the guinea-pig ileum where C5a des Arg is inactive (Jose *et al.*, 1981). However, the requirement for circulating neutrophils in the oedema response to C5a des Arg in the guinea-pig is unknown. We have now shown that i.d. injection of ZAP, as a source of guinea-pig C5a des Arg, in guinea-pig skin induces local oedema formation that is largely independent of circulating neutrophils, as assessed by the small inhibitory effect of the anti-CD18 mAb 6.5E. In the same skin sites in 6.5E-treated animals, ZAP-induced neutrophil accumulation was very effectively reduced. This is consistent with other studies which have clearly demonstrated that neutrophil accumulation into inflammatory sites in the skin is dependent on CD18 (Arfors *et al.*, 1987; Nourshargh *et al.*, 1989; Doerschuk *et al.*, 1990; Mulligan *et al.*, 1992). Most of the ZAP-induced oedema response in guinea-pig skin was attributed to endogenous histamine, probably deriving from cutaneous mast cells, although at the higher ZAP doses a component of the response was independent of histamine and neutrophils. We have previously shown that local oedema formation in the PCA reaction is blocked by a combination of an H_1 anti-histamine, a PAF antagonist and a leukotriene D_4 antagonist (Weg *et al.*, 1991) and oedema formation induced by CH and cCTF is due to endogenous bradykinin generation (Teixeira *et al.*, 1993a). As these mediators are all direct-acting (i.e. neutrophil-independent), it was not surprising that oedema in the former reactions was not abrogated in 6.5E-treated animals. We also found, that despite 6.5E inhibiting PAF- or LTB_4-induced leukocyte accumulation by up to 93%, local oedema formation in the same skin sites was similar in control and 6.5E-treated animals (data not shown).

There is considerable evidence derived from experimental models which indicates that neutrophil accumulation at sites of inflammation in tissues, including skin, is dependent on the β_2 integrin CD11/CD18 (reviewed in Rossi & Hellewell, 1994). In addition, patients who suffer from leukocyte adhesion deficiency (LAD), whose leukocytes lack the CD18 molecule, show an inability to mount an accumulation of neutrophils to infected tissue (Bowen *et al.*, 1982; Hawkins *et al.*, 1992) The most likely explanation for the inhibitory effect of anti-CD18 mAbs on neutrophil accumulation in experimental models is that they prevent the firm adhesion of neutrophils to venular endothelium and/or their subsequent endothelial transmigration (Smith *et al.*, 1989; Furie *et al.*, 1991). Compared with neutrophils, the role of CD11/CD18

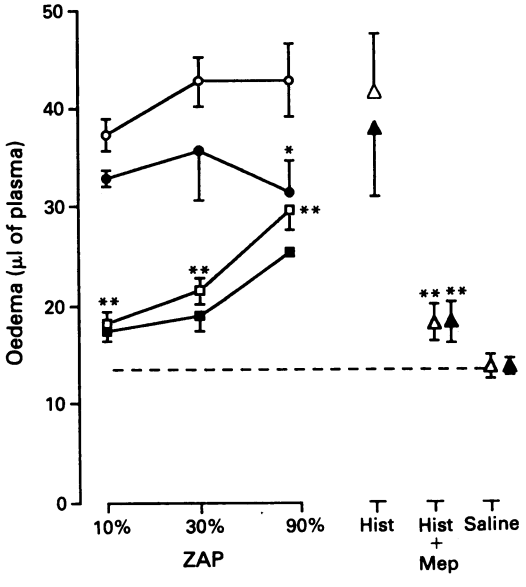


Figure 3 Effect of 6.5E $F(ab')_2$ and local mepyramine on oedema formation induced by i.d. injection of zymosan activated plasma (ZAP) and histamine in guinea-pig skin. Animals were treated with saline (1 ml kg^{-1}, i.v.) or 6.5E $F(ab')_2$ (2.4 mg kg^{-1}, i.v.). ZAP (10–90% in saline) was injected i.d. in saline-treated animals (○), in 6.5E-treated animals (●), in the presence of local mepyramine (Mep, 2.5×10^{-8} mol per site) in saline-treated animals (□) and in the presence of mepyramine in 6.5E-treated animals (■). Histamine (Hist, 2.5×10^{-8} mol per site), with or without mepyramine, and saline were injected i.d. in saline-treated (△) or 6.5E-treated guinea-pigs (▲). Local oedema formation was assessed over a 2 h period. Results are expressed as the mean ± s.e.mean of five animals. The dashed lines represent the background values in sites injected with saline alone. Significant differences between responses in control and 6.5E-treated animals, or at sites with and without local mepyramine are indicated by * for $P<0.05$ and ** for $P<0.01$.

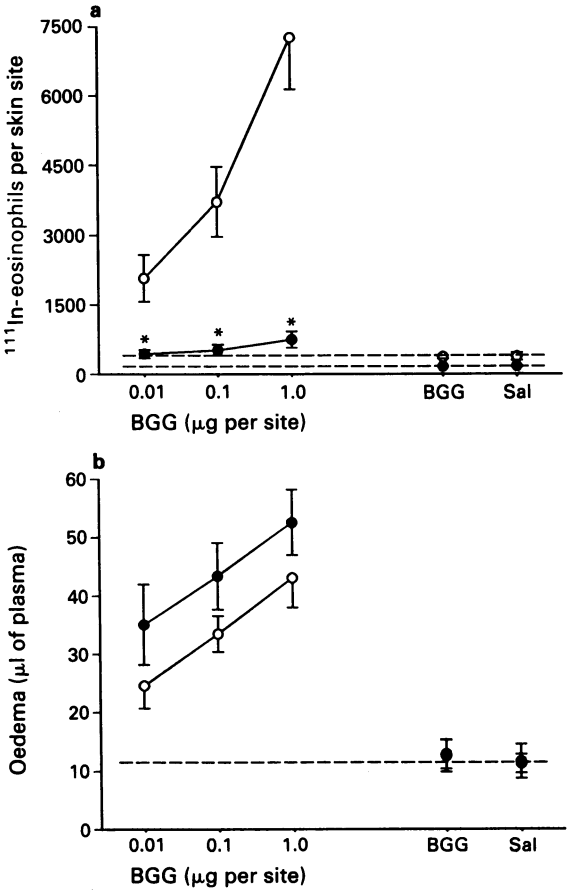


Figure 4 Effect of 6.5E $F(ab')_2$ on the local accumulation of (a) ^{111}In-eosinophils and (b) local oedema formation induced in passive cutaneous anaphylactic (PCA) reaction in guinea-pig skin. Animals were treated with saline (1 ml kg^{-1}, i.v.; ○) or 6.5E $F(ab')_2$ (2.4 mg kg^{-1}, i.v., ●). BGG and saline were injected i.d. and radiolabelled eosinophil accumulation and oedema formation were assessed over a 2 h period. Results are expressed as the mean ± s.e.mean of six animals. The dashed lines represent the background values in sites injected with saline (Sal) alone. Responses to injection of BGG into naive sites are also shown. *$P<0.01$ when responses in control and 6.5E $F(ab')_2$-treated guinea-pigs are compared.

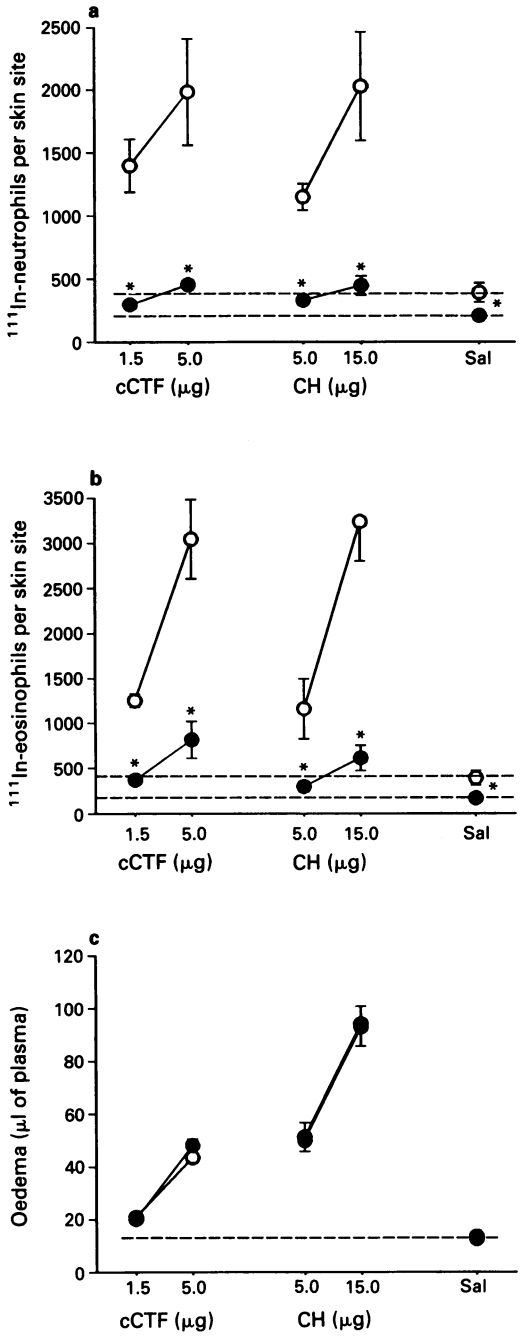


Figure 5 Effect of 6.5E F(ab')$_2$ on the local accumulation of (a) ^{111}In-neutrophils and (b) ^{111}In-eosinophils and (c) local oedema formation induced by i.d. injection of extracts of *Schistosoma mansoni* larvae in guinea-pig skin. Animals were treated with saline (1 ml kg^{-1}, i.v.; ○) or 6.5E F(ab')$_2$ (2.4 mg kg^{-1}, i.v., ●). Concentrated cercarial transformation fluid (cCTF; 1.5 and 5 μg per site), cercarial homogenate (CH; 5 and 15 μg per site) and saline were injected i.d. and radiolabelled leukocyte accumulation and oedema formation were assessed over a 2 h period. Results are expressed as the mean ± s.e.mean of 4–6 animals. The dashed lines represent the background values in sites injected with saline (Sal) alone. *$P < 0.01$ when responses in control and 6.5E F(ab')$_2$-treated guinea-pigs are compared.

recent study from our department (Weg *et al.*, 1993) showed that accumulation of ^{111}In-eosinophils to sites of cutaneous inflammation in the guinea-pig were attenuated by a mAb to the β_1 integrin, very late antigen-4 (VLA-4). Nevertheless, there are some data in the literature which indicate that CD18 may also be involved in eosinophil accumulation *in vivo*. For example, Wegner and colleagues demonstrated that antigen-induced eosinophil accumulation in the lungs of sensitized primates was attenuated by an antibody to one of the CD11/CD18 ligands, ICAM-1 (Wegner *et al.*, 1990) and preliminary studies in the sensitized guinea-pig showed that eosinophil migration into the airways 24 h following antigen challenge was reduced by 80% by an anti-CD18 mAb (Noonan *et al.*, 1991). However, in neither of these studies was a possible mAb-induced leukopaenia excluded as the mechanism of action of mAb.

In vitro data have indicated that eosinophils can adhere to endothelial cells through binding to adhesion molecules such as ICAM-1, VCAM-1 and E-selectin (Bochner *et al.*, 1991; Dobrina *et al.*, 1991; Walsh *et al.*, 1991; Weller *et al.*, 1991). It is also clear that CD11/CD18 is important for subsequent transendothelial migration (Moser *et al.*, 1992; Kuijpers *et al.*, 1993), presumably binding to its endothelial cell ligands ICAM-1 and ICAM-2. A recent study (Kuijpers *et al.*, 1993) demonstrated that VLA-4 in combination with other β_1 integrins was also important for eosinophil migration across endothelial cell monolayers and a combination of an anti-β_1 and anti-β_2 mAbs reduced migration by 97%. In the latter study, the ligand for VLA-4 was subendothelial matrix and not VCAM-1. Data from the present study and the study of Weg *et al.* (1993) suggest that both CD18 and VLA-4 may be required for effective migration of eosinophils *in vivo*; blocking either of these adhesion molecules results in a substantial, but not complete inhibition of eosinophil accumulation. In future studies it will be interesting to compare the inhibitory effects of combinations of these mAbs with either mAb tested alone.

The mAb 6.5E inhibited in a dose-dependent manner PMA-stimulated adhesion of guinea-pig neutrophils and eosinophils to serum-coated plastic. This strongly suggested that the anti-human CD18 mAb was able to bind and block a functional epitope on the guinea-pig CD18 molecule since human leukocyte adhesion to serum-coated plastic is known to be mediated by CD18 (Harlan *et al.*, 1985; Tonnesen, 1989). The same mAb also blocks rabbit CD18 (Rutter *et al.*, 1992; Galea-Lauri *et al.*, 1993). When administered i.v., 6.5E had no significant effect on the total number of circulating leukocytes although it effectively reduced the circulation of ^{111}In-labelled cells suggesting clearance via the reticulo-endothelial system. In keeping with this suggestion, ^{111}In counts in the liver of the 6.5E-treated animals were substantially increased compared with controls. In addition, this enhanced clearance of radiolabelled cells was prevented if F(ab')$_2$ fragments of 6.5E were used.

In summary, we have found that the accumulation of neutrophils and eosinophils at inflammatory sites in guinea-pig skin involves the leukocyte β_2 integrin, CD18. The results also demonstrate that local oedema formation induced by C5a des Arg is largely independent of neutrophil accumulation. Unlike oedema responses in the rabbit, we found no evidence for neutrophil-dependent oedema formation in the guinea-pig.

in mediating eosinophil accumulation *in vivo* is less established although in LAD patients, relatively large numbers of eosinophils have been found in tissues (Anderson *et al.*,1985) suggesting that a CD18-independent pathway for eosinophil migration may exist. In support of this latter suggestion, a

We thank the National Asthma Campaign, the British Heart Foundation, The Wellcome Trust and Sandoz, Switzerland for support. We also thank Dr M.J. Doenhoff and Mr C. McNeice, University College of North Wales, Bangor for generating and supplying CH and cCTF.

References

ANDERSON, D.C., SCHMALSTEIG, F.C., FINEGOLD, M.J., HUGHES, B.J., ROTHLEIN, R., MILLER, L.J., KOHL, S., TOSI, M.F., JACOBS, R.L., WALDROP, T.C., GOLDMAN, A.S., SHEARER, W.T. & SPRINGER, T.A. (1985). The severe and moderate phenotypes of heritable Mac-1, LFA-1, deficiency: their quantitative definition and relation to leukocyte dysfunction and clinical features. *J. Infect. Dis.*, **152,** 668–689.

ANDREW, D., SHOCK, A., BALL, E., ORTLEPP, S., BELL, J. & ROBINSON, M. (1993). KIM 185, a monoclonal antibody to CD18 which induces a change in the conformation of CD18 and promotes both LFA-1- and CR3-dependent adhesion. *Eur. J. Immunol.*, **23,** 2217–2222.

ARFORS, K.-E., LUNDBERG, C., LINDBOM, L., LUNDBERG, K., BEATTY, P.G. & HARLAN, J.M. (1987). A monoclonal antibody to the membrane glycoprotein complex CD18 inhibits polymorphonuclear leukocyte accumulation and plasma leakage *in vivo*. *Blood*, **69,** 338–340.

BJORK, J., HUGLI, T.E. & SMEDEGARD, G. (1983). Microvascular effects of anaphylatoxins C3a and C5a. *J. Immunol.*, **134,** 1115–1119.

BOCHNER, B.S, LUSCINSKAS, F.W., GIMBRONE, M.A., NEWMAN, W., STERBINSKY, S.A., DERSE-ANTHONY, C.P., KLUNK, D. & SCHLEIMER, R.P. (1991). Adhesion of human basophils, eosinophils, and neutrophils to interleukin 1-activated human vascular endothelial cells: contributions of endothelial cell adhesion molecules. *J. Exp. Med.*, **173,** 1553–1556.

BOWEN, T.J., OCHS, H.D., ALTMAN, L.C., PRICE, T.H., VAN EPPS, D.E., BRAUTIGAN, D.L., ROSIN, R.E., PERKINS, W.D., BABIOR, B.M., KLEBANOFF, S.J. & WEDGWOOD, R.J. (1982). Severe recurrent bacterial infections associated with defective adherence and chemotaxis in two patients with neutrophils deficient in a cell-associated glycoprotein. *J. Pediatrics*, **101,** 932–940.

COCHRANE, G. & MULLER-EBERHARD, H.J. (1968). The derivation of two distinct anaphylatoxin activities from the third and fifth components of human complement. *J. Exp. Med.*, **127,** 371–386.

COLLINS, P.D., WEG, V.B., FACCIOLI, L.H., WATSON, M.L., MOQBEL, R. & WILLIAMS, T.J. (1993). Eosinophil accumulation induced by human interleukin-8 in the guinea pig in vivo. *Immunology*, **79,** 312–318.

DAVIES, G.E. & LOWE, J.S. (1960). A permeability factor released from guinea-pig serum by antigen-antibody precipitates. *Br. J. Exp. Pathol.*, **XLI,** 335–344.

DAVIES, G.E. & LOWE, J.S. (1962). Further studies on a permeability factor released from guinea-pig serum by antigen-antibody precipitates: relationship to serum complement. *Int. Arch. Allergy*, **20,** 235–250.

DIAS DA SILVA, W. & LEPOW, I.H. (1967). Complement as a mediator of inflammation. II. Biological properties of anaphylatoxin prepared with purified components of human complement. *J. Exp. Med.*, **125,** 921–932.

DOBRINA, A., MENEGAZZI, R., CARLOS, T.M., NARDON, E., CRAMER, R., ZACCHI, T., HARLAN, J.M. & PATRIARCA, P. (1991). Mechanisms of eosinophil adherence to cultured vascular endothelial cells. Eosinophils bind to the cytokine-induced endothelial ligand vascular cell adhesion molecule-1 via the very late activation antigen-4 integrin receptor. *J. Clin. Invest.*, **88,** 20–26.

DOERSCHUK, C.M., WINN, R.K., COXSON, H.O. & HARLAN, J.M. (1990). CD18-dependent and -independent mechanisms of neutrophil emigration in the pulmonary and systemic microcirculation of rabbits. *J. Immunol.*, **144,** 2327–2333.

FACCIOLI, L.H., NOURSHARGH, S., MOQBEL, R., WILLIAMS, F.M., SEHMI, R., KAY, A.B. & WILLIAMS, T.J. (1991). The accumulation of ^{111}In-eosinophils induced by inflammatory mediators in vivo. *Immunology*, **73,** 222–227.

FERNANDEZ, H.N., HENSON, P.M., OTANI, A. & HUGLI, T.E. (1978). Chemotactic response to human C3a and C5a anaphylatoxins: 1. Evaluation of C3a and C5a leukotaxis in vitro and under stimulated in vivo conditions. *J. Immunol.*, **120,** 109–115.

FIGDOR, C.G. & VAN KOOYK, Y. (1992). Regulation of cell adhesion. In *Adhesion: Its Role in Inflammatory Disease*. ed. Harlan, J.M. & Liu, D.Y. pp. 151–182. New York: W.H. Freeman and Company.

FURIE, M.B., TANCINCO, M.C.A. & SMITH, C.W. (1991). Monoclonal antibodies to leukocyte integrins CD11a/CD18 and CD11b/CD18 or intercellular adhesion molecule-1 inhibit chemoattractant-stimulated neutrophil transendothelial migration in vitro. *Blood*, **78,** 2089–2097.

GALEA-LAURI, J., BLACKFORD, J. & WILKINSON, J.M. (1993). The expression of CD11/CD18 molecules on rabbit leucocytes: identification of monoclonal antibodies to CD18 and their effects on cellular adhesion processes. *Mol. Immunol.*, **30,** 529–537.

HARLAN, J.M., KILLEN, P.D., SENECAL, F., SCHWARTZ, B.R., YEE, E.K., TAYLOR, R.F., BEATTY, P.G., PRICE, T. & OCHS, H.D. (1985). The role of neutrophil membrane glycoprotein GP-150 in neutrophil adherence to endothelium in vitro. *Blood*, **66,** 167–178.

HAWKINS, H.K., HEFFELFINGER, S.C. & ANDERSON, D.C. (1992). Leukocyte adhesion deficiency: clinical and postmortem observations. *Pediatric Pathol.*, **12,** 119–130.

HUDSON, L. & HAY, F.C. (1989). *Practical Immunology*. Oxford: Blackwell Scientific Publications.

ISSEKUTZ, A.C. (1981). Vascular responses during acute neutrophilic inflammation. Their relationship to in vitro neutrophil emigration. *Lab. Invest.*, **45,** 435–441.

JOSE, P.J., FORREST, M.J. & WILLIAMS, T.J. (1981). Human C5a des Arg increases vascular permeability. *J. Immunol.*, **127,** 2376–2380.

KUIJPERS, T.W., MUL, F.P.J., BLOM, M., KOVACH, N.L., GAETA, F.C.A., TOLIEFSON, V., ELICES, M.J. & HARLAN, J.M. (1993). Freezing adhesion molecules in a state of high-avidity binding blocks eosinophil migration. *J. Exp. Med.*, **178,** 279–284.

MOSER, R., FEHR, J., OLIGIATI, L. & BRUIJNZEEL, P.L.B. (1992). Migration of primed human eosinophils across cytokine-activated endothelial cell monolayers. *Blood*, **79,** 2937–2943.

MULLIGAN, M.S., VARANI, J., WARREN, J.S., TILL, G.O., SMITH, C.W., ANDERSON, D.C., TODD, R.F. & WARD, P.A. (1992). Roles of β_2 integrins of rat neutrophils in complement and oxygen radical-mediated acute inflammatory injury. *J. Immunol.*, **148,** 1847–1857.

NOONAN, T.C., GUNDEL, R.H., DESAI, S.N., STEARNS, C., BARTON, R.W., ROTHLEIN, R., LETTS, L.G. & PIPER, P.J. (1991). The effects of an anti-CD18 antibody (R15.7) in antigen-induced airway hyperresponsiveness (AH) and cell influx in guinea pigs. *Agents Actions*, **34,** 211–213.

NOURSHARGH, S., RAMPART, M., HELLEWELL, P.G., JOSE, P.J., HARLAN, J.M., EDWARDS, A.J. & WILLIAMS, T.J. (1989) Accumulation of ^{111}In-neutrophils in rabbit skin in allergic and non-allergic inflammatory reactions in vivo: inhibition by neutrophil pretreatment in vitro with a monoclonal antibody recognising the CD18 antigen. *J. Immunol.*, **142,** 3193–3198.

ROSSI, A.G. & HELLEWELL, P.G. (1994). Mechanisms of neutrophil accumulation in tissues. In *Immunopharmacology of Neutrophils*. ed. Hellewell, P.G. & Williams, T.J. London: Academic Press, (in press).

RUTTER, J.A., MINION, T., HOWAT, D., ROBINSON, M., HIGGS, G., ANDREW, D., CLEMENTS, G. & HUGHES, B. (1992). In vivo administration of an anti-CD18 monoclonal antibody inhibits leukocyte-dependent plasma exudation in rabbit skin. *Br. J. Pharmacol.*, **106,** 70P.

SMITH, C.W., MARLIN, S.D., ROTHLEIN, R., TOMAN, C. & ANDERSON, D.C. (1989). Co-operative interactions of LFA-1 and Mac-1 with intercellular adhesion molecule-1 in facilitating adherence and transendothelial migration of human neutrophils in vitro. *J. Clin. Invest.*, **83,** 2008–2017.

TEIXEIRA, M.M., DOENHOFF, M.J., MCNEICE, C., WILLIAMS, T.J. & HELLEWELL, P.G. (1993a). Mechanisms of the inflammatory response induced by extracts of Schistosoma mansoni larvae in guinea pig skin. *J. Immunol.*, **151,** 5525–5534.

TEIXEIRA, M.M., WILLIAMS, T.J. & HELLEWELL, P.G. (1993b). E-type prostaglandins enhance local oedema formation and neutrophil accumulation but suppress eosinophil accumulation in guinea pig skin. *Br. J. Pharmacol.*, **110,** 416–422.

TONNESEN, M.G., ANDERSON, D.C., SPRINGER, T.A., KNEDLER, A., AVDI, N. & HENSON, P.M. (1989). Adherence of neutrophils to cultured human microvascular endothelial cells. Stimulation by chemotactic peptides and lipid mediators and dependence upon the Mac-1, LFA-1, p150,95 glycoprotein family. *J. Clin. Invest.*, **83,** 637–646.

WALSH, G.M., MERMOD, J.-J., HARTNELL, A., KAY, A.B. & WARDLAW, A.J. (1991). Human eosinophil, but not neutrophil, adherence to IL-1-stimulated human umbilical vascular endothelial cells is $\alpha_4\beta_1$ (very late antigen-4) dependent. *J. Immunol.*, **146,** 3419–3423.

WEBSTER, R.O., HONG, S.R., JOHNSTON, R.B. & HENSON, P.M. (1980). Biological effects of the human complement fragments C5a and $C5a_{des\ Arg}$ on neutrophil function. *Immunopharmacology*, **2**, 201–209.

WEDMORE, C.V. & WILLIAMS, T.J. (1981). Control of vascular permeability by polymorphonuclear leukocytes in inflammation. *Nature*, **289**, 646–650.

WEG, V.B., WATSON, M.L., CORDEIRO, R.S.B. & WILLIAMS, T.J. (1991). Histamine, leukotriene D_4 and platelet activating factor in guinea pig passive cutaneous anaphylaxis. *Eur. J. Pharmacol.*, **204**, 157–163.

WEG, V.B., WATSON, M.L., FACCIOLI, L.H. & WILLIAMS, T.J. (1992). [^{111}In]-eosinophil accumulation during passive cutaneous anaphylaxis in the guinea pig. *Br. J. Pharmacol.*, **105**, 127P.

WEG, V.B., WILLIAMS, T.J., LOBB, R.R. & NOURSHARGH, S. (1993). A monoclonal antibody recognising very late activation antigen-4 (VLA-4) inhibits eosinophil accumulation in vivo. *J. Exp. Med.*, **177**, 561–566.

WEGNER, C.D., GUNDEL, R.H., REILLY, P., HAYNES, N., LETTS, L.G. & ROTHLEIN, R. (1990). Intercellular adhesion molecule-1 (ICAM-1) in the pathogenesis of asthma. *Science*, **247**, 456–459.

WELLER, P.F., RAND, T.H., GOELZ, S.E., CHI-ROSSO, G. & LOBB, R.R. (1991). Human eosinophil adherence to vascular endothelium mediated by binding to vascular cell adhesion molecule 1 and endothelial leukocyte adhesion molecule 1. *Proc. Natl. Acad. Sci. U.S.A.*, **88**, 7430–7433.

WILLIAMS, T.J. & JOSE, P.J. (1981). Mediation of increased vascular permeability after complement activation: histamine-independent action of rabbit C5a. *J. Exp. Med.*, **153**, 136–153.

WILLIAMSON, L.M., SHEPPARD, K., DAVIES, J.M. & FLETCHER, J. (1986). Neutrophils are involved in the increased vascular permeability produced by activated complement in man. *Br. J. Haematol.*, **64**, 375–384.

(Received September 28, 1993
Revised November 12, 1993
Accepted November 22, 1993)

Br. J. Pharmacol. (1994), **111**, 819–824 © Macmillan Press Ltd, 1994

α_{1b}-Adrenoceptors mediate renal tubular sodium and water reabsorption in the rat

Abdelhamid M. Elhawary & [1]Catherine C.Y. Pang

Department of Pharmacology & Therapeutics, Faculty of Medicine, The University of British Columbia, Vancouver B.C., Canada, V6T 1Z3

1 It is known that activation of α_1-adrenoceptors causes renal vasoconstriction and increased tubular Na^+ and water reabsorption, with the α_{1a}-subtype mediating the constrictor effect.

2 This study examines which subtype of α_1-adrenoceptors mediates tubular Na^+ and water reabsorption in pentobarbitone-anaesthetized rats. In order to avoid systemic effects, phenylephrine (0.3 to 30 $\mu g\ kg^{-1}$), methoxamine (0.1–10 $\mu g\ kg^{-1}$) and vehicle were infused into the right renal artery (via the suprarenal artery) of three groups of rats. Two other groups of rats were continuously infused with the irreversible selective α_{1b}-adrenoceptor antagonist, chloroethylclonidine (3 $mg\ kg^{-1}\ h^{-1}$) for 1 h, prior to the construction of dose-response curves to phenylephrine or methoxamine. Another group was continuously infused with the irreversible selective α_{1a}-adrenoceptor antagonist, SZL-49 (10 $\mu g\ kg^{-1}\ h^{-1}$) for 1 h, prior to the construction of dose-response curves to phenylephrine. Mean arterial pressure (MAP), heart rate (HR), urine flow, Na^+ and K^+ excretion, and urine osmolality were monitored.

3 Phenylephrine and methoxamine did not affect MAP or HR but dose-dependently and significantly decreased urine flow, urine osmolality as well as Na^+ excretion and, slightly increased K^+ excretion, although this was significant only for phenylephrine.

4 The antidiuretic, antinatriuretic and kaliuretic effects of phenylephrine were abolished by pretreatment with chloroethylclonidine, but were not inhibited by SZL-49. The inhibitory effects of methoxamine on urine flow and Na^+ excretion were also almost totally abolished by chloroethylclonidine.

5 Our results show that α_{1b}-adrenoceptors mediate renal tubular Na^+ and water reabsorption.

Keywords: α_1-Adrenoceptor subtype; chloroethylclonidine; SZL-49; renal tubules; sodium and water reabsorption

Introduction

α_1-Adrenoceptors are known to mediate renal vasoconstriction as well as sodium and water reabsorption induced by the stimulation of renal sympathetic nerves (DiBona, 1985; Jeffries & Pettinger, 1989). The antidiuresis and antinatriuresis mediated by α_1-adrenoceptors can occur in the absence of changes in the glomerular filtration rate of the whole kidney or single nephron, renal blood flow or intrarenal distribution of blood flow, and it is not dependent on intrarenal actions of prostaglandins or angiotensin II (DiBona & Sawin, 1982; Gottschalk *et al.*, 1985). Radioligand binding studies (Schmitz *et al.*, 1981; Snavely & Insel, 1982), autoradiographic analyses (Summers, 1984; Muntz *et al.*, 1985) as well as microdissection studies using radioligand binding techniques (Kusano *et al.*, 1984) have quantified α_1-adrenoceptors in the rat renal membrane. These studies have shown the existence of a high density of α_1-adrenoceptors in the cortex, especially in proximal tubules and ascending thick limb of the loop of Henle, a lower density in the medulla and no apparent binding in the collecting ducts.

Multiple subtypes of α_1-adrenoceptors are known to exist. Separate genes for α_{1a}- (Lomasney *et al.*, 1991), α_{1b}- (Cotecchia *et al.*, 1988; Voigt *et al.*, 1990) and α_{1c}-adrenoceptors (Schwinn *et al.*, 1990) were cloned from different tissues, despite the recent controversy as to whether the cloned 'α_{1a}' is indeed α_{1a}, or rather, a novel α_{1d}-adrenoceptor-subtype (Perez *et al.*, 1992). Pharmacological agents with apparent selectivity for α_{1a}- and α_{1b}-adrenoceptors have been used to identify, functionally and biochemically, these subtypes of receptors. These include the alkylating agent, chloroethylclonidine (CEC) which selectively inactivates α_{1b}-adrenoceptors (Han *et al.*, 1987; Minneman, 1988; Minneman *et al.*, 1988) and SZL-49, an analogue of prazosin, which alkylates CEC-resistant α_1-adrenoceptors, presumably the α_{1a}-subtype (Babich *et al.*, 1987; Kusiak *et al.*, 1989; Piascik *et al.*, 1989).

The rat renal artery has been shown to contain only α_{1a}-adrenoceptors *in vitro* (Han *et al.*, 1990). Elhawary *et al.* (1992) showed that the inactivation of rat renal α_{1a}-adrenoceptors abolished *in vivo* α_1-adrenoceptor-mediated renal vasoconstriction, indicating the inclusive invovlement of α_{1a}-adrenoceptors in renal vasoconstriction. The subtype of α_1-adrenoceptors mediating renal tubular sodium and water reabsorption has not yet been identified. High densities of both α_{1a}- and α_{1b}-adrenoceptors are present in the rat renal membrane (Han *et al.*, 1987). This suggests the possible involvement of both adrenoceptor subtypes in the mediation of renal tubular responses. The aim of this study was to investigate the effect of selective alkylation of α_1-adrenoceptor subtypes on antidiuretic and antinatriuretic actions of α_1-adrenoceptor agonists.

Methods

Male Sprague Dawley rats (300–350 g) were anaesthetized with sodium pentobarbitone (50 $mg\ kg^{-1}$, i.p.). A rectal thermometer connected to an Animal Blanket Control Unit was used to maintain body temperature at 37.5°C. Cannulae (PE50) were inserted into the left femoral artery, for the continuous measurement of mean arterial pressure (MAP) with a Statham pressure transducer (Model P23 DB, Gould Statham, CA), and into the left femoral vein, for continuous infusion of saline (30 $\mu l\ min^{-1}$) throughout the experiment. Heart rate (HR) was derived electronically from the upstroke of the arterial pulse pressure with a tachograph (Grass, model 7P4G). MAP and HR responses were monitored by a Grass polygraph (Grass, model RP57C8). The abdominal cavity was opened through a ventral midline incision. The right suprarenal artery was located and its origin from the renal artery was verified. A tapered PE-10 tube was inserted retrogradely into the suprarenal artery as described by Smits

[1] Author for correspondence.

et al. (1983), and connected to a syringe pump (SAGE 341A) for the infusion of drugs. A PE-50 cannula was inserted into the right ureter for the collection of urine every 10 min in pre-weighed vials. The rats were given 1 h for stabilization after surgery before the study began.

Experimental protocol

Six groups of rats ($n = 7-9$ each, except for groups II and V, where $n = 5$) were used. Groups I, II and III were infused with the vehicle (0.45% NaCl) for 1 h followed by the construction of dose-response curves to phenylephrine (PE, 0.3–30 $\mu g\,kg^{-1}$; 10 min each dose), methoxamine (Methox, 0.1–10 $\mu g\,kg^{-1}$; 10 min each dose) and an equal volume of the vehicle (0.45% NaCl), respectively. In Groups IV and V, chloroethylclonidine (CEC; 3 $mg\,kg^{-1}\,h^{-1}$) was infused into the renal artery for 1 h followed by the infusions of various doses of PE and Methox, respectively. Group VI was given continuous renal arterial infusion of SZL-49 (10 $\mu g\,kg^{-1}\,h^{-1}$) for 1 h followed by PE. The doses of the CEC and SZL-49 selected were those which maximally alkylated and blocked renal vascular responses to stimulation of α_{1b}- and α_{1a}-adrenoceptors, respectively (Elhawary *et al.*, 1992). Urine was collected at the end of each 10 min infusion period. A blood sample was obtained at the end of the stabilization period and after the completion of the study to monitor any changes in the haematocrit, plasma osmolality and levels of sodium (Na^+) and potassium (K^+) during the course of the study. The duration of the studies was approximately 2 h, counting from the end of the stabilization period to the completion of drug infusions. Urine volume was determined gravimetrically. Urine Na^+ and K^+ concentrations were determined by flame photometry (Fisher Scientific IL 143) and urine osmolality was measured by a WESCOR 5500 vapour pressure osmometer.

Materials

SZL-49, {1-(4-amino-6, 7-dimethoxy-2-quinazolnyl)-4- (2-bicyclo [2,2,2] octa-2,5-dienylcarbonyl)-piperazine}, and CEC were purchased from Research Biomedicals, Inc. (Natick, MA, U.S.A.). PE and Methox were obtained from the Sigma Chemical Co (St. Louis, MO, U.S.A.). All drugs were dissolved in 0.45% NaCl solution except SZL-49, which was first solubilized in 80% ethanol and then diluted with 0.45% NaCl solution to make a final concentration of 0.3% ethanol (v/v).

Statistics

All data are expressed as mean ± s.e.mean. The results were analysed by analysis of variance followed by Duncan's multiple range test, with $P < 0.05$ as the level of statistical significance.

Results

The infusion of the vehicle into the renal artery caused minimal and insignificant changes in MAP, HR, urine volume, urine Na^+/K^+ or urine osmolality (Table 1). Intra-renal arterial infusion of PE also caused negligible changes in MAP and HR (Figure 1). PE dose-dependently and signifi-

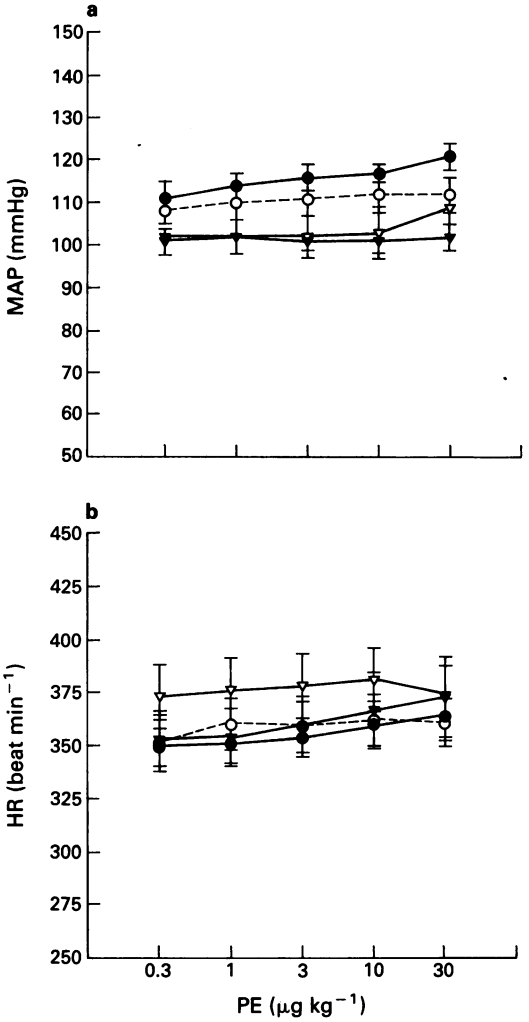


Figure 1 Dose-response effects on mean arterial pressure (MAP, a) and heart rate (HR, b) following renal arterial infusions of vehicle (○, 0.45% NaCl, $n = 8$), phenylephrine (●, PE, $n = 7$), PE after infusion of SZL-49 (▽, 10 $\mu g\,kg^{-1}\,h^{-1}$, $n = 9$), and PE after infusion of CEC (▼, 3 $mg\,kg^{-1}\,h^{-1}$, $n = 7$) in four groups of pentobarbitone-anaesthetized rats. Data are shown as mean ± s.e.mean. For abbreviations, see text.

Table 1 Effect of vehicle (0.45% NaCl) on mean arterial pressure (MAP, mmHg), heart rate (HR, beats min^{-1}), urine flow (UF, $\mu l\,min^{-1}$), Na^+ and K^+ excretions (mEq l^{-1}) and urine osmolality (Osm, mOsm kg^{-1}) during the six sampling periods (C1 to C6) in pentobarbitone-anaesthetized rats

	Time control					
	C1	*C2*	*C3*	*C4*	*C5*	*C6*
MAP	108 ± 3	108 ± 3	110 ± 3	111 ± 4	112 ± 4	112 ± 4
HR	349 ± 13	350 ± 12	351 ± 10	354 ± 9	360 ± 11	364 ± 11
UF	5.1 ± 0.3	4.9 ± 0.3	4.6 ± 0.3	4.8 ± 0.3	4.5 ± 0.4	4.9 ± 0.6
Na	59 ± 5	55 ± 4	56 ± 8	54 ± 7	56 ± 7	62 ± 8
K	163 ± 17	156 ± 20	167 ± 20	171 ± 19	172 ± 18	170 ± 15
Osm	1408 ± 97	1415 ± 109	1447 ± 107	1477 ± 111	1446 ± 112	1460 ± 111

$n = 8$.

cantly reduced urine flow (Figure 2a), urine osmolality (Figure 2b) and Na^+ excretion (Figure 3a) but slightly increased K^+ excretion, which, for the third and fifth PE doses, were significantly different from the corresponding readings in control rats given the vehicle (Figure 3b). Neither 1 h of close arterial infusion of CEC nor of SZL-49 affected baseline values of MAP, HR, urinary flow, urine values of Na^+, K^+ or osmolality, haematocrit or, blood values of Na^+, K^+ or osmolality (Table 2). CEC and SZL-49 also did not affect either MAP or HR response to PE (Figure 1a,b). CEC abolished the effects of PE on urine flow (Figure 2a), urine osmolality (Figure 2b) and K^+ excretion (Figure 3b). In the

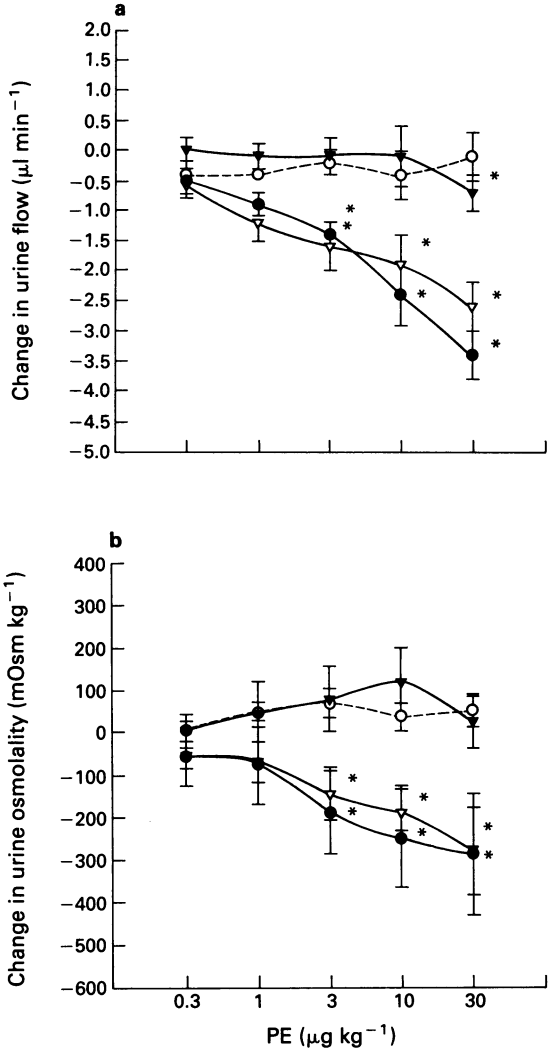


Figure 2 Dose-response effects on urine flow (a) and osmolality (b) following renal arterial infusions of vehicle (○, 0.45% NaCl, $n = 8$), phenylephrine (●, PE, $n = 7$), PE after infusion of SZL-49 (▽, 10 μg kg^{-1} h^{-1}, $n = 9$), and PE after infusion of CEC (▼, 3 mg kg^{-1} h^{-1}, $n = 7$) in four groups of pentobarbitone-anaesthetized rats. Data are shown as mean ± s.e.mean. *Significantly different from values in vehicle-treated rats. For abbreviations, see text.

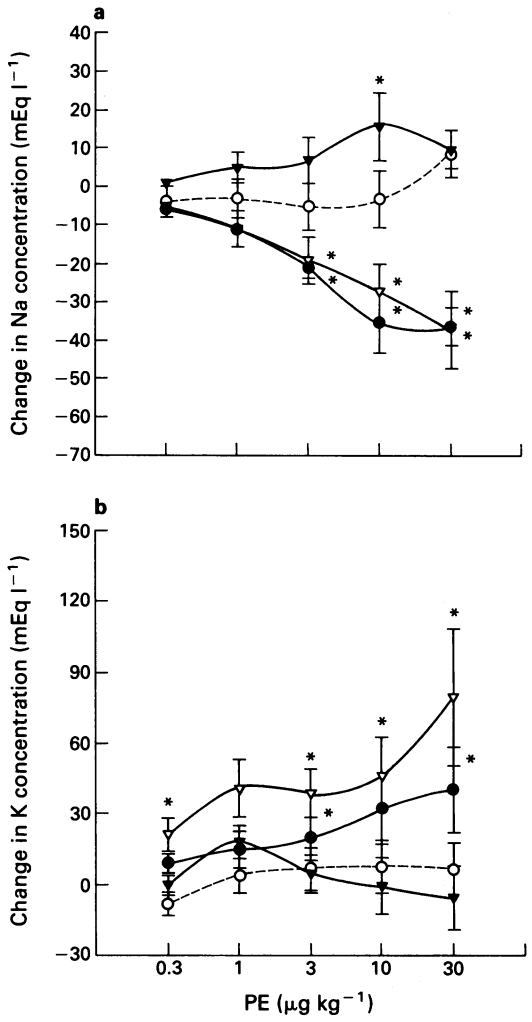


Figure 3 Dose-response effects on urinary excretions of Na^+ (a) and urinary K^+ (b) following renal arterial infusions of vehicle (○, 0.45% NaCl, $n = 8$), phenylephrine (●, PE, $n = 7$), PE after infusion of SZL-49 (▽, 10 μg kg^{-1} h^{-1}, $n = 9$), and PE after infusion of CEC (▼, 3 mg kg^{-1} h^{-1}, $n = 7$) in four groups of pentobarbitone-anaesthetized rats. Data are shown as means ± s.e.mean. *Significantly different from values in vehicle-treated rats. For abbreviations, see text.

Table 2 Baseline values of mean arterial pressure (MAP, mmHg), heart rate (HR, beats min^{-1}), urine flow (UF, μl min^{-1}), urine sodium (U Na, mEq l^{-1}), urine potassium (U K, mEq l^{-1}), urine osmolality (U Osm, mOsm kg^{-1}), haematocrit (HC%), blood sodium (Bl Na, mEq l^{-1}), blood potassium (Bl K, mEq l^{-1}) and blood osmolality (Bl Osm, mOsm kg^{-1}) following 1 h infusion of vehicle (0.45% NaCl), SZL-49 (10 μg kg^{-1} h^{-1}) or CEC (3 mg kg^{-1} h^{-1}) in five groups of pentobarbitone-anaesthetized rats to be infused with phenylephrine (PE) or methoxamine (Methox)

Group	*MAP*	*HR*	*UF*	*U Na*	*U K*	*U Osm*	*HC%*	*Bl Na*	*Bl K*	*Bl Osm*
Vehicle, PE	108 ± 4	347 ± 13	5.3 ± 0.4	62 ± 7	173 ± 19	1507 ± 33	48 ± 2%	137 ± 4	3.3 ± 0.5	295 ± 7
SZL, PE	102 ± 2	372 ± 13	5.3 ± 0.6	74 ± 11	164 ± 23	1537 ± 171	47 ± 2%	136 ± 7	3.4 ± 0.5	298 ± 5
CEC, PE	102 ± 1	348 ± 11	5.3 ± 0.4	50 ± 7	166 ± 16	1370 ± 151	49 ± 1%	138 ± 8	3.6 ± 0.8	297 ± 7
Vehicle, Methox	103 ± 3	380 ± 15	4.7 ± 0.8	53 ± 5	194 ± 14	1695 ± 90	48 ± 1%	137 ± 2	3.4 ± 0.3	297 ± 6
CEC, Methox	108 ± 3	370 ± 12	4.9 ± 0.8	68 ± 13	225 ± 7	1634 ± 180	45 ± 4%	134 ± 6	2.9 ± 0.6	296 ± 8

$n = 7$–9 per group.

Table 3 Dose-response effects of 10 min i.a. infusion of methoxamine on mean arterial pressure (MAP, mmHg), heart rate (HR, beats min^{-1}), urine flow (UF, $\mu l\ min^{-1}$), urine sodium (Na, $mEq\ l^{-1}$), urine potassium (K, $mEq\ l^{-1}$) and urine osmolality (Osm, $mOsm\ kg^{-1}$) in pentobarbitone-anaesthetized rats in the absence ($n = 5$) and presence ($n = 5$) of i.a. infused chloroethylclonidine (CEC, $3\ mg\ kg^{-1}\ h^{-1}$)

	Methoxamine ($\mu g\ kg^{-1}$)						*Methoxamine* ($\mu g\ kg^{-1}$) + *CEC* ($3\ mg\ kg^{-1}\ h^{-1}$)					
	C	0.1	0.3	1	3	10	C	0.1	0.3	1	3	10
MAP	103 ± 3	102 ± 3	102 ± 4	101 ± 5	101 ± 5	103 ± 6	108 ± 3	107 ± 4	109 ± 3	108 ± 4	108 ± 5	109 ± 5
HR	380 ± 15	380 ± 15	351 ± 10	354 ± 9	360 ± 11	364 ± 11	370 ± 12	360 ± 17	364 ± 15	368 ± 15	376 ± 19	382 ± 23
UF	4.7 ± 0.7	4.1 ± 0.7	3.5 ± 0.6*	2.8 ± 0.7*	2.1 ± 0.4*	1.2 ± 0.6*	4.9 ± 0.8	5.8 ± 0.8	5.6 ± 0.8	5.7 ± 0.7	5.8 ± 0.7	6.0 ± 0.9
Na	53 ± 5	45 ± 7	42 ± 6*	29.8 ± 4*	24.8 ± 3*	19 ± 2*	68 ± 13	67 ± 12	64 ± 11	72 ± 16	74 ± 15	75 ± 15
K	194 ± 14	200 ± 12	198 ± 15	219 ± 14	222 ± 16	206 ± 26	225 ± 7	234 ± 6	242 ± 6	234 ± 8	214 ± 21	213 ± 24
Osm	1695 ± 90	1566 ± 97	1490 ± 97	1417 ± 101*	1350 ± 49*	1238 ± 123*	1634 ± 180	1408 ± 97	1415 ± 109	1506 ± 208	1447 ± 247	1440 ± 246

*Indicates significant difference from the baseline value.

presence of CEC, PE slightly increased Na^+ excretion, which was significantly different from the vehicle effect at the fourth dose (Figure 3a). SZL-49, in contrast, did not inhibit the effects of PE on urine osmolality, flow (Figure 2a,b) or Na^+ (Figure 3a) and it slightly but insignificantly potentiated the effect of PE on K^+ excretion, as K^+ excretions in the presence were not different from those in the absence of SZL-49 (Figure 3b). To ascertain that the renal tubular effects of PE were mediated via the activation of α_1-adrenoceptors, Methox was also infused into the renal artery. Like PE, Methox significantly and dose-dependently reduced urine flow, urine osmolality and urine Na^+, slightly but insignificantly increased urine K^+ and did not affect MAP or HR (Table 3). CEC completely inhibited the effects of Methox on urine flow and Na^+ but it incompletely, though significantly, suppressed the effect on urine osmolality (Table 3). Haematocrit and blood values of Na^+, K^+ and osmolality at the end of the experiments were similar to the corresponding values (Table 2) after the stabilization period (results not shown).

Discussion

The results of this study show that renal arterial infusion of PE induced dose-dependent reductions in urine flow and Na^+ excretion. This reduction was accompanied by a decrease in urine osmolality and a slight increase in K^+ excretion. Pretreatment with the irreversible and selective α_{1b}-adrenoceptor antagonist, CEC, abolished the antidiuretic and antinatriuretic effects of PE, suggesting that these responses were mediated via the activation of α_{1b}-adrenoceptors. The infusion of Methox into the renal artery also caused similar dose-dependent decreases in urine flow, osmolality as well as Na^+ and, slight (but insignificant) increases in urine K^+. Since all these changes were inhibited by CEC, it suggests that renal tubular effects of Methox were also mediated via the activation of α_{1b}-adrenoceptors. In contrast, pretreatment with the alkylating agent, SZL-49, did not inhibit the effects of PE on urine volume, osmolality or Na^+. Accordingly, our results indicate that α_{1b}-adrenoceptors are the primary α_1-adrenoceptors involved in the mediation of renal tubular Na^+ and water reabsorption.

In the present study, the renal tubular effects of PE and Methox were not due to alterations in systemic haemodynamics, since these drugs caused negligible systemic effects. It was also unlikely that CEC inhibited the tubular effects of PE via actions on the renal vasculature since CEC only weakly suppressed renal vasoconstriction elicited by α_1-adrenoceptor stimulation (Elhawary *et al.*, 1992). Furthermore, SZL-49 (Elhawary *et al.*, 1992) and the Ca^{2+} entry blocker, nifedipine (Han *et al.*, 1990) produced marked rightward shifts of the dose-renal pressor response curve of PE but SZL-49 did not inhibit renal tubular effects of PE in the present study. Therefore, the subtype of α_1-adrenoceptors mediating renal vasoconstriction are different from those mediating tubular effects.

The effect of α_1-adrenoceptor activation, either by renal nerve stimulation or selective agonists, on renal function has been extensively studied (for review see DiBona, 1985) and this includes: increased Na^+ and water reabsorption in the proximal tubules, increased Na^+ and Cl^- reabsorption in the thick ascending limb of the Loop of Henle (DiBona & Sawin, 1982), increased Ca^{2+} (Jones & Manitius, 1986) and bicarbonate reabsorption (Osborn & Harland, 1988), stimulation of gluconeogenesis (Kessar & Saggerson, 1980) and, increased renovascular resistance (Cooper & Malik, 1985; Wolff *et al.*, 1987; DiBona & Sawin, 1987; Jeffries *et al.*, 1987). Intrarenal arterial infusion of PE in anaesethetized rabbits, at a dose which did not alter renal haemodynamics, significantly reduced urine flow and absolute and fractional Na^+ excretion by about 15, 23, and 23% respectively (Hesse & Johns, 1985). Higher doses of PE, which caused 11% decrease of blood flow and 15% decrease in filtration rate,

were found to decrease urine flow, absolute and fractional Na^+ excretion by 43%, 49% and 42% respectively. In the same study, a low dose of Methox, which had no effect on MAP, HR, renal blood flow or glomerular filteration rate, significantly reduced urine flow, absolute and fractional Na^+ excretion by about 33%, 30 and 28% respectively. The high dose of Methox, which significantly reduced blood flow (by 15%) and filtration rate (by 26%), decreased urine flow, absolute and fractional Na^+ excretion by 79%, 76% and 65%, respectively. These results are in accordance with our present results in anaesthetized rats of PE ($30\ \mu g\ kg^{-1}$) and Methox ($10\ \mu g\ kg^{-1}$), in reducing urine flow, by 64 and 74%, and Na^+ excretion, by 52 and 64%, respectively.

Our results of the involvement of α_{1b}- but not α_{1a}-adrenoceptors in renal tubular Na^+ and water resorption are in accordance with the anatomical distribution of these receptors in the kidney. Feng *et al.* (1991) reported a distinct pattern of distribution of the two subtypes of α_1-adrenoceptors in the rat kidney. Both α_{1a}- and α_{1b}-adrenoceptors are found in equal proportions in the renal cortex and outer strip of the medulla; however, the α_{1b}-subtype predominates in the inner strip of the medulla. According to the anatomical structure of the nephron, the vascular tissue mass diminishes from the cortex to the medulla, the proximal convoluted tubules exist in the cortex and outer strip of the medulla (Sundaresan *et al.*, 1987), and the thick ascending limb of the loop of Henle predominates in the inner strip of the medulla (Kriz, 1981). Therefore, the regional distribution of subtypes of α_1-adrenoceptors and the anatomical distribution of vascular and tubular tissues is consistent with the results of functional studies which show that renal vasoconstrictor and tubular effects are mediated by α_{1a}- and α_{1b}-adrenoceptors, respectively.

In conclusion, our results suggest discrete physiological function for each subtype of α_1-adrenoceptors in rats: α_{1a}-adrenoceptors for renal vasoconstriction and α_{1b}-adrenoceptors for renal tubular Na^+ and water reabsorption.

This work was supported by the Heart & Stroke Foundation of B.C. & Yukon. We thank Dr Ralph Keeler of Department of Physiology for technical advice.

References

BABICH, M., PEDIGO, N.W., BUTLER, B.T. & PIASCIK, M.T. (1987). Heterogeneity of alpha1 receptors associated with vascular smooth muscle. Evidence from functional and ligand binding studies. *Life Sci.*, **41**, 663–674.

COOPER, C.L. & MALIK, K.U. (1985). Prostaglandin synthesis and renal vasoconstriction elicited by adrenergic stimuli are linked to activation of alpha-1 adrenergic receptors in the isolated rat kidney. *J. Pharmacol. Exp. Ther.*, **233**, 24–31.

COTECCHIA, S., SCHWINN, D.A., RANDALL, R.R., LEFKOWITZ, R.J., CARON, M.G. & KOBILKA, B.K. (1988). Molecular cloning and expression of the cDNA for the hamster alpha1-adrenergic receptor. *Proc. Natl. Acad. Sci. U.S.A.*, **85**, 7159–7163.

DIBONA, G.F. (1985). Neuronal control of renal function: role of renal alpha adrenoceptors. *J. Cardiovasc. Pharmacol.*, **7** (Suppl. 8), S18–S23.

DIBONA, G.F. & SAWIN, L.L. (1982). Effect of renal nerve stimulation on NaCl and H_2O transport in Henle's loop of the rat. *Am. J. Physiol.*, **243**, F576–F580.

DIBONA, G.F. & SAWIN, L.L. (1987). Role of renal α2-adrenergic receptors in spontaneously hypertensive rats. *Hypertension*, **9**, 41–48.

ELHAWARY, A.M., PETTINGER, W.A. & WOLFF, D.W. (1992). Subtype-selective alpha1-adrenoceptor alkylation in the rat kidney and its effect on the vascular pressor response. *J. Pharmacol. Exp. Ther.*, **260**, 2, 709–713.

FENG, F., PETTINGER, W.A., ABEL, P. & JEFFRIES, W.B. (1991). Regional distributon of alpha1-adrenoceptor subtypes in rat kidney. *J. Pharmacol. Exp. Ther.*, **258**, 1, 263–268.

GOTTSCHALK, C.W., MOSS, N.G. & COLINRES, R.E. (1985). Neuronal control of renal function in health and disease. In *The Kidney: Physiology and Pathophysiology*. ed. Seldin, D.W. & Giebisch, G. pp. 581–611. New York: Raven Press.

HAN, C., ABEL, P.W. & MINNEMAN, K.P. (1987). Heterogeneity of alpha1-adrenergic receptors revealed by chloroethylclonidine. *Mol. Pharmacol.*, **32**, 505–510.

HAN, C., LI, J. & MINNEMAN, K.P. (1990). Subtypes of alpha1-adrenoceptors in rat blood vessels. *Eur. J. Pharmacol.*, **190**, 97–104.

HESSE, I.F.A. & JOHNS, E.J. (1985). The role of α-adrenoceptors in the regulation of renal tubular sodium reabsorption and renin secretion in the rabbit. *Br. J. Pharmacol.*, **84**, 715–724.

JEFFRIES, W.B. & PETTINGER, W.A. (1989). Adrenergic signal transduction in the kidney. *Miner. Electrolyte Metab.*, **15**, 5–15.

JEFFRIES, W.B., TAM, L.T., WANG, Y, SMYTH, D.D. & PETTINGER, W.A. (1987). Prazosin-induced alterations in renal α-adrenergic receptor function. *Hypertension*, **9** (Suppl. 3), III-125–III-129.

JOHNS, E.J. & MANITIUS, J. (1986). A study in the rat of the renal actions of nitrendipine and diltiazem on the adrenergic regulation of the Ca++ and Na reabsorption. *Br. J. Pharmacol.*, **89**, 99–107.

KESSAR, P. & SAGGERSON, E.D. (1980). Evidence that catecholamines stimulate renal gluconeogenesis through an alpha1-type of adrenoceptor. *Biochem. J.*, **190**, 119–123.

KRIZ, W. (1981). Structural organization of renal medulla: comparative and functional aspects. *Am. J. Physiol.*, **241**, R3–R16.

KUSANO, E., NAKAMURA, R., ASANO, Y. & IMAI, M. (1984). Distribution of α-adrenergic receptors in the rabbit nephron. *Tohoku J. Exp. Mech.*, **142**, 275–282.

KUSIAK, J.W., PITHA, J. & PIASCIK, M.T. (1989). Interaction of a chemically reactive prazosin analog with alpha-1 adrenoceptors of rat tissues. *J. Pharmacol. Exp. Ther.*, **249**, 70–77.

LOMASNEY, J.W., COTECCHIA, S., LORENZ, W., LEUNG, W.-Y., SCHWINN, D.A., YANG-FENG, T.L., BROWNSTEIN, M., LEFKOWITZ, R.J. & CARON, M.G. (1991). Molecular cloning and expression of the cDNA for the alpha1A-adrenergic receptor. *J. Biol. Chem.*, **266**, 6365–6369.

MINNEMAN, K.P. (1988). Alpha1-Adrenergic receptor subtypes, inositol phosphates, and sources of cell calcium. *Pharmacol. Rev.*, **40**, 87–120.

MINNEMAN, K.P., HAN, C. & ABEL, P.W. (1988). Comparison of alpha1-adrenoceptor subtypes distinguished by CEC and WB 4101. *Mol. Pharmacol.*, **33**, 509–514.

MUNTZ, K.H., GARCIA, C. & HAGLER, H.K. (1985). Alpha1-receptor localization in rat heart and kidney using autoradiography. *Am. J. Physiol.*, **249**, H512–H519.

OSBORN, J.L. & HARLAND, R.W. (1988). $Alpha_1$-adrenoceptor mediation of urinary bicarbonate excretion. *Am. J. Physiol,*. **255**, F1116–F1121.

PEREZ, D.M., PIASCIK, M.T. & GRAHAM, R.M. (1992). Solution phase library screening for the identification of rare clones: Isolation of an alpha1D-adrenergic receptor cDNA. *Mol. Pharmacol.*, **40**, 876–883.

PIASCIK, M.T., BUTLER, B.T., KUSIAK, J.W., PITHA, J. & HOLTMAN, J.R. Jr (1989). Effect of an alkylating analog of prazosin on alpha-1 adrenoceptor subtypes and arterial blood pressure. *J. Pharmacol. Exp. Ther.*, **251**, 878–883.

SCHMITZ, J.M., GRAHAM, R.M., SAGALOWSKY, A. & PETTINGER, W.A. (1981). Renal $alpha_1$- and α_2-adrenergic receptors: Biochemical and pharmacological correlations. *J. Pharmacol. Exp. Ther.*, **219**, 400–406.

SCHWINN, D.A., LOMASNEY, J.W., LORENZ, W., SZKLUT, P.J., FREMEAU, R.T. Jr, YANG-FENG, T.L., CARON, M.G., LEFKOWITZ, R.J. & COTECCHIA, S. (1990). Molecular cloning and expression of the cDNA for a novel alpha1-adrenergic receptor subtype. *J. Biol. Chem.*, **265**, 8183–8189.

SMITS, J.F.M., KASBERGEN, C.M., VAN ESSEN, H., KLEINJANS, J.C.S. & STRUYKER-BOUDIER, H.A.J. (1983). Chronic local infusion into the renal artery of unrestrained rats. *Am. J. Physiol.*, **244**, H304–H306.

SNAVELY, M.D. & INSEL, P.A. (1982). Characterization of alpha adrenoceptors subtypes in the rat renal cortex. *Mol. Pharmacol.*, **22,** 532–546.

SUMMERS, R.J. (1984). Renal α-adrenoceptors. *Fed. Proc.*, **43,** 2917–2922.

SUNDARESAN, P.R., FORTIN, T.L. & KELVIE, S.L. (1987). α- and β-adrenoceptors in proximal tubules of the rat kidney. *Am. J. Physiol.*, **253,** F848–F856.

VOIGT, M.M., KISPERT, J. & CHIN, H. (1990). Sequence of a rat brain c DNA encoding an alpha1B-adrenergic receptor. *Nucleic Acids Res.*, **18,** 1053.

WOLFF, D.W., GESEK, F.A. & STRANDHOY, J.W. (1987). *In vivo* assessment of rat renal alpha adrenoceptors. *J. Pharmacol. Exp. Ther.*, **241,** 472–476.

(Received September 3, 1993
Revised November 9, 1993
Accepted November 23, 1993)

Br. J. Pharmacol. (1994), **111**, 825–828

© Macmillan Press Ltd, 1994

Detection of nitric oxide in exhaled air during administration of nitroglycerin *in vivo*

[1,]*M.G. Persson, *P. Agvald & *†L.E. Gustafsson

*Department of Physiology and Pharmacology and †Institute of Environmental Medicine, Karolinska Institute, S-171 77 Stockholm, Sweden

1 Direct evidence for nitric oxide (NO) formation from nitroglycerin (GTN) was obtained by measurements of NO concentrations in exhaled air in artifically-ventilated, pentobarbitone-anaesthetized rabbits.

2 The concentration of endogenously formed NO was 23 ± 5 parts per billion (p.p.b.). Infusions of GTN (1–100 μg kg^{-1} min^{-1}, i.v.) induced dose-dependent and biphasic increments in exhaled NO and concomitant reductions in systemic blood pressure.

3 Tolerance to the blood pressure reduction developed in parallel with a decrease in GTN-induced exhaled NO, a pattern which was unaffected by administration of N^{ω}-nitro-L-arginine methyl ester (L-NAME, 30 mg kg^{-1}), L-cysteine (200 mg kg^{-1}), N-acetylcysteine (200 mg kg^{-1}) or glutathione (200 mg kg^{-1}).

4 Intravenous infusions of adenosine (0.7 mg ml^{-1}, 250 μl kg^{-1} min^{-1}) and GTN (1 mg ml^{-1}, 250 μl kg^{-1} min^{-1}) elicited similar decrements in pulmonary vascular resistance. GTN elicited a substantial increase in exhaled NO (50 ± 10 p.p.b.) whereas adenosine evoked a markedly smaller increase (7 ± 1 p.p.b.). L-NAME (30 mg kg^{-1}, i.v.) abolished NO in exhaled air, and evoked an increase in pulmonary vascular resistance from 116 ± 19 to 147 ± 9 pulmonary vascular resistance units. After L-NAME the change in pulmonary vascular resistance induced by adenosine or GTN was increased to a similar degree. However, while the increase in exhaled NO induced by nitroglycerin was unaffected, the response to adenosine was abolished.

5 The present data demonstrate that NO is formed from GTN *in vivo*. Furthermore, thiol availability, or nitric oxide synthase activity are not limiting factors in the conversion of nitroglycerin to NO *in vivo*. Finally, pulmonary haemodynamic changes *per se* do not explain the observed increase in NO upon nitroglycerin infusion.

Keywords: Nitroglycerin; nitric oxide; thiol; cysteine; glutathione; NO production *in vivo*; adenosine; blood pressure; respiratory system; lung

Introduction

Nitroglycerin (GTN) has been used in the treatment of angina pectoris for more than a century. The mode of action has been suggested to be thiol-dependent activation (cf. Needleman & Johnson, 1973; Andersson & Ahlner, 1987) of vascular smooth muscle guanylate cyclase (Diamond & Blissard, 1976). In the presence of sulphydryls, GTN is metabolized to nitric oxide (NO) *in vitro* (Feelisch & Noack, 1987), possibly via formation of a nitrosocysteine-intermediate (Ignarro *et al.*, 1980), which, like NO, is a potent smooth muscle relaxant and activator of guanylate cyclase.

An intriguing characteristic of GTN is the rapid development of tolerance observed *in vitro*, as well as in clinical use, which may be due to decreased vascular biotransformation, reduced availability of tissue free thiols, metabolite inhibition, or desensitization of guanylate cyclase (cf. Andersson & Ahlner, 1987).

Nitric oxide, the tentative common final mediator of all nitrovasodilators, is known to be formed from the naturally occurring amino acid, L-arginine, in many mammalian cells (cf. Moncada, 1992) and can be detected in the exhaled air from experimental animals and man (Gustafsson *et al.*, 1991).

The aim of the present investigation was to establish a model for studies of the conversion of GTN to NO *in vivo*, and to investigate NO concentrations during development of tolerance.

[1] Author for correspondence.

Methods

The experiments were approved by the local animal ethics committee. New Zealand White rabbits (2–3 kg) were anaesthetized with sodium pentobarbitone (6 mg ml^{-1}, 50–60 mg kg^{-1} body weight) via an ear vein. Breathing was facilitated by tracheal cannulation, and the animals were ventilated with a Harvard Apparatus (South Natick, Massachusetts, USA) model 683 rodent ventilator adjusted to keep blood gases normal (40 breaths min^{-1}, tidal volume 6–8 ml kg^{-1}, F_IO_2 = 0.21, synthetic air containing less than one part per billion [p.p.b.] NO). Heparinized (100 iu ml^{-1}) catheters were inserted in the left carotid artery for blood pressure recordings, and in the right jugular vein for administration of a continuous infusion, containing glucose (2.5 g 100 ml^{-1}), dextran 70 (3.0 g 100 ml^{-1}), $NaHCO_3$ (0.7 g 100 ml^{-1}) and pentobarbitone sodium (360 mg 100 ml^{-1}), at a rate of 5 ml kg^{-1} h^{-1}, by means of a STC-521 syringe pump (Terumo Corp., Tokyo, Japan). Blood pressure was recorded by a Statham pressure transducer. Rectal temperature was maintained at 37–38°C by means of a heating pad connected to a thermostat (Wittman-Hereaus, Heidelberg, Germany). Drugs were infused via the venous catheter and administered by a microinfusion pump (CMA 100, Carnegie Medical, Stockholm, Sweden). Nitroglycerin or adenosine were administered for 15 min with 30 min pauses between each infusion.

Pulmonary vascular resistance was measured as previously described (Persson *et al.*, 1990). Briefly, a median sternotomy was performed and a catheter (umbilical artery catheter, 3.5 Fr, Sherwood Medical, Belgium) was introduced via the left jugular vein into the pulmonary artery for recording of pulmonary arterial pressure (Statham pressure transducer). An ultrasonic flow probe (R6, Transonic Systems Inc., Cornell

Research Park, Ithaca, NY, U.S.A.) was applied on the ascending aorta and connected to a blood flow meter (Transonic T-201). Blood flow in the ascending aorta was taken as a measure of cardiac output. A flanged polythene catheter was placed in the left atrium, via a puncture wound in the auricle, for recordings of mean left atrial pressure. Pressures were recorded by means of Statham pressure transducers and a Grass polygraph. Pulmonary vascular resistance was calculated from the expression ([(mean pulmonary arterial pressure – mean left atrial pressure)/cardiac output]/1000), and was expressed in $cmH_2O\ ml^{-1}\ min^{-1}$, which was designated milliRU$_L$ (mRU$_L$). In all cases, 45 min were allowed before experimentation to obtain stable circulatory conditions.

Nitric oxide was analyzed on a Sievers NOA 270 chemiluminescence system (Sievers, Boulder, CO, U.S.A.) set at an integration time of 0.12 s. A gas flow of 150 ml min^{-1}, controlled by a precision flow meter (Brooks Instrument B.V., Veenendaal, Netherlands) and a working pressure of 7–9 torr was obtained by a vacuum pump (Edwards 18 Two Stage, Edwards High Vacuum Int., Crawley, Sussex, U.K.). The NO analyser was, by means of mass flow controllers (Bronkhorst, Ruurlo, Holland), calibrated with dilutions in synthetic air of a certified NO standard gas in N_2 (AGA Specialgas, Lidingö, Sweden). The final concentration of NO in the calibration gas was 2, 5, 10, 50, 100 and 200 p.p.b. (accuracy ± 5%).

Drugs

The following were used: adenosine, L-cysteine and L-NAME (N^{ω}-nitro-L-arginine methyl ester) purchased from Sigma; heparin and acetylcysteine from Kabi Pharmacia, Stockholm, Sweden; pentobarbitone sodium (Mebubal Vet.) from Nord Vacc, Uppsala, Sweden; nitroglycerin (Perlinganit) was a kind gift from Schwartz-Pharma, Monheim, Germany.

Statistical data are given as mean ± s.e.mean, and statistical significance was calculated by means of Student's *t* test. Correlation was analyzed by linear regression.

Results

Blood pressure, heart rate and NO concentrations in exhaled air remained at 64.8 ± 5.9 mmHg, 196 ± 8 min^{-1} and 15.3 ± 2.0 p.p.b. respectively during a 30 min control period. Dose-dependent increments of NO in exhaled air were found upon infusion of GTN (1–100 μg $kg^{-1}min^{-1}$, $n = 6$). The increase in NO reached a peak within 3 min after starting the infusion; thereafter the NO concentrations decreased to a markedly lower plateau level and were not different at 15 min of infusion compared to 10 min (Figures 1 and 2). At the same time as the changes in exhaled NO during infusion of GTN, there was an initial sharp and dose-dependent blood pressure fall, after which the blood pressure returned to values closer to control (Figures 1 and 2). There was a correlation ($r = 0.80$, $P < 0.001$) between the increments in exhaled NO and the reduction of systemic blood pressure upon infusion of GTN. When the GTN-infusion (100 μg $kg^{-1}\ min^{-1}$) was repeated at 30 min intervals slight inter-infusion reductions in the blood pressure effect, as well as in the GTN-induced increments in NO in exhaled air, were observed (NS). In addition, 15 min after the repeated GTN infusions (eight times, 15 min each) the concentration of *endogenous* exhaled NO was stable and at a significantly lower concentration than prior to GTN-infusions (11.8 ± 1.4 vs. 14.9 ± 2.2 p.p.b., $P < 0.05$, $n = 6$).

Administration of L-cysteine (200 mg kg^{-1}, i.v., $n = 6$), N-acetyl-cysteine (200 mg kg^{-1}, i.v., $n = 6$), or glutathione (200 mg kg^{-1}, i.v., $n = 5$) 15 min prior to GTN affected neither the blood pressure response nor the NO response in exhaled air induced by GTN (Table 1). The ratio of NO in exhaled air at the end of a GTN-infusion (plateau concentration) compared to the initial peak value was taken as a measure of within-infusion ('acute') tolerance in NO formation. This ratio was similar in control animals and in animals treated with L-cysteine, N-acetyl-cysteine or glutathione (0.54 ± 0.07, 0.59 ± 0.07, 0.59 ± 0.08 and 0.57 ± 0.07, respectively, NS, $n =$ 5–6 in each group).

The inhibitor of endogenous NO synthesis N^{ω}-nitro-L-arginine methyl ester (L-NAME, 30 mg kg^{-1}, i.v.) abolished *endogenous* NO in exhaled air (below detection limit; 1 p.p.b.). However, the GTN-induced NO excretion in exhaled air was not significantly affected by L-NAME ($n = 4$).

In three experiments pulmonary vascular resistance was measured. In the absence of L-NAME, intravenous infusions of adenosine (0.7 mg ml^{-1}, 250 μl $kg^{-1}\ min^{-1}$) or GTN (1 mg ml^{-1}, 250 μl $kg^{-1}\ min^{-1}$) elicited similar and limited decrements in pulmonary vascular resistance. GTN elicited a substantial increase in exhaled NO (50 ± 10 p.p.b.) whereas

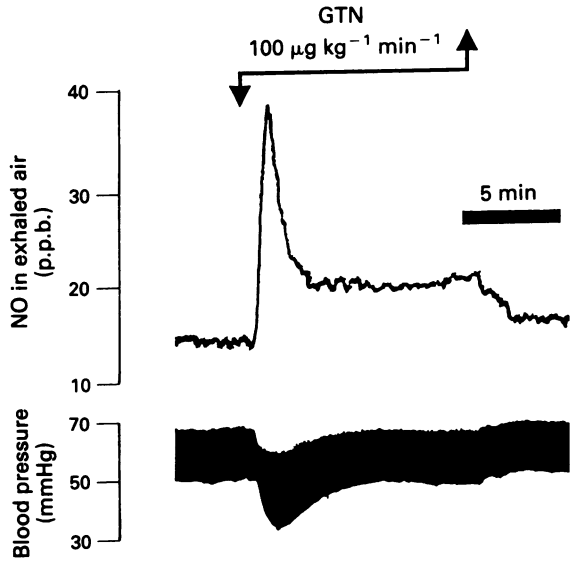


Figure 1 Artifically-ventilated, pentobarbitone-anaesthetized rabbit: recordings of NO in exhaled air (upper panel) and systemic blood pressure (lower panel). Effect of a 15 min infusion of nitroglycerin (GTN, 100 μg $kg^{-1}\ min^{-1}$, i.v.) is shown.

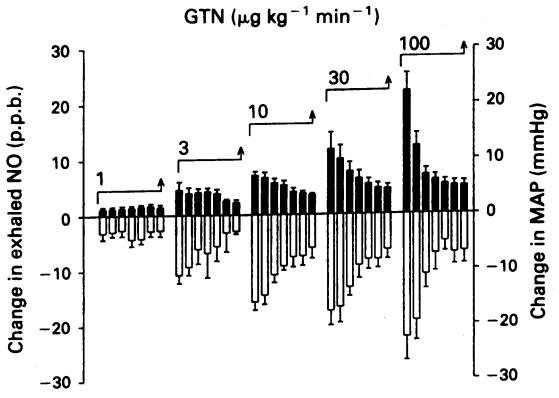


Figure 2 Artificially-ventilated, pentobarbitone-anaesthetized rabbits: increments in NO in exhaled air (black columns, left ordinate scale) and decrements in mean arterial blood pressure (MAP, open columns, right ordinate scale) in response to 15 min infusions of nitroglycerin (GTN, 1–100 μg $kg^{-1}\ min^{-1}$, i.v., as indicated in figure) compared to control values obtained immediately prior to GTN-infusion. Thirty-min resting periods were allowed between the infusions. Values were obtained at the time when the NO concentration peaked and at 1, 2, 3, 5, 10 and 15 min thereafter. Means ± s.e. mean, $n = 6$.

Table 1 Effect of thiols on exhaled NO and blood pressure in rabbits

	Control	*L-Cysteine* (200 mg kg^{-1})	*N-acetyl-cysteine* (200 mg kg^{-1})	*Glutathione* (200 mg kg^{-1})
NO at peak (p.p.b.)	39.4 ± 5.5	36.7 ± 4.2	37.9 ± 4.3	36.0 ± 2.7
NO at plateau (p.p.b.)	20.1 ± 2.2	19.7 ± 1.6	21.0 ± 2.1	18.8 ± 1.6
MAP at peak (mmHg)	39.8 ± 7.5	40.5 ± 5.3	40.2 ± 5.2	37.1 ± 5.3
MAP at plateau (mmHg)	54.3 ± 9.1	51.9 ± 7.5	46.2 ± 8.2	46.6 ± 8.9

Artificially ventilated pentobarbitone-anaesthetized rabbits: nitric oxide (NO) in exhaled air and mean arterial blood pressure (MAP) during infusions of GTN (100 μg kg^{-1} min^{-1}, i.v.) in the absence (control), or presence of L-cysteine (200 mg kg^{-1}, i.v.). N-acetyl-cysteine (200 mg kg^{-1}, i.v.), or glutathione (200 mg kg^{-1}, i.v.) 15 min prior to GTN. Thirty-min resting periods were allowed between the infusions. Values were obtained at the time when the NO concentration peaked and at the end of a 15 min infusion period. There were no statistically significant differences between responses in the control group, compared to the groups which had been pretreated with L-cysteine, N-acetyl-cysteine or glutathione, respectively. Means ± s.e.mean, $n = 5$–6.

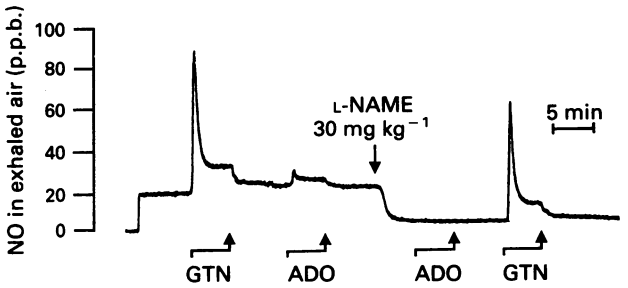


Figure 3 Artificially-ventilated, pentobarbitone-anaesthetized rabbit: recordings of NO in exhaled air. Effect of 5 min infusions of nitroglycerin (GTN, 1 mg ml^{-1}) or adenosine (0.7 mg ml^{-1}, 250 μl kg^{-1} min^{-1}, i.v.) before and after the NO-synthase inhibitor N$^{\omega}$-nitro-L-arginine methyl ester (L-NAME, 30 mg kg^{-1}, i.v.) is shown. The first min of the recording indicates the NO concentration in the inhaled synthetic air.

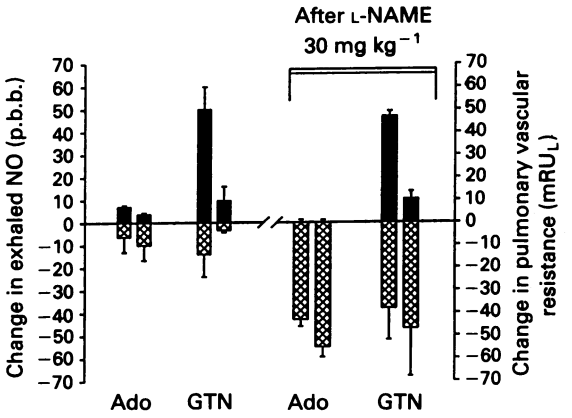


Figure 4 Artificially-ventilated, pentobarbitone-anaesthetized rabbits: changes in NO in exhaled air (filled columns, left ordinate scale) and pulmonary vascular resistance (crosshatched columns, right ordinate scale). Effects of 5 min infusions of nitroglycerin (GTN, 1 mg ml^{-1}, 250 μl kg^{-1} min^{-1}, i.v.) or adenosine (Ado, 0.7 mg ml^{-1}, 250 μl kg^{-1} min^{-1}, i.v.) before and after the NO-synthase inhibitor N$^{\omega}$-nitro-L-arginine methyl ester (L-NAME, 30 mg kg^{-1}, i.v.) are shown. The changes, compared to values immediately prior to each infusion, in NO concentration and pulmonary vascular resistance during the initial peak and at the end of infusion are shown for each infusion. Means ± s.e.mean, $n = 3$.

adenosine evoked a markedly smaller ($P<0.05$) increase (7 ± 1 p.p.b.) (Figure 3). L-NAME (30 mg kg^{-1}, i.v.) evoked an increase in pulmonary vascular resistance from 116 ± 19 to 147 ± 9 mRU$_L$ ($P<0.05$). After L-NAME the drop in pulmonary vascular resistance induced by adenosine or GTN was increased to a similar degree. However, while the increase in exhaled NO by GTN was unaffected by L-NAME, the small increase in exhaled NO concentration by adenosine was abolished (Figures 3 and 4).

Discussion

The present findings demonstrate that NO is formed upon infusion of GTN *in vivo* and that there is a correlation between the increased NO formation and the reduction in systemic blood pressure. This supports the hypothesis that NO is the active metabolite of GTN and suggests that bioconversion of GTN can be studied *in vivo*. Furthermore, the lack of effect of L-NAME on the GTN-induced NO production indicates that GTN, rather than L-arginine (cf. Moncada, 1992), was the source of the increased NO detected in exhaled air.

The concentration of exhaled NO, as well as the blood pressure response, exhibited biphasic patterns with an early peak, and a later and markedly less pronounced plateau. This observation suggests the participation of a rapidly activated mechanism in the development of tolerance to GTN which may result from inhibition of the enzymatic bioactivation pathway of nitrovasodilators (cf. Needleman & Krantz, 1965; Noack & Feelisch, 1991) or interference with the non-enzymatic, sulphydryl-dependent bioactivation (Noack & Feelisch, 1991). Since, in the present study, three different thiols failed to affect the response, the availability of thiols is apparently not the main restraint on formation of NO from GTN *in vivo*. In addition, the present findings also imply that tolerance is not exclusively due to direct interference with guanylate cyclase activity (Andersson & Axelsson, 1983). Pulmonary vasodilatation accompanied by increased clearance of NO from the alveolar space by blood haemoglobin (cf. Borland & Higenbottam, 1989; Persson *et al.*, 1993) is not likely to explain the decrement and plateau concentration of NO during GTN-infusion since adenosine at a dose that induced similar pulmonary vasodilatation only to a very limited degree affected the concentration of *endogenous* NO in exhaled air. This finding also makes it unlikely that increased endothelial shear stress is a major stimulus for the increased concentrations of NO in exhaled air upon GTN infusions. Thus, our findings rather point to decreased biotransformation of GTN to NO (Brien *et al.*,

1986), possibly as a consequence of metabolite inhibition (cf. Cossum & Roberts, 1985; Andersson & Ahlner, 1987), as an important mechanism for tolerance towards GTN. Furthermore, we found that the concentration of endogenous NO in exhaled air was reduced after repeated infusions of GTN or inhibition of NO synthesis from L-arginine (cf. Moncada, 1992) by GTN or its metabolites.

In conclusion, direct evidence for NO formation from GTN *in vivo* was found, and the NO generation correlated with the blood pressure effects. A rapid tolerance to GTN was observed, which was due largely to reduced NO formation and was unaffected by administration of thiols.

We would like to thank Mr Armin Guhl for excellent technical assistance. This study was supported by the Swedish National Environmental Protection Board (Proj. No. 11321), the Swedish Society Against Asthma and Allergy, the Swedish Medical Research Council (7919), the Karolinska Institute, the IEM, Tore Nilsson's Fund, Stiftelsen Ragnhild och Einar Lundströms Minne and Stiftelsen Lars Hiertas Minne.

References

ANDERSSON, K.L. & AHLNER, J. (1987). Nitrate tolerance from a biochemical point of view. *Drugs*, **33** (suppl 4), 63–68.

ANDERSSON, K.L. & AXELSSON, R.G.G. (1983). Tolerance towards nitroglycerin, induced in vivo, is correlated to a reduced cGMP response and an alteration in cGMP turnover. *Eur. J. Pharmacol.*, **88**, 71–79.

BORLAND, C.D.R. & HIGENBOTTAM, T.W. (1989). A simultaneous single breath measurement of pulmonary diffusing capacity with nitric oxide and carbon monoxide. *Eur. Resp. J.*, **2**, 56–63.

BRIEN, J.F., MCLAUGHLIN, B.E., BREEDON, T.H., BENNET, B.M., NAKATSU, K. & MARKS, G.S. (1986). Biotransformation of glyceryl trinitrate occurs concurrently with relaxation of rabbit aorta. *J. Pharmacol. Exp. Ther.*, **237**, 608–614.

COSSUM, P.A. & ROBERTS, M.S. (1985). Metabolite inhibition of nitroglycerin metabolism in sheep tissue homogenates. *J. Pharmaceut. Pharmacol.*, **37**, 807–809.

DIAMOND, J. & BLISSARD, K.S. (1976). Effects of stimulant and relaxant drugs on tension and cyclic nucleotide levels in canine femoral artery. *Mol. Pharmacol.*, **12**, 688–692.

FEELISCH, M. & NOACK, E. (1987). Correlation between nitric oxide formation during degradation of organic nitrates and activation of guanylate cyclase. *Eur. J. Pharmacol.*, **139**, 19–30.

GUSTAFSSON, L.E., LEONE, A.M., PERSSON, M.G., WIKLUND, N.P. & MONCADA, S. (1991). Endogenous nitric oxide is present in the exhaled air of rabbits, guinea pigs and humans. *Biochem. Biophys. Res. Commun.*, **181**, 852–857.

IGNARRO, L.J., LIPPTON, H., EDWARDS, J.C., BARICOS, W.H., HYMAN, A.L., KADOWITZ, P.J. & GRUETTER, C.A. (1980). Mechanism of vascular smooth muscle relaxation by organic nitrates, nitrites, nitroprusside, and nitric oxide: evidence for the involvement of S-nitrosothiols as active intermediates. *J. Pharmacol. Exp. Ther.*, **218**, 739–749.

MONCADA, S. (1992). The 1991 Ulf v Euler lecture, The L-arginine: nitric oxide pathway. *Acta Physiol. Scand.*, **145**, 201–227.

NEEDLEMAN, P. & KRANTZ, J.C. (1965). The biotransformation of nitroglycerin. *Biochem. Pharmacol.*, **14**, 1225–1230.

NEEDLEMAN, P. & JOHNSON, E.M.Jr. (1973). Mechanism of tolerance development to organic nitrates. *J. Pharmacol. Exp. Ther.*, **184**, 709–715.

NOACK, E. & FEELISCH, M. (1991). Molecular aspects of nitrovasodilator bioactivation. *Basic Res. Cardiol.*, **86** (suppl 2), 37–50.

PERSSON, M.G., GUSTAFSSON, L.E., WIKLUND, N.P., MONCADA, S. & HEDQVIST, P. (1990). Endogenous nitric oxide as a probable modulator of pulmonary circulation and hypoxic pressor response *in vivo*. *Acta Physiol. Scand.*, **140**, 449–457.

PERSSON, M.G., WIKLUND, N.P. & GUSTAFSSON, L.E. (1993). Endogenous nitric oxide in single exhalations, and change during exercise. *Am. Rev. Resp. Dis.*, **148**, 1210–1214.

(Received November 8, 1993
Accepted November 23, 1993)

Br. J. Pharmacol. (1994), **111**, 829–836 © Macmillan Press Ltd, 1994

Differential action of (+)-amphetamine on electrically evoked dopamine overflow in rat brain slices containing corpus striatum and nucleus accumbens

[1]Walter J. Wieczorek & Zygmunt L. Kruk

Department of Pharmacology, Queen Mary & Westfield College, Mile End Road, London E1 4NS

1 The effects of (+)-amphetamine on electrically evoked dopamine overflow were examined in the rat brain slice containing either anterior caudate putamen (aCPu) or nucleus accumbens (NAc), by fast cyclic voltammetry.

2 (+)-Amphetamine (1 μM) caused a time-dependent increase in the extracellular concentration of dopamine ($[dopamine]_{ex}$) due to displacement of dopamine from terminal sites. After a 40 min superfusion, $[dopamine]_{ex}$ in the aCPu was 0.617 ± 0.117 μM and in the NAc was 0.270 ± 0.04 μM. Pretreatment with (−)-sulpiride (1 μM) did not affect this action of (+)-amphetamine.

3 (+)-Amphetamine (1 μM) exhibited a complex and time-dependent effect on electrically stimulated dopamine overflow, evoked by 1p, 4p/10 Hz and 20p/20 Hz.

4 In the aCPu, (+)-amphetamine (1 μM) resulted in attenuation of dopamine overflow due to 1p and 4p/10 Hz but potentiation of dopamine overflow to 20p/20 Hz. (−)-Sulpiride (1 μM) prior to (+)-amphetamine (1 μM) reversed the attenuation of dopamine overflow evoked by 1p and 4p/10 Hz but had no significant effect on dopamine overflow evoked by 20p/20 Hz.

5 (+)-Amphetamine (1 μM) potentiated dopamine overflow in the NAc to all three stimuli. (−)-Sulpiride (1 μM) prior to (+)-amphetamine (1 μM), resulted initially, in a further potentiation of overflow, followed by a time-dependent attenuation of dopamine overflow to all three stimuli.

6 $t_{1/2}$, the rate of removal of $[dopamine]_{ex}$ following electrical stimulation was not significantly different in the aCPu and NAc for any of the stimulation conditions. After a 40 min superfusion with (+)-amphetamine (1 μM), $t_{1/2}$ for 1p, 4p/10 Hz and 20p/20 Hz was significantly increased in both the aCPu and NAc, the increase in $t_{1/2}$ being significantly greater in the aCPu than in the NAc.

7 In conclusion, this study indicates that the dopamine displacement and uptake inhibitory actions of (+)-amphetamine result in complex and differential effects on electrically evoked dopamine overflow in the aCPu and NAc.

Keywords: Fast cyclic voltammetry; dopamine; brain slices; nucleus accumbens; caudate putamen; (+)-amphetamine; D_2 autoreceptors

Introduction

The psychostimulant effects of (+)-amphetamine are believed to be mediated by its actions on dopaminergic neurotransmission. The increased locomotor and stereotypy behaviour produced by (+)-amphetamine are attributed to increased extracellular levels of dopamine in the nucleus accumbens and corpus-striatum respectively (Moore, 1978; Kuczenski, 1983; McMillan, 1983). It has been proposed that dopamine is distributed heterogenously within two distinct intraneuronal storage compartments, a newly-synthesized, α-methyl-*p*-tyrosine-sensitive, cytoplasmic pool and a reserpine-sensitive, vesicular pool that is involved in neurogenic dopamine release (Glowinski, 1975; McMillan *et al.*, 1980). These two storage compartments are thought to be in dynamic equilibrium with each other (Parker & Cubeddu, 1986b).

(+)-Amphetamine displaces dopamine from synaptosomes or brain slices containing dopaminergic nerve terminals by a mechanism which is not related to calcium-dependent exocytotic events (Azzaro & Rutledge, 1973; Fischer & Cho, 1979; Raiteri *et al.*, 1979; Jacocks & Cox, 1992). Although (+)-amphetamine can enter the nerve by passive diffusion, a functional carrier system is a prerequisite for displacement of dopamine into the extracellular space by (+)-amphetamine, as this displacement can be inhibited by dopamine neuronal uptake inhibitors (Fischer & Cho, 1979; Raiteri *et al.*, 1979; Parker & Cubeddu, 1988; Jacocks & Cox, 1992).

It has been suggested that (+)-amphetamine displaces dopamine into the extracellular space by the reversal of the dopamine neuronal uptake system (Fischer & Cho, 1979; Parker & Cubeddu, 1988; Jacocks & Cox, 1992). The hypothesis states that (+)-amphetamine acts as a substrate for the carrier molecule and accelerates the inward movement of the carrier, making it available for the outward transport of cytoplasmic free dopamine. The increase in the cytoplasmic concentration of (+)-amphetamine results in an elevation of cytoplasmic free dopamine due to both the displacement of dopamine from intraneuronal stores (Moore, 1978; McMillan, 1983; Sulzer *et al.*, 1993) and the monoamine oxidase inhibitory action of (+)-amphetamine (Miller *et al.*, 1980). As a substrate for the dopamine carrier system, (+)-amphetamine also acts as a dopamine neuronal uptake inhibitor (Horn *et al.*, 1970; Heikilla *et al.*, 1975; Hyttel, 1978; Parker & Cubeddu, 1988).

Although the mechanisms of action of (+)-amphetamine on dopaminergic neurotransmission are well documented, relatively few studies have investigated the effect of (+)-amphetamine on electrically evoked dopamine efflux and these studies have yielded conflicting results. *In vivo*, electrical stimulation of the median forebrain bundle in the presence of (+)-amphetamine resulted in an increase in the efflux of [^{3}H]-dopamine from the caudate nucleus (Von Voigtlander & Moore, 1973). By contrast, Kuhr *et al.* (1986) using a voltammetric technique, showed that (+)-amphetamine attenuated electrically evoked endogenous dopamine efflux in the caudate nucleus but had no effect on dopamine efflux in the

[1] Author for correspondence.

nucleus accumbens. *In vitro*, (+)-amphetamine either enhanced electrically evoked dopamine efflux, when measured by high performance liquid chromatography (h.p.l.c.) (Parker & Cubeddu, 1986b), or reduced the release of [^{3}H]-dopamine (Kamal *et al.*, 1983) from brain slices containing striatum. This lack of consensus may be due to the differing techniques used. The results obtained using radiolabelled dopamine or precursor to demonstrate the effect of drugs on different dopamine storage pools have been shown not to parallel the action of these drugs on endogenous dopamine (Herdon *et al.*, 1985). The use of h.p.l.c. (Parker & Cubeddu, 1986b) required a 35 min incubation and 15 min collection period of perfusate after electrical stimulation. Actions of (+)-amphetamine on electrical stimulation during the 35 min period could not be measured. In the *in vivo* voltammetric study (Kuhr *et al.*, 1986), the effect of (+)-amphetamine on dopamine release was monitored every 20 min.

The problem of monitoring the action of (+)-amphetamine more frequently during the course of an experiment can be overcome by using fast cyclic voltammetry in brain slices. Fast cyclic voltammetry is a technique that can measure electrically evoked endogenous dopamine overflow from anatomically precise regions, in real time and over a wide range of stimulation frequencies (Trout & Kruk, 1992). This technique has been used to study the action of D_2 autoreceptor agonists, antagonists and dopamine neuronal uptake inhibitors on electrically evoked dopamine overflow in various regions of the rat brain (Bull *et al.*, 1990; Trout & Kruk, 1992; Patel *et al.*, 1992; Wieczorek & Kruk, 1992).

In this study we set out to examine the time course of action of (+)-amphetamine on (i) extracellular concentration of dopamine arising from exchange diffusion and (ii) on electrically evoked dopamine overflow, in brain slices of the rat anterior caudate putamen and nucleus accumbens. The electrical stimulation parameters used were a single pulse (a stimulation that does not cause autoinhibition; Limberger *et al.*, 1991); 20 pulses at 20 Hz, the maximum stimulus at which consistent responses could be obtained and 4 pulses at 10 Hz, a stimulus closer to reported physiological rates of firing of dopamine neurones in the substantia nigra and ventral tegmental area (Freeman *et al.*, 1985). As (+)-amphetamine elevates extracellular concentrations of dopamine there is the possibility that D_2 autoreceptors may be activated. We therefore studied the role of D_2 autoreceptors in modulating the effect of (+)-amphetamine on electrically evoked dopamine efflux using the D_2 receptor antagonist, (−)-sulpiride.

Methods

Male Sprague Dawley rats (200–300 g) were killed and the brain rapidly removed into ice-cold artificial cerebrospinal fluid (ACSF). Blocks of tissue containing anterior caudate putamen (aCPu) and nucleus accumbens (NAc) were prepared. Slices, 350 μm thick, corresponding to the coronal sections described by Paxinos & Watson (1986), were prepared from the aCPu and NAc, (1.7 and 2.2 mm anterior to bregma respectively) using an Oxford Vibratome. The brain slice was transferred to a full immersion bath, made to a design of Richards & Tegg (1977), placed on a stainless steel grid and held in place by a nylon mesh. The slice was superfused with ACSF at 1 ml min^{-1}, 32°C. Following 1 h equilibration, the carbon fibre recording microelectrode (7 μm diam., 30–50 μm long) was placed into the desired region. A bi-polar tungsten wire stimulating electrode was placed in white matter 200–300 μm from the recording electrode. Both electrodes were placed 80 μm below the slice surface.

Fast cyclic voltammetry (FCV) at the carbon fibre microelectrode, as described by Trout & Kruk (1992), was used to detect changes in extracellular concentrations of dopamine following electrical stimulation of the brain slice. FCV was performed with a Millar voltammeter (PD system Ltd., West Moseley, Surrey) using a triangular waveform, applied at 480 Vs^{-1}. Each scan lasted 15 ms and was repeated at 2 Hz. The stainless steel grid served as an auxillary electrode and a silver/silver chloride reference electrode was included in the potentiostat circuit. Changes at the peak oxidation potential for dopamine (+600 mV) were monitored using a sample and hold circuit in the voltammeter with an output to a Y-t chart recorder and to a Cambridge Electronic Design Ltd (CED) 1401 interface. Data were stored as files using CED software (SIGNAL AVERAGER and CHART). Each carbon fibre microelectrode was calibrated in a standard solution of dopamine.

Electrical stimulation was controlled using Neurolog signal conditioning apparatus with constant voltage stimulation provided by a DS2 stimulator. The stimulus applied consisted of either a single square wave pulse (1p) (0.1 ms, 20 V) or trains of pulses at the following frequencies; 4 pulses at 10 Hz (4p/10 Hz) and 20 pulses at 20 Hz (20p/20 Hz). The following stimulation protocol was used: time 0 min: 1p; 2.5 min: 4p/10 Hz; 5 min: 1p; 7.5 min: 20p/20 Hz; and repeated until reproducible responses were obtained (usually 4 cycles).

Superfusion of brain slices with ACSF containing drug commenced immediately after the last control response. Slices were superfused with (i) (+)-amphetamine (1 μM) for 40 min; (ii) (−)-sulpiride (1 μM) for 50 min followed by a combined solution of (+)-amphetamine (1 μM) and (−)-sulpiride (1 μM) for 40 min or (iii) benztropine (1 μM) for 60 min. During each of these superfusion procedures the tissues were electrically stimulated according to the above stimulation protocol. Preliminary experiments indicated that (+)-amphetamine (1 μM) was the lowest concentration at which consistent effects on electrically evoked dopamine overflow could be observed. The concentration and duration of the superfusion with (−)-sulpiride and benztropine were those required to give a maximum effect.

Drugs and solutions

ACSF was prepared fresh every day according to following formula (all values are mM): NaCl 125, KCl 2, KH_2PO_4 1.25, $MgSO_4$ 7 H_2O 2.0, $NaHCO_3$ 25, D-glucose 11, $CaCl_2$ 2 H_2O 2.0, in distilled water and equilibrated at 32°C for at least 1 h with 95% O_2:5% CO_2 before use. (+)-Amphetamine sulphate (Sigma) and benztropine methane-sulphonate (Sigma) were dissolved in distilled water. (−)-Sulpiride (Sigma) was dissolved in 1 ml of tartaric acid (10^{-2} M, Sigma) and made up to 10 ml with distilled water. All drugs were diluted in ACSF to the final concentration used.

Statistics

Results are expressed as arithmetic means ± standard error of the mean (s.e.mean). Groups were compared with Student's unpaired *t* test (two-tailed) if analysis of variance tests indicated a significant difference. *n* = number of brain slices.

Terminology

FCV measures the concentration of dopamine that has overflowed from the synapse into the extracellular space and the term 'overflow' will be used to denote dopamine release due to electrical stimulation. The dopamine overflow evoked by electrical stimulation resulted in a rapid but transient increase in current flow at the peak oxidation potential. For any given stimulation the point at which there is maximum current flow, is termed the 'peak dopamine overflow' (Figure 3). The dopamine overflow for 1p in the two regions is variable (see Results). To normalize the results, peak dopamine overflows to 4p/10 Hz and 20p/20 Hz were expressed as a ratio of peak dopamine overflow for 1p.

Results

(+)-Amphetamine and baseline response

The changes in oxidation current monitored in a non stimulated tissue (i.e. no electrical stimulation and no drug) are small and result in a flat Y-t trace. This is referred to as the baseline response. A 40 min superfusion with (+)-amphetamine (1 μM) produced a time dependent rise in the baseline, in both the aCPu and NAc. The rise in baseline was due to an increase in the extracellular dopamine concentration. This was confirmed by the electronic subtraction of the charging current immediately before and after a 40 min superfusion with (+)-amphetamine, resulting in a faradaic current waveform which was indistinguishable from that obtained in a solution of dopamine (1 μM) (Figure 1c,d). The increase in extracellular dopamine concentration after a 40 min superfusion with (+)-amphetamine (1 μM) was significantly greater in the aCPu (0.617 ± 0.117 μM) than in the NAc (0.270 ± 0.047 μM; $P<0.001$), as shown in Figure 2. Superfusion of the brain slice with (−)-sulpiride (1 μM) for 50 min did not alter the baseline response and did not significantly alter the rise in baseline response to (+)-amphetamine (1 μM) (results not shown).

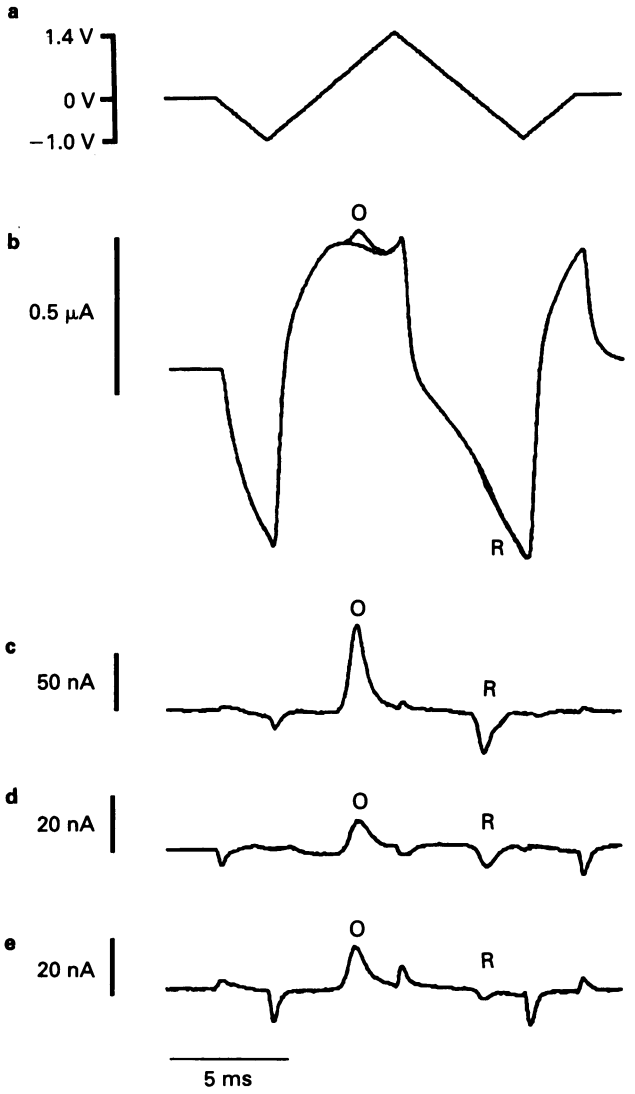


Figure 1 Fast cyclic voltammetry in rat brain slices: (a) One and a half cycles of a symmetrical 100 Hz saw-tooth waveform with a voltage ramp of 480 Vs^{-1}, are applied to a carbon fibre microelectrode twice a second, sweeping from zero volts (relative to a silver/silver chloride reference electrode) to −1.0 V, +1.4 V, −1.0 V and back to 0.0 V. (b) The charging current waveform is shown. When dopamine is present, oxidation (O) and reduction (R) peaks appear superimposed on the charging current waveform at a position corresponding to the oxidation potential (600 mV) and reduction potential (−200 mV) for dopamine, respectively. The subtraction of the charging current waveform in the absence from that in the presence of dopamine results in a faradaic waveform characteristic for dopamine. (c) Faradaic waveform obtained in a solution of dopamine (1 μM) in artificial cerebrospinal fluid. (d) Faradaic waveform due to displacement of neurotransmitter in the anterior caudate putamen after a 40 min superfusion with (+)-amphetamine (1 μM). (e) Faradaic waveform following electrical stimulation with 25 pulses at 50 Hz in the anterior caudate putamen. The vertical calibration bars indicate the current detected at the carbon fibre microelectrode. The time bar provides a calibration for the duration of the voltammetric scan in ms.

Electrically stimulated dopamine overflow

The substance detected at the carbon fibre electrode following electrical stimulation of nerve terminals in either the aCPu or NAc was confirmed as dopamine by electronic subtraction of the charging current before and after stimulation with 25 pulses at 50 Hz (25p/50 Hz). This resulted in a faradaic current waveform which was indistinguishable from that obtained in a solution of dopamine (1 μM) (Figure 1c,e). Although the recording microelectrode was placed visually into the selected area, confirmation was made by comparing the ratio of the peak dopamine overflow for 25p/50 Hz: 1p. The peak dopamine overflow to 25p/50 Hz is the maximum in both regions. The ratio of peak dopamine overflow for 25p/50 Hz: 1p in the NAc (8.66:1(± 0.52)) is significantly greater than in the aCPu (2.12:1(± 0.12), $P<0.001$). Only sites at which the ratios were approximately 2:1 in the aCPu and greater than 6:1 in the NAc were used in this study.

The extracellular concentration of dopamine after an electrical stimulation of 1p in the aCPu (0.081 ± 0.01 μM; range 0.03 to 0.18 μM; $n = 16$) was not significantly different from

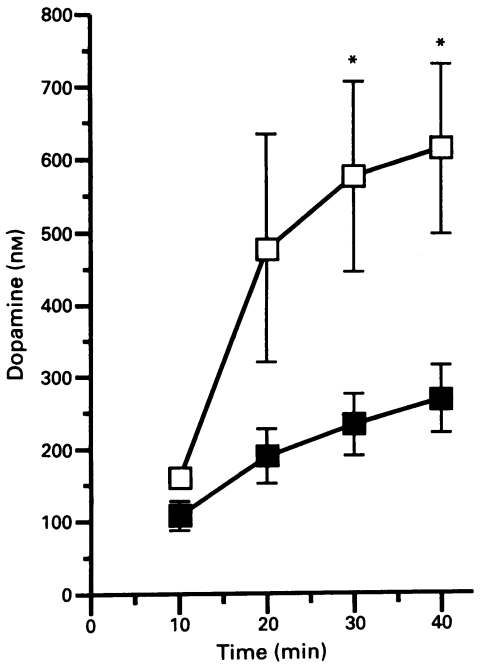


Figure 2 Time-dependent increase in the extracellular concentration of dopamine, as a consequence of exchange diffusion, due to a 40 min superfusion with (+)-amphetamine (1 μM). Superfusion started at time 0 and measurements were made at 10 min intervals in both the anterior caudate putamen (□) and nucleus accumbens (■). Each point is a mean ± s.e.mean, $n = 4–5$; *$P<0.05$ (aCPu *v* NAc).

that due to 1p in the NAc (0.093 ± 0.01 μM; range 0.038 to 0.17 μM; $n = 17$). A representative trace of the responses to electrical stimulation in both the aCPu and NAc is shown in Figure 3, which also illustrates how the various measurements referred to in this paper were made.

The ratios of peak dopamine overflow for 4p/10 Hz:1p and 20p/20 Hz:1p differed between the aCPu and NAc, in that the ratio for 20p/20 Hz:1 was higher in the NAc than in the aCPu (Trout & Kruk, 1992) (Figure 4). Pretreatment with (−)-sulpiride (1 μM), a D_2 receptor antagonist, did not significantly alter the peak dopamine overflow to 1p in either the aCPu or NAc. The ratio of peak dopamine overflow for 4p/10 Hz:1p was not significantly increased in either region but that for 20p/20 Hz:1p was significantly increased in both the aCPu and NAc (Figure 4).

(+)-Amphetamine and electrically stimulated overflow of dopamine

The effect of (+)-amphetamine (1 μM) on electrically stimulated dopamine overflow depended upon the region and stimulation parameter. In the aCPu, (+)-amphetamine (1 μM) produced a time-dependent decrease in peak dopamine overflow to electrical stimulation with 1p and 4p/10 Hz. The peak dopamine overflow evoked by 20p/20 Hz was increased two fold for the duration of the experiment (Figure 5). After pretreatment with (−)-sulpiride (1 μM) for 50 min, peak dopamine overflow to 1p, in the presence of (+)-amphetamine (1 μM), was initially potentiated followed by a time-dependent attenuation of overflow (Figure 5a). The peak dopamine overflow to 1p in the presence of (−)-sulpiride (1 μM) and (+)-amphetamine (1 μM) was significantly greater at all time points than that observed with (+)-amphetamine (1 μM) alone.

Pretreatment with (−)-sulpiride (1 μM) resulted in significantly increased peak dopamine overflow to 4p/10 Hz in the presence of (+)-amphetamine (1 μM) when compared to (+)-amphetamine (1 μM) alone (Figure 5b).

Initially, superfusion with (−)-sulpiride (1 μM) increased the peak dopamine overflow to 20p/20 Hz by 50%, subsequent superfusion with (+)-amphetamine (1 μM) did not result in a further significant increase in peak dopamine overflow (Figure 5c).

In the NAc, the peak dopamine overflow to 4p/10 Hz and 20p/20 Hz was potentiated by (+)-amphetamine (1 μM) for the duration of experiment. Although the peak dopamine overflow to 1p was initially increased by (+)-amphetamine (1 μM), it rapidly declined to its pre-drug level (Figure 6). After pretreatment with (−)-sulpiride (1 μM) for 50 min, superfusion with (+)-amphetamine (1 μM) resulted, initially, in a significant potentiation of dopamine overflow to 1p, 4p/10 Hz and 20p/20 Hz, after which peak dopamine overflow to all three stimuli was significantly attenuated when compared to overflow in the presence of (+)-amphetamine (1 μM) alone (Figure 6).

(+)-Amphetamine and rate of dopamine re-uptake

Comparisons of the rate at which electrically evoked dopamine is removed from extracellular space can be made by measuring $t_{1/2}$ (the time in s for a peak dopamine overflow to decline by 50%); this is illustrated for raw data in Figure 2.

$t_{1/2}$ measurements following 1p, 4p/10 Hz and 20p/20 Hz stimulations were obtained at the end of each control or drug superfusion period. The $t_{1/2}$ for 1p, 4p/10 Hz and 20p/20 Hz was not significantly different in the aCPu and NAc (Table 1) and these values were not altered by superfusion with (−)-sulpiride (1 μM). (+)-Amphetamine (1 μM) significantly increased $t_{1/2}$ for all stimulation parameters, in both aCPu and NAc, when compared with control. The increase in $t_{1/2}$ was significantly greater in the aCPu than in the NAc (Table 1). Pretreatment with (−)-sulpiride (1 μM) further increased the

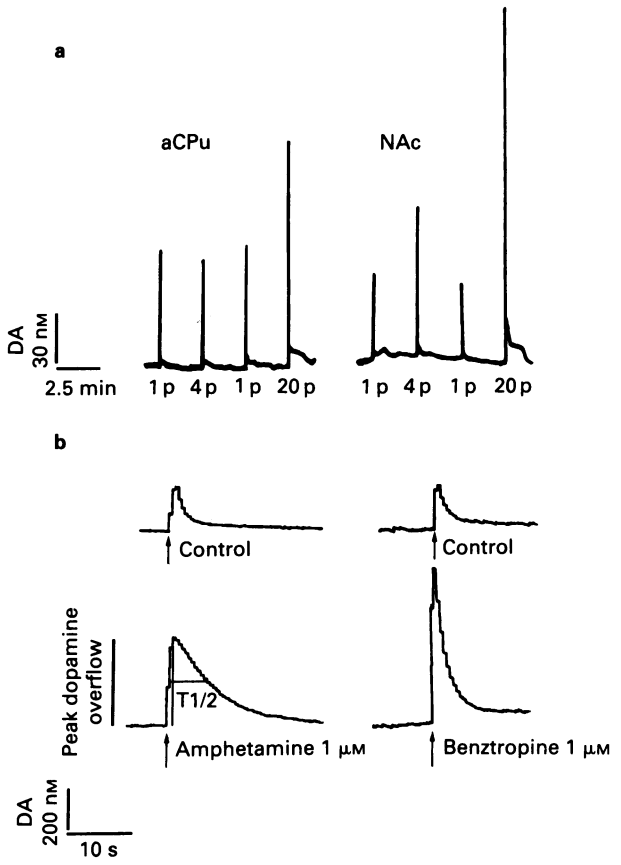


Figure 3 (a) Typical sample and bold trace from a Y–t recorder, illustrating changes in dopamine (DA) overflow following stimulation with a single pulse (1p), 4p/10 Hz (4p) and 20p/20 Hz (20p) in the anterior caudate putamen (aCPu) and nucleus accumbens (NAc). The figure also illustrates the stimulation protocol which was used for this series of experiments. (b) Typical set of sample and hold traces obtained using the CED 1401 interface, recorded on a faster time base than in (a), illustrating the effects of pretreatment with (+)-amphetamine (1 μM) for 40 min or benztropine (1 μM) for 60 min on the peak dopamine overflow and $t_{1/2}$ to electrical stimulation of 20p/20 Hz (↑ arrow) in the anterior caudate putamen (aCPu).

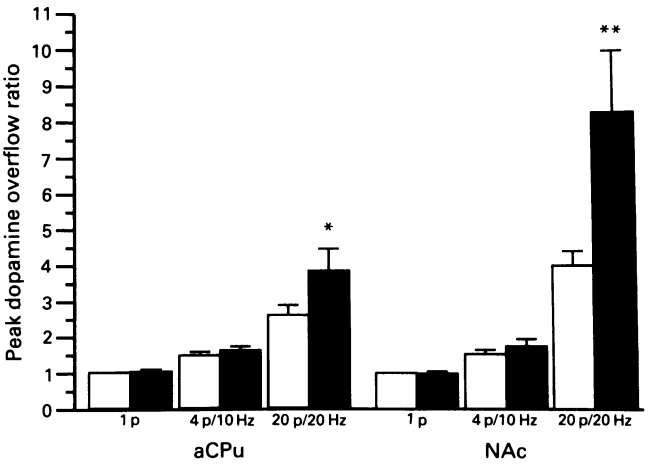


Figure 4 A comparison of the peak dopamine overflow evoked by electrical stimulation with 1p, 4p/10 Hz and 20p/20 Hz expressed as peak dopamine overflow ratios relative to 1p. Control (open columns) and after 50 min superfusion with (−)-sulpiride (1 μM) (solid columns), in the anterior caudate putamen (aCPu) and nucleus accumbens (NAc). Each column is a mean ± s.e.mean, $n = 5–6$; $^*P < 0.05$; $^{**}P < 0.001$ (control *v* sulpiride at that frequency and brain region).

effect of (+)-amphetamine (1 μM) on $t_{1/2}$ in both the aCPu and NAc.

By comparison, benztropine (1 μM), a dopamine uptake inhibitor with no indirect dopamine releasing action or monoamine oxidase inhibitory activity, significantly increased $t_{1/2}$ for all three stimulations in the aCPu, although the increases were relatively small compared to those observed with (+)-amphetamine (1 μM), but had no effect on $t_{1/2}$ in the NAc (Table 1). Benztropine (1 μM) increased peak dopamine overflow to 1p, 4p/10 Hz and 20p/20 Hz in the aCPu by 162 ± 13%; 339 ± 69%; 519 ± 110% and in the NAc by 114 ± 28%; 118 ± 28%; 93 ± 27% (mean ± s.e.mean; $n = 4$) respectively.

Discussion

The behavioural effects of (+)-amphetamine in the central nervous system are considered to be primarily mediated by its action on dopaminergic neurotransmission. Activation of

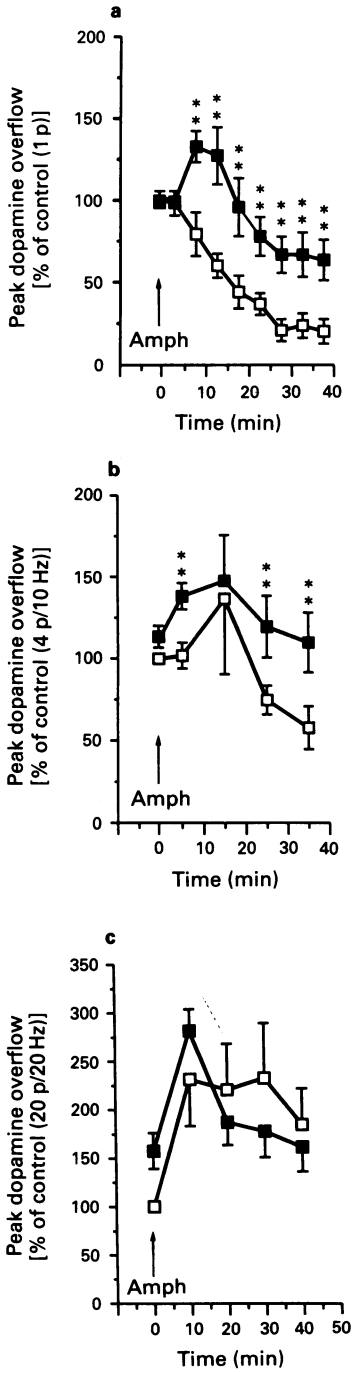


Figure 5 The time course of action of (+)-amphetamine (1 μM) added at time 0 (↑ Amph), alone (□) or after superfusion with (−)-sulpiride (1 μM) for 50 min (■) on peak dopamine overflow to electrical stimulation of (a) 1p; (b) 4p/10 Hz and (c) 20p/20 Hz in the anterior caudate putamen. In any given brain slice, the peak dopamine overflow to 1p, 4p/10 Hz and 20p/20 Hz obtained prior to superfusion with either drug was considered to be control values (100%) against which all subsequent responses were compared. All points are a mean ± s.e.mean, $n = 4$–6. $^{**}P < 0.001$.

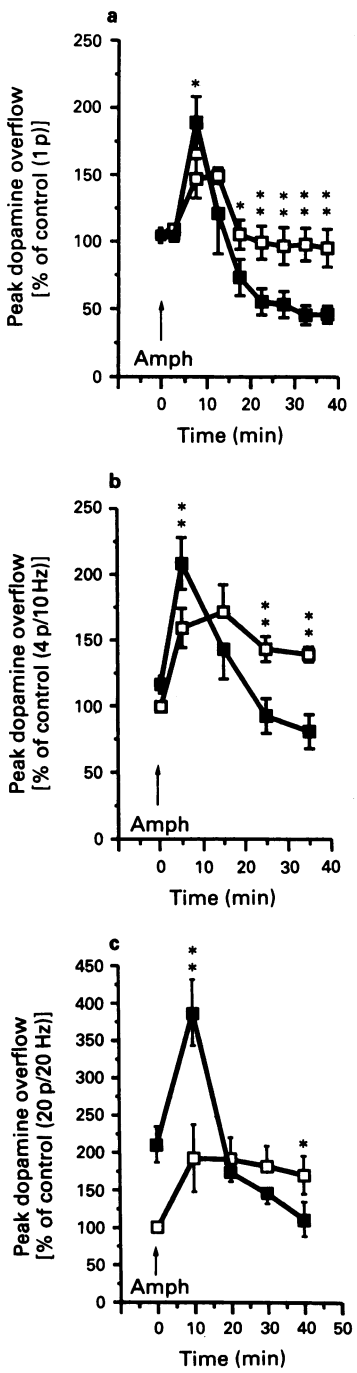


Figure 6 The time course of action of (+)-amphetamine (1 μM) added at time 0 (↑ Amph) alone (□) or after superfusion with (−)-sulpiride (1 μM) for 50 min (■), on peak dopamine overflow to electrical stimulation of (a) 1p; (b) 4p/10 Hz and (c) 20p/20 Hz in the nucleus accumbens. In any given brain slice, the peak dopamine overflow to 1p, 4p/10 Hz and 20p/20 Hz obtained prior to superfusion with either drug was considered to be the control value (100%) against which all subsequent responses were compared. All points are a mean ± s.e.mean, $n = 4$–6. $^{*}P < 0.05$; $^{**}P < 0.001$.

Table 1 Effect of (+)-amphetamine, (−)-sulpiride and benztropine on $t_{1/2}$ (s) in the anterior caudate putamen (aCPu) and nucleus accumbens (NAc)

	1p	*4p/10 Hz*	*20p/20 Hz*	n
aCPu				
Control	1.36 ± 0.18	1.35 ± 0.1	1.92 ± 0.12	14
(+)-Amphetamine (1 μM)	10.8 ± 3.9**†	10.8 ± 2.9**†	18.1 ± 3.9**†	4
Sulpiride (1 μM)	1.16 ± 1.3	1.50 ± 0.18	1.83 ± 0.11	6
(+)-Amphetamine (1 μM) + Sulpiride (1 μM)	8.31 ± 1.3	20.4 ± 8.2	35.9 ± 15.6	6
Benztropine (1 μM)	1.78 ± 0.14	1.84 ± 0.2*	2.34 ± 0.18	4
NAc				
Control	1.28 ± 0.11	1.51 ± 0.13	2.12 ± 0.14	14
(+)-Amphetamine (1 μM)	4.32 ± 0.7**	5.20 ± 0.7**	10.2 ± 3.0**	5
Sulpiride (1 μM)	1.40 ± 0.1	1.50 ± 0.16	2.20 ± 0.2	5
(+)-Amphetamine (1 μM) + Sulpiride (1 μM)	6.35 ± 0.4*	9.60 ± 2.24*	34.0 ± 16	5
Benztropine (1 μM)	1.34 ± 0.18	1.98 ± 0.4	2.84 ± 0.5	4

All values are mean ± s.e.mean.
**$P<0.001$ versus control: *$P<0.05$ versus (+)-amphetamine (1 μM): †$P<0.05$ aCPu (+)-amphetamine (1 μM) *v* NAc (+)-amphetamine (1 μM).

the mesolimbic and mesostriatal systems are manifested via the nucleus accumbens and caudate putamen as locomotion and stereotyped behaviour, respectively (Moore, 1977; Kuczenski, 1983; McMillan, 1983). Recent studies indicate that somatodendritic dopamine sites are important for the expression of (+)-amphetamine activity (Kalivas, 1993) but these will not be considered here as this study was confined to the examination of the effects of (+)-amphetamine on dopamine axon terminals in the brain slice, physically separated from the nerve cell bodies.

The mechanisms by which (+)-amphetamine facilitates dopaminergic transmission include (i) displacement of dopamine from storage sites in the nerve terminals, resulting in carrier-mediated efflux of dopamine (Azzaro & Rutledge, 1973; Raiteri *et al.*, 1979; Parker & Cubeddu, 1986a,b); (ii) inhibition of re-uptake of dopamine (Horn *et al.*, 1970; Heikilla *et al.*, 1975; Parker & Cubeddu, 1988); (iii) stimulation of dopamine synthesis by removing end-product inhibition (Connor & Kuczenski, 1986) and (iv) inhibition of monoamine oxidase (Miller *et al.*, 1980).

Applying a range of anatomical, electrochemical and pharmacological criteria, it has previously been shown that the voltammetric signal, as measured in this study, following electrical stimulation in striatal brain slices can be attributed to a transient increase in extracellular dopamine concentration (Palij *et al.*, 1990; Bull *et al.*, 1990; Patel *et al.*, 1992; Trout & Kruk, 1992). By use of fast cyclic voltammetry it is possible to measure dopamine overflow evoked by a wide range of electrical stimuli, ranging from a single pulse to long trains applied over a wide range of frequencies with a time resolution which approaches real time (Bull *et al.*, 1990; Limberger *et al.*, 1991; Trout & Kruk, 1992).

Electrical stimulation of a brain slice resulted in a rapid, but transient rise in the extracellular dopamine concentration. However, when dopamine was displaced from nerve terminals by (+)-amphetamine (1 μM), there was a slow sustained rise in extracellular dopamine, resulting in a maximum extracellular dopamine concentration of 0.617 μM and 0.270 μM in the aCPu and NAc respectively. As dopamine is ionized at physiological pH, it cannot readily pass through membranes by diffusion in the absence of specific carrier molecules. Therefore, dopamine leaves the nerve terminal either by calcium-dependent exocytosis from vesicular stores, or by exchange diffusion, induced by displacement of dopamine from stores by drugs such as (+)-amphetamine (Sulzer *et al.*, 1993). For exchange diffusion to operate, the dopamine uptake system must be functional, as inhibitors of the dopamine uptake system prevent dopamine displacement by (+)-amphetamine (Raiteri & Levi, 1978; Fisher & Cho, 1979; Parker & Cubeddu, 1988).

In this study (+)-amphetamine induced significantly greater overflow of dopamine by exchange diffusion, from nerve terminals situated in the aCPu than from those in the NAc (Figure 2). These results agree with those obtained *in vivo* using microdialysis and h.p.l.c. (Jacocks & Cox, 1992; Guix *et al.*, 1992). The tissue content of dopamine in both areas is not significantly different (Beal & Martin, 1985; Marshall *et al.*, 1990); however, there is a a two fold greater number of dopamine uptake sites in the aCPu than in the NAc (Marshall *et al.*, 1990). This greater number of dopamine uptake sites in the aCPu would indicate a greater number of carrier molecules available for transferring the cyotplasmic free dopamine to the extracellular fluid and could account for the greater displacement of dopamine in the aCPu compared with the NAc.

When (+)-amphetamine was present in the superfusion fluid, it was possible to monitor electrically evoked dopamine overflow superimposed upon a baseline rise due to displacement of dopamine by the (+)-amphetamine. (+)-Amphetamine caused variable effects on electrically stimulated dopamine overflow in the aCPu and NAc dependent on the electrical stimulation parameters. In the aCPu, (+)-amphetamine produced a time-dependent attenuation of dopamine overflow evoked by 1p and 4p/10 Hz, whereas an increase in dopamine overflow was observed with 20p/20 Hz. In the NAc, in the presence of (+)-amphetamine, dopamine overflow was potentiated during 4p/10 Hz and 20p/20 Hz stimulation but with 1p after an initial increase in dopamine overflow there was a gradual return to control values.

The variable effects of (+)-amphetamine on electrically evoked dopamine overflow can be explained in terms of (i) activation of dopamine D_2 autoreceptors by the displaced endogenous dopamine, (ii) inhibition of dopamine uptake into neuronal and extraneuronal sites and (iii) depletion of dopamine stores by (+)-amphetamine and electrical stimulation.

In both the aCPu and NAc, the elevated extracellular dopamine concentrations due to displacement by (+)-amphetamine, exerted a D_2-mediated inhibitory action on electrically evoked dopamine overflow. This was indicated when pretreatment with (−)-sulpiride initially potentiated all responses to electrical stimulation in the presence of (+)-amphetamine, in both regions, whereas (−)-sulpiride alone, had a significant effect only at the non-physiological frequency (20p/20 Hz) in both regions. In the aCPu, at the lower stimulation parameters of 1p and 4p/10 Hz, the D_2-mediated inhibitory action of the extracellular dopamine (displaced by (+)-amphetamine) on electrically stimulated dopamine overflow, was the dominant action of (+)-amphetamine because the attenuation of the dopamine

overflow evoked by 1p and 4p/10 Hz in the presence of (+)-amphetamine was transformed to a potentiation after pretreatment with (−)-sulpiride.

In the NAc, the dopamine overflow evoked by 1p, 4p/10 Hz or 20p/20 Hz was potentiated in the presence of (+)-amphetamine, indicating that the inhibitory action of (+)-amphetamine on uptake was the dominant effect, even though D_2 receptor-mediated inhibition of release was present. In the NAc, in the presence of (−)-sulpiride and (+)-amphetamine, dopamine overflow following 20p/20 Hz stimulation was significantly greater than with (+)-amphetamine alone. Subsequent stimulations with 20p/20 Hz resulted in a markedly attenuated dopamine overflow. It is likely that under these conditions (i.e. (−)-sulpiride and (+)-amphetamine) repeated stimulation with 20p/20 Hz leads to a marked depletion of the vesicular storage pool. Dopamine overflow following 1p and 4p/10 Hz stimulation was also decreased; this may be a consequence of the stimulation protocol used throughout this study, whereby all three stimulation parameters were tested in each brain slice and therefore the depletion of the vesicular storage pool by 20p/20 Hz would be reflected in subsequent responses to 1p and 4p/10 Hz stimulations.

These observations indicate that D_2 autoreceptors play an important role in limiting dopamine release from terminal sites, particularly in the NAc. The apparently greater importance of D_2 autoreceptor modulation in the NAc was indicated when (−)-sulpiride produced a greater potentiation of dopamine overflow evoked by 20p/20 Hz in the NAc than in the aCPu. No significant effects of (−)-sulpiride on dopamine overflow were seen following 1p or 4p/10 Hz stimulation in either brain region. This accords with previous findings, where it was observed that dopamine released by electrical stimulation exerts an autoinhibitory action on its own release only if the stimulus lasts (and dopamine is present in the extracellular fluid) for more than 500 ms (Limberger *et al.*, 1991; Trout & Kruk, 1992).

In the brain slice, the rate at which dopamine, released by electrical stimulation, is removed from the extracellular medium is governed primarily by the neuronal uptake system into nerve terminals and the extraneuronal uptake systems into glial cells (Pelton *et al.*, 1981). The relative importance of these two uptake systems is not established. Fast cyclic voltammetry measures dopamine which has overflowed into the extracellular space and for this to occur, it is suggested that both neuronal and extraneuronal uptake systems are required to be, at least briefly, saturated. An index of the rate at which dopamine is subsequently removed from the extracellular space, used in this study and by other authors, is provided by $t_{1/2}$ (O'Connor & Kruk, 1991; Hafizi *et al.*, 1992).

The relatively small increases in $t_{1/2}$ for 1p, 4p/10 Hz and 20p/10 Hz, obtained in the presence of benztropine (Table 1), when compared to the large increases in electrically stimulated dopamine overflow, suggest that the increases in dopamine overflow may indicate inhibition of the neuronal dopamine uptake system, whereas substantial increases in $t_{1/2}$ indicate a reduction in the ability of the extraneuronal system to remove dopamine. Results with (+)-amphetamine support this idea because the greater increases in $t_{1/2}$ values are paralleled by the substantial increase in the extracellular concentration of dopamine as a result of displacement by (+)-amphetamine. These results indicate that the extraneuronal uptake system is equally important in regulating extracellular concentrations of dopamine.

In conclusion, we have shown that fast cyclic voltammetry can be used to monitor in real time and simultaneously (i) dopamine displacement by (+)-amphetamine, (ii) electrically stimulated dopamine overflow in the presence of (+)-amphetamine and (iii) inhibition of endogenous dopamine uptake by (+)-amphetamine. In addition, we have assessed the role of dopamine D_2 autoreceptor activation by endogenous dopamine displaced by (+)-amphetamine on electrically evoked dopamine efflux. We have attempted to evaluate the relative importance of these mechanisms at the axon terminal sites in the mesolimbic and mesostriatal dopamine systems by studying these processes in rat brain slices containing either the NAc or aCPu and their modification in the presence of a single dose of (+)-amphetamine and (−)-sulpiride.

References

AZZARO, A.J. & RUTLEDGE, C.O. (1973). Selectivity of release of norepinephrine, dopamine and 5-hydroxytryptamine by amphetamine in various regions of rat brain. *Biochem. Pharmacol.*, **22**, 2801–2813.

BEAL, M.F. & MARTIN, J.B. (1985). Topographical dopamine and serotonin distribution and turnover in the rat striatum. *Brain Res.*, **358**, 10–15.

BULL, D.R., PALIJ, P., SHEEHAN, M.J., MILLAR, J., STAMFORD, J.A., KRUK, Z.L. & HUMPHREY, P.P.A. (1990). Application of fast cyclic voltammetry to measurement of electrically evoked dopamine overflow from brain slices in vitro. *J. Neurosci. Methods*, **32**, 37–44.

CONNOR, C.E. & KUCZENSKI, R. (1986). Evidence that amphetamine and Na^+ gradient reversal increase striatal synaptosomal dopamine synthesis through carrier mediated efflux of dopamine. *Biochem. Pharmacol.*, **35**, 3123–3130.

FISCHER, J.F. & CHO, A.K. (1979). Chemical release of dopamine from striatal homogenates: evidence for an exchange diffusion model. *J. Pharmacol. Exp. Ther.*, **208**, 203–209.

FREEMAN, S.A., MELTZER, L.T. & BUNNEY, B.S. (1985). Firing properties of substantia nigra dopaminergic neurons in freely moving rats. *Life Sci.*, **36**, 1983–1994.

GLOWINSKI, J. (1975). Properties and functions of intraneuronal monoamine compartments in central aminergic neurones. In *Handbook of Psychopharmacology*, vol.3, pp. 139–167, ed. Iversen, L.L., Iversen, S.D. & Snyder, S.H. New York: Plenum Press.

GUIX, T., HURD, Y.L. & UNGERSTEDT, U. (1992). Amphetamine enhances extracellular concentrations of dopamine and acetylcholine in dorsolateral striatum and nucleus accumbens of freely moving rats. *Neurosci. Lett.*, **138**, 137–140.

HAFIZI, S., PALIJ, P. & STAMFORD, J.A. (1992). Activity of two human metabolites of nomifensine on stimulated efflux and uptake of dopamine in the striatum: in vitro voltammetric data in slices of rat brain. *Neuropharmacol.*, **31**, 817–824.

HEIKILLA, R.E., ORLANSKY, H. & COHEN, G. (1975). Studies on the distinction between uptake inhibition and release of ^{3}H-dopamine in rat brain slices. *Biochem. Pharmacol.*, **24**, 84–92.

HERDON, H., STRUPISH, J. & NAHORSKI, S.R. (1985). Differences between the release of radiolabelled and endogenous dopamine from superfused rat brain slices: effects of depolarizing stimuli, amphetamine and synthesis inhibitors. *Brain Res.*, **348**, 309–320.

HORN, A.S., COYLE, J.T. & SNYDER, S.H. (1970). Catecholamine uptake by synaptosomes from rat brain: structure-activity of drugs with differential effects on dopamine and norepinephrine neurones. *Mol. Pharmacol.*, **7**, 66–80.

HYTTEL, J. (1978). Inhibition of [^{3}H] dopamine accumulation in rat striatal synaptosomes by psychotropic drugs. *Biochem. Pharmacol.*, **27**, 1063–1068.

JACOCKS III, H.M. & COX, B.M. (1992). Serotonin-stimulated release via reversal of the dopamine transporter in rat striatum and nucleus accumbens: a comparison with release elicited by potassium, N-methyl-d-aspartic acid, glutamic acid and d-amphetamine. *J. Pharmacol. Exp. Ther.*, **262**, 356–364.

KALIVAS, P.W. (1993). Neurotransmitter regulation of dopamine neurones in the ventral tegmental area. *Brain. Res.*, **18**, 75–113.

KAMAL, L.A., ARABILLA, S., GALZIN, A.-M. & LANGER, S.Z. (1983) Amphetamine inhibits electrically evoked release of [^{3}H] dopamine from slices of the rabbit caudate. *J. Pharmacol. Exp. Ther.*, **227**, 446–458.

KUCZENSKI, R. (1983). Biochemical actions of amphetamine and other stimulants. In *Stimulants: Neurochemical, Behavioural and Clinical Perspectives*. ed. Creese, I., pp. 31–61, New York: Raven Press.

KUHR, W.G., BIGELOW, J.C. & WIGHTMAN, R.M. (1986). In vivo comparison of the regulation of releasable dopamine in the caudate nucleus and the nucleus accumbens of the rat brain. *J. Neurosci.*, **6,** 974–982.

LIMBERGER, N., TROUT, J.S., KRUK, Z.L. & STARKE, K. (1991). 'Real time' measurement of endogenous dopamine release during short trains of pulses in slices of rat neostriatum and nucleus accumbens: role of autoinhibition. *Naunyn-Schmied. Arch. Pharmacol.*, **344,** 623–629.

MARSHALL, J.F., O'DELL, S.J., NAVARRETE, R. & ROSENSTEIN, A.J. (1990). Dopamine high-affinity transport site topography in rat brain: major differences between dorsal and ventral striatum. *Neuroscience*, **37,** 11–21.

MCMILLAN, B.A. (1983). CNS stimulants. Two distinct mechanisms of action for amphetamine-like drugs. *Trends Pharmacol. Sci.*, **5,** 387–390.

MCMILLAN, B.A., GERMAN, D.C. & SHORE, P.A. (1980). Functional and pharmacological significance of brain dopamine and norepinephrine storage pools. *Biochem. Pharmacol.*, **29,** 3045–3050.

MILLER, H.H., SHORE, P.A. & CLARKE, D.E. (1980). In vivo monoamine oxidase inhibition by d-amphetamine. *Biochem. Pharmacol.*, **29,** 1347–1354.

MOORE, K.E. (1977). The actions of amphetamine on neurotransmitters: a brief review. *Biol. Psychiatry*, **12,** 451–456.

MOORE, K.E. (1978). Amphetamines: biochemical and behavioral actions in animals. In *Handbook of Psychopharmacology*, vol. 11, ed. Iversen, S.D. & Snyder, S.H., pp. 41–98. New York: Plenum Press.

O'CONNOR, J.J. & KRUK, Z.L. (1991). Fast cyclic voltammetry can be used to measure stimulated endogenous 5-hydroxytryptamine release in untreated rat brain slices. *J. Neurosci. Methods*, **88,** 25–33.

PALIJ, P., BULL, D.R., SHEEHAN, M.J., MILLAR, J., STAMFORD, J.A., KRUK, Z.L. & HUMPHREY, P.P.A. (1990). Presynaptic regulation of dopamine release in corpus striatum monitored in vitro in real time by fast cyclic voltammetry. *Brain Res.*, **509,** 172–174.

PARKER, E.M. & CUBEDDU, L.X. (1986a). Effects of d-Amphetamine and dopamine synthesis inhibitors on dopamine and acetylcholine neurotransmission in the striatum. 1. Release in the absence of vesicular transmitter stores. *J. Pharmacol. Exp. Ther.*, **237,** 179–192.

PARKER, E.M. & CUBEDDU, L.X. (1986b). Effects of d-Amphetamine and dopamine synthesis inhibitors on dopamine and acetylcholine neurotransmission in the striatum. 11. Release in the presence of vesicular transmitter stores. *J. Pharmacol. Exp. Ther.*, **237,** 193–203.

PARKER, E.M. & CUBEDDU, L.X. (1988). Comparative effects of amphetamine and related drugs on dopamine efflux, dopamine uptake and mazindol binding. *J. Pharmacol. Exp. Ther.*, **245,** 199–210.

PATEL, J., TROUT, S.J. & KRUK, Z.L. (1992). Regional differences in evoked dopamine efflux in brain slices of rat anterior and posterior caudate putamen. *Naunyn-Schmied. Arch. Pharmacol.*, **346,** 267–276.

PAXINOS, G. & WATSON, C. (1986). *The Rat Brain Stereotaxic Coordinates*. Second edition. London: Academic Press.

PELTON II, E.W., KIMELBERG, H.K., SHIPHERD, S.V. & BOURKE, R.S. (1981). Dopamine and norepinephrine uptake and metabolism by astroglial cells in culture. *Life Sci.*, **28,** 1655–1663.

RAITERI, M., CERRITO, F., CERVONI, A.M. & LEVI, G. (1979). Dopamine can be released by two mechanisms differentially affected by the dopamine transport inhibitor nomifensine. *J. Pharmacol. Exp. Ther.*, **208,** 195–202.

RAITERI, M. & LEVI, G. (1978). Release mechanism for catecholamine and serotonin in synaptosomes. In *Review of Neurosciences*. ed. Ehrenpreis, S. & Kopin, I. pp. 70–130. New York: Raven Press.

RICHARDS, C.D. & TEGG, W.J.B. (1977). A superfusion chamber suitable for maintaining mammalian brain tissue slices for electrical recording. *Br. J. Pharmacol.*, **59,** 526P.

SULZER, D., MAIDMENT, N.T. & RAYPORT, S. (1993). Amphetamine and other weak bases act to promote reverse transport of dopamine in ventral midbrain neurones. *J. Neurochem.*, **60,** 527–535.

TROUT, S.J. & KRUK, Z.L. (1992). Differences in evoked dopamine efflux from the rat caudate putamen, nucleus accumbens and tuberculum olfactorium in the absence of uptake inhibition: influence of autoreceptors. *Br. J. Pharmacol.*, **106,** 452–458.

VON VOIGTLANDER, P.F. & MOORE, E.K. (1973). Involvement of the nigro-straital neurones in the in vivo release of dopamine by amphetamine, amantadine and tyramine. *J. Pharmacol. Exp. Ther.*, **184,** 542–552.

WIECZOREK, W.J. & KRUK, Z.L. (1992). Differential action of (+)-amphetamine on electrically-evoked dopamine efflux in the rat caudate putamen and nucleus accumbens. *Br. J. Pharmacol.*, **107,** 212P.

(Received June 25, 1993
Revised October 23, 1993
Accepted November 24, 1993)

Br. J. Pharmacol. (1994), **111**, 837–842 © Macmillan Press Ltd, 1994

Effect of L-arginine/nitric oxide pathway on MPP^+-induced cell injury in the striatum of rats

Marti Santiago, Alberto Machado & [1]Josefina Cano

Departamento de Bioquímica, Facultad de Farmacia, E-41012 Sevilla, Spain

1 Protection against 1-methyl-4-phenylpyridinium ion (MPP^+) neurotoxicity by two nitric oxide-related compounds, N^{ω}-nitro-L-arginine (L-NOARG) and L-arginine, was studied in the corpus striatum by means of two MPP^+ perfusions separated by 24 h. Dopamine extracellular output after the second MPP^+ (1, 5 and 10 mM) perfusion was considered as an index of the dopaminergic neurone damage produced by the first MPP^+ (1, 5 and 10 mM) perfusion.

2 L-NOARG, systemically administered (10 mg kg^{-1}, i.p., every 12 h for 4 days), failed to prevent the neurotoxic action of MPP^+ (1 and 10 mM). On the contrary, the neurotoxic effect of MPP^+ was increased by L-NOARG administration.

3 L-Arginine (10 mM) perfused 2 h before MPP^+ perfusion did not protect against the neurotoxic action of high MPP^+ concentrations (5 and 10 mM). At the highest MPP^+ concentration used (10 mM), the increase in the extracellular output of dopamine after the second MPP^+ perfusion was slower in L-arginine-treated rats than in control and L-NOARG-treated rats.

4 When MPP^+ (1 mM) was perfused 2 h after L-arginine (10 mM) perfusion, there was a clear protection against MPP^+ neurotoxicity. In the second MPP^+ (1 mM) perfusion, the increase in the extracellular output of dopamine in L-arginine-treated rats was twice as high as for the control rats.

5 The results indicate that NO may exert a protective mechanism in the presence of a low ambient redox.

Keywords: Dopamine; microdialysis; striatum; 1-methyl-4-phenylpyridinium ion (MPP^+); L-arginine; N^{ω}-nitro-L-arginine

Introduction

The neurotoxin, 1-methyl-4-phenyl-1,2,3,6-tetrahydropyridine (MPTP) induces an extensive and quite selective destruction of dopaminergic neurones in the substantia nigra pars compacta and dramatic decrease of dopamine content in the caudate and putamen nuclei (Burns *et al.*, 1983; Langston *et al.*, 1984). The toxic action of MPTP is ultimately due to its principal metabolite, 1-methyl-4-phenylpyridinium ion (MPP^+) (Langston *et al.*, 1984; Markey *et al.*, 1984). MPP^+ is accumulated intraneuronally by a high-affinity dopamine uptake mechanism (Javitch *et al.*, 1985; Schinelli *et al.*, 1988). The toxic mechanism of MPP^+ may involve its accumulation within mitochondria (Ramsay *et al.*, 1986) and inhibition of mitochondrial respiration supported by NADH-linked substrates (Nicklas *et al.*, 1985). Intrastriatal MPP^+ perfusion causes a massive release of glutamate and aspartate (Westerink *et al.*, 1987). Therefore, the involvement of excitatory amino acids in the mechanism of MPTP/MPP^+ neurotoxicity has been postulated. The effects of MK-801, a non-competitive antagonist of the N-methyl-D-aspatate (NMDA)-type receptor, on MPTP and MPP^+ toxicity are still controversial. It was reported that MK-801 was able to prevent the dopamine neuronal degeneration induced by intranigral (Turski *et al.*, 1991) and striatal (Santiago *et al.*, 1992) perfusion of MPP^+ in rats, and the MPTP-induced Parkinsonism in primates (Zuddas *et al.*, 1992). In contrast, it was also noted that MPTP-induced neurotoxicity was not prevented by MK-801 (Sonsalla *et al.*, 1992). The activation of NMDA receptors stimulates, via calcium-calmodulin-dependent mechanisms, the synthesis of nitric oxide (NO), which, in turn, increases guanosine 3':5'-cyclic monophosphate (cyclic GMP) formation (East & Garthwaite, 1991; Garthwaite, 1991). For this reason, NO is actually considered as a putative mediator of neurotoxicity. Studies in a stroke model in mice have shown that 1 mg of N^{ω}-nitro-L-arginine (L-NOARG) per kilogram of body weight provides up to 75% protection, whereas MK-801 provides only 50–60% protection (Nowicki *et al.*, 1991). In order to verify a possible involvement of NO in NMDA-mediated neurotoxicity, we have investigated, using the microdialysis technique, a potential protective effect against MPP^+ perfusion of either a 4 day systemic treatment with L-NOARG or perfusion with 10 mM L-arginine.

[1] Author for correspondence.

Methods

Animals and drug treatment

Male albino Wistar rats were used for the experiments. The rats were housed in plastic cages (35 × 35 × 40 cm) and allowed free access to food and water.

The following drugs were used: MPP^+ iodide (Research Biochemical Inc., Natick, MA, U.S.A.) and L-arginine and N^{ω}-nitro-L-arginine (Sigma Chemical Co., St. Louis, MO, U.S.A.). MPP^+ iodide (1, 5 and 10 mM) and L-arginine (10 mM) were dissolved in the perfusion fluid. N^{ω}-nitro-L-arginine was dissolved in saline and injected intraperitoneally (10 mg kg^{-1}, every 12 h) for 4 days before MPP^+ perfusion. L-Arginine perfusion started 2 h before and lasted 3 h after each MPP^+ perfusion.

Surgery and brain dialysis

Microdialysis in the corpus striatum was performed with an I-shaped cannula (Santiago & Westerink, 1990). The exposed tip of the dialysis membrane was 4 mm. The dialysis tube (i.d.: 0.22 mm; o.d.: 0.31 mm) was prepared from polyacrylonitrile/sodium methalyl sulphonate copolymer (AN 69, Hospal, Bologna, Italy). The *in vitro* recovery of the membrane ($n = 5$) was: 20.3 ± 1.6%, for dopamine; 32.4 ± 2.7%, for 3,4-dihydroxyphenylacetic acid (DOPAC); and 30.5 ± 2.8%, for homovanillic acid (HVA). The probe was implanted into the corpus striatum [A/P 0.6, L/M 2.8, V/D 6.0, from bregma point and dura] during general chloral hydrate (400 mg kg^{-1}, i.p.) and local lignocaine (10% w/v in water) anaesthesia.

The perfusion experiments were carried out 24–48 h after implantation of the probe. Brain dialysis was performed with a fully automated on-line system as has been described previously (Westerink *et al.*, 1987). In brief, two polyethylene tubes (i.d. = 0.28 mm) were connected to the outlets of the dialysis tube. One tube (45 cm in length) was connected to the perfusion pump, and the other (45 cm in length) to the injection valve of the high performance liquid chromatography (h.p.l.c.) apparatus. From the time drugs (MPP^+ or L-arginine) were included in the Ringer solution delivered by the perfusion pump to the time when the first sample with drugs was injected onto the column, there was a time lag of about 30 min; the data presented are corrected to account for this time lag. With the help of an electronic timer, the injection valve was held in the load position for 15 min, during which the sample loop (40 μl) was filled with dialysate. The valve then switched automatically to the injection position for 15 s. This procedure was repeated every 15 min – the time needed to record a complete chromatogram. The corpus striatum was perfused with Ringer solution at a flow rate of 3.0 μl min^{-1} (perfusor VI, B. Braun, Melsungen, Germany). The composition of the Ringer solution was (in mM): NaCl 140, KCl 4.0, $CaCl_2$ 1.2 and $MgCl_2$ 1.0.

At the end of the experiment, the rat was given an overdose of chloral hydrate, and the brain was fixed with 4% paraformaldehyde via intracardiac perfusion. Coronal sections (40 μm thick) were cut, and placement of the dialysis probe localized according to the atlas of Paxinos & Watson (1986).

Chemical assays

Dopamine, DOPAC and HVA were quantitated by h.p.l.c. with electrochemical detection. A Kontron 420 pump was used in conjunction with a glassy carbon electrode set at – 780 mV (ANTEC, The Netherlands). A Merck Lichrocart cartridge (125 mm × 4 mm) column filled with Lichrospher reverse-phase C_{18} 5 μM material was used. The mobile phase consisted of a mixture of 0.05 M sodium acetate, 0.4 mM 1-octanesulphonic acid, 0.3 mM Na_2EDTA and 70 ml methanol l^{-1}, adjusted to pH 4.1 with acetic acid. The flow rate was 0.8 ml min^{-1} and the detection limit for dopamine, DOPAC and HVA was 5, 5 and 20 fmol per injection, respectively.

Expression of results and statistics

The average of the last four stable samples before drug-treatment was used as the basal value and was defined as 100%. All values given are expressed as percentages of basal values. Difference between the average dialysate concentrations of the basal values and drugs treatment was compared by Kruskal-Wallis analysis of variance by ranks, and, where appropriate (H value greater than the 95% confidence level),

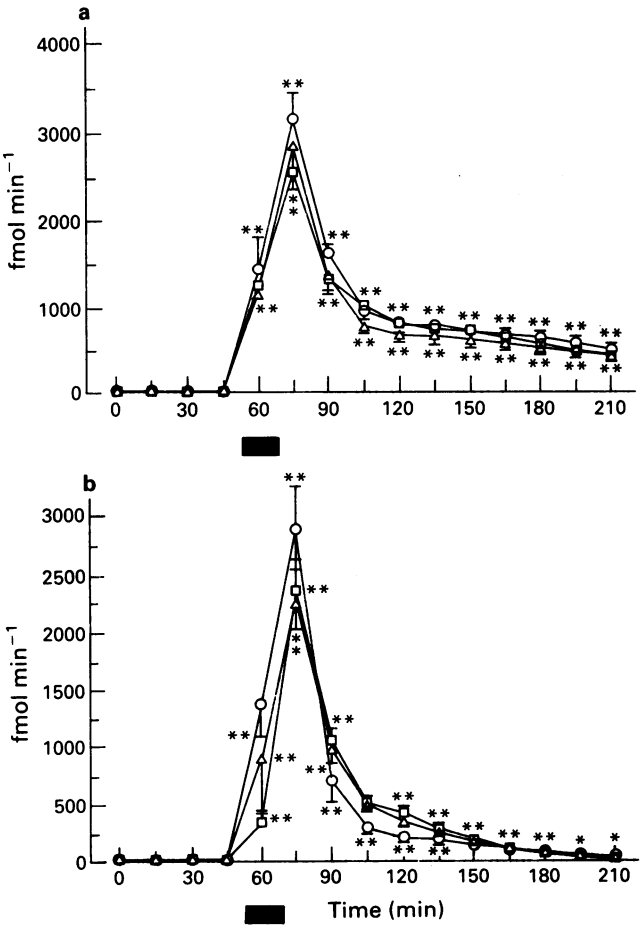


Figure 1 Effect of 1-methyl-4-phenylpyridinium ion (MPP^+) perfusion (black bar), at concentrations of 10 mM (a) and 1 mM (b), on the extracellular output of dopamine in control (□), N^{ω}-nitro-L-arginine-L (Δ) and L-arginine- (○) treated rats. Data are mean ± s.e.mean, expressed as fmol min^{-1} ($n = 4–6$). $^*P<0.05$; $^{**}P<0.01$, compared with the basal values (Kruskal-Wallis followed by the Mann-Whitney's test).

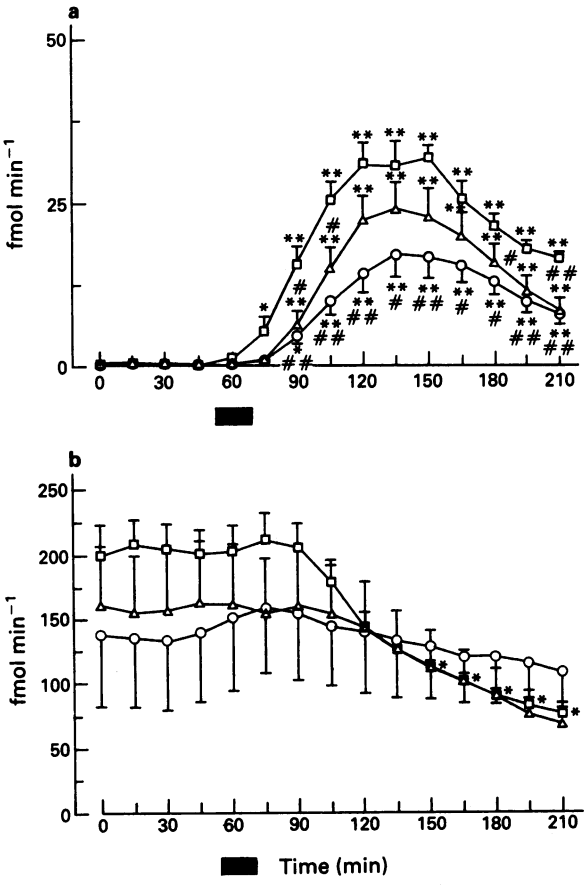


Figure 2 Effect of 1-methyl-4-phenylpyridinium ion (MPP^+) (10 mM) perfusion (black bar), 24 h after a first MPP^+ (10 mM) perfusion, on the extracellular output of dopamine (a) and DOPAC (b) in control (□), N^{ω}-nitro-L-arginine (L-NOARG) (Δ) and L-arginine- (○) treated rats. Data are mean ± s.e.mean, expressed as fmol min^{-1} ($n = 4–6$). $^*P<0.05$; $^{**}P<0.01$, compared with the basal values (Kruskal-Wallis followed by the Mann-Whitney's test). $^{\#}P<0.05$; $^{\#\#}P<0.01$, comparing control data with L-NOARG or L-arginine data at the same collection time (Student's *t* test).

means were compared by the Mann-Whitney U-test. Student's t test was used to compare control and L-NOARG or L-arginine data at the same collection time.

Results

Basal release of dopamine was unaffected by either the systemic administration of L-NOARG (10 mg kg^{-1}, i.p., every 12 h) for 4 days or the perfusion of L-arginine (10 mM) for 2 h prior to MPP$^+$ perfusion. The dopamine basal release values were as follows (in fmol min^{-1}): 19.0 ± 2.8 (n = 16), for control rats; 16.8 ± 1.5 (n = 9), for L-NOARG-treated rats; and 24.1 ± 2.5 (n = 14), for L-arginine-treated rats.

The first perfusion of MPP$^+$, for 15 min, produced a similar increase in the extracellular output of dopamine for all concentrations of MPP$^+$ used (1, 5 and 10 mM) both in control animals and in those treated with L-NOARG or L-arginine. Figure 1 shows the effect of MPP$^+$ (1 and 10 mM) perfusion on the extracellular output of dopamine in control, L-NOARG- and L-arginine-treated rats. However, after MPP$^+$ perfusion, there were similar decreases in the extracellular outputs of DOPAC and HVA, the extent of which was dependent upon the concentration of MPP$^+$ used, regardless of the treatment of the rats (data not shown).

After the perfusion of MPP$^+$ (1, 5 or 10 mM), L-NOARG-treated rats received two further intraperitoneal injections of L-NOARG (10 mg kg^{-1}, every 12 h) and L-arginine-treated rats were perfused with L-arginine (10 mM) for 3 h.

One day later, every experimental group received the same treatment as on the previous day. In the control animals, the second perfusion with MPP$^+$ (1 mM) resulted in a maximum output of dopamine of approximately 16% of that after the first MPP$^+$ (1 mM) perfusion. However, this output was 10 times higher than that induced by the second perfusion with MPP$^+$ (10 mM), which was in turn only 2.5% of the level induced by the first perfusion with MPP$^+$ (10 mM). Similar trends were found for DOPAC. The basal levels of DOPAC output after the second MPP$^+$ perfusion with respect to the first one, were about 50% and 15% for doses of MPP$^+$ 1 and 10 mM, respectively.

Figure 2 shows that the second 15 min perfusion with MPP$^+$ (10 mM), performed 24 h after perfusion with the same, induced a significant increase in the extracellular output of dopamine (Figure 2a). Dopamine content in control animals reached the highest levels, and although they were not statistically significant when compared with the maximum output of dopamine in L-NOARG-treated rats, they were statistically significant with respect to the levels in L-arginine-treated rats. Basal levels of DOPAC were higher in control rats (corresponding to the highest release of dopamine) compared with L-NOARG- and L-arginine-treated rats (Figure 2b), but the difference was not significant. After perfusion with MPP$^+$ (10 mM), DOPAC output underwent a

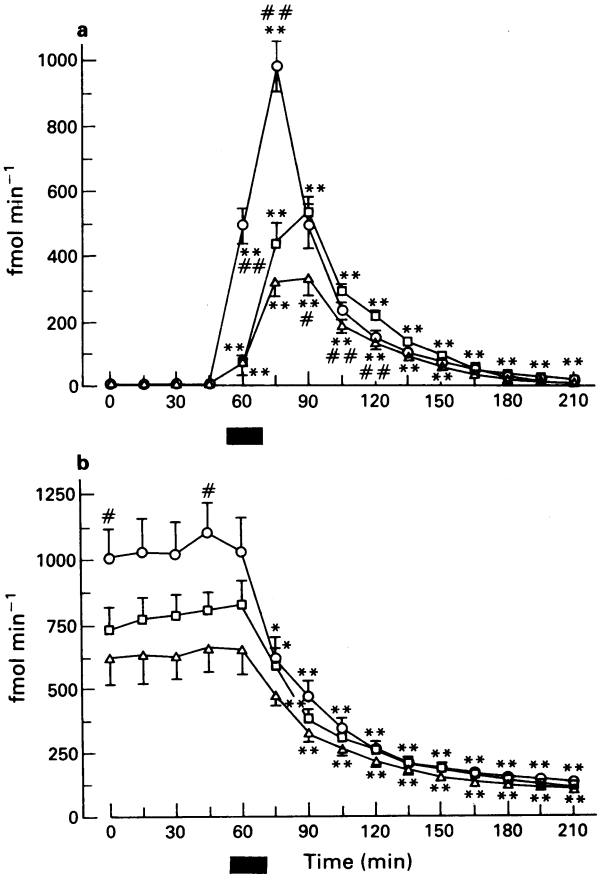


Figure 3 Effect of 1-methyl-4-phenylpyridinium ion (MPP$^+$, 1 mM) perfusion (black bar), 24 h after a first MPP$^+$ (1 mM) perfusion, on the extracellular output of dopamine (a) and DOPAC (b) in control (□), N$^\omega$-nitro-L-arginine (L-NOARG) (△) and L-arginine- (○) treated rats. Data are mean ± s.e.mean, expressed as fmol min^{-1} (n = 5–6). *P<0.05; **P<0.01, compared with the basal values (Kruskal-Wallis followed by the Mann-Whitney's test). #P<0.05; ##P<0.01, comparing control data with L-NOARG or L-arginine data at the same collection time (Student's t test).

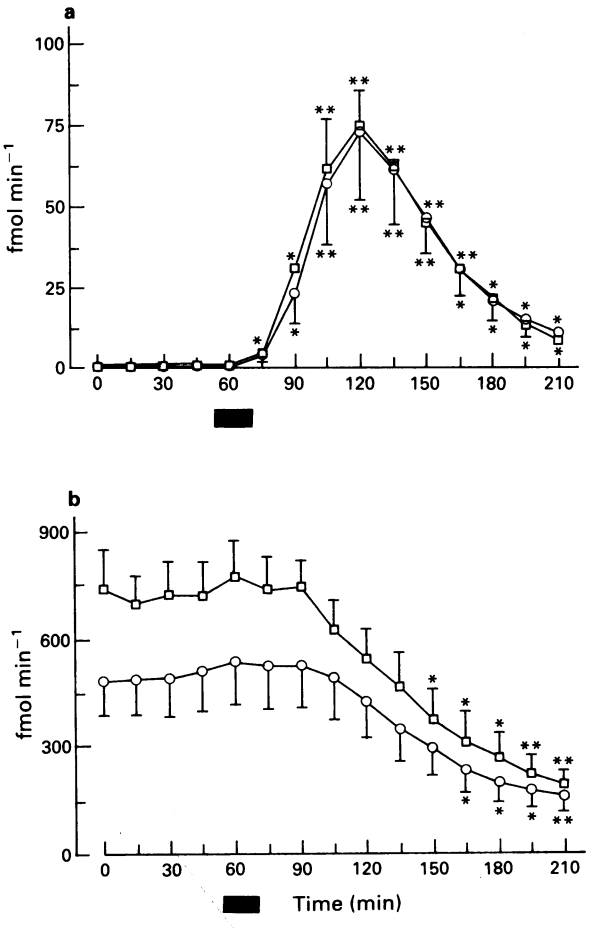


Figure 4 Effect of 1-methyl-4-phenylpyridinium ion (MPP$^+$, 5 mM) perfusion (black bar), 24 h after a first MPP$^+$ (5 mM) perfusion, on the extracellular output of dopamine (a) and DOPAC (b) in control (□) and L-arginine (○) treated rats. Data are mean ± s.e.mean, expressed as fmol min^{-1} (n = 4–6). *P<0.05; **P<0.01, compared with the basal values (Kruskal-Wallis followed by the Mann-Whitney's test).

decrease. This decrease was statistically significant in control animals (Figure 2b). The effect of MPP^+ perfusion (1, 5 and 10 mM) on HVA output was similar to the effect on extracellular output of DOPAC (data not shown).

Perfusion with MPP^+ (1 mM) for 15 min, performed 24 h after the first perfusion with MPP^+ (1 mM) showed marked differences in the maximum extracellular output of dopamine between the different experimental groups studied (Figure 3a). When compared at the same collection time, control and L-NOARG-treated rats had similar profiles of dopamine, although dopamine output was higher and statistically significant in the former with respect to the latter group. The increase in the extracellular output of dopamine due to MPP^+ perfusion was higher and faster in rats treated with L-arginine. The maximum output of dopamine took place 15 min after MPP^+ perfusion in L-arginine-treated rats and lasted 15 min more in control and L-NOARG-treated rats (Figure 3a). As observed for the maximum output of dopamine after MPP^+ perfusion, the highest basal value of DOPAC after the second MPP^+ perfusion was found in rats treated with L-arginine, followed by that of control rats. The lowest basal value of DOPAC was found in rats treated with L-NOARG (Figure 3b). The effect of perfusion with MPP^+ (1 mM) on the DOPAC output was similar for the three experimental groups (Figure 3b). Treatment with L-arginine produced a different effect on dopamine extracellular output depending on the concentration of MPP^+ used (1 and 10 mM). For this reason, 24 h after a first perfusion with MPP^+ (5 mM) for 15 min, control and L-arginine-treated rats underwent a second perfusion with the same. Under these conditions, there were no statistical differences in the maximum extracellular output of dopamine between either group (Figure 4a). Basal DOPAC output was higher in control rats, but not statistically significant compared with L-arginine-treated rats (Figure 4b).

Discussion

It is well documented that MPP^+, as an active metabolite of MPTP, causes damage to dopaminergic neurones. It is plausible that this effect is related to the amount of dopamine released after MPP^+ perfusion. Working on this assumption, we have perfused MPP^+ twice with an interval of 24 h between them. On the first day, MPP^+ perfusion produced a maximum output of dopamine which remained fairly constant for the three doses applied (1, 5 and 10 mM). The toxic effect, with cellular death, produced by the first MPP^+ perfusion is indicated by the output of dopamine and its metabolites produced with a second MPP^+ perfusion 24 h later. This second MPP^+ perfusion showed that the maximum output of dopamine differed, depending on the dose applied. The maximum output of dopamine with 1 mM MPP^+ perfusion in control rats was 10 times higher than that produced with 10 mM MPP^+, which was about 2.5% of that of the first day. Similar behaviour was found for DOPAC and HVA output. These results indicate that the toxic effect of MPP^+ depends on its concentration.

It has been reported that the toxic effect of MPP^+ is due to its accumulation in the dopaminergic neurones (Ramsay *et al.*, 1986), its inhibitory action on the respiratory chain (Nicklas *et al.*, 1985) and the generation of cytotoxic hydroxyl free radicals (Chiueh *et al.*, 1992). However, a massive release of glutamate and aspartate could be involved in the toxic effect of MPP^+ (Carboni *et al.*, 1990). Moreover, MK-801, a non-competitive antagonist of the glutamate NMDA-type receptor, is able to prevent the dopamine neuronal degeneration induced by MPTP/MPP^+ neurotoxicity (Turski *et al.*, 1991; Santiago *et al.*, 1992). Activation of NMDA receptors stimulates the synthesis of nitric oxide (NO), which is actually considered as a putative mediator of neurotoxicity (East & Garthwaite, 1991; Garthwaite, 1991). Therefore, probably through NO increase, there is a MPP^+ secondary toxicity due to glutamate. Taking into account the protective effect of MK-801 (Turski *et al.*, 1991; Santiago *et al.*, 1992), we expect that the inhibition of the enzyme, nitric oxide synthase (NOS), should give similar results to those described in other circumstances. Ischaemia produces, like MPP^+, neuronal death with a previous high output of dopamine and excitatory amino acids (Baker *et al.*, 1991). Likewise, it has been reported that MK-801 protects against neuronal death produced by ischaemia (Rod *et al.*, 1989; Demerlé-Pallardi *et al.*, 1991). Nowicki *et al.* (1991) have reported a higher protective effect for L-NOARG than for MK-801 in a stroke model in mice.

We inhibited the NOS by systemic administration of L-NOARG for 4 days (Dwyer *et al.*, 1991). After this treatment, animals were perfused twice with MPP^+ (1 or 10 mM). Under these conditions, we found an increase in the toxicity with both MPP^+ concentrations assayed. The second MPP^+ perfusion produced greater damage in animals treated with L-NOARG than in control animals, the output of dopamine in the former group being about 75% of the latter group in both cases (1 or 10 mM). Likewise, DOPAC basal levels were lower in animals treated with L-NOARG than in control animals.

These data seem to demonstrate that the toxic action provoked by MPP^+ through activation of NMDA receptors is not produced by an increase of NO synthesis. Similar data have been given for other neurodegenerative processes. Lener-Natoli *et al.* (1992) showed that the NOS inhibitors failed to protect hippocampal neurones against NMDA toxicity in diethylether anaesthetized rats. Moncada *et al.* (1992) failed to demonstrate any protective effect of N^{ω}-nitro-L-arginine methyl ester (L-NAME) in the ischaemic model. In addition, in a comparative study of the effect of NOS inhibitors, MK-801, and methyl blue (guanylate cyclase inhibitor), Demerlé-Pallardy *et al.* (1991) found that, while all these compounds decreased the cyclic GMP levels, only MK-801 was able to reduce neuronal death.

Our results with L-NOARG treatment seem to indicate that this inhibitor of NOS fails to protect against the neuronal death produced by MPP^+ and, in some cases, increases the damage. For this reason, we have tried to study, in similar conditions, the effect of L-arginine, a substrate of NOS. We have found that the effect of L-arginine depends on the MPP^+ concentration used.

Perfusion of MPP^+ (10 mM) seems to produce higher damage in animals treated with L-arginine than in control animals. The maximum output of dopamine was lower (half) in the former compared with the latter animals. This damage was also higher than that produced in L-NOARG-treated rats. Twenty-four hours after the first MPP^+ perfusion, DOPAC output was lower in L-arginine-treated rats compared to control and L-NOARG-treated rats. However, opposite effects seemed to be observed, when a lower MPP^+ concentration (1 mM) was used. After the second MPP^+ (1 mM) perfusion, the maximum output of dopamine in L-arginine-treated rats was twice that of control animals. It is worthwhile noting that the immediate rise of dopamine seen after MPP^+ perfusion in L-arginine-treated rats is probably caused by the death of the neuronal elements surrounding the cannula. It is, therefore, of interst that, after MPP^+ (1 mM) perfusion the maximum output of dopamine in L-arginine-treated rats had a similar time-profile on the first and second days, but, with 5 and 10 mM of MPP^+, there was a delay in the maximum output of dopamine on the second day compared with the first day. These results seem to indicate that the higher delay in dopamine maximum output on the second day demonstrates higher neuronal death surrounding the cannula on the first day. Therefore, there is a protection with L-arginine against MPP^+ (1 mM) neurotoxicity. Likewise, DOPAC basal levels, 24 h after the first MPP^+ (1 mM) perfusion, were significantly higher than in control animals.

All of these findings are consistent with the neuroprotec-

tive and neurotoxic role of NO. The redox versatility of NO allows for its interconversion from neuroprotective to neurotoxic species by change in the ambient redox milieu. It has been recently reported (Lipton *et al.*, 1993) that NO· mediated neurotoxicity is engendered by reaction with superoxide anion (O_2^-) and not by NO· alone. In contrast, the neuroprotective effects of NO result from downregulation of NMDA-receptor activity by reaction with thiol group(s) of the receptor's modulatory site. This reaction is not mediated by NO· itself, but occurs under conditions supporting S-nitrosylation of NMDA receptor thiol.

Free radical formation enhanced by MPP^+ in the striatum appears to be dose-dependent (1–10 mM) (Chiueh *et al.*, 1992). Therefore, there is an ambient redox that is higher with MPP^+ 10 mM than with MPP^+ 1 mM. Taken together with our results, it is inferred that, after arginine and MPP^+ 10 mM perfusion, the NO produced could be chemically reduced to NO· and react with superoxide anion and become neurotoxic. In contrast, with arginine and MPP^+ 1 mM the NMDA receptor's redox modulatory site can be downregulated by the NO· produced and thus prevent excessive influx of Ca^{2+} and its associated neurotoxic effects (Lei *et al.*, 1992; Stamler *et al.*, 1992).

In conclusion, these results seem to indicate that the NO could be an important protector mechanism when there is not a high ambient redox, since with a low concentration of MPP^+ (1 mM) the neurotoxic action mediated by glutamate release, through NMDA receptors, could be regulated by NO. In fact, nitroprusside (which spontaneously generates NO) and L-arginine inhibit NMDA receptors (Manzoni *et al.*, 1992; Manzoni & Bockaert, 1993) and protect cerebellar cells from oxygen radical-induced damage (Garthwaite & Garthwaite, 1988).

This research was supported by a grant from DGICYT PM91-0097. M.S. thanks Ministerio de Educación y Ciencia, Spain, for a Contrato de Reincorporación.

References

BAKER, A.J., ZORNOW, M.H., SCHELLER, M.S., YAKSH, T.L., SKILLING, S.R., SMULLIN, D.H., LARSON, A.A. & KUCZENSKI, R. (1991). Changes in extracellular concentrations of glutamate, aspartate, glycine, dopamine, serotonin, and dopamine metabolites after transient global ischemia in the rabbit brain. *J. Neurochem.*, **57**, 1370–1379.

BURNS, R.S., CHIUEH, C.C., MARKEY, S.P., EBERT, M.H., JACOBOWITZ, D.M. & KOPIN, I.J. (1983). A primate model of parkinsonism: selective destruction of dopaminergic neurons in the pars compacta of the substantia nigra. *Proc. Natl. Acad. Sci. U.S.A.*, **80**, 4546–4550.

CARBONI, S., MELIS, F., PANI, L., HADJICONSTANTINOU, M. & ROSSETTI, Z.L. (1990). The non-competitive NMDA-receptor antagonist MK-801 prevents the massive release of glutamate and aspartate from rat striatum induced by 1-methyl-4-phenylpyridinium (MPP^+). *Neurosci. Lett.*, **117**, 129–133.

CHIUEH, C.C., KRISHNA, G., TULSI, P., OBATA, T., LANG, K., HUANG, S.-J. & MURPHY, D.L. (1992). Intracranial microdialysis of salicyclic acid to detect hydroxyl radical generation through dopamine autooxidation in the caudate nucleus: effect of MPP^+. *Free Radical Biol. Med.*, **13**, 581–583.

DEMERLÉ-PALLARDY, C., LONCHAMPT, M.O., CHABRIER, P.E. & BRAQUET, P. (1991). Absence of implication of L-arginine/nitric oxide pathway on neuronal cell injury induced by L-glutamate or hypoxia. *Biochem. Biophys. Res. Commun.*, **181**, 456–464.

DWYER, M.A., BREDT, S. & SNYDER, S.H. (1991). Nitric oxide synthase: irreversible inhibition by L-NG-nitroarginine in brain in vitro and in vivo. *Biochem. Biophys. Res. Commun.*, **176**, 1136–1141.

EAST, S.J. & GARTHWAITE, J. (1991). NMDA receptor activation in rat hippocampus induces cyclic GMP formation through the L-arginine nitric oxide pathway. *Neurosci. Lett.*, **123**, 17–19.

GARTHWAITE, J. (1991). Glutamate, nitric oxide and cell-cell signalling in the nervous system. *Trends Neurosci.*, **14**, 60–67.

GARTHWAITE, G. & GARTHWAITE, J. (1988). Cyclic AMP and cell death in rat cerebellar slices. *Neuroscience*, **26**, 321–326.

JAVITCH, J.A., D'AMATO, R.J., STRITTMATTER, S.M. & SNYDER, S.H. (1985). Parkinson-inducing neurotoxin 1-methyl-1,2,3,6-tetrahydropyridine: uptake of the metabolite N-methyl-4-phenylpyridine by dopamine neurons explains selective toxicity. *Proc. Natl. Acad. Sci. U.S.A.*, **82**, 2173–2177.

LANGSTON, J.W., FORNO, L.S., REBERT, C.S. & IRWIN, I. (1984). Selective nigral toxicity after systemic administration of 1-methyl-4-phenyl-1,2,3,6-tetrahydropyridine (MPTP) in the squirrel monkey. *Brain Res.*, **292**, 390–394.

LEI, S.Z., PAN, Z.-H., AGGARWAL, S.K., CHEN, H.-S.V., HARTMAN, J., SUCHER, N.J. & LIPTON, S.A. (1992). Effect of nitric oxide production on the redox modulatory site of the NMDA receptor-channel complex. *Neuron*, **8**, 1087–1099.

LENER-NATOLI, M., RONDOUIN, G., DE BOCK, F. & BOCKAERT, J. (1992). Chronic NO synthase inhibition fails to protect hippocampal neurones against NMDA toxicity. *NeuroReport*, **3**, 1109–1112.

LIPTON, S.A., CHOI, Y.-B., PAN, Z.-H., LEI, S.Z., CHEN, H.-S.V., SUCHER, N.J., LOSCALZO, J., SINGEL, D.J. & STAMLER, J.S. (1993). A redox-based mechanism for the neuroprotective and neurodestructive effects of nitric oxide and related nitroso-compounds. *Nature*, **364**, 626–632.

MANZONI, O. & BOCKAERT, J. (1993). Nitric oxide synthase activity endogenously modulates NMDA receptors. *J. Neurochem.*, **61**, 368–370.

MANZONI, O., PREZEAU, L., MARIN, P., DESHAGER, S., BOCKAERT, J. & FAGNI, L. (1992). Nitric oxide-induced blockade of NMDA receptors. *Neuron*, **8**, 653–662.

MARKEY, S.P., JOHANNESSEN, J.N., CHIUEH, C.C., BURNS, R.S. & HERKENHAM, M.A. (1984). Intraneuronal generation of a pyridinium metabolite may cause drug-induced parkinsonism. *Nature*, **311**, 464–467.

MONCADA, C., LEKIEFFRE, D., ARVIN, B. & MELDRUM, B. (1992). Effect of NO synthase inhibition on NMDA-induced and ischaemia-induced hippocampal lesions. *NeuroReport*, **3**, 530–532.

NICKLAS, W.J., VYAS, I. & HEIKKILA, R.E. (1985). Inhibition of NADH-linked oxidation in brain mitochondria by 1-methyl-4-phenylpyridine, a metabolite of the neurotoxin, 1-methyl-4-phenyl-1,2,3,6-tetrahydropyridine. *Life Sci.*, **36**, 2503–2508.

NOWICKI, J.P., DUVAL, D., POIGNET, H. & SCATTON, B. (1991). Nitric oxide mediates neuronal death after focal cerebral ischemia in the mouse. *Eur. J. Pharmacol.*, **204**, 339–341.

PAXINOS, G. & WATSON, C. (1986). *The Rat Brain in Stereotaxic Coordinates* (second edition). San Diego: Academic Press.

RAMSAY, R.R., DADGAR, J., TREVOR, A. & SINGER, T.P. (1986). Energy driven uptake of 1-methyl-4-phenyl-1,2,3,6-tetrahydropyridine by brain mitochondria mediates the neurotoxicity of MPTP. *Life Sci.*, **39**, 581–588.

ROD, M.R. & AUER, R.N. (1989). Pre- and postischemic administration of dizocilpine (MK-801) reduces cerebral necrosis in the rat. *Can. J. Neurol. Sci.*, **16**, 340–344.

SANTIAGO, M., VENERO, J.L., MACHADO, A. & CANO, J. (1992). In vivo protection of striatum from MPP^+ neurotoxiciy by N-methyl-D-aspartate antagonists. *Brain Res.*, **586**, 203–207.

SANTIAGO, M. & WESTERINK, B.H.C. (1990). Characterization of the in vivo release of dopamine as recorded by different types of intracerebral microdialysis probes. *Naunyn-Schmied. Arch. Pharmacol.*, **342**, 407–414.

SCHINELLI, S., ZUDDAS, A., KOPIN, I.J., BARKER, J.L. & DI PORCIO, H. (1988). 1-methyl-4-phenyl-1,2,3,6-tetrahydropyridine metabolism and 1-methyl-4-phenylpyridinium uptake in dissociated cell cultures from the embrionic mesencephalon. *J. Neurochem.*, **50**, 1900–1907.

SONSALLA, P.K., ZEEVALK, G.D., MANZINO, L., GIOVANNI, A. & NICKLAS, W.J. (1992). MK-801 fails to protect against the dopaminergic neuropathology produced by systemic 1-methyl-1-phenyl-1,2,3,6-tetrahydropyridine in mice or intranigral 1-methyl-4-phenylpyridinium in rats. *J. Neurochem.*, **58**, 1979–1982.

STAMLER, J.S., SINGEL, D.J. & LOSCALZO, J. (1992). Biochemistry of nitric oxide and its redox-activated forms. *Science*, **258**, 1898–1902.

TURSKI, L., BRESSLER, K., RETTIG, K.J., LÖSCHMANN, P.A. & WACHTEL, H. (1991). Protection of substantia nigra from MPP^+ neurotoxicity by N-methyl-D-aspartate antagonists. *Nature*, **349**, 414–418.

WESTERINK, B.H.C., DAMSMA, G., ROLLEMA, H., DE VRIES, J.B. & HORN, A.S. (1987). Scope and limitations of in vivo brain dialysis: a comparison of its applications to various neurotransmitter systems. *Life Sci.*, **41**, 1763–1776.

ZUDDAS, A., OBERTO, G., VAGLINI, F., FASCETTI, F., FORNAI, F. & CORSINI, G.U. (1992). MK-801 prevents 1-methyl-4-phenyl-1,2,3,6-tetrahydropyridine-induced Parkinsonism in primates. *J. Neurochem.*, **59**, 733–739.

(Received July 20, 1993
Revised October 1, 1993
Accepted October 25, 1993)

Br. J. Pharmacol. (1994), **111**, 843–851 © Macmillan Press Ltd, 1994

Central and peripheral actions of the novel κ-opioid receptor agonist, EMD 60400

[1]A. Barber, G.D. Bartoszyk, H.E. Greiner, F. Mauler, R.D. Murray, C.A. Seyfried, *M. Simon, R. Gottschlich, J. Harting & I. Lues

Preclinical Pharmaceutical Research, E. Merck, Frankfurter Strasse 250, 64271 Darmstadt, Germany and *Merck-Clevenot S.A., 5/9 Rue Anquetil, 94731 Nogent-sur-Marne, France

1 The pharmacological characteristics of the κ-opioid receptor agonist, EMD 60400, have been investigated, with particular reference to its central and peripheral sites of action and its ability to influence nociception. The κ agonists ICI 197067 and ICI 204448 were tested for purposes of comparison.

2 EMD 60400 and ICI 197067 bind with high affinity (IC_{50} values of 2.8 and 1.5 nM, respectively) and high selectivity to κ-opioid receptors. ICI 204448 has a lower binding affinity (IC_{50} 13.0 nM) and selectivity for κ-opioid receptors.

3 EMD 60400, ICI 197067, and ICI 204448 are full and potent agonists in the rabbit vas deferens *in vitro* assay for κ-opioid receptors (IC_{50} values of 41.8, 15.7 and 15 nM, respectively).

4 *Ex vivo* binding experiments in mice revealed that EMD 60400 and ICI 197067 were well taken up after s.c. administration. Brain levels of EMD 60400 were lower than those of ICI 197067 at comparable doses, indicating that EMD 60400 does not penetrate into the CNS as well as ICI 197067.

5 Haloperidol-induced DOPA accumulation in the nucleus accumbens of the rat was dose-dependently reversed by s.c. application of EMD 60400 and ICI 197067 at doses of and above 3 and 0.3 mg kg^{-1}, respectively. ICI 204448 had no effect on DOPA accumulation at 30 mg kg^{-1}, s.c.

6 Prolongation of hexobarbitone-induced sleeping time in mice and motor impairment in the rat rotarod test were observed for EMD 60400 at doses above 3 and 2.5 mg kg^{-1}, s.c., respectively, and for ICI 197067 at doses above 0.3 and 0.25 mg kg^{-1}, s.c., respectively. ICI 204448 was inactive in these tests at doses of 30 and 100 mg kg^{-1}, s.c., respectively.

7 EMD 60400 applied s.c. produced dose-dependent naloxone-reversible antinociception in the mouse formalin test (1st and 2nd phase ID_{50} 0.44 and 0.47 mg kg^{-1}, respectively) and rodent writhing test (ID_{50} mouse 0.55 mg kg^{-1} and rat 0.3 mg kg^{-1}). Furthermore, EMD 60400 was considerably more potent in the rat pressure pain test after the induction of inflammation with carrageenin than under normalgesic conditions (ID_{50} values 0.1 μg kg^{-1} and 4.0 mg kg^{-1}, s.c., respectively). The action of EMD 60400 (50 μg kg^{-1}, s.c.) in the hyperalgesic pressure pain test was completely antagonized by injection of the κ-opioid antagonist, norbinaltorphimine (100 μg) into the inflamed tissue, thus demonstrating the peripheral opioid nature of this effect.

8 EMD 60400 produced dose-dependent inhibition of neurogenic plasma extravasation elicited by antidromic electrical stimulation of the rat saphenous nerve (ID_{50} value 0.3 mg kg^{-1}, i.v.). This inhibition was completely antagonized by intraplantar injection of norbinaltorphimine (50 μg).

9 EMD 60400, ICI 197067, and ICI 204448 have diuretic effects in rats at doses of and above 0.1, 0.01, and 0.3 mg kg^{-1}, s.c., respectively. An antidiuretic action was also observed with ICI 197067 at very low doses (3 and 6 μg kg^{-1}, s.c.).

10 Pharmacological and biochemical data therefore indicate that the three κ-opioid receptor agonists tested here have different tendencies to elicit centrally-mediated sedation and putative aversion (ICI 197067 > EMD 60400 > ICI 204448) which correspond to their ability to cross the blood-brain barrier. EMD 60400 combines high affinity and selectivity for the κ receptor with a degree of peripheral selectivity. The peripheral actions of systemically-applied EMD 60400 against hyperalgesic pressure pain and neurogenic inflammation are very probably mediated by opioid receptors on the endings of sensory nerve fibres.

Keywords: EMD 60400; ICI 197067; ICI 204448; κ-opioid agonist; antinociceptive; diuretic; antidiuretic; peripherally-selective

Introduction

It has been recognised for a number of years that analgesic actions of opiates can be produced by agonists acting at opioid-receptor subtypes (μ, κ and δ) in the brain and spinal cord. However, this action is often accompanied by undesirable central side effects. In the case of κ-opioid agonists these central side effects include dysphoria and sedation (Pfeiffer *et al.*, 1986), which severely limit the usefulness of these compounds in the clinical setting. Evidence has recently become available that opiates can also have peripheral antinociceptive actions, in particular when inflammation is present (see Barber & Gottschlich, 1992, for recent review). An opiate agonist which is unable to cross the blood-brain barrier should under inflammatory or hyperalgesic conditions be able to produce a peripheral analgesic effect which is not coupled with unacceptable central side effects.

In this study we have examined some biochemical and pharmacological properties of the novel κ-agonist, EMD 60400 and compared them with those of ICI 204448 and ICI 197067. ICI 204448 (Shaw *et al.*, 1989) is a κ-opioid receptor agonist which has been described as having only limited access to the CNS, though there have been few tests of its antinociceptive effectiveness in animal models of pain (Barber *et al.*, 1992; Rogers *et al.*, 1992). In contrast, ICI 197067 (Costello *et al.*, 1988) is a κ agonist which readily

[1] Author for correspondence.

penetrates the blood-brain barrier (Shaw *et al.*, 1989). Our aim was to investigate whether EMD 60400 can have peripherally-mediated actions at systemic doses which do not produce centrally-mediated side effects. Some of these results have been presented as a preliminary communication (Barber *et al.*, 1992).

Methods

In vitro *tests*

Binding Opioid receptor binding was determined in the presence of 1.5 nM [^{3}H]-U-69593 (κ), 0.5 nM [^{3}H]-PL-017 (μ), or 1.0 nM [^{3}H]-[D-Pen^{2,5}]enkephalin (δ) in 50 mM Tris (2-amino-2-hydroxymethyl-propan-1,3-diol) buffer (pH 7.7) using membranes prepared from guinea-pig cerebellum (κ) or rat cerebrum (μ and δ). Assays were run for 30 min at 25°C and non-specific binding was measured by use of 10 μM naloxone (κ), 0.3 μM morphine (μ), or 1 μM [D-Ala^2, D-Leu^5]enkephalin (DADLE; δ).

Rabbit vas deferens This assay was performed in a manner similar to that of Oka *et al.* (1980). Briefly, vasa deferentia were isolated from New Zealand white rabbits (ca. 2.5 kg) and were mounted in organ baths containing 50 ml oxygenated Krebs Henseleit solution at 30°C. The tissue was stimulated electrically with square-wave pulses (0.1 Hz, 2 ms, 40–60 V) via platinum field-stimulating electrodes and contractions were recorded isometrically under a load of 0.5 g. Test substances were dissolved in Krebs Henseleit solution and applied in increasing concentrations at 15 min intervals.

Tests for demonstrating central actions of κ *agonists*

Ex vivo *determination of brain and plasma levels* These assays were performed as described by Shaw *et al.* (1989) with a few modifications. Briefly, groups of six female NMRI mice (22–24 g) were injected with vehicle, or test compound dissolved in saline. Thirty minutes later the animals were decapitated, their brains removed and plasma samples collected.

Ex vivo κ-opioid receptor binding was performed in HEPES buffer (pH 7.4) using [^{3}H]-ethylketocyclazocine (0.5 nM). Assays were run for 40 min at 25°C in the presence of 3 μM DADLE, along with 200 μl pooled mouse brain homogenate, or the equivalent of 20 μl pooled blood plasma together with 200 μl of homogenized guinea-pig brain. Ethylketocyclazocine (10 μM) was used to define non-specific binding.

Calibration curves were generated by adding the test compound *in vitro* to brain homogenates or plasma samples from control animals. Specific binding values were then obtained for vehicle and treated mice, and the inhibition of binding due to the test compound was used to calculated the concentration of test compound in the brain or plasma of the treated mouse from the corresponding calibration curve. Each estimate of brain and plasma concentration represents mean ± s.d. from at least six determinations.

Reversal of haloperidol-induced DOPA (3,4-dihydroxyphenylalanine) accumulation This method was adopted with minor modifications from Manzanares *et al.* (1991). Groups of 4 male Wistar rats (150–200 g) were treated orally with 0.3 mg kg^{-1} haloperidol suspended in methocel (E. Merck, Darmstadt, Germany). After 1 h the animals were injected s.c. with opiates dissolved in propandiol (E. Merck, Darmstadt, Germany), or propandiol alone. Twenty-five minutes later the animals were injected i.p. with 100 mg kg^{-1} of the DOPA-decarboxylase inhibitor, NSD 1015, dissolved in physiological saline. After a further 35 min the animals were decapitated, the nucleus accumbens from both brain halves was removed rapidly, weighed, homogenized and centrifuged. Thereafter, the DOPA content of the samples was analysed by high performance liquid chromatography (Seyfried *et al.*, 1986).

Hexobarbitone-induced sleeping time Groups of 10 male NMRI mice (20–30 g) were injected s.c. with test substances dissolved in distilled water. Thirty minutes later the mice were injected with hexobarbitone (Serva, Heidelberg, Germany; 100 mg kg^{-1}, i.p.) and the duration of narcosis was defined as the time till recovery of the righting reflex.

Rotarod Groups of 3–6 male Wistar rats (160–220 g) were selected for their ability to balance on a rotating rod (diameter 9 cm; rate of rotation 7 revolutions per min). Selected rats were then injected s.c. with test compounds dissolved in distilled water (EMD 60400 and ICI 197067) or 20% dimethylsulphoxide (DMSO; E. Merck, Darmstadt, Germany; ICI 204448). The animals were tested again 30 min after treatment; a rat falling off the bar more than twice within 2 min was considered to be showing motor impairment.

Antinociceptive tests

Formalin test Male NMRI mice (20–30 g) were injected s.c. with test compound dissolved in distilled water (EMD 60400 and ICI 197067), 25% DMSO (ICI 204448) or vehicle. After 30 min 20 μl of a 3% solution of formalin (E. Merck, Darmstadt, Germany) was injected into a hind paw. The amount of time spent licking the injected paw was measured 0–5 and 20–25 min after the injection of formalin (i.e., in the non-inflammatory first phase and the inflammatory second phase of the reaction, respectively; Hunskaar & Hole, 1987) and expressed as % inhibition compared to the respective vehicle group.

Writhing test Male NMRI mice (20–30 g) and Wistar rats (150–180 g) were injected s.c. with test compound or vehicle (physiological saline or distilled water). Thirty minutes later the animals were injected with a saturated aqueous solution of 2-phenyl-1,4-benzoquinone (E. Merck, Darmstadt, Germany) into the abdominal cavity. The number of writhing movements made in the subsequent 20 min were counted and expressed as % inhibition compared to the respective vehicle group.

Carrageenin-induced hyperalgesia Male Wistar rats (250–370 g) were fitted with a tail cuff and injected with a 1% solution of carrageenin (Marine Colloids Inc., Springfield N.J., U.S.A.) into the base of the tail at the level of the cuff. Three hours later the proportion of freely-moving animals responding to a standard painful pressure (2.5 bar) delivered to the inflamed tissue via a pin built into the cuff was compared in groups of animals receiving different doses of the test substance. The response consisted of vocalisation, turning and/or biting the cuff. The κ-opioid receptor agonists were dissolved in distilled water and applied s.c. at the same time as carrageenin. Peripheral antinociceptive effects of systemically-applied EMD 60400 were demonstrated by applying 100 μg norbinaltorphimine dissolved in 25 μl saline into the inflamed portion of the tail.

Experiments were also carried out on freely-moving rats which had not been injected with carrageenin. In this case the pain response to a pressure of 4 bar was tested 30 min after the s.c. application of the opiates.

Other in vivo *tests*

Neurogenic inflammation Male Wistar rats (270–330 g) were anaesthetized with pentobarbitone sodium (Sanofi, Paris; 60 mg kg^{-1}, i.p.) and their saphenous nerves were exposed and sectioned at the level of the thigh, the right nerve being hung in paraffin over a pair of stimulating electrodes, the

other serving as an internal control. Evans blue (E. Merck, Darmstadt, Germany; 50 mg kg^{-1}, i.v.) and κ agonists were dissolved in a 0.9% solution of NaCl and applied simultaneously through a cannula in a tail vein. After 15 min the saphenous nerve was stimulated antidromically with square-wave electrical pulses (5 mA, 1 ms, 2 Hz) for 10 min, following which the animal was killed with an overdose of anaesthetic. The skin of both hindpaws was then removed and incubated for 90 h in formamide (E. Merck, Darmstadt, Germany) at room temperature. Extracted dye was measured with an LKB Ultrospec spectrophotometer at 620 nm. Comparisons were made of the mean amounts of extracted dye (expressed as μg dye per 100 mg skin) on stimulated and control sides for groups of animals treated with saline (vehicle) or test compound. Alternatively, the mean of differences between stimulated and control sides were used for analysis.

Local inhibitory actions of systemically-applied EMD 60400 were tested for by injecting 50 μg norbinaltorphimine dissolved in 25 μl saline into the paw (intraplantar, i.pl.) 10 min after the application of Evans blue and agonist and 5 min before the beginning of nerve stimulation. The control side was injected with 25 μl saline at the same time.

In other experiments substance P (10 μg) was dissolved in 25 μl saline and injected into the paw 15 min after the injection of Evans blue and EMD 60400. It was allowed to act for 10 min before the experiment was terminated. Investigations into the role of the adrenal glands were performed on rats adrenalectomized immediately prior to preparation of the saphenous nerves.

Urinary volume in conscious rats Male Wistar rats (180–250 g) received water *ad libitum* and were deprived of food for 18 h before experiments. Groups of three rats had their urinary bladders emptied by light pressure and were placed in metabolism cages for 6 h. The volume of urine produced in this time was expressed as ml per 100 g body weight. In additional experiments with volume-loaded rats, a 0.6% solution of NaCl (10 ml per 100 g, i.p.) was injected just before the beginning of the experiment. Agonists were dissolved in distilled water and injected s.c. in a volume of 0.1 ml per 100 g immediately before the start of the measurements.

Substances

The following substances were used: [D-Ala^2, D-Leu^5]enkephalin acetate (Bachem), EMD 60400 (N-methyl-*N*-[(1S)-1-phenyl-2-((3S)-3-hydroxypyrrolidine-1-yl)-ethyl]-2-aminophenylacetamide 2HCl, E. Merck, Darmstadt, Germany; Figure 1), ethylketocyclazocine methanesulphonate (Sterling Winthrop), haloperidol HCl (E. Merck, Darmstadt, Germany), ICI 197067 ((2S)-N- [2-(*N*-methyl-3, 4-dichlorphenylacetamido)-3-methylbutyl]-pyrrolidine HCl (E. Merck, Darmstadt, Germany; Cambridge Research Biochemicals; Figure 1), ICI 204448 (2-[3-(1-(3,4-dichlorphenyl-*N*-methylacetamido)-2-pyrrolidonoethyl)-phenoxy]acetic acid HCl; E. Merck, Darmstadt, Germany; Figure 1), morphine HCl (E. Merck, Darmstadt, Germany), naloxone HCl (Sigma), norbinaltorphimine 2HCl (Research Biochemicals Inc.), NSD 1015 (*m*-hydroxybenzylhydrazine 2HCl; Sigma), substance P tetratrifluracetate (Bachem) and U 69593 ((5-α,7-α,8-β)-(−)-N-methyl-*N*-(7-(1-pyrrolidinyl)-1-oxaspiro (4,5)-dec-8-yl)-phenylacetamide; Upjohn, Kalamazoo, U.S.A). The ligands [^{3}H]-U 69593, [^{3}H]-PL 017 ([N-MePhe^3, D-Pro^4]morphiceptin), [^{3}H]-[D-Pen^{2,5}] enkephalin, [^{3}H]-[D-Ala^2, D-Leu^5]enkephalin acetate and [^{3}H]-ethylketocyclazocine were from NEN Research Products, Dreieich.

Statistics

Tests of statistical significance were made with the Dunnett test for multiple comparisons with control; 95% confidence intervals were calculated by the method of Litchfield & Wilcoxon (1949), except in the case of the rotarod and pressure pain tests, where the method of Dixon & Mood (1948) was used.

Results

In vitro *tests*

Binding Experiments with radiolabelled ligands revealed that EMD 60400 and ICI 197067 bind potently to κ-opioid receptors, with IC_{50} values (mean ± s.d.) of 2.8 ± 1.3 and 1.5 ± 0.2 nM, respectively; ICI 204448 had an IC_{50} value for binding to κ-opioid receptors of 13.0 ± 5.7 nM (all $n = 3$). The corresponding figures for μ and δ binding were 500 ± 115, 100 ± 57 and 233 ± 60 nM, and 333 ± 88, 1200 ± 400 and 167 ± 33 nM, respectively (all $n = 3$).

Electrically-stimulated rabbit vasa deferentia EMD 60400, ICI 197067, and ICI 204448 were full and potent κ-opioid receptor agonists which were able to produce concentration-dependent inhibition of electrically-induced contractions of rabbit isolated vasa deferentia. IC_{50} values (means with 95% confidence intervals) were 41.8 (35.1–49.9; $n = 4$), 15.7 (5.2–47; $n = 4$), and 15 (12–19; $n = 3$) nM, respectively.

Central actions of systemically-applied κ agonists

Ex vivo *determination of brain and plasma levels* Results from this test indicated that EMD 60400 is absorbed well into blood plasma following its s.c. administration (see Table 1 for comparison with ICI 197067). The concentration of EMD 60400 in the brains of treated mice increased from a threshold between 1.0 and 10 mg kg^{-1}, whereas for ICI 197067 this threshold lay between 0.1 and 1.0 mg kg^{-1} (Table 1). The brain concentration of ICI 204448 was below 2 pg mg^{-1} after s.c. application at a dose of 10 mg kg^{-1}.

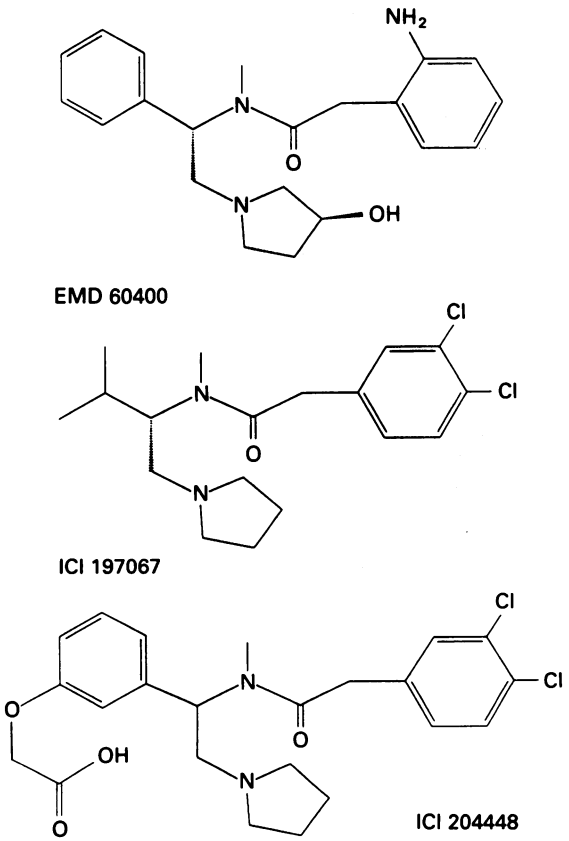


Figure 1 Chemical structures of EMD 60400, ICI 197067 and ICI 204448.

Table 1 Estimation of brain and plasma concentrations (mean ± s.d.) by *ex vivo* binding in the mouse

	Dose (mg kg^{-1} s.c.)	*Brain level* (pg mg^{-1})	*Plasma concentration* (ng ml^{-1})
EMD 60400	0.1	<1	3.1 ± 0.2
	1.0	2.6 ± 3.5	20.4 ± 5.9
	10	120.0 ± 18.0	403.0 ± 35.0
	50	470.0 ± 166.0	1200.0 ± 117.0
ICI 197067	0.1	21.5 ± 3.5	23.6 ± 5.0
	1.0	167.4 ± 37.0	175.6 ± 8.4
	10	848.0 ± 27.0	626.8 ± 44.5

Haloperidol-induced DOPA accumulation Levels of DOPA in haloperidol-treated control groups (mean ± s.e.mean) were 4,547 ± 126 ($n = 13$), 5,258 ± 238 ($n = 14$), and 4,089 ± 247 ($n = 3$) ng g^{-1} for EMD 60400, ICI 197067, and ICI 204448, respectively. Statistically significant inhibition of haloperidol-induced DOPA accumulation was obtained with EMD 60400 at doses of and above 3.0 mg kg^{-1}, s.c. and with ICI 197067 at doses of and above 0.3 mg kg^{-1}, s.c. (see Table 2 for ID_{50} values). ICI 204448, on the other hand, produced no significant reduction in DOPA accumulation at a dose of 30 mg kg^{-1}, s.c. (Table 2).

Sleeping time Sleeping times in the vehicle-treated groups (mean ± s.e.mean) were 73.6 ± 3.6 ($n = 30$), 71.9 ± 3.2 ($n = 29$), and 82.0 ± 5.9 ($n = 15$) min for EMD 60400, ICI 197067, and ICI 204448, respectively. EMD 60400 prolonged hexobarbitone-induced sleeping in mice at doses above 3.0 mg kg^{-1}, s.c., whereas narcosis-potentiation after pretreatment with ICI 197067 was observed at doses above 0.3 mg kg^{-1} (see Table 2 for ID_{50} values). ICI 204448 was ineffective in this test at a dose of 30 mg kg^{-1}, s.c. (Table 2).

Rotarod The threshold dose for sedation 30 min after treatment with EMD 60400 lay between 2.5 and 5.0 mg kg^{-1}, s.c. and for ICI 197067 between 0.25 and 0.55 mg kg^{-1}, s.c. (see Table 2 for ID_{50} values). ICI 204448 was completely inactive in this test at doses of 50 and 100 mg kg^{-1}, s.c. (Table 2).

Antinociceptive actions of the κ agonists

Mouse formalin-induced paw licking All three compounds produced dose-dependent antinociception against the non-inflammatory (1st) and inflammatory (2nd) phases of the nociceptive response to formalin (Figure 2; Table 3). When applied at a high enough dose these compounds were able to abolish completely the response to inflammatory and non-inflammatory pain.

The effect of naloxone on the opiate action was also tested. Licking was inhibited (mean ± s.e.mean; 1st phase/2nd phase) by 53 ± 9.6/52 ± 16.7% ($n = 6$) in mice treated with 1.0 mg kg^{-1} EMD 60400, s.c., by − 13 ± 16.7/21 ± 15.5% ($n = 10$) in mice injected 20 min before formalin with 1.0 mg kg^{-1} naloxone, s.c., and by − 4 ± 14.6/15 ± 25.8% ($n = 6$) in mice injected with both EMD 60400 and naloxone.

Mouse and rat writhing ICI 197067, EMD 60400 and ICI 204448 also had dose-dependent antinociceptive effects in mouse and rat writhing tests, with each substance being equieffective in the two species (Figure 3; Table 3). The antinociceptive action of EMD 60400 in this test in mice was inhibited by the s.c. application of naloxone given 30 min prior to phenylbenzoquinone. The number of pain symptoms (mean ± s.e.mean) in the vehicle-treated group was 53.3 ± 4.1

Table 2 Summary of ID_{50} values (with 95% confidence intervals) in tests of central activity

Test	*EMD 60400*	*ICI 197067*	*ICI 204448*
DOPA accumulation	5.0 (0.7–35)	2.0 (0.02–168)	>30
Hexobarbitone sleeping	16 (10.0–25.6)	3.3 (1.5–7.3)	>30
Rotarod	6.1 (4.3–8.7)	0.71 (0.45–1.12)	>100

ID_{50} values (mg kg^{-1}, s.c.).

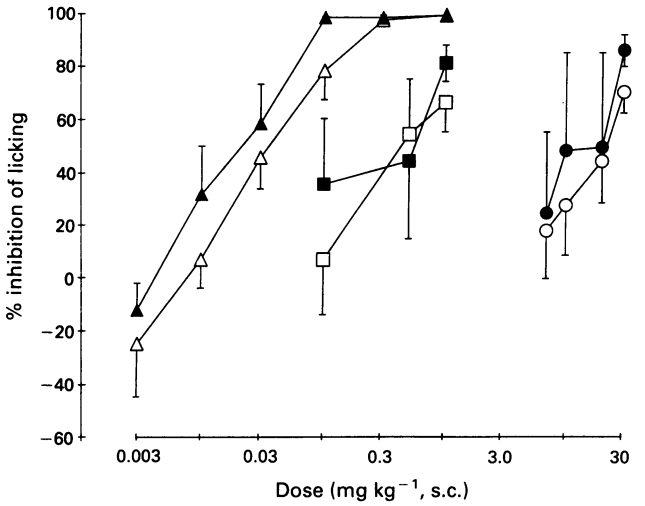


Figure 2 Effects of κ agonists on formalin-induced paw licking observed 0–5 (open symbols) and 20–25 (closed symbols) min after the intraplantar injection of formalin. The κ agonists, EMD 60400 (□, ■), ICI 197067 (△, ▲) and ICI 204448 (○, ●) were applied s.c. 30 min before formalin. Absolute licking times (mean ± s.e.mean; 1st phase/2nd phase) in the vehicle-treated groups were 51.3 ± 2.2/53.5 ± 12.4 ($n = 12$), 49.7 ± 4.1/57.5 ± 5.4 ($n = 15$), and 51.6 ± 5.1/26.3 ± 6.7 ($n = 19$) s for EMD 60400, ICI 197067, and ICI 204448, respectively. Each point in the figure represents the mean ± s.e.mean of measurements from 5–11 mice.

Table 3 Summary of ID_{50} values (with 95% confidence intervals) in antinociceptive and related tests

Test	*EMD 60400*	*ICI 197067*	*ICI 204448*
Formalin			
1st phase	0.44 (0.17–1.1)	0.04 (0.02–0.1)	18.9 (7.3–49.1)
2nd phase	0.47 (NC)	0.02 (0.01–0.04)	12.6 (8.4–18.9)
Writhing			
Mouse	0.55 (0.41–0.75)	0.02 (0.01–0.03)	1.9 (0.6–5.9)
Rat	0.3 (0.2–0.5)	0.04 (0.01–0.11)	4.5 (0.6–31.5)
Pressure pain			
Hyperalgesic	0.1 μg kg^{-1} (0.02–0.47)	4.4 μg kg^{-1} (1.3–14.9)	0.8 (0.3–2.4)
Normalgesic	4.0 (2–8)	77 μg kg^{-1} (24–246)	>30
Neurogenic inflammation	0.3* (0.1–1.0)	1.8* (0.64–5.0)	1.5* (0.4–4.9)

ID_{50} values (mg kg^{-1}, s.c. or i.v.*). NC = not calculable.

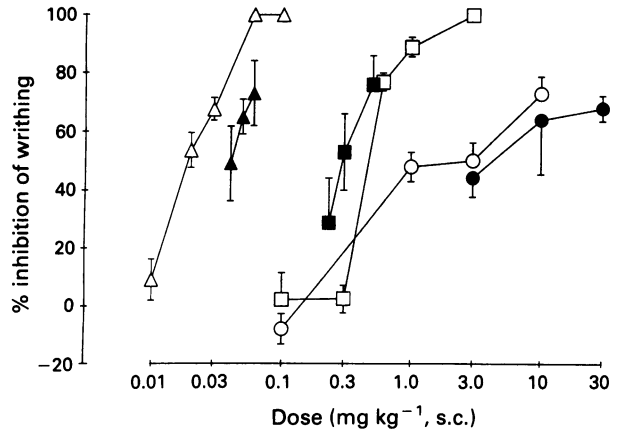


Figure 3 Effects of κ agonists on writhing movements observed 0–20 min after the i.p. injection of 2-phenyl-1,4-benzoquinone. The κ agonists EMD 60400 (□, ■), ICI 197067 (△, ▲) and ICI 204448 (○, ●) were applied s.c. 30 min before 2-phenyl-1,4-benzoquinone. The numbers of writhing movements (mean ± s.e.mean) in the vehicle-treated groups in mice were 51.6 ± 4.5, 36 ± 2.2 and 41.1 ± 1.1 (all $n = 15$) and rats were 53.6 ± 4.3 ($n = 12$), 43.4 ± 2.8 ($n = 16$), and 48.2 ± 4.6 ($n = 11$) for EMD 60400, ICI 197067, and ICI 204448, respectively. Each point in the figure represents the mean ± s.e.mean of measurements from 4 rats (closed symbols) or 10 mice (open symbols).

($n = 15$), in the group treated with 1.0 mg kg^{-1} naloxone, s.c., was 53.6 ± 4.1 ($n = 10$), in the group injected with 0.6 mg kg^{-1} EMD 60400 was 12.0 ± 1.7 ($n = 10$), and in the group given both EMD 60400 and naloxone was 37.5 ± 4.8 ($n = 10$; there was no difference between this group and the vehicle-treated group, $P > 0.05$).

Carrageenin-induced hyperalgesia Both EMD 60400 and ICI 197067 proved extraordinarily effective at inhibiting pressure pain under conditions of inflammatory hyperalgesia, with ID_{50} values in the μg kg^{-1} range (Figure 4; Table 3). ICI 204448 was not as potent, but nevertheless had a dose-dependent antinociceptive effect in this test (Figure 4; Table 3). The antinociceptive effectiveness (number of rats not responding to painful pressure) was four out of six animals treated 30 min before testing with EMD 60400 0.5 μg kg^{-1}, s.c., 0 out of three animals injected with naloxone 0.2 mg kg^{-1}, i.p. 20 min before testing, and 0 out of six animals treated with EMD 60400 and naloxone.

The opiate action against pressure pain was weaker in normalgesic rats, i.e. animals which had not been injected with carrageenin (Figure 4). In these animals EMD 60400 and ICI 197067 were 40,000 and 17.5 times less effective, respectively, than under conditions of inflammatory hyperalgesia, whereas ICI 204448 was ineffective at doses of 10 and 30 mg kg^{-1}, s.c. (Figure 4; Table 3).

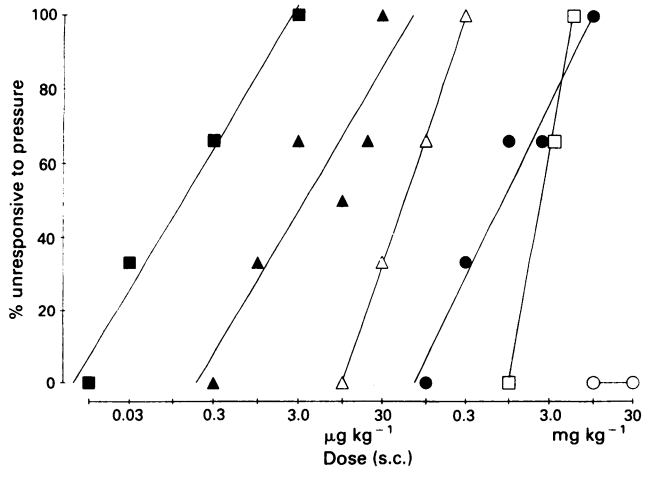


Figure 4 Effects of the κ agonists EMD 60400 (□, ■), ICI 197067 (△, ▲) and ICI 204448 (○, ●) on pressure pain in the rat. Measurements were either made 30 min after the application of the κ agonist in rats without inflammation (open symbols), or 3 h after the injection of carrageenin into the tail (closed symbols), in which case the κ agonists were applied at the same time as carrageenin. Each point represents the % of animals ($n = 3$–6) which did not respond to a standard noxious press.

Other in vivo *effects*

Neurogenic inflammation Neurogenic plasma extravasation in anaesthetized rats was dose-dependently inhibited by the i.v. administration of all three κ-opioid receptor agonists (Figure 5; Table 3), whereby EMD 60400 was most effective

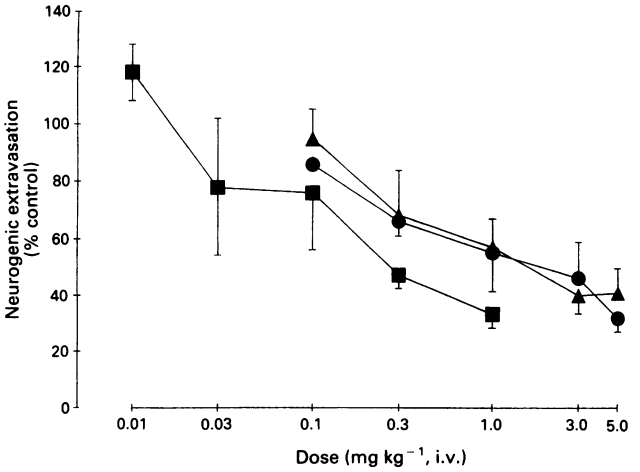


Figure 5 Effects of κ agonists on neurogenic plasma extravasation evoked by 10 min antidromic electrical stimulation of the saphenous nerve. The κ agonists, EMD 60400 (■), ICI 197067 (▲) and ICI 204448 (●) were applied i.v. 15 min before the beginning of nerve stimulation. Neurogenic inflammation was defined as the difference between dye levels in stimulated and control paws. Dye levels (mean ± s.e.mean) in paws from vehicle-treated rats were 3.4 ± 0.3 ($n = 21$), 3.7 ± 0.4 ($n = 23$), and 3.9 ± 0.5 ($n = 22$) μg dye per 100 mg skin for EMD 60400, ICI 197067, and ICI 204448, respectively. Each point in the figure represents the mean ± s.e.mean from 7 animals.

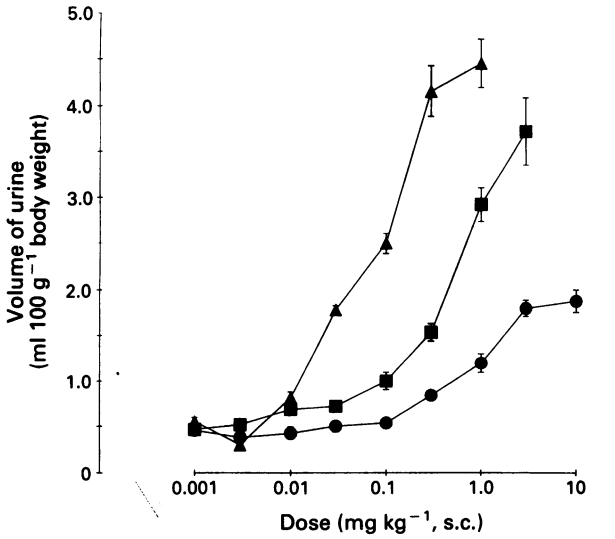


Figure 6 Effects of κ agonists on urinary volume in non-hydrated rats in the 6 h following s.c. application of EMD 60400 (■), ICI 197067 (▲) and ICI 204448 (●).The amount of urine (mean ± s.e. mean) in the vehicle-treated groups were 0.56 ± 0.05 ($n = 30$), 0.49 ± 0.03 ($n = 20$) and 0.44 ± 0.03 ($n = 30$) ml 100 g^{-1} body weight for EMD 60400, ICI 197067, and ICI 204448, respectively. Each point in the figure represents the mean ± s.e.mean of 5 or 10 measurements.

and ICI 204448 and ICI 197067 were equipotent.

The i.v. application of EMD 60400 did not reduce the mean (± s.e.mean) amount of dye measured in the paw after i.pl. injection of 10 μg substance P (control animals had 18.8 ± 1.74 μg dye per 100 mg skin, $n = 13$; animals treated with 1 mg kg^{-1} EMD 60400 had 18.4 ± 2.72 μg dye per 100 mg skin, $n = 7$). Furthermore, the action of EMD 60400 was not blocked by acute adrenalectomy. EMD 60400 at a dose of 1.0 mg kg^{-1} produced a 33 ± 4.7% (mean ± s.e.mean) inhibition of neurogenic extravasation in intact animals (Figure 4) and a 40 ± 6.3% inhibition in adrenalectomised animals ($n = 7$).

Diuresis All three κ-opioid receptor agonists were able to produce large (between 3 and 9 fold) increases in total urinary volume (Figure 6) after s.c. application in non-hydrated conscious rats. ICI 197067 was the most potent of these compounds, with a diuretic effect at doses of and above 10 μg kg^{-1} (Figure 6). EMD 60400 produced diuresis at doses of and above 100 μg kg^{-1} (Figure 6). Diuresis was increased following doses of ICI 204448 of and above 0.3 mg kg^{-1}, though it was noticeable that this compound was not able to raise urinary volume to the extent of ICI 197067 or EMD 60400.

ICI 197067 at very low doses elicited antidiuresis in hydrated rats. Vehicle-treated animals produced 3.5 ± 0.09 ml urine per 100 g (mean ± s.e.mean), whereas rats treated with 1, 3 and 6 μg kg^{-1} ICI 197067, s.c., produced 3.7 ± 0.09, 3.0 ± 0.04 and 3.1 ± 0.08 ml urine per 100 g (all $n = 5$), of which the latter two values are significantly less than control ($P < 0.01$).

Peripheral actions of systemically-applied EMD 60400

The antinociceptive action of systemically-applied EMD 60400 in the hyperalgesic pressure pain test was completely antagonized by small doses of the κ-opioid receptor antagonist, norbinaltorphimine, applied directly into the inflamed portion of the tail. Six out of six rats responded to painful pressure 30 min after receiving vehicle s.c. and 5 min after an injection of 100 μg norbinaltorphimine into the tail, two out of six rats responded after the application of 50 μg kg^{-1} EMD 60400 s.c. and vehicle into the tail, whereas six out of six animals responded to pressure after receiving EMD 60400 s.c. and norbinaltorphimine in the tail. There was no evidence that norbinaltorphimine at this dose can produce systemic inhibition of κ antinociception. Two out of six animals responded to pressure 30 min after the injection of EMD 60400 0.5 μg kg^{-1}, s.c. and vehicle i.p., while one out of six rats responded after the application of EMD 60400 s.c. and norbinaltorphimine 100 μg, i.p.

The cutaneous locus of action of EMD 60400 against neurogenic inflammation was demonstrated by the i.pl application of norbinaltorphimine. The inhibitory action of EMD 60400 (1 mg kg^{-1}, i.v.) in the skin of the hind paw could be completely antagonized by the i.pl application of 50 μg norbinaltorphimine (Figure 7). This dose of norbinaltorphimine had no significant effect on neurogenic plasma extravasation on its own (Figure 7) and also did not antagonize the opiate action when given by the i.v. route of administration. The amount of dye in the skin (mean ± s.e. mean of the difference between stimulated and unstimulated paws expressed as μg dye per 100 mg skin) was 6.3 ± 0.7 ($n = 5$) in vehicle-treated animals, 5.7 ± 0.7 ($n = 4$) after 50 μg norbinaltorphimine i.v., 2.6 ± 0.8 ($n = 5$) after 1.0 mg kg^{-1} EMD 60400 i.v., and 2.8 ± 1.1 ($n = 5$) after EMD 60400 and norbinaltorphimine.

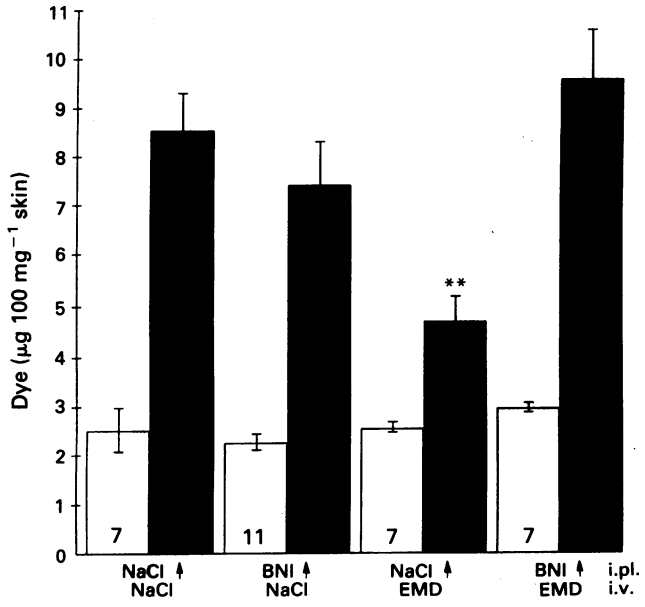


Figure 7 Reversal of EMD 60400-induced inhibition of neurogenic extravasation by intraplantar (i.pl.) norbinaltorphimine. Shown are mean amounts of dye (± s.e.mean) measured in skin from paws in which the saphenous nerve was stimulated antidromically (solid columns) and from control paws which were all injected with 25 μl NaCl (open columns). Stimulated paws were either injected with 25 μl NaCl solution or 50 μg norbinaltorphimine (BNI), while rats were treated with either NaCl or 1 mg kg^{-1} EMD 60400 i.v. The number of animals in each group is shown in the corresponding open column. The amount of dye measured on the stimulated side of rats injected with EMD 60400 was significantly different from control (**$P < 0.01$), otherwise differences from control were not statistically significant.

Discussion

There have been a number of reports that centrally-active κ-opioid receptor agonists can have direct, peripheral antinociceptive actions in inflamed tissue (see Barber & Gottschlich, 1992, for recent review). These findings, along with the recognition that the systemic application of such agonists in humans has unacceptable central side effects (Pfeiffer *et al.*, 1986), have led to interest in the development of 'peripherally-selective' κ-opioid receptor agonists for the treatment of inflammatory hyperalgesia. EMD 60400 (Barber *et al.*, 1992), ICI 197067 (Costello *et al.*, 1988) and ICI 204448 (Shaw *et al.*, 1989) are κ agonists which were expected to have different degrees of access to the CNS following their systemic application.

The results from the present *in vitro* experiments indicate that EMD 60400 and ICI 197067 are potent, selective and full κ-opioid receptor agonists. We were able to confirm the low κ binding affinity of ICI 204448 relative to ICI 197067 reported on the basis of inhibition of [^{3}H]-bremazocine binding by Shaw *et al.* (1989; 33.2 and 1.19 nM, respectively). Under the present experimental conditions the binding affinities of ICI 204448 and ICI 197067 for the κ-opioid receptor were 13.0 and 1.5 nM, respectively. The present binding studies further indicate that ICI 204448 is not particularly selective in its affinity for the κ-opioid receptor, with a κ:μ:δ binding ratio of 1:17.9:12.8 (this ratio was 1:179:119 and 1:67:800 for EMD 60400 and ICI 197067, respectively). Our IC_{50} value for the agonist potency of ICI 204448 in the rabbit vas deferens preparation (15 nM) is also similar to the 10.8 nM found by Shaw *et al.* (1989). On the other hand, the κ:μ selectivity of ICI 197067 calculated in the present experiments on the basis of [^{3}H]-U-69593:[^{3}H]-PL-017 binding (1:67) is much less than that reported by Costello *et al.* (1988) using [^{3}H]-bremazocine:[^{3}H]-naloxone binding (1:1900).

We have tried to obtain a measure of the ability of EMD 60400, ICI 197067 and ICI 204448 to induce the centrally-mediated side effects, aversion and sedation. The increase in DOPA accumulation in the nucleus accumbens induced by the block of inhibitory D_2 receptors with halo-

peridol is known to be reversed by centrally-active κ-opioid receptor agonists (Manzanares *et al.*, 1991) because dopamine release in the accumbens is also subject to presynaptic inhibition from κ agonists (Smith *et al.*, 1992). Since the κ agonists used here have only very poor affinity for dopamine receptors (C.A. Seyfried, unpublished observations), results with this method can be taken as a measure of activity at central κ-opioid receptors in that neurotransmitter system and area of the brain in which κ agonists are believed to mediate their aversive effects (Di Chiara & Imperato, 1988; Spanagel *et al.*, 1990). The sedative effects of the κ-opioid receptor agonists were investigated in the mouse hexobarbitone narcosis and rodent rotarod tests, in which centrally-active κ agonists are known to be active (e.g. Hayes *et al.*, 1990; Fürst, 1991).

These methods have produced similar results. Systemically-applied ICI 204448 gave no sign of activating central κ-opioid receptors in rats and mice even at high doses. Thus ICI 204448 was not detected in *ex vivo* binding experiments after s.c. application of 10 mg kg^{-1}. Thirty mg kg^{-1} ICI 204448 s.c. produced no reduction in DOPA accumulation in the nucleus accumbens (Table 2) or prolongation of hexobarbitone-induced sleeping (Table 2), and 100 mg kg^{-1} ICI 204448 s.c. did not impair motor performance in the rotarod test (Table 2). Since ICI 204448 is as potent in the rabbit vas deferens assay as the other κ agonists used here it is likely that these results are indicative of poor penetration into the CNS due to the polar zwitterionic stucture of ICI 204448 (Shaw *et al.*, 1989).

ICI 197067 displays a greater ability to penetrate into the CNS than ICI 204448 (Shaw *et al.*, 1989). Our results in the *ex vivo* binding test (Table 1) are comparable with those of Shaw *et al.* (1989), who found a brain concentration of 119 pg mg^{-1} tissue after the s.c. application of ICI 197067 at a dose of 0.23 mg kg^{-1}. In our experiments ICI 197067 began to increase its concentration in the brain substantially at s.c. doses between 0.1 and 1.0 mg kg^{-1} (Table 1). This compound also produced significant inhibition of DOPA accumulation at doses of 0.3 mg kg^{-1}, s.c. and above, prolonged hexobarbitone-induced sleeping at doses above 0.3 mg kg^{-1}, s.c., and impaired performance on the rotarod at doses above 0.25 mg kg^{-1}, s.c. The data therefore suggest that ICI 197067 penetrates the blood-brain barrier in sufficient amounts to elicit the centrally-mediated side effects, sedation and putative aversion, at a threshold dose of around 0.3 mg kg^{-1}, s.c.

The threshold dose for these effects with EMD 60400 is in the order of 10 fold higher since inhibition of DOPA accumulation, prolongation of sleeping time and impaired rotarod performance were all observed at doses beginning around 3.0 mg kg^{-1}, s.c. Results from the *ex vivo* experiments also indicate that the concentration of EMD 60400 in the brain began to increase markedly only after doses between 1 and 10 mg kg^{-1}, s.c. (Table 1). We interpret these findings as being due to a reduced tendency of EMD 60400 to cross the blood-brain barrier, as compared to ICI 197067. The structural characteristics of EMD 60400, namely the inclusion of 2 polar groups (NH_2 and OH; Figure 1), therefore appear to allow the combination of high affinity and selectivity for the κ-opioid receptor with a relatively high threshold for producing central side effects.

Centrally-acting κ-opioid receptor agonists generally induce sedative effects at higher doses than central antinociceptive actions (Hayes *et al.*, 1990; Hunter *et al.*, 1990). The three κ agonists we tested were effective in the rodent writhing test (Figure 3), and the present ID_{50} values for ICI 197067 and ICI 204448 in the mouse writhing test (0.02 and 1.9 mg kg^{-1}, s.c., respectively) are in good agreement with those published previously by others (0.05 (0.02–0.06) and 4.4 (2.5–7.4) mg kg^{-1}, s.c., respectively; Costello *et al.*, 1988; Rogers *et al.*, 1992).

EMD 60400, ICI 197067 and ICI 204448 were also effective in the mouse formalin test against both non-inflammatory (1st phase) and inflammatory (2nd phase) pain, although we, in contrast to Rogers *et al.* (1992) who used the rat, saw no evidence of more pronounced inhibition of the 2nd than the 1st phase by the peripherally-selective compound ICI 204448 (Figure 2; Table 3). The dose-response relationships indicate that all three κ agonists produce their antinociceptive actions in this test in dose-ranges in which antinociceptive effects can be found in the writhing test.

The sites of action of the κ agonists in these tests are still unclear. Rogers *et al.* (1992) concluded on the basis of their experiments with s.c. and i.c.v. application that systemic antinociceptive effects of the peripherally-selective κ agonist, GR 94839, in the mouse writhing test were probably due to penetration of this compound into the CNS. Moreover, the fact that the antinociceptive action of GR 94839 after systemic application in the formalin test was only partially antagonized by i.pl. application of the opiate antagonists, naltrexone (1 μg) or norbinaltorphimine (100 μg; Rogers *et al.*, 1992) may indicate that GR 94839 is having central and peripheral actions in this test. Both central and peripheral inhibitory effects of κ agonists have been reported previously in the formalin test (Haley *et al.*, 1990; Pelissier *et al.*, 1990).

The antinociceptive actions of the κ agonists in the normalgesic pressure pain test reported here (Figure 4) also correspond well to their effectiveness in the writhing test (with the exception of ICI 204448; Figure 3). However, EMD 60400 and ICI 204448 become much more potent antinociceptive agents in tissue inflamed by the injection of carrageenin, as do GR 94839 and ICI 204448 in the zymosan-induced hyperalgesia model in the rat paw (Rogers *et al.*, 1992). It seems very probable that under these conditions EMD 60400 is producing antinociception in the periphery rather than the CNS since the action of this compound can be completely inhibited by injection of the κ-opioid receptor antagonist, norbinaltorphimine, directly into the tail at a dose (100 μg) which produces no systemic inhibition of κ-mediated antinociception.

Independent of where it is acting, the selectivity of EMD 60400 for κ-opioid receptors means that its antinociceptive actions in the writhing and formalin tests are most probably mediated by these receptors. We found that the action of EMD 60400 in these tests could be reversed by pretreatment with naloxone (1 mg kg^{-1}, s.c.), like Hunter *et al.* (1990) who found that this dose of naloxone completely antagonized antinociception produced by CI-977, PD 117302, U 69593, U 50488 and other κ-agonists in the rat paw pressure test. The observation that the action of EMD 60400 in the hyperalgesic pressure pain test can be completely antagonized by 0.2 mg kg^{-1} naloxone s.c. may, however, indicate that this compound can also have activity at μ-opioid receptors under some *in vivo* experimental conditions.

In the present study we have shown that systemically-applied EMD 60400 also inhibits neurogenic inflammation (Figure 5). This is probably achieved via a purely peripheral opioid mechanism in the skin because the inhibitory action of this compound can be completely reversed by 50 μg norbinaltorphimine applied directly into the paw (Figure 7). This dose of norbinaltorphimine produces no systemic inhibition of the opiate effect. Similar effects have been obtained with ICI 204448 using 10 μg naloxone as the antagonist (A. Barber, unpublished observations) and previous studies have shown that the inhibitory action of systemically-applied ethylketocyclazocine in this test can be antagonized by the systemic application of the quaternised opiate antagonist, N-methyl nalorphine (Smith & Buchan, 1984).

The diuretic effects of EMD 60400, ICI 197067 and ICI 204448 described here are typical for κ-opioid receptor agonists (Vonvoightlander *et al.*, 1983; Leander *et al.*, 1983). Antidiuretic effects of κ agonists at high doses (e.g. 10 mg kg^{-1} U 69593, s.c.; Hayes *et al.*, 1990; 10 mg kg^{-1} U 50488, i.p.; Bianchi, 1991) and in the 1st hour following the blockade of α_2-adrenoceptors with idazoxan or yohimbine (Bianchi, 1991) have also been observed. But antidiuretic actions of substances of this class at such very low doses relative to

effective doses in the mouse writhing test have not been documented previously.

Diuretics have been described as having weak antinociceptive effects in rats in the hot plate test (Poggioli *et al.*, 1985) but it is unclear to what extent the diuretic action of the κ agonists contributes to the antinociception reported here, for instance, by reducing swelling. Antinociception and diuresis following the application of EMD 60400 and ICI 197067 occur in the same dose-range in the formalin, writhing and normalgesic pressure pain tests (Figures 2,3,4 and 6). However, these compounds are effective in the hyperalgesic pressure pain test at doses too low to cause diuresis (Figure 4), which therefore rules out the possibility of a pseudo-antinociceptive effect through loss of body fluid.

An important mechanism of the peripheral antinociceptive action of κ-opiate agonists in the hyperalgesic pressure pain model is likely to be the reduction in the flow of tonic sensory information from the painful area (Russell *et al.*, 1987; Haley *et al.*, 1990). Such a peripheral inhibitory action of systemically-applied EMD 60400 on the spontaneous and evoked activity of slowly-conducting afferents from the inflamed knee joint of the cat has recently been demonstrated (Meßlinger *et al.*, 1993).

In the present study it was found that systemically-applied EMD 60400 did not reduce the effectiveness of i.pl. substance P in eliciting plasma extravasation in rat skin. Since substance P is the main putative neurotransmitter mediating neurogenic inflammation (Holzer, 1988), this indicates that the opiates have a pre- rather than a postjunctional mechanism of action in this test. The results with adrenalectomized animals also demonstrated that EMD 60400 does not exert an indirect action via the adrenal glands (Carey *et al.*, 1987). The most likely mechanism involves the presynaptic inhibition of the release of substance P from primary afferent fibres in the skin (Yonehara *et al.*, 1992). Peripheral opiate receptors on small diameter sensory neurones capable of mediating inhibition of impulse flow and substance P release have been documented (Stein *et al.*, 1990).

The results of our experiments therefore indicate that EMD 60400 and ICI 197067 are potent and selective κ-opioid receptor agonists which display different tendencies to cross the blood-brain barrier, as measured by *ex vivo* binding. This is reflected in their relative abilities to elicit the centrally-mediated side effects, sedation and putative aversion (ICI 197067 > EMD 60400 > ICI 204448). Furthermore, EMD 60400 inhibits hyperalgesic pressure pain and neurogenic inflammation through a peripheral mechanism of action. This could involve inhibition of the flow of tonic and evoked sensory information from inflamed areas to the CNS, and inhibition of the peripheral release of the inflammatory mediator substance P, presumably through the activation of peripheral κ-opioid receptors on primary sensory neurones. Systemic application of these agonists also produced antinociception in the writhing, normalgesic pressure pain, and formalin tests, though the relative contribution of central and peripheral antinociceptive components in these models remains to be determined. The development of peripherally-selective κ agonists may allow novel treatment of inflammatory pain in man which is not accompanied by unacceptable central side effects.

References

BARBER, A. & GOTTSCHLICH, R. (1992). Opioid agonists and antagonists: an evaluation of their peripheral actions in inflammation. *Med. Res. Rev.*, **12**, 525–562.

BARBER, A., GOTTSCHLICH, R., HARTING, J., LUES, I., MAULER, F. & STOHRER, M. (1992). Pharmacological characteristics of the peripherally-selective κ-opioid agonists EMD 60400 and ICI 204448. *Naunyn-Schmied. Arch. Pharmacol.*, **345S**, 456.

BIANCHI, G. (1991). Antidiuretic effect of bremazocine and U-50,488 in rats after α_2-adrenoceptor blockade. *J. Pharm. Pharmacol.*, **43**, 212–216.

CAREY, F., HAWORTH, D., STONE, M.A., HERON, J.R.M., WAYNE, J., JAMIESON, A. & RUSSELL, N.J.W. (1987). Involvement of corticosterone in the antiinflammatory activity of the opioid κ-agonists tifluadom and U 50488. *Br. J. Pharmacol.*, **92**, 629P.

COSTELLO, G.F., MAIN, B.G., BARLOW, J.J., CARROLL, J.A. & SHAW, J.S. (1988). A novel series of potent and selective agonists at the opioid κ-receptor. *Eur. J. Pharmacol.*, **151**, 475–478.

DI CHIARA, G. & IMPERATO, A. (1988). Opposite effects of mu and kappa opiate agonists on dopamine release in the nucleus accumbens and in the dorsal caudate of freely moving rats. *J. Pharmacol. Exp. Ther.*, **244**, 1067–1080.

DIXON, W.J. & MOOD, A.M. (1948). A method for obtaining and analyzing sensitivity data. *J. Am. Stat. Ass.*, **43**, 109–126.

FÜRST, S. (1991). Pharmacological interactions of opiates with various classes of centrally acting dopaminergic drugs. *Drug Metabol. Drug Interactions*, **9**, 77–102.

HALEY, J., KETCHUM, S. & DICKENSON, A. (1990). Peripheral κ-opioid modulation of the formalin response: an electrophysiological study in the rat. *Eur. J. Pharmacol.*, **191**, 437–446.

HAYES, A.G., BIRCH, P.J., HAYWARD, N.J., SHEEHAN, M.J., ROGERS, H., TYERS, M.B., JUDD, D.B., SCOPES, D.I.C. & NAYLOR, A. (1990). A series of novel, highly potent and selective agonists for the κ-opioid receptor. *Br. J. Pharmacol.*, **101**, 944–948.

HOLZER, P. (1988). Local effector functions of capsaicin-sensitive sensory nerve endings: involvement of tachykinins, calcitonin gene-related peptide and other neuropeptides. *Neurosci.*, **24**, 739–768.

HUNSKAAR, S. & HOLE, K. (1987). The formalin test in mice: dissociation between inflammatory and non-inflammatory pain. *Pain*, **30**, 103–114.

HUNTER, J.C., LEIGHTON, G.E., MEECHAM, K.G., BOYLE, S.J., HORWELL, D.C., REES, D.C. & HUGHES, J. (1990). CI-977, a novel and selective agonist for the κ-opioid receptor. *Br. J. Pharmacol.*, **101**, 183–189.

LEANDER, J.D. (1983). A kappa opioid effect: increased urination in the rat. *J. Pharmacol. Exp. Ther.*, **224**, 89–94.

LITCHFIELD, J.T. & WILCOXON, F. (1949). A simplified method of evaluating dose-effect experiments. *J. Pharmacol. Exp. Ther.*, **96**, 99–113.

MANZANARES, J., LOOKINGLAND, K.J. & MOORE, K.E. (1991). Kappa opioid receptor-mediated regulation of dopaminergic neurons in rat brain. *J. Pharmacol. Exp. Ther.*, **256**, 500–505.

MEßLINGER, K., PAWLAK, M., LUKAS, A. & SCHMIDT, R.F. (1992). Peripheral action of EMD 60400, a new kappa-opioid agonist, on the activity of slowly conducting afferents in the inflamed knee joint of the cat. Abstract 42 *7th World Congress on Pain, Paris*, Seattle: IASP Publications.

OKA, T., NEGISHI, K., SUDA, M., MATSUMIYA, T., INAZU, T. & UEKI, M. (1980). Rabbit vas deferens: a specific bioassay for opioid κ-receptor agonists. *Eur. J. Pharmacol.*, **73**, 235–236.

PELISSIER, T., PAEILE, C., SOTO-MOYANO, R., SAAVEDRA, H. & HERNANDEZ, A. (1990). Analgesia produced by intrathecal administration of the κ opioid agonist, U-50,488H, on formalin-evoked cutaneous pain in the rat. *Eur. J. Pharmacol.*, **190**, 287–293.

PFEIFFER, A., BRANTL, V., HERZ, A. & EMRICH, H.M. (1986). Psychomimesis mediated by κ opiate receptors. *Science*, **233**, 774–776.

POGGIOLI, R., VERGONI, A.V. & BERTOLINI, A. (1985). Influence of hydrochlorothiazide on the pain threshold and on the antinociceptive activity of morphine, in rats. *Experientia*, **41**, 265–266.

ROGERS, H., BIRCH, P.J., HARRISON, S.M., PALMER, E., MANCHEE, G.R., JUDD, D.B., NAYLOR, A., SCOPES, D.I.C. & HAYES, A.G. (1992). GR94839, a κ-opioid agonist with limited access to the central nervous system, has antinociceptive activity. *Br. J. Pharmacol.*, **106**, 783–789.

RUSSELL, N.J.W., SCHAIBLE, H.-G. & SCHMIDT, R.F. (1987). Opiates inhibit the discharges of fine afferent units from inflamed knee joint of the cat. *Neurosci. Lett.*, **76**, 107–112.

SEYFRIED, C.A., ADAM, G. & GREVE, T. (1986). An automated direct-injection HPLC-method for the electrochemical/fluorimetric quantitation of monoamines and related compounds for the screening of large numbers of animals. *Biomed. Chromatogr.*, **1**, 78–88.

SHAW, J.S., CARROLL, J.A., ALCOCK, P. & MAIN, B.G. (1989). ICI 204448: a κ-opioid agonist with limited access to the CNS. *Br. J. Pharmacol.*, **96**, 986–992.

SMITH, T.W. & BUCHAN, P. (1984). Peripheral opioid receptors located on the rat saphenous nerve. *Neuropeptides*, **5**, 217–220.

SMITH, J.A.M., LOUGHLIN, S.E. & LESLIE, F.M. (1992). κ-Opioid inhibition of [^{3}H] dopamine release from rat ventral mesencephalic dissociated cell cultures. *Mol. Pharmacol.*, **42**, 575–583.

SPANAGEL, R., HERZ, A. & SHIPPENBERG, T.S. (1990). The effect of opioid peptides on dopamine relase in the nucleus accumbens: an in vivo microdialysis study. *J. Neurochem.*, **55**, 1734–1740.

STEIN, C., HASSAN, A.H.S., PRZEWLOCKI, R., GRAMSCH, C., PETER, K. & HERZ, A. (1990). Opioids from immunocytes interact with receptors on sensory nerves to inhibit nociception in inflammation. *Proc. Natl. Acad. Sci. U.S.A.*, **87**, 5935–5939.

VONVOIGHTLANDER, P.F., LAHTI, R.A. & LUDENS, J.H. (1983). U-50,488: a selective and structurally novel non-mu (kappa) opioid agonist. *J. Pharmacol. Exp. Ther.*, **224**, 7–12.

YONEHARA, N., IMAI, Y., CHEN, J.-Q., TAKIUCHI, S. & INOKI, R. (1992). Influence of opioids on substance P release evoked by antidromic stimulation of primary afferent fibers in the hind instep of rats. *Regul. Pept.*, **38**, 13–22.

(Received April 5, 1993
Revised October 5, 1993
Accepted October 22, 1993)

Br. J. Pharmacol. (1994), **111**, 852–860

© Macmillan Press Ltd, 1994

Autocrine enhancement of leukotriene synthesis by endogenous leukotriene B_4 and platelet-activating factor in human neutrophils

Patrick P. McDonald, Shaun R. McColl, *Pierre Braquet & [1]Pierre Borgeat

Centre de recherche en Inflammation, immunologie et rhumatologie, Institut de recherche du CHUL et Université Laval, 2705 boul. Laurier, Ste-Foy, Québec, Canada, G1V 4G2 and *Institut Henri-Beaufour, Le Plessis-Robinson, France

1 Platelet-activating factor (PAF) and leukotriene B_4 (LTB_4), two potent lipid mediators synthesized by activated neutrophils, are known to stimulate several neutrophil functional responses. In this study, we have determined that endogenous LTB_4 and PAF exert autocrine effects on LT synthesis, as well as the underlying mechanism involved.

2 Pretreatment of neutrophils with either pertussis toxin (PT), or with receptor antagonists for LTB_4 and PAF, resulted in an inhibition of LT synthesis induced by calcium ionophore, A23187. This inhibition was most marked at submaximal (100– 300 nM) A23187 concentrations, whilst it was least at ionophore concentrations which induce maximal LT synthesis (1–3 μM). Thus newly-synthesized PAF and LTB_4 can enhance LT synthesis induced by A23187 under conditions where the LT-generating system is not fully activated.

3 In recombinant human (rh) granulocyte-macrophage colony-stimulating factor (GM-CSF)-primed neutrophils, LT synthesis in response to chemoattractants (fMet-Leu-Phe or rhC5a) was also significantly inhibited by the LTB_4 receptor antagonist, and to a lesser extent by PAF receptor antagonists.

4 Further investigation revealed that LTB_4 and/or PAF exert their effects on LT synthesis via an effect on arachidonic acid (AA) availability, as opposed to 5-lipoxygenase (5-LO) activation. Indeed, the receptor antagonists, as well as PT, inhibited LT synthesis and AA release to a similar extent, whereas 5-LO activation (assessed with an exogenous 5-LO substrate) was virtually unaffected under the same conditions. Accordingly, we showed that addition of exogenous LTB_4 could enhance AA availability in response to chemoattractant challenge in rhGM-CSF-primed cells, without significantly affecting the 5-LO activation status.

5 Our data show that newly-generated PAF and LTB_4 have the ability to positively feedback on LT synthesis by acting at the level of the phospholipase A_2/re-esterification component of the LT biosynthetic pathway in neutrophils. Such autocrine affects are likely to represent an important amplification step of LT synthesis, and may as such contribute to the rapid onset, as well as to the evolution, of inflammatory responses.

Keywords: Arachidonate 5-lipoxygenase; phospholipase A_2; leukotriene B_4 receptor; PAF receptor; guanine nucleotide-binding proteins; pertussis toxin; receptor antagonists

Introduction

Leukotriene B_4 (LTB_4) and platelet activating factor (PAF) are potent activators of various phagocyte responses, such as chemotaxis, aggregation, adherence, degranulation, and oxygen radical generation (O'Flaherty *et al.*, 1981; Lad *et al.*, 1985; Filep & Foldes-Filep, 1990; Hirafuji & Shinoda, 1991), and are thus considered as important lipid mediators of inflammation. Both LTB_4 and PAF are synthesized in large amounts upon activation of polymorphonuclear leukocytes (PMN) by calcium ionophores such as A23187, or by phagocytic stimuli such as zymosan or inflammatory microcrystals (Borgeat & Samuelsson, 1979; Chilton *et al.*, 1984; Poubelle *et al.*, 1987; 1989; Riches *et al.*, 1990). Receptor-dependent soluble stimuli such as N-formyl-methionyl-leucyl-phenylalanine (fMLP), C5a and interleukin-8, as well as LTB_4 and PAF themselves, also have the ability to induce PAF synthesis, a process that is amplified following PMN treatment with granulocyte-macrophage colony-stimulating factor (GM-CSF) (Tessner *et al.*, 1989; Wirthmueller *et al.*, 1989; Gomez-Cambronero *et al.*, 1989; Bussolino *et al.*, 1992; McDonald *et al.*, 1993). Similarly, receptor-dependent agonists induce a significant production of LTB_4 in PMN primed with GM-CSF (Dahinden *et al.*, 1988; McColl *et al.*, 1991; McDonald *et al.*, 1993).

Previous studies have indicated that PAF and LTB_4 may act as autocrine activators of cell functions. For instance, it has been reported that the polymerisation of actin in response to calcium ionophores can be prevented following PMN treatment with pertussis toxin (PT) or the LTB_4 receptor antagonist, LY-223982, or (to a lesser extent) with PAF receptor antagonists (Shefeyk *et al.*, 1985; Downey *et al.*, 1990). It has also been shown that selective 5-lipoxygenase (5-LO) inhibitors profoundly inhibit degranulation in macrophages undergoing phagocytosis, whilst exogenous LTB_4 or LTC_4 enhance degranulation, suggesting an autocrine effect of LTs on these processes (Lew *et al.*, 1991). Similarly, a recent study showed that PAF receptor antagonists inhibit LT synthesis and superoxide anion generation in response to fMLP in rabbit PMN (Stewart & Harris, 1991a). With respect to LT synthesis in human PMN, it is known that exogenous PAF and LTB_4 both have the ability to stimulate LT synthesis (Lin *et al.*, 1982; McDonald *et al.*, 1992). Accordingly, we have recently shown that PAF and LTB_4 are potent activators of the human neutrophil 5-LO (McDonald *et al.*, 1991; 1992). Finally, we have also reported that endogenous LTB_4 partially accounts for several of the stimulatory effects of exogenous arachidonic acid (AA) on human PMN, including calcium mobilisation and LT synthesis (McColl *et al.*, 1989; Naccache *et al.*, 1989). Together,

[1] Author for correspondence.

these observations suggest that endogenous PAF and/or LTB_4 may modulate LT synthesis in an autocrine fashion.

PAF and LTB_4 exert their effects on PMN responses after binding to specific cell-surface receptors. Once occupied, these receptors interact with PT-sensitive, guanine nucleotide-binding proteins (G proteins) to simulate phospholipases A_2, C and/or D, resulting in the generation of second messengers, which participate in triggering functional responses. Thus an autocrine effect of endogenous PAF abd LTB_4 may take place at any of these levels. That LT synthesis ultimately depends upon precursor availability however, makes phospholipase A_2 (PLA_2) a likely target for such autocrine effects. In addition, the neutrophil 5-LO may represent another potential target for autocrine modulation of LT synthesis by PAF and LTB_4, since both products are potent 5-LO activators (McDonald *et al.*, 1991; 1992). Evidence for autocrine effects could be obtained by blocking either the first step of the signal transduction cascade (i.e. the LTB_4 or PAF receptors), or the second step (i.e. the PT-sensitive G proteins). In the current study, we used both approaches to characterize the autocrine effects of PAF and LTB_4 on LT synthesis in human PMN.

Methods

Cell separation

Blood from healthy donors was collected by venepuncture using heparin as anticoagulant. PMN were purified as previously described (Boyum, 1968), with modifications (McDonald *et al.*, 1992), and were resuspended at a final concentration of 5×10^6 PMN ml^{-1}, in HBSS buffered with HEPES (1 mM final). The percentage of PMN in the cell suspensions used in this study exceeded 95%, and cell viability was greater than 98%, as determined by trypan blue exclusion.

Cell incubations

Cell suspensions were supplied with $CaCl_2$ and $MgCl_2$ (1.6 mM and 1.0 mM final concentrations, respectively), and warmed to 37°C for 10 min prior to incubation with substrate and/or stimulus. All agonists were dissolved in dimethyl sulphoxide (DMSO), except for recombinant human (rh)C5a, which was dissolved in PBS plus 0.01% bovine serum albumen (BSA), and added to 0.1 ml aliquots of the cell suspension. The final concentration of DMSO (maximum of 0.3%) consistently failed to stimulate any detectable LT synthesis. The stock solution of 15(S)-hydroperoxy-5,8,11,13 (Z,Z,Z,E)-eicosatetraenoic acid (15-HpETE) (3 mM in ethanol) was diluted 10 fold in 0.6 mM sodium carbonate solution (to form the sodium salt of the fatty acid), and 10 µl of the resulting sodium salt solution was added to 1.0 ml of the cell suspensions, to yield a final concentration of 3.0 µM. After the desired incubation time with the stimuli, samples were processed for reverse-phase high performance liquid chromatography (r.p.-h.p.l.c.) analysis, as described earlier (McDonald *et al.*, 1992). When AA release was determined, reactions were stopped by the addition of 1.0 ml ice-cold methanol containing 25 ng 5,6,8,9,11,12,14,15-octadeutero-AA (D_8-AA) as internal standard.

In the experiments involving PT, cell suspensions were pre-incubated with the toxin at a final concentration of 0.5 µg ml^{-1} for 3 h at 37°C. During this time, the cells were swirled in a rotary water bath (New Brunswick Scientific, Edison, New Jersey, U.S.A.). Calcium and magnesium were added 15 min prior to stimulation. Pretreatment of PMN with rhGM-CSF (1 nM, for 30 min at 37°C) was also performed in this manner. These conditions were chosen from the results of previous studies, for optimal priming (McColl *et al.*, 1991; McDonald *et al.*, 1993). In the experiments involving LTB_4 or PAF receptor antagonists, or MK-886, the compounds were added to the cells 5 min prior to stimulation. The receptor antagonists and MK-886 were dissolved in DMSO.

Analysis of lipoxygenase products by r.p.-h.p.l.c.

Analysis of lipoxygenase products was performed by r.p.-h.p.l.c. as described previously, using an on-line extraction procedure (Borgeat *et al.*, 1990). The lower limit of detection was 0.2 ng at 280 nm and 1 ng at 229 nm.

Analysis of free AA by l.c.-m.s.

Denatured samples were processed by r.p.-h.p.l.c. as described previously (Borgeat *et al.*, 1990). AA-containing fractions were collected, evaporated under reduced pressure in a Speed Vac (model SVC 100D, Savant Instruments Inc., Farmingdale, NY, U.S.A.) and redissolved into 100 µl of acetonitrile. AA was assayed by liquid chromatography-mass spectrometry (l.c.-m.s.), using a nebuliser-assisted electrospray (ion spray) interface coupled to a triple-quadrupole m.s. (API-III, PE Sciex, Thornhill, Ontario, Canada). Aliquots (6 µl) of the samples were injected into the electrospray interface via the 20-µl loop of a Rheodyne injector (model 9125, Rheodyne, Cotati, CA, U.S.A.) connected to a short column (2 × 30 mm, packed with 5 µm octadodecylsilyl silica particles), using acetonitrile:H_2O (87.5:12.5, v:v, containing 0.1% acetic acid) as solvent, at a flow rate of 150 µl min^{-1}. Samples were analysed in negative ion mode. The ions at m/z 303 and 311 (representing the carboxylate anions of AA and D_8-AA, respectively) were monitored. Quantitation was performed using a calibration curve generated by l.c.-m.s. analysis of mixtures of AA and D_8-AA standards.

Statistical analyses

Where mentioned, statistical significance was assessed by Student's paired *t* test (one-tailed).

Materials

Calcium ionophore A23187, fMLP, HEPES, soybean lipoxygenase and PT were obtained from the Sigma Chemical Company (St-Louis, Missouri, U.S.A.). HBSS was from GIBCO (Burlington, Ontario, Canada), and all solvents were h.p.l.c. grade from Anachemia (Montréal, Québec, Canada). 15-HpETE was synthesized and purified as previously described (McDonald *et al.*, 1992). LTB_4 and the LT synthesis inhibitor, MK-886 (3-[3-(4-chlorobenzyl)-3-t-butyl-thio-5-isopropylindol-2-yl]2,2-dimethylpropanoic acid), were generous gifts from Dr Robert N. Young of the Merck-Frosst Centre for Therapeutic Research (Pointe-Claire, Québec, Canada). The PAF receptor antagonists, L-659,989 ((±)-trans-2-(3-methoxy-5-methylsulphonyl-4-propoxyphenyl)-5-(3,4,5-trimethoxyphenyl)tetrahydrofuran) and BN 50730 (tetrahydro-4,7,8,10-methyl-1-(chloro-2-phenyl)-6-(methoxy-4-phenylthiocarbamoyl)-9-pyrido[4',3'-4,5]thieno[3,2-f]triazolo-1,2,4[4,3-α] diazepine-1,4), were respectively provided by Dr W.H. Parsons of Merck Sharp & Dohme (Rahway, New Jersey, U.S.A.), and by Dr Pierre Braquet (Laboratoires Henri-Beaufour, Le Plessis-Robinson, France). The LTB_4 receptor antagonist, LY-223982 ((E)-5-(3-carboxybenzoyl)-2-{[6-(4-methoxyphenyl)-5-henenyl]oxy}benzenepropanoic acid), was obtained from Dr M.H. Niedenthal of Lilly Research Laboratories (Indianapolis, Indiana, U.S.A.). rhGM-CSF was donated by The Genetics Institute (Boston, Massachusetts, U.S.A.), and rhC5a was kindly provided by Dr Henry Showell of the Pfizer Central Research Center (Groton, Connecticut, U.S.A.).

Results

Autocrine effects of endogenous LTB_4 and PAF on A23187-induced LT synthesis

In the course of previous studies, we have observed that PT pretreatment partially inhibited LT synthesis in PMN challenged with submaximal A23187 concentrations, suggesting that the effect of the ionophore may involve G protein-dependent events. Since PAF and LTB_4 are actively synthesized upon ionophore stimulation, we investigated the possibility that a feedback stimulation by these products may account, at least partially, for the inhibitory effect of PT. PMN were pre-incubated with PT or its diluent, or with a combination of the LTB_4 receptor antagonist, LY-223982, and of the PAF receptor antagonist, BN 50730, and stimulated with increasing concentrations of A23187. These concentrations of the receptor antagonists were used on the basis of their being found to inhibit by ≈80% the elevation in free intracellular calcium elicited by either 30 nM LTB_4 or PAF (data not shown). Cells exposed to A23187 alone required a minimal dose of 100 nM to allow the detection of 5-LO products derived from endogenous AA, with a maximal response being achieved at between 1 and 3 μM A23187 (Figure 1). In cells pretreated with either PT or with the LTB_4 and PAF receptor antagonists however, the formation of all AA-derived 5-LO products (i.e. LTB_4, its ω-oxidation products, and the LTA_4 non-enzymatic degradation products) was markedly inhibited in the 100–300 nM range, the inhibition being less evident at A23187 concentrations which induced a maximal response. A parallel effect was consistently observed between the inhibition by PT and that by both receptor antagonists, suggesting that newly synthesized PAF and/or LTB_4 contribute to ongoing LT synthesis induced by submaximal concentrations of A23187, and that they account for most of the G protein-mediated effects of A23187 on LT synthesis.

To determine the respective contributions of endogenous PAF and LTB_4 to LT synthesis in ionophore-challenged PMN, we investigated the effect of the PAF receptor antagonists, BN 50730 and L-659,989, and of the LTB_4 receptor antagonist, LY-223982, either individually or in combination, as well as the effect of PT. At concentrations of A23187 which elicit a nearly maximal LT synthesis (i.e. 1.0 μM), the receptor antagonists had a moderate inhibitory effect on LT synthesis (Figure 2a). In contrast, when a submaximal dose of A23187 was used (i.e. 200 nM), pretreatment with individual receptor antagonists yielded a profound inhibition of LT synthesis (Figure 2b). The combination of BN 50730 and LY-223982, as well as PT pretreatment, consistently led to a somewhat greater inhibition of LT synthesis.

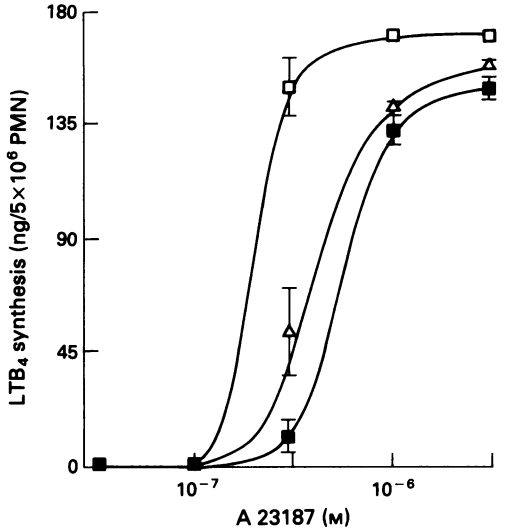


Figure 1 Concentration-dependence of A23187-elicited LTB_4 generation in human PMN, and the effect of pertussis toxin or of receptor blockade. PMN were stimulated (5 min, 37°C) with the indicated concentrations of A23187, following pre-incubation (3 h, 37°C) with 0.5 μg ml^{-1} PT (■), or with the PT diluent (□), or following pretreatment with a combination of 1.0 μM LY-223982 and 100 nM BN 50730 (▲). Samples were analysed by r.p.-h.p.l.c., as described in Methods. Mean ± s.e.mean of triplicate determinations from a single experiment representative of 4. The amounts of LTB_4 represent the sum of LTB_4 and of its ω-oxidation products, 20-hydroxy- and 20-carboxy-LTB_4. For abbreviations, see text.

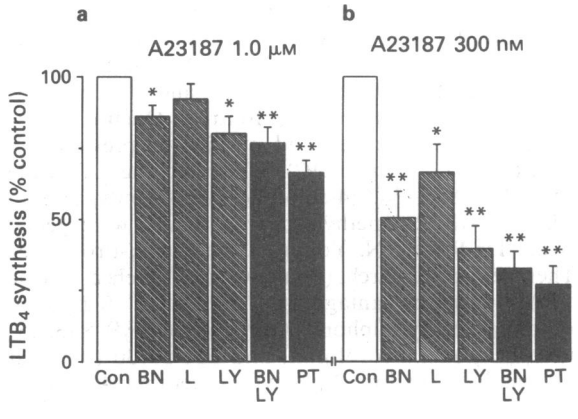


Figure 2 Effect of pertussis toxin, and of PAF and LTB_4 receptor antagonists, on A23187-induced LT synthesis in human PMN. PMN were stimulated (5 min, 37°C) with 1.0 μM (a) or 300 nM (b) A23187, in the presence or absence (5 min before stimulation) of 1.0 μM LY-223982 (LY), 100 nM BN 50730 (BN) or 100 nM L-659,989 (L), or following pre-treatment with PT (0.5 μg ml^{-1}, 3 h at 37°C). Samples were analysed by r.p.-h.p.l.c., as described in Methods. Mean ± s.e.mean of averaged triplicate determinations from at least 5 independent experiments. The 100% control (Con) values, representing the sum of LTB_4 and of its ω-oxidation products, averaged 162 ± 10 ng per 5 × 10^6 PMN (a, $n = 7$) and 123 ± 8 ng per 5 × 10^6 PMN (b, $n = 8$). *$P < 0.04$; **$P < 0.01$. For abbreviations, see text.

Table 1 Effect of pertussis toxin or of PAF and LTB_4 receptor antagonists on A23187-elicited 5-LO activation under conditions where neither PAF nor LTs are synthesized in detectable amounts

Compound	*5-LO activation* (% of control)	*Number of experiments*	P
BN 50730 100 nM	104.2 ± 6.6	3	0.296
L-659,989 100 nM	103.7 ± 4.1	3	0.234
LY-223982 1.0 μM	98.2 ± 4.3	5	0.347
BN + LY	101.7 ± 9.1	5	0.429
PT 0.5 μg ml^{-1}	92.7 ± 9.4	7	0.233

PMN suspensions were pretreated with the receptor antagonists (5 min, 37°C), or with PT (3 h, 37°C) and subsequently incubated for 10 min at 37°C with 3.0 μM 15-HpETE, either alone or with 30 nM A23187. The conversion of 15-HpETE into 5,15-DiHETE (reflecting 5-LO activation) was then determined by r.p.-h.p.l.c. analysis, as described in Methods. Comparisons of 5-LO activity (expressed as % of control) have been calculated after subtracting the 5,15-DiHETE levels resulting from exposure of PMN to 15-HpETE only (± antagonists or PT). Values are the mean ± s.e.mean from the indicated number of experiments, each performed in triplicate. The 100% control values averaged 21 ± 1 ng 5,15-DiHETE per 5 × 10^6 PMN for A23187 30 nM ($n = 7$). BN + LY, simultaneous exposure to 100 nM BN 50730 and 1.0 μM LY-223982. For abbreviations, see text.

To rule out possible nonspecific effects of the antagonists or of PT on 5-LO activity, we investigated whether these compounds would affect 5-LO activation induced by a low concentration (30 nM) of A23187, which allows 5-LO activation without triggering a detectable LTB_4 or PAF synthesis. For this purpose, we used exogenous 15-HpETE, which is converted into 5(S),15(S)-dihydroxy-6,8,11,13 (E,Z,Z,E)-eicosatetraenoic acid (5,15-DiHETE) by the 5-LO. We have shown previously that this approach allows the determination of 5-LO activation independently of endogenous substrate release (McDonald *et al.*, 1991). PMN were therefore incubated with 15-HpETE and/or 30 nM A23187, following treatment with the receptor antagonists or PT (Table 1). A23187 alone did not elicit the formation of 5-LO products or of PAF in detectable amounts (data not shown). Under all conditions tested, no significant inhibition of the A23187-induced transformation of 15-HpETE into 5,15-DiHETE (reflecting 5-LO activation) was observed. Similarly, the 5,15-DiHETE synthesis resulting from exposure of the cells to 15-HpETE alone was unaffected by prior treatment with the antagonists or with PT (data not shown).

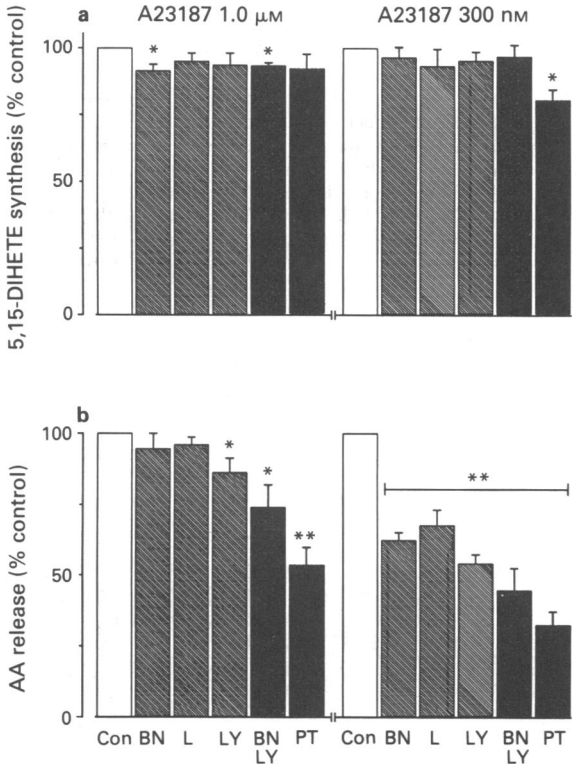


Figure 3 Effect of pertussis toxin, and of PAF and LTB_4 receptor antagonists, on A23187-induced 5-LO activation and AA release in human PMN. Incubation conditions are as in Figure 2. (a) Ionophore-induced 5-LO activation (as determined by the 5-LO-mediated conversion of exogenous 15-HpETE into 5,15-DiHETE). Samples were analysed by r.p.-h.p.l.c., as described in Methods. The given percentages have been calculated after subtraction of the 5,15-DiHETE synthesis resulting from exposures of PMN to 15-HpETE only (± receptor antagonists or PT). Mean ± s.e.mean of averaged triplicate determinations from at least 3 independent experiments. The 100% control (Con) values averaged 512 ± 33 ng 5,15-DiHETE per 5×10^6 PMN (left panel, $n = 3$) and 270 ± 31 ng per 5×10^6 PMN (right panel, $n = 5$). (b) Ionophore-induced AA release (2.5 min stimulations). Samples were analysed by l.c.-m.s., as described in Methods. Mean ± s.e.mean of averaged triplicate determinations from 5 independent experiments. The 100% control values averaged 203 ± 27 ng AA per 5×10^6 PMN (left panel, $n = 5$) and 94 ± 3 ng per 5×10^6 PMN (right panel, $n = 5$). BN, BN 50730; L, L-659,989; LY, LY-223982. $^*P < 0.04$; $^{**}P < 0.01$. For abbreviations, see text.

Effect of endogenous LTB_4 and PAF on A23187-induced 5-LO activation and AA release

Our previous observation, that both PAF and LTB_4 are potent 5-LO activators (McDonald *et al.*, 1991; 1992), led us to determine whether the amplification of A23187-induced LT synthesis by endogenous LTB_4 and PAF could take place at the 5-LO level. PMN were pretreated with PT or the receptor antagonists (individually or in combination), and then stimulated with 300 nM or 1.0 μM A23187, along with 15-HpETE. Figure 3a shows that regardless of the ionophore concentration used, PAF and/or LTB_4 receptor antagonists had no significant effect on A23187-induced conversion of 15-HpETE into 5,15-DiHETE in all but two cases, where a minor inhibition was noted, whilst PT had a moderate inhibitory effect at 300 nM A23187.

We next examined whether A23187-induced AA release would be affected upon pretreatment of the cells with the receptor antagonists or PT. In these experiments, PMN were stimulated with either 1.0 μM or 300 nM A23187. At the higher ionophore concentration, the PAF receptor antagonists failed to alter AA release significantly, whereas LY-223982 and PT exerted a moderate inhibition (Figure 3b, left panel). In contrast, all compounds potently inhibited AA release induced by 300 nM A23187 (Figure 3b, right panel).

Autocrine effects of endogenous LTB_4 and PAF on LT synthesis induced by chemoattractants in rhGM-CSF-primed PMN

Having shown that endogenous LTB_4 and PAF enhance A23187-induced LT synthesis in an autocrine fashion, we determined to what extent these neutrophil products may contribute to LT synthesis elicited under physiologically-relevant conditions. PMN were pretreated with rhGM-CSF or its diluent, and during the last 5 min of pre-incubation, the cells were exposed to the PAF and LTB_4 receptor antagonists, individually or in combination. Cells were then stimulated with either fMLP or rhC5a, and LT synthesis was measured. The effect of PT pretreatment was not investigated in these experiments, as it would have prevented PMN

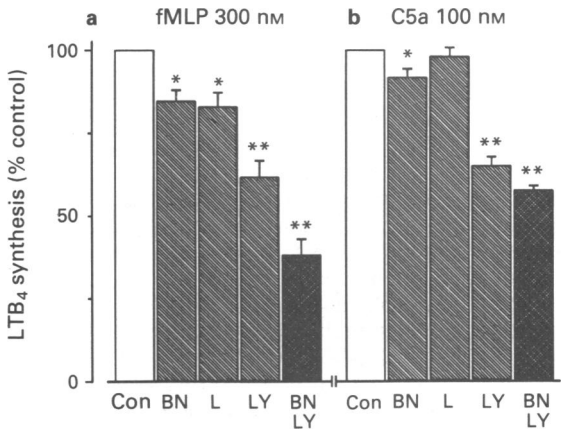


Figure 4 Effect of PAF and LTB_4 receptor antagonists on LT synthesis induced by fMLP (a) or rhC5a (b) in rhGM-CSF-primed PMN. PMN were pretreated with 1 nM rhGM-CSF or its diluent (30 min, 37°C) and stimulated for 10 min at 37°C with 300 nM fMLP or 100 nM rhC5a, in the presence or absence of 1.0 μM LT-223982 (LY), 100 nM BN 50730 (BN) or 100 nM L-659,989 (L) in the last 5 min of pre-incubation. Samples were analysed by r.p.-h.p.l.c., as described in Methods. Mean ± s.e.mean of averaged triplicate determinations from at least 4 independent experiments. The 100% control values (Con), representing the sum of LTB_4 and of its ω-oxidation products, averaged 2.1 ± 0.2 ng per 5×10^6 PMN (fMLP, $n = 10$) and 1.6 ± 0.2 ng per 5×10^6 PMN (C5a, $n = 5$). $^*P < 0.05$; $^{**}P < 0.003$. For abbreviations, see text.

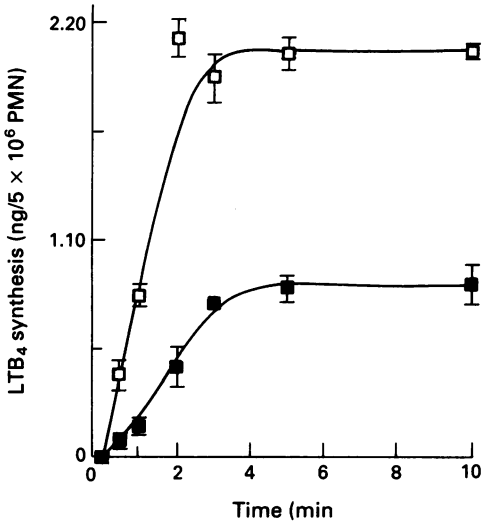


Figure 5 Effect of PAF and LTB_4 receptor antagonists on the time course of chemoattractant-induced LT synthesis in rhGM-CSF-primed PMN. PMN were pretreated with 1 nM rhGM-CSF or its diluent (30 min, 37°C) and stimulated with 300 nM fMLP for varying lengths of time, in the presence (■) or absence (□) of 1.0 μM LY-223982 and 100 nM BN 50730 in the last 5 min of pre-incubation. Samples were analysed by r.p.-h.p.l.c., as described in Methods. Mean ± s.e.mean of triplicate determinations from a single experiment representative of 4. The amounts of LTB_4 represent the sum of LTB_4 and of its ω-oxidation products. For abbreviations, see text.

stimulation by fMLP and C5a. Figure 4 shows that the PAF receptor antagonists exerted a significant but moderate inhibition of LT synthesis. In contrast, the LTB_4 receptor antagonist was found to inhibit potently LT synthesis, whilst the combination of both types of receptor antagonists yielded the highest degree of inhibition.

We next examined the effect of receptor antagonist pretreatment on the kinetics of chemoattractant-elicited LT synthesis in rhGM-CSF-primed cells. PMN were pretreated with rhGM-CSF, with or without a combination of LY-223982 and BN 50730 in the last 5 min of pre-incubation, and were stimulated with fMLP for increasing lengths of time. In the absence of the receptor antagonists, LTB_4 synthesis was detectable by 30 s, and reached a plateau between 2 and 5 min (Figure 5), depending on the donor. In the presence of the receptor antagonists, the pattern of synthesis was similar, with the exception that the initial rate of LT synthesis was lower, resulting in markedly decreased total amounts of LTB_4 at later time points.

To rule out possible nonspecific effects of the receptor antagonists on PMN stimulation by the chemoattractants, in particular at the level of 5-LO activation, we assessed the effect of these compounds on the 5-LO-mediated conversion of 15-HpETE into 5,15-DiHETE, under conditions where LT synthesis is not detected, i.e. in the absence of GM-CSF. PMN were incubated with 15-HpETE and/or 30 nM of fMLP, rhC5a, LTB_4 or PAF, following treatment with individual receptor antagonists (Table 2). By themselves, the agonists did not elicit the formation of 5-LO products from endogenous AA in detectable amounts (data not shown). Except for the expected blockade of the effect of LTB_4 by LY-223982, no significant inhibition of LTB_4-, rhC5a- or fMLP-elicited 5-LO activation by any antagonist was observed. In the case of PAF-induced 5-LO activation however, the LTB_4 receptor antagonist, LY-223982, was found to antagonize the response significantly, albeit less potently than the PAF receptor antagonists (see discussion).

Table 2 Effect of PAF and LTB_4 receptor antagonists on chemoattractant-elicited 5-LO activation under conditions where no detectable LT synthesis occurs

Conditions	*5-LO activation* (% of control)	*Number of experiments*	P
fMLP 30 nM + BN	99.3 ± 5.4	3	0.456
fMLP 30 nM + L	94.1 ± 2.6	3	0.078
fMLP 30 nM + LY	101.7 ± 10.7	4	0.441
C5a 30 nM + BN	101.5 ± 1.7	3	0.244
C5a 30 nM + L	96.9 ± 4.3	3	0.275
C5a 30 nM + LY	108.3 ± 6.6	3	0.170
LTB_4 30 nM + BN	98.7 ± 7.3	3	0.439
LTB_4 30 nM + L	97.7 ± 4.2	3	0.316
LTB_4 30 nM + LY	23.9 ± 2.6	4	0.001
PAF 30 nM + BN	7.6 ± 8.7	3	0.005
PAF 30 nM + L	21.1 ± 6.8	3	0.005
PAF 30 nM + LY	41.7 ± 3.7	3	0.002

PMN suspensions were pretreated with the receptor antagonists (5 min, 37°C), and subsequently incubated for 10 min at 37°C with 3.0 μM 15-HpETE, either alone or with the 5-LO agonists at the indicated concentrations. The conversion of 15-HpETE into 5,15-DiHETE (reflecting 5-LO activation) was then determined by r.p.-h.p.l.c. analysis, as described in Methods. Comparisons of 5-LO activity (expressed as % of control) have been calculated after subtracting the 5,15-DiHETE levels resulting from exposure of PMN to 15-HpETE only (± antagonists). Values are the mean ± s.e.mean from the indicated number of experiments, each performed in triplicate. The 100% control values, representing 5,15-DiHETE synthesis per 5×10^6 PMN, averaged 29 ± 1 ng (fMLP, $n = 4$), 35 ± 3 ng (C5a, $n = 4$), 33 ± 4 ng (LTB_4, $n = 4$), and 40 ± 2 ng (PAF, $n = 5$). BN, 100 nM BN 50730; L, 100 nM L-659,989; LY, 1.0 μM LY-223982. For abbreviations, see text.

Table 3 Effect of exogenous LTB_4 on AA release and 5-LO activation resulting from fMLP stimulation of rhGM-CSF-primed PMN

Added LTB_4	*AA release*[1] (% of control)	P	*5-LO activation*[2] (% of control)	P
10 nM	107.7 ± 4.4	0.077	–	–
100 nM	129.2 ± 7.1	0.007	101.4 ± 3.5	0.360

[1]PMN were pretreated with 1 nM rhGM-CSF or its diluent (30 min, 37°C) and stimulated for 2.5 min at 37°C with 300 nM fMLP, either alone or with exogenous LTB_4, in the presence of 100 nM MK-886 (added in the last 5 min of pre-incubation). Free AA levels were determined by l.c.-m.s., as described in Methods. Mean ± s.e.mean of averaged triplicate determinations from 5 independent experiments. [2]PMN were pretreated with 1 nM rhGM-CSF or its diluent (30 min, 37°C) and stimulated for 10 min at 37°C with 300 nM fMLP, either alone or with exogenous LTB_4, in the presence of 3.0 μM 15-HpETE. The conversion of 15-HpETE into 5,15-DiHETE (reflecting 5-LO activation) was then determined by r.p.-h.p.l.c. analysis, as described in Methods. The % control have been calculated after subtraction of the 5,15-DiHETE synthesis resulting from exposure of PMN to 15-HpETE only. Mean ± s.e. mean of averaged triplicate determinations from 3 independent experiments. For abbreviations, see text.

Effect of endogenous LTB_4 and PAF on chemoattractant-induced 5-LO activation and AA release in rhGM-CSF-primed PMN

We next investigated whether the autocrine amplification of chemoattractant-induced LT synthesis by endogenous LTB_4 or PAF occurred at the 5-LO level, or at the level of AA

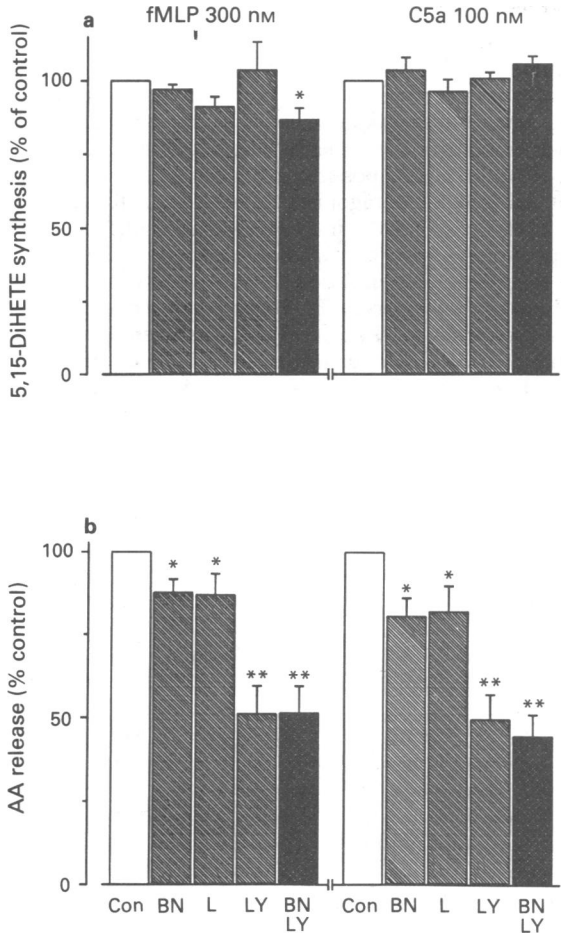


Figure 6 Effect of PAF and LTB_4 receptor antagonists on 5-LO activation and AA release induced by chemoattractants in rhGM-CSF-primed PMN. Incubation conditions are as in Figure 4. (a) Chemoattractant-induced 5-LO activation (as determined by the 5-LO-mediated conversion of exogenous 15-HpETE into 5,15-DiHETE). Samples were analysed by r.p.-h.p.l.c., as described in Methods. The given percentages have been calculated after subtraction of the 5,15-DiHETE synthesis resulting from exposure of PMN to 15-HpETE only ($\pm$ receptor antagonists). Mean $\pm$ s.e.mean of averaged triplicate determinations from at least 3 independent experiments. The 100% control values (Con) averaged 98 ± 9 ng, 5,15-DiHETE per 5×10^6 PMN (fMLP, $n = 6$) and 94 ± 11 ng per 5×10^6 PMN (C5a, $n = 4$). (b) Chemoattractant-induced AA release (2.5 min stimulations). Samples were analysed by l.c.-m.s., as described in Methods. Mean $\pm$ s.e.mean of averaged triplicate determinations from at least 4 independent experiments. The 100% control values (Con) averaged 24 ± 2 ng AA per 5×10^6 PMN (fMLP, $n = 5$) and 17 ± 2 ng per 5×10^6 PMN (C5a, $n = 4$). BN, BN 50730; L, L-659,989; LY, LY-223982. $^*P < 0.05$; $^{**}P < 0.003$. For abbreviations, see text.

availability. PMN were pretreated with rhGM-CSF, in the presence or absence of the receptor antagonists in the last 5 min of pre-incubation, and then stimulated with either fMLP or rhC5a, along with 15-HpETE. Figure 6a shows that chemoattractant-elicited 5-LO activation was slightly inhibited only in the case of fMLP-treated cells exposed to the combined antagonists for LTB_4 and PAF. In a second series of experiments, PMN were pre-incubated and stimulated as described above, and AA release was determined. As observed for LT synthesis under the same conditions, the PAF receptor antagonists were markedly less potent than the LTB_4 receptor antagonist in inhibiting AA release (Figure 6b).

Effect of exogenous LTB_4 on chemoattractant-induced AA release and 5-LO activation in rhGM-CSF-primed PMN

Finally, we examined whether the autocrine amplification by LTB_4 of chemoattractant-induced AA release could be mimicked by use of exogenous LTB_4. PMN primed with rhGM-CSF were stimulated with fMLP, in the presence or absence of added LTB_4, and AA release was determined. To ensure that changes in AA availability would exclude the participation of endogenous LTB_4, these experiments were performed in the presence of the LT synthesis inhibitor, MK-886. The combined presence of fMLP and of 100 nM LTB_4 resulted in significantly increased free AA levels, relative to cells stimulated with fMLP only (Table 3). In the same experiments, we also examined the effect of exogenous LTB_4 on 5-LO activation under the same conditions, using 15-HpETE as exogenous substrate. No significant effect of exogenous LTB_4 could be demonstrated (Table 3).

Discussion

In recent years, it has been proposed that since PAF and LTB_4 are both neutrophil products and activators, these lipid mediators may exert autocrine effects on neutrophil functions (O'Flaherty, 1985; Stewart *et al.*, 1990; Stewart & Harris, 1991a; Lew *et al.*, 1991). In particular, we recently reported that endogenous LTB_4 accounts, at least partially, for the induction of calcium mobilisation and LT synthesis by exogenous AA in human PMN (McColl *et al.*, 1989; Naccache *et al.*, 1989). We now report that newly-generated LTB_4 and PAF both have the ability to stimulate LT synthesis, and that this autocrine amplification of LT synthesis occurs primarily at the level of AA availability.

Evidence for an autocrine effect of LTB_4 and PAF on LT synthesis was first obtained under conditions where both compounds are synthesized in large amounts, i.e. upon A23187 challenge of PMN. The LTB_4 receptor antagonist, LY-223982 (a dicarboxylic benzophenone derivative), and the structurally unrelated PAF receptor antagonists, BN 50730 (a triazolodiazepine derivative) and L-659,989 (a tetrahydrofuran derivative), as well as PT, all markedly inhibited LT synthesis in PMN stimulated by 100–300 nM A23187. This indicated that endogenously-generated LTB_4 and/or PAF could substantially amplify LT synthesis at submaximal A23187 concentrations, after binding to their cell-surface receptors, in a process involving PT-sensitive G proteins. In comparison, PT or the receptor antagonists had but a moderate effect on LT synthesis induced by micromolar A23187 concentrations, suggesting that newly synthesized PAF and LTB_4 cannot further stimulate the LT-generating system once it is strongly activated. Consistent with this conclusion is the fact that no greater inhibition was observed when cells were exposed to 10 fold higher concentrations of the receptor antagonists (data not shown). In a second series of experiments, we examined the effect of the PAF and LTB_4 receptor antagonists on LT synthesis under physiologically-relevant stimulatory conditions, using chemoattractants in GM-CSF-primed PMN. Under these conditions, the total quantities of LTB_4 being generated (and accordingly, the amount of AA being released) were much smaller than those yielded in ionophore-challenged neutrophils. Given the known requirement for calcium of both 5-LO and PLA_2 activities, this difference may reflect the fact that chemoattractants (even following GM-CSF treatment of PMN) induce calcium transients of relatively small amplitude, in comparison to the larger and sustained increase in intracellular calcium that occurs following A23187 stimulation of neutrophils. In GM-CSF-treated PMN stimulated by chemotactic agonists, it was also found that both endogenous LTB_4 and PAF can modulate LT synthesis, with endogenous LTB_4 being implicated to a greater extent than PAF. This

contrasts again with the results obtained with PMN stimulated by submaximal concentrations of A23187, where PAF and LTB_4 appeared equally effective in enhancing LT synthesis. Such a difference could be related to the fate of endogenous PAF, depending upon the type of cell stimulation. Indeed, it was reported that most of the PAF generated upon A23187 challenge remains intracellular, whereas newly-synthesized PAF is mostly released upon activation of GM-CSF-primed PMN by chemoattractants (Riches *et al.*, 1990; DeNichilo *et al.*, 1991; Stewart & Harris, 1991b). In light of many reports which suggest that the PAF receptors are located intracellularly (Hwang & Lam, 1991; Rogers *et al.*, 1991), the intracellular retention of endogenous PAF occurring in A23187-stimulated PMN could facilitate its interaction with its receptors, thereby providing a basis for the autocrine effects of PAF on LT synthesis under such conditions.

LT synthesis principally relies on the activity of two key enzymes, 5-LO and PLA_2. By investigating the effect of the combined receptor antagonists on the time course of LT synthesis in respect to fMLP, it was shown that endogenous LTB_4 and PAF modulate LT synthesis by increasing the initial synthesis rate, which results in greater synthesis levels overall. Similar observations were made on PMN undergoing LT synthesis in response to A23187 (data not shown). This suggested a stimulatory effect on the enzymatic activity of either PLA_2 or 5-LO, or both. We therefore examined which step may be modulated by endogenous PAF and LTB_4. It was found that prior treatment with receptor antagonists or PT had but a slight effect on 5-LO activation under the same stimulatory conditions where they inhibited LT synthesis, be it in response to A23187, or to chemoattractants. These observations indicate that the autocrine amplification of LT synthesis by LTB_4 and PAF probably does not occur at the level of the 5-LO. In contrast, the receptor antagonists and PT inhibited AA availability to a similar extent as they affected LT synthesis under the same stimulatory conditions. Thus endogenous LTB_4 and PAF amplify LT synthesis mainly through enhanced AA availability, implying that they act by stimulating PLA_2 activation and/or by inhibiting the re-esterification of released AA, thereby enhancing its availability for conversion into LTs. That exogenous LTB_4 enhanced the AA availability resulting from fMLP stimulation of GM-CSF-primed PMN, while 5-LO activation remained unaffected in the same experiments, further supports this view. Consistent with our conclusion, it was recently reported that 5-LO activation is nearly maximal under stimulatory conditions which constitute a threshold for PLA_2 activity in human PMN (Schatz-Munding *et al.*, 1991).

The exact mechanism whereby endogenous PAF and LTB_4 enhance AA availability remains to be determined. On the one hand, it is known that AA release is associated with the calcium-dependent translocation of cytosolic PLA_2 to cell membranes in human PMN, macrophages and U937 cells (Diez & Mong, 1990; Goldman *et al.*, 1992; Smith & Waite, 1992). However, the mobilization of intracellular calcium induced by 100 nM ionomycin (a non-fluorescent calcium ionophore used instead of A23187 in the fura-2 calcium mobilization assay) is only marginally affected by PAF and LTB_4 receptor antagonists in PMN (P.P.McD., unpublished data), whereas the latter potently inhibit LT synthesis under the same conditions. Thus it does not appear likely that endogenous PAF and LTB_4 could increase cytosolic PLA_2 translocation to an extent sufficient to account for their modulatory effects on LT synthesis. On the other hand, it has been recently reported that phosphorylation of the PLA_2 by the microtubule-associated protein kinase or MAPK (a serine-threonine protein kinase) positively correlates with its enzymatic activity (Wijkander & Sundler, 1992; Xing & Mattera, 1992; Nemenoff *et al.*, 1993). Given the known ability of PAF and LTB_4 to induce tyrosine phosphorylation of several PMN proteins (Dryden *et al.*, 1992), and in particular that of the neutrophil MAPK (Gomez-Cambronero *et al.*, 1992), resulting in its activation, it is possible that endogenous PAF and LTB_4 could enhance LT synthesis through increased PLA_2 phosphorylation.

In investigating cell responses, conclusions based upon the use of pharmacological tools must take into consideration the generally limited specificity of these compounds. Hence, numerous control experiments were performed in the current study to rule out the possibility that nonspecific effects of PT or of the receptor antagonists could account for their inhibition of LT synthesis. First, we examined the effect of the compounds on 5-LO activation in response to 30 nM A23187 – an ionophore concentration that does not elicit a detectable synthesis of LTB_4 or PAF. Under these conditions, where autocrine effects of PAF and LTB_4 are unlikely to occur, neither the receptor antagonists nor PT significantly affected the 5-LO-mediated conversion of 15-HpETE into 5,15-DiHETE. Therefore, the inhibition of LT synthesis by these compounds seen at higher ionophore concentrations (100–300 nM) is not likely to reflect nonspecific inhibitory effects of the antagonists or of PT at the level of the 5-LO. Similarly, to ensure that the inhibition by the receptor antagonists of chemoattractant-induced LT synthesis was not due to their interfering with GM-CSF priming, we compared the effect of adding the antagonists either before GM-CSF, or in the last 5 min of pre-incubation with the cytokine. That no significant difference was noted (data not shown) is consistent with a recent report, which excluded the participation of endogenous LTB_4 or PAF in the priming of LT synthesis by GM-CSF (Stewart *et al.*, 1991). Additionally, to ascertain that the inhibition of chemoattractant-induced LT synthesis by the receptor antagonists did not reflect a possible interference with the fMLP or C5a receptors, we assessed the effect of these compounds on 5-LO activation induced by 30 nM fMLP or rhC5a in the absence of GM-CSF, i.e. under conditions where LT synthesis is not detected. Since no significant inhibition of the 5-LO-mediated conversion of 15-HpETE into 5,15-DiHETE was observed, it can be concluded that the receptor antagonists exert their inhibitory effects on LT synthesis neither through nonspecific blockade of C5a or fMLP receptors, nor at the level of the post-receptor events which lead to 5-LO activation. Similarly, the PAF receptor antagonists did not affect 5-LO activation in response to 30 nM LTB_4, thus further confirming their specificity. In contrast, 5-LO activation induced by 30 nM PAF was significantly antagonized by the LTB_4 receptor antagonist LY-223982, albeit to a lesser extent than when 10 fold lower concentrations of PAF receptor antagonists were used. The mobilization of intracellular calcium in response to PAF was also similarly inhibited by LY-223982 (data not shown). This is in agreement with a recent study, which reported that concentrations of LY-223982 similar to those used in the current study antagonized PMN chemotaxis towards PAF (Boyd & Jackson, 1988). Thus the inhibitory properties of LY-223982 on LT synthesis may partially reflect a contribution of PAF to LT synthesis. This is of little consequence insofar as the results obtained with chemoattractants in GM-CSF-primed PMN are concerned, since the PAF antagonists inhibited LT synthesis only slightly. The autocrine effects observed under such conditions therefore remain mostly attributable to endogenous LTB_4. In the case of A23187 stimulation, it also remains likely that the inhibitory effects of LY-223982 principally reflect the blockade of LTB_4 receptors, since the BN 50730 plus LY-223982 combination achieved a higher degree of inhibition than that seen with LY-223982 alone. Finally, it must be stated that the receptor antagonists and/or PT could possibly exert nonspecific effects at the level of PLA_2 activation. Nevertheless, the minor inhibition exerted by the antagonists or PT on LT synthesis induced by 3 μM A23187 (Figure 1) suggests that eventual nonspecific effects at the level of AA availability be equally minor. That 10 fold higher concentrations of the receptor antagonists failed to induce a significantly greater inhibition of LT synthesis under the same conditions, further supports this assertion.

In summary, the preceding findings show that in activated PMN, the autocrine enhancement of ongoing LT synthesis by endogenous PAF and/or LTB_4 represents an important amplification mechanism of LT synthesis, regardless of the type of stimulus used. Consistent with this assertion is that both PAF and LTB_4 receptor antagonists inhibit LT synthesis in response to particulate PMN agonists, namely zymosan and serum-opsonized zymosan (P.P.McD., unpublished data). Therefore, the modulatory effects of endogenous PAF and LTB_4 described herein are likely to be a general feature of LT synthesis regulation in PMN. That such autocrine effects take place at the level of AA availability raises the possibility that PAF synthesis may also be subject to autocrine stimulation by newly-generated LTB_4 and PAF, should PLA_2 be the actual target. Accordingly, it was recently reported that the PAF receptor antagonist, WEB 2086, inhibits the formation of PAF in response to fMLP (Müller & Nigam, 1992). In a broader context, the autocrine stimulation by LTB_4 and PAF of ongoing PMN responses may represent a general characteristic of neutrophil activation.

This work was supported by grants from the Arthritis Society of Canada and by the Medical Research Council of Canada. P.P.McD. is the recipient of a studentship from the Fonds de la recherche en santé du Québec (FRSQ); P.B. and S.R.M. are FRSQ scholars. We also wish to thank Dr Paul H. Naccache for fruitful discussions, and especially Serge Picard for outstanding technical assistance in the l.c.-m.s. analyses.

References

BORGEAT, P., PICARD, S., VALLERAND, P., BOURGOIN, S., ODEIMAT, A., SIROIS, P. & POUBELLE, P.E. (1990). Automated on-line extraction and profiling of lipoxygenase products of arachidonic acid by high-performance liquid chromatography. In *Methods in Enzymology*. ed. Murphy, R.C. & Fitzpatrick, F.A. pp. 98–116. New York: Academic Press.

BORGEAT, P. & SAMUELSSON, B. (1979). Arachidonic acid metabolism in polymorphonuclear leukocytes: Effects of ionophore A23187. *Proc. Natl. Acad. Sci. U.S.A.*, **76,** 2148–2152.

BOYD, R.J. & JACKSON, W.T. (1988). Specific inhibition of leukotriene B_4-induced chemotaxis by LY255282 and LY223982. *FASEB J.*, **2,** A1110.

BOYUM, A. (1968). Isolation of mononuclear cells and granulocytes from human blood. *Scand. J. Lab. Invest.*, **97,** 77.

BUSSOLINO, F., SIRONI, M., BOCCHIETTO, E. & MANTOVANI, A. (1992). Synthesis of platelet-activating factor by polymorphonuclear neutrophils stimulated with interleukin-8. *J. Biol. Chem.*, **267,** 14598–14603.

CHILTON, F.H., ELLIS, J.M., OLSON, S.C. & WYKLE, R.L. (1984). 1-O-alkyl-2-arachidonoyl-*sn*-glycero-3-phosphocholine: A common source of platelet-activating factor and arachidonate in human polymorphonuclear leukocytes. *J. Biol. Chem.*, **259,** 12014–12019.

DAHINDEN, C.A., ZINGG, J., MALY, F.E. & DE WECK, A.L. (1988). Leukotriene production in human neutrophils primed by rhGM-CSF and stimulated with the complement component C5a and fMLP as second signals. *J. Exp. Med.*, **167,** 1281–1295.

DENICHILO, M.O., STEWART, A.G., VADAS, M.A. & LOPEZ, A.F. (1991). Granulocyte-macrophage colony-stimulating factor is a stimulant of platelet-activating factor and superoxide anion generation by human neutrophils. *J. Biol. Chem.*, **266,** 4896–4902.

DIEZ, E. & MONG, S. (1990). Purification of a phospholipase A_2 from human monocytic leukemic U937 cells – Calcium-dependent activation and membrane association. *J. Biol. Chem.*, **265,** 14654–14661.

DOWNEY, G.P., CHAN, C.K., TRUDEL, S. & GRINSTEIN, S. (1990). Actin assembly in electropermeabilized neutrophils – Role of intracellular calcium. *J. Cell Biol.*, **110,** 1975–1982.

DRYDEN, P., DURONIO, V., MARTIN, L., HUDSON, A.T. & SALARI, H. (1992). Inhibition of human neutrophil responses by α-cyano-3,4-dihydroxythiocinnamamide – a protein tyrosine kinase inhibitor. *Br. J. Pharmacol.*, **106,** 656–664.

FILEP, J.G. & FOLDES-FILEP, E. (1990). Inhibition by calcium channel blockers of the binding of platelet-activating factor to human neutrophil granulocytes. *Eur. J. Pharmacol.*, **190,** 67–73.

GOLDMAN, R., FERBER, E. & ZORT, U. (1992). Reactive oxygen species are involved in the activation of cellular phospholipase A_2. *FEBS Lett.*, **309,** 190–192.

GOMEZ-CAMBRONERO, J., DURSTIN, M., MOLSKI, T.F.P., NACCACHE, P.H. & SHA'AFI, R.I. (1989). Calcium is necessary but not sufficient for platelet-activating factor release in human neutrophils stimulated by physiological stimuli. *J. Biol. Chem.*, **264,** 21699–21704.

GOMEZ-CAMBRONERO, J., HUANG, C.K., GOMEZ-CAMBRONERO, T.M., WATERMAN, W.H., BECKER, E.L. & SHA'AFI, R.I. (1992). Granulocyte-macrophage colony-stimulating factor-induced protein tyrosine phosphorylation of microtubule-associated protein kinase in human neutrophils. *Proc. Natl. Acad. Sci. U.S.A.*, **89,** 7551–7555.

HIRAFUJI, M. & SHINODA, H. (1991). Platelet-leukocyte interaction in adhesion to endothelial cells induced by platelet-activating factor *in vitro*. *Br. J. Pharmacol.*, **103,** 1333–1338.

HWANG, S.B. & LAM, M.H. (1991). L-659,989 – A useful probe in the detection of multiple conformational states of PAF receptors. *Lipids*, **26,** 1148–1153.

LAD, P.M., OLSON, C.V. & GREWAL, I.S. (1985). Platelet-activating factor-mediated effects on human neutrophil function are inhibited by pertussis toxin. *Biochem. Biophys. Res. Commun.*, **129,** 632–638.

LEW, D.B., LESLIE, C.C., HENSON, P.M. & RICHES, D.W.H. (1991). Role of endogenously derived leukotrienes in the regulation of lysosomal enzyme expression in macrophages exposed to β(1,3)-glucan. *J. Leuk. Biol.*, **49,** 266–276.

LIN, A.H., MORTON, D.R. & GORMAN, R.R. (1982). Acetyl glyceryl ether phosphorylcholine stimulates leukotriene B_4 synthesis in human polymorphonuclear leukocytes. *J. Clin. Invest.*, **70,** 1058–1065.

MCCOLL, S.R., KRUMP, E., NACCACHE, P.H., CAON, A.C. & BORGEAT, P. (1989). Activation of the human neutrophil 5-lipoxygenase by exogenous arachidonic acid: involvement of pertussis toxin-sensitive guanine nucleotide-binding proteins. *Br. J. Pharmacol.*, **97,** 1265–1273.

MCCOLL, S.R., KRUMP, E., NACCACHE, P.H., POUBELLE, P.E., BRAQUET, P., BRAQUET, M. & BORGEAT, P. (1991). Granulocyte-macrophage colony-stimulating factor increases the synthesis of leukotriene B_4 by human neutrophils in response to platelet-activating factor - Enhancement of both arachidonic acid availability and 5-lipoxygenase activation. *J. Immunol.*, **146,** 1204–1211.

MCDONALD, P.P., MCCOLL, S.R., NACCACHE, P.H. & BORGEAT, P. (1991). Activation of the human neutrophil 5-lipoxygenase by natural agonists and Ca^{2+} ionophore A23187. *Biochem. J.*, **280,** 379–385.

MCDONALD, P.P., MCCOLL, S.R., NACCACHE, P.H. & BORGEAT, P. (1992). Activation of the human neutrophil 5-lipoxygenase by leukotriene B_4. *Br. J. Pharmacol.*, **107,** 226–232.

MCDONALD, P.P., POULIOT, M., BORGEAT, P. & MCCOLL, S.R. (1993). Induction by chemokines of lipid mediator synthesis in GM-CSF-treated human neutrophils. *J. Immunol.* (in press).

MÜLLER, S. & NIGAM, S. (1992). Enhancement by staurosporine of platelet-activating factor formation in N-formyl peptide-challenged human neutrophils is mediated by intracellular platelet-activating factor binding sites. *Biochem. Biophys. Res. Commun.*, **189,** 771–776.

NACCACHE, P.H., MCCOLL, S.R., CAON, A.C. & BORGEAT, P. (1989). Arachidonic acid-induced mobilization of calcium in human neutrophils: evidence for a multicomponent mechanism of action. *Br. J. Pharmacol.*, **97**, 461–168.

NEMENOFF, R.A., WINITZ, S., QIAN, N.X., VAN PUTTEN, V., JOHNSON, G.L. & HEASLEY, L.E. (1993). Phosphorylation and activation of a high molecular weight form of phospholipase A_2 by p42 microtubule-associated protein-2 kinase and protein kinase C. *J. Biol. Chem.*, **268**, 1960–1964.

O'FLAHERTY, J.T. (1985). Neutrophil degranulation: Evidence pertaining to its mediation by the combined effects of leukotriene B_4, platelet-activating factor, and 5-HETE. *J. Cell. Physiol.*, **122**, 229–239.

O'FLAHERTY, J.T., WYKLE, R.L., LEES, C.J., SHEWMAKE, T., MCCALL, C.E. & THOMAS, M.J. (1981). Neutrophil-degranulating action of 5.12-dihydroxy-6,8,11,14-eicosatetraenoic acid and 1-O-alkyl-2-O-acetyl-*sn*-glycero-3-phosphocholine. Comparison with other degranulating agents. *Am. J. Pathol.*, **105**, 264–269.

POUBELLE, P.E., DE MÉDICIS, R. & NACCACHE, P.H. (1987). Monosodium urate and pyrophosphate crystals differentially activate the excitation-response coupling sequence of human neutrophils. *Biochem. Biophys. Res. Commun.*, **149**, 649–657.

POUBELLE, P.E., BOURGOIN, S., NACCACHE, P.H. & BORGEAT, P. (1989). Granulocyte-macrophage colony-stimulating factor and opsonization synergistically enhance leukotriene B_4 synthesis induced by phagocytosis in human neutrophils. *Agents Actions*, **27**, 388–390.

RICHES, D.W.H., YOUNG, S.K., SECCOMBE, J.F., HENSON, J.E., CLAY, K.L. & HENSON, P.M. (1990). The subcellular distribution of platelet-activating factor in stimulated human neutrophils. *J. Immunol.*, **145**, 3062–3070.

ROGERS, J.E., DURONIO, V., WONG, S.I., MCNEIL, M. & SALARI, H. (1991). Solubilization of a functionally active platelet-activating factor receptor from rabbit platelets. *Biochem. J.*, **278**, 405–410.

SCHATZ-MUNDING, M., HATZELMANN, A. & ULLRICH, V. (1991). The involvement of extracellular calcium in the formation of 5-lipoxygenase metabolites by human polymorphonuclear leukocytes. *Eur. J. Biochem.*, **197**, 487–493.

SHEFEYK, J., YASSIN, R., VOLPI, M., MOLSKI, T.F.P., NACCACHE, P.H., MUNOZ, J.J., BECKER, E.L., FEINSTEIN, M.B. & SHA'AFI, R.I. (1985). Pertussis toxin, but not cholera toxin, inhibits the stimulated increase in actin association with the cytoskeleton in rabbit neutrophils: Role of 'G proteins' in stimulus-response coupling. *Biochem. Biophys. Res. Commun.*, **126**, 1174–1181.

SMITH, D.M. & WAITE, M. (1992). Phosphatidylinositol hydrolysis by phospholipase A_2 and phospholipase C activities in human peripheral blood neutrophils. *J. Leuk. Biol.*, **52**, 670–678.

STEWART, A.G., DUBBIN, P.N., HARRIS, T. & DUSTING, G.J. (1990). Platelet-activating factor may act as a second messenger in the release of icosanoids and superoxide anions from leukocytes and endothelial cells. *Proc. Natl. Acad. Sci. U.S.A.*, **87**, 3215–3219.

STEWART, A.G. & HARRIS, T. (1991a). Platelet-activating factor may participate in signal transduction processes in rabbit leukocytes. *Lipids*, **26**, 1044–1049.

STEWART, A.G. & HARRIS, T. (1991b). Involvement of platelet-activating factor in endotoxin-induced priming of rabbit polymorphonuclear leukocytes. *J. Lipid Med.*, **3**, 125–138.

STEWART, A.G., HARRIS, T., DENICHILO, M. & LOPEZ, A.F. (1991). Involvement of leukotriene B_4 and platelet-activating factor in cytokine priming of human polymorphonuclear leucocytes. *Immunology*, **72**, 206–212.

TESSNER, T.G., O'FLAHERTY, J.T. & WYKLE, R.L. (1989). Stimulation of PAF synthesis by a nonmetabolizable bioactive analog of PAF and influence of arachidonic acid metabolites. *J. Biol. Chem.*, **264**, 4794–4799.

WIJKANDER, J. & SUNDLER, R. (1992). Regulation of arachidonate-mobilizing phospholipase A_2 by phosphorylation via protein kinase C in macrophages. *FEBS Lett.*, **311**, 299–301.

WIRTHMUELLER, U., DE WECK, A.L. & DAHINDEN, C.A. (1989). Platelet-activating factor production in human neutrophils by sequential stimulation with granulocyte-macrophage colony-stimulating factor and the chemotactic factors C5a and formyl-methionyl-leucyl-phenylalanine. *J. Immunol.*, **142**, 3213–3218.

XING, M.Z. & MATTERA, R. (1992). Phosphorylation-dependent regulation of phospholipase A_2 by G proteins and Ca^{2+} in HL-60 granulocytes. *J. Biol. Chem.*, **267**, 25966–25975.

(Received September 9, 1993
Revised October 18, 1993
Accepted October 25, 1993)

Br. J. Pharmacol. (1994), **111**, 861–865 © Macmillan Press Ltd, 1994

Effect of lithium on plasma glucose, insulin and glucagon in normal and streptozotocin-diabetic rats: role of glucagon in the hyperglycaemic response

[1]O. García Hermida, T. Fontela, *M. Ghiglione & *L.O. Uttenthal

Centro de Investigaciones Biológicas, C.S.I.C., Velázquez 144, 28006 Madrid, Spain, and *Departamento de Bioquímica y Biología Molecular, Facultad de Medicina, Universidad de Salamanca, Avenida del Campo Charro s/n, 37007 Salamanca, Spain

1 Lithium salts, used in the treatment of affective disorders, may have adverse effects on glucose tolerance in man, and suppress glucose-stimulated insulin secretion in rats.

2 To study the interaction of these effects with pre-existing diabetes mellitus, plasma glucose and insulin responses to lithium chloride were measured in male Wistar rats made diabetic with intraperitoneal streptozotocin, and in normal controls.

3 In both normal and diabetic anaesthetized rats, intravenous lithium (4 mEq kg^{-1}) caused a rise in plasma glucose. In absolute terms, the rise was greater in diabetic (5.2 mmol l^{-1}) than in normal rats (2.3 mmol l^{-1}).

4 Plasma insulin concentrations were reduced by lithium in normal rats, but the low insulin concentrations measured in the diabetic rats were not significantly changed.

5 After intravenous glucose (0.5 g kg^{-1}), lithium-treated diabetic rats showed a second rise in plasma glucose at 60–90 min without any insulin response, while normal rats showed typically reduced insulin responses and initial glucose disappearance rates.

6 Intravenous glucose reduced plasma glucagon concentrations to a greater extent in normal than in diabetic rats, but lithium induced an equal rise in plasma glucagon in both groups, with a time-course similar to that of the hyperglycaemic effect.

7 The hyperglycaemic action of lithium is greater in the hypoinsulinaemic diabetic rats and appears to involve a stimulation of glucagon secretion in both normal and diabetic animals.

Keywords: Lithium; streptozotocin; diabetes mellitus; glucose; insulin; glucagon

Introduction

Lithium has become widely used in the treatment of mono- and bipolar affective disorders and its cellular mechanisms of action have been the subject of extensive research (Birch, 1991), both in relation to its therapeutic effect and its many unwanted secondary effects. Among the latter are variable effects on glucose tolerance and interactions with pre-existing diabetes mellitus (reviewed by Lazarus, 1986). While there have been several reports of a decrease in glucose tolerance in human patients on lithium, a similar number of studies have shown an increased tolerance; and whereas there are isolated reports of the development or deterioration of diabetes mellitus of type 1 or 2 during lithium treatment, a controlled study of type 2 diabetic patients showed a diminished plasma glucose response to a 50 g carbohydrate breakfast after 1 week of lithium administration (Jones *et al.*, 1983).

In normal rats, lithium administration causes a rise in plasma glucose while plasma insulin concentrations remain unchanged or are slightly suppressed (Fontela *et al.*, 1986). Glucose-stimulated insulin release is inhibited both *in vivo* and *in vitro* (Anderson & Blackard, 1978; Shah & Pishdad, 1980; Fontela *et al.*, 1986; 1987), and these effects appear to be mediated by central opiate and by neural and endocrine catecholamine pathways, the latter acting on the pancreatic β cell through its α_2-adrenoceptors (Fontela *et al.*, 1990; García-Hermida *et al.*, 1991). The aim of the present study was to investigate how this 'diabetogenic' effect of lithium in rats interacts with pre-existing diabetes mellitus, using streptozotocin-induced diabetes as the experimental model. The ultimate aim was to obtain data that might, with due caution, help in the interpretation of the highly disparate findings in human patients.

[1] Author for correspondence.

Methods

Animals

Male Wistar rats (160–220 g) were kept under standard conditions previously described (Fontela *et al.*, 1990). Randomly chosen rats were injected i.p. with 1 ml kg^{-1} of a solution of streptozotocin (Sigma, U.S.A.) 65 mg ml^{-1} in 0.1 M sodium citrate buffer, pH 4.5, while control rats were injected with the corresponding volume of buffer alone. The streptozotocin-treated rats were separated, and their urine tested after 48 h with BM-Test-Glucose strips (Boehringer Mannheim, Germany). Animals showing 1% glycosuria were kept for a further 12 days before being used. Food was withdrawn the night before each experiment, but free access to water was maintained.

Experimental protocol

To compensate for possible effects arising from performing experiments on different days, each day's experiments were carried out simultaneously on streptozotocin-diabetic and non-diabetic control rats. Animals were anaesthetized with pentobarbitone sodium, 60 mg kg^{-1}, i.p., and the previously described experimental protocol was followed (Fontela *et al.*, 1990). Venous blood samples (0.5 ml) were collected before and at 5, 30, 60, 90 and 120 min after rapid (30 s) i.v. infusion of 0.5 M LiCl or control 0.5 M NaCl (4 mEq kg^{-1}), or after the further i.v. infusion (5 min later) of 0.55 M glucose (0.5 g kg^{-1}) for studies of i.v. glucose tolerance and glucose-stimulated insulin secretion. For glucagon determination, blood samples were collected into tubes containing 20 μg aprotinin (Sigma, U.S.A.), equivalent to 400 kallikrein inhibitory units per ml of blood. Samples were kept at 4°C, centrifuged, and a small aliquot of plasma was removed for immediate glucose determination by the glucose oxidase me-

Table 1 Characteristics of streptozotocin-treated and control rats

	Body wt. (g)		*Plasma glucose* (mmol l^{-1})	*Plasma insulin* (μu ml^{-1})
	Day 0	Day 14	Day 14	Day 14
Control rats	186 ± 17	276 ± 22	8.0 ± 1.3	24 ± 9
Streptozotocin-diabetic rats	178 ± 9	201 ± 28	21.8 ± 4.7	12 ± 4

Male Wistar rats were injected i.p. with streptozotocin 65 mg kg^{-1} or vehicle alone on Day 0 and used on Day 14. Diabetic rats were selected on the basis of persistent glycosuria >1%. Results are given as mean ± s.d., $n = 36$.

thod. The remaining plasma was frozen at − 18°C for the subsequent determination of insulin (Amersham, Bucks) and pancreatic glucagon (Novo-Nordisk, Denmark; antiserum K 5563) by radioimmunoassay following the suppliers' instructions.

Analysis of data

The initial rate of fall of the plasma glucose concentration after i.v. glucose administration (the 'K value') was calculated as the percentage fall in plasma glucose per minute during the period 5 to 30 min after the injection of glucose. Results are expressed as means ± s.d. or s.e.mean. Within-group and between-group differences were analysed by Wilcoxon's rank sum tests for paired and unpaired data respectively.

Results

Characteristics of experimental animals

The streptozotocin-diabetic rats, selected on the criterion of >1% glycosuria, showed a markedly reduced weight-gain and elevated basal plasma glucose (Table 1). The mean basal plasma insulin concentration was reduced to half that of controls.

Effects of lithium on plasma glucose and insulin

The effects of i.v. lithium (4 mEq kg^{-1}) on plasma glucose and insulin concentrations in streptozotocin-diabetic and control rats are shown in Figures 1 and 2. Both groups showed a rise in plasma glucose that reached a maximum at 60 min. In absolute terms, the mean rise in streptozotocin-diabetic rats was greater (5.2 mmol l^{-1}) than that in the non-diabetic controls (2.3 mmol l^{-1}). Because of considerable variation in individual responses the rises were of borderline statistical significance in both groups ($0.1 > P > 0.05$, $n = 8$). The non-diabetic controls showed an early reduction of plasma insulin concentrations (Figure 2), maximal at 5 min ($P < 0.05$) and recovering to control levels by 90 min. The low insulin concentrations recorded in the streptozotocin-diabetic rats were unchanged after lithium.

Effects of lithium on i.v. glucose tolerance

Plasma glucose The effects of i.v. lithium on plasma glucose changes after i.v. glucose tolerance tests in streptozotocin-diabetic and non-diabetic control rats are shown in Figure 3. Whereas the K value for glucose-disappearance was reduced by lithium from 1.52 ± s.e.mean 0.06 to 1.23 ± 0.17 (NS, $n = 7$) in the non-diabetic controls, lithium administration increased the K value in the streptozotocin-diabetic rats from 0.15 ± 0.05 to 0.33 ± 0.07 ($P < 0.05$, $n = 7$ and 11). However, there was a second rise of plasma glucose in the streptozotocin-diabetic rats that reached a maximum at 90 min, whereas the non-diabetic controls showed only a minor reduction in the slope of glucose-disappearance around the 60 min time-point.

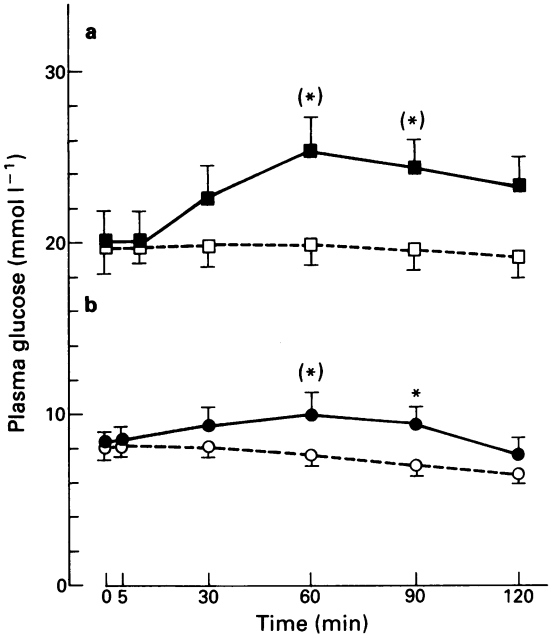


Figure 1 Effect of i.v. LiCl 4 mEq kg^{-1} (closed symbols) or the same dose of NaCl (open symbols) on plasma glucose concentrations in (a) streptozotocin-diabetic (□, ■) and (b) non-diabetic control rats (○, ●). Each result represents the mean ± s.e.mean of 8 rats. Statistical significance of differences from saline controls: (*)$0.1 > P > 0.05$; *$P < 0.05$.

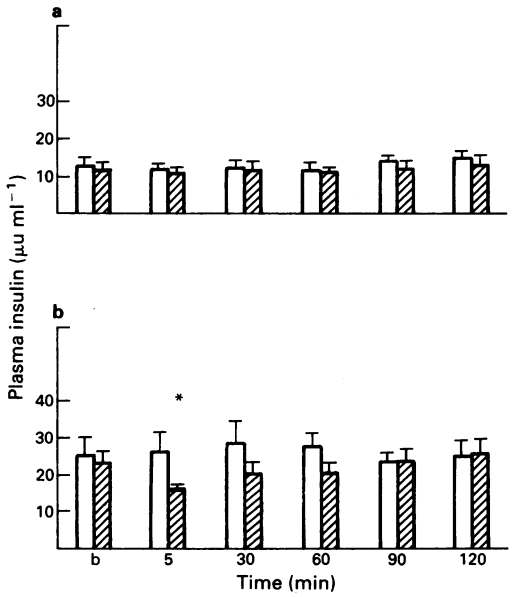


Figure 2 Effect of i.v. LiCl 4 mEq kg^{-1} (hatched columns) or the same dose of NaCl (open columns) on plasma insulin concentrations in streptozotocin-diabetic rats (a) and non-diabetic control rats (b). Each result represents the mean with s.e.mean of 8 rats. Statistical significance of difference from saline controls: *$P < 0.05$.

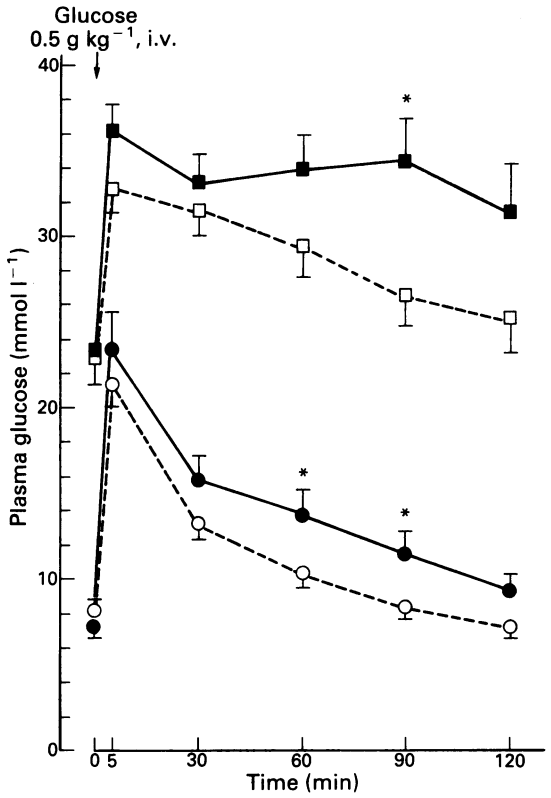


Figure 3 Effect of prior i.v. administration of LiCl 4 mEq kg^{-1} (closed symbols) or the same dose of NaCl (open symbols) on plasma glucose concentrations after i.v. glucose 0.5 g kg^{-1} in streptozotocin-diabetic (■, □) and non-diabetic control rats (●, ○). Each result represents the mean of 7 rats ± s.e.mean (11 for lithium-treated streptozotocin-diabetic rats). Statistical significance of differences from saline controls: *$P<0.05$.

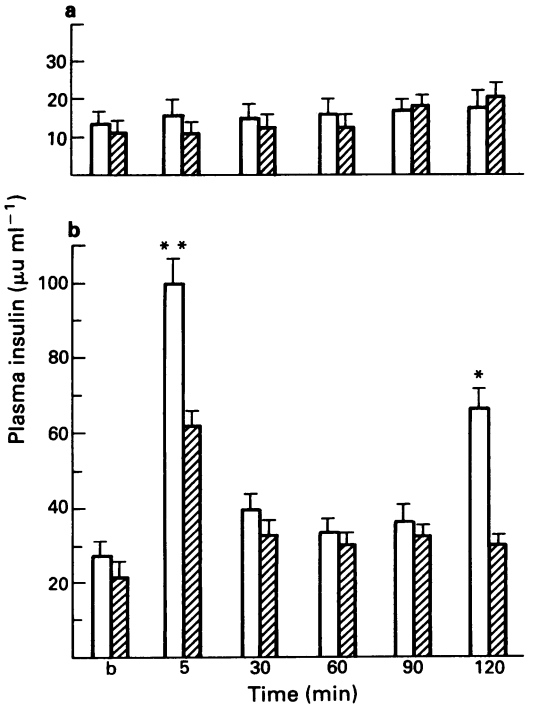


Figure 4 Effect of prior i.v. administration of LiCl 4 mEq kg^{-1} (hatched columns) or the same dose of NaCl (open columns) on plasma insulin concentrations after i.v. glucose 0.5 g kg^{-1} in streptozotocin-diabetic (a) and non-diabetic control rats (b). Each result represents the mean with s.e.mean of 7 rats (11 for lithium-treated streptozotocin-diabetic rats). Statistical significance of differences from saline controls: *$P<0.05$; **$P<0.01$.

Plasma insulin Plasma insulin responses to i.v. glucose are shown in Figure 4. In the non-diabetic controls the insulin response was markedly suppressed by lithium, the mean plasma concentration at 5 min being reduced by 37.6 ± 2.8% s.e.mean ($P<0.01$). A second rise of insulin observed at 120 min in the saline control group was completely absent in the lithium-treated group ($P<0.05$). In the streptozotocin-diabetic rats there was no immediate insulin response to glucose in either lithium-treated or saline control groups, but both groups showed a tendency for plasma insulin concentrations to rise during the 120 min post-glucose period ($P<0.01$ for within-group comparison of 0 and 120 min time-points). There were no significant between-group differences in the plasma insulin levels of the diabetic rats.

Effect of lithium on plasma glucagon

The liberation of endogenous glucose into the circulation in response to lithium, which was particularly apparent at the 60 and 90 min time-points in the diabetic rats, directed attention to the possible role of insulin counter-regulatory hormones. Plasma concentrations of pancreatic glucagon were therefore measured during the i.v. glucose tolerance test, when glucagon secretion would normally be suppressed. The results are shown in Figure 5. In the saline-treated, non-diabetic control rats, mean plasma glucagon fell from 35 ± 10 to 10 ± 1 pmol l^{-1} within 5 min of i.v. glucose ($P<0.05$, $n=6$), remained low at 60 min and then rose slightly by 120 min ($P<0.05$). Lithium treatment superimposed on this a rise in glucagon at 30 and 60 min, reaching a maximum of 14 pmol l^{-1} above corresponding saline control values at 60 min ($P<0.01$). A further rise was observed at 120 min. The saline-treated, streptozotocin-diabetic rats had a slightly lower mean basal glucagon level (25 ± 3 pmol l^{-1}) which was less markedly reduced by i.v. glucose, falling to a minimum of 16 ± 3 pmol l^{-1} at 30 to 60 min, and thereafter again rising. On this response, lithium treatment superimposed a rise in glucagon of the same magnitude and time-course as that seen in the non-diabetic rats, reaching a maximum of 14 pmol l^{-1} at 60 min ($P<0.02$, $n=8$).

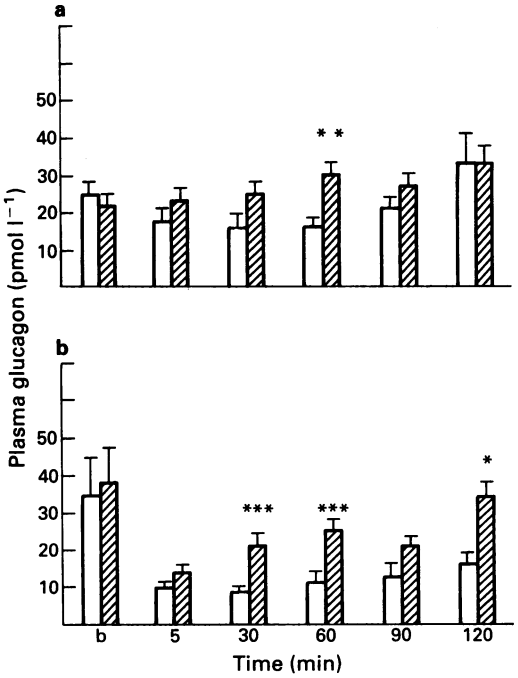


Figure 5 Effect of prior i.v. administration of LiCl 4 mEq kg^{-1} (hatched columns) or the same dose of NaCl (open columns) on plasma concentrations of pancreatic glucagon after i.v. glucose 0.5 g kg^{-1} in streptozotocin-diabetic (a) and non-diabetic control rats (b). Each result represents the mean with s.e.mean of 6 to 8 rats Statistical significance of differences from saline controls: *$P<0.05$; **$P<0.02$; ***$P<0.01$.

Discussion

The results of the present study can be interpreted in the light of the following effects of lithium administration in the intact rat:

(1) Activation of the sympatho-adrenal system

This involves both neural and humoral catecholamine pathways, as shown by the partial reversal of the effects of lithium on plasma glucose and glucose-stimulated insulin secretion by bilateral adrenalectomy (Fontela *et al.*, 1986), the elevation of plasma adrenaline and noradrenaline in response to lithium (Fontela *et al.*, 1991), and the reversal by adrenoceptor antagonists (specifically by the α_2-selective antagonist, yohimbine) of the inhibitory effect of lithium on the second phase of glucose-stimulated insulin secretion from isolated islets (Fontela *et al.*, 1987; 1990). The rise in plasma glucose may thus be attributed to the stimulatory effect of adrenaline and noradrenaline on glycogenolysis, combined with an inhibition of insulin secretion mediated by α_2-adrenoceptors of the pancreatic B cell.

(2) Stimulation of glucose uptake

The 'insulin-like' effect of lithium in promoting glucose uptake by muscle tissue *in vitro* (Bhattacharya, 1959; 1961; Clausen, 1968) is also seen as increased glucose disposal *in vivo*, both in patients on lithium treatment (Vendsborg & Rafaelsen, 1973; Vendsborg, 1979) and in diabetic rats, where lithium can restore insulin-sensitivity and muscle glycogen synthesis (Rossetti, 1989).

The overall results of lithium administration in the intact animal may therefore be expected to reflect the interaction, at different time-courses, of these effects with the capacity of the organism to respond in terms of insulin and its counter-regulatory hormones. Thus, while the adrenergic response to lithium predominates in the intact rat, producing hyperglycaemia, in the adrenalectomized rat the stimulation of glucose disposal produces hypoglycaemia (Fontela *et al.*, 1986). A high incidence of reactive hypoglyceamia during glucose tolerance tests in lithium-treated, non-diabetic patients has also been reported (Shah *et al.*, 1986).

The fact that lithium administration produced a greater rise of plasma glucose in streptozotocin-diabetic rats than in non-diabetic controls may, at least in part, be attributed to their low prevailing insulin levels and lower rates of glucose disposal. In these circumstances the stimulation of glucose disposal by lithium is evidently insufficient to compensate for the liberation of glucose into the circulation that is induced by the stimulation of counter-regulatory hormones.

The results of the i.v. glucose tolerance test show the different balance of effects of lithium on glucose disposal and insulin secretion particularly clearly. In the control rats the potent inhibition of glucose-stimulated insulin secretion outweighed any enhancing effect of lithium on glucose disposal. However, in the diabetic rats, characterized by low insulin levels that are unaffected by lithium, the initial rate of glucose disposal was significantly increased.

While much attention has been directed at the effects of lithium on catecholaminergic systems, there has been relatively little work on its possible effects on other important insulin counter-regulatory hormones. In view of the importance of disturbances in the normal regulation of basal and stimulated glucagon levels in diabetes mellitus (Unger & Orci, 1981), we decided to measure plasma glucagon responses to lithium after i.v. glucose. Under these conditions, glucagon secretion should be suppressed in normal rats, reducing the considerable individual variations in the fasting 'basal' levels seen in anaesthetized and cannulated animals and facilitating the demonstration of secretory responses due to other mechanisms. In diabetic rats, the glucagon-secreting A cells have to some extent escaped from the inhibitory effect of high plasma glucose concentrations. Nevertheless, the basal glucagon levels of the streptozotocin-diabetic rats were slightly lower than those of the non-diabetic controls ($0.1 > P > 0.05$), and were still significantly suppressed by i.v. glucose, although to a much lesser extent than in the controls. Despite these differences, however, the glucagon responses to lithium were identical in magnitude in the diabetic and control rats.

The existence of a glucagon response to lithium, previously suggested by Mellerup *et al.* (1970), has, as far as we know, not hitherto been substantiated by more recent work. In the present state of knowledge, it may be regarded as a consequence of activation of the sympatho-adrenal system. The A cells of the pancreatic islets carry β-adrenoceptors, demonstrated in isolated A cells by Schuit & Pipeleers (1986), and in isolated, perfused rat pancreas by Filipponi *et al.* (1986). The effect of β-adrenoceptor agonists is to stimulate glucagon secretion, and the blockage of this effect by metoprolol indicates that the receptors are of the β_1-type (Gregorio *et al.*, 1986). While the work of Gross *et al.* (1991) showed that A-cell responses to isoprenaline were completely suppressed after 5 weeks of streptozotocin-induced diabetes, the present results demonstrate an intact response to lithium after 2 weeks. The time during which the A cells have been subjected to hyperglycaemia and/or insulin deficiency may be significant in this respect. Our findings suggest that, after lithium administration, the induction of glucagon secretion co-operates with catecholamines in stimulating glycogenolysis.

Any application of these results to the use of lithium in man must be extremely cautious. Chronic treatment with slow-release oral lithium carbonate will not produce rapid changes in plasma lithium concentrations and may therefore have less effect on peripheral catecholamine pathways, whereas the potentiating effect of lithium on glucose disposal seems to persist. Our results suggest that the hyperglycaemic effect of lithium is enhanced when it is acutely administered in animals with low insulin levels and intact insulin counter-regulatory systems, including the glucagon response. This would imply that it is in inadequately treated diabetes that initiation of lithium treatment may contribute to hyperglycaemia.

This work was supported by grants from the Dirección General de Investigación Científica y Técnica (no. PM-89-0005) and from the Fundación Rodríguez Pascual.

References

ANDERSON, J.H.Jr. & BLACKARD, W.G. (1978). Effect of lithium on pancreatic islet insulin-release. *Endocrinology*, **102**, 291–295.

BHATTACHARYA, G. (1959). Influence of ions on the uptake of glucose and on the effect of insulin on it by rat diaphragm. *Nature*, **183**, 324–325.

BHATTACHARYA, G. (1961). Effects of metal ions on the utilization of glucose and on the influence of insulin on it by the isolated rat diaphragm. *J. Biochem.*, **79**, 369–377.

BIRCH, N.J. Ed. (1991). *Lithium and the Cell: Pharmacology and Biochemistry*. London: Academic Press.

CLAUSEN, T. (1968). The relationship between the transport of glucose and cations across cell membranes in isolated tissues. IV. The 'insulin-like' effect of Li^+. *Biochim. Biophys. Acta*, **150**, 66–72.

FILIPPONI, P., GREGORIO, F., FERRANDINA, C., NICOLETTI, I., MANNARELLI, C., PIPPI, R. & SANTEUSANIO, F. (1986). Alpha-adrenergic system in the modulation of pancreatic A and B cell function in normal rats. *Diabetes Res. Clin. Pract.*, **2**, 325–336.

FONTELA, T., GARCIA HERMIDA, O. & GOMEZ-ACEBO, J. (1986). Blocking effect of naloxone, dihydroergotamine and adrenalectomy on lithium-induced hyperglycaemia and glucose intolerance in the rat. *Acta Endocrinol.*, **111**, 342–348.

FONTELA, T., GARCIA HERMIDA, O. & GOMEZ-ACEBO, J. (1987). Dihydroergotamine, but not naloxone, counteracts lithium as an inhibitor of glucose-induced insulin release in isolated rat islets in vitro. *Diabetologia*, **30**, 183–187.

FONTELA, T., GARCIA HERMIDA, O. & GOMEZ-ACEBO, J. (1990). Role of adrenoceptors *in vitro* and *in vivo* in the effects of lithium on blood glucose levels and insulin secretion in the rat. *Br. J. Pharmacol.*, **100**, 283–288.

FONTELA, T., GARCIA HERMIDA, O., MENA, M.A. & UTTENTHAL, L.O. (1991). Effect of acute lithium administration on plasma catecholamines in rats. *Lithium*, **2**, 185–186.

GARCIA HERMIDA, O., FONTELA, T., GHIGLIONE, M. & UTTENTHAL, L.O. (1991). Effect of *pertussis* pretreatment on plasma glucose and insulin responses to lithium in rats. *Br. J. Pharmacol.*, **103**, 1309–1312.

GREGORIO, F., FILIPPONI, P., CRISTALLINI, S., CARLONI, C., MORETTI, I., FERRANDINA, C., PIPPI, R. & PIETROPAOLO, M. (1986). Effects of beta non-selective and beta 1 selective adrenergic blocking agents on glucagon secretion from isolated perfused rat pancreas. *J. Endocrinol. Invest.*, **9**, 209–215.

GROSS, R., HILLAIRE-BUYS, D., RIBES, G. & LOUBATIERES-MARIANI, M.M. (1991). Diabetes alters the responses of glucagon-secreting cells and vascular bed to isoprenaline and forskolin in vitro in rat pancreas. *Life Sci.*, **48**, 2349–2358.

JONES, G.R., LAZARUS, J.H., DAVIES, C.J. & GREENWOOD, R.H. (1983). The effect of short term lithium carbonate in type II diabetes mellitus. *Horm. Metabol. Res.*, **15**, 422–424.

LAZARUS, J.H. (1986). *Endocrine and Metabolic Effects of Lithium*. New York: Plenum Medical Book Co.

MELLERUP, E.T., GRÖNLUND THOMSEN, H., PLENGE, P. & RAFAELSEN, O.J. (1970). Lithium effect on plasma glucagon, liver phosphorylase-a and liver glycogen in rats. *J. Psychiatr. Res.*, **8**, 37–42.

ROSSETTI, L. (1989). Normalization of insulin sensitivity with lithium in diabetic rats. *Diabetes*, **38**, 648–652.

SCHUIT, F.C. & PIPELEERS, D.G. (1986). Differences in adrenergic recognition by pancreatic A and B cells. *Science*, **232**, 875–877.

SHAH, J.H., DELEON-JONES, F.A., SCHICKLER, R., NASR, S., MAYER, M. & HURKS, C. (1986). Symptomatic reactive hypoglycemia during glucose tolerance test in lithium-treated patients. *Metabolism*, **35**, 634–639.

SHAH, J.H. & PISHDAD, G. (1980). The effect of lithium on glucose and tolbutamide-induced insulin release and glucose tolerance in the intact rat. *Endocrinology*, **107**, 1300–1304.

UNGER, R.H. & ORCI, L. (1981). Glucagon and the A cell: Physiology and pathophysiology. *N. Engl. J. Med.*, **304**, 1518–1524.

VENDSBORG, P.B. (1979). Lithium treatment and glucose tolerance in manic-melancholic patients. *Acta Psychiatr. Scand.*, **59**, 306–316.

VENDSBORG, P.B. & RAFAELSEN, O.J. (1973). Lithium in man: effect on glucose tolerance and serum electrolytes. *Acta Psychiatr. Scand.*, **49**, 601–610.

(Received July 19, 1993
Revised October 21, 1993
Accepted October 27, 1993)

Br. J. Pharmacol. (1994), **111**, 866–872

© Macmillan Press Ltd, 1994

Classical and atypical binding sites for β-adrenoceptor ligands and activation of adenylyl cyclase in bovine skeletal muscle and adipose tissue membranes

[1]M.N. Sillence & M.L. Matthews

Tropical Cattle Research Centre, CSIRO Division of Tropical Animal Production, Rockhampton, Queensland 4702, Australia

1 The radioligand [^{125}I]-iodocyanopindolol ([^{125}I]-ICYP) was used under standard ligand binding conditions, to detect β_1- and β_2-adrenoceptors in membrane preparations from bovine skeletal muscle and adipose tissue. High concentrations of [^{125}I]-ICYP were also used, to identify an 'atypical' binding site in skeletal muscle. Finally, adenosine 3':5'-cyclic monophosphate (cyclic AMP) production was measured in the same membrane preparations, to determine the relationship between the β-adrenoceptor sub-types present and the production of this second-messenger.

2 According to the results of radioligand binding studies, both skeletal muscle and adipose tissue membranes have β_2-adrenoceptors, characterized by a high affinity for the β_2-selective antagonist, ICI 118551 (pK 8.3 and 8.6 respectively); and a low affinity for the β_1-selective antagonist CGP 20712A (pK 5.2 in both tissues). Antagonism of (−)-isoprenaline-stimulated cyclic AMP production by low concentrations of ICI 118551, yielded pseudo pA_2 values in muscle and adipose tissue of 7.6 and 8.7 respectively, confirming that β_2-adrenoceptors in these tissues are linked to the production of the second-messenger.

3 Although β_1-adrenoceptors could not be detected in either skeletal muscle or adipose tissue membranes by use of ligand binding techniques, high pseudo pA_2 values were obtained (8.0 and 8.2 respectively), when CGP 20712A was used to block the stimulation of cyclic AMP production by (−)-isoprenaline. This finding is consistent with the presence in both tissues of a population of β_1-adrenoceptors which is small, but efficiently coupled to the second-messenger.

4 In addition to identifying standard β_1- and β_2-adrenoceptors, it was also established that skeletal muscle membranes have an 'atypical' binding site which has a relatively low affinity for [^{125}I]-ICYP (pK 8.84), but which exists in abundance. At high concentrations of radioligand, the 'atypical' site accounted for 89% of the total [^{125}I]-ICYP binding sites present.

5 The results of second-messenger studies do not support the hypothesis that skeletal muscle or adipose tissue membranes contain functional β_3-adrenoceptors: based on the failure of a β_3-adrenoceptor-selective agonist (BRL 37344) to stimulate cyclic AMP production, the absence of a biphasic response to (−)-isoprenaline, and the observation that cyclic AMP production was not resistant to blockade by either ICI 118551 or CGP 20712A.

6 It is concluded that data from radioligand binding studies do not accurately reflect the contribution made by β_1- and β_2-adrenoceptors to cyclic AMP production in bovine skeletal muscle and adipose tissue membranes. Furthermore, the 'atypical' [^{125}I]-ICYP binding site identified in bovine skeletal muscle does not represent a functional bovine β_3-adrenoceptor.

Keywords: cyclic AMP; skeletal muscle; adipose tissue; β-adrenoceptor ligands; β_1 and β_2-adrenoceptors

Introduction

The role of classical β-adrenoceptors in controlling skeletal muscle and adipose tissue metabolism was thought to be well understood. There is a perception that in skeletal muscle, the β_2-adrenoceptor is the only β-adrenoceptor sub-type present (Ijzerman *et al.*, 1984; Liggett *et al.*, 1988; Disatnik *et al.*, 1990); whereas in adipose tissue, β_1-adrenoceptors are believed to govern lipolysis, with an additional contribution from β_2-adrenoceptors in some species (Arner, 1992). This perception is now changing.

Following the discovery that functional adrenoceptors of the putative β_3-sub-type are present in rat adipose tissue (Arch *et al.*, 1984; Wilson *et al.*, 1984), the control of lipolysis by β-adrenoceptors has been re-examined in a number of different laboratory animal species. A few comparative studies have been conducted on human adipose tissue (Hollenga *et al.*, 1991a; Langin *et al.*, 1991), but to our knowledge there have been no previous studies using adipose tissue from domestic animals.

Although most studies of putative β_3-adrenoceptors have focussed on adipose tissue, there is also some evidence that β_3-adrenoceptors may be found in skeletal muscle. Three years after a report that a propranolol-resistant, 'atypical' β-adrenoceptor might be involved in the control of glycogen synthesis in rat soleus muscle (Challiss *et al.*, 1988), a propranolol-resistant 'atypical' binding site for the radioligand [^{125}I]-iodocyanopindolol ([^{125}I]-ICYP) was identified in the same tissue (Molenaar *et al.*, 1991). Subsequently, this site was shown to be identical to a putative β_3-adrenoceptor binding site found in rat brown adipose tissue (BAT) (Sillence *et al.*, 1993), and to display a strong resemblance to the cloned human β_3-adrenoceptor expressed in Chinese hamster ovary cells (Fève *et al.*, 1991). However, low pK values observed for the binding of β-adrenoceptor agonists to the 'atypical' site, caused uncertainty about whether the binding site was indeed an authentic β_3-adrenoceptor (Sillence *et al.*, 1993).

Establishing whether or not skeletal muscle contains putative β_3-adrenoceptors might help to improve our understanding of the control of skeletal muscle growth, and could be particularly important in relation to the clinical use of β_3-

[1] Author for correspondence at: CSIRO Division of Tropical Animal Production, P.O. Box 5545, Rockhampton Mail Centre, Queensland, Australia, 4702.

adrenoceptor-selective drugs. So far, the principal therapeutic benefit derived from using these compounds, seems to be an improvement in glucose tolerance, seen in patients suffering from non-insulin-dependent diabetes. This effect is thought to be mediated by an increase in the sensitivity of skeletal muscle to insulin-stimulated glucose uptake (Smith *et al.*, 1990).

In the present study, our aim was to examine the β-adrenoceptor population found in bovine skeletal muscle. By using both conventional and modified radioligand binding techniques, we aimed to identify both classical and 'atypical' β-adrenoceptor binding sites, and then determine which of the receptor sub-types present are linked to the production of the second-messenger adenosine 3':5'-cyclic monophosphate (cyclic AMP). The responsiveness of skeletal muscle membranes to a β_3-adrenoceptor-selective agonist was examined, as well as to (−)-isoprenaline, in the presence and absence of β_1- and β_2-adrenoceptor-selective antagonists. For comparative purposes, we report the results of similar experiments on bovine adipose tissue.

Methods

Preparation of tissue homogenates

Four young brahman (*Bos indicus*) heifers (150 kg) were stunned with a captive-bolt pistol, then exsanguinated. Samples (2 g) longissimus dorsi muscle and peri-renal white adipose tissue were quickly removed and placed in buffer (50 mM Tris 7.0, 0.25 M sucrose, 1 mM EGTA; pH 7.4 at 4°C) which was either ice cold (for skeletal muscle) or at room temperature (for adipose tissue). The tissues were minced with scissors, then homogenized separately; each in 10 ml of buffer with an Ultra-Turrax tissue homogenizer set at half-maximum speed and run for 10–20 s.

Cell membrane fragments were prepared by centrifugation at 4°C as described by Sillence *et al.* (1993). Briefly, the homogenates were centrifuged for 10 min at 1,000 *g*. The supernatants were filtered through gauze, then centrifuged for a further 15 min at 10,000 *g*. Next, the supernatants were centrifuged for 30 min at 100,000 *g* and the pellets obtained from this centrifugation were resuspended in 3 ml of ice-cold buffer (50 mM Tris 7.0, 5 mM $MgCl_2$, 1 mM EGTA; pH 7.4 at 4°C). After a further centrifugation, again at 100,000 *g* for 30 min, the supernatants were discarded and the pellets stored dry at − 80°C. Cell membrane fragments prepared for adenylyl cyclase assays were used within 1 week of preparation, whereas those prepared for ligand binding assays were used within 4 weeks.

Radioligand binding assays

The same procedure was applied to adipose tissue and muscle membranes and was identical to that described previously for the characterization of rat brown adipose tissue and soleus muscle (Sillence *et al.*, 1993). Frozen cell membrane pellets were thawed, pooled and resuspended in 5 ml of assay buffer (50 mM Tris 7.7, 10 mM $MgCl_2$, 0.15 M NaCl; pH 7.4 at 37°C) using three strokes of the tissue homogenizer. Protein concentration was determined by the Bradford Protein Assay (Bio-Rad, Richmond, U.S.A.) with bovine serum albumin standards. The membrane suspension was diluted to a working strength of 0.1 mg protein ml^{-1} (incubation concentration 0.04 mg protein ml^{-1}) after preliminary experiments had shown that binding of the radioligand to both standard and atypical sites was linear over the protein concentration range of 0.05 to 0.3 mg protein ml^{-1} (working strength).

Assays were performed in triplicate by incubating 100 μl cell membrane suspension with 50 μl [^{125}I]-ICYP, 50 μl guanylylimidodiphosphate (GppNHp) and 50 μl of various drugs, in polystyrene tubes (12 mm × 75 mm). Assays were initiated by the addition of cell membranes, and tubes were incubated for 90 min in a shaking water bath set at 37°C and 120 cycles min^{-1}. All components of the assay were in Tris assay buffer. Ascorbic acid (final concentration 2.8 mM) was added to the Tris buffer when isoprenaline was used in the assay. Separation of bound from free radioligand was achieved by filtering through Whatman GF-C glass fibre filter papers using a Brandel cell harvester (Beckman Instruments, Brisbane, Australia). Radioactivity remaining on the filters was determined in a Gammamaster gamma counter (Linbrook, Brisbane, Australia) at a counting efficiency of 68.3%.

To determine a p*K* value for the binding of [^{125}I]-ICYP to standard β_1- and β_2-adrenoceptors, a range of [^{125}I]-ICYP concentrations from 1 to 250 pM was used, and nonspecific binding was fixed at the level defined by 1 μM (−)-propranolol. The p*K* value for the binding of [^{125}I]-ICYP to putative β_3-adrenoceptors was determined using a radioligand concentration range of 5 to 2,000 pM, with nonspecific binding defined by 0.5 mM (−)-propranolol. Results were analysed by the Ligand computer programme (Munson & Rodbard, 1980).

Competition studies were performed under three sets of conditions, as described by Sillence *et al.* (1993). To characterize binding to β_1- and β_2-adrenoceptors, low concentrations of radioligand (30 pM) were used, and nonspecific binding was fixed at the level defined by 1 μM (−)-propranolol. To examine the binding of ligands to putative β_3-adrenoceptors, higher concentrations of radioligand were used (300 pM). In this case, nonspecific binding was defined using the Ligand curve-fitting programme, allowing this paramater to float about an initial estimate obtained in the presence of 0.5 mM (−)-propranolol. For ligands which were selective between standard adrenoceptors and putative β_3-adrenoceptors, p*K* values were obtained from multiple-site binding models generated by Ligand. A third set of binding conditions was necessary to characterize certain drugs which did not discriminate between standard β-adrenoceptors and putative β_3-adrenoceptors. These were the compounds which described a level of nonspecific binding similar to that defined by 0.5 mM (−)-propranolol, but gave displacement curves which were best described by one-site binding models. To determine p*K* values for these ligands at putative β_3-adrenoceptors, competition studies were repeated using 300 pM [^{125}I]-ICYP, but with all tubes containing 1 μM (−)-propranolol to block binding of the radioligand to β_1- and β_2-adrenoceptors.

Cyclic AMP assays

Frozen cell membranes were thawed, pooled and resuspended in 1 ml buffer (50 mM Tris 7.0, 5 mM $MgCl_2$, 1 mM EGTA; pH 7.0 at 25°C) using the tissue homogenizer. Following protein determination, the membrane suspension was diluted to a concentration of 0.6 mg protein ml^{-1}, and left at room temperature for approximately 30 min in order to prevent a lag-phase in cyclic AMP production, which would otherwise occur at the beginning of the incubation. Drugs were prepared in a buffer containing 50 mM Tris 7.7 and 100 μM ascorbic acid (pH 7.4 at 37°C). A third buffer was made immediately before the incubation, and contained: 50 mM Tris 7.7; 10 mM $MgCl_2$; 2 mM EGTA; 2 mM isobutylmethylxanthine; 0.4 mg bacitracin ml^{-1}; 6 mg bovine serum albumin ml^{-1}; 40 nM phosphocreatine, 2 mM ATP; 0.2 mM GTP; and 0.6 mg creatine phosphokinase ml^{-1}. A small volume (1 ml) of the latter 'incubation buffer' was reserved for the addition of 1.7 mg NaF.

All incubations were performed in triplicate. At the beginning of the incubation period 50 μl of incubation buffer was placed in 12 mm × 75 mm glass tubes along with 25 μl of drug solution. The incubation was initiated by the addition of 25 μl of membrane suspension and was carried out for 10 min in a shaking water bath set at 30°C. To determine the basal level of adenylyl cyclase activity, one set of tubes contained 25 μl drug-dilution buffer with no drug added. To determine maximum adenylyl cyclase activity, a second set of

tubes contained 50 μl NaF-incubation buffer, instead of standard incubation buffer.

At the end of the incubation period, the tubes were placed in a bath of boiling water for 4 min. Next, they were transferred to an ice-cold water bath and allowed to cool. The extraction of cyclic AMP from the samples was performed by adding 2 ml of ice-cold 65% ethanol to all tubes, mixing, then leaving the tubes to stand for 5 min at 4°C. The tubes were then centrifuged for 15 min at 2,000 *g* and 4°C. The supernatant was transferred to a second glass tube and a further 1 ml of cold ethanol was added to the pellet. The tubes containing pellet were vortexed and centrifuged again for 15 min at 2,000 *g*. Finally, the supernatants from both extractions were combined, and evaporated in a vacuum oven overnight at 60°C.

The samples were assayed in duplicate for cyclic AMP concentration with an assay kit (Amersham, North Ryde, Australia), after being resuspended in 3 ml of assay buffer supplied with the kit.

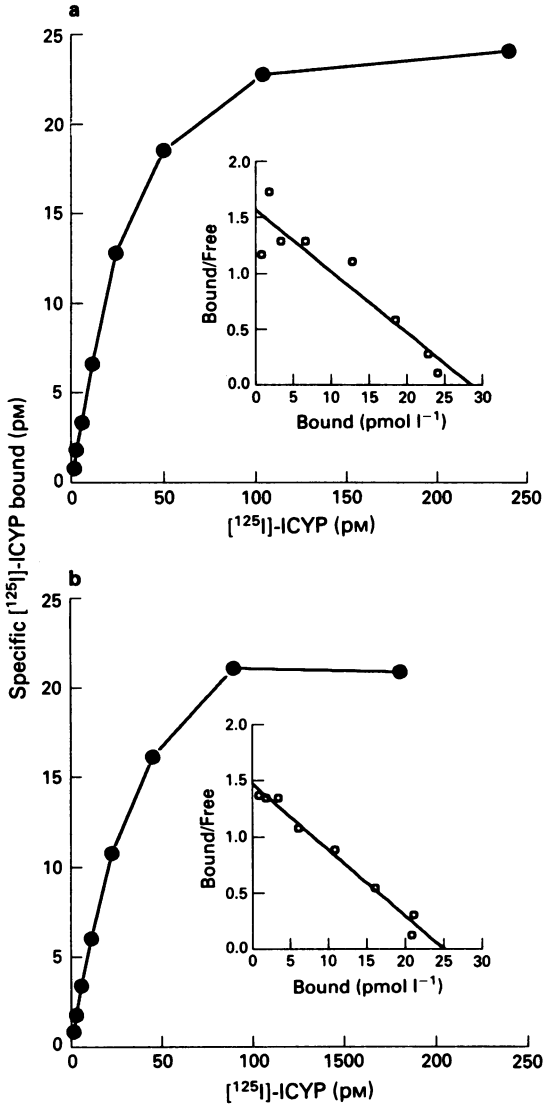


Figure 1 Specific binding of (−)-[^{125}I]-iodocyanopindolol ([^{125}I]-ICYP) to bovine cell membranes prepared from skeletal muscle (a) and adipose tissue (b). Assay conditions were designed to assess binding to β_1- and β_2-adrenoceptors: a low range of radioligand concentration was used, and binding to non-β_1/β_2-adrenoceptor sites was defined by use of 1 μM (−)-propranolol. Inset shows a Scatchard plot of the data.

Table 1 Dissociation constants for β_2-adrenoceptor binding sites in bovine skeletal muscle membranes

Ligand	*pK*[a]
(−)-[^{125}I]-iodocyanopindolol	10.7 ± 0.02
(−)-Propranolol	8.58 ± 0.06
(±)-Oxprenolol	7.71 ± 0.03
(±)-BRL 37344	5.96 ± 0.04
(−)-Isoprenaline	5.84 ± 0.04
(+)-Isoprenaline	3.77 ± 0.02

[a]Negative log of the dissociation constant. Values are means ± s.e.mean (n = 3).

Data analysis

Data presented as means ± s.e.mean. Curves were fitted to the cyclic AMP concentration-response data by eye, to allow the estimates of EC_{50} values. Pseudo pA_2 values were calculated by the dose-ratio method according to: $pA_2 = -\log$ {[antagonist]/(DR − 1)} (Mackay, 1978). The non-additive nature of multiple receptor responses, combined with insufficient data, precluded more rigorous Schild analysis.

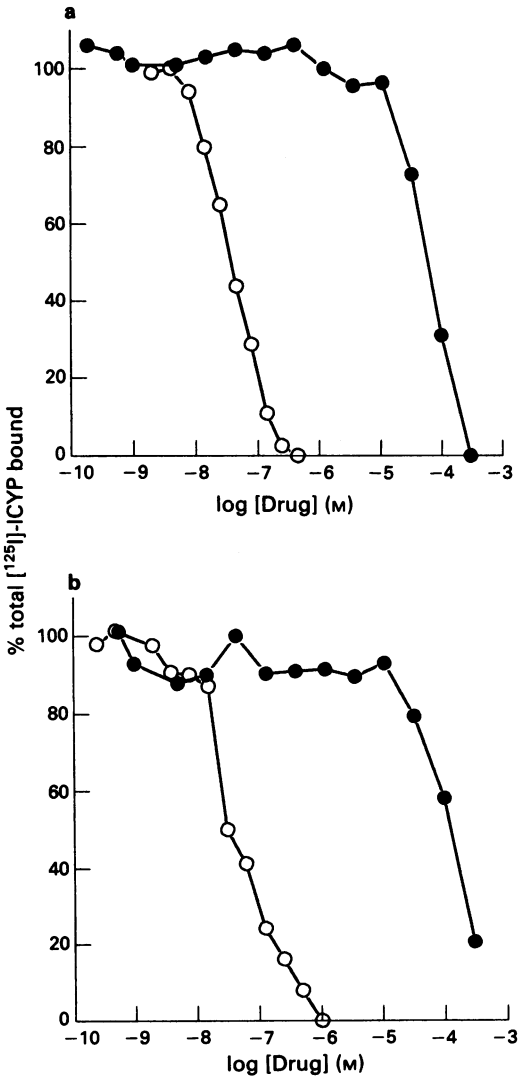


Figure 2 Representative curves showing the displacement of (−)-[^{125}I]-iodocyanopindolol ([^{125}I]-ICYP) (30 pM) from bovine skeletal muscle (a) and white adipose tissue (b) membranes by ICI 118551 (○) and CGP 20712A (●). Binding to non-β_1/β_2-adrenoceptor sites was determined by use of 1 μM (−)-propranolol and has been subtracted from the data.

Table 2 Dissociation constants and pseudo pA_2 values for the antagonism of (−)-isoprenaline-stimulated cyclic AMP production in bovine cell membrane fragments

	Skeletal muscle		*Adipose tissue*	
	pK^a	pA_2^b	pK^a	pA_2^b
ICI 118551	8.26 ± 0.03	7.57 ± 0.17	8.56 ± 0.06	8.69 ± 0.37
CGP20712A	5.16 ± 0.07	8.03 ± 0.21	5.15 ± 0.07	8.20 ± 0.37

[a]Negative log of the dissociation constant.
[b]Pseudo pA_2 values determined from the shift in concentration-response curve caused by a low concentration of antagonist. Note that Schild plots with a slope of unity were not obtained.
Values are means ± s.e.mean ($n = 3$).

Drugs

(−)-Isoprenaline, (−)-propranolol hydrochloride, (±)-oxprenolol hydrochloride and all buffer salts were purchased from Sigma Chemical Co (St Louis, U.S.A.). Bovine serum albumin was from Armour (Kanakee, U.S.A.). (−)-[^{125}I]-iodocyanopindolol (2200 Ci mmol^{-1}) was from Dupont (North Ryde, Australia). Guanylylimidodiphosphate (GppNHp) was from Boehringer Mannheim (New Farm, Australia). The following drugs were received as gifts: CGP 20712A (2-hydroxy-5-(2-[{2-hydroxy-3-(4-[1-methyl-4-trifluoromethyl-2-imidazolyl]phenoxy]propyl}amino]ethoxy)benzamide) (Ciba Geigy, Basel, Switzerland); ICI 118551 (erythro-1-(7-methylindan-4-yloxy)-3-(isopropylamino)-butan-2-ol) (ICI, Macclesfield, England); BRL 37344 (sodium-4-(2-[2-hydroxy-{3-chlorophenyl} ethylamino] propyl) phenoxyacetate) (SmithKline Beecham, Epsom, England); (+)-isoprenaline (Sterling Winthrop, Rensselaer, U.S.A.).

Results

Ligand binding studies in skeletal muscle membranes

In saturation studies using low concentrations of [^{125}I]-ICYP (Figure 1), a single saturable binding site was revealed which had a high affinity for the radioligand (Table 1) and a relatively low density (B_{max} 619 ± 35 fmol mg^{-1} protein), characteristic of a population of β_1- or β_2-adrenoceptors. In displacement studies, both agonists and antagonists yielded pK values consistent with binding to either β_1- or β_2-adrenoceptors, with greater than 100 fold stereoselectivity being demonstrated by the enantiomers of isoprenaline (Table 1). When the β_1-/β_2-adrenoceptor sub-type-selective ligands CGP 20712A and ICI 118551 were used, both compounds gave pK values consistent with binding to β_2-adrenoceptors (Table 2). Although the displacement of [^{125}I]-ICYP by low concentrations of CGP 20712A was erratic, neither drug could be modelled to reveal the presence of any β_1-adrenoceptors (Figure 2).

Next, the binding conditions were modified to detect putative β_3-adrenoceptors. Saturation studies using high concentrations of [^{125}I]-ICYP (Figure 3) revealed a binding site of high density (B_{max} 5 ± 0.48 pmol mg^{-1} protein) with relatively low affinity for the radioligand (Table 3), consistent with the putative β_3-adrenoceptor. Displacement studies using five different competing ligands also gave results characteristic of the putative β_3-adrenoceptor, as seen by a comparison of pK values with those from an earlier study of rat brown adipose tissue (Table 3).

Ligand binding studies in adipose tissue membranes

Although the characterization of adipose tissue membranes was less extensive than that of skeletal muscle, the results obtained in both tissues were strikingly similar (Figures 1 and 2). Saturation studies using low concentrations of [^{125}I]-ICYP revealed a single radioligand binding site (pK 10.78 ± 0.04, B_{max} 648 ± 43 fmol kg^{-1} protein) and pK values obtained using the sub-type-selective compounds CGP 20712A and ICI 118551 were also consistent with the presence of a homogeneous population of β_2-adrenoceptors (Table 2).

Table 3 Dissociation constants for atypical ligand binding sites in bovine skeletal muscle and rat brown adipose tissue (BAT)[a] membranes

	pK^b	
Ligand	*Bovine muscle*	*BAT*
(−)-[^{125}I]-iodocyanopindolol	8.84 ± 0.06	8.77 ± 0.11
(±)-ICI 118551	5.04 ± 0.11	5.00 ± 0.10
(−)-Propranolol	4.82 ± 0.02	4.93 ± 0.10
(±)-BRL 37344	3.47 ± 0.07	3.87 ± 0.03
(−)-Isoprenaline[c]	<3	3.14 ± 0.16
(±)-Phentolamine[c]	3.64 ± 0.01	3.58 ± 0.04

[a]Results taken from Sillence *et al.* (1993).
[b]Negative log of the dissociation constant.
[c]Ligands tested in the presence of 1 μM (−)-propranolol.
Values are means ± s.e.mean ($n = 3$).

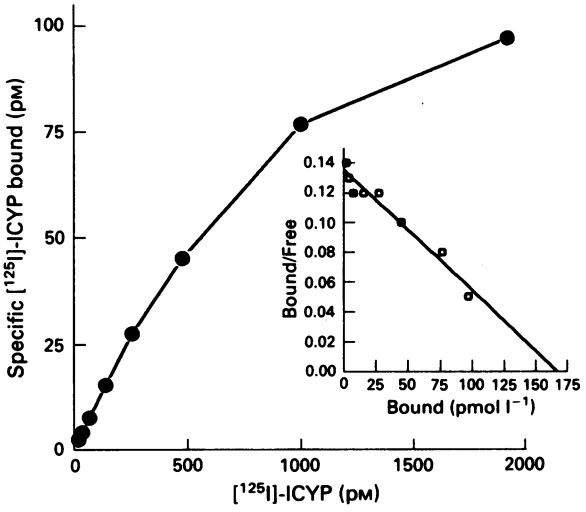


Figure 3 Representative curve showing the binding of (−)-[^{125}I]-iodocyanopindolol ([^{125}I]-ICYP) to skeletal muscle membranes. Assay conditions were designed to assess binding to putative β_3-adrenoceptors rather than to β_1- or β_2-adrenoceptors. Thus, high concentrations of radioligand were used, and nonspecific binding was determined in the presence of 0.5 mM (−)-propranolol. Inset shows a Scatchard plot of these data.

Second-messenger studies

The basal rates of cyclic AMP production were similar in skeletal muscle (1.71 ± 0.22 pmol mg^{-1} protein min^{-1}) and

adipose tissue membranes (2.07 ± 0.41 pmol mg^{-1} protein min^{-1}), whereas the stimulation of cyclic AMP production by NaF was markedly greater in adipose tissue membranes (6.8 ± 0.13 pmol mg^{-1} protein min^{-1}) than in skeletal muscle (4.55 ± 0.26 pmol mg^{-1} protein min^{-1}). The effects of (−)-isoprenaline and BRL 37344 are shown in Figure 4. (−)-Isoprenaline caused a dose-dependent stimulation of cyclic AMP production with mean pD_2 values ($-\log EC_{50}$) of 5.74 ± 0.14 and 5.7 ± 0.17 in skeletal muscle and adipose tissue membranes respectively. The pD_2 values for (−)-isoprenaline were in close agreement with the pK value determined in ligand binding studies, consistent with there being no receptor reserve for the response to this agonist. In contrast to (−)-isoprenaline, the β_3-adrenoceptor-selective agonist, BRL 37344, failed to stimulate cyclic AMP production in either tissue, and at high concentrations caused a slight fall in the output of second-messenger, most noticeable in skeletal muscle.

In both tissues the antagonists CGP 20712A and ICI 118551 caused a rightward shift of the concentration-response curve to (−)-isoprenaline (Figure 5). For CGP 20712A, the pseudo pA_2 values calculated from the shift

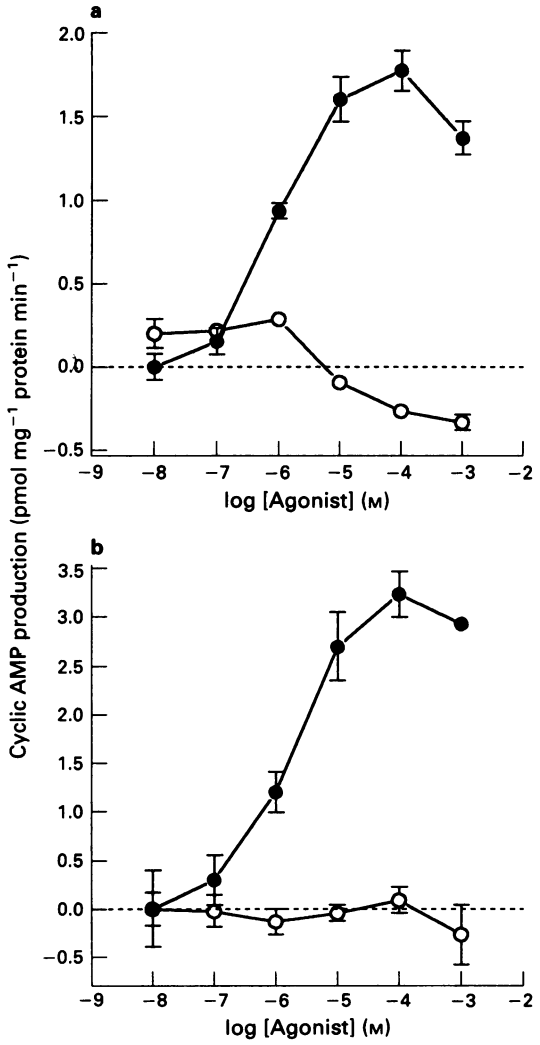


Figure 4 Effects of (−)-isoprenaline (●) and BRL 37344 (○) on the production of adenosine 3′:5′-cyclic monophosphate (cyclic AMP) in bovine cell membrane fragments: from (a) skeletal muscle and (b) white adipose tissue. Incubations were for 10 min. Each point represents the mean (± s.e.mean) value for three observations. Where standard errors are not visible, they are less than the size of the symbols. The results are presented relative to the basal amount of cyclic AMP produced in the absence of drug.

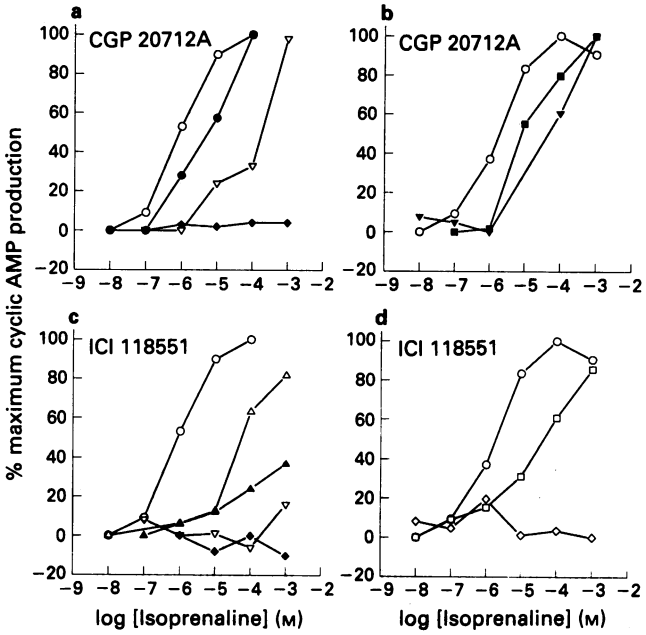


Figure 5 Effects of CGP 20712A and ICI 118551 on the stimulation of adenosine 3′:5′-cyclic monophosphate (cyclic AMP) production in bovine cell membranes by (−)-isoprenaline (○). Results are expressed relative to the maximum response to (−)-isoprenaline, after the subtraction of basal rates of production determined in the absence of agonist. Each point represents the mean of three observations. Standard errors are omitted for the sake of clarity, but were always less than 10% of the mean. Concentrations of CGP 20712A used in skeletal muscle (a) were 36 nM (●), 10 μM (▽), and 1 mM (◆); concentrations used in adipose tissue (b) were 100 nM (■) and 37 μM (▼). Concentrations of ICI 118551 used in skeletal muscle (c) were 1 μM (△), 2.7 μM (▲), 10 μM (▽) and 1 mM (◆); concentrations used in adipose tissue (d) were 38 nM (□) and 48 μM (◇).

produced by low concentrations of antagonist (36 and 100 nM) were similar in both tissues (Table 2), and were consistent with the activation of β_1-adrenoceptors by (−)-isoprenaline. However, when higher concentrations of the β_1-antagonist were used (in the range 10 to 37 μM), the shift in the concentration-response curve to isoprenaline was less than that expected from the activation of β_1-adrenoceptors alone. The shift was apparently greater in skeletal muscle than in adipose tissue, being reflected by pseudo pA_2 values of 7 and 6.5 respectively (determined from a single experiment in each tissue). Cyclic AMP production in skeletal muscle membranes was abolished by 1 mM CGP 20712A.

Next, pseudo pA_2 values were calculated from the shift in concentration-response curves caused by ICI 118551 (Table 2). The pseudo pA_2 value determined at 38 nM ICI 118551 in adipose tissue was higher than that determined using 1 μM in skeletal muscle. However, both values were closer to that expected for blockade of β_2-adrenoceptors, than for blockade of β_1- or β_3-adrenoceptors. Concentrations of ICI 118551 above 1 μM caused a non-parallel shift in the concentration-response curve to isoprenaline, and at anatagonist concentrations above 10 μM, cyclic AMP production was abolished.

Discussion

The results of this study show that bovine skeletal muscle has a low-affinity, 'atypical' [^{125}I]-ICYP binding site, which has binding characteristics almost identical to those of the 'atypical' site described in rat soleus muscle (Roberts *et al.*, 1993; Sillence *et al.*, 1993) and brown adipose tissue (Sillence *et al.*, 1993). The 'atypical' binding site is similarly abundant in bovine and rat skeletal muscle: representing 89% and 81%

respectively, of the total population of [^{125}I]-ICYP binding sites in muscle from these two species.

Having identified the 'atypical' binding site, our next aim was to test the hypothesis that this site represents a functional β_3-adrenoceptor coupled to adenylyl cyclase. The most extensive studies of β_3-adrenoceptor-mediated cyclic AMP responses are those which have been conducted on rat adipose tissue (Granneman, 1990; 1992; Hollenga *et al.*, 1991a,b). This tissue can be stimulated by BRL 37344 and in the presence of (−)-isoprenaline, gives a bi-phasic response which is resistant to blockade by either CGP 20712A or ICI 118551, yielding pA_2 values of 4.53 (Hollenga *et al.*, 1991b) and 5.49 (Hollenga & Zaagsma, 1989) respectively. None of these features were observed in the present study, suggesting that β_3-adrenoceptors are not expressed at a functional level in either bovine skeletal muscle or adipose tissue membranes.

This finding contrasts with the results of studies in rat soleus muscle (Challis *et al.*, 1988) and white adipose tissues (Hollenga & Zaagsma, 1989; Granneman, 1992), but is similar to the results of functional studies in human tissue. More specifically, human subcutaneous adipose tissue shows little or no response to BRL 37344 (Hollenga *et al.*, 1991a; Langin *et al.*, 1991), whereas functional β_3-adrenoceptors can be detected in human omental adipose tissue, with a lipolysis assay of appropriate sensitivity (Lonnqvist *et al.*, 1993). The second-messenger assay employed in the present study is not particularly sensitive, and bovine β_3-adrenoceptors may be expressed to a greater degree in other adipose tissue depots. Nevertheless, the results of the present study do not support the hypothesis that the abundant 'atypical' [^{125}I]-ICYP binding sites described above, represent functional bovine β_3-adrenoceptors.

The possibility that the 'atypical' [^{125}I]-ICYP binding sites represent β_3-adrenoceptors which are not coupled to cyclic AMP, is suggested from ligand binding data using adrenoceptor antagonists. The pK value for [^{125}I]-ICYP at the 'atypical' bovine site (8.84) is not only similar to that seen in our earlier experiments (Sillence *et al.*, 1993) using rat brown adipose tissue (8.77), but is also in close agreement with the value reported for a putative β_3-adrenoceptor in cultured murine adipocytes (8.82) (Fève *et al.*, 1991), and with those pK values for cloned human (8.72) and mouse (9.06) β_3-adrenoceptors expressed in Chinese hamster ovary (CHO) cells (Féve *et al.*, 1991; Nahmias *et al.*, 1991). In previous papers, we and others discussed further similarities between the 'atypical' [^{125}I]-ICYP binding site, and the putative rat β_3-adrenoceptor (Sillence *et al.*, 1993; Roberts *et al.*, 1993). However, despite these similarities, the pK values for the binding of agonists to the 'atypical' site are disturbingly low. Because β-agonists are generally less lipophilic than antagonists, it might be argued that the 'atypical' [^{125}I]-ICYP binding site is simply a nonspecific, lipophilic binding site. Rademaker *et al.* (1985) identified such a site in Cheng liver cells, by observing a strong correlation between binding affinity and hydrophobicity for 10 ligands, and a high affinity for the lipophilic α-adrenoceptor antagonist, phentolamine (pK 5.5), relative to that of the hydrophilic β-agonist isoprenaline. Our own analysis of log P and pK values for 11 ligands tested in rat skeletal muscle, shows a correlation which is not stronger for the 'atypical' binding site than for binding to classical β_2-adrenoceptors (unpublished data). Furthermore, the pK value for phentolamine observed in the present study (3.64) is not consistent with that reported in Cheng liver cells, so we conclude that the 'atypical' rat and bovine [^{125}I]-ICYP binding sites are not the same as the non-β-adrenoceptor site described by Rademaker *et al.* (1985). As well as binding to lipophilic sites, [^{125}I]-ICYP has been shown to label 5-HT receptors (Hoyer *et al.*, 1985) and to be susceptible to tissue peroxidases, which cause the nonspecific incorporation of iodide free radicles into tyrosine residues of membrane proteins (Rigby *et al.*, 1988). However, in contrast to these non-β-adrenoceptor binding sites, the site described in this and in our previous study, is not sensitive either to 5-HT (Sillence *et al.*, 1993) or to ascorbic acid concentration (unpublished observation).

Despite having shown that our 'atypical' [^{125}I]-ICYP site does not correspond to a number of previously-identified non-β-adrenoceptor binding sites, the low affinity observed for the binding of β-adrenoceptor agonists and the lack of a functional β_3-adrenoceptor-mediated response in tissues which express this binding site, are of concern. Further studies will need to be performed, therefore, before the nature of this 'atypical' site can be fully understood.

As well as identifying 'atypical' [^{125}I]-ICYP binding sites by using high concentrations of radioligand, we showed in the present study that under more conventional binding conditions, both skeletal muscle and white adipose tissue appear to have homogeneous populations of β_2-adrenoceptors. The present results for muscle agree with those of earlier studies in cattle (Ijzerman *et al.*, 1984; Sillence *et al.*, 1991), guinea-pigs (Elfellah & Reid, 1989), humans (Liggett *et al.*, 1988), and rat plantaris muscle (Kim *et al.*, 1991); whereas in rat soleus muscle, a minor population of β_1-adrenoceptors was identified with the highly sensitive technique of autoradiography (Kim *et al.*, 1991). In contrast to skeletal muscle, white adipose tissue from a number of species including pigs (Coutinho *et al.*, 1992), hamsters (Bjorgell & Belfrage, 1982) and man (Mauriege *et al.*, 1988), is well-recognised as being a source of both β_1- and β_2-adrenoceptors. The β_1-adrenoceptor is thought to govern lipolysis, whereas the contribution of β_2-adrenoceptors is thought to vary according to the species of animal (Arner, 1992). Thus, the present finding that no β_1-adrenoceptors could be detected in bovine adipose tissue with ligand binding techniques was surprising, and to our knowledge is in accord with only one previous study which examined sheep adipose tissue (R.G. Vernon, personal communication).

Our finding that no β_1-adrenoceptors could be detected in bovine muscle or adipose tissue using ligand binding techniques, is clearly at variance with the results of our adenylyl cyclase experiments. Although we have not attempted to quantify the relative contribution of β_1- and β_2-adrenoceptors to the production of cyclic AMP, our results show clearly that both adrenoceptor sub-types are involved, because the selective antagonists of CGP 20712A and ICI 118551 were both effective at low concentrations in causing a rightward shift in the concentration-response curve to (−)-isoprenaline. In addition, it was apparent that the generation of second-messenger by the two adrenoceptor sub-types was not additive. For this reason we have not attempted to generate Schild plots from our data, nor to define precisely pA_2 values for the antagonists used. The pseudo pA_2 values we report are estimates made with the lower concentrations of antagonists tested. Under these conditions, the occupation of either receptor sub-type attenuates the response of the tissue to (−)-isoprenaline markedly. However, when one or other receptor subtype is blocked to an extent greater than 99% by using high concentrations of antagonist e.g. 10 to 37 μM CGP 20712A, then maximum cyclic AMP production is still achievable, presumably through the agonist interacting with the unbound receptor sub-type. Our results suggest that the generation of second-messenger in these tissues involves a system which is more complex than can be described using standard pharmacological equations and we propose that this system warrants further investigation.

At the outset of this study, our primary aim was to determine which β-adrenoceptor subtypes are functional in bovine skeletal muscle. A secondary aim was to characterize bovine adipose tissue. The role of β_2-adrenoceptors in skeletal muscle is well-established for many species, and the results of the present work confirm the presence and coupling to second-messenger of this sub-type in cattle. We have also demonstrated that bovine skeletal muscle contains a small population of β_1-adrenoceptors, which are undetectable by ligand binding methods, but which nevertheless are strongly

coupled to the production of cyclic AMP. It remains to be determined whether β_1-adrenoceptors are present in skeletal muscle from other species, and whether these receptors have a physiological role, or represent a potential therapeutic target. As in skeletal muscle, both β_1- and β_2-adrenoceptors contribute to the production of second-messenger in bovine adipose tissue. Finally, although we have identified a binding site for [^{125}I]-ICYP which shares certain characteristics with the putative β_3-adrenoceptor, our second-messenger data do not support the hypothesis that functional β_3-adrenoceptors are present in either bovine skeletal muscle or adipose tissue.

The authors thank Professor M.J. Stock for supplying the method for the adenylyl cyclase assay, and are grateful to the pharmaceutical companies who kindly supplied ligands for this work. This study was supported by grants from the Australian Meat Research Corporation and the Australian Research Council.

References

ARCH, J.R.S., AINSWORTH, A.T., CAWTHORNE, M.A., PIERCY, V., SENNITT, M.V., THODY, V.E., WILSON, C. & WILSON, S. (1984). Atypical β-adrenoceptor on brown adipocytes as target for anti-obesity drugs. *Nature*, **309**, 163–165.

ARNER, P. (1992). Adrenergic receptor function in fat cells. *Am. J. Clin. Nutr.*, **55**, 228S–236S.

BJORGELL, P. & BELFRAGE, P. (1982). Characteristics of the lipolytic beta-adrenergic receptors in hamster adipocytes. *Biochim. Biophys. Acta*, **713**, 80–85.

CHALLISS, R.A.J., LEIGHTON, B., WILSON, S., THURLBY, P.L. & ARCH, J.R.S. (1988). An investigation of the β-adrenoceptor that mediates metabolic responses to the novel agonist BRL 28410 in rat soleus muscle. *Biochem. Pharmacol.*, **37**, 947–950.

COUTINHO, L.L., BERGEN, W.G., MERKEL, R.A. & SMITH, C.K. (1992). Quantitative characterization of beta-adrenergic receptor subtypes in porcine adipocytes. *Comp. Biochem. Physiol.*, **101C**, 481–485.

DISATNIK, M.H., SAMPSON, S.R. & SHAINBERG, A. (1990). Characterization of β-adrenoceptors on rat skeletal muscle cells grown *in vitro*. *Biochem. Pharmacol.*, **40**, 1043–1048.

ELFELLAH, M.S. & REID, J.L. (1989). Regulation of β_1- and β_2-adrenoceptors following chronic treatment with β-adrenoceptor antagonists. *Eur. J. Pharmacol.*, **173**, 85–92.

FEVE, B., EMORINE, L.J., LASNIER, F., BLIN, N., BAUDE, B., NAHMIAS, C., STROSBERG, A.R. & PAIRAULT, J. (1991). Atypical β-adrenergic receptor in 3T3-F442A adipocytes: pharmacological and molecular relationship with the human β_3-adrenergic receptor. *J. Biol. Chem.*, **266**, 20329–20336.

GRANNEMAN, J.G. (1990). Norepinephrine and BRL 37344 stimulate adenylate cyclase by different receptors in rat brown adipose tissue. *J. Pharmacol. Exp. Ther.*, **254**, 508–513.

GRANNEMAN, J.G. (1992). Effects of agonist exposure on the coupling of $beta_1$ and $beta_3$ adrenergic receptors to adenylyl cyclase in isolated adipocytes. *J. Pharmacol. Exp. Ther.*, **261**, 638–642.

HOLLENGA, C., BROUWER, F. & ZAAGSMA, J. (1991a). Differences in functional cyclic AMP compartments mediating lipolysis by isoprenaline and BRL 37344 in four adipocyte types. *Eur. J. Pharmacol.*, **200**, 325–330.

HOLLENGA, Ch., BROUWER, F. & ZAAGSMA, J. (1991b). Relationship between lipolysis and cyclic AMP generation mediated by atypical β-adrenoceptors in rat adipocytes. *Br. J. Pharmacol.*, **102**, 577–580.

HOLLENGA, Ch. & ZAAGSMA, J. (1989). Direct evidence for the atypical nature of functional β-adrenoceptors in rat adipocytes. *Br. J. Pharmacol.*, **98**, 1420–1424.

HOYER, D., ENGLE, G. & KALKMAN, H.O. (1985). Characterization of the 5-HT_{1B} recognition site in rat brain; binding studies with (−)[^{125}I]iodocyanopindolol. *Eur. J. Pharmacol.*, **118**, 1–12.

IJZERMAN, A.P., BULTSMA, T., TIMMERMAN, H. & ZAAGSMA, J. (1984). The relationship between ionization and affinity of β-adrenoceptor ligands. *Naunyn-Schmied. Arch. Pharmacol.*, **327**, 293–298.

KIM, Y.S., SAINZ, R.D., MOLENAAR, P. & SUMMERS, R.J. (1991). Characterization of β_1- and β_2-adrenoceptors in rat skeletal muscles. *Biochem. Pharmacol.*, **42**, 1783–1789.

LANGIN, D., PORTILLO, M.P., SAULINER-BLACHE, J.S. & LAFONTAN, M. (1991). Coexistence of three β-adrenoceptor subtypes in white fat cells of various mammalian species. *Eur. J. Pharmacol.*, **199**, 291–301.

LIGGETT, S.B., SHAH, S.D. & CRYER, P.E. (1988). Characterization of β-adrenergic receptors of human skeletal muscle obtained by needle biopsy. *Am. J. Physiol.*, **254**, (Endocrinol. Metab. 17), E795–798.

LONNQVIST, F., KRIEF, S., STROSBERG, A.D., NYBERG, B., EMORINE, L.J. & ARNER, P. (1993). Evidence for a functional β_3-adrenergic receptor in man. *Br. J. Pharmacol.* (in press).

MACKAY. D. (1978). How should values of pA_2 and affinity constants for pharmacological competitive antagonists be estimated? *J. Pharm. Pharmacol.*, **30**, 312–313.

MAURIEGE, P., DEPERGOLA, G., BERLAN, M. & LAFONTAN, M. (1988). Human fat cell beta-adrenergic receptors: beta-agonist-dependent lipolytic responses and characterization of beta-adrenergic binding sites on human fat cell membranes with highly selective beta-antagonists. *J. Lipid Res.*, **29**, 587–601.

MOLENAAR, P., ROBERTS, S.J., KIM, Y.S., PAK, H.S., SAINZ, R.D. & SUMMERS, R.J. (1991). Localization and characterizaton of two propranolol resistant (−)-[^{125}I] cyanopindolol binding sites in rat skeletal muscle. *Eur. J. Pharmacol.*, **209**, 257–262.

MUNSON, P.J. & RODBARD, D. (1980). Ligand: a versatile computerized approach for characterization of ligand-binding studies. *Anal. Biochem.*, **107**, 220–239.

NAHMIAS, C., BLIN, N., ELALOUF, J.M., MATTEI, M.G., STROSBERG, A.D. & EMORINE, L.J. (1991). Molecular characterization of the mouse β_3-adrenoceptor: relationship with the atypical receptor of adipocytes. *EMBO J.*, **10**, 3721–3727.

RADEMAKER, B., KRAMER, K., STROES, J.W., VLUG, J., KRIELAART, M. & ZAAGSMA, J. (1985). High affinity non-β-adrenoceptor binding of β-adrenergic ligands. *Eur. J. Pharmacol.*, **111**, 31–36.

RIGBY, P.J., PASSARELLI, M.C., SELF, G.J., PREUSS, J.M.H. & GOLDIE, R.G. (1988). Ascorbic acid-induced binding of [^{125}I]I-iodocyanopindolol to non-beta-adrenoceptor sites in guinea-pig trachea. *Biochem. Pharmacol.*, **37**, 1421–1424.

ROBERTS, S.J., MOLENAAR, P. & SUMMERS, R.J. (1993). Characterization of propranolol-resistant (−)-[^{125}I]-cyanopindolol binding sites in rat soleus muscle. *Br. J. Pharmacol.*, **109**, 344–352.

SILLENCE, M.N., MOORE, N.G., PEGG, G.G. & LINDSAY, D.B. (1993). Ligand binding properties of putative β_3-adrenoceptors compared in brown adipose tissue and in skeletal muscle membranes. *Br. J. Pharmacol.*, **109**, 1157–1163.

SILLENCE, M.N., PEGG, G.G. & LINDSAY, D.B. (1991). Affinity of clenbuterol analogues for β_2-adrenoceptors in bovine skeletal muscle and the effect of these compounds on urinary nitrogen excretion in female rats. *Naunyn-Schmied. Arch. Pharmacol.*, **344**, 442–448.

SMITH, S.A., SENNITT, M.V. & CAWTHORNE, M.A. (1990). BRL 35135: an orally active antihyperglycaemic agent with weight reducing effects. In *New Antidiabetic Drugs*. ed. Bailey, C.J. & Flatt, P.R. pp. 177–189. London: Smith-Gordon.

WILSON, C., WILSON, S., PIERCY, V., SENNITT, M.W. & ARCH, J.R.S. (1984). The rat lipolytic β-adrenoceptor studies using novel β-adrenoceptor agonists. *Eur. J. Pharmacol.*, **100**, 309–319.

(Received September 1, 1993
Revised October 27, 1993
Accepted October 29, 1993)

Br. J. Pharmacol. (1994), **111**, 873–879 © Macmillan Press Ltd, 1994

Effects of disopyramide and flecainide on the kinetics of inward rectifier potassium channels in rabbit heart muscle

Donald K. Martin, *Yutaka Nakaya, Kenneth R. Wyse & [1]Terence J. Campbell

Departments of Cardiology & Clinical Pharmacology, St. Vincent's Hospital, Victoria St. Darlinghurst, Sydney N.S.W. 2010, Australia and *Second Department of Internal Medicine, Tokushima University, Tokushima, Japan

1 Standard patch-clamp techniques were used to study the interaction of therapeutic concentrations of flecainide and disopyramide with single inwardly-rectifying potassium channels in cell-attached membrane patches from rabbit ventricular myocytes.

2 Under drug-free conditions, the potassium channels had a conductance of 31 ± 2 pS ($n = 13$), a mean open time of 230 ± 6 ms ($n = 11$) recorded at the resting cell potential, and an open probability of 0.66 ± 0.20 ($n = 39$). The resting potential of the cells studied was -68.5 ± 3.6 mV ($n = 32$).

3 Disopyramide did not reduce the open probability of the channel when the cell was voltage-clamped at the resting cell potential. However, disopyramide increased the mean open time of the channel, recorded at the resting cell potential, by 15% at 5 μM and by 29% at 20 μM. The action potential prolonging actions of disopyramide in therapeutic concentrations appear not to be due to blocking the inward rectifier K^+ channel.

4 Flecainide (3.0 μM, but not at 0.5 μM) decreased the open probability without changing the conductance of the channel, at 3 μM ($51.0 \pm 7.2\%$, $n = 6$, $P = 0.03$) at the resting cell potential. Flecainide increased the mean open time of the channel, recorded at the resting cell potential, by 12% at 3.0 μM.

5 We propose that flecainide stabilized the inward rectifier K^+ channel in an inactivated state, without plugging the conducting pore. In addition, it appeared to bind to an open conformation of the channel, since some of the reduction in open probability could be accounted for by the lengthening of the mean open time. The changes in open-state kinetics suggest that this binding may be in the region of the activation gate.

Keywords: Disopyramide; flecainide; potassium channel; inward rectification; single myocyte; conductance; open probability; kinetics

Introduction

The Cardiac Arrhythmia Suppression Trial (Echt *et al.*, 1991) reported that the use of the Class IC antiarrhythmic agents, flecainide and encainide increased mortality compared to placebo in patients with asymptomatic or mildly symptomatic ventricular arrhythmias following myocardial infarction. This trial greatly accelerated the search for antiarrhythmic agents that act by mechanisms other than sodium channel blockade. In particular drugs which prolong action potential duration (APD) by blocking potassium channels have received much attention. This effect is usually designated as the Class III antiarrhythmic action (Campbell, 1993). There are, however, at least seven different potassium channels reported in myocardium, and the relevant importance of each of these in controlling APD is poorly understood (Coraboeuf, 1978; Noble, 1984; Colatsky *et al.*, 1990; Hondeghem, 1992; Escande & Cavero, 1992). Channels which have particularly attracted much attention as possible targets for antiarrhythmic action include the transient outward current (I_{to}), the ATP-dependent potassium channel (I_{KATP}) and the delayed recitifier current (I_K), and a number of recent publications have highlighted the effects of various agents on one or more of these currents. It is known however, that the inwardly rectifying potassium channel (I_{K1}) also contributes significantly to repolarization, and carries the main current responsible for maintaining the resting potential of cardiac myocytes (Arena *et al.*, 1990; Martin & Chinn, 1992; Escande & Cavero, 1992). Additionally, specific blockade of this channel has very recently been reported to show prolongation of repolarization, measured as the QT interval on the ECG, and to be associated with potent antiarrhythmic properties in various animal models (Rees & Curtis, 1993). For these reasons we felt it important to characterize the effects on I_{K1} of therapeutic concentrations of antiarrhythmic agents in current clinical use. We also felt it important to use single channel recording methods, since only by these techniques can the individual potassium channels responsible for carrying the various currents be separated cleanly from each other and studied systematically.

Balser *et al.* (1991) had already shown that quinidine in a supratherapeutic concentration (50 μM) reduced the open probability of inwardly rectifying potassium channels by 20% without altering the channel conductance or kinetics. We were interested in the effects of the very similar agent, disopyramide on this current. Coraboeuf *et al.* (1988) reported data which suggested a modest effect on I_{K1} for a concentration of disopyramide three times the upper limit of the therapeutic range (60 μM). We therefore set out to confirm, using single channel recording techniques, whether disopyramide in therapeutic concentrations did in fact produce significant blockade of I_{K1}. We were also interested in the effects of flecainide on I_{K1} for a number of reasons. This agent is traditionally regarded as being primarily a sodium channel blocker and does not normally prolong the QT interval or the ventricular action potential duration. However, it has recently been reported to prolong atrial action potential duration (Wang *et al.*, 1990) and also to block the delayed rectifier (I_K) in ventricular myocytes. We therefore wanted to see whether flecainide in therapeutic concentrations would significantly depress I_{K1}. We have taken 8 to 22 μM as the therapeutic range for disopyramide (Niarchos, 1976), 0.3 to 2.0 μM for flecainide (Hodges *et al.*, 1982).

[1] Author for correspondence.

Methods

Preparation of myocytes

New Zealand White rabbits of either sex were anaesthetized with pentobarbitone sodium (Nembutal, Boehringer-Ingelheim, 45 mg kg^{-1}) and the anticoagulant heparin (500 units) infused via an ear vein. After removal of the heart, the ascending aorta was cannulated and mounted on a modified Langendorff perfusion apparatus, where it was maintained at 37°C. Remaining blood was washed from the heart for 5 min with a bicarbonate-buffered Ringer solution. Collagenase (76 u ml^{-1}, Worthington Type II) was added to this solution and the heart perfused for 20 min. After removing the atria and connective tissue, the ventricles were cut into 3–4 large pieces, which were agitated gently in the perfusing collagenase solution for a further 5 min at 37°C. Single myocytes were dispersed by gently agitating these pieces in a HEPES-buffered Ringer solution that contained 1% w/v bovine serum albumin (Sigma, No A-7906).

Solutions and drugs

The bicarbonate-buffered Ringer solution used to rinse the blood from the heart contained (mM): NaCl 130, KCl 4.8, $MgCl_2$ 1.0, NaH_2PO_4 0.35, KH_2PO_4 0.3, $NaHCO_3$ 25 and glucose 12.5. The pH was maintained at 7.4 by bubbling with Carbogen (5% CO_2/95% O_2). The HEPES-buffered Ringer solution (pH = 7.4) used for dispersion of the myocytes following the perfusion of the heart, and for superfusion of the cells during experiments contained (mM): NaCl 130, KCl 4.8, $MgCl_2$ 1.0, NaH_2PO_4 0.35, KH_2PO_4 0.3, HEPES 10 and glucose 12.5 The solution (pH = 7.2) used to fill the recording pipette for the patch-clamp experiments contained (mM): KCl 140, $MgCl_2$ 1.2, EGTA 5.0 and HEPES 10. The drugs used in the experiments were made as stock solutions dissolved in the HEPES-buffered Ringer solution and stored at 4°C. Roussel Laboratories supplied disopyramide, as free base, and Riker Laboratories supplied flecainide acetate.

Electrophysiological recording and analysis

Single-channel currents were recorded by standard patch-clamp techniques at room temperature (20–23°C). The channel currents were amplified and filtered at 500 Hz (– 3dB point) using an Axopatch 1B amplifier (Axon Instruments) and sampled on-line by a microcomputer (IBM 486 compatible) using commercial software and associated A/D hardware (pClamp 5.5.1/Labmaster TL-1-125, Axon Instruments Inc. and Scientific Solutions Inc.). Patch pipettes (7–10 MΩ) were fabricated from thin-walled borosilicate glass (Vitrex Microhæmatocrit Tubes, Modulohm I/S, Denmark). The recordings were made in the cell-attached configuration to preserve the intracellular milieu and to minimize the possibility of inward rectifier channel run-down that occurs with isolated membrane patches (Balser et al., 1991). All single-channel currents in this paper are referred to the trans-patch membrane potential (V_m). This was determined from the pipette potential (V_p), measured cell resting potential (E_m) and the liquid junction potential (E_L) between the bath and pipette solutions. The liquid junction potential was calculated using commercial software (JPCalc, A/Prof P.H. Barry, University of New South Wales; Barry & Lynch, 1991). The cell resting potential (E_m), measured by rupturing the membrane patch to obtain a whole-cell configuration, was -68.5 ± 3.6 mV ($n = 32$) with the solutions as described. Thus

$$V_m = (E_m - V_p) + E_L \quad (1)$$

Channel open probability was determined from steady-state recordings of 2 min duration, with the cell clamped at the resting membrane potential ($V_p = 0$ mV), and quantified as follows

$$P_o = \frac{1}{M} \sum_{m=1}^{M} m.P_m \quad (2)$$

where P_o = single channel open probability, M = total number of channels in the patch, m = each channel in the range 1 to M, and P_m = the open probability associated with the mth channel in the patch. The values for P_m were obtained as the area-under-the-curve for Gaussian curves fitted to each of the channel peaks in amplitude histograms constructed for each patch.

Channel kinetics were determined from distributions of dwell times, compiled from recordings containing only one channel, using the 50% amplitude threshold criterion, and filtered at 250 Hz (– 3dB). Sojourns in substates, except in the state of 1/8 of the main conductance, were considered to be open times during compilation of the histograms. The bin-size for this analysis was 16 ms, which was chosen to exclude brief openings which may have been artifactually modified due to the limited time resolution of the patch clamp amplifier and recording system. This combination of bin-size and low-pass filtering provides information on burst duration rather than individual channel openings within bursts (Sakmann & Trube, 1984b). Any errors due to our finite sampling times were negligible, since the data sampling period (1 ms) was much less than 10–20% of the dead time and fastest time constant of the interval distributions. Also, errors due to binning promotion during the construction of the histograms were negligible since the bin-widths were much less than 20–30% of the time constants (McManus et al., 1987). To optimize resolution of any changes in the kinetics of burst durations, we pooled data obtained from 2 min recordings at the resting membrane potential from multiple cells. Such recordings were made at steady-state, before and 20 min after addition of drug. All curve-fitting was performed with the pStat section of the pClamp software.

Statistical methods

The statistical significance of drug effects on open probability was assessed by the Wilcoxon rank sum test. Open-time distributions from multiple cells were pooled, and time constants derived from them using the non-linear least-squares Levenberg-Marquandt algorithm in the pClamp software. Ninety-nine percent confidence intervals (λ) were also generated for these fitted time-constants as follows (Dr P. Cooke, personal communication).

$$\lambda = 2.33 \left[\frac{\tau_1^2}{n_1} + \frac{\tau_2^2}{n_2} \right]^{\frac{1}{2}} \quad (3)$$

where $\tau_{1,2}$ = fitted time constants before and after addition of drug and $n_{1,2}$ = numbers of events in each distribution. Drug effects on t were considered significant if their confidence intervals did not overlap. That is, if

$$\lambda < \tau_1 - \tau_2 \quad (4)$$

No data were recorded until consistent channel activity had been observed for at least 10 min. In our experience channel open-probabilty in such cells did not change significantly over the subsequent 20 min (the maximum time required to observe drug effects). Similarly, there was no significant change in open-time kinetics during this period. For example, in three cells not exposed to drug, mean open-time was 234 ± 14 ms ($n = 734$ events) at 10 min after seal formation, and 228 ± 7 ms ($n = 553$ events) 20 min later. All the experiments described were approved by the Committee for the Use of Animals in Research and Training of the University of New South Wales and the Animal Ethics Committee of St Vincent's Hospital.

Results

Channel characteristics in drug-free solution

The resting membrane potential was -68.5 ± 2.6 mV, recorded from 32 cells (drug-free conditions) in which the cell-attached patch was ruptured. The potassium channel recorded in cell-attached patches showed inward rectification between membrane potentials of -24 mV and -190 mV, with a chord conductance for inward current within these potentials of 31 ± 2 pS ($\pm$ s.d., $n = 13$, Figure 1). Outward currents were hardly ever observed even at potentials up to $+55$ mV. In most cell-attached patches (drug-free) there were 2 to 6 channels present at the resting membrane potential, with very few patches (e.g. 2 out of 24 consecutive patches from separate cells) containing only one channel. Some recordings contained substates of the main conductance level, which were clustered around either 1/8, 1/4, or 1/2 of the main level (Figure 1). Cells which predominantly expressed these smaller conductance states were not included in the analysis. The open probability of this channel was 0.66 ± 0.20 ($\pm$ s.d., $n = 39$ cells) at the cell membrane potential. The distribution of open-times was well fitted by a single exponential curve. For example, the mean channel open-time (burst duration) for a sample of 11 cells (drug-free conditions) was 230 ± 6 ms ($n = 3541$ events), determined by pooling the dwell-times for all cells. The χ^2 value for this fit was 879.76 ($P < 0.001$).

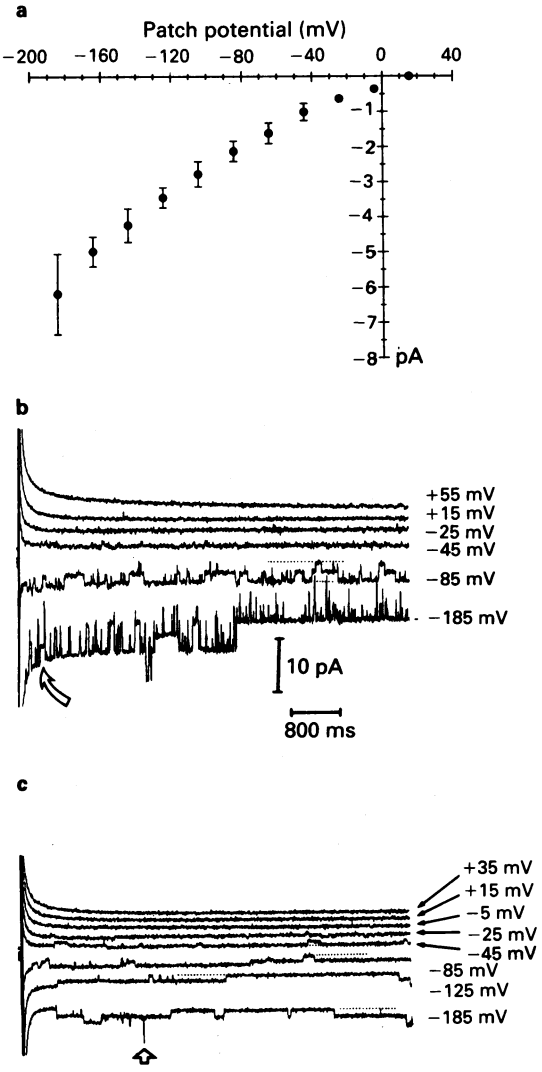


Figure 1 (a) Average current-voltage relation in cell-attached patches (conductance = 31 ± 2 pS; mean $\pm$ s.d.; $n = 13$). The potential on the abscissa scale is the trans-patch potential (see Methods). Inward currents are shown as negative values on the ordinate scale. The trans-patch reversal potential is around 0 mV since the pipette contained 140 mM K^+. (b) Representative single-channel recordings of the inwardly rectifying K^+ channel in a cell-attached patch. The trans-patch potential is shown next to the corresponding current record. Inward cell currents are shown as downward deflections. The dotted line indicates no current flow through the channel, when it was either in a closed or inactivated state. There were rare and brief openings of the channel when the patch was depolarized (potentials more positive than the resting cell potential, -68.5 mV). A substance level is indicated by the arrow. (c) Representative single-channel recordings from another cell where the inward rectifying currents were either carried by a different channel or a subconductance level of the channel shown in (b). A brief opening of the studied channel (b) is indicated by the arrow. There were fewer cells which showed this type of channel opening (slower, smaller conductance), and they were not included in the analysis.

Disopyramide

Disopyramide (1 μM) had no effect on the open probability of the inward rectifier at the resting membrane potential (Figure 2). Reductions in open probability were seen at 5 μM ($-32.4 \pm 18.8\%$, $n = 6$) and 20 μM ($-15.9 \pm 25.1\%$, $n = 6$) but the response was quite variable from cell to cell and, overall, did not achieve statistical significance ($P = 0.48$ at 5 μM, and $P = 0.94$ at 20 μM). Disopyramide did not affect the single-channel current at the resting cell potential (Table 1).

Disopyramide increased the mean open time of the channel (Figure 3). The mean open time was determined from distributions constructed from two experiments in which we recorded only 1 channel. The mean burst duration was

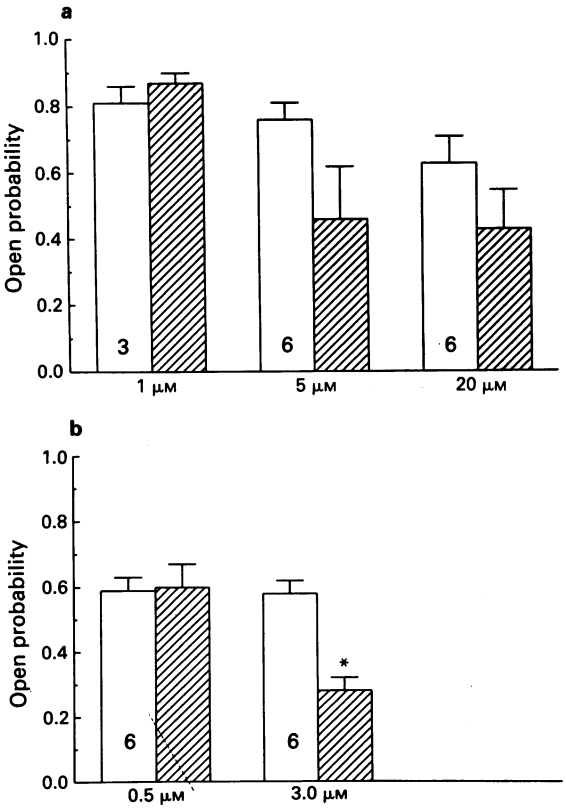


Figure 2 Inhibition of channel activity recorded in cell-attached patches voltage-clamped at the cell resting potential. The data are summarized for disopyramide (a) and flecainide (b). The number of observations is indicated in the histograms. Error bars indicate standard error of the mean. The asterisk indicates a significant change from control at the $P = 0.05$ level.

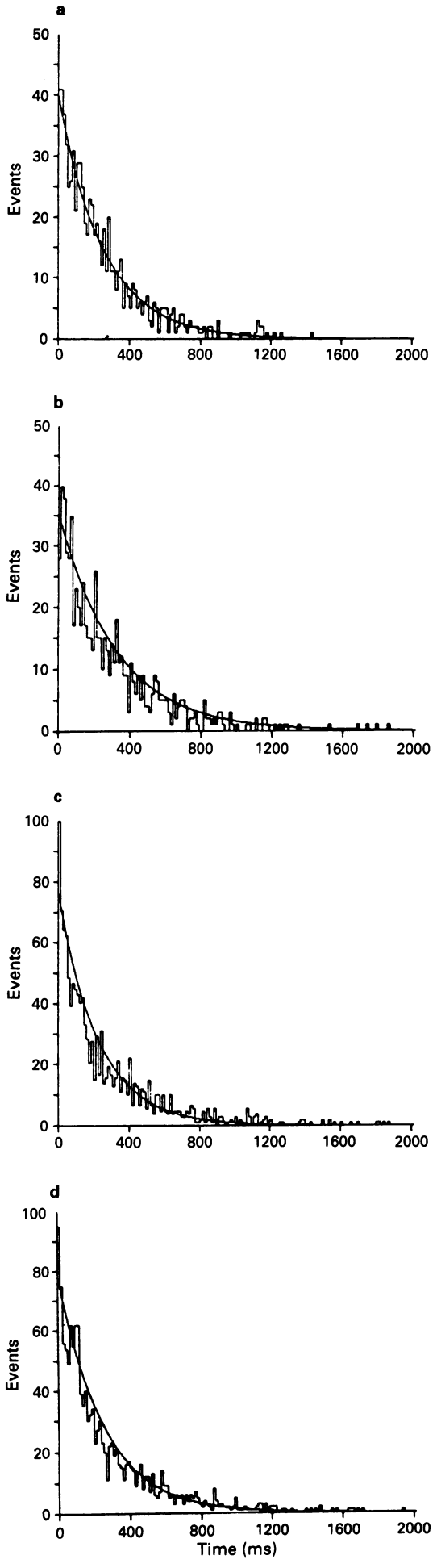


Table 1 Single-channel currents (pA) before and after application of the drugs

Drug	*Concentration*	*Control*	*20 min*
Disopyramide	1 μM	1.70 ± 0.06	1.72 ± 0.23
	5 μM	1.69 ± 0.36	1.89 ± 0.36
	20 μM	1.55 ± 0.49	1.76 ± 0.33
Flecainide	0.5 μM	1.99 ± 0.17	2.04 ± 0.35
	3.0 μM	1.73 ± 0.23	1.81 ± 0.18

Data are presented for recordings made at the resting membrane potential ($V_m = -68.5$ mV).

347 ± 16 ms ($n = 550$ events) at a concentration of 5 μM, and 387 ± 16 ms ($n = 733$ events) at 20 μM. Both of these values were significantly larger than the control value of 301 ± 9 ms ($n = 749$), with $\Delta\tau_{5\mu M} = 49$ ms, $\lambda_{5\mu M} = 40$ ms, $\Delta\tau_{20\mu M} = 86$ ms, $\lambda_{20\mu M} = 40$ ms.

Flecainide

The open probability of the channel was not affected by flecainide at 0.5 μM, but was significantly reduced by flecainide at 3.0 μM (51.0 ± 7.2%, $n = 6$, $P = 0.03$; Figure 2). Open probability was reduced in all six of the cells tested with 3.0 μM flecainide. This effect of flecainide is illustrated with records from a representative experiment (Figure 4). In the cell shown in Figure 4, the lower concentration reduced the activity of a subconductance level with no change in the main conductance level. The higher concentration of flecainide reduced the activity of all conductance levels. There was no significant change in the single-channel current following drug application (Table 1).

Flecainide also increased the burst duration of the channel (Figure 3). The mean open time was determined from distributions constructed from three experiments in which we recorded only 1 channel. The mean burst duration of 302 ± 10 ms ($n = 1399$ events) at a concentration of 3.0 μM was significantly longer than the control value of 269 ± 10 ms ($n = 1376$ events), with $\Delta\tau_{3.0\mu M} = 33$ ms and $\lambda_{3.0\mu M} = 25$ ms. In separate cells, the mean burst duration of 342 ± 14 ms ($n = 561$ events) at a concentration of 0.5 μM was significantly longer than the control value of 257 ± 16 ms ($n = 610$ events), with $\Delta\tau_{0.5\mu M} = 85$ ms and $\lambda_{0.5\mu M} = 41$ ms.

Discussion

In this study we have assessed the effects of therapeutic concentrations of disopyramide and flecainide on single inwardly rectifying potassium channels in rabbit ventricular myocytes using patch clamp techniques. The channel we describe very closely resembles that reported in guinea-pig ventricular myocytes by Sakmann & Trube (1984a,b). Specifically, the single-channel conductance at 20°C to 23°C in symmetrical transmembrane potassium concentrations was 31 ± 2 pS, and the open probability of the channel at the resting membrane potential (− 69 mV), was 0.66 ± 0.20. Sakmann & Trube reported a single-channel conductance under the same conditions of 27.5 ± 0.7 pS, and an open probability at − 72 mV of 0.63 ± 0.40. The similarity of these parameters allows us to be confident that the inwardly rec-

Figure 3 Change in channel open time following drug application. (a) Control for disopyramide (301 ± 9 ms, $n = 749$); (b) effect of 20 μM disopyramide (387 ± 16 ms, $n = 733$), (c) control for flecainide (269 ± 10 ms, $n = 1376$), (d) effect of 3 μM flecainide (302 ± 10 ms, $n = 1399$).

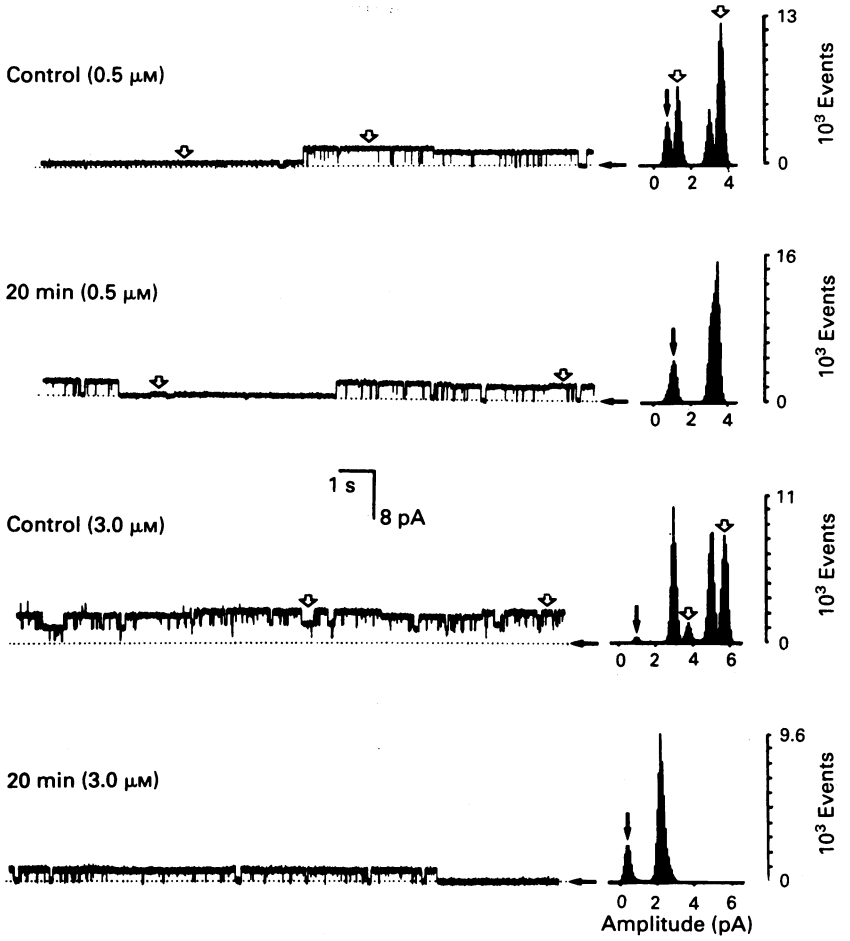


Figure 4 Representative recording of the channel activity in a cell-attached patch which was voltage-clamped (steady-state for 2 min) at the resting cell potential . The channel opening is shown as upward, for this figure only, even though it is an inward current. The dotted line (and solid arrow) indicates no current flow through the channel, when it was either in a closed or inactivated state. The peak in the amplitude histogram corresponding to this level is indicated by the solid arrow. A subconductance level in the single-channel record is indicated by the hollow arrow, which shows the corresponding peaks in the amplitude histogram.

tifying potassium channel we have studied corresponds to that described by Sakmann & Trube. It also closely resembles other descriptions of the equivalent current by Josephson & Brown (1986) in rat ventricular myocytes, and Matsuda (1988), in guinea-pig ventricular muscle.

Essentially we have shown that, at the resting membrane potential, flecainide at a concentration of 3.0 μM produced a 51% reduction in open probability ($P<0.05$; $n=6$). No effect was seen with 0.5 μM flecainide, and disopyramide did not significantly reduce open probability (at the resting membrane potential) at any of the three concentrations used. Both agents on the other hand, produced significant increases in the mean open time of the inward rectifier channel at all concentrations used (except 1 μM disopyramide). Channel conductance at the resting membrane potential was unaltered by either drug, suggesting that the effects observed were not due to simple plugging of the conducting pore.

To our knowledge, these are the first data obtained with single channel techniques which relate to the effects of flecainide and disopyramide on the inward rectifying potassium channel. In a multicellular preparation of sheep cardiac Purkinje fibres, Coraboeuf *et al.* (1988), reported that 60 μM disopyramide decreased the 'background potassium current'. While it is possible to identify a macroscopic inwardly rectifying current using this technique, it is not possible to tell with certainty which specific channel or channels carry this current. This is true even if isolated single cells are employed in the whole-cell voltage clamp mode, and the potential for accurate identification of individual channels is reduced further in multicellular preparations such as Purkinje fibres, which may exhibit significant artifactual depletion or accumulation currents (DiFrancesco, 1981). Flecainide has also been studied in this context, using freshly dissociated cat ventricular myocytes in whole-cell voltage clamp mode (Follmer & Colatsky, 1990), and reported to have no effect on the steady-state current measured at the end of 300 ms hyperpolarizing steps.

The concept that drugs such as flecainide and disopyramide, which are traditionally classifed as sodium channel blocking agents (Vaughan Williams Class I), might also affect potassium currents is not novel. Both agents have been shown to depress significantly the delayed rectifier, I_K, thought to be a major determinant of action potential duration in many cardiac myocyte types (Elharrar, 1988; Follmer & Colatsky, 1990). In addition to that, flecainide and disopyramide have both been shown to reduce the ATP-dependent potassium current, measured as dinitrophenol-induced outward current, in guinea-pig isolated ventricular cells by whole-cell voltage clamp techniques (Wu *et al.*, 1992). It is interesting therefore, to note that while disopyramide is well known to prolong the action potential duration in ventricular myocardium (Campbell, 1983), flecainide normally only produces slight lengthening (Ikeda *et al.*, 1985; Colatsky *et al.*, 1990). The solution to this apparent inconsistency lies no

doubt in the fact that Class I antiarrhythmic drugs produce opposing effects on action potential duration, with sodium channel blockade tending to shorten it and potassium channel blockade tending to lengthen it (Colatsky, 1991; Wyse *et al.*, 1993).

Possible mechanisms

Despite being relatively modest, the effects on I_{K1} of disopyramide and flecainide described above can be used to obtain some insight into the mechanisms by which these agents may modulate channel gating. We propose that flecainide binds to an 'inactivated' state of I_{K1}, in a similar manner to that proposed by Balser *et al.* (1991) for quinidine, and also affects the 'open state' of I_{K1} without reducing conductance.

Disopyramide, however, did not significantly reduce the open probability of I_{K1} in therapeutic concentrations. We propose that, since the only effect of disopyramide was to lengthen mean open time, this drug may only alter channel gating mechanisms for the open state. This interaction may be in the region of the activation gate of the channel. Such an interaction has been proposed for the effect of N-bromoacetamide on sodium channels (Patlak & Horn, 1982). The apparent difference between our data on disopyramide and those of Balser *et al.* (1991) for quinidine may relate to the relatively much higher drug concentration used by these workers (50 μM, or more than three times the upper limit of the therapeutic range for quinidine). It should be noted that both 5 μM and 20 μM disopyramide produced reductions in open probability which, while not statistically significant, were quite compatible with the modest 20% reduction reported by Balser *et al.* (Figure 2).

Clinical implications of I_{K1} blockade

The inward rectifier, I_{K1}, plays the major role in maintaining the resting membrane potential of the cardiac myocyte during diastole. It is largely inactivated on depolarization, but reactivates during repolarization, and plays a significant part in determining the duration of the later phases of the action potential in many cell types (Kass *et al.*, 1990; Shimoni *et al.*, 1992; Martin & Chinn, 1992).

Hondeghem (1992), has pointed out that there are basically two ways of prolonging the action potential duration leading to an increase in refractory period. These are by prolonged activation of inward currents during the plateau, or by blocking one or more of the outward currents leading to repolarization. The second of these comprises the mechanism of action of most of the known Class III antiarrhythmic agents. This action in turn however is not very specific, as there are at least seven described outward potassium currents involved in the generation of the cardiac action potential. The most important of these include the delayed rectifier I_K, and the ATP-sensitive potassium channel, both of which have been referred to above as well as the transient outward current I_{to}, and the inward rectifier I_{K1}. In the same review, Hondeghem postulated that blockade of the inward rectifier might be proarrhythmic, in that it would result in depolarization, and prolongation of the terminal phase of the action potential. He suggested that I_{K1} blockade was unlikely to be clinically useful. It has been shown, however, that reduction of I_{K1} by up to approximately 50% does not result in significant depolarization, and is manifest mainly as prolongation of the terminal phases of the action potential (Kass *et al.*, 1990; Martin & Chinn, 1992). Furthermore, Rees & Curtis (1993), have reported potent antiarrhythmic activity in a number of animal models of arrhythmias for RP58866, a specific I_{K1} blocking agent. This certainly raises the possibility that I_{K1} blockade might contribute to the antiarrhythmic effects of some of the Class III antiarrhythmic agents in current clinical use, most of which appear to block more than one potassium channel (Colatsky *et al.*, 1990). This paradox of a specific antiarrhythmic action having the potential to lead to either proarrhythmic or antiarrhythmic effects has a number of parallels. For example, the fact that sodium channel blockade can produce antiarrhythmic effects has been known, (and used clinically), for many years. There is no doubt however, following the results of the CAST study, that this action can also be proarrhythmic. Similarly, blockade of the delayed rectifier I_K, if excessive, may lead to the development of early afterdepolarizations and triggered activity, thought to be the mechanism underlying torsades des points.

The effects on I_{K1} we have demonstrated for flecainide are of comparable magnitude to those discussed by Kass *et al.* (1990), Martin & Chinn (1992) and Rees & Curtis (1993). It is quite possible therefore, that they may play some role in the overall electrophysiological actions of this agent, particularly in view of recent reports of a rate-dependent prolongation of duration of human atrial action potentials by flecainide (Wang *et al.*, 1990). While the (nonsignificant) reductions in the open probability of I_{K1} we observed for disopyramide were consistent with the 20% reduction reported by Balser *et al.* (1991) for quinidine, it would seem unlikely that such modest effects would contribute to the electrophysiological actions of either of these drugs.

This work was supported by the National Heart Foundation of Australia (D.K.M., K.R.W., T.J.C.) and The Japanese Ministry of Education, Science and Culture (Y.N.). Dr Peter Cooke from the School of Mathematics, University of New South Wales, advised us concerning the statistical testing of the time constants derived from the distributions of channel open-times.

References

ARENA, J.P., WALSH, K.B. & KASS, R.S. (1990). Measurement, block and modulation of potassium channel currents in the heart. *Prog. Clin. Biol. Res.*, **334**, 43–64.

BALSER, J.R., RODEN, D.M. & BENNETT, P.B. (1991). Single inward rectifier potassium channels in guinea pig ventricular myocytes – effects of quinidine. *Biophys. J.*, **59**, 150–161.

BARRY, P.H. & LYNCH, J.M. (1991). Liquid junction potentials and small cell effects in a patch-clamp analysis. *J. Membr. Biol.*, **121**, 101–117.

CAMPBELL, T.J. (1983). Kinetics of onset of rate-dependent effects of class I antiarrhythmic drugs are important in determining their effects on refractoriness in guinea-pig ventricle, and provide a theoretical basis for their subclassification. *Cardiovasc. Res.*, **17**, 344–352.

CAMPBELL, T.J. (1993). Class III antiarrhythmic action: the way forward? *Med. J. Aust.*, **158**, 732.

COLATSKY, T.J. (1991). Modulation of cardiac repolarization currents by antiarrhythmic drugs. In *Cardiac Electrophysiology: A Textbook*. ed. Rosen, M.R., Janse, M.J. & Wit, A.L. pp. 1043–1062. New York: Futura.

COLATSKY, T.J., FOLLMER, C.H. & STARMER, C.F. (1990). Channel specificity in antiarrhythmic drug action. *Circulation*, **82**, 2235–2242.

CORABOEUF, E. (1978). Ionic basis of electrical activity in cardiac tissues. *Am. J. Physiol.*, **234**, H101–H116.

CORABOEUF, E., DEROUBAIX, E., ESCANDE, D. & COULOMBE, A. (1988). Comparative effects of three class I antiarrhythmic drugs on plateau and pacemaker currents of sheep Purkinje fibres. *Cardiovasc. Res.*, **22**, 375–384.

DIFRANCESCO, D. (1981). A study of the ionic nature of the pacemaker current in Purkinje fibres. *J. Physiol.*, **314**, 359–393.

ECHT, D.S., LIEBSON, P.R., MITCHELL, L.B., PETERS, R.W., OBIAS-MANNO, D., BARKER, A.H., ARENSBERG, D., BAKER, A., FRIED-MAN, L., GREENE, L., HUTHER, M.L., RICHARDSON, D.W. & CAST INVESTIGATORS. (1991). Mortality and morbidity in patients receiving encainide, flecainide, or placebo. *N. Engl. J. Med.*, **324,** 781–788.

ELHARRAR, V. (1988). Recovery from use-dependent block of Vmax and restitution of action potential duration in canine cardiac Purkinje fibers. *J. Pharmacol. Exp. Ther.*, **246,** 235–242.

ESCANDE, D. & CAVERO, I. (1992). K^+ channel openers and 'natural' cardioprotection. *Trends. Pharmacol. Sci.*, **13,** 269–271.

FOLLMER, C.H. & COLATSKY, T.J. (1990). Block of delayed rectifier potassium current, Ikl, by flecainide and E-4031 in rat ventricular myocytes. *Circulation*, **82,** 289–293.

HODGES, M., HANGLAND, J.M., GRANRUD, G., CONARD, G.J., ASINGER, R.W., MIKELL, F.L. & KREJCI, J. (1982). Suppression of ventricular entropic depolarisations by flecainide acetate, a new antiarrhythmic drug. *Circulation*, **65,** 879–885.

HONDEGHEM, L.M. (1992). Development of class III antiarrhythmic agents. *J. Cardiovasc. Pharmacol.*, **20** (Suppl. 2), S17–S22.

IKEDA, N., SINGH, B.H., DAVIS, L.D. & HAUSWIRTH, O. (1985). Effects of flecainide on the electrophysiologic properties of isolated canine and rabbit myocardial fibers. *J. Am. Coll. Cardiol.*, **5,** 303–310.

JOSEPHSON, I.R. & BROWN, A.M. (1986). Inwardly rectifying single-channel and whole cell K^+ currents in rat ventricular myocytes. *J. Membr. Biol.*, **94,** 19–35.

KASS, R.S., ARENA, J.P. & WALSH, B. (1990). Measurement and block of potassium channel currents in the heart: importance of channel type. *Drug Dev. Res.*, **19,** 115–127.

MCMANUS, O.B., BLATZ, A.L. & MAGLEBY, K.L. (1987). Sampling, log binning, fitting and plotting durations of open and shut intervals from single channels and the effects of noise. *Pflügers Arch.*, **410,** 530–553.

MARTIN, C.L. & CHINN, K. (1992). Contribution of delayed rectifier and inward rectifier to repolarization of the action potential: pharmacologic separation. *J. Cardiovasc. Pharmacol.*, **19,** 830–837.

MATSUDA, H. (1988). Open-state substructure of inwardly rectifying potassium channels revealed by magnesium block in guinea-pig heart cells. *J. Physiol.*, **397,** 237–258.

NIARCHOS, A.P. (1976). Disopyramide: serum level and arrhythmia conversion. *Am. Heart J.*, **92,** 57–64.

NOBLE, D.N. (1984). The suprising heart: a review of recent progress in cardiac electrophysiology. *J. Physiol.*, **353,** 1–50.

PATLAK, J. & HORN, R. (1982). Effect of N-bromoacetamide on single sodium channel currents in excised membrane patches. *J. Gen. Physiol.*, **79,** 333–351.

REES, S.A. & CURTIS, M.J. (1993). Specific Ik1 blockade: a new antiarrhythmic mechanism? *Circulation*, **87,** 1979–1989.

SAKMANN, B. & TRUBE, G. (1984a). Conductance properties of single inwardly rectifying potassium channels in ventricular cells from guinea-pig heart. *J. Physiol.*, **347,** 641–657.

SAKMANN, B. & TRUBE, G. (1984b). Voltage-dependent inactivation of inward-rectifying single-channel currents in the guinea-pig heart cell membrane. *J. Physiol.*, **347,** 659–683.

SHIMONI, Y., CLARK, R.B. & GILES, W.R. (1992). Role of an inwardly rectifying potassium current in rabbit ventricular action potential. *J. Physiol.*, **448,** 109–727.

WANG, Z., PELLETIER, L.C., TALAJIC, M. & NATTEL, S. (1990). Effects of flecainide and quinidine on human atrial action potentials. *Circulation*, **82,** 274–283.

WU, B., SATO, T., KIYOSUE, T. & ARITA, M. (1992). Blockade of the 2,4-dinitrophenol induced ATP-sensitive potassium current in guinea-pig ventricular myocytes by class I antiarrhythmic agents. *Cardiovasc. Res.*, **26,** 1095–1101.

WYSE, K.R., YE, V., CAMPBELL, T.J. (1993). Action potential prolongation exhibits simple dose-dependence for sotalol, but reverse dose-dependence for quinidine and disopyramide: implications for proarrhthymia due to triggered activity. *J. Cardiovasc. Pharmacol.*, **21,** 316–322.

(Received April, 5, 1993
Revised September 1, 1993
Accepted November 1, 1993)

Br. J. Pharmacol. (1994), **111**, 880–886 © Macmillan Press Ltd, 1994

Potentiation by endogenously released ATP of spontaneous transmitter secretion at developing neuromuscular synapses in *Xenopus* cell cultures

[1]Wen-Mei Fu & Fu-Lei Huang

Pharmacological Institute, College of Medicine, National Taiwan University, Taipei, Taiwan

1 Previously we have shown that extracellular application of ATP, a substance co-stored and co-released with acetylcholine (ACh) in the peripheral nervous system, markedly potentiated the frequency of spontaneous synaptic currents (SSCs) produced by ACh. In the present study, we have further characterized the purinoceptor which mediates the potentiation effect of ATP and the role of endogenously released ATP.

2 Pretreatment with a P_2-purinoceptor antagonist, suramin (0.3 mM), but not a P_1-purinoceptor antagonist, 8-phenyltheophylline (0.1 mM), prevented the potentiating effect of ATP.

3 We studied the role of endogenously released ATP by examining the effect of a specific P_2-purinoceptor antagonist on the frequency of spontaneous synaptic events at high-activity synapses ($\geqslant 3$ Hz) and found that suramin, but not 8-phenyltheophylline markedly reduced the frequency of SSCs at these high-activity synapses. In addition, desensitizing the P_2-purinoceptor with α,β-methylene ATP also produced similar effects to suramin.

4 Extracellular application of the L-type Ca^{2+} channel blockers, verapamil, nifedipine or diltiazem (10 μM each) reduced SSC frequency of high-activity synapses, while the N-type Ca^{2+} channel blocker, omega-conotoxin had no appreciable effect. The potentiating effect of ATP was further prevented by pretreatment with the L-type Ca^{2+} channel blockers. On the other hand, Bay K 8644, which is a depolarization-dependent L-type Ca^{2+} channel agonist, potentiated SSC frequency at these high-activity synapses.

5 These results suggest that endogenous release of ATP at developing neuromuscular synapses is responsible for the maintenance of high levels of spontaneous ACh release, which is known to play a crucial role in regulating postsynaptic differentiation.

Keywords: ATP; L-type Ca^{2+} channel; ACh release; neuromuscular synapses; *Xenopus* cell cultures

Introduction

Development, maintenance and modulation of synapses depends on molecular interactions between the pre- and postsynaptic cells (Purves, 1986). At developing neuromuscular junctions, factors secreted from the presynaptic nerve terminals may affect the development of postsynaptic acetylcholine (ACh) receptor clusters (Nitkin *et al.*, 1987; Usdin & Fishbach, 1986) and muscle contractile properties (Kidokoro & Saito, 1988). Adenosine 5'-triphosphate (ATP) has long been considered a potential candidate for a neurotrophic factor, since ATP is known to be co-stored and co-released with ACh in the vertebrate peripheral nervous system (Silinsky & Hubbard, 1973; Dowdall *et al.*, 1974; Meunier *et al.*, 1975; Zimmerman, 1978). Muscle cells are also known to secrete substantial amounts of ATP in response to electrical activity (Smith & Lindgren, 1986). Exogenously applied ATP and its derivative, adenosine, at mature synapses have been shown to inhibit the evoked and spontaneous ACh release (Ribeiro & Walker, 1975; Silinsky & Ginsborg, 1983). More recent results have shown that exogenous application of ATP potentiates the spontaneous secretion of ACh at developing neuromuscular synapses both in *Xenopus* cell cultures and tadpoles (Fu & Poo, 1991; Fu *et al.*, 1993). We here report the first evidence that *endogenous* release of ATP at developing neuromuscular synapses is responsible for the maintenance of high levels of spontaneous ACh release, which is known to play a crucial role in regulating postsynaptic differentiation (Kidokoro & Saito, 1988).

[1] Author for correspondence.

Methods

Culture preparation

Xenopus nerve-muscle cultures were prepared as previously reported (Spitzer & Lamborghini, 1976; Anderson *et al.*, 1977; Sanes & Poo, 1989). Briefly, the neural tube and the associated myotomal tissue of 1-day-old *Xenopus* embryos (stage 20–22; Nieuwkoop & Faber, 1967) were dissociated in Ca^{2+}- and Mg^{2+}-free Ringer supplemented with EDTA. The cells were plated on clean glass coverslips and were used for experiments after 24 h at room temperature (20–22°C). The culture medium consisted of 50% (vol/vol) Ringer solution (composition: mM: NaCl 115, $CaCl_2$ 2, KCl 1.5, HEPES 10, pH 7.6), 49% L-15 Leibovitz medium (Sigma), and 1% foetal bovine serum (Gibco).

Electrophysiology

Gigaohm-seal whole-cell patch-clamp recording methods followed those described previously (Hamill *et al.*, 1981; Young & Poo, 1983; Evers *et al.*, 1989). Synaptic currents were recorded from innervated myocytes by whole-cell recording in the voltage-clamp mode. Recordings were made at room temperature in culture medium. For whole-cell recordings, the solution inside the recording pipette contained mM: KCl 150, NaCl 1, $MgCl_2$ 1 and HEPES 10 (pH 7.2). In all recordings, the membrane currents were monitored by a patch-clamp amplifier (Dagan 8900, filtered at 10 kHz). The data were stored on a videotape recorder for later playback onto a storage oscilloscope (Tektronix 5113) or an oscillographic recorder (Gould RS3200). The Data 6100 waveform

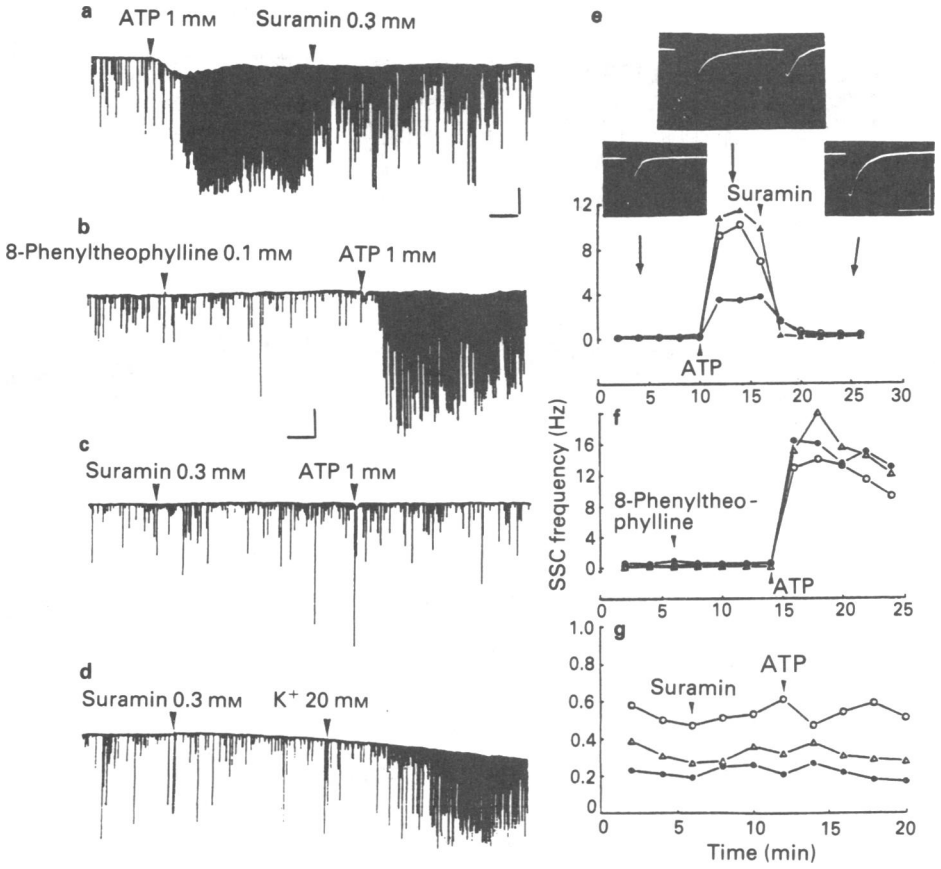


Figure 1 Effect of purinoceptor antagonists on the potentiation action of spontaneous acetylcholine (ACh) release by ATP. The continuous trace depicts the membrane current recorded from the innervated muscle cell in 1-day-old *Xenopus* culture. The cell was whole-cell voltage-clamped at a membrane potential of − 60 mV. Downward deflection represents inward currents (filtered at 150 Hz). (a) ATP was applied to the culture medium at the time marked by the arrow. Note the marked increase in spontaneous synaptic current (SSC) frequency after ATP application. Addition of suramin after ATP treatment inhibited the ATP effect, samples of synaptic currents are shown in the insets of (e) at higher time resolution (filtered at 10 kHz). (b) Pretreatment with P_1-purinoceptor antagonist, 8-phenyltheophylline, did not affect the potentiating action of ATP. However, the P_2-purinoceptor antagonist, suramin, significantly inhibited the potentiating action of ATP (c) but not that of high-K^+ (d). The time course-response curves of (a) (b) and (c) are shown in (e), (f) and (g), respectively. Each curve represents data collected from 1 synapse. Scale bar: 560 pA, 100 s and 400 pA, 20 ms for the slow and fast traces, respectively.

analyser (Data Precision) was used to analyse the frequency of the spontaneous synaptic currents.

The following chemicals were used: adenosine 5′-triphosphate (ATP), 8-phenyltheophylline (8-PT), α,β-methylene ATP, nifedipine, diltiazem and verapamil (Sigma), suramin (FBA, Germany), omega-conotoxin (Biomol) and Bay K 8644 (methyl-1, 4-dihydro-2, 6-dimethyl-5-nitro-4-[(2-trifluoromethyl)phenyl)]-3-pyridine-5-carboxylate, Research Biochemicals Incorporated). H-7 (1-(5-isoquinoline-sulphonyl)-2-methylpiperazine dihydrochloride; Seikgaku, Kogyo, Japan).

Results

Effects of selective purinoceptor antagonists on the potentiation of ACh release by ATP

Cultures of embryonic spinal neurones and myotomal muscle cells were prepared from 1-day-old *Xenopus* embryos. Functional synaptic contacts between the nerve and muscle cells are established within 24 h after cell plating. Spontaneous synaptic currents (SSCs) were recorded from myocytes innervated by co-cultured spinal neurones by the whole-cell voltage-clamp recording method. These currents resulted from spontaneous quantal ACh secretion from the neurone, since they are abolished by bath application of (+)-tubocurarine (Xie & Poo, 1986). It has been shown previously that *exogenous* application of ATP to these synapses triggers a marked increase in the frequency of SSCs (Fu & Poo, 1991). In the present study, we found that the potentiating effect of ATP is mediated specifically by P_2-purinoceptors. As shown in Figure 1, pretreatment with a P_2-purinoceptor antagonist, suramin (0.3 mM), but not a P_1-purinoceptor antagonist, 8-phenyltheophylline (0.1 mM), prevented the potentiating effect of ATP (1 mM) (Figure 1b,c,f and g). The effect of suramin was not due to a non-selective blockade of transmitter release, since it did not inhibit the potentiation of ACh release by high-K^+ (20 mM)-induced depolarization (Figure 1d). Moreover, addition of suramin after ATP treatment also reversed the ATP effect (Figure 1a and e). As the mean amplitude of spontaneous synaptic currents was not altered by suramin (0.3 mM) (357.8 ± 50.6 pA and 334.1 ± 43.2 pA before and after treatment with suramin, respectively, $n = 8$, $P > 0.05$, t test), its inhibitory effect on ATP does not result from postsynaptic inhibition.

Effects of endogenously released ATP on the spontaneous ACh release

Spontaneous ACh release at the developing neuromuscular synapse may play a trophic function in regulating synapse maturation and muscle differentiation. In these *Xenopus* cul-

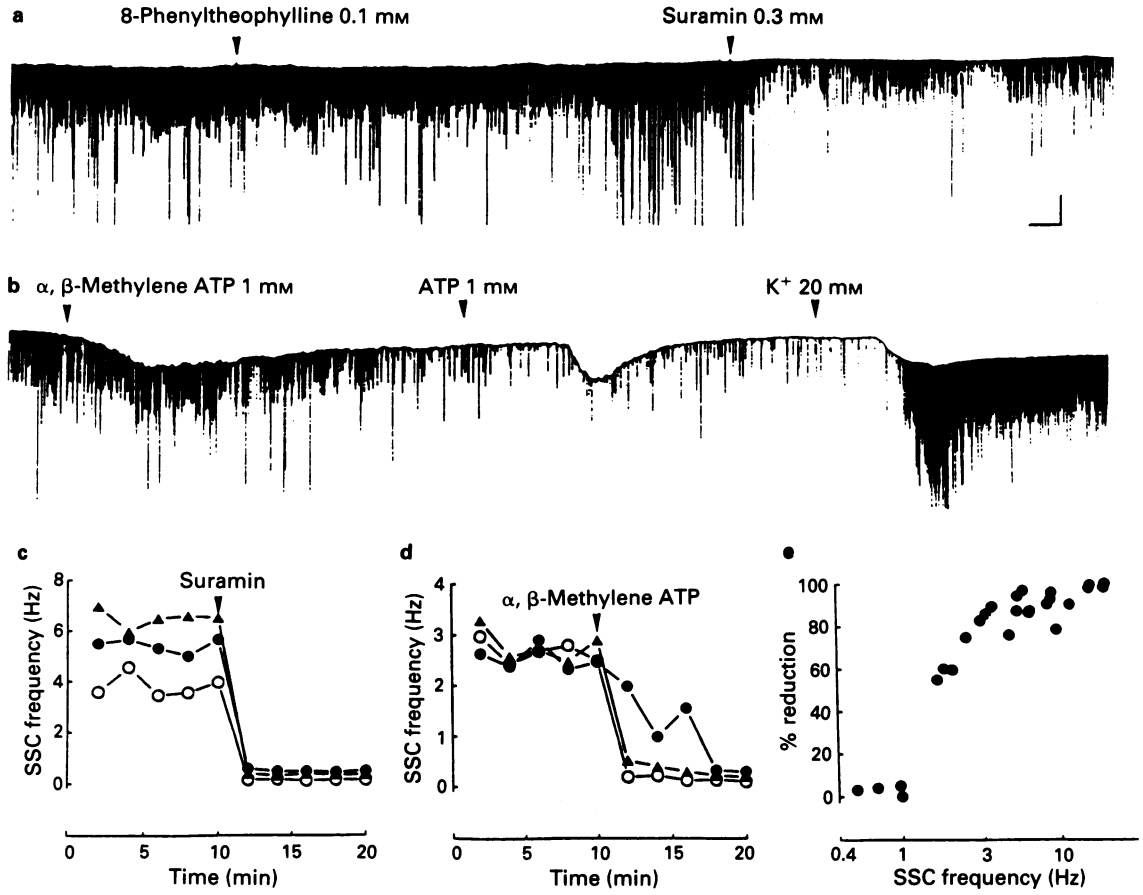


Figure 2 Effect of purinoceptor antagonists on the spontaneous acetylcholine (ACh) release at high-activity synapses. The synapses with frequency of spontaneous ACh release higher than 3 Hz were chosen for the following experiments. (a) Suramin but not 8-phenyltheophylline inhibited spontaneous ACh secretion. (b) α,β-Methylene ATP which was used to desensitize P_2-purinoceptor also inhibited the spontaneous secretion of ACh. The potentiating effect of ATP but not of high-K^+ on spontaneous ACh release was further inhibited by α,β-methylene ATP pretreatment. The time course-response curves of (a) and (b) were shown in (c) and (d), respectively. Each curve represents data collected from 1 synapse. (e) Correlation of the suramin effect with the frequency of spontaneous synaptic currents (SSCs) of the synapses. Note that the higher SSC frequency, the greater inhibitory effect of suramin. Scale bar: 560 pA, 100 s.

tures, many of the spontaneous synaptic potentials are capable of eliciting action potentials and contractions in the muscle cell and such contractions accelerate the development of muscle striation (Kidokoro & Saito, 1988). Two previous observations had led to our present study on the role of endogenously released ATP. First, the frequency of spontaneous synaptic events was found to vary greatly from cell to cell, over two orders of magnitude (Evers *et al.*, 1989). Second, synapses with a high frequency of spontaneous events and contractions resemble those induced by exogenous application of ATP. It seems likely that synapses with high frequency events are under the influence of endogenously released ATP. This notion was tested by examining the effect of a specific P_2-purinoceptor antagonist on the frequency of spontaneous synaptic events at high-activity synapses ($\geqslant 3$ Hz). We found that suramin (0.3 mM), but not 8-phenyltheophylline (0.1 mM), markedly reduced the frequency of spontaneous synaptic current at these high-activity synapses (Figure 2a and c). The effect of suramin on low-activity synapses, however, was much less apparent (Figure 1c and g). Figure 2e summarizes the result of all experiments. There is a clear correlation of the suramin effect with the frequency of spontaneous synpatic currents. Furthermore, we found that α,β-methylene ATP, a slowly degradable analogue of ATP that is known to desensitize P_2-purinoceptor, also decreased SSC frequency at high-activity synapses (Figure 2b and d). The effect of α,β-methylene ATP was not due to a non-selective blockade of ACh secretion from the nerve terminals, since substantial release can be triggered by further application of high external-K^+ (20 mM) medium but not of ATP (Figure 2b). Taken together, these results indicate that tonic activation of P_2-purinoceptors, presumably due to endogenous ATP released from the nerve terminals and/or the muscle cells, is responsible for the maintenance of high levels of spontaneous ACh release at these developing neuromuscular synapses.

Effects of Ca^{2+} channel blockers on the spontaneous ACh release at high-activity synapses

Extracellular Ca^{2+} influx is required for the maintenance of high spontaneous synaptic activity, since application of high Mg^{2+} (5 mM) depressed the spontaneous ACh release from 4.8 ± 1.4 Hz to 0.3 ± 0.1 Hz ($n = 8$) within 10 min. Co^{2+} (2.5 mM) which also blocks Ca^{2+} channels exerted a similar effect to high Mg^{2+} (from 4.6 ± 0.3 Hz to 0.2 ± 0.1 Hz, $n = 4$). Furthermore, L-type Ca^{2+} channels are found to be involved in the regulation of spontaneous transmitter release in *Xenopus* developing neuromuscular synapses (Fu & Huang, 1993). The potentiating effect of endogenous ATP on the spontaneous synaptic activity at these high-activity synapses appears to be mediated by the opening of L-type Ca^{2+}-channels in the plasma membrane. Extracellular application of the L-type Ca^{2+} channel blockers, verapamil, nifedipine or

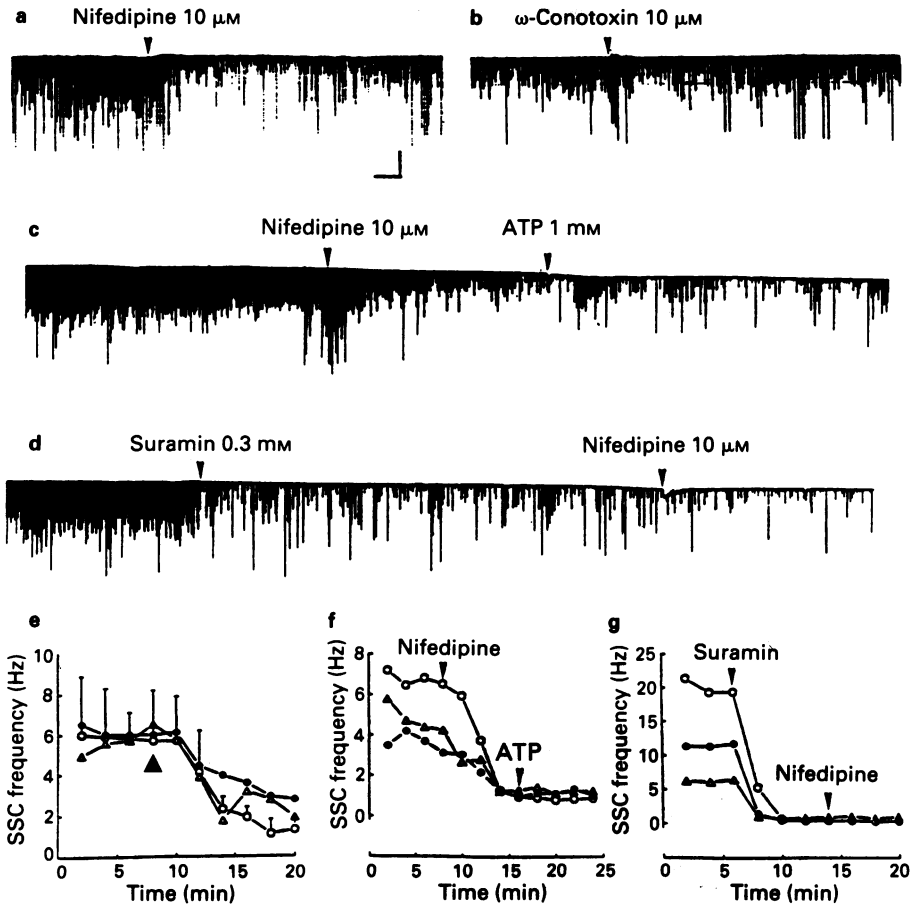


Figure 3 Inhibitory effect of L-type Ca^{2+} channel blockers on the spontaneous acetylcholine (ACh) release at high-activity synapses. (a) Application of the L-type Ca^{2+} channel blocker, nifedipine, inhibited spontaneous ACh release, whereas, omega-conotoxin, a N-type Ca^{2+} channel blocker had no effect (b). The inhibitory effects of three L-type Ca^{2+} channel blockers (10 μM each) on spontaneous synaptic currents (SSCs) are shown quantitatively in (e). The data points of nifedipine-treated groups (●) were obtained from 4 cells (mean ± s.e.mean) and only one representative example of 4 experiments is shown for the verapamil (Δ) and diltiazem-treated (○) groups. (c) The potentiating effect of ACh release by extracellular application of ATP was totally abolished by pretreatment with nifedipine. (d) Nifedipine did not further inhibit SSC frequency after the maximal inhibitory effects of suramin at high-activity synapses. The time course-response curves of (c) and (d) are shown in (f) and (g), respectively. Each curve represents data collected from 1 synapse. Scale bar: 560 pA and 100 s.

diltiazem (10 μM each) reduced SSC frequency of high-activity synapses, while the N-type Ca^{2+}-channel blocker, omega-conotoxin, had no appreciable effect (Figure 3a,b and e). The following evidence supports the idea that the tonic opening of the L-type Ca^{2+} channels results from the presence of endogenously released ATP. First, we found that the potentiation of spontaneous synaptic activity by ATP is totally abolished in the presence of the L-type Ca^{2+} channel blocker, nifedipine (Figure 3c and f). Second, application of nifedipine following the blockade of the P_2-purinoceptors by suramin produced no further reduction of SSC frequency (Figure 3d and g). These results are consistent with the notion that the activation of P_2-purinoceptor by ATP results in the opening of presynaptic L-type Ca^{2+} channels. Moreover, they suggest the existence of a basal level of spontaneous synpatic activity (SSC frequency $\leqslant$ 1 Hz) that is independent of the ATP action and Ca^{2+} influx.

The effects of the L-type Ca^{2+} channel agonist, Bay K 8644, provides further evidence in support of the involvement of L-type Ca^{2+} channels in regulating spontaneous release of ACh. As shown in Figure 4a, Bay K 8644 did not affect the transmitter secretion at synapses of low-activity ($\leqslant$ 1 Hz). However, at synapses with medium-activity as shown in Figure 4b (1–3 Hz), Bay K 8644 enhanced the spontaneous ACh release which was further inhibited by the addition of nifedipine. At synapses of much higher activity as shown in Figure 4c ($\geqslant$ 3 Hz), Bay K 8644 competed with high Mg^{2+} to reverse the inhibitory effects of high Mg^{2+}. The time course-response curves of three representative cells were shown in Figure 4d. We have shown previously that protein kinase C activation is involved in the action mechanism of ATP (Fu & Poo, 1991). Application of H-7, a kinase inhibitor, also reduced spontaneous ACh release of high-activity synapses (Figure 5). Whereas, tetrodotoxin, which is a Na^+ channel blocker, did not affect the spontaneous ACh release, indicating that ACh release at these high-activity synapses resulted from spontaneous but not evoked secretion (Figure 5).

Discussion

The presence of ATP in the synaptic vesicle (Dowdall *et al.*, 1974) and its release upon electrical stimulation of presynaptic nerve (Zimmerman, 1978) suggests that ATP is co-stored and co-released with ACh from presynaptic nerve terminals. However, ATP may also be released from stimulated post-synaptic cells. This has been observed in crayfish (Smith & Lindgren, 1986); frog (Abood *et al.*, 1962) and human muscle (Forrester, 1972) as well as in *Torpedo* electric organ (Israel

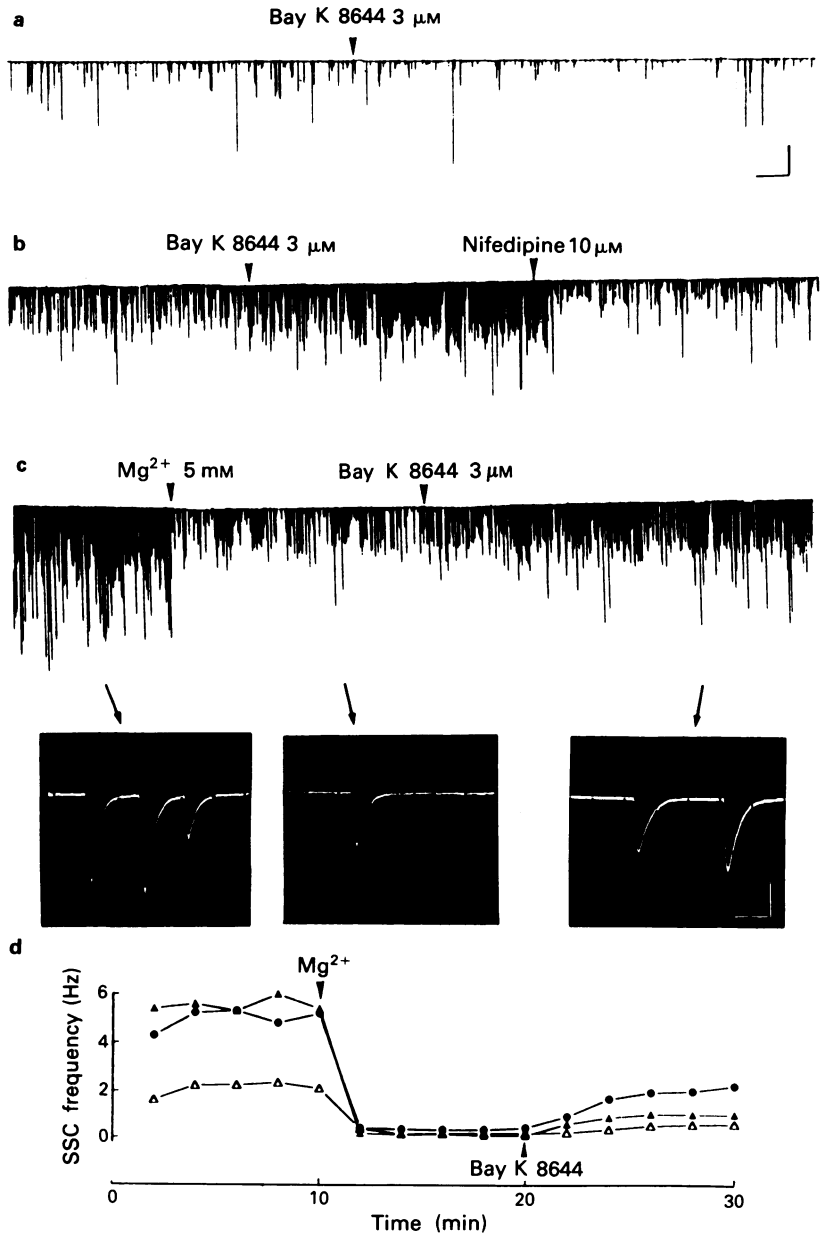


Figure 4 Enhancement by Bay K 8644 of the spontaneous acetylcholine (ACh) release of high-activity synapses. (a) Bay K 8644, an L-type Ca^{2+} channel agonist, had no effect on spontaneous ACh secretion at synapses of low-activity ($\leqslant$ 1 Hz). (b) Bay K 8644 enhanced the spontaneous ACh release at synapses which exhibit medium-activity of spontaneous ACh release (1–3 Hz) and the potentiation was reversed by the L-type Ca^{2+} channel blocker, nifedipine. (c) Application of high Mg^{2+} inhibited spontaneous ACh release at synapses of high-activity ($\geqslant$ 3 Hz), which was competitively reversed by Bay K 8644. Samples of synaptic currents before and after drug treatment are shown below the trace at higher time resolution (filtered at 10 kHz). Note that only the frequency but not the amplitude and decay time of synaptic currents was significantly changed. Scale bars are 560 pA, 100 s, and 400 pA, 20 ms for the slow and fast traces, respectively. Time course-response curves of three cells were shown in (d). Each curve represents data collected from 1 synapse.

et al., 1976). The effects of extracellular ATP on ACh release at mature synapses have been examined in the past. Exogenous ATP has been shown to reduce transmitter release from presynaptic terminals of preganglionic sympathetic neurones (Silinksy & Ginsborg, 1983) and motoneurones (Ribeiro & Walker, 1975). We are the first to show that ATP potentiates spontaneous ACh release at embryonic developing neuromuscular synapses (Fu & Poo, 1991; Fu *et al.*, 1993). In the present study, we have further demonstrated that the endogenously released ATP potentiates ACh secretion and maintains the high levels of spontaneous synaptic activity.

In a previous study, we have shown that ATP but not ADP, AMP or adenosine potentiates spontaneous ACh secretion, indicating that the P_2-purinoceptor is probably involved in the action of ATP (Fu & Poo, 1991). Results of the present study further support the notion that the potentiation of ACh release by exogenously applied ATP is mediated by a P_2-purinoceptor, since suramin, a P_2-purinoceptor antagonist (Hoyle *et al.*, 1990), but not 8-phenyltheophylline, a P_1-purinoceptor antagonist (Griffith *et al.*, 1981), antagonized the potentiating effect of ATP. The lack of measurable effect on the mean amplitude of SSCs by suramin indicates that its inhibitory effect on ATP does not result from postsynaptic inhibition. Taking advantage of the selectivity of these purinoceptor antagonists, we inves-

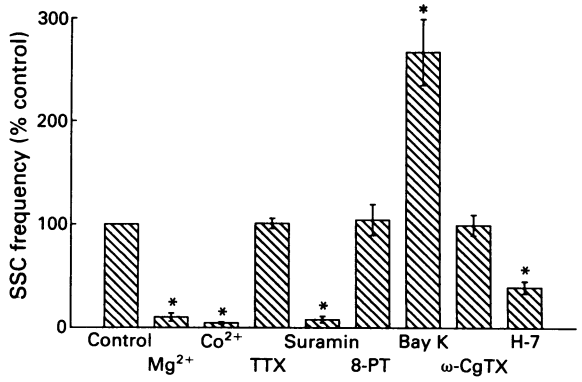


Figure 5 Summary of the effects of various drugs on the spontaneous acetylcholine (ACh) release at medium- or high-activity synapses. The effects of drugs are represented as % of control SSC frequency before drug treatment (mean ± s.e.mean, $n = 3-5$). Mg^{2+} (5 mM), Co^{2+} (2.5 mM), suramin (0.3 mM) and H-7 (10 μM) inhibited and Bay K 8644 (3 μM) potentiated the spontaneous ACh release, whereas tetrodotoxin (TTX, 0.3 μM) and omega-conotoxin (ω-CgTx, 10 μM) had no effect. $^*P < 0.05$ as compared with control.

tigated the physiological role of endogenously released ATP on spontaneous ACh release. The ACh released spontaneously in *Xenopus* culture is capable of eliciting action potentials and contractions in muscle cells (Chow & Poo, 1985) and the application of ATP increased markedly the frequency of these spontaneous contractions (Fu & Poo, 1991). However, even without drug treatment, many synapses have a high frequency of spontaneous contractions resembling those induced by exogenous application of ATP. It seems likely that synapses with high frequency events are under the influence of endogenously released ATP. We thus chose these high-activity synapses to do the following experiments. Surprisingly, the application of suramin but not 8-phenyltheophylline inhibited the SSC frequency of these high-activity synapses. Additionally, desensitizing the P_2-purinoceptor with the slowly degradable ATP analogue, α,β-methylene ATP also inhibited the SSC frequency of high-activity synapses. The desensitization of the P_2-purinoceptor was further supported by the finding that the potentiation effect of ATP but not high-K^+ was abolished by the application of α,β-methylene ATP. The frequency-dependent inhibitory effect of suramin on the SSCs, indicating that more endogenously released ATP acts at synapses of higher activity.

Extracellular Ca^{2+} influx is required for the maintenance of high spontaneous synaptic activity, since application of high Mg^{2+} and Co^{2+} depressed the spontaneous ACh release at these high-activity synapses. There are at least four types of voltage-dependent Ca^{2+} channel demonstrated in neurones which have been termed L-, N-, T- and P- (Tsien *et al.*, 1988; Bertolino & Llinas, 1992). The N-type Ca^{2+} channels may link action potentials to neurotransmitter release at many vertebrate fast-transmitting synapses (Perney *et al.*, 1986; Hirning *et al.*, 1988; Stanley & Atrakchi, 1990). However, the P-type Ca^{2+} channels mediate transmitter release in mammalian neuromuscular junction (Uchitel *et al.*, 1992). On the other hand, in peptide-secreting presynaptic (Perney *et al.*, 1986; Rane *et al.*, 1987; Holz *et al.*, 1988; Loudes *et al.*, 1988) and neurosecretory (Drouva *et al.*, 1988; Lemos & Nowycky, 1989) terminals, dihydropyridine-sensitive L-type Ca^{2+} channels appear to dominate. The physiological role of L-type Ca^{2+} channels in fast-transmitting synapses is still unknown. However, the potentiating effect of ATP on ACh release requires the influx of Ca^{2+} through the plasma membrane (Fu & Poo, 1991). More recently, we found that the presynaptic L-type Ca^{2+} channels are involved in the high K^+-, TPA (12-O-tetradecanoyl-phorbol-13-acetate)- and ATP-enhanced spontaneous ACh release in embryonic *Xenopus* cell cultures (Fu & Huang, 1993). We thus examined the effects of L-type Ca^{2+} channel blockers on the SSC frequency of high-activity synapses. Nifedipine, verapamil and diltiazem inhibited the SSC frequency of high-activity but not that of low-activity synapses. Bay K 8644, which is a depolarization-dependent L-type Ca^{2+} channel agonist (Garcia *et al.*, 1984), enhanced the ACh release at medium- or high-activity synapses but not that of low-activity synapses. Omega-conotoxin which is reported to block selectively the N-type Ca^{2+} channels inhibits L as well as N currents in neurones (McCleskey *et al.*, 1987; Plummer *et al.*, 1989). Although in our previous study, we found that pretreatment with omega-conotoxin also inhibited the potentiating effect of spontaneous ACh release by high K^+, TPA and ATP (Fu & Huang, 1993), we could not show an inhibitory effect of omega-conotoxin on the SSC frequency of high-activity synapses, probably because omega-conotoxin is more effective in preventing the opening of the Ca^{2+} channels than in inhibiting the Ca^{2+} channel which is already in the open state. Taken together, these results suggest that the opening of the L-type Ca^{2+} channels is involved in the maintenance of high levels of spontaneous release.

In conclusion, we have provided evidence that the endogenous release of ATP potentiates spontaneous ACh release at developing neuromuscular synapses. Through the activation of P_2-purinoceptors, ATP potentiates the spontaneous ACh release by opening the presynaptic L-type Ca^{2+} channels and allowing Ca^{2+} influx into the presynaptic nerve terminals. It has been shown that Ca^{2+} current will increase survival and promote differentiation of neurones (Collins & Lile, 1989). Moreover, the spontaneous ACh released in *Xenopus* culture is capable of eliciting action potentials and contractions in the muscle cell (Chow & Poo, 1985). This frequent suprathreshold excitation produces a global influence on the development of the muscle cell, as shown by the acceleration of myofibril striation (Kidokoro & Saito, 1988). In addition, all spontaneous synaptic potentials bring about a localized influx of ions at the subsynaptic site of the muscle, especially Ca^{2+} (Decker & Dani, 1990). Local Ca^{2+} accumulation and the consequent Ca^{2+}-dependent enzymatic reactions are likely to play an important role in the development of postsynaptic structures. Modulation of the L-type Ca^{2+} channels in embryonic motor nerve terminals by endogenously released ATP would allow a highly localized control of Ca^{2+} entry and subsequent transmitter release; ATP may thus serve as an important trophic factor at developing neuromuscular synapses.

This work was supported by a grant from the Institute of Biomedical Science, Academia Sinica, Taiwan (IBMS-CRC83-T18).

References

ABOOD, L.G., KOKETSU, K. & MIYAMOTO, S. (1962). Outflux of various phosphates during membrane depolarization of excitable tissues. *Am. J. Physiol.*, **202**, 469–474.

ANDERSON, M.J., COHEN, M.W. & ZORYCHTA, E. (1977). Effects of innervation on the distribution of acetylcholine receptors on cultured muscle cells. *J. Physiol.*, **268**, 731–756.

BERTOLINO, M. & LLINAS, R.R. (1992). The central role of voltage-activated and receptor-operated channels in neuronal cells. *Annu. Rev. Pharmacol. Toxicol.*, **32**, 399–421.

CHOW, I. & POO, M.M. (1985). Release of actylcholine from embryonic neurons upon contact with the muscle cell. *J. Neurosci.*, **5**, 1076–1082.

COLLINS, F. & LILIE, J.D. (1989). The role of dihydropyridine-sensitive voltage-gated calcium channels in potassium-mediated neuronal survival. *Brain Res.*, **502**, 99–108.

DECKER, E.R. & DANI, J.A. (1990). Calcium permeability of the nicotinic acetylcholine receptor: the single channel calcium influx is significant. *J. Neurosci.*, **10**, 3413–3420.

DOWDALL, J.J., BOYNE, A.F. & WHITTAKER, V.P. (1974). Adenosine triphosphate: a constituent of cholinergic synaptic vesicles. *Biochem. J.*, **140**, 1–13.

DROUVA, S.V., RERAT, E., BIHOREAU, C., LAPLANTE, E., RASOLONJANAHARY, R., CLAUSER, H. & KORDON, C. (1988). Dihydropyridine-sensitive calcium channel activity related to prolactin, growth hormone, and luteinizing hormone release from anterior pituitary cells in culture: interactions with somatostatin, dopamine, and estrogen. *Endocrinology*, **123**, 2762–2773.

EVERS, J., LASER, M., SUN, Y., XIE, Z. & POO, M.M. (1989). Studies of nerve-muscle interactions in *Xenopus* cell culture: analysis of early synaptic currents. *J. Neurosci.*, **9**, 1523–1539.

FORRESTER, T. (1972). An estimate of adenosine triphosphate release into the venous effluent from exercising human forearm muscle. *J. Physiol.*, **224**, 611–628.

FU, W.M. & HUANG, F.L. (1993). L-type Ca^{2+} channel is involved in the regulation of spontaneous transmitter release at developing neuromuscular synapses. *Neuroscience*, (in press).

FU, W.M. & POO, M.M. (1991). ATP potentiates spontaneous transmitter release at developing neuromuscular synapses. *Neuron*, **6**, 837–843.

FU, W.M., YANG, S.H. & LIN-SHIAU, S.Y. (1993). Potentiation of miniature endplate potential frequency by ATP in *Xenopus* tadpoles. *Br. J. Pharmacol.*, **108**, 236–241.

GARCIA, A.G., SALA, F., REIG, J.A., VINIEGRA, S., FRIAS, J., FONTERIZ, R. & GANDIA, L. (1984). Dihydropyridine Bay K 8644 activates chromaffin cell calcium channels. *Nature*, **309**, 69–71.

GRIFFITH, S.G., MEGHJI, P., MOODY, C.J. & BURNSTOCK, G. (1981). 8-Phenyltheophylline: a potent P_1-purinoceptor antagonist. *Eur. J. Pharmacol.*, **75**, 61–64.

HAMILL, O.P., MARTY, A., NEHER, E., SAKMANN, B. & SIGWORTH, F.J. (1981). Improved patch-clamp techniques for high-resolution current recording from cell and cell-free membrane patches. *Pflügers Arch.*, **391**, 85–100.

HIRNING, L.D., FOX, A.F., MCCLESKEY, E.W., OLIVERA, B.M., THAYER, S.A., MILLER, R.J. & TSIEN, R.W. (1988). Dominant role of N-type Ca channels in evoked release of norepinephrine from sympathetic neurons. *Science*, **239**, 57–60.

HOLZ, G.G., IV, DUNLAP, K. & KREAM, R.M. (1988). Characterization of the electrically evoked release of substance P from dorsal root ganglion neurons: methods and dihydropyridine sensitivity. *J. Neurosci.*, **8**, 463–471.

HOYLE, C.H.V., KNIGHT, G.E. & BURNSTOCK, G. (1990). Suramin antagonizes responses to P_2-purinoceptor agonists and purinergic nerve stimulation in the guinea-pig urinary bladder and taenia coli. *Br. J. Pharmacol.*, **99**, 617–621.

ISRAEL, M., LESBATS, B., MEUNIER, F.M. & STINNAKRE, J. (1976). Postsynaptic release of adenosine triphosphate induced by single impulse transmitter action. *Proc. R. Soc. B.*, **193**, 461–468.

KIDOKORO, Y. & SAITO, M. (1988). Early cross-striation formation in twitching *Xenopus* myocytes in culture. *Proc. Natl. Acad. Sci. U.S.A.*, **85**, 1978–1982.

LEMOS, J.R. & NOWYCKY, M.C. (1989). Two types of calcium channels coexist in peptide-releasing vertebrate nerve terminals. *Neuron*, **2**, 1419–1426.

LOUDES, C., FAIVRE-BAUMAN, A., PATTE, C. & TIXIER-VIDAL, A. (1988). Involvement of DHP voltage-sensitive calcium channels and protein kinase C in thyroliberin (TRH) release by developing hypothalamic neurons in culture. *Brain Res.*, **456**, 324–332.

MCCLESKLEY, E.W., FOX, A.P., FELDMAN, D., CRUZ, L.Y, OLIVERA, B.M., TSIEN, R.W. & YOSHIKAMI, D. (1987). ω-Conotoxin direct and persistent blockade of specific types of calcium channels in neurons but not muscle. *Proc. Natl. Acad. Sci. U.S.A.*, **84**, 4327–4331.

MEUNIER, F.-M., ISRAEL, M. & LESBATS, B. (1975). Release of ATP from stimulated nerve electroplaque junctions. *Nature*, **257**, 407–409.

NIEUWKOOP, P.D. & FABER, J. (1967). *Normal Table of* Xenopus laevis, Second Edition. Amsterdam: North Holland.

NITKIN, R.M., SMITH, M.A., MAGILL, C., FALLON, J.R., YAO, Y.M., WALLACE, B.G. & MCMAHAN, J.J. (1987). Identification of agrin: a synaptic organizing protein from Torpedo electric organ. *J. Cell. Biol.*, **105**, 2471–2478.

PERNEY, T.M., HIRNING, L.D., LEEMAN, S.Z. & MILLER, R.J. (1986). Multiple calcium channels mediate neurotransmitter release from peripheral neurons. *Proc. Natl. Acad. Sci. U.S.A.*, **83**, 6656–6659.

PLUMMER, M.R., LOGOTHETIS, D.E. & HESS, P. (1989). Elementary properties and pharmacological sensitivities of calcium channels in mammalian peripheral neurons. *Neuron*, **1**, 1453–1463.

PURVES, D. (1986). The trophic theory of neuronal connections. *Trends Neurosci.*, **9**, 486–488.

RANE, S.G., HOLZ, G.G. IV & DUNLAP, K. (1987). Dihydropyridine inhibition of neuronal calcium current and substance P release. *Pflügers Arch.*, **409**, 361–366.

RIBEIRO, J.A. & WALKER, J. (1975). The effect of adenosine triphosphate and adenosine diphosphate on transmission at the rat and frog neuromuscular junctions. *Br. J. Pharmacol.*, **54**, 213–218.

SANES, D.H. & POO, M.M. (1989). In vitro analysis of position- and lineage-dependent selectivity in the formation of neuromuscular synapse. *Neuron*, **2**, 1237–1244.

SILINSKY, E.M. & GINSBORG, B.L. (1983). Inhibition of acetylcholine release from preganglionic frog nerves by ATP but not adenosine. *Nature*, **305**, 237–238.

SILINSKY, E.M. & HUBBARD, J.I. (1973). Release of ATP from rat motor nerve terminals. *Nature*, **243**, 404–405.

SMITH, D.O. & LINDGREN, C.A. (1986). Modulation of presynaptic transmitter release by ATP derived from postsynaptic sources. In *Calcium, Neuronal Function and Transmitter Release*. ed. Rahamimoff, R. & Katz, B. pp. 357–374. Boston, MA: Martinus Nijhoff Pub.

SPITZER, N.C. & LAMBORGHINI, J.C. (1976). The development of the action potential mechanism of amphibian neurons isolated in culture. *Proc. Natl. Acad. Sci. U.S.A.*, **73**, 1641–1645.

STANLEY, E.F. & ATRAKCHI, A.H. (1990). The calcium current in the presynaptic nerve terminal of the chick giant synapse is insensitive to the dihydropyridine nifedipine. *Proc. Natl. Acad. Sci. U.S.A.*, **87**, 9683–9687.

TSIEN, R.W., LIPSCOMBE, D., MADISON, D.V., BLEY, K.R. & FOX, A.P. (1988). Multiple types of neuronal calcium channels and their selective modulation. *Trends Neurosci.*, **11**, 431–438.

UCHITEL, O.D., PROTTI, D.A., SANCHEZ, V., CHERKSEY, B.D., SUGIMORI, M. & LLINAS, R. (1992). P-type voltage-dependent calcium channel mediates presynaptic calcium influx and transmitter release in mammalian synapses. *Proc. Natl. Acad. Sci. U.S.A.*, **89**, 3330–3333.

USDIN, T.B. & FISCHBACH, G.D. (1986). Purification and characterization of a polypeptide from chick brain that promotes the accumulation of acetylcholine receptors in chick myotubes. *J. Cell Biol.*, **103**, 493–507.

XIE, A. & POO, M.M. (1986). Initial events in the formation of neuromuscular synapse. *Proc. Natl. Acad. Sci. U.S.A.*, **83**, 7069–7073.

YOUNG, S.H. & POO, M.M. (1983). Spontaneous release of transmitter from growth cones of embryonic neurons. *Nature*, **305**, 634–637.

ZIMMERMAN, H. (1978). Turnover of adenine nucleotides in cholinergic synaptic vesicles of the Torpedo electric organ. *Neuroscience*, **3**, 827–836.

(Received June 9, 1993
Revised October 21, 1993
Accepted November 1, 1993)

Br. J. Pharmacol. (1994), **111**, 887–893 © Macmillan Press Ltd, 1994

Beneficial effect of the Ca^{2+} antagonist, nimodipine, on existing diabetic neuropathy in the BB/Wor rat

A.C. Kappelle, G. Biessels, B. Bravenboer, T. van Buren, *J. Traber, D.J. de Wildt & [1]W.H. Gispen

Department of Medical Pharmacology, Rudolf Magnus Institute, University of Utrecht, Vondellaan 6 3521 GD, Utrecht, The Netherlands and *Institute for Neurobiology, Troponwerke, Cologne, Germany

1 Neuropathy is a frequently diagnosed complication of diabetes mellitus. Effective pharmacotherapy is not available.

2 The spontaneously diabetic BB/Wor rats develop secondary complications like neuropathy as do human diabetic patients.

3 BB/Wor rats treated with insulin via a subcutaneous implant show a significant impairment of sensory and motor nerve conduction velocity 6 weeks after the onset of diabetes mellitus.

4 Intraperitoneal treatment of diabetic BB/Wor rats with the Ca^{2+} antagonist, nimodipine (20 mg kg^{-1}), from week 6 onwards every 48 h for a period of 6 weeks resulted in a significant increase of sensory and motor nerve conduction velocity.

5 Twelve weeks after the onset of diabetes mellitus BB/Wor rats show a 40% impairment of sciatic nerve blood flow as compared to the non-diabetic age-matched controls. Treatment with nimodipine (20 mg kg^{-1}) from week 6 onwards significantly increased the sciatic nerve blood flow as compared to placebo-treated diabetic BB/Wor rats.

6 The adrenergic responsiveness of the vasa nervorum of the sciatic nerve to tyramine and phenylephrine was investigated as a parameter for autonomic neuropathy.

7 The fact that nimodipine treatment restored the reduced response to tyramine independently of the reduced postsynaptic phenylephrine responsiveness indicates that nimodipine improves adrenergic responsiveness mainly at the presynaptic level.

Keywords: Diabetes mellitus; neuropathy; nerve conduction velocity; nerve blood flow; adrenergic responsiveness; peripheral nerve regeneration; Ca^{2+} antagonist; nimodipine

Introduction

Patients with diabetes mellitus may suffer from a number of chronic complications. It remains to be determined to what extent chronic hyperglycaemia itself is responsible for these complications. With respect to diabetic neuropathy, Pirart (1978) has demonstrated that the prevalence of this complication is increased in patients with poor metabolic control. Although maintenance of normoglycaemia may certainly have a beneficial effect on diabetic complications such as the neuropathy, the pathogenesis of these complications seems to involve additional factors (Strowig & Raskin, 1992). A major focus of research is the prevention and treatment of complications such as neuropathy. The somatic and autonomic nervous system is affected during diabetes mellitus, resulting in functional disturbances and clinical morbidity (Thomas & Eliasson, 1984; Horowitz *et al.*, 1986; Watkins, 1990; Smout *et al.*, 1991).

Most of our current knowledge on diabetic neuropathy is based on the results of animal studies. The streptozotocin (STZ)-induced diabetic rat is the most frequently used model to study experimental diabetes mellitus (Mayer & Tomlinson, 1983). The spontaneously diabetic BB/Wor rat, however, mimics human diabetes mellitus in a superior way and has proved to be a promising animal model of insulin-dependent diabetes mellitus (IDDM) (Mordes *et al.*, 1987; Crisá *et al.*, 1992).

Diabetic BB/Wor rats gradually develop secondary complications as do human patients with diabetes mellitus. Complications such as pathological changes in the retina (Fitzgerald & Caldwell, 1990), kidneys (Cohen *et al.*, 1987), nerves (Sima & Thibert, 1982; Sima *et al.*, 1990; Zhang *et al.*, 1990) have been reported.

We used the BB/Wor rat to study the pathogenesis of diabetic neuropathy and to determine the effect of the Ca^{2+} antagonist, nimodipine, on the affected nervous system. Nimodipine (isopropyl-(2-methoxy-ethyl)-1,4-dihydro-2,6-dimethyl-4-(3-nitrophenyl)-3,5-pyridinic dicarboxylate) is an L-type Ca^{2+} channel blocker (Scriabine *et al.*, 1989) which exerts profound neuropharmacological effects (Traber & Gispen, 1989). Recently, we demonstrated beneficial effects of nimodipine on nerve conductance velocity in STZ-induced diabetic rats (Kappelle *et al.*, 1992; 1993b).

Decreased nerve blood flow (NBF) appears to be a crucial factor in the pathogenesis of diabetic neuropathy (Cameron *et al.*, 1991; Hotta *et al.*, 1992); therefore the question was raised whether vascular effects of nimodipine (Betz *et al.*, 1985) contribute to its ameliorative effect in experimental diabetic neuropathy (Kappelle *et al.*, 1993a). In addition to NBF, blood flow control mechanisms are an important issue in the study of diabetic neuropathy. In the present study, we investigated the influence of diabetes mellitus and the effect of nimodipine treatment on three targets: sensory and motor nerve conduction velocity, NBF and autonomic sympathetic function of the nervi vasorum. In this way we attempted to obtain insight into the functioning of the peripheral somatic and autonomic nerve and the vasa nervorum of the diabetic BB/Wor rat and the mechanism of action of nimodipine in experimental diabetic neuropathy.

Methods

Animals

Twenty-five BB/Wor rats and 12 WB/Prone, non-diabetic, age-matched control rats were obtained from the Møllengard

[1] Author for correspondence.

Institute, Skensved, Denmark. The rats were housed on sawdust in macrolon cages, 2 rats per cage and maintained on a 12:12 h light-dark cycle with food and water *ad libitum*. Insulin treatment was started immediately after the development of hyperglycaemia (blood glucose > 15 mmol l^{-1}) ($n = 22$). Since continuous subcutaneous insulin infusion in human diabetics has received more and more attention, slow release insulin implants were used instead of daily subcutaneous injections. Implants (Møllengard Institute, Skensved, Denmark), containing 17% bovine insulin (0.5% Zn) and 83% palmitic acid, weight about 26 mg and dimensions of 2 mm in diameter and 7 mm in length were placed subcutaneously. Slow surface erosion of the implant *in vivo* gradually releases the entrapped insulin at a rate of 2 u per day for more than 40 days. The implant was removed after 40 days and a new implant was inserted. Body weight was measured every week. Blood glucose was controlled every third week. Blood samples were obtained from the tail vein. Blood glucose was monitored with a Minilab (Bayer GmbH, Munich, Germany).

Electrophysiology

Sensory nerve conduction velocity (SNCV) and motor nerve conduction velocity (MNCV) were measured every 2 weeks from the start of the treatment. The method used has been described in detail by De Koning & Gispen (1987). In short, the sciatic and tibial nerves were stimulated at the sciatic notch and the ankle, respectively, by monopolar needle electrodes. Responses were recorded from the small muscles of the foot by means of surface electrodes. SNCV and MNCV were calculated from the latencies of these responses and the distance between the two stimulation points.

Nerve blood flow measurements

The rats were anaesthetized with 10% urethane, 1.2 ml 100 g^{-1}, i.p., and placed on a homiothermic heating blanket. Rectal temperature was maintained at $\pm$ 37°C. Urethane was used instead of barbiturates in order to ensure minimal anaesthetic interference with the cardiovascular system and to leave autonomic reflexes intact. The left sciatic nerve was exposed and the fascia surrounding the nerve was carefully removed. The nerve was positioned on a perspex holder just at the place where the nerve emerges from the musculus gluteus maximus. The part of the nerve positioned on the holder was cleaned of remaining fascia tissue, disturbing the epineurial blood vessels as little as possible. The sciatic nerve was kept moist with saline solution at 37°C. Blood flow was monitored with a laser-Doppler flowmeter (Perimed Sweden, Periflux PF3). The flowmeter was equipped with a 2 mW Helium-Neon laser with a wave length of 632.8 nm. Flow is expressed in arbitrary units (perfusion units (PU)). The low pass filter was set at a cut-off frequency of 4 kHz. The laser probe (Perimed needle probe PF302, tip diameter of 0.45 mm) was positioned on the nerve just contacting the saline film covering the nerve. The flow signal was averaged at 0.2 s periods. Care was taken to avoid placing the probe in the proximity of larger blood vessels. Basal sciatic NBF was determined by taking the average of 10 out of 14 consecutive flow measurements at different locations on the nerve (the two lowest and two highest values were excluded). At the end of the experiment the background LDF value was assessed by monitoring thte LDF output signal after the rat had been killed with i.v. administered pentobarbitone. Background values were subtracted from the values obtained during the experiment.

Assessment of nervi vasorum sympathetic autonomic function

LDF allows the continuous measurement of microvascular blood flow. This makes this technique especially suitable for monitoring rapid flow changes resulting from adrenergic stimulation. The response to phenylephrine was used as a measure of adrenergic postsynaptic function. The NBF response to tyramine is a result of combined pre- and postsynaptic effects. A polyethylene catheter, containing 50 iu ml^{-1} sodium heparin in isotonic saline, was implanted in the right common iliac artery, its tip positioned just at the bifurcation of the abdominal aorta, after the basal sciatic NBF was quantified. The right artery was closed around the catheter with ligatures, to allow all vasoactive agents applied via the catheter to end up in the left common iliac artery. The arterial catheter was connected to a pressure transducer (Viggo-Spectramed disposable DTX/plus^{tm}) via a Y-shaped injection system. Vasoactive agents could be administered locally through this system to the left hind paw of the animal, without interruption of blood pressure recording.

Responses of sciatic NBF to phenylephrine (1, 2 and 3 $\mu g\ kg^{-1}$) and tyramine (75, 150 and 300 $\mu g\ kg^{-1}$) were recorded in each animal. The number of doses was rather limited because of an irreversible decline in responsiveness after more than 10 doses (Zochodne & Low, 1990). Blood pressure is expressed as mean arterial pressure (MAP) in mmHg (MAP = (systolic pressure + 2 × diastolic pressure)/3).

Phenylephrine and tyramine had minor effects on MAP. Therefore, the responses to phenylephrine and tyramine are expressed as '% flow change'. This measure was calculated by correcting the change in flow for effects on MAP, since minor changes in MAP are followed passively by NBF (Sundqvist *et al.*, 1985).

$$\%\ \text{flow change} = \frac{NBF_{post} * (MAP_{pre}/MAP_{post}) - NBF_{pre}}{NBF_{pre}} * 100\%$$

Drugs

Nimodipine 20 mg kg^{-1} (a gift from Bayer AG, Elberfeld, Germany) as a micronized powder was dissolved in polyethylene glycol (PEG 400) 1 ml kg^{-1} under dim light and injected intraperitoneally (i.p.) as a freshly prepared solution.

Phenylephrine, an α-adrenoceptor agonist ((−)-phenylephrine hydrochloride, Sigma, St. Louis, MO, U.S.A.), was dissolved in saline (0.9%) at doses of 1, 2 and 3 $\mu g\ kg^{-1}$ respectively and tyramine, which releases endogenous noradrenaline from presynaptic terminals (tyramine hydrochloride, Regis Chemical Co., Chicago, IL, U.S.A.), was dissolved in saline (0.9%) at doses of 75, 150 and 300 $\mu g\ kg^{-1}$. The drugs were administered i.v. at a rate of 200 $\mu l\ min^{-1}$ with an infusion pump.

Data analysis

Data are presented as means $\pm$ standard error of the mean (s.e.mean), unless indicated otherwise. Experiments were carried out in a blind fashion. The treatment code was partially broken at the end of the experiment to allow analysis of data for the various treatment groups. The results of SNCV, MNCV and adrenergic responsiveness were analysed by multivariate analysis of variance for repeated measurements (MANOVA) followed by t tests. Group differences in NBF were assessed by an analysis of variance (ANOVA) followed by t tests. The correlation between changes in NBF and SNCV/MNCV was determined by regression analysis, using the NCV values of week 12. The final treatment code was broken only after the analysis of the data was completed.

Outline of the study

Six weeks after the development of diabetes mellitus the rats were randomly divided into two groups. Group 1 (nimodipine, $n = 11$) received nimodipine, 20 mg kg^{-1} dissolved in PEG i.p. every 48 h. Group 2 (placebo, $n = 11$) received PEG, 1 ml kg^{-1} i.p. every 48 h. Group 3 consisted of non-diabetic WB/prone rats (control, $n = 12$), receiving PEG

Table 1 Mean blood glucose levels (Gluc) (mmol l^{-1}) at wk 0 (onset of diabetes mellitus), wk 6 (start treatment) and wk 12 (end of the experiment), body weight (BW) in (g) at wk 0 and wk 12, and systolic (P_{syst}) and diastolic pressure (P_{diast}) at wk 12 (mmHg) ± s.e.mean of the non-diabetic controls, the placebo-treated diabetic rats and the nimodipine-treated diabetic rats.

	Gluc wk 0	*Gluc* wk 6	*Gluc* wk 12	*BW* wk 0	*BW* wk 12	P_{syst} wk 12	P_{diast} wk 12
Control	6.7 (1.0)	5.9 (0.9)	6.3 (1.1)	292 (4)	385 (7)	118 (5)	91 (4)
Placebo	23 (1.1)*	21 (1.1)*	18 (1.0)*	274 (4)	313 (5)*	115 (6)	87 (7)
Nimodipine	23 (1.1)*	23 (2.3)*	18 (0.9)*	279 (4)	306 (6)*	121 (5)	89 (6)

*$P<0.001$ as compared to control.

1 ml kg^{-1} i.p. every 48 h. SNCV and MNCV were measured every 2 weeks from the start of treatment. After 6 weeks of treatment (12 weeks after the development of diabetes mellitus) sciatic NBF was assessed by laser-Doppler flowmetry. Thereafter the response of sciatic NBF to local application of tyramine and phenylephrine was tested.

Results

Blood glucose, body weight and blood pressure

The glucose levels of 22 rats increased to levels >15 mmol l^{-1} and remained stable throughout the study (Table 1). The mean body weight of the non-diabetic control rats and of the diabetic rats increased during the experiment (Table 1). Neither systolic nor diastolic blood pressure differed significantly among the three experimental groups at the end of the experiment (Table 1).

Sensory and motor nerve conduction velocity

SNCV and MNCV of the age-matched controls showed an increase until week 6 and remained relatively stable thereafter. The diabetic rats showed a smaller increase in SNCV and MNCV. The difference in SNCV and MNCV between the diabetic and non-diabetic rats reached significance within 6 weeks. Over the treatment period placebo-treated diabetic rats had significantly impaired SNCV and MNCV as compared to the non-diabetic, age-matched controls (SNCV: $F(1,21) = 243.5$, $P<0.001$; MNCV: $F(1,21) = 172.3$, $P<0.001$). Treatment with nimodipine resulted in an increase in SNCV and MNCV as compared to the placebo treatment (SNCV: $F(1,20) = 40.63$, $P<0.001$; MNCV: $F(1,20) = 18.20$, $P<0.001$) (Figure 1). Nimodipine treatment prevented a further increase in the diabetic SNCV and MNCV deficit. However, nimodipine was not able to restore the deficit to the level of the age-matched, control rats (SNCV: $F(1,21) = 137.77$, $P<0.001$; MNCV: $F(1,21) = 197.5$, $P<0.001$) (Figure 1). Throughout the experimental period there was no significant difference in body weight between the nimodipine-treated and the placebo-treated diabetic rats (Table 1). Blood pressure was measured just before vas nervorum adrenergic responsiveness was measured and did not significantly differ between the three groups (Table 1).

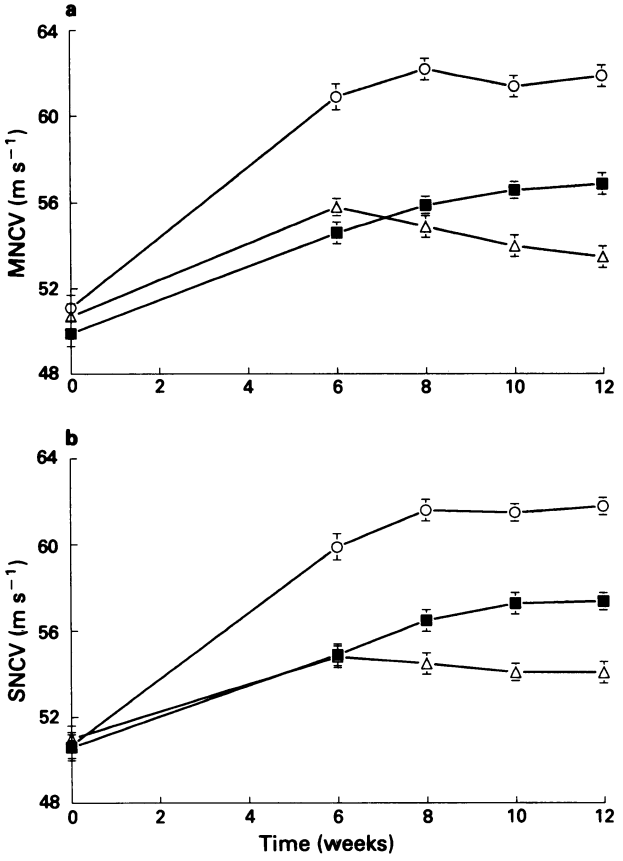


Figure 1 Motor (a) and sensory (b) nerve conduction velocity: treatment started 6 weeks after the development of diabetes mellitus. Over the treatment period placebo-treated diabetic rats (Δ, $n = 11$) had significantly impaired SNCV and MNCV as compared to the non-diabetic age-matched controls (○, $n = 12$) (SNCV: $F(1,21) = 243.5$, $P<0.001$; MNCV: $F(1,21) = 172.3$, $P<0.001$). Chronic nimodipine treatment of BB/Wor, diabetic rats (■, $n = 11$) significantly ameliorated the deficit observed in placebo-treated rats after 12 weeks of diabetes mellitus (SNCV: $F(1,20) = 40.63$, $P<0.001$; MNCV: $F(1,20) = 18.20$, $P<0.001$) but could not completely restore the deficit as comapred to the non-diabetic, age-matched control group (SNCV: $F(1,21) = 137.77$, $P<0.001$; MNCV: $F(1,21) = 197.5$, $P<0.001$).

Measurement of sciatic nerve blood flow

Sciatic NBF was measured 12 weeks after the development of diabetes mellitus. At this time, the diabetic rats had been treated with nimodipine or placebo for 6 weeks. The sciatic NBF of the non-diabetic controls was significantly higher than the sciatic NBF of the placebo-treated diabetic rats ($P<0.001$) (Figure 2). Treatment with nimodipine significantly ameliorated the deficit observed in the diabetic rats ($P<0.001$) but could not completely restore the deficit to the level of the age-matched controls ($P<0.001$) (Figure 2). Furthermore, NBF significantly correlated with nerve conduction velocities in the animal studied (Figure 3; MNCV × NBF: R = 0.81, $P<0.001$; SNCV × NBF: R = 0.78, $P<0.001$).

Measurement of nervi vasorum sympathetic autonomic function

The response of sciatic NBF to locally applied phenylephrine and tyramine was significantly smaller in the placebo-treated diabetic group as compared to the age-matched con-

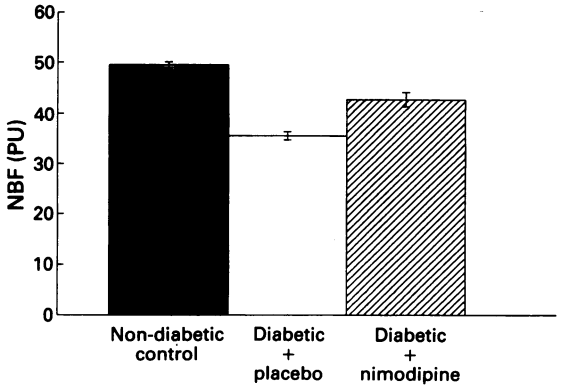


Figure 2 Sciatic nerve blood flow (NBF) ± s.e.mean 12 weeks after the development of diabetes mellitus. Treatment started 6 weeks after the development of diabetes mellitus. ANOVA revealed significant differences between the three treatment groups ($F(2,31) = 54.29$, $P < 0.001$). Placebo-treated rats ($n = 11$) showed a significant decrease in NBF as compared to the non-diabetic, age-matched control rats ($n = 12$) ($P < 0.001$). Chronic nimodipine treatment ($n = 11$) of BB/Wor diabetic rats significantly ameliorated the deficit observed in placebo-treated rats after 12 weeks of diabetes mellitus ($P < 0.001$) but could not completely restore the deficit as compared to the non-diabetic, age-matched control group ($P < 0.001$).

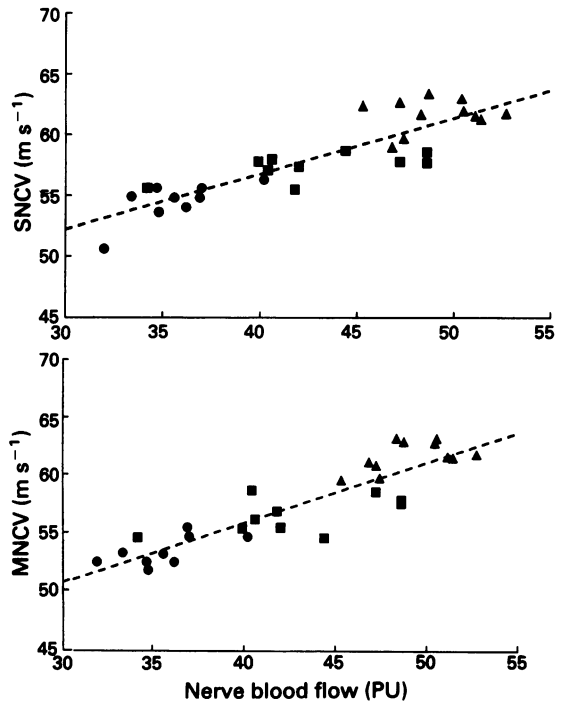


Figure 3 Correlation between nerve blood flow (NBF) and motor nerve conduction velocity (MNCV) and sensory nerve conduction velocity (SNCV) of the age-matched control rats, the nimodipine-treated diabetic rats and the placebo-treated diabetic rats, 12 weeks after the induction of diabetes mellitus. MNCV = 34.79 + 0.53 × NBF. R = 0.81, $F(1,28) = 121$, $P < 0.001$. SNCV = 38.40 + 0.46 × NBF. R = 0.78, $F(1,28) = 100$, $P < 0.001$. (▲ = age-matched control, $n = 11$; ● = diabetes placebo, $n = 9$; ■ = diabetes + nimodipine, $n = 10$).

trols (phenylephrine: $F(1,18) = 36.26$, $P < 0.001$; tyramine: $F(1,18) = 6.92$, $P < 0.05$) (Figure 4). Chronic nimodipine treatment did not significantly affect the response to phenylephrine. However, the response to tyramine was significantly increased compared to that of the placebo-treated

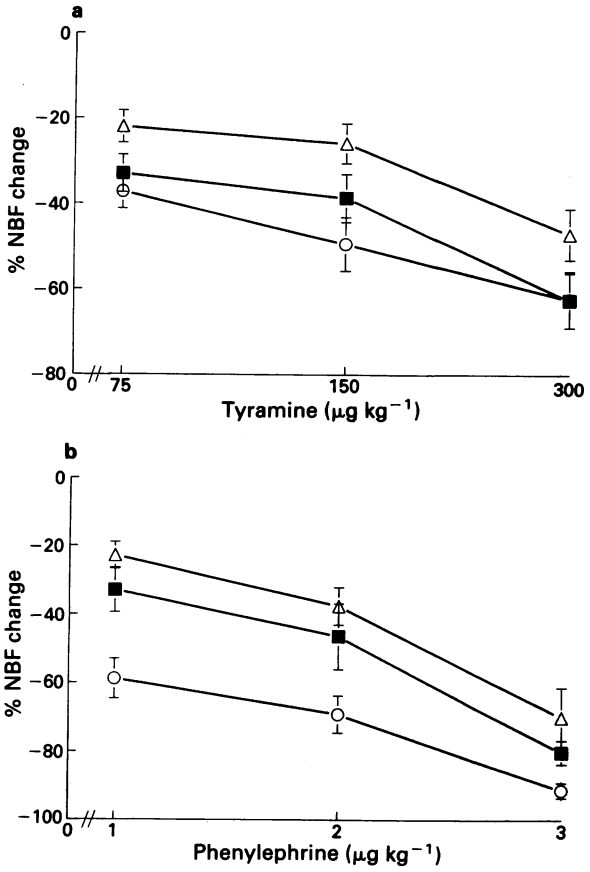


Figure 4 Response of the sciatic nerve blood flow (NBF) to local tyramine (a) (75, 150 and 300 μg kg^{-1}) and to local phenylephrine (b) (1, 2 and 3 μg kg^{-1}) application. The response of the sciatic NBF to local tyramine and phenylephrine administration in the placebo-treated diabetic rats (Δ, $n = 10$) was significantly smaller than in the age-matched control rats (○, $n = 10$), (tyramine: $F(1,18) = 6.92$, $P < 0.05$; phenylephrine: $F(1,18) = 36.26$, $P < 0.001$). Chronic nimodipine treatment in diabetic rats (■, $n = 10$) did not increase the response to phenylephrine administration as compared to the placebo treatment in the diabetic rats but significantly increased the response to tyramine as compared to placebo treatment in diabetic rats ($(F1,18) = 6.17$, $P < 0.05$).

diabetic group ($F(1,18) = 6.17$, $P < 0.05$). The response to tyramine in the nimodipine-treated diabetic group was not significantly different from the response of the age-matched controls (Figure 4).

Discussion

Over the years many studies from several laboratories have demonstrated the beneficial effects of different pharmacotherapeutic agents in experimental diabetic neuropathy (Tomlinson, 1992; Bravenboer *et al.*, 1992; 1993). The present study confirms and extends the results of previous STZ-diabetic rat studies (Robertson *et al.*, 1992; Kappelle *et al.*, 1993a,b) in which Ca^{2+} antagonists improved existing experimental diabetic neuropathy.

The beneficial action of nimodipine has been documented in post lesion recovery of function in the peripheral nervous system (Van der Zee *et al.*, 1987; 1991; Bär *et al.*, 1990; Gispen *et al.*, 1991) in the central nervous system (Nyakas *et al.*, 1989), in cisplatin-induced peripheral neuropathy (Hamers *et al.*, 1991) and in counteracting the age-related decline in sensorimotor function and cognition (Schuurman *et al.*, 1987; Gispen *et al.*, 1988; Disterhoft *et al.*, 1989; Van

der Zee *et al.*, 1989). Recently, a preventive effect of nimodipine on the development of STZ-induced diabetic neuropathy was observed (Kappelle *et al.*, 1992). Additional experiments demonstrated that nimodipine ameliorated an existing neuropathy in the STZ-induced diabetic rat (Kappelle *et al.*, 1993b). The beneficial action of nimodipine has been attributed to its direct protective effect on the neurone (Traber & Gispen, 1989; Bär *et al.*, 1990; 1993).

A reduced NBF and associated endoneurial hypoxia in diabetes mellitus have been demonstrated in several studies and are thought to play a role in the pathogenesis of diabetic neuropathy (Tuck *et al.*, 1984; Yasuda *et al.*, 1989; Cameron *et al.*, 1991; Hotta *et al.*, 1992). Furthermore, endoneurial vascular abnormalities have been demonstrated in sural nerve biopsies of diabetic patients (Dyck *et al.*, 1985; Sima *et al.*, 1988; Britland *et al.*, 1990). A putative role of hypoxia in diabetic neuropathy is supported by the fact that longstanding hypoxia *per se* can induce severe damage and slowing of nerve conduction velocity in peripheral nerves (Hendriksen *et al.*, 1992).

Nimodipine, a Ca^{2+} antagonist has relaxing effects on cerebral vessels in animal models (Haws *et al.*, 1983; Towart & Kazda, 1985) and counteracts vasospasms in man (Allen *et al.*, 1983). We measured sciatic NBF in order to clarify whether nimodipine could affect experimental diabetic neuropathy by influencing NBF (Tuck *et al.*, 1984; Low *et al.*, 1987). Nimodipine improved sciatic NBF as compared to the placebo-treated diabetic rats although it could not restore NBF to control levels. It should be noted that chronic nimodipine treatment, in the current dose-regimen, influences neither NBF (data not shown), nor nerve conduction velocity in non-diabetic control rats (Hamers *et al.*, 1991). The improvement of sciatic NBF may well have contributed to the amelioration of experimental diabetic neuropathy, since regression analysis of the data revealed that improvement of NBF correlated with enhanced NCV (Figure 3). The effect of nimodipine on NBF is probably caused by a local vasodilator effect since very little effect on systemic blood pressure was measured. Nimodipine prevents Ca^{2+} influx into vascular smooth muscle (Bevan & Hwa, 1985) leading to a reduced vascular tone (Triggle, 1982; Flaim, 1982) and eventually to an improvement of local blood flow (Flaim & Kanda, 1982). Since vasoconstriction, induced by calcium, is enhanced in diabetes mellitus (White & Carrier, 1990) this could be a factor in the beneficial effect of nimodipine in experimental diabetic neuropathy.

Perhaps the beneficial effect of chronic nimodipine treatment is related to an increased endoneurial capillary density as well, since nimodipine promotes microvessel growth (Yuan *et al.*, 1990). Thus, in addition to direct neuroprotective effects (Traber & Gispen, 1989; Bär *et al.*, 1990; 1993), nimodipine probably has a beneficial effect on the vasa nervorum of the diabetic peripheral nerve.

Several investigators have demonstrated substantial innervation of the vasa nervorum and thus a mechanism of neurogenic control (Amenta *et al.*, 1983; Appenzeller *et al.*, 1984; Renkin, 1984; Milner *et al.*, 1992). Autoregulation of NBF in response to systemic blood pressure changes, as observed in the brain, seems to be negligible (Low & Tuck, 1984; Sundqvist *et al.*, 1985; Monafo *et al.*,1988; Zochodne & Low, 1990). Little research has been carried out on the nervi vasorum of the diabetic nerve and the results obtained are inconsistent (Dhital *et al.*, 1986; Koistinaho *et al.*, 1990). In the present study a hyporesponsiveness of the vasa nervorum to both tyramine and phenylephrine application was demonstrated in placebo-treated diabetic rats. The hyporesponsiveness to phenylephrine demonstrated postsynaptic defects confirming other observations of decreased noradrenaline responsiveness (Foy & Lucas, 1976; Jackson & Carrier, 1983; Ramos, 1988; Van der Zee *et al.*, 1990) in diabetes mellitus. Increased noradrenaline responsiveness has also been described (White & Carrier, 1990; Morff, 1990). As we are the first to measure noradrenaline responsiveness in the vasa nervorum of diabetic rats, comparison of our results with previous research in other vascular systems is difficult. Since the phenylephrine response is seriously disturbed in diabetic rats it is not possible to quantify presynaptic defects based on the impaired response to tyramine application in diabetic rats.

Chronic nimodipine treatment revealed no difference in the response to phenylephrine administration. This implies that the effect of chronic nimodipine treatment on postsynaptic adrenergic responsiveness if any, is limited. The response to tyramine was restored to the non-diabetic level. These results indicate that nimodipine has a beneficial effect on the presynaptic function of the nervi vasorum of the sciatic nerve of the diabetic rat.

Our results do not allow us to answer all the questions about the mechanism of action of nimodipine in experimental diabetic neuropathy. However, besides its direct neuronal effects and the amelioration of NBF, nimodipine seems to have beneficial effect on the autonomic nerves which innervate the vasa nervorum.

In conclusion, NBF and the neural control of the vasa nervorum are seriously affected in experimental diabetic neuropathy. Nimodipine ameliorated the nerve conduction velocity deficits, the decreased NBF and the decreased vasa nervorum adrenergic responsiveness in BB/Wor diabetic rats. Nimodipine may act at at least three levels; directly on the neurone (Traber & Gispen, 1989; Bär *et al.*,1990; 1993), on the vasa nervorum and on the nervi vasorum of the affected sciatic nerve. Whether these mechanisms of action depend on the specific blockade of Ca^{2+} influx into the neurone, on direct vascular effects, on long-term effects on microvessel growth (Yuan *et al.*, 1990) or on a combination of these factors remains to be elucidated and is currently under investigation. However, it is clear that the nimodipine is a promising putative pharmacotherapeutic agent against experimental diabetic neuropathy and since other diabetic complications could be ameliorated by Ca^{2+} antagonists (Afzal *et al.*, 1988) it would be interesting to investigate the effects of nimodipine treatment in diabetic patients.

References

AFZAL, N., GANGULY, P.K., DHALLA, K.S., PIERCE, G.N., SINGAL, P.K. & DHALLA, N.S. (1988). Beneficial effects of verapamil in diabetic cardiomyopathy. *Diabetes*, **37**, 936–942.

ALLEN, G.S., AHN, H.S., PREZIOSI, T.J., BATTYE, R., BOONE, S.C., CHOU, S.N., KELLY, D.L., WEIR, B.K., CRABBE, R.A., LAVIK, P.J., ROSENBLOOM, S.B., DORSEY, F.C., INGRAM, C.R., MELLITS, D.E., BERTSCH, L.A., BOISVERT, D.P.J., HUNDLEY, M.B., JOHNSON, R.K., STORM, J.A. & TRANSOU, R.N. (1983). Cerebral arterial spasm – a controlled trial of nimodipine in patients with subarachnoid hemorrhage. *New Engl. J. Med.*, **308**, 619–624.

AMENTA, F., MIONE, M.C. & NAPOLEONE, P. (1983). The autonomic innervation of the vasa nervorum. *J. Neural Transm.*, **58**, 291–297.

APPENZELLER, O., DHITAL, K.K., COWEN, T. & BURNSTOCK, G. (1984). The nerves to blood vessels supplying blood to nerves: the innervation of vasa nervorum. *Brain Res.*, **304**, 383–386.

BÄR, P.R., RENKEMA, G.H., VERAART, C.M.H.H.M. & GISPEN, W.H. (1993). Nimodipine prevents depolarization-induced inhibition of neurite outgrowth from cultured rat spinal cord slices. *Cell Calcium*, **14**, 293–299.

BÄR, P.R., TRABER, J., SCHUURMAN, T. & GISPEN, W.H. (1990). CNS and PNS effects of nimodipine. *J. Neural Transm.*, **31**, 55–71.

BETZ, E., DECK, K. & HOFFMEISTER, F. (1985) *Nimodipine: Pharmacological and Clinical Properties*. Stuttgart, New York: Schattauer.

BEVAN, J.A. & HWA, J.T. (1985). Calcium blockers and vascular tone. In *Nimodipine Pharmacological and Clinical Properties*. ed. Betz, E., Deck, K., Hoffmeister, F. pp. 9–16. Stuttgart, New York: Schattauer.

BRAVENBOER, B., KAPPELLE, A.C., HAMERS, F.P.T., VAN BUREN, T., ERKELENS, D.W. & GISPEN, W.H. (1992). Potential use of glutathione for the prevention and treatment of diabetic neuropathy in the streptozotocin-induced diabetic rat. *Diabetologia*, **35**, 813–817.

BRAVENBOER, B., KAPPELLE, A., VAN BUREN, T., ERKELENS, D.W. & GISPEN, W.H. (1993). ACTH-analogue Org 2766 can improve existing neuropathy in diabetic rats. *Acta Diabetologia*, **30**, 21–24.

BRITLAND, S.F., YOUNG, F.J. & SHARMA, A.K. (1990). Relationship of endoneurial capillary abnormalities to type and severity of diabetic polyneuropathy. *Diabetes*, **39**, 909–913.

CAMERON, N.E., COTTER, M.A. & LOW, P.A. (1991a). Nerve blood flow in early experimental diabetes in rats: relation to conduction deficits. *Am. J. Physiol.*, **261**, E1–E8.

COHEN, A.J., MCGILL, P.D., ROSETTI, R.G., GUBERSKI, D.L. & LIKE, A.A. (1987). Glomerulopathy in the spontaneously, diabetic rat. Impact of glycaemic control. *Diabetes*, **36**, 944–951.

CRISÁ, L., MORDES, J.P. & ROSSINI, A.A. (1992). Autoimmune diabetes mellitus in the BB rat. *Diabetes Met. Rev.*, **8**, 9–37.

DE KONING, P. & GISPEN, W.H. (1987). Org 2766 improves functional and electrophysiological aspects of regenerating sciatic nerve in the rat. *Peptides*, **8**, 415–422.

DHITAL, K., LINCOLN, J., APPENZELLER, O. & BURNSTOCK, G. (1986). Adrenergic innervation of vasa and nervi nervorum of optic, sciatic, vagus and sympathetic nerve trunks in normal and streptozotocin-diabetic rats. *Brain Res.*, **367**, 39–44.

DISTERHOFT, J.F., DEYO, R.A., BLACK, J., DE JONGE, M., STRAUBE, K.T. & THOMPSON, L.T. (1989). Associative learning in aging rabbits is facilitated by nimodipine. In *Nimodipine and Central Nervous System Function: New Vistas*. ed. Traber, J. & Gispen, W.H. pp. 209–226. Stuttgart, New York: Schattauer.

DYCK, P.J., HANSEN, S., KARNES, J., O'BRIEN, P., YASUDA, H., WIDEBANK, A.J. & ZIMMERMAN, B. (1985). Capillary number and percentage closed in human diabetic sural nerve. *Proc. Natl. Acad. Sci. U.S.A.*, **82**, 2513–2517.

FITZGERALD, M.E.C. & CALDWELL, R.B. (1990). The retinal microvasculature of spontaneously diabetic BB rats: structure and luminal surface properties. *Microvasc. Res.*, **39**, 15–27.

FLAIM, S.F. (1982). Comparative pharmacology of calcium blockers based on studies of vascular smooth muscle. In *Calcium Blockers: Mechanism of Action and Clinical Applications*. ed. Flaim, S.F. & Zelis, R. pp. 155–178. Baltimore: Williams & Wilkins.

FLAIM, S.F. & KANDA, K. (1982). Comparative pharmacology of calcium blockers based on studies of cardiac output distribution. In *Calcium Blockers: Mechanism of Action and Clinical Applications*. ed. Flaim, S.F. & Zelis, R. pp. 179–192. Baltimore: Williams & Wilkins.

FOY, J.M. & LUCAS, P.D. (1976). Effect of experimental diabetes, food deprivation and genetic obesity on the sensitivity of pithed rats to autonomic agents. *Br. J. Pharmacol.*, **57**, 229–234.

GISPEN, W.H., SCHUURMAN, T. & TRABER, J. (1988). Nimodipine and neural plasticity in the peripheral nervous system of adult and aged rats. In *The Calcium Channel: Function and Implications*. ed. Morad, M., Nayler, W., Kazda, S. & Schramm, M. pp. 491–502. Berlin, Heidelberg: Springer-Verlag.

GISPEN, W.H., SPOREL-ÖZAKAT, E., DUCKERS, H.J. & EDWARDS, P.M. (1991). The Ca^{2+} antagonist nimodipine and recovery of function following peripheral nerve damage in the rat. *Neurosci. Res. Commun.*, **8**, 175–184.

HAMERS, F.P.T., GERRRITSEN VAN DER HOOP, R., STEERENBURG, P.A., NEIJT, J.P. & GISPEN, W.H. (1991). Putative neurotrophic factors in the protection of cisplatin-induced peripheral neuropathy in rats. *Toxicol. Appl. Pharmacol.*, **111**, 514–522.

HAWS, C.W., GOURLEY, J.K. & HEISTAD, D.R. (1983). Effects of nimodipine on cerebral blood flow. *J. Pharmacol. Exp. Ther.*, **225**, 24–28.

HENDRIKSEN, P.H., OEY, P.L., WIENEKE, G.H., VAN HUFFELEN, A.C. & GISPEN, W.H. (1992). Hypoxic neuropathy versus diabetic neuropathy – an electrophysiological study in rats. *J. Neurol. Sci.*, **110**, 99–106.

HOROWITZ, M., HARDING, P.E., MADDOX, A., MADDEREN, G.J., COLLINS, P.J., CHATTERTON, B.E., WISHART, J. & SHEARMAN, D.J.C. (1986). Gastric and oesophageal emptying in insulin-dependent diabetes mellitus. *J. Gastroenterol. Hepatol.*, **1**, 97–113.

HOTTA, N., KAKUTA, H., FUKASAWA, H., KOH, N., SAKAKIBARA, F., KOMORI, H. & SAKAMOTO, N. (1992). Effect of niceritrol on streptozocin-induced diabetic neuropathy in rats. *Diabetes*, **41**, 587–591.

JACKSON, C.V. & CARRIER, G.O. (1983). Influence of short-term experimental diabetes on blood pressure and heart rate in response to norepinephrine and angiotensin II in the conscious rat. *J. Cardiovascular Pharmacol.*, **5**, 260–265.

KAPPELLE A.C., BIESSELS, G., VAN BUREN, T., ERKELENS, D.W., DE WILDT, D.J. & GISPEN, W.H. (1993a). Effects of nimodipine in sciatic nerve blood flow and vasa nervorum responsiveness in the diabetic rat. *Eur. J. Pharmacol.* (in press).

KAPPELLE, A.C., BRAVENBOER, B., TRABER, J., ERKELENS, D.W. & GISPEN, W.H. (1992). The Ca^{2+} antagonist nimodipine counteracts the onset of an experimental neuropathy in streptozotocin-induced diabetic rats. *Neurosc. Res. Commun.*, **10**, 95–104.

KAPPELLE, A.C., BRAVENBOER, B., VAN BUREN, T., TRABER, J., ERKELENS, D.W. & GISPEN, W.H. (1993b). The Ca^{2+} antagonist, nimodipine, ameliorates an existing neuropathy in the streptozotocin-induced diabetic rat model. *Br. J. Pharmacol.*, **108**, 780–785.

KOISTINAHO, J., WADHWANI, K.C. & RAPOPORT, S.I. (1990). Adrenergic innervation in the tibial and vagus nerves of rats with streptozotocin-induced diabetes. *Brain Res.*, **513**, 106–112.

LOW, P.A. & TUCK, R.R. (1984). Effects of changes of blood pressure, respiratory acidosis and hypoxia on nerve blood flow in the sciatic nerve of the rat. *J. Physiol.*, **347**, 513–519.

LOW, P.A., TUCK, R.R. & TAKEUCHI, M. (1987). Nerve microenvironment in diabetic neuropathy. In *Diabetic Neuropathy*. ed. Dyck, P.J., Thomas, P.K., Asbury, A.K., Winegrad, A.I. & Porte, D. pp. 266–278. Philadelphia: Saunders.

MAYER, J.H. & TOMLINSON, D.R. (1983). Prevention of defects of axonal transport and nerve conduction velocity by oral administration of myo-inositol or an aldose-reductase inhibitor in streptozotocin-diabetes rats. *Diabetologia*, **25**, 433–438.

MILNER, P., APPENZELLER, O., QUALLS, C. & BURNSTOCK, G. (1992). Differential vulnerability of neuropeptides in nerves of the vasa nervorum to streptozotocin-induced diabetes. *Brain Res.*, **574**, 56–62.

MONAFO, W.W., ELIASSON, S.G., SHIMAZAKI, S. & SUGIMOTO, H. (1988). Regional blood flow in resting and stimulated sciatic nerve of diabetic rats. *Exp. Neurol.*, **99**, 607–614.

MORDES, J.P., DESEMONE, J. & ROSSINI, A.A. (1987). The BB rat. *Diabetes/Metab. Rev.*, **3**, 725–750.

MORFF, R.J. (1990). Microvascular reactivity to norepinephrine at different arteriolar levels and durations of streptozotocin-induced diabetes. *Diabetes*, **39**, 354–360.

NYAKAS, C., MARKEL, E., KRAMERS, R.J.K., GASPAR, E., BOHUS, B. & LUYTEN, P.G.M. (1989). Effect of nimodipine on hypoxia-induced learning and memory deficits. In *Nimodipine and Central Nervous System Function: New Vistas*. ed. Trabere, J. & Gispen, W.H. pp. 175–194. Stuttgart, New York: Schattauer.

PIRART, J. (1978). Diabetes mellitus and its degenerative complications: a prospective study of 4400 patients observed between 1947 and 1973. *Diabetes Care*, **1**, 168–252.

RAMOS, O.L. (1988). Diabetes mellitus and hypertension. *Hypertension*, **11**, I,14–I,18.

RENKIN, E.M. (1984). Control of microcirculation and blood-tissue exchange. In *Handbook of Physiology, section 2, The Cardiovascular System*, Vol 4, *Microcirculation*, part 2. ed. Renkin, E.M. & Michel, C.C. pp. 627–687. Bethesda, MD: Am. Physiol. Soc.

ROBERTSON, S., CAMERON, N.E. & COTTER, M.A. (1992). The effect of the calcium antagonist nifedipine on peripheral nerve function in streptozotocin-diabetic rats. *Diabetologia*, **35**, 1113–1117.

SCHUURMAN, T., KELIN, H., BENEKE, M. & TRABER, J. (1987). Nimodipine and motor deficits in the aged rat. *Neurosci. Res. Commun.*, **1**, 9–15.

SCRIABINE, A., SCHUURMAN, T. & TRABER, J. (1989). Pharmacological basis for the use of nimodipine. *Ann. N.Y. Acad. Sci.*, **522**, 698–706.

SIMA, A.A.F., BRIL, V., NATHANIEL, V., BRIL, V., MCEWEN, T.A.J., BROWN, M.B., LATTIMER, S. & GREENE, D.A. (1988). Regeneration and repair of myelinated fibers in sural-nerve biopsy specimens from patients with diabetic neuropathy treated with sorbinil. *N. Engl. J. Med.*, **319**, 548–555.

SIMA, A.A.F., PRASHAR, A., ZHANG, W.-X., CHAKRABATI, S. & GREENE, D.A. (1990). Preventive effect of long-term aldose reductase inhibition (ponalrestat) on nerve conduction and sural nerve structure in the spontaneously diabetic Bio-Breeding rat. *J. Clin. Invest.*, **85**, 1410–1420.

SIMA, A.A.F. & THIBERT, P. (1982). Proximal motor neuropathy in the BB-Wistar rat. *Diabetes*, **31**, 784–788.

SMOUT, A.J.P.M., JEBBINK, H.J.A. & BRAVENBOER, B. (1991). Gastrointestinal manifestations of diabetic autonomic neuropathy. *Neth. J. Med.*, **39**, 329–332.

STROWIG, S. & RASKIN, P. (1992). Glycemic control and diabetic complications. *Diabetes Care*, **15**, 1126–1140.

SUNDQVIST, T., ÖBERG, P.Å. & RAPPAPORT, S.I. (1985). Blood flow in rat sciatic nerve during hypotension. *Exp. Neurol.*, **90**, 139–148.

THOMAS, P.K. & ELIASSON, S.G. (1984). Diabetic neuropathy. In *Peripheral Neuropathy*. ed. Dyck, P.J., Thomas, P.K. & Lambert, E.M. pp. 1173–1810. Philadelphia PA: Saunders.

TOMLINSON, D.R. (1992). The pharmacology of diabetic neuropathy. *Diabetes/Metab. Rev.*, **8**, 67–84.

TOWART, R. & KAZDA, S. (1985). Effects of calcium antagonist nimodipine on isolated cerebral vessels. In *Nimodipine Pharmacological and Clinical Properties*. ed. Betz, E., Deck, K. & Hoffmeister, F. pp. 207–215. Stuttgart, New York: Schattauer.

TRABER, J. & GISPEN, W.H. (1989). *Nimodipine and the Central Nervous System: New Vistas*. Stuttgart, New York: Schattauer.

TRIGGLE, D.J. (1982). Biochemical pharmacology of calcium blockers. In *Calcium Blockers: Mechanism of Action and Clinical Applications*. ed. Flaim, S.F. & Zelis, R. pp. 121–134. Baltimore: Williams & Wilkins.

TUCK, P.R., SCHMELZER, J.D. & LOW, P.A. (1984). Endoneurial blood flow and oxygen tension in the sciatic nerves of rats with experimental diabetic neuropathy. *Brain*, **107**, 935–950.

VAN DER ZEE, C.E.E.M., SCHUURMAN, T., TRABER, J. & GISPEN, W.H. (1987). Oral administration of nimodipine accelerates functional recovery following peripheral nerve damage in the rat. *Neurosci. Lett.*, **83**, 143–148.

VAN DER ZEE, C.E.E.M., SCHUURMAN, T., GERRITSEN VAN DER HOOP, R., TRABER, J. & GISPEN, W.H. (1989). Beneficial effect of nimodipine on peripheral nerve function in aged rats. *Neurobiol. Aging*, **11**, 451–456.

VAN DER ZEE, C.E.E.M., VAN DER BUUSE, M. & GISPEN, W.H. (1990). Beneficial effect of an $ACTH_{4-9}$ analog on peripheral neuropathy and blood pressure response to tyramine in streptozotocin-diabetic rats. *Eur. J. Pharmacol.*, **177**, 211–213.

VAN DER ZEE, C.E.E.M., BRAKKEE, J.H. & GISPEN, W.H. (1991). Putative neurotrophic factors and functional recovery from nerve damage in the rat. *Br. J. Pharmacol.*, **103**, 1041–1046.

WATKINS, P.J. (1990). Diabetic autonomic neuropathy. *N. Engl. J. Med.*, **322**, 1078–1079.

WHITE, R.E. & CARRIER, G.O. (1990). Vascular contraction induced by activation of membrane calcium ion channels is enhanced by streptozotocin-diabetes. *J. Pharmacol. Exp. Ther.*, **253**, 1057–1062.

YASUDA, H., SONOBE, M., YAMASHITA, M., TERADA, M., HATANAKA, H., HUITIAN, Z. & SHIGETA, Y. (1989). Effect of prostaglandin E_1 analogue TFC 612 on diabetic neuropathy in streptozotocin-induced diabetic rats. *Diabetes*, **38**, 832–838.

YUAN, X.Q., SMITH, T.L., PROUGH, D.S., DE WITT, D.S., DUSSEAU, J.W., LYNCH, C.D., FULTON, J.M. & HUTCHINS, P.M. (1990). Long-term effects of nimodipine in pial microvasculature and systemic circulation in conscious rats. *Am. J. Physiol.*, **258**, H1395–1401.

ZHANG, W.-X., CHAKRABATI, S., GREENE, D.A. & SIMA, A.A.F. (1990). Diabetic autonomic neuropathy in BB rats and effect of ARI treatment on heart-rate variability and vagus nerve structure. *Diabetes*, **39**, 613–618.

ZOCHODNE, D.W. & LOW, P.A. (1990). Adrenergic control of nerve blood flow. *Exp. Neurol.*, **109**, 300–307.

(Received June 28, 1993
Revised October 26, 1993
Accepted November 4, 1993)

Br. J. Pharmacol. (1994), **111**, 894–902

© Macmillan Press Ltd, 1994

Evidence that nitric oxide is an endogenous antiangiogenic mediator

[1]Eva Pipili-Synetos, Eleni Sakkoula, G. Haralabopoulos, Paraskevi Andriopoulou, P. Peristeris & M.E. Maragoudakis

Department of Pharmacology, Medical School, University of Patras, Patras 261 10, Greece

1 The involvement of nitric oxide (NO) in the regulation of angiogenesis was examined in the *in vivo* system of the chorioallantoic membrane (CAM) of the chick embryo and in the matrigel tube formation assay.

2 Sodium nitroprusside (SNP) (0.37–28 nmol/disc), which releases NO spontaneously, caused a dose-dependent inhibition of angiogenesis in the CAM *in vivo* and reversed completely the angiogenic effects of α-thrombin (6.7 nmol/disc) and the protein kinase C (PKC) activator 4-β-phorbol-12-myristate-13-acetate (PMA) (0.97 nmol/disc). In addition, SNP (28×10^{-6} M) stimulated the release of guanosine 3′-5′-cyclic monophosphate (cyclic GMP) from the CAM *in vitro*.

3 In the matrigel tube formation assay, an *in vitro* assay of angiogenesis, both SNP ($1-3 \times 10^{-6}$ M) and the cell permeable cyclic GMP analogue, Br-cGMP ($0.3-1.0 \times 10^{-3}$ M) reduced tube formation.

4 The inhibitors of NO synthase, N^G-monomethyl-L-arginine (L-NMMA) (3.8–102 nmol/disc) and N^G-nitro-L-arginine methylester (L-NAME) (1.3–34.2 nmol/disc) stimulated angiogenesis in the CAM *in vivo*, in a dose-dependent fashion. D-NMMA and D-NAME on the other hand had no effect on angiogenesis in this system.

5 L-Arginine (10.9 nmol/disc), although it had a modest antiangiogenic effect by itself, was capable of abolishing the angiogenic effects of L-NMMA (34.2 nmol/disc) and of L-NAME (3.8 nmol/disc).

6 Dexamethasone, an inhibitor of the induction of NO synthase, at 0.2–116.1 nmol/disc, stimulated angiogenesis in the CAM, whereas at 348.4–1161 nmol/disc it inhibited this process. Combination of 38.7 nmol/disc dexamethasone with L-NAME (9.3 nmol/disc) resulted in a potentiation of the angiogenic effect of the former. It appears therefore that both the constitutive and the inducible NO synthase may contribute to the NO-mediated inhibition of angiogenesis.

7 Superoxide dismutase (SOD), which prevents the destruction of NO, at 300 i.u./disc had a modest antiangiogenic effect in the CAM, by itself. In addition, SOD, prevented α-thrombin (6.7 nmol/disc) and PMA (0.97 nmol/disc) from stimulating angiogenesis in the CAM.

8 These results suggest that NO may be an endogenous antiangiogenic molecule of pathophysiological importance.

Keywords: Nitric oxide; angiogenesis; sodium nitroprusside; thrombin; 4-β-phorbol-12-myristate-13-acetate; chick chorioallantoic membrane; neovascularization; cyclic GMP; platelet activation; collagenous protein biosynthesis

Introduction

Nitric oxide (NO) is an endogenous mediator which is released from a variety of cell types including endothelial cells, smooth muscle cells, platelets, macrophages and nerve cells of the peripheral and central nervous system (Marletta *et al.*, 1988; Moncada *et al.*, 1991; Lowenstein & Snyder, 1992). This very interesting molecule subserves an evergrowing number of functions including vasodilatation (Amezcua *et al.*, 1989), cytotoxicity (Hibbs *et al.*, 1988), inhibition of protein synthesis (Nakaki *et al.*, 1990), neurotransmission (Snyder & Bredt, 1992), inhibition of messangial cell proliferation (Garg & Hassid, 1989) and inhibition of platelet aggregation (Radomski *et al.*, 1990).

Angiogenesis is a multi-step process of great pathophysiological significance as it is associated with proliferative states with the notable example of tumour growth (Maragoudakis, 1993). Recently, it was shown that thrombin, one of the most potent activators of platelets (Fenton *et al.*, 1991), is capable of stimulating angiogenesis in the chorioallantoic membrane (CAM) of the chick embryo *in vivo* (Tsopanoglou *et al.*, 1993a) in a process which is mediated mainly via its catalytic site and can occur independently of fibrin formation. In the same system, 4-β-phorbol-12-myristate-13-acetate (PMA) a well known activator of protein kinase C (Castagna *et al.*, 1982) and of platelet aggregation (Sano *et al.*, 1983; Rink *et al.*, 1983) was also shown to stimulate angiogenesis (Tsopanoglou *et al.*, 1993b) specifically and reversibly. Based on the above observations and in view of the fact that many angiogenesis-dependent diseases, such as tumour growth and psoriasis are accompanied by increased thrombogenesis (Rickles & Edwards, 1983; McDonald, 1991), the possibility was considered that platelet activation may be an important step in the angiogenic cascade. Since NO is an inhibitor of platelet activation, its role as an endogenous antiangiogenic molecule was investigated. Preliminary data suggested that NO may indeed be involved in the angiogenic process (Pipili-Synetos *et al.*, 1993).

The objective of the present study was to provide evidence that increasing the availability of NO results in inhibition of angiogenesis and inversely, limiting its availability results in promotion of angiogenesis. The experimental systems used were (a) the *in vivo* CAM model (Folkman, 1985) and (b) the matrigel tube formation assay (Kubota *et al.*, 1988; Grant *et al.*, 1989) where endothelial cells when grown on a solid gel of laminin-rich basement membrane proteins differentiate and form capillary-like structures.

[1] Author for correspondence.

Methods

The *in vivo* CAM angiogenesis model, initially described by Folkman (1985) and modified as previously reported (Maragoudakis *et al.*, 1988) was used. Briefly, fresh fertilized eggs were incubated for 4 days at 37°C when a window was opened on the egg shell exposing the CAM. The window was covered with sterile cellophane tape and the eggs were returned to the incubator until day 9 when the test materials were applied. The test materials or vehicle and 0.5 μCi U-^{14}C-labelled proline, were placed on sterile plastic discs and were allowed to dry under sterile conditions. The control discs (containing vehicle and radiolabelled proline) were placed on the CAM 1 cm away from the disc containing the test material. A sterile solution of cortisone acetate (249 nmol/disc) was routinely incorporated in all discs in order to prevent an inflammatory response. The loaded and dried discs were inverted and placed on the CAM, the windows were covered and the eggs incubated until day 11 when assessment of angiogenesis took place.

Biochemical evaluation of angiogenesis

Collagenous proteins represent 80% of the total basement membrane proteins formed by the CAM during the chick embryo development (Maragoudakis *et al.*, 1988). The extent of their biosynthesis has been shown to correlate well with new vessel formation. This biosynthesis reaches a maximum between days 8 and 11 and coincides with maximal angiogenesis in the CAM as shown by morphological evaluation of vascular density. Furthermore, at day 10, collagenous protein biosynthesis is 11 fold higher than that of day 15 when angiogenesis has reached a plateau. Biochemical evaluation of newly formed vessels was performed by determining the extent of collagenous protein biosynthesis in the CAM lying directly under the discs. Briefly, the area under the disc was cut off, placed in an appropriate buffer and protein biosynthesis was stopped. Non protein bound radioactivity was removed by washing with trichloroacetic acid. The tissue containing radioactivity was resuspended and subjected to collagenase digestion. The resulting radiolabelled tripeptides corresponding to basement membrane collagen and other collagenous material synthesized by the CAM from [U-^{14}C]-proline, were counted and expressed as c.p.m. mg^{-1} protein.

Morphological evaluation of angiogenesis

For morphological evaluation, eggs were treated as above in the absence of radiolabelled proline. At day 11 the eggs were flooded with 10% buffered formalin, the plastic discs were removed and the eggs were kept at 37°C until dissection. A large area around the discs was cut off and placed on a glass slide and the vascular density index (expressed as number of blood vessels) was measured by the method of Harris-Hooker *et al.* (1983). Representative specimens were mounted on a stereoscope (magnification × 16) and photographed. Harris-Hooker evaluation underestimates by approximately 10% (compared to the biochemical evaluation of angiogenesis) the changes in the vascular network. This is an expected limitation of this method as some vessels are probably collapsed and do not show up under the stereoscope.

Matrigel tube formation assay and assessment of the area

Human umbilical vein endothelial cells were isolated from freshly obtained umbilical cords according to the method previously described by Jaffe *et al.* (1987). Cells were maintained in medium (supplemented with ECGS, FBS, and antibiotics) at 37°C, 95% humidity, and 5% CO_2. Matrigel consists of reconstituted basement membrane enriched with laminin extracted from the Engelbredt-Holm Swarm (EHS) tumour (Timpl *et al.*, 1979). When endothelial cells are cultured on this material, they stop proliferating, they align and within 12–18 h they form an anastomosing network of tube-like structures resembling a capillary plexus (Grant *et al.*, 1989). The Matrigel tube formation assay was performed as previously described (Kubota *et al.*, 1988). Briefly, 300 μl/well Matrigel was used to coat 24-well Limbro cluster plates at 4°C. After the Matrigel had formed a gel, approximately 40,000 cells were seeded in each well in medium containing the test substances and 10% FBS. After 18 h of incubation the wells were fixed, stained and the tube area was quantified using the MCID image analysis system from Brock University, Ontario, Canada, according to Grant *et al.* (1989).

Determination of cyclic GMP release from the CAM in vitro

At day 4 the windows were opened as described above and the eggs were returned for a further 7 days to the incubator without placing any discs on the exposed surface. At day 11, the exposed CAM from 15 eggs were dissected into 4 pieces each and divided between two petri dishes (control and treatment group) containing ice-cold Krebs physiological salt solution (PSS) and 0.5 mM isobutyl-methyl-xanthine (IBMX) to prevent the degradation of cyclic GMP. Subsequently, they were placed in round-bottomed polypropylene centrifuge tubes standing on ice and containing 5 ml of Krebs PSS and IBMX with or without 2.8×10^{-6} M SNP. The zero time sample was transferred immediately to a deep freeze (– 40°C) until further processing. The remaining samples (with or without SNP) were incubated for 2, 5 and 10 min at 37°C in a shaking water bath. At the end of the incubation period, all samples were homogenized in a Polytron Homogenizer at 4°C in the presence of 6% trichloroacetic acid (TCA) and centrifuged at 2,000 *g* for 15 min at 4°C. The supernatant was recovered, and washed 4 times with 5 volumes of water saturated diethyl ether. The aqueous extract remaining was lyophillized and reconstituted in a suitable volume of assay buffer immediately prior to analysis. Cyclic GMP determination was performed by radioimmunoassay (RIA) using a commerically available kit (cGMP[^{125}I] assay system, Amersham, U.K.). Results are expressed as pmol mg^{-1} protein.

Materials

The composition of the Krebs PSS was (mM): NaCl 118.4, KCl 4.7, $CaCl_2$ 2.5, $MgSO_4.7H_2O$ 1.2, $NaHCO_3$ 24.9, KH_2PO_4 1.2 and glucose 11.1. The following drugs were used: collagenase type VII from *Clostridium histolyticum*, cortisone acetate, 4-β-phorbol-12-myristate-13-acetate (4-β-PMA), sodium nitroprusside (SNP), N^G-nitro-L-arginine methyl ester (L-NAME), D-NAME, superoxide dismutase (SOD), isobutyl-methyl-xanthine (IBMX), L-arginine, were obtained from Sigma Chemical Co. (Poole, Dorset, U.K.). Dexamethasone was obtained from Organon (Holland). L-[U-^{14}C]-proline (specific activity 273 mCi mmol^{-1}) was obtained from New England Nuclear (Boston, MA, U.S.A.). N^G-monomethyl-L-arginine (L-NMMA) and D-NMMA were a gift from Dr S. Moncada. α-Thrombin was a gift from Dr J.W. Fenton and had the following characteristics: specific activity 3287 units mg^{-1} protein, active site concentration 5.3×10^{-5} M (Fenton *et al.*, 1991). Foetal bovine serum (FBS), endothelial cell growth supplement (ECGS), M199, penicillin, streptomycin, L-glutamine, gentamycin, heparin, trypsin-EDTA were obtained from ICN Flow Lab. (U.K.). Matrigel was a gift from Dr Hynda Kleinman, Lab. of Dev. Biol., NIH (Bethesda, MD, U.S.A.).

Plastic discs used were 13 mm round tissue culture coverslips from Nunc Inc. (Naperville, IL, U.S.A.).

Fresh fertilized eggs were obtained locally (Ioannina, Greece) and kept at 10°C before incubaton at 37°C.

Calculations and statistics

For each egg, collagenous protein biosynthesis under the disc containing the test material or vehicle, was calculated as c.p.m. mg^{-1} protein. Collagenous protein biosynthesis, or number of vessels, under the disc containing the test material, was then expressed as % of that under the control disc. The results were analysed by Student's paired or unpaired t test and n signifies the number of eggs for each treatment. The graphics were performed using the Cricket Graph computer programme on a Mackintosh SE.

Results

In each experiment 2–4 eggs were included where both discs contained only vehicle (control-control), in order to assess (a) the variability in the amount of radioactive collagenous protein biosynthesis synthesized by two adjacent areas of the CAM and (b) the variability in collagenous protein biosynthesis synthesized under the control disc. It was shown that there was no statistically significant difference in this parameter (expressed as c.p.m. mg^{-1} protein) under the two discs (14900 ± 1192 and 14903 ± 1194, $n = 32$) and that the standard error was less than 10% of the mean in both cases.

Effect of SNP on angiogenesis in the CAM in vivo *and on cyclic GMP production from the CAM* in vitro

Sodium nitroprusside from 0.37–28 nmol/disc and in agreement with previous observations (Pipili-Synetos *et al.*, 1993), caused a dose-dependent inhibition in basal (unstimulated) angiogenesis as evidenced by a decrease in collagenous protein biosynthesis (Figure 1). This inhibition ranged between $11.8 \pm 3.8\%$–$34 \pm 3.2\%$ of control ($n = 5$–33). In these experiments, morphological evaluation performed by the method of Harris-Hooker *et al.* (1983), showed that the vascular density under the discs containing 9.3 nmol was reduced by $26.4 \pm 2.2\%$, $n = 13$, $P < 0.01$, compared to controls. Photographs of the area of the CAM lying directly under the control and the test disc, in the same egg, provide visual confirmation of the antiangiogenic effect of SNP (Figure 2a,b).

In order to establish that SNP inhibits angiogenesis in the CAM via NO formation, it was important to determine that

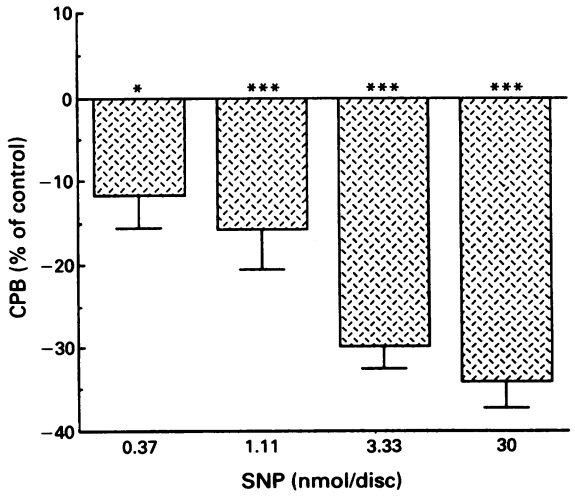


Figure 1 Effect of sodium nitroprusside (SNP) on angiogenesis in the chick chorioallantoic membrane *in vivo*, expressed as collagenous protein biosynthesis (CPB). Results are expressed as mean ($\pm$ s.e.mean)% of control ($n = 5$–33) and are compared by paired t test. Asterisks denote statistical significance of the calculated percentage difference between control and test: $*P < 0.05$ and $***P < 0.01$.

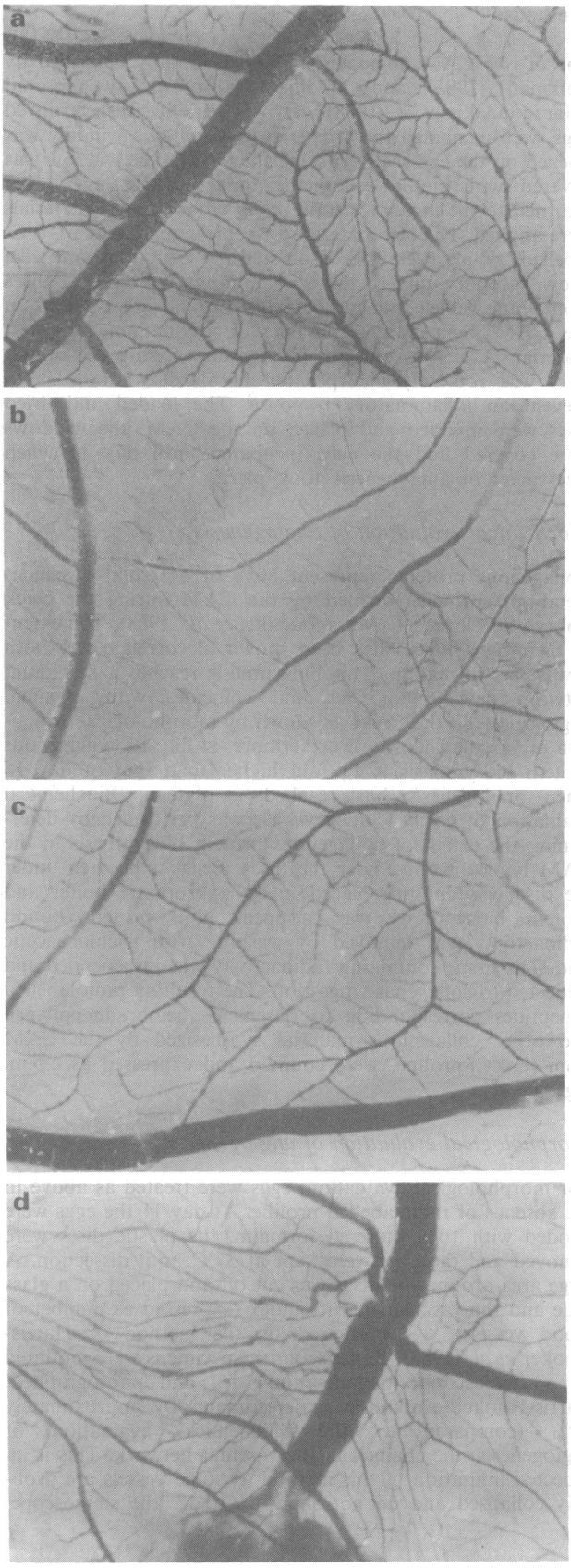


Figure 2 Effect of sodium nitroprusside and N^G-monomethyl-L-arginine on angiogenesis in the chick chorioallantoic membrane *in vivo*. Specimens processed as for morphological evaluation, were mounted on a stereoscope (calibration bar = 1 mm) and photographed. Area under the control discs (a and c). Area under the discs containing 3.9 nmol of sodium nitroprusside (b) and 34.2 nmol N^G-monomethyl-L-arginine (d).

SNP is capable of stimulating cyclic GMP production, the NO second messenger (Arnold *et al.*, 1977) in this tissue. When the CAM *in vitro*, was preincubated for various time intervals with SNP (28×10^{-6} M), cyclic GMP production was shown to increase progressively (Figure 3) and at 10 min, it reached 35.3 ± 3.0 pmol mg^{-1} protein compared to 15.2 ± 4.0 pmol mg^{-1} protein, ($n = 3$, $P < 0.01$) in the control CAM. It should be mentioned that 15 eggs were used in each of the three (3) experiments, i.e. these observations were obtained from a total of 45 eggs.

Effects of L-NMMA and L-NAME on angiogenesis in the CAM in vivo

Since SNP inhibited angiogenesis, inhibitors of NO synthase (Moncada *et al.*, 1991) were subsequently examined to see whether they had the opposite effect. The NO synthase inhibitors L-NMMA (3.8–102 nmol/disc) (in agreement with previous observations, Pipili-Synetos *et al.*, 1993) and L-NAME (1.3–34.2 nmol/disc) caused a dose-dependent increase in basal collagenous protein biosynthesis (Figure 4a,b) which ranged between $5.6 \pm 5.4\%$–$29.8 \pm 4.8\%$ of control ($n = 7$–48) for L-NMMA and $22.2 \pm 5.3\%$–$54.4 \pm 11.8\%$ of control ($n = 8$–15) for L-NAME. L-NAME was 3 times more potent in stimulating angiogenesis than L-NMMA. The D-isomers of both compounds D-NMMA (11.4–102 nmol/disc) and D-NAME (1.3–34.2 nmol/disc) had no effect on basal collagenous protein biosynthesis which ranged between $1.55 \pm 6.0\%$–$2.8 \pm 2.9\%$ of control ($n = 6$–7) for D-NMMA and $6.2 \pm 4.9\%$–$11.2 \pm 6.1\%$ of control ($n = 7$–8) for D-NAME.

Photographs of the area of the CAM lying directly under the control and the test disc, in the same egg, provide visual confirmation of the angiogenic effect of L-NMMA (34.2 nmol/disc) (Figure 2c,d). Morphological evaluation showed that the same amount of L-NMMA caused a $29.0 \pm 4.9\%$, $n = 12$, $P < 0.01$ increase in vascular density.

Reversal of the effect of L-NMMA or L-NAME by L-arginine

In order to establish that the angiogenic effect of L-NMMA and L-NAME were due to inhibition of NO synthase, it was attempted to reverse the effect of these agents with L-arginine, the endogenous substrate for NO synthase (Palmer *et al.*, 1988). L-Arginine (2.1–10.9 nmol/disc) caused a small but significant decrease in collagenous protein biosynthesis ($13.9 \pm 3.6\%$ inhibition, $n = 25$, $P < 0.01$, at the highest dose). Under these conditions and at the 10.9 nmol/disc dose, there was a non significant decrease in vascular density ($9.8 \pm 3.0\%$ of control, $n = 5$). However, when L-arginine (10.9 nmol/disc) was combined with either L-NMMA (34.2 nmol/disc, $n = 13$) or L-NAME (3.8 nmol/disc, $n = 7$), the angiogenic effects of both compounds were completely abolished (Figure 5a,b) and a small inhibition of angiogenesis was observed ($7.7 \pm 5.5\%$ of control, NS and $4.1 \pm 1.5\%$ of control, $P < 0.05$, inhibition respectively).

Effect of dexamethasone, alone and in combination with L-NAME, on angiogenesis in the CAM

Dexamethasone, an inhibitor of the induction of NO synthase (O'Connor & Moncada, 1991), at 0.2–38.7 nmol/disc ($n = 6$–17) was found to increase angiogenesis in the CAM dose-dependently (Figure 6a). This increase ranged between $19.6 \pm 3.7\%$ and $41.7 \pm 6.4\%$ of control. In these experiments, morphological evaluation by the method of Harris-

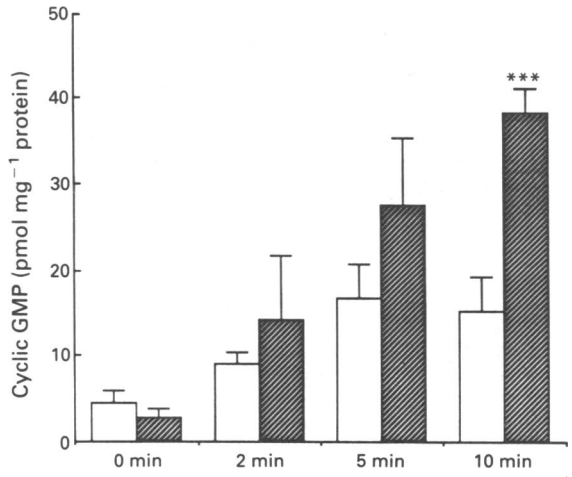


Figure 3 Effect of sodium nitroprusside on cyclic GMP production. Results are expressed as mean ($\pm$ s.e.mean)pmol mg^{-1} protein ($n = 3$) produced from the chick chorioallantoic membrane *in vitro*, at various time intervals and in the absence (control, open columns) and presence of sodium nitroprusside (28×10^{-6} M, hatched columns). Asterisks denote statistical significance between control and test: ***$P < 0.01$.

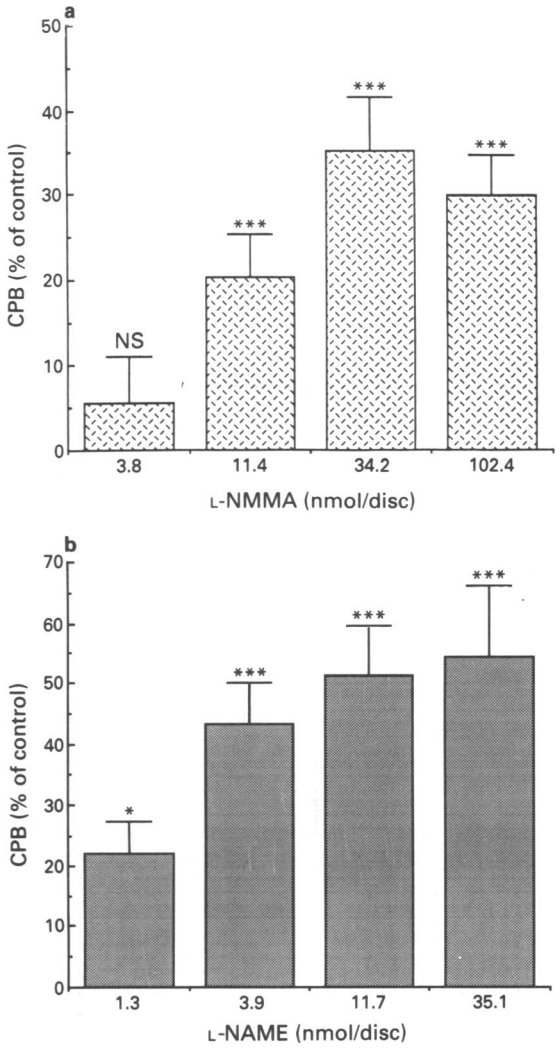


Figure 4 Effect of increasing amounts of (a) N^G-monomethyl-L-arginine and of (b) N^G-nitro-L-arginine methyl ester on angiogenesis in the chick chorioallantoic membrane *in vivo*, expressed as collagenous protein biosynthesis (CPB). Results are expressed as mean ($\pm$ s.e.mean)% of control ($n = 7$–48, a and $n = 8$–15, b) and are compared by paired t test. Asterisks denote statistical significance of the calculated percentage difference between control and test: *$P < 0.05$ and ***$P < 0.01$.

Hooker et al. (1983) showed that the vascular density under the disc containing 38.7 nmol of dexamethasone increased by 31.5 ± 4.4%, $n = 6$, $P < 0.01$. At 116.1 nmol/disc, the angiogenic effect of dexamethasone was reduced to 18.2 ± 4.6%, $n = 7$ and at 348.4 and 1161 nmol/disc it caused a 24.8 ± 9.5%, $n = 6$ ($P < 0.05$) and 65.0 ± 4.9%, $n = 7$ ($P < 0.01$) decrease in collagenous protein biosynthesis (Figure 6a).

When 38.7 nmol/disc of dexamethasone were combined with L-NAME (9.3 nmol/disc, $n = 13$), a 68.8 ± 9.4%, $n = 10$, increase in collagenous protein biosynthesis was observed. This increase was significantly greater than that seen with dexamethasone ($P < 0.05$) or L-NAME ($P < 0.05$) alone (Figure 6b).

Reversal of the angiogenic effects of α-thrombin and PMA by SNP

α-Thrombin has been shown to be a potent activator of angiogenesis in the CAM *in vivo* (Tsopanoglou *et al.*, 1993a). In this system α-thrombin at 6.7 nmol/disc, caused a 64.1 ± 5.7%, $n = 57$, increase in basal collagenous protein biosynthesis (Figure 7a) and a 43.6 ± 5.3%, $n = 5$, $P < 0.01$, increase in vascular density. This latter result rules out the possibility that the morphologically evaluated decrease of angiogenesis caused by SNP might be due to vasoconstriction. α-Thrombin is a vasoconstrictor agent in vascular preparations such as the rabbit aorta (Haver & Namm, 1984; De Blois *et al.*, 1992). Furthermore, L-NMMA which caused an increase in vascular density in the CAM (see above), as well as other arginine analogues, induces contraction of vascular tissue *in vitro* and a dose-related hypertensive response (Moncada & Palmer, 1990).

The combination of α-thrombin with SNP (28 nmol/disc) failed to stimulate angiogenesis in the CAM and resulted in a non significant inhibition of collagenous protein biosynthesis (14.8 ± 8.2% of control, $n = 12$) (Figure 7a). Similar results were obtained when PMA, a PKC activator (Castagna *et al.*, 1982) and a potent angiogenic molecule in the CAM

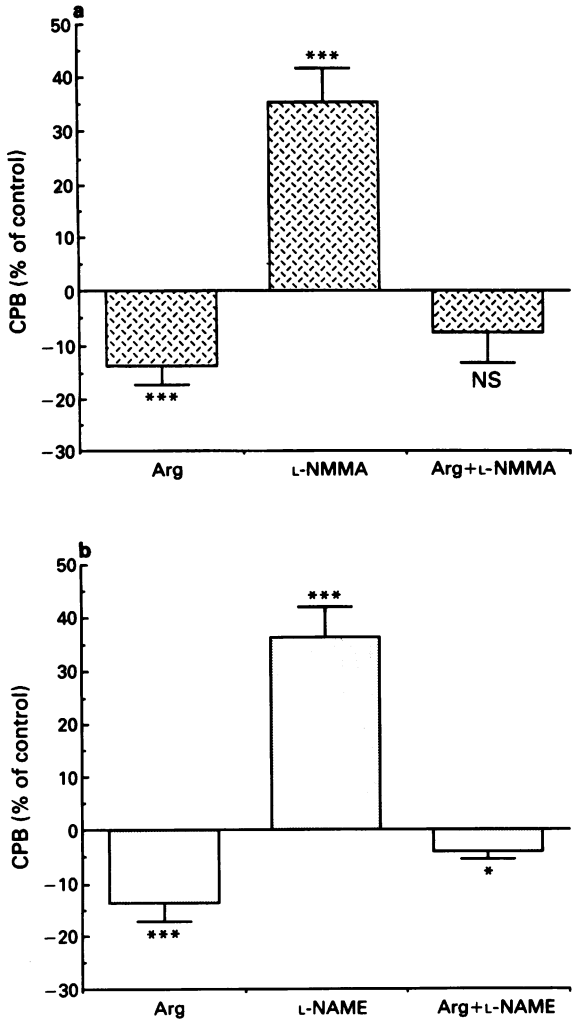


Figure 5 Reversal of the angiogenic effects (expressed as collagenous protein biosynthesis, CPB) of (a) N^G-monomethyl-L-arginine (L-NMMA) (34.2 nmol/disc, $n = 13$) and of (b) N^G-nitro-L-arginine methyl ester (L-NAME) (3.8 nmol/disc, $n = 7$) by N^G-L-arginine (L-Arg) (10.9 nmol/disc, $n = 25$) in the chick chorioallantoic membrane *in vivo*. Results are expressed as mean (± s.e.mean)% of control and are compared by paired t test. Asterisks denote statistical significance of the calculated percentage difference between control and test: $*P < 0.05$ and $***P < 0.01$.

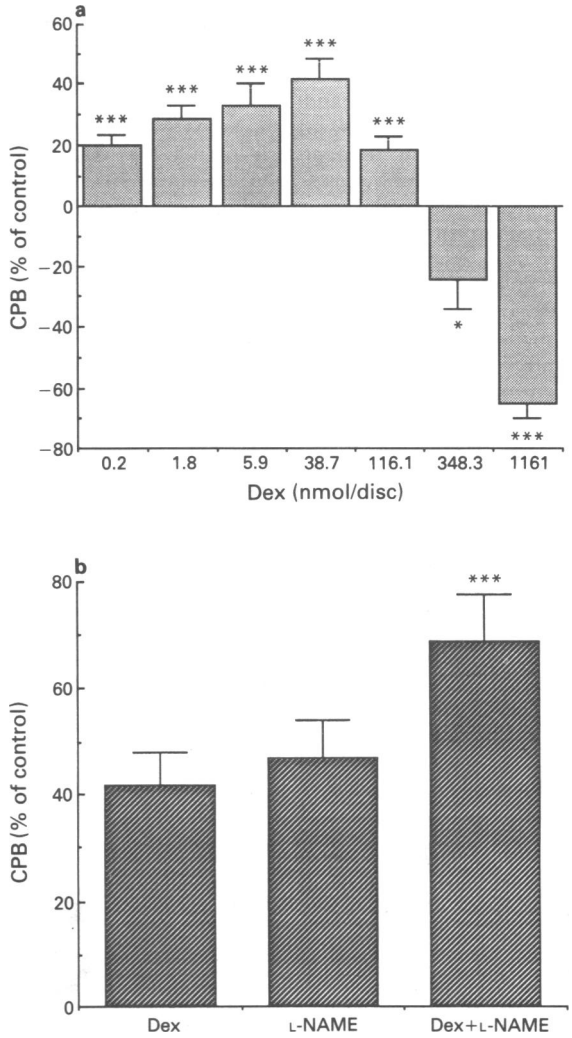


Figure 6 (a) Effect of increasing amounts of dexamethasone (Dex) on angiogenesis in the chick chorioallantoic membrane *in vivo*, expressed as collagenous protein biosynthesis (CPB). Results are expressed as mean (± s.e.mean)% of control ($n = 6$–17) and are compared by paired t test. Asterisks denote statistical significance of the calculated percentage difference between control and test: $*P < 0.05$ and $***P < 0.01$. (b) Effect of the combination of dexamethasone (Dex) (38.7 nmol/disc) with N^G-nitro-L-arginine methyl ester (L-NAME) (9.3 nmol/disc) on angiogenesis in the chick chorioallantoic membrane *in vivo*, expressed as collagenous protein biosynthesis (CPB). Results are expressed as mean (± s.e.mean)% of control and are compared by unpaired t test. $n = 12$ for dexamethasone alone, $n = 12$ for L-NAME alone and $n = 10$ for the combination of dexamethasone and L-NAME (Dex-L-NAME). Asterisks denote a statistical difference from dexamethasone-L-NAME (Dex-L-NAME): $*P < 0.05$.

(Tsopanoglou *et al.*, 1993b) was combined with SNP (Figure 7b). While PMA alone (0.97 nmol/disc) caused a 64.2 ± 15.3% of control, $n = 7$, stimulation in collagenous protein biosynthesis (Figure 7b) and a 38.4 ± 4.5%, $n = 5$, $P < 0.01$, increase in vascular density, its combination with SNP (28 nmol/disc) resulted in a 27 ± 6.4%, $n = 13$, $P < 0.01$, inhibition. The extent of this inhibition again was comparable to that seen with SNP alone (Figure 7b). In these experiments, when either α-thrombin or PMA were combined with SNP, there was no significant difference in vascular density assessed with the Harris-Hooker method (data not shown).

Inhibition of the angiogenic effects of α-thrombin and PMA by SOD

Superoxide dismutase is known to prolong the NO half life by preventing its destruction by the superoxide anion (Gryglewski *et al.*, 1986). In the present study, this agent at 300 i.u. caused a modest but statistically signficant inhibition of collagenous protein biosynthesis (17.8 ± 4.2%, $n = 11$, $P < 0.01$, Figure 8a). Under these conditions there was a non significant decrease in vascular density (7.2 ± 2.5% of control, $n = 4$). When SOD (300 i.u./disc) was combined with α-thrombin (6.7 nmol/disc), it reduced the angiogenic effect of the former and resulted in a small non significant increase (8.6 ± 6.6% of control, $n = 10$) in collagenous protein biosynthesis (Figure 8a). Furthermore, combination of PMA with SOD (300 i.u./disc) abolished the angiogenic effect of the former (0.18 ± 14%, $n = 9$) (Figure 8b). In these experiments, when either α-thrombin or PMA were combined with SOD, there was no significant difference in vascular density assessed with the Harris-Hooker method (data not shown).

These results suggest that prolonging the half life of the endogenous NO, may have drastic effects in the regulation of angiogenesis.

Effects of SNP and of Br-cGMP on relative tube area on the matrigel tube formation assay

When human umbilical vein endothelial cells (HUVECs) were cultured on matrigel in the presence of either SNP

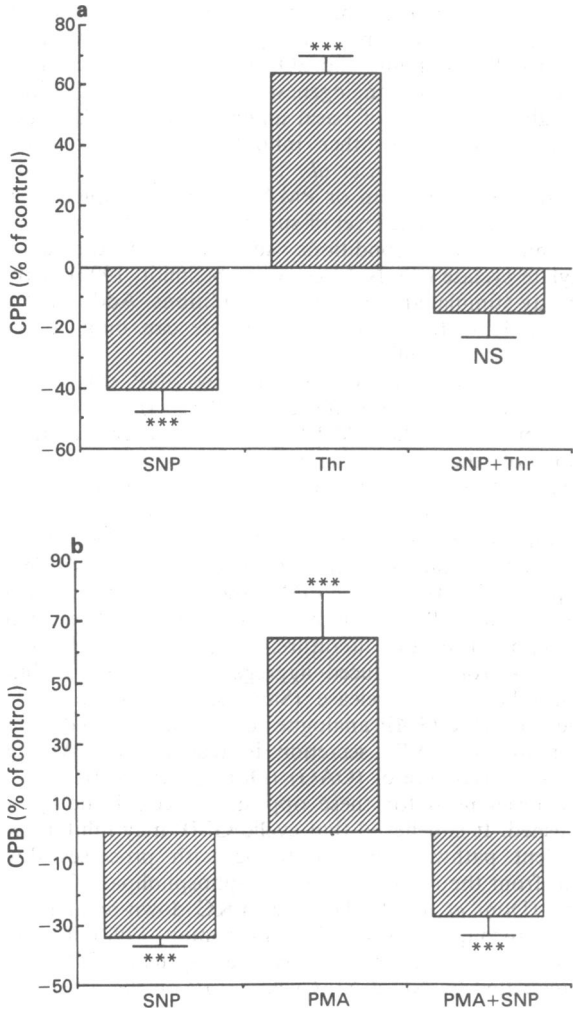


Figure 7 Reversal of the angiogenic effects (expressed as collagenous protein biosynthesis, CPB) of (a) α-thrombin (Thr) (6.7 nmol/disc) and of (b) 4-β-phorbol-12-myristate-13-acetate (PMA) by sodium nitroprusside (SNP) (28 nmol/disc) in the chick chorioallantoic membrane *in vivo*. Results are expressed as mean (± s.e.mean)% of control and are compared by paired *t* test. $n = 57$ for α-thrombin alone, $n = 7$ for PMA alone, $n = 22$ for SNP alone, $n = 12$ for the combination of α-thrombin and SNP (Thr + SNP) and $n = 13$ for the combination of PMA and SNP (PMA + SNP). Asterisks denote statistical significance of the calculated percentage difference between control and test: ***$P < 0.01$.

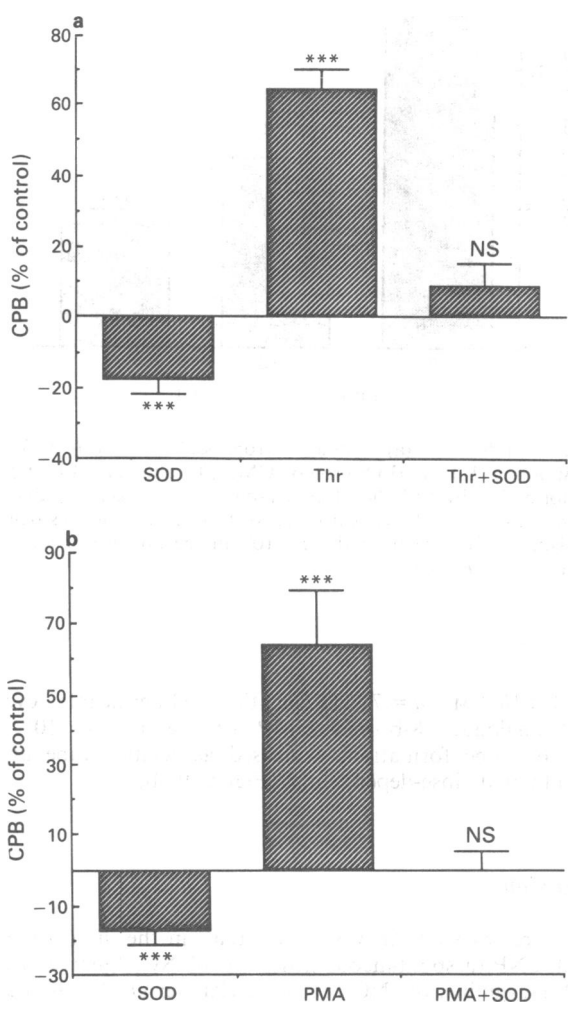


Figure 8 Inhibition of the angiogenic effects (expressed as collagenous protein biosynthesis, CPB) of (a) α-thrombin (Thr) (6.7 nmol/disc) and of (b) 4-β-phorbol-12-myristate-13-acetate (PMA) (0.97 nmol/disc) by superoxide dismutase (SOD) (300 i.u./disc) in the chick chorioallantoic membrane *in vivo*. Results are expressed as mean (± s.e.mean)% of control and are compared by paired *t* test. $n = 57$ for α-thrombin alone, $n = 7$ for PMA alone, $n = 11$ for SOD alone, $n = 10$ for the combination of α-thrombin and SOD (Thr + SOD) and $n = 9$ for the combination of PMA and SOD (PMA + SOD). Asterisks denote statistical significance of the calculated percentatge difference between control and test: ***$P < 0.01$.

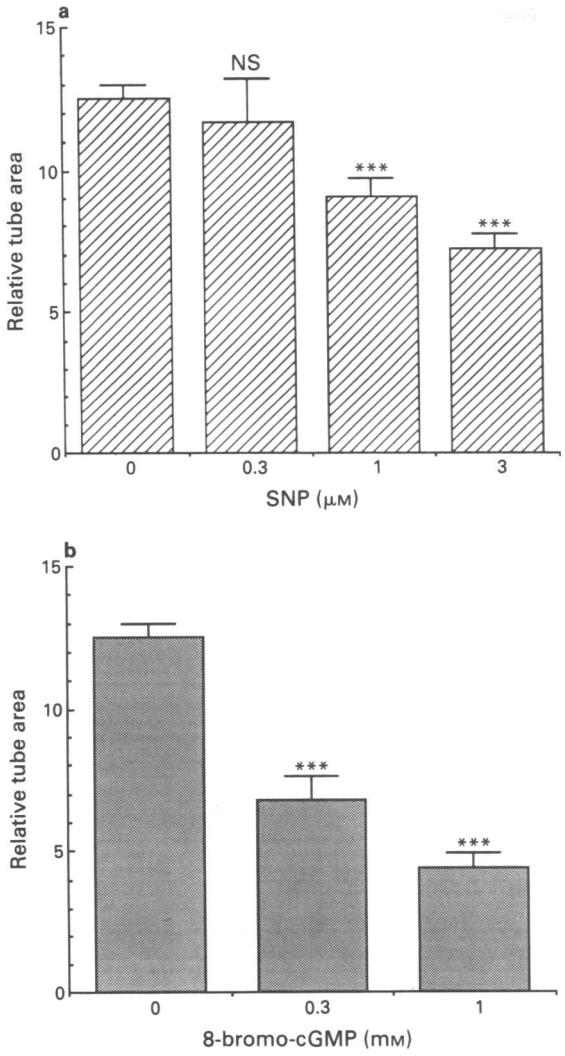


Figure 9 Effect of (a) sodium nitroprusside (SNP) ($0.3-3.0 \times 10^{-6}$ M, $n = 7-11$) and (b) 8-bromo-cGMP (0.3 and 1.0×10^{-3} M) on tube formation by endothelial cells grown on matrigel. Results are expressed as mean (± s.e.mean) relative tube area. Asterisks denote a statistical difference from the control (in the absence of any test substance): $***P < 0.01$.

($0.3-3 \times 10^{-6}$ M, $n = 7-11$) or the cell-permeable cyclic GMP analogue, 8-bromo-cGMP (0.3 and 1.0×10^{-3} M, $n = 4-6$), tube formation, expressed as relative tube area, was inhibited dose-dependently (Figure 9a,b).

Discussion

In the present study it was shown that, in the *in vivo* CAM model, SNP (a spontaneous generator of NO, Ignarro *et al.*, 1981), L-arginine, the NO precursor (Palmer *et al.*, 1988) and SOD which prevents destruction of the endogenous NO (Gryglewski *et al.*, 1986), inhibited angiogenesis. In contrast, the NO-synthase inhibitors L-NMMA and L-NAME (Moncada *et al.*, 1991), caused a significant stimulation in angiogenesis. The effects of both inhibitors of NO synthase on angiogenesis were abolished by L-arginine. This observation coupled with the fact that D-NMMA and D-NAME were ineffective in the CAM, suggests that the angiogenic effects of L-NMMA and L-NAME were mediated through an action on NO synthase. Dexamethasone, an inhibitor of the induction of NO synthase (O'Connor & Moncada, 1991) also stimulated angiogenesis in the CAM. This effect of dexamethasone was potentiated by combination with L-NAME. These observations suggest that increasing or limiting the availability of endogenous NO, inhibits or promotes angiogenesis, respectively. It appears therefore that in the CAM, NO is a suppressor of angiogenesis.

The amounts of L-arginine used in the present study, were three times higher than the respective amounts of L-NAME. L-Arginine, on the other hand, was capable of overcoming the angiogenic effect caused by a three fold higher amount of L-NMMA. Reports in the literature suggest that the dose of L-arginine required to reverse the effects of L-NMMA or L-NAME (Amezcua *et al.*, 1989; Brizzolara *et al.*, 1993) was 3–100 times the amount of the respective inhibitor. In these studies, the effect of the antagonist had been established for a period of time before L-arginine was added. In our experiments the two agents were added simultaneously. In the former case L-arginine conferred its effect by displacement whereas in the latter by competition. When in fact Amezcua *et al.* (1989) added L-arginine at the same time as L-NMMA, L-arginine was much more effective in overcoming the effect of the antagonist.

NO formation appears to be an important regulator of the angiogenic process under basal conditions in the CAM, since L-NAME can stimulate this process by 54%. On the other hand, all three agents which act by increasing the availability of NO (SNP, L-arginine and SOD) could not exceed a 34% inhibitory effect on angiogenesis under basal conditions. Although suppression of basal angiogenesis by NO appears modest compared to other inhibitors such as the PKC inhibitors (Tsopanoglou *et al.*, 1993b), when angiogenesis is promoted by α-thrombin or PMA, NO can completely suppress this process. The level of suppression of angiogenesis by NO under basal conditions suggests that the soluble guanylate cyclase (the NO 'receptor', Schmidt, 1992), activity is already stimulated, under these conditions. Additional NO made available to the system therefore can only confer a limited additional effect.

Stimulation of guanylate cyclase by SNP can only be inferred because of the limitations of the *in vivo* system since measurement of cyclic GMP levels 2 days after the administration of the test materials to the CAM, would be irrelevant. The fact however that SNP can increase cyclic GMP formation *in vitro*, indicates that in the CAM, as in most other systems examined, SNP confers its effects through NO formation and subsequent increase in cyclic GMP levels.

Opposing effects of cyclic GMP, the NO second messenger (Arnold *et al.*, 1977) and thrombin or PMA have already been reported in the literature. In platelets, cyclic GMP inhibits γ-thrombin-induced aggregation through inhibition of thromboxane A_2 release (Sane *et al.*, 1989). SNP or permeable cyclic GMP analogues on the other hand, inhibit aggregation and ATP secretion in response to PMA and 1-oleyl-2-acetyl-glycerol (OAG) (Doni *et al.*, 1991).

The mechanism for these opposing effects is not clearly established. It is believed that cyclic GMP may inhibit PKC-dependent pathways by interfering with processes downstream from the receptor-G protein-phospholipase C effector system (Doni *et al.*, 1991). Since PKC down-regulates NO synthase through phosphorylation (Schmidt, 1992), it appears that there may exist a positive feedback system in NO formation regulated by NO itself. Cyclic GMP on the other had is believed to inhibit γ-thrombin-induced thromboxane A_2 release through interfering with the coupling between phospholipase A_2 and a G protein (Sane *et al.*, 1989). In both reports cited above, irrespective of the underlying mechanism, the net result of SNP or cyclic GMP was to inhibit agonist-induced platelet aggregation an effect which may also be due to a decreased availability of intracellular Ca^{2+} caused by cyclic GMP (Lang & Lewis, 1991).

The above observations, coupled with the results of the present study, indicate that the interaction between elevated cyclic GMP and thrombin or PMA, proceeds in a similar

fashion in platelets and in the CAM. It is therefore likely that NO inhibits angiogenesis at least partly, via inhibition of platelet activation. The question arises as to how could platelets be involved in the promotion of the angiogenic process? Activated platelets may adhere to the vascular endothelium, increase cell permeability and initiate proliferative phenomena through the release of growth factors (Page, 1988) which are well characterized angiogenic molecules (Folkman & Shing, 1992).

Another target for the antiangiogenic effect of NO may be the endothelial cell itself where NO may inhibit (a) proliferation as it does in messangial cells (Garg & Hassid, 1989) or (b) the switch from the quiescent to the activated secretory and migratory phenotype. The fact that both SNP and Br-cGMP inhibited tube formation in the matrigel assay, indicates that NO may affect this latter process.

In an attempt to identify the isoforms of NO synthase responsible for the NO-mediated suppression of angiogenesis, L-NMMA and L-NAME which inhibit both the constitutive and the inducible forms (Moncada *et al.*,1991) and dexamethasone, which inhibits the induction of the latter (O'Connor & Moncada, 1991), were used. The nitro-analogues of L-arginine are more potent than L-NMMA in inhibiting the constitutive (compared to the inducible) NO synthase in brain and endothelial cells (Forstermann *et al.*, 1991). In the present study L-NAME was found to be more potent than L-NMMA in producing an angiogenic effect, suggesting that the constitutive NO synthase was mostly responsible for the NO-mediated antiangiogenic effects in the CAM.

A role for the inducible NO synthase however cannot be excluded since dexamethasone, the most potent inhibitor of induction of this form of the enzyme (O'Connor & Moncada, 1991), at the low end of the dose-range, promoted angiogenesis. This action was potentiated by L-NAME. Synergism between glucocorticoids and inhibitors of NO synthase in a system has been regarded as indicating participation of the inducible enzyme in NO formation (O'Connor & Moncada, 1991). At a higher dose-range, dexamethasone inhibited angiogenesis in agreement with previous observations (Nakamura *et al.*, 1992; Wolff *et al.*, 1992; 1993). In the day 4 shell-less egg, Nakamura *et al.* (1992) reported that dexamethasone produced an avascular zone in the CAM. In addition Wolff *et al.* (1992; 1993) showed that dexamethosone inhibited the *in vitro* C6 astroglial cell-induced microvessel morphogenesis and the vascular density in 9L rat brain tumours (Wolff *et al.*, 1993). Hydrocortisone (unpublished data) as well as cortisone acetate, which is routinely incorporated in the discs to avoid an inflammatory response, are not angiogenic (Maragoudakis *et al.*, 1989). This observation suggests that not all glucocorticoids share the angiogenic activity of dexamethasone. Lack of angiogenic activity in hydrocortisone and cortisone acetate might be due to different potencies of these agents, dexamethasone > hydrocortisone > cortisone acetate, against the inducible NO synthase. It is possible that more than one mechanism accounts for the observed angiogenic effect of dexamethasone in the present study. In addition to inhibiting the direct induction of NO synthase, dexamethasone may confer its action by inhibiting the production of the cytokines interleukines-1, 6 and 8 (Fantuzzi & Ghezzi, 1993). Although some of these cytokines have been reported to be angiogenic (Mahadevan & Lewis, 1989; Hu *et al.*, 1993) they also induce NO synthase (Moncada *et al.*, 1991; Schneeman *et al.*, 1993). Since NO appears to be antiangiogenic, the end effect will depend on the balance between these two opposing actions under the conditions where a particular experiment is conducted.

In conclusion, NO formation appears to be an important determinant of the angiogenic process in the CAM under basal conditions and a powerful inhibitor of the effect of promoters of angiogenesis. The underlying mechanism of the NO effects may involve inhibition of platelet activation. Since angiogenesis-dependent disease states are often accompanied by increased thrombogenesis (Rickles & Edwards, 1983; McDonald, 1991), the proposed mechanism may offer a new insight in the series of events involved in the initiation of pathological angiogenesis and an alternative approach for controlling this process.

The present study was supported by grants from the Ministry of Health and the National Drug Organization. The authors wish to thank Dr M. Markianos for the determination of cGMP levels at the Aeginition Hospital, Athens.

References

AMEZCUA, J.L., PALMER, R.M.J., DE SOUZA, B.M. & MONCADA, S. (1989). Nitric oxide synthesized from L-arginine regulates vascular tone in the coronary circulation of the rabbit. *Br. J. Pharmacol.*, **97**, 1119–1124.

ARNOLD, W.P., MITTAL, C.K., KATSUKI, S. & MURAD, F. (1977). Nitric oxide activates guanylate cyclase and increases 3'-5'-cyclic monophosphate levels in various tissue preparations. *Proc. Natl. Acad. Sci. U.S.A.*, **74**, 3203–3207.

BRIZOLLARA, A.L., CROW, R. & BURNSTOCK, G. (1993). Evidence for the involvement of both ATP and nitric oxide in non-adrenergic, non-cholinergic inhibitory neurotransmission in the rabbit portal vein. *Br. J. Pharmacol.*, **109**, 606–608.

CASTAGNA, M., TAKAI, Y., KAIBUCHI, K., SANO, K., KIKKAWA, U. & NISHIZUKA, Y. (1982). Direct activation of calcium-activated, phospholipid-dependent protein kinase by tumor-promoting phorbol esters. *J. Biol. Chem.*, **257**, 7847–7851.

DE BLOIS, D., DRAPEAU, G., PETITCLERC, E. & MARCEAU, F. (1992). Synergism between the contractile effect of epidermal growth factor and that of des-Arg^9-bradykinin or of α-thrombin in rabbit aortic rings. *Br. J. Pharmacol.*, **105**, 959–967.

DONI, M.G., DEANA, R., PADOIN, E., RUZZENE, M. & ALEXANDRE, A. (1991). Platelet activation by diacylglycerol or ionomycin is inhibited by nitroprusside. *Biochim. Biophys. Acta*, **1094**, 323–329.

FANTUZZI, G. & GHEZZI, P. (1993). Glucocorticoids as cytokine inhibitors: role in neuroendocrine control and therapy of inflammatory diseases. *Mediat. Inflamm.*, **2**, 263–270.

FENTON II, J.W., OFOSU, F.A., MOON, D.G. & MARAGANORE, J.M. (1991). Thrombin structure and function: why thrombin is the primary target for antithrombotics. *Blood Coag. Fibrinolysis*, **2**, 69–75.

FOLKMAN, J. (1985) Tumor angiogenesis. *Adv. Cancer Res.*, **43**, 172–203.

FOLKMAN, J. & SHING, Y. (1992). Angiogenesis. A minireview. *J. Biol. Chem.*, **267**, 10931–10934.

FORSTERMANN, U., SCHMIDT, H.H.H.W., POLLOCK, J.S., SHENG, H., MITCHELL, J.A., WARNER, T.D., NAKANE, M. & MURAD, F. (1991). Commentary. Isoforms of nitric oxide synthase. Characterization and purification from different cell types. *Biochem. Pharmacol.*, **42**, 1849–1857.

GARG, U.C. & HASSID, A. (1989). Inhibition of rat messanghial cell mitogenesis by nitric oxide-generating vasodilators. *Am. J. Physiol.*, **257**, F60–F66.

GRANT, D.S., TASHIRO, K.I., SEGUI-REAL, B., YAMADA, Y., MARTIN, G.R. & KLEINMAN, H.K. (1989). Two different laminin domains mediate the differentiation of human endothelial cells into capillary-like structures in vitro. *Cell*, **58**, 933–943.

GRYGLEWSKI, R.J., PALMER, R.M.J. & MONCADA, S. (1986). Superoxide anion is involved in the breakdown of endothelium-derived vascular relaxing factor. *Nature*, **320**, 454–456.

HARRIS-HOOKER, S.A., GAJDUSEC, C.M., WIGHT, T.N. & SCHWARTZ, S.M. (1983). Neovascular response induced by cultured aortic endothelial cells. *J. Cell Physiol.*, **114**, 302–310.

HAVER, V.M. & NAMM, D.H. (1984). Characterization of the thrombin-induced contraction of vascular smooth muscle. *Blood Vessels*, **21**, 53–63.

HIBBS, J.B., TAINTOR, R.R., VAVRIN, Z. & RACHLIN, E.M. (1988). Nitric oxide: a cytotoxic activated macrophage effector molecule. *Biochem. Biophys. Res. Commun.*, **157**, 87–94.

HU, D.E., HORI, Y. & FAN, T.P. (1983). Interleukin 8 stimulates angiogenesis in rats. *Inflammation*, **17**, 135–143.

IGNARRO, L.J., LIPPTON, H., EDWARDS, J.C., BARICOS, W.H., HYMAN, A.L., KADOWITZ, P.J. & GRUETTER, C.A. (1981). Mechanism of vascular smooth muscle relaxation by organic nitrates, nitrites, nitroprusside and nitric oxide: evidence for the involvement of S-nitrosothiols as active intermediates. *J. Pharmacol. Exp. Ther.*, **218**, 739–749.

JAFFE, E.A., GRULICH, J., WEKSLER, B.B., HAMPEL, G. & WATANABE, K. (1987). Correlation between thrombin-induced prostacyclin production and inositol triphosphate and cytosolic free calcium levels in cultured human endothelial cells. *J. Biol. Chem.*, **262**, 8557–8565.

KUBOTA, Y., KLEINMAN, H.K., MARTIN, G.R. & LAWLEY, T.J. (1988). The role of laminin and basement membrane in the morphological differentiation of human endothelial cells into capillary-like structures. *J. Cell Biol.*, **107**, 1589–1598.

LANG, D. & LEWIS, M.J. (1991). Inhibition of inositol 1,4,5-trisphosphate formation by cyclic GMP in cultured aortic endothelial cells of the pig. *Br. J Pharmacol.*, **102**, 277–281.

LOWENSTEIN, C.J. & SNYDER, S.H. (1992). Nitric oxide, a novel biologic messenger. *Cell*, **70**, 705–707.

MAHADEVAN, V., HART, I.R. & LEWIS, G.P. (1989). Factors influencing blood supply in wound granuloma quantitated by a new *in vivo* technique. *Cancer Res.*, **49**, 415–419.

MARAGOUDAKIS, M.E. (1993). Angiogenesis. In *Annual of Cardiac Surgery*, ed. Yakoub, M. & Pepper, J., pp. 13–19. London: Current Science, Ltd.

MARAGOUDAKIS, M.E., SARMONIKA, M. & PANOUTSAKOPOULOU, M. (1988). Rate of basement membrane biosynthesis as an index to angiogenesis. *Tissue Cell*, **20**, 531–539.

MARAGOUDAKIS, M.E., SARMONIKA, M. & PANOUTSAKOPOULOU, M. (1989). Antiangiogenic action of heparin plus cortisone is associated with decreased collagenous protein synthesis in the chick chorioallantoic membrane system. *J. Pharmacol. Exp. Ther.*, **251**, 679–682.

MARLETTA, M.A., YOON, P.S., IYENKAR, R., LEAF, C.D. & WISHNIK, J.S. (1988). Macrophage oxidation of L-arginine to nitrite and nitrate: nitric oxide is an intermediate. *Biochemistry*, **27**, 8706–8711.

McDONALD, C.J. (1991). Cardiovascular complications of psoriasis. In *Psoriasis*. ed. Roenigk, H.H. & Mailbach, H.J. pp. 97–111. New York-Basel-Hong Kong: Marcel Dekker Inc.

MONCADA, S. & PALMER, R.M.J. (1990). In *Nitric Oxide from L-Arginine: A Bioregulatory System*. ed. Moncada, S. & Higgs, E.A. pp. 17–31. Amsterdam: Elsevier.

MONCADA, S., PALMER, R.M.J. & HIGGS, E.A. (1991). Nitric oxide: physiology, pathophysiology and pharmacology. *Pharmacol. Rev.*, **43**, 109–142.

NAKAKI, T., MAKAYAMA, M. & KATO, R. (1990). Inhibition by nitric oxide and nitric oxide-producing vasodilators of DNA synthesis in vascular smooth muscle cells. *Eur. J. Pharmacol.*, **189**, 347–353.

NAKAMURA, O., UEKI, K., HIBI, T., SHITARA, N., MATSUTANI, M., TAKAKURA, K. & OIKAWA, T. (1992). Inhibition of neovascularization and tumor growth by dexamethasone. *Brain Nerve*, **44**, 37–41.

O'CONNOR, K.J. & MONCADA, S. (1991). Glucocorticoids inhibit the induction of nitric oxide synthase and the related cell damage in adenocarcinoma cells. *Biochim. Biophys. Acta*, **1097**, 227–231.

PAGE, C.P. (1988). The involvement of platelets in non-thrombotic processes. *Trends Pharmacol Sci.*, **9**, 66–71.

PALMER, R.M.J., ASHTON, D.S. & MONCADA, S. (1988). Vascular endothelial cells synthesize nitric oxide from L-arginine. *Nature*, **333**, 664–666.

PIPILI-SYNETOS, E., SAKKOULA, E. & MARAGOUDAKIS, M.E. (1993). Nitric oxide is involved in the regulation of angiogenesis. *Br. J. Pharmacol.*, **108**, 855–857.

RADOMSKI, M.W., PALMER, R.M.J. & MONCADA, S. (1990). An L-arginine/nitric oxide pathway present in human platelets regulates aggregation. *Proc. Natl. Acad. Sci. U.S.A.*, **87**, 5193–5197.

RICKLES, F.R. & EDWARDS, R.L. (1983). Activation of blood coagulation in cancer: Trousseau's syndrome revised. *Blood*, **62**, 14–31.

RINK, T.J., SANCHEZ, A. & HALLAM, T.J. (1983). Diacylglycerol and phorbol ester stimulate secretion without raising cytoplasmic free calcium in human platelets. *Nature*, **305**, 317–319.

SANE, D.C., BIELAWSKA, A., GREENBERG, C.S. & HANNUN, Y.A. (1989). Cyclic GMP analogs inhibit gamma thrombin-induced arachidonic acid release in human platelets. *Biochem. Biophys. Res. Commun.*, **165**, 708–714.

SANO, K., TAKAI, Y., YAMANISHI, J. & NISHIZUKA, Y. (1983). A role of calcium-activated phospholipid-dependent protein kinase in human platelet activation. *J. Biol. Chem.*, **258**, 2010–2013.

SCHMIDT, H.H.H.W. (1992). NO·, CO and ·OH. Endogenous soluble guanylate cyclase-activating factors. *FEBS Lett.*, **307**, 102–107.

SCHNEEMAN, M., SCHOEDON, G., FREI, K. & SCHAFFNER, A. (1993). Immunovascular communication. Activation and destruction of murine endothelial cell nitric oxide synthase by cytokines. *Immunol. Lett.*, **35**, 159–162.

SNYDER, S.H. & BREDT, D.S. (1992). Biological roles of nitric oxide. *Scientific American*, May, 28–35.

TIMPL, R., RHODE, H., GEHRON ROBEY, P., RENNARD, S.I., FOIDART, J.M. & MARTIN, G.R. (1979). Laminin – a glycoprotein from basement membranes. *J. Biol. Chem.*, **254**, 9933–9937.

TSOPANOGLOU, N.E., PIPILI-SYNETOS, E. & MARAGOUDAKIS, M.E. (1993a). Thrombin promotes angiogenesis by a mechanism independent of fibrin formation. *Am. J. Physiol.*, **264** (Cell Physiol. 33), C1302–C1307.

TSOPANOGLOU, N.E., PIPILI-SYNETOS, E. & MARAGOUDAKIS, M.E. (1993b). Protein kinase C involvement in the regulation of angiogenesis. *J. Vasc. Res.*, (in press).

WOLFF, J.E.A., LATERRA, J. & GOLDSTEIN, G.W. (1992). Steroid inhibition of neural microvessel morphogenesis in vitro: receptor-mediation and astroglial-dependence. *J. Neurochem.*, **58**, 1023–1032.

WOLFF, J.E.A., GUERIN, C., LATERRA, J., BRESSLER, J., INDURTI, R.R., BREM, H. & GOLDSTEIJN, G.W. (1993). Dexamethasone reduces vascular density and plasminogen activator activity in 9L rat brain tumors. *Brain Res.*, **604**, 79–85.

(Received August 2, 1993
Revised October 22, 1993
Accepted November 4, 1993)

Br. J. Pharmacol. (1994), **111**, 903–905

© Macmillan Press Ltd, 1994

Specific inhibition of Ca-activated K channels in red cells by selected dihydropyridine derivatives

[1]J.C. Ellory, S.J. Culliford, P.A. Smith, [2]*the late M.W. Wolowyk & *E.E. Knaus

Department of Physiology, University of Oxford, Parks Road, Oxford OX1 3PT and *Faculty of Pharmacy, University of Alberta, Edmonton, Alberta, Canada T6G 2N8

1 Thirty two dihydropyridine derivatives were screened as potential inhibitors of the Ca-activated K-channel in human red cells.

2 Three derivatives (26, 29, 32 see Tables 1 and 2) with high activity were then characterized in detail, and also tested against the smooth muscle Ca-channel and shown to have varying potencies.

3 One of the more potent derivatives (32) and nitrendipine were also tested on the Ca-activated K-channel, Maxi-K channel, from mouse pancreatic beta-cells.

4 We conclude from our results that it may be possible to develop selective Gardos-channel inhibitors based on these molecules, which may be of benefit in the treatment of sickle cell disease.

Keywords: Dihydropyridine; gardos channel; maxi-K channel; L-type Ca-channel; erythrocyte; β-cell; ileal smooth muscle

Introduction

It has been shown recently that dihydropyridines (DHP) not only inhibit L-type calcium channels, but are potent antagonists of the Ca-activated K-channel (Gardos-channel, Gardos, 1958) in human red cells (Kaji, 1990; Ellory *et al.*, 1992). In particular, nitrendipine is effective at 100 nM as a blocker of this channel. This finding is of potential therapeutic importance in sickle cell disease, where repeated oxygenation and deoxygenation of HbSS red cells raise intracellular calcium and activate the Gardos-channel causing significant K^+ loss, cell shrinkage, an increase in MCHC, and an enhanced probability of the formation of irreversibly sickled cells.

An obvious disadvantage of DHP derivatives in sickle cell therapy is their direct inhibition of L-type Ca^{2+}-channels in other tissues, especially heart and vascular smooth muscle. We have therefore investigated the potency of a number of DHP derivatives against the red cell Gardos-channel, the Maxi-K channel in pancreatic β-cells and the L-type Ca^{2+}-channel in smooth muscle in the hope of identifying specific structural characteristics which would allow a greater functional separation of activity of these derivatives. Initially 32 molecules based on the substituted DHP nitrendipine were assayed at a single dose (5 μM) against the red cell Gardos-channel. Subsequently, three active molecules (**26, 29, 32**) were selected and their IC_{50} measured both as inhibitors of Ca-dependent smooth muscle contraction (ileal muscle), and as inhibitors of the red cell Gardos channel. Finally, the ability of both nitrendipine (10 μM) and molecule number **32** (10 μM) to block the classical Maxi-K channel in pancreatic β-cells was tested. The results indicate selective differences in the pharmacology which may form a basis for the development of more specific Gardos-channel inhibitors in the future.

Methods

Erythrocytes

Blood (HbAA) from three healthy donors was taken into heparin and then washed three time by centrifugation (5 min at 3,000 *g*) in MOPS-buffered saline (MBS) composition (mM): NaCl 134.4, KCl 5, $MgCl_2$ 0.4, MOPS 15, and glucose 10, pH 7.4).

K^+ ($^{86}Rb^+$) flux measurements

The flux measurements were performed in the low-K^+ washing solution (as above) as previously described (Ellory *et al.*, 1992). Briefly, the final samples had a volume of 1.0 ml and a haematocrit of approximately 5%. Each sample contained ouabain (0.1 mM), bumetanide (0.1 mM) and $CaCl_2$ (0.4 mM). The nitrendipine derivatives were added to give the required final concentration of 5 μM, and the samples incubated at 37°C for 10 min. The Gardos K^+-channel was activated by the addition of the calcium ionophore, ionomycin and for experimental convenience, K^+ influx was estimated from the uptake of $^{86}Rb^+$ over a 60s incubation period. The flux was terminated by the addition of 300 μl of quinine (0.87 mM in ice-cold MBS), then four 300 μl aliquots were transferred immediately to microcentrifuge tubes containing quinine (0.1 mM in MBS) layered over dibutylphthalate. The tubes were then centrifuged (14000 *g* for 10 s) to form a pellet of red cells below the oil and the supernatant removed. The tubes were then rinsed three times with water and the dibutylphthalate aspirated. The red cells were then lysed with 0.5 ml Triton-X-100 (0.1% v/v) and deproteinised with 0.5 ml TCA (5% w/v). The $^{86}Rb^+$ in the supernatant was then measured by Cerenkov counting.

Calcium channel antagonist assay

The calcium channel antagonist activities of molecules **26, 29** and **32** were determined as the concentration required to produce 50% of the muscarinic receptor-mediated (carbachol, 1.6×10^{-7} M) Ca^{2+}-dependent contraction of guinea-pig ileal longitudinal smooth muscle. This was measured according to the procedure described by Dagnino *et al.* (1987).

Measurement of block of Maxi-K channels from pancreatic β-cells

Pancreatic β-cells possess Ca^{2+}-activated K^+-channels with biophysical properties highly similar to the classical Maxi-K type of K^+-channel (Latorre *et al.*, 1989; Ashcroft & Rors-

[1] Author for correspondence.

[2] Dedicated to the memory of Professor Michael W. Wolowyk, who died on January 31, 1992.

man, 1989). The actions of molecule **32**, nitrendipine and nifedipine were tested on the activity of Maxi-K channels by the patch-clamp technique. Single-channel activity of the Maxi-K channel was recorded in outside-out membrane patches excised from pancreatic β-cells, isolated from mouse pancreas, using the methods described by Bokvist *et al.* (1990a,b). The pipette (intracellular) solution contained (in mM): KCl 140, $MgCl_2$ 1, $CaCl_2$ 0.2, MGATP 3 and K-HEPES 10 (pH 7.2). The bath (extracellular) solution contained (in mM) NaCl 138, KCl 5.6, $MgCl_2$ 1.2, $CaCl_2$ 2.6 and Na-HEPES 10 (pH 7.4). The membrane potential was held at 0 mV and experiments conducted at room temperature. Under these conditions only potassium currents flowing through the Maxi-K type of K-channels are recorded (Bokvist *et al.*, 1990b). The effect of the dihydropyridine on channel activity was determined by normalizing the channel activity in the test solution (NP) to the average of its value in the control solution before and after exposure to the dihydropyridine.

Materials

$^{86}RbCl$ was supplied by NEN (UK). Ouabain, nifedipine and bumetanide were from Sigma Chemical Co. Nitrendipine was a gift from Bayer. The 1,4-dihydropyridyl derivatives (**1–32**) were prepared using the literature procedures as follows: **8–10**, **16** (Dagnino *et al.*, 1986); **1–5**, **18**, **20**, **22** (Akula *et al.*, 1989); **26–27**, **29**, **31–32** (Wynn *et al.*, 1988); **6**, **11–13** (Akula *et al.*, 1990a); **7**, **14** (Akula *et al.*, 1990b); **19**, **21** (Ramesh *et al.*, 1987); **15**, **17**, **23–25**, **28**, **30** (Knaus & Wolowyk, unpublished results). Ionomycin and charybdotoxin were from Calbiochem Corporation (CA, U.S.A.). All other reagents were of analytical grade.

Results

Table 1 presents the results of experiments screening 32 dihydropyridine derivatives at a single dose (5 μM) as inhibitors of the Ca-activated K^+ efflux from normal (HbAA) red cells. Molecules **26**, **29**, **32** were then selected for detailed study, and dose-response curves generated for inhibition of both the red cell Gardos-channel, and an ileal smooth muscle preparation. The results of these experiments are presented in Table 2. It can be seen that differences in potency against the two systems were found. Thus, **29** was more potent against the Gardos-channel than the L-type Ca-channel; conversely **32** was a much more effective inhibitor of the L-type Ca-channel, than against the red cell Gardos-channel.

Activity of Maxi-K channels could be readily recorded, single-channel current amplitude 5 ± 0.2 pA, in outside-out patches held at a membrane potential of 0 mV. Application of 100 nM charybdotoxin slowly and reversibly reduced the activity of the channel to 46 ± 8% of control activity ($n = 6$). In all 9 patches tested, external 1 mM TEA produced a rapid, reversible and almost complete block of Maxi-K channel activity ($K_d = 140$ μM, Bokvist *et al.*, 1990b). Molecule **32** (10 μM) had no effect on the activity of the Maxi-K channel (activity 106 ± 7% of control, $n = 8$) whereas 10 μM nitrendipine increased the activity of the Maxi-K channel to 120 ± 7% of its control value ($n = 9$, $P = 0.02$). In two patches tested, 10 μM nifedipine which blocks the Gardos-channel with a K_d of 4 μM (Kaji, 1990) was without effect on the activity of the Maxi-K channel.

Drugs **29**, **32** and nitrendipine were also tested against HbSS cells and no significant differences in the IC_{50} between normal and HbSS cells were found.

Table 1 The inhibition of the Gardos channel in normal HbAA erythrocytes by derivatives of nitrendipine at a concentration of 5 μM

No.	R^1	R^2	R^3	*% inhibition*
1	ethyl	cyclohexyl	2-pyridyl	− 4.6 ± 2.6
2	cyclohexyl	cyclohexyl	2-pyridyl	13.7 ± 7.5
3	*t*-butyl	cyclohexyl	2-pyridyl	− 10.8 ± 4.1
4	methoxyethyl	cyclohexyl	2-pyridyl	− 3.8 ± 3.5
5	isopropyl	cyclopentyl	2-pyridyl	3.7 ± 4.0
6	isopropyl	4-chlorophenylethyl	2-pyridyl	8.4 ± 3.2
7	isopropyl	2-furanylmethyl	2-pyridyl	− 0.7 ± 5.9
8	isobutyl	methyl	2-pyridyl	3.1 ± 7.0
9	methyl	methyl	3-pyridyl	9.8 ± 6.8
10	isobutyl	isobutyl	3-pyridyl	− 0.2 ± 3.1
11	isopropyl	4-fluorophenylethyl	3-pyridyl	− 6.6 ± 7.4
12	isopropyl	4-chlorophenylethyl	3-pyridyl	8.1 ± 5.6
13	isopropyl	4-methoxyphenylethyl	3-pyridyl	2.6 ± 1.6
14	isopropyl	2-furanylmethyl	3-pyridyl	43.9 ± 3.5
15	ethyl	2-cyanoethyl	3-pyridyl	− 16.8 ± 13
16	isopropyl	isopropyl	3-pyridyl	− 14.9 ± 7.3
17	methyl	2-cyanoethyl	3-pyridyl	− 14.8 ± 17
18	cyclohexyl	cyclohexyl	3-pyridyl	− 14.1 ± 12.5
19	*t*-butyl	t-butyl	3-pyridyl	− 3.4 ± 6.5
20	methyl	cyclohexyl	3-pyridyl	12.8 ± 9.8
21	methyl	t-butyl	3-pyridyl	− 14.3 ± 17.9
22	cyclohexyl	cyclohexyl	4-pyridyl	− 6.3 ± 14.9
23	isopropyl	3-pyridylmethyl	2-nitrophenyl	− 15.9 ± 18.3
24	isopropyl	3-pyridylmethyl	3-nitrophenyl	− 4.8 ± 8.1
25	ethyl	ethyl	phenyl	43.2 ± 1.7
26	methyl	methyl	cyclohexyl	97.0 ± 0.8
27	methyl	methyl	methyl	2.5 ± 4.0
28	methyl[a]	methyl	H	0.5 ± 4.3
29	methyl	methyl	4-nitrophenyl	98.7 ± 0.7
30	methyl[b]	methyl	H	1.8 ± 3.5
31	methyl[c]	methyl	phenyl	24.4 ± 3.0
32	methyl	methyl	phenyl	82.5 ± 3.1

The compounds in this table have the general structure (1) except for (a) which is a mixture of compounds of general structure (1) and (2) (1:1 ratio, $R^1 = R^2 = Me$, $R^3 = H$), (b) has general structure (2) ($R^1 = R^2 = Me$, $R^3 = H$) and (c) has general structure (2) ($R^1 = R^2 = Me$, $R^3 = Ph$).

Table 2 Comparison of calcium channel antagonist activity and Gardos channel inhibition of selected derivatives

No.	R^1	R^2	R^3	*Calcium channel antagonist activity* (ID_{50}, M)	*Gardos channel inhibition* (ID_{50}, M)
26	methyl	methyl	cyclohexyl	$3.05 \pm 1.07 \times 10^{-7}$	$3.22 \pm 0.74 \times 10^{-7}$
29	methyl	methyl	4-nitrophenyl	$1.21 \pm 0.20 \times 10^{-6}$	$2.29 \pm 0.90 \times 10^{-7}$
32	methyl	methyl	phenyl	$2.61 \pm 0.04 \times 10^{-8}$	$1.44 \pm 0.51 \times 10^{-6}$

The compounds in this table have the general structure (1) shown in footnote to Table 1.

Discussion

A number of structure-activity correlations were observed that produce superior Gardos-channel inhibition, these include: (1) The 1,4-dihydropyridine ring is essential since 3,5-dimethyl 1,4-dihydro-2,6-dimethyl-4-phenyl-3,5-pyridinedicarboxylate (**32**) is more active than the aromatic pyridine compound 3,5-dimethyl 2,6-dimethyl-4-phenyl-3,5-pyridinedicarboxylate **31**; (2) Increasing the size of the alkyl ester substituents decreases activity since the 3,5-dimethyl compound **32** ($R^1 = R^2 = Me$) was more potent than the 3,5-diethyl analogue **25** ($R^1 = R^2 = Et$); (3) Compounds having a C-4 cycloalkyl **26** (R^3 = cyclohexyl), aryl **29** (R^3 = 4-nitrophenyl) or phenyl substituent (R^3 = phenyl) as in **32** provided more potent activity than compounds having a pyridyl substituent such as **9** (R^3 = 3-pyridyl); (4) The nature of the C-4 substituent appears to be a selective determinant of both L-type Ca-channel and Gardos-channel antagonism since the 4-cyclohexyl compound **26** was equipotent in both assays, whereas the 4-nitrophenyl compound **29** was more active as a Gardos-channel inhibitor than as a L-type Ca-channel antagonist, whilst the 4-phenyl compound, **32**, was a more potent antagonist of the L-type Ca-channel then the Gardos-channel. Both compound **32** and nifedipine, potent antagonists of both the L-type Ca-channel and the Gardos-channel were without effect on the Maxi-K channel suggesting that nonspecific block of Maxi-K in other tissues by these compounds is unlikely. We have not attempted to explain the surprising ability of nitrendipine to activate the Maxi-K channel, a phenomenon that warrants further investigation.

These structure-activity correlations indicate that 3,5-dimethyl 1,4-dihydro-2,6-dimethyl-4-(4-nitrophenyl)-3,5-pyridinedicarboxylate (**29**) is a good 'lead component' for further structural manipulation in the design of a selective 1,4-dihydropyridine antagonist for the Gardos-channel.

Our original hypothesis in screening these molecules was that the nitro group may be less important in the context of Gardos-channel inhibition than in blocking the L-type Ca-channel. This idea, however, is not completely borne out by the results, since compound **29** with the 4-nitrophenyl group proved more useful than the simple unsubstituted phenyl compound **32**.

These results confirm earlier experiments indicating that DHP derivatives are effective Gardos-channel inhibitors. They also offer prospects for the development of modifications to these molecules to increase the efficacy of red cell Gardos-channel inhibition whilst avoiding significant effects on L-type Ca-channels and Maxi-K channels. The final goal of therapy for sickle cell disease relies on the development of more specific inhibitors of the Gardos-channel which would avoid the hypotensive effects of the DHP class of drugs.

We are grateful for financial support from the Medical Research Council of Canada (Grant no. MT-8892) (to E.E.K.) and the Wellcome Trust.

References

AKULA, M.R., MATOWE, W.C., WOLOWYK, M.W. & KNAUS, E.E. (1989). Synthesis and calcium channel antagonist activity of alkyl cycloalkyl esters of nifedipine containing pyridinyl substituents. *Drug Design Del.*, **5**, 117–123.

AKULA, M.R., MATOWE, W.C., WOLOWYK, M.W. & KNAUS, E.E. (1990a). Synthesis and calcium channel antagonist activity of nifedipine analogues containing 4-pyridyl and 3-arylethyloxycarbonyl substituents. *Drug Design Del.*, **7**, 11–17.

AKULA, M.R., MATOWE, W.C., WOLOWYK, M.W. & KNAUS, E.E. (1990b). Synthesis and calcium channel antagonist activity of 3-arylmethyl 5-isopropyl 1,4-dihydro-2,6-dimethyl-4-(pyridyl)-3,5-pyridinedicarboxylates. *Pharmacol. Res.*, **7**, 919–922.

ASHCROFT, F.M. & RORSMAN, P. (1989). Electrophysiology of the pancreatic β-cell. *Pro. Biol. Mol. Res.*, **54**, 87–144.

BOKVIST, K., RORSMAN, P. & SMITH, P.A. (1990a). Effects of external tetraethylammonium ions and quinine on delayed rectifying K-channels in mouse pancreatic β-cells. *J. Physiol.*, **423**, 311–325.

BOKVIST, K., RORSMAN, P. & SMITH, P.A. (1990b). Block of ATP-regulated and Ca-activated K-channels in mouse pancreatic β-cells by external tetraethylammonium and quinine. *J. Physiol.*, **423**, 327–342.

DAGNINO, L., LI-KWON-KEN, M.C., WOLOWYK, M.W., WYNN, H., TRIGGLE, C.R. & KNAUS, E.E. (1986). Synthesis and calcium channel antagonist activity of dialkyl 1,4-dihydro-2,6-dimethyl-4-(pyridinyl)-3,5-pyridinedicarboxylates. *J. Med. Chem.*, **29**, 2524–2529.

DAGNINO, L., LI-KWON-KEN, M.C., WYNN, H., WOLOWYK, M.W., TRIGGLE, C.R. & KNAUS, E.E. (1987). Synthesis and calcium channel antagonist activity of dialkyl 4-(dihydropyridinyl)1,4-dihydro-2,6-dimethyl-3,5-pyridinedicarboxylates. *J. Med. Chem.*, **30**, 640–646.

ELLORY, J.C., KIRK, K., CULLIFORD, S.J., NASH, G.B. & STUART, J. (1992). Nitrendipine is a potent inhibitor of the Ca^{2+}-activated K^+ channel of human erythrocytes. *FEBS Lett.*, **296**, 219–221.

GARDOS, G. (1958). The function of calcium in the potassium permeability of human erythrocytes. *Biochem. Biophys. Acta*, **30**, 653–654.

KAJI, D.M. (1990). Nifedipine inhibits calcium activated K transport in human erythrocytes. *Am. J. Physiol.*, **259**, C332–C339.

LATORRE, R., OBERHAUSER, A., LABARCA, P. & ALVAREZ, O. (1989). Varieties of calcium-activated potassium channels. *Annu. Rev. Physiol.*, **51**, 385–399.

RAMESH, M., MATOWE, W.C., WOLOWYK, M.W. & KNAUS, E.E. (1987). Synthesis and calcium channel antagonist activity of alkyl *t*-butyl esters of nifedipine analogues containing pyridinyl substituents. *Drug Design Del.*, **2**, 79–89.

WYNN, H., RAMESH, M., MATOWE, W.C., WOLOWYK, M.W & KNAUS, E.E. (1988). Synthesis and calcium channel antagonist activity of dihydropyridyl analogues of nifedipine. *Drug Design Del.*, **3**, 245–256.

(Received September 14, 1993
Accepted November 5, 1993)

Br. J. Pharmacol. (1994), **111**, 906–912 © Macmillan Press Ltd, 1994

Pharmacological characterization of cinnamophilin, a novel dual inhibitor of thromboxane synthase and thromboxane A_2 receptor

[1]Sheu-Meei Yu, *Tian-Shung Wu & Che-Ming Teng

Department of Pharmacology, Chang Gung Medical College, Kwei-San, Tao-Yuan and *Department of Chemistry, National Cheng-Kong University, Tainan and Pharmacological Institute, College of Medicine, National Taiwan University, Taipei, Taiwan

1 The pharmacological effects of cinnamophilin, a new lignan, isolated from *Cinnamomum philippinense*, was determined *in vitro* in human platelet, rat isolated aorta and guinea-pig isolated trachea and *in vivo* in mice and guinea-pigs.

2 Cinnamophilin inhibited dose-dependently human platelet-rich plasma (PRP) aggregation induced by arachidonic acid (AA), collagen and U-46619 with IC_{50} of 5.0 ± 0.4, 5.6 ± 0.6 and $3.0 \pm 0.4\,\mu M$, respectively. The second wave of ADP- or adrenaline-induced platelet aggregation was inhibited by cinnamophilin, while the first wave was only slightly inhibited by cinnamophilin above $30\,\mu M$.

3 Cinnamophilin was found to be a thromboxane A_2 (TXA_2) receptor blocking agent in human platelet, rat aorta and guinea-pig trachea as revealed by its competitive antagonism of U-46619-induced aggregation of human-PRP, contraction of rat aortic rings and guinea-pig tracheal rings with pA_2 values of 7.3 ± 0.2, 6.3 ± 0.1 and 5.2 ± 0.2, respectively.

4 [^{3}H]-inositol monophosphate formation and the rise of intracellular Ca^{2+} caused by U-46619 in human platelet was suppressed by cinnamophilin ($10\,\mu M$).

5 Cinnamophilin induced a dose-dependent inhibition of thromboxane B_2 (TXB_2) formation, while the prostaglandin E_2 (PGE_2) formation was increased. Cinnamophilin did not affect unstimulated platelet adenosine 3':5'-cyclic monophosphate (cyclic AMP) levels. When the platelets were challenged with AA, a dose-dependent rise in cyclic AMP was observed. Dazoxiben (a pure TX synthase inhibitor) and SQ 29548 (a pure TXA_2 receptor antagonist) did not affect cyclic AMP levels in AA-treated platelets.

6 A high concentration of cinnamophilin ($100\,\mu M$), failed to attenuate the contractile response of rat aorta to endothelin-1, angiotensin II, 5-hydroxytryptamine or noradrenaline. Contraction of tracheal rings induced by histamine, carbachol or KCl was also not inhibited by cinnamophilin ($100\,\mu M$).

7 Thirty min after intraperitoneal (i.p.) administration of cinnamophilin ($100\,\mu g\,kg^{-1}$), tail bleeding time of mice was prolonged more markedly than with indomethacin, dazoxiben or SQ 29548.

8 Intravenous administration of AA ($50\,\mu g\,kg^{-1}$) to guinea-pig induced bronchoconstriction. Cinnamophilin ($0.1\,mg\,kg^{-1}$, i.v.) was administered 1 min before AA, the bronchoconstriction response to AA was abolished.

9 It is concluded that cinnamophilin is a novel dual TX synthase inhibitor and TXA_2 receptor antagonist and that it may be a useful tool for the investigation and treatment of diseases involving TXA_2 disorders.

Keywords: Cinnamophilin; thromboxane A_2 (TXA_2) receptor antagonist; thromboxane synthase inhibitor

Introduction

The discovery of thromboxane A_2 (TXA_2) (Hamberg *et al.*, 1975) and prostacyclin (PGI_2) (Moncada *et al.*, 1976) has generated a great deal of interest in these highly potent derivatives of arachidonic acid (AA). TXA_2 is the major cyclo-oxygenase product derived from AA in blood platelets. It is an extremely potent platelet aggregator, vasoconstrictor and bronchoconstrictor (Moncada & Vane, 1987a). PGI_2 is produced by vascular endothelium and has potent biological actions opposing those of TXA_2 (Gryglewski *et al.*, 1976). Normally there is a homaeostatic balance maintained between TXA_2 and PGI_2. However, in some pathological conditions (e.g. thrombosis), the normal balance is upset allowing the detrimental properties of TXA_2 to predominate (Moncada & Vane, 1978b). Thus, drugs that inhibit TXA_2 formation or action may have a potential as antithrombotic agents.

Cyclo-oxygenase inhibitors (e.g. aspirin) have been criticized for their alleged capability of suppressing the synthesis not only of TXA_2 but also of PGI_2, a powerful antiaggregatory and vasodilator substance. The use of the more recently introduced thromboxane (TX) synthase inhibitors has been questioned on the basis of a possible proaggregatory activity of prostaglandin endoperoxides (PGG_2, PGH_2) accumulating after the block of TX synthase (Bertele *et al.*, 1981). TXA_2 receptor antagonists have the advantage of inhibiting the pro-aggregatory action of both TXA_2 and prostaglandin endoperoxides and also of antagonizing the effects of these agonists on smooth muscle cells (Gresele *et al.*, 1984). However, they do not suppress platelet activation mediated by TXA_2-independent agonists (high dose collagen, thrombin). Drugs with combined TX synthase inhibitory and TXA_2 receptor antagonistic properties may overcome several of the shortcomings of the pharmacological classes discussed above. Indeed, while TX synthase inhibition enhances the endogenous synthesis of antiaggregatory prostaglandins (PGI_2 and PGD_2) (Gresele *et al.*, 1987), TXA_2 receptor antagonism prevents accumulated endoperoxides from activating platelets and smooth muscle cells. The summation of these effects may theoretically lead to an increase of adenosine 3':5'-cyclic monophosphate (cyclic AMP) in platelets and smooth muscle

[1] Author for correspondence.

cells, a phenomenon associated with strong platelet inhibition and smooth muscle relaxation.

Medicinal plants have been widely used as traditional remedies in oriental countries for hundreds of years. Recently, in a large scale screening test, we have found that cinnamophilin, a new lignan (Figure 1), isolated from *Cinnamomum philippinense*, possessed both TX synthase inhibitory and TXA_2 receptor antagonizing properties. In this study, the pharmacological effect of cinnamophilin was determined *in vitro* in human platelet, rat isolated aorta and guinea-pig isolated trachea and *in vivo* in mice and guinea-pigs.

Methods

Human platelet aggregation

Platelet-rich plasma (PRP) was obtained from blood collected from healthy individuals with sodium citrate (3.8%, 1:14) added as anticoagulant, and centrifuged for 10 min at 90 *g*. Three minutes before the addition of the aggregation inducer, PRP was preincubated with various concentrations of cinnamophilin and stirred at 1200 r.p.m. The absorbance of PRP was taken as 0% aggregation and the absorbance of platelet-poor plasma (PPP) as 100% aggregation. Adenosine 5'-triphosphate (ATP) released from platelets was detected by the bioluminescence method (DeLuca & McElory, 1978). ATP at a known concentration was used to calibrate the intensity of bioluminescence. Both the aggregation and release of ATP were simultaneously measured by a Lumi-aggregometer (Chrono-Log Co. U.S.A.) connected to a dual channel recorder. In order to eliminate the effect of the solvent on aggregation, the final concentration of dimethylsulphoxide (DMSO) was fixed at 0.5%.

Measurement of [^{3}H]-inositol monophosphate

The method was modified from those of Huang & Detwiler (1986) and Neylon & Summers (1987). Citrated human-PRP was centrifuged at 500 *g* for 10 min; the platelet pellets were then suspended in 700 µl of Ca^{2+}-free and bovine serum albumin (BSA)-free Tyrode solution (mM: NaCl 136.8, KCl 2.8, $MgCl_2$ 2.1, NaH_2PO_4 0.33, $NaHCO_3$ 11.9) containing 75 µCi ml^{-1} of [^{3}H]-*myo*-inositol. After incubation for 2 h at 37°C, the platelets were collected by centrifugation (500 *g* for 4 min) and suspended in Ca^{2+}-free Tyrode solution. Phosphoinositides breakdown was induced by adding aggregating agents to 1 ml of platelet suspension in a 3.5 ml cuvette with a stirring bar driven at 900 r.p.m., 37°C for 6 min. An equal volume of 10% (w/v) trichloroacetic acid was added to stop the reaction. After centrifugation at 1000 *g* for 10 min, 1 ml of supernatant was pooled and trichloroacetic acid was removed by washing with 5 × 2 vol. of diethylether. The aqueous phase containing the inositol phosphates was adjusted to pH 7–8 and diluted to 4 ml with distilled water before application to a Dowex-1 ion-exchange column for separation of the inositol phosphates as described previously by Neylon & Summers (1987). All the experiments were carried out in the presence of 5 mM LiCl to inhibit inositol-monophosphate phosphatase. Because the levels of inositol bisphosphate and inositol trisphosphate were very low, we measured the inositol monophosphate as an index of the total inositol phosphates formation.

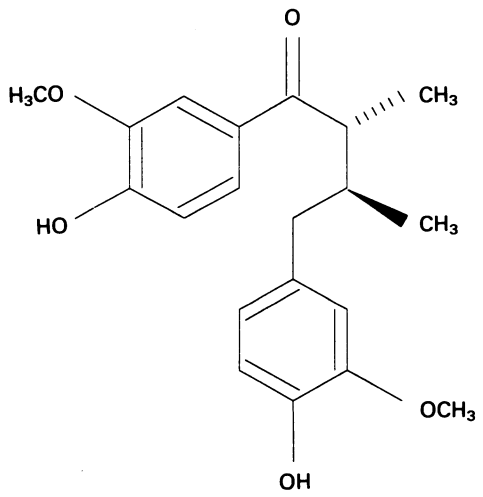


Figure 1 Chemical structure of cinnamophilin.

Measurement of intracellular Ca^{2+} in platelets

The method described by Rink *et al.* (1983) was used: citrated human-PRP was incubated with quin-2/AM (20 µM) for 40 min and then washed and suspended in the above Tyrode solution. Fluorescence was measured with a Hitachi Fluorescence Spectrophotometer (Ex. 339 nm, Em. 492 nm).

Measurement of platelet cyclic AMP

Platelet cyclic AMP was assayed with a commercially available RIA kit. Human-PRP was incubated with cinnamophilin or its vehicle for 3 min at 37°C with stirring, then AA (800 µM) or saline was added. After 3 min, the proteins were precipitated with 0.5 M trichloroacetic acid containing [^{3}H]-cyclic AMP for assessment of recovery. After centrifugation and chromatography the samples were assayed by RIA for cyclic AMP.

Measurement of TXB_2 and PGE_2 in human PRP

The effects of cinnamophilin on TXB_2 and PGE_2 production were determined in human PRP. Human PRP was preincubated with DMSO or various concentrations of cinnamophilin for 15 min, then AA (800 µM) was added for another 6 min incubation. The platelets were then spun down at 12,000 *g* for 5 min and the plasma was frozen until assay. Immunoreactive TXB_2 and PGE_2 were measured in unextracted, highly diluted serum samples by RIA kits.

Rat aortic contraction

Wistar rats of either sex weighing 250 to 300 g were killed by a blow to the head. The thoracic aorta was isolated and excess fat and connective tissue were removed. Vessels were cut into rings of about 5 mm in length and mounted in organ baths containing 5 ml Krebs solution of the following composition (mM): NaCl 118.4, KCl 4.7, $CaCl_2$ 1.9, $MgSO_4$ 1.2, KH_2PO_4 1.2, $NaHCO_3$ 25.0 and glucose 11.7. The tissue bath solution was maintained at 37°C and gassed with 95% O_2:5% CO_2 mixture. Two stainless steel hooks were inserted into the aortic lumen, one was fixed while the other was connected to a transducer. Aortae were equilibrated in the medium for 90 min with three changes of Krebs solution and maintained under an optimal tension of 1 g before specific experimental protocols were initiated. Contractions were recorded isometrically via a force-displacement transducer connected to a Grass polygraph. Aortae were allowed to preincubate for 15 min with cinnamophilin before generating the cumulative concentration-response curve with each agonist for 15–30 min at 3 min intervals. Results are expressed as a percentage of the maximal control response for each agonist.

Guinea-pig tracheal contraction

Tracheae from guinea-pigs were dissected out, transferred to a dish containing Krebs solution and cut transversely between the segments of cartilage. Several of these, usually

about 5, were tied together so as to form a chain, which was then mounted in Krebs solution at 37°C, gassed with 95% O_2 plus 5% CO_2. One end of the chain was attached to a fixed pin in the bath and the other to a transducer connected to a Grass polygraph. Resting tension on each tissue was set at 1 g. Tracheae were allowed to equilibrate for at least 1 h and washed periodically. Cumulative concentration-response curves were obtained by application of various concentrations of spasmogens for 15–18 min at 3 min intervals. Tracheal rings were preincubated with cinnamophilin for 15 min, then various concentrations of spasmogens were added for 15–18 min at 3 min intervals. Results were expressed as percentage of the maximal control response for each agonist.

In vivo *studies*

Tail bleeding time in conscious mice Thirty minutes after the intraperitoneal (i.p.) administration of drugs, mice were placed in a tube holder with the tail allowed to protrude. The tail was transected at 1.5 mm from the tip and 1.5 cm of the distal portion was vertically immersed into saline at 37°C and the bleeding time was measured as described by Hornstra *et al.* (1981).

AA-induced bronchoconstriction in anaesthetized guinea-pigs

The method as previously described by Pretolani *et al.* (1987) was followed. Male Hartley guinea-pigs (350–400 g) were anaesthetized with sodium pentobarbitone (30 mg kg^{-1}, i.p.). The carotid artery (for monitoring blood pressure), jugular vein (for drug administration) and trachea were cannulated. Mechanical ventilation was started (Harvard Rodent Ventilator, Model 683; 60 strokes min^{-1}) and spontaneous breathing abolished with pancuronium (2 mg kg^{-1}, i.v.). Bronchial resistance was recorded with a Bronchospasm Transducer (Ugo Basile, Model 7020) connected to a polygraph (Gould, Model 2400).

Drugs

Cinnamophilin (Figure 1) was isolated from *Cinnamomum philippinense* (unpublished data), and its purity (>99%) was confirmed by n.m.r., mass, IR and proton spectrophotometer. The following drugs were used: arachidonic acid, collagen (type I, bovine achilles tendon), ADP (tris salt), A23187, indomethacin, (−)-noradrenaline HCl, endothelin-1, angiotensin II, carbachol, quin-2/AM, histamine, luciferase-luciferin, trichloroacetic acid, bovine serum albumin (BSA), EDTA, sodium citrate and Dowex-1 (100–200 mesh: ×8, chloride) were obtained from Sigma Chemical. Co.; U-46619 (9,11-dideoxymethanoepoxy-9α,11α-$PGF_{2\alpha}$) from Biomol. cyclic AMP, *myo*-[2-^{3}H]-inositol, TXB_2 and PGE_2 RIA kits were purchased from Amersham. If drugs were dissolved in dimethylsulphoxide (DMSO), the final concentration of DMSO in the bathing solution did not exceed 0.1% and had no effect on the muscle contraction.

Data analysis

In each experiment, agonist dose-response curves in the presence of cinnamophilin were related to the control dose-response curves, of which the maximum response was taken as 100%. In most experiments, three or four concentrations of cinnamophilin were tested and the slopes of the resulting Schild plots were used to assess competitive antagonism. The pA_2 values were calculated for each concentration of cinnamophilin according to: $pA_2 = -\log([\text{antagonist}]/[\text{dose ratio} - 1])$ (Mackay, 1978).

The experimental results are expressed as the mean ± s.e. mean and accompanied by the number of observations. Statistical significance was assessed by Student's t test and P values less than 0.05 were considered significant.

Results

Effects of cinnamophilin on platelet aggregation and ATP release

Cinnamophilin inhibited dose-dependently human platelet-rich plasma (PRP) aggregation induced by arachidonic acid (AA) (800 μM), collagen (10 μM) and the prostaglandin endoperoxide analogue, U-46619 (1 μM) with IC_{50} of 5.0 ± 0.4 μM, 5.6 ± 0.6 μM and 3.0 ± 0.4 μM, respectively (Table 1). In human PRP, ADP (5 μM) and adrenaline (10 μM) caused biphasic aggregation. The second wave of ADP- or adrenaline-induced platelet aggregation was suppressed by cinnamophilin (IC_{50} = 6.0 ± 0.6 and 7.6 ± 0.9 μM, respectively), while the first wave was only slightly reduced by cinnamophilin above 30 μM. The release of ATP from platelets challenged by AA, collagen, U-46619, ADP or adrenaline was also inhibited by cinnamophilin; this inhibition was paralleled by its inhibitory effect on aggregation (Table 1). The aggregation and ATP release induced by the calcium ionophore, A23187, was slightly affected by cinnamophilin concentrations up to 30 μM (Table 1).

Cinnamophilin (0.3–10 μM) produced a parallel shift to the right of the concentration-response curve of U-46619; there was no depression of the maximum response to U-46619 even with the highest dose of cinnamophilin (10 μM) tested (Figure 2a). When the data were represented as a Schild plot, pA_2 and pA_{10} values of 7.3 (7.1–7.5 for 95% confidence limits) and 6.3 (6.1–6.5) with a slope of 0.95 were obtained (Figure 2b). At various times after the platelet aggregation trigged by U-46619 (1 μM), deaggregation of platelets was caused by cinnamophilin (3 μM) but not by indomethacin (20 μM). The earlier the addition of cinnamophilin, the more rapid was the reversal of platelet aggregation (Figure 3).

Effects of cinnamophilin on platelet phosphoinositides breakdown and intracellular Ca^{2+}

To see if signal transduction after TXA_2 receptor activation was blocked by cinnamophilin, human PRP were labelled with [^{3}H]-*myo*-inositol and quin-2/AM. Phosphoinositides breakdown was observed in platelets activated by many agonists. We found that thrombin (0.1 u ml^{-1}), collagen (10 μM), PAF (20 ng ml^{-1}) and U-46619 (1 μM) increased inositol monophosphate formation 280 ± 30%, 150 ± 20%, 180 ± 30% and 160 ± 20%, respectively (after subtraction of basal levels). Only the formation of inositol monophosphate by U-46619 was almost completely inhibited by cinnamophilin (10 μM) (Figure 4). In quin-2/AM-loaded platelets, the net increases of intracellular Ca^{2+} caused by thrombin, collagen,

Table 1 Effects of cinnamophilin on platelet aggregation and ATP release in human platelet-rich plasma (PRP)

Inducer	*Aggregation* IC_{50} (μM)	*ATP release* IC_{50} (μM)
Arachidonic acid (800 μM)	5.0 ± 0.4	4.3 ± 0.2
Collagen (10 μM)	5.6 ± 0.6	5.0 ± 0.5
U-46619 (1 μM)	3.0 ± 0.4	2.5 ± 0.2
A23187 (5 μM)	>30	>30
ADP (5 μM)		
first wave	>30	–
second wave	6.0 ± 0.6	5.0 ± 0.4
Adrenaline (10 μM)		
first wave	>30	–
second wave	7.6 ± 0.9	7.1 ± 0.3

Human PRP was incubated with cinnamophilin for 3 min, then arachidonic acid (800 μM), collagen (10 μM), U-46619 (1 μM), A23187 (5 μM), ADP (5 μM) or adrenaline (10 μM) was added to trigger the aggregation and ATP release.

PAF and U-46619 were 380 ± 20 nM, 225 ± 15 nM, 338 ± 30 nM and 316 ± 10 nM, respectively. Only the increase of intracellular Ca^{2+} by U-46619 was almost completely suppressed by cinnamophilin (10 μM) (net increase about 20 ± 15 nM).

Effects of cinnamophilin on arachidonic acid metabolism

In human PRP, cinnamophilin induced a dose-dependent inhibition of TXB_2 producton; PGE_2 formation, instead, was dose-dependently increased by the cinnamophilin (Figure 5).

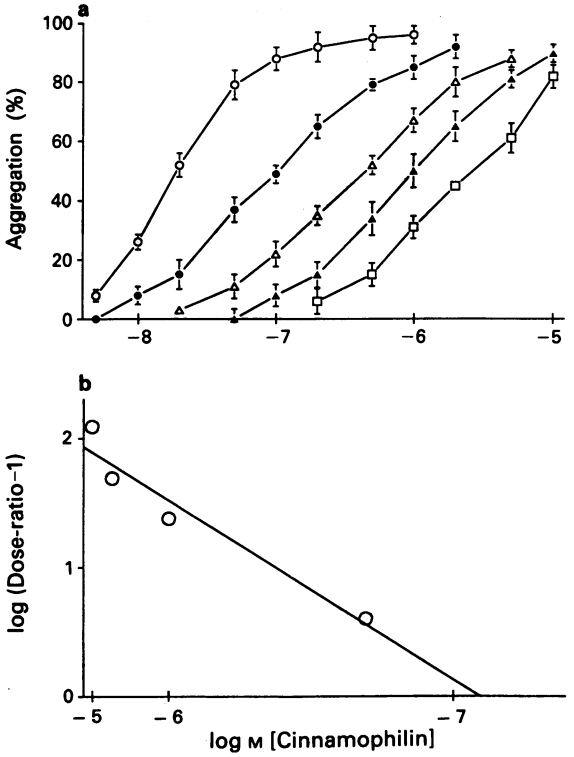


Figure 2 (a) Concentration-dependent shift induced by cinnamophilin on platelet aggregation induced by U-46619. Human platelet-rich plasma were incubated with dimethylsulphoxide (0.5%, ○) or various concentrations of cinnamophilin (0.3 μM, ●; 1 μM, △; 3 μM, ▲; 10 μM, □) for 3 min, then various concentrations of U-46619 were added to trigger the aggregation. Each point represents the mean ± s.e.mean ($n = 6$). (b) Schild plot of (a). The equation of the regression line was $y = -0.95 \times + 6.9$ with $r = 0.99$.

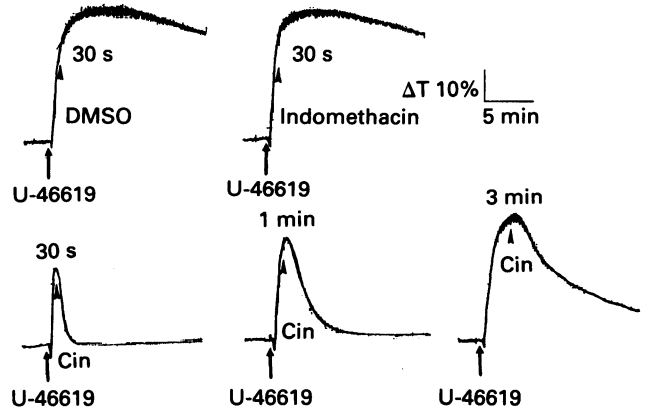


Figure 3 Reversal effect of cinnamophilin on the aggregation of human platelet-rich plasma induced by U-46619. Platelet aggregation was induced by U-46619 (1 μM) for 30 s, 1 min or 3 min, then dimethylsulphoxide (DMSO, 0.5%), indomethacin (20 μM) or cinnamophilin (Cin, 3 μM) was added.

In sheep seminal vesicle microsomes, cinnamophilin also induced a dose-dependent increase of PGE_2 formation (data not shown). Thus cinnamophilin was an inhibitor of platelet TX synthase, but had no effect on cyclo-oxygenase activity.

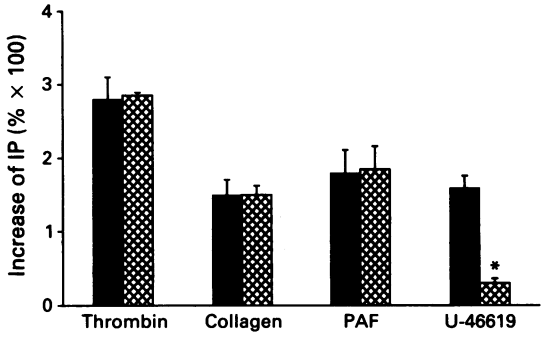


Figure 4 Effect of cinnamophilin on the formation of inositol monophosphate caused by thrombin, collagen, PAF and U-46619 in human platelet-rich plasma (PRP). [^{3}H]-*myo*-inositol-labelled platelets were incubated with DMSO (solid columns) or cinnamophilin (10 μM, cross-hatched columns) for 3 min, then thrombin (0.1 u ml^{-1}), collagen (10 μM), PAF (20 ng ml^{-1}) or U-46619 (1 μM) was added for another 6 min. Percentage increases of inositol monophosphate (IP) (after subtraction of basal levels) are expressed as the mean ± s.e.mean ($n = 6$). *$P < 0.001$ denotes significantly different from stimulated platelets which were not cinnamophilin-treated.

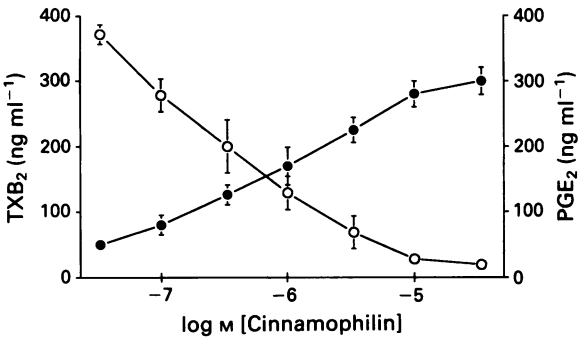


Figure 5 Effects of cinnamophilin on the thromboxane B_2 (○) and prostaglandin E_2 (●) synthesis induced by arachidonic acid (AA) in human PRP. Cinnamophilin was preincubated with platelets for 15 min, then AA (800 μM) was added. Each point represents the mean ± s.e.mean ($n = 4$).

Table 2 Effects of cinnamophilin, dazoxiben and SQ 29548 on platelet cyclic AMP levels

	Unstimulated	*AA-stimulated*
	(pmol ml^{-1})	
Control	28 ± 4	21 ± 4
Cinnamophilin (μM)		
1	–	22 ± 3
3	–	29 ± 3*
10	29 ± 5	35 ± 2**
Dazoxiben (μM)		
30	29 ± 4	22 ± 3
SQ 29548 (μM)		
30	28 ± 5	21 ± 3

Human platelet-rich plasma (PRP) were incubated with drugs for 3 min at 37°C with stirring, then saline or AA (800 μM) was added. Values are expressed as mean ± s.e.mean ($n = 5$–7). *$P < 0.05$, **$P < 0.01$ as compared with the respective control.

Effects of cinnamophilin on platelet cyclic AMP

In control experiments, 28 ± 4 pmol ml^{-1} of cyclic AMP in human PRP was measured. Cinnamophilin did not affect platelet cyclic AMP levels up to 10 μM (Table 2). When the platelets were preincubated with cinnamophilin and challenged with AA, a dose-dependent rise in cyclic AMP was observed (Table 2). Dazoxiben (a specific TX synthase inhibitor) and SQ 29548 (a specific TXA_2 receptor antagonist) did not affect cyclic AMP levels in AA-untreated or AA-treated platelets.

Effects of cinnamophilin on U-46619-induced rat aorta and guinea-pig contractions

Cumulative addition of U-46619 (0.005–10 μM) caused a stepwise increase of contractions of rat aorta and guinea-pig trachea. Cinnamophilin inhibited these responses in a concentration-dependent manner and shifted the dose-response curve to the right in a parallel fashion. The pA_2 values for cinnamophilin toward U-46619-induced responses in rat aorta and guinea-pig trachea were 6.3 ± 0.1 and 5.2 ± 0.2, respectively. (Figure 6a,b).

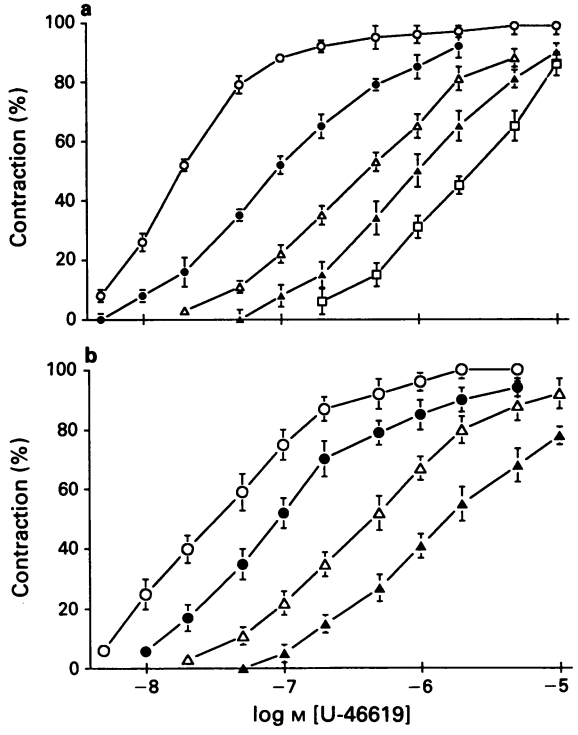


Figure 6 Antagonism of U-46619-induced contractions by cinnamophilin in rat aorta and guinea-pig trachea. Rat aortic rings were preincubated with 0.1% dimethylsulphoxide (DMSO, ○) or cinnamophilin (3 μM, ●; 10 μM, △; 30 μM, ▲; 100 μM, □) at 37°C for 15 min (a). Tracheal rings were preincubated with 0.1% DMSO (○) or cinnamophilin (10 μM, ●; 30 μM, △; 100 μM, ▲) for 15 min (b). Cumulative concentrations of U-46619 were used in (a) and (b). Each point represent the mean ± s.e.mean ($n = 6$).

Table 3 Effect of cinnamophilin on mice tail bleeding time

	Tail bleeding time (s)
Control	60.3 ± 5.4
Cinnamophilin 100 μg kg^{-1}	160.6 ± 17.5***
Indomethacin 100 μg kg^{-1}	110.9 ± 19.9*
Dazoxiben 100 μg kg^{-1}	96.8 ± 10.8**
SQ 29548 100 μg kg^{-1}	99.6 ± 11.9**

Drugs were administered i.p. 30 min before test. Values are expressed as mean ± s.e.mean ($n = 8$–12). *$P<0.05$, **$P<0.01$, ***$P<0.001$ denote values significantly different from the control values (DMSO-treated).

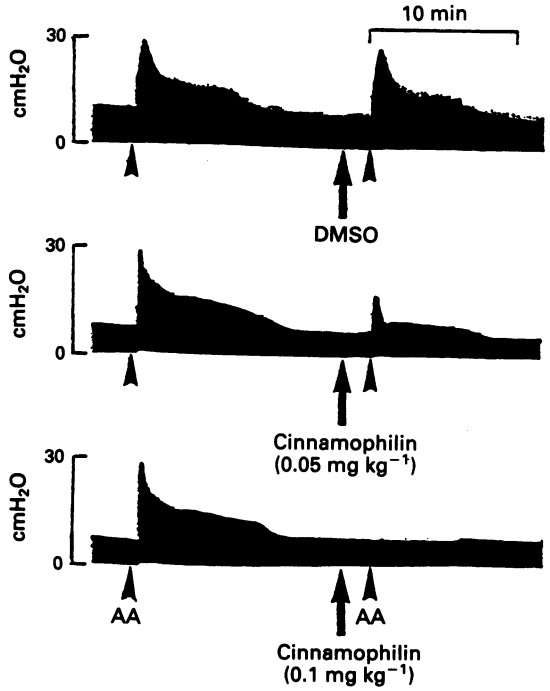


Figure 7 Inhibition by cinnamophilin of the bronchoconstriction induced by arachidonic acid (AA) in guinea-pigs. Cinnamophilin (0.05, 0.1 mg kg^{-1}, i.v.) was administered 1 min before AA (50 μg kg^{-1}, i.v.). Data from one of the three experiments are presented.

To determine the specificity of cinnamophilin on other receptors of rat aorta, endothelin-1 (3 nM), angiotensin II (300 nM), 5-hydroxytryptamine (5-HT) (10 μM) or noradrenaline (3 μM) was used. Cinnamophilin, at a concentration (100 μM) sufficient to inhibit the U46619-induced contraction of the aorta, failed to attenuate the contractile response of rat aorta to endothelin-1, angiotensin II, 5-HT or noradrenaline. Tracheal ring contraction induced by histamine, carbachol or KCl was also not antagonized by cinnamophilin (100 μM) (data not shown).

Effects of cinnamophilin on tail bleeding time of mice

Thirty minutes after i.p. administration of cinnamophilin, tail bleeding time of mice was prolonged more markedly than after indomethacin, dazoxiben and SQ 29548 (Table 3).

Effects of cinnamophilin on AA-induced bronchoconstriction in guinea-pig

Intravenous administration of AA (50 μg kg^{-1}) to guinea-pig induced a reversible bronchoconstriction. When cinnamophilin (0.1 mg kg^{-1}) was administered (i.v.) 1 min before AA, the bronchoconstrictor response to AA was blocked (Figure 7). In contrast, the bronchoconstriction induced by PAF (50 ng kg^{-1}) was not affected by cinnamophilin (1 mg kg^{-1}).

Discussion

The present study has demonstrated that cinnamophilin has both TX synthase inhibitory and TXA_2 receptor antagonizing activities. Thromboxane-dependent pathways of platelet acti-

vation (AA, collagen, second wave of ADP and adrenaline) were inhibited, whereas the independent ones (first wave of ADP, adrenaline and A23187) were not inhibited by cinnamophilin. TX synthase inhibition was determined as a drop in the formation of TXB_2 in AA-stimulated PRP. Furthermore, this inhibition was accompanied by an increase in the formation of PGE_2. Cinnamophilin did not affect basal cyclic AMP levels, therefore excluding a direct action of cinnamophilin on adenylate cyclase or cyclic AMP-dependent phosphodiesterase. This whole series of effects is a typical feature of TX synthase inhibition (Gresele *et al.*, 1984; 1988). Cinnamophilin also behaves as a TXA_2 receptor antagonist. The profiles of action of cinnamophilin upon U-46619-induced contraction of rat aortic rings, guinea-pig tracheal rings and aggregation of human platelets (with pA_2 value of 6.3 ± 0.1, 5.2 ± 0.2 and 7.3 ± 0.2, respectively), indicate that cinnamophilin is a competitive TXA_2 receptor antagonist. This conclusion is supported by the lack of depression of the maximum responses to U-46619 and slopes of the Schild regression not significantly different from unity. Cinnamophilin does not exert any antagonism on the endothelin-1-, angiotensin II- or noradrenaline-induced contraction of the rat aorta and histamine-, carbachol- or KCl-induced contraction of the guinea-pig trachea. This indicated that cinnamophilin is a selective antagonist of the TXA_2 receptor. AA has been shown to cause TXA_2-mediated bronchoconstriction in the anaesthetized guinea-pig (Vargaftig & Doa Hai, 1972; Greenberg *et al.*, 1984). Cinnamophilin significantly inhibited AA-induced increases in airways resistance. *In vivo*, cinnamophilin produced a more marked prolongation of the tail bleeding time in mice than indomethacin, dazoxiben and SQ 29548. These results indicate that cinnamophilin is an effective inhibitor of TX synthase and TXA_2 receptor not only *in vitro*, but also *in vivo*.

TXA_2 plays a pivotal role in platelet activation and is involved in the development of thrombosis. TX synthase inhibitors suppress TXA_2 formation and increase the synthesis of the antiaggregatory prostaglandins (PGI_2 and PGD_2); however, accumulated PGH_2 may interact with platelet and vessel wall TXA_2 receptors, thus reducing the antithrombotic effects of this class of drug. TXA_2 receptor antagonists block the activity of both TXA_2 and PGH_2 on platelets and the vessel wall. Recently, ridogrel and picotamide have been developed (Gresele *et al.*, 1991). Both drugs reduce formation of TXA_2 and increase levels of PGI_2 and PGD_2, and competitively inhibit the binding and action of TXA_2. However, ridogrel shows a dissociation between the TX synthase inhibitory activity ($IC_{50} = 15$ nM) and the receptor antagonistic activity ($IC_{50} = 2$ μM) (De Clerck *et al.*, 1989; Hoet *et al.*, 1990). Indeed, in an ideal agent the two pharmacological activities should be balanced to allow both a suppression of TX synthase and antagonism of TXA_2 receptors of >95% at equivalent plasma concentrations. The potency ratio of cinnamophilin as a TX synthase inhibitor and as a receptor antagonist is approximately 1; thus cinnamophilin is likely to exert simultaneously both effects at active concentrations. Picotamide is relatively weak ($IC_{50} = 100$ μM) (Gresele *et al.*, 1989); in addition, this drug may possess other pharmacological actions beyond its activities on TXA_2 (Gresele *et al.*, 1990).

Dazoxiben (a pure TX synthase inhibitor) and SQ 29548 (a pure TXA_2 receptor antagonist) did not increase intraplatelet cyclic AMP in AA-stimulated platelets. However, cinnamophilin possessing the combination of a TX synthase inhibitory activity with a TXA_2 receptor antagonistic action may lead to an increase in cyclic AMP levels in activated platelets. This enhancement is probably caused by the simultaneous stimulation of platelet adenylate cyclase by PGE_2 produced in increased amounts after TX synthase inhibition (Gresele *et al.*, 1984; 1987), and by the neutralization of the adenylate cyclase inhibitory effects of accumulated prostaglandin endoperoxides (Avdonin *et al.*, 1985).

A potentiation of the platelet-suppressing activity of a TX synthase inhibitor by a TXA_2 receptor antagonist *in vitro* has been described (FitzGerald *et al.*, 1985). Thus, cinnamophilin acting at more than one level of the AA-metabolic pathway appears to be a promising approach to antithrombotic therapy.

All of these data indicate that cinnamophilin is a novel dual TX synthase inhibitor and TXA_2 receptor antagonist and that it may be a useful tool for the investigation and treatment of diseases involving TXA_2 disorders.

This work was supported by research grants of CMRP 377 from Chang Gung Medical Research Foundation and the National Science Council of the Republic of China (NSC 83-0412-B182-032).

References

AVDONIN, P.V., SVITINA-ULUTINA, I.V., LEYTIN, V.L. & THACHUK, V.A. (1985). Interaction of stable prostaglandin endoperoxide analogs U-46619 and U-44069 with human platelet membranes: coupling of receptors with high affinity GTPase and adenylate cyclase. *Thromb. Res.*, **40**, 101–112.

BERTELE, V., CERLETTI, C., SCHIEPPATI, A., DI MINNO, G. & DE GAETANO, G. (1981). Inhibition of thromboxane synthetase does not necessarily prevent platelet aggregation. *Lancet*, **i**, 1057–1058.

DE CLERCK, F., BEETENS, J., VAN DE WATER, A., VERCAMMEN, E. & JANSSEN, P.A.J. (1989). R68070: Thromboxane A2 synthetase inhibition and thromboxane A_2/prostaglandin endoperoxide receptor blockade combined in one molecule-II. Pharmacological effects in vivo and ex vivo. *Thromb. Haemost.*, **61**, 43–49.

DELUCA, M. & MCELORY, W.D. (1978). Purification and properties of firefly luciferase. *Methods Enzymol.*, **57**, 3–15.

FITZGERALD, G.A., REILLY, I.A.G. & PEDERSEN, A.K. (1985). The biochemical pharmacology of thromboxane synthase inhibition in man. *Circulation*, **72**, 1194–1201.

GREENBERG, R., STENBACHER, T.E., HARRIS, D.N. & HASLANGER, M.F. (1984). Thromboxane receptor antagonist properties of SQ 27427 in the anaesthetized guinea-pig. *Eur. J. Pharmacol.*, **103**, 19–24.

GRESELE, P., ARNOUT, J., DECKMYN, H., HUYBRECHTS, E., PIETERS, G. & VERMYLEN, J. (1987). Role of proaggregatory and antiaggregatory prostaglandins in hemostasis. Studies with combined thromboxane synthase inhibition and thromboxane receptor antagonism. *J. Clin. Invest.*, **80**, 1435–1445.

GRESELE, P., BLOCKMANS, D., DECKMYN, H. & VERMYLEN, J. (1988). Adenylate cyclase activation determines the effect of thromboxane synthase inhibitors on platelet aggregation in vitro. Comparison of platelets from responders and non-responders. *J. Pharmacol. Exp. Ther.*, **246**, 301–307.

GRESELE, P., CORONA, C., ALBERTI, P. & NENCI, G.G. (1990). Picotamide protects mice from death in a pulmonary embolism model by a mechanism independent from thromboxane suppression. *Thromb. Haemost.*, **64**, 80–86.

GRESELE, P., DECKMYN, H., ARNOUT, J., LEMMENS, J., JANSSENS, W. & VERMYLEN, J. (1984). BM 13177, a selective blocker of platelet and vessel wall thromboxane receptors, is active in man. *Lancet*, **i**, 991–994.

GRESELE, P., DECKMYN, H., ARNOUT, J., NENCI, G.G. & VERMYLEN, J. (1989). Characterization of N,N'-bis(3-picolyl)-4-methoxy-isophtalamide (picotamide) as a dual thromboxane synthase inhibitor/thromboxane A_2 receptor antagonist in human platelets. *Thromb. Haemost.*, **61**, 479–484.

GRESELE, P., DECKMYN, H., NENCI, G.G. & VERMYLEN, J. (1991). Thromboxane synthase inhibitors, thromboxane receptor antagonists and dual blockers in thrombotic disorders. *Trends Pharmacol. Sci.*, **12**, 158–163.

GRYGLEWSKI, R.J., BUNTING, S., MONCADA, S., FLOWER, R.J. & VANE, J.R. (1976). Arterial walls are protected against deposition of platelet thrombi by a substance (prostaglandin X) which they make from prostaglandin endoperoxidase. *Prostaglandins*, **12**, 685–713.

HAMBERG, M., SVENSSEN, J. & SAMUELSSON, B. (1975). Thromboxanes: A new group of biologically active compounds derived from prostaglandin endoperoxides. *Proc. Natl. Acad. Sci. U.S.A.*, **72**, 2994–2998.

HOËT, B., FALCON, C., DEREYS, S., ARNOUT, J., DECKMYN, H. & VERMYLEN, J. (1990). R68070, combined thromboxane/endoperoxide receptor antagonist and thromboxane synthase inhibitor, inhibits human platelet activation in vitro and in vivo, a comparison with aspirin. *Blood*, **75**, 646–653.

HORNSTRA, G., CHRIST-HAZELHOLF, E., HADDEMAN, E., TEN, H.F. & NUGSTEREN, D.H. (1981). Fish oil feeding lower thromboxane and prostacyclin production by rat platelets or aorta and does not result in the formation of prostaglandin I_3. *Prostaglandin*, **21**, 727–738.

HUANG, E.M. & DETWILER, W.D. (1986). The effect of lithium on platelet phosphoinositide metabolism. *Biochem. J.*, **236**, 895–901.

MACKAY, D. (1978). How should values of pA_2 and affinity constants for pharmacological competitive antagonists be estimated? *J. Pharm. Pharmacol.*, **30**, 312–313.

MONCADA, S., GRYGLEWSKI, R.J., BUNTING, S. & VANE, J.R. (1976). An enzyme isolated from arteries transform prostaglandin endoperoxides to an unstable substance that inhibits platelet aggregation. *Nature*, **263**, 663–665.

MONCADA, S. & VANE, J.R. (1978a). Pharmacology and endogenous roles of prostaglandin endoperoxides, thromboxane A_2 and prostacyclin. *Pharmacol. Rev.*, **30**, 293–331.

MONCADA, S. & VANE, J.R. (1978b). Unstable metabolites of arachidonic acid and their role in haemostasis and thrombosis. *Br. Med. Bull.*, **34**, 129–135.

NEYLON, C.B. & SUMMERS, R.J. (1987). Stimulation of α1-adrenoceptors in rat kidney mediates increased inositol phospholipid hydrolysis. *Br. J. Pharmacol.*, **91**, 367–376.

PRETOLANI, M., LEFORT, J., MALANCHERE, E. & VARGAFTIG, B.B. (1987). Interference by the novel PAF-acether antagonist WEB 2086 with the bronchopulmonary responses to PAF-acether and to active and passive anaphylactic shock in guinea-pigs. *Eur. J. Pharmacol.*, **140**, 311–321.

RINK, J.J., SANCHEZ, A. & HALLAM, J.J. (1983). Diacylglycerol and phorbol ester stimulate secretion without rasing cytoplasmic free calcium in human platelets. *Nature*, **305**, 317–319.

VARGAFTIG, B.B. & DOA HAI, N. (1972). Selective inhibition by mepacrine of the release of rabbit aorta contracting substance evoked by the administration of bradykinin. *J. Pharm. Pharmacol.*, **24**, 159–161.

(Received August 24, 1993
Revised October 27, 1993
Accepted November 9, 1993)

Br. J. Pharmacol. (1994), **111**, 913–917 © Macmillan Press Ltd, 1994

Investigation of the actions of PPADS, a novel P_{2X}-purinoceptor antagonist, in the guinea-pig isolated vas deferens

G.J. McLaren, *G. Lambrecht, *E. Mutschler, †H.G. Bäumert, [1]P. Sneddon & C. Kennedy

Department of Physiology and Pharmacology, Royal College, 204 George St, University of Strathclyde, Glasgow, G1 1XW and Departments of *Pharmacology and †Biochemistry, University of Frankfurt, Biocenter Niederursel, Marie-Curie-Strasse 9, Geb. N260, D-60053 Frankfurt, Germany

1 Pyridoxalphosphate-6-azophenyl-2',4'-disulphonic acid (PPADS) was investigated for its ability to act as an antagonist at P_{2X}-purinoceptors which mediate neurogenic excitatory junction potentials (e.j.ps) and contractions in the guinea-pig isolated vas deferens.

2 PPADS (10^{-7} M) caused a small potentiation of the phasic, predominantly purinergic component of contractions evoked by symapthetic nerve stimulation, but higher concentrations of PPADS (3×10^{-6}–3×10^{-5} M) elicited a substantial and significant concentration-dependent inhibition. In contrast, over the same concentration-range, PPADS had no effect on the tonic, predominantly noradrenergic phase.

3 PPADS (3×10^{-5} M) also inhibited contractile responses to exogenous α,β-methyleneATP (10^{-8}–10^{-3} M), a P_{2X}-purinoceptor agonist, without affecting the responses to exogenous noradrenaline (10^{-8}–10^{-3} M), carbachol (10^{-5} M) or histamine (10^{-4} M).

4 PPADS (10^{-7}–3×10^{-5} M) produced a concentration-dependent reduction in e.j.p. magnitude and resting membrane potential. The maximum effect was seen at 10^{-5} M PPADS, which reduced e.j.p. magnitude from 13.7 ± 0.6 mV ($n = 12$) to 1.8 ± 0.7 mV ($n = 12$) and membrane potential from -64.8 ± 0.6 mV ($n = 51$) to -55.0 ± 1.8 mV ($n = 12$).

5 The PPADS-induced depolarization was not inhibited by the P_{2X}-purinoceptor antagonist, suramin (10^{-4} M). This indicates that the depolarization was not due to an agonist action of PPADS at P_{2X}-purinoceptors.

6 The results support the proposal that PPADS is a selective antagonist at P_{2X} purinoceptors as opposed to non-P_2-purinoceptors in the guinea-pig vas deferens, but its ability to cause membrane depolarization independently of P_{2X}-purinoceptors and also, at a low concentration, to potentiate the phasic component of the neurogenic contraction indicates that it has other actions.

Keywords: Pyridoxalphosphate-6-azophenyl-2'-4'-disulphonic acid (PPADS); P_{2X}-purinoceptor; vas deferens; cotransmitter; purinergic; sympathetic

Introduction

There is considerable evidence to indicate that in many tissues adenosine 5'-triphosphate (ATP) is released from sympathetic nerves and acts as a cotransmitter with noradrenaline (for recent reviews see Burnstock, 1990; von Kügelgen & Starke, 1991). For example, stimulation of the sympathetic nerves in the vas deferens of the mouse, rat and guinea-pig produces a biphasic contractile response which is thought to result from the combined action of ATP and noradrenaline released as cotransmitters. The initial phase of the neurogenic contraction is blocked by arylazidoaminopropyionyl-ATP ($ANAPP_3$) (guinea-pig) (Fedan *et al.*, 1981), by selective desensitization of P_{2X}-purinoceptors with α,β-methyleneATP (guinea-pig, rat and mouse) (Meldrum & Burnstock, 1983; Allcorn *et al.*, 1986) and by the P_2-purinoceptor antagonist, suramin (mouse and rat) (Dunn & Blakeley, 1988; von Kügelgen *et al.*, 1989; Blakeley *et al.*, 1991; Mallard *et al.*, 1992) and is therefore considered to be mediated by ATP acting on P_{2X}-purinoceptors (Burnstock & Kennedy, 1985; Kennedy, 1990). The secondary component of the neurogenic response is blocked by α-adrenoceptor antagonists such as prazosin and so is thought to be due to the action of noradrenaline acting on α_1-adrenoceptors.

The underlying electrical response to sympathetic nerve stimulation in the vas deferens is a rapid, transient excitatory junction potential (e.j.p.) which is also blocked by $ANAPP_3$ (Sneddon *et al.*, 1982), α,β-methyleneATP (Sneddon & Burnstock, 1984; Stjärne & Åstrand, 1984; Allcorn *et al.*, 1986) and suramin (Sneddon, 1992; Sneddon & Machaly, 1992), but not by α-adrenoceptor antagonists. Indeed the e.j.p. is particularly useful for monitoring P_{2X}-purinoceptor-mediated responses since it appears to be produced solely by ATP, whereas the mechanical responses are composed of two phases which can be described as predominantly noradrenergic or predominantly purinergic, but each of which has some contribution from both transmitters (for details see Amobi & Smith, 1990).

Recently, the compound pyridoxalphosphate-6-azophenyl-2',4'-disulphonic acid (PPADS), has been proposed as a selective P_{2X}-purinoceptor antagonist in the rabbit isolated vas deferens (Lambrecht *et al.*, 1992). PPADS was found to inhibit the contractile response to exogenous α,β-methylene-ATP, a selective P_{2X}-purinoceptor agonist, but not that to exogenous noradrenaline. PPADS also inhibited selectively the initial phasic contraction to sympathetic nerve stimulation, thought to be predominantly mediated by ATP acting through P_{2X}-purinoceptors, without having any effect on the later, secondary component, which is thought to be mainly due to noradrenaline acting at α_1-adrenoceptors. Responses mediated through muscarinic cholinoceptors, P_1-purinoceptors and H_1-histamine receptors were also unaffected by PPADS. In addition, PPADS was found to inhibit selectively P_{2X}-purinoceptor-mediated contractions in guinea-pig submucosal arterioles (Bungardt *et al.*, 1992). Thus, as far as it has been tested, PPADS appears to display selectivity for the P_{2X}-purinoceptor.

In this study we have examined the effect of PPADS on mechanical and electrical responses of the guinea-pig vas deferens in order to investigate further its selectivity in blocking responses to P_{2X}-purinoceptors. A preliminary account of these results has been published (McLaren *et al.*, 1993).

[1] Author for correspondence.

Methods

Albino male guinea-pigs (300–400 g) were killed with CO_2 and subsequent exanguination. The vasa deferentia were dissected out, cleaned of connective tissue, mounted for recording and allowed to equilibrate at 35°C for 1 h. A physiological salt solution of the following composition was used throughout (mM): NaCl 118, KCl 5.4, NaH_2PO_4 1.16, $NaHCO_3$ 25, $MgSO_4$ 1.16, $CaCl_2$ 2.5 and glucose 11.1, bubbled with 95% O_2, 5% CO_2.

In isometric tension recording experiments, the vas deferens was suspended in a 2 ml organ bath, under a resting tension of 0.5–0.75 g and connected to a Gould Metrigram transducer which was coupled to a Gould 2200s pen recorder via a Gould universal preamplifier. The sympathetic axons in the tissue were stimulated by electrical field stimulation using a Scientific Research Instruments stimulator giving a stimulus of 4 Hz for 20 s with a pulse width of 0.5 ms and supramaximal voltage every 10 min. In individual tissues the effect of a range of concentrations of PPADS (10^{-7}–3×10^{-5} M) on neurogenic contractions were examined. Initially, sympathetic nerves were stimulated until two consecutive contractions of similar magnitude were evoked. The lowest concentration of PPADS used was then applied to the tissue for 15 min, in which time steady state inhibition was reached. Thereafter, progressively higher concentrations of PPADS were administered and the inhibition allowed to reach equilibrium. Each concentration of PPADs was tested in each of six tissues.

Concentration-response curves to α,β-methyleneATP were obtained by direct addition to the bath. Shortly after the contraction had reached a peak the drug was washed out by several changes of the bathing solution. Care was taken to avoid desensitization of the muscle to α,β-methyleneATP by leaving a time interval of 30 to 45 min before the next concentration of agonist was added. Concentration-response curves to noradrenaline were obtained in a similar manner. For either agonist, a concentration-response curve was first obtained followed by a test curve in the presence of PPADS. Contractile responses to histamine and carbachol were obtained with concentrations that had been shown in preliminary experiments to be near EC_{50} for either agonist. PPADS was allowed to equilibrate for at least 15 min before addition of agonists.

In the electrophysiological studies the vasa deferentia were pinned out in a 2 ml organ bath and maintained as described above for the mechanical experiments. Intracellular recording of the transmembrane potential was carried out with glass microelectrodes of 30–50 MΩ resistance. The signal was recorded on a storage oscilloscope (Tektronix) and a tape recorder (Racal) via a preamplifier (Cell Explorer 800, Dagan). Impalements were accepted if the resting potential maintained a stable level of at least − 60 mV. E.j.ps were evoked continuously by field stimulation at 0.5 Hz, 0.2 ms pulse width and at a voltage lower than that necessary to initiate a contraction. As with the mechanical recordings, each tissue was exposed to increasing concentrations of PPADS (10^{-7}–3×10^{-5} M). Initially, the lowest concentration used was applied for 15 min before measurements of the e.j.p. magnitude and membrane potential were taken. Progressively higher concentrations were then administered and steady state e.j.p. magnitude and membrane potential recorded. In several experiments suramin (10^{-4} M) was added to the bath 30 min before the addition of PPADS (10^{-5} M).

Statistics

Values in the text refer to mean ± s.e.mean or geometric mean with 95% confidence limits for EC_{50} values (after Fleming *et al.*, 1972). Statistical comparison of the results was tested by Student's *t* test for paired or unpaired data, as appropriate. Differences were considered significant when $P<0.05$. In some cases (Figure 2b), concentration-response curves were fitted to the data by logistic (Hill equation), non-linear regression analysis (FigP, Biosoft, Cambridge, UK).

Drugs

α,β-methyleneATP (lithium salt), carbachol (carbamylcholine chloride), histamine dihydrochloride (all Sigma) and suramin (Bayer, U.K.) were dissolved in distilled water and kept as 10^{-1} M stock solutions. (−)-Noradrenaline bitartrate (Sigma) was dissolved in acid saline and frozen as a 10^{-1} M stock solution. PPADS was synthesized in one of our laboratories (starting materials aniline-2,4-disulphonic acid and pyridoxalphosphate). The structure of PPADS was confirmed by ^1H n.m.r. spectroscopy and its purity investigated by thin-layer chromatography on high-performance silica gel plates (developing solvent: 1-propanol/aqueous ammonia (33%)/water, 6:3:2 v/v. The final product showed only one spot and the two starting materials could not be detected. PPADS was dissolved in distilled water as a 10^{-2} M stock solution and kept frozen in darkness.

Results

Contractile responses to sympathetic nerve stimulation

Field stimulation of the sympathetic nerves of the guinea-pig vas deferens with trains of pulses for 20 s at 4 Hz, produced a characteristic biphasic response (Figure 1a). PPADS (10^{-7}

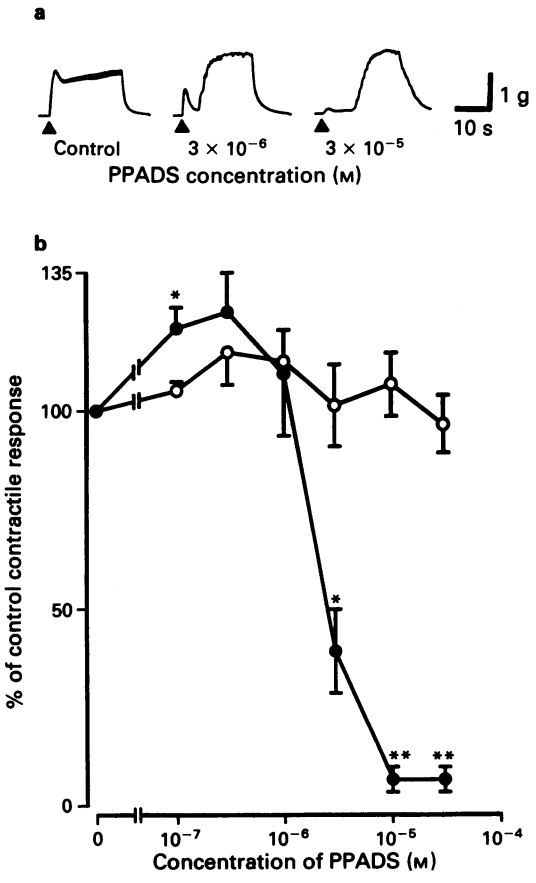


Figure 1 The effects of PPADS on the biphasic contractile response of the guinea-pig vas deferens to sympathetic nerve stimulation elicited by a train of pulses for 20 s at 4 Hz (▲-start of stimulation). (a) The upper panel shows contractions elicited in the same tissue in the absence and presence of PPADS (3×10^{-6} and 3×10^{-5} M). (b) The lower panel shows the mean data ± s.e.mean ($n = 6$) for the effect of PPADS (10^{-7}–3×10^{-5} M) on the initial phasic response (●) and the secondary tonic response (○). $^*P<0.05$, $^{**}P<0.01$.

M -3×10^{-5} M) did not alter the resting tension, but had two effects on the phasic, predominantly purinergic, component of the neurogenic contraction. At 10^{-7} M, PPADS caused a small, but significant, potentiation of the phasic response, whilst at higher concentrations PPADS evoked a substantial, concentration-dependent inhibition, which was significant at 3×10^{-6} M and greater, 50% inhibition was seen at approximately 2.5×10^{-6} M PPADS. In contrast, over the same concentration-range, PPADS had no significant effect on the secondary, predominantly noradrenergic phase of the response (Figure 1a,b).

Concentration-response curves to α,β-methyleneATP and noradrenaline

Next, the effect of a concentration of PPADS (3×10^{-5} M), which was maximally effective against the phasic contraction was tested against exogenously applied agonists.

The P_{2X}-purinoceptor agonist, α,β-methyleneATP (10^{-8}–10^{-3} M) evoked rapidly developing, concentration-dependent, transient contractions. Concentration-response curves to α,β-methyleneATP in the absence and presence of PPADS (3×10^{-5} M) are shown in Figure 2a. Since there were was no clear maximum achieved in these curves, it was not possible to calculate EC_{50} values, so the effect of PPADS was examined statistically at each individual concentration of α,β-methyleneATP. PPADS caused a significant inhibition of contractions induced by lower concentrations of α,β-methyleneATP (10^{-8}–10^{-5} M), but this was overcome by the highest concentrations of α,β-methyleneATP (10^{-4}–10^{-3} M). These results suggest that PPADS could be acting as a competitive antagonist here. When measured at the level equal to 50% of the contraction induced by 10^{-3} M α,β-methyleneATP, PPADS (3×10^{-5} M) induced a 13.5-fold shift to the right, giving an apparent pK_B of 5.62.

Noradrenaline (10^{-8}–10^{-3} M) caused concentration-dependent, biphasic contractions consisting of a small initial twitch, followed by a larger, slowly developing maintained contraction. In the absence of PPADS noradrenaline had an EC_{50} of 1.4×10^{-5} M (95% confidence limits = 2.7×10^{-6}–7.4×10^{-5} M) with a maximum response of 2.9 ± 0.1 g ($n = 5$), while in the presence of PPADS (3×10^{-5} M) the EC_{50} was 7.6×10^{-6} M (95% confidence limits = 2.2×10^{-6}–2.6×10^{-5} M) and the maximum contraction 3.5 ± 0.2 g ($n = 5$) (see Figure 2b; values derived from sigmoid curve fitting). Neither value was significantly different from the control.

Responses to carbachol and histamine

Contractions to carbachol and histamine were evoked to determine further the selectivity of PPADS. In the presence of PPADS (3×10^{-5} M) the contraction to 10^{-5} M carbachol (1.6 ± 0.4 g) was not significantly different from the control value (1.2 ± 0.3 g, $n = 6$). Similarly, PPADS (3×10^{-5} M) had no significant effect on contractions evoked by 10^{-4} M histamine (control, 1.1 ± 0.3 g; + PPADS, 0.8 ± 0.2 g, $n = 4$).

Electrophysiological studies

The mean resting membrane potential of control cells was -64.8 ± 0.6 mV and the mean size of fully facilitated e.j.ps recorded from these cells at 0.5 Hz was 13.7 ± 0.6 mV ($n = 51$). PPADS (10^{-7}–3×10^{-5} M) caused a significant and concentration-dependent depolarization and reduction in e.j.p. magnitude (Figure 3a, b); 50% inhibition of e.j.p. magnitude was seen at approximately 7×10^{-7} M PPADS. After washout of PPADS for 1 h the e.j.p. magnitude recovered to 11.2 ± 1.3 mV ($n = 17$) and the resting membrane potential to -65.4 ± 1.4 mV ($n = 17$), which were not significantly different from the control values.

Since activation of P_{2X}-purinoceptors elicits depolarization in the guinea-pig vas deferens (Sneddon & Westfall, 1984), PPADS may be acting here as a partial agonist at the P_{2X}-purinoceptor. To test this possibility we examined the effect of PPADS when present with the P_2-purinoceptor antagonist suramin. In the presence of suramin (10^{-4} M) the resting membrane potential was -66.8 ± 0.9 mV ($n = 5$), which was not significantly different from control cells. In the continued presence of suramin, subsequent addition of PPADS (10^{-5} M) still produced a significant reduction in membrane potential to -54.6 ± 0.6 mV ($n = 8$), which was similar to that seen in the absence of suramin (-55.0 ± 1.8 mV, $n = 12$).

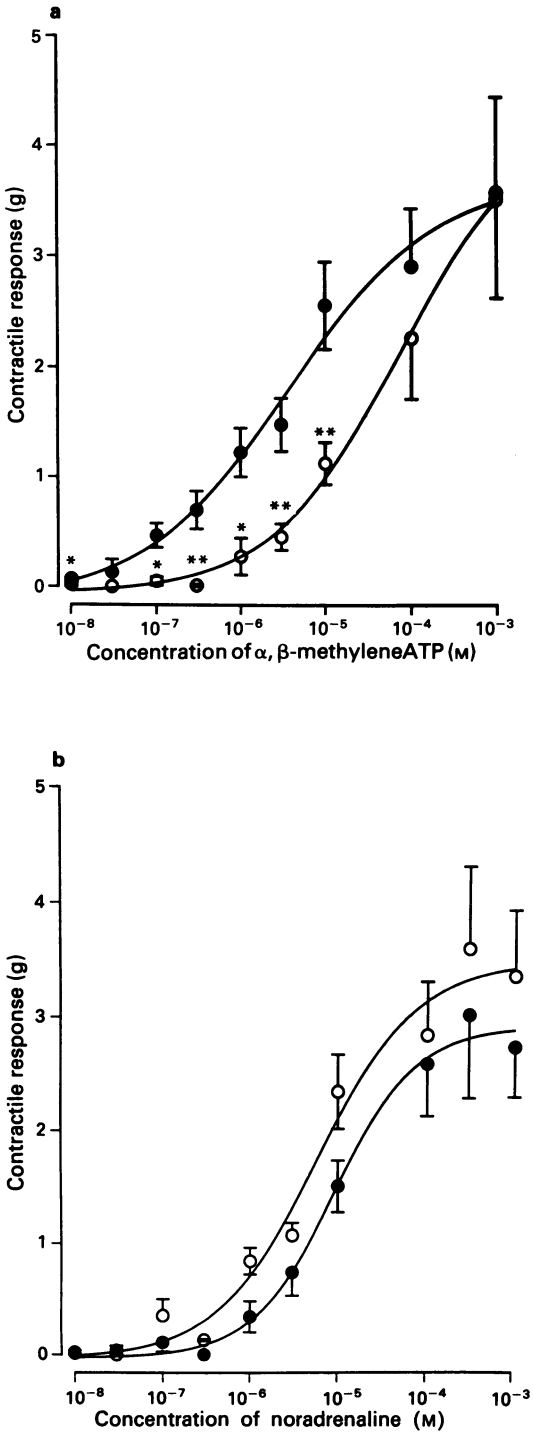


Figure 2 The effect of PPADS on the concentration-response curves to exogenously applied (a), α,β-methyleneATP (10^{-8}–10^{-3} M, $n = 7$) an (b) noradrenaline (10^{-8}–10^{-3} M, $n = 5$) in the absence (●) and presence (○) of PPADS (3×10^{-5} M). Mean with s.e.mean, $*P < 0.05$, $**P < 0.01$.

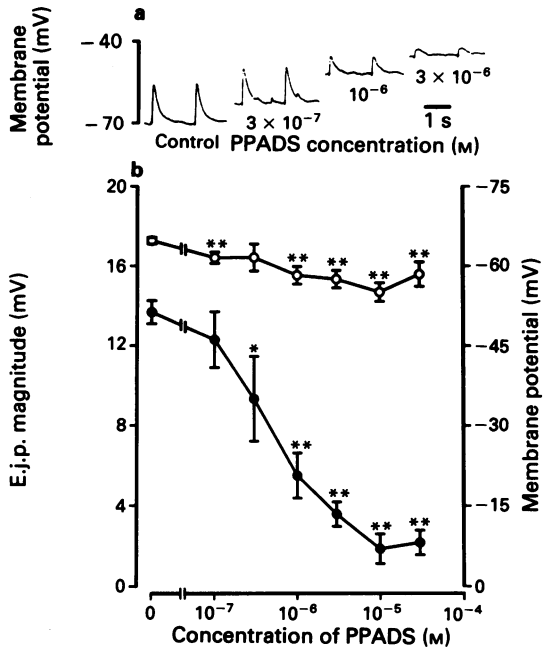


Figure 3 The effect of PPADS on the magnitude of fully facilitated e.j.ps (0.5 Hz, 0.2 ms pulse width, submaximal voltage) and the membrane potential. (a) The upper panel shows recordings in a single cell of the membrane potential and e.j.ps, initially in the absence and then in the presence of increasing concentrations of PPADS (3×10^{-7}–3×10^{-6} M). (b) The lower panel shows the mean data ± s.e.mean ($n = 5$–51) for the effects of PPADS (10^{-7}–3×10^{-5} M) on e.j.p. magnitude (●) and membrane potential (○). $^{*}P<0.05$, $^{**}P<0.01$.

Discussion

The results of this study show that PPADS selectively inhibits those responses in the guinea-pig vas deferens which are mediated by P_{2X}-purinoceptors, but has no effect on contractions mediated by α_1-adrenoceptors, muscarinic cholinoceptors or histamine receptors. In general, this is consistent with the initial reports of the actions of PPADS in the rabbit vas deferens (Lambrecht *et al.*, 1992) and guinea-pig submucosal arterioles (Bungardt *et al.*, 1992), where it was found that PPADS selectively inhibited responses mediated by P_{2X}-purinoceptors. However, in the present study we also found that PPADS has additional excitatory actions, depolarization of the smooth muscle cells, which is independent of P_{2X}-purinoceptors and, at a low concentration, a small potentiation of the phasic component of the neurogenic contraction through an unknown mechanism.

PPADS selectively modulated the phasic, predominantly purinergic component of neurogenic contractions of the guinea-pig vas deferens while having no effect on the tonic, mainly noradrenergic component. PPADS also selectively inhibited contractions to α,β-methyleneATP, but had no effect on those elicited by noradrenaline, carbachol or histamine. The PPADS-induced inhibition of contractions evoked by α,β-methyleneATP was overcome by increasing the concentration of the agonist, suggesting that PPADS could be acting here as a competitive antagonist at P_{2X}-purinoceptors. This contrasts with the study in rabbit vas deferens (Lambrecht *et al.*, 1992) where, at lower concentrations than used here, PPADS appeared to cause a non-competitive antagonism of contractions evoked by α,β-methyleneATP.

In the electrophysiological studies PPADS caused a reduction in the magnitude of e.j.ps which underlie the phasic, purinergic contraction in the guinea-pig vas deferens (Sneddon *et al.*, 1982) and this is consistent with the view that PPADS is an antagonist at P_{2X}-purinoceptors. However, PPADS also induced a membrane depolarization, which may also contribute to the reduction in the amplitude of the e.j.ps due to a decrease in driving force (but see Sjöstrand, 1973). One possible explanation for this depolarization is that PPADS is a partial agonist at P_{2X}-purinoceptors, which are known to mediate depolarization in this tissue (Sneddon & Westfall, 1984). We investigated this by determining whether suramin, which is also a P_{2X}-purinoceptor antagonist (Dunn & Blakeley, 1988; Blakeley *et al.*, 1991; Mallard *et al.*, 1992; Sneddon, 1992), would alter the depolarization caused by PPADS. PPADS still caused a depolarization when suramin was present, indicating that the depolarization was not due to an excitatory action of PPADS at P_{2X}-purinoceptors.

Although PPADS depolarized the smooth muscle cells, this did not lead to a contraction. Presumably, the depolarization was not great enough to induce sufficient calcium influx to initiate contraction. How PPADS depolarized the smooth muscle cells was not studied further here. One possibility is that PPADS was acting non-selectively to disrupt the membrane of the cell. However, this is unlikely as the effects of PPADS on the contractile responses to noradrenaline, histamine and carbachol were not reduced. Another possibility is that PPADS could modify the activity of ion channels in the membrane of the smooth muscle, e.g. by blocking potassium channels, or less likely, by activating sodium, calcium or chloride channels. However, this was not examined here and the exact mechanism requires further investigation. Likewise, the mechanism through which a low concentration of PPADS potentiated the phasic component of the neurogenic contraction is not clear. One possibility is that the potentiation was due to the small depolarization induced by PPADS, as has been found for other agonists in this tissue (Sjöstrand, 1973).

In conclusion, PPADS selectively inhibits responses in the guinea-pig vas deferens which are mediated by the P_{2X}-purinoceptor as opposed to responses mediated by non-P_2-purinoceptors, but its ability to depolarize the smooth muscle cells independently of P_{2X}-purinoceptors and also, at a low concentration, to potentiate the phasic component of neurogenic contractions, shows that it has other actions.

This work was supported by a grant from the Wellcome Trust. G.J. McL. is funded by an M.R.C. studentship. Furthermore, the authors thank the Fonds der Chemischen Industrie (Germany) (G.L., E.M.) and the Deutsche Forschungsgemeinschaft (H.G.B., SFB 169) for financial support.

References

ALLCORN, R.J., CUNNANE, T.C. & KIRKPATRICK, K. (1986). Actions of α,β-methyleneATP and 6-hydroxydopamine on sympathetic neurotransmission in the vas deferens of the guinea-pig, rat and mouse: support for cotransmission. *Br. J. Pharmacol.*, **89**, 647–659.

AMOBI, N. & SMITH, I.C. (1990). Effects of α,β-methyleneATP on biphasic responses of rat vas deferens. *Eur. J. Pharmacol.*, **133**, 75–82.

BLAKELEY, A.G.H., BROCKBANK, J.E., KELLY, S.S & PETERSEN, S.A. (1991). Effects of suramin on the concentration-response relationship of α,β-methyleneATP on the mouse vas deferens. *J. Auton. Pharmacol.*, **11**, 45–49.

BUNGARDT, E., MOSER, U., SPATZ-KUMBEL, G., BÄUMERT, H.G., LAMBRECHT, G. & MUTSCHLER, E. (1992). Characterization of purinoceptors in guinea-pig ileum resistance vessels by the use of computer-assisted videomicroscopy. *Int. J. Purine Pyrimidine Res.*, **3**, 66 (abstract).

BURNSTOCK, G. (1990). Noradrenaline and ATP as cotransmitters in sympathetic nerves. *Neurochem. Int.*, **17**, 357–368.

BURNSTOCK, G. & KENNEDY, C. (1985). Is there a basis for distinguishing two types of P_2-purinoceptor? *Gen. Pharmacol.*, **5**, 433–440.

DUNN, P.M. & BLAKELEY, A.G.H. (1988). Suramin: a reversible P_{2X}-purinoceptor antagonist in the mouse vas deferens. *Br. J. Pharmacol.*, **93**, 243–245.

FEDAN, J.S., HOGABOOM, G.K., WESTFALL, D.P. & O'DONNELL, J.P. (1981). Comparison of the effects of arylazido aminopropionyl ATP ($ANAPP_3$), an ATP antagonist, on responses of the smooth muscle of the guinea-pig vas deferens to ATP and related nucleotides. *Eur. J. Pharmacol.*, **81**, 193–204.

FLEMING, W.W., WESTFALL, D.P., DE LA LANDE, I.S. & JELLETT, L.B. (1972). Log-normal distribution of equieffective doses of norepinephrine and acetylcholine in several tissues. *J. Pharmacol. Exp. Ther.*, **181**, 339–345.

KENNEDY, C. (1990). P_1 and P_2-purinoceptor subtypes – an update. *Arch. Int. Pharmacodyn.*, **303**, 30–50.

LAMBRECHT, G., FRIEBE, T., GRIMM, U., WINDSCHEIF, U., BUNGARDT, E., HILDEBRANDT, C., BÄUMERT, H.G., SPATZ-KÜMBEL, G. & MÜTSCHLER, E. (1992). PPADS, a novel functionally selective antagonist of P_2 purinoceptor-mediated responses. *Eur. J. Pharmacol.*, **217**, 217–219.

MALLARD, N., MARSHALL, R., SITHERS, A. & SPRIGGS, B. (1992). Suramin: a selective inhibitor of purinergic neurotransmission in the rat isolated vas deferens. *Eur. J. Pharmacol.*, **220**, 1–10.

McLAREN, G.J., SNEDDON, P., KENNEDY, C., LAMBRECHT, G., BURNSTOCK, G., MUTSCHLER, E., BAUMERT, H.G. & HOYLE, C.H.V. (1993). Investigation of a putative P_{2X}-purinoceptor antagonist in the guinea-pig vas deferens. *Br. J. Pharmacol.*, **109**, 109P.

MELDRUM, L.A. & BURNSTOCK, G. (1983). Evidence that ATP acts as a cotransmitter with noradrenaline in the sympathetic nerves supplying the guinea-pig vas deferens. *Eur. J. Pharmacol.*, **92**, 161–163.

SJÖSTRAND, N.O. (1973). Effects of acetylcholine and some other smooth muscle stimulants on the electrical and mechanical responses of the guinea-pig vas deferens to nerve stimulation. *Acta Physiol. Scand.*, **89**, 1–9.

SNEDDON, P. (1992). Suramin inhibits excitatory junction potentials in the guinea-pig isolated vas deferens. *Br. J. Pharmacol.*, **107**, 101–103.

SNEDDON, P. & BURNSTOCK, G. (1984). Inhibition of excitatory junction potentials in the guinea-pig vas deferens by α,β-methyleneATP: further evidence for ATP and noradrenaline as cotransmitters. *Eur. J. Pharmacol.*, **100**, 85–90.

SNEDDON, P. & MACHALY, M. (1992). Regional variation in purinergic and adrenergic responses in isolated vas deferens of rat, rabbit and guinea-pig. *J. Auton. Pharmacol.*, **12**, 421–428.

SNEDDON, P. & WESTFALL, D.P. (1984). Pharmacological evidence that adenosine triphosphate and noradrenaline are cotransmitters in the guinea-pig vas deferens. *J. Physiol.*, **347**, 561–580.

SNEDDON, P., WESTFALL, D.P. & FEDAN, J.S. (1982). Cotransmitters in the motor nerves of the guinea-pig vas deferens: electrophysiological evidence. *Science*, **218**, 693–695.

STJÄRNE, L. & ASTRAND, P. (1984). Discrete events measure single quanta of adenosine 5′-triphosphate secreted from sympathetic nerves of guinea-pig and mouse vas deferens. *Neuroscience*, **13**, 21–28.

VON KÜGELGEN, I. & STARKE, K. (1991). Noradrenaline-ATP cotransmission in the sympathetic nervous system. *Trends Pharmacol. Sci.*, **12**, 319–324.

VON KÜGELGEN, I., BÜLTMANN, R. & STARKE, K. (1989). Interaction of adenine nucleotides. UTP and suramin in mouse vas deferens: suramin-sensitive and suramin-insensitive components in the contractile effect of ATP. *Naunyn-Schmied. Arch. Pharmacol.*, **342**, 198–205.

(Received August 7, 1993
Revised November 4, 1993
Accepted November 9, 1993)

Br. J. Pharmacol. (1994), **111**, 918–922 © Macmillan Press Ltd, 1994

Effect of sodium metabisulphite on bronchial blood flow in conscious sheep: pharmacological modulation

G.M. Nichol, G.H. Parsons & [1]K.F. Chung

Department of Thoracic Medicine, National Heart and Lung Instititute, Royal Brompton National Heart & Lung Hospital, London SW3 and Division of Pulmonary Critical Care, University of California, Davis CA 95616, U.S.A.

1 Sodium metabisulphite (MBS) can induce bronchoconstriction in patients with asthma. We investigated the effects of MBS aerosol on bronchial blood velocity (V_{br}) and pulmonary resistance in intubated conscious sheep.

2 Bronchial blood velocity was measured by implanting a 20 MHz ultrasonic Doppler flow probe on the common bronchial branch of the bronchoesophageal artery.

3 Inhaled MBS induced a dose-dependent, transient increase in V_{br} lasting for a few minutes without any changes in aortic and pulmonary artery pressures. There was some tachyphylaxis of the V_{br} response to successive inhalations of MBS.

4 The cholinoceptor antagonist, ipratropium bromide and the H_1 and H_2 histamine antagonists, chlorpheniramine and cimetidine, had no significant effect on MBS-induced increase on V_{br}. The loop diuretic, frusemide, and the anti-inflammatory drug, nedocromil sodium, which both inhibit MBS-induced bronchoconstriction in patients with asthma, were also without effect.

5 We conclude that MBS induces bronchial vasodilatation in conscious sheep, and that this effect is not dependent on the release of histamine or other mediators, or an activation of cholinergic pathways.

Keywords: Bronchial blood flow; histamine; sodium metabisulphite; nedocromil sodium; frusemide; ipratropium bromide; sheep

Introduction

Sulphites and sulphur dioxide (SO_2) have been shown to induce bronchoconstriction in patients with asthma (Sheppard *et al.*, 1980; Koenig *et al.*, 1981). Sodium metabisulphite (MBS), a sulphite frequently used as a preservative, can cause bronchoconstriction in a minority of asthmatics when ingested (Stevenson & Simon, 1981). On the other hand, inhalation of MBS aerosol or SO_2 induces bronchoconstriction in most asthmatics (Schwartz & Chester, 1984). The mechanisms by which MBS aerosol or SO_2 induce airway narrowing are unclear. Because MBS itself does not directly induce contractile responses on airway smooth muscle preparations such as guinea-pig tracheal strips (Sun *et al.*, 1993), we examined whether indirect mechanisms could be responsible for the airway narrowing. In asthmatic subjects, anticholinoceptor agents have various inhibitory effects on the bronchoconstrictor response to SO_2 or MBS in asthmatic subjects, implying that cholinergic nerves are not involved in this response (Tan *et al.*, 1982; Snashall & Baldwin, 1982; Seale *et al.*, 1988; Nichol *et al.*, 1989). Sodium metabisulphite aerosol can induce bronchoconstriction in the anaesthetized guinea-pig, an effect partly mediated through the endogenous release of tachykinins (Sakamoto *et al.*, 1992).

Another possibility by which MBS may influence airway calibre could be through an effect on the airway vasculature. Several agents such as histamine, bradykinin, prostaglandins and substance P are known to increase both tracheal and bronchial blood flow (Laitinen *et al.*, 1987; Parsons *et al.*, 1992a,b) and it is possible that this vasodilatation could encroach on the inner luminal diameter particularly in intrapulmonary airways. We have characterized the effects of MBS aerosol on bronchial blood flow in conscious sheep using a method we have previously described (Parsons *et al.*, 1992a). In addition, we studied the pharmacological modulation of MSB-induced bronchial blood flow by an anticholinoceptor agent and by H_1 and H_2 histamine receptor blockade. In order to determine the contribution of mediator release during MBS airway challenge, we examined the effects of nedocromil sodium and of frusemide which are both able to inhibit the release of histamine or leukotrienes from inflammatory cells (Leung *et al.*, 1988; Bruinjzeel *et al.*, 1989; Anderson *et al.*, 1991).

[1] Author for correspondence at London address.

Methods

Preparatory surgery

Two to three weeks before the experimental observations, 10 adult sheep (body weight, 31 ± 3 kg, mean ± s.d.) were anaesthetized with thiamylal (10–15 mg kg^{-1}, i.v.). The trachea was intubated, and the lungs were ventilated with 1–2% halothane in oxygen by a Harvard ventilator. Using sterile procedure, we opened the chest in the left 5th intercostal space, and cleared the ventral surface of the descending thoracic aorta to reveal the short bronchoesophageal artery. The artery has two major branches, the oesophageal branch directed caudally, and the common bronchial branch (hereafter called the bronchial artery) directed ventrally to supply the bronchi and the distal trachea (Magno *et al.*, 1987). A Doppler flow probe 2.5 mm in diameter (Crystal-Biotech, Hopkinton, MA, U.S.A.) was secured around the bronchial artery. Wires from the probe were led through the chest wall and tunnelled subcutaneously to exit between the scapulae. The chest was closed, the pneumothorax reduced, and the sheep allowed to recover the anaesthesia.

Use of pulsed Doppler flow probes

The Doppler flow meter is essentially a velocity meter but can be used as a volume flowmeter when the transducer is implanted chronically. Its lightweight probes are suitable for chronic implantation around small arteries (1.0–2.5 mm in diameter) (Hartley & Cole, 1974; White *et al.*, 1974; Vatner *et al.*, 1982) so that the bronchial blood flow can be monitored in spontaneously breathing animals. The probe

output (δF) is the shift between an emitted frequency (F_e, 20 MHz) and the frequency reflected from moving blood components (F_r). Doppler flow probes provide a signal proportional to the velocity of blood flow, according to the equation:

$$\delta F = F_e - F_r = (2F_e\ V/c)\ \cos\ \alpha$$

where δF is the Doppler shift, V is blood flow velocity, c is the velocity of sound in blood, and α is the angle between the flow axis and the acoustic axis (Hartley & Cole, 1974). Since F_e, c and α are constants, blood velocity (V, cm s^{-1}) can be calculated. Velocity is related linearly to blood flow provided that the velocity profile and the cross-sectional area of the vessel on which the probe is implanted remains constant (White *et al.*, 1974). This condition is met in preparations such as ours (in which the probes are implanted chronically on small arteries) by the formation of granulation tissue between the cuff in which the crystals are set and the output of the probe to measure bronchial arterial blood velocity (V_{br}, cm s^{-1}) and thereby monitor changes in bronchial blood flow relative to control.

Two to three weeks after the probe had been implanted, it was tested by connecting it to an ultrasonic (20 MHz) pulsed Doppler flowmeter (Valpey-Fisher, Hopkinton, MA, U.S.A.). In all sheep, the probe provided a signal that was judged to be satisfactory on the basis of its auditory quality, the presence of a pronounced cardiac modulation in the undamped signal, and the elicitation of an increased signal by the intravenous injection of 0.1 μg kg^{-1} histamine base. Zero flow is readily determined by disconnecting the probe because a Doppler shift of zero is equivalent to zero flow. The linearity of the signal to flow has been previously demonstrated (Parsons *et al.*, 1992b). When examined at post-mortem after the experimental observations had been completed, the bronchial artery within the flow probe was invariably found to be firmly embedded in granulation tissue.

Drug preparation and delivery

Sodium metabisulphite (Sigma, Dorset) was dissolved freshly each day in 0.9% NaCl in increasing doubling concentrations from 25 to 400 mg ml^{-1} (0.13 M to 2.1 M). Control solutions were prepared by titrating 0.9% NaCl with hydrochloric acid to a pH of 3.8 similar to the 400 mg ml^{-1} MBS solution, and dissolving sodium sulphate in a 0.9% NaCl solution (100 mg ml^{-1} or 0.7 M) so as to obtain a solution of similar osmolarity at 100 mg ml^{-1} MBS solution. MBS, ipratroprium bromide (Boehringer Ingleheim, Bracknell), frusemide (Antigen, Roscrea, Republic of Ireland), nedocromil sodium (Fisons Pharmaceuticals Ltd, Leics) and histamine diphosphate (0.02 M; 0.5% in 0.9% NaCl; Sigma, Dorset) were delivered by continuous jet nebulisation. The nebuliser (System 22, Medic-Aid Limited, West Sussex) was driven by a 6 l min^{-1} flow of compressed air and generated aerosol droplets with a mass median aerodynamic diameter of 3.4 μm (Malvern Instruments Laser particle sizer, model 2600D). Aerosols were generated into the inspiratory tubing via a T-piece connected to the endotracheal tube, and during the period of exposure to drugs the animals were connected to a Harvard ventilator (Harvard Apparatus, South Natick, MA, U.S.A.) set at a tidal volume of 10 ml kg^{-1} and a frequency of 12 breaths per min in order to overdrive spontaneous breathing. The H_1 receptor antagonist used was chlorpheniramine maleate (Sigma Chemical Co. Dorset, U.S.A.) and H_2 receptor antagonist was cimetidine hydrochloride (Smith Kline Beecham Corp, Philadelphia, PA, U.S.A.), both administered intravenously.

Protocols

Dose-response, time-course and tachyphylaxis Following restraint, baseline recordings of bronchial blood flow velocity, airway resistance and aortic and pulmonary pressures were made. These sheep were then exposed to the following aerosols in the following order: control solutions, histamine, increasing concentrations of MBS, a repeat nebulisation of the MBS dose that caused approximately 50% of the maximal bronchial blood-flow response (EC_{50} dose) and a repeat histamine. All nebulizations lasted 2 min (i.e. 24 breaths) except for histamine of which only 10 breaths were given. Bronchial blood flow and haemodynamic parameters were recorded prior to and continuously for 15 min after each nebulisation, by which time they had invariably returned to baseline.

Effect of drugs on MBS airway response In preliminary experiments, we established that two submaximal inhalations of MBS 5–30 min apart induced similar increases in bronchial blood flow. We performed studies on separate days with MBS inhalations before and after dosing with the appropriate drug. MBS was inhaled for 2 min followed by 10 min of continuous recording of bronchial blood velocity with 5 min rest afterwards. The dose of MBS administered was that which caused a 50% increase of the maximal value of bronchial blood flow (EC_{50} dose) as previously determined for each individual sheep.

The drugs studied were as follows:

(a) *Cholinoceptor blockade:* In six sheep, challenge with an EC_{50} dose of MBS before and immediately after receiving atropine (1 mg or 1.44 mmol i.v.) and ipratropium bromide (750 μg or 1.74 mmol by aerosol) was performed. This dose was chosen because we have shown it to be effective in sheep (Coleridge *et al.*, 1992; Mansour *et al.*, 1992).

(b) *Combined H_1- and H_2-histamine receptor blockade:* In seven sheep, challenge with an EC_{50} dose of MBS before and 20 min after receiving chlorpheniramine (3 mg kg^{-1} or 7.7 mmol kg^{-1}, i.v.) and cimetidine (5 mg kg^{-1} or 20 mmol kg^{-1}, i.v.) was performed. The doses used have been previously shown to be effective in inhibiting histamine-induced increases in V_{br} in the sheep (Parsons *et al.*, 1992b).

(c) *Inhaled frusemide:* In six sheep, challenge with an EC_{50} dose of MBS before and immediately after inhaling frusemide (30 mg dissolved in 3 ml of 0.9% NaCl or 91 mmol delivered into the airways) was performed. This dose of frusemide has been shown to inhibit the bronchoconstrictor effects of inhaled MBS in asthmatic volunteers (Nichol *et al.*, 1990).

(d) *Inhaled nedocromil sodium:* In six sheep, a dose of 1 mg kg^{-1} (2.4 mmol kg^{-1}) was administered by aerosol after the effects of an EC_{50} dose of MBS was measured, followed by repeat MBS challenge (Abraham *et al.*, 1988).

Data analysis

Data are expressed as mean ± s.e.mean. Paired results were compared by Student's *t* test for paired data. Repeated measurements were analysed by the two-way analysis of variance for repeated measures. A significance level of 5% was used to reject the null hypothesis.

Results

Time course of V_{br} to MBS

The bronchial blood velocity response to inhaled MBS followed a characteristic time-course, rising progressively during, and for a further minute after, the 2 min period. Bronchial velocity then returned steadily towards baseline over the ensuing 10 min. Figure 1 illustrates the average time-course of the response to EC_{50} doses of MBS in eight animals. Inhalation of either acidified saline or hypertonic sodium sulphate did not change bronchial blood flow despite the induction of coughing during inhalation of sodium sulphate solution.

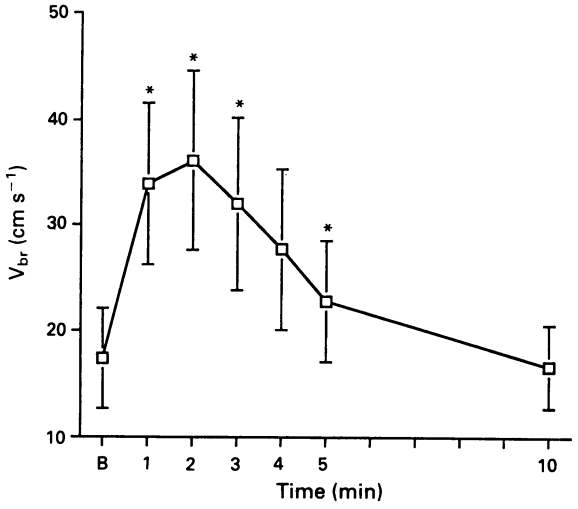


Figure 1 Time-course of bronchial artery blood velocity (V_{br}, cm s^{-1}) before (baseline) and for the 10 min immediately following completion of the metabisulphite (MSB) aerosol inhalation at the EC_{50} dose. Values are mean ± s.e.mean in eight sheep. The EC_{50} dose was 64.8 mg ml^{-1} (g.s.e.mean 1.25). *$P<0.05$ compared to baseline.

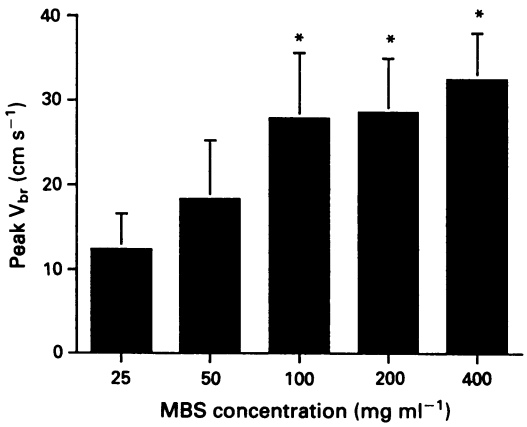


Figure 2 Peak changes in bronchial arterial blood velocity (V_{br}) in response to increasing doses of metabisulphite (MSB) aerosol, delivered at 12 breaths min^{-1} for 2 min. The baseline bronchial blood velocities prior to MBS at 25, 50, 100, 200 and 400 mg ml^{-1} were 21.0 ± 5.5, 18.2 ± 5.3, 16.4 ± 4.5, 16.1 ± 4.6 and 15.4 ± 4.1, respectively. Values are mean ± s.e.mean in eight sheep. *$P<0.05$ compared to the 25 mg ml^{-1} concentration.

Dose-response of V_{br} to MBS

The baseline V_{br} before the MBS-induced increase in V_{br} for 25, 50, 100, 200 and 400 mg ml^{-1} of MBS were 21.0 ± 5.5, 18.2 ± 5.3, 16.4 ± 4.5, 16.1 ± 4.6 and 15.5 ± 4.1 cm s^{-1} respectively. Peak responses to increasing doses of MBS in eight animals are shown in Figure 2. The increase in V_{br} was 12.4 ± 4.2 cm s^{-1} after 25 mg ml^{-1} and 32.5 ± 5.5 after 400 mg ml^{-1} MBS. Systemic and pulmonary blood pressure responses to MBS challenge are shown for five instrumented animals in Figure 3. There was a non-significant trend for higher doses of MBS to produce elevations in peak aortic pressure amounting at most to an increase of 30 mmHg. Individual increases in aortic pressure did not correlate with increases in V_{br} ($r = -0.08$; NS). There was no significant increase in pulmonary artery pressure.

Tachyphylaxis of V_{br} response

The geometric mean EC_{50} dose of MBS was 64.8 mg ml^{-1} (g.s.e.mean 1.25) in eight sheep. Inhalation of the EC_{50} dose produced a greater response during the cumulative dose-response (peak response: 20.5 ± 3.9 cm s^{-1}) than immediately after it (peak response: 6.7 ± 2.7 cm s^{-1}; $P<0.05$). In contrast, histamine produced a similar response whether given before (peak response: 17.4 ± 4.2 cm s^{-1}) or after (peak response: 18.1 ± 4.6 cm s^{-1}) the cumulative MBS challenges.

Effect of drug treatment

There were no significant effects of any of the drugs on V_{br} evoked by MBS at the EC_{50} dose. Prior to cholinoceptor blockade, the baseline V_{br} of 23.3 ± 6.4 cm s^{-1} increased by 25.4 ± 6.4 cm s^{-1} following MBS. Post-cholinoceptor blockade, baseline V_{br} of 16.7 ± 5.6 increased by 30.1 ± 7.4 cm s^{-1} in response to MBS. The increase in V_{br} in response to MBS was not affected by cholinoceptor blockade.

Prior to histamine H_1 and H_2 receptor blockade, the baseline V_{br} of 27.9 ± 7.4 cm s^{-1} increased by 20.8 ± 6.0 cm s^{-1} when MBS aerosol was delivered. Following histamine receptor blockade, the baseline V_{br} of 20.1 ± 7.3 increased by 20.9 ± 5.8 cm s^{-1} in response to MBS.

Before sheep were given the frusemide aerosol, the baseline V_{br} of 27.4 ± 7.6 cm s^{-1} increased by 21.7 ± 4.4 cm s^{-1} in response to MBS. Following frusemide, baseline V_{br} increased by 25.5 ± 4.0 cm s^{-1} in response to MBS, which was not significantly different from the pre-frusemide values.

The baseline V_{br} of 25.7 ± 6.5 cm s^{-1} increased by 23.3 ± 3.5 cm s^{-1} in response to MBS before nedocromil sodium. Following nedocromil sodium, the baseline V_{br} of 24.6 ± 6.8 cm s^{-1} increased by 22.3 ± 3.4 cm s^{-1}, which is not different from pre-nedocromil values.

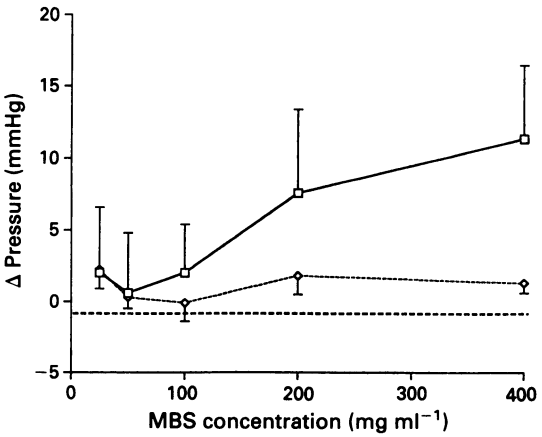


Figure 3 Peak changes in haemodynamic parameters, mean aortic pressure (ΔP_{aorta}, □) or mean pulmonary artery pressure (ΔP_{pa}, ◇), after sodium metabisulphite (MBS) aerosol inhalation at increasing doses. Values are mean ± s.e.mean in five sheep. Changes are not statistically significant.

Discussion

We have shown that sodium metabisulphite when delivered as an aerosol caused a dose-dependent increase in bronchial blood velocity in conscious sheep. This effect was transient lasting for up to 5 min and showed some degree of tachyphylaxis to repeated dosing. Sodium metabisulphite-induced vasodilatation did not appear to be modulated by histamine release or by activation of cholinergic pathways. Nedocromil sodium and frusemide which inhibit sodium metabisulphite-induced bronchoconstriction in patients with asthma were

also inactive against metabisulphite-induced increases in bronchial blood velocity.

The increases in bronchial blood flow induced by sodium metabisulphite are unlikely to be secondary to the physical properties of the aerosol such as acidity or hyperosmolality, because the control solutions with similar pH and osmolality as the metabisulphite solutions had no effect on bronchial blood flow. Although infusion of hypertonic solutions into the trachea may induce tracheal vasodilatation (Deffebach *et al.*, 1989), inhalation of hypertonic saline solutions does not alter tracheobronchial blood flow (Godden *et al.*, 1988), as we have demonstrated. We therefore examined mechanisms other than those involving hyperosmolarity by studying the effect of various pharmacological agents. As both acetylcholine and histamine are potent stimulators of bronchial blood flow in the sheep, we administered inhaled ipratropium bromide, and intravenous chlorpheniramine and cimetidine which have been shown to inhibit to a large extent the increases in bronchial blood flow induced by acetylcholine and histamine respectively so that the potential contribution of these mediators could be determined (Parsons *et al.*, 1992b; Coleridge *et al.*, 1992). These agents failed to affect significantly the sodium metabisulphite response, indicating that acetylcholine release from cholinergic efferent nerves or release of histamine from mast cells or basophils are unlikely to mediate metabisulphite-induced vasodilatation.

The loop diuretic frusemide has recently been shown to inhibit the bronchoconstrictor responses to a wide range of indirectly-acting agents or stimuli such as distilled water, exercise, allergen, adenosine and sodium metabisulphite in patients with mild asthma (Bianco *et al.*, 1988; 1989; Robuschi *et al.*, 1989; Nichol *et al.*, 1990). However, it is inactive against the direct constrictors such as methacholine and histamine (Nichol *et al.*, 1990; O'Connor *et al.*, 1991), suggesting that frusemide may inhibit the release of secondary bronchoconstrictor mediators when the indirectly-acting agents are inhaled. *In vitro*, frusemide inhibited the release of histamine and of slow-reacting substance of anaphylaxis (SRS-A) from sensitized human lung fragments challenged with allergen (Anderson *et al.*, 1991). Frusemide has also been shown to reduce the activation of cholinergic and of non-adrenergic non-cholinergic constrictor nerves in the guinea-pig airway probably through the inhibition of the release of acetylcholine and of tachykinins respectively (Elwood *et al.*, 1990). Nedocromil sodium, an inhaled drug used for the prophylaxis of asthma, has also been shown to inhibit bronchoconstriction induced by sodium metabisulphite in mild asthmatic subjects (Dixon & Ind, 1990), in addition to attenuating the constrictor effect of the tachykinin, neurokinin A (Joos *et al.*, 1989). The negative results we have observed with both frusemide and nedocromil sodium therefore suggest that sodium metabisulphite is unlikely to activate such nerves in the airways of conscious sheep. However, the use of more direct pharmacological agents such as specific antagonists of the neurokinin receptors will be necessary to confirm this.

In summary, we have shown that sodium metabisulphite aerosol induces a dose-dependent increase in bronchial blood flow in the conscious sheep. The underlying mechanism for the increase in bronchial blood flow does not appear to involve histamine release or cholinergic pathways.

References

ABRAHAM, W.M., STEVENSON, J.S., ELDRIDGE, M., GARRIDO, R. & NIEVES, L. (1988). Nedocromil sodium in allergen-induced bronchial responses and airway hyperresponsiveness in allergic sheep. *J. Appl. Physiol.*, **65**, 1062–1068.

ANDERSON, S.D., HE, W. & TEMPLE, D.M. (1991). Inhibition of frusemide of inflammatory mediators from lung fragments. *N. Engl. J. Med.*, **324**, 131.

BIANCO, S., PIERONI, M.G., REFINI, R.M., ROTTOLI, L. & SIESTINI, P. (1989). Protective effect of inhaled frusemide on allergen-induced early and late asthmatic reactions. *N. Engl. J. Med.*, **32**, 1069–1073.

BIANCO, S., VAGHI, A., ROBUSCHI, M. & PASARGIKLIAN, M. (1988). Prevention of exercise-induced bronchoconstriction by inhaled frusemide. *Lancet*, **ii**, 252–255.

BRUIJNZEEL, P.L.B., HAMELINK, M.L. & KOK, P.T.M. (1989). Nedocromil sodium inhibits the A23187- and opsonised zymosan-induced leukotriene formation by human eosinophils but not by human neutrophils. *Br. J. Pharmacol.*, **96**, 631–636.

COLERIDGE, H.M., COLERIDGE, J.C.G., GREEN, J.F. & PARSONS, G.H. (1992). Pulmonary c-fiber stimulation by capsaicin evokes reflex cholinergic bronchial vasodilation in sheep. *J. Appl. Physiol.*, **72**, 770–778.

DEFFEBACH, M.E., SALONEN, R.O., WEBBER, S.E. & WIDDICOMBE, J.G. (1989). Cold and hyperosmolar fluids in canine trachea: vascular and smooth muscle and albumin flux. *J. Appl. Physiol.*, **63**, 1309–1315.

DIXON, C.M.S. & IND, P.W. (1990). Inhaled sodium metabisulphite induced bronchoconstriction: inhibition by nedocromil sodium and sodium cromoglycate. *Br. J. Clin. Pharmacol.*, **30**, 371–376.

ELWOOD, W., LOTVALL, J.O., BARNES, P.J. & CHUNG, K.F. (1991). Loop diuretics inhibit cholinergic and non-cholinergic nerves in guinea-pig airways. *Am. Rev. Respir. Dis.*, **143**, 1340–1344.

GODDEN, D.J., BAILE, E.M., OKAZAWA, M. & PARE, P.D. (1988). Hypertonic aerosol inhalation does not alter central airway blood flow in dogs. *J. Appl. Physiol.*, **65**, 1990–1994.

HARTLEY, C.J. & COLE, J.S. (1974). An ultrasonic pulsed Doppler system for measuring blood flow in small vessels. *J. Appl. Physiol.*, **37**, 626–629.

JOOS, G.F., PAUWELS, R.A. & VAN DER STRAETEN, M.E. (1989). The effect of nedocromil sodium on the bronchoconstrictor effect of neurokinin A in subjects with asthma. *J. Allergy Clin. Immunol.*, **83**, 663–668.

KOENIG, J.Q., PIERSON, W.E., HORIKE, M. & FRANK, R. (1981). Effects of SO2 plus NaCl aerosol combined with moderate exercise on pulmonary function in asthmatic adolescents. *Environ. Res.*, **25**, 340–348.

LAITINEN, A., LAITINEN, L.A. & WIDDICOMBE, J. (1987). Effects of inflammatory and other mediators on airway vascular beds. *Am. Rev. Respir. Dis.*, **135**, S67–S70.

LEUNG, K.B.P., FLINT, K.C., BROSTOFF, J., HUDSPITH, B.N., JOHNSON, N.McI., LAU, H.Y.A., LIU, W.L. & PEARCE, F.L. (1988). Effects of sodium cromoglycate and nedocromil sodium on histamine secretion from human lung mast cells. *Thorax*, **43**, 756–761.

MAGNO, M., CHARAN, N,. PARSONS, G.H., BAILE, L., ALBERTINE, K.H. & BUTLER, J. (1974). Nomenclature for the bronchial circulation (Letter to the Editor). *J. Appl. Physiol.*, **37**, 626–629.

MANSOUR, E., AHMED, A., CORTES, A., CAPLAN, J., BURCH, R.M. & ABRAHAM, W.M. (1992). Mechanisms of metabisulphite-induced bronchoconstriction: evidence for bradykinin B2-receptor stimulation. *J. Appl. Physiol.*, **7**, 1831–1837.

NICHOL, G.M., ALTON, E., NIX, A., GEDDES, D.M., CHUNG, K.F. & BARNES, P.J. (1990). Effect of inhaled furosemide on metabisulphite and methacholine-induced bronchoconstriction and nasal potential difference in asthmatic subjects. *Am. Rev. Respir. Dis.*, **142**, 576–580.

NICHOL, G.M., NIX, A., CHUNG, K.F. & BARNES, P.J. (1989). Characterisation of bronchoconstrictor responses to sodium metabisulphite aerosol in atopic subjects with and without asthma. *Thorax*, **44**, 102–107.

O'CONNOR, B.J., CHUNG, K.F., CHEN-WORDSELL, Y., FULLER, R.W. & BARNES, P.J. (1991). Effect of inhaled furosemide and bumetanide on adenosine-5'-monophosphate and sodium metabisulphite-induced bronchoconstriction in asthmatic subjects. *Am. Rev. Respir. Dis.*, **143**, 1329–1333.

PARSONS, G.H., NICHOL, G.M., BARNES, P.J. & CHUNG, K.F. (1992a). Effect of neuropeptides on bronchial blood flow and lung resistance in conscious sheep. *J. Appl. Physiol.*, **72,** 1118–1122.

PARSONS, G.H., VILLABLANCA, A.C., BROCK, J.M, HOWARD, R.S., COLBERT, S.R., NICHOL, G.M. & CHUNG, K.F. (1992b). Bronchial vasodilatation by histamine in sheep: characterization of receptor subtype. *J. Appl. Physiol.*, **72,** 2090–2098.

ROBUSCHI, M., GAMBARD, G., SPAGNOTTO, S., VAGHI, A. & BIANCO, S. (1991). Inhaled frusemide is highly effective in preventing ultrasonically nebulised water bronchoconstriction. *Pulm. Pharmacol.*, **1,** 187–191.

SAKAMOTO, T., ELWOOD, W., BARNES, P.J. & CHUNG, K.F. (1992). Pharmacological modulation of inhaled sodium metabisulphite-induced bronchoconstriction and airway microvascular leakage in guinea-pig. *Br. J. Pharmacol.*, **107,** 481–487.

SCHWARTZ, H.J. & CHESTER, E.H. (1984). Bronchospastic responses to aerosolized metabisulphite in sensitive asthmatics: potential mechanisms and clinical implications. *J. Allergy Clin. Immunol.*, **74,** 511.

SEALE, J.P., TEMPLE, D.M. & TENNANT, C.M. (1988). Bronchoconstriction by nebulised metabisulphite solutions (SO_2) and its modification by ipratropium bromide. *Ann. Allergy*, **61,** 209–213.

SHEPPARD, D., WONG, S.C., UEHARA, C.F., NADEL, J.A. & BOUSHEY, H.A. (1980). Lower threshold and greater bronchomotor responsiveness of asthmatic subjects to sulphur dioxide. *Am. Rev. Respir. Dis.*, **122,** 873–878.

SNASHALL, P.D. & BALDWIN, C. (1982). Mechanisms of sulphur dioxide induced bronchoconstriction in normal and asthmatic man. *Thorax*, **37,** 671–674.

STEVENSON, D.D. & SIMON, R.A. (1981). Sensitivity to ingested metabisulfites in asthmatic subjects. *J. Allergy Clin. Immunol.*, **68,** 26.

SUN, J., SAKAMOTO, T., BARNES, P.J. & CHUNG, K.F. (1993). Effect of sodium metabisulfite on guinea-pig airway smooth muscle contraction in vitro. *Am. Rev. Resp. Dis.*, **147,** A812.

TAN, W.C., CRIPPS, E., DOUGLAS, N. & SUDLOW, M.F. (1982). Protective effect of drugs on bronchoconstriction induced by sulphur dioxide. *Thorax*, **37,** 671–674.

VATNER, S.F., PATRICK, T.A. & MURRAY, P.A. (1982). Monitoring of cardiovascular dynamics in conscious animals. In *Cardiovascular Toxicology*, ed. Van Stee, E.W. pp. 35–55. New York: Raven Press.

WHITE, S.W., ANGUS, J.A., McRITCHIE, R.J. & PORGES, W.L. (1974). Evaluation of the Doppler flowmeter for the measurement of blood flow in small vessels of unanesthetized animals. *Clin. Exp. Pharmacol. Physiol*, **1 Suppl,** 79–92.

(Received July 8, 1993
Revised October 21, 1993
Accepted November 18, 1993)

Br. J. Pharmacol. (1994), **111**, 923–929

© Macmillan Press Ltd, 1994

Selective antagonism by PPADS at P_{2X}-purinoceptors in rabbit isolated blood vessels

*,†Airat U. Ziganshin, *Charles H.V. Hoyle, §Günter Lambrecht, §Ernst Mutschler, ‡Hans G. Bäumert & [1,]*Geoffrey Burnstock

*Department of Anatomy and Developmental Biology and Centre for Neuroscience, University College London, Gower Street, London WC1E 6BT; †Kazan Medical Institute, 49 Butlerov Street, Kazan, 420012, Russia and Departments of §Pharmacology and ‡Biochemistry, University of Frankfurt, Theodor-Stern-Kai 7, Geb. 75A, D-6000 Frankfurt/M, Germany

1 Pyridoxalphosphate-6-azophenyl-2',4'-disulphonic acid (PPADS), a P_2-purinoceptor antagonist, was investigated for its ability to antagonize: (1) P_{2X}-purinoceptor-mediated contractions of the rabbit central ear artery and saphenous artery evoked by either α,β-methylene ATP (α,β-MeATP) or electrical field stimulation (EFS); (2) P_{2Y}-purinoceptor-mediated relaxations of the rabbit mesenteric artery; (3) endothelium-dependent and endothelium-independent, P_{2Y}-purinoceptor-mediated relaxations of the rabbit aorta.

2 α,β-MeATP (0.1–100 μM) caused concentration-dependent contractions of the rabbit ear and saphenous arteries. The negative log[α,β-MeATP] that produced a contraction equivalent to the EC_{25} for noradrenaline (ear artery) or histamine (saphenous artery) in the absence of PPADS was 6.60 ± 0.18 (9) and 6.18 ± 0.17 (9) in the ear artery and saphenous artery, respectively. These effects of exogenous α,β-MeATP were concentration-dependently inhibited by PPADS (1–30 μM). In the ear artery, the negative log[α,β-MeATP] producing a contractile response equivalent to the EC_{25} of noradrenaline, in the presence of PPADS at 1, 3 and 10 μM was 6.16 ± 0.18 (8), 5.90 ± 0.18 (8) and 4.72 ± 0.36 (8), respectively ($P<0.01$). In the saphenous artery, the negative log[α,β-MeATP] values equivalent to the EC_{25} for histamine in the presence of PPADS at concentrations of 1, 3, 10 and 30 μM were 5.90 ± 0.19 (8), 5.73 ± 0.16 (8), 4.99 ± 0.14 (8) and 4.51 ± 0.13 (8), respectively ($P<0.01$).

3 PPADS at a concentration of 1 μM had no effect on contractions of the ear artery evoked by EFS (4–64 Hz; 1 μM phentolamine present). At higher concentrations (3–30 μM) it caused concentration-dependent inhibition of neurogenic contractions. In the saphenous artery, PPADS (1–30 μM) concentration-dependently inhibited contractions evoked by EFS at frequencies of 4, 8 and 16 Hz. Contractions evoked by EFS at frequencies of 32 and 64 Hz were significantly inhibited by PPADS only at concentrations of 10 and 30 μM.

4 PPADS (30 μM) had no effect on relaxations to 2-methylthio ATP (3 nM–3 μM) in rabbit mesenteric artery and to ATP (1 μM–1 mM) in rabbit aorta (with endothelium intact or removed). In addition, PPADS (30 μM) had no significant influence on the contractile potency of noradrenaline and histamine in rabbit ear and saphenous artery, respectively.

5 In conclusion, these results support the evidence that PPADS is a selective antagonist of P_{2X}-purinoceptor-mediated responses.

Keywords: PPADS; P_{2X}-purinoceptors; P_{2Y}-purinoceptors; rabbit blood vessels; α,β-methylene ATP; electrical field stimulation; 2-methylthio ATP

Introduction

The pharmacology of purinoceptors has advanced rapidly during the last 10 years (Hoyle & Burnstock, 1991; Abbracchio *et al.*, 1993), and there are now some adenosine receptor (P_1) agonists and antagonists that are selective for different subtypes of the P_1-purinoceptor (Williams, 1991; Mast, 1992). However, so far there is a lack of selective and reversible P_2-purinoceptor antagonists. Suramin has fairly specific antagonistic activity at P_2-purinoceptors but does not discriminate between P_{2X}- and P_{2Y}-subtypes (Hoyle *et al.*, 1990). Reactive blue 2 is only useful within a narrow range of concentrations and for limited time of exposure, above or after which it has non-specific effects (Burnstock & Warland, 1987b). Arylazidoaminopropionyl ATP ($ANAPP_3$), a photoaffinity ATP analogue, is a selective antagonist at P_{2X}-purinoceptors after photolysis, but its action is irreversible (Hogaboom *et al.*, 1980). α,β-Methylene ATP (α,β-MeATP) desensitization of P_{2X}-purinoceptors (Kasakov & Burnstock, 1983), although often used successfully (see Hoyle, 1992), does not provide competitive antagonism.

Recently we found that pyridoxalphosphate-6-azophenyl-2',4'-disulphonic acid (PPADS) selectively inhibits P_{2X}-purinoceptor-mediated contractions in guinea-pig ileum resistance vessels (Bungardt *et al.*, 1992) and in the rabbit vas deferens (Lambrecht *et al.*, 1992). With this in mind, the present study was undertaken to investigate the selectivity of PPADS in inhibiting the P_{2X}-purinoceptor-mediated response in several rabbit isolated blood vessels.

P_2-purinoceptors in blood vessels are located both on endothelial cells and on smooth muscle cells (see Pearson & Gordon, 1989; Burnstock, 1990a). Generally, P_{2X}-purinoceptors found in vascular smooth muscles mediate contractile responses, while P_{2Y}-purinoceptors, present either on endothelial cells or on smooth muscle cells, mediate vasodilatation (Burnstock, 1988; Ralevic & Burnstock, 1991a). Recently it has been reported that in some tissues, for example rat mesenteric arterial bed (Ralevic & Burnstock, 1991b) and rabbit aorta smooth muscle (Chinelatto *et al.*, 1992) other, non-classical, types of P_{2Y}-purinoceptor exist at which UTP as well as ATP are effective in producing endothelium-independent vasodilatation.

In the present study we have tested the activity of PPADS in the rabbit central ear artery and saphenous artery for inhibition of P_{2X}-purinoceptor-mediated contractions (Ken-

[1] Author for correspondence.

nedy & Burnstock, 1985; Warland & Burnstock, 1987; Burnstock & Warland, 1987a; O'Connor et al., 1990; MacDonald et al., 1992); in the rabbit mesenteric artery for antagonism of endothelium-independent relaxations mediated via P_{2Y}-purinoceptors in smooth muscle (Mathieson & Burnstock, 1985; Burnstock & Warland, 1987b); in the rabbit aorta for inhibition of either endothelium-dependent or endothelium-independent P_{2Y}-purinoceptor-mediated relaxation (Chinellato et al., 1992).

Methods

General procedure

Male New Zealand White rabbits (2–3 kg) were killed by an overdose of sodium pentobarbitone (Sagatal), which was injected via the marginal ear vein, and exsanguination. All vessels were suspended horizontally in 5 ml organ baths for isometric recording of mechanical activity (Bevan & Osher, 1972). An initial load of 750–1000 mg was applied to the vessels which were then allowed to equilibrate for at least 60 min. The Krebs solution had the following composition (mM): NaCl 133, KCl 4.7, $NaHCO_3$ 16.4, $MgSO_4$ 0.6, NaH_2PO_4 0.8, $CaCl_2$ 2.5 and glucose 7.7, and was gassed with 95% O_2/5% CO_2 (pH 7.3–7.4) and maintained at 37 ± 1°C. In experiments with electrical field stimulation (EFS), phentolamine (1 μM) was included in the Krebs solution in order to block the adrenergic component of contraction. Contractions were recorded by either a Dynamometer UF1 or Grass FT0C3 force-displacement transducer and were displayed on a Grass 79D ink-writing oscillograph.

Single concentrations of agonists (noradrenaline at 1 μM for the ear artery and aorta, noradrenaline at 10 μM for the mesenteric artery and histamine at 10 μM for the saphenous artery) were added repeatedly at intervals of 20 min, until reproducible increases in tone were obtained. Then these agonists were added cumulatively to determine the maximal contractile response of the blood vessels.

Central ear artery and saphenous artery

The proximal regions of the central ear artery and saphenous artery were removed and ring segments 4 mm in length were prepared and used as described above.

α,β-MeATP (0.1–100 μM) was added directly to the organ bath and washed out after a maximum contraction had been reached. In order to avoid desensitization, intervals of at least 30 min, with a wash every 10 min, were allowed between consecutive applications of α,β-MeATP. Concentration-response relationships for α,β-MeATP were constructed before and after incubation with PPADS (1–30 μM, at least 30 min).

EFS was applied via two platinum wire electrodes placed parallel to, and on each side of, the vessel, and was provided by a Grass S9 stimulator. Stimuli were applied at a given frequency (4–64 Hz) with a pulse width of 0.1 ms and supramaximal voltage for a period of 1 s. These parameters provide stimulation of intramural nerves without direct stimulation of muscle (Burnstock & Warland, 1987a; Stewart-Lee et al., 1991). Frequency-response relationships were determined before and after incubation with PPADS (1–30 μM) for at least 20 min.

When PPADS was tested against contractile responses induced by noradrenaline in the ear artery, the cumulative concentration-response relationships for noradrenaline (0.1–100 μM) were determined in parallel on two preparations from each animal. Then one preparation was incubated with PPADS at a concentration of 30 μM for at least 20 min, and the concentration-response relationships for noradrenaline on both preparations were determined again. Thus, the preparation without PPADS was considered as a time-matched control. The same procedure was used for histamine (1 μM–1 mM) in the saphenous artery.

Mesenteric artery

Side branches of the superior mesenteric artery were dissected and two ring segments 5 mm long were prepared. The initial maximum response to noradrenaline was established, the preparations were washed several times with fresh Krebs solution and were allowed to rest for at least 20 min. Then the segments were contracted by the approximate EC_{50} of noradrenaline (20 or 30 μM) and relaxant cumulative concentration-response relationships for 2-methylthio ATP (2-MeSATP, 3 nM–3 μM) were determined. One preparation was incubated with 30 μM PPADS for at least 20 min and a second concentration-response relationship for 2-MeSATP was constructed on each preparation. The parallel preparation, in which two concentration-response relationships for 2-MeSATP were determined without incubation with PPADS, was considered as a time-matched control.

Aorta

The thoracic aorta was removed, and after dissecting away connective tissue, two ring preparations 4 mm in length were prepared. The endothelium of one of the preparations was removed by gently rubbing with a silk thread passed through the lumen. After the maximum response to noradrenaline had been established, both preparations were precontracted by the approximate EC_{50} of noradrenaline (0.3 or 1 μM) and relaxant concentration-response relationships for ATP (1 μM –1 mM) were determined cumulatively. The concentration-response relationships were determined on the same preparations again after incubation with PPADS at 30 μM (at least 20 min). In the time-control preparations, the first and second relationships for ATP were determined with an interval of at least 20 min. At the end of the experiments, the preparations were opened longitudinally, and treated with a silver staining technique (Nakatsu et al., 1988) to examine the presence of endothelial cells under a microscope. In rubbed preparations the endothelium had been successfully removed, and in unrubbed preparations it was intact.

Drugs used

Rogitine (phentolamine sulphate) was obtained from Ciba. α,β-Methylene ATP lithium salt, adenosine 5'-triphosphate disodium salt (ATP), (−)-arterenol (noradrenaline) bitartrate and histamine dihydrochloride were obtained from Sigma Chemical Co. Ltd. 2-Methylthio ATP tetrasodium salt was obtained from Research Biochemicals Inc. (U.S.A.). Sagatal was supplied by May and Baker. PPADS was synthesized in one of our laboratories.

Solutions of noradrenaline were prepared in ascorbic acid (100 μM); other drug solutions were made up in distilled water.

Analysis of results

In the experiments with α,β-MeATP, responses were expressed as a percentage of the maximum contraction evoked by noradrenaline (ear artery) or histamine (saphenous artery). Because it was not practicable to construct complete concentration-response relationships for α,β-MeATP in the presence of PPADS, the negative log[α,β-MeATP] that produced a contraction equivalent to that produced by the EC_{25} for noradrenaline or histamine was calculated in controls and compared with the negative log[α,β-MeATP] that caused, in the presence of PPADS, contractions equivalent to the EC_{25} for noradrenaline or histamine.

In the experiments with EFS, responses were expressed as a percentage of the contraction evoked by stimulation at a frequency of 32 Hz (maximal contraction obtained) in the absence of PPADS.

When concentration-response curves for noradrenaline in the ear artery were constructed, responses were calculated as

a percentage of the maximal noradrenaline contraction. The mean response of the preparations from each animal was calculated at each concentration of noradrenaline applied. These mean responses for each animal were then subjected to a probit transformation (Bliss, 1935; Finney, 1971) which converts the sigmoidal log concentration curve to a straight line. Linear regression of the probit values against log concentration was then carried out in order to interpolate the log-concentrations yielding 1, 5, 10, 20, 35, 50, 65, 80, 90, 95 and 99% responses (Hoyle & Greenberg, 1988). The means and standard errors of the log concentrations for each of these percentage points were calculated and used to plot the summed concentration-response curve. The pD_2 values (negative logarithm of EC_{50}) in the absence and presence of PPADS and in time-control preparations were calculated from the concentration-response relationships and were then used in Student's paired t tests. The concentration-response histamine relationships for histamine were constructed in the saphenous artery in the same way.

The relaxant responses of 2-MeSATP on precontracted mesenteric arteries were expressed as a percentage of the maximal relaxation induced by 2-MeSATP, and were then used for probit analysis as described above.

In the aorta, the relaxant responses to ATP were expressed relative to the contraction evoked by the EC_{50} of noradrenaline. In preparations with intact endothelium, the $-$ log[ATP] that caused a 50% relaxation of the noradrenaline-induced contraction was calculated. In the cases when 50% relaxation was not reached in some endothelium-denuded preparations, the $-$ log[ATP] that caused 25% relaxation was calculated.

Means were compared by Student's paired and unpaired t tests. A probability of less than or equal to 0.05 was considered as significant. Data are presented as mean ± s.e.mean (n).

Results

In the rabbit isolated central ear artery, α,β-MeATP (0.1–100 μM) caused concentration-dependent contractions with a maximum response of 57.7 ± 4.3% (9) relative to the maximum contraction evoked by noradrenaline (Figure 1a). The negative log concentration of α,β-MeATP that caused a contraction equivalent to the EC_{25} for noradrenaline, was 6.60 ± 0.18 (9). PPADS at concentrations of 1–30 μM caused a concentration-dependent shift to the right of the concentration-response curve for α,β-MeATP (Figure 1a). The negative log[α,β-MeATP] producing a contractile response equivalent to the EC_{25} of noradrenaline, in the presence of PPADS at 1, 3 and 10 μM was 6.16 ± 0.18 (8), 5.90 ± 0.18 (8) and 4.72 ± 0.36 (8), respectively. All these values were significantly different from control ($P<0.01$, paired t tests). In the presence of PPADS at a concentration of 30 μM, the highest concentration of α,β-MeATP used (100 μM) did not produce an effect equivalent to the EC_{25} for noradrenaline.

In the saphenous artery, α,β-MeATP (0.1–100 μM) caused concentration-dependent contractions with a $-$ log[α,β-MeATP] that produced a contraction equivalent to the EC_{25} for histamine of 6.18 ± 0.17 (9) (Figure 1b). PPADS (1–30 μM) concentration-dependently shifted the concentration-response curve for α,β-MeATP to the right (Figure 1b). The negative log[α,β-MeATP] values equivalent to the EC_{25} for histamine in the presence of PPADS at concentrations of 1, 3, 10 and 30 μM were significantly less than control values being 5.90 ± 0.19 (8), 5.73 ± 0.16 (8), 4.99 ± 0.14 (8) and 4.51 ± 0.13 (8), respectively ($P<0.01$, paired t tests).

In the presence of phentolamine (1 μM), EFS of the intramural nerves caused frequency-dependent contraction of the rabbit ear artery, which although almost neglible at a frequency of 4 Hz, was maximal at a frequency of 32 Hz (Figure 2a). PPADS at a concentration of 1 μM did not significantly affect contractions of the ear artery evoked by EFS, but at 3–30 μM it caused significant inhibition. In the

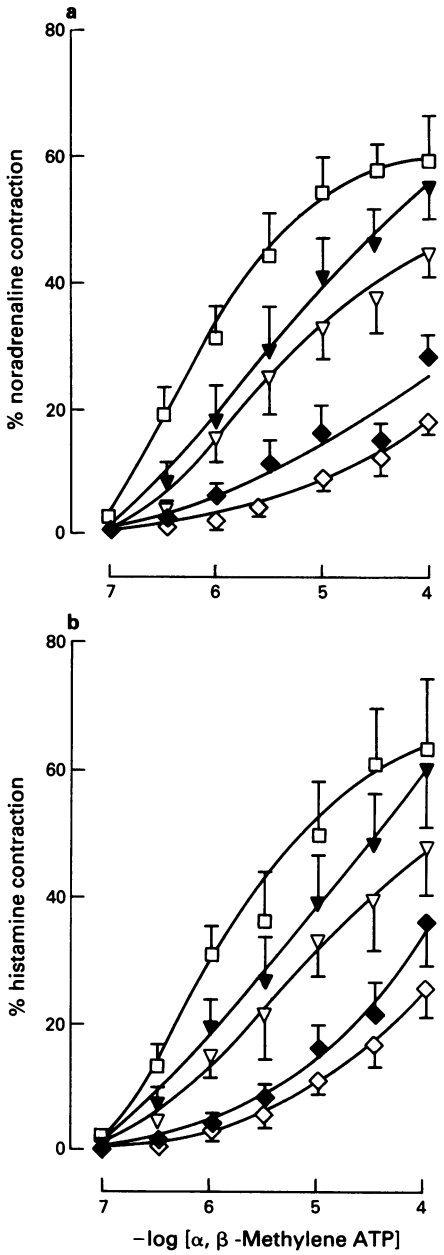


Figure 1 Concentration-response relationships for α,β-methylene ATP in the presence and absence of PPADS on rabbit isolated central ear artery (a) and saphenous artery (b). Responses (ordinate axis) are expressed as a percentage relative to the maximum contraction evoked by noradrenaline (ear artery) or histamine (saphenous artery). Concentration-response curves are shown for α,β-methylene ATP in the absence of PPADS (□, $n=8$ or 9) and presence of PPADS at concentrations of 1 μM (▼, $n=7$ or 8), 3 μM (▽, $n=7$ or 8), 10 μM (◆, $n=7$ or 8) and 30 μM (◇, $n=7$ or 8). The values shown represent the mean ± s.e.mean.

presence of 30 μM PPADS, the contractile response evoked by EFS at a frequency of 32 Hz was decreased by 80.0 ± 4.5% (8) relative to that in the absence of PPADS ($P<0.001$, paired t tests). The log EF_{50} (i.e. the frequency that causes a 50% contraction of the maximum response) of 1.00 ± 0.07 (8) in the absence of PPADS was significantly increased by PPADS at concentrations of 10 and 30 μM, being 1.22 ± 0.04 (7) and 1.31 ± 0.03 (6), respectively ($P<0.05$, paired t tests).

In the saphenous artery, EFS produced frequency-dependent contractions at all applied frequencies (4–64 Hz) being maximal at a frequency of 32 Hz (Figure 2b). PPADS (1–30

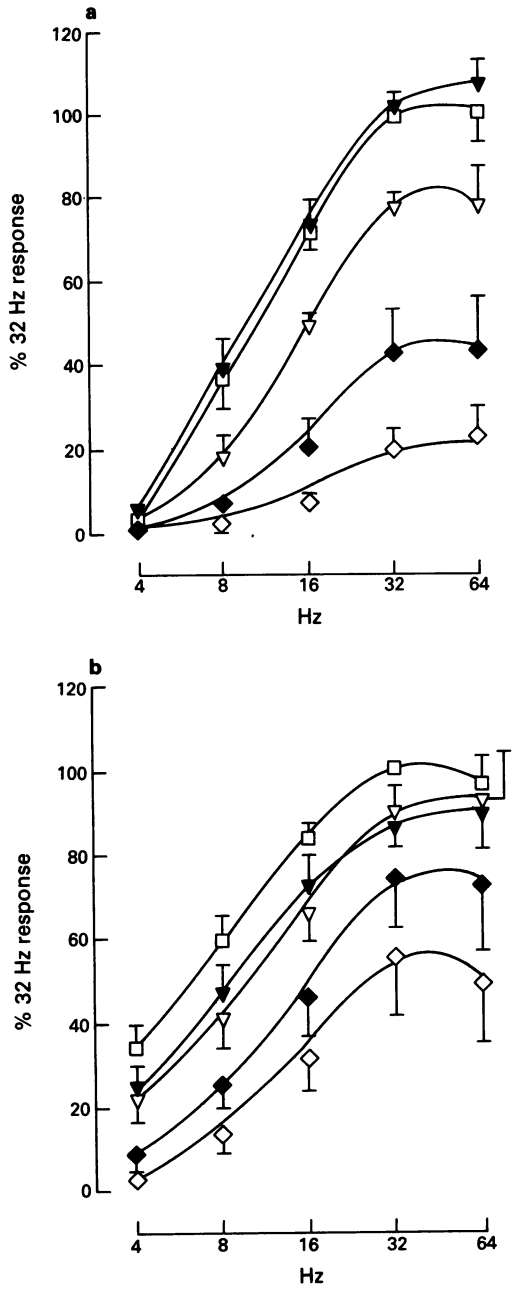


Figure 2 Frequency-response relationships for electrical field stimulation in rabbit isolated central ear artery (a) and saphenous artery (b). The Krebs solution contained 1 μM phentolamine. Responses (ordinate axis) are expressed as a percentage of contraction evoked by electrical field stimulation at a frequency of 32 Hz in controls. Frequency-response curves are shown for PPADS at zero (□, $n = 7$ or 8), 1 μM (▼, $n = 7$ or 8), 3 μM (▽, $n = 7$ or 8), 10 μM (◆, $n = 7$ or 8) and 30 μM (◇, $n = 7$ or 8). Values shown are mean ± s.e.mean. The abscissae are on a logarithmic scale.

μM) caused a concentration-dependent inhibition of neurogenic contractions of the saphenous artery at frequencies of 4, 8 and 16 Hz. Contractions evoked by EFS at frequencies of 32 and 64 Hz were significantly inhibited by PPADS only at concentrations of 10 and 30 μM. In the presence of PPADS at a concentration of 30 μM, contractions induced by EFS at 32 Hz were decreased by 44.7 ± 12.8% (9) relative to the control value. The log EF_{50} of 1.10 ± 0.03 (8) and 1.19 ± 0.03 (8) obtained in the presence of PPADS at concentrations of 10 and 30 μM, respectively, were significantly different from that of 0.89 ± 0.05 (8) obtained in the absence of PPADS ($P < 0.01$, paired t tests).

In mesenteric artery preparations in which tone has been raised with the EC_{50} of noradrenaline, 2-MeSATP at concentrations of 3–300 nM caused concentration-dependent sustained relaxations usually after an initial small transient contraction, but at concentrations of 1 μM and above it caused marked contractions without additional relaxation. In time-matched control preparations, the second concentration-response curve for 2-MeSATP was significantly shifted to the right with pD_2 values of 7.32 ± 0.17 (4) and 6.77 ± 0.13 (4) for the first and second curves, respectively ($P < 0.001$, paired t tests). In preparations incubated with 30 μM PPADS, there was also a significant rightward shift of the concentration-response curve with the pD_2 value being 7.42 ± 0.16 (4) in the absence and 6.73 ± 0.09 (4) in the presence of PPADS ($P < 0.01$, paired t tests). However, the shift of the second concentration-response curves for 2-MeSATP in preparations without and with incubation with PPADS were not significantly different being 0.55 ± 0.04 (4) and 0.69 ± 0.10 (4) log units, respectively ($P > 0.05$, unpaired t tests).

In preparations of the rabbit aorta with intact endothelium precontracted by the EC_{50} of noradrenaline, ATP (1 μM–1 mM) caused a concentration-dependent fast transient relaxation with a $-\log[ATP]$ that caused 50% relaxation of 4.13 ± 0.07 (6). In the presence of PPADS at a concentration of 30 μM, there was no significant change in this value, which was 3.89 ± 0.15 (6) (Figure 3a). Further, no significant difference was found when the slopes of the concentration-response curves for ATP were calculated, being 44.3 ± 3.4 (6) and 37.0 ± 3.4 (6)% log unit^{-1} in the presence and absence of PPADS, respectively ($P > 0.005$, paired t tests).

ATP (10 μM–1 mM) caused a slow, sustained relaxation of the precontracted endothelium-denuded preparations of the aorta, with a significantly smaller maximum response than in the endothelium-intact preparations at all concentrations of ATP. The $-\log[ATP]$, that caused 25% relaxation, 3.84 ± 0.12 (6), obtained before incubation with PPADS, was not significantly different from that obtained after 20 min incubation with PPADS at a concentration of 30 μM which was 4.00 ± 0.09 (6) (Figure 3b). No significant difference was found between the slopes of the concentration-response curves for ATP before and after incubation with PPADS being 35.0 ± 2.9 (6) and 34.0 ± 1.5 (6)% log unit^{-1}, respectively.

In time-matched control preparations, either with or without endothelium, there were no significant differences between any points of the concentration-response curves, or the $-\log[ATP]$ values causing 50% or 25% relaxation, or the slopes of the curves.

Noradrenaline, added cumulatively (0.1–100 μM), caused concentration-dependent contraction of the rabbit ear artery. The pD_2 values calculated for the first and second concentration-response curves in the time-matched control preparations were not significantly different being 6.07 ± 0.13 (4) and 5.99 ± 0.16 (4), respectively. PPADS (30 μM) had no effect on the potency of noradrenaline (Figure 4a). The pD_2 values in the absence and in the presence of PPADS were 6.08 ± 0.07 (4) and 5.95 ± 0.11 (4), respectively. There was no significant difference between these values. In addition, PPADS did not significantly change the maximum response to noradrenaline, which was 3.68 ± 0.35 (4) g before and 3.59 ± 0.32 (4) g after incubation with PPADS.

Histamine, added cumulatively (1 μM–1 mM), concentration-dependently contracted the rabbit saphenous artery. In the time-control preparations, the first pD_2 value was significantly greater than the second one being 5.46 ± 0.22 (4) and 5.12 ± 0.26 (4), respectively ($P < 0.05$, paired t tests). However, there was no significant difference between the pD_2 values calculated in the absence (5.46 ± 0.19, $n = 4$) and presence (5.27 ± 0.22, $n = 4$) of PPADS at a concentration of 30 μM (Figure 4b). Further, there was no significant difference between the shift in the concentration-response curve due to time alone and that due to PPADS as well, these values being 0.19 ± 0.07 (4) and 0.34 ± 0.10 (4) log units, respectively ($P > 0.05$, unpaired t tests). No significant differ-

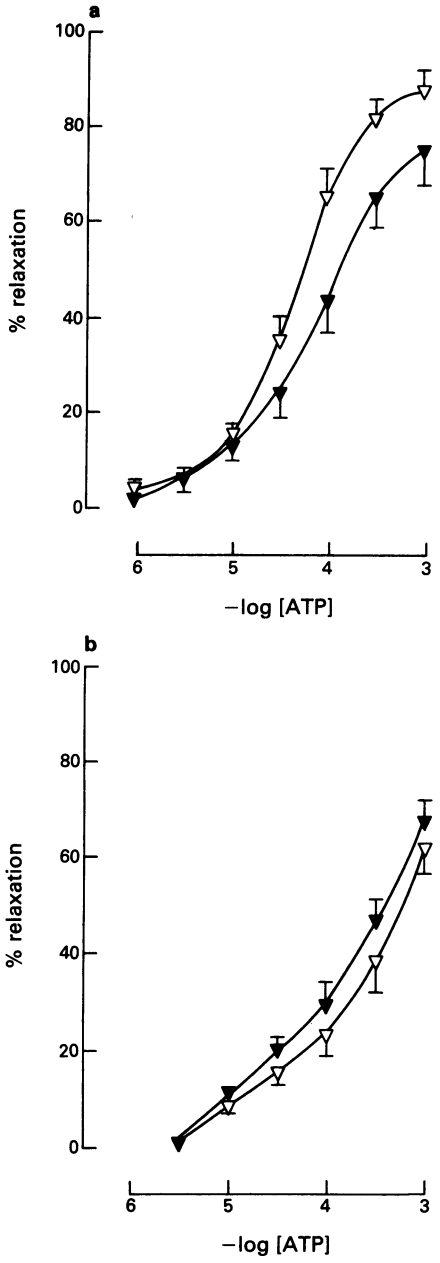


Figure 3 Concentration-response relationships for ATP in the rabbit aorta with (a) and without endothelium (b). Curves are shown in the absence (▽, $n = 4$) and presence of PPADS at 30 μM (▼, $n = 4$). Values shown are mean ± s.e.mean. $^*P < 0.05$.

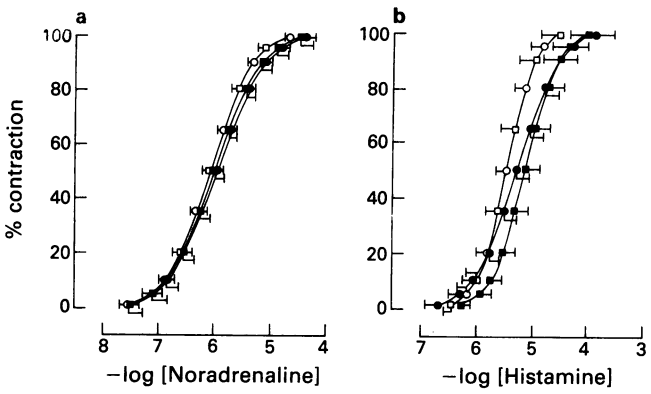


Figure 4 Rabbit isolated arteries: concentration-response relationships for noradrenaline in central ear artery (a) and for histamine in saphenous artery (b) calculated using probit analysis. Curves are shown for the first (□, $n = 4$) and the second (■, $n = 4$) relationships in time-control preparations, and in the absence (○, $n = 4$) and in the presence of PPADS at 30 μM (●, $n = 4$). Values shown are mean with s.e.mean.

ence was found when the maximum responses for histamine were calculated in the presence and absence of PPADS, being 3.08 ± 0.25 (4) g and 3.25 ± 0.29 (4) g, respectively.

Discussion

The results described in this study demonstrate that PPADS selectively antagonized responses mediated via P_{2X}-purinoceptors in the rabbit central ear artery and saphenous artery without significantly affecting responses mediated via P_{2Y}-purinoceptors in the rabbit mesenteric artery and aorta. Further, PPADS did not antagonize α-adrenoceptor or histamine receptor-mediated responses. These results are consistent with those of Bungardt *et al.* (1992) who showed that PPADS strongly inhibited contractions to exogenous α,β-MeATP (mediated via P_{2X}-purinoceptors) in guinea-pig ileum resistance vessels, without any action on the resting vessel diameter or the diameter after preconstriction with noradrenaline. In addition, our findings are also consistent with those of Lambrecht *et al.* (1992) who observed that PPADS caused selective inhibition of neurogenic contractions in the rabbit vas deferens, which also possesses postjunctional excitatory P_{2X}-purinoceptors (Kennedy & Burnstock, 1985).

Both the rabbit central ear and saphenous arteries possess P_{2X}-purinoceptors on the smooth muscle cells, which mediate the contractile actions of α,β-MeATP and purinergic nerve stimulation (Kennedy *et al.*, 1986; Burnstock & Warland, 1987a; Saville & Burnstock, 1988). In both preparations, PPADS caused a concentration-dependent inhibition of the contractile effects of α,β-MeATP. However, from our results it is difficult to decide whether or not the antagonism is competitive, since in both tissues the maximum effect of α,β-MeATP had not been reached in the presence of PPADS.

During the last few years sympathetic purinergic excitatory co-transmission in various blood vessels has been established (Burnstock, 1990b; Von Kügelgen & Starke, 1991; Hoyle 1992). Burnstock & Warland (1987a), using EFS, established the involvement of noradrenaline and ATP in sympathetic co-transmission in the rabbit saphenous artery, where there is a large prazosin-resistant purinergic component. Similar co-transmission has been demonstrated in the rabbit central ear artery (Kennedy *et al.*, 1986; Saville & Burnstock, 1988), however, in this preparation the prazosin-resistant component is much less dominant. In our experiments with EFS, the contractile responses were purinergic because the α-adrenoceptors had been blocked by phentolamine. At the highest PPADS concentration tested (30 μM), the inhibition of contractions evoked by EFS at frequencies of 32 and 64 Hz was about 2 times greater in the ear artery than in the saphenous artery. However, the changes of the EF_{50} due to PPADS in both the arteries were approximately the same, as were the shifts in concentration-response curves for α,β-MeATP in both tissues. Thus, it seems that the greater % inhibition due to PPADS in the ear artery is because the total amount of purinergic transmitter released by EFS in the ear artery is less than that in the saphenous artery at any given frequency, but the affinity of PPADS for P_{2X}-purinoceptors in the two arteries is the same. When PPADS was tested against the direct action of histamine in the saphenous artery there was no effect that did not occur with time in any case.

In order to determine the selectivity of PPADS for P_{2X}-purinoceptors, it was also tested on vessels that possess other subtypes of purinoceptors. P_{2Y}-purinoceptors in the rabbit

mesenteric artery are present, unlike many other vessels, not on endothelial cells, but on smooth muscle cells (Burnstock & Warland, 1987b). In the present study, we have shown that P_{2Y}-purinoceptor-mediated relaxations of the mesenteric artery are susceptible to desensitization, since there was a highly significant difference between the two pD_2 values for 2-MeSATP obtained in the time-control experiments. However, PPADS did not significantly affect this relationship, indicating an absence of inhibitory action on these P_{2Y}-purinoceptors.

The purinoceptors that mediate relaxation in the rabbit aorta appear to be different from those in the mesenteric artery. There are P_{2Y}-purinoceptors on endothelial cells, but another type of ATP-receptor, which is not a P_{2X}-purinoceptor, is present on the smooth muscle cells (O'Connor *et al.*, 1991; Chinellato *et al.*, 1992). At endothelial P_{2Y}-purinoceptors the rank order of potency of agonists is 2-MeSATP >> ATP = ADP >> UTP (O'Connor *et al.*, 1991), which is inherent for 'classical' P_{2Y}-purinoceptors as in the guinea-pig taenia coli (Burnstock & Kennedy, 1985). However, the order of potency of agonists at the aorta smooth muscle receptors is ATP = UTP > ADP > 2-MeSATP, which is not consistent with a classical P_{2Y}-purinoceptor (O'Connor *et al.*, 1991). Whatever the subtypes of P_2-purinoceptor, in testing the effects of PPADS in the aorta, the concentration-response relationship for ATP in preparations either with or without endothelium was not significantly altered by PPADS.

Thus, in the present study we have established that PPADS is a selective antagonist of vascular P_{2X}-purinoceptors having no effect at P_{2Y}-purinoceptors, α-adrenoceptors or histamine receptors. This is in line with previous observations (Lambrecht *et al.*, 1992; Bungardt *et al.*, 1992).

Note added in proof

Since this Manuscript was submitted and accepted for publication we have also shown that PPADS antagonizes P_{2X}-purinoceptors in the rabbit urinary bladder. (Ziganshin, A.U., Hoyle, C.H.V., Bo, X., Lambrecht, G., Mutschler, E., Bäumert, H.G. & Burnstock, G. (1993). PPADS selectively antagonizes P_{2X}-purinoceptor-mediated responses in the rabbit urinary bladder. *Br. J. Pharmacol.*, **110**, 1491–1495.)

The authors thank the Wellcome Trust (A.U.Z.), the Fonds der Chemischen Industrie (Germany) (G.L., E.M.), the Deutsch Forschungsgemeinschaft (H.G.B., SFB 169) and the British Heart Foundation for financial support. The authors would like to thank Dr W.R. Stones for assistance with the histochemistry and Dr A.L. Brizzolara for assistance with preparation of the vessels.

References

ABBRACCHIO, M.P., CATTABENI, F., FREDHOLM, B.B. & WILLIAMS, M. (1993). Purinoceptor nomenclature. A status report. *Drug Dev. Res.*, **28**, 207–213.

BLISS, C.I. (1935). The calculation of the dosage-mortality curve. *Ann. Appl. Biol.*, **22**, 134–167.

BEVAN, J.A. & OSHER, J.V. (1972). A direct method for recording tension changes in the wall of small blood vessels in vitro. *Agents Actions*, **2**, 257–260.

BUNGARDT, E., MOSER, U., SPATZ-KÜMBEL, G., BÄUMERT, H.G., LAMBRECHT, G. & MUTSCHLER, E. (1992). Characterization of purinoceptors in guinea-pig ileum resistance vessels by the use of computer-assisted videomicroscopy. *Int. J. Purine Pyrimidine Res.*, **3**, 66.

BURNSTOCK, G. (1988). Sympathetic purinergic transmission in small blood vessels. *Trends Pharmacol. Sci.*, **9**, 116–117.

BURNSTOCK, G. (1990a). Dual control of local blood flow by purines. In *Annals of New York Academy of Science*, Vol. 603. *Biological Action of Extracellular ATP*. ed. Dubyak, G.R. & Fedan, J.S. pp. 31–45. New York: N.Y. Acad. Sci.

BURNSTOCK, G. (1990b). Noradrenaline and ATP as co-transmitters in sympathetic nerves. *Neurochem. Int.*, **17**, 357–368.

BURNSTOCK, G. & KENNEDY, C. (1985). Is there a basis for distinguishing two types of P_2-purinoceptor? *Gen. Pharmacol.*, **16**, 433–440.

BURNSTOCK, G. & WARLAND, J.J.I. (1987a). A pharmacological study of the rabbit saphenous artery *in vitro*: a vessel with a large purinergic contractile response to sympathetic nerve stimulation. *Br. J. Pharmacol.*, **90**, 111–120.

BURNSTOCK, G. & WARLAND, J.J.I. (1987b). P_2-purinoceptors of two subtypes in the rabbit mesenteric artery: reactive blue 2 selectively inhibits responses mediated via the P_{2Y}-but not P_{2X}-purinoceptor. *Br. J. Pharmacol.*, **90**, 383–391.

CHINELLATO, A., RAGAZZI, E., PANDOLFO, L., FROLDI, G., CAPARROTA, L. & FASSINA, G. (1992). Pharmacological characterization of ATP receptors mediating vasodilation on isolated rabbit aorta. *Gen. Pharmacol.*, **23**, 861–865.

FINNEY, D. (1971). *Probit Analysis*. 3rd edition. Cambridge: Cambridge University Press.

HOGABOOM, G.K., O'DONNELL, J.P. & FEDAN, J.S. (1980). Purinergic receptors: A photoaffinity analog of adenosine triphosphate is a specific adenosine triphosphate antagonist. *Science*, **208**, 1273–1276.

HOYLE, C.H.V. (1992). Transmission: Purines. In *Autonomic Neuroeffector Mechanisms*. ed. Burnstock, G. & Hoyle, C.H.V. pp. 367–407. Chur: Harwood Academic Publishers.

HOYLE, C.H.V. & BURNSTOCK, G. (1991). ATP receptors and their physiological roles. In *Adenosine in the Nervous System*. ed. Stone, T.W. pp. 43–76. London: Academic Press Ltd.

HOYLE, C.H.V. & GREENBERG, M.J. (1988). Actions of adenylyl compounds in invertebrates from several phyla: evidence for internal purinoceptors. *Comp. Biochem. Physiol.*, **90C**, 113–122.

HOYLE, C.H.V., KNIGHT, G.E. & BURNSTOCK, G. (1990). Suramin antagonizes responses to P_2-purinoceptor agonists and purinergic nerve stimulation in the urinary bladder and taenia coli. *Br. J. Pharmacol.*, **99**, 617–621.

KASAKOV, L. & BURNSTOCK, G. (1983). The use of the slowly degradable analog, α,β-methylene ATP, to produce desensitization of the P_2-purinoceptor: effect on non-adrenergic, non-cholinergic responses of the guinea-pig urinary bladder. *Eur. J. Pharmacol.*, **86**, 291–294.

KENNEDY, C. & BURNSTOCK, G. (1985). ATP produces vasodilation via P_1-purinoceptors and vasoconstriction via P_2-purinoceptors in the isolated rabbit central ear artery. *Blood Vessels*, **22**, 145–155.

KENNEDY, C., SAVILLE, V.L. & BURNSTOCK, G. (1986). The contribution of noradrenaline and ATP to the responses of the rabbit central ear artery to sympathetic nerve stimulation depend on the parameters of stimulation. *Eur. J. Pharmacol.*, **122**, 291–300.

LAMBRECHT, G., FRIEBE, T., GRIMM, U., WINDSCHEIF, U., BUNGARDT, E., HILDEBRANDT, C., BÄUMERT, H.G., SPATZ-KÜMBEL, G. & MUTSCHLER, E. (1992). PPADS, a novel functionally selective antagonist of P_2 purinoceptor-mediated responses. *Eur. J. Pharmacol.*, **217**, 217–219.

MACDONALD, A., DALY, C.J., BULLOCH, J.M. & MCGRATH, J.C. (1992). Contributions of α_1-adrenoceptors, α_2-adrenoceptors and P_{2X}-purinoceptors to neurotransmission in several rabbit isolated blood vessels: role of neuronal uptake and autofeedback. *Br. J. Pharmacol.*, **105**, 347–354.

MAST, S.G. (1992). Therapeutic opportunities from purinergic transmission. *Drugs News Perspect.*, **5**, 378–383.

MATHIESON, J.J.I. & BURNSTOCK, G. (1985). Purine-mediated relaxation and constriction of isolated rabbit mesenteric artery are not endothelium-dependent. *Eur. J. Pharmacol.*, **118**, 221–229.

NAKATSU, K., KAWAMOTO, J.H., BRIEN, J.F. & MARKS, G.S. (1988). A facile, reliable method for staining blood vessel endothelium. *J. Pharmacol. Methods*, **19**, 149–154.

O'CONNOR, S.E., WOOD, B.E. & LEFF, P. (1990). Characterization of P_{2X}-purinoceptors in rabbit isolated ear artery. *Br. J. Pharmacol.*, **101**, 640–644.

O'CONNOR, S.E., DAINTY, I.A. & LEFF, P. (1991). Further subclassification of ATP receptors based on agonist studies. *Trends Pharmacol. Sci.*, **12**, 137–141.

PEARSON, J.D. & GORDON, J.L. (1989). P_2-purinoceptors in the blood vessel wall. *Biochem. Pharmacol.*, **38**, 4157–4163.

RALEVIC, V. & BURNSTOCK, G. (1991a). Roles of P_2-purinoceptors in the cardiovascular system. *Circulation*, **84**, 1–14.

RALEVIC, V. & BURNSTOCK, G. (1991b). Effects of purines and pyrimidines in the rat mesenteric arterial bed. *Circ. Res.*, **69**, 1583–1590.

SAVILLE, V.L. & BURNSTOCK, G. (1988). Use of reserpine and 6-hydroxydopamine supports evidence for purinergic cotransmission in the rabbit ear artery. *Eur. J. Pharmacol.*, **155**, 271–277.

STEWART-LEE, A.L., MAYNARD, K.I., LINCOLN, J. & BURNSTOCK, G. (1991). Sympathetic neurotransmission in the rabbit isolated central ear artery is affected as early as one week following a single dose of X-irradiation. *Br. J. Pharmacol.*, **102**, 23–26.

VON KÜGELGEN, I. & STARKE, K. (1991). Noradrenaline-ATP cotransmission in the sympathetic nervous system. *Trends Pharmacol. Sci.*, **12**, 319–324.

WARLAND, J.J.I. & BURNSTOCK, G. (1987). Effects of reserpine and 6-hydroxydopamine on the adrenergic and purinergic component of sympathetic nerve responses of the rabbit saphenous artery. *Br. J. Pharmacol.*, **92**, 871–880.

WILLIAMS, M. (1991). Adenosine receptor agonists and antagonists. In *Adenosine in the Nervous System.*, ed. Stone, T.W. pp. 137–171. London: Academic Press.

(Received July 5, 1993
Revised October 30, 1993
Accepted November 18, 1993)

Br. J. Pharmacol. (1994), **111**, 930–934 © Macmillan Press Ltd, 1994

Reversal of CRF- and dopamine-induced stimulation of colonic motility by CCK and igmesine (JO 1784) in the rat

[1]*Michèle Gué, Chantal Gleïzes-Escala, Chantal Del Rio-Lacheze, *Jean-Louis Junien & Lionel Buéno

[1]Department of Pharmacology, INRA, 180 Chemin de Tournefeuille, B.P.3, 31931 Toulouse Cedex, France and *Institut de Recherche Jouveinal, 3-9, Rue de la Loge, B.P.100, 94265 Fresnes Cedex, France

1 The role of dopamine in the genesis of corticotropin releasing factor (CRF)- and emotional stress (ES)-induced stimulation of colonic motility, as well as the mechanism of antagonistic action of cholecystokinin octapeptide (CCK-8s) and igmesine (a σ receptor ligand, formerly JO 1784) on dopamine-induced colonic hypermotility, have been investigated in the rat.

2 ES and i.c.v. injection of CRF (0.5 $\mu g\,kg^{-1}$) increased the frequency of colonic spike bursts by 63% and 114%, respectively. Prior i.c.v. administration of (+)-SCH 23390 (a D_1 receptor antagonist, 10 $\mu g\,kg^{-1}$) significantly ($P<0.05$) reduced the CRF- and ES-induced increase in colonic spike burst; whereas, sulpiride (a D_2 receptor antagonist, 10 $\mu g\,kg^{-1}$) blocked the CRF-induced stimulation of colonic spike bursts but had no effect on the colonic response to stress.

3 I.c.v. injection of dopamine (100 $\mu g\,kg^{-1}$), increased colonic spike burst frequency by 54%. (+)-SKF 38393 (5 $\mu g\,kg^{-1}$), a selective D_1 receptor agonist, and quinpirole (5 $\mu g\,kg^{-1}$), a selective D_2 receptor agonist, increased colonic spike burst frequency by 71% and 70% respectively. CCK-8s (0.1 $\mu g\,kg^{-1}$) and igmesine (0.1 $\mu g\,kg^{-1}$) injected i.c.v. completely prevented the stimulatory effects of dopamine, (+)-SKF 38393 and quinpirole.

4 Previous i.c.v. injection of devazepide, a CCK_A receptor antagonist, (10 $\mu g\,kg^{-1}$) antagonized the inhibitory effects of both CCK-8s and igmesine injected i.c.v. on dopamine-induced colonic hyperkinesia.

5 These results show that CRF stimulates colonic motility through activation of central dopaminergic mechanisms in response to stress; furthermore, CCK-8s inhibits dopamine-induced colonic hyperkinesia through a mechanism involving D_1 and D_2 receptors. The σ receptor ligand igmesine, blocks the CRF- and ES-induced colonic hyperactivity via an interaction with central CCK mechanisms.

Keywords: Stress; corticotropin releasing factor (CRF); dopamine; sigma ligands; CCK-8s; rat colon

Introduction

Stressful situations are known to activate dopamine metabolism in mesolimbic and mesocortical structures as well as in the striatum in rats and mice (Deutch *et al.*, 1985; Cabib *et al.*, 1988). In rats, emotional stress (ES) induced by the fear of receiving electric footshocks increases dopamine turnover in mesoprefrontal dopaminergic neurones originating in the ventral tegmental area (VTA, A 10) (Kaneyuki *et al.*, 1991). ES stimulates colonic motility in rats through a mechanism involving the central release of corticotropin-releasing factor (CRF) (Gué *et al.*, 1991) and we have recently shown that ES-induced stimulation of colonic motility is mediated through activation of central dopaminergic neurones (Buéno *et al.*, 1992). Consequently, in the first part of this study, we have examined the involvement of dopamine pathways in the CRF-induced stimulation of colonic motility in rats using the selective D_1 and D_2 receptor antagonists, SCH 23390 and sulpiride, respectively.

Several drugs, such as benzodiazepines (Gué *et al.*, 1991), buspirone (Martinez & Buéno, 1991) σ ligands (Junien *et al.*, 1991), neuropeptide Y (Jimenez & Buéno, 1990), cholecystokinin octapeptide (CCK-8s, Gue *et al.*, 1992) and 5-HT_{1A} receptor agonists (Gué *et al.*, 1993), prevent ES- and CRF-induced stimulation of colonic motility. The effects of σ ligands, neuropeptide Y and 5-HT_{1A} receptor agonists are blocked by CCK receptor antagonists suggesting that their mechanism of action is through the release of CCK or the modulation of CCK pathways. CCK and dopamine are colocalized in several brain structures and particularly in mesencephalic neurones (Hökfelt *et al.*, 1980). Exogenously applied and endogenous CCK-8s modify the postsynaptic action of dopamine in the nucleus accumbens (Yim & Mogenson, 1991) and also modulate the release of dopamine (Lane *et al.*, 1986; Voight *et al.*, 1986). σ Receptor binding sites are present in high density in the zona compacta of the substantia nigra where dopamine containing neurones are abundant (Gundlach *et al.*, 1985; 1986), and σ ligands are involved in the regulation of neuronal activity of midbrain dopaminergic neurones (Freeman & Bunney, 1984). This suggests that the 'antistress' action of σ ligands and CCK-8 on ES-induced colonic motor disturbances may be mediated via an inhibitory action on dopaminergic pathways. In the second part of this study, we have investigated the influence of the σ ligand, (+)-N-cyclopropyl-methyl-1, 4-diphenyl-1-ethyl-but-3-en-1-ylamine hydrochloride (igmesine, formerly JO 1784) and CCK-8s on dopamine- and selective D_1 and D_2 receptor agonist-induced stimulation of colonic motility.

Methods

Animal preparation

Male Wistar rats (Centre d'élevage R. Janvier, Route des Chênes Secs, 53940 Le Genest Saint Isle, France) weighing 250–300 g were used for these experiments. Animals were housed individually in polypropylene cages (37.5 × 17 × 15 cm) and kept in a temperature controlled room (21 ± 1°C, 50 ± 5% relative humidity) on a 12 h light-dark cycle (light on at 08 h:00 min). The rats were allowed access to water *ad libitum* and rat chow from 08 h:00 min to 24 h:00 min.

[1] Author for correspondence at present address: Department of Pharmacology, INRA, 180 Chemin de Tournefeuille, B.P.3; 31931 Toulouse Cedex, France.

Motility recordings

Under ketamine (Imalgene 1000, Rhône Merieux, Lyon, France; 100 mg kg^{-1}, i.p.) anaesthesia, the animals were surgically prepared with Nickel/Chrome electrodes implanted into the muscular layers of the proximal colon at 2 and 4 cm distal from the ileo-colonic junction according to the method of Ruckebush & Fioramonti (1975). The animals were also fitted with a permanent polyethylene catheter (PE 10) inserted into the lateral ventricle of the brain (L: 1.8; A: − 1.3; H: − 3.5) according to the atlas of Paxinos & Watson (1986). Bipolar recordings of myoelectric activity (time constant, 0.03 s), using an electromyographic recorder (Minihuit, ALVAR, Paris, France), began 5 days after surgery. The rats were fasted for 12 h before each experiment and colonic myoelectric activity was recorded from 30 min before the first injection to 30 min after the last i.c.v. injection or the beginning of the ES session.

Emotional stress session procedure

The emotional stress (ES) involved displacement of the animals from their home cage to a closed box (test-cage) in which they had previously received electric shocks as described by Gué *et al.* (1991). Briefly, each rat was placed in the test-cage for 5 min and received six series of electric footshocks (1.4 mA, 180 ms) supplied to the grid floor by pulse generated scrambler (Campden, England). Each series of shocks lasted 8 s and was administered at 45 s intervals. As the resistance, with the animal in the cage, varied between 10 and 250 kΩ, each rat received an electric footshock in the range of 1.2 to 3.0 mA, a value producing discomfort, but not pain as judged by the lack of any jump response. Placement of the rat in the same cage, without electric shock was considered to be a form of ES (Nabeshima *et al.*, 1988; Gué *et al.*, 1991). In order to eliminate the ability of the rats to differentiate between the electric footshocks session and the ES session without electric footshocks, reinforcement was performed at two-day intervals with each rat in a randomized fashion (for details se Gué *et al.*, 1991). The study was approved by the Midi-Pyrénées experimentation committee (agreement No 9224).

Experimental design

In a first series of experiments, a group of rats ($n = 10$) was injected i.c.v. with CRF (0.5 μg kg^{-1}) and in a second group, rats ($n = 10$) were placed in the test cage for 30 min, 15 min after i.c.v. administration of sterilized water alone (control) or containing sulpiride or SCH 23390 at 10 μg kg^{-1}. Doses were chosen according to a previous study (Buéno *et al.*, 1992).

In a second series of experiments, rats ($n = 10$), were injected i.c.v. either with (+)-N-cyclopropyl-methyl-1, 4-diphenyl-1-ethyl-but-3-en-1-ylamine hydrochloride (igmesine) (0.01 μg kg^{-1}) or CCK-8s (0.01 μg kg^{-1}), 15 min before i.c.v. injection of either dopamine (100 μg kg^{-1}), (+)-SKF 38393 (15 μg kg^{-1}), a selective D_1 receptor agonist or quinpirole (5 μg kg^{-1}), a selective D_2 receptor agonist.

In a third series of experiments, rats ($n = 10$) received 3 μl of dimethylsulphoxide (DMSO, 5%) alone (control) or with devazepide, (1 and 10 μg kg^{-1}) a selective CCK_A receptor antagonist, injected i.c.v. 15 min before igmesine or CCK-8s or their respective vehicle. Dopamine (100 μg kg^{-1}) was injected i.c.v. 15 min later.

CRF, CCK-8s and dopamine were purchased from Sigma (La Verpillière, France); sulpiride, SCH 23390 (R(+)-7-chloro-8 hydroxy-3 methyl-1-phenyl-2,3,4,5-tetrahydro-1H-3-benzazepine hydrochloride, SKF 38393 ((1-phenyl-7,8-dihydroxy-2,3,4,5-tetrahydro-1H-3 benzazepine) hydrochloride) and quinpirole were purchased from Research Biochemicals Inc., (Natick, MA, U.S.A.); all these compounds were dissolved in sterilized water. Igmesine was synthesized by the Institut de Recherche Jouveinal, (Fresnes, France) and dissolved in bovine serum albumin (0.5%); devazepide was a gift from Merck Sharp and Dohme (West Point, PA, U.S.A.) and was dissolved in DMSO (Sigma, La Verpillière, France).

Colonic motility evaluation and statistics

The frequency of colonic spike bursts, expressed as the number of spike bursts occurring in 10 min periods, was determined from direct electromyographic recording obtained from 30 min before the first i.c.v. administration to 30 min after either the beginning of the stress session or the last central administration. The mean values obtained before and during emotional stress or after treatment, as well as their differences, were compared by Student's paired t test or two way analysis of variance (ANOVA) followed by a paired t test for each treatment when appropriate. Differences were considered to be significant when $P \leqslant 0.05$.

Results

Influence of dopamine receptor antagonists on emotional stress- and CRF-induced stimulation of colonic motility

During the control period, the number of spike bursts occurring on the proximal colon was 7.9 ± 0.7 and 8.3 ± 0.5 spike bursts 10 min^{-1} at 2 and 4 cm from the ileo-cecal junction, respectively, and these values were not significantly ($P = 0.23$) different from one another. Consequently, we considered only the values obtained at 2 cm from the ileo-cecal junction for the following experiments.

Placement of the animals in the test-cage for 30 min, i.e. emotional stress, increased the mean frequency of colonic spike bursts by 141% over the entire period of exposure, 19.5 ± 1.7 spike bursts 10 min^{-1} vs 8.1 ± 0.8 spike bursts 10 min^{-1} in controls (Figure 1).

I.c.v. administration of CRF (0.5 μg kg^{-1}, i.c.v.) significantly ($P < 0.01$) increased the occurrence of colonic spike bursts from 7.9 ± 0.7 to 12.9 ± 1.3 spike bursts 10 min^{-1} observed between 5 and 15 min after administration (Figure 1).

I.c.v. injection of (+)-SCH 23390 (10 μg kg^{-1}) and sulpiride (10 μg kg^{-1}) did not modify *per se* the colonic spike burst frequency (Figure 1); SCH 23390 injected 15 min before either ES or CRF administration (0.5 μg kg^{-1} i.c.v.) prevented both ES- and CRF-induced stimulation of colonic motility (Figure 1); in contrast, sulpiride injected 15 min before

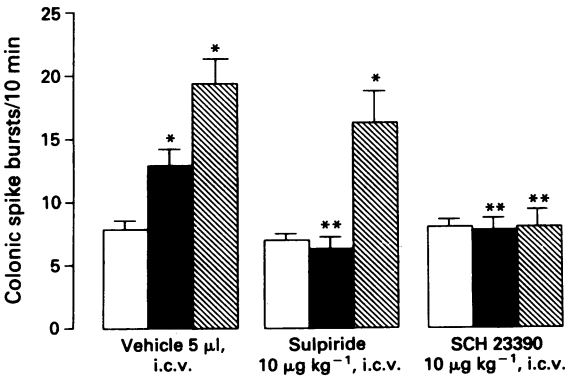


Figure 1 Comparative influence of i.c.v. pretreatment with (+)-SCH 23390 and sulpiride on corticotropin releasing factor (CRF)- and emotional stress-induced increase in frequency of colonic spike bursts in rats (mean ± s.d.; $n = 10$). Significantly different (*$P < 0.05$) from corresponding control values; significantly different (**$P < 0.05$) from CRF values (analysis of variance followed by t test). Open columns, vehicle, 3 μl i.c.v.; solid columns, CRF 0.5 μg kg^{-1}, i.c.v.; hatched columns, emotional stress.

Table 1 Comparative influence of intracerebroventricular (i.c.v.) injection of σ ligand (igmesine) and cholecystokinin octapeptide (CCK-8s) on the increase of colonic spike bursts induced by dopamine, quinpirole and (+)-SKF 38393 centrally administered in rats

Substances (i.c.v.)	*Basal*	*Frequency of colonic spike burst (10 min^{-1})* *Dopamine* (100 μg kg^{-1}, i.c.v.)	*Quinpirole* (5 μg kg^{-1}, i.c.v.)	*(+)-SKF 38393* (5 μg kg^{-1}, i.c.v.)
BSA 0.5% (5 μl)	7.6 ± 0.4	11.7 ± 0.6*	12.9 ± 1.1*	13.0 ± 1.2*
Igmesine (0.1 μg kg^{-1})	7.5 ± 0.8	7.4 ± 0.6	8.5 ± 0.8	6.4 ± 1.1
Sterilized water (5 μl)	7.4 ± 0.9	12.1 ± 0.7*	13.1 ± 0.4*	12.9 ± 0.8*
CCK-8s (0.1 μg kg^{-1})	7.8 ± 1.1	8.5 ± 1.3	9.4 ± 1.2	6.5 ± 1.6

Values significantly (*$P \leq 0.05$) different from corresponding basal values.
Values are mean ± s.d.; $n = 10$.

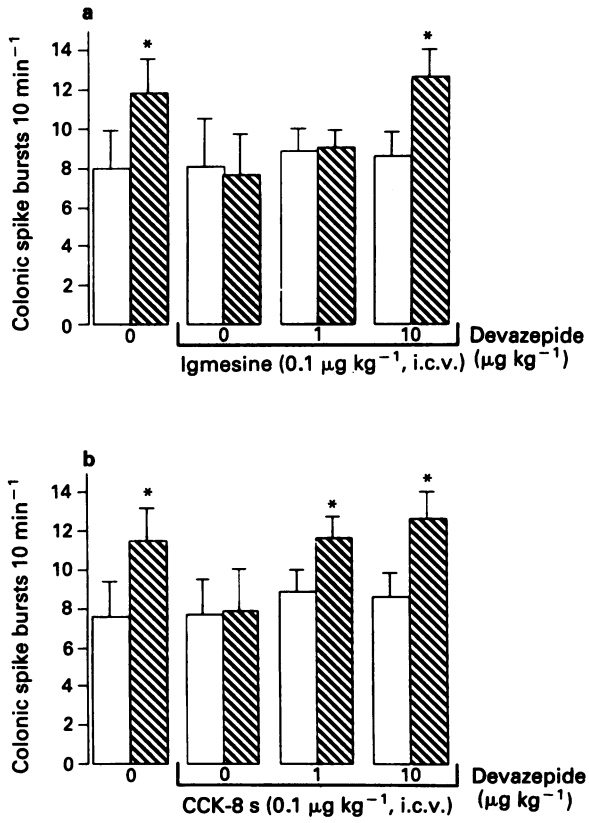


Figure 2 Influence of i.c.v. pretreatment with devazepide on the blockade by igmesine (a) and cholecystokinin octapeptide (CCK-8s) (b) of dopamine-induced increase in colonic spike bursts frequency (mean ± s.d., $n = 10$). Significantly different (*$P < 0.05$) from corresponding control values (analysis of variance followed by t test). Open columns, basal; hatched columns, dopamine 100 μg kg^{-1}, i.c.v.

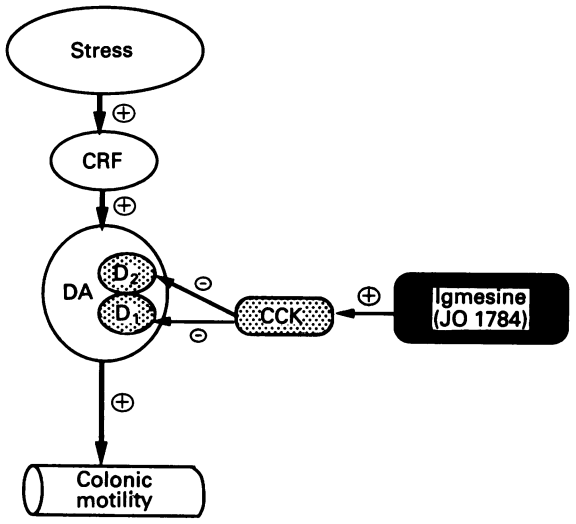


Figure 3 Schematic representation of the pathways involved in blockade of corticotropin releasing factor (CRF)- and dopamine (DA)-induced colonic hypermotility by igmesine.

CRF antagonized CRF-induced increase in colonic spike bursts but had no effect on ES-induced stimulation of colonic motility.

Influence of igmesine and CCK-8s on stimulation by dopamine of colonic myoelectrical activity

During the control period, i.e. 30 min before any treatment, the number of spike bursts occurring in the proximal colon was 7.6 ± 0.4 spike bursts 10 min^{-1}. I.c.v. injection of vehicle (5 μl) did not change the colonic spike burst frequency. Dopamine injected i.c.v. (100 μg kg^{-1}) increased the frequency of colonic spike bursts from 7.6 ± 0.4 to 11.7 ± 0.6 spike bursts 10 min^{-1}. Similarly, (+)-SKF 38393 (5 μg kg^{-1}, i.c.v.) and quinpirole (5 μg kg^{-1}, i.c.v.) increased by 71% and 70% respectively, the frequency of colonic spike bursts (Table 1).

Igmesine (0.1 μg kg^{-1}) injected i.c.v., 15 min before central administration of dopamine, at a dose which had no effect *per se* on colonic myoelectrical activity, abolished the colonic motor stimulation induced by dopamine, since, the frequency of colonic spike bursts was similar to that observed before dopamine injection (7.4 ± 0.6 vs 7.5 ± 0.8 spike burst 10 min^{-1}) (Table 1). Similarly, igmesine (0.1 μg kg^{-1}, i.c.v.) blocked the stimulatory effects of both (+)-SKF 38393 (5 μg kg^{-1}, i.c.v.) and quinpirole (5 μg kg^{-1}, i.c.v.); in these cases the values are similar ($P > 0.05$) to those recorded during the control period (Table 1).

CCK-8s injected i.c.v., also suppressed the stimulation of colonic motility induced by i.c.v. dopamine (100 μg kg^{-1}) (dopamine, 11.7 ± 0.6 spike bursts 10 min vs CCK-8s + dopamine, 8.5 ± 1.3 spike bursts 10 min^{-1}) (Table 1). Similarly, the stimulatory effects of (+)-SKF 38393 and quinpirole (5 μg kg^{-1}, i.c.v.) on colonic spike activity were significantly reduced ($P < 0.05$) by prior i.c.v. injection of CCK-8s (0.1 μg kg^{-1}) (Table 1).

Influence of devazepide on CCK-8s- and igmesine-induced blockade of dopamine stimulation of colonic myoelectrical activity

I.c.v. injection of DMSO (3 μl) had no effect on the colonic spike bursts frequency (8.0 ± 0.7 spike bursts 10 min^{-1}). Furthermore, this group of rats in control conditions, i.e. 3 i.c.v. injections of vehicle, did not show a significant ($P > 0.05$) difference in the frequency of colonic spike bursts as compared with rats not receiving injections.

Devazepide injected i.c.v. (10 $\mu g\,kg^{-1}$) did not modify the colonic spike burst frequency (8.3 ± 0.9 spike bursts 10 min^{-1}) or the increase in the frequency of colonic spike bursts produced by dopamine (Figure 2). However, devazepide (10 $\mu g\,kg^{-1}$, i.c.v.) abolished the antagonistic action of both CCK-8s and igmesine on dopamine-induced colonic motor hyperactivity (Figure 2). In contrast, devazepide injected i.c.v. at a lower dose (1 $\mu g\,kg^{-1}$) antagonized the inhibitory effect of CCK-8s on dopamine-induced colonic hyperkinesia but had no effect on the blocking effect of igmesine (Figure 2).

Discussion

The increase in colonic motility associated with ES has previously been shown to depend upon the central release of CRF, since it is blocked by a CRF antagonist and mimicked by i.c.v. administration of CRF (Gué *et al.*, 1991). Furthermore, these effects are not mediated through the stimulation of the hypothalamo-pituitary adrenal (HPA) axis and persisted in hypophysectomized rats (Gué *et al.*, 1991).

Dopaminergic mechanisms are known to play a key role in the central response to stress. The mesocortical, mesolimbic and to a lesser extent, the nigrostriatal dopaminergic systems are known to be activated by most forms of stress (Fadda *et al.*, 1978; Herman *et al.*, 1982). Furthermore, dopamine receptor antagonists block the suppression of locomotor activity associated with mental stress (Katoh *et al.*, 1991). The present work shows that the release of dopamine and/or the activation of dopaminergic pathways are involved in the genesis of CRF-induced colonic motor alterations, because these effects are blocked by central injection of D_1 and D_2 receptor antagonists, such as (+)-SCH 23390 and sulpiride, respectively. Furthermore, as we have previously shown (Buéno *et al.*, 1992), ES stimulates colonic motility through the activation of dopaminergic pathways, since D_1 receptor antagonists block the stimulation of colonic motility associated with mental stress. However, our results also show that both D_1 and D_2 receptor antagonists inhibit the CRF-induced stimulation of colonic motility, while only the D_1 receptor antagonist blocks the colonic response to stress. These data suggest that CRF activates dopaminergic stimulation of both pathways via a mechanism involving both types of dopamine receptor, whereas ES activates dopaminergic pathways only via an activation of D_1 receptors to stimulate colonic motility. Such discrepancies could be explained by the fact that stress induces CRF release from specific brain structures, such as the paraventricular nuclei, which interfere with D_1 receptor activating pathways to stimulate colonic motility. In contrast, exogenously administered CRF reaches the receptors present in several brain structures, which are not specifically activated during stress, and which may interact with dopaminergic pathways through both D_1 and D_2 receptors to activate colonic motility.

In the present study, we also found that a σ ligand (igmesine), known to block the emotional stress-induced increase in colonic myoelectrical activity (Junien *et al.*, 1991), is able to abolish dopamine-induced colonic motor stimulation as well as that induced by either D_1 or D_2 receptor agonists injected centrally. Since activation of a dopaminergic system is involved in the neurotransmission of emotional stress-induced colonic myoelectrical activity (Buéno *et al.*, 1992), our results suggest that σ ligands act, at least at this level, to block the effects of emotional stress on colonic motility. Previously, we have shown that igmesine exerts its colonic anti-stress effect through CCK neurones (Gué *et al.*, 1992). Our present data indicate that igmesine also exerts its antagonist effect on dopamine-induced stimulation of colonic motility via a mechanism involving the central activation of CCK release or neuronal pathways. This hypothesis is reinforced by the fact that CCK blocks the stimulatory action of dopamine as well as those of D_1 and D_2 receptor agonists, on colonic motility. These findings could be explained by the co-localization of CCK and dopamine in neurones which have been described in brain structures known to be activated during stress. Furthermore, since CCK is present within dopamine containing neurones of the rat ventral midbrain (Hökfelt *et al.*, 1980) and because CCK-8s modulates the dopamine release (Lane *et al.*, 1986; Voight *et al.*, 1986), we can suppose that CCK-8s and related substances act by modulating dopaminergic neurotransmission in the midbrain to inhibit the CRF- and emotional stress-induced colonic motor activation. This hypothesis is in agreement with evidence that CCK-8s alters dopaminergic transmission at this level (Bunney *et al.*, 1982; Skirboll & Hommer, 1985). However, the nature of the effects of CCK-8s on dopaminergic transmission is not clearly defined; indeed, it has been suggested that CCK-8s may have opposite effects on dopamine release from the anterior and posterior nucleus accumbens depending on the CCK receptor type involved i.e. CCK_A or CCK_B (Marshall *et al.*, 1991). However, other studies suggest that CCK acts mainly as an endogenous antagonist of dopamine (Crawley, 1991; Liang *et al.*, 1991).

Regarding the interaction between σ receptors and dopaminergic systems, several reports also provide evidence that σ ligands modulate dopaminergic pathways. However, some controversy exists regarding the effect of σ ligands, such as (+)-N-allyl-nor-metazocine (d-NANM), on the firing rate of A9 and A10 dopaminergic neurones. Indeed, Freeman & Bunney (1984) report an increase in the firing rates of midbrain (A9 and A10) dopaminergic neurones after acute intravenous d-NANM administration, while the same σ receptor ligand produces either an increase, a decrease or no effect on the firing rates of midbrain dopaminergic neurones after microiontophoretic application (Freeman & Bunney, 1984; Steinfels & Tam, 1988). Since in the present study, igmesine was injected centrally, our findings of an inhibitory action of this σ ligand on dopamine-induced stimulation of colonic motility could be compared to the microiontophoretic application studies rather than to the systemic injection of σ ligands. Therefore, our results agree with the known modulatory role of σ ligands on dopaminergic neuronal activity. Taken together, these data support the hypothesis that σ ligands interact with central dopaminergic mechanisms through activation of CCK receptors or CCK release.

In summary, our study suggests (1) that CRF released by emotional stress stimulates colonic motility through the central activation of dopaminergic neuronal pathways and involves stimulation of both D_1 and D_2 receptor types, (2) that CCK-8s inhibits dopamine induced colonic hyperkinesia through D_1 and D_2 receptors and (3) that igmesine, a selective σ ligand, blocks the CRF- and ES-induced colonic motor response through central CCK release and/or activation of CCK supraspinal pathways (Figure 3).

References

BUÉNO, L., GUÉ, M., FABRE, C. & JUNIEN, J.L. (1992). Involvement of central dopamine and D1 receptors in stress-induced colonic motor alterations in rats. *Brain Res. Bull.*, **29**, 135–140.

BUNNEY, B.S., GRACE, A.A., HOMMER, D.W. & SKIRBOLL, L.R. (1982). Effect of cholecystokinin of the activity of midbrain dopaminergic neurons. *Adv. Biochem. Psychopharmacol.*, **33**, 429–436.

CABIB, S., KEMPF, E., SCHLEEF, C., OLIVERIO, A. & PUGLISI-ALLEGRA, S. (1988). Effects of immobilization stress on dopamine and its metabolites in different brain areas of the mouse: role of genotype and stress duration. *Brain Res.*, **441**, 153–160.

CRAWLEY, J.N. (1991). Cholecystokinin-dopamine interactions. *Trends Pharmacol. Sci.*, **12**, 232–235.

DEUTCH, A.Y., TAM, S. & ROTH, R. (1985). Footshock and conditioned stress increase 3,4-dihydroxyphenylacetic acid (DOPAC) in the ventral tegmental area but not in the substantia nigra. *Brain Res.*, **33**, 143–146.

FADDA, F., ARGIOLAS, A., MELIS, M.R., TISSARI, A.H., ONALI, P.L. & GESSA, G.L. (1978). Stress-induced increase in 3-4-dihydroxyphenylacetic acid (DOPAC) levels in the cerebral cortex and in accumbens: reversal by diazepam. *Life Sci.*, **23**, 2219–2224.

FREEMAN, A.S. & BUNNEY, B.S. (1984). The effects of phencyclidine and N-allylnormetazocine on midbrain dopamine neuronal activity. *Eur. J. Pharmacol.*, **104**, 287–293.

GUÉ, M., ALARY, C., DEL RIO-LACHEZE, C., JUNIEN, J.L. & BUÉNO, L. (1993). Comparative involvement of 5-HT1, 5-HT2 and 5-HT3 receptors in stress-induced colonic motor alterations in rats. *Eur. J. Pharmacol.*, **233**, 193–199.

GUÉ, M., JUNIEN, J.L. & BUÉNO, L. (1991). Conditioned emotional response in rats enhances colonic motility through the central release of corticotropin-releasing factor. *Gastroenterology*, **100**, 964–970.

GUÉ, M., JUNIEN, J.L., DEL RIO, C. & BUÉNO, L. (1992). Neuropeptide Y and sigma ligand (JO 1784) suppress stress-induced colonic motor disturbances in rats through sigma and CCK receptors. *J. Pharmacol. Exp. Ther.*, **261**, 850–855.

GUNDLACH, A.L., LARGENT, B.L. & SNYDER, S.H. (1985). Phencyclidine and σ opiate receptors in brain: biochemical and autoradiographical differentiation. *Eur. J. Pharmacol.*, **113**, 465–472.

GUNDLACH, A.L., LARGENT, B.L. & SNYDER, S.H. (1986). Autoradiographic localization of σ receptors binding sites in guinea pig and rat central nervous system with (+)3H-3(3-hydroxyphenyl)-N-(1-propyl)piperidine. *J. Neurosci.*, **6**, 1757–1762.

HERMAN, J.P., GUILLONNEAU, D., DANTZER, R., SCATTON, B., SEMERDJIAN-ROUQUIER, L. & LE MOAL, M. (1982). Differential effects of inescapable footschoks on dopamine turnover in cortical and limbic areas of the rat. *Life Sci.*, **30**, 2207–2214.

HÖKFELT, T., REHFELD, J.F., SKIRBOL, L., IVEMARK, B., GOLSTEIN, M. & MARKEY, M. (1980). Evidence of coexistence of dopamine and CCK in mesolimbic neurons. *Nature*, **285**, 476–478.

JIMENEZ, M. & BUÉNO, L. (1990). Inhibitor effects of neuropeptide Y on CRF and stress-induced caecal motor response in rats. *Life Sci.*, **47**, 205–212.

JUNIEN, J.L., GUÉ, M. & BUÉNO, L. (1991). Neuropeptide Y and sigma ligand (JO 1784) act through a Gi protein to block the psychological stress and corticotropin-releasing factor-induced colonic motor activation in rats. *Neuropharmacol.*, **30**, 1119–1124.

KANEYUKI, H., YOKOO, H., TSUDA, A., YOSHIDA, M., MIZULI, Y., YAMADA, M. & TANAKA, M. (1991). Psychological stress increases dopamine turnover selectively in mesoprefrontal dopamine neurons of rats: Reversal by diazepam. *Brain Res.*, **557**, 154–161.

KATOH, A., NABESHIMA, T. & KAMEYAMA, T. (1991). Interactions between enkephalinergic and dopaminergic systems in stressful situations. *Eur. J. Pharmacol.*, **193**, 95–99.

LANE, R.F., BLAHA, C.D. & PHILLIPS, A.G. (1986). In vivo electrochemical analysis of cholecystokinin-induced inhibition of dopamine release in nucleus accumbens. *Brain Res.*, **397**, 200–204.

LIANG, R.Z., WU, M., YIM, C.C.Y. & MOGENSON, G.J. (1991). Effects of dopamine agonists on excitatory inputs to nucleus accumbens neurons from the amygdala: modulatory actions of cholecystokinin. *Brain Res.*, **554**, 85–94.

MARSHALL, F.H., BARNES, S., HUGHES, J., WOODDRUFF, G.N. & HUNTER, J.C. (1991). Cholecystokinin modulates the release of dopamine from the anterior and posterior nucleus accumbens by two different mechanisms. *J. Neurochem.*, **56**, 917–922.

MARTINEZ, J.A. & BUÉNO, L. (1991). Buspirone inhibits corticotropin-releasing factor and stress-induced cecal motor response in rats by acting through 5-HT_{1A} receptors. *Eur. J. Pharmacol.*, **202**, 379–383.

NABESHIMA, T., KATOH, A. & KAMEYAMA, T. (1988). Inhibition of enkephalin degradation attenuated stress-induced motor suppression (conditioned suppression of motility). *J. Pharmacol. Exp. Ther.*, **244**, 303–309.

PAXINOS, G. & WATSON, C. (1986). *The Rat Brain in Stereotaxic Coordinates*. 2nd Ed. pp. 1–116. Orlando: Academic Press.

RUCKEBUSH, M. & FIORAMONTI, J. (1975). Electrical spiking activity and propulsion in small intestine in fed and fasted rats. *Gastroenterology*, **68**, 1500–1508.

SKIRBOLL, L.R. & HOMMER, D.W. (1985). Electrophysiological studies of the role of cholecystokinin in the substantia nigra and its interactions with dopamine. *Ann. N.Y. Acad. Sci.*, **448**, 275–282.

STEINFELS, G.F. & TAM, S.W. (1988). Electrophysiological action of selective sigma receptor agonists and antagonists on midbrain dopamine neurones. *Soc. Neurosci. Abst.*, **14**, 214–218.

VOIGHT, M, WANG, R.Y., KASSER, R.J. & HU, X.T. (1986). Cholecystokinin octapeptide alters the release of endogenous dopamine from the rat nucleus accumbers in vitro. *J. Pharmacol. Exp. Ther.*, **237**, 147–153.

YIM, C.C. & MOGENSON, G.J. (1991). Electrophysiological evidence of modulatory interaction between dopamine and cholecystokinin in the nucleus accumbens. *Brain Res.*, **541**, 12–20.

(Received July 2, 1993
Revised October 29, 1993
Accepted November 22, 1993)

Br. J. Pharmacol. (1994), **111**, 935–941 © Macmillan Press Ltd, 1994

Inhibitory effects of caffeine on secretagogue-induced catecholamine secretion from adrenal chromaffin cells of the guinea-pig

[1]Yoshikazu Nakazato, Yuichiro Tani, *Hiroki Teraoka, Takeshi Sugawara, Tadashi Asano, Toshio Ohta & Shigeo Ito

Department of Pharmacology, Faculty of Veterinary Medicine, Hokkaido University, Sapporo 060, and *Department of Veterinary Pharmacology, Faculty of Dairy Science, Rakuno Gakuen University, Ebetsu 069, Japan

1 The inhibitory action of caffeine on catecholamine secretion induced by secretagogues was investigated in perfused adrenal glands and dispersed chromaffin cells of the guinea-pig.

2 Caffeine (10 mM) caused a reversible inhibition of catecholamine secretion evoked by acetylcholine (ACh, 50 μM), KCl (56 mM, high K^+) and veratridine (100 μM) and that induced by muscarinic receptor activation in the absence of extracellular Ca^{2+} in perfused adrenal glands.

3 In dispersed chromaffin cells, caffeine caused a dose-dependent inhibition of the secretory responses to 100 μM ACh and veratridine. Forskolin (30 μM), dibutyryl cyclic AMP (1 mM) and 8-bromo cyclic AMP (1 mM) did not mimic the action of caffeine.

4 In the voltage-clamp, whole-cell recording mode (at a holding potential of −60 mV or −70 mV), ACh (100 μM) evoked an inward current, and depolarizing pulses elicited inward Na^+, Ca^{2+} and outward K^+ currents. All these responses were partially inhibited by caffeine (20 mM).

5 ACh rapidly increased the intracellular concentration of Ca^{2+} ($[Ca^{2+}]_i$) in fura-2-loaded cells in either the presence or the absence of external Ca^{2+}, though its magnitude was decreased by about 50% in Ca^{2+}-free conditions. Caffeine (20 mM) inhibited these ACh-induced increases in $[Ca^{2+}]_i$.

6 In permeabilized chromaffin cells, caffeine (20 mM) caused an inhibition of catecholamine secretion evoked by Ca^{2+} (10 μM).

7 These results suggest that caffeine inhibits evoked catecholamine secretion through mechanisms such as the blockade of voltage-dependent Na^+ and Ca^{2+} currents and ACh receptor current, and reduction of the release of intracellularly stored Ca^{2+} and/or Ca^{2+}-sensitivity of the secretory apparatus.

Keywords: Acetylcholine currents; caffeine; Ca^{2+} transient; intracellular concentration of Ca^{2+}; whole cell patch clamp

Introduction

Caffeine is known to be a potentiator of Ca^{2+}-induced Ca^{2+} release (CICR) in muscle cells (Endo, 1977). It has been demonstrated that caffeine causes a much larger increase in catecholamine secretion in the absence of extracellular Ca^{2+} and/or Na^+ than in their presence in perfused adrenal glands of the cat and guinea-pig (Yamada *et al.*, 1988; 1989; Teraoka *et al.*, 1990; Nakazato *et al.*, 1992), and in cultured bovine adrenal chromaffin cells (Teraoka *et al.*, 1991). Caffeine was also found to increase the cytosolic free Ca^{2+} level ($[Ca^{2+}]_i$) and catecholamine secretion, both of which were abolished after combined treatment with caffeine and ryanodine (Teraoka *et al.*, 1991; Nakazato *et al.*, 1992). These results suggest that caffeine stimulates Ca^{2+} mobilization from ryanodine-sensitive intracellular Ca^{2+} stores through the CICR mechanism, resulting in an increase in catecholamine secretion from adrenal chromaffin cells. Apart from these stimulant actions, we also found that caffeine decreased catecholamine secretion evoked by Ca^{2+} in digitonin-permeabilized bovine adrenal chromaffin cells, suggesting that caffeine reduces the susceptibility of the secretory apparatus to Ca^{2+} (Teraoka *et al.*, 1991). However, there has been no further information about the mode of inhibitory action of caffeine on adrenal catecholamine secretion.

The primary object of this study was to determine whether caffeine caused inhibition of catecholamine secretion evoked by various secretagogues in perfused adrenal glands and dispersed chromaffin cells of the guinea-pig. The results showed that caffeine decreased the evoked catecholamine secretion irrespective of the kind of secretagogue used. Therefore, possible mechanisms underlying this inhibitory action were examined by studying the effects of caffeine on membrane currents and $[Ca^{2+}]_i$ using the whole-cell mode of the patch clamp technique and monitoring $[Ca^{2+}]_i$ by fura-2, respectively.

[1] Author for correspondence.

Methods

Experiments with perfused adrenal glands

Guinea-pigs of either sex, weighing 350–450 g, were anaesthetized with sodium pentobarbitone (40 mg kg^{-1}) intraperitoneally. Both adrenal glands were perfused and isolated following the general procedure described previously (Ito *et al.*, 1979). The glands were perfused at a flow rate of 0.5 to 0.6 ml min^{-1} and maintained at room temperature (approximately 25°C). The adrenal effluent was collected continuously in 5 min aliquots into glass tubes kept on ice.

The standard perfusion medium was modified Locke solution of the following composition (mM): NaCl 154, KCl 5.6, $CaCl_2$ 2.2, $MgCl_2$ 1.2, Na_2HPO_4-NaH_2PO_4 buffer 3 (pH 7.0). When ACh was used as a secretagogue, perfusion solutions contained 0.2 μM physostigmine. All solutions used were bubbled with 100% O_2 throughout the experiments.

Experiments were started about 40 min after isolation of adrenal glands. Secretagogues were administered for 1 min, beginning 1 min before the following 5 min collection periods because of the 1 min dead time of the arterial cannula. Samples collected were acidified with 8 M perchloric acid to a final concentration of 0.4 M and stored on ice until assayed.

Experiments with dispersed chromaffin cells

Guinea-pigs of either sex weighing 250–400 g were stunned and bled to death. Adrenal glands were isolated and freed from surrounding tissues in Ca^{2+}-free Krebs solution and then sliced with a razor blade. Sliced adrenal glands were incubated with Ca^{2+}-free Krebs solution containing collagenase (1.5–2 mg ml^{-1}) according to the methods of Hochman & Perlman (1976). The isolated chromaffin cells were suspended in modified Krebs solution (1 ml) containing bovine serum albumin (5 mg ml^{-1}) and incubated in a shaking bath (150 oscillations min^{-1}) with drugs at 37°C for 20 min under 100% O_2. Cells were then rapidly chilled on ice and removed by centrifugation, after which the catecholamine content in the supernatant and pellet was measured. Catecholamine release from the isolated cells was expressed as a percentage of catecholamine content in the cells. The modified Krebs solution contained (mM): NaCl 118, KCl 4.7, KH_2PO_4 1.2, MOPS 25 (pH 7.2 adjusted with NaOH), $CaCl_2$ 2.5, $MgSO_4$ 1.2 and glucose 10.

Experiments with permeabilized chromaffin cells

Permeabilized adrenal chromaffin cells of guinea-pigs were prepared by the method of Dunn & Holz (1983). Cells were preincubated with a solution of the following composition (mM): potassium glutamate 139, PIPES 20 (pH 6.8, adjusted with KOH), $MgSO_4$ 5, ATP-Na_2 5, EGTA 5, glucose 5, (K^+ glutamate solution) at 37°C for 30 min. Then the cells were washed twice with K^+ glutamate solution and incubated with this solution containing β-escin (20 μM) and caffeine (20 mM) with or without Ca^{2+} (10 μM) at room temperature for 20 min.

Assay of catecholamine

Adrenaline and noradrenaline were separated by high performance liquid chromatography (h.p.l.c., Jasco, Japan) and detected by an electochemical detector (840-EC, Jasco). The detection limit was 10 nM (0.01 nmol ml^{-1}) for either adrenaline or noradrenaline. The treatment of samples for h.p.l.c. was carried out according to the method of Salzman & Sellers (1982).

Membrane current recording

Whole-cell membrane currents were measured with standard patch clamp techniques (Hamill *et al.*, 1981) using a patch clamp amplifier (CEZ-2300, Nihon-Koden, Japan) at room temperature. The patch pipette resistance ranged from 3 to 5 MΩ. Data recording and illustration were carried out as described previously (Ohta *et al.*, 1992). The ionic composition of the external solution used for this experiment was as follows (mM): NaCl 126, KCl 6, $MgCl_2$ 1.2, $CaCl_2$ 1.7, HEPES 10, glucose 14. The K^+-containing pipette solution contained (mM): KCl 132, $MgCl_2$ 1.2, HEPES 10 (pH 7.2, with KOH), EGTA 10, ATP-Na_2 2. The K^+-free, Cs^+-containing pipette solution was prepared by substitution of equimolar CsCl for KCl.

Flourescence measurements

The intracellular concentration of Ca^{2+}, $[Ca^{2+}]_i$, was estimated from fura-2 fluorescence by the ratio method using dual-wavelength excitation and single emission (Grynkiewicz *et al.*, 1985). Dispersed chromaffin cells attached to a cover glass were loaded with fura-2 by incubating with the external solution described above, containing fura-2AM (5 μM) and bovine serum albumin (0.05%) at room temperature for 30 min. Then the cells and the cover glass were transferred to a small chamber (volume 0.6 ml) placed on the stage of a fluorescence microscope (TMD, Nikon, Japan) attached to a fluorimeter (CAM-200, Jasco). The cells were superfused with the external solution at a flow rate of 1.5–2 ml min^{-1} and waste solution was continuously drained. The fluorescence signal was detected with a Nikon CF u.v. (Fluor, × 40 oil-immersion objective) lens and the emission light, which was passed through a pinhole diaphragm slightly larger than a cell, was collected by a photomultiplier through a 500 nm filter. The ratio of the fluorescence due to excitation at 340 nm to that at 380 nm (F340/F380) was calculated from successive illumination periods and stored on videotape through a PCM data recording system (RP-880, NF Electronic Instruments, Japan).

Chemicals

The following chemicals were used: acetylcholine chloride (Ovisort, Daiichi, Tokyo), adenosine-5′-triphosphate (ATP, Boehringer-Manheim-Yamanouchi, Tokyo), β-escin, bovine serum albumin, forskolin, N6,2′-O-dibutyryladenosine 3′,5′-cyclic monophosphate (dibutyryl cyclic AMP), 8-bromoadenosine 3′,5′-cyclic monophosphate (8-bromo cyclic AMP), veratridine (Sigma, St. Louis, MO), ethylenediaminetetraacetic acid (EDTA), glycoletherdiamine-*N,N, N′,N′*-tetraacetic acid (EGTA), N-2-hydroxyethyl-piperazine-*N′*-2-ethanesulphonic acid (HEPES), 3-(N-morpholino) propanesulphonic acid (MOPS), fura-2AM (Dojindo Laboratories, Kumamoto), caffeine monohydrate, collagenase, theophylline (Wako Pure Chem, Tokyo), sodium 1 octanesulphonate (Nacalai Tesque, Kyoto) and tetrodotoxin (Mitsui, Tokyo).

Statistics

The data are presented as arithmetic mean ± s.e.mean. Significance was assessed with Student's *t* test.

Results

Effects of caffeine on catecholamine secretion induced by secretagogues in perfused adrenal glands

The effect of caffeine on catecholamine secretion evoked by various secretagogues was investigated with perfused adrenal glands. Acetylcholine (ACh, 50 μM), KCl (56 mM, high K^+) and veratridine (100 μM) were sequentially applied to the adrenal gland for 1 min at 20 min intervals before, during and after infusion of caffeine (10 mM). Caffeine showed almost no consistent effect on the resting catecholamine secretion during perfusion with standard Locke solution as reported previously (Teraoka *et al.*, 1990; Nakazato *et al.*, 1992). However, the secretory responses to ACh, high K^+ and veratridine all were partially inhibited in the presence of caffeine (Figure 1).

Previously we demonstrated that both nicotinic and muscarinic receptors almost equally contribute to catecholamine secretion evoked by ACh with concentrations of 50 μM and 100 μM (Nakazato *et al.*, 1988). Furthermore, unlike nicotinic receptor activation, muscarinic activation mobilizes intracellulary stored Ca^{2+} to increase catecholamine secretion (Nakazato *et al.*, 1984; 1988; Yamada *et al.*, 1988; Teraoka *et al.*, 1990). Thus, the effect of caffeine on ACh-evoked catecholamine secretion through muscarinic receptor activation was studied in the adrenal glands perfused with Ca^{2+}-free Locke solution containing hexamethonium (0.5 mM). ACh (100 μM) applied for 1 min caused increases in catecholamine secretion repeatedly during perfusion with Ca^{2+}-free solution, as long as the adrenal glands were loaded with 2.2 mM Ca^{2+} for 20 to 25 min between stimuli. It was also noted that the Ca^{2+} loading produced a tonic increase in catecholamine secretion which declined on repetition (Figure 2a). In Figure 2b, ACh (100 μM) was first applied during perfusion with the standard Locke solution, and then the same protocol of experiment as shown in Figure 2a was carried out in the presence of caffeine (10 mM) during the

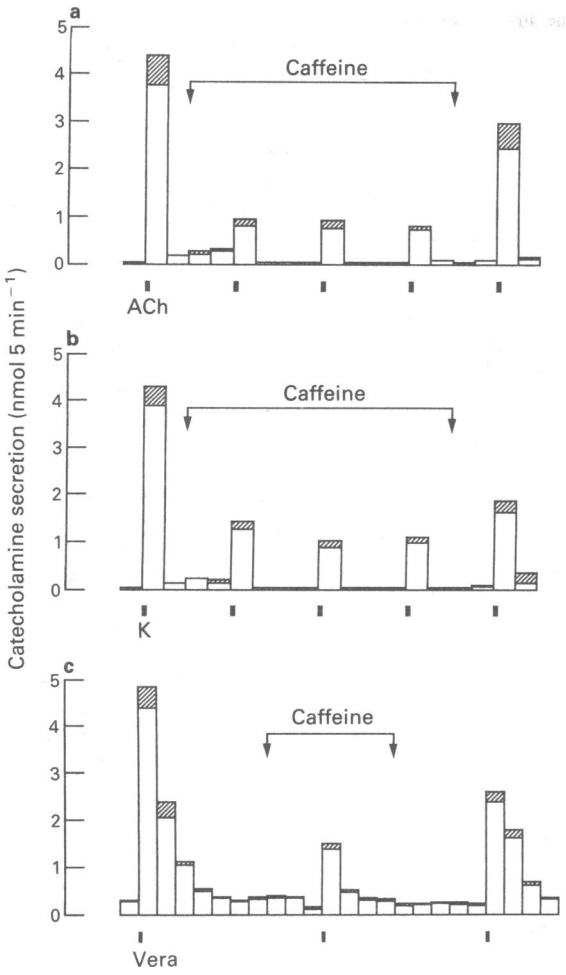


Figure 1 Inhibitory effect of caffeine on secretagogue-induced catecholamine secretion. Acetylcholine (ACh, 50 μM) (a), KCl (K, 56 mM) (b) and veratridine (Vera, 100 μM) (c) were sequentially applied for 1 min before, during and after infusion of caffeine (10 mM) (↓——↓) in perfused adrenal glands of the guinea-pig. The standard Locke solution was used for perfusion. Representative data are shown. Columns show the amount of adrenaline (open) and noradrenaline (hatched) released in nmol 5 min^{-1}.

second and third exposure to Ca^{2+}-free solution. The magnitude of ACh-induced catecholamine secretion in the absence of extracellular Ca^{2+} was about 25% of that in the presence of Ca^{2+}. Caffeine caused a significant inhibition of ACh-induced catecholamine secretion which completely recovered after its removal. In addition, there was almost no increase in catecholamine secretion in response to the Ca^{2+} loading.

Effects of caffeine on catecholamine secretion induced by ACh and veratridine in dispersed chromaffin cells

By use of dispersed chromaffin cells, the potency of caffeine to inhibit the agonist-induced catecholamine secretion was estimated. The dispersed chromaffin cells were incubated for 20 min at 37°C with ACh (100 μM) or veratridine (100 μM) in combination with various concentrations of caffeine (1–40 mM). Caffeine caused a dose-dependent inhibition of both secretory responses (Figure 3). The rate of inhibition was about 10% at 1 mM caffeine and increased as its concentration increased, attaining a maximum at 20 mM for both the responses to ACh and those to veratridine. The IC_{50} values for caffeine were about 4.4 mM in ACh- and 6.0 mM in vertridine-induced catecholamine secretions.

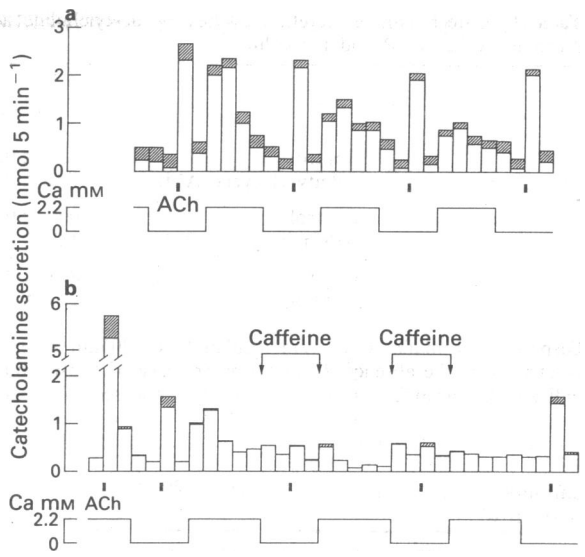


Figure 2 Inhibitory effect of caffeine on catecholamine secretion induced by acetylcholine in the absence of extracellular Ca^{2+}. The adrenal glands were perfused with the standard Locke and Ca^{2+}-free Locke solutions alternately as indicated below the records. Acetylcholine (ACh, 100 μM) was applied for 1 min as indicated by vertical heavy bars. (a) Shows control experiment and in (b) caffeine (10 mM) was present for the periods indicated (↓——↓). Representative data are illustrated. Columns show the amount of adrenaline (open) and noradrenaline (hatched) released in nmol 5 min^{-1}.

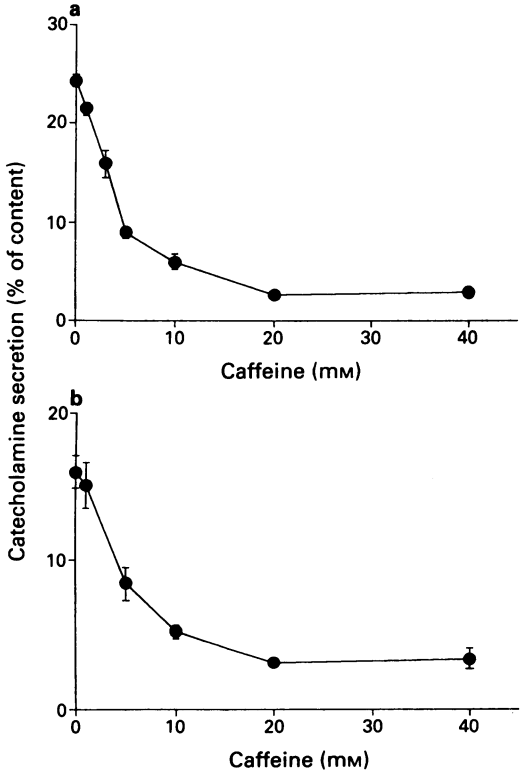


Figure 3 Dose-dependent inhibition of secretagogue-induced catecholamine secretion by caffeine. Dispersed chromaffin cells were incubated with acetylcholine (ACh, 100 μM) (a) and veratridine (100 μM) (b) for 20 min at 37°C in the absence and presence of various concentrations of caffeine (1–40 mM). Modified Krebs solution was used for incubation. Symbols indicate the mean ± s.e.mean (if vertical lines are present) of adrenaline released as a percentage of total cell content in the presence of the secretagogues obtained from 8 experiments.

Table 1 Catecholamine secretion evoked by acetylcholine and veratridine in the presence or absence of dibutyryl cyclic AMP, 8-bromo cyclic AMP and forskolin

	Catecholamine secretion (%)		
	Resting	*Acetylcholine*	*Veratridine*
Control	0.75 ± 0.46 (4)	9.11 ± 0.86 (5)	8.66 ± 0.67 (5)
Dibutyryl cyclic AMP	1.88 ± 0.70 (5)	14.07 ± 1.24 (5)	9.10 ± 1.64 (4)
Control	0.61 ± 0.36 (5)	12.91 ± 0.72 (6)	14.88 ± 1.44 (4)
8-Bromo cyclic AMP	1.23 ± 0.49 (5)	13.35 ± 0.80 (4)	11.76 ± 1.67 (4)
Control	2.00 ± 0.49 (5)	15.10 ± 0.74 (5)	18.20 ± 0.43 (5)
Forskolin	2.70 ± 0.29 (5)	19.59 ± 0.76 (5)	16.59 ± 0.79 (5)

Dispersed chromaffin cells were incubated for 20 min at 37°C with modified Krebs solutions containing 100 μM acetylcholine or veratridine in the absence (Control) or presence of 1 mM dibutyryl cyclic AMP, 8-bromo cyclic AMP and 30 μM forskolin. Numbers indicate the mean ± s.e.mean of adrenaline released as a percentage of total cell contents (no. of experiments in parentheses).

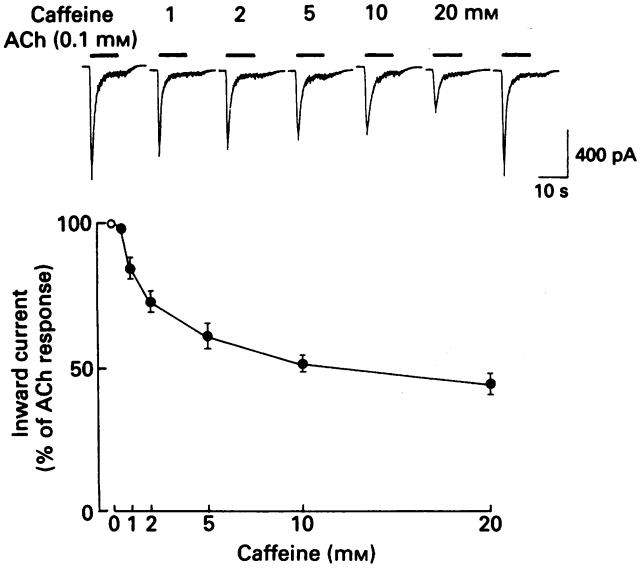


Figure 4 Dose-dependent inhibition of acetylcholine (ACh)-induced inward current in single chromaffin cells. Cells were dialyzed with K^+-rich (KCl, 132 mM) pipette solution and superfused with the normal external solution at a holding potential of − 60 mV. ACh (100 μM) was sequentially applied for 10 s (horizontal bars) through a pipette placed close to the cell in the presence and absence of caffeine, which was added to the superfused solution in the concentrations indicated above the current responses. Representative records are shown in (a) and the data obtained from different experiments are sumarized in (b). The symbols indicate the mean ± s.e.mean of peak amplitude, if vertical lines are present, as a percentage of control in the presence (●) and absence (○) of caffeine.

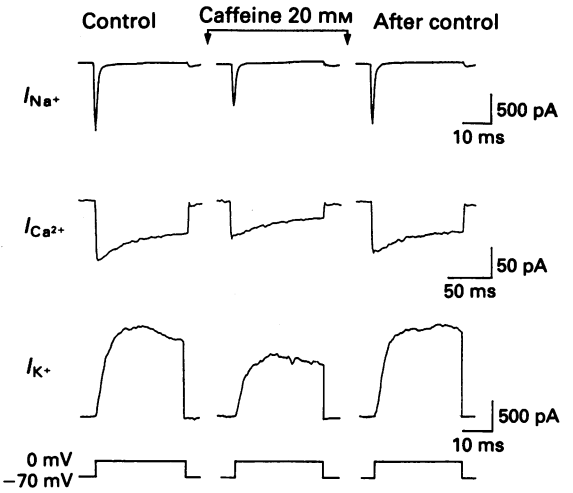


Figure 5 Inhibitory effect of caffeine on depolarization-induced membrane currents in single chromaffin cells. Traces from top to bottom: inward Na^+ (I_{Na^+}), Ca^{2+} ($I_{Ca^{2+}}$), outward K^+ currents (I_{K^+}) and depolarization pulse. Depolarizing pulses from holding potential, − 70 mV to 0 mV were applied using a patch pipette which contained CsCl (132 mM) instead of KCl for Na^+ and Ca^{2+} currents and KCl (132 mM) for K^+ current before (control), during and after (after control) the addition of caffeine (20 mM). The duration of the pulse was 30 ms for Na^+ and K^+ currents and 100 ms for Ca^{2+} current. When K^+ and Ca^{2+} currents were recorded, tetrodotoxin (0.5 μM) was added to the bathing solution to prevent the initiation of Na^+ current.

Like caffeine, theophylline (5–10 mM) also caused a dose-dependent inhibition of ACh-evoked catecholamine secretion (data not shown).

Effects of membrane-permeant analogues of cyclic AMP and forskolin

To determine whether caffeine or theophylline caused inhibition of secretagogue-induced catecholamine secretion by increasing the amount of cyclic AMP, chromaffin cells were stimulated with ACh (100 μM) and veratridine (100 μM) in the presence or absence of dibutyryl cyclic AMP (1 mM), 8-bromo cyclic AMP (1 mM) or forskolin (30 μM). The results are summarized in Table 1. Both membrane-permeant cyclic AMP analogues and forskolin caused a small increase in the resting catecholamine secretion, but no consistent effect on ACh- and veratridine-evoked catecholamine secretions. Forskolin (30 μM) also failed to inhibit sequentially evoked catecholamine secretion by ACh (100 μM) or high K^+ in perfused adrenal glands (data not shown).

Effects of caffeine on membrane currents

The effects of caffeine on membrane current were observed using single chromaffin cells under voltage clamp conditions. After achieving the whole-cell configuration by rupture of the membrane patch, ACh (100 μM) was added to the external solution for 10 s every 3 or 4 min. At a holding potential of − 60 mV, ACh repeatedly evoked a transient inward current together with an increase in the background noise. This transient current was abolished by hexamethonium, indicating that the current was mediated by the activation of nicotinic receptors. When caffeine was added to the external solution, ACh-evoked inward current was inhibited depending on the concentration of caffeine (1–20 mM). The inhibitory action of caffeine started to occur at 1 mM and progressively increased with the concentration of caffeine, attaining a maximum, a little less than 50% of the control, at 20 mM and recovered after its removal. A representative

Table 2 Effects of caffeine on Ca^{2+} transient and membrane current induced by acetylcholine (ACh) and on depolarization-evoked membrane currents

	n	*Control*	*Caffeine*	*After control*
ACh-induced				
Inward current	8	100	37.3 ± 2.3	87.9 ± 3.7
Ca^{2+} transient	9	100	44.8 ± 6.7	86.6 ± 2.7
Voltage-dependent				
Na^+ current	7	100	62.8 ± 4.2	101.7 ± 9.1
Ca^{2+} current	6	100	44.5 ± 6.3	77.4 ± 6.5
K^+ current	5	100	70.9 ± 2.6	100.6 ± 3.1

Numbers indicate the mean ± s.e.mean of peak amplitude of Ca^{2+} transient and current responses, as a percentage of each control, obtained before (Control), during (Caffeine) and after (After control), application of caffeine (20 mM). Numbers of experiments (*n*) are shown.

result and the summarized data from different experiments are shown in Figure 4a and b, respectively.

To study the effect of caffeine on voltage-dependent membrane currents, depolarization pulses of 30 ms duration to evoke inward Na^+ and outward K^+ currents, and of 100 ms duration to elicit inward Ca^{2+} current from a holding potential of − 70 mV to test potential of 0 mV were applied at 20 s intervals before, during and after addition of caffeine (20 mM). Figure 5 shows that all current responses were partially, but reversibly inhibited by caffeine. The effects of different preparations on the inhibitory action of caffeine are summarized as percentages of control values in Table 2. The data show that caffeine is more effective in decreasing Ca^{2+} current than Na^+ and K^+ currents.

Effects of caffeine on the intracellular concentration of Ca^{2+}

The effect of caffeine on ACh-induced changes in $[Ca^{2+}]_i$ was observed on single chromaffin cells loaded with fura-2. ACh (100 μM) added to the external solution for 10 s rapidly increased $[Ca^{2+}]_i$. In about half of the cells tested, the addition of caffeine (20 mM) to the external solution also caused an increase in $[Ca^{2+}]_i$ which progressively declined toward the resting level even if caffeine was still infused. When the caffeine-induced increase in $[Ca^{2+}]_i$ attained the resting level, ACh (100 μM) was applied. Regardless of whether or not caffeine increased $[Ca^{2+}]_i$, subsequent ACh-induced Ca^{2+} transient was reversibly inhibited by caffeine to about 45% of the control (Figure 6a, b and Table 2). In agreement with previous results (Teraoka *et al.*, 1991), caffeine-induced increase in $[Ca^{2+}]_i$ was blocked by pretreatment with caffeine plus ryanodine (data not shown).

Next, it was determined whether ACh was effective in increasing $[Ca^{2+}]_i$ in the absence of external Ca^{2+} and if so, whether it was affected by caffeine. ACh (100 μM) was applied for 10 s at 3 min intervals before and during exposure to Ca^{2+}-free solution containing EGTA (0.5 mM). As shown in Figure 6c and d, ACh still increased $[Ca^{2+}]_i$ in the absence of external Ca^{2+}, though the magnitude was decreased by about 50% of the control value. After readmission of Ca^{2+}, the ACh-induced Ca^{2+} transient recovered completely and then caffeine (20 mM) was added to the external medium. Two minutes after the start of exposure to caffeine, external Ca^{2+} was replaced by EGTA (0.5 mM) and ACh was applied.

Under these conditions, ACh completely failed to evoke Ca^{2+} transient regardless of whether or not caffeine itself caused increase in $[Ca^{2+}]_i$.

Effect of caffeine on Ca^{2+}-sensitivity of the secretory apparatus

In cultured bovine adrenal chromaffin cells permeabilized by treatment with digitonin, caffeine decreased catecholamine

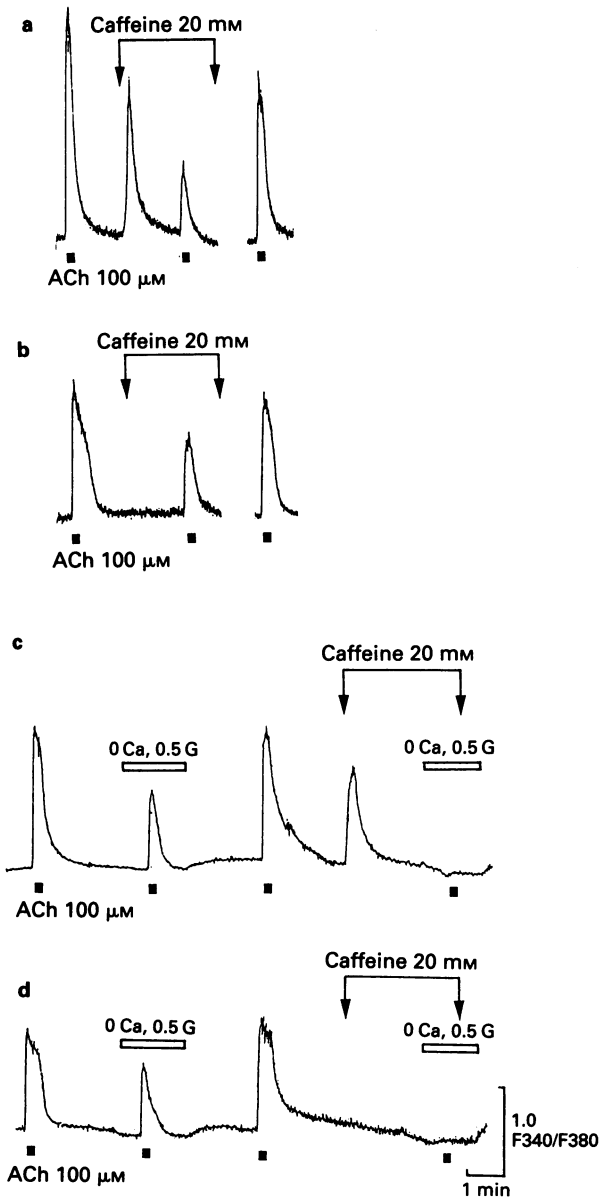


Figure 6 Inhibitory effect of caffeine on acetylcholine (ACh)-induced Ca^{2+} transients in a single chromaffin cell. Traces show intracellular Ca^{2+} concentration ($[Ca^{2+}]_i$). ACh (100 μM) was sequentially applied for 10 s (■) in the presence (a, b) and absence (c, d) of external Ca^{2+} through a pipette placed close to the cell before, during and after the addition of caffeine (20 mM) (↓——↓). Caffeine itself caused a Ca^{2+} transient in (a) and (c), but not in (b) and (d). In Ca^{2+}-free solution, Ca^{2+} was omitted and 0.5 mM EGTA was added (0Ca, 0.5G; □).

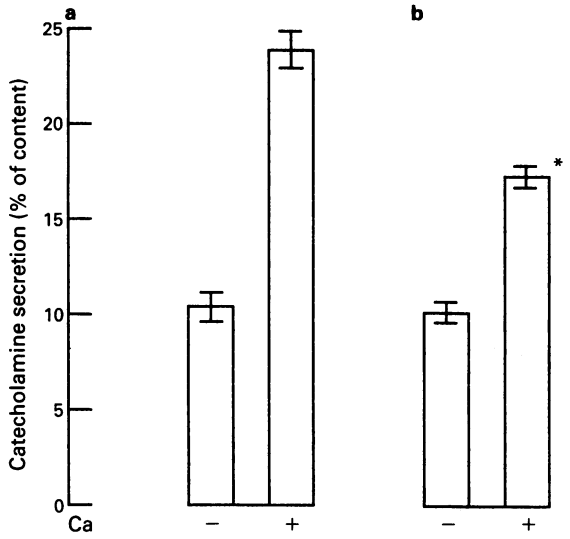


Figure 7 Inhibitory effect of caffeine on catcholamine secretion evoked by Ca^{2+} in permeabilized chromaffin cells. Dispersed chromaffin cells were incubated in K^+ glutamate solution containing β-escin (20 μM) with (+) or without (−) Ca^{2+} (10 μM) for 20 min at room temperature (approximately 25°C) in the absence (a) and presence (b) of caffeine (20 mM). Columns indicate the mean ± s.e.mean of adrenaline released as a percentage of total cell contents obtained from 19 experiments. $*P<0.01$, when compared with the response to Ca^{2+} in control (a).

secretion directly evoked by Ca^{2+}, suggesting a reduction of the Ca^{2+}-sensitivity of the secretory apparatus in the presence of caffeine (Teraoka *et al.*, 1991). We therefore examined whether the same was true in the case of the guinea-pig. Dispersed chromaffin cells were incubated with K^+ glutamate solution containing β-escin (20 μM) for 20 min with or without Ca^{2+} (10 μM) in the presence and absence of caffeine (20 mM). Figure 7 shows that Ca^{2+} caused an increase in catecholamine secretion, which was significantly inhibited by caffeine.

Discussion

The present study showed that caffeine causes a marked inhibition of catecholamine secretion evoked by ACh, veratridine and high K^+ in perfused adrenal glands and isolated chromaffin cells of the guinea-pig. The mechanism of action inducing catecholamine secretion is different among the secretagogues. ACh, veratridine and high K^+ have been considered to depolarize the chromaffin cell and to increase Ca^{2+} influx through voltage-dependent Ca^{2+} channels, resulting in an increase in catecholamine secretion (Douglas & Rubin, 1961; Ito *et al.*, 1978; 1979; Kilpatrick *et al.*, 1981; Knight & Baker, 1983; Knight & Kesteven, 1983; Wakade & Wakade, 1983). However, the mechanism underlying the depolarization is different between stimulants, ACh and veratridine cause depolarization resulting mainly from the activation of nicotinic receptor channels and voltage-dependent, tetrodotoxin-sensitive Na^+ channels, respectively. High K^+ depolarizes the membrane directly by changing the equilibrium potential for K^+. On the other hand, muscarinic receptor activation is assumed to mobilize intracellularly stored Ca^{2+} responsible for catecholamine secretion (Nakazato *et al.*, 1984; 1988; Yamada *et al.*, 1988; Teraoka *et al.*, 1990).

In the present experiments, caffeine was found to decrease Na^+, Ca^{2+} and K^+ currents evoked by depolarizing voltage steps. The inhibition of the Ca^{2+} current was much greater than that of Na^+ and K^+ currents. Caffeine is also reported to block voltage-operated Ca^{2+} channels in smooth muscle cells (Hughes *et al.*, 1990; Watanabe *et al.*, 1992). Therefore, the inhibitory effect of caffeine on the secretory responses to veratridine and high K^+ may be due partly to the action on voltage-dependent Na^+ and/or Ca^{2+} channels. Caffeine also inhibited both ACh-induced inward currents through nicotinic receptor channels and Ca^{2+} transients, indicating that the inhibitory action of caffeine on catecholamine secretion induced by ACh can be attributed mainly to the inhibition of increase in $[Ca^{2+}]_i$ through nicotinic receptor channels and voltage-dependent Ca^{2+} channels. However, it was noted that the rate of inhibition by caffeine was much larger in catecholamine secretion than in either inward currents or Ca^{2+} transients, suggesting the involvement of some additional mechanisms in the inhibition of the evoked catecholamine secretion.

Caffeine was found to block catecholamine secretion induced by muscarinic receptor activation in adrenal glands perfused with Ca^{2+}-free Locke solution in the present experiments. In addition, caffeine abolished the ACh-induced increase in $[Ca^{2+}]_i$ in the absence of external Ca^{2+} regardless of whether or not caffeine itself evoked Ca^{2+} transient. It therefore seems unlikely that caffeine inhibits ACh-induced Ca^{2+} transient by depleting intracellular Ca^{2+} stores. It has been reported that caffeine causes non-specific inhibition of inositol 1,4,5-trisphosphate ($InsP_3$)-induced Ca^{2+} release from rat cerebellar microsomes (Brown *et al.*, 1992) and mouse pancreatic acinar cells (Toescu *et al.*, 1992). One of the possible mechanisms involved in the inhibitory effect of caffeine on secretagogue-induced catecholamine secretions is the inhibition of Ca^{2+} release from intracellular Ca^{2+} stores. Another possibility is that caffeine may decrease the Ca^{2+}-sensitivity of the secretory apparatus, because caffeine reduced catecholamine secretion induced by Ca^{2+} in permeabilized chromaffin cells of the guinea-pig. Our results are in accord with reports that caffeine decreases the Ca^{2+}-sensitivity of secretory apparatus in bovine adrenal chromaffin cells (Teraoka *et al.*, 1991) and of contractile proteins in smooth muscle cells (Sato *et al.*, 1988; Ahn *et al.*, 1988; Savineau & Mironneau, 1990). The inhibitory effect of caffeine on the Ca^{2+}-sensitivity of the secretory apparatus may account for the failure of a continuous infusion of caffeine to increase catecholamine secretion, even if $[Ca^{2+}]_i$ rose in response to the caffeine infusion.

Xanthine derivatives are well known to increase the cyclic AMP concentration as a result of inhibition of cyclic AMP phosphodiesterase activity (Butcher & Sutherland, 1962). In the present experiments theophylline was also shown to cause inhibition of ACh-evoked catecholamine secretion. However, neither membrane-permeant analogues of cyclic AMP, such as dibutyryl cyclic AMP and 8-bromo cyclic AMP nor forskolin showed consistent effects on evoked catecholamine secretion from both perfused adrenal glands and isolated chromaffin cells, indicating that cyclic AMP does not play a role in the inhibitory action of caffeine.

Furthermore, the inhibitory effect of caffeine on various ionic channels should not be due to a secondary action of increased cytosolic free Ca^{2+} level, because the inhibitory effects still occurred long after the end of the Ca^{2+} transient evoked by caffeine. The inhibitory action of caffeine observed in this study was observed to recover quickly after washout of the drug. Such rapid recovery seems to provide an important clue for determining the mechanism of inhibitory action of xanthine derivatives on ionic channels. Further studies are certainly required to solve this problem.

In conclusion, caffeine causes inhibition of secretagogue-induced catecholamine secretion by inhibiting nicotinic receptor channel currents, voltage-dependent Ca^{2+} and Na^+ currents and by decreasing the mobilization of intracellularly stored Ca^{2+} and/or the sensitivity of the secretory apparatus to Ca^{2+}.

This work was supported by grants from the Japanese Ministry of Education, Science and Culture and the Japanese Society for the Promotion of Science for Japanese Junior Scientists.

References

AHN, H.Y., KARAKI, H. & URAKAWA, N. (1988). Inhibitory effects of caffeine on contractions and calcium movement in vascular and intestinal smooth muscle. *Br. J. Pharmacol.*, **93**, 267–274.

BROWN, G.R., SAYERS, L.G., KIRK, C.J., MICHELL, R.H. & MICHELANGELI, F. (1992). The opening of the inositol 1,4,5-trisphosphate-sensitive Ca^{2+} channel in rat cerebellum is inhibited by caffeine. *Biochem. J.*, **282**, 309–312.

BUTCHER, R.W. & SUTHERLAND, E.W. (1962). Adenosine 3′, 5′-phosphate in biological materials. I. Purification and properties of cyclic 3′, 5′-nucleotide phosphodiesterase and use of this enzyme to characterize adenosine 3′, 5′-phosphate in human urine. *J. Biol. Chem.*, **237**, 1244–1250.

DOUGLAS, W.W. & RUBIN, R.P. (1961). The role of calcium in the secretory response of the adrenal medulla to acetylcholine. *J. Physiol.*, **159**, 40–57.

DUNN, L.A. & HOLZ, R.W. (1983). Catecholamine secretion from digitonin-treated adrenal medullary chromaffin cells. *J. Biol. Chem.*, **258**, 4989–4993.

ENDO, M. (1977). Calcium release from the sarcoplasmic reticulum. *Physiol. Rev.*, **57**, 71–108.

GRYNKIEWICZ, G., POENIE, M. & TSIEN, R.Y. (1985). A new generation of Ca^{2+} indicators with greatly improved fluorescence properties. *J. Biol. Chem.*, **260**, 3440–3450.

HAMILL, O.P., MARTY, A., NEHER, E., SAKMANN, B. & SIGWORTH, F.J. (1981). Improved patch-clamp techniques for high-resolution current recording from cells and cell-free membrane patches. *Pflügers Arch.*, **391**, 85–100.

HOCHMAN, J. & PERLMAN, R.L. (1976). Catecholamine secretion by isolated adrenal cells. *Biochim. Biophys. Acta*, **421**, 168–175.

HUGHES, A.D., HERING, S. & BOLTON, T.B. (1990). The action of caffeine on inward barium current through voltage-dependent calcium channels in single rabbit ear artery cells. *Pflügers Arch.*, **416**, 462–466.

ITO, S., NAKAZATO, Y. & OHGA, A. (1978). Pharmacological evidence for the involvement of Na^{+} channels in the release of catecholamines from perfused adrenal glands. *Br. J. Pharmacol.*, **62**, 359–361.

ITO, S., NAKAZATO, Y. & OHGA, A. (1979). The effect of veratridine on the release of catecholamines from the perfused adrenal gland. *Br. J. Pharmacol.*, **65**, 319–330.

KILPATRICK, D.L., SLEPETIS, R. & KIRSHNER, N. (1981). Ion channels and membrane potential in stimulus-secretion coupling in adrenal medulla cells. *J. Neurochem.*, **36**, 1245–1255.

KNIGHT, D.E. & BAKER, P.F. (1983). Stimulus-secretion coupling in isolated bovine adrenal medullary cells. *Q.J. Exp. Physiol.*, **68**, 123–143.

KNIGHT, D.E. & KESTEVEN, N.T. (1983). Evoked transient intracellular free Ca^{2+} changes and secretion in isolated bovine adrenal medullary cells. *Proc. R. Soc. B.*, **218**, 177–199.

NAKAZATO, Y., HAYASHI, H. & TERAOKA, H. (1992). Comparisons of the effects of ryanodine on catecholamine secretion evoked by caffeine and acetylcholine in perfused adrenal glands of the guinea-pig. *Br. J. Pharmacol.*, **105**, 597–602.

NAKAZATO, Y., OHGA, A., OLESHANSKY, M., TOMITA, U. & YAMADA, Y. (1988). Voltage-independent catecholamine release mediated by the activation of muscarinic receptors in guinea-pig adrenal glands. *Br. J. Pharmacol.*, **93**, 101–109.

NAKAZATO, Y., YAMADA, Y., TOMITA, U. & OHGA, A. (1984). Muscarinic agonists release adrenal catecholamine by mobilizing intracellular Ca^{2+}. *Proc. Jpn. Acad.*, **60**, 314–317.

OHTA, T., ITO, S., NOTO, T., TACHIBANA, R., NAKAZATO, Y. & OHGA, A. (1992). The inhibitory action of cyclic AMP on responses to carbachol dependent on calcium stores in rat gastric smooth muscle. *J. Physiol.*, **453**, 367–384.

SALZMAN, S.K. & SELLERS, M.S. (1982). Determination of norepinephrine in brain perfusates using high performance liquid chromatography with electrochemical detection. *J. Chromatogr.*, **232**, 29–37.

SATO, K., OZAKI, H. & KARAKI, H. (1988). Multiple effects of caffeine on contraction and cytosolic free Ca^{2+} levels in vascular smooth muscle of rat aorta. *Naunyn-Schmied. Arch. Pharmacol.*, **338**, 443–448.

SAVINEAU, J.P. & MIRONNEAU, J. (1990). Caffeine acting on pregnant rat myometrium: analysis of its relaxant action and its failure to release Ca^{2+} from intracellular stores. *Br. J. Pharmacol.*, **99**, 261–266.

TERAOKA, H., NAKAZATO, Y. & OHGA, A. (1990). Sodium ions inhibit the stimulant action of caffeine on catecholamine secretion from adrenal chromaffin cells of the guinea pig. *Neurosci. Lett.*, **108**, 179–182.

TERAOKA, H., NAKAZATO, Y. & OHGA, A. (1991). Ryanodine inhibits caffeine-evoked Ca^{2+} mobilization and catecholamine secretion from cultured bovine adrenal chromaffin cells. *J. Neurochem.*, **57**, 1884–1890.

TOESCU, E.C., O'NEILL, S.C., PETERSEN, O.H. & EISNER, D.A. (1992). Caffeine inhibits the agonist-evoked cytosolic Ca^{2+} signal in mouse pancreatic acinar cells by blocking inositol trisphosphate production. *J. Biol. Chem.*, **267**, 23467–23470.

WAKADE, A.R. & WAKADE, T.D. (1983). Contribution of nicotinic and muscarinic receptors in the secretion of catecholamines evoked by endogenous and exogenous acetylcholine. *Neuroscience*, **10**, 973–978.

WATANABE, C., YAMAMOTO, H., HIRANO, K., KOBAYASHI, S. & KANAIDE, H. (1992). Mechanisms of caffeine-induced contraction and relaxation of rat aortic smooth muscle. *J. Physiol.*, **456**, 193–213.

YAMADA, Y., NAKAZATO, Y. & OHGA, A. (1989). The mode of action of caffeine on catecholamine release from perfused adrenal glands of cat. *Br. J. Pharmacol.*, **98**, 351–356.

YAMADA, Y., TERAOKA, H., NAKAZATO, Y. & OHGA, A. (1988). Intracellular Ca^{2+} antagonist TMB-8 blocks catecholamine secretin evoked by caffeine and acetylcholine from perfused cat adrenal glands in the absence of extracellular Ca^{2+}. *Neurosci. Lett.*, **90**, 338–342.

(Received July 26, 1993
Revised November 15, 1993
Accepted November 23, 1993)

Br. J. Pharmacol. (1994), **111**, 942–950

© Macmillan Press Ltd, 1994

Characterization and possible function of adenosine 5′-triphosphate receptors in activated rat microglia

[1]W. Nörenberg, J.M. Langosch, *P.J. Gebicke-Haerter & [1]P. Illes

Department of Pharmacology, University of Freiburg, Hermann-Herder-Strasse 5, and *Department of Psychiatry, University of Freiburg, Hauptstrasse 5, D-79104 Freiburg, Germany

1 Purinoceptor agonist-induced currents in untreated (proliferating) and lipopolysaccharide (LPS; 100 ng ml^{-1})-treated (non-proliferating) rat microglial cells in culture were recorded by the whole-cell patch-clamp technique. These cells have two preferred resting membrane potentials, one at − 35 mV and another one at − 70 mV.

2 Most experiments were carried out in non-proliferating cells. ATP, ATP-γ-S and α,β-MeATP (1–1000 μM in all cases) evoked an inward current at a holding potential of − 70 mV, followed, in some experiments, by an outward current. At − 70 mV 2-methylthio ATP (1–1000 μM) evoked an inward current, whereas at − 35 mV it produced an outward current only.

3 When K^+ was replaced in the pipette solution by an equimolar concentration of Cs^+ (150 mM), the main outward component of the ATP-γ-S (10 μM) induced response disappeared. Instead, an inward current was obtained. Replacement of K^+ by Cs^+ did not affect the inward current evoked by 2-methylthio ATP (300 μM). 4-Aminopyridine (1–10 mM), however, almost abolished this current and unmasked a smaller outward current.

4 The rank order of agonist potency was 2-methylthio ATP > ATP > α,β-MeATP. Adenosine and UTP were inactive. Suramin (300 μM) and reactive blue 2 (50 μM) antagonized the effect of 2-methylthio ATP (300 μM).

5 *I–V* relations were determined by delivering fast voltage ramps before and during the application of 2-methylthio ATP (300 μM). In the presence of extra- (1 mM) and intracellular (150 mM) Cs^+, the 2-methylthio ATP-evoked current crossed the zero current level near 0 mV. When both Cs^+ (1 mM) and 4-aminopyridine (1 mM) were present in the bath medium, the intersection of the 2-methylthio ATP current with the zero current level was near − 75 mV.

6 2-Methylthio ATP (1–1000 μM) induced the same inward current both in proliferating and non-proliferating microglia. However, the depolarizing response to 2-methylthio ATP (300 μM) was larger and longer-lasting in the proliferating cells. When the free Ca^{2+} concentration in the pipettes was increased from the standard 0.01 to 1 μM, the amplitude and duration of this depolarization was increased in non-proliferating cells. 4-Aminopyridine (1 mM) enhanced the duration, but not the amplitude of responses.

7 ATP and its structural analogues stimulate microglial purinoceptors of the P_{2Y}-type. This leads to the opening of non-selective cationic channels and potassium channels. Depending on the resting membrane potential, depolarization or hyperpolarization prevails. Although the inward current produced by 2-methylthio ATP is of similar amplitude in proliferating and non-proliferating microglia, the resulting depolarization is smaller in the latter cell type because of the presence of voltage-sensitive, outwardly rectifying potassium channels.

Keywords: Microglia; lipopolysaccharide; P_2-purinoceptor; ATP; suramin; non-selective cationic channel; potassium channel

Introduction

Microglia originate from monocytes/macrophages entering the brain during the early embryonic development (Jordan & Thomas, 1988; Theele & Streit, 1993). These resident immunocytes are capable of regressive metamorphosis in pathological processes and thereby represent a major source of endogenous brain macrophages (Rieske *et al.*, 1989; Thomas, 1992). Resting (ramified) microglia differentiate into fully activated macrophages through a number of transitional states. In tissue culture systems, cells become initially activated by the isolation procedure and are capable of both proliferation and phagocytosis (Rieske *et al.*, 1989; Gebicke-Haerter *et al.*, 1989). They can be driven further into macrophage-like (amoeboid) microglia by stimuli such as bacterial lipopolysaccharide (LPS) (Adams & Hamilton, 1987). These cells present major histocompatibility antigen (MHC) type I and II, secrete cytokines (e.g. interleukin-1 and 6) and produce superoxide anions (Bignami, 1991; Dickson *et al.*, 1991). They no longer proliferate but are still involved in phagocytosis.

The predominant voltage-dependent current in proliferating rat microglia is potassium-selective and inwardly rectifying (Kettenmann *et al.*, 1990; Banati *et al.*, 1991). LPS-treatment leads to the expression of previously lacking outwardly rectifying potassium channels (Nörenberg *et al.*, 1992; 1993a,b). In addition to voltage-dependent currents, proliferating microglia were shown to exhibit an ATP-induced non-selective cationic conductance (Kettenmann *et al.*, 1993).

Three major types of adenosine 5′-triphosphate- (ATP) sensitive P_2-purinoceptors have been described, principally based on the rank order of agonist potencies (Gordon, 1986). The P_{2X}-(α,β-methylene ATP [α,β-MeATP] > ATP = 2-methylthio ATP) and P_{2Y}-(2-methylthio ATP > ATP > α,β-MeATP) subtypes occur in muscle and exocrine glands (Burnstock & Kennedy, 1985; Kennedy, 1990). Peripheral and central neurones are endowed with P_{2Y}-purinoceptors only (Illes & Nörbenberg, 1993). Receptors of mast cells and possibly lymphocytes are termed P_{2z}; they recognize the tet-

[1] Authors for correspondence.

rabasic form of ATP^{4-} (Gordon, 1986). ATP itself may be degraded to adenosine, which stimulates adenosine receptors, also named P_1-purinoceptors (Burnstock & Kennedy, 1985). Finally, separate pyrimidinoceptors have been described at which UTP is the prototypic agonist (Kügelgen *et al.*, 1987; Seifert & Schulz, 1989).

The aim of the present study was to characterize P_2-purinoceptors of rat microglial cells by the use of pharmacological agents, to investigate the ionic mode of ATP action, and to compare ATP effects in proliferating and non-proliferating microglia.

Methods

Cell cultures

Mixed astroglial-microglial cell cultures were prepared from cerebral hemispheres of newborn Wistar rats as described previously (Keller *et al.*, 1985). In brief, animals were killed by decapitation, meninges were removed, and forebrains were minced and gently dissociated by trituration in Hank's balanced salt solution. Cells were collected by centrifugation at 200 *g* for 10 min, resuspended in Dulbecco's modified Eagle's medium (DMEM), supplemented with 10% foetal calf serum (FCS), plated onto 35 mm Falcon culture dishes (5×10^5 cells/dish), and incubated at 37°C in a humidified atmosphere of 95% air, 5% CO_2. Media were prepared taking extreme care to avoid all potential sources of LPS contaminations. After 14 days of culture under LPS-free conditions, floating microglial cells were harvested and reseeded into 35 mm Petri dishes to give pure microglial cultures (Gebicke-Haerter *et al.*, 1989). Small cells (diameter, 5–8 μm) with unipolar or bipolar processes were observed under phase contrast optics immediately after reseeding. When LPS (100 ng ml^{-1}) was added for 12–24 h, the microglial cells became circular in shape with ruffled edges (diameter, 15–23 μm).

Patch-clamp experiments

Membrane currents of microglial cells were measured with the patch-clamp method in the whole-cell configuration (Hamill *et al.*, 1981). The bath (extracellular) solution contained (mM): NaCl 160, KCl 4.5, $CaCl_2$ 2, $MgCl_2$ 1, HEPES (N-[2-hydroxyethyl]piperazine-N'-[2-ethanesulphonic acid]) 5, glucose 11, pH 7.4 adjusted with NaOH. A nominally Mg^{2+}-free medium was prepared by omitting MgCl. A Na^+-free, high Ca^{2+} (100 mM) medium was obtained by replacement of NaCl by 98 mM $CaCl_2$ plus 60 mM tris (2-amino-2-[hydroxymethyl]-1,3-propanediol), and by setting the pH to 7.4 with HCl. The pipette (internal) solution contained (mM): KCl 150, $MgCl_2$ 2, $CaCl_2$ 1 (free Ca^{2+}, 0.01 μM), EGTA 11, HEPES 10, pH 7.3 adjusted with KOH. The free Ca^{2+} concentration was increased to 1 μM by decreasing the concentration of EGTA to 1.1 mM and leaving the other components of the solution unchanged. In some experiments the intracellular KCl was replaced by CsCl and the pH was set to 7.3 by adding CsOH. Pipettes pulled from borosilicate capillaries (Vitrex BRI/E, Poly-Labo-Strasbourg, France) were coated with beeswax and dipped in Sigmacote (Sigma, Deisenhofen, Germany) to minimize associated capacitive currents. The resistance of the electrodes was 2–5 MΩ.

Compensation of capacitance and series resistance was achieved with the inbuilt circuitry of the patch amplifier (List EPC-7, Darmstadt, Germany). Voltage-clamp protocols were generated with a laboratory computer (ESCOM/486, Heppenheim, Germany). Data were digitized at 1–7 kHz (Cambridge Electronic Devices 1401, Cambridge, UK) and then stored on and analyzed with the computer. Experiments were carried out at room temperature (20–24°C). Data illustrated are non-leak subtracted.

After whole-cell configuration was achieved, the membrane potential was determined in the current-clamp mode. Then the system was left for 5–10 min to allow stabilization of the voltage-dependency of various parameters. During this time the membrane potential of single cells alternated between two preferred values of approximately − 70 and − 35 mV. When currents induced by ATP and its structural analogues (I_{ATP}) were measured, the cells were held at − 70 mV. Purinoceptor agonists and uridine 5'-triphosphate (UTP) were locally microperfused for 10 s by means of separate, wide-bore, pressurized (10 kPa) puffer pipettes, placed about 50 μm away from the cell under examination.

Each agonist concentration was applied only once (T_1) to a cell, except in some cases when two subsequent applications (T_1,T_2) separated by 3 or 10 min intervals were made. During these intervals, the 3 ml bath was superfused with drug-free medium, or with medium containing purinoceptor antagonists. Puffer application of drug-free extracellular solution had no effect. All other compounds were superfused at a flow rate of 2 ml min^{-1}. Suramin and reactive blue 2 were present in the bath for 8 min before, and during T_2. When the effects of two consecutive administrations of purinoceptor agonists were compared, the current induced by T_2 was normalized with respect to the current induced by T_1. In some experiments, Cs^+ and/or 4-aminopyridine were added for 10 min before the pressure application of 2-methylthio ATP.

Voltage-dependent currents were evoked by voltage pulses of 300 ms duration delivered every 8 s from a holding potential of − 70 mV in 20 mV increments. Step range was from − 150 to + 50 mV. I–V relations were determined by using fast voltage ramps (− 70 mV holding potential, 1 s duration, from − 140 to + 40 mV). Ramps were generated both before the application of 2-methylthio ATP (300 μM) and during the peak response to the agonist. The 2-methylthio ATP current was obtained by digital subtraction.

Materials

The following materials and drugs were used: suramin hexasodium salt (Bayer, Leverkusen, Germany); reactive blue 2 trisodium salt (EGA-Chemie, Steinheim, Germany); Dulbecco's modified Eagle's medium, Hank's balanced salt solution, foetal calf serum (Gibco, Eggenstein, Germany); 2-methylthioadenosine 5'-triphosphate tetrasodium salt (RBI, Natick, MA, U.S.A.); lipopolysaccharide from *Salmonella typhimurium* (Sebak, Aidenbach, Germany); adenosine, adenosine 5'-triphosphate disodium salt (ATP), adenosine 5'-O-(3-thio)-triphosphate tetralithium salt (ATP-γ-S), 4-aminopyridine, α,β-methyleneadenosine 5'-triphosphate lithium salt (α,β-Me-ATP), uridine 5'-triphosphate sodium salt (UTP) (Sigma, Deisenhofen, Germany).

LPS, dissolved in distilled water (1 mg ml^{-1}), was further diluted into DMEM. 4-Aminopyridine was dissolved in the bath medium. Stock solutions (10–100 mM) of purinoceptor agonists and antagonists were prepared with distilled water and further diluted with medium.

Statistics

Means ± s.e.mean of *n* trials are shown. The Student's paired or unpaired *t* test was used to compare means as appropriate. Multiple comparisons were carried out by one way analysis of variance followed by the Student-Newman-Keuls test. A probability level of 0.05 or less was considered to be statistically significant.

Results

The present data were obtained from 41 proliferating and 247 non-proliferating microglial cells kept in primary culture.

Measurements of ionic currents

Effects of P_2-purinoceptor agonists Most of the experiments were carried out on proliferating microglia treated with LPS

(100 ng ml^{-1}) for 12–24 h. This treatment had driven the cells into a more activated, non-proliferating state. ATP (100 μM) was pressure-applied for 10 s every 3 min at a holding potential of − 70 mV (T_1–T_4: Figure 1a). In five out of seven cells, T_1 evoked an inward current only. The size of this response markedly decreased within the 10 s ejection period. In the residual two cells, the initial response rapidly disappeared and gave rise to a slowly developing and non-desensitizing outward current. Since the outward component was not present in all cells, only the inward component was statistically evaluated (Figure 5a).

The ATP-(100 μM) induced inward current appeared to decrease from T_1 to T_4 (Figure 1a), with a major and statistically significant decline from T_1 to T_2 only (see legend to Figure 1). When the interval between T_1 (− 46.2 ± 8.6 pA) and T_2 (− 33.0 ± 6.1 pA; $n = 8$; $P > 0.05$) was increased from 3 to 10 min, the responses became rather stable.

Puffer application of ATP-γ-S (100 μM) for 10 s every 3 min also resulted in a decrease of the inward current from T_1 to T_2 (Figure 1b). At the same time the outward current increased (Figure 1b). ATP-γ-S at 10 μM caused a transient inward current (which was sometimes missing; Figure 2a, left panel), followed by a more marked and slowly declining outward current (Figure 2a, right panel). The outward component tended to decrease when the concentration of ATP-γ-S was increased from 10 μM (10.6 ± 3.0 pA; $n = 8$) to 100 μM (3.9 ± 1.8 pA; $n = 7$; $P > 0.05$); at 1 mM ATP-γ-S only the inward component was present (Figure 5a). 2-Methylthio ATP (10–100 μM; $n = 5$–7) and α,β-MeATP (10–100 μM; $n = 6$) caused less outward current than ATP-γ-S (10–100 μM).

Ionic nature of P_2-purinoceptor agonist-induced currents When K^+ was replaced in the pipette solution by an equimolar concentration of Cs^+ (150 mM), the main outward component of the ATP-γ-S (10 μM)-induced response disappeared (Figure 2a). Instead, an inward current was obtained. By contrast, replacement of K^+ by Cs^+ did not affect the current evoked by 2-methylthio ATP (300 μM; $n = 6$). Apparently, intracellular Cs^+ selectively interfered with the outward component and, thereby, increased or even unmasked the inward component. 4-Aminopyridine (10 mM), however, almost abolished the inward current evoked by 2-methylthio ATP (300 μM) and unmasked a smaller outward current response (Figure 2b). A lower concentration of 4-aminopyridine (1 mM) also inhibited the 2-methylthio ATP (300 μM)-induced inward current (control, − 67.4 ± 12.8 pA; $n = 6$; 4-aminopyridine, − 9.7 ± 3.7 pA, $n = 5$; $P < 0.01$), but revealed only in some cells an outward current (17.9 ± 13.0 pA; $n = 5$).

At a holding potential of − 70 mV (the higher preferred membrane potential of microglia), 2-methylthio ATP (100 μM) caused an inward current (− 33.1 ± 6.5 pA; $n = 7$), whereas at a holding potential of − 35 mV (the lower preferred membrane potential of microglia) it caused an outward current (54.8 ± 8.9 pA; $n = 5$). This suggests that the inward and outward currents may be differentiated by their respective reversal potentials.

Therefore, I–V relations of non-proliferating microglial cells were determined by applying fast voltage ramps (− 70 mV holding potential, 1 s duration, from − 140 to + 40 mV) before and during the administration of 2-methylthio ATP (300 μM). The 2-methylthio ATP-evoked current was obtained by subtraction. The control I–V relation determined in a normal bath-medium with K^+-containing pipettes, exhibits both inward and outward rectification (Figure 3a, inset). This rectification is characteristic for non-proliferating microglia and can be elicited also by applying a series of hyperpolarizing and depolarizing voltage steps from a holding potential of − 70 mV (Figure 6a). The 2-methylthio ATP current crossed the zero current value at three points (− 76.4 ± 5.2 mV, − 28.8 ± 2.0 mV and − 18.6 ± 2.9 mV; $n = 8$ each), the two last points being rather similar (Figure 3a). Hence, the I–V curves of non-proliferating microglial cells appear to represent the sum of two ionic currents with two distinct

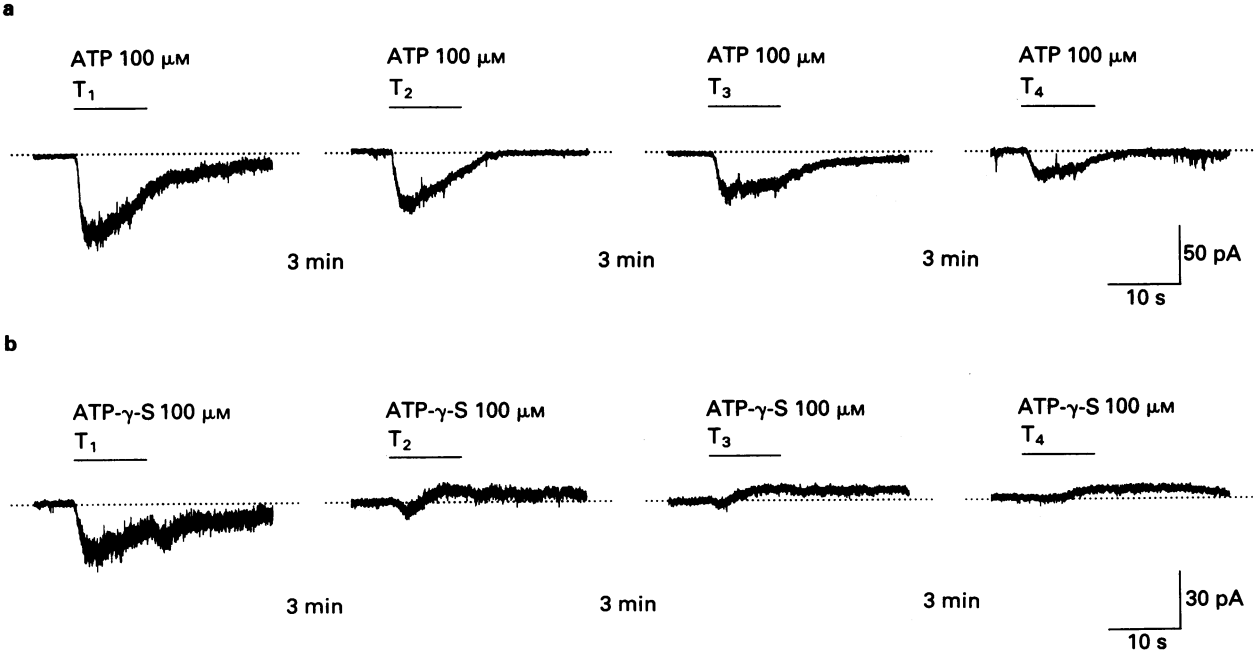


Figure 1 Inward currents activated by consecutive applications of ATP or ATP-γ-S in non-proliferating rat microglia. The holding potential was − 70 mV. Both ATP and ATP-γ-S were pressure-applied onto the same cell for 10 s and at 3 min intervals. (a) Currents evoked by 4 consecutive applications (T_1–T_4) of ATP (100 μM). The inward current appeared to decrease from T_1 to T_4, with a major and statistically significant decline from T_1 (− 26.7 ± 8.5 pA) to T_2 (− 11.9 ± 4.9 pA; $n = 7$; $P < 0.05$) only. (b) Currents evoked by 4 consecutive applications (T_1–T_4) of ATP-γ-S (100 μM). The inward current decreased from T_1 (− 16.8 ± 5.0 pA) to T_2 (− 6.9 ± 2.2 pA; $n = 7$; $P < 0.05$). At the same time the outward current increased (T_1, 3.9 ± 1.8 pA; T_2, 6.9 ± 1.7 pA; $n = 7$; $P < 0.05$). Representative tracings from 7 similar experiments in both (a) and (b). The dotted lines indicate the zero current levels.

reversal potentials. The slope conductance of the curve was determined, as in all similar experiments, between − 130 and − 110 mV and amounted to 1.7 ± 0.4 nS ($n = 8$).

The application of Cs^+ (1 mM) to the bath-medium abolished the inward rectification of voltage-dependent control currents (Figure 3b, inset). When 4-aminopyridine (1 mM) was also applied to block outward rectification, the 2-methylthio ATP current crossed the zero current level at a single point only, in the range of the calculated K^+ equilibrium potential (− 89 mV) at − 75.0 ± 5.3 mV ($n = 6$) (Figure 3b). This may be due to the fact that 4-aminopyridine blocks in addition to the voltage-dependent outward rectification (Figure 3b, inset) also the 2-methylthio ATP-induced inward, cationic component (Figure 2b). The slope conductance of the curve was 3.6 ± 1.3 nS ($n = 6$).

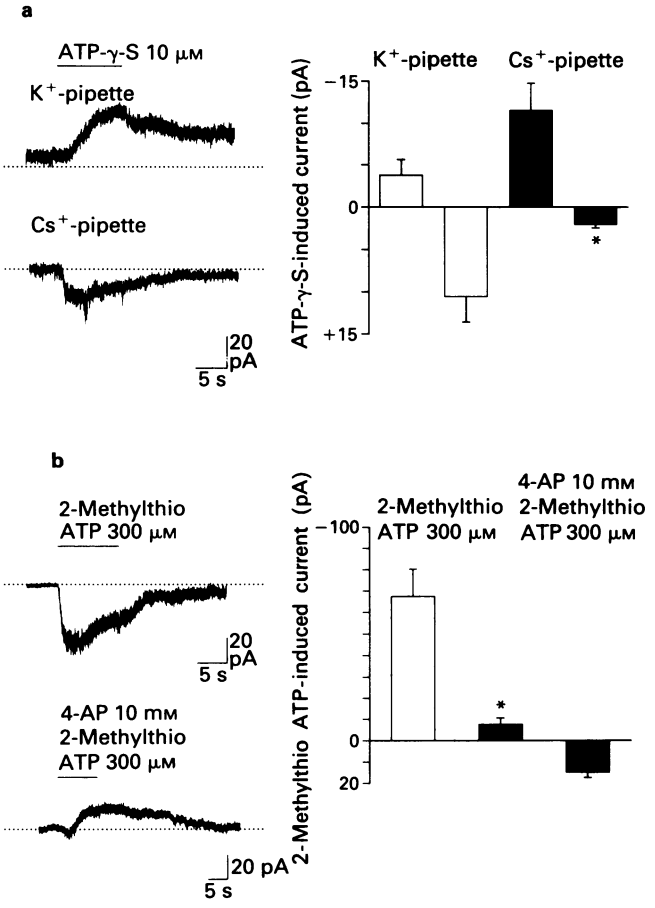


Figure 2 Selective blockade of the outward or inward components of the ATP-γ-S- and 2-methylthio ATP-evoked currents in non-proliferating rat microglia. Both purinoceptor agonists were pressure applied for 10 s at a holding potential of − 70 mV. Each agonist concentration was applied only once and to different cells. (a) Currents induced by ATP-γ-S (10 μM) were recorded with pipette solutions in which K^+ (150 mM; open columns) or Cs^+ (150 mM; solid columns) were the main intracellular cation, respectively. Representative tracings (left panel). Means ± s.e.mean from 7 experiments are shown in the right panel similar to those shown in the left panel. $*P < 0.05$; significant difference between the outward currents in the 1st and 2nd sets of columns. (b) Currents induced by 2-methylthio ATP (300 μM) were recorded either in the absence ($n = 6$; open columns) or presence ($n = 8$; solid columns) of 4-aminopyridine (4-AP; 10 mM). Representative tracings are shown in the left panel. Means ± s.e.mean from n experiments similar to those in the left panel are shown in the right panel. $*P < 0.05$; significant difference between the inward currents in the absence and presence of 4-aminopyridine. The dotted lines indicate the zero current levels both in (a) and (b). Note that inward currents are indicated by upward columns, while outward currents are indicated by downward columns.

Replacement of K^+ in the pipettes by Cs^+ (150 mM) and the simultaneous presence of Cs^+ (1 mM) in the bath medium were another means of blocking all voltage-dependent conductances (Figure 4a, inset). However, the 2-methylthio ATP current crossed now the zero current level near 0 mV (7.3 ± 1.8 mV; $n = 6$) and showed inward rectification (Figure 4a). Apparently extracellular Cs^+ abolished the outward, K^+-component of this current (Figure 2a). The slope conductance of the curve (2.2 ± 0.8 nS; $n = 6$; $P > 0.05$) did not differ from that measured in the combined presence of extracellular 4-aminopyridine (1 mM) and Cs^+ (1 mM).

Finally, the experimental conditions in Figure 4b are similar to those in Figure 4a in that Cs^+ is present both intra- and extracellularly. In a Na^+-free, high Ca^{2+} (100 mM) bath medium, the 2-methylthio ATP current crossed the zero current level at − 4.2 ± 2.6 mV ($n = 5$) and differed from I_{ATP} determined in a normal Na^+ (160 mM), normal Ca^{2+} (2 mM) bath medium by its failure to exhibit inward rectification (Figure 4b). Thus, Ca^{2+} was able to substitute for Na^+ as a charge carrier of the 2-methylthio ATP-induced inward, cationic component. The slope conductance (4.2 ± 2.1 nS; $n = 5$; $P > 0.05$) was similar to that of the reference curve in Figure 4a.

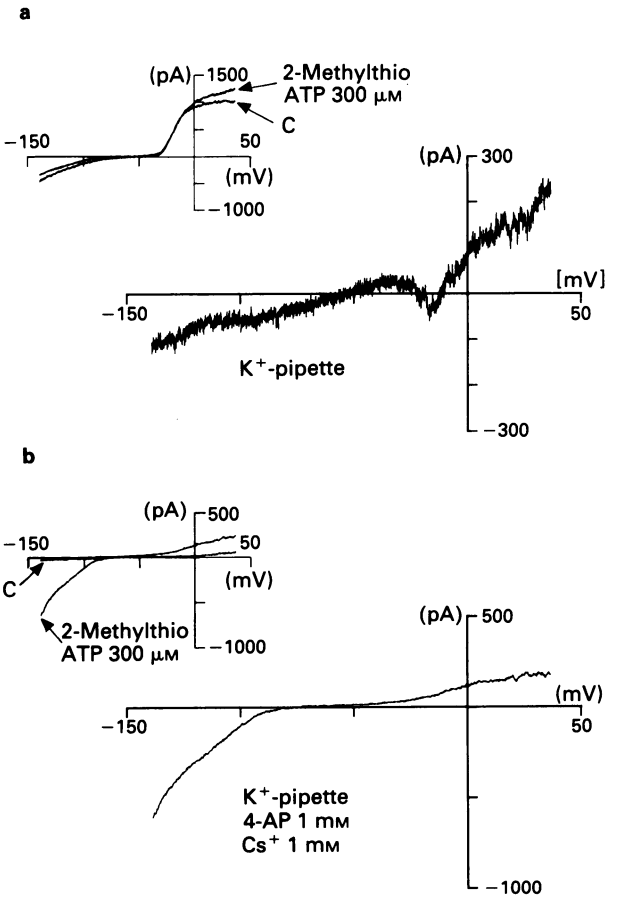


Figure 3 Current-voltage ($I-V$) relations of the 2-methylthio ATP-induced dual conductance (a) or potassium conductance (b) in non-proliferating microglia. $I-V$ relations of microglial cells were determined by applying depolarizing voltage ramps (− 70 mV holding potential, 1 s duration, from − 140 to + 40 mV) before a 10 s pressure application of 2-methylthio ATP (300 μM) and during the peak response to the agonist (indicated in the insets of a and b). The 2-methylthio ATP current was obtained by subtraction. (a) 2-Methylthio ATP current recorded with a K^+-pipette in a normal bath medium; (b) 2-methylthio ATP current recorded with a K^+-pipette in the presence of extracellular 4-aminopyridine (4-AP; 1 mM) and Cs^+ (1 mM). Representative tracings from 8 (a) and 6 (b) similar experiments.

Rank order of P_2-purinoceptor agonist potencies and blockade of agonist effects by P_2-purinoceptor antagonists Figure 5a shows concentration-response curves of various purinoceptor agonists and UTP in non-proliferating microglia. Of the compounds investigated, adenosine and UTP were inactive. At a concentration of 1 mM, 2-methylthio ATP induced the largest inward current (-100.5 ± 14.6 pA; $n = 8$), followed by ATP-γ-S (-30.7 ± 8.9 pA; $n = 7$) and ATP (-30.1 ± 6.5 pA; $n = 5$); α,β-MeATP had the lowest activity (-6.7 ± 3.1 pA; $n = 7$). Only the concentration-response curves of ATP and α,β-MeATP exhibited a clear maximum. The concentration causing a half maximal effect (EC_{50} value) was 25.1 μM for ATP. In the case of 2-methylthio ATP and ATP-γ-S there were no maximal effects and, therefore, EC_{50} values could not be determined. Finally, 2-methylthio ATP (300 μM) produced the same inward current both in the presence and absence of Mg^{2+} (1 mM) in the bath-medium (Figure 5a, inset).

When 2-methylthio ATP (300 μM) was applied twice, spaced 10 min apart, constant responses were obtained (Figure 5b). Incubation with suramin (300 μM) or reactive blue 2 (50 μM) for 8 min markedly reduced the effect of 2 methylthio ATP. Higher concentrations of the purinoceptor antagonists were not investigated.

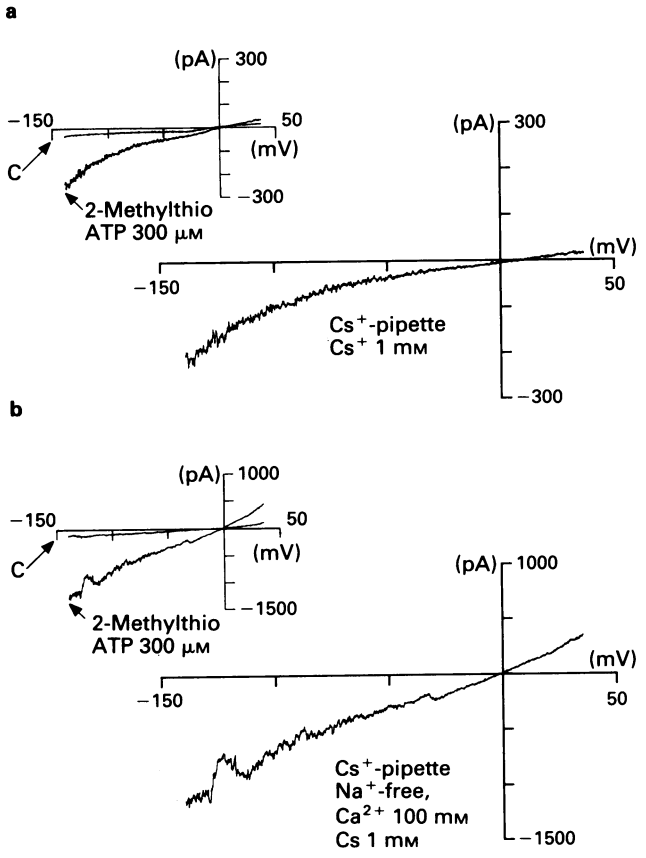


Figure 4 Current-voltage ($I-V$) relations of the 2-methylthio ATP-induced cationic conductance (a,b) in non-proliferating microglia. $I-V$ relations of microglial cells were determined by applying depolarizing voltage ramps (− 70 mV holding potential, 1 s duration, from − 140 to + 40 mV) before a 10 s pressure application of 2-methylthio ATP (300 μM) and during the peak response to the agonist (indicated in the insets of a and b). The 2-methylthio ATP current was obtained by subtraction. (a) 2-Methylthio ATP current recorded with a Cs^+ (150 mM) pipette and in the additional presence of extracellular Cs^+ (1 mM); (b) 2-methylthio ATP current recorded with a Cs^+-pipette and in the additional presence of extracellular Cs^+ (1 mM). A Na^+-free medium also containing Ca^{2+} (100 mM) was used. Representative tracings out of 6 (a) and 5 (b) similar experiments.

Comparison of ATP-induced inward currents in proliferating and non-proliferating microglia In a subsequent series of experiments currents were elicited by both negative and positive voltage pulses given in steps of 20 mV from a holding potential of − 70 mV (Figure 6a). Proliferating microglial cells exhibited only a hyperpolarization-evoked inward current; depolarizing steps were without effect ($n = 3$; Figure 6a, left panel). In contrast, non-proliferating cells responded to depolarizing pulses with an outward current, although the inwardly rectifying channels were also present ($n = 3$; Figure 6a, right panel). In spite of the different pattern of voltage-dependent current responses, 2-methylthio ATP (1–1000 μM) induced the same inward current in the two types of microglial cells (Figure 6b).

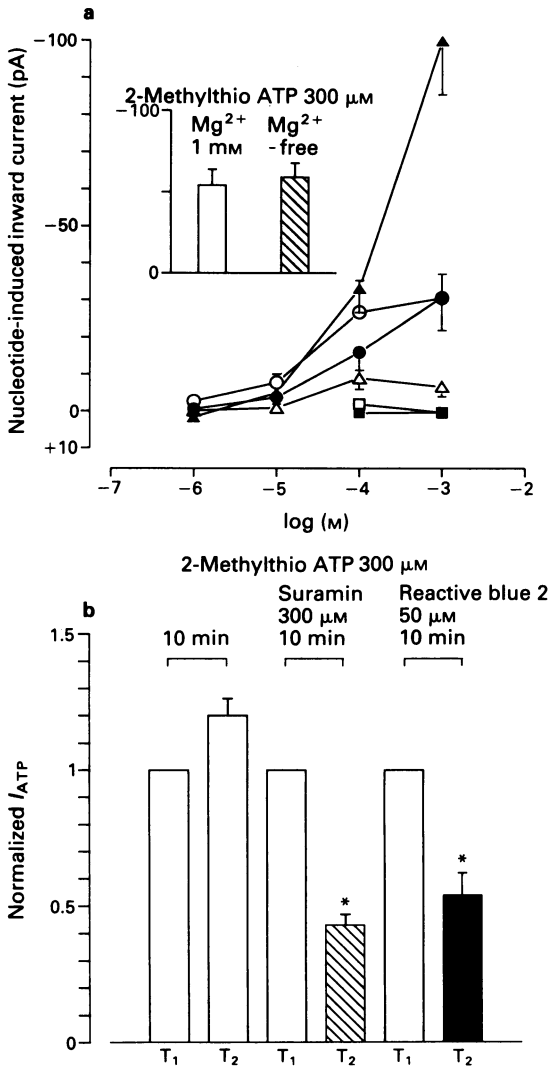


Figure 5 Pharmacological characterization of ATP-sensitive receptors in non-proliferating rat microglia. Inward currents obtained at a holding potential of − 70 mV were evaluated only. (a) Concentration-response curves to ATP (○), ATP-γ-S (●), α,β-methylene ATP (α,β-MeATP; △), 2-methylthio ATP (▲), adenosine (□) and UTP (■). The current induced by 2-methylthio ATP (300 μM) was the same both in the presence ($n = 6$) and absence of Mg^{2+} (2 mM; $n = 7$) (inset). Each concentration was pressure applied for 10 s, only once and to different cells. (b) Antagonism of the 2-methylthio ATP-(300 μM) induced current by suramin (300 μM; hatched column) or reactive blue 2 (50 μM; solid column). 2-Methylthio ATP (300 μM) was pressure applied twice for 10 s with 10 min interval (T_1-T_2), either in the absence (open columns) or presence of the antagonists. The effects of T_2 were normalized with respect to the effects of T_1. $^*P < 0.01$: significant difference between T_1 and T_2 in the 2nd and 3rd sets of columns.

Measurements of membrane potential changes

Comparison of ATP-induced depolarizing effects in proliferating and non-proliferating microglia The membrane potential of microglial cells, 5–10 min after gaining access to the cell interior was continuously recorded in the current-clamp mode of the patch-clamp amplifier. Random alterations of the membrane potential between two preferred values near − 35 and − 70 mV were observed. In most experiments, 2-methylthio ATP was pressure applied when the membrane potential was in the range of − 70 mV (see legend to Figure 7). 2-Methylthio ATP (300 μM) caused a large and long-lasting depolarization in proliferating microglia (Figures 6c, left panel and 7b). In contrast, the majority of non-proliferating cells responded to 2-methylthio ATP (300 μM) with a rapidly declining small depolarization (Figures 6c, right panel, 7a, upper panel and 7b). A few non-proliferating cells with a low membrane potential (− 39.4 ± 1.6 mV), were hyperpolarized by 2-methylthio ATP (300 μM) (− 10.1 ± 1.4 mV; $n = 5$).

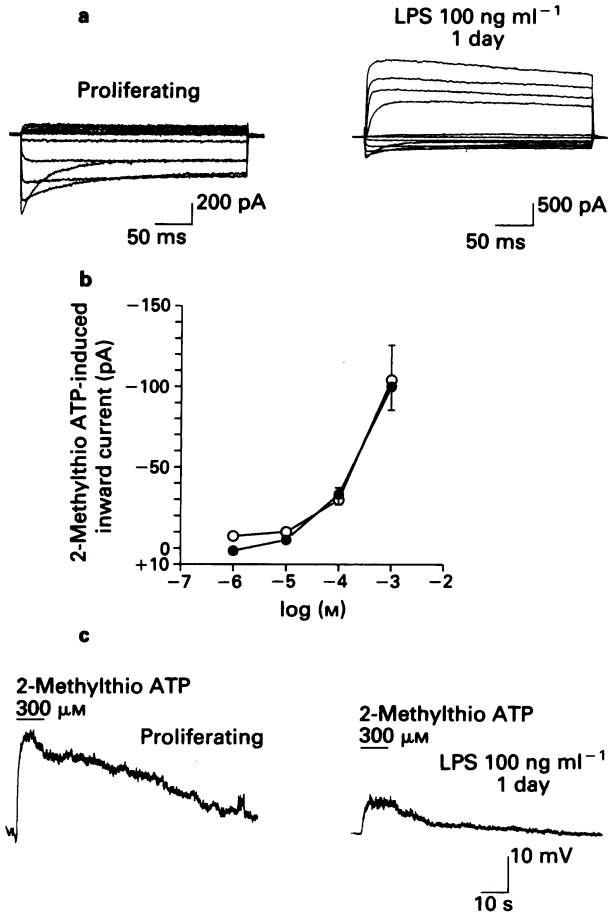


Figure 6 Voltage-sensitive and 2-methylthio ATP-evoked currents in proliferating and non-proliferating rat microglia. (a) Voltage pulses were applied every 8 s from a holding potential of − 70 mV in 20 mV increments. Step range was from − 170 to + 50 mV. Proliferating ($n = 3$; left panel) and lipopolysaccharide (LPS)- (100 ng ml^{-1} for 12–24 h) treated (non-proliferating; $n = 3$; right panel) cells were used. (b) Concentration-response curves to 2-methylthio ATP in proliferating (○) and non-proliferating (●) microglia. Inward currents obtained by 10 s pressure applications at a holding potential of − 70 mV were evaluated. Each concentration was applied only once and to different cells. Means ± s.e.mean from 5–8 (proliferating) and 5–7 (non-proliferating) cells. (c) Depolarization induced by a 10 s pressure application of 2-methylthio ATP (300 μM) to proliferating ($n = 8$) and non-proliferating ($n = 14$) rat microglial cells.

Role of voltage-sensitive potassium channels in ATP-induced depolarizations The normal pipette solution contained 0.01 μM free Ca^{2+}. Elevation of the internal free Ca^{2+} concentration to 1 μM, increased the amplitude and duration of 2-methylthio ATP- (300 μM) induced depolarizations (Figures 7a, lower panel and 7b). Recordings with 0.01 and 1 μM internal Ca^{2+} were carried out alternately on cells from the same culture dishes. The application of 4-aminopyridine (1 mM) increased the duration, but not the amplitude of the depolarizing response to 2-methylthio ATP (300 μM) (Figure 7b).

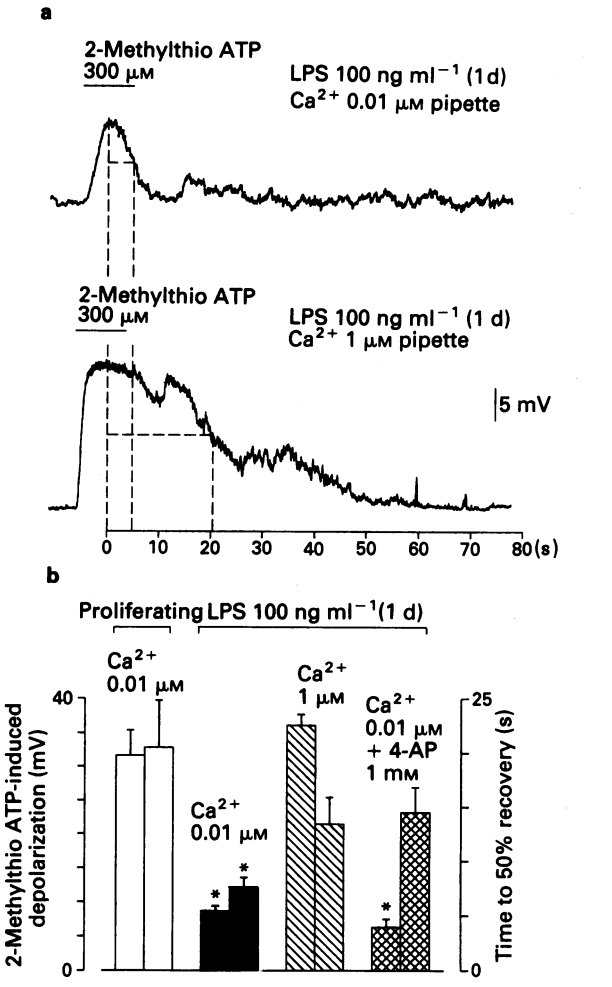


Figure 7 Role of voltage-sensitive potassium channels in the 2-methylthio ATP-induced depolarization. 2-Methylthio ATP (300 μM) was pressure applied for 10 s to proliferating and lipopolysaccharide (LPS)- (100 ng ml^{-1} for 12–24 h) treated (non-proliferating) rat microglial cells. (a) Representative depolarizations recorded with pipettes containing 0.01 μM (upper panel) or 1 μM (lower panel) Ca^{2+} in non-proliferating cells. The time to 50% recovery of depolarization was calculated as indicated. (b) Amplitude (left column of each pair) and time to 50% recovery (right column of each pair) of the 2-methylthio ATP-(300 μM) induced depolarization. Recordings were with 0.01 μM free Ca^{2+}-containing pipettes in proliferating (open column; membrane potential, − 61.0 ± 5.4 mV; $n = 8$) or non-proliferating microglia (solid column; membrane potential, − 61.7 ± 4.6 mV; $n = 14$). Other recordings were with 0.01 μM free Ca^{2+}-containing pipettes in the presence of 4-aminopyridine (4-AP; hatched columns; membrane potential, − 79.3 ± 1.2 mV; $n = 8$) or with 1 μM free Ca^{2+}-containing pipettes (cross-hatched columns: membrane potential, − 69.5 ± 4.9 mV; $n = 8$) in non-proliferating microglia. $^*P < 0.05$; significant difference from the amplitude and time to 50% recovery of 2-methylthio ATP-induced depolarization in proliferating microglia, respectively.

Discussion

The membrane potential of proliferating and non-proliferating rat microglial cells exhibits two stable values resulting in random switching between approximately − 35 mV and − 70 mV (Nörenberg *et al.*, 1993b). The reason for this behaviour is a negative slope region of the *I–V* curves reported also for mouse macrophages (Gallin, 1981) and human T-lymphocytes (Maltsev, 1993). In most experiments of this study, microglial cells were held at the preferred membrane potential of − 70 mV.

The predominant membrane current induced by ATP and its structural analogues was inward at − 70 mV. However, intermediate concentrations of ATP-γ-S and, to a minor extent, of 2-methylthio ATP and ATP, evoked an additional outward current, which followed the rapidly desensitizing inward current. Moreover, the repetitive application of ATP-γ-S, which appears to cause a stronger desensitization of P_2-purinoceptors than 2-methylthio ATP, led to the disappearance of the inward component and, thereby, to the enhancement or even unmasking of a non-desensitizing outward component. This outward component was inhibited when Cs^+ instead of K^+ was the main intracellular cation. Furthermore, with Cs^+-containing pipettes, the inward component became larger or, in some cases, a previously absent inward component emerged. The likely explanation for these changes is the blockade of K^+ outward currents by occlusion of the inner channel mouth by Cs^+ (Bezanilla & Armstrong, 1972).

In contrast, Cs^+ was unable to alter 2-methylthio ATP-elicited inward currents. However, in the presence of 4-aminopyridine, the inward current was nearly abolished and an outward component became unmasked. Apparently, in addition to the well-known ability of 4-aminopyridine to block both delayed rectifier and transient potassium channels (Adams & Nonner, 1990), this compound may inhibit ATP-activated cation channels as well. This novel effect of 4-aminopyridine was unexpected, but firmly established in two independent series of experiments. Hence, P_2-agonists may initiate a conductance increase both towards cations and potassium ions, which predominate at − 70 mV and − 35 mV, respectively. The present findings agree with the reported occurrence of an ATP-induced non-selective cationic conductance in proliferating microglia (Kettenmann *et al.*, 1993). A recent study of the same group, published during the preparation of this manuscript, demonstrated an additional increase of K^+ conductance by ATP in proliferating microglia (Walz *et al.*, 1993). We observed both types of conductances also in non-proliferating cells.

The *I–V* relation of non-proliferating microglial cells exhibited strong inward and outward rectification (Nörenberg *et al.*, 1992; 1993b). The ATP-evoked current obtained by subtraction crossed the zero current level in the range of the potassium equilibrium potential (− 89 mV) and additionally near the equilibrium potential for non-selective cationic conductances (0 mV). A combination of intra- and extracellular Cs^+ appears to inhibit voltage-sensitive, inwardly and outwardly rectifying K^+ channels of microglia (Nörenberg *et al.*, 1993b). Furthermore, intracellular Cs^+ has been shown to block 2-methylthio ATP-induced outward K^+ currents (see above). In fact, only when Cs^+ was present both intra- and extracellularly did the ATP current cross the zero current level near 0 mV and exhibited inward rectification similar to that described for I_{ATP} in neurones and smooth muscle cells (Bean & Friel, 1990).

It is interesting to note that when K^+ channels were blocked by Cs^+, and a Na^+-free, high Ca^{2+} bath medium was used, the ATP current persisted, but its inward rectification disappeared. Hence, the channels were permeable not only to Na^+, but also to Ca^{2+}, as reported previously for various cell types (Bean & Friel, 1990; Bean, 1992). The permeability of Ca^{2+} relative to that of Na^+ varies widely from 3:1 in ear artery smooth muscle (Benham & Tsien, 1987) to 0.3:1 in sensory neurones (Bean *et al.*, 1990). No attempt was undertaken in the present study to determine the permeability ratio of these two cations. In contrast to conditions which block the potassium component of the ATP current, extracellular application of 4-aminopyridine abolished the cationic component. In the additional presence of extracellular Cs^+, an increased K^+ conductance was left behind with the expected intersection of the zero current level in the range of the K^+ equilibrium potential.

In view of the monocytic origin of microglia it is interesting to note that ATP is able to permeabilize to cations the plasma membranes of rat (Naumov *et al.*, 1992) and mouse peritoneal macrophages (Steinberg *et al.*, 1987), and of the murine macrophage-like cell-line J774 (Sung *et al.*, 1985; Steinberg *et al.*, 1987). This effect is associated with depolarization (Sung *et al.*, 1985; Buisman *et al.*, 1988) and an increase in membrane conductance (Buisman *et al.*, 1988). Membrane permeabilization also leads to an enhanced entry of Ca^{2+} into macrophages (Sung *et al.*, 1985), although an additional release of Ca^{2+} from intracellular stores may be also involved (Greenberg *et al.*, 1988). ATP has been shown to increase the intracellular Ca^{2+} concentration of mouse peritoneal macrophages and, in consequence, may activate Ca^{2+}-dependent K^+ channels (Hara *et al.*, 1990). All these effects are due to the stimulation of P_{2z}-purinoceptors by ATP^{4-} (Steinberg *et al.*, 1987; Greenberg *et al.*, 1988).

The present experiments were principally aimed at elucidating the receptors involved in the microglial I_{ATP}. The lack of effect of adenosine and UTP excluded the presence of P_1-purinoceptors and pyrimidinoceptors. In contrast, ATP and its analogues were effective and appeared to increase the permeability of the membrane by receptor-stimulation, rather than by phosphorylation of extracellular proteins. ATP-induced phosphorylation is Mg^{2+}-dependent (see e.g. Christie *et al.*, 1992) and, therefore, the similar amplitudes of inward currents induced by 2-methylthio ATP both in the presence and absence of extracellular Mg^{2+} (1 mM) favour a receptor-mediated effect. Additional arguments also support this conclusion: (1) The ATP-induced inward current strongly desensitized both during contact with the agonists and on repetitive agonist applications; this phenomenon was observed previously in muscle preparations and neurones (Bean & Friel, 1990; Illes & Nörenberg, 1993). (2) Suramin and reactive blue 2 antagonized the effect of 2-methylthio ATP. Suramin is an antagonist at both P_{2X}- and P_{2Y}-purinoceptors, while reactive blue 2 appears to display some preference for the latter receptor-type (Kennedy, 1990). (3) The rank order of agonist potency (2-methylthio ATP > ATP > α,β-MeATP) was also compatible with the presence of P_{2Y}-purinoceptors (Burnstock & Kennedy, 1985; Kennedy, 1990). This strongly suggests that peripheral macrophages (P_{2Z}) and resident brain macrophages (microglia; P_{2Y}) are endowed with a distinct population of purinoceptors.

ATP has been reported to cause a long-lasting depolarization in proliferating rat microglia, because voltage-dependent, outwardly rectifying K^+ channels are absent and there are no efficient means of repolarizing the membrane (Kettenmann *et al.*, 1993). Cellular damage may both activate microglia (Dickson *et al.*, 1991), and allow leakage of ATP from neurones and glial cells into the extracellular space (White & Hoehn, 1991). In the present study, proliferating microglia were incubated with LPS in order to drive them into a more activated state (Adams & Hamilton, 1987). It was confirmed that non-proliferating microglial cells express previously missing, outwardly rectifying K^+ channels (Nörenberg *et al.*, 1992; 1993b) which are able to restore efficiently the resting membrane potential after depolarization. Thus, although in proliferating and non-proliferating cells 2-methylthio ATP produced identical inward current amplitudes, the depolarizing response to 2-methylthio ATP was much larger in proliferating than in non-proliferating cells. Moreover, manipulations known to block this type of K^+ channel, such as an enhanced intracellular Ca^{2+} concentration and extracellular

4-aminopyridine (Nörenberg *et al.*, 1993b), increased the extent and/or duration of the ATP-induced depolarization. The amplitude of the depolarization did not increase after the application of 4-aminopyridine, because this compound has a dual effect. It blocks voltage-dependent potassium conductances but seems to inhibit the cationic current initiated by P_2-purinoceptors as well.

In conclusion, ATP and its structural analogues stimulate P_{2Y}-purinoceptors in rat microglia. The mode of action of these receptors is the opening of cationic channels, which causes depolarization at the preferred membrane potential of − 70 mV. The concomitant opening of potassium channels causes hyperpolarization at the other preferred membrane potential of − 35 mV. The expression of outwardly rectifying K^+ channels in activated microglia decreases the sensitivity of these cells towards the depolarizing, excitatory effect of ATP.

The authors are grateful to Dr I. von Kügelgen for helpful discussions. This work was supported by grants of the Deutsche Forschungsgemeinschaft to P.I. (SFB 325; A2) and P.J.G.-H. (Ge 486/6-1).

References

ADAMS, D.O. & HAMILTON, T.A. (1987). Molecular transductional mechanisms by which IFNγ and other signals regulate macrophage development. *Immunol. Rev.*, **97**, 5–27.

ADAMS, D.O. & NONNER, W. (1990). Voltage dependent potassium channels: gating, ion permeation and block. In *Potassium Channels: Structure, Classification, Function and Therapeutic Potential.* ed. Cook, N.S. pp. 40–69. Chichester: Ellis Horwood.

BANATI, R.B., HOPPE, D., GOTTMANN, K., KREUTZBERG, G.W. & KETTENMANN, H. (1991). A subpopulation of bone marrow-derived macrophage-like cells shares a unique ion channel pattern with microglia. *J. Neurosci. Res.*, **30**, 593–600.

BEAN, B.P. (1992). Pharmacology and electrophysiology of ATP-activated ion channels. *Trends Pharmacol. Sci.*, **13**, 87–90.

BEAN, B.P. & FRIEL, D.D. (1990). ATP-activated channels in excitable cells. In *Ion Channels*, vol. II. ed. Narahashi, T. pp. 169–203. New York: Plenum Press.

BEAN, B.P., WILLIAMS, C.A. & CEELEN, P.W. (1990). ATP-activated channels in rat and bullfrog sensory neurons: current-voltage relation and single-channel behavior. *J. Neurosci.*, **10**, 11–19.

BENHAM, C.D. & TSIEN, R.W. (1987). A novel receptor-operated Ca^{2+}-permeable channel activated by ATP in smooth muscle. *Nature*, **328**, 275–278.

BEZANILLA, F. & ARMSTRONG, C.M. (1972). Negative conductance caused by entry of sodium and cesium ions into the potassium channels of squid axons. *J. Gen. Physiol.*, **60**, 588–608.

BIGNAMI, A. (1991). Glial cells in the central nervous system. *Disc. Neurosci.*, **8**, 11–45.

BUISMAN, H.P., STEINBERG, T.H., FISCHBARG, J., SILVERSTEIN, S.C., VOGELZANG, S.A., INCE, C., YPEY, D.L. & LEIJH, P.C.J. (1988). Extracellular ATP induces a large nonselective conductance in macrophage plasma membranes. *Proc. Natl. Acad. Sci. U.S.A.*, **85**, 7988–7992.

BURNSTOCK, G. & KENNEDY, C. (1985). Is there a basis for distinguishing two types of P_2-purinoceptor? *Gen. Pharmacol.*, **5**, 433–440.

CHRISTIE, A., SHARMA, V.K. & SHEU, S.-S. (1992). Mechanism of extracellular ATP-induced increase of cytosolic Ca^{2+} concentration in isolated rat ventricular myocytes. *J. Physiol.*, **445**, 369–388.

DICKSON, D.W., MATTIACE, L.A., KURE, K., HUTCHINS, K., LYMAN, W.D. & BROSNAN, C.F. (1991). Biology of disease. Microglia in human disease, with an emphasis on acquired immune deficiency syndrome. *Lab. Invest.*, **64**, 135–156.

GALLIN, E.K. (1981). Voltage clamp studies in macrophages from mouse spleen cultures. *Science*, **214**, 458–460.

GEBICKE-HAERTER, P.J., BAUER, J., SCHOBERT, A. & NORTHOFF, H. (1989). Lipopolysaccharide-free conditions in primary astrocyte cultures allow growth and isolation of microglial cells. *J. Neurosci.*, **9**, 183–194.

GORDON, J.L. (1986). Extracellular ATP: effects, sources and fate. *Biochem. J.*, **233**, 309–319.

GREENBERG, S., DI VIRGILIO, F., STEINBERG, T.H. & SILVERSTEIN, S.C. (1988). Extracellular nucleotides mediate Ca^{2+} fluxes in J774 macrophages by two distinct mechanisms. *J. Biol. Chem.*, **263**, 10337–10343.

HAMILL, O.P., MARTY, E., NEHER, E., SAKMANN, B. & SIGWORTH, F.J. (1981). Improved patch-clamp techniques for high-resolution current recording from cells and cell-free membrane patches. *Pflügers Arch.*, **391**, 85–100.

HARA, N., ICHINOSE, M., SAWADA, M., IMAI, K. & MAENO, T. (1990). Activation of single Ca^{2+}-dependent K^+ channels by external ATP in mouse macrophages. *FEBS Lett.*, **267**, 281–284.

ILLES, P. & NÖRENBERG, W. (1993). Neuronal ATP receptors and their mechanism of action. *Trends Pharmacol. Sci.*, **14**, 50–54.

JORDAN, F.L. & THOMAS, W.E. (1988). Brain macrophages: questions of origin and interrelationship. *Brain Res. Rev.*, **13**, 165–178.

KELLER, M., JACKISCH, R., SEREGI, A. & HERTTING, G. (1985). Comparison of prostanoid forming capacity of neuronal and astroglial cells in primary culture. *Neurochem. Int.*, **7**, 655–665.

KENNEDY, C. (1990). P_1- and P_2-purinoceptor subtypes – an update. *Arch. Int. Pharmacodyn. Ther.*, **303**, 30–50.

KETTENMANN, H., BANATI, R. & WALZ, W. (1993). Electrophysiological behaviour of microglia. *Glia*, **7**, 93–101.

KETTENMANN, H., HOPPE, D., GOTTMANN, K., BANATI, R. & KREUTZBERG, G. (1990). Cultured microglial cells have a distinct pattern of membrane channels different from peritoneal macrophages. *J. Neurosci. Res.*, **26**, 278–287.

KÜGELGEN, I.v., HÄUSSINGER, D. & STARKE, K. (1987). Evidence for a vasoconstriction-mediating receptor for UTP, distinct from the P_2 purinoceptor, in rabbit ear artery. *Naunyn-Schmied. Arch. Pharmacol.*, **336**, 556–560.

MALTSEV, V.A. (1993). A negative resistance region underlies the triggering property of membrane potential of human T-lymphocytes. *Cell. Sign.*, **4**, 697–707.

NAUMOV, A.P., KRUYSHEV, Y.A., KAZNACHEYEVA, E.V. & MOZHAYEVA, G.N. (1992). ATP-activated Ca^{2+}-permeable channels in rat peritoneal macrophages. *FEBS Lett.*, **313**, 285–287.

NÖRENBERG, W., APPEL, K., BAUER, J., GEBICKE-HAERTER, P.J. & ILLES, P. (1993a). Expression of an outwardly rectifying K^+ channel in rat microglia cultivated on teflon. *Neurosci. Lett.*, **160**, 69–72.

NÖRENBERG, W., GEBICKE-HAERTER, P.J. & ILLES, P. (1992). Inflammatory stimuli induce a new K^+ outward current in cultured rat microglia. *Neurosci. Lett.*, **147**, 171–174.

NÖRENBERG, W., GEBICKE-HAERTER, P.J. & ILLES, P. (1993b). Voltage-dependent potassium channels in activated rat microglia. *J. Physiol.* (in press).

RIESKE, E., GRAEBER, M.B., TETZLAFF, W., CZLONKOWSKA, A., STREIT, W.J. & KREUTZBERG, G.W. (1989). Microglia and microglia-derived brain macrophages in culture: generation from axotomized rat facial nuclei, identification and characterization in vitro. *Brain Res.*, **492**, 1–14.

SEIFERT, R. & SCHULZ, G. (1989). Involvement of pyrimidinoreceptors in the regulation of cell function by uridine and by uracil nucleotides. *Trends Pharmacol. Sci.*, **10**, 365–369.

STEINBERG, T.H., NEWMAN, A.S., SWANSON, J.A. & SILVERSTEIN, S.C. (1987). ATP^{4-} permeabilizes the plasma membrane of mouse macrophages to fluorescent dyes. *J. Biol. Chem.*, **262**, 8884–8888.

SUNG, S.-S.J., YOUNG, J.D.-E., ORIGLIO, A.M., HEIPLE, J.M., KABACK, H.R. & SILVERSTEIN, S.C. (1985). Extracellular ATP perturbs transmembrane ion fluxes, elevates cytosolic $[Ca^{2+}]$, and inhibits phagocytosis in mouse macrophages. *J. Biol. Chem.*, **260**, 13442–13449.

THEELE, D.P. & STREIT, W. (1993). A chronicle of microglial ontogeny. *Glia*, **7**, 5–8.

THOMAS, W.E. (1992). Brain macrophages: evaluation of microglia and their functions. *Brain Res. Rev.*, **17**, 61–74.

WALZ, W., ILSCHNER, S., OHLEMEYER, C., BANATI, R. & KETTENMANN, H. (1993). Extracellular ATP activates a cation conductance and a K^+ conductance in cultured microglial cells from mouse brain. *J. Neurosci.*, **13**, 4403–4411.

WHITE, T.D. & HOEHN, K. (1991). Release of adenosine and ATP from nervous tissue. In *Adenosine in the Nervous System.* ed. Stone, T.W. pp. 173–195. London: Academic Press.

(Received August 23, 1993
Revised November 15, 1993
Accepted November 23, 1993)

Br. J. Pharmacol. (1994), **111**, 951–955

© Macmillan Press Ltd, 1994

Possible NMDA antagonist properties of drugs that affect high pressure neurological syndrome

M. Anthony Shuker, Frank Bowser-Riley & [1]Stephen N. Davies

Department of Biomedical Sciences, Marischal College, University of Aberdeen, Aberdeen AB9 1AS

1 Previous studies have suggested that a series of drugs modelled on part of the strychnine molecule interfere with the development of high pressure neurological syndrome (HPNS) and it was presumed that this effect was via an action on inhibitory glycinergic transmission. We have now used the rat hippocampal slice preparation to examine the possibility that some of these drugs might instead have an action at the strychnine-insensitive (SI) glycine binding site associated with the NMDA receptor.

2 D-2-Amino-5-phosphonovalerate (AP5) and 7-chlorokynurenate (7CK) had no significant effect on the height of the population spike recorded from the CA1 region in 1 mM Mg^{2+} medium, but both blocked the multiple population spikes recorded in Mg^{2+}-free medium. The effect of 7CK, but not AP5, was reversed by 200 μM D-serine which is consistent with the known antagonist action of 7CK at the SI-glycine site.

3 A derivative of benzimidazole, which shows the clearest structural similarities to known SI-glycine site antagonists and ameliorates HPNS, mirrored the effects of 7CK although it was considerably less potent.

4 Gramine, which exacerbates HPNS, significantly increased the number of population spikes evoked in Mg^{2+}-free medium.

5 Mephenesin, which is the most potent known drug in ameliorating HPNS, had no significant effect on the response recorded in 1 mM Mg^{2+} and significantly reduced the number of population spikes recorded in Mg^{2+}-free medium, but this effect was only partially reversed by the addition of D-serine.

6 The results are consistent with the benzimidazole derivative, but not gramine, being an antagonist at the SI-glycine receptor. The results with mephenesin are equivocal but leave open the possibility that some of the drugs which are effective against HPNS act via an effect on excitatory NMDA receptor-mediated transmission, rather than on inhibitory glycine-mediated transmission.

Keywords: High pressure neurological syndrome; N-methyl-D-aspartate; glycine; strychnine-insensitive glycine site; mephenesin; gramine

Introduction

High pressure neurological syndrome (HPNS) describes the collection of symptoms including tremor and convulsions that are observed when animals or man are exposed to high barometric pressures (Halsey, 1982). Previous studies have shown that strychnine acts strictly additively with pressure in producing convulsions in mice (Bowser-Riley *et al.*, 1988) and that a series of drugs with molecular structures related to strychnine affect the threshold pressure for producing convulsions (Bowser-Riley *et al.*, 1989b). These observations led to the theory that increased hydrostatic pressure depresses inhibitory glycinergic synaptic transmission and that the drugs tested exert their effects via an action at the strychnine-sensitive glycine receptor.

More recently we observed that several of these drugs also show structural similarities with drugs known to be active at the strychnine-insensitive (SI) glycine binding site which is associated with the NMDA receptor (Thomson, 1990; Kemp & Leeson, 1993). This presents the possibility that the drugs which affect HPNS do so not by an action on inhibitory glycinergic transmission but by modulating excitatory NMDA receptor-mediated transmission.

As a preliminary way of testing this hypothesis we have examined the effects of a number of drugs on extracellular population spikes recorded in rat hippocampal slices. Under normal experimental conditions stimulation of the Schaffer collateral-commissural fibres at a low frequency evokes a single population spike recorded in the cell body region of the CA1 neurones. NMDA antagonists do not reduce the amplitude of the population spike and therefore the underlying excitatory postsynaptic potential (e.p.s.p.) under these conditions is thought to be mediated almost entirely by non-NMDA receptors (Collingridge *et al.*, 1983). However, perfusion with Mg^{2+}-free medium unblocks the NMDA gated channels so that stimulation evokes multiple population spikes that are blocked by NMDA antagonists (Coan & Collingridge, 1985). If the antagonist acts competitively at the glycine site then its efficacy is reduced by adding increased concentrations of glycine or the more selective agonist, D-serine (Bashir *et al.*, 1990). A profile showing (a) no effect on the single population spike evoked in normal medium, (b) blockade of the multiple population spikes evoked in Mg^{2+}-free medium and (c) a reduced effect in the presence of added D-serine, would therefore be consistent with that of an NMDA antagonist acting at the SI-glycine site.

In the present study we have chosen to investigate three test drugs; (i) a benzimidazole derivative which shows the clearest structural similarities to known SI-glycine site antagonists and is also effective against HPNS (Helliwell, 1990); (ii) gramine which has the opposite effect and facilitates HPNS (Bowser-Riley *et al.*, 1989b) and (iii) mephenesin which is the most effective drug against HPNS (Bowser-Riley *et al.*, 1989b). We have also compared the effects of these drugs with those of the competitive NMDA antagonist D-2-amino-5-phosphonovalerate (AP5), and a known antagonist at the SI-glycine site, 7-chlorokynurenic acid (7CK). Some of these results have previously been published in abstract form (Shuker *et al.*, 1992).

[1] Author for correspondence.

Methods

Transverse rat hippocampal slices (400 μm thick) were cut and maintained in a recording chamber at the interface between a humidified oxygen enriched atmosphere and a modified Krebs solution. The CA3 region of the slice was routinely removed to prevent the propagation of spreading depression which often originates in this area. The composition of the Krebs was (mM): NaCl 124, KCl 3, $NaHCO_3$ 26, NaH_2PO_4 1.25, $CaCl_2$ 2, $MgSO_2$ 1, D-glucose 10, which was continuously bubbled with 95% O_2/5% CO_2, maintained at 30°C, and perfused through the chamber at approximately 2 ml min^{-1}. Mg^{2+}-free Krebs solution consisted of the same solution with no added $MgSO_4$. The Schaffer collateral-commissural pathway was stimulated with bipolar silver electrodes and extracellular population spikes were recorded from the cell bodies of the CA1 region by use of 3 M NaCl filled glass electrodes (resistance approx. 5 MΩ). AP5, D-serine and 7CK (all from Tocris Neuramin, U.K.) were made up as 1000 × concentrated stock solutions and diluted into the perfusing medium, whereas gramine (Sigma), mephenesin (Sigma) and the benzimidazole derivative (HCl salt from Dr J. Lewis, University of Aberdeen Chemistry Department) were all dissolved directly in the Krebs solution. The structures of these three compounds are shown in Figure 1. Slices were always left for at least 60 min after changing to Mg^{2+}-free solution, or to D-serine containing solution, to allow full equilibration. Where possible, to exclude the effects of inter slice variation, the effects of the test drug were examined under the three conditions (i.e. in 1 mM Mg^{2+} medium, in Mg^{2+}-free medium, and in Mg^{2+}-free medium in the presence of added D-serine) on the same slice. In the case of mephenesin, where two doses of the test drug were used, this usually made the experiments impractically long. Therefore, in most instances, on any one slice the effect of mephenesin in 1 mM Mg^{2+} ws compared with that in Mg^{2+}-free medium, *or* the effect in Mg^{2+}-free medium was compared with that in Mg^{2+}-free medium with added D-serine. Data in the text are expressed as mean ± s.e.mean and tests of statistical significance were made by a paired Wilcoxon matched pairs test on the original data.

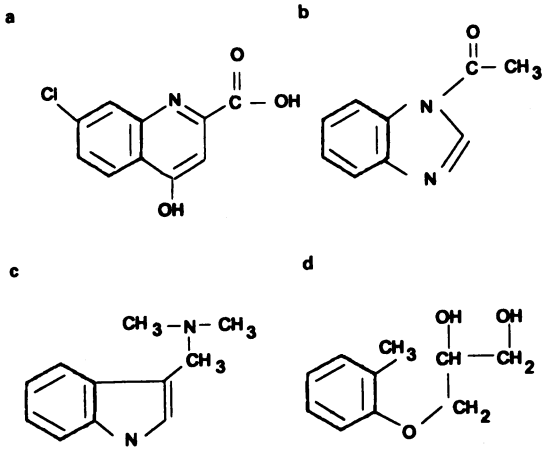


Figure 1 Structures of the compounds used in the present study: (a) 7-chlorokynurenic acid (7CK); (b) benzimidazole derivative; (c) gramine; (d) mephenesin.

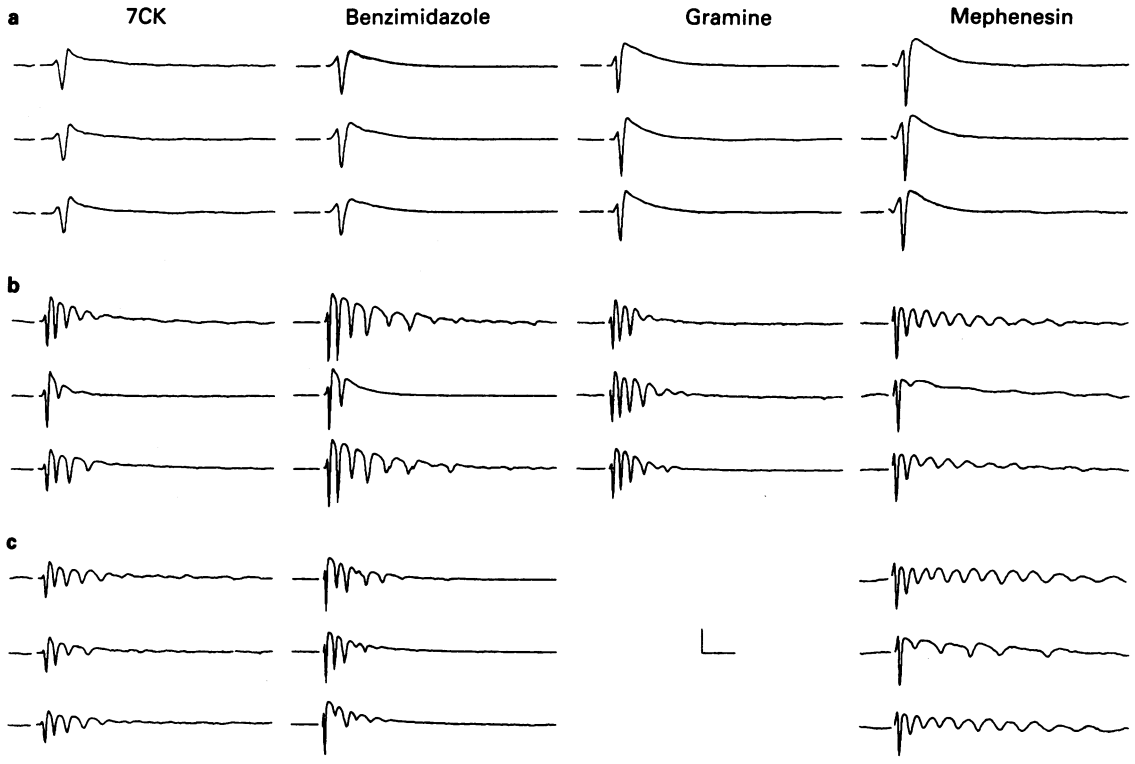


Figure 2 Representative traces showing the effects of a single dose of, 7-chlorokynurenic acid (7CK) (40 μM), the benzimidazole derivative (2 mM), gramine (500 μM), and mephenesin (1 mM) on synaptic responses recorded in 1 mM Mg^{2+} (a); Mg^{2+}-free medium (b); and in Mg^{2+}-free medium containing 200 μM D-serine (c). Each set of 3 traces shows control, drug and wash responses. Each drug was tested on 1 slice under all three perfusing conditions, except for mephenesin where the responses in 1 mM Mg^{2+} medium come from a separate slice. Each trace is the average of 3–5 consecutive recordings and stimulation artifacts have been blanked for clarity. Scale bar represents: (a) 10 ms; (b) and (c) 20 ms; 7CK, 2 mV; benzimidazole derivative, 10 mV; gramine, 5 mV; mephenesin, 2 mV.

Results

Effects of AP5 and 7CK

Stimulation in 1 mM Mg^{2+} medium evoked a single population spike 4–13 mV in amplitude and this was not significantly affected by perfusion of 20 μM AP5 (control: 8.4 ± 1.5, AP5: 7.8 ± 1.5 mV, $n = 5$) or by 20 or 40 μM 7CK (7.1 ± 0.4 to 6.2 ± 0.2 mV, $n = 4$ (2 each at 20 μM and 40 μM) Figures 2 and 3). Stimulation in Mg^{2+}-free medium evoked between 2 and 16 population spikes and these were significantly blocked by both 20 μM AP5 (5.1 ± 1.1 and 1.4 ± 0.3 spikes, $n = 7$) and by 20 or 40 μM 7CK (6.0 ± 0.6 to 2.2 ± 0.6 spikes, $n = 4$, Figures 2 and 3) with good recovery after washout. Over the course of the experiments we noticed that D-serine tended to increase the number of population spikes recorded in Mg^{2+}-free medium, but with a dose of 200 μM D-serine this was not statistically significant in any of the groups tested. The multiple population spikes evoked in Mg^{2+}-free medium and 200 μM D-serine were still effectively blocked by 20 μM AP5 (10.0 ± 2.0 to 2.5 ± 1.5 spikes, $n = 2$), but not by 20 or 40 μM 7CK (7.0 ± 0.6 to 5.7 ± 1.1 spikes, $n = 4$, Figures 2 and 3).

Effects of the benzimidazole derivative

Perfusion of the benzimidazole derivative (2 mM) had no significant effect on the height of the single population spike recorded in 1 mM Mg^{2+}-medium (11.9 ± 1.6 to 11.5 ± 1.5 mV, $n = 6$). In the same group of slices the derivative significantly reduced the number of population spikes evoked in Mg^{2+}-free medium (9.3 ± 1.2 to 4.0 ± 0.8 spikes, $n = 6$) in a reversible manner. However, also in the same group of slices, in the presence of D-serine the effect of the derivative was attenuated such that it was no longer statistically significant (8.2 ± 1.3 to 6.8 ± 1.0 spikes, $n = 6$, Figures 2 and 3).

Effects of gramine

Perfusion of gramine (250 and 500 μM, cumulative doses) had no significant effect on the height of the single population spike evoked in 1 mM Mg^{2+}-medium (6.3 ± 0.9 to 6.8 ± 1.0 to 6.9 ± 1.1 mV, $n = 9$). However, gramine (250 and 500 μM) consistently increased the number of population spikes evoked in Mg^{2+}-free medium and this was statistically significant at the 250 μM dose (3.6 ± 0.8 to 5.7 ± 1.2 to 5.3 ± 0.6, $n = 8$, Figures 2 and 3). Little or no recovery from this effect of gramine was observed over the course of 1 h. The effect of gramine in Mg^{2+}-free medium with added D-serine was not examined.

Effects of mephenesin

Perfusion of mephenesin (0.5 and 1 mM, cumulative doses) in 1 mM Mg^{2+} medium had no significant effect on the height of the single population spike (9.4 ± 1.0 to 8.1 ± 0.7 to 7.9 ± 0.8 mV, $n = 7$, Figures 2 and 3), however in the same 7 slices perfused with Mg^{2+}-free medium, mephenesin significantly and reversibly reduced the number of population spikes evoked (6.3 ± 1.4 to 3.3 ± 0.9 to 1.2 ± 0.4 spikes, Figures 2 and 3). In a separate group of 8 slices the same 2 doses of mephenesin significantly reduced the number of population spikes evoked in Mg^{2+}-free medium (8.0 ± 0.7 to 5.1 ± 1.2 to 3.0 ± 0.7 spikes), and had a smaller, but still statistically significant effect, in the presence of 200 μM D-serine (10.0 ± 1.6 to 8.0 ± 1.4 to 6.3 ± 1.0 spiked). In this group of 8 slices, as in all other groups, the increase in number of population spikes induced by perfusion of D-serine alone was not statistically significant (10.0 ± 1.6 compared to 8.0 ± 0.7 spikes); however, the number of spikes recorded in 1 mM mephenesin was significantly higher in the presence, as compared to the absence, of D-serine (6.3 ± 1.0 compared to 3.0 ± 0.7 spikes). There is therefore some evidence for a partial reversal of the effect of mephenesin by D-serine.

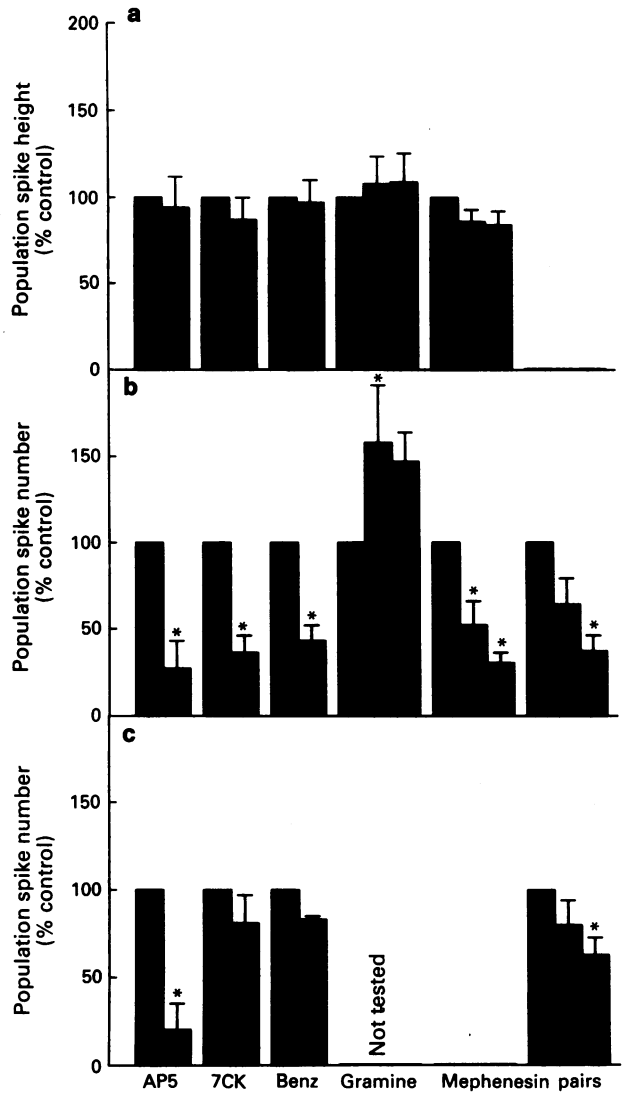


Figure 3 Effects of D-2-amino-5-phosphonovalerate (AP5, 20 μM), 7-chlorokynurenate (7CK, 20 or 40 μM), the benzimidazole derivative (2 mM), gramine (250 and 500 μM) and mephenesin (0.5 and 1 mM) on the population spike amplitude recorded in 1 mM Mg^{2+} (a), the number of population spikes evoked in Mg^{2+}-free medium (b), and the number of population spikes evoked in Mg^{2+}-free medium containing 200 μM D-serine (c). In order to aid comparison, the data are expressed as percentage of control, calculated from the figures given in the text. Each pair (or triplet) of histograms represents the normalized control response, together with the response in the presence of 1 (or 2) concentrations of drug. Bars denote s.e.mean. *Indicates $P < 0.05$, as determined by the Wilcoxon matched pairs test on the original data.

Discussion

The results with AP5 and 7CK agree with those of previous authors (Bashir *et al.*, 1990) and confirm that our preparation reveals the expected profile for known competitive NMDA antagonists and SI-glycine site antagonists respectively.

The effects of the benzimidazole derivative closely mirrored those of 7CK (see Figure 3) and are therfore consistent with the benzimidazole derivative having an antagonist action at

the SI-glycine site, although it was considerably less potent than 7CK in our preparation.

The results with mephenesin were somewhat equivocal. Like 7CK and the benzimidazole derivative, mephenesin selectively reduced the number of population spikes recorded in Mg^{2+}-free medium, but the 1 mM dose still had a significant effect in the presence of 200 μM D-serine. However, a comparison of the number of spikes evoked in the presence of 1 mM mephenesin with or without D-serine, shows that significantly more spikes were evoked in the presence of D-serine and that this could not be explained by an action of D-serine on the control responses. Of course, not all drugs that are effective against HPNS need work by the same mechanism; mephenesin is used as a centrally acting muscle relaxant, which may indicate an action at $GABA_B$ receptors, and this could explain some of its effects against HPNS. We are also aware of one report that the weak NMDA antagonist properties of mephenesin are not reversed by D-serine in a grease-gap preparation of the rat spinal cord (Pralong *et al.*, 1992).

In our experiments gramine significantly increased the number of population spikes evoked in Mg^{2+}-free medium. Therefore, this drug, which lowers the threshold pressure for convulsions, clearly did not show the profile expected of an NMDA antagonist at any site.

Structure-activity relationships

Structure activity relationships triggered this study; the test drugs used being modelled on the strychnine molecule and in particular a negatively charged group spaced 4.5 angstroms from an aromatic group (Bowser-Riley *et al.*, 1989b), but it transpired that this shows marked similarities to the more recently proposed antagonist pharmacophore at the SI-glycine site associated with the NMDA receptor (Moselley *et al.*, 1992; Kemp & Leeson, 1993). The benzimidazole derivative closely fits the model whereas gramine clearly does not. Compared to the other drugs used, mephenesin is conformationally unrestricted, and one of the possible conformations (Figure 1) approximates to the model, but in this case the negatively charged group lies too far away from the aromatic group. This may explain the equivocal results obtained in our experiments. The obvious similarities between the strychnine-sensitive and SI-glycine sites make it likely that some drugs (e.g. glycine) will have activity at both. In the context of ameliorating HPNS, a combined action of agonist at the inhibitory strychnine-sensitive site, and antagonist at the excitatory SI-site, would theoretically be most effective.

Mechanism of effect of pressure

The initial observation that the effect of strychnine was strictly additive with pressure led to the theory that increased hydrostatic pressure might have some effect on inhibitory glycinergic transmission (Bowser-Riley *et al.*, 1988). However, the present experiments suggest that some of these drugs might instead act at the excitatory SI-glycine site associated with the NMDA receptor. How can this be reconciled with the observation that strychnine and pressure act strictly additively? There are two possibilities that might account for a common mechanism between the two treatments: (i) There is evidence that increased hydrostatic pressure directly potentiates NMDA receptor-mediated responses (Fagni *et al.*, 1987; Zinebi *et al.*, 1988). In addition, NMDA receptor gated channels are indirectly regulated by the state of GABAergic (and presumably glycinergic) inhibition which affects the voltage-dependent Mg^{2+} block of the channels (Nowak *et al.*, 1984; Collingridge *et al.*, 1988). Thus the common mechanism might be the opening of NMDA receptor gated channels by pressure acting directly on the NMDA receptor gated channels, and by strychnine acting on the state of glycinergic inhibition. (ii) Alternatively, high hydrostatic pressure might, as initially suggested, affect glycinergic inhibition itself. Here the common mechanism would still be the opening of NMDA receptor-gated channels, but in this case by pressure and strychnine both blocking the glycinergic inhibition.

Both these hypotheses predict that NMDA antagonists would be effective against HPNS, and indeed they are (Meldrum *et al.*, 1983; Milan *et al.*, 1990). However, the facts that bicuculline (Bowser-Riley *et al.*, 1989a) and picrotoxin (Bowser-Riley *et al.*, 1988) do *not* act additively with pressure, and that pressure selectively inhibits currents evoked by glycine (as opposed to GABA or kainate (Daniels *et al.*, 1993)), both favour the second hypothesis; that pressure reduces glycinergic inhibition and hence indirectly regulates the NMDA gated channel.

The results presented here suggest that an antagonist action at the SI-glycine site might have a role to play in the HPNS protecting effects of some of these drugs. However, none of the results using this preparation can be considered conclusive, but only consistent or inconsistent with an action at the SI-glycine site. For instance, due to the time course of the excitatory and inhibitory components of the synaptic response, it is possible that a drug which potentiates $GABA_B$ receptor-mediated responses would have little effect on the single population spike evoked in Mg^{2+} containing medium, but would affect the multiple population spikes evoked in Mg^{2+}-free medium. These pilot studies have, however, encouraged us to set up a grease-gap recording preparation in which to study more quantitatively the pharmacological actions of these and other drugs that interfere with HPNS.

We wish to thank Dr John Lewis of the University of Aberdeen Chemistry Department for synthesis of drugs, and the Wellcome Trust for financial support.

References

BASHIR, Z.I., TAM, B. & COLLINGRIDGE, G.L. (1990). Activation of the glycine site in the NMDA receptor is necessary for the induction of LTP. *Neurosci. Lett.*, **108**, 261–266.

BOWSER-RILEY, F., DANIELS, S., HILL, W.A.G., LEARNER, T.S. & SMITH, E.B. (1989a). The additive effects of pressure and chemical convulsants in mice. *J. Physiol.*, **409**, 36P.

BOWSER-RILEY, F., DANIELS, S., HILL, W.A.G. & SMITH, E.B. (1989b). An evaluation of the structure-activity relationships of a series of analogues of mephenesin and strychnine on the response to pressure in mice. *Br. J. Pharmacol.*, **96**, 789–794.

BOWSER-RILEY, F., DANIELS, S. & SMITH, E.B. (1988). Investigations into the origin of the high pressure neurological syndrome: the interaction between pressure, strychnine and 1,2-propandiols in the mouse. *Br. J. Pharmacol.*, **94**, 1069–1076.

COAN, E.J. & COLLINGRIDGE, G.L. (1985). Magnesium ions block an N-methyl-D-aspartate receptor-mediated component of synaptic transmission in rat hippocampus. *Neurosci. Lett.*, **53**, 21–26.

COLLINGRIDGE, G.L., HERRON, C.E. & LESTER, R.A.J. (1988). Synaptic activation of N-methyl-D-aspartate receptors in the Schaffer collateral-commisural pathway of rat hippocampus. *J. Physiol.*, **399**, 283–300.

COLLINGRIDGE, G.L., KEHL, S.J. & MCLENNAN, H. (1983). Excitatory amino acids in synaptic transmission in the Schaffer collateral-commissural pathway of the rat hippocampus. *J. Physiol.*, **334**, 33–46.

DANIELS, S., SHELTON, C.J. & SMITH, E.B. (1993). The effect of high pressure on ligand gated ion channels. *Proc. XXXII IUPS*, **37.3**

FAGNI, L., ZINEBI, F. & HUGON, M. (1987). Helium pressure potentiates the N-methyl-D-aspartate- and D,L-homocysteate-induced decreases of field potentials in the rat hippocampal slice preparation. *Neurosci. Lett.*, **81**, 285–290.

HALSEY, M.J. (1982). Effects of high pressure on the central nervous system. *Physiol. Rev.*, **62**, 1341–1377.

HELLIWELL, F.M. (1990). The actions of muscle relaxants and general anaesthetics on the effects of raised hydrostatic pressure in mice. *BSc Thesis: University of Aberdeen.*

KEMP, J.A. & LEESON, P.D. (1993). The glycine site of the NDMA receptor – five years on. *Trends Pharmacol. Sci.*, **14,** 20–25.

MELDRUM, B., WARDLEY-SMITH, B., HALSEY, M.J. & ROSTAIN, J.-C. (1983). 2-amino-phosphonoheptanoic acid protects against the high pressure neurological syndrome. *Eur. J. Pharmacol.*, **87,** 501–502.

MILAN, M.H., WARDLEY-SMITH, B., HALSEY, M.J. & MELDRUM, B.S. (1990). Effects of NMDA and 2-amino-7-phosphono-heptanoate focal injection into the ventrolateral thalamic nucleus on the high pressure neurological syndrome in the rat. *Brain Res.*, **507,** 354–356.

MOSELLEY, A.M., BAKER, R., FOSTER, A.C., GRIMWOOD, S., KEMP, J.A. & MARSHALL, G.R. (1992). 2-Carboxytetrahydroquinolines – conformational and stereochemical requirements for antagonism of the glycine site on the NMDA receptor. *J. Med. Chem.*, **35,** 1942–1953.

NOWAK, L., BREGESTOVSKI, P., ASCHER, P., HERBET, A. & PROCHIANTZ, A. (1984). Magnesium gates glutamate-activated channels in mouse central neurones. *Nature*, **307,** 462–465.

PRALONG, E., MILLAR, J.D. & LODGE, D. (1992). Specificity and potency of N-methyl-D-aspartate glycine site antagonists and of mephenesin on the rat spinal cord in vitro. *Neurosci. Lett.*, **136,** 56–58.

SHUKER, M.A., BOWSER-RILEY, F. & DAVIES, S.N. (1992). NMDA antagonist properties of drugs that affect high pressure neurological syndrome in the rat hippocampal slice. *J. Physiol.*, **446,** 46P.

THOMSON, A.M. (1990). Glycine is a coagonist at the NMDA receptor/channel comlex. *Prog. Neurobiol.*, **35,** 53–74.

ZINEBI, F., FAGNI, L. & HUGON, M. (1988). The influence of helium pressure on the reduction induced in field potentials by various amino acids and on the GABA-mediated inhibition in the CA1 region of hippocampal slices in the rat. *Neuropharmacology*, **27,** 57–65.

(Received September 1, 1993
Revised November 19, 1993
Accepted November 24, 1993)

Br. J. Pharmacol. (1994), **111**, 956–960 © Macmillan Press Ltd, 1994

Antidepressant-like effects of CCK_B antagonists in mice: antagonism by naltrindole

M. Derrien, C. Durieux & [1]B.P. Roques

Département de Pharmacochimie Moléculaire et Structurale, INSERM U266, CNRS URA D 1500, UFR des Sciences Pharmaceutiques et Biologiques, 4, avenue de l'Observatoire, 75270 Paris Cedex 06, France

1 The effects of selective CCK_B agonists, BC 264 and BC 197 were investigated in the conditioned suppression of motility test in mice, an animal model used to select antidepressant drugs. The results showed that both CCK_B agonists at doses of 3 and 30 $\mu g\ kg^{-1}$, accentuated the suppression of motility in shocked mice and did not modify the behaviour of non-shocked mice. The effects of BC 264 were suppressed by L-365,260.

2 L-365,260 alone, at doses of 0.2 and 2 $mg\ kg^{-1}$ decreased motor inhibition in shocked mice and had no effect in non-shocked mice.

3 The effects of L-365,260 observed in shocked mice were suppressed by naltrindole, a selective antagonist for δ-opioid receptors, suggesting the occurrence of physiological adverse interactions between CCK and opioid systems.

4 Together, these results suggest that CCK_B antagonists could block centrally located CCK_B receptors to produce antidepressant-like effects which could indirectly involve δ-opioid receptor stimulation.

Keywords: Conditioned suppression of motility: antidepressant-like effects of CCK_B antagonists; CCK_B receptors; CCK_B agonists; CCK_B antagonists; δ-opioid receptors

Introduction

It has been estimated that in the general population the incidence of anxiety disorders is between 2 and 5% (Togersen, 1983). Recent clinical studies reported that, when intravenously injected to healthy volunteers or to patients with panic disorders, the C-terminal tetrapeptide or cholecystokinin (CCK-4), which is a selective CCK_B agonist, induces panic attacks that are suppressed by L-365,260, a selective CCK_B antagonist (De Montigny, 1989; Bradwejn *et al.*, 1991; 1992; Lydiard *et al.*, 1992). In agreement with this, antagonists selective for CCK_B receptors were shown to induce anxiolytic-like effects and to suppress the anxiogenic-like responses of CCK agonists in animal models for anxiety (Hughes *et al.*, 1990; Harro & Vasar, 1991; Singh *et al.*, 1991). Antidepressant drugs and monoamine oxidase inhibitors are also efficient in the treatment of panic attacks, particularly those associated with agoraphobia (Den Boer & Westenberg, 1990; see also Rosenberg *et al.*, 1991 for a review).

It has also been suggested that the endogenous opioid peptides, enkephalins (but not β-endorphins) might be involved in the aetiology of depression (Kameyama & Nagasaka, 1982; Wise, 1983; Roques *et al.*, 1985; Willner, 1990; Katoh *et al.*, 1992). In line with this, increasing the level of endogenous enkephalins by RB 101, a mixed inhibitor of enkephalin metabolizing enzymes (Fournié-Zaluski *et al.*, 1992) induced antidepressant-like effects in the conditioned suppression of motility test in mice (Baamonde *et al.*, 1992). In this animal model of depression, mice react to the adverse situation (electric footshocks) by motor immobility which is reduced by antidepressants such as imipramine, desipramine and amitryptiline (Kameyama & Nagasaka, 1982; Kameyama *et al.*, 1985). The effects of RB 101 were suppressed by both the δ-opioid antagonist, naltrindole (NTI) and the dopamine D_1 antagonist, SCH 23390 (Baamonde *et al.*, 1992).

Enkephalins and CCK behave as endogenous tonically active antagonists (Faris *et al.*, 1983; Wiertelak *et al.*, 1992; Noble *et al.*, 1993). Thus, CCK_B antagonists have been shown to enhance antinociceptive responses induced by opiates (Dourish *et al.*, 1990; Wiesenfeld-Hallin *et al.*, 1991) or by endogenous enkephalins (Maldonado *et al.*, 1993). It was therefore of interest to investigate the possible existence of CCK-mediated processes which would counteract the antidepressant effects of opioids. With this aim, selective CCK_B agonists, BC 264 and BC 197 (Charpentier *et al.*, 1988a,b; Daugé *et al.*, 1990) and the selective antagonist L-365,260 (Bock *et al.*, 1989) have been administered peripherally to mice and the behavioural responses of the animals studied by use of the conditioned suppression of motility test.

Methods

Animals

Male Swiss albino mice (Charles River, France) weighing 30 g were used. Animals were housed in groups and placed in the room in which behavioural experiments were performed, at least two days before the experiments were started. Food and water were available *ad libitum*. All studies were performed between 10 h 00 min and 19 h 00 min. Each animal was used only once.

Conditioned suppression of motility

The assay was performed as previously described by Kameyama & Nagasaka (1982). Mice were placed in a transparent rectangular cage (30 × 26 × 30 cm) with a metallic grid floor. Twelve squares were drawn on the floor to count animal displacements. The apparatus was located in a sound-proof room illuminated by a 75 W bulb.

On the first day, the mouse was left in the test cage for 6 min and received electric footshocks (0.1 Hz, 200 ms, 100 V) through an isolated stimulator (GL 260T, Société Ravia, Bordeaux, France). Each animal received electric shocks in a range of 1.2 to 3 mA. On the second day, the mouse was placed in the same cage without receiving electric footshocks and motility changes were observed by counting

[1] Author for correspondence.

the number of squares crossed, plus the number of rears during 6 min. On the first day, mice in the control group were treated in the same way as those in the conditioned suppression group except that they did not receive electric footshocks.

In all experiments, the CCK_B agonists, BC 264 and BC 197 or their vehicle were administered intraperitoneally (i.p.) 30 min before the tests. L-365,260 was injected i.p. 15 min before BC 264 (45 min before experiments) or 30 min before the test in the second experiment (proper effect of CCK_B antagonists). Naltrindole was administered s.c. 35 min before testing (5 min before L-365,260). In all cases the volume of injection was 0.1 ml per 10 g of body weight except in the experiments with antagonist where injections of 0.1 ml per 20 g of body weight were used in order to minimize the total volume injected.

Chemicals

BC 264 (Boc-Tyr(SO_3H)-gNle-mGly-Trp-(NMe)Nle-Asp-Phe-NH_2), BC 197 (Boc-D-Asp-Tyr(SO_3H)-Nle-D-Lys-Trp-Nle-Asp-Phe-NH_2) (Charpentier *et al.*, 1988a,b) and naltrindole (NTI, 17-cyclopropylmethyl-6,7-dehydro-4,5α-epoxy-3,14-dihydroxy-6,7,2′,3′-indolomorphinan) were dissolved in saline (NaCl 0.9%); L-365,260: (3R-(+)-2,3-dihydro-1-methyl-2-oxo-5-phenyl-1*H*-1,4-benzodiazepin-3-yl)-*N*′-(3 methylphenyl)-urea) (Bock *et al.*, 1989) was suspended in carboxymethyl cellulose (0.5%).

Statistical analysis

Individual group comparisons were made by a two-way analysis of variance (ANOVA). The factors of variation were dose (between subjects) and shock (between subjects). Individual dose-effects within a given group (shocked or non-shocked) were analysed by one way analysis of variance (ANOVA). *Posthoc* comparisons were made with Dunnett's *t* or Newman Keuls tests.

Results

Effects of CCK_B agonists in the conditioned suppression of motility in mice

Mice injected with vehicle or BC 264 were tested for their motility in the same test cage in which they had previously received, or not, electrical footshocks. Two way analysis of variance showed no significant effects for the treatment. $F(7,164) = 1.78$, $P = 0.09$; significant effects for shocks, $F(1,164) = 672$, $P < 0.01$ and interaction, $F(7,164) = 3.31$, $P < 0.01$. In the group of non-shocked mice, BC 264 did not change the locomotor activity at all doses tested. $F(7,74) = 1.33$, $P < 0.01$ (Figure 1a).

In the group of shocked mice treated with vehicle, (conditioned suppression group), the animals exhibited a significant suppression of motility as previously reported by Kameyama & Nagasaka (1982) and by Baamonde *et al.* (1992). In the group of shocked mice, BC 264, 3 and 30 μg kg^{-1} i.p. 30 min before the test, increased the conditioned suppression of motility: $F(7,90) = 4.90$, $P < 0.01$ (Figure 1a).

In the case of BC 197, a two way analysis of variance showed significant effects for the treatment, $F(3,70) = 3.45$, $P < 0.05$; significant effects for shocks, $F(1,70) = 448$, $P < 0.01$ and interaction, $F(3,70) = 2.64$, $P < 0.05$. In the group of non-shocked mice, BC 197 did not change the locomotor activity at all doses tested: $F(3,34) = 0.04$, $P = 0.98$ (Figure 1b). In the group of shocked mice, BC 197, 3 and 30 μg kg^{-1} i.p. 30 min before the test, increased the conditioned suppression of motility: $F(3,36) = 11.93$, $P < 0.01$ (Figure 1b).

In the experiment with L-365,260, i.p. administered 15 min before BC 264 (30 μg kg^{-1}, i.p.), two way analysis of variance

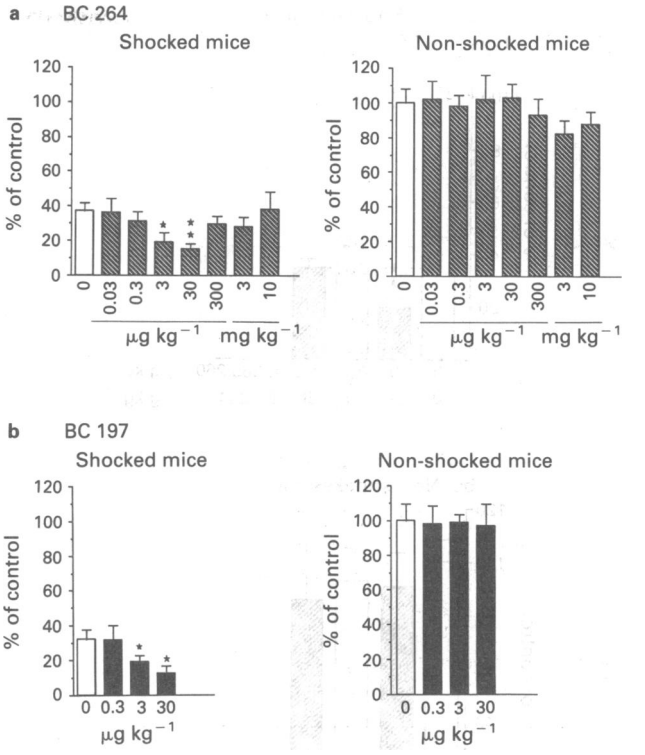


Figure 1 Depressant-like effects of CCK_B agonists, BC 264 and BC 197; 30 min before observation, mice placed in an environment previously paired (or not) with inescapable electric footshocks, were administered intraperitoneally either with saline or with CCK_B agonists. The doses administered were 0.03 μg kg^{-1} to 10 mg kg^{-1} for BC 264 (a) and 0.3, 3 and 30 μg kg^{-1} for BC 197 (b). Locomotor activity, measured for 6 min, was assessed by measuring the total number of rearings and of squares crossed. Two way analysis of variance indicated, in each experiment, a significant ($P < 0.01$) difference between shocked and non shocked mice as well as an interaction between treatment and shocks ($P < 0.05$). The results are expressed as a percentage of control ± s.e.mean. $^*P < 0.05$; $^{**}P < 0.01$ as compared to control groups, Dunnett's test.

indicated a significant effect for the treatment $F(3,66) = 2.50$, $P < 0.05$; shocks, $F(1,66) = 322$, $P < 0.01$; but not for interaction, $F(3,66) = 2.35$, $P = 0.08$. L-365,260 (0.1 mg kg^{-1}, s.c., 45 min before the test or 15 min before BC 264) suppressed the decreased locomotion induced by 30 μg kg^{-1} of BC 264 in the conditioned suppression group: $F(3,33) = 8.47$, $P < 0.01$, whereas the antagonist was devoid of intrinsic effects (Figure 2). These treatments were without effect in the group of non-shocked mice: $F(3,33) = 0.70$, $P = 0.55$ (Figure 2).

Effects of L-365,260 in the conditioned suppression of motility in mice

In an attempt to measure the intrinsic effects of the CCK_B antagonist, vehicle (carboxymethyl cellulose) or L-365,260 were administered 30 min before the test. Two way analysis of variance showed no significant effects for the treatment, $F(3,99) = 1.31$, $P = 0.27$; significant effects for shocks, $F(1,99) = 216$, $P < 0.01$ and interaction, $F(3,99) = 2.73$, $P < 0.05$. In the group of non-shocked mice, L-365,260 did not change the locomotor activity at all tested doses: $F(3,49) = 0.23$, $P = 0.87$ (Figure 3a).

In the group of shocked mice, 0.2 and 2 mg kg^{-1} i.p. of L-365,260 injected 30 min before the test, decreased the conditioned suppression of motility (Figure 3a): $F(3,50) = 5.87$, $P < 0.01$.

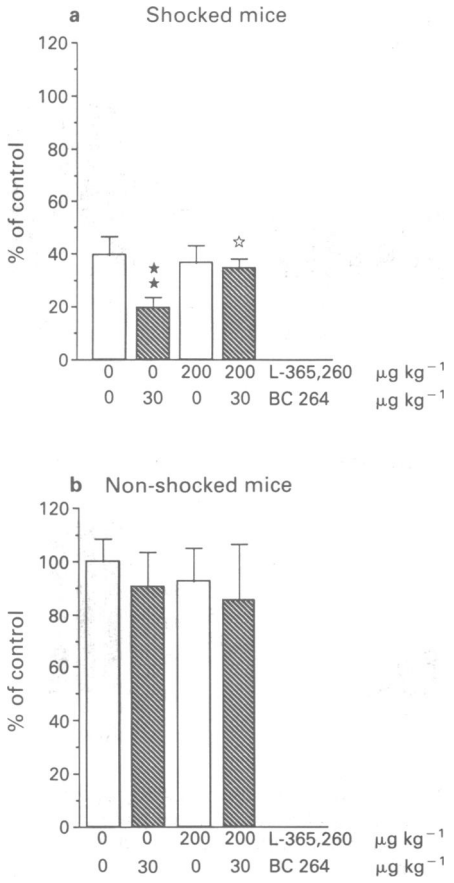


Figure 2 Effect of the CCK_B antagonist L-365,260 (0.2 mg kg^{-1}, i.p., administered 45 min before the experiment) on the behavioural response induced by BC 264 (30 μg kg^{-1}, i.p., administered 30 min before the experiment) in shocked (a) and non-shocked mice (b). Locomotor activity, measured for 6 min, was assessed by counting the total number of rearings and of squares crossed. Two way analysis of variance indicated in each experiment a significant ($P<0.01$) difference between shocked and non-shocked mice. The results are expressed as a percentage of control ± s.e.mean. $^{**}P<0.01$ as compared to control group; ☆$P<0.05$ as compared to BC 264 group, Newman Keuls' test.

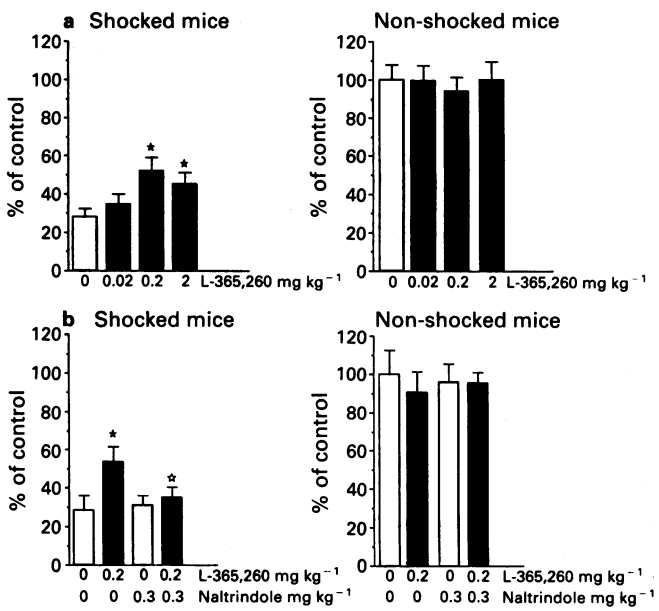


Figure 3 Antidepressant-like effects of L-365,260 (a) and reversal of the effect of L-365,260 by naltrindole (b), a selective δ-opioid receptor antagonist. Thirty minutes before observation, mice placed in an environment previously paired (or not) with inescapable electric footshocks were given intraperitoneally either carboxymethycellulose or L-365,260. The administered doses were 0.02, 0.2 and 2 mg kg^{-1}. In the study of the effect of naltrindole on the antidepressant-like response induced by L-365,260, the selective δ-opioid antagonists, naltrindole (0.3 mg kg^{-1}, s.c.) was administered 35 min before the experiments (or 5 min before L-365,260, 0.2 mg kg^{-1}, i.p.). Locomotor activity, measured for 6 min, was assessed by counting the total number of rearings and of squares crossed. Two way analysis of variance indicated, in each experiment, a significant ($P<0.01$) difference between shocked and non shocked mice. The results are expressed as a percentage of control ± s.e.mean. $^{*}P<0.05$ as compared to control group; ☆$P<0.05$ as compared to L-365,260 group, Newman Keul's test.

Effects of the selective δ-opioid antagonist naltrindole on L-365,260-induced decrease in the conditioned suppression of motility in mice

Two way analysis of variance showed no significant effects for the treatment, $F(3,48)=0.65$, $P=0.55$; significant effects for shocks, $F(1,48)=164$, $P<0.01$ and interaction, $F(3,48)=2.70$, $P=0.05$. In the group of non-shocked mice, no change in locomotor activity was observed irrespective of the treatment: $F(3,24)=0.27$, $P=0.84$ (Figure 3b).

In the group of vehicle-treated, shocked mice, 0.2 mg kg^{-1} i.p. of L-365,260 injected 30 min before the test, decreased the conditioned suppression of motility. This effect was suppressed by the selective δ-opioid receptor antagonist, naltrindole, 0.3 mg kg^{-1} i.p. injected 5 min before L-365,260: $F(3,24)=4.74$, $P<0.01$ (Figure 3b).

Discussion

Potential antidepressant drugs are selected by using several animal models of depression, such as the conditioned suppression of motility in mice, the forced swimming test or the learned helplessness assay in rat (Willner, 1990).

The present results show that CCK_B agonists such as BC 264 or BC 197 potentiate the decrease in motor activity measured in mice which have received electric footshocks the day before, but do not modify the activity in non-shocked mice. Moreover, the effects of BC 264 and BC 197 (not shown) were suppressed by the selective CCK_B antagonist, L-365,260. The two CCK_B agonists produced similar effects at similar doses of 3 and 30 μg kg^{-1}.

The possibility that CCK_B antagonists alone induce behavioural responses in the conditioned suppression of motility was studied by administration of L-365,260, 30 min before the test. The motor activity of non-shocked mice remained comparable to that of control group, whereas shocked mice treated with the CCK_B antagonist exhibited a significant reduction in the suppression of motility. These results strongly suggest that in stressed mice a phasic stimulation of CCK_B receptors by endogenous CCK could occur. In agreement with this, Siegel *et al.* (1984) have reported that stressful situations increase CCK levels in rat brain. It is also possible that the binding characteristics of CCK receptors may be modified in shocked mice since exposure to a novel environment has been shown to modulate the levels of these receptors (Harro *et al.*, 1990).

These results show that CCK_B antagonists are able to induce antidepressant-like effects in mice. The possible involvement of CCK in behavioural responses associated with anticipatory stress has already been demonstrated and the importance of external stimuli, such as a novel environment, in revealing the behavioural effects induced by CCK

agonists or antagonists has been emphasized in several studies (Crawley, 1984; Daugé *et al.*, 1989; O'Neill *et al.*, 1991; Lavigne *et al.*, 1992). Under the present conditions, anticipatory stress might increase the sensitivity of the CCK system, allowing the effects of CCK_B agonists and antagonists to be detected. In agreement with this hypothesis, a recent study has shown that CCK immunoreactivity is elevated in marathon runners under prerun conditions, which was considered as an anticipatory stress (Philipp *et al.*, 1992). Moreover, abnormalities in the CCK concentrations of patients with psychiatric disorders have been reported (Garver *et al.*, 1990; Lydiard *et al.*, 1992). Thus, the CCK system could act as a counteracting 'anxiogenic' system, aimed at ensuring a sufficient level of emotional vigilance (Wiertelak *et al.*, 1992).

In this study, CCK_B agonists have been found to accentuate the immobility of shocked mice. In contrast, it has been shown that an increase in extracellular levels of endogenous enkephalins by RB 101, a mixed inhibitor of enkephalin metabolizing enzymes, attenuates the conditioned suppression of motility (Baamonde *et al.*, 1992). The antidepressant-like effect of RB 101 was blocked by naltrindole, a selective δ-opioid receptor antagonist and by the selective D_1 dopamine antagonist, SCH 23390. Opposing responses of CCK and enkephalins have often been described and in most studies CCK has been found to behave as an anti-opioid peptide. Thus, administration of CCK agonists suppressed opioid analgesia (Itoh *et al.*, 1982; Faris *et al.*, 1983; Noble *et al.*, 1993) while CCK_B antagonists potentiated the antinociceptive effects produced by opioids (Dourish *et al.*, 1990; Wiesenfeld-Hallin *et al.*, 1991; Lavigne *et al.*, 1992; Wiertelak *et al.*, 1992) or by endogenous enkephalins (Maldonado *et al.*, 1993).

The antidepressant-like effects of L-365,260 observed in shocked mice were antagonized by naltrindole. This strongly supports the occurrence of direct or indirect interactions between endogenous enkephalins and CCK, interacting with δ-opioid and CCK_B receptor types respectively. Several lines of evidence indicate that the reinforcing properties of opioids are mediated in the mesolimbic dopamine system (Bozarth & Wise, 1984; Cooper, 1991) and very probably through D_1 dopamine receptors (Baamonde *et al.*, 1992). The complex behavioural sequence observed in shocked mice may involve motivational and rewarding processes in which δ-opioid receptor participation has been suggested (Amalric *et al.*, 1987; Shippenberg *et al.*, 1987; Calenco-Choukroun *et al.*, 1991). Thus, it has been found that stimulation of δ-opioid receptors by exogenous agonists (Latimer *et al.*, 1987; Calenco-Choukroun *et al.*, 1991) or endogenous enkephalins (Kalivas & Richardson-Carlson, 1986; Daugé *et al.*, 1992) increases the dopamine system activity (Wood, 1983; Daugé *et al.*, 1992). One of the neuroanatomical structures involved in this response could be the ventral tegmental area, since microinjection of BC 264 in this structure was found to potentiate dopamine-induced hypolocomotion (Daugé *et al.*, 1990) while local infusion of selective δ-opioid agonists or kelatorphan, a peptidase inhibitor increasing the level of endogenous enkephalins were shown to enhance motor activity (Calenco-Choukroun *et al.*, 1991). Endogenous CCK, acting on CCK_B receptors, could inhibit, directly or indirectly through GABA interneurones activation, the facilitatory effect of endogenous enkephalins on dopamine system activity (Wolf *et al.*, 1978). The involvement of other brain areas such as the amygdala, where antagonism of CCK and enkephalin systems has been reported (Flood *et al.*, 1993), could also account for these effects.

In summary, these results suggest that CCK_B agonists induce depressant-like properties in mice placed in an environment previously associated with inescapable electric shocks, through stimulation of brain CCK_B receptors. The CCK_B antagonist-induced antidepressant-like effects observed in this test suggest that CCK released during stress may contribute to modulate arousal needed to counteract stressful situations. Studies are now warranted to evaluate the therapeutic potential of these CCK antagonists as new antidepressant drugs, alone, or in association with classical treatments.

References

AMALRIC, M., CLINE, E.J., MARTINEZ Jr. J.L., BLOOM, F.E. & KOOB, G.F. (1987). Rewarding properties of β-endorphin as measured by conditioned place preference. *Psychopharmacol.*, **91**, 14–19.

BAAMONDE, A., DAUGÉ, V., RUIZ-GAYO, M., FULGA, I.G., TURCAUD, S., FOURNIÉ-ZALUSKI, M.C. & ROQUES, B.P. (1992). Antidepressant-type effects of endogenous enkephalins protected by systemic RB101 are mediated by opioid δ and dopamine D_1 receptor stimulation. *Eur. J. Pharmacol.*, **216**, 157–166.

BOCK, M.G., DIPARDO, R.M., EVANS, B.E., RITTLE, K.E., WHITTER, W.L., VEBER, D.F., ANDERSON, P.S. & FREIDINGER, R.M. (1989). Benzodiazepine gastrin and brain cholecystokinin ligands: L-365,260. *J. Med. Chem.*, **32**, 13–16.

BOZARTH, M.A. & WISE, R.A. (1984). Anatomically distinct opiate receptor fields mediate reward and physical dependence. *Science*, **224**, 516–517.

BRADWEJN, J., KOSZYCKI, D., COUSTOUX-DUTERTRE, A., VAN MEGEN, H., DEN BOER, J., WESTENBERG, H., KARKANIAS, C. & HAIGH, J. (1992). L-365,260, a CCK_B antagonist, blocks CCK-4-panic disorder. *Clin. Neuropharmacol.*, **15** Suppl. 1, 5.

BRADWEJN, J., KOSZYCKI, D. & SHRIQUI, C. (1991). Enhanced sensitivity to cholecystokinin tetrapeptide in panic disorder. Clinical and behavioural findings. *Arch. Gen. Psychiatry*, **48**, 603–610.

CALENCO-CHOUKROUN, G., DAUGÉ, V., GACEL, G. & ROQUES, B.P. (1991). Lesion of dopaminemesolimbic neurons blocks behavioural effects induced by the endogenous enkephalins but not by a μ-opioid receptor agonist. *Eur. J. Pharmacol.*, **209**, 267–271.

CHARPENTIER, B., DURIEUX, C., PÉLAPRAT, D., DOR, A., REIBAUD, M., BLANCHARD, J.-C. & ROQUES, B.P. (1988a). Enzyme-resistant CCK analogs with high affinities for central receptors. *Peptides*, **9**, 835–841.

CHARPENTIER, B., PÉLAPRAT, D., DURIEUX, C., DOR, A., REIBAUD, M., BLANCHARD, J.-C. & ROQUES, B.P. (1988b). Cyclic cholecystokinin analogues with high selectivity for central receptors. *Proc. Natl. Acad. Sci. U.S.A.*, **85**, 1968–1972.

COOPER, S.J. (1991). Interactions between endogenous opioids and dopamine: implications for reward and aversion. In *The Mesolimbic Dopaminergic System: from Motivation to Action*, ed. Willner, P. & Scheel-Kruger, J. 331–366, pp. Chichester: John Wiley.

CRAWLEY, J.N. (1984). Cholecystokinin accelerates the rate of habituation to a novel environment. *Pharmacol. Biochem. Behav.*, **20**, 23–27.

DAUGÉ, V., BÖHME, G.A., CRAWLEY, J.N., DURIEUX, C., STUTZMAN, J.M., FÉGER, J., BLANCHARD, J.C. & ROQUES, B.P. (1990). Investigation of behavioural and electrophysiological responses induced by selective stimulation of CCKB receptors by using a new highly potent CCK analog, BC 264. *Synapse*, **6**, 73–80.

DAUGÉ, V., DOR, A., FÉGER, J. & ROQUES, B.P. (1989). The behavioural effects of CCK8 injected into the medial accumbens are dependent on the motivational state of the rat. *Eur. J. Pharmacol.*, **163**, 25–32.

DAUGÉ, V., KALIVAS, P.W., DUFFY, T. & ROQUES, B.P. (1992). Effect of inhibiting enkephalin catabolism in the VTA on motor activity and extracellular dopamine. *Brain Res.*, **599**, 209–214.

DEMONTIGNY, C. (1989). Cholecystokinin tetrapeptide induces panic-like attacks in healthy volunteers. *Arch. Gen. Psychiatry*, **46**, 511–517.

DEN BOER, J.A. & WESTENBERG, H.G.M. (1990). Serotonin function in panic disorder: a double blind placebo controlled study with fluvoxamine and ritanserin. *Psychopharmacol.*, **102**, 85–94.

DOURISH, C.T., O'NEILL, M.F., COUGHLAN, J., KITCHENER, S.J., HAWLEY, D. & IVERSEN, S.D. (1990). The selective CCK-B receptor antagonist L-365,260 enhances morphine analgesia and prevents morphine tolerance in the rat. *Eur. J. Pharmacol.*, **176**, 35–44.

FARIS, P.L., KOMISARUK, B.R., WATKINS, L.R. & MAYER, D.J. (1983). Evidence for the neuropeptide cholecystokinin as an antagonist of opiate analgesia. *Science*, **219**, 310–312.

FLOOD, J.F., GARLAND, J.S. & MORLEY, J.E. (1992). Evidence that cholecystokinin-enhanced retention is mediated by changes in opioid activity in the amygdala. *Brian Res.*, **585**, 94–104.

FOURNIÉ-ZALUSKI, M.C., CORIC, P., TURCAUD, S., LUCAS, E., NOBLE, F., MALDONADO, R. & ROQUES, B.P. (1992). 'Mixed-inhibitor-prodrug' as a new approach toward systemically active inhibitors of enkephalin-degrading enzymes. *J. Med. Chem.*, **35**, 2473–2481.

GARVER, D.L., BEINFELD, M.C. & YAO, J.K. (1990). Cholecystokinin, dopamine and schizophrenia. *Psychopharmacol. Bull.*, **26**, 377–380.

HARRO, J., KIIVET, R.-A., LANG, A. & VASAR, E. (1990). Rats with anxious and non-anxious type of exploratory behaviour differ in their brain CCK-8 and benzodiazepine receptor characteristics. *Behavioural Brain Res.*, **39**, 63–71.

HARRO, J. & VASAR, E. (1991). Evidence that CCK_B receptors mediate the regulation of exploratory behaviour in the rat. *Eur. J. Pharmacol.*, **193**, 379–381.

HUGHES, J., BODEN, P., COSTALL, B., DOMENEY, A., KELLY, E., HORWELL, D.C., HUNTER, J.C., PINNOCK, R.D. & WOODRUFF, G.N. (1990). Development of a class of selective cholecystokinin type B receptor antagonists having potent anxiolytic activity. *Proc. Natl. Acad. Sci. U.S.A.*, **87**, 6728–6732.

ITOH, S., KATSUURA, G. & MAEDA, Y. (1982). Caerulein and cholecystokinin suppress β-endorphin-induced analgesia in the rat. *Eur. J. Pharmacol.*, **80**, 421–425.

KALIVAS, P.W. & RICHARDSON-CARLSON, R. (1986). Endogenous enkephalin modulation of dopamine neurons in the ventral tegmental area. *Am. J. Physiol.*, **251**, R243–R249.

KAMEYAMA, T. & NAGASAKA, M. (1982). Effects of apomorphine and diazepam on a quickly learned conditioned suppression in rats. *Pharmacol. Biochem. Behav.*, **17**, 59–63.

KAMEYAMA, T., NAGASAKA, M. & YAMADA, K. (1985). Effects of antidepressant drugs on a quickly learned conditioned suppression responses in mice. *Neuropharmacol.*, **24**, 285–290.

KATOH, A., NABESHIMA, T., UKAI, R. & KAMEYAMA, T. (1992). Endorphins do not affect behavioural stress responses in mice. *Peptides*, **13**, 737–739.

LATIMER, L.G., DUFFY, P. & KALIVAS, P.W. (1987). Mu opioid receptor involvement in enkephalin activation of dopamine neurons in the ventral tegmental area. *J. Pharmacol. Exp. Ther.*, **241**, 328–337.

LAVIGNE, G.J., MILLINGTON, W.R. & MUELLER, G.P. (1992). The CCK-A and CCK-B receptor antagonists, devazeptide and L-365,260, enhance morphine antinociception only in non-acclimated rats exposed to a novel environment. *Neuropeptides*, **21**, 119–129.

LYDIARD, R.B., BALLENGER, J.C., LARAIA, M.T., FOSSEY, M.D. & BEINFELD, M.C. (1992). CSF cholecystokinin concentrations in patients with panic disorder and in normal comparison subjects. *Am. J. Psychiatry*, **149**, 691–693.

MALDONADO. R., DERRIEN, M., NOBLE, F. & ROQUES, B.P. (1993). Association of the peptidase inhibitor RB 101 and a CCK-B antagonist strongly enhances antinociceptive responses. *NeuroReport*, **4**, 947–950.

NOBLE, F., DERRIEN, M. & ROQUES, B.P. (1993). Modulation of opioid antinociception by CCK at the supraspinal level: evidence of regulatory mechanisms between CCK and enkephalin systems in the control of pain. *Br. J. Pharmacol.*, **109**, 1064–1070.

O'NEILL, M.F., DOURISH, C.T. & IVERSEN, S.D. (1991). Hypolocomotion induced by peripheral or central injection of CCK in the mouse is blocked by the CCK_A receptor antagonist devazepide but not by the CCK_B receptor antagonist L-365,260. *Eur. J. Pharmacol.*, **193**, 203–208.

PHILIPP, E., WILCKENS, T., FRIESS, E., PLATTE, P. & PIRKE, K.-M. (1992). Cholecystokinin, gastrin and stress hormone responses in marathon runners. *Peptides*, **13**, 125–128.

ROQUES, B.P., DAUGÉ, V., GACEL, G. & FOURNIÉ-ZALUSKI, M.C. (1985). Selective agonists and antagonists of delta opioid receptors and inhibitors of enkephalin metabolism. Potential use in treatment of mental illness. In *Biological Psychiatry Developments in Psychiatry*, Vol. 7. ed. Josiassen, R.C., Bridger, W.H., Weiss, K.J., Stoff, D. & Simpson, G.M. pp. 287–289. New York: Elsevier.

ROSENBERG, R., OTTOSSON, J.-O., BECH, P., MELLERGÄRD, M. & ROSENBERG, N.K. (1991). Validation criteria for panic disorder as a nosological entity. *Acta Psychiatr. Scand.*, Supp. 365, 7–17.

SIEGEL, R.A., DÜKER, E.-M., FUCHS, E., PAHNKE, U. & WUTTKE, W. (1984). Responsiveness of mesolimbic, mesocortical, septal and hippocampal cholecystokinin and substance P neuronal systems to stress, in the male rat. *Neurochem. Int.*, **6**, 783–789.

SINGH, L., LEWIS, A.S., FIELD, M.J., HUGHES, J. & WOODRUFF, G.N. (1991). Evidence for an involvement of the brain cholecystokinin B receptor in anxiety. *Proc. Natl. Acad. Sci. U.S.A.*, **88**, 1130–1133.

SHIPPENBERG, T.S., BALS-KUBIK, R. & HERZ, A. (1987). Motivational properties of opioids: evidence that an activation of δ-receptors mediates reinforcement processes. *Brain Res.*, **436**, 234–239.

TOGERSEN, S. (1983). Genetic factors in anxiety disorders. *Arch. Gen. Psychiatry*, **40**, 1085–1089.

WIERTELAK, E.P., MAIER, S.F. & WATKINS, L.R. (1992). Cholecystokinin antianalgesia: safety cues abolish morphine analgesia. *Science*, **256**, 830–833.

WIESENFELD-HALLIN, Z., XU, X.-J., HUGHES, J., HORWELL, D.C. & HÖKFELT, T. (1990). PD 134308, a selective antagonist of cholecystokinin type B receptor, enhances the analgesic effect of morphine and synergistically interacts with intrathecal galanin to depress spinal nociceptive reflexes. *Proc. Natl. Acad. Sci. U.S.A.*, **87**, 7105–7109.

WILLNER, P. (1990). Animal models of depression: an overview. *Pharmacol. Ther.*, **45**, 425–455.

WISE, R.A. (1983). Brain neuronal systems mediating reward processes. In *Neurobiologie of Opiate Reward Processes*. ed. Smith, J.E. & Lane, J.D. pp. 405–437. Elsevier/North Holland Biomedical Press, Amsterdam.

WOLF, P., OLPE, H.R., AVRITH, D. & HAAS, H.L. (1978). GABAergic inhibition of neurons in the ventral tegmental area. *Experientia*, **34**, 73–74.

WOOD, P.L. (1983). Opioid regulation of CNS dopaminergic pathways: a review of methodology, receptor types, regional variations and species differences. *Peptides*, **4**, 595–601.

(Received August 9, 1993
Revised November 5, 1993
Accepted November 24, 1993)

Br. J. Pharmacol. (1994), **111**, 961–967 © Macmillan Press Ltd, 1994

Inhibition of nitric oxide biosynthesis and carotid arteriovenous anastomotic shunting in the pig

[2]E. Marcel van Gelderen & [1]Pramod R. Saxena

Department of Pharmacology, Cardiovascular Research Institute 'COEUR', Faculty of Medicine and Health Sciences, Erasmus University Rotterdam, P.O. Box 1738, 3000 DR Rotterdam, The Netherlands

1 The role of nitric oxide (NO) biosynthesis in the regulation of blood flow through arteriovenous anastomoses was evaluated in the carotid circulation of the anaesthetized pig. For this purpose, the effect of intracarotid (i.c.) administration of the NO synthase inhibitor, N^G-nitro-L-arginine methyl ester (L-NAME; 0.1, 0.3 and 1.0 mg kg^{-1}; $n = 6$) or saline ($n = 6$) was studied on the distribution of common carotid blood flow, using the radioactive microsphere method.

2 Apart from the highest dose, L-NAME caused no major changes in the systemic haemodynamic variables. Both cardiac output and systemic vascular conductance were reduced by L-NAME (1 mg kg^{-1}), being reversed partly by L-arginine (100 mg kg^{-1}, i.c.). In both groups, L-arginine slightly reduced mean arterial blood pressure.

3 Total common carotid artery blood flow as well as its distribution over the capillary and arteriovenous anastomotic fraction remained stable after saline injection. In contrast, L-NAME caused a dose-dependent decline in common carotid artery blood flow and conductance and this decline was confined entirely to its arteriovenous anastomotic part.

4 Subsequent intracarotid injection of L-arginine (100 mg kg^{-1}) reversed the reduction in total carotid conductance almost completely and that in the arteriovenous anastomotic region partially. Additionally, L-arginine increased capillary conductance significantly in the L-NAME – as well as the saline-treated animals.

5 These results indicate that the L-arginine-NO pathway contributes little to the regulation of tissue perfusion in the porcine carotid circulation. In contrast, NO seems to play an important role in shunting arterial blood through arteriovenous anastomoses in the anaesthetized pig.

Keywords: Arteriovenous anastomoses; endothelium; N^G-nitro-L-arginine methyl ester; nitric oxide; nitrite; blood flow in pig

Introduction

Arteriovenous anastomoses have been found in animals and man, although their precise physiological function is not yet fully understood. Cutaneous arteriovenous anastomoses may be implicated in the regulation of the body temperature and blood pressure (Hales & Molyneux, 1988). Furthermore, dilatation of cranial arteriovenous anastomoses has been proposed to contribute to the pathogenesis of migraine headache (Heyck, 1969; Saxena, 1978; 1990).

Little is known of the mechanisms involved in opening arteriovenous anastomoses, which are normally under a constrictor tone. However, for several reasons nitric oxide (NO), which is formed from L-arginine by the calcium/calmodulin dependent enzyme NO-synthase (Palmer *et al.*, 1988; Bredt & Snyder, 1990; Förstermann *et al.*, 1991), may be a potential candidate: (i) as indicated by the inhibition of NO biosynthesis using N^G-nitro-L-arginine methyl ester (L-NAME), continuous production of NO apparently contributes to the regulation of arterial blood pressure and tissue perfusion (Gardiner *et al.*, 1990; Rees *et al.*, 1990; Van Gelderen *et al.*, 1991); (ii) compounds that act via the NO system (e.g. nitroglycerin, isosorbide mononitrate) cause headache as well as temporal artery dilatation in man (Iversen, 1992; Iversen *et al.*, 1992); and (iii) we have recently found that systemic administration of L-NAME in anaesethetized pigs decreased the number of microspheres detected in the lungs after left atrial injection (i.e. bronchial plus systemic arteriovenous anastomotic blood flow); however, in these experiments cardiac output was also concomitantly reduced (Van Gelderen *et al.*, 1993).

The present investigation was devoted to study the effect of L-NAME, administered directly into the common carotid artery to avoid changes in cardiac output, on the distribution of the common carotid artery blood flow into arteriovenous and capillary (tissue) parts in the anaesthetized pig. Furthermore, jugular venous nitrite content was analysed to establish whether the inhibition of NO biosynthesis is reflected by a reduction in plasma nitrite (NO_2) and nitrate (NO_3) levels *in vivo*; NO is rapidly decomposed to finally yield nitrite and nitrate, both detected in biological fluids (Green *et al.*, 1982; Furchgott *et al.*, 1990; Kelm & Schrader, 1990). Preliminary data from the present investigation were presented at the winter meeting of the British Pharmacological Society (Van Gelderen & Saxena, 1993).

Methods

General

Twelve domestic pigs (Yorkshire x Landrace; 15–18 kg) were anaesthetized with azaperone (120 mg, i.m.) and metomidate (150 mg, i.v.), intubated and connected to a respirator (Bear 2E, BeMeds AG, Baar, Switzerland) for intermittent positive pressure ventilation with a mixture of room air and oxygen. Arterial blood gas values were kept within physiological range (pH 7.39–7.49; P_{CO_2} 37–44; P_{O_2} 100–130) by adjusting oxygen supply, respiratory rate and tidal volume. Anaesthesia was maintained by continuous i.v. infusion of pentobarbitone sodium (20 mg kg^{-1} h^{-1} during the first hour followed by 12 mg kg^{-1} h^{-1}) in the right femoral vein. A catheter was introduced into the aortic arch via the left femoral artery, connected to a pressure transducer (Statham P23, Hato Rey, Puerto Rico) for measurement of arterial blood pressure and blood sample withdrawal to determine blood gases (ABL-510, Radiometer, Copenhagen, Denmark). Cardiac output

[1] Author for correspondence.
[2] Author for reprint requests.

and pulmonary arterial blood pressure were measured with a 6F-Swan-Ganz thermodilution catheter (Corodyn, Braun Melsungen AG, Melsungen, Germany) introduced into the pulmonary artery via the left femoral vein and connected to a cardiac output computer (WTI, Rotterdam, The Netherlands) as well as to a pressure transducer. Mean arterial (MAP) and mean pulmonary artery (MPAP) pressures were calculated from respective systolic (SBP) and diastolic (DBP) blood pressures as: MAP or MPAP = DBP + (SBP-DBP)/3. Heart rate was counted from the blood pressure signals. Systemic and pulmonary vascular conductances were calculated by dividing cardiac output by MAP and MPAP, respectively, with the assumption that the pulmonary capillary wedge pressure remained stable throughout the experiment. The right common carotid artery was dissected free and the total carotid blood flow at the ipsilateral side was measured with a flow probe (internal diameter: 2.5 or 3 mm) connected to a sine-wave electromagnetic flow meter (Transflow 600-system, Skalar, Delft, The Netherlands). Two hubless needles (external diameter 0.5 mm), connected to polyethylene tubing, were inserted into the common carotid artery against the direction of the blood flow for administration of radioactive microspheres or drugs. The right jugular vein was cannulated in order to collect venous blood samples to determine venous blood gases and to analyse nitrite levels. All catheters were filled with a heparin sodium solution (80 iu ml^{-1}) to prevent blood clotting. During the experiment, body temperature was kept above 37°C and physiological saline was infused to compensate for fluid loss. The animals were allowed to stabilize for at least 45 min before the start of experiments.

Distribution of the common carotid blood flow

The distribution of the common carotid blood flow as measured by repeated injections of radioactive microspheres (mean ± s.d. diameter: 15 ± 1 μm; NEN Company, Dreieich, Germany) with different labels (^{141}Ce, ^{113}Sn, ^{103}Ru, ^{95}Nb or ^{46}Sc) (Johnston & Saxena, 1978). A suspension of approximately 250,000 microspheres was vortexed before each measurement and injected into the common carotid artery against the direction of the blood flow to ensure uniform mixing. At the end of the experiment the animals were killed and the heart, kidneys, lungs and the different cranial tissues were dissected out, weighed and put in vials. The radioactivity in these vials was counted for 10 min in a gamma-scintillation counter (Packard, Minaxi Autogamma 5000) using suitable windows for discriminating between the different isotopes.

Tissue blood flow (capillary blood flow) was calculated by multiplying the ratio between tissue radioactivity and the total radioactivity with the total carotid blood flow at the time of injection. Since radioactivity was absent in the heart and kidneys, all radioactive microspheres reaching the venous side of the circulation had passed through arteriovenous anastomoses to be ultimately sieved in the lungs. Therefore, the amount of radioactivity in the lungs served as an index for the arteriovenous anastomotic fraction of the common carotid blood flow.

Nitrite analysis

The nitrite content of venous blood samples, withdrawn from the ipsilateral jugular vein, was measured by a modification of the colorimetric procedure using the Griess reagent (0.5% sulphanilamide with 0.05% N-(naphthyl)-ethylenediamine in 2% H_3PO_4) (Green *et al.*, 1982). This assay is based on the diazotization of a sulphanilamide by nitrite and a subsequent coupling with N-(naphthyl)-ethylenediamine to yield a azochromophore which can be detected spectrophotometrically. Briefly, following centrifugation 150 μl of the supernatant was mixed with an equal amount of the Griess reagent in a 96-wells plate and incubated for 10 min at room temperature. Extinction was measured at 540 nm using a microplate reader (BIORAD, Model 3550) against a blank containing sulphanilamide. Sample nitrite concentration was calculated from a standard absorption curve constructed with several concentrations of sodium nitrite. Since nitrite is converted rapidly to nitrate in the presence of oxygen, samples were analysed immediately after blood withdrawal.

Additionally, total nitrite and nitrate content in deproteinized samples was measured using Griess reagent following reduction of nitrates with a *Klebsiella penumoniae* suspension (BBD 900990, RIVM-Pharmacology, Bilthoven, The Netherlands) into nitrites, detected by measuring the absorbance at 540 nm with a spectrophotometer (Perkin-Elmer lambda 15 UV/VIS) against a blank (Phizackerley & Al-Dabbagh, 1983).

Experimental protocol

After the stabilization period the animals were randomly assigned to either the treatment or control group, finally consisting of six animals each. At the start of the experiments, baseline haemodynamic parameters, venous nitrite levels, blood gases as well as the distribution of the common carotid blood flow was measured. Thereafter, the first group was treated with three consecutive doses of L-NAME (0.1, 0.3 and 1.0 mg kg^{-1}, i.c.), whereas an equal volume of saline was injected three times into the control animals group. In both groups, L-arginine (100 mg kg^{-1}, i.c.) was injected after the last dose of L-NAME or saline. Ten minutes after each dose all parameters were reassessed and blood samples collected.

Data presentation and analysis

All data, calculated with a personal computer (Olivetti PCS 286) using a set of specially developed computer programmes (Saxena *et al.*, 1980), are presented in the text as mean ± s.e.mean. The effect of treatment was analysed in each group by a repeated measurement of analysis of variance. When the samples represented different populations, the values after the different treatments were compared to baseline values by use of a Duncan's new multiple range test. Subsequently, the changes to baseline values among the two groups were tested using a Student's t test. Statistical significance was accepted at a level of $P \leqslant 0.05$.

Chemicals

The chemicals used in this study were: azaperone, metomidate (both from Janssen Pharmaceutica, Beerse, Belgium), L-arginine, N-(naphthyl)-ethylenediamine, N^G-nitro-L-arginine methyl ester (L-NAME), sulphanilamide (All from Sigma Chemical Co., St. Louis, U.S.A.), pentobarbitone sodium (Narcovet, Apharmo, Arnhem, The Netherlands) and heparin sodium (Thromboliquine, Organon Teknika B.V., Boxtel, The Netherlands). Both L-arginine and L-NAME were dissolved in saline. All doses refer to their respective salts.

Results

Systemic haemodynamics

The systemic haemodynamic variables in both groups at baseline, followed by either saline or L-NAME (0.1, 0.3 and 1.0 mg kg^{-1}, i.c.), and L-arginine (100 mg kg^{-1}, i.c.) are depicted in Table 1. There were no significant differences between the two groups in the systemic haemodynamic values at baseline, and no major changes were observed in the saline-treated animals. L-NAME also did not significantly affect heart rate or mean arterial blood pressure but after the highest dose, pulmonary artery pressure increased (18 ± 5%) and cardiac output decreased (− 20 ± 3%) significantly. Consequently, the calculated systemic (21 ± 6%) and pulmonary

Table 1 Systemic haemodynamic variables measured at baseline and after intracarotid injections of saline (control; $n = 6$) or N^G-nitro-L-arginine methyl ester (L-NAME) ($n = 6$), followed by L-arginine (100 mg kg^{-1})

		Saline or L-NAME (mg kg^{-1})			
	Baseline	0.1	0.3	1.0	*L-Arginine*
HR (beats min^{-1})					
Saline	93 ± 7	91 ± 6	91 ± 6	91 ± 6	91 ± 6
L-NAME	104 ± 5	102 ± 5	100 ± 6	94 ± 3	92 ± 4
MAP (mmHg)					
Saline	96 ± 5	95 ± 7	94 ± 6	90 ± 5	82 ± 4†
L-NAME	100 ± 2	100 ± 5	104 ± 6	109 ± 8	91 ± 6†
MPAP (mmHg)					
Saline	21.5 ± 1.0	21.7 ± 0.9	23.2 ± 1.3	22.2 ± 1.6	21.5 ± 1.3
L-NAME	20.7 ± 0.5	21.3 ± 0.4	23.0 ± 0.7	24.5 ± 1.4*	21.2 ± 0.7†
CO (l min^{-1})					
Saline	2.01 ± 0.2	1.94 ± 0.2	1.90 ± 0.2	1.83 ± 0.1	1.86 ± 0.1
L-NAME	2.10 ± 0.2	1.97 ± 0.2	1.83 ± 0.1	1.68 ± 0.1*	1.80 ± 0.1
SVC (ml min^{-1} mmHg^{-1})					
Saline	21.3 ± 2.7	20.9 ± 2.2	20.4 ± 1.7	20.7 ± 1.7	22.7 ± 1.1
L-NAME	21.1 ± 1.9	19.6 ± 1.4	17.7 ± 1.6	16.2 ± 1.0*	19.9 ± 0.5†
PVC (ml min^{-1} mmHg^{-1})					
Saline	96.3 ± 14	89.6 ± 7.0	81.8 ± 3.5	84.0 ± 7.2	87.0 ± 4.1
L-NAME	102.5 ± 10	92.6 ± 9.8	80.7 ± 7.0	70.6 ± 8.9*	84.9 ± 5.3

Data are mean ± s.e.mean. *$P < 0.05$ versus baseline; †$P < 0.05$ L-arginine versus L-NAME (1.0 mg kg^{-1}) or saline. HR, heart rate; MAP, mean arterial blood pressure; MPAP, mean pulmonary artery pressure; CO, cardiac output; SVC, systemic vascular conductance; PVC, pulmonary vascular conductance.

(37 ± 7%) vascular conductances were significantly decreased at the highest dose of L-NAME (1 mg kg^{-1}). L-Arginine (100 mg kg^{-1}, i.c.) reversed the L-NAME-induced increase in mean pulmonary artery pressure as well as the reduction in systemic vascular conductance, and it also moderately lowered mean arterial blood pressure in both groups.

Carotid haemodynamics

As shown in Figure 1, no significant effects were observed in either total carotid blood flow or its distribution in saline-treated animals. In contrast, L-NAME caused a dose-dependent decline in total common carotid artery blood flow (maximum change: − 37 ± 3%). This effect was confined entirely to the arteriovenous anastomotic part with little change in the capillary part. The effects of L-NAME were partially reversed by L-arginine.

The effects of saline and L-NAME on carotid vascular bed conductance are shown in Figure 2. While no changes were observed with saline, intracarotid injections of the three consecutive doses of L-NAME (0.1 to 1.0 mg kg^{-1}) elicited dose-dependent decreases in total carotid conductance; the maximum change following the highest dose was − 41 ± 4%. Coincident with this reduction, a decrease in arteriovenous anastomotic conductance was observed (− 64 ± 2%), whereas capillary conductance was unaffected. Subsequent intracarotid injection of L-arginine (100 mg kg^{-1}) reversed the reduction in total carotid conductance almost completely (93 ± 16%) and the arteriovenous anastomotic conductance partially (50 ± 6%). Additionally, L-arginine increased capillary conductance significantly in the L-NAME-treated animals (+ 50 ± 18%), whereas in the saline-treated animals the conductance was increased when compared to baseline (+ 55 ± 18%; Figure 2).

Regional carotid blood flow

Although L-NAME failed to alter capillary blood flow, tissue blood flow to the eyes was reduced by L-NAME (0.3 and 1.0 mg kg^{-1}); the maximum changes observed from baseline (21 ± 4 ml min^{-1} 100 g^{-1}) were 52 ± 7% and 43 ± 17%, respectively. No significant changes were observed in all other dissected extracerebral tissues. L-Arginine restored blood flow to the eyes (16 ± 2 ml min^{-1} 100 g^{-1}). As depicted in Figure 3, total brain flow increased following L-NAME (261 ± 106%)

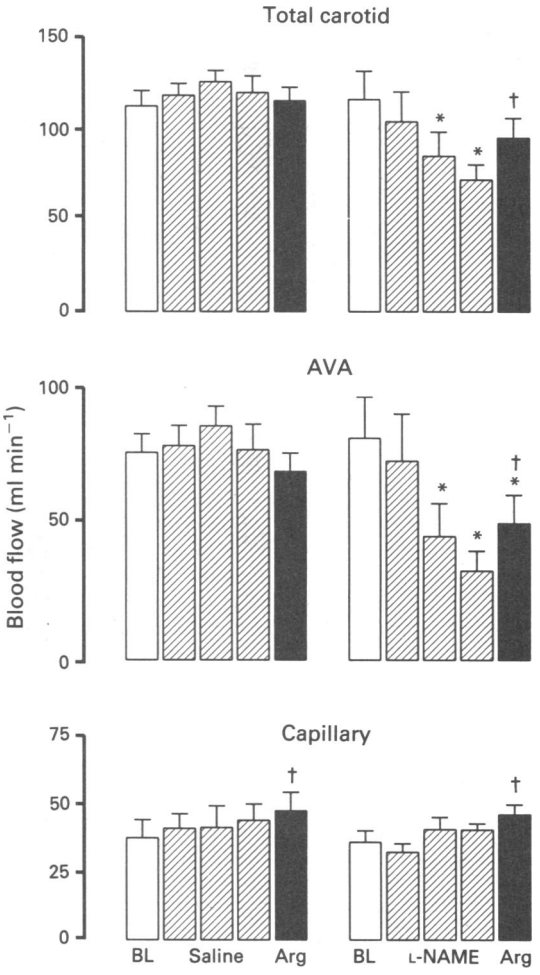


Figure 1 Total carotid, arteriovenous (AVA) and capillary blood flow at baseline (BL), after the three intracarotid injections with either saline (left panels; $n = 6$) or N^G-nitro-L-arginine methyl ester (L-NAME) (right panels; 0.1, 0.3 and 1.0 mg kg^{-1}; $n = 6$) and following L-arginine (Arg, 100 mg kg^{-1}; solid columns). In each set of panels, the hatched columns represent three increasing doses of saline or L-NAME. Values are given as mean ± s.e.mean. †$P < 0.05$ versus BL; *$P < 0.05$ versus saline.

and this was unaffected by L-arginine. A further subdivision of the brain revealed a similar increase in all parts, also unaffected by L-arginine.

Similarly, L-NAME failed to alter total capillary conductance, but reduced vascular conductance in the eyes significantly by 54 ± 6% (baseline: 1.6 ± 0.3 ml min^{-1} mmHg × 100) following L-NAME (0.3 and 1.0 mg kg^{-1}), whereas no significant changes were observed in all other dissected extracerebral tissues. L-Arginine reversed the vascular conductance in the eyes (1.3 ± 0.2 ml min^{-1} mmHg^{-1} × 100). Furthermore, as shown in Figure 4, total brain conductance was enhanced by L-NAME (maximum: 212 ± 77%), which was unaffected by L-arginine. A further subdivision of the brain revealed a similar increase in all parts, also being unaffected by L-arginine (Figure 4).

Arteriovenous oxygen saturation difference and nitrite content

In both groups arterial oxygen tension and carbon dioxide tension remained stable throughout the experiments. The difference in arteriovenous oxygen saturation increased significantly following the highest dose of L-NAME with 92 ± 33%, whereas no changes were observed in the saline-treated control group (Table 2). Similarly, a reduction in venous oxygen pressure was observed with this dose (19 ± 4%), whereas venous carbon dioxide pressure remained stable. At baseline, total venous nitrite and nitrate content was 125 ± 20 nmol ml^{-1} (n = 12, 6 each in saline and L-NAME groups), which remained stable throughout the experiment in both saline and L-NAME-treated animals (Table 2). At baseline, plasma nitrite content varied largely between saline and L-NAME-treated animals; the pooled nitrite level was 3.3 ± 0.6 nmol ml^{-1} (n = 8; 4 each in saline and L-NAME groups). The nitrite level remained essentially unchanged in both groups, though with L-NAME (1.0 mg kg^{-1}; n = 4) some decrease (34 ± 19%) was observed compared to baseline values. L-Arginine restored venous nitrite levels fully in the L-NAME-treated animals, but was without effect in the control group (Table 2).

Discussion

Systemic haemodynamics and distribution of the common carotid blood flow

Using the radioactive microsphere technique, we have previously shown that inhibition of NO biosynthesis in the anaesthetized pig by systemic administration of L-NAME reduces blood flow and vascular conductance in a number of tissues as well as the microsphere content of the lungs (i.e. a sum of bronchial artery and total systemic arteriovenous anastom-

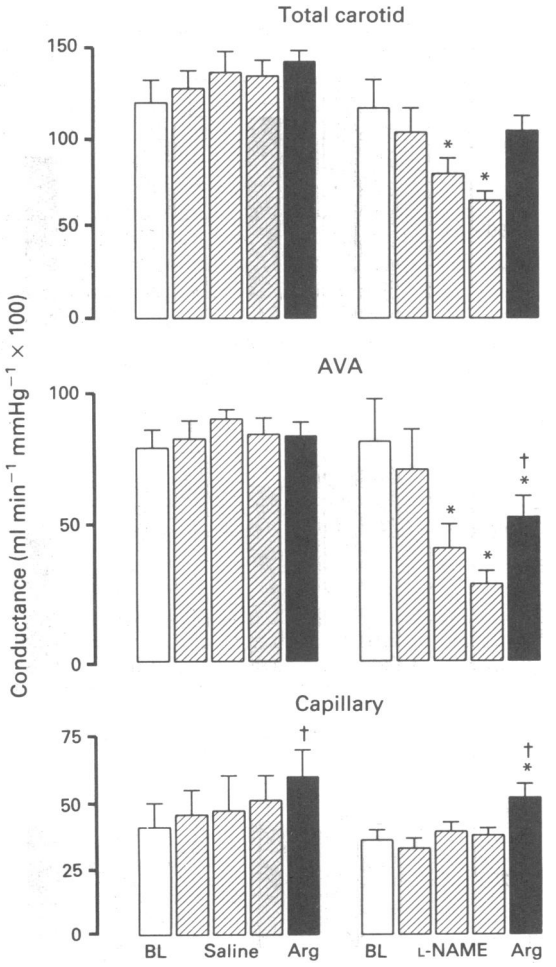


Figure 2 Total carotid, arteriovenous (AVA) and capillary vascular conductance at baseline (BL), after the three intracarotid injections with either saline (left panels; n = 6) or N^G-nitro-L-arginine methyl ester (L-NAME) (right panels: 0.1, 0.3 and 1.0 mg kg^{-1}; n = 6) and following L-arginine (Arg, 100 mg kg^{-1}; solid columns). In each set of panels, the hatched columns represent three increasing doses of saline or L-NAME. Values are given as mean ± s.e.mean. †P < 0.05 versus BL; *P < 0.05 versus saline.

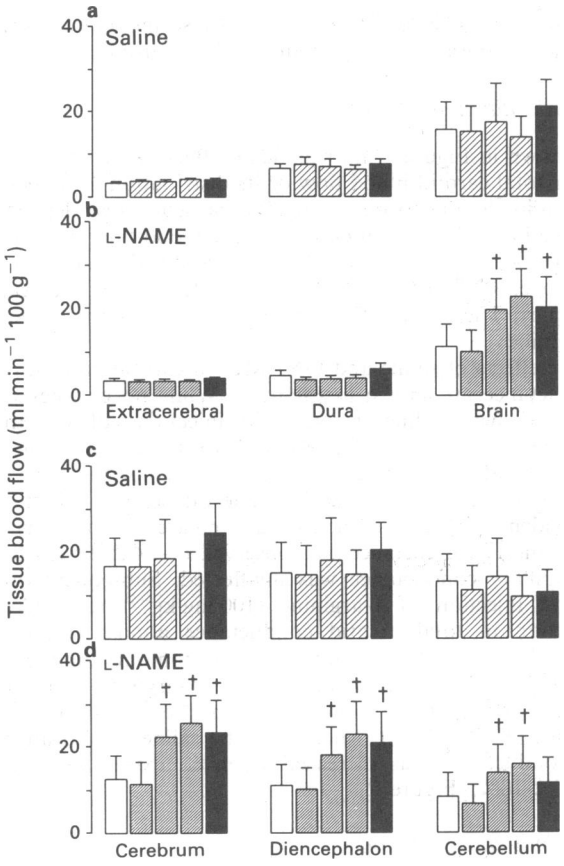


Figure 3 Blood flow distribution to cerebral and extracerebal tissues and to dura mater at baseline (BL), after the three intracarotid injections with either saline (a, c; n = 6) or N^G-nitro-L-arginine methyl ester (L-NAME) b,d; 0.1, 0.3 and 1.0 mg kg^{-1}; n = 6) and following L-arginine (100 mg kg^{-1}; solid columns). In each set of panels, the hatched columns represent three increasing doses of saline or L-NAME. Values are given as mean ± s.e.mean. †P < 0.05 versus BL.

otic flows) (Van Gelderen *et al.*, 1993). In these experiments the reduction in arteriovenous anastomotic blood flow was not unequivocal and, moreover, it was accompanied by a decline in cardiac output. Therefore, in the present study we evaluated the effects of local intra-arterial injections of L-NAME (0.1, 0.3 and 1 mg kg^{-1}) on the porcine carotid vascular bed, where arteriovenous anastomoses are abundant (Saxena & Verdouw, 1982). Indeed, the effects of i.c. application of L-NAME were largely confined to the carotid vascular bed, since little changes in systemic haemodynamic variables were observed; only the highest dose significantly affected mean pulmonary artery pressure, cardiac output and systemic and pulmonary vascular conductances. It is unlikely that these changes were due to the carotid haemodynamic effects of L-NAME and, therefore, it seems that pharmacologically effective concentrations of L-NAME were present in the systemic circulation following its highest i.c. dose. These changes as well as the ability of L-arginine to reverse them are in accordance with our previous observations following systemic administration of L-NAME (Van Gelderen *et al.*, 1993).

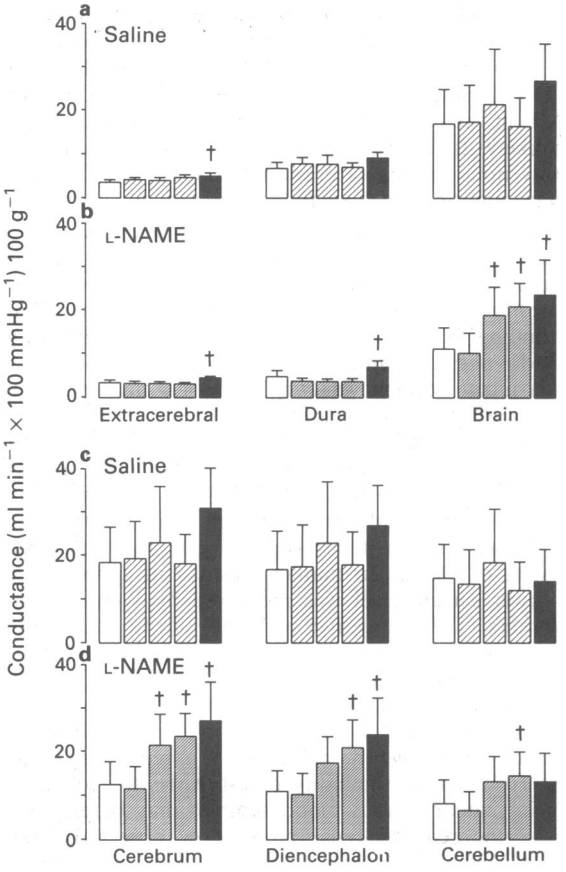


Figure 4 Vascular conductance in cerebral and extracerebral tissues and dura mater at baseline (BL), after the three intracarotid injections with either saline (a,c; $n = 6$) or N^G-nitro-L-arginine methyl ester (L-NAME) (b,d; 0.1 0.3 and 1.0 mg kg^{-1}; $n = 6$) and following L-arginine (100 mg kg^{-1}; solid columns). In each set of panels, the hatched columns represent three increasing doses of saline or L-NAME. Values are given as mean ± s.e.mean. †$P < 0.05$ versus BL.

Independent of any systemic haemodynamic effect, total common carotid blood flow and conductance were decreased by L-NAME. Moreover, it is remarkable that L-NAME caused no change in the capillary part of the carotid circulation and that the reductions in carotid blood flow and conduction were entirely confined to the arteriovenous anastomotic part. The carotid arteriovenous anastomoses have been localized, as demonstrated by simultaneous injections of radioactive microspheres of different sizes, particularly in the skin, ears and dura mater, but also in the eyes and tongue (Saxena & Verdouw, 1985; Den Boer *et al.*, 1992). Although arteriovenous anastomoses are anatomically distinct from the rest of the microvasculature, light and electron microscopy studies have shown the presence of an endothelial layer in both human and rabbit peripheral arteriovenous anastomoses (Gorgas *et al.*, 1977; Fujiwara & Iijima, 1990). The finding that L-arginine, the endogenous substrate for NO-synthase, partly reversed the L-NAME-induced reductions in the carotid arteriovenous anastomotic blood flow and conductance suggests that NO, released from the endothelium, may provide a vasodilator tone in these specialized vessels. Interestingly, it has also been reported that sodium nitroprusside, which releases NO spontaneously (Feelisch & Noack, 1987), tends to increase systemic arteriovenous anastomotic shunt flow in anaesthetized rabbits (Hof & Hof, 1989).

Regional carotid blood flow

Total capillary and extracerebral blood flow were unaffected by L-NAME and L-arginine caused no significant increases in blood flows to or conductances in the various tissues, though

Table 2 Jugular venous blood P_{O_2} (V P_{O_2}), P_{CO_2} (V P_{CO_2}), difference in arterial and jugular venous oxygen saturation (A-V O_2 sat) and jugular venous blood nitrite levels, both as nitrite alone (NO_2) and as nitrate and nitrite (NO_x) measured at baseline and after intracarotid injection of either saline or N^G-nitro-L-arginine methyl ester (L-NAME) and following L-arginine (100 mg kg^{-1})

		Saline or L-NAME (mg kg^{-1})			
	Baseline	0.1	0.3	1.0	*L-Arginine*
VP_{O_2} (mmHg)					
Saline	58 ± 3	56 ± 4	54 ± 5	59 ± 4	53 ± 5
L-NAME	60 ± 5	60 ± 8	57 ± 6	47 ± 3*	50 ± 4
VP_{CO_2} (mmHg)					
Saline	43 ± 2	46 ± 6	45 ± 2	42 ± 2	44 ± 2
L-NAME	43 ± 1	39 ± 2	43 ± 1	45 ± 2	43 ± 2
A-V O_2 sat (%)					
Saline	15.2 ± 3	17.6 ± 4	19.1 ± 4	14.9 ± 3	19.3 ± 4
L-NAME	15.5 ± 4	16.4 ± 6	17.4 ± 5	24.8 ± 4*	18.5 ± 4
NO_x (nmol ml^{-1})					
Saline	134 ± 34	135 ± 28	127 ± 29	120 ± 28	116 ± 23
L-NAME	117 ± 23	93 ± 29	133 ± 32	116 ± 26	128 ± 27
NO_2 (nmol ml^{-1})					
Saline	2.4 ± 1	2.7 ± 1	2.7 ± 1	2.6 ± 1	2.3 ± 1
L-NAME	4.2 ± 1	3.8 ± 1	4.4 ± 1	3.1 ± 1†	3.5 ± 1

Data are means ± s.e.mean.
*$P < 0.05$ versus corresponding saline value; †$P < 0.05$ versus baseline value ($n = 4$).

total capillary conductance was increased by the latter in both saline and L-NAME treated animals. It therefore seems that, unlike the arteriovenous anastomoses, a NO-dependent vascular tone is absent in the capillary part of the cranial circulation of the anaesthetized pig. However, it may be noted that under pentobarbitone anaesthesia, capillary blood flow is approximately one-third of the total carotid blood flow (Saxena & Verdouw, 1982; 1985; Den Boer *et al.*, 1992; present results) and thus the basal release of NO may already be too low to detect a significant decrease.

In contrast to a number of studies which reported a moderate reduction in cerebral blood flow following NO-synthase inhibition, suggesting a basal NO-release in this part of the cranial circulation (Kovách *et al.*, 1992; Prado *et al.*, 1992; Seligsohn & Bill, 1993), in our present experiments L-NAME failed to reduce the cerebral component of carotid blood flow. The absence of an endothelial NO-dependent dilator tone is supported by the recent finding that cultured rat brain microvessel endothelial cells do not show basal release of NO (Durieu-Trautmann *et al.*, 1993). Morever in our experiments, L-NAME increased blood flow to the brain as well as to its constituent parts. This increase cannot be explained by hypercapnia, since arterial carbon dioxide tension remained unchanged. One possible explanation may be a redistribution of blood from the constricted arteriovenous anastomoses towards the cerebral blood vessels. If this is the case, it is of interest that the redistribution is solely confined to the brain tissue without affecting extracerebral blood flow. Since the increase in cerebral blood flow was not susceptible to L-arginine, a NO-independent mechanism seems likely. Finally, the inability of L-NAME to reduce cerebral blood flow is probably not due to the low doses used, since 1 mg kg^{-1} of L-NAME has been shown to block NO-production, as reflected by the increase in mean arterial blood pressure and blood flow reductions in a number of peripheral tissues (e.g. Gardiner *et al.*, 1990; Van Gelderen *et al.*, 1991). In doses up to 30 mg kg^{-1}, both L-NAME and N^G-nitro-L-arginine (L-NOARG) are without effect on brain blood flow (Van Gelderen *et al.*, 1991; Faraci & Heistad, 1992), though in higher doses these agents can significantly reduce cerebral blood flow (Kovách *et al.*, 1992; Prado *et al.*, 1992; Seligsohn & Bill, 1993). It is tempting to speculate that at high doses NO-synthase inhibitors may act at a different site within the brain. Apart from the endothelium, NO-synthase is abundantly present in neural tissues including perivascular nerves surrounding cerebral vessels (Bredt *et al.*, 1990; Nozaki *et al.*, 1993). The activity of these nerves, denoted as nitroxidergic, is inhibited by L-NOARG (Toda *et al.*, 1993) and topical application of N^G-monomethyl L-arginine (L-NMMA) reduces the diameter of cerebral arteries (Faraci, 1991). Hence, it is conceivable that these NO-synthase inhibitors do not readily pass the blood brain barrier and can only inhibit the activity of nitrergic nerves when used in high doses.

Changes in arteriovenous oxygen saturation difference and nitrite content

L-NAME caused an increase in arteriovenous oxygen saturation difference which is in keeping with an effect on arteriovenous anastomoses. A reduced difference between arterial and venous oxygen has been observed by Heyck (1969) in migraine patients and the difference is increased by ergot alkaloids together with a reduction in arteriovenous anastomoses blood flow (Johnston & Saxena, 1978; Den Boer *et al.*, 1992). Since no changes were observed following L-NAME in the capillary fraction of the carotid blood flow, it is unlikely that the increase in percentage difference in arteriovenous oxygen saturation is due to an enhanced oxygen consumption in the capillaries.

Concomitant with the decrement in arteriovenous anastomotic blood flow by L-NAME, a reduction of the plasma nitrite content in jugular venous blood was observed, which was restored by endogenous substrate L-arginine. Though this finding is in line with the proposed competition of L-NAME and L-arginine for the enzyme NO-synthase, basal plasma nitrite content was within the low micromolar range and a marked difference between the saline and L-NAME group was observed. Since NO may bind to haemeproteins or be converted into nitrite and nitrate it is not clear if this is a true reflection of the basal endothelial NO release. In contrast, total nitrite and nitrate content was approximately 40 times higher than nitrite levels and no changes were observed following L-NAME. In human plasma, an approximately 3 fold lower nitrate level was measured by Wennamalm and co-workers (1992), together with low nitrite concentrations. These authors suggested that NO is converted predominantly within red blood cells to nitrate. If this is the case, it is still unclear to what extent endothelial NO release contributes to the plasma nitrate content. Therefore, NO-synthase inhibition may not be *per se* reflected by a reduction in nitrate levels. However, the inability of L-NAME to reduce nitrate levels in jugular venous blood samples may be explained in part by the reduced renal blood flow observed following L-NAME (Van Gelderen *et al.*, 1993). An augmented nitrate elimination due to a reduced renal perfusion may oppose the expected reduction in plasma nitrate levels.

In conclusion, the results of the present investigation indicate that, under resting conditions, the L-arginine-NO pathway has little contribution to the regulation of tissue perfusion within the carotid circulation of the anaesthetized pig. In contrast, NO may participate in controlling shunting of arterial blood through arteriovenous anastomoses.

The authors wish to thank Mr Jan Heiligers for his skilful technical assistance and Dr Jan van Amsterdam and Mr Corné Tak for performing the nitrite analyses.

References

BREDT, D.S., HWANG, P.M. & SNYDER, S.H. (1990). Localization of nitric oxide synthase indicating a neural role for nitric oxide. *Nature*, **347**, 768–770.

BREDT, D.S. & SNYDER, S.H. (1990). Isolation of nitric oxide synthetase, a calmodulin-requiring enzyme. *Proc. Natl. Acad. Sci. U.S.A.*, **87**, 682–685.

DEN BOER, M.O., SOMERS J.A.E. & SAXENA, P.R. (1992). Lack of effect of the antimigraine drugs sumatriptan, ergotamine and dihydroergotamine in the pig on arteriovenous anastomotic shunting in the dura mater of the pig. *Br. J. Pharmacol.*, **107**, 577–583.

DURIEU-TRAUTMANN, O., FÉDÉRICI, C., CRÉMINON, C,. FOIGNANT-CHAVEROT, N., ROUX, F., CLAIRE, M., STROSBERG, A.D. & COURAUD, P.O. (1993). Nitric oxide and endothelin secretion by brain microvessel endothelial cells: regulation by cyclic nucleotides. *J. Cell. Physiol.*, **155**, 104–111.

FARACI, F.M. (1991). Role of endothelium-derived relaxing factor in cerebral circulation: large arteries vs. microcirculation. *Am. J. Physiol.*, **261**, H1038–1042.

FARACI, F.M. & HEISTAD, D.D. (1992). Does basal production of nitric oxide contribute to regulation of brain-fluid balance? *Am. J. Physiol.*, **262**, H340–344.

FEELISCH, M. & NOACK, E. (1987). Nitric oxide (NO) formation from nitrovasodilators occurs independently of haemoglobin or non-heme iron. *Eur. J. Pharmacol.*, **142**, 465–469.

FÖRSTERMANN, U., POLLOCK, J.S., SCHMIDT, H.H.H.W., HELLER, M. & MURAD, F. (1991). Calmodulin-dependent endothelium-derived relaxing factor/nitric oxide synthase is present in the particulate and cytosolic fractions of bovine aortic endothelial cells. *Proc. Natl. Acad. Sci.*, **88**, 1788–1792.

FUJIWARA, T. & IIJIMA, T. (1990). Three-dimensional cytoarchitecture of the media of arteriovenous anastomoses in the rabbit ear. *Am. J. Anat.*, **189**, 253–260.

FURCHGOTT, R.F., JOTHIANANDAN, D. & FREAY, A.D. (1990). Endothelium-derived relaxing factor: some old and new findings. In *Nitric Oxide from L-arginine: a Bioregulatory System*. Ed. Moncada, S. & Higgs, E.A. pp. 5–1). Amsterdam: Elsevier.

GARDINER, S.M., COMPTON, A.M., KEMP, P.A. & BENNETT, T. (1990). Regional and cardiac effects of N^G-nitro-L-arginine methyl ester in conscious, Long Evans rats. *Br. J. Pharmacol.*, **101**, 625–631.

GORGAS, K., BÖCK, P., TISCHENDORF, F. & CURRI, S.B. (1977). The fine structure of human arterio-venous anastomoses (Hoyer-Grosser's organs). *Anat. Embryol.*, **150**, 269–289.

GREEN, L.C., WAGNER, D.W., GLOGOWSKI, J., SKIPPER, P.L., WISHNOK, J.S. & TANNENBAUM, S.R. (1982). Analysis of nitrate, nitrite and [^{15}N] nitrate in biological fluids. *Anal. Biochem.*, **126**, 131–138.

HALES, J.R.S. & MOLYNEUX, G.S. (1988). Control of cutaneous arteriovenous anastomoses. In *Vasodilatation: Vascular Smooth Muscle, Peptides, Autonomic Nerves and Endothelium.* Vanhoutte, P.M. pp. 321–332. New York: Raven Press.

HEYCK, H. (1969). Pathogenesis of migraine. *Res. Clin. Stud. Headache*, **2**, 1–28.

HOF, R.P. & HOF, A. (1989). Differential effects of antihypertensive drugs on nutritive and nonnutritive blood flow in anaesthetized rabbits. *J. Cardiovasc. Pharmacol.*, **13**, 565–571.

IVERSEN, H.K. (1992). N-acetylcysteine enhances nitroglycerin-induced headache and cranial arterial responses. *Clin. Pharmacol. Ther.*, **52**, 125–133.

IVERSEN, H.K., NIELSEN, T.H., GARRE, K., TFELT-HANSEN, P. & OLESEN, J. (1992). Dose-dependent headache response and dilatation of limb and extracranial arteries after three doses of 5-isosorbide-mononitrate. *Eur. J. Clin. Pharmacol.*, **42**, 31–35.

JOHNSTON, B.M. & SAXENA, P.R. (1978). The effect of ergotamine on tissue blood flow and the arteriovenous shunting of radioactive microspheres in the head. *Br. J. Pharmacol.*, **63**, 541–549.

KOVÁCH, A.G.B., SZABÓ, C., BENYÓ, CSÁKI, C., GREENBERG, J.H. & REIVICH, M. (1992). Effects of N^G-nitro-L-arginine and L-arginine on regional cerebral blood flow in the cat. *J. Physiol.*, **449**, 183–196.

KELM, M. & SCHRADER, J. (1990). Control of coronary vascular tone by nitric oxide. *Circ. Res.*, **66**, 1561–1575.

NOZAKI, K., MOSKOWITZ, M.A., MAYNARD, K.I., KOKETSU, N, DAWSON, T.M., BREDT, D.S. & SNYDER, S.H. (1993). Possible origins and distribution of immunoreactive nitric oxide synthase-containing nerve fibers in cerebral arteries. *J. Cereb. Blood Flow Metab.*, **13**, 70–79.

PALMER, R.M.J., ASHTON, D.S. & MONCADA, S. (1988). Vascular endothelial cells synthesize nitric oxide from L-arginine. *Nature*, **333**, 664–666.

PHIZACKERLEY, P.J. & AL-SABBAGH, S.A. (1983). The estimation of nitrate and nitrite in saliva and urine. *Anal. Biochem.*, **131**, 242–245.

PRADO, R., WATSON, B.D., KULUZ, J. & DIETRICH, W.D. (1992). Endothelium-derived nitric oxide synthase inhibition, effects on cerebral blood flow, pial artery diameter and vascular morphology in rats. *Stroke*, **23**, 1118–1124.

REES, D.D., PALMER, R.M.J., SCHULTZ, R., HODSON, H.F. & MONCADA, S. (1990). Characterization of three inhibitors of endothelial nitric oxide synthase *in vitro* and *in vivo*. *Br. J. Pharmacol.*, **101**, 746–752.

SAXENA, P.R. (1978). Arteriovenous shunting and migraine. *Res. Clin. Stud. Headache*, **6**, 89–102.

SAXENA, P.R. (1990). Is there still a case for the shunt hypothesis in migraine? In: *Migraine: A Spectrum of Ideas.* ed. Sandler, M. & Collins, G.M. pp. 191–199. Oxford: Oxford University Press.

SAXENA, P.R., SCHAMHARDT, H.C., FORSYTH, R.P. & LOEVE, J. (1980). Computer programs for the radioactive microsphere technique. *Comp. Programs Biomed.*, **12**, 63–84.

SAXENA, P.R. & VERDOUW, P.D. (1982). Redistribution by 5-hydroxytryptamine of carotid arterial blood at the expense of arteriovenous anastomotic blood flow. *J. Physiol.*, **332**, 501–520.

SAXENA, P.R. & VERDOUW, P.D. (1985). Tissue blood flow and localization of arteriovenous anastomoses in pigs with microspheres of four different sizes. *Pflügers Arch.*, **403**, 128–135.

SELIGSOHN, E.E. & BILL, A. (1993). Effects of N^G-nitro-L-arginine methyl ester on the cardiovascular system of the anaesthetized rabbit and on the cardiovascular response to thyrotropin-releasing hormone. *Br. J. Pharmacol.*, **109**, 1219–1225.

TODA, N., AYAJIKI, K., YOSHIDA, K., KIMURA, H. & OKAMURA, (1993). Impairment by damage of the pterygopalatine ganglion of nitroxidergic vasodilator nerve function in canine cerebral and retinal arteries. *Circ. Res.*, **72**, 206–213.

VAN GELDEREN, E.M., HEILIGERS, J.P.C. & SAXENA, P.R. (1991). Haemodynamic changes and acetylcholine-induced hypotensive responses after N^G-nitro-L-arginine methyl ester in rats and cats. *Br. J. Pharmacol.*, **103**, 1899–1904.

VAN GELDEREN, E.M., DEN BOER, M.O. & SAXENA, P.R. (1993). N^G-nitro-L-arginine methyl ester: systemic and pulmonary haemodynamics, tissue blood flow and arteriovenous shunting in the pig. *Naunyn-Schmied. Arch. Pharmacol.*, **348**, 417–423.

VAN GELDEREN, E.M. & SAXENA, P.R. (1993). Nitric oxide synthesis inhibition and arteriovenous anastomoses shunting in the pig. *Br. J. Pharmacol.*, **108**, 7P.

WENNMALM, Å., BENTHIN, G. & PETERSSON, A.-S. (1992). Dependence of the metabolism of nitric oxide (NO) in healthy human whole blood on the oxygenation of its red cell haemoglobin. *Br. J. Pharmacol.*, **106**, 507–508.

(Received September 13, 1993
Revised November 17, 1993
Accepted November 24, 1993)

 © Macmillan Press Ltd, 1994

Erratum

Br. J. Pharmacol. (1993) **110**, 1483–1490

R.G. Pertwee, L.A. Stevenson & G. Griffin. Cross-tolerance between delta-9-tetrahydrocannabinol and the cannabimimetic agents, CP 55,940, WIN 55,212-2 and anandamide.

In the above article, which appeared in the December issue of the journal, Table 2 was omitted and replaced by a duplication of Table 3.

Table 2 is reproduced here.

Table 2 Effect of various pretreatments with delta-9-tetrahydrocannabinol (delta-9-THC) on the ability of this drug to induce hypothermia by intravenous injection (1.0 mg kg^{-1})

Experiment	*Drug*	*Pretreatment dose* (mg kg^{-1}, i.p.)	*Number of i.p. injections*	*Mean rectal temperature* at −5 min (°C ± s.e.mean)	*Mean rectal temperature* at T1 (°C ± s.e.mean)	*Mean hypothermia* at T1 (°C ± s.e.mean)	T1 (min)
1	Δ^9-THC	20	2	37.39 ± 0.13	37.20 ± 0.20	0.19 ± 0.13††	15
	Tween 80	40	2	37.74 ± 0.18	34.98 ± 0.34**	2.77 ± 0.43	20
2	Δ^9-THC	10	2	37.72 ± 0.29	36.46 ± 0.34*	1.26 ± 0.42†	15
	Tween 80	20	2	38.05 ± 0.11	35.22 ± 0.57**	2.83 ± 0.52	20
3	Δ^9-THC	5	2	37.77 ± 0.13	35.87 ± 0.32**	1.90 ± 0.27††	15
	Tween 80	10	2	37.98 ± 0.12	34.28 ± 0.24**	3.71 ± 0.16	20
4	Δ^9-THC	2	2	37.93 ± 0.15	36.62 ± 0.46*	1.32 ± 0.37	15
	Tween 80	4	2	37.87 ± 0.09	35.55 ± 0.34**	2.32 ± 0.32	20
5	Δ^9-THC	1	2	37.95 ± 0.17	35.95 ± 0.35**	2.00 ± 0.39	20
	Tween 80	2	2	37.85 ± 0.14	35.40 ± 0.35**	2.45 ± 0.31	15
6	Δ^9-THC	20	1	37.94 ± 0.17	35.88 ± 0.40**	2.07 ± 0.26††	15
	Tween 80	40	1	38.00 ± 0.13	34.83 ± 0.11**	3.17 ± 0.22	20
7	Δ^9-THC	10	1	37.62 ± 0.14	36.02 ± 0.48*	1.60 ± 0.40	15
	Tween 80	20	1	37.76 ± 0.13	35.54 ± 0.17**	2.22 ± 0.25	15
8§	Δ^9-THC	20	2	37.66 ± 0.18	37.08 ± 0.20*	0.57 ± 0.15††	10
	Tween 80	40	2	37.87 ± 0.11	35.13 ± 0.37**	2.74 ± 0.37	20

Each mouse received an intravenous injection of delta-9-THC at time zero, 24 h after the final intraperitoneal injection of delta-9-THC or Tween 80. Control animals received the same amount of Tween 80 as delta-9-THC treated animals (see Methods). T1 is the time after intravenous injection of delta-9-THC at which mean hypothermia was maximal. Mean rectal temperature at −5 min has been compared with the corresponding value at T1 min using Student's *t* test for paired data (*$P<0.05$; **$P<0.01$). For each experiment, Student's *t* test for unpaired data has been used to compare the mean hypothermic responses to delta-9-THC of drug and vehicle pretreated groups (†$P<0.05$; ††$P<0.01$). In none of the experiments did the pairs of mean rectal temperature values listed in the −5 min column deviate significantly from each other (Student's *t* test for unpaired data).

§In experiment 8, the mice were exposed to an ambient temperature of 34°C for 3 h immediately after each i.p. pretreatment with delta-9-THC or Tween 80. Groups of six mice were used.

British Journal of Pharmacology

VOLUME 111 (3) MARCH 1994

OBITUARY

G.W. Bisset. Wilhelm Feldberg, CBE, FRS (1900–1993) 649

SPECIAL REPORT

I. Pörsti, A.T. Bara, R. Busse & M. Hecker. Release of nitric oxide by angiotensin-(1-7) from porcine coronary endothelium: implications for a novel angiotensin receptor 652

PAPERS

H. Moritoki, T. Hisayama, S. Takeuchi, W. Kondoh & M. Imagawa. Relaxation of rat thoracic aorta induced by the Ca^{2+}-ATPase inhibitor, cyclopiazonic acid, possibly through nitric oxide formation 655

J. Cuevas & D.J. Adams. Local anaesthetic blockade of neuronal nicotinic ACh receptor-channels in rat parasympathetic ganglion cells 663

Y. Dohi, M. Kojima & K. Sato. Vasorelaxant effect of mexiletine in mesenteric resistance arteries of rats 673

M.K. Herbert & P. Holzer. Interleukin-1β enhances capsaicin-induced neurogenic vasodilatation in the rat skin 681

C.A. Maggi, S. Giuliani & P. Santicioli. Effect of cromakalim and glibenclamide on spontaneous and evoked motility of the guinea-pig isolated renal pelvis and ureter 687

P.B.S. Clarke, M. Reuben & H. El-Bizri. Blockade of nicotinic responses by physostigmine, tacrine and other cholinesterase inhibitors in rat striatum 695

K.K.C. Tan, M.J. Brown, J. Longmore, C. Plumpton & R.G. Hill. Demonstration of the neurotransmitter role of calcitonin gene-related peptides (CGRP) by immunoblockade with anti-CGRP monoclonal antibodies 703

C. Jiang & P. Collins. Inhibition of hypoxia-induced relaxation of rabbit isolated coronary arteries by N^G-monomethyl-L-arginine but not glibenclamide 711

O. Pérez, C. Valenzuela, E. Delpón & J. Tamargo. Class I and III antiarrhythmic actions of prazosin in guinea-pig papillary muscles 717

J.R. Purkiss, G.F. Wilkinson & M.R. Boarder. Differential regulation of inositol 1,4,5-trisphosphate by co-existing P_{2Y}-purinoceptors and nucleotide receptors on bovine aortic endothelial cells 723

D.M. Pollock & T.J. Opgenorth. ET_A receptor-mediated responses to endothelin-1 and big endothelin-1 in the rat kidney 729

G.J. Molderings, E. Colling, J. Likungu, J. Jakschik & M. Göthert. Modulation of noradrenaline release from the sympathetic nerves of the human saphenous vein and pulmonary artery by presynaptic EP_3- and DP-receptors 733

S. Meini, R. Patacchini &. C.A. Maggi. Tachykinin NK_1 receptor subtypes in the rat urinary bladder 739

S.S. Kelly & C.B. Ferry. The origin of the effects of an anticholinesterase on the latencies of action potentials in mouse skeletal muscles 747

J.M. Hunt, R.S. Redman & E.M. Silinsky. Reduction by intracellular calcium chelation of acetylcholine secretion without occluding the effects of adenosine at frog motor nerve endings 753

A. Floch, V. Fardin & I. Cavero. Characterization of NK_1 and NK_2 tachykinin receptors in guinea-pig and rat bronchopulmonary and vascular systems 759

J. Cortijo, C.M. Sanz, V. Villagrasa, E.J. Morcillo & R.C. Small. The effects of phorbol 12,13-diacetate on responses of guinea-pig isolated trachea to methylxanthines, isoprenaline and ryanodine 769

C.M. Yang, Y.-L. Yo, J.-T. Hsieh & R. Ong. 5-Hydroxytryptamine receptor-mediated phosphoinositide hydrolysis in canine cultured tracheal smooth muscle cells 777

R. Atcheson, D.G. Lambert, R.A. Hirst & D.J. Rowbotham. Studies on the mechanism of [^{3}H]-noradrenaline release from SH-SY5Y cells: the role of Ca^{2+} and cyclic AMP 787

C.J. Bailey & K.J. Mynett. Insulin requirement for the antihyperglycaemic effect of metformin 793

G.A. Kennett, M.D. Wood, A. Glen, S. Grewal, I. Forbes, A. Gadre & T.P. Blackburn. *In vivo* properties of SB 200646A, a $5\text{-}HT_{2C/2B}$ receptor antagonist 797

D. Bowie & T.G. Smart. Species-dependent functional properties of non-NMDA receptors expressed in *Xenopus laevis* oocytes injected with mammalian and avian brain mRNA 803

M.M. Teixeira, S. Reynia, M. Robinson, A. Shock, T.J. Williams, F.M. Williams, A.G. Rossi & P.G. Hellewell. Role of CD18 in the accumulation of eosinophils and neutrophils and local oedema formation in inflammatory reactions in guinea-pig skin 811

A.M. Elhawary & C.C.Y. Pang. α_{1b}-Adrenoceptors mediate renal tubular sodium and water reabsorption in the rat 819

M.G. Persson, P. Agvald & L.E. Gustafsson. Detection of nitric oxide in exhaled air during administration of nitroglycerin *in vivo* 825

W.J. Wieczorek & Z.L. Kruk. Differential action of (+)-amphetamine on electrically evoked dopamine overflow in rat brain slices containing corpus striatum and nucleus accumbens 829

M. Santiago, A. Machado & J. Cano. Effect of L-arginine/nitric oxide pathway on MMP^+-induced cell injury in the striatum of rats 837

A. Barber, G.D. Bartoszyk, H.E. Griener, F. Mauler, R.D. Murray, C.A. Seyfried, M. Simon, R. Gottschlich, J. Harting & I. Lues. Central and peripheral actions of the novel κ-opioid receptor agonist, EMD 60400 843

P.P. McDonald, S.R. McColl, P. Braquet & P. Borgeat. Autocrine enhancement of leukotriene synthesis by endogenous leukotriene B_4 and platelet-activating factor in human neutrophils 852

O.G. García Hermida, T. Fontela, M. Ghiglione & L.O. Uttenthal. Effect of lithium on plasma glucose, insulin and glucagon in normal and streptozotocin-diabetic rats: role of glucagon in the hyperglycaemic response 861

M.N. Sillence & M.L. Matthews. Classical and atypical binding sites for β-adrenoceptor ligands and activation of adenylyl cyclase in bovine skeletal muscle and adipose tissue membranes 866

D.K. Martin, Y. Nakaya, K.R. Wyse & T.J. Campbell. Effects of disopyramide and flecainide on the kinetics of inward rectifier potassium channels in rabbit heart muscle 873

W.-M. Fu & F.-L. Huang. Potentiation by endogenously released ATP of spontaneous transmitter secretion at developing neuromuscular synapses in *Xenopus* cell cultures **880**

A.C. Kappelle, G. Biessels, B. Bravenboer, T. van Buren, J. Traber, D.J. De Wildt & W.H. Gispen. Beneficial effect of the Ca^{2+} antagonist, nimodipine, on existing diabetic neuropathy in the BB/Wor rat **887**

E. Pipili-Synetos, E. Sakkoula, G. Haralabopoulos, P. Andriopoulou, P. Peristeris & M.E. Maragoudakis. Evidence that nitric oxide is an endogenous antiangiogenic mediator **894**

J.C. Ellory, S.J. Culliford, P.A. Smith, the late M.W. Wolowyk & E.E. Knaus. Specific inhibition of Ca-activated K channels in red cells by selected dihydropyridine derivatives **903**

S.-M. Yu, T.-S. Wu & C.-M. Teng. Pharmacological characterization of cinnamophilin, a novel dual inhibitor of thromboxane synthase and thromboxane A_2 receptor **906**

G.J. McLaren, G. Lambrecht, E. Mutschler, H.G. Bäumert, P. Sneddon & C. Kennedy. Investigation of the actions of PPADS, a novel P_{2X}-purinoceptor antagonist, in the guinea-pig isolated vas deferens **913**

G.M. Nichol, G.H. Parsons & K.F. Chung. Effect of sodium metabisulphite on bronchial blood flow in conscious sheep: pharmacological modulation **918**

A.U. Ziganshin, C.H.V. Hoyle, G. Lambrect, E. Mutschler, H.G. Bäumert & G. Burnstock. Selective antagonism by PPADS at P_{2X}-purinoceptors in rabbit isolated blood vessels **923**

M. Gué, C. Gleïzes-Escala, C. Del Rio-Lacheze, J.-L. Junien & L. Buéno. Reversal of CRF- and dopamine-induced stimulation of colonic motility by CCK and igmesine (JO 1784) in the rat **930**

Y. Nakazato, Y. Tani, H. Teraoka, T. Sugawara, T. Asano, T. Ohta & S. Ito. Inhibitory effects of caffeine on secretagogue-induced catecholamine secretion from adrenal chromaffin cells of the guinea-pig **935**

W. Nörenberg, J.M. Langosch, P.J. Gebicke-Haerter & P. Illes. Characterization and possible function of adenosine 5′-triphosphate receptors in activated rat microglia **942**

M.A. Shuker, F. Bowser-Riley & S.N. Davies. Possible NMDA antagonist properties of drugs that affect high pressure neurological syndrome **951**

M. Derrien, C. Durieux & B.P. Roques. Antidepressant-like effects of CCK_B antagonists in mice: antagonism by naltrindole **956**

E.M. van Gelderen & P.R. Saxena. Inhibition of nitric oxide biosynthesis and carotid arteriovenous anastomotic shunting in the pig **961**

ERRATUM **968**

Br. J. Pharmacol. (1993), **110,** 1483–1490

R.G. Pertwee, L.A. Stevenson & G. Griffin. Cross-tolerance between delta - 9 - tetrahydrocannabinol and the cannabimimetic agents, CP 55,940, WIN 55,212-2 and anandamide

BRITISH JOURNAL OF PHARMACOLOGY

The *British Journal of Pharmacology* welcomes contributions in all fields of experimental pharmacology including neuroscience, biochemical, cellular and molecular pharmacology. The Board of Editors represents a wide range of expertise and ensures that well-presented work is published as promptly as possible, consistent with maintaining the overall quality of the journal.

Edited for the British Pharmacological Society by

A.T. Birmingham
(Chairman)

R.W. Horton **W.A. Large**
(Secretaries)

Editorial Board

J.A. Angus *Melbourne, Australia*
M.L.J. Ashford *Cambridge*
G.W. Bennett *Nottingham*
W.C. Bowman *Glasgow*
N.G. Bowery *London*
Alison F. Brading *Oxford*
S.D. Brain *London*
K.D. Butler *Horsham*
M. Caulfield *London*
R. Chess-Williams *Sheffield*
M.K. Church *Southampton*
T. Cocks *Melbourne, Australia*
S.J. Coker *Liverpool*
R.A. Coleman *Ware*
Helen M. Cox *London*
A.J. Cross *London*
V. Crunelli *Cardiff*
T.C. Cunnane *Oxford*
F. Cunningham *London*
A. Dray *London*
J.R. Docherty *Dublin*
J.M. Edwardson *Cambridge*
P.C. Emson *Cambridge*
W. Feniuk *Cambridge*
J.R. Fozard *Basle, Switzerland*
Allison D. Fryer *Baltimore, USA*
Sheila M. Gardiner *Nottingham*
C.J. Garland *Bristol*
L.G. Garland *Beckenham*
A. Gibson *London*
R. W. Gristwood *Cambridge*
D.W.P. Hay *Philadelphia, USA*
P.G. Hellewell *London*
P.E. Hicks *Edinburgh*
S.J. Hill *Nottingham*
S.M.O. Hourani *Guildford*
J.C. Hunter *Cambridge*
C.C. Jordan *Ware*
D.A. Kendall *Nottingham*
P. Leff *Loughborough*
H.D. Lux *Planegg, Germany*
R. McMillan *Macclesfield*
J. Maclagan *London*
C.A. Maggi *Florence, Italy*
Janice M. Marshall *Birmingham*
G. Martin *Beckenham*
W. Martin *Glasgow*
A. Mathie *London*
D.N. Middlemiss *Harlow*
P.K. Moore *London*
R.J. Naylor *Bradford*
C.D. Nicholson *Oss, The Netherlands*
C.P. Page *London*
A.N. Payne *Beckenham*
F.L. Pearce *London*
J.D. Pearson *London*
A.G. Renwick *Southampton*
M.H.T. Roberts *Cardiff*
C. Robinson *London*
G.J. Sanger *Harlow*
M.A. Simmonds *London*
J.M. Sneddon *Sunderland*
P. Sneddon *Glasgow*
K. Starke *Freiburg, Germany*
R.J. Summers *Melbourne, Australia*
P.V. Taberner *Bristol*
J. Tamargo *Madrid, Spain*
C. Thiemermann *London*
M.D. Tricklebank *Harlow*
M.B. Tyers *Ware*
S.P. Watson *Oxford*
K.J. Watling *Cambridge*
A.H. Weston *Manchester*
B.J.R. Whittle *Beckenham*
Eileen Winslow *Riom, France*
B. Woodward *Bath*
E.H.F. Wong *California, USA*

Corresponding Editors

P.R. Adams *Stony Brook, U.S.A.*
C. Bell *Melbourne, Australia*
F.E. Bloom *La Jolla, U.S.A.*
A.L.A. Boura *Newcastle, Australia*
N.J. Dun *Toledo, U.S.A.*
R.F. Furchgott *New York, U.S.A.*
T. Godfraind *Brussels, Belgium*
S.Z. Langer *Paris, France*
R.J. Miller *Chicago, U.S.A.*
R.C. Murphy *Denver, U.S.A.*
E. Muscholl *Mainz, Germany*
R.A. North *Portland, U.S.A.*
M. Otsuka *Tokyo, Japan*
M.J. Rand *Melbourne, Australia*
S. Rosell *Södertalje, Sweden*
P. Seeman *Toronto, Canada*
L. Szekeres *Szeged, Hungary*
B. Uvnas *Stockholm, Sweden*
P.A. Van Zwieten *Amsterdam, Netherlands*
V.M. Varagič *Belgrade, Yugoslavia*
G. Velo *Verona, Italy*
Wang Zhen Gang *Beijing, China*
M.B.H. Youdim *Haifa, Israel*

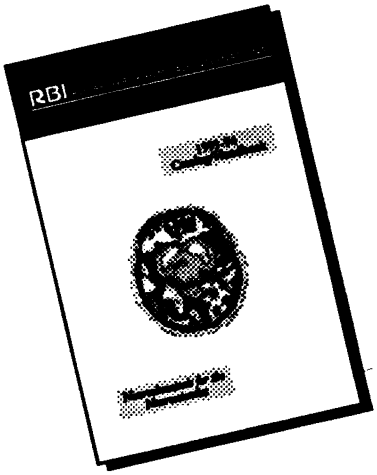
Submission of manuscripts: Manuscripts (two copies) should be sent to The Editorial Office, British Journal of Pharmacology, St. George's Hospital Medical School, Cranmer Terrace, London SW17 0RE.

Authors should consult the Instructions to Authors and the Nomenclature Guidelines for Authors in Vol. **111,** 378–387. These Instructions and Guidelines also appear with the journal Index for Volumes **108–110**, 1993. A checklist of the essential requirements is summarised in each issue of the journal, or as the last page of the issue.

RBI THE RESEARCHER'S GOLD STANDARD

Look here first for new...

- Adenosines/Purinergics
- Adrenergics
- β-Amyloid Proteins
- Benzodiazepines
- Cholecystokinins
- Cholinergics
- Cocaine Receptor Ligands
- Controlled Substances
- Dopaminergics
- Drug Metabolites
- Enzyme Inhibitors
- Excitatory Amino Acids
- GABA-ergics
- Gangliosides
- Histaminergics
- Ion Channel Modulators
- Neuropeptides
- Neurotoxins
- Neurosteroids
- Opioids
- PCP/Sigma Receptor Ligands
- PET/SPECT Agents
- Reference Standards
- Serotonergics
- Signal Transduction Agents
- Tachykinins



Fax or write for our NEW 1993-94 Catalog/Handbook, *Neurochemicals for the Neuroscientist*, listing 1,000 pharmacologically active compounds.

RBI RESEARCH BIOCHEMICALS INTERNATIONAL

One Strathmore Road, Natick, MA 01760 USA • 800-736-3690 • 508-651-8151 • Fax 508-655-1359

Denmark, Roedovre • 044-948822
France, Illkirch • 88-67-14-14
Germany, Köln • 0221-497-2034
Italy, Milano • 02-50-97-720
Japan, Tokyo • 03-5684-1622
Switzerland, Zurich • 01-312-2124
Taiwan, Taipei • 2-595-9225
United Kingdom, St. Albans • 0727-8-41414

The *British Journal of Pharmacology* is published monthly by the Scientific & Medical Division, Macmillan Press Ltd.

The journal is covered by *Current Contents*, *Excerpta Medica* and *Index Medicus*.

All business correspondence and reprint requests should be addressed to the Scientific & Medical Division, Macmillan Press Ltd., Houndmills, Basingstoke, Hampshire RG21 2XS, UK. Telephone: (0256) 29242; Fax: (0256) 810526.

Enquiries concerning advertising space or rates should be addressed to: Michael Rowley, Advertisement Manager, Macmillan Press Ltd., 4 Little Essex Street, London WC2R 3LF. Telephone: 071 836 6633; Fax: 071 379 0820.

Annual subscription prices for 1993 EC £540, elsewhere £595/US$950 (sterling rate is definitive). Orders must be accompanied by remittance. Cheques should be made payable to Macmillan Press, and sent to: Macmillan Press Ltd., Subscription Department, Brunel Road, Houndmills, Basingstoke, Hampshire RG21 2XS, UK.
Overseas subscribers may make payments into UK Post Office Giro Account No. 5192455. Full details must accompany the payment.

British Journal of Pharmacology (ISSN 0007–1188) is published monthly by Macmillan Publishers Ltd, c/o Mercury Airfreight International Ltd, 2323 Randolph Avenue, Avenel, NJ 07001, USA. Subscription price is $950.00 per annum. 2nd class postage is paid at Rahway NJ. *Postmaster*: send address corrections to Macmillan Publishers, c/o Mercury Airfreight International Ltd, 2323 Randolph Avenue, Avenel NJ 07001.

All rights of reproduction are reserved in respect of all papers, articles, illustrations, etc., published in this journal in all countries of the world.

All material published in this journal is protected by copyright, which covers exclusive rights to reproduce and distribute the material. No material published in this journal may be reproduced or stored on microfilm or in electronic, optical or magnetic form without the written authorisation of the Publisher.

Authorization to photocopy items for internal or personal use, or the internal or personal use of specific clients, is granted by Macmillan Press Ltd for libraries and other users registered with the Copyright Clearance Center (CCC) Transactional Reporting Service, provided that the base fee of $9.00 per copy is paid directly to CCC, 21 Congress St., Salem, MA 01970, USA.

Apart from any fair dealing for the purposes of research or private study, or criticism or review, as permitted under the Copyright, Designs and Patent Act 1988, this publication may be reproduced, stored or transmitted, in any form or by any means, only with the prior permission in writing of the publishers, or in the case of reprographic reproduction, in accordance with the terms of licences issued by the Copyright Licensing Agency.

© The British Pharmacological Society & Macmillan Press Ltd, 1994.

ISSN 0007–1188
0007–1188/94 $9.00 + $0.00

PREPARATION OF MANUSCRIPTS

Authors are strongly recommended to read the full *Instructions to Authors* and *Nomenclature Guidelines for Authors* (*Br. J. Pharmacol.* 1993, **108,** 275–284) before submitting a manuscript for publication in the *British Journal of Pharmacology*. The manuscript and cover letter should be checked against the following list before mailing.

The original and one copy of the manuscript must be supplied. Manuscripts must be typed in double-line spacing on one side of A4 paper, in type not smaller than 12 characters per inch or 10 point. Both copies to include Tables and a set of labelled Figures. One set of Figures without numbers or letters is also to be included. The text to be arranged in the following subsections:

1. **Title**—To have no more than 150 characters on a separate page, which should also include a Short Title (50 characters maximum) and the name and address of the author for correspondence.
2. **Summary**—To be arranged in numbered paragraphs (Full Papers) or a single paragraph (Special Reports).
   —to include aims, principal results and conclusions.
   —to include Key words (10 maximum) at end of summary.
3. **Introduction**—To contain concise statements of the problem and the aims of the investigation.
4. **Methods**—To have brief but adequate account of the procedures; *full names of drugs* (*including those referred to by manufacturer's code*), sources of drugs and statistical tests to be stated.
5. **Results**—To have no repetition of data in Figures, Tables and text.
6. **Discussion**—Findings and conclusions to be placed in context of other relevant work.
   NB Simple repetition of results and unwarranted speculation are not acceptable.
7. **Acknowledgements**—Sources of support. Sources of drugs not widely available commercially.
8. **References**—All references in the text to be included in the Reference List and *vice versa*. References in alphabetical order with complete citations; Journals publishing 'in press' papers identified.
   References to manuscripts submitted to other journals but not yet accepted are not allowed.
9. **Tables**—Each on a separate page and prepared in accordance with current requirements of the Journal.
10. **Figures**—Both labelled and non-labelled Figures to be prepared in accordance with current requirements of the Journal (see *Instructions to Authors*, 1993, **108,** 275–281) and provided with Figure Number and Authors' names on back (*in pencil*).
    —each legend to be typed on a separate page and carrying keys to symbols.
    —keys to symbols and histograms must not appear on the figures themselves, but in the respective legends.
    —'box style' figures are not in keeping with the Journal style; line drawings etc must have only left-hand and bottom axes.
11. **Manuscripts**—To be accompanied by a declaration signed by each author that
    (a) results are original
    (b) approval of all persons concerned has been given to submit manuscripts for consideration (see also 12b)
    (c) the same material is neither 'in press' (i.e. is in proof or has definitely been accepted for publication) nor under consideration elsewhere. Furthermore it will not be submitted or published elsewhere before a decision has been reached by the Editorial Board of the *British Journal of Pharmacology* and will not be submitted elsewhere if accepted by the *British Journal of Pharmacology*.
    (d) Copyright assignment is included.
12. **Cover letter**—To state clearly
    (a) Corresponding author's full postal address, telephone, telex or Fax number
    (b) where appropriate, that *either* ethical approval has been given for investigation *or* Company or Institutional permission to publish work has been received.
13. **Reminder**—Packaging to be sufficiently robust to protect Figures and to withstand mailing.

Failure to comply with *Instructions to Authors* may lead to substantial delays in processing, review and publication and may even jeopardize acceptance of the manuscript.

NOMENCLATURE

Authors are reminded that accepted receptor and associated terminology is laid out in *Nomenclature Guidelines for Authors*, as published in the *British Journal of Pharmacology*, *Br. J. Pharmacol.*, 1994, **111,** 385–387.

SPECIAL REPORTS

The purpose of *Special Reports* is to provide rapid publication for **new** and **important** results which the Editorial Board considers are likely to be of special pharmacological significance. *Special Reports* will have publication priority over all other material and so authors are asked to consider carefully the status of their work before submission.

In order to speed publication there is normally no revision allowed beyond very minor typographical or grammatical corrections. If significant revision is required, the Board may either invite rapid re-submission or, more probably, propose that it be re-written as a Full Paper and be re-submitted for consideration. In order to reduce delays, proofs of *Special Reports* will be sent to authors but **essential corrections must reach the Production Office within 48 hours of receipt.** Authors should ensure that their submitted material conforms exactly to the following requirements.

Special Reports should normally occupy no more than two printed pages of the Journal; two illustrations (Figures or Tables, with legends) are permitted. As a guideline, with type face of 12 pitch and double-line spacing, a page of A4 paper could contain about 400 words. The absolute maximum length of the *Special Report* is 1700 words. For each Figure or Table, please deduct 200 words. The manuscript should comprise a Title page with key words (maximum of 10), a Summary consisting of a single short paragraph, followed by Introduction, Methods, Results, Discussion and References (maximum of 10). In all other respects, the requirements are the same as for Full Papers (see current 'Instructions to Authors').

BRITISH JOURNAL OF PHARMACOLOGY VOLUME 111 (3) 1994

OBITUARY

G.W. Bisset. Wilhelm Feldberg, CBE, FRS (1900–1993) 649

SPECIAL REPORT

I. Pörsti, A.T. Bara, R. Busse & M. Hecker. Release of nitric oxide by angiotensin-(1-7) from porcine coronary endothelium: implications for a novel angiotensin receptor 652

PAPERS

H. Moritoki, T. Hisayama, S. Takeuchi, W. Kondoh & M. Imagawa. Relaxation of rat thoracic aorta induced by the Ca^{2+}-ATPase inhibitor, cyclopiazonic acid, possibly through nitric oxide formation 655

J. Cuevas & D.J. Adams. Local anaesthetic blockade of neuronal nicotinic ACh receptor-channels in rat parasympathetic ganglion cells 663

Y. Dohi, M. Kojima & K. Sato. Vasorelaxant effect of mexiletine in mesenteric resistance arteries of rats 673

M.K. Herbert & P. Holzer. Interleukin-1β enhances capsaicin-induced neurogenic vasodilatation in the rat skin 681

C.A. Maggi, S. Giuliani & P. Santicioli. Effect of cromakalim and glibenclamide on spontaneous and evoked motility of the guinea-pig isolated renal pelvis and ureter 687

P.B.S. Clarke, M. Reuben & H. El-Bizri. Blockade of nicotinic responses by physostigmine, tacrine and other cholinesterase inhibitors in rat striatum 695

K.K.C. Tan, M.J. Brown, J. Longmore, C. Plumpton & R.G. Hill. Demonstration of the neurotransmitter role of calcitonin gene-related peptides (CGRP) by immunoblockade with anti-CGRP monoclonal antibodies 703

C. Jiang & P. Collins. Inhibition of hypoxia-induced relaxation of rabbit isolated coronary arteries by N^G-monomethyl-L-arginine but not glibenclamide 711

O. Pérez, C. Valenzuela, E. Delpón & J. Tamargo. Class I and III antiarrhythmic actions of prazosin in guinea-pig papillary muscles 717

J.R. Purkiss, G.F. Wilkinson & M.R. Boarder. Differential regulation of inositol 1,4,5-trisphosphate by co-existing P_{2Y}-purinoceptors and nucleotide receptors on bovine aortic endothelial cells 723

D.M. Pollock & T.J. Opgenorth. ET_A receptor-mediated responses to endothelin-1 and big endothelin-1 in the rat kidney 729

G.J. Molderings, E. Colling, J. Likungu, J. Jakschik & M. Göthert. Modulation of noradrenaline release from the sympathetic nerves of the human saphenous vein and pulmonary artery by presynaptic EP_3- and DP-receptors 733

S. Meini, R. Patacchini &. C.A. Maggi. Tachykinin NK_1 receptor subtypes in the rat urinary bladder 739

S.S. Kelly & C.B. Ferry. The origin of the effects of an anticholinesterase on the latencies of action potentials in mouse skeletal muscles 747

J.M. Hunt, R.S. Redman & E.M. Silinsky. Reduction by intracellular calcium chelation of acetylcholine secretion without occluding the effects of adenosine at frog motor nerve endings 753

A. Floch, V. Fardin & I. Cavero. Characterization of NK_1 and NK_2 tachykinin receptors in guinea-pig and rat bronchopulmonary and vascular systems 759

J. Cortijo, C.M. Sanz, V. Villagrasa, E.J. Morcillo & R.C. Small. The effects of phorbol 12,13-diacetate on responses of guinea-pig isolated trachea to methylxanthines, isoprenaline and ryanodine 769

C.M. Yang, Y.-L. Yo, J.-T. Hsieh & R. Ong. 5-Hydroxytryptamine receptor-mediated phosphoinositide hydrolysis in canine cultured tracheal smooth muscle cells 777

R. Atcheson, D.G. Lambert, R.A. Hirst & D.J. Rowbotham. Studies on the mechanism of [^{3}H]-noradrenaline release from SH-SY5Y cells: the role of Ca^{2+} and cyclic AMP 787

C.J. Bailey & K.J. Mynett. Insulin requirement for the antihyperglycaemic effect of metformin 793

G.A. Kennett, M.D. Wood, A. Glen, S. Grewal, I. Forbes, A. Gadre & T.P. Blackburn. *In vivo* properties of SB 200646A, a 5-$HT_{2C/2B}$ receptor antagonist 797

D. Bowie & T.G. Smart. Species-dependent functional properties of non-NMDA receptors expressed in *Xenopus laevis* oocytes injected with mammalian and avian brain mRNA 803

M.M. Teixeira, S. Reynia, M. Robinson, A. Shock, T.J. Williams, F.M. Williams, A.G. Rossi & P.G. Hellewell. Role of CD18 in the accumulation of eosinophils and neutrophils and local oedema formation in inflammatory reactions in guinea-pig skin 811

A.M. Elhawary & C.C.Y. Pang. α_{1b}-Adrenoceptors mediate renal tubular sodium and water reabsorption in the rat 819

M.G. Persson, P. Agvald & L.E. Gustafsson. Detection of nitric oxide in exhaled air during administration of nitroglycerin *in vivo* 825

W.J. Wieczorek & Z.L. Kruk. Differential action of (+)-amphetamine on electrically evoked dopamine overflow in rat brain slices containing corpus striatum and nucleus accumbens 829

M. Santiago, A. Machado & J. Cano. Effect of L-arginine/nitric oxide pathway on MMP^+-induced cell injury in the striatum of rats 837

A. Barber, G.D. Bartoszyk, H.E. Griener, F. Mauler, R.D. Murray, C.A. Seyfried, M. Simon, R. Gottschlich, J. Harting & I. Lues. Central and peripheral actions of the novel κ-opioid receptor agonist, EMD 60400 843

P.P. McDonald, S.R. McColl, P. Braquet & P. Borgeat. Autocrine enhancement of leukotriene synthesis by endogenous leukotriene B_4 and platelet-activating factor in human neutrophils 852

O.G. García Hermida, T. Fontela, M. Ghiglione & L.O. Uttenthal. Effect of lithium on plasma glucose, insulin and glucagon in normal and streptozotocin-diabetic rats: role of glucagon in the hyperglycaemic response 861

M.N. Sillence & M.L. Matthews. Classical and atypical binding sites for β-adrenoceptor ligands and activation of adenylyl cyclase in bovine skeletal muscle and adipose tissue membranes 866

D.K. Martin, Y. Nakaya, K.R. Wyse & T.J. Campbell. Effects of disopyramide and flecainide on the kinetics of inward rectifier potassium channels in rabbit heart muscle 873

W.-M. Fu & F.-L. Huang. Potentiation by endogenously released ATP of spontaneous transmitter secretion at developing neuromuscular synapses in *Xenopus* cell cultures 880

A.C. Kappelle, G. Biessels, B. Bravenboer, T. van Buren, J. Traber, D.J. De Wildt & W.H. Gispen. Beneficial effect of the Ca^{2+} antagonist, nimodipine, on existing diabetic neuropathy in the BB/Wor rat 887

E. Pipili-Synetos, E. Sakkoula, G. Haralabopoulos, P. Andriopoulou, P. Peristeris & M.E. Maragoudakis. Evidence that nitric oxide is an endogenous antiangiogenic mediator 894

J.C. Ellory, S.J. Culliford, P.A. Smith, the late M.W. Wolowyk & E.E. Knaus. Specific inhibition of Ca-activated K channels in red cells by selected dihydropyridine derivatives 903

S.-M. Yu, T.-S. Wu & C.-M. Teng. Pharmacological characterization of cinnamophilin, a novel dual inhibitor of thromboxane synthase and thromboxane A_2 receptor 906

G.J. McLaren, G. Lambrecht, E. Mutschler, H.G. Bäumert, P. Sneddon & C. Kennedy. Investigation of the actions of PPADS, a novel P_{2X}-purinoceptor antagonist, in the guinea-pig isolated vas deferens 913

G.M. Nichol, G.H. Parsons & K.F. Chung. Effect of sodium metabisulphite on bronchial blood flow in conscious sheep: pharmacological modulation 918

A.U. Ziganshin, C.H.V. Hoyle, G. Lambrect, E. Mutschler, H.G. Bäumert & G. Burnstock. Selective antagonism by PPADS at P_{2X}-purinoceptors in rabbit isolated blood vessels 923

M. Gué, C. Gleizes-Escala, C. Del Rio-Lacheze, J.-L. Junien & L. Buéno. Reversal of CRF- and dopamine-induced stimulation of colonic motility by CCK and igmesine (JO 1784) in the rat 930

Y. Nakazato, Y. Tani, H. Teraoka, T. Sugawara, T. Asano, T. Ohta & S. Ito. Inhibitory effects of caffeine on secretagogue-induced catecholamine secretion from adrenal chromaffin cells of the guinea-pig 935

Contents continue inside back cover

Typeset by Elite Typesetting Techniques, Southampton, Hampshire
and printed in Great Britain by Unwin Brothers Ltd., The Gresham Press, Old Woking, Surrey

W. Nörenberg, J.M. Langosch, P.J. Gebicke-Haerter & P. Illes. Characterization and possible function of adenosine 5'-triphosphate receptors in activated rat microglia **942**

M.A. Shuker, F. Bowser-Riley & S.N. Davies. Possible NMDA antagonist properties of drugs that affect high pressure neurological syndrome **951**

M. Derrien, C. Durieux & B.P. Roques. Antidepressant-like effects of CCK_B antagonists in mice: antagonism by naltrindole **956**

E.M. van Gelderen & P.R. Saxena. Inhibition of nitric oxide biosynthesis and carotid arteriovenous anastomotic shunting in the pig **961**

ERRATUM **968**

Br. J. Pharmacol. (1993), **110,** 1483–1490

R.G. Pertwee, L.A. Stevenson & G. Griffin. Cross-tolerance between delta - 9 - tetrahydrocannabinol and the cannabimimetic agents, CP 55,940, WIN 55,212-2 and anandamide